

The background of the cover features a stylized brain composed of various colored segments (yellow, orange, red, purple, blue, green) arranged in a circular pattern. Overlaid on this brain is a network of white lines connecting small white dots, resembling a neural network or a web. The top half of the cover has a solid blue background, while the bottom half is white.

PERIPHERAL NERVE REGENERATION

EDITED BY: Giovanna Gambarotta, Kirsten Haastert-Talini, Esther Udina,
Stefania Raimondo and James Phillips
PUBLISHED IN: Frontiers in Cellular Neuroscience



frontiers

Frontiers eBook Copyright Statement

The copyright in the text of individual articles in this eBook is the property of their respective authors or their respective institutions or funders. The copyright in graphics and images within each article may be subject to copyright of other parties. In both cases this is subject to a license granted to Frontiers.

The compilation of articles constituting this eBook is the property of Frontiers.

Each article within this eBook, and the eBook itself, are published under the most recent version of the Creative Commons CC-BY licence.

The version current at the date of publication of this eBook is CC-BY 4.0. If the CC-BY licence is updated, the licence granted by Frontiers is automatically updated to the new version.

When exercising any right under the CC-BY licence, Frontiers must be attributed as the original publisher of the article or eBook, as applicable.

Authors have the responsibility of ensuring that any graphics or other materials which are the property of others may be included in the CC-BY licence, but this should be checked before relying on the CC-BY licence to reproduce those materials. Any copyright notices relating to those materials must be complied with.

Copyright and source acknowledgement notices may not be removed and must be displayed in any copy, derivative work or partial copy which includes the elements in question.

All copyright, and all rights therein, are protected by national and international copyright laws. The above represents a summary only. For further information please read Frontiers' Conditions for Website Use and Copyright Statement, and the applicable CC-BY licence.

ISSN 1664-8714

ISBN 978-2-88963-268-8

DOI 10.3389/978-2-88963-268-8

About Frontiers

Frontiers is more than just an open-access publisher of scholarly articles: it is a pioneering approach to the world of academia, radically improving the way scholarly research is managed. The grand vision of Frontiers is a world where all people have an equal opportunity to seek, share and generate knowledge. Frontiers provides immediate and permanent online open access to all its publications, but this alone is not enough to realize our grand goals.

Frontiers Journal Series

The Frontiers Journal Series is a multi-tier and interdisciplinary set of open-access, online journals, promising a paradigm shift from the current review, selection and dissemination processes in academic publishing. All Frontiers journals are driven by researchers for researchers; therefore, they constitute a service to the scholarly community. At the same time, the Frontiers Journal Series operates on a revolutionary invention, the tiered publishing system, initially addressing specific communities of scholars, and gradually climbing up to broader public understanding, thus serving the interests of the lay society, too.

Dedication to Quality

Each Frontiers article is a landmark of the highest quality, thanks to genuinely collaborative interactions between authors and review editors, who include some of the world's best academicians. Research must be certified by peers before entering a stream of knowledge that may eventually reach the public - and shape society; therefore, Frontiers only applies the most rigorous and unbiased reviews.

Frontiers revolutionizes research publishing by freely delivering the most outstanding research, evaluated with no bias from both the academic and social point of view. By applying the most advanced information technologies, Frontiers is catapulting scholarly publishing into a new generation.

What are Frontiers Research Topics?

Frontiers Research Topics are very popular trademarks of the Frontiers Journals Series: they are collections of at least ten articles, all centered on a particular subject. With their unique mix of varied contributions from Original Research to Review Articles, Frontiers Research Topics unify the most influential researchers, the latest key findings and historical advances in a hot research area! Find out more on how to host your own Frontiers Research Topic or contribute to one as an author by contacting the Frontiers Editorial Office: researchtopics@frontiersin.org

PERIPHERAL NERVE REGENERATION

Topic Editors:

Giovanna Gambarotta, University of Turin, Italy

Kirsten Haastert-Talini, Hannover Medical School, Germany

Esther Udina, Autonomous University of Barcelona, Spain

Stefania Raimondo, University of Turin, Italy

James Phillips, University College London, United Kingdom

Citation: Gambarotta, G., Haastert-Talini, K., Udina, E., Raimondo, S., Phillips, J., eds. (2019). Peripheral Nerve Regeneration. Lausanne: Frontiers Media SA.
doi: 10.3389/978-2-88963-268-8

Table of Contents

- 05 Editorial: Peripheral Nerve Regeneration**
Giovanna Gambarotta, Stefania Raimondo, Esther Udina, James B. Phillips and Kirsten Haastert-Talini
- 08 Factors Within the Endoneurial Microenvironment Act to Suppress Tumorigenesis of MPNST**
Jo Anne Stratton, Peggy Assinck, Sarthak Sinha, Ranjan Kumar, Aaron Moulson, Natalya Patrick, Eko Raharjo, Jennifer A. Chan, Rajiv Midha, Wolfram Tetzlaff and Jeff Biernaskie
- 19 Nerve Repair Using Decellularized Nerve Grafts in Rat Models. A Review of the Literature**
Arianna B. Lovati, Daniele D'Arrigo, Simonetta Odella, Pierluigi Tos, Stefano Geuna and Stefania Raimondo
- 39 Inhibition of RhoA-Subfamily GTPases Suppresses Schwann Cell Proliferation Through Regulating AKT Pathway Rather Than ROCK Pathway**
Dandan Tan, Jinkun Wen, Lixia Li, Xianghai Wang, Changhui Qian, Mengjie Pan, Muhua Lai, Junyao Deng, Xiaofang Hu, Haowen Zhang and Jiasong Guo
- 49 Mitochondrial Damage-Associated Molecular Patterns of Injured Axons Induce Outgrowth of Schwann Cell Processes**
Andrea Korimová, Ilona Klusáková, Ivana Hradilová-Svíženská, Marcela Kohoutková, Marek Joukal and Petr Dubový
- 60 In vivo Evaluation of Nanostructured Fibrin-Agarose Hydrogels With Mesenchymal Stem Cells for Peripheral Nerve Repair**
Jesús Chato-Astrain, Fernando Campos, Olga Roda, Esther Miralles, Daniel Durand-Herrera, José Antonio Sáez-Moreno, Salomé García-García, Miguel Alaminos, Antonio Campos and Víctor Carriel
- 79 Long-Term Denervated Rat Schwann Cells Retain Their Capacity to Proliferate and to Myelinate Axons in vitro**
Tessa Gordon, Patrick Wood and Olawale A. R. Sulaiman
- 90 The Role of BDNF in Peripheral Nerve Regeneration: Activity-Dependent Treatments and Val66Met**
Claire Emma McGregor and Arthur W. English
- 112 The Success and Failure of the Schwann Cell Response to Nerve Injury**
Kristjan R. Jessen and Rhona Mirsky
- 126 Cholesterol Depletion Regulates Axonal Growth and Enhances Central and Peripheral Nerve Regeneration**
Cristina Roselló-Busquets, Natalia de la Oliva, Ramón Martínez-Mármol, Marc Hernaiz-Llorens, Marta Pascual, Ashraf Muhaisen, Xavier Navarro, Jaume del Valle and Eduardo Soriano
- 142 Role of Noradrenergic Inputs From Locus Coeruleus on Changes Induced on Axotomized Motoneurons by Physical Exercise**
Ariadna Arbat-Plana, Maria Puigdomenech, Xavier Navarro and Esther Udina
- 154 The Complex Work of Proteases and Secretases in Wallerian Degeneration: Beyond Neuregulin-1**
Marta Pellegatta and Carla Taveggia

- 167** *Ascorbic Acid Facilitates Neural Regeneration After Sciatic Nerve Crush Injury*
Lixia Li, Yuanyuan Li, Zhihao Fan, Xianghai Wang, Zhenlin Li, Jinkun Wen, Junyao Deng, Dandan Tan, Mengjie Pan, Xiaofang Hu, Haowen Zhang, Muhua Lai and Jiasong Guo
- 184** *Relevance and Recent Developments of Chitosan in Peripheral Nerve Surgery*
A. Boecker, S. C. Daeschler, U. Kneser and L. Harhaus
- 199** *Beyond Trophic Factors: Exploiting the Intrinsic Regenerative Properties of Adult Neurons*
Arul Duraikannu, Anand Krishnan, Ambika Chandrasekhar and Douglas W. Zochodne
- 221** *Spatiotemporal Differences in Gene Expression Between Motor and Sensory Autografts and Their Effect on Femoral Nerve Regeneration in the Rat*
David Hercher, Markus Kerbl, Christina M. A. P. Schuh, Johannes Heinzel, László Gal, Michaela Stainer, Robert Schmidhammer, Thomas Hausner, Heinz Redl, Antal Nógrádi and Ara Hacobian
- 240** *Two-Chambered Chitosan Nerve Guides With Increased Bendability Support Recovery of Skilled Forelimb Reaching Similar to Autologous Nerve Grafts in the Rat 10 mm Median Nerve Injury and Repair Model*
Nina Dietzmeyer, Maria Förthmann, Julia Leonhard, Olaf Helmecke, Christina Brandenberger, Thomas Freier and Kirsten Haastert-Talini
- 257** *The Effects of Surgical Antiseptics and Time Delays on RNA Isolated From Human and Rodent Peripheral Nerves*
Matthew Wilcox, Tom J. Quick and James B. Phillips
- 266** *Peripheral Nerve Regeneration is Independent From Schwann Cell p75^{NTR} Expression*
Nádia P. Gonçalves, Simin Mohseni, Marwa El Soury, Maj Ulrichsen, Mette Richner, Junhua Xiao, Rhiannon J. Wood, Olav M. Andersen, Elizabeth J. Coulson, Stefania Raimondo, Simon S. Murray and Christian B. Vægter
- 280** *The Median Nerve Injury Model in Pre-clinical Research – A Critical Review on Benefits and Limitations*
Giulia Ronchi, Michela Morano, Federica Fregnan, Pierfrancesco Pugliese, Alessandro Crosio, Pierluigi Tos, Stefano Geuna, Kirsten Haastert-Talini and Giovanna Gambarotta



Editorial: Peripheral Nerve Regeneration

Giovanna Gambarotta¹, Stefania Raimondo^{1,2}, Esther Udina³, James B. Phillips^{4,5} and Kirsten Haastert-Talini^{6,7*}

¹ Department of Clinical and Biological Sciences, University of Torino, Orbassano, Italy, ² Neuroscience Institute of the "Cavalieri Ottolenghi" Foundation (NICO), University of Torino, Orbassano, Italy, ³ Department of Cell Biology, Physiology and Immunology, Centro de Investigación Biomédica en Red sobre Enfermedades Neurodegenerativas, Institute of Neurosciences, Universitat Autònoma de Barcelona, Bellaterra, Spain, ⁴ Department of Pharmacology, UCL School of Pharmacy, University College London, London, United Kingdom, ⁵ UCL Centre for Nerve Engineering, University College London, London, United Kingdom, ⁶ Institute of Neuroanatomy and Cell Biology, Hannover Medical School, Hannover, Germany, ⁷ Center for Systems Neuroscience (ZSN) Hannover, Hannover, Germany

Keywords: axotomy, nerve guide, nerve graft, nerve sheath tumor, Schwann cells, dorsal root ganglion neurons, motoneurons, functional recovery

Editorial on the Research Topic

Peripheral Nerve Regeneration

The Research Topic entitled "Peripheral Nerve Regeneration" is focused on strategies to promote and improve the same. Injuries to peripheral nerves have variable causation such as metabolic or hereditary poly-neuropathies, nerve sheath tumors, or nerve trauma resulting from occupational or car accidents or combat activities. Although knowledge on the processes allowing peripheral nerve regeneration after degeneration or injury has been significantly increased over the last decades, and although (micro-)surgical methods have been refined considerably, more research is still needed to minimize consequences for patients and society. Treatment of acutely or chronically injured peripheral nerves is far from being optimal. Patients suffer from severe impairment of their quality of life due to continuous disabilities and their treatment is still affiliated with high socio-economic costs.

We are very grateful to the 123 authors from 14 different countries and five continents that contributed to the current Research Topic with seven review articles and 12 original research articles. These publications look from different angles into the current challenges for the field. For more than 100 years investigative surgeons and basic researchers have revealed solid knowledge on (1) key events orchestrating the process of peripheral nerve regeneration, and (2) basic mechanisms and pathways that need to be activated or blocked for axonal regeneration and correct reinnervation of peripheral target tissue. They have also discovered (3) cellular key players and how lineage reprogramming is generating them, and, not to forget, (4) surgical approaches and biomaterials supporting successful recovery.

This collection of articles adds insights to the aforementioned knowledge and also provides technical information worth considering in future research. In the following we first give an overview about the included review articles before shortly reporting on the original research articles.

Ronchi et al. analyzed the potential applications, advantages and limitations of the rat median nerve injury and repair model in pre-clinical research. They provide a synthetic overview of a variety of methods that can be applied in this model for assessing functional nerve regeneration and present informative tables about the research that has made use of this model. Also the article of Lovati et al. considers pre-clinical work performed in rat models. They performed a systematic review of the literature (from January 2007 to October 2017) regarding the different

OPEN ACCESS

Edited and reviewed by:

Arianna Maffei,
Stony Brook University, United States

*Correspondence:

Kirsten Haastert-Talini
Haastert-Talini.Kirsten@
mh-hannover.de

Specialty section:

This article was submitted to
Cellular Neurophysiology,
a section of the journal
Frontiers in Cellular Neuroscience

Received: 24 September 2019

Accepted: 30 September 2019

Published: 15 October 2019

Citation:

Gambarotta G, Raimondo S, Udina E,
Phillips JB and Haastert-Talini K
(2019) Editorial: Peripheral Nerve
Regeneration.
Front. Cell. Neurosci. 13:464.
doi: 10.3389/fncel.2019.00464

decellularization protocols used and aimed, through assessment of the results from histological and functional read-outs, to compare the effectiveness of the different nerve grafts. Boecker et al. reviewed the clinical relevance of chitosan derived nerve guides for short gap repair in human patients. They give an overview on the physiologic properties of chitosan in comparison to other nerve guide materials and discuss actual and future translation of chitosan into clinical practice.

In their article Duraikannu et al. review the regenerative capacity of adult neurons and novel intrinsic pathways that have impact on axonal regrowth, downstream from growth factor receptors. They thereby describe a novel approach to enhance the intrinsic growth of adult neurons, targeting neuronal inhibitors of regeneration, like tumor suppressor molecules, by means of non-viral siRNA. Orchestration of proteases and secretases during Wallerian degeneration and setting-up of a pro-regenerative environment is the focus of the article contributed by Pellegatta and Taveggia. They describe the role of different proteases and secretases in controlling, on a post-translational level, the activity of transmembrane proteins involved in peripheral nerve regeneration, among which the neurotrophin receptor p75^{NTR}, the receptor Notch, the growth factor Neuregulin-1, and how this creates a permissive environment to allow successful regeneration of injured axons. Jessen and Mirsky review the remarkable plasticity of Schwann cells and the characteristics of the denervated repair Schwann cell population. Knowledge about their distinct properties and cell-type specific control mechanisms can potentially be used to foster the development of effective treatments, further increasing regenerative potential and maintaining repair capacity for the extended periods that are required for substantial nerve regeneration.

Neurotrophic factors and especially brain derived neurotrophic factor (BDNF) are known to modulate axonal regeneration. McGregor and English put a particular focus on discussing the role of BDNF in activity-dependent treatments to enhance regeneration such as electrical stimulation, exercise, and optogenetic stimulation. The authors further discuss the impact of a common single nucleotide polymorphism in the human *bdfn* gene, Val66Met, on the effectiveness of these treatments and emphasize the need for personalized regenerative medicine.

The original research articles included into this Research Topic, again, cover versatile aspects of peripheral nerve regeneration research.

The characteristic properties of the graft material will have an important impact on the outcome of functional recovery after nerve gap repair. This is not only true for bioartificial grafts, but also for autografts that are commonly harvested from sensory nerves and implanted into motor (mixed) nerves. In this context Hercher et al. evaluated regeneration-associated gene expression in homotopic or heterotopic 6 mm rat femoral nerve grafts. They describe evident spatiotemporal differences in the expression of some trophic factors and cell adhesion molecules between grafts from sensory and motor branches. Although differences in the capabilities of these grafts to sustain motor regeneration in their short gap repair model were minor, the paper contributes to the debate about the concerns of using sensory donor nerves

as the gold standard to repair especially long nerve defects. The paper of Wilcox et al. considers a technical issue for going beyond rodent models in peripheral nerve research. For ethical and practical reasons, research of nerve injury and repair is focused to rodent models. Nevertheless, during reconstructive nerve repair it is sometimes possible to obtain human nerve samples. These samples are, however, exposed to the complex surgical environment, bringing them in contact with chemical and physical factors which are not present when sampling animal tissues in a research laboratory. With the aim of optimizing protocols for the efficient extraction of RNA for quantitative analysis, the authors characterized the effect of time delays before cryopreservation and the effect of contact with antiseptic surgical reagents on the quantity and quality of RNA isolated from human samples in comparison to rat nerve samples.

The efficacy of two novel bioartificial nerve grafts has been investigated by other groups in two different models, the 10 mm rat median nerve and the 10 mm rat sciatic nerve model. Dietzmeyer et al. report their analysis of a more bendable 2-chambered chitosan nerve guide. Bendability was increased by a corrugated outer wall and the chambers were formed by longitudinally introducing a perforated chitosan film to assist axonal outgrowth. The authors evaluated functional regeneration with three methods in the advanced rat median nerve model and demonstrate that the device represents a promising and innovative alternative for nerve repair in mobile body parts such as digits. Chato-Astrain et al. describe their attempt to produce a tissue engineered nerve graft from mesenchymal stem cells integrated into a nanostructured hydrogel. They evaluated their graft alone or introduced into clinically approved collagen type I nerve guides in the rat sciatic nerve model. The results presented suggest that the novel nanostructured fibrin-agarose bio-artificial nerve substitutes support nerve tissue regeneration and functional recovery to an extent similar to the autograft control.

As also discussed in the review by McGregor and English, already mentioned above, physical exercise has been shown to add positive effects on motor recovery after nerve transection and repair. In this context Arbat-Plana et al. investigated how physical exercise can modulate the synaptic stripping and other spinal changes that spinal motoneurons undergo after axotomy in a rat model of end-to-end sciatic nerve repair. They describe that in addition to the activity-dependent modulation of the BDNF system, noradrenergic projections of the *locus coeruleus* are important for some but not all the effects that exercise induces on the spinal cord after peripheral nerve injury. Besides physical exercise, also supplementation of specific nutrients is frequently discussed to support peripheral nerve regeneration. The paper of Li et al. investigated the effects of ascorbic acid (vitamin C), an essential micronutrient, on nerve regeneration *in vivo* in mice and *in vitro*. The study showed that ascorbic acid improved regeneration and functional recovery following sciatic nerve crush, promoted neurite outgrowth in dorsal root ganglion (DRG) neuron cultures, enhanced proliferation and migration behavior in primary Schwann cell cultures, and positively modulated the polarization of primary macrophages in culture toward the pro-regenerative phenotype.

Since sufficient peripheral nerve regeneration obviously depends on axonal outgrowth and its support by Schwann cells, we have included into this special issue also basic research papers reporting novel knowledge about these topics. The critical role of micro domains in cell membranes, specifically cholesterol-rich lipid rafts which cluster proteins and other molecules together, is explored by Roselló-Busquets et al. using a series of *in vitro* and mouse *in vivo* models. This study showed that cholesterol depletion disrupted lipid rafts, altered growth cone morphology, and resulted in increased axonal growth during development and after axotomy, with implications for both peripheral and central nervous system research.

It is widely accepted that the neurotrophin receptor p75^{NTR} is a central component in nerve regeneration, but since it is expressed in both neurons and glia and has been associated with a wide range of cellular behaviors its specific role remains elusive. Gonçalves et al. generated a conditional knockout mouse model to silence expression of p75^{NTR} specifically in Schwann cells, subsequently showing that Schwann cell p75^{NTR} is not critical for axonal regrowth or remyelination following crush injury, although its absence did reduce nerve conduction velocity.

Following injury, the axons and their terminals release mitochondrial DNA (mtDNA) fragments and proteins known as “mitochondrial damage-associated molecular patterns” (mtDAMPs). In their paper, Korimová et al. hypothesized that mtDAMPs might stimulate Schwann cells to put out cytoplasmic processes through the action of the corresponding receptors and tested their hypothesis *in vitro* in RT4-D6P2T schwannoma cells.

Schwann cell proliferation is an important component of the peripheral nerve injury response and Tan et al. explored the effect of inhibiting RhoA-subfamily GTPases with C3 transferase on this process, since RhoA inhibition is an established target used for improving neural regeneration. Using an *in vitro* model they showed that the C3 transferase CT04 suppressed primary Schwann cell proliferation, but that this was likely to be independent of the ROCK pathway and instead involved inactivation of the AKT pathway. Also related to the topic of Schwann cell proliferation, Gordon et al. analyzed the proliferative capacity of rat Schwann cells obtained from distal nerve stumps subjected to acute denervation of 7 days or

chronic denervation of either 7 weeks or 17 months, showing *in vitro* that these cells retained their capacity to myelinate DRG neurites, although with a reduced capacity. They hypothesized that, although these Schwann cells retain their ability to respond to axonal signals and to elaborate myelin, their low numbers and their reduced capacity to proliferate might account, at least in part, for the poor functional recovery observed after delayed surgical repair of injured peripheral nerves.

The last, but not least, publication included into this Research Topic, is a contribution of Stratton et al. who elucidated the role of the microenvironment to sustain/suppress malignant peripheral nerve sheath tumors (MPNST) that usually lead to aggressive nerve resections. Therefore, strategies aimed to suppress proliferation of these tumors would limit the functional loss derived from these malignancies. The authors present a novel *in vitro* model for studying MPNST by using isolated adult rodent Schwann cells and their results strengthen the finding that balanced properties of the tissue environment are crucial for tumor-suppression and point out to the high importance of the endoneurial tissue in this context.

We, the guest editors, thank all authors one more time for their valuable contributions and hope that the readers of this Research Topic will, as much as we did, enjoy learning the expert opinions and excellent research results presented.

AUTHOR CONTRIBUTIONS

All the authors have contributed to this editorial, writing comments to the different articles. KH-T has connected them all within the Editorial.

Conflict of Interest: The authors declare that the research was conducted in the absence of any commercial or financial relationships that could be construed as a potential conflict of interest.

Copyright © 2019 Gambarotta, Raimondo, Udina, Phillips and Haastert-Talini. This is an open-access article distributed under the terms of the Creative Commons Attribution License (CC BY). The use, distribution or reproduction in other forums is permitted, provided the original author(s) and the copyright owner(s) are credited and that the original publication in this journal is cited, in accordance with accepted academic practice. No use, distribution or reproduction is permitted which does not comply with these terms.



Factors Within the Endoneurial Microenvironment Act to Suppress Tumorigenesis of MPNST

Jo Anne Stratton^{1,2,3}, Peggy Assinck^{4,5}, Sarthak Sinha², Ranjan Kumar², Aaron Moulson⁴, Natalya Patrick², Eko Raharjo², Jennifer A. Chan^{6,7}, Rajiv Midha^{8*}, Wolfram Tetzlaff⁴ and Jeff Biernaskie^{1,2,3*}

¹ Hotchkiss Brain Institute, University of Calgary, Calgary, AB, Canada, ² Department of Comparative Biology and Experimental Medicine, Faculty of Veterinary Medicine, University of Calgary, Calgary, AB, Canada, ³ Alberta Children's Hospital Research Institute, University of Calgary, Calgary, AB, Canada, ⁴ Department of International Collaboration on Repair Discoveries, The University of British Columbia, Vancouver, BC, Canada, ⁵ Graduate Program in Neuroscience, The University of British Columbia, Vancouver, BC, Canada, ⁶ Arnie Charbonneau Cancer Institute, University of Calgary, Calgary, AB, Canada, ⁷ Department of Pathology and Laboratory Medicine, University of Calgary, Calgary, AB, Canada, ⁸ Department of Clinical Neurosciences, Cumming School of Medicine, University of Calgary, Calgary, AB, Canada

OPEN ACCESS

Edited by:

Esther Udina,
Autonomous University of Barcelona,
Spain

Reviewed by:

Hugo Guerrero-Cazares,
Mayo Clinic, United States
Doychin N. Angelov,
Universität zu Köln, Germany

*Correspondence:

Rajiv Midha
rajmidha@ucalgary.ca
Jeff Biernaskie
jeff.biernaskie@ucalgary.ca;
jabierna@ucalgary.ca

Received: 10 July 2018

Accepted: 21 September 2018

Published: 11 October 2018

Citation:

Stratton JA, Assinck P, Sinha S, Kumar R, Moulson A, Patrick N, Raharjo E, Chan JA, Midha R, Tetzlaff W and Biernaskie J (2018) Factors Within the Endoneurial Microenvironment Act to Suppress Tumorigenesis of MPNST. *Front. Cell. Neurosci.* 12:356. doi: 10.3389/fncel.2018.00356

Background: Deciphering avenues to adequately control malignancies in the peripheral nerve will reduce the need for current, largely-ineffective, standards of care which includes the use of invasive, nerve-damaging, resection surgery. By avoiding the need for en bloc resection surgery, the likelihood of retained function or efficient nerve regeneration following the control of tumor growth is greater, which has several implications for long-term health and well-being of cancer survivors. Nerve tumors can arise as malignant peripheral nerve sheath tumors (MPNST) that result in a highly-aggressive form of soft tissue sarcoma. Although the precise cause of MPNST remains unknown, studies suggest that dysregulation of Schwann cells, mediated by the microenvironment, plays a key role in tumor progression. This study aimed to further characterize the role of local microenvironment on tumor progression, with an emphasis on identifying factors within tumor suppressive environments that have potential for therapeutic application.

Methods: We created GFP-tagged adult induced tumorigenic Schwann cell lines (iSCs) and transplanted them into various *in vivo* microenvironments. We used immunohistochemistry to document the response of iSCs and performed proteomics analysis to identify local factors that might modulate divergent iSC behaviors.

Results: Following transplant into the skin, spinal cord or epineurial compartment of the nerve, iSCs formed tumors closely resembling MPNST. In contrast, transplantation into the endoneurial compartment of the nerve significantly suppressed iSC proliferation. Proteomics analysis revealed a battery of factors enriched within the endoneurial compartment, of which one growth factor of interest, ciliary neurotrophic factor (CNTF) was capable of preventing iSCs proliferation *in vitro*.

Conclusions: This dataset describes a novel approach for identifying biologically relevant therapeutic targets, such as CNTF, and highlights the complex relationship that tumor cells have with their local microenvironment. This study has significant implications for the development of future therapeutic strategies to fight MPNSTs, and, consequently, improve peripheral nerve regeneration and nerve function.

Keywords: peripheral nerve, sarcoma, Schwann cell, MPNST, CNTF, endoneurium, epineurium, microenvironment

IMPORTANCE OF STUDY

These studies provide several major findings. First, we develop a reproducible *in vitro* model to study MPNST from isolated adult rodent Schwann cells (termed iSCs) that following transplantation, share striking phenotypic resemblance to human MPNST tumors. Second, our results underscore the importance of tissue microenvironment in promoting tumorigenic growth and identify the endoneurial compartment within the peripheral nerve as a unique microenvironment enriched in tumor suppressive factors. Third, by probing uniquely expressed proteins within the endoneurial compartment, we demonstrated an autonomous role for CNTF to block proliferation of iSCs mimicking the inhibition observed when grafted iSCs are contained within the endoneurial compartment *in vivo*. Together, these experiments provide evidence for a tumor suppressive endoneurial niche that functions to repress proliferation and identifies CNTF signaling as a potential therapeutic avenue for MPNST.

INTRODUCTION

Malignancies within the peripheral nerve usually arise from aberrant Schwann cell proliferation (Miller et al., 2006; Chen et al., 2014) giving rise to malignant peripheral nerve sheath tumors (MPNST), a highly aggressive and largely untreatable form of soft tissue sarcoma, often culminating in patient death within ten years (LaFemina et al., 2013). MPNSTs occur in association with inherited syndromes, such as Neurofibromatosis Type 1 (NF1) but can also occur sporadically (46–48% of cases) (LaFemina et al., 2013). Although numerous treatment modalities have been assessed for treating MPNSTs (i.e., radiation therapy, surgical resection) they show moderate to poor results long term (LaFemina et al., 2013).

Deciphering avenues to adequately control malignancies in the peripheral nerve will potentially improve the current standard of care. More effective adjunctive drug therapy may allow modification of en block procedures, toward a nerve-sparing approach, to permit function to be retained.

There is strong evidence to suggest that distinct locations within the peripheral nervous system are prone to tumor formation and progression. For example, several studies have reported the capacity of nerve sheath tumors to form, with increased tumor burden, within the proximal nerves and plexus compared to the distal nerves (Plotkin et al., 2012) and are increasingly metastatic in the intrathoracic and dorsal root ganglion (DRG) regions compared to subdiaphragmatic

regions (Kourea et al., 1998). One potential difference between these anatomical regions is the presence of distinct local microenvironments unique to each location (Le et al., 2010; Lavasani et al., 2013). Moreover, transplanting NF1-mutant cells into several distinct locations within healthy rodents revealed that aberrant cell growth was especially pronounced when introduced into distinct regions (Le et al., 2010). The factors responsible for these divergent effects remain to be elucidated.

In line with this, others have observed similar phenomena following injury (Ribeiro et al., 2013; Schulz et al., 2016). Recently, Ribeiro and his colleagues found that when NF1 mutation was induced in adult Schwann cells, tumors formed in the nerve, but intriguingly *only* post-injury, and were restricted *only* to the injury site. In this context, the authors concluded that tumor formation must involve an interplay between Schwann cell-associated NF1 mutation and injury environments. They suggested that although the nerve is generally a “tumor suppressive environment,” an insult can locally alter the composition and concentration of factors present at the injury site, consequently allowing unregulated cell growth. Indeed, cytokine-releasing mast cells at the injury site have been shown to play a role in nerve tumor progression by introducing factors that are not typically present within the intact nerve (Yang et al., 2008). Importantly, the authors also noted that tumors did not form distal to the injury site – an area of the nerve that undergoes Wallerian degeneration post-injury. Since this area is subjected to similar injury cues, including the presence of mast cells (Gaudet et al., 2011), such findings suggest that injury-associated factors are not the sole mediators of tumorigenicity in this context.

Another plausible explanation for the formation of tumors at the injury site is the breakdown of connective tissue barriers as a result of the mechanical force exerted at the injury site itself (Olsson and Kristensson, 1973). The perineurial barrier, a thin layer of perineurial cells and collagen (Riccardi, 2007), acts as a specialized blood-nerve barrier in health (similar to that of the central nervous systems blood-brain barrier) (Allt and Lawrenson, 2000), but becomes compromised at sites of nerve injury (Haftek and Thomas, 1968). In homeostatic conditions, this specialized perineurial barrier with tight junctions prevents components from the endoneurium, where axons and Schwann cells reside, to diffuse freely into the epineurium, where large amounts of connective tissue resides (Olsson and Kristensson, 1973), as well as vice versa. Importantly, long term compromised perineurial barrier function post-injury is spatially confined *only* to the site of injury and does not extend distally (Olsson and Kristensson, 1973).

The potential contribution of a compromised barrier function to tumor progression becomes especially plausible when the types of cells and factors present within each defined compartment are considered. The epineurium harbors fibroblasts, adipocytes, endothelial cells, blood vessels, mast cells and large amounts of collagen (Norris et al., 1985; Verheijen et al., 2003). On the other hand, the endoneurial compartment mainly harbors Schwann cells (90%) and axons as well as a small number of neural-crest derived fibroblasts, endothelial cells, immune cells and small amounts of collagen (Sunderland, 1945; Riccardi, 2007; Weiss et al., 2016). Interestingly, several studies have shown that factors/cells known to be present within the epineurium enhance tumor progression (Fang et al., 2014; Kuzet and Gaggioli, 2016; McDonald et al., 2016), while several factors known to be present within the endoneurial compartment suppress Schwann cell proliferation (Parrinello et al., 2008). As such, one might hypothesize that Schwann cell-derived tumorigenesis is a consequence of perineurium breakdown and consequent exposure of latent tumorigenic cells to factors previously restricted to the epineurial compartment competing with suppressive factors within the endoneurium.

To elucidate the role of microenvironment on tumor progression, we subjected healthy adult Schwann cells to a mutagenic environment *in vitro* following which they were transplanted into various *in vivo* anatomical microenvironments. Following transplantation, mutagenic Schwann cells share striking phenotypic resemblance to human MPNST tumors. Intriguingly, when these same mutagenic induced tumor Schwann cells (iSCs) are injected and contained within the endoneurial compartment, they exit cell cycle and down-regulate tumor markers. Using quantitative proteomics to screen for factors that were uniquely present within the endoneurial compartment, we identified ciliary neurotrophic factor (CNTF), a growth factor known for promoting Schwann cell differentiation (Reynolds and Woolf, 1993), as a factor that was not only enriched within the endoneurium, but exhibited an autonomous capacity to inhibit proliferation of mutagenic Schwann cells. Uncovering the signals in the endoneurial niche that bias Schwann cells against hyperproliferation can safeguard against nerve malignancies and pave the path for regeneration and return of nerve function for cancer survivors.

MATERIALS AND METHODS

In vitro Induction of Tumor-Forming Adult Schwann Cells (iSCs)

Sciatic nerves were collected from three adult Sprague Dawley rats, then Schwann cells were isolated using a modified protocol from previously described methods (Mirfeizi et al., 2017). Briefly, nerves were dissected and minced, and subsequently incubated in collagenase Type IV (Worthington) at 37°C for 40 min. Samples were then centrifuged (1000 rpm for 5 min), then re-suspended in Schwann cell media containing DMEM and F12 (3:1), neuregulin-1 type III (50 ng/ml), forskolin (5 μ M), B27 supplement (1%), and penicillin (100 μ g/ml)/streptomycin (100 units/ml). Cells were plated on poly-D-Lysine (20 μ g/ml)

and laminin (4 μ g/ml) coated surfaces (BD Bioscience) and cultured at 37°C in a 5% CO₂ incubator. Cultures were also supplemented with plasmocin (25 μ g/mL, Invitrogen) and fungizone (40 ng/ml, Invitrogen) for the first month of culturing to prevent mycoplasma and fungal growth. Triple-filtered fetal bovine serum (1–5% FBS; Hyclone) was added for the first 5 days of culturing. Cells were maintained *in vitro* for 3–4 months. For passaging, media was removed and TrypLE-express (Invitrogen) was added to cultures and incubated at 37°C for 5 min. All detached cells were collected and plated at a density of 50,000 cells/ml for further maintenance. Tumor-forming characteristics of adult Schwann cells were induced by extended growth and repeated passage *in vitro* as previously described (Funk et al., 2007). Spherical colony formation (loss of contact mediated growth inhibition) and growth factor independence was observed by 3 months in culture. Cells were fed every 4th day and treated identically.

Lenti-Viral Labeling

To track cells following *in vivo* transplantation, cells were transduced with a GFP-expressing lenti-viral vector as previously described (Mirfeizi et al., 2017). All lentivirus work was undertaken in a biohazard level 2+ laboratory using previously established protocols. Cells (70% confluence) were incubated overnight in DMEM containing GFP-expressing lentiviral particles and polybrene (8 μ g/ml). The next day, fresh media was applied and cells were left to grow to 100% confluence. Cells were then dissociated and FACs sorted (BD FACS Aria III) to further purify the GFP+ cell fraction.

Karyotyping

To assess chromosomal integrity, karyotyping was performed on iSCs using previously described methods (Fan et al., 2014). Cultures (70% confluence) were treated with KaryoMAX Colcemid solution (30 ng/mL, Gibco) for 4 h at 37°C. Schwann cells were then detached from dishes, centrifuged, then re-suspended in cell hypotonic solution (CHS; 40 mM KCl, 20 mM HEPES, 0.5 mM EGTA and 9 mM NaOH) and incubated for 1 h at 37°C. After 1 h, the mix was fixed with acetic acid/methanol (1:3) and G-banding analysis was performed in the Clinical Genetics Facility at the Alberta Children's Hospital.

In vitro Treatments, Immunocytochemistry and Imaging

To assess the response of iSCs to different environmental stimuli, iSCs were plated onto 96-well plates at 10,000 cells/mL. Cells were treated with base media in the presence of neuregulin (100 ng/ml, R&D), CNTF (0–100 ng/ml, Peprotech), or media pre-conditioned with epineurial tissue, endoneurial tissue or spinal cord tissue. To prepare media for conditioned media experiments, equal wet weights of healthy epineurial tissue or endoneurial tissue from sciatic nerves, or white matter from thoracic spinal cords was dissected from C57BL/6 mice ($n = 8–10$), then maintained in DMEM and F12 (3:1), B27 supplement (1%), penicillin (100 μ g/ml)/streptomycin (100 units/ml) and 10% FBS for 4–6 days before filtering (0.4 μ m), and snap

freezing at -80°C until iSCs 96-well experiments were ready. Depleted media alone controls were treated identically except no explants were added. Three days post-treatment, cells were washed with sterile PBS and then fixed in 4% paraformaldehyde (PFA) for 5–10 min. For immunocytochemistry, cells were permeabilized using 0.5% triton X-100 and 5% BSA for 1–2 h at room temperature. Primary antibodies (rat anti-Ki67 (clone SolA15, 14569882, eBiosciences), mouse anti-nestin (SC23927, Santa Cruz) were incubated overnight (1:200) at room temperature. Unbound primary antibodies were washed and cells were subsequently incubated with Alexa-conjugated secondary antibodies (1:200, Invitrogen) at room temperature for 1–2 h, washed, and nuclei were counterstained with Hoechst (1:1000, Sigma) and imaged using ImageXpress (Molecular Devices). The sum of cells (Ki67+ NES+ Hoechst+ versus NES+ Hoechst+) in 12 images (20 \times) per well was obtained, then normalized to obtain a percentage value for each well. This value was subsequently averaged across three replicates per condition. Experiments were replicated on 3 independent days.

Animal Care and Surgery

Animal procedures were approved by the University of Calgary and University of British Columbia Animal Care Committees in compliance with the Guidelines of the Canadian Council of Animal Care. To assess the impact of *in vivo* microenvironments on the capacity of iSCs to form tumors, adult 8–12 weeks immune-deficient Foxn1^{nu}, NOD/CB17-Prkdc^{scid}/NcrCrl mice (for nerve and skin injections), or Sprague Dawley rats (for spinal cord injections) were used [Charles River Laboratories (Senneville, QC, Canada)]. Rats were treated with Cyclosporin A and GM1 natural killer cell antibodies for immunosuppression. Rodents were maintained on a 12-h light cycle in a temperature-controlled environment with unlimited food and water. For cell transplants, rodents were anesthetized using isoflurane (5% induction and 2% maintenance) and given subcutaneous injections of 0.1 mL (0.03 mg/mL) buprenorphine for pain relief. For nerve and spinal cord transplants, an injury was first induced prior to transplants in order to create an environment permissive for tumor formation (Ribeiro et al., 2013). Surgery sites were sterilized and then the sciatic nerve (including endoneurial and epineurial compartments) or spinal cords were exposed and crush injured using #5 forceps (nerve) or an Infinite Horizon Impactor, 200 KD (spinal cord). Immediately after (nerve) or 2 weeks after (spinal cord) injury, each distal nerve received a 2 μL volume injection (100,000 cells) and each spinal cord received a 5 μL volume injection (500,000 cells) of GFP+ve nerve or skin-derived iSCs ($n = 3\text{--}4$ rodent per donor, 2–3 donors) using a 33-gauge Hamilton syringe. iSCs were suspended in neuregulin (500 ng/mL) and fast green (1%) in DMEM at a density of 50,000 cells/ μL . Importantly, this injection strategy resulted in the presence of iSCs in the endoneurial (tibial fascicles) and epineurial (surrounding the fascicles) compartments. For skin transplants, GFP transduced iSCs were injected intradermally into the back skin of NOD/CB17-Prkdc^{scid}/NcrCrl mice. In all cases, tissue was collected within 2–4 months of surgeries.

Tissue Processing, Immunohistochemistry and Imaging

Briefly, nerve, skin, and spinal cord tissue was harvested at 2–4 months post-transplant, then fixed overnight with 4% PFA. For spinal cords, 4% PFA cardiac perfusion was also performed. Tissue was then left in 30% sucrose overnight, then frozen in OCT (VWR International) and stored at -80°C . For comparisons to MPNST, archived human and rodent samples were fixed overnight in 10% neutral buffered formalin, processed through graded ethanol's and xylene, and embedded in paraffin. Sections were cut at 4 μm thickness and stained with hematoxylin and eosin (H&E). For IHC, heat-induced antigen retrieval was performed in 10 mM sodium citrate for 25 min in microwave prior to staining with the following primary antibodies: S100 (DAKO) rabbit polyclonal 1:3,000 dilution and Desmin (DAKO) mouse monoclonal D33 1:400 dilution. Detection of staining was performed using Envision+ DAB kit (DAKO) per manufacturer's protocol with hematoxylin as a counterstain. Archival material from MPNST surgical samples were obtained from the Clark Smith Tumor Bank at the University of Calgary (in collaboration with Calgary Laboratory Services) with ethics approval from the Health Research Ethics Board of Alberta – Cancer Committee. For immunohistochemistry for PFA fixed tissue, sections were cut using a Leica cryotome at 10–20 μm . Sections were then permeabilized with 0.5% triton-X 100 and blocked with 5% BSA or 10% NDS. Primary antibodies were incubated overnight (rabbit anti-Ncad, AB12221 Abcam; rat anti-Ki67, 14569882, eBiosciences; goat anti-CNTF, AB557 R&D; sheep anti-ErbB3, AF4518 R&D), washed with PBS, and then Alexa-conjugated secondary antibodies (1:200, Invitrogen) were applied for 2 h at room temperature. Hoechst was used to stain nuclei (1:1000, Sigma) and mounted with Permafluor (Thermo Fisher Scientific). Image collection and quantification was done using a Leica SP8 confocal microscope. Two images per condition at 4 mm distal to the injury site was collected using a 63 \times objective lens and Z-stack (eight planes) features. Images (maximum projection) were analyzed using ImageJ (NIH). These counts were then expressed as a ratio (i.e., GFP+ve Ki67+ve cells/GFP+ve cells) and averaged within each animal ($n = 5$ animals/group).

Proteomics

In order to assess the protein composition of the fascicular portion of the nerve, sciatic nerves were firstly extracted from healthy adult C57BL/6 mice ($n = 8$). Using fine forceps the outer sheaths (ie. epineurium and perineurium) of the sciatic nerves were carefully removed. At this stage the contents of the endoneurium (individual myelinated axons) were clearly distinguishable, and were minced and incubated before processing for protein collection. Equal wet weights of the dorsal column from the same mice were also collected as a comparison. Protein was extracted with SDS gel sample buffer [0.2 M Tris, 5 mM EDTA, 1 M Sucrose, SDS and dithiothreitol (DTT)]. Protein was then run on 10% acrylamide gel containing SDS to separate out proteins that were most likely of interest (10–60 kDa).

Gel plugs were washed in 50 mM ammonium bicarbonate/acetonitrile (50:50, v/v) then incubated in 100% acetonitrile. After being air dried, proteins were reduced with DTT (10 mM) at 56°C and alkylated with iodoacetamide (50 mM) at 24°C. Gel plugs were washed then rehydrated with a trypsin solution (Promega; 0.02 µg/ul, 10% acetonitrile) for 2 h at 0°C then placed in buffer for 16 h at 37°C. Supernatant (tryptic peptides) was transferred to acidifying solution [acetonitrile/water/10% trifluoroacetic acid (60:30:10, v/v)]. Gel plugs were washed with the same acidifying solution and combined. Samples were then lyophilized and resuspended in 1% formic acid. The tryptic peptides were analyzed by liquid chromatography (LC; Agilent 1260 Infinity chip cube interface) tandem mass spectrometry (MS/MS) on an Agilent 6550 iFunnel quadrupole (Q)-time-of-flight (TOF) mass spectrometer. The LC and the Q-TOF were both controlled by MassHunter (B.05.00). The capillary pump used: A1 (97% water, 2.9% acetonitrile, 0.1% formic acid) and B1 (90% acetonitrile, 9.9% water, 0.1% formic acid) solutions; and, the nanopump used: A1 (97% water, 2.9% acetonitrile, 0.1% formic acid) and B1 (97% acetonitrile, 2.9% water, 0.1% formic acid) solutions. Tryptic peptides (1 µl) were loaded onto a C18 trap column of an Agilent chip operating in enrichment mode using the capillarity pump of the LC system at a flow rate of 2.5 µl/min. Elution of the peptides was performed using a 25 min linear gradient from 3% to 50% B1 generated by the nanopump operated at 0.3 µl/min. The peptides were electrosprayed into the Q-TOF using an ionization voltage of 1950V and a 275°C heated drying gas at a flow of 13 l/min. The Q-TOF was operated in positive auto MS/MS mode. The precursor ions with a m/z comprised between 275 and 1700 were acquired at a scan rate of 250 ms/spectrum and the 10 most abundant precursors for each cycle having a charge higher than 1, an intensity of at least 1000 counts and a peptidic isotopic model were fragmented by collision induced dissociation. Fragment ions having a m/z comprised between 50 and 1700 were acquired at a scan rate of 333.3 ms/spectrum. The collision energy was calculated for each precursor based on its charge and its mass. An active exclusion which was released after 1 spectrum and 0.2 min was applied to avoid re-acquiring the same precursor.

For data extraction, a peptidic isotopic model with a maximum charge state of 6 was used. The peak filtering for MS/MS data was set up at an absolute height of at least 10 counts and relative height of the most abundant peak of at least 0.1%. Using Mascot algorithm (2.4), NCBI database search was performed. Parameters included: trypsin as enzyme, maximum number of missed cleavage of 1, a peptide charge of 2+, 3+, and 4+, cysteine carbamidomethylation as fixed modification, methionine oxidation as variable modification and a mass error tolerance of 20 ppm. A mass error tolerance of 0.2 Da was selected for the fragment ions. Only peptides identified with a score having a confidence higher than 95% were kept for further analysis.

Statistical Analysis

All statistical analysis was performed using GraphPad Prism (v5.0). Statistical comparisons were performed using a two-tailed unpaired Student's *t*-test or One-way ANOVA

followed by Tukey's *posthoc* test. A *p*-value of <0.05 was considered statistically significant. All graphs are presented as mean ± standard error of mean (SEM).

RESULTS

The Development of a Model for MPNST

To develop an MPNST model, we isolated primary Schwann cells from adult uninjured nerves (*n* = 3) and subjected these cells to identical mutagenic *in vitro* conditions as described by Funk and colleagues rodent experiments (Funk et al., 2007). Following 3–4 months of *in vitro* processing, adult Schwann cells consistently demonstrated features typical to tumor cell lines, including growth factor independent growth, loss of contact-mediated growth suppression, and abnormal chromosomes (Figure 1). Immunocytochemical assessment of proliferation kinetics indicated that iSCs were capable of proliferating at similar rates even in the absence of growth factors (neuregulin and forskolin; Figures 1A,B); indicating a loss of growth factor-dependent growth (Funk et al., 2007). Subsequent quantification revealed that the percentage of Ki67+ iSCs did not statistically differ between iSCs cultured in the presence or absence of growth factors critical to SC survival (Student's *t*-test, *n* = 4, *p* = 0.3). Also, iSCs formed non-adherent spherical colonies indicating a loss of contact-mediated cell cycle arrest—another common feature of uncontrolled proliferation (Figure 1C). Finally, we also demonstrated that there were several chromosomal abnormalities, including polyploidy and monosomy present within all iSC cultures (Figure 1D). Together, such findings indicate that Schwann cells exposed to extended *in vitro* cell culture exhibit reproducible transformation of otherwise healthy Schwann cells.

In order to determine the subtype of tumors generated by iSCs, we assessed several *in vivo* features of iSC-generated tumors following transplantation into the skin and compared these to human MPNST tumor biopsies collected at the Clark Smith Tumor Bank at the University of Calgary. Following subcutaneous injection of iSCs, 10/12 (83%) of cases showed a dermal growth at the injection site (Figure 1E). Consistent with MPNST (Figure 1F–I), iSC-generated tumors consisted of solid sheets and fascicles comprising elongated spindled cells with enlarged atypical oval and tapered nuclei, and moderate amounts of cytoplasm (Figures 1J,K). Tumor cells were mitotically active and displayed foci of intratumoral necrosis. Immunohistochemical staining showed that the tumor cells were focally immunoreactive for S100 (Figure 1L) and were negative for desmin (Figure 1M). Together, the histologic and immunophenotypic findings of iSC-generated tumors recapitulate those of human MPNST.

Endoneurial Microenvironment Suppresses Tumorigenesis of MPNST

To assess the effect of distinct nerve microenvironments on iSC tumor progression, GFP-labeled iSCs were injected into specific compartments (eg. endoneurium and epineurium) within the sciatic nerves of immune deficient rodents. Within 2 months

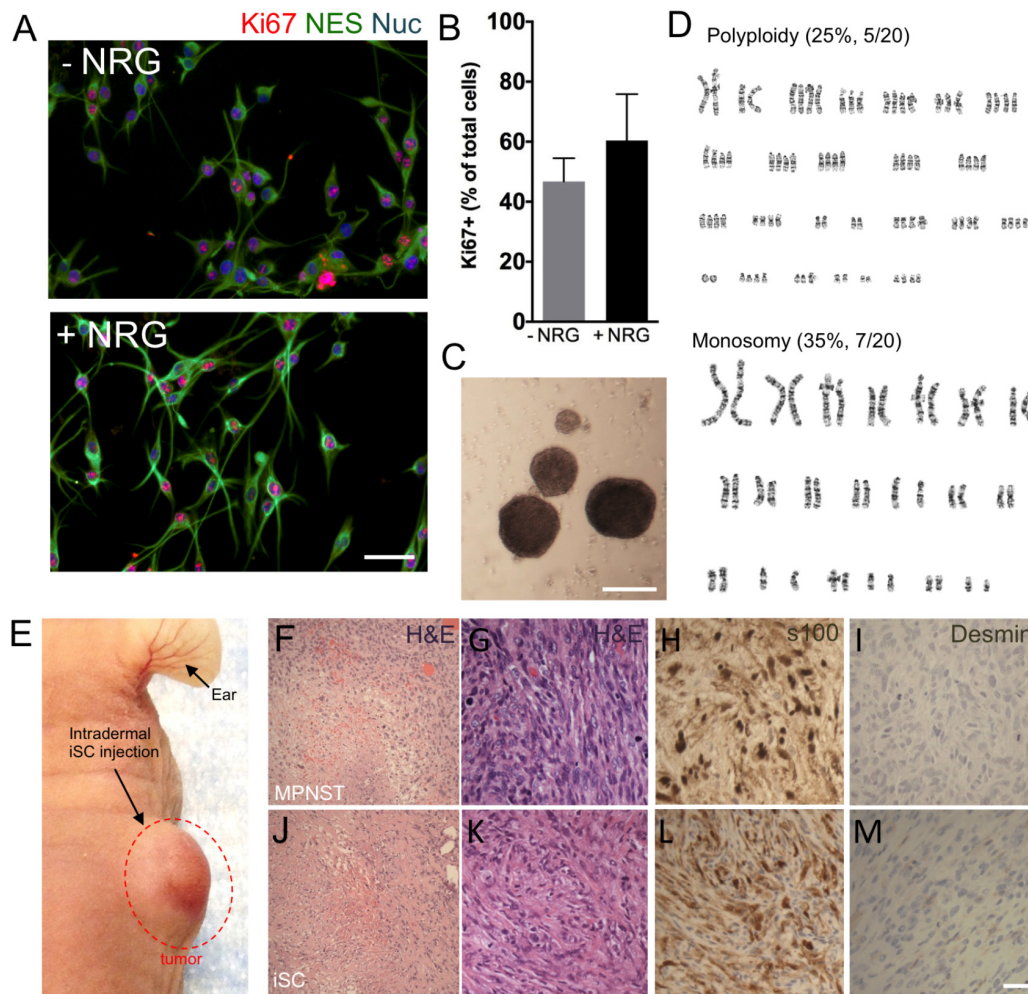


FIGURE 1 | The development of a malignant peripheral nerve sheath tumors (MPNST) model. **(A)** Representative immunocytochemical images of induced tumor Schwann cells (iSCs) either deprived of growth factors (–NRG) or treated with neuregulin and forskolin (+NRG, 50 ng/ml neuregulin, 5 mM Forskolin). Note the similar numbers of Nestin+ (green, NES), Hoechst+ (blue) iSCs that express Ki67 (red) across both conditions. **(B)** Quantification of percentage of Ki67+ cells revealed no difference between groups (Student's *t*-test, $n = 4$, $P = 0.3$). **(C)** Note the presence of sphere formation when iSCs are grown in growth factor deprived conditions. **(D)** Karyotyping analysis indicates multiple chromosomal abnormalities, including polyploidy and monosomy cells. **(E)** Intradermal iSC injections into back skin resulted in the development of tumors within 16 weeks. **(F–M)** Representative histological images of H&E (**F,G,J,K**), s100 (**H,L**) and Desmin (**I,M**) from a biopsied sample of human MPNSTs (**F–I**) and from a sample from iSCs (**J–M**). Note the presence of necrosis, mitosis and spindle-shaped cells in both samples (**F,G** and **J,K**). Also note the presence of S100 (**H,L**) immunoreactivity, as well as the lack of Desmin immunoreactivity (**I,M**) in both samples. Scale bars = **A** (50 μ m), **C** (200 μ m), **G–I** (20 μ m).

post-transplant, in 88% of cases (8/9 animals), we observed the formation of tumors (**Figure 2A**). Importantly, there was a robust presence of Ki67+ GFP+ iSCs (Watanabe et al., 2001) and their location was strictly confined to the epineurial compartment (**Figure 2B**). Quantification of the percentage of Ki67+ GFP+ iSCs demonstrated a fourfold decrease in proliferation in the endoneurial compartment compared to the epineurial compartment (One-way ANOVA with Tukey's *posthoc* test, $n = 6$, $p < 0.001$, **Figure 2E**). We also noted reduced expression of other cancer-associated proteins in iSCs within the endoneurial compartment compared to those within the epineurial compartment, including ErbB3 (Stonecypher et al., 2005) and N-cadherin (Flaiz et al., 2008), both associated

with dysregulated growth factor signaling in tumor growth (Aplin et al., 1998; Hanahan and Weinberg, 2000) (**Figure 3**). We also performed identical injections of iSCs into the spinal cord. Similar to the epineurial compartment, highly proliferative and invasive iSC tumors formed in 88% of cases (9/10) (**Figures 2C–E**).

Finally, we asked whether secreted factors may be responsible for this context-dependent growth inhibition. To do this, we exposed iSCs to conditioned media from microdissected adult nerve endoneurium, epineurium or spinal cord tissues. Intriguingly, there was a ~40% reduction in the percentage of proliferative iSCs when subjected to conditioned media from endoneurial tissue compared to media conditioned with

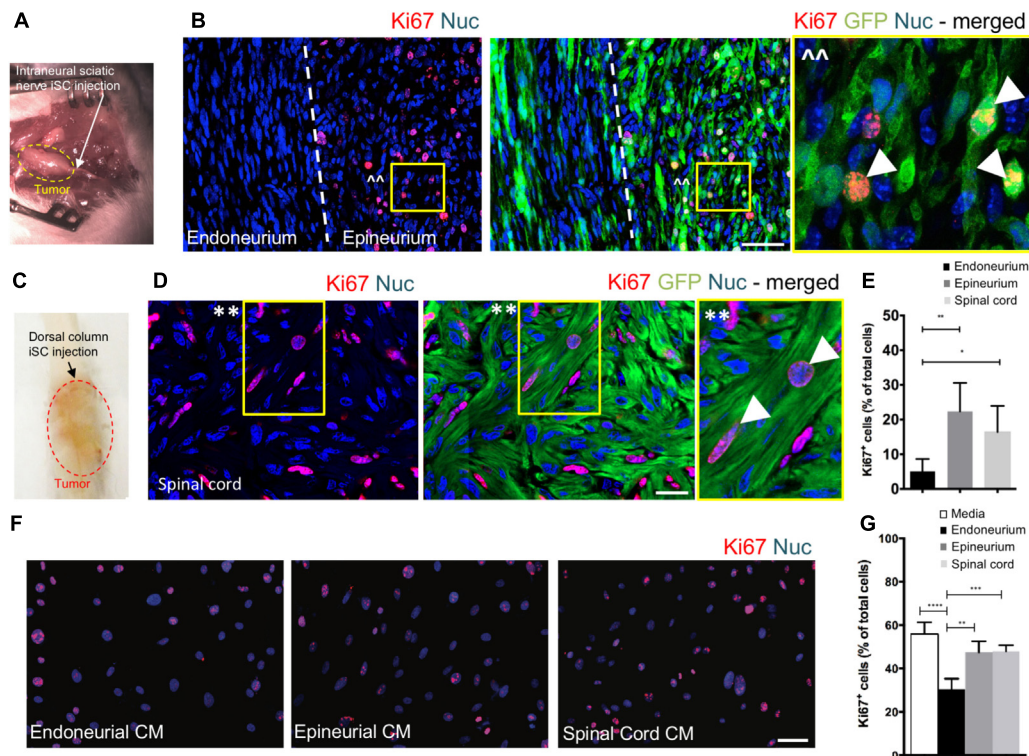


FIGURE 2 | The endoneurial microenvironment suppresses tumorigenesis of MPNST. **(A)** Intraneural iSC injections into the sciatic nerve resulted in the development of tumors within 2 months. **(B)** Representative immunohistochemical images of the endoneurial and epineurial compartments. Note the presence of widespread Ki67+ (red), Hoechst+ (blue) proliferative iSC (green) in the epineurial compartment compared to the endoneurial compartment. See inset (*) for high-resolution example of localization (arrowheads). **(C)** iSCs injected into the dorsal column of the spinal cord formed tumors within 2 months. **(D)** Representative immunohistochemical images of the spinal cord. Note the presence of widespread Ki67+ (red), Hoechst+ (blue) proliferative iSC (green) in the spinal cord. See inset (**) for high-resolution example of localization (arrowheads). **(E)** Quantification of the percentage of Ki67+ iSCs in the endoneurial compartment, epineurial compartment and spinal cord demonstrated a significant decrease in endoneurial compartment compared to other regions (One-way ANOVA, Tukey's *posthoc* test, $n = 6-8$, $*p < 0.01$, $**p < 0.001$). **(F)** Representative immunocytochemical images of iSCs treated with conditioned media (CM). Note there are less Ki67+ (red) Hoechst+ (blue) iSCs in the cultures treated with endoneurial CM compared to epineurial, spinal cord or base media. **(G)** Quantification of the percentage of Ki67+ iSCs demonstrated a significant decrease in the percentage of Ki67+ iSCs under endoneurial CM conditions compared to all other groups (One-way ANOVA, Tukey's *posthoc* test, $n = 3$, $****p < 0.0001$, $***p < 0.001$, $**p < 0.01$). Scale bars = **B** (50 μm), **E** (20 μm), **F** (50 μm).

epineurium or spinal cord tissue homogenates (One-way ANOVA, Tukey's *posthoc* test, $n = 3$, endoneurium vs; depleted, $p < 0.0001$; spinal cord, $p < 0.001$; epineurium, $p < 0.01$, **Figures 2F,G**). Taken together, these findings suggest that endoneurial microenvironments are uniquely suppressive for Schwann cells predisposed for oncogenic growth.

The Identification of Suppressive Factors in the Endoneurial Compartment

To identify potential repressive signaling proteins (10–60 kDa) enriched in endoneurial tissue of the adult mouse sciatic nerve we employed tandem mass spectrometry to perform unbiased proteomic analysis. We found that CNTF—a growth factor known for promoting Schwann cell differentiation (Reynolds and Woolf, 1993), was 5.5-fold enriched in endoneurial tissue compared to spinal cord tissue (**Figure 4A**). We validated CNTF expression with immunohistochemistry on mouse and human adult uninjured nerves and found CNTF immunoreactivity restricted to cytoplasmic-rich regions of myelinating Schwann

cells – most obviously at the perinuclear area (**Figure 4B**). Most importantly, we found that application of CNTF alone on iSCs *in vitro* caused a striking dose-dependent reduction in proliferation (**Figure 4C**). Quantification of this effect revealed up to a sixfold reduction in the percentage of Ki67+ iSCs when treated with 100ng/ml CNTF (One-way ANOVA, Tukey's *posthoc* test, $n = 3$, $**p < 0.05$) (**Figure 4D**). Taken together, CNTF appears to be an important regulator of oncogenic Schwann cells and this data suggests that CNTF or small molecules targeting its downstream targets, may offer some therapeutic value toward controlling aberrant Schwann cells and MPNSTs.

DISCUSSION

These studies provide several major findings that has implications for MPNST and consequently peripheral nerve regeneration. First, we developed a reproducible *in vitro* model to study MPNST from isolated adult Schwann cells (termed iSCs) that following transplantation, share striking phenotypic resemblance

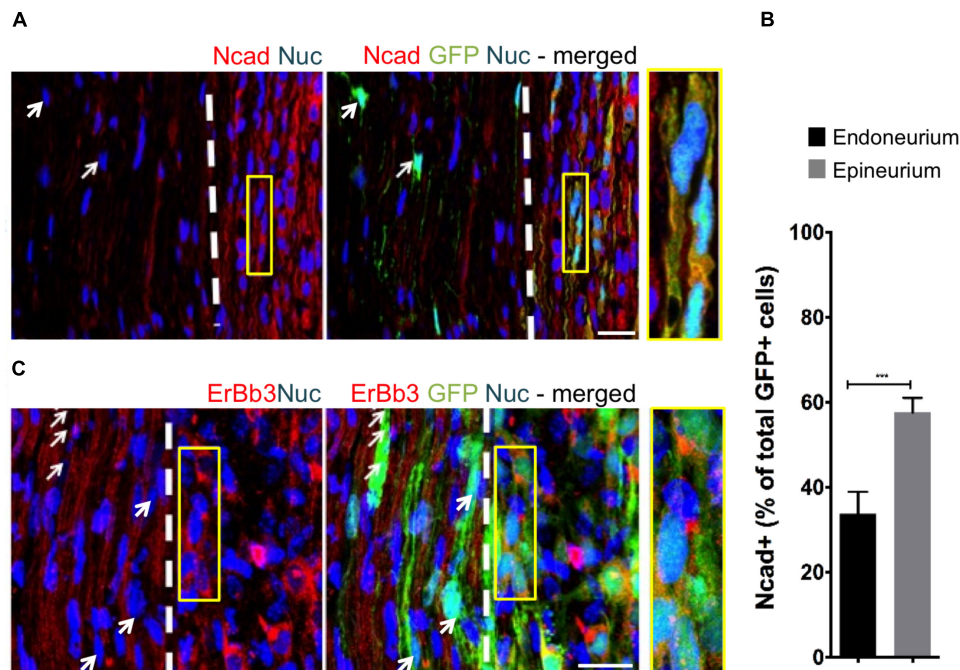


FIGURE 3 | The fascicular microenvironment suppresses tumor-associated protein expression in MPNST. **(A)** Representative immunohistochemical images of the endoneurial and epineurial compartments. Note the presence of widespread Ncad+ (red), Hoechst+ (blue) iSC (green) in the epineurial compartment (inset) compared to the endoneurial compartment (arrow). See inset for high-resolution example of colocalization of proteins. **(B)** Quantification of the percentage of Ncad+ iSCs in endoneurial and epineurial compartments demonstrated a significant decrease in endoneurial compartment (Student's *t*-test, $n = 4$, *** $p < 0.0008$). **(C)** Representative immunohistochemical images of the endoneurial and epineurial compartment. Note the presence of widespread ErbB3+ (red), Hoechst+ (blue) iSC (green) in the epineurium (inset) compared to the endoneurium (arrows). See inset for high-resolution example of colocalization of proteins. Scale bars = **A** (20 μ m), **C** (10 μ m), Insets (10 μ m, **A**; 5 μ m, **C**).

to primary human MPNST tumors. Second, our results underscore the importance of regional microenvironments in promoting tumorigenic growth and identify the endoneurial compartment within the peripheral nerve as a unique microenvironment enriched in tumor suppressive factors. Third, by probing uniquely expressed proteins within the endoneurial compartment, we demonstrated an autonomous role for CNTF to block proliferation of iSCs mimicking the inhibition observed when grafted iSCs are contained within the endoneurial compartment *in vivo*. Together, these experiments underscore the plasticity of iSC, highlights their sensitivity to microenvironment, and identifies CNTF signaling as a potential therapeutic avenue for MPNST.

Therapeutic approaches that take advantage of the responsiveness of tumor forming cells to CNTF offers a promising approach to treat MPNST. First, tumor-forming cells remain responsive to this growth factor—which is already a potentially valuable finding given the large amount of pathogenic pathways present within cancer cells (Birindelli et al., 2001). Moreover, given the well-described role of CNTF-induced differentiation in healthy cells (Rathje et al., 2011; Johnson et al., 2014), we suspect that CNTF-induced cell cycle arrest in iSCs likely takes advantage of differentiation-induced cell cycle arrest, which has for a long time been a promising avenue to treat cancer (Nguyen et al., 2016). Like in MPNST, in normal health

following nerve injury, proliferation of Schwann cells also occurs. But in contrast to the uncontrollable Schwann cell proliferation that occurs in MPNST, in normal health, these Schwann cells have the capacity to transition back into a mature differentiated myelinating state and contribute to regeneration. It is possible that CNTF-induced cell cycle arrest of iSCs piggy-backs on similar molecular pathways as regenerative-induced cell cycle arrest in normal health, but further study is needed.

Malignant peripheral nerve sheath tumors are mostly resistant to current standards of treatment (Ferner and Gutmann, 2002; Zehou et al., 2013), and surgical removal is often inadequate and debilitating as major nerves are sacrificed, given that the MPNST is often in close proximity to or in association with major nerves (Plotkin et al., 2013). At present, there are few early-stage diagnostic features that can adequately predict the risk of MPNST. In recent years, there have been several attempts to better understand the genetic bases of MPNST with the hope that this knowledge could be used for early detection, better predictions, and the discovery of new therapeutic targets. Recently, Rahrman et al. (2013) used an animal model approach to investigate several likely genetic links (NF1, Pten, and EGFR) for PNSTs, finding that a subset of genes were key players in the formation of high-grade PNSTs (otherwise known as MPNST). Unfortunately, identified genes only partially accounted for the progression of benign tumors toward high-grade PNST

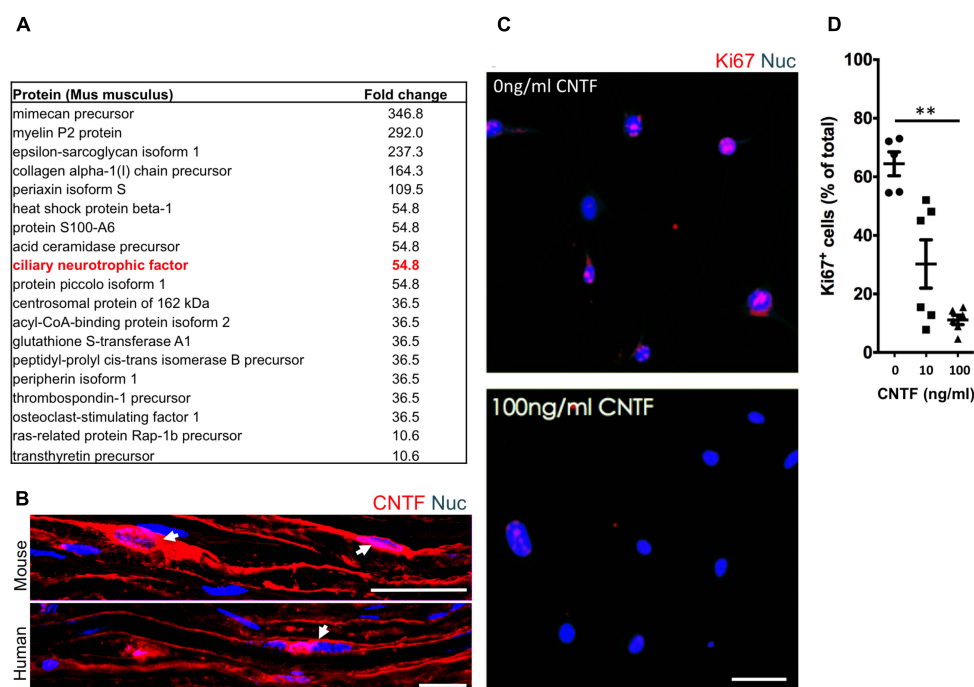


FIGURE 4 | The identification of suppressive factors in the endoneurial compartment. **(A)** Fold change in candidate proteins (10–60 kDa) enriched in the endoneurium compared to spinal cord tissue. Ciliary neurotrophic factor (CNTF, red box), a growth factor known for its role in promoting differentiation of Schwann cells, was found at levels 5.5-fold higher in endoneurium tissue compared to spinal cord tissue. **(B)** Representative immunohistochemical images of uninjured mouse and human sciatic nerves demonstrating the presence of CNTF (red) in the cytoplasm of Schwann cells (blue). Note the presence of CNTF around the peri-nuclear area adjacent to nuclei (blue)—a cytoplasmic rich region of the myelinating Schwann cell. **(C)** Representative immunocytochemical images of iSCs (blue) treated with 0 ng/ml and 100 ng/ml CNTF. Note the reduction in Ki67+ (red) cells in CNTF treated conditions. **(D)** Quantification of the percentage of Ki67+ cells treated with 0, 10, or 100 ng/ml CNTF revealed a reduction in ki67+ cells at 100 ng/ml compared to 0 ng/ml (One-way ANOVA, Tukey's *posthoc* test, $n = 3$, $**p < 0.05$). Scale bars = **B** (25 μ m), **C** (50 μ m).

formation and in most cases only when there was a combination of forced genetic mutations. Rodents generally formed either benign PNSTs, such as neurofibromas, or no tumors at all. Taken together, such findings suggest that, although there may be some genetic characteristics of MPNST, these characteristics do not autonomously dictate outcome. Rather, additional contributors, such as, epigenetic and environmental factors, must also play a role in MPNST development.

Our results support the notion that the cellular microenvironment plays a key role in predictability of tumor formation. When Ribeiro and colleagues first made the seminal discovery that NF1-mutant Schwann cells *only* formed tumors post-injury, a logical conclusion for this phenomenon was an environmental cue associated with the injury must also play a role. Indeed there are several factors associated with injury (Gaudet et al., 2011) as well as associated with tumor progression (Brossier and Carroll, 2012) that overlap. Most researched, in relation to PNST, is the mast cell (Yang et al., 2008). But, in addition to mast cells, there are many other injury-associated factors that influence cancer cells. Regulatory T-cells thrive in the cancerous microenvironment, producing excess TGF β 1, preventing the proliferation of other immune cells reducing immune responses to tumors, as well as enhancing tumor cell proliferation (Franco et al., 2016). In addition,

cancer associated fibroblasts (CAFs) have the ability to regulate malignant growth (Erez et al., 2010; Xing et al., 2010). Finally, another influencing factor for tumor progression is low pH (Jahde et al., 1982)—also known to be regulated in injury (Lengheden and Jansson, 1995). The fact that there is so much overlap with injury-associated factors and factors known to promote tumorigenesis, presupposes relationships between these factors and tumor progression (Brossier and Carroll, 2012). Interestingly, though Ribeiro et al. (2013) found that tumors did not form distal to the injury site – an area of the nerve that undergoes Wallerian degeneration post-injury and is, therefore, subject to similar injury cues, including the presence of mast cells and much of the factors described above (Gaudet et al., 2011). Such findings suggest that injury-associated factors are not the only mechanism at play in injury-associated Schwann cell-derived nerve sheath tumor progression. Consistent with Ribeiro et al. (2013), our results demonstrate that iSCs injected into the endoneurium of the distal stump, where injury cues are widespread, does not result in tumor formation. Together, such findings suggest that exposure to other factors at the injury site may be triggering malignant growth.

The fact that the perineurium is compromised when nerve injury occurs, resulting in long term dysfunction of the

perineurium, including a chronic increase in permeability, *but* only at the injury site and not distally (Haftak and Thomas, 1968; Olsson and Kristensson, 1973) makes it plausible that a compromised nerve-barrier might contribute to Schwann cell-derived tumor formation and progression. Usually this specialized perineurial barrier prevents fibroblast-derived and adipocyte-derived factors, as well as large amounts of collagen in the epineurium (Sunderland, 1945; Riccardi, 2007; Weiss et al., 2016) to diffuse freely within the endoneurium where widespread Schwann cells are present (Norris et al., 1985; Verheijen et al., 2003). Given that several papers have shown that factors within the epineurial compartment can lead to tumor progression (Fang et al., 2014; Kuzet and Gaggioli, 2016; McDonald et al., 2016); and that factors within the endoneurial compartment reduce Schwann cell proliferation (Parrinello et al., 2008), including CNTF, it is not surprising that we have found that iSCs are highly tumorigenic in the epineurial compartment compared to the endoneurial compartment. Taken together, this dataset suggests that in order for tumor progression to occur, the growth-promoting factors within the epineurium override suppressive factors within the endoneurium, ultimately driving tumor formation in peripheral nerves.

Finally, our data offers a cautionary note regarding the use of adult Schwann cells for stem cell transplant-based therapies to treat nervous system injury and disease. Our work demonstrates that these cells can exhibit genomic instability and readily acquire aberrations following repeated

in vitro expansion resulting in uncontrolled growth. As such, we strongly believe that adult Schwann cells, isolated from patients for subsequent autologous nervous system transplants, should undergo minimal *in vitro* processing, and be subjected to rigorous genetic screening before re-introduction into patients.

AUTHOR CONTRIBUTIONS

JAS, PA, NP, AM, RK, SS, ER, and JC contributed to execution of experiments. JAS, JB, RM, and WT designed the study and interpreted the data. JAS and JB prepared the manuscript.

FUNDING

This work was funded by an Alberta Innovates Health Solutions CRIO Project grant #201200859 (RM and JB) and a Stem Cell Network grant (WT and JB).

ACKNOWLEDGMENTS

We acknowledge the support provided by personnel in the regeneration unit in neurobiology (RUN) facility, and the Southern Alberta Mass Spectrometry (SAMS) Centre at the University of Calgary.

REFERENCES

- Allt, G., and Lawrenson, J. (2000). The blood–nerve barrier: enzymes, transporters and receptors—a comparison with the blood–brain barrier. *Brain Res. Bull.* 52, 1–12. doi: 10.1016/S0361-9230(00)00230-6
- Aplin, A. E., Howe, A., Alahari, S. K., and Juliano, R. L. (1998). Signal transduction and signal modulation by cell adhesion receptors: the role of integrins, cadherins, immunoglobulin-cell adhesion molecules, and selectins. *Pharmacol. Rev.* 50, 197–263.
- Birindelli, S., Perrone, F., Oggionni, M., Lavarino, C., Pasini, B., Vergani, B., et al. (2001). Rb and TP53 pathway alterations in sporadic and NF1-related malignant peripheral nerve sheath tumors. *Lab. Invest.* 81, 833–844. doi: 10.1038/labinvest.3780293
- Brossier, N. M., and Carroll, S. L. (2012). Genetically engineered mouse models shed new light on the pathogenesis of neurofibromatosis type I-related neoplasms of the peripheral nervous system. *Brain Res. Bull.* 88, 58–71. doi: 10.1016/j.brainresbull.2011.08.005
- Chen, Z., Liu, C., Patel, A. J., Liao, C. P., Wang, Y., and Le, L. Q. (2014). Cells of origin in the embryonic nerve roots for NF1-associated plexiform neurofibroma. *Cancer Cell* 26, 695–706. doi: 10.1016/j.ccell.2014.09.009
- Erez, N., Truitt, M., Olson, P., Arron, S. T., and Hanahan, D. (2010). Cancer-associated fibroblasts are activated in incipient neoplasia to orchestrate tumor-promoting inflammation in an NF- κ B-dependent manner. *Cancer Cell* 17, 135–147. doi: 10.1016/j.ccr.2009.12.041
- Fan, Y., Hsiung, M., Cheng, C., and Tzanakakis, E. S. (2014). Facile engineering of xeno-free microcarriers for the scalable cultivation of human pluripotent stem cells in stirred suspension. *Tissue Eng. A* 20, 588–599. doi: 10.1089/ten.TEA.2013.0219
- Fang, M., Yuan, J., Peng, C., and Li, Y. (2014). Collagen as a double-edged sword in tumor progression. *Tumour Biol.* 35, 2871–2882. doi: 10.1007/s13277-013-1511-7
- Ferner, R. E., and Gutmann, D. H. (2002). International consensus statement on malignant peripheral nerve sheath tumors in neurofibromatosis. *Cancer Res.* 62, 1573–1577.
- Flaiz, C., Utermark, T., Parkinson, D. B., Poetsch, A., and Hanemann, C. O. (2008). Impaired intercellular adhesion and immature adherens junctions in merlin-deficient human primary schwannoma cells. *Glia* 56, 506–515. doi: 10.1002/glia.20629
- Franco, O. E., Tyson, D. R., Konvinse, K. C., Udyavar, A. R., Estrada, L., Quaranta, V., et al. (2016). Altered TGF- β signaling drives cooperation between breast cancer cell populations. *FASEB J.* 30, 3441–3452. doi: 10.1096/fj.201500187RR
- Funk, D., Fricke, C., and Schlosshauer, B. (2007). Aging Schwann cells in vitro. *Eur. J. Cell Biol.* 86, 207–219. doi: 10.1016/j.ejcb.2006.12.006
- Gaudet, A. D., Popovich, P. G., and Ramer, M. S. (2011). Wallerian degeneration: gaining perspective on inflammatory events after peripheral nerve injury. *J. Neurotrauma* 28, 110. doi: 10.1186/1742-2094-28-110
- Haftak, J., and Thomas, P. K. (1968). Electron-microscope observations on the effects of localized crush injuries on the connective tissues of peripheral nerve. *J. Anat.* 103, 233–243.
- Hanahan, D., and Weinberg, R. (2000). The hallmarks of cancer. *Cell* 100, 57–70. doi: 10.1016/S0092-8674(00)81683-9
- Jahde, E., Rajewsky, M. F., and Baumgartl, H. (1982). pH distributions in transplanted neural tumors and normal tissues of BDIX rats as measured with pH microelectrodes. *Cancer Res.* 42, 1498–1504.
- Johnson, R. W., White, J. D., Walker, E. C., Martin, T. J., and Sims, N. A. (2014). Myokines (muscle-derived cytokines and chemokines) including ciliary neurotrophic factor (CNTF) inhibit osteoblast differentiation. *Bone* 64, 47–56. doi: 10.1016/j.bone.2014.03.053
- Kourea, H. P., Bilsky, M. H., Leung, D. H. Y., Lewis, J. J., and Woodruff, J. M. (1998). Subdiaphragmatic and intrathoracic paraspinal malignant peripheral nerve sheath tumors: a clinicopathologic study of 25 patients and 26 tumors.

- Cancer* 82, 2191–2203. doi: 10.1002/(SICI)1097-0142(19980601)82:11<2191::AID-CNCR14>3.0.CO;2-P
- Kuzet, S.-E., and Gaggioli, C. (2016). Fibroblast activation in cancer: when seed fertilizes soil. *Cell Tissue Res.* 365, 607–619. doi: 10.1007/s00441-016-2467-x
- LaFemina, J., Qin, L. X., Moraco, N. H., Antonescu, C. R., Fields, R. C., Crago, A. M., et al. (2013). Oncologic outcomes of sporadic, neurofibromatosis-associated, and radiation-induced malignant peripheral nerve sheath tumors. *Ann. Surg. Oncol.* 20, 66–72. doi: 10.1245/s10434-012-2573-2
- Lavasani, M., Pollett, J. B., Usas, A., Thompson, S. D., Pollett, A. F., and Huard, J. (2013). The microenvironment-specific transformation of adult stem cells models malignant triton tumors. *PLoS One* 8:e82173. doi: 10.1371/journal.pone.0082173
- Le, L. Q., Shipman, T., Burns, D. K., and Parada, L. F. (2010). Cell of origin and microenvironment contribution for NF1-associated dermal neurofibromas. *Stem Cell* 4, 453–463. doi: 10.1016/j.stem.2009.03.017
- Lengheden, A., and Jansson, L. (1995). PH effects on experimental wound healing of human fibroblasts in vitro. *Eur. J. Oral Sci.* 103, 148–155. doi: 10.1111/j.1600-0722.1995.tb00016.x
- McDonald, M. M., Fairfield, H., Falank, C., and Reagan, M. R. (2016). Adipose, bone, and myeloma: contributions from the microenvironment. *Calcif. Tissue Int.* 100, 433–448. doi: 10.1007/s00223-016-0162-2
- Miller, S. J., Rangwala, F., Williams, J., Ackerman, P., Kong, S., Jegga, A. G., et al. (2006). Large-scale molecular comparison of human Schwann cells to malignant peripheral nerve sheath tumor cell lines and tissues. *Cancer Res.* 66, 2584–2591. doi: 10.1158/0008-5472.CAN-05-3330
- Mirfeizi, L., Stratton, J. A., Kumar, R., Shah, P., Agabalyan, N., Stykel, M. G., et al. (2017). Serum-free bioprocessing of adult human and rodent skin-derived Schwann cells: implications for cell therapy in nervous system injury. *J. Tissue Eng. Regen. Med.* 11, 3385–3397. doi: 10.1002/term.2252
- Nguyen, P. H., Giraud, J., Staedel, C., Chambonnier, L., Dubus, P., Chevret, E., et al. (2016). All-trans retinoic acid targets gastric cancer stem cells and inhibits patient-derived gastric carcinoma tumor growth. *Oncogene* 35, 5619–5628. doi: 10.1038/onc.2016.87
- Norris, J. F., Smith, A. G., Fletcher, P. J., Marshall, T. L., and Hand, M. J. (1985). Neurofibromatous dermal hypoplasia: a clinical, pharmacological and ultrastructural study. *Br. J. Dermatol.* 112, 435–441. doi: 10.1111/j.1365-2133.1985.tb02317.x
- Olsson, Y., and Kristensson, K. (1973). The perineurium as a diffusion barrier to protein tracers following trauma to nerves. *Acta Neuropathol.* 23, 105–111. doi: 10.1007/BF00685764
- Parrinello, S., Noon, L. A., Harrisingh, M. C., Wingfield, Digby P., Rosenberg, L. H., Cremona, C. A., et al. (2008). NF1 loss disrupts Schwann cell-axonal interactions: a novel role for semaphorin 4F. *Genes Dev.* 22, 3335–3348. doi: 10.1101/gad.490608
- Plotkin, S. R., Blakeley, J. O., Evans, D. G., Hanemann, C. O., Hulsebos, T. J., Hunter-Schaedle, K., et al. (2013). Update from the 2011 international Schwannomatosis workshop: from genetics to diagnostic criteria. *Am. J. Med. Genet. A* 161, 405–416. doi: 10.1002/ajmg.a.35760
- Plotkin, S. R., Bredella, M. A., Cai, W., Kassarian, A., Harris, G. J., Esparza, S., et al. (2012). Quantitative assessment of whole-body tumor burden in adult patients with neurofibromatosis. *PLoS One* 7:e35711. doi: 10.1371/journal.pone.0035711
- Rahrmann, E. P., Watson, A. L., Keng, V. W., Choi, K., Moriarity, B. S., Beckmann, D. A., et al. (2013). Forward genetic screen for malignant peripheral nerve sheath tumor formation identifies new genes and pathways driving tumorigenesis. *Nat. Genet.* 45, 756–766. doi: 10.1038/ng.2641
- Rathje, M., Pankratova, S., Nielsen, J., Gotfryd, K., Bock, E., and Berezin, V. (2011). A peptide derived from the CD loop-D helix region of ciliary neurotrophic factor (CNTF) induces neuronal differentiation and survival by binding to the leukemia inhibitory factor (LIF) receptor and common cytokine receptor chain gp130. *Eur. J. Cell Biol.* 90, 990–999. doi: 10.1016/j.ejcb.2011.08.001
- Reynolds, M. L., and Woolf, C. J. (1993). Reciprocal Schwann cell-axon interactions. *Curr. Opin. Neurobiol.* 3, 683–693. doi: 10.1016/0959-4388(93)90139-P
- Ribeiro, S., Napoli, I., White, I. J., Parrinello, S., Flanagan, A. M., Suter, U., et al. (2013). Injury signals cooperate with Nf1 loss to relieve the tumor-suppressive environment of adult peripheral nerve. *Cell Rep.* 5, 126–136. doi: 10.1016/j.celrep.2013.08.033
- Riccardi, V. M. (2007). The genetic predisposition to and histogenesis of neurofibromas and neurofibrosarcoma in neurofibromatosis type 1. *Neurosurg. Focus* 22:E3.
- Schulz, A., Büttner, R., Hagel, C., Baader, S. L., Kluwe, L., Salamon, J., et al. (2016). The importance of nerve microenvironment for schwannoma development. *Acta Neuropathol.* 132, 289–307. doi: 10.1007/s00401-016-1583-8
- Stonecypher, M. S., Byer, S. J., Grizzle, W. E., and Carroll, S. L. (2005). Activation of the neuregulin-1/ErbB signaling pathway promotes the proliferation of neoplastic Schwann cells in human malignant peripheral nerve sheath tumors. *Oncogene* 24, 5589–5605. doi: 10.1038/sj.onc.1208730
- Sunderland, S. (1945). The adipose tissue of peripheral nerves. *Brain* 68, 118–122. doi: 10.1093/brain/68.2.118
- Verheijen, M. H. G., Chrast, R., Burrola, P., and Lemke, G. (2003). Local regulation of fat metabolism in peripheral nerves. *Genes Dev.* 17, 2450–2464. doi: 10.1101/gad.1116203
- Watanabe, T., Oda, Y., Tamiya, S., Kinukawa, N., Masuda, K., and Tsuneyoshi, M. (2001). Malignant peripheral nerve sheath tumours: high Ki67 labelling index is the significant prognostic indicator. *Histopathology* 39, 187–197. doi: 10.1046/j.1365-2559.2001.01176.x
- Weiss, T., Taschner-Mandl, S., Bileck, A., Slany, A., Kromp, F., Rifategovic, F., et al. (2016). Proteomics and transcriptomics of peripheral nerve tissue and cells unravel new aspects of the human schwann cell repair phenotype. *Glia* 64, 2133–2153. doi: 10.1002/glia.23045
- Xing, F., Saidou, J., and Watabe, K. (2010). Cancer associated fibroblasts (CAFs) in tumor microenvironment. *Front. Biosci.* 15:166–179. doi: 10.2741/3613
- Yang, F. C., Ingram, D. A., Chen, S., Zhu, Y., Yuan, J., Li, X., et al. (2008). Nf1-dependent tumors require a microenvironment containing Nf1 +/– and c-kit-dependent bone marrow. *Cell* 135, 437–448. doi: 10.1016/j.cell.2008.08.041
- Zehou, O., Fabre, E., Zelek, L., Sbidian, E., Ortonne, N., Banu, E., et al. (2013). Chemotherapy for the treatment of malignant peripheral nerve sheath tumors in neurofibromatosis 1: a 10-year institutional review. *Orphanet J. Rare Dis.* 8:127. doi: 10.1186/1750-1172-8-127

Conflict of Interest Statement: The authors declare that the research was conducted in the absence of any commercial or financial relationships that could be construed as a potential conflict of interest.

Copyright © 2018 Stratton, Assinck, Sinha, Kumar, Moulson, Patrick, Raharjo, Chan, Midha, Tetzlaff and Biernaskie. This is an open-access article distributed under the terms of the Creative Commons Attribution License (CC BY). The use, distribution or reproduction in other forums is permitted, provided the original author(s) and the copyright owner(s) are credited and that the original publication in this journal is cited, in accordance with accepted academic practice. No use, distribution or reproduction is permitted which does not comply with these terms.



Nerve Repair Using Decellularized Nerve Grafts in Rat Models. A Review of the Literature

Arianna B. Lovati^{1*†}, Daniele D'Arrigo^{1†}, Simonetta Odella², Pierluigi Tos², Stefano Geuna³ and Stefania Raimondo³

¹ Cell and Tissue Engineering Laboratory, IRCCS Istituto Ortopedico Galeazzi, Milan, Italy, ² UOC Hand Surgery and Reconstructive Microsurgery Unit, ASST G. Pini-CTO, Milan, Italy, ³ Department of Clinical and Biological Sciences, San Luigi Gonzaga Hospital, University of Turin, Turin, Italy

OPEN ACCESS

Edited by:

James Phillips,
University College London,
United Kingdom

Reviewed by:

Valerio Magnaghi,
Università degli Studi di Milano, Italy
Tatsuro Mutoh,
Fujita Health University, Japan

*Correspondence:

Arianna B. Lovati
arianna.lovati@grupposandonato.it

[†]These authors have contributed
equally to this work

Received: 02 August 2018

Accepted: 30 October 2018

Published: 19 November 2018

Citation:

Lovati AB, D'Arrigo D, Odella S,
Tos P, Geuna S and Raimondo S
(2018) Nerve Repair Using
Decellularized Nerve Grafts in Rat
Models. A Review of the Literature.
Front. Cell. Neurosci. 12:427.
doi: 10.3389/fncel.2018.00427

Peripheral nerve regeneration after severe traumatic nerve injury is a relevant clinical problem. Several different strategies have been investigated to solve the problem of bridging the nerve gap. Among these, the use of decellularized nerve grafts has been proposed as an alternative to auto/isografts, which represent the current gold standard in the treatment of severe nerve injury. This study reports the results of a systematic review of the literature published between January 2007 and October 2017. The aim was to quantitatively analyze the effectiveness of decellularized nerve grafts in rat experimental models. The review included 33 studies in which eight different decellularization protocols were described. The decellularized nerve grafts were reported to be immunologically safe and able to support both functional and morphological regeneration after nerve injury. Chemical protocols were found to be superior to physical protocols. However, further research is needed to optimize preparation protocols, including recellularization, improve their effectiveness, and substitute the current gold standard, especially in the repair of long nerve defects.

Keywords: nerve injury, nerve regeneration, allograft, decellularized nerve graft, rat model

INTRODUCTION

Traumatic injury of peripheral nerves is of considerable clinical importance due to its high incidence. The estimated incidence is upward of 300,000 cases per year in Europe (Kingham and Terenghi, 2006) and more than one million per year worldwide (Daly et al., 2012). Peripheral nerve lesions are five times more frequent than spinal cord lesions and results in decreased or complete loss of sensitivity and/or motor activity. The ability of peripheral nerves to regenerate has been recognized for more than a century; however, clinical and experimental evidence shows that regeneration is often unsatisfactory, especially following severe injury (Navarro et al., 2007; Sun et al., 2009; Pfister et al., 2011). For treating mild injury, direct suturing is the most common surgical technique. For nerve substance loss, nerve autograft (transplantation of an autologous nerve)

Abbreviations: AG, autograft/isograft; AP, authors' (in-house) protocol; AP-T, authors' protocol using triton-X; AP-TPA, authors' protocol using triton-X and peracetic acid; AP-TS, authors' protocol using triton-X and SDS; AP-W, authors' protocol using Wallerian degeneration; CMAP, compound muscle action potential; CV, conduction velocity; FTP, freeze and thaw protocol; HP, Hudson's protocol; NP, Neubauer's protocol; PBS, phosphate-buffered saline; SDS, sodium dodecyl sulfate; SFI, Sciatic Functional Index; SP, Sondell's protocol.

is currently the gold standard (Battiston et al., 2009) despite its limitations (e.g., additional surgery, scarring, and donor-site morbidity, limited source of donor nerves) (Hoben et al., 2018). There is a strong need to find innovative therapies.

Recent research has focused on the use of biological and synthetic conduits. Progress in materials sciences, with the availability of new biomaterials and innovative manufacturing procedures (Siemionow et al., 2013) has led to the development of innovative artificial conduits. However, as the translation of synthetic nerve grafts from bench to bedside is still limited, biological tubulization remains the mainstay approach. Albert (1885) first used a nerve graft from a donor (allograft) to reconstruct a damaged nerve after resection of a sarcoma. Although devoid of the drawbacks of autografts, allografts can be rejected by the recipient body and therefore require systemic immunosuppressive therapy. Advances in tissue engineering in the last decade have led to the realization of decellularized nerve allografts (Hundepool et al., 2017; Philips et al., 2018). Unlike conventional allografts, they are cleaned of their antigenic component yet retain their 3D structure which serves as scaffolds for axonal growth. Decellularized nerve allografts could thus represent a potentially ideal alternative.

The aim of this review was to quantitatively analyze the relevant scientific literature for comparative assessment of the effectiveness of nerve allografts in relation to decellularized grafts.

METHODS

The PubMed database was searched for articles published in English between January 2007 and October 2017. The search terms were “decellularization, decellularized, decellular, acellularization, acellular, acellularized” combined with the keyword “nerve.” The present study was focused on the integration of decellularized nerve grafts and tissue repair in rat models of peripheral nerve defects. Rat and mouse models are often the first choice for nerve regeneration studies. For this study we focused on the rat model because there is a marked predominance of rat use in nerve regeneration studies. Also, because rat nerves are larger and more resilient than the corresponding mouse nerves, standardized functional tests can be performed and the anatomy of rat nerves is better known (Greene, 1935; Tos et al., 2008). A total of 185 studies were retrieved, of which 149 full-text articles were excluded: 25 review articles; 30 articles because they concerned decellularization of tissue or matrices other than nerves; 12 studies on engineered nerve tissue with different cell sources unrelated to any decellularization protocol; 12 studies on the repair of spinal cord injuries but not peripheral nerve lesions; 23 studies on the clinical use of commercial products for which decellularization techniques are not described; 9 studies described only *in vitro* approaches and investigations; 7 were unrelated to nerve regeneration and/or integration; 8 involved animal species other than rats; 26 lacked specific control groups, such as the absence of autograft or pure decellularized nerve graft implantation, making it impossible to verify the efficacy of the decellularization protocols compared to the selected studies.

Ultimately, a total of 33 studies performed in rat models met our inclusion criteria for this review of the literature (Figure 1 and Table 1).

RESULTS AND DISCUSSION

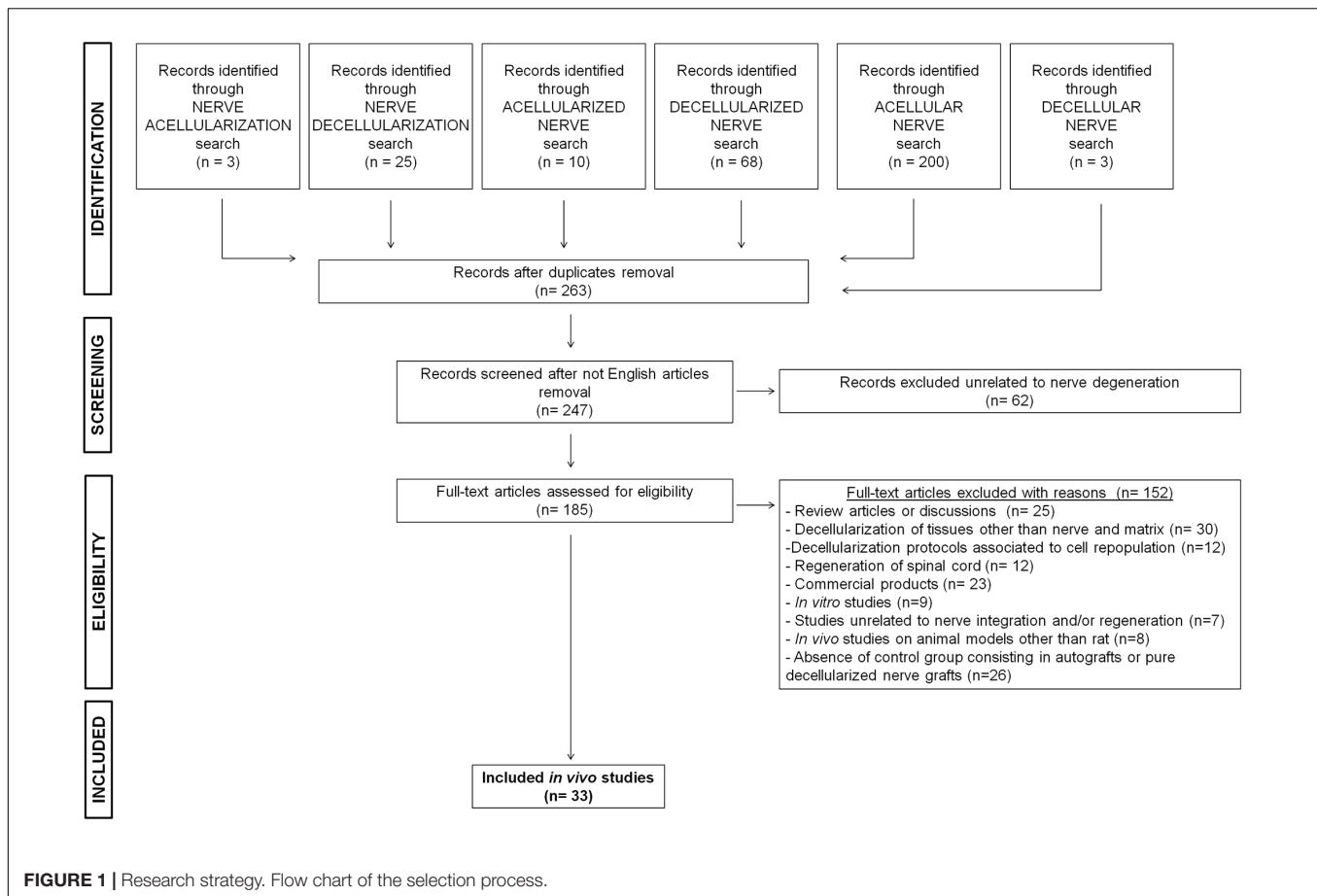
Decellularization Protocols

Several studies described the attempt to repair severe nerve damage by means of biologically derived scaffolds, such as decellularized nerve grafts. There are three main decellularization protocols for the creation of a functional graft: the one described by Sondell et al. (1998) and Hudson et al. (2004), and the combined Hudson protocol added with chondroitinase ABC by Krekoski et al. (2001). SP was used in 33% of the studies (Jia et al., 2012, 2017; Wang et al., 2012; Zhang et al., 2014; Zheng et al., 2014; Zhou et al., 2014; Zhu and Weihua, 2014; Huang et al., 2015; Garcia-Pérez et al., 2017; Zhu et al., 2015, 2017); HP was used in 24% (Saheb-Al-Zamani et al., 2013; Gao et al., 2014a; Hoben et al., 2015; Marquardt et al., 2015; Kim et al., 2016; Tajdaran et al., 2016; Yan et al., 2016; Cai et al., 2017), and a combined HP was used in 12% (Whitlock et al., 2009; Vasudevan et al., 2014; Wood et al., 2014; Jiang et al., 2016). Other studies (6%) used a FTP with or without the addition of chondroitinase ABC as introduced by Krekoski et al. (2001; Godinho et al., 2013; Wang H. et al., 2016). Moreover, others still (21%) developed an in-house decellularization protocol and tested its efficacy against autografts (Liu et al., 2011; Zhang and Lv, 2013; Wakimura et al., 2015; Kusaba et al., 2016; Wang W. et al., 2016; Wang et al., 2017b; Xiang et al., 2017). One study (3%) compared the efficacy of Hudson's, Sondell's, and the FTP in the same experimental setup (Nagao et al., 2011).

The most widely used protocol was developed by Sondell et al. (1998) (SP), who demonstrated *in vitro* good removal of the myelin sheath and cells, along with satisfying nerve regeneration in the absence of inflammatory response *in vivo*. This method is based on two sequential steps with a 3% Triton X-100 solution followed by a 4% sodium deoxycholate solution, in which the combination of a non-ionic surfactant with an anionic detergent is considered efficient to chemically lyse cells.

Several years later, Hudson et al. (2004) proposed a milder chemical treatment to better preserve the structure of the extracellular matrix (ECM). HP requires several steps repeated twice. In particular, an amphoteric detergent consisting of 125 mM sulfobetaine-10 (SB-10) solution is followed by an anionic detergent solution of 0.14% Triton X-200 and 0.6 mM sulfobetaine-16 (SB-16). The use of detergents with a demonstrated mild toxicity at low concentrations allowed Hudson and co-workers to efficiently disrupt the cell membranes while maintaining the ECM intact.

In order to eliminate chondroitin sulfate proteoglycans, which are known to inhibit axonal growth and the growth-promoting cues derived from the ECM components, Krekoski et al. (2001) introduced a step of proteoglycan degradation by means of the chondroitinase ABC enzyme, thus developing the so-called NP. By adopting this improvement, many authors were able to optimize their protocols by adding this degradation step



at the end of the decellularization process, especially after HP and the FTP. The original NP started the process with thermal decellularization, which is one of the most common methods to produce biological acellular grafts. In this process, tissues usually undergo three to five repeated freeze–thaw cycles.

In the various in-house protocols (Author's protocol, AP), three chemicals are employed to obtain nerve decellularization: Triton-X100 or 200 (Liu et al., 2011; Zhang and Lv, 2013; Kim et al., 2016; Wang et al., 2017b; Xiang et al., 2017) (AP-T; 50% of all AP), its combination with SDS (Wakimura et al., 2015; Kusaba et al., 2016; Wang H. et al., 2016) (AP-TS, 30% of AP) or with peracetic acid (Cai et al., 2017) (AP-TPA, 10% of AP). Moreover, Vasudevan et al. (2014) cultured explanted nerves *in vitro* with normal culture media to initiate the Wallerian degeneration and then in PBS to decellularize them and abruptly remove nutrient supply (AP-W, 10% of AP). SDS is an anionic surfactant with amphiphilic properties that lyses cells and denatures proteins. Peracetic acid is a potent oxidizing agent used to sterilize collagen tissues (Kemp, 1994; Gilbert et al., 2006). In decellularization, it acts by enhancing tissue permeability, allowing detergent penetration and subsequent cell colonization (Bottagisio et al., 2016).

The first parameter in the choice of a decellularization protocol is its duration. Duration is important for the time needed to obtain the results, for the structural maintenance

of the biological scaffolds, and for the cost of the procedure. In fact, the reduction of the entire process diminishes or eventually avoids the need for sterilization techniques, such as gamma irradiation, which has a controversial effect on decellularized matrix integrity (Boriani et al., 2017). Another issue is the use of numerous chemical detergents with reduced incubation times during the decellularization protocol. Indeed, the combination of different chemicals augments the deprivation of ECM components (Alhamdani et al., 2010) but also permits use of lower doses of detergents and shortens the incubation time, thus facilitating the complete removal of detergents, which results in a more suitable graft for cell repopulation (Rieder et al., 2004; Serghei et al., 2010; Crapo et al., 2011) and makes the procedure less time-consuming. In our analysis of the original version of the protocols considered here, the FTP was found to be the quickest and least laborious: it consists of three to five brief freeze and thaw cycles and takes a few minutes to complete without the need for chemical detergents and devoid of chemical remains with toxic side effects (Serghei et al., 2010; Crapo et al., 2011). All the other protocols take considerably longer: the HP needs almost 69.5 h and the SP 86 h to complete. Besides its shorter duration, the HP requires a lower percentage of chemical detergents, making their elimination more easy. The NP entails the chondroitinase ABC incubation step, which lasts 16 h, so the total duration of decellularization before this step is increased by

TABLE 1 | *In vivo* studies of nerve tissue decellularization and graft implantation.

Decellularization protocol	Implantation time (week)	Graft length (mm)	Investigations	Results	Reference
SP; HP; FTP	52	15	Sciatic functional index	AG = HP HP > FTP and SP	Nagao et al., 2011
SP	8	10	Conduction velocity, latency period, wave amplitude, muscle wet weight ratio, myelinated fiber density, axon diameter, myelin sheath thickness	AG > SP	Jia et al., 2012
SP	2,12	20	Muscle wet weight and tension ratio, myelinated fiber number, myelin sheath thickness, Von Frey hair sensitivity test	AG > SP	Wang et al., 2012
SP	1,2,4,8,12	15	Sciatic functional index, conduction velocity, myelinated fiber density, myelinated fiber number, myelin sheath thickness, immunostaining	AG > SP	Zhou et al., 2014
SP	8	10	Sciatic functional index, conduction velocity, latency period, wave amplitude, muscle wet weight ratio, myelinated fiber number, myelin sheath thickness	AG > SP	Zhang et al., 2014
SP	12	15	Sciatic functional index, conduction velocity, muscle wet weight and tension ratio, myelinated fiber density, axon diameter, myelin sheath thickness, immunostaining, gene expression (nerve growth factor, glial-derived neurotrophic factor, growth-associated protein 43, neurofilament heavy)	AG > SP, AG = SP in the first 6 weeks for sciatic functional index. Expression of all genes: AG > SP	Zheng et al., 2014
SP	20	6	Latency period, wave amplitude, myelinated fiber density, axon diameter, myelin sheath thickness	SP = AG	Zhu and Weihua, 2014
SP	1,2,4	15	Myelinated fiber density, axon diameter, myelin sheath thickness Immunostaining Gene expression (angiogenesis-related genes)	AG > SP Expression of angiogenesis-related genes: AG > SP	Zhu et al., 2015
SP	12	10	Conduction velocity Myelinated fiber density, myelinated fiber number, axon diameter, myelin sheath thickness Immunostaining	AG > SP, AG = SP myelinated fiber number Number of Schwann cells: AG > SP	Huang et al., 2015
SP	15	15	Sciatic functional index Immunostaining	AG = SP Presence of myelin in AG but not in SP	Garcia-Pérez et al., 2017
SP	8	10	Latency period, conduction velocity, wave amplitude Muscle wet weight ratio Myelinated fiber density, axon diameter, myelin sheath thickness	AG > SP Presence of laminin and myelin in AG, in SP only laminin	Jia et al., 2017
SP	1,2,3,4	10	Immunostaining	AG > SP	Zhu et al., 2017
HP + NP	6,12,22	14,28	Sciatic functional index Muscle wet weight ratio Myelinated fiber number, axon diameter	14-mm graft: AG = HP + NP, AG > HP + NP for myelinated fiber number at 6 weeks. AG = HP + NP at 12 weeks 28-mm graft: AG > HP + NP at 6 and 22 weeks HP + NP resulted non-immunogenic and maintained laminin structure	Whitlock et al., 2009
HP	10,20	20,40,60	Muscle wet weight and tension ratio Myelinated fiber number, axon diameter Immunostaining Gene expression (senescence markers)	AG > HP Senescence: AG < HP	Saheb-Al-Zamani et al., 2013

(Continued)

TABLE 1 | Continued

Decellularization protocol	Implantation time (week)	Graft length (mm)	Investigations	Results	Reference
HP	6,12	10	Sciatic functional index Conduction velocity Muscle wet weight ratio Axon diameter, myelin sheath thickness	AG > HP	Gao et al., 2014a
HP + NP; AP-W	12	35	Muscle wet weight and tension ratio Myelinated fiber number, myelin sheath thickness	AG > HP + NP and AP-W, HP + NP = AP-W	Vasudevan et al., 2014
HP + NP	12	14	Myelinated fiber number, axon diameter, myelin sheath thickness Retrograde nerve tracking	AG > HP + NP, AG = HP + NP for myelinated fiber number Regenerating nerves: AG = HP + NP, allograft > xenograft	Wood et al., 2014
HP	10	20	Myelinated fiber density, myelinated fiber number, axon diameter	AG > HP	Hoben et al., 2015
HP	8	30	Muscle wet weight ratio Myelinated fiber density, myelinated fiber number	AG > HP	Marquardt et al., 2015
HP	8	20	Muscle wet weight and tension ratio Myelinated fiber number Gene expression (Glial-derived neurotrophic factor)	AG > HP, AG = HP for muscle tension ratio Glial-derived neurotrophic factor expression: AG > HP	Yan et al., 2016
HP	8	10	Myelinated fiber number, axon diameter, myelin sheath thickness Retrograde nerve tracking	AG = HP, AG > SP for myelinated fiber number Regenerating neurons: AG > HP	Tajdaran et al., 2016
HP; HP + NP	12	15	Conduction velocity Muscle wet weight ratio Myelinated fiber density, myelin sheath thickness	AG > HP and HP + NP, HP + NP > HP, HP + NP = HP for myelin sheath thickness	Jiang et al., 2016
HP; AP-T	12	15	Muscle wet weight ratio Myelinated fiber density, myelin sheath thickness	AG > HP and AP-T, AP-T > HP	Kim et al., 2016
HP; AP-TPA Triton-X200 in sulfobetaine 10 + sulfobetaine 16 + 4% sodium deoxycholate + 0.1% peracetic acid	1,8	15	Muscle wet weight ratio Myelinated fiber number, axon diameter, myelin sheath thickness Thermosensitivity Immunological response	AG = AP-TPA, AG and AP-TPA > HP, AP-TPA = HP for myelinated fiber number <i>In vivo</i> host immune response: AP-TPA < HP	Cai et al., 2017
NP	8,12	20	Sciatic functional index Muscle wet weight and tension ratio Myelinated fiber number, axon diameter, myelin sheath thickness ELISA (collagen I and III)	AG = NP Collagen III expression: AG = NP Collagen I: AG < NP	Wang H. et al., 2016
FTP (5 cycles)	10	10	Myelinated fiber number Unmyelinated/myelinated axons ratio, area of individual myelinated axon, number of axons in unmyelinated bundle	AG = FTP	Godinho et al., 2013
AP-T	3 days,12	15	Sciatic functional index Conduction velocity, latency period, wave amplitude Myelinated fiber number, axon diameter, myelin sheath thickness Immunostaining	AG > AP-T	Liu et al., 2011
AP-T	12	15	Conduction velocity Muscle wet weight ratio Immunostaining	AG > AP-T Presence of acetyl cholinesterase-positive nerve fibers in motor endplates in AG and AP-T	Zhang and Lv, 2013
AP-TS	4,24	10,15	Latency period, wave amplitude Myelinated fiber density, myelin sheath thickness, axon diameter Immunostaining Von Frey's hair sensitivity test, toe spread factor	AG = AP-TS Basal lamina preserved in AG and AP-TS Limited presence of macrophage in both AG and AP-TS	Wakimura et al., 2015

(Continued)

TABLE 1 | Continued

Decellularization protocol	Implantation time (week)	Graft length (mm)	Investigations	Results	Reference
AP-TS	4,24	10,15	Latency period, wave amplitude Myelinated fiber density, axon diameter, myelin sheath thickness Immunostaining Von Frey's hair sensitivity test, toe spread factor	AG = AP-TS Basal lamina preserved in AG and AP-TS Limited presence of macrophage in both AG and AP-TS	Wang W. et al., 2016
AP-TS	25	15	Latency period, wave amplitude Myelinated fiber density, axon diameter Von Frey's hair sensitivity test, toe spread factor	AG = AP-TS Basal lamina preserved in AG and AP-TS	Kusaba et al., 2016
AP-T	11	10	Muscle wet weight and tension ratio Axon diameter, myelin sheath thickness	AG > AP-T, AG < AP-T for axon diameter	Wang et al., 2017b
AP-T	2,12	15	Sciatic functional index Conduction velocity, latency period Muscle wet weight ratio Retrograde nerve tracking	AG > AP-T, AG = AP-T for sciatic functional index at 2 weeks Cellularity and regenerating fibers: AG > AP-T	Xiang et al., 2017

AG, Autograft or isograft; HP, Hudson Protocol; NP, Neubauer Protocol; SP, Sondell Protocol; FTP, Freeze/Thaw Protocol; AP-T, Authors' Protocol using Triton X; AP-TS, Authors' Protocol using Triton X + SDS; AP-TPA, Authors' Protocol using Triton X + Peracetic Acid; AP-W, Authors' Protocol using Wallerian degeneration.

16 h. In the group of AP, the AP-TPA was the quickest protocol, taking 84.5 h, similar to the SP. The AP-T protocols varied in the amount of time required for decellularization: from 70 h in the protocol developed by Xiang et al. (2017) to 200 h in the protocol by Wang et al. (2017b), with an average duration of 128 h. The longest protocol was based on Wallerian degeneration developed by Vasudevan et al. (2014) which required 2 weeks of culture in complete culture medium and then another week of incubation in PBS in order to deprive cells of nutrients.

Evaluation of Parameters to Measure and Compare Nerve Decellularization Protocols After *in vivo* Implantation

The efficacy of nerve regeneration with decellularized nerve grafts was evaluated using quantitative analyses and standardized parameters to compare study outcomes after *in vivo* transplantation in rat models. We examined the SFI, the von Frey hair sensitivity test, and the toe spread factor which, altogether, indicate functional recovery after nerve grafting. The SFI comprises values between -100 (complete loss of functionality) to 0 (normal functionality). The von Frey hair sensitivity test entails stimulation of the animal's paw by means of increasingly stiff nylon monofilaments; paw withdrawal and flinch are considered positive responses and the test results are presented as a correlation between stimulus intensity and type of response (Chaplan et al., 1994). The toe spread factor is calculated on the basis of the distance from the first to the fifth toe (Geuna et al., 2009).

Among the various electrophysiological tests that evaluate *ex vivo* recovery of the graft's electrical functionality after implantation, conduction velocity (CV, m/s) through the graft and compound muscle action potential (CMAP, mV), and two features derived from CMAP, i.e., latency period (μ sec) and wave amplitude (mV), were analyzed. CMAP records the summation

of all muscle fiber action potentials derived from the activation of a group of motor neurons within a nerve bundle by means of a brief electrical stimulation. The latency period is the time between the application of an electrical stimulus to a nerve and muscle contraction. The wave amplitude represents the maximum value measured from baseline in the CMAP-resulting curve.

To assess muscle atrophy and functional recovery of the muscles most commonly analyzed (gastrocnemius, triceps surae, extensor digitorum, and tibialis anterior), muscle wet weight and maximum contraction tension were considered. Both parameters were analyzed by the studies *ex vivo* and mainly expressed as the ratio between the operated and the uninjured side. Moreover, since functional recovery is based on restoration of physiological neuronal morphology (Geuna et al., 2009), histomorphometric parameters were examined, including myelinated axon number, density (number of fibers/mm²), total fiber number, axon diameter (μ m), and myelin sheath thickness (μ m).

Morphological and Functional Comparison of Autografts and Sham Control of Nerve Gap Reconstruction in Rat Models

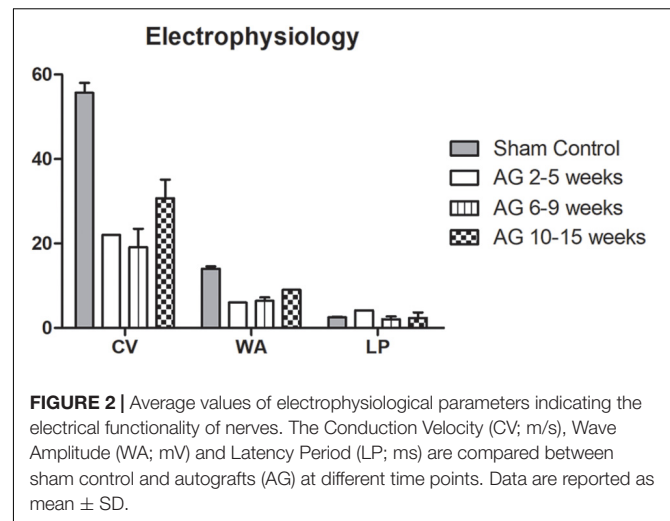
For a quantitative assessment of the functional and morphological recovery of the nerve graft, all manuscripts published in the literature and reporting numerical values for nerve recovery in terms of functionality and morphology over time were analyzed. Specifically, three different time points were considered: 2–5, 6–9, and 10–15 weeks after implantation. Comparable results from week 2 after graft implantation – the time in which nerve regeneration begins – until week 15 after surgery were evaluated. After surgical grafting, 3–6 weeks are necessary for Schwann cells and macrophages to arrive at the injury site and clear it of cellular and myelin debris (Geuna et al., 2009). The Schwann cells then start to proliferate,

organizing themselves in columns to permit the association of the regenerating axons. The choice of 15 weeks as the last time point was based on the study by Waitayawinyu et al. (2007), who reported that analyzing the outcomes of nerve recovery beyond 15 weeks may lead to misleading interpretations because differences between the experimental groups might be lost, also given the high regenerative capacity of the rodent model.

Most studies (Liu et al., 2011; Wang et al., 2012; Zhang and Lv, 2013; Gao et al., 2014a; Vasudevan et al., 2014; Wood et al., 2014; Zheng et al., 2014; Zhou et al., 2014; Huang et al., 2015; Jiang et al., 2016; Kim et al., 2016; Wang H. et al., 2016; Xiang et al., 2017) (39% of the studies included) set week 12 as the last endpoint and a few went beyond the 15th week. For instance, Zhou et al. (2014) and Saheb-Al-Zamani et al. (2013) evaluated the regenerative process until week 20, Whitlock et al. (2009) until week 22, Wakimura et al. (2015), Kusaba et al. (2016), and Wang W. et al. (2016) until week 24, and Nagao et al. (2011) until week 52.

As autografting represents the gold standard procedure for peripheral nerve reconstruction, we first analyzed its outcomes and then compared them with those obtained from sham procedures on healthy nerves. Only five studies included a sham control (Nagao et al., 2011; Tajdaran et al., 2016; Wang H. et al., 2016; Wang et al., 2017b; Garcia-Pérez et al., 2017), in which a slight decrease in nerve functionality after sham surgery (sham control) was found compared to that of the native nerves. This small number of studies could constitute a limitation of the present literature review and preclude comparison of the parameters analyzed. Taking into account that evaluation based on the SFI could vary widely depending on artifacts and operator ability (Varejao et al., 2001; Nichols et al., 2005; Monte-Raso et al., 2008; Fricker et al., 2016), the mean SFI of the sham controls was -8.16 at week 15 (Nagao et al., 2011; Wang H. et al., 2016; Wang et al., 2017a; Garcia-Pérez et al., 2017). Only one study reported a SFI of -2 , which approached the normal value at 52 weeks after surgery (Nagao et al., 2011). The SFI of autografts was expected to be lower than the sham surgery. The average SFI values were, in fact, significantly lower for the autografts than the sham controls at all time points. These data indicate that also sham surgery affects nerve functionality, albeit to a lesser extent. Differently, although autografting compromised nerve functionality initially, there was a predictable improvement in the SFI over time, indicating that nerve regeneration and recovery processes had begun.

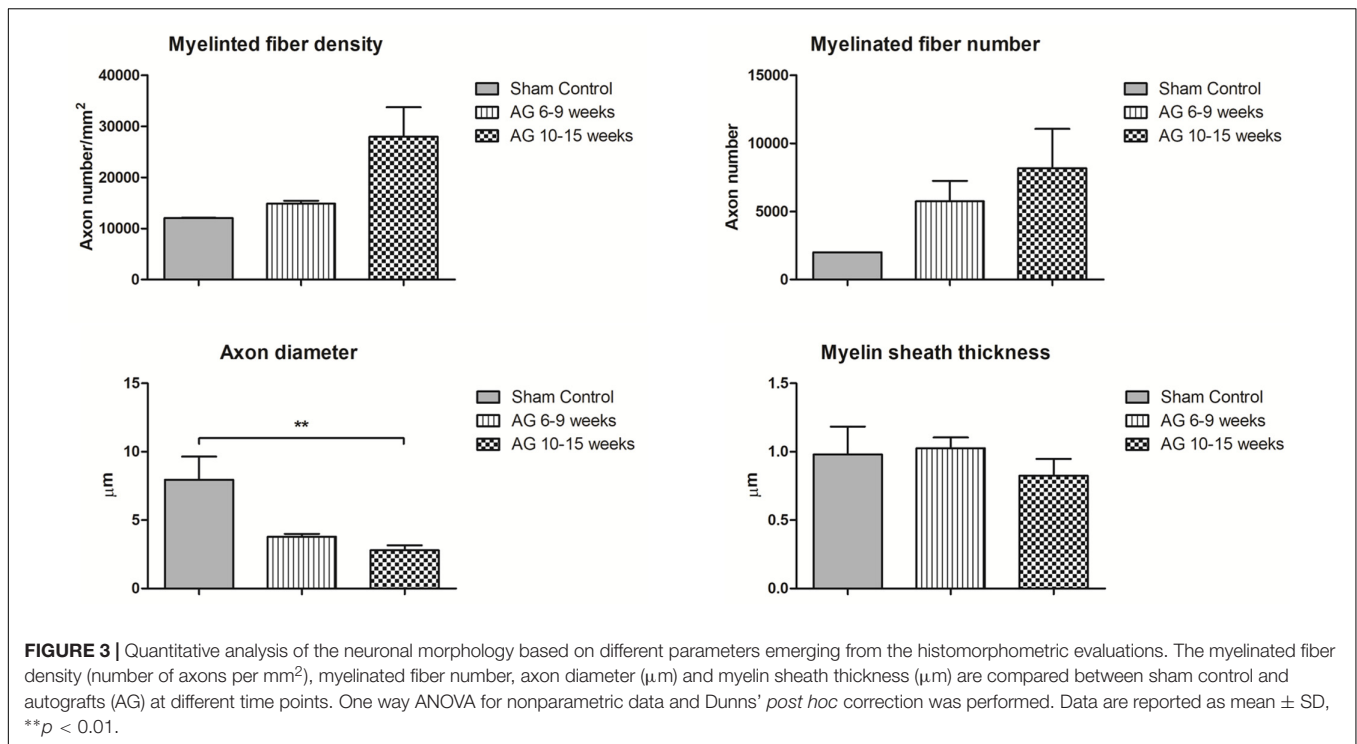
The electrophysiological parameters (CV, WA, and LP) reported in **Figure 2** were compared among studies, obtaining data for the sham controls and AG 2–5 weeks from one study (Wang H. et al., 2016), for AG 6–9 weeks from four studies (Jia et al., 2012; Zhang et al., 2014; Wang H. et al., 2016; Jia et al., 2017), and for AG 10–15 weeks from six studies (Liu et al., 2011; Zhang and Lv, 2013; Zheng et al., 2014; Huang et al., 2015; Jiang et al., 2015; Wang H. et al., 2016). The low amount of recorded data did not permit to statistically analyze the differences in the results. However, the trend of the electrophysiological parameters (**Figure 2**) showed higher CV and wave amplitude values for the sham control, while the latency period in the autografts was longer during the first 5 weeks after surgery and almost the same



for the two groups at the later time points. At 6–9 weeks, this parameter was even lower for the autografts, probably because only one study reported data for the sham control (Wang H. et al., 2016). The three parameters showed improvement over time, with an increase in CV and wave amplitude at the last time point, reaching half that of the sham control values. Otherwise, the latency period shortened over time, similar to the sham control value.

Muscle functionality, reported as the muscle wet weight and tension ratio, was greater in the sham control compared to autografts at all time points. The average muscle wet weight ratio in the sham control was 82% of that of the native limb (Wang H. et al., 2016), while the ratio obtained with the autografts was increased over time, from a mean of 46.3–51.6% from weeks 6–9 to 10–15, though none of the studies analyzed this parameter during the first 5 weeks (Whitlock et al., 2009; Liu et al., 2011; Jia et al., 2012, 2017; Wang et al., 2012, 2017a; Zhang and Lv, 2013; Vasudevan et al., 2014; Zheng et al., 2014; Marquardt et al., 2015; Jiang et al., 2016; Kim et al., 2016; Wang H. et al., 2016; Yan et al., 2016; Cai et al., 2017). The average muscle tension was 75% for the sham control and 54.7% for the autografts at the last time point; no analyses were performed at earlier time points. These results demonstrated that the autografts supported and strengthened reinnervation along the graft over time, resulting in a decrease in muscle atrophy and reinforcement of the tension that the muscles were able to elicit.

In the case of histomorphometric analyses, several authors reported evaluable data to be analyzed through non-parametric statistical tests, as reported in **Figure 3**. Indeed, for the sham controls, five authors reported quantitative parameters (Jia et al., 2012, 2017; Zhang et al., 2014; Wang H. et al., 2016; Wang et al., 2017b). For AG at 6–9 weeks, seven records indicated values for myelin and axon morphology (Whitlock et al., 2009; Jia et al., 2012; Zhang et al., 2014; Marquardt et al., 2015; Tajdaran et al., 2016; Cai et al., 2017; Jia et al., 2017), as well as, fourteen records detailed values for AG at 10–15 weeks (Whitlock et al., 2009; Liu et al., 2011; Wang et al., 2012, 2017b; Godinho et al., 2013; Vasudevan et al., 2014; Wood et al., 2014; Zheng et al., 2014;



Zhou et al., 2014; Hoben et al., 2015; Huang et al., 2015; Jiang et al., 2015; Kim et al., 2016; Wang H. et al., 2016).

As expected, myelinated fiber density and number were lower in the sham control than with the autograft at 6–9 and 10–15 weeks (**Figure 3**). The axon diameter in the sham controls showed a normal opposite trend, with a significant difference compared to the autografts at 10–15 weeks ($p < 0.01$). Unexpectedly, myelin sheath thickness was comparable between the sham controls and autografts and over time was decreased for the autografts. These data are far higher than normal estimated for a regenerating nerve, in which myelin sheath thickness is expected to be lower than in sham controls and directly proportional to the regenerating axon diameter, especially during the first weeks of regeneration.

There was a fluctuating trend for myelinated fiber density in the autografts owing to the study by Zhou et al. (2014) who reported a value of 53876 at weeks 2–5 (data not shown). Moreover, the myelinated fiber density in the autografts continued to increase, reaching 29000 myelinated fibers/mm² at 24 weeks, as reported by Wakimura et al. (2015) and Wang W. et al. (2016). These authors also reported an average myelin sheath thickness of 1 μm at 24 weeks after surgery (Wakimura et al., 2015; Wang W. et al., 2016). In addition, the axon diameter increased, reaching 5.6 μm (Wakimura et al., 2015; Kusaba et al., 2016; Wang W. et al., 2016). The data reported in **Figure 3** do not include the results reported by Godinho et al. (2013) because they seem to differ greatly (23000 myelinated fiber number) from the physiological parameters of a healthy nerve.

Interestingly, Godinho et al. (2013) evaluated three more parameters that could be useful for gaining a broader perspective on nerve function recovery at 8 weeks after surgery. The first

parameter was the unmyelinated and myelinated axon ratio, which was 6 in the sham control and 3 in the autograft. The second was the average number of axons in unmyelinated bundles, which was 3.5 in both groups. Moreover, in the same study, the sectional area of the myelinated axons was greater in the sham control than in the autograft group (9.5 vs. 3.6 μm²).

Overall, most of the studies reported consistent and comparable results for SFI, muscle wet weight ratio, and wave amplitude. Only a few reported values that substantially differed from the mean. In the autograft group, Wang et al. (2017b) reported a SFI markedly lower than average at all three time points, with a value of −48 at weeks 2–5, −45 at weeks 6–9, and −40 at weeks 10–15. Zhang et al. (2014) reported a much higher SFI and muscle wet weight ratio, with an increase from −32.3 after 2 weeks to −18.7 after 8 weeks and a muscle weight ratio of 89.5% at 8 weeks after surgery. Also, Xiang et al. (2017) reported a SFI value higher (−17) compared to the autograft average at 12 weeks. Liu et al. (2011) found a wave amplitude of 29.5 mV at 12 weeks after autografting, which was twice the mean value obtained for the sham control.

As expected, the overall values for the autografts were lower than the sham controls. In the majority of the parameters, there was a positive trend for the autografts over time, indicating a progressive recovery in nerve functionality and morphology. This recovery is due to the autografts providing viable Schwann cells and neurotrophic factors that support nerve axon regeneration (Flores et al., 2000; Siemionow and Brzezicki, 2009). Autografts are, in fact, effective and employed in the treatment of severe nerve injury in clinical practice (Rinker and Vyas, 2014). Based on this premise, the outcomes with autografts were compared with the results obtained with the different

decellularization protocols and were considered as benchmark values for evaluating the recovery of graft functionality and morphology.

Morphological and Functional Outcomes of Nerve Grafts Obtained With Decellularization Protocols

In order to evaluate the functional and morphological efficacy of decellularized nerve grafts at the three time points (2–5, 6–9, and 10–15 weeks after implantation), these parameters were analyzed and compared with respect to the decellularization protocols and to autografts or isografts used as the gold standard.

Also, the implanted graft length was considered. The success of regeneration has been shown to be proportional to the extent of the interstump zone and of the advancing sprouting cell protrusions. Nerve regeneration takes place through the extension of Schwann cell protrusions rather than axonal growth; Schwann cells guide and support the regenerating axons and regulate the rate of the recovery process (Son and Thompson, 1995). Lundborg et al. (1982) experimentally fixed at 10 mm the length beyond which the nerve injury is considered a critical defect in the rat model. This limit was corroborated by Saheb-Al-Zamani et al. (2013) who found it difficult to regenerate with the use of decellularized grafts longer than 20 mm and reported no regeneration in grafts in 60 mm long. Therefore, graft length is a crucial feature, as are its functional and morphological recovery properties, for developing a suitable alternative to autografts. Moreover, as stated by Hare et al. (1992) and demonstrated by Whitlock et al. (2009), the use of a very long nerve graft (28 mm) could produce misleading results in the evaluation of nerve functionality due to the poor reinnervation process along the distal edges of the grafts.

In the studies that used the classic decellularization protocols (SP, HP, NP, and FTP), the majority (75.8%) used grafts ranging in length from 10 to 15 mm (Whitlock et al., 2009; Liu et al., 2011; Nagao et al., 2011; Jia et al., 2012, 2017; Godinho et al., 2013; Zhang and Lv, 2013; Gao et al., 2014a; Wood et al., 2014; Zhang et al., 2014; Zheng et al., 2014; Zhou et al., 2014; Huang et al., 2015; Wakimura et al., 2015; Zhu et al., 2015; Jiang et al., 2016; Kim et al., 2016; Kusaba et al., 2016; Tajdaran et al., 2016; Wang W. et al., 2016; Wang et al., 2017b; Cai et al., 2017; Garcia-Pérez et al., 2017; Xiang et al., 2017). Among the others, only Zhu and Weihua (2014) used a shorter graft (6 mm), while others still used longer grafts: a 20-mm graft in five studies (Wang et al., 2012; Saheb-Al-Zamani et al., 2013; Hoben et al., 2015; Yan et al., 2016; Wang H. et al., 2016); a 30-mm graft in two (Whitlock et al., 2009; Marquardt et al., 2015); a 35–40 mm graft in two (Saheb-Al-Zamani et al., 2013; Vasudevan et al., 2014), and a 60-mm graft in one study (Saheb-Al-Zamani et al., 2013). The mean graft length used with the SP was 12.6 mm, 16.7 mm with the HP, 21 mm with the NP, and 12.5 mm with the FTP. Regarding the various in-house protocols, the average graft length was 14.3 mm (range, from 10 to 15 mm), except for the 35-mm-long graft developed by Vasudevan et al. (2014). The average length of the AP-T grafts

was 14 mm and that of the AP-TS and AP-TPA grafts was 15 mm. In general, the average length of the autografts and isografts was 14.8 mm.

Sciatic Functional Index

Like the autografts, all the decellularized grafts, except for those produced using the NP, showed an improvement in the SFI (Table 2). In particular, the results of the grafts produced using the SP seemed to be closer to those obtained with the autografts. It has to be taken into account, however, that the average SP graft length was 4 mm shorter than that of the autografts or the HP grafts and 9 mm shorter than the NP grafts. This difference could influence the SFI, although no studies examined whether length difference had an impact on the SFI. Zhang et al. (2014) reported a value of -33.39 for SP grafts at 8 weeks after surgery, a value much higher than the SP or the autograft average. Only two studies calculated the SFI of the NP grafts (Whitlock et al., 2009; Wang H. et al., 2016a). Wang H. et al. (2016) reported higher positive values than Whitlock et al. (2009) which could explain the opposite trend observed in this protocol. Only Nagao et al. (2011) calculated the SFI in HP and FTP grafts, while only Liu et al. (2011) evaluated it in AP-T grafts. This lack of relevant data precluded analysis of this parameter. Therefore, our analysis focused on the study by Nagao et al. (2011) who evaluated and compared the SFI for the SP, HP, and FTP grafts in the same experimental procedure. They found that the grafts reached a plateau in the recovery of SFI at 12 weeks, and that from week 12 until week 52 the SFI for the HP grafts was statistically superior compared to the SP and FTP grafts. In brief, a more rapid recovery during the first weeks after surgery was noted for the HP grafts, which then maintained a higher SFI over time.

Extensively employed in nerve injury and recovery studies, this parameter is generally considered to be highly accurate and reliable in describing sciatic nerve function (Varejao et al., 2001; Nichols et al., 2005). Nonetheless, SFI has certain disadvantages: frequent footprint artifacts and distortions produced by smearing of the ink when applied to the rats' paws (Fricker et al., 2016); the footprint key points have to be adequately recognized and analyzed, which are operator dependent (Monte-Raso et al., 2008). For these reasons, together with the lack of data, this parameter was insufficient to describe functional recovery, but it was used to complete the evaluation of functional restoration in association with other parameters.

Electrophysiology

In our analysis of the electrophysiological features of decellularized nerve grafts, sufficient data for a comparison were available only for CV at 10–15 weeks (Table 3). Electrophysiological measurement allows for a meaningful evaluation of the effective re-innervation of the graft over time. For instance, latency period and CV are correlated with the myelination rate and the size of the regenerating axons (Geuna et al., 2009). The CV can be subject to high variability during recording, however (Geuna et al., 2009). Nonetheless, it is a reliable factor for the evaluation of nerve regeneration (Booth and Gollnick, 1983). The CV in nerve grafts obtained with NP, HP, and AP was nearly half that of the SP grafts, which showed

TABLE 2 | Average values of the Sciatic Functional Index evaluated from 2 to 15 weeks after surgery.

Sciatic Functional Index									
Time point	AG	Well-established protocols				Authors' (in-house) protocols			
		SP	HP	NP	FTP	AP-T	AP-TS	AP-TPA	AP-W
2–5 weeks	–83.9 (Whitlock et al., 2009; Nagao et al., 2011; Zheng et al., 2014; Zhou et al., 2014; Wang H. et al., 2016; García-Pérez et al., 2017)	–88.2 (Whitlock et al., 2009; Nagao et al., 2011; Zheng et al., 2014; Zhou et al., 2014; Wang H. et al., 2016; García-Pérez et al., 2017)	–96.5 (Nagao et al., 2011)	–71.5 (Whitlock et al., 2009; Wang H. et al., 2016)	–97.5 (Nagao et al., 2011)	–94 (Liu et al., 2011)	n.d.	n.d.	n.d.
6–9 weeks	–74.4 (Whitlock et al., 2009; Nagao et al., 2011; Zheng et al., 2014; Zhou et al., 2014; Wang H. et al., 2016; García-Pérez et al., 2017)	–75.1 (Nagao et al., 2011; Zheng et al., 2014; Zhou et al., 2014; García-Pérez et al., 2017)	–86.5 (Nagao et al., 2011)	–74.7 (Whitlock et al., 2009; Wang H. et al., 2016)	–88.5 (Nagao et al., 2011)	–88.5 (Liu et al., 2011)	n.d.	n.d.	n.d.
10–15 weeks	–64.5 (Whitlock et al., 2009; Liu et al., 2011; Nagao et al., 2011; Zheng et al., 2014; Zhou et al., 2014; Wang H. et al., 2016; García-Pérez et al., 2017)	–66 (Nagao et al., 2011; Zheng et al., 2014; Zhou et al., 2014; García-Pérez et al., 2017)	–75.7 (Nagao et al., 2011)	–77 (Whitlock et al., 2009; Wang H. et al., 2016)	–79.5 (Nagao et al., 2011)	–80.5 (Liu et al., 2011)	n.d.	n.d.	n.d.

The average SFI values of the autograft (AG) are also reported. n.d., not declared.

TABLE 3 | Average conduction velocity recorded in decellularized grafts and in autografts (AG).

Time point	Conduction velocity (m/s)				
	Well-established protocols			Authors' (in-house) protocols	
	AG	SP	HP	NP	FTP
10–15 weeks	30.7 (Liu et al., 2011; Zhang and Lv, 2013; Zheng et al., 2014; Huang et al., 2015; Jiang et al., 2016; Wang H. et al., 2016)	27 (Zheng et al., 2014; Huang et al., 2015)	12.2 (Jiang et al., 2016)	15.5 (Jiang et al., 2016)	n.d.
					12.9 (Liu et al., 2011; Zhang and Lv, 2013; Xiang et al., 2017)
					n.d.
					n.d.
					n.d.

Only the values measured at the last time point are reported. *n.d.*, not declared.

CV values slightly below those of the autografts. CV in the HP and NP grafts was measured only in one study (Jiang et al., 2016). The wave amplitude is correlated with the number and size of effectively regenerated axons, in which electrical impulses can be propagated. Also, CV is influenced by the graft distance (Geuna et al., 2009). The best results were obtained with the AP-T grafts, with higher values than those of the autografts. The amplitude of the SP grafts was half that measured for the autografts, although evaluated at the previous time point (data not shown). Given the longer average length of the AP-T grafts, this outcome was remarkable, notwithstanding its being calculated only by Liu et al. (2011). In contrast, the latency period was shorter in the SP than the AP-T grafts, indicating greater fiber maturation in the SP than in the AP-T grafts (Wang W. et al., 2016) (data not shown).

All the studies on AP-TS grafts evaluated the wave amplitude and latency period at 25 weeks after surgery. The results were expressed in percentage (43.2 and 46.9%, respectively) with respect to the contralateral non-operated limb, precluding their comparison with the other groups (Wakimura et al., 2015; Kusaba et al., 2016; Wang W. et al., 2016).

Due to the variability in the CV recordings and the absence of data for wave amplitude and latency period, the electrophysiological parameters need to be correlated with other functional and morphological data in order to evaluate the whole regeneration process.

Muscle Functionality

Evaluation of muscle functionality is the key to assessment of the progress of nerve regeneration. The muscle wet weight ratio is related to muscle atrophy: without physiological innervations, muscles would undergo atrophy and loss of functionality and lose weight. Therefore, an increase in muscle weight and tension reflects the effective reinnervation of a graft able to conduct and deliver electrical stimuli to the target effector muscle (Zhao et al., 2014; Wang et al., 2015). The peripheral nervous system is capable of a certain degree of self-regeneration (Cerri et al., 2014). But when nerve continuity is interrupted, and particularly when the gap defect is large, complete reinnervation will be difficult. For this reason, we considered the muscle functionality parameter as being highly relevant for predicting effective functional recovery. Restoration of muscle function implies that the regenerating nerve fibers have effectively crossed the graft and reached the target muscle. In the present analysis, the best result was obtained with AP-TPA grafts, which showed the best muscle mass recovery similar to that of autografts (Table 4). This represents a remarkable result because it was evaluated at 8 weeks after surgery with a 15-mm-long graft (Cai et al., 2017). Unfortunately, no data on muscle tension were reported for AP-TPA grafts. Among the other protocols, the HP grafts came the closest to the autografts at the last time point, with increasing improvement over time and good recovery from muscle atrophy. The NP grafts started at a value similar to the HP grafts at weeks 6–9 but the rate of improvement fell behind that of the HP grafts over the following weeks, probably due to the higher average length of the grafts. In contrast, no increase was observed for the SP grafts. Moreover, Zhu and Weihua (2014) found some

TABLE 4 | The average muscle wet weight ratio evaluated in autografts (AG) and decellularized grafts.

Time point	Muscle wet weight ratio (% on healthy limb)									
	Well-established protocols					Authors' (in-house) protocols				
	AG	SP	HP	NP	FTP	AP-T	AP-TS	AP-TPA	AP-W	
6–9 weeks	46.4% (Whitlock et al., 2009; Jia et al., 2012, 2017; Zhang et al., 2014; Marquardt et al., 2015; Yan et al., 2016; Cai et al., 2017)	33.1% (Jia et al., 2012, 2017; Zhang et al., 2014)	34.8% (Gao et al., 2014a; Marquardt et al., 2015; Yan et al., 2016; Cai et al., 2017)	33% (Whitlock et al., 2009)	n.d.	n.d.	n.d.	47% (Cai et al., 2017)	n.d.	
10–15 weeks	51.6% (Whitlock et al., 2009; Liu et al., 2011; Wang et al., 2012, 2017b; Zhang and Lv, 2013; Vasudevan et al., 2014; Zheng et al., 2016; Kim et al., 2016; Wang H. et al., 2016)	31.5% (Wang et al., 2012; Zheng et al., 2014)	44.8% (Gao et al., 2014a; Jiang et al., 2016; Kim et al., 2016)	37.3% (Whitlock et al., 2009; Jiang et al., 2016; Wang H. et al., 2016)	n.d.	39.8% (Liu et al., 2011; Zhang and Lv, 2013; Kim et al., 2016; Wang et al., 2017b)	n.d.	n.d.	25% (Vasudevan et al., 2014)	

Only the values at 6–9 weeks and 10–15 weeks are reported. n.d., not declared.

motoneuron endplate activity in the SP grafts also on the operated side, but Zheng et al. (2014) reported that these motor endplates were scarce and characterized by serious atrophy. Vasudevan et al. (2014) calculated the muscle wet weight ratio for AP-W grafts and reported the lowest outcomes of all the decellularization protocols.

The muscle tension ratio was evaluated only for the SP, NP, and AP-T grafts at weeks 10–15 (Table 5). It reflected the same trend of the previous parameter, in which the muscle tension ratio for the AP-T grafts was slightly higher than that of the NP grafts, which was greater than that of the SP grafts, albeit to a lesser extent. This parameter was calculated only by one author for both NP (Wang H. et al., 2016) and AP-T grafts (Wang et al., 2017b).

Further evidence of recovery of muscle functionality was presented by Zhang and Lv (2013) and Zhu and Weihua (2014) who demonstrated, in SP and AP-T grafts, respectively, the presence of fibers positive to acetylcholinesterase immunostaining in some motoneuron endplates.

Morphology

Quantitative histomorphology is an essential method to investigate nerve regeneration, as numerous morphological parameters can be associated with functional outcomes (Geuna et al., 2004; Vleggeert-Lankamp, 2007). Table 6 presents the morphological data, in which only values at 10–15 weeks are included since the results at this time point were richer. AP-TPA is an exception because it had better and promising outcomes than the other decellularization protocols. It has been included in the table even if it was evaluated at 6–9 weeks.

Myelinated fiber density

The number of myelinated neurons in a regenerating nerve reflects the rate of functional recovery (Geuna et al., 2009). Regenerating nerves are initially characterized by a shortage of myelin, but, thanks to the action of Schwann cells, the fibers will be surrounded in a myelin layer (Flores et al., 2000). Myelinated fiber density is also related to a nerve's electrophysiological characteristics and provides a meaningful measure of the recovery process (Russell et al., 1996).

The highest myelinated fiber density, comparable to autograft values, was measured in FTP grafts, and it was evaluated only in one study (Godinho et al., 2013). Comparable results were obtained with SP and HP grafts, in which the fiber density was almost half that of the autografts. Some studies published very variable values for myelinated fiber density. Zhu et al. (2015) and Zhou et al. (2014) reported unexpectedly higher density values for SP grafts with respect to autografts at 2–5 (48231) and 10–15 (40523) weeks, while Zhu and Weihua (2014) reported a lower density of 2090 at week 20. The average density of the NP grafts, calculated only at 10–15 weeks, was the lowest among the decellularized grafts.

Among the grafts produced with an in-house protocol, the AP-T grafts had an intermediate value between the SP/HP and the NP grafts. For the same group (AP-T), Liu et al. (2011) reported only 0.03 myelinated fibers per mm² at week 12, considerably lower than those reported by other studies. The myelinated fiber density of AP-W grafts, reported only by Vasudevan et al. (2014),

TABLE 5 | Average muscle tension ratio evaluated in autografts and decellularized grafts.

Time point	Muscle tension ratio (% in healthy limb)									
	Well-established protocols					Authors' (in-house) protocols				
	AG	SP	HP	NP	FTP	AP-T	AP-TS	AP-TPA	AP-W	
10–15 weeks	54.7% (Wang et al., 2012, 2017b; Vasudevan et al., 2014; Zheng et al., 2014; Wang H. et al., 2016)	42.8% (Wang et al., 2012; Zheng et al., 2014)	n.d.	45% (Wang H. et al., 2016)	n.d.	48.8% (Wang et al., 2017b)	n.d.	n.d.	n.d.	

The reported values were measured only at the last time point. n.d., not declared.

was out of range since it was almost twice that of the autografts. However, the same study reported a density value out of range also for the NP grafts (75000), which was greater than that of the AP-W grafts. The AP-TS grafts had a higher density (17050) than the HP grafts, though this difference might have resulted from the late time point considered in these studies (Wakimura et al., 2015; Kusaba et al., 2016; Wang W. et al., 2016).

Myelinated fiber number

Since some studies evaluated either myelinated fiber density or myelinated fiber number, we examined both these parameters even if their functional significance is identical. Unlike myelinated fiber density, myelinated fiber number was similar in NP grafts and autografts. As seen for other parameters, already at weeks 6–9, the fiber number in the AP-TPA grafts was higher than in those produced with other decellularization protocols and was only slightly lower than the autografts (5743 at week 6–9). The grafts with the lowest number of myelinated fibers were produced with AP-T (Kim et al., 2016) and SP (Huang et al., 2015), though only one study evaluated both types of grafts.

Axon diameter

The average axon diameter in a regenerating nerve is an important parameter; it is the determining factor that influences CV and defines the capacity of nerves to transmit electrical stimuli (Hoffman, 1995; Assaf et al., 2008). During the regeneration phase in the first weeks after injury, the axon diameter increases. Evaluation of this parameter during the very early phases may be challenging, however, because it is difficult to discern between small successfully regenerated fibers from small atrophic or dying fibers (Ikeda and Oka, 2012). For this reason, we compared the results measured at the last time point. Axon diameter in AP-TS grafts was the largest (5.4 μm) since it was evaluated at week 25. Once again, AP-TPA had the best outcome among the other protocols, although evaluated only at 8 weeks after surgery. This value was even slightly greater than that for autografts measured at the same time point (3.8 μm), meaning that this graft type probably also had a high CV, which was not experimentally measured, however. The NP grafts had the largest diameter, reflecting the outcome derived from CV recording. HP grafts were evaluated only by one study (Hoben et al., 2015), which found an intermediate value, confirming the graft's average velocity in the conduction of electrical stimuli. The SP grafts were re-innervated by axons with a diameter among the lowest, higher only than that of the AP-T grafts. In addition, Zhu and Weihua (2014) demonstrated that axon diameter was increased slightly in the SP grafts, reaching 2.5 μm at week 20. A discrepancy was noted in the comparison with the CV recorded for SP grafts: while these grafts had the fastest CV, their axon diameter was among the lowest. This cannot be elucidated by the reported data, since the parameters were evaluated by different studies and were nearly comparable, albeit with low variance. Finally, in line with CV outcomes, the axons in the AP-T grafts had the smallest diameter.

Myelin sheath thickness

Myelin sheath thickness has been shown to correlate with the functional recovery of regenerating nerves (Kanaya et al., 1996). During the early period after injury, the axon diameter

TABLE 6 | Histomorphometric parameters at 10–15 weeks.

Histomorphology									
Parameter	Well-established protocols					Authors' (in-house) protocols			
	AG	SP	HP	NP	FTP	AP-T	AP-TS	AP-TPA	AP-W
Myelinated fiber density (myelinated fibers/mm ²)	27950.7 (Vasudevan et al., 2014; Zheng et al., 2014; Zhou et al., 2014; Jiang et al., 2016; Kim et al., 2016; Wang H. et al., 2016)	12500 (Zheng et al., 2014)	12748 (Hoben et al., 2015; Jiang et al., 2016; Kim et al., 2016)	6799 (Wood et al., 2014; Jiang et al., 2016)	27000 (Godinho et al., 2013)	9893 (Kim et al., 2016)	n.d.	n.d.	50000 (Vasudevan et al., 2014)
	12939.6 (Whitlock et al., 2009; Godinho et al., 2013; Wood et al., 2014; Huang et al., 2015; Kim et al., 2016)	1400 (Huang et al., 2015)	n.d.	12332 (Whitlock et al., 2009)	n.d.	5211 (Kim et al., 2016)	n.d.	5600* (Cai et al., 2017)	n.d.
Axon diameter (μm)	2.8 (Liu et al., 2011; Wood et al., 2014; Zheng et al., 2014; Zhou et al., 2014; Hoben et al., 2015; Huang et al., 2015; Wang H. et al., 2016; Wang et al., 2017b)	2.1 (Zheng et al., 2014; Zhou et al., 2014; Huang et al., 2015)	2.7 (Hoben et al., 2015)	3.8 (Wood et al., 2014; Wang H. et al., 2016)	n.d.	1.5 (Liu et al., 2011; Wang et al., 2017b)	n.d.	4.1* (Cai et al., 2017)	n.d.
	0.8 (Liu et al., 2011; Wang et al., 2012, 2017b; Vasudevan et al., 2014; Wood et al., 2014; Zheng et al., 2014; Zhou et al., 2014; Huang et al., 2015; Jiang et al., 2016; Kim et al., 2016; Wang H. et al., 2016)	0.6 (Wang et al., 2012; Zheng et al., 2014; Zhou et al., 2014; Huang et al., 2015)	0.8 (Jiang et al., 2016)	0.6 (Vasudevan et al., 2014; Wood et al., 2014; Jiang et al., 2016; Wang H. et al., 2016)	n.d.	2.1 [§] (Liu et al., 2011; Kim et al., 2016; Wang et al., 2017b)	n.d.	1* (Cai et al., 2017)	0.6 (Vasudevan et al., 2014)

* Outcomes with AP-TPA grafts are included though calculated at the previous time point in order to facilitate comparison of the results, as the grafts produced with this protocol showed good recovery. [§] Off-the-scale data. n.d., not declared.

decreases and then later increases over time (Sanders, 1948). The decrease in axon diameter is associated with a mild increase in myelin sheath thickness, maintaining the size of the entire fiber steady. The axons then start to increase their diameter, causing the surrounding myelin sheath to decrease in thickness (Sanders, 1948). The correlation between these two parameters is useful for interpreting the results. For instance, in the AP-TPA grafts, despite measurement at an earlier time point, myelin sheath thickness and axon diameter were nearly comparable to those of the autografts, meaning that these two types of grafts were probably almost at the same regeneration phase. This comparison was not possible with NP grafts, as myelin sheath thickness was evaluated only at the last time point. Its low value, together with the increased axon diameter, suggested that the grafts were further along in the regeneration process than the HP grafts. In fact, axon diameter was smaller, while myelin sheath thickness remained substantially unchanged, indicating that the HP grafts were probably still in an intermediate phase of regeneration. Kim et al. (2016) reported a myelin sheath thickness of 4 μm in HP grafts at 12 weeks after the graft procedure, which was much higher and out of the range, even when compared with autografts. Differently, a slight increase in axon diameter and a slight decrease in myelin sheath thickness was observed in SP grafts, suggesting that they were probably at the beginning of the second phase of regeneration. The AP-TS grafts were re-innervated by large axons (5.4 μm in diameter) and had a lower myelin sheath thickness (0.8 μm), indicating good progress in the regeneration process, as expected, given the time point at which they were evaluated. Conversely, the myelin sheath was thickest in the AP-T grafts, in which the axon diameter was among the smallest. In this case, the myelin sheath thickness reported for this graft type appeared to be outside the expected physiological range, as mentioned in Section “Morphological and Functional Comparison of Autografts and Sham Control of Nerve Gap Reconstruction in Rat Models.” Unfortunately, some of the studies (Liu et al., 2011; Kim et al., 2016) reported unforeseen and off-the-scale values due to possible methodological sampling errors or, more commonly, insufficient methodological information to obtain significant results, as demonstrated elsewhere (Geuna et al., 2004; Geuna and Herrera-Rincon, 2015).

Other histomorphological parameters

The unmyelinated/myelinated axon ratio, the number of axons in the unmyelinated bundle, and the sectional area of single myelinated axons were evaluated by Godinho et al. (2013) in FTP grafts at weeks 10–15. The unmyelinated/myelinated axon ratio was also evaluated in AP-TS grafts (Wang W. et al., 2016). Unmyelinated axons are physiologically present in the peripheral nervous system and can result locally abundant, accounting for about 75% of axons in the cutaneous nerves of mammals (Geuna et al., 2009). They are usually small; given the lack of a myelin sheath, they do not permit saltatory conduction, resulting in a lower CV. Both FTP (with an unmyelinated/myelinated axon ratio of 4) and especially AP-TS grafts (with a ratio of 5.3) seemed to be re-innervated by a higher number of unmyelinated neurons compared with autografts, in which the ratio was 3.5. This implies

that the CV was slower in these grafts, though evidence for this parameter was not directly evaluated.

Godinho et al. (2013) observed a difference in axon sectional area between FTP grafts and autografts (2.1 μm^2 vs. 3.6 μm^2), supporting the hypothesis that CV in FTP grafts is slower. In addition, the two parameters correlating with functional recovery were evaluated in AP-TS grafts (Wakimura et al., 2015; Kusaba et al., 2016; Wang W. et al., 2016): the von Frey hair sensitivity test and the toe spread factor, both as compared to the healthy limb and expressed as a percentage. The mean von Frey hair sensitivity value was 13.8% and the toe spread factor ratio was 46.3%, consistent with the values for autografts measured in other studies (Wang et al., 2012; Wakimura et al., 2015; Kusaba et al., 2016; Wang W. et al., 2016), indicating comparable functional recovery for AP-TS grafts and autografts at week 20.

Vascularization and Inflammation

Nerve grafts obtained with decellularization protocols often proved inadequate for clinical application, and this inadequacy was noted to increase linearly with graft length (He et al., 2012, 2014; Hayashida et al., 2015). A chief reason is that, ischemia, degeneration, and necrosis can occur in the non-vascularized parts of long, decellularized nerve grafts, associated with slow regeneration and risk of graft failure (Hayashida et al., 2015; Rbia and Shin, 2017). In conventional approaches with autografts or isografts, revascularization is simpler and more direct, based on reconnection with the existing vasculature (Best et al., 1999). Differently, the native cells in decellularized grafts, including endothelial cells, are removed, thus impeding adequate and rapid support to the decellularized nerve scaffold. Given the importance of this issue, and in order to better understand the process of vascularization in decellularized grafts, we analyzed two studies. Zhu et al. (2017) evaluated patterns of microangiogenesis in decellularized grafts, while Farber et al. (2016) completed the study by Saheb-Al-Zamani et al. (2013) investigating the difference in vascularization between long auto/isografts and decellularized grafts. Zhu et al. (2017) studied short grafts (10 mm in length) and demonstrated that nutrient supply relies on fluid permeation from the surrounding tissues during the early stages after the graft procedure. Microvessels started to grow at the graft extremities and then penetrated into the decellularized nerve matrix along the long axis. Moreover, they calculated that the microvessels grew more rapidly in the autografts than in the decellularized nerves. After 14 days, newly formed microvessels were anastomosed at the midgraft in the autografts AG, whereas the decellularized grafts needed 21 days for this process.

Farber et al. (2016) demonstrated that long nerve grafts (60 mm) need different times for complete vascularization, depending on the approach used. Auto/isografts take about 5 days before the first signs of vascularization in the midgraft appear, whereas decellularized nerves need about 20 days, as shown in Zhu et al.'s (2017) study. The longer time to obtain adequate vascularization might be the cause of cell damage and senescence, oxidative stress, and other numerous pathological processes. Hence, one of the main reasons why better outcomes

are achieved with auto/isografts is this faster and higher microvascularization capability of autografts. Angiogenesis and the formation of new vascularization within the nerve graft are two processes necessary for successful nerve regeneration and must be taken into account in the development of functional nerve grafts.

Another fundamental issue in decellularization is graft biocompatibility, i.e., the risk of eliciting an inflammatory response or immunological rejection of the transplanted nerve matrix. During the decellularization process, a great quantity of cells, myelin sheath, and ECM debris is generated, which is theoretically able to activate inflammatory and macrophage response that could damage the basement membrane and thus delay regeneration (Gao et al., 2014b). Moreover, some of these fragments might result immunogenic and able to activate lymphocyte T cells, promoting their migration within the graft and leading to its destruction. Therefore, it is important to consider the pro-inflammatory and immunologic potential of decellularized nerves used as a graft. In the present review, six studies described immunological response to decellularized grafts (Jia et al., 2011; Godinho et al., 2013; Fan et al., 2014; Jiang et al., 2015; Wakimura et al., 2015; Poppler et al., 2016; Wang W. et al., 2016; Cai et al., 2017; Kaizawa et al., 2017). All six studies used immunostaining to detect T lymphocyte (CD3, CD4, CD8) and macrophage (CD68) activity. The majority of the studies showed a slight increase in these cells as compared with autografts within and in the immediate proximity of the graft, especially during the first days after grafting, though there was no statistical difference between these values. Only Cai et al. (2017) reported a significant difference between autografts and decellularized nerve grafts. Jiang et al. (2015) quantified the serum concentration of inflammatory cytokines (IL-2, TNF- α , and IFN- γ) after a grafting procedure but found no significant increase in inflammatory cytokines in animals grafted with a decellularized nerve graft and those that received an autograft. These outcomes indicated no apparent graft rejection during the early recovery period but only a restrained inflammatory response. This means that decellularized nerves are not subject to the cytotoxic effect of T lymphocytes and macrophage degradation, making them fairly safe for *in vivo* use.

CONCLUSION

With this literature review, we wanted to quantitatively analyze the effectiveness of decellularized nerve grafts as possible substitutes for auto/isografts, which currently represent the current gold standard procedure in the treatment of severe nerve injury. We evaluated functional and morphological parameters that reflect the progressive recovery of nerve function. The parameters were selected because they are the ones most commonly used in the studies and the most representative of the regeneration process. Among these parameters, muscle functionality and histomorphometric analysis (axon diameter and myelin sheath thickness) best predicted effective recovery of nerve function. Restoration of muscle weight and tension

entails effective crossing of the nerve gap to reach the target muscle. The histomorphometric evaluations not only highlighted the graft's morphological features but also its functional and electrophysiological characteristics. Overall, histomorphometric evaluations are subject to methodological sampling errors, which may induce bias in the interpretation of the results. We noted, for example, that myelin sheath thickness was frequently overrated, supporting the hypothesis of common errors in the evaluation of histomorphometric parameters, as pointed out in our previously studies (Geuna et al., 2004; Geuna and Herrera-Rincon, 2015). In contrast, SFI evaluation and electrophysiological measurements are useful in the assessment of nerve regeneration, though they, too, may be subject to error and high variability (Monte-Raso et al., 2008; Geuna et al., 2009; Fricker et al., 2016).

The main limitation of the present study was the lack of data for numerous investigations: not all parameters were evaluated for all decellularization protocols at all time points. Moreover, only one evaluation reported by a single study was available in many cases, making complete and exhaustive comparison between the protocols not always possible.

Overall, although reported in only one study (Cai et al., 2017), the most promising outcomes were obtained with the grafts produced with the AP-TPA protocol. This protocol had the best data for muscle wet weight ratio, myelinated fiber number, axon diameter, and myelin sheath thickness, with all values comparable to those of autografts evaluated at 8 weeks after surgery. Moreover, the effectiveness of this protocol was notable also for the length of the graft (15 mm, longer than the critical size) and the time needed for decellularization (the quickest among the in-house protocols and similar to that of SP). Based on the promising results of AP-TPA, further investigations should be carried out to confirm these outcomes.

Among the well-established protocols, NP, especially when performed after HP, seemed to be the most effective. In fact, it resulted in grafts with sufficient muscle weight and tension ratio, axon diameter, myelin sheath thickness, myelinated fiber number, CV, and SFI (until week 9). Given that the NP grafts were the longest on average (21 mm), the outcomes appeared even more remarkable. This protocol is, in fact, used in the manufacture of Avance® processed nerve grafts (AxoGen, Inc., Alachua, FL, United States), which is a decellularized nerve graft currently employed in clinical practice. The protocol was developed with the idea to improve on the effectiveness of the previously developed, well-established protocols (SP and HP) by removing chondroitin sulfate proteoglycans, which were demonstrated to inhibit axonal growth (Krekoski et al., 2001; Jiang et al., 2016); this improvement was confirmed in our analysis. The HP and the SP showed similar results; however, based on specific parameters, mainly muscle functionality, outcomes with the HP grafts were slightly superior. This observation was confirmed by Nagao et al. (2011) who compared SP, HP, and FTP grafts in the same experimental procedure and reported a significantly better improvement in SFI with use of HP grafts as compared to those obtained with the other two protocols. Moreover, HP takes less time to complete than SP. This can be explained by the fact

that SP was the first decellularization protocol to be developed, while HP is a later improvement with better preservation of the ECM structure and an easier detergent removal step using lower doses of chemicals (Hudson et al., 2004; Rieder et al., 2004; Alhamdani et al., 2010; Serghei et al., 2010; Crapo et al., 2011). Evaluation of FTP grafts was scarce, since it was evaluated only by two studies (Nagao et al., 2011; Godinho et al., 2013) that reported the lowest values for SFI, statistically lower than the HP grafts (Nagao et al., 2011). Moreover, in the same experimental design, the myelinated fiber density was lower in the FTP than in the NP grafts (Godinho et al., 2013). Three major advantages of FTP are that it is the quickest decellularization protocol, it requires no chemicals, and the effect of decellularization is uniform on the entire tissue, without depending on diffusion or perfusion (Crapo et al., 2011). Nonetheless, the protocol has many limitations, which explains the worse outcomes obtained. First the technique causes rapid tissue expansion and contraction that can damage basal lamina continuity, making axonal regeneration difficult. Moreover, FTP kills cells in the tissue. Since it does not have a washing step, the debris is not eliminated (Gulati and Cole, 1994; Sondell et al., 1998; Szyndrak et al., 2013), which might activate inflammatory or immunological response (Gao et al., 2014b).

Concerning the other in-house protocols, the AP-T protocol employed a longer time for decellularization and the outcomes were generally slightly worse than with HP, particularly for morphology. Finally, the AP-W protocol ranked last; its long duration (2 weeks) makes it less attractive and effective than the other protocols.

Table 7 summarizes the advantages and disadvantages of the different techniques used to decellularize nerve grafts for potential clinical use.

In conclusion, decellularized nerve grafts are a promising, alternative to auto/isografts for the treatment of nerve injury, even in the repair of defects with large gaps. They are immunologically safe and some more than others support the functional and morphological recovery of the injured nerve. Although the use of peracetic acid showed very promising outcomes, it needs to be further analyzed. The use of chondroitinase ABC, introduced with NP, seems to effectively improve the outcomes obtained with SP and HP. The use of triton-X alone or in association with SDS did not seem to improve the outcomes with the HP or the SP grafts. The worst results were obtained with physical techniques (freeze/thaw or Wallerian degeneration protocol); therefore, chemicals and washing steps

TABLE 7 | Advantages and disadvantages of the various protocols to decellularize nerve grafts.

Decellularization protocol	Advantages	Disadvantages
Sondell (SP)	<ul style="list-style-type: none"> • SFI similar to autograft • CV similar to autograft 	<ul style="list-style-type: none"> • Motor endplates seriously atrophied and low recovery of muscle functionality • Very few regenerated myelinated nerve fibers
Hudson (HP)	<ul style="list-style-type: none"> • Low percentage of chemical detergents • Good muscle wet weight ratio at 10–15 weeks • Axon diameter and myelinated sheath thickness comparable to autografts at 10–15 weeks 	<ul style="list-style-type: none"> • Low CV values 10–15 weeks after repair
Neubauer (NP)	<ul style="list-style-type: none"> • Satisfying SFI • Satisfying muscle weight and tension ratio • Satisfying quantitative histomorphological parameters (myelinated fiber number, axon diameter, myelin sheath thickness) 	<ul style="list-style-type: none"> • CV values halved of that registered in autografts • Low myelinated fiber density
Freeze-and-thaw (FTP)	<ul style="list-style-type: none"> • Quickest and less laborious protocol, no chemicals are needed 	<ul style="list-style-type: none"> • Low values of SFI • Low myelinated fiber density • Cell debris are not eliminated • Damaged basal lamina and difficult axonal regeneration
Triton-X (AP-T)	<ul style="list-style-type: none"> • Remarkable electrophysiological outcome (considering the higher average graft length) • Muscle tension ratio recovery similar to autografts 	<ul style="list-style-type: none"> • Long time to the decellularization process • Low values of SFI recovery
Triton-X + SDS (AP-TS)	<ul style="list-style-type: none"> • Good progress in nerve regeneration (large axons at 25 weeks) • Basal lamina preserved 	<ul style="list-style-type: none"> • Few data comparable to the other protocols
Triton-X + peracetic acid (AP-TPA)	<ul style="list-style-type: none"> • Quickest protocol between in-house protocols • Muscle mass recovery (muscle wet weight ratio) at 8 weeks similar to autografts • Quantitative histomorphological parameters (myelinated fiber number, axon diameter, myelin sheath thickness) at 8 weeks comparable with those of the autograft at 10–15 weeks 	<ul style="list-style-type: none"> • Only one paper describing this protocol
Wallerian degeneration (AP-W)	<ul style="list-style-type: none"> • Myelin thickness of regenerating fibers similar to autografts 	<ul style="list-style-type: none"> • Longest protocol • Muscle wet weight ratio recovery half than autografts

are needed to obtain an effective decellularized nerve graft. Finally, in order to further improve process performance, a recellularization step could be introduced to produce a graft that is able to substitute the current gold standard of auto/isografts.

AUTHOR CONTRIBUTIONS

AL, PT, SG, and SR contributed to the conception and design of the study. AL, DD'A, SO, SG, and SR collected and analyzed the data, interpreted the results, and wrote the article. All authors analyzed the data and interpreted the results, and critically revised the manuscript. All authors approved the publication of the contents and verified that

all parts of the work were appropriately investigated and described.

FUNDING

This work was funded by the Fondazione Cassa di Risparmio di Torino (Turin, Italy), protocol number 2017.AI190.U219, RF: 2016.2388.

ACKNOWLEDGMENTS

The authors wish to thank Dr. Kenneth Adolf Britsch for the English revision of the manuscript.

REFERENCES

- Albert, E. (1885). *Einige Operationen an Nerven*. Wien: Wien Med Press, 26.
- Alhamdani, M. S. S., Schröder, C., Werner, J., Giese, N., Bauer, A., and Hoheisel, J. D. (2010). Single-step procedure for the isolation of proteins at near-native conditions from mammalian tissue for proteomic analysis on antibody microarrays. *J. Proteome Res.* 9, 963–971. doi: 10.1021/pr900844q
- Assaf, Y., Blumenfeld-Katzir, T., Yovel, Y., and Basser, P. J. (2008). AxCaliber: a method for measuring axon diameter distribution from diffusion MRI. *Magn. Reson. Med.* 59, 1347–1354. doi: 10.1002/mrm.21577
- Battiston, B., Raimondo, S., Tos, P., Gaidano, V., Audisio, C., Scevola, A., et al. (2009). Chapter 11: tissue engineering of peripheral nerves. *Int. Rev. Neurobiol.* 87, 227–249. doi: 10.1016/S0074-7742(09)87011-6
- Best, T. J., Mackinnon, S. E., Midha, R., Hunter, D. A., and Evans, P. J. (1999). Revascularization of peripheral nerve autografts and allografts. *Plast. Reconstr. Surg.* 104, 152–160. doi: 10.1097/00006534-199907000-00021
- Booth, F. W., and Gollnick, P. D. (1983). Effects of disuse on the structure and function of skeletal muscle. *Med. Sci. Sports Exerc.* 15, 415–420.
- Boriani, F., Fazio, N., Fotia, C., Savarino, L., Nicoli Aldini, N., Martini, L., et al. (2017). A novel technique for decellularization of allogenic nerves and in vivo study of their use for peripheral nerve reconstruction. *J. Biomed. Mater. Res. – Part A* 105, 2228–2240. doi: 10.1002/jbm.a.36090
- Bottagisio, M., Pellegata, A. F., Boschetti, F., Ferroni, M., Moretti, M., and Lovati, A. B. (2016). A new strategy for the decellularisation of large equine tendons as biocompatible tendon substitutes. *Eur. Cells Mater.* 32, 58–73. doi: 10.22203/eCM.v032a04
- Cai, M., Huang, T., Hou, B., and Guo, Y. (2017). Role of demyelination efficiency within acellular nerve scaffolds during nerve regeneration across peripheral defects. *Biomed. Res. Int.* 2017:10. doi: 10.1155/2017/4606387
- Cerri, F., Salvatore, L., Memon, D., Boneschi, F. M., Madaghiele, M., Brambilla, P., et al. (2014). Peripheral nerve morphogenesis induced by scaffold micropatterning. *Biomaterials* 35, 4035–4045. doi: 10.1016/j.biomaterials.2014.01.069
- Chaplan, S. R., Bach, F. W., Pogrel, J. W., Chung, J. M., and Yaksh, T. L. (1994). Quantitative assessment of tactile allodynia in the rat paw. *J. Neurosci. Methods* 53, 55–63. doi: 10.1016/0165-0270(94)90144-9
- Crapo, P. M., Gilbert, T. W., and Badylak, S. F. (2011). An overview of tissue and whole organ decellularization processes. *Biomaterials* 32, 3233–3243. doi: 10.1016/j.biomaterials.2011.01.057
- Daly, W. T., Yao, L., Abu-rub, M. T., O'Connell, C., Zeugolis, D. I., Windebank, A. J., et al. (2012). The effect of intraluminal contact mediated guidance signals on axonal mismatch during peripheral nerve repair. *Biomaterials* 33, 6660–6671. doi: 10.1016/j.biomaterials.2012.06.002
- Fan, L., Yu, Z., Li, J., Dang, X., and Wang, K. (2014). Immunoregulation effects of bone marrow-derived mesenchymal stem cells in xenogeneic acellular nerve grafts transplant. *Cell. Mol. Neurobiol.* 34, 999–1010. doi: 10.1007/s10571-014-0076-3
- Farber, S. J., Hoben, G. M., Hunter, D. A., Yan, Y., Johnson, P. J., Mackinnon, S. E., et al. (2016). Vascularization is delayed in long nerve constructs compared with nerve grafts. *Muscle Nerve* 54, 319–321. doi: 10.1002/mus.25173
- Flores, A. J., Lavernia, C. J., and Owens, P. (2000). Anatomy and physiology of peripheral nerve injury and repair. *Am. J. Orthop.* 29, 167–173.
- Fricker, L., Penna, V., Lampert, F., Stark, G. B., Witzel, C., and Kouloxouidizis, G. (2016). A self-made, low-cost infrared system for evaluating the sciatic functional index in mice. *Neural Regen. Res.* 11, 829–834. doi: 10.4103/1673-5374.182712
- Gao, S., Zheng, Y., Cai, Q., Deng, Z., Yao, W., Wang, J., et al. (2014a). Combination of acellular nerve graft and schwann cells-like cells for rat sciatic nerve regeneration. *Neural Plast.* 2014:9. doi: 10.1155/2014/139085
- Gao, S., Zheng, Y., Cai, Q., Yao, W., Wang, J., Zhang, P., et al. (2014b). Comparison of morphology and biocompatibility of acellular nerve scaffolds processed by different chemical methods. *J. Mater. Sci. Mater. Med.* 25, 1283–1291. doi: 10.1007/s10856-014-5150-3
- García-Pérez, M. M., Martínez-Rodríguez, H. G., Lópoez-Guerra, G. G., Soto-Domínguez, A., Said-Fernández, S.-L., Morales-Avalos, R., et al. (2017). A modified chemical protocol of decellularization of rat sciatic nerve and its recellularization with mesenchymal differentiated schwann-like cells: morphological and functional assessments. *Histol. Histopathol.* 32, 779–792.
- Geuna, S., Gigo-Benato, D., and De Castro Rodrigues, A. (2004). On sampling and sampling errors in histomorphometry of peripheral nerve fibers. *Microsurgery* 24, 72–76. doi: 10.1002/micr.10199
- Geuna, S., and Herrera-Rincon, C. (2015). Update on stereology for light microscopy. *Cell Tissue Res.* 360, 5–12. doi: 10.1007/s00441-015-2143-6
- Geuna, S., Tos, P., and Battiston, B. (2009). *Essays on Peripheral Nerve Repair and Regeneration*, 1st Edn. Cambridge, MA: Academic Press.
- Gilbert, T. W., Sellaro, T. L., and Badylak, S. F. (2006). Decellularization of tissues and organs. *Biomaterials* 27, 3675–3683. doi: 10.1016/j.biomaterials.2006.02.014
- Godinho, M. J., Teh, L., Pollett, M. A., Goodman, D., Hodgetts, S. I., Sweetman, I., et al. (2013). Immunohistochemical, ultrastructural and functional analysis of axonal regeneration through peripheral nerve grafts containing schwann cells expressing BDNF, CNTF or NT3. *PLoS One* 8:e69987. doi: 10.1371/journal.pone.0069987
- Greene, E. C. G. (1935). *Anatomy of the Rat*. Philadelphia, PA: Eunice Chace Greene Transactions of the American Philosophical Society, 339. doi: 10.1002/ar.1090650112
- Gulati, A. K., and Cole, G. P. (1994). Immunogenicity and regenerative potential of acellular nerve allografts to repair peripheral nerve in rats and rabbits. *Acta Neurochir. (Wien)* 126, 158–164.
- Hare, G. M., Evans, P. J., Mackinnon, S. E., Best, T. J., Bain, J. R., Szalai, J. P., et al. (1992). Walking track analysis: a long-term assessment of peripheral nerve recovery. *Plast. Reconstr. Surg.* 89, 251–258.
- Hayashida, K., Hiroto, S., Morooka, S., Kuwabara, K., and Fujioka, M. (2015). The vascularized sural nerve graft based on a peroneal artery perforator for

- reconstruction of the inferior alveolar nerve defect. *Microsurgery* 35, 244–248. doi: 10.1002/micr.22346
- He, B., Zhu, Q., Chai, Y., Ding, X., Tang, J., Gu, L., et al. (2012). Outcomes with the use of human acellular nerve graft for repair of digital nerve defects: a prospective multicenter controlled clinical trial. *J. Tissue Eng. Regen. Med.* 6:76.
- He, B., Zhu, Z., Zhu, Q., Zhou, X., Zheng, C., Li, P., et al. (2014). Factors predicting sensory and motor recovery after the repair of upper limb peripheral nerve injuries. *Neural Regen. Res.* 9, 661–672. doi: 10.4103/1673-5374.130094
- Hoben, G., Yan, Y., Iyer, N., Newton, P., Hunter, D. A., Moore, A. M., et al. (2015). Comparison of acellular nerve allograft modification with schwann cells or VEGF. *Hand* 10, 396–402. doi: 10.1007/s11552-014-9720-0
- Hoben, G. M., Ee, X., Schellhardt, L., Yan, Y., Hunter, D. A., Moore, A. M., et al. (2018). Increasing nerve autograft length increases senescence and reduces regeneration. *Plast. Reconstr. Surg.* 142, 952–961. doi: 10.1097/PRS.00000000000004759
- Hoffman, P. N. (1995). Review: the synthesis, axonal transport, and phosphorylation of neurofilaments determine axonal caliber in myelinated nerve fibers. *Neuroscience* 1, 76–83. doi: 10.1177/107385849500100204
- Huang, H., Xiao, H., Liu, H., Niu, Y., Yan, R., and Hu, M. (2015). A comparative study of acellular nerve xenografts and allografts in repairing rat facial nerve defects. *Mol. Med. Rep.* 12, 6330–6336. doi: 10.3892/mmr.2015.4123
- Hudson, T. W. T., Zawko, S., Deister, C., Lundy, S., Hu, C. C. Y., Lee, K., et al. (2004). Optimized acellular nerve graft is immunologically tolerated and supports regeneration. *Tissue Eng.* 10, 1641–1651. doi: 10.1089/ten.2004.10.1641
- Hundepool, C. A., Nijhuis, T. H. J., Kotsougiani, D., Friedrich, P. F., Bishop, A. T., and Shin, A. Y. (2017). Optimizing decellularization techniques to create a new nerve allograft: an in vitro study using rodent nerve segments. *Neurosurg. Focus* 42, 1–7. doi: 10.3171/2017.1.FOCUS16462
- Ikedo, M., and Oka, Y. (2012). The relationship between nerve conduction velocity and fiber morphology during peripheral nerve regeneration. *Brain Behav.* 2, 382–390. doi: 10.1002/brb3.61
- Jia, H., Wang, Y., Tong, X. J., Liu, G. B., Li, Q., Zhang, L. X., et al. (2011). Biocompatibility of acellular nerves of different mammalian species for nerve tissue engineering. *Artif. Cells Blood Substit. Biotechnol.* 39, 366–375. doi: 10.3109/10731199.2011.618133
- Jia, H., Wang, Y., Tong, X. J., Liu, G. B., Li, Q., Zhang, L. X., et al. (2012). Sciatic nerve repair by acellular nerve xenografts implanted with BMSCs in rats xenograft combined with BMSCs. *Synapse* 66, 256–269. doi: 10.1002/syn.21508
- Jia, H., Wang, Y., Wang, T., Dong, Y., Li, W. L., Li, J. P., et al. (2017). Synergistic effects of G-CSF and bone marrow stromal cells on nerve regeneration with acellular nerve xenografts. *Synapse* 71:e21974. doi: 10.1002/syn.21974
- Jiang, L., Zheng, Y., Chen, O., Chu, T., Ding, J., and Yu, Q. (2016). Nerve defect repair by differentiated adipose-derived stem cells and chondroitinase ABC-treated acellular nerves. *Int. J. Neurosci.* 126, 568–576. doi: 10.3109/00207454.2015.1048547
- Jiang, L. F., Chen, O., Chu, T. G., Ding, J., and Yu, Q. (2015). T lymphocyte subsets and cytokines in rats transplanted with adipose-derived mesenchymal stem cells and acellular nerve for repairing the nerve defects. *J. Korean Neurosurg. Soc.* 58, 101–106. doi: 10.3340/jkns.2015.58.2.101
- Kaizawa, Y., Kakinoki, R., Ikeguchi, R., Ohta, S., Noguchi, T., Takeuchi, H., et al. (2017). A nerve conduit containing a vascular bundle and implanted with bone marrow stromal cells and decellularized allogenic nerve matrix. *Cell Transplant.* 26, 215–228. doi: 10.3727/096368916X692951
- Kanaya, F., Firrell, J. C., and Breidenbach, W. C. (1996). Sciatic function index, nerve conduction tests, muscle contraction, and axon morphometry as indicators of regeneration. *Plast. Reconstr. Surg.* 98, 1264–1271; discussion 1272–1274.
- Kemp, P. (1994). *Peracetic Acid Sterilization of Collagen or Collagenous Tissue*. US Grant: US5460962A.
- Kim, J. K., Koh, Y., Do, Kim, J. O., and Seo, D. H. (2016). Development of a decellularization method to produce nerve allografts using less invasive detergents and hyper/hypotonic solutions. *J. Plast. Reconstr. Aesthetic Surg.* 69, 1690–1696. doi: 10.1016/j.bjps.2016.08.016
- Kingham, P. J., and Terenghi, G. (2006). Bioengineered nerve regeneration and muscle reinnervation. *J. Anat.* 209, 511–526. doi: 10.1111/j.1469-7580.2006.00623.x
- Krekoski, C. A., Neubauer, D., Zuo, J., and Muir, D. (2001). Axonal regeneration into acellular nerve grafts is enhanced by degradation of chondroitin sulfate proteoglycan. *J. Neurosci.* 21, 6206–6213.
- Kusaba, H., Terada-Nakaishi, M., Wang, W., Itoh, S., Nozaki, K., Nagai, A., et al. (2016). Comparison of nerve regenerative efficacy between decellularized nerve graft and nonwoven chitosan conduit. *Biomed. Mater. Eng.* 27, 75–85.
- Liu, G., Cheng, Y., Guo, S., Feng, Y., Li, Q., Jia, H., et al. (2011). Transplantation of adipose-derived stem cells for peripheral nerve repair. *Int. J. Mol. Med.* 28, 565–572. doi: 10.3892/ijmm.2011.725
- Lundborg, G., Dahlin, L. B., Danielsen, N., Gelberman, R. H., Longo, F. M., Powell, H. C., et al. (1982). Nerve regeneration in silicone chambers: influence of gap length and of distal stump components. *Exp. Neurol.* 76, 361–375. doi: 10.1016/0014-4886(82)90215-1
- Marquardt, L. M., Ee, X., Iyer, N., Hunter, D., Mackinnon, S. E., Wood, M. D., et al. (2015). Finely tuned temporal and spatial delivery of GDNF promotes enhanced nerve regeneration in a long nerve defect model. *Tissue Eng. Part A* 21, 2852–2864. doi: 10.1089/ten.tea.2015.0311
- Monte-Raso, V. V., Barbieri, C. H., Mazzer, N., Yamasita, A. C., and Barbieri, G. (2008). Is the sciatic functional index always reliable and reproducible? *J. Neurosci. Methods* 170, 255–261. doi: 10.1016/j.jneumeth.2008.01.022
- Nagao, R. J., Lundy, S., Khaing, Z. Z., and Schmidt, C. E. (2011). Functional characterization of optimized acellular peripheral nerve graft in a rat sciatic nerve injury model. *Neurol. Res.* 33, 600–608. doi: 10.1179/1743132810Y.0000000023
- Navarro, X., Vivó, M., and Valero-Cabré, A. (2007). Neural plasticity after peripheral nerve injury and regeneration. *Prog. Neurobiol.* 82, 163–201. doi: 10.1016/j.pneurobio.2007.06.005
- Nichols, C. M., Myckatyn, T. M., Rickman, S. R., Fox, I. K., Hadlock, T., and Mackinnon, S. E. (2005). Choosing the correct functional assay: a comprehensive assessment of functional tests in the rat. *Behav. Brain Res.* 163, 143–158. doi: 10.1016/j.bbr.2005.05.003
- Pfister, B. J., Gordon, T., Loverde, J. R., Kochar, A. S., Mackinnon, S. E., and Cullen, D. K. (2011). Biomedical engineering strategies for peripheral nerve repair: surgical applications, state of the art, and future challenges. *Crit. Rev. Biomed. Eng.* 39, 81–124.
- Philips, C., Campos, F., Roosens, A., Sanchez-Quevedo, M. D. C., Declercq, H., and Carriel, V. (2018). Qualitative and quantitative evaluation of a novel detergent-based method for decellularization of peripheral nerves. *Ann. Biomed. Eng.* doi: 10.1007/s10439-018-2082-y [Epub ahead of print].
- Poppler, L. H., Ee, X., Schellhardt, L., Hoben, G. M., Pan, D., Hunter, D. A., et al. (2016). Axonal growth arrests after an increased accumulation of schwann cells expressing senescence markers and stromal cells in acellular nerve allografts. *Tissue Eng. Part A* 22, 949–961. doi: 10.1089/ten.tea.2016.0003
- Rbia, N., and Shin, A. Y. (2017). The role of nerve graft substitutes in motor and mixed motor/sensory peripheral nerve injuries. *J. Hand Surg. Am.* 42, 367–377. doi: 10.1016/j.jhbsa.2017.02.017
- Rieder, E., Kasimir, M.-T., Silberhumer, G., Seebacher, G., Wolner, E., Simon, P., et al. (2004). Decellularization protocols of porcine heart valves differ importantly in efficiency of cell removal and susceptibility of the matrix to recellularization with human vascular cells. *J. Thorac. Cardiovasc. Surg.* 127, 399–405. doi: 10.1016/j.jtcvs.2003.06.017
- Rinker, B., and Vyas, K. S. (2014). Clinical applications of autografts, conduits, and allografts in repair of nerve defects in the hand: current guidelines. *Clin. Plast. Surg.* 41, 533–550. doi: 10.1016/j.cps.2014.03.006
- Russell, J. W., Karnes, J. L., and Dyck, P. J. (1996). Sural nerve myelinated fiber density differences associated with meaningful changes in clinical and electrophysiologic measurements. *J. Neurol. Sci.* 135, 114–117. doi: 10.1016/0022-510X(95)00243-U
- Saheb-Al-Zamani, M., Yan, Y., Farber, S. J., Hunter, D. A., Newton, P., Wood, M. D., et al. (2013). Limited regeneration in long acellular nerve allografts is associated with increased schwann cell senescence. *Exp. Neurol.* 247, 165–177. doi: 10.1016/j.expneurol.2013.04.011
- Sanders, F. K. (1948). The thickness of the myelin sheaths of normal and regenerating peripheral nerve fibres. *Proc. R. Soc. London. Ser. B – Biol. Sci.* 135, 323–357.
- Serghei, C., Igor, T., Thomas, J., Andres, H., Suzanne, D., Waldemar, T., et al. (2010). Detergent decellularization of heart valves for tissue engineering:

- toxicological effects of residual detergents on human endothelial cells. *Artif. Organs* 34, 206–210. doi: 10.1111/j.1525-1594.2009.00796.x
- Siemionow, M., and Brzezicki, G. (2009). “Current techniques and concepts in peripheral nerve repair,” in *International Review of Neurobiology* (Cambridge, MA: Academic Press), 141–172. doi: 10.1016/S0074-7742(09)87008-6
- Siemionow, M., Uygur, S., Ozturk, C., and Siemionow, K. (2013). Techniques and materials for enhancement of peripheral nerve regeneration: a literature review. *Microsurgery* 33, 318–328. doi: 10.1002/micr.22104
- Son, Y. J., and Thompson, W. J. (1995). Schwann cell processes guide regeneration of peripheral axons. *Neuron* 14, 125–132. doi: 10.1016/0896-6273(95)90246-5
- Sondell, M., Lundborg, G., and Kanje, M. (1998). Regeneration of the rat sciatic nerve into allografts made acellular through chemical extraction. *Brain Res.* 795, 44–54. doi: 10.1016/S0006-8993(98)00251-0
- Sun, W., Sun, C., Lin, H., Zhao, H., Wang, J., Ma, H., et al. (2009). The effect of collagen-binding NGF- β on the promotion of sciatic nerve regeneration in a rat sciatic nerve crush injury model. *Biomaterials* 30, 4649–4656. doi: 10.1016/j.biomaterials.2009.05.037
- Szynkaruk, M., Kemp, S. W. P., Wood, M. D., Gordon, T., and Borschel, G. H. (2013). Experimental and clinical evidence for use of decellularized nerve allografts in peripheral nerve gap reconstruction. *Tissue Eng. Part B. Rev.* 19, 83–96. doi: 10.1089/ten.TEB.2012.0275
- Tajdaran, K., Gordon, T., Wood, M. D., Shoichet, M. S., and Borschel, G. H. (2016). A glial cell line-derived neurotrophic factor delivery system enhances nerve regeneration across acellular nerve allografts. *Acta Biomater.* 29, 62–70. doi: 10.1016/j.actbio.2015.10.001
- Tos, P., Ronchi, G., Nicolino, S., Audisio, C., Raimondo, S., Fornaro, M., et al. (2008). Employment of the mouse median nerve model for the experimental assessment of peripheral nerve regeneration. *J. Neurosci. Methods* 169, 119–127. doi: 10.1016/j.jneumeth.2007.11.030
- Varejao, A. S., Meek, M. F., Ferreira, A. J., Patricio, J. A., and Cabrita, A. M. (2001). Functional evaluation of peripheral nerve regeneration in the rat: walking track analysis. *J. Neurosci. Methods* 108, 1–9.
- Vasudevan, S., Huang, J., Botterman, B., Matloub, H. S., Keefer, E., and Cheng, J. (2014). Detergent-free decellularized nerve grafts for long-gap peripheral nerve reconstruction. *Plast. Reconstr. Surg. Glob. Open* 2:e81. doi: 10.1097/GOX.0000000000000118
- Vleggeert-Lankamp, C. L. (2007). The role of evaluation methods in the assessment of peripheral nerve regeneration through synthetic conduits: a systematic review, laboratory investigation. *J. Neurosurg.* 107, 1168–1189. doi: 10.3171/JNS-07/12/1168
- Waitayawinyu, T., Parisi, D. M., Miller, B., Luria, S., Morton, H. J., Chin, S. H., et al. (2007). A comparison of polyglycolic acid versus type I collagen bioabsorbable nerve conduits in a rat model: an alternative to autografting. *J. Hand Surg. Am.* 32, 1521–1529. doi: 10.1016/j.jhbsa.2007.07.015
- Wakimura, Y., Wang, W., Itoh, S., Okazaki, M., and Takakuda, K. (2015). An experimental study to bridge a nerve gap with a decellularized allogeneic nerve. *Plast. Reconstr. Surg.* 136, 319e–327e. doi: 10.1097/PRS.0000000000001556
- Wang, H., Wu, J., Zhang, X., Ding, L., and Zeng, Q. (2016). Study of synergistic role of allogenic skin-derived precursor differentiated schwann cells and heregulin-1 β in nerve regeneration with an acellular nerve allograft. *Neurochem. Int.* 97, 146–153. doi: 10.1016/j.neuint.2016.04.003
- Wang, W., Itoh, S., and Takakuda, K. (2016). Comparative study of the efficacy of decellularization treatment of allogenic and xenogeneic nerves as nerve conduits. *J. Biomed. Mater. Res. – Part A* 104, 445–454. doi: 10.1002/jbm.a.35589
- Wang, Q., Chen, C., Liu, W., He, X., Zhou, N., Zhang, D., et al. (2017a). Levofloxacin loaded mesoporous silica microspheres/nanohydroxyapatite/polyurethane composite scaffold for the treatment of chronic osteomyelitis with bone defects. *Sci. Rep.* 7:41808. doi: 10.1038/srep41808
- Wang, Q., Chen, J., Niu, Q., Fu, X., Sun, X., and Tong, X. (2017b). The application of graphene oxidized combining with decellularized scaffold to repair of sciatic nerve injury in rats. *Saudi Pharm. J.* 25, 469–476. doi: 10.1016/j.jsps.2017.04.008
- Wang, Y., Ma, M., Tang, Q., Zhu, L., Koleini, M., and Zou, D. (2015). The effects of different tensile parameters for the neurodynamic mobilization technique on tricipital muscle wet weight and MuRf-1 expression in rabbits with sciatic nerve injury. *J. Neuroeng. Rehabil.* 12, 1–7. doi: 10.1186/s12984-015-0034-4
- Wang, Y., Zhao, Z., Ren, Z., Zhao, B., Zhang, L., Chen, J., et al. (2012). Recellularized nerve allografts with differentiated mesenchymal stem cells promote peripheral nerve regeneration. *Neurosci. Lett.* 514, 96–101. doi: 10.1016/j.neulet.2012.02.066
- Whitlock, E. L., Tuffaha, S. H., Luciano, J. P., Yan, Y., Hunter, D. A., Magill, C. K., et al. (2009). Processed allografts and type I collagen conduits for repair of peripheral nerve gaps. *Muscle Nerve* 39, 787–799. doi: 10.1002/mus.21220
- Wood, M. D., Kemp, S. W. P., Liu, E. H., Szynkaruk, M., Gordon, T., and Borschel, G. H. (2014). Rat-derived processed nerve allografts support more axon regeneration in rat than human-derived processed nerve xenografts. *J. Biomed. Mater. Res. – Part A* 102, 1085–1091. doi: 10.1002/jbm.a.34773
- Xiang, F., Wei, D., Yang, Y., Chi, H., Yang, K., and Sun, Y. (2017). Tissue-engineered nerve graft with tetramethylpyrazine for repair of sciatic nerve defects in rats. *Neurosci. Lett.* 638, 114–120. doi: 10.1016/j.neulet.2016.12.026
- Yan, Y., Wood, M. D., Hunter, D. A., Ee, X., Mackinnon, S. E., and Moore, A. M. (2016). The effect of short nerve grafts in series on axonal regeneration across isografts or acellular nerve allografts. *J. Hand Surg. Am.* 41, e113–e121. doi: 10.1016/j.jhbsa.2016.01.009
- Zhang, C., and Lv, G. (2013). Repair of sciatic nerve defects using tissue engineered nerves. *Neural Regen. Res.* 8, 1985–1994. doi: 10.3969/j.issn.1673-5374.2013.21.007
- Zhang, Y., Zhang, H., Katiella, K., and Huang, W. (2014). Chemically extracted acellular allogeneic nerve graft combined with ciliary neurotrophic factor promotes sciatic nerve repair. *Neural Regen. Res.* 9, 1358–1364. doi: 10.4103/1673-5374.137588
- Zhao, Z., Wang, Y., Peng, J., Ren, Z., Zhang, L., Guo, Q., et al. (2014). Improvement in nerve regeneration through a decellularized nerve graft by supplementation with bone marrow stromal cells in fibrin. *Cell Transplant.* 23, 97–110. doi: 10.3727/096368912X658845
- Zheng, C., Zhu, Q., Liu, X., Huang, X., He, C., Jiang, L., et al. (2014). Improved peripheral nerve regeneration using acellular nerve allografts loaded with platelet-rich plasma. *Tissue Eng. Part A* 20, 3228–3240. doi: 10.1089/ten.tea.2013.0729
- Zhou, X., He, B., Zhu, Z., He, X., Zheng, C., Xu, J., et al. (2014). Etifoxine provides benefits in nerve repair with acellular nerve grafts. *Muscle Nerve* 50, 235–243. doi: 10.1002/mus.24131
- Zhu, G., and Weihua, L. (2014). Regeneration of facial nerve defects with xenogeneic acellular nerve grafts in a rat model. *Head Neck* 36, 481–486.
- Zhu, Z., Huang, Y., Zou, X., Zheng, C., Liu, J., Qiu, L., et al. (2017). The vascularization pattern of acellular nerve allografts after nerve repair in Sprague-Dawley rats. *Neurol. Res.* 39, 1014–1021. doi: 10.1080/01616412.2017.1365423
- Zhu, Z., Zhou, X., He, B., Dai, T., Zheng, C., Yang, C., et al. (2015). Ginkgo biloba extract (EGb 761) promotes peripheral nerve regeneration and neovascularization after acellular nerve allografts in a rat model. *Cell. Mol. Neurobiol.* 35, 273–282. doi: 10.1007/s10571-014-0122-1

Conflict of Interest Statement: The authors declare that the research was conducted in the absence of any commercial or financial relationships that could be construed as a potential conflict of interest.

The handling Editor and author SR declared their involvement as co-editors in the Research Topic, and confirm the absence of any other collaboration.

Copyright © 2018 Lovati, D'Arrigo, Odella, Tos, Geuna and Raimondo. This is an open-access article distributed under the terms of the Creative Commons Attribution License (CC BY). The use, distribution or reproduction in other forums is permitted, provided the original author(s) and the copyright owner(s) are credited and that the original publication in this journal is cited, in accordance with accepted academic practice. No use, distribution or reproduction is permitted which does not comply with these terms.



Inhibition of RhoA-Subfamily GTPases Suppresses Schwann Cell Proliferation Through Regulating AKT Pathway Rather Than ROCK Pathway

Dandan Tan^{1,2}, Jinkun Wen^{1,2}, Lixia Li^{1,2}, Xianghai Wang^{1,2}, Changhui Qian^{1,2,3}, Mengjie Pan^{1,2}, Muhua Lai^{1,2}, Junyao Deng^{1,2}, Xiaofang Hu^{1,2}, Haowen Zhang^{1,2} and Jiasong Guo^{1,2,4*}

¹Guangdong Provincial Key Laboratory of Construction and Detection in Tissue Engineering, Southern Medical University, Guangzhou, China, ²Department of Histology and Embryology, Southern Medical University, Guangzhou, China, ³Department of Histology and Embryology, Fujian University of Traditional Chinese Medicine, Fuzhou, China, ⁴Key Laboratory of Mental Health of the Ministry of Education, Southern Medical University, Guangzhou, China

OPEN ACCESS

Edited by:

Giovanna Gambarotta,
Università di Torino, Italy

Reviewed by:

Pablo Hector Horacio Lopez,
Instituto de Investigación Médica
Mercedes y Martín Ferreyra (INIMEC),
Argentina
Barbara Hausott,
Innsbruck Medical University, Austria

*Correspondence:

Jiasong Guo
jiasongguo@aliyun.com

Received: 21 July 2018

Accepted: 05 November 2018

Published: 20 November 2018

Citation:

Tan D, Wen J, Li L, Wang X, Qian C, Pan M, Lai M, Deng J, Hu X, Zhang H and Guo J (2018) Inhibition of RhoA-Subfamily GTPases Suppresses Schwann Cell Proliferation Through Regulating AKT Pathway Rather Than ROCK Pathway.
Front. Cell. Neurosci. 12:437.
doi: 10.3389/fncel.2018.00437

Inhibiting RhoA-subfamily GTPases by C3 transferase is widely recognized as a prospective strategy to enhance axonal regeneration. When C3 transferase is administered for treating the injured peripheral nerves, Schwann cells (SCs, important glial cells in peripheral nerve) are inevitably impacted and therefore SC bioeffects on nerve regeneration might be influenced. However, the potential role of C3 transferase on SCs remains elusive. Assessed by cell counting, EdU and water-soluble tetrazolium salt-1 (WST-1) assays as well as western blotting with PCNA antibody, herein we first found that CT04 (a cell permeable C3 transferase) treatment could significantly suppress SC proliferation. Unexpectedly, using Y27632 to inhibit ROCK (the well-accepted downstream signal molecule of RhoA subfamily) did not impact SC proliferation. Further studies indicated that CT04 could inactivate AKT pathway by altering the expression levels of phosphorylated AKT (p-AKT), PI3K and PTEN, while activating AKT pathway by IGF-1 or SC79 could reverse the inhibitory effect of CT04 on SC proliferation. Based on present data, we concluded that inhibition of RhoA-subfamily GTPases could suppress SC proliferation, and this effect is independent of conventional ROCK pathway but involves inactivation of AKT pathway.

Keywords: Schwann cell, proliferation, RhoA-subfamily GTPase, C3 transferase, AKT, ROCK

INTRODUCTION

Rho family small guanosine triphosphatases (Rho-GTPases) are essential in the regulation of diverse cellular functions such as regulation of actin cytoskeleton, vesicular trafficking and transcriptome dynamics (Hu and Selzer, 2017; Nomikou et al., 2017). Rho-GTPases cycle between an active GTP-bound and an inactive GDP-bound form, regulated by the opposing actions of guanine nucleotide exchange factors (GEFs) and GTPase-activating proteins (GAPs; Bai et al., 2015). The best characterized members of Rho family are classified into three subgroups, the RhoA (RhoA, B, C), Cdc42 (Cdc42, Tc10 and TcL) and Rac (Rac1, 2, 3 and RhoG) subfamilies, respectively (Erschbamer et al., 2005). RhoA subfamily is widely recognized as a crucial molecular switch to initiate growth cone collapse and inhibit axonal regrowth in the nervous system (Antoine-Bertrand et al., 2011; Matsukawa et al., 2018).

Peripheral nerve injury (PNI) is a common global clinical problem which involves approximate 2.8% clinic trauma patients, and it significantly affects the life quality of patients and arouses an enormous socioeconomic burden (Wang et al., 2017). Recently, inhibiting RhoA subfamily has been accepted as a prospective strategy to facilitate axonal regrowth and functional recovery after PNI (Hiraga et al., 2006; Auer et al., 2012; Hynds, 2015; Joshi et al., 2015). Due to C3 transferase is able to selectively inactivate RhoA-subfamily GTPases, it is widely used to promote neural regeneration (Auer et al., 2012, 2013; Zhou et al., 2012; Forgione and Fehlings, 2014; Gutekunst et al., 2016).

Peripheral nerves are composed not only of axons but also of Schwann cells (SCs), which wrap around the axons and form myelin sheath (Tricaud, 2017). SCs are the first cells activated following PNI and play vital roles in nerve regeneration through dedifferentiation and proliferation (Pan et al., 2017). The proliferated SCs can organize the clearance of broken axons and myelin debris by promoting macrophage recruitment or via phagocytosis by themselves, secrete neurotrophins to facilitate the axonal regrowth, form bands of Bungers in the distal stump to provide a permissive microenvironment for axon regeneration and ensuing remyelination (Monk et al., 2015; Jessen and Mirsky, 2016; Wong et al., 2017). Thus, SC proliferation is regarded as a crucial part of the nerve injury and regeneration (Jessen et al., 2015). When C3 transferase is administered to promote the axonal regeneration in the injured peripheral nerves, SCs are inevitably impacted and their bioeffects on nerve regeneration might be influenced. However, the potential roles of C3 transferase on SCs remain elusive. To figure out this issue, the present project was firstly designed to reveal the effect of CT04 (a cell permeable C3 transferase) on SC proliferation and then the underlying mechanisms were also studied.

MATERIALS AND METHODS

Primary Cultures of Schwann Cells

The procedures of this study were performed in accordance with National Institutes of Health (NIH) guidelines for the care and use of laboratory animals (NIH Publications) and approved by the Animal Experimental Ethics Committee of the Southern Medical University (SMU), Guangdong Province, China. All efforts were made to minimize animal suffering and usage. Primary rat SCs were isolated and cultured according to our previous reports (Wen et al., 2017a,b). Briefly, spinal and sciatic nerves were aseptically isolated from 3-day to 5-day postnatal Sprague-Dawley (SD) rats (provided by the Experimental Animal Center of SMU). The collected nerves were dissociated by 0.25% Trypsin-EDTA (Gibco) at 37°C for 30 min and single cells were obtained by gentle pipetting. Following digestion and dissociation, the cells were centrifuged for 10 min at 1,000 rpm and re-suspended in DMEM/F12 (Corning) containing 10% fetal bovine serum (FBS, Corning). Then cells were plated onto poly-L-lysine (PLL, Sigma-Aldrich)-coated petri dish (Jet Biofil). The next day, 10 μ M of cytosine arabinoside (Sigma-Aldrich) was added into the medium and incubated with the cells to eliminate

fibroblasts. Forty-eight hours later, the medium was replaced by SC medium (DMEM/F12) containing 3% FBS, 3 μ M forskolin (Sigma-Aldrich), 10 ng/ml heregulin (PeproTech) and 100 mg/ml penicillin-streptomycin (Gibco) to expand the cells. And all experiments of the present study were routinely performed using SCs collected at passages 3–5th. In designed experiments, 2 μ g/ml CT04 (RhoA-subfamily GTPases inhibitor, Cytoskeleton), 50 μ M Y27632 (ROCK inhibitor, Selleck), 150 ng/ml IGF-1 (AKT activator, PeproTech) or 20 μ M SC79 (AKT activator, Selleck) was added into the culture medium and maintained for 24 h.

Immunofluorescence Staining

To characterize the primary isolated cells, the cultured cells of passage 3 were fixed by 4% (*w/v*) paraformaldehyde for 20 min and washed three times with 0.01 M PBS. The fixed cells were permeabilized by 0.5% Triton X-100 (Sigma) for 30 min and then blocked with 5% bovine serum albumin (BSA, GBCBIO Technologies) in PBS for 1 h at room temperature, followed by the incubation with primary antibodies diluted in 1% BSA overnight at 4°C. The dilutions of the primary antibodies are as follows: rabbit anti-GFAP (1:400, Sigma-Aldrich); mouse anti-S100 (1:200, Millipore); and mouse anti-P75 (1:400, Millipore). Alexa 488 fluorescent conjugated secondary antibodies (1:400, Molecular Probes) were applied for 2 h at room temperature, and the nuclei were counterstained by 1 μ g/ml 4',6-diamidino-2-phenylindole (DAPI, Sigma) for 2 min. After immunofluorescence staining, the cultures were mounted using the anti-fading mounting medium (Vector) and images were captured with a fluorescent microscope (Leica).

Schwann Cell Proliferation Assays

EdU Incorporation Assay

The EdU incorporation assay was conducted according to the manufacturer's instructions (RiboBio). In brief, the cells were seeded at 1×10^4 /well in 96-well plates and incubated overnight to allow cell adherence. Cells were exposed to various drug treatments as designed for 24 h and then incubated with 50 μ M EdU labeling reagent for 3 h prior to fixation. Following permeabilization in 0.5% Triton X-100, the cells underwent EdU staining. The cell nuclei were counterstained with DAPI. EdU-positive nuclei were determined under a fluorescence microscope (Leica). Five images were captured at the center and four quadrants in each plate using a fluorescent microscope. The EdU positive ratio was calculated as the number of EdU-positive cells divided by the number of total cells (positive for DAPI). Meanwhile, the cell density of each group was calculated and defined as the number of cells (positive for DAPI) in each captured image. The number of cells was counted using Image-Pro Plus software (Media Cybernetics).

WST-1 Assay

The cell proliferation was also evaluated by the water-soluble tetrazolium salt-1 (WST-1) assay using a Quick Cell Proliferation Assay Kit II (Abcam). SCs were prepared as described above (EdU incorporation assay). According to the manufacturer's instructions, 10 μ l of the WST reagent was added to each

well of the 96-well plates for 3 h at 37°C. The absorbance was measured at 450 nm by using a microplate reader (BioTek). $A_{\text{background}}$ is the absorbance of culture medium plus WST in the absence of cells. The actual absorbance of the control cells (A_{control}) is the absorbance of A_{control} minus the absorbance of $A_{\text{background}}$. The actual absorbance of the treated cells ($A_{\text{experimental}}$) is the absorbance of $A_{\text{experimental}}$ minus the absorbance of $A_{\text{background}}$.

Western Blotting

For western blotting, SCs were treated with various drugs as designed for 24 h. The subjected cells were washed twice with ice-cold PBS, scraped and lysed in RIPA buffer (GBCBIO) containing protease inhibitor cocktail (1:100, Cell Signaling). Lysates were incubated on ice for 30 min and centrifuged (14,000 rpm, 20 min, 4°C) in order to collect the supernatant. Extracts were combined with SDS-PAGE sample buffer (400 mM Tris/HCl, pH 6.8, 10% SDS, 50% glycerol, 500 mM DTT, 2 µg/ml bromophenol blue) and denatured by boiling for 10 min. Equal protein samples were loaded and resolved by 10% SDS-PAGE gels and transferred to polyvinylidene difluoride (PVDF) membrane (Bio-Rad) by liquid transfer. Membranes were blocked with 5% BSA for 1 h at room temperature and incubated with primary antibodies overnight at 4°C. The following primary antibodies were used in western blotting: rabbit anti-GAPDH (1:3,000, Multi Science); rabbit anti-PCNA (1:500, Cell Signaling Technology); rabbit anti-PTEN (1:1,000, Cell Signaling Technology); rabbit anti-PI3K (1:1,000, Cell Signaling Technology); rabbit anti-phospho-AKT (1:1,000, Cell Signaling Technology); rabbit anti-AKT (1:1,000, Cell Signaling Technology). After washed three times with Tris-buffered saline containing 0.05% Tween-20, the membranes were incubated with respective

HRP-conjugated secondary antibodies (1:2,000, Cell Signaling Technology) for 2 h at room temperature. Immunoreactive proteins bands were detected and imaged by enhanced chemiluminescence (ECL, Millipore) using Lumazone system (Roper). After exposure, membranes were washed by stripping buffer (Thermo) for further incubation of another antibody if needed. Integrated optical density (IOD) of each lane was quantified with Image-Pro Plus software and the expression levels of targeted proteins were normalized by the IOD of GAPDH.

Cytotoxicity Assay by Live/Dead Cell Staining

In order to assess whether the effect of CT04 on cell proliferation is attributed to the cytotoxicity of CT04, an assay with Live/Dead cell staining kit (BestBio) was conducted according to the manufacturer's instructions. In brief, the cells were seeded at 1×10^4 /well in 96-well plates and incubated overnight to allow cell adherence. The culture media were supplemented with 2 µg/ml CT04 or 30% DMSO for 24 h and then incubated for 30 min with the Live/Dead cell staining solution which was prepared with the reagents A, B and C of the kit. After that, the cultures were observed with a fluorescence microscope to detect the live cells (stained by Calcein-AM with green fluorescence) and dead cells (stained by PI with red fluorescence). Five images were captured at the center and four quadrants in each culture. Then the live cell ratio was calculated as the number of Calcein-AM positive cells divided by the number of total cells (Calcein-AM-positive cells plus PI-positive cells).

Statistical Analysis

All statistical analyses and calculations were carried out using SPSS 20.0 software (IBM, Armonk, NY, USA). Statistics for

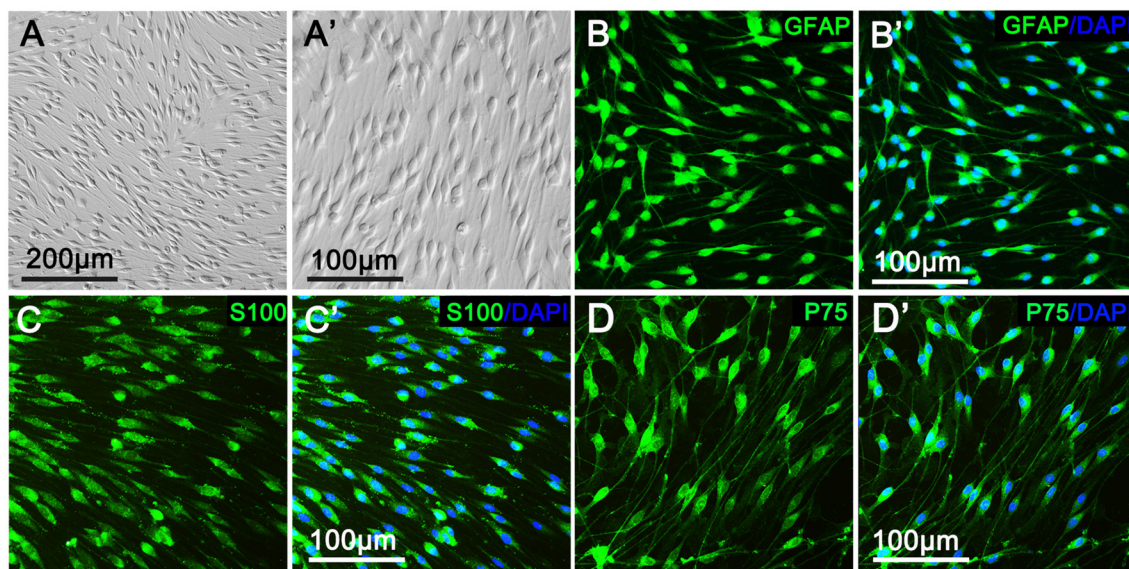


FIGURE 1 | Characterization and identification of primary cultured Schwann cells (SCs). (A,A') Primary cultured SCs showed a bipolar spindle shape under phase contrast microscope. More than 95% of the cells were positive for the SC specific markers, including GFAP (B,B'), S100 (C,C') and P75 (D,D').

multiple comparisons were generated using one-way ANOVA followed by Bonferroni *post hoc* tests. Independent samples *t*-test was used to analyze values between two groups. All statistical graphs were plotted with the Graph Pad Prism 6.0 (Graph Pad software), and quantitative data were presented as mean \pm standard deviation (SD). Differences were considered statistically significant with P -value < 0.05 .

RESULTS

CT04 Suppresses Schwann Cell Proliferation

As shown in **Figure 1**, primary cultured SCs exhibited a bipolar spindle shape (**Figures 1A,A'**) and were positive for SC-specific markers, including GFAP, S100 and P75 (**Figures 1B–D,B'–D'**). To illustrate the effect of CT04 on SC proliferation, SCs were treated by CT04 for 24 h. Then, the EdU and WST-1 measurements were conducted. The EdU assay displayed that the ratio of EdU positive cells was significantly reduced in the presence of CT04 (**Figures 2A–G**). Furthermore, the statistical analysis of cell density indicated that the number of total cells was also decreased by CT04 treatment (**Figure 2H**). The WST-1 results revealed that CT04 markedly decreased the absorbance value compared

to the control group (**Figure 2I**). Meanwhile, the level of PCNA, determined using western blotting, was remarkably down-regulated by CT04 treatment (**Figures 2J,K**). Taken together, all these results confirm that CT04 can suppress SC proliferation.

Further experiment with Live/Dead cell staining assay was designed to test the potential cytotoxicity of CT04 in the SC cultures. In order to confirm the efficiency and reliability of this assay, we set up a positive control (30% DMSO treatment) and a negative control (no drug treatment) to do the parallel experiment with the CT04 treatment. The results illustrated that the overwhelming majority of cells in both of the negative control group and CT04 group were live cells, only very few of cells in these two groups were dead cells (**Figures 3A–F,J**). However, almost all cells in the positive control group were dead cells (**Figures 3G–J**). These results demonstrate that the effect of CT04 on SC proliferation is not caused by cytotoxicity.

Inhibition of ROCK Does Not Affect Schwann Cell Proliferation

To identify whether CT04 modulates SC proliferation through ROCK which is the most well-known downstream effector of RhoA-subfamily GTPases, the SCs were treated with Y27632 (a widely used specific ROCK inhibitor) for 24 h. Unexpectedly,

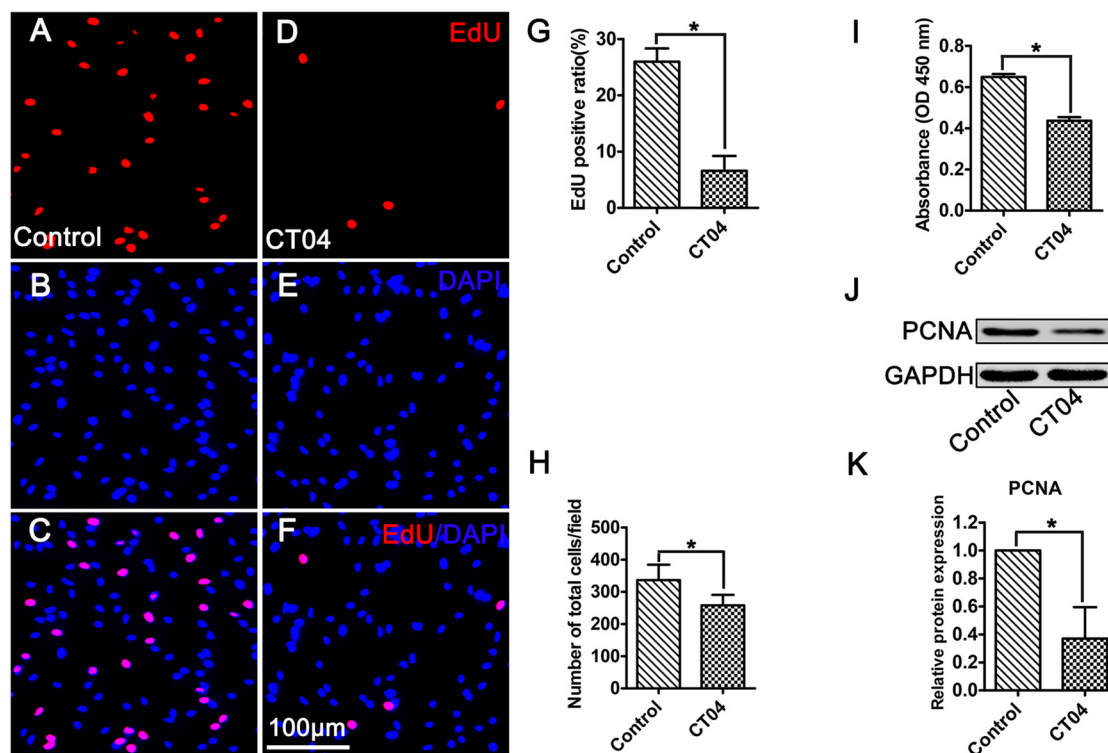


FIGURE 2 | CT04 suppresses SC proliferation. (**A–G**) EdU staining showed that EdU positive ratio was suppressed by CT04 treatment ($n = 15$, $*P < 0.05$). (**H**) Statistical graph of cell density indicated that the number of total cells (positive for 4',6-diamidino-2-phenylindole (DAPI)) was decreased in the presence of CT04 ($n = 15$, $*P < 0.05$). (**I**) Water-soluble tetrazolium salt-1 (WST-1) measurement revealed that CT04 markedly decreased the absorbance value compared to the control group ($n = 4$, $*P < 0.05$). (**J,K**) Western blotting displayed that the expression of PCNA was remarkably down-regulated in the CT04 treated cells ($n = 6$, $*P < 0.05$). The blots were cropped from different parts of the same gel. The expression level of PCNA in the control group was normalized to 1.

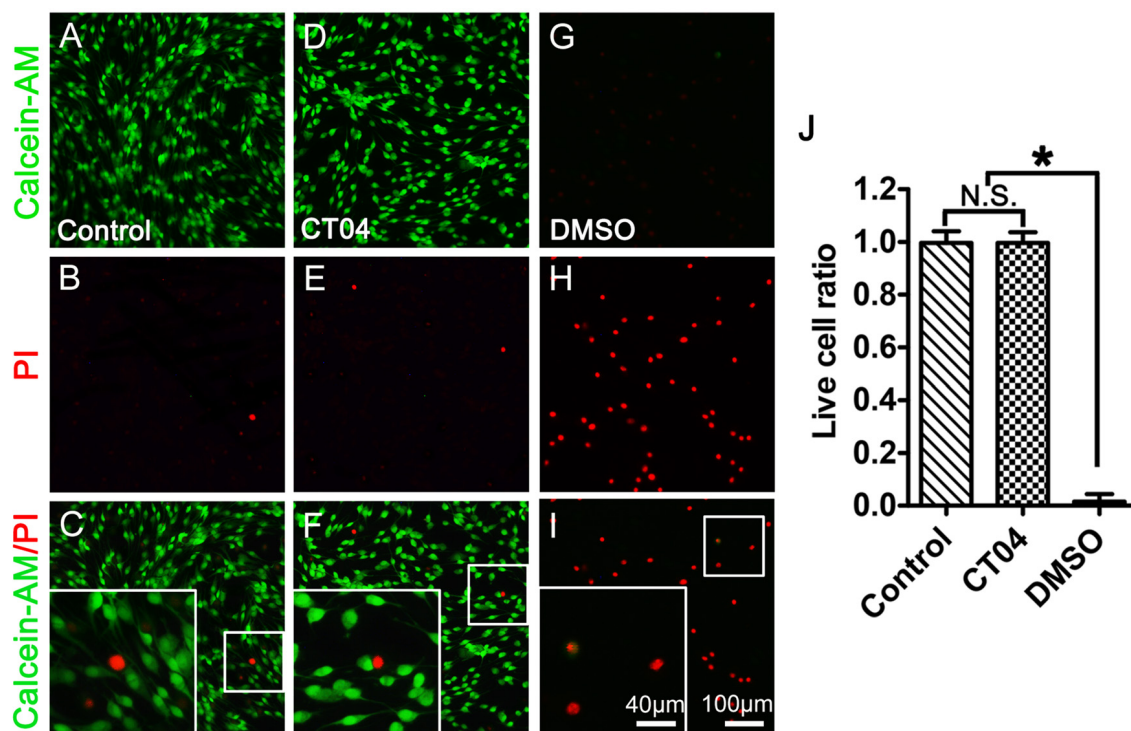


FIGURE 3 | CT04 does not induce toxic effect on SC. The cytotoxicity of CT04 was evaluated using Live/Dead cell staining. (A–J) The Live/Dead cell staining and statistical diagrams suggested that addition of CT04 did not induce cell death in the SCs cultures ($n = 20$, $*P < 0.05$). N.S. as non-significance.

Y27632 did not result in the same effect on SC proliferation as CT04. As shown in **Figure 4**, the EdU assay indicated that the ratio of EdU positive cells as well as the cell density was not affected in the presence of Y27632 (**Figures 4A–G,H**). Meanwhile, WST-1 assay showed no difference in absorbance value between Y27632 and control groups (**Figure 4I**). In addition, the expression level of PCNA was similar between two groups (**Figures 4J,K**). These data strongly implicate that ROCK is not involved in the regulation of SC proliferation.

CT04 Inactivates AKT Signaling Pathway

According to previous reports (He et al., 2011; Chen et al., 2016; Wu et al., 2016), AKT pathway is one of the most important pathways involved in regulating SC proliferation. To determine whether this pathway is responsible for mediating the CT04-induced suppression on SC proliferation, the total AKT, phosphorylated AKT (p-AKT) as well as AKT's critical upstream regulator—PI3K (Gaesser and Fyffe-Maricich, 2016) and its crucial inhibitor—PTEN (Liu et al., 2017) were detected. Western blotting verified that the p-AKT was significantly decreased in CT04 group, while the total AKT was unaffected (**Figures 5A,B**). Furthermore, the expression of PI3K was down-regulated in the presence of CT04 (**Figures 5C,D**), while the expression of PTEN was up-regulated (**Figures 5E,F**). These data drew us to hypothesize that AKT pathway might be involved in the inhibitory effect of CT04 on SC proliferation.

Activation of AKT Reverses the Inhibitory Effect of CT04 on SC Proliferation

To ascertain the potential role of AKT pathway on CT04-mediated inhibition of SC proliferation, we treated the SCs with CT04 in the presence or absence of AKT activators (IGF-1 (Jo et al., 2012; Sabater et al., 2017) or SC79 (Wu et al., 2017; Yang et al., 2018; Zhou et al., 2018)), respectively. Western blotting indicated that IGF-1 dramatically increased the level of p-AKT while the level of total AKT was not affected (**Figures 6A,B**). Subsequently, the EdU assay showed that CT04-induced suppression of EdU positive ratio of SCs and the cell density were obviously restored by IGF-1 (**Figures 6C–L,M**). The effect of IGF-1 on SC proliferation was also verified by the change in absorbance value detected by WST-1 measurement (**Figure 6N**). What's more, the down-regulation of PCNA expression caused by CT04 treatment was also significantly alleviated by IGF-1 as shown in western blots (**Figures 6O,P**). Similar findings were observed when SCs were treated with CT04 in the presence of SC79, another specific activator of AKT. The results of cell density, EdU, WST-1 and western blotting assays also revealed that the addition of SC79 partly reversed CT04-mediated suppression of SC proliferation (**Figure 7**).

DISCUSSION

Collectively, overall data of the present study demonstrate that: (1) data got from the assessments of cell density, EdU,

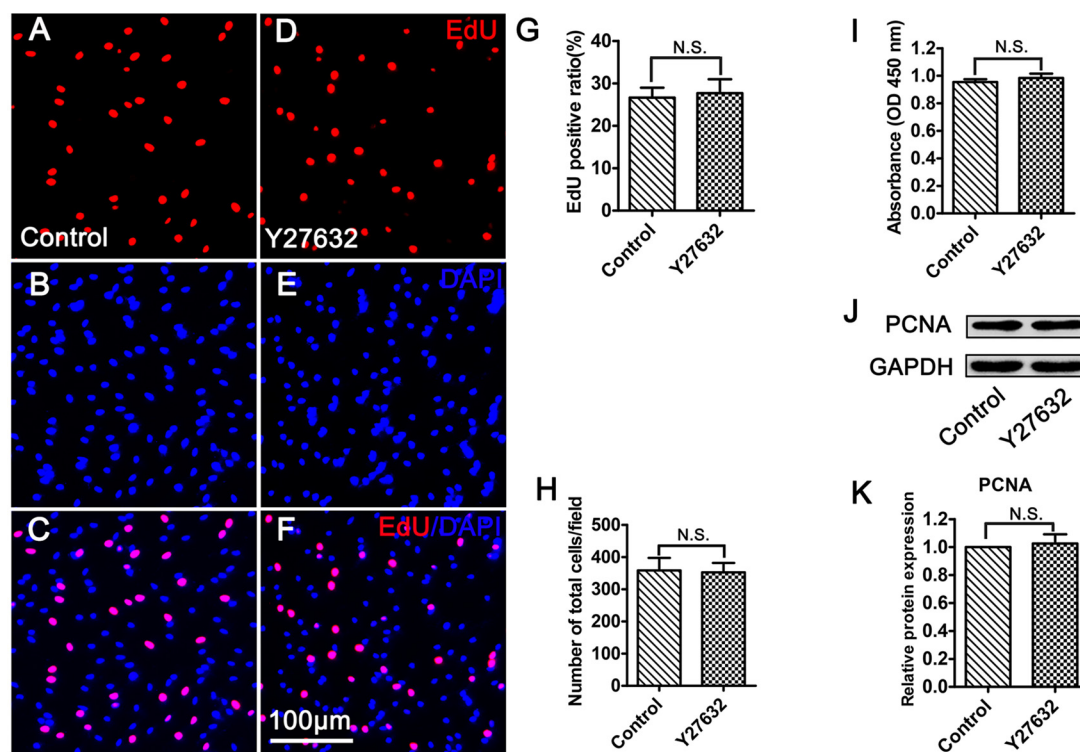


FIGURE 4 | Inhibition of ROCK does not affect SC proliferation. **(A–G)** EdU assay showed that EdU positive ratio was not affected by Y27632 treatment ($n = 15$). **(H)** Statistical diagram of cell density suggested that the number of total cells was not altered in the presence of Y27632 ($n = 15$). **(I)** WST-1 measurement revealed that there was no significant difference in the absorbance value between the control group and Y27632 group ($n = 4$). **(J,K)** Western blotting indicated that the expression of PCNA was unaffected in the Y27632 treated cells ($n = 6$). The blots were cropped from different parts of the same gel. The expression level of PCNA in the control group was normalized to 1. N.S. as non-significance.

WST-1 and PCNA expression indicate that the inhibition of RhoA-subfamily GTPases by C3 transferase (CT04) can suppress the SC proliferation; (2) Live/Dead cell staining assay indicates CT04 does not induce cell death in the SCs cultures, which means the effect of CT04 on SC proliferation was not related to the cytotoxicity; (3) Y27632 (a widely used specific ROCK inhibitor) does not affect the SC proliferation. By which excludes the possibility of RhoA-subfamily GTPases regulating SC proliferation via ROCK pathway; (4) the level of p-AKT is significantly decreased in the CT04 treated SCs, while the total AKT is unaffected. Since AKT activation (phosphorylation) is involved in regulating the proliferation of many kinds of cells including SCs, these results suggest AKT inactivation might play a role in CT04 negative effects on SC proliferation; (5) CT04 treatment results in down-regulation of PI3K and up-regulation of PTEN, which can confirm and verify the results of CT04 suppressing the AKT activation; and (6) reversing the AKT activation by IGF-1 or SC79 (two kinds of widely used AKT activators) can significantly alleviate the inhibitory effect of CT04 on SC proliferation. These data confirm that AKT pathway is involved in the mechanisms of CT04-induced suppression on SC proliferation.

Since SCs are important glial cells in peripheral nerve and they have attractive application prospects in cell transplantation for

the therapy of nervous system injury, the biology and application of SCs have been attracting a great deal of attention (Belin et al., 2017). Recent decades, lots of publications focused on the study of SC proliferation (Atanasoski et al., 2004; Deng et al., 2017; Pan et al., 2017; Piñero et al., 2017). As molecular switches that control the organization and dynamics of the actin cytoskeleton, Rho GTPases are considered to be key regulators of proliferation of various cells (Hu et al., 2014; Wang et al., 2014). Our previous study indicated that lentivirus-mediated RhoA knocking down to reduce the total protein level of RhoA could significantly slack the proliferation of SCs (Wen et al., 2017a). In this study, we aimed to reveal whether inhibiting the activation of RhoA-subfamily GTPases can impact the SC proliferation. CT04 is able to specifically and irreversibly inhibit activation of RhoA-subfamily GTPases by ADP ribosylation, our recent study proved CT04 treatment could reduce the level of activated GTP-RhoA in cultured SCs (Wen et al., 2018). Combined with the present data of cell density, EdU assay, WST-1 assessment and western blotting of PCNA, we can safely draw the conclusion that inhibition of RhoA-subfamily GTPases by CT04 can significantly slow down the SC proliferation.

Up to now, the most well-known downstream effector of RhoA-subfamily GTPases is ROCK. In existing reports, RhoA subfamily plays roles in various biologic effects including

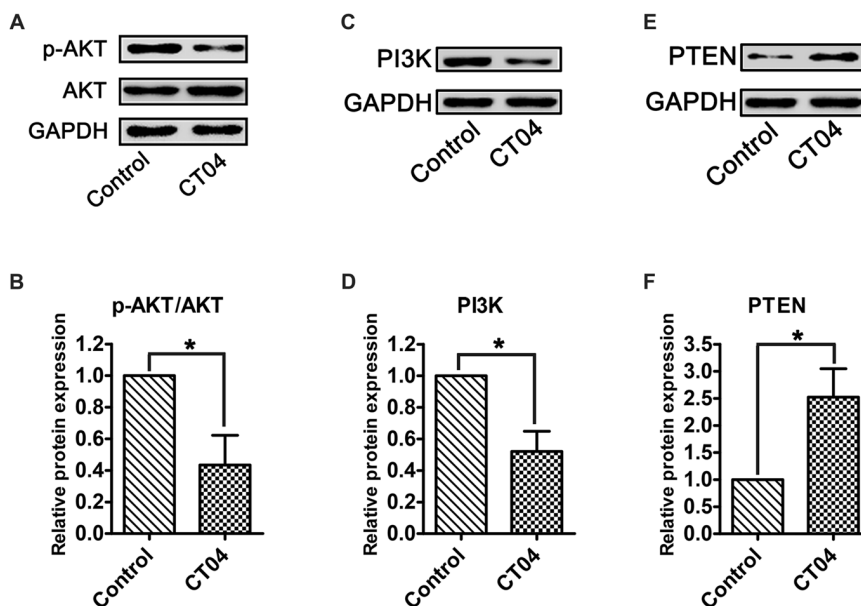


FIGURE 5 | CT04 regulates the AKT signaling pathway. **(A,B)** The western blots indicated that the phosphorylation of AKT was markedly decreased in the presence of CT04 ($n = 12$, $*P < 0.05$). **(C–F)** Immunoblot assays and statistical diagrams also revealed that addition of CT04 resulted in down-regulation of PI3K and up-regulation of PTEN ($n = 4$, $*P < 0.05$). The blots were cropped from different parts of the same gel. The expression levels of target proteins in the control group were normalized to 1.

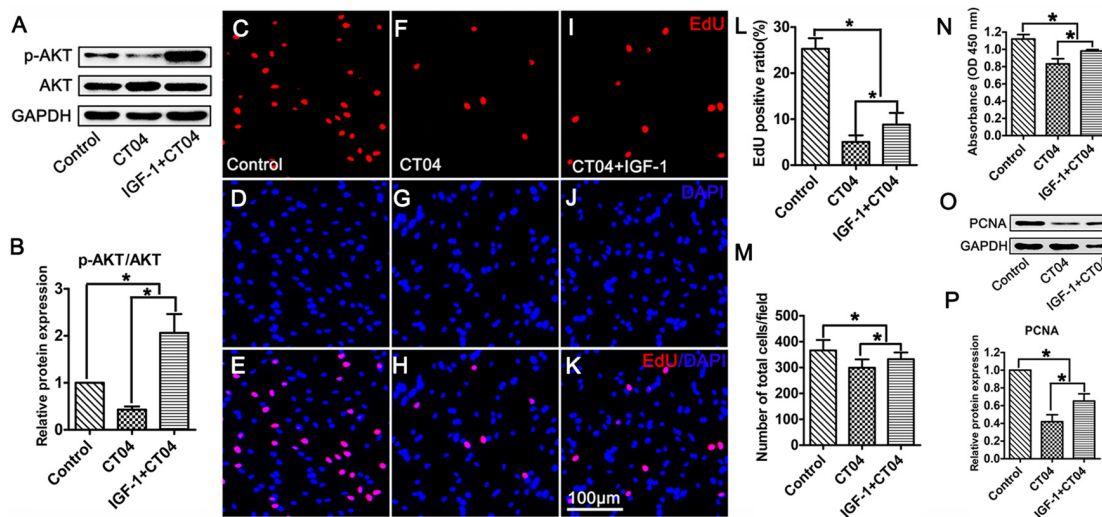


FIGURE 6 | Activation of AKT by IGF-1 reverses the inhibitory effect of CT04 on SC proliferation. The SCs were treated with CT04 in the presence or absence of IGF-1 for 24 h. **(A,B)** Western blotting was performed to confirm the effect of IGF-1 on activation of AKT. GAPDH was used as the loading control ($n = 4$, $*P < 0.05$). **(C–L)** Analysis of EdU incorporation indicated that IGF-1 partly restored the declined EdU positive ratio in CT04 treated cells ($n = 15$, $*P < 0.05$). **(M)** Statistics of cell density displayed that CT04-mediated inhibition of SC density was reversed by IGF-1 ($n = 15$, $*P < 0.05$). **(N)** WST-1 assay revealed that IGF-1 treatment partly restored the change in absorbance value caused by CT04 ($n = 4$, $*P < 0.05$). **(O)** Western blots showed that application of IGF-1 up-regulated the expression of PCNA in the CT04 treated cells. The blots were cropped from different parts of the same gel. **(P)** Statistical diagram of relative protein expression of PCNA ($n = 4$, $*P < 0.05$). The expression levels of target proteins in the control group were normalized to 1.

cell proliferation always by regulating actin dynamics via ROCK pathway. Thus, we naturally consider CT04 may also influence SC proliferation through ROCK pathway. However, the treatment of Y27632, a widely used inhibitor of ROCK,

has no significant impact on the parameters of SC proliferation including cell density, EdU, WST-1 and western blotting of PCNA. Therefore, ROCK is impossible taking part in the regulation of RhoA subfamily on SC proliferation.

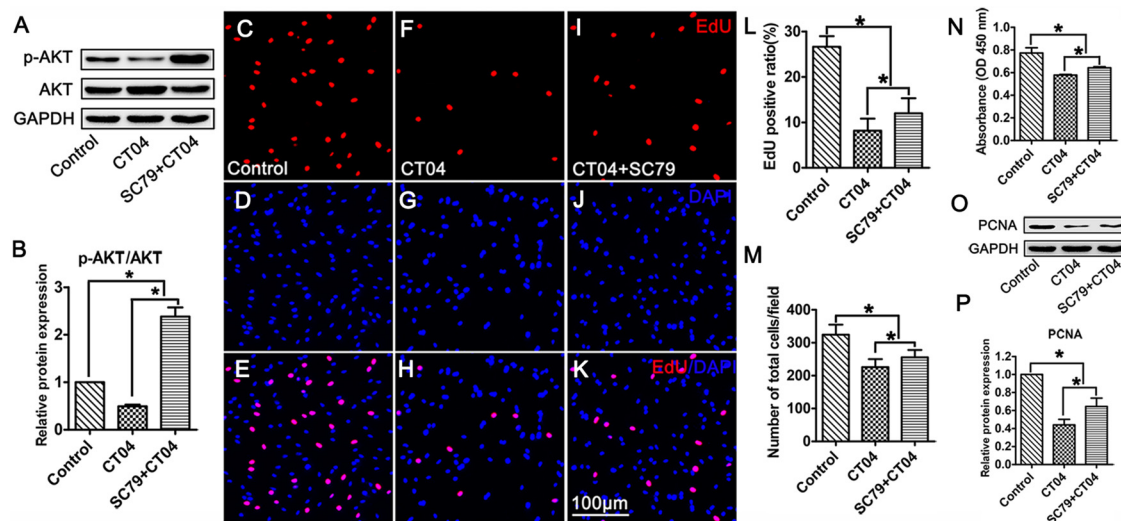


FIGURE 7 | Activation of AKT by SC79 counteracts the inhibitory effect of CT04 on SC proliferation. SCs were treated with DMSO as vehicle control. The SCs were treated with CT04 with or without SC79 for 24 h. **(A,B)** Western blotting was performed to confirm the effect of SC79 on activation of AKT ($n = 4$, $*P < 0.05$). **(C-L)** The EdU incorporation assay suggested that application of SC79 increased the EdU positive ratio in CT04 treated cells ($n = 15$, $*P < 0.05$). **(M)** The statistics showed that CT04-mediated suppression of SC density was partly restored by SC79 ($n = 15$, $*P < 0.05$). **(N)** Assessment of cell proliferation by WST-1 assay displayed that SC79 counteracted the inhibitory effect of CT04 on SC proliferation ($n = 4$, $*P < 0.05$). **(O,P)** Western blots and statistical data indicated that the addition of SC79 increased the expression of PCNA in the CT04 treated cells ($n = 4$, $*P < 0.05$). The blots were cropped from different parts of the same gel. The expression levels of target proteins in the control group were normalized to 1.

AKT pathway is demonstrated as an important signaling pathway in the regulation of cell proliferation, including SCs (Wu et al., 2016; Liu et al., 2017; Zhao et al., 2017). This drew us to think whether CT04 treatment modulated SC proliferation via AKT pathway. In order to test this hypothesis, the phosphorylation of AKT was firstly evaluated. The results demonstrated that CT04 treatment significantly reduced the level of p-AKT. Moreover, the expression level of PI3K, which is the crucial positive upstream molecule of AKT, was markedly decreased. It has been shown in several researches that in the PTEN/PI3K/AKT signaling pathway, PI3K can catalyze 3,4,5-phosphatidylinositol triphosphate phosphorylation and then activate AKT to promote the proliferation of cells (Zhang et al., 2015). In addition, we found that the expression of PTEN was dramatically up-regulated. PTEN is an important negative regulator of AKT pathway, it can antagonize PI3K and then weaken the activation of AKT (Zhang et al., 2015; Ahmed et al., 2016). Therefore, the up-regulation of PTEN and down-regulation of PI3K further confirmed that AKT pathway could be inactivated by CT04. To further validate whether the inactivation of AKT pathway was responsible for CT04-mediated suppression of SC proliferation, two kinds of activators of AKT pathway (IGF-1 and SC79) were used to do the rescue experiments. As expected, both IGF-1 and SC79 could reverse the AKT inactivation by CT04 and significantly alleviate the inhibitory effect of CT04 on SC proliferation.

Taken together, we can conclude that: (1) C3 transferase (CT04) treatment can significantly suppress the SC proliferation. Considering SCs are important glial cells in peripheral nerves

and C3 transferase is widely used to promote axonal regeneration in the injured peripheral nerve, the present study indicates further studies are needed to explore new strategies to avoid this side-effect when using this drug to treat the injured nerve; and (2) the effect of CT04 on SC proliferation involves the AKT pathway. While ROCK, the most well-known downstream molecule of Rho subfamily, is independent of the effect of CT04 on the SC proliferation. Considering the complicate signaling networks of Rho GTPases in most kinds of cells, and combining with present data, we believe that AKT is not the only downstream of RhoA subfamily on SC proliferation. The clear mechanism needs further studies in the future.

AUTHOR CONTRIBUTIONS

JG and DT designed the study. DT, JW, LL and XW performed experiments. CQ, MP and ML participated in collecting and analyzing experimental data. JD, XH and HZ contributed for double blind analyzing data and doing statistics. The manuscript was written by JG, DT and reviewed by all authors.

FUNDING

This work is supported by the National Natural Science Foundation of China (81870982, 81571182 and 81371354), the Program for Changjiang Scholars and Innovative Research Team in University (IRT-16R37), National Key Basic Research Program of China (2014CB542202), the Science and Technology Project of Guangdong Province (2015A020212024) and Natural Science Foundation of Guangdong Province (2017A030312009).

REFERENCES

- Ahmed, M. W., Kayani, M. A., Shabbir, G., Ali, S. M., Shinwari, W.-U.-D., and Mahjabeen, I. (2016). Expression of PTEN and its correlation with proliferation marker Ki-67 in head and neck cancer. *Int. J. Biol. Markers* 31, e193–e203. doi: 10.5301/jbm.5000196
- Antoine-Bertrand, J., Villemure, J.-F., and Lamarche-Vane, N. (2011). Implication of Rho GTPases in neurodegenerative diseases. *Curr. Drug Targets* 12, 1202–1215. doi: 10.2174/138945011795906543
- Atanasoski, S., Notterpek, L., Lee, H.-Y., Castagner, F., Young, P., Ehrenguber, M. U., et al. (2004). The protooncogene *Ski* controls Schwann cell proliferation and myelination. *Neuron* 43, 499–511. doi: 10.1016/j.neuron.2004.08.001
- Auer, M., Allodi, I., Barham, M., Udina, E., Neiss, W. F., Navarro, X., et al. (2013). C3 exoenzyme lacks effects on peripheral axon regeneration *in vivo*. *J. Peripher. Nerv. Syst.* 18, 30–36. doi: 10.1111/jns.12004
- Auer, M., Schweigreiter, R., Hausott, B., Thongrong, S., Hölte, M., Just, I., et al. (2012). Rho-independent stimulation of axon outgrowth and activation of the ERK and Akt signaling pathways by C3 transferase in sensory neurons. *Front. Cell. Neurosci.* 6:43. doi: 10.3389/fncel.2012.00043
- Bai, Y., Xiang, X., Liang, C., and Shi, L. (2015). Regulating Rac in the nervous system: molecular function and disease implication of Rac GEFs and GAPs. *Biomed. Res. Int.* 2015:632450. doi: 10.1155/2015/632450
- Belin, S., Zuloaga, K. L., and Poitelon, Y. (2017). Influence of mechanical stimuli on Schwann cell biology. *Front. Cell. Neurosci.* 11:347. doi: 10.3389/fncel.2017.00347
- Chen, M.-S., Kim, H., Jagot-Lacoussiere, L., and Maurel, P. (2016). *Cadm3* (Nccl-1) interferes with the activation of the PI3 kinase/Akt signaling cascade and inhibits Schwann cell myelination *in vitro*. *Glia* 64, 2247–2262. doi: 10.1002/glia.23072
- Deng, Y., Wu, L. M. N., Bai, S., Zhao, C., Wang, H., Wang, J., et al. (2017). A reciprocal regulatory loop between TAZ/YAP and G-protein *Gαs* regulates Schwann cell proliferation and myelination. *Nat. Commun.* 8:15161. doi: 10.1038/ncomms15161
- Erschbamer, M. K., Hofstetter, C. P., and Olson, L. (2005). RhoA, RhoB, RhoC, Rac1, Cdc42 and Tc10 mRNA levels in spinal cord, sensory ganglia and corticospinal tract neurons and long-lasting specific changes following spinal cord injury. *J. Comp. Neurol.* 484, 224–233. doi: 10.1002/cne.20471
- Forgione, N., and Fehlings, M. G. (2014). Rho-ROCK inhibition in the treatment of spinal cord injury. *World Neurosurg.* 82, e535–e539. doi: 10.1016/j.wneu.2013.01.009
- Gaesser, J. M., and Fyffe-Maricich, S. L. (2016). Intracellular signaling pathway regulation of myelination and remyelination in the CNS. *Exp. Neurol.* 283, 501–511. doi: 10.1016/j.expneurol.2016.03.008
- Gutekunst, C.-A., Tung, J. K., McDougal, M. E., and Gross, R. E. (2016). C3 transferase gene therapy for continuous conditional RhoA inhibition. *Neuroscience* 339, 308–318. doi: 10.1016/j.neuroscience.2016.10.022
- He, B., Liu, S.-Q., Chen, Q., Li, H.-H., Ding, W.-J., and Deng, M. (2011). Carboxymethylated chitosan stimulates proliferation of Schwann cells *in vitro* via the activation of the ERK and Akt signaling pathways. *Eur. J. Pharmacol.* 667, 195–201. doi: 10.1016/j.ejphar.2011.06.001
- Hiraga, A., Kuwabara, S., Doya, H., Kanai, K., Fujitani, M., Taniguchi, J., et al. (2006). Rho-kinase inhibition enhances axonal regeneration after peripheral nerve injury. *J. Peripher. Nerv. Syst.* 11, 217–224. doi: 10.1111/j.1529-8027.2006.00091.x
- Hu, J., and Selzer, M. E. (2017). RhoA as a target to promote neuronal survival and axon regeneration. *Neural Regen. Res.* 12, 525–528. doi: 10.4103/1673-5374.205080
- Hu, X., Yu, J., Zhou, X., Li, Z., Xia, Y., Luo, Z., et al. (2014). A small GTPase-like protein fragment of *Mycoplasma* promotes tumor cell migration and proliferation *in vitro* via interaction with Rac1 and Stat3. *Mol. Med. Rep.* 9, 173–179. doi: 10.3892/mmr.2013.1766
- Hynds, D. (2015). Subcellular localization of Rho GTPases: implications for axon regeneration. *Neural Regen. Res.* 10, 1032–1033. doi: 10.4103/1673-5374.160064
- Jessen, K. R., and Mirsky, R. (2016). The repair Schwann cell and its function in regenerating nerves. *J. Physiol.* 594, 3521–3531. doi: 10.1113/jp270874
- Jessen, K. R., Mirsky, R., and Lloyd, A. C. (2015). Schwann cells: development and role in nerve repair. *Cold Spring Harb. Perspect. Biol.* 7:a020487. doi: 10.1101/cshperspect.a020487
- Jo, H., Mondal, S., Tan, D., Nagata, E., Takizawa, S., Sharma, A. K., et al. (2012). Small molecule-induced cytosolic activation of protein kinase Akt rescues ischemia-elicited neuronal death. *Proc. Natl. Acad. Sci. U S A* 109, 10581–10586. doi: 10.1073/pnas.1202810109
- Joshi, A. R., Bobylev, I., Zhang, G., Sheikh, K. A., and Lehmann, H. C. (2015). Inhibition of Rho-kinase differentially affects axon regeneration of peripheral motor and sensory nerves. *Exp. Neurol.* 263, 28–38. doi: 10.1016/j.expneurol.2014.09.012
- Liu, G.-L., Yang, H.-J., Liu, B., and Liu, T. (2017). Effects of microRNA-19b on the proliferation, apoptosis and migration of Wilms' tumor cells via the PTEN/PI3K/AKT signaling pathway. *J. Cell. Biochem.* 118, 3424–3434. doi: 10.1002/jcb.25999
- Matsukawa, T., Morita, K., Omizu, S., Kato, S., and Koriyama, Y. (2018). Mechanisms of RhoA inactivation and CDC42 and Rac1 activation during zebrafish optic nerve regeneration. *Neurochem. Int.* 112, 71–80. doi: 10.1016/j.neuint.2017.11.004
- Monk, K. R., Feltri, M. L., and Taveggia, C. (2015). New insights on Schwann cell development. *Glia* 63, 1376–1393. doi: 10.1002/glia.22852
- Nomikou, E., Stournaras, C., and Kardassis, D. (2017). Functional analysis of the promoters of the small GTPases RhoA and RhoB in embryonic stem cells. *Biochem. Biophys. Res. Commun.* 491, 754–759. doi: 10.1016/j.bbrc.2017.07.114
- Pan, B., Shi, Z.-J., Yan, J.-Y., Li, J.-H., and Feng, S.-Q. (2017). Long non-coding RNA NONMUG014387 promotes Schwann cell proliferation after peripheral nerve injury. *Neural Regen. Res.* 12, 2084–2091. doi: 10.4103/1673-5374.221168
- Piñero, G., Berg, R., Andersen, N. D., Setton-Avruj, P., and Monje, P. V. (2017). Lithium reversibly inhibits Schwann cell proliferation and differentiation without inducing myelin loss. *Mol. Neurobiol.* 54, 8287–8307. doi: 10.1007/s12035-016-0262-z
- Sabater, A. L., Andreu, E. J., García-Guzmán, M., López, T., Abizanda, G., Perez, V. L., et al. (2017). Combined PI3K/Akt and Smad2 activation promotes corneal endothelial cell proliferation. *Invest. Ophthalmol. Vis. Sci.* 58, 745–754. doi: 10.1167/iovs.16-20817
- Tricaud, N. (2017). Myelinating Schwann cell polarity and mechanically-driven myelin sheath elongation. *Front. Cell. Neurosci.* 11:414. doi: 10.3389/fncel.2017.00414
- Wang, C., Lu, C.-F., Peng, J., Hu, C.-D., and Wang, Y. (2017). Roles of neural stem cells in the repair of peripheral nerve injury. *Neural Regen. Res.* 12, 2106–2112. doi: 10.4103/1673-5374.221171
- Wang, L., Wang, T., Song, M., and Pan, J. (2014). Rho plays a key role in TGF- β 1-induced proliferation and cytoskeleton rearrangement of human periodontal ligament cells. *Arch. Oral Biol.* 59, 149–157. doi: 10.1016/j.archoralbio.2013.11.004
- Wen, J., Qian, C., Pan, M., Wang, X., Li, Y., Lu, Y., et al. (2017a). Lentivirus-mediated RNA interference targeting RhoA slacks the migration, proliferation and myelin formation of Schwann cells. *Mol. Neurobiol.* 54, 1229–1239. doi: 10.1007/s12035-016-9733-5
- Wen, J., Tan, D., Li, L., and Guo, J. (2017b). Isolation and purification of Schwann cells from spinal nerves of neonatal rat. *Bio-protocol* 7:e2588. doi: 10.21769/bioprotoc.2588
- Wen, J., Tan, D., Li, L., Wang, X., Pan, M., and Guo, J. (2018). RhoA regulates Schwann cell differentiation through JNK pathway. *Exp. Neurol.* 308, 26–34. doi: 10.1016/j.expneurol.2018.06.013
- Wong, K. M., Babetto, E., and Beirowski, B. (2017). Axon degeneration: make the Schwann cell great again. *Neural Regen. Res.* 12, 518–524. doi: 10.4103/1673-5374.205000
- Wu, K.-C., Cheng, K.-S., Wang, Y.-W., Chen, Y.-F., Wong, K.-L., Su, T.-H., et al. (2017). Perturbation of Akt signaling, mitochondrial potential and ADP/ATP ratio in acidosis-challenged rat cortical astrocytes. *J. Cell. Biochem.* 118, 1108–1117. doi: 10.1002/jcb.25725
- Wu, W., Liu, Y., and Wang, Y. (2016). Sam68 promotes Schwann cell proliferation by enhancing the PI3K/Akt pathway and acts on regeneration after sciatic nerve crush. *Biochem. Biophys. Res. Commun.* 473, 1045–1051. doi: 10.1016/j.bbrc.2016.04.013

- Yang, Q., Wen, L., Meng, Z., and Chen, Y. (2018). Blockage of endoplasmic reticulum stress attenuates nilotinib-induced cardiotoxicity by inhibition of the Akt-GSK3 β -Nox4 signaling. *Eur. J. Pharmacol.* 822, 85–94. doi: 10.1016/j.ejphar.2018.01.011
- Zhang, L.-L., Mu, G.-G., Ding, Q.-S., Li, Y.-X., Shi, Y.-B., Dai, J.-F., et al. (2015). Phosphatase and tensin homolog (PTEN) represses colon cancer progression through inhibiting paxillin transcription via PI3K/AKT/NF- κ B pathway*. *J. Biol. Chem.* 290, 15018–15029. doi: 10.1074/jbc.m115.641407
- Zhao, Z., Li, X., and Li, Q. (2017). Curcumin accelerates the repair of sciatic nerve injury in rats through reducing Schwann cells apoptosis and promoting myelination. *Biomed. Pharmacother.* 92, 1103–1110. doi: 10.1016/j.biopha.2017.05.099
- Zhou, J., Chen, J., and Yu, H. (2018). Targeting sphingosine kinase 2 by ABC294640 inhibits human skin squamous cell carcinoma cell growth. *Biochem. Biophys. Res. Commun.* 497, 535–542. doi: 10.1016/j.bbrc.2018.02.075
- Zhou, Z., Peng, X., Chiang, P., Kim, J., Sun, X., Fink, D. J., et al. (2012). HSV-mediated gene transfer of C3 transferase inhibits Rho to promote axonal regeneration. *Exp. Neurol.* 237, 126–133. doi: 10.1016/j.expneurol.2012.06.016
- Conflict of Interest Statement:** The authors declare that the research was conducted in the absence of any commercial or financial relationships that could be construed as a potential conflict of interest.

Copyright © 2018 Tan, Wen, Li, Wang, Qian, Pan, Lai, Deng, Hu, Zhang and Guo. This is an open-access article distributed under the terms of the Creative Commons Attribution License (CC BY). The use, distribution or reproduction in other forums is permitted, provided the original author(s) and the copyright owner(s) are credited and that the original publication in this journal is cited, in accordance with accepted academic practice. No use, distribution or reproduction is permitted which does not comply with these terms.



Mitochondrial Damage-Associated Molecular Patterns of Injured Axons Induce Outgrowth of Schwann Cell Processes

Andrea Korimová, Ilona Klusáková[†], Ivana Hradilová-Sviženská[†], Marcela Kohoutková, Marek Joukal[†] and Petr Dubový*

Department of Anatomy, Division of Neuroanatomy, Faculty of Medicine, Masaryk University, Brno, Czechia

OPEN ACCESS

Edited by:

Giovanna Gambirotta,
Università di Torino, Italy

Reviewed by:

Giulia Ronchi,
Università degli Studi di Torino, Italy
Michela Rigoni,
Università degli Studi di Padova, Italy

*Correspondence:

Petr Dubový
pdubový@med.muni.cz

[†]These authors have contributed
equally to this work

Received: 19 September 2018

Accepted: 12 November 2018

Published: 27 November 2018

Citation:

Korimová A, Klusáková I,
Hradilová-Sviženská I,
Kohoutková M, Joukal M and
Dubový P (2018) Mitochondrial
Damage-Associated Molecular
Patterns of Injured Axons Induce
Outgrowth of Schwann
Cell Processes.
Front. Cell. Neurosci. 12:457.
doi: 10.3389/fncel.2018.00457

Activated Schwann cells put out cytoplasmic processes that play a significant role in cell migration and axon regeneration. Following nerve injury, axonal mitochondria release mitochondrial damage-associated molecular patterns (mtDAMPs), including formylated peptides and mitochondrial DNA (mtDNA). We hypothesize that mtDAMPs released from disintegrated axonal mitochondria may stimulate Schwann cells to put out cytoplasmic processes. We investigated RT4-D6P2T schwannoma cells (RT4) *in vitro* treated with N-formyl-L-methionyl-L-leucyl-phenylalanine (fMLP) or cytosine-phospho-guanine oligodeoxynucleotide (CpG ODN) for 1, 6 and 24 h. We also used immunohistochemical detection to monitor the expression of formylpeptide receptor 2 (FPR2) and toll-like receptor 9 (TLR9), the canonical receptors for formylated peptides and mtDNA, in RT4 cells and Schwann cells distal to nerve injury. RT4 cells treated with fMLP put out a significantly higher number of cytoplasmic processes compared to control cells. Preincubation with PBP10, a selective inhibitor of FPR2 resulted in a significant reduction of cytoplasmic process outgrowth. A significantly higher number of cytoplasmic processes was also found after treatment with CpG ODN compared to control cells. Pretreatment with inhibitory ODN (INH ODN) resulted in a reduced number of cytoplasmic processes after subsequent treatment with CpG ODN only at 6 h, but 1 and 24 h treatment with CpG ODN demonstrated an additive effect of INH ODN on the development of cytoplasmic processes. Immunohistochemistry and western blot detected increased levels of tyrosine-phosphorylated paxillin in RT4 cells associated with cytoplasmic process outgrowth after fMLP or CpG ODN treatment. We found increased immunofluorescence of FPR2 and TLR9 in RT4 cells treated with fMLP or CpG ODN as well as in activated Schwann cells distal to the nerve injury. In addition, activated Schwann cells displayed FPR2 and TLR9 immunostaining close to GAP43-immunopositive regenerated axons and their growth cones after nerve crush. Increased FPR2 and TLR9 immunoreaction was associated with activation of p38 and NFκB, respectively. Surprisingly, the growth cones displayed also FPR2 and TLR9 immunostaining.

These results present the first evidence that potential mtDAMPs may play a key role in the induction of Schwann cell processes. This reaction of Schwann cells can be mediated via FPR2 and TLR9 that are canonical receptors for formylated peptides and mtDNA. The possible role for FPR2 and TLR9 in growth cones is also discussed.

Keywords: RT4-D6P2T schwannoma cells, *in vitro*, fMLP, CpG ODN, FPR2, TLR9, growth cones, nerve injury

INTRODUCTION

Wallerian degeneration (WD) is the highly orchestrated cascade of cellular and molecular events distal to injury of nerve fibers, and is considered to be a kind of innate immune reaction or sterile inflammation (Stoll et al., 2002; Gaudet et al., 2011). These events comprise, among others, invasion of macrophages and other immune cells, axon fragmentation, as well as activation and inflammatory profiling of Schwann cells (Stoll et al., 2002; Dubový et al., 2013). Schwann cells of the injured nerve and the so-called terminal Schwann cells overlying denervated neuromuscular junctions elaborate processes that guide the sprouts of regenerated axons (Son and Thompson, 1995a,b; Gomez-Sanchez et al., 2017). Thus, cytoplasmic extensions of Schwann cells are crucial for axon regeneration in the peripheral nervous system. However, the stimuli that trigger the elaboration of Schwann cell processes have still not been precisely characterized.

Degeneration of a distal nerve stump is the source of a broad spectrum of damage-associated molecular patterns (DAMPs) produced by the digestion of the endoneurial extracellular matrix as well as fragmentation of axons and their myelin sheaths (Karanth et al., 2006; Boivin et al., 2007; Kato and Svensson, 2015). These DAMPs are ligands for pattern recognition receptors such as the toll-like receptors (TLRs) that regulate WD and Schwann cell inflammatory profiling (Boivin et al., 2007; Goethals et al., 2010; Boerboom et al., 2016; Dubový, 2017).

The axons and their terminals contain abundant mitochondria which are disintegrated distal to a peripheral nerve lesion. The disintegrated mitochondria release specific mitochondrial DNA (mtDNA) fragments and proteins like formyl peptides generally termed mitochondrial damage-associated molecular patterns (mtDAMPs; Krysko et al., 2011). Formylated peptides are ligands for the formylpeptide receptor 2 (FPR2; Le et al., 2002) while mtDNA activates the toll-like receptor 9 (TLR9; Zhang et al., 2010).

We hypothesize that mtDAMPs of disintegrated axonal mitochondria in the immediate aftermath of WD can stimulate Schwann cells to put out cytoplasmic processes through the action of the corresponding receptors. In the experiments presented here, we used the rat RT4-D6P2T schwannoma cell line as a model for studying the elaboration of cytoplasmic processes induced by the potential mtDAMPs, formyl-methionyl-leucyl-phenylalanine (fMLP) and cytosine-phospho-guanine oligodeoxynucleotide (CpG ODN) known to be the prototypical ligands of FPR2 and TLR9, respectively (Le et al., 2002; Chen et al., 2011). In addition, we detected FPR2 and TLR9 in activated Schwann cells distal to the nerve injury but close to regenerated axons.

MATERIALS AND METHODS

Cell Culture and Treatment

Rat RT4-D6P2T schwannoma cell line (RT4) was provided by ATCC. RT4 cells were cultivated in Dulbecco's Modified Eagle's Medium/Nutrient F-12 Ham (DMEM/F12) at 37°C in a 5% CO₂ atmosphere. The medium was supplemented with 10% Fetal Bovine Serum (FBS), 2 mM L-glutamine and antibiotics (100 U/ml penicillin and 100 µg/ml streptomycin; all obtained from Sigma Aldrich). At approximately 90% confluency, cells were seeded at a density of 1×10^4 cells/cm² and harvested in serum-free medium before treatment.

To determine changes in cytoplasmic process extension, RT4 cells were stimulated with the appropriate mtDAMPs. fMLP (Sigma-Aldrich) dissolved in dimethyl sulfoxide (DMSO) as a 100 mM stock solution and maintained at −20°C was used in 100 nM, 10 µM and 50 µM concentration for 1, 6 and 24 h and equivalent volumes of DMSO (0.02%, 0.2% and 1%) were used in controls. To test if the fMLP effect is mediated by FPR2, a set of cells was preincubated with 1 µM PBP10 (Tocris), a selective inhibitor of FPR2 (Forsman et al., 2012), for 20 min before treatment with 50 µM fMLP.

RT4 cells were treated for the same durations, with immunostimulatory 1 µM CpG ODN (ODN D-SL03, a C class CpG ODN, 5'-tcg cgaacgttcgccgcttcgaacgcgg-3', Invivogen) directly or following a pretreatment with 1- or 10-fold amounts of inhibitory ODN (INH ODN) (1 or 10 µM, ODN 4084-F, 5'-cctggatgggaa-3', Invivogen) for 30 min. Oligonucleotides tested for absence of bacterial contamination were separately resuspended in endotoxin-free water to 500 µM stock solution according to the manufacturer's instructions, aliquoted and stored at −20°C until used.

Immunofluorescent Staining and Quantitative Analysis of Cytoplasmic Processes

At the end of the treatments described, cells cultured on slides in 12-well plates were fixed with 4% paraformaldehyde in phosphate-buffered saline (PBS) for 5 min, washed three times with PBS, and permeabilized with cold methanol:acetone (1:1). The cells were then immunostained with rabbit monoclonal anti-β-actin (1:200; Cell Signaling) overnight and FITC-conjugated donkey anti-rabbit affinity-purified secondary antibody (1:100; Millipore) for 90 min at room temperature. The slides with cells were washed extensively in PBS and mounted with the anti-fading medium Mowiol.

To detect FPR2, TLR9 or paxillin expression, portions of the RT4 cells were immunostained overnight with rabbit

polyclonal anti-FPR2 (1:100; Novusbio), anti-TLR9 antibody (1:500; Acris) or a mouse monoclonal antibody recognizing tyrosine-phosphorylated paxillin (1:1,000; Chemicon). The immunohistochemical reaction was visualized using TRITC-conjugated donkey anti-rabbit or anti-mouse affinity-purified secondary antibodies (1:100; Millipore) for 90 min at room temperature. Control cells for immunohistochemical staining were incubated without primary antibody or by substituting the primary antibodies with the donkey IgG isotype. Cell nuclei were stained with Hoechst 33342, and the slides were mounted in aqueous mounting medium (Vectashield; Vector Laboratories, Burlingame, CA, USA). The stained RT4 cells were analyzed, and pictures captured using an epifluorescence microscope (Nikon Eclipse NI-E Motorized Microscope System) equipped with a Nikon DS-Ri1 camera (Nikon, Prague, Czechia).

Actin immunostained RT4 cells were used for quantitative analysis of cytoplasmic processes in response to stimuli. At least 50 cells were randomly chosen for each experimental group and the number of cytoplasmic processes per cell was manually counted using the Count and Taxonomy module of NIS-Elements software (Nikon, Prague, Czechia) following curve fitting detection of cell body boundaries. The number of cytoplasmic processes was measured by a person blind to the experimental conditions.

Dimethyl sulfoxide was used as a solvent and vehicle for fMLP. Because it was demonstrated that medium supplemented with DMSO was enough to induce changes in cell surface area (Lemieux et al., 2011), we compared number of cell processes after fMLP treatment to those of cells cultivated in medium supplemented with DMSO of a corresponding concentration used for dissolution of fMLP and for the appropriate durations.

Western Blot Analysis

As activated paxillin is involved in the initiation of cytoplasmic processes outgrowth in the cell (López-Colomé et al., 2017), we quantified the level of paxillin phosphorylated in tyrosine positions by western blot analysis in RT4 cells after potential mtDAMP action. After cultivation in the presence or absence of stimulants or inhibitors, RT4 cells were washed twice with ice-cold PBS, mechanically harvested from the culture dishes and sonicated for 30 s. The samples were centrifuged at 2,000 rpm for 5 min and lysed at 4°C in buffer containing 80 mM HEPES, pH 7.5; 2.5 M urea, 1 mM EDTA, 0.5% Triton X-100 and 20 mM β -mercaptoethanol as well as cocktails of protease and phosphatase inhibitors (Roche, Germany). Equal amounts of proteins from cell lysates (50 μ g/lane) were separated by SDS-polyacrylamide gel electrophoresis and transferred to a nitrocellulose membrane (Bio-Rad). After blocking of nonspecific binding sites with 5% bovine serum albumin (BSA) in TRIS-buffered saline (pH 7.2) for 2 h, membranes were incubated with mouse monoclonal anti-tyrosine-phosphorylated paxillin (1:1,000; Chemicon) at 4°C overnight, followed by peroxidase-conjugated anti-mouse IgG (1:1,000; Sigma, Ronkonkoma, NY, USA) at room temperature for 1 h. Protein bands were visualized using the ECL detection kit (Bio-Rad) on a PXi chemiluminometer reader and analyzed

using the GeneTools densitometry software (Syngene). All analyzed proteins were normalized to β -actin.

Animals and Surgical Treatment

The *in vivo* experiments were performed in 15 adult male rats (Wistar, 250–280 g, Anlab, Brno, Czechia) housed on 12 h light/dark cycles at a temperature of 22–24°C under specific pathogen-free conditions in the animal housing facility of Masaryk University. Sterilized standard rodent food and water were available *ad libitum*. Animals for surgical treatments were anesthetized using a mixture of ketamine (40 mg/ml) and xylazine (4 mg/ml) administered intraperitoneally (0.2 ml/100 g body weight). All surgical procedures were carried out under sterile conditions by the same person according to protocols approved by the Animal Investigation Committee of the Faculty of Medicine, Brno, Czechia.

The right ulnar nerve of three rats was exposed in mid-thigh, ligated with two ligatures and cut. The proximal nerve stump was buried and fixed in muscles to protect the distal stump from reinnervation. The right ulnar nerve of three other rats was exposed for a short segment and crushed with clamp of a defined force of 1.9 N twice for 1 min (Ronchi et al., 2010) under a stereological microscope. The distal margin of the crush injury was indicated with Indian ink and the skin wound was closed with 5/0 sutures. The ulnar nerve of sham-operated rats ($n = 3$) was carefully exposed without any lesion. To demonstrate a role of p38 and NF κ B in downstream signaling pathways of FPR2 and TLR9, the right ulnar nerve of four rats was crushed as described above and 10 μ l of PBP10 (1 μ M; Tocris) or chloroquine (50 μ M; InvivoGen) was injected via a micro syringe into the subarachnoid space of the cisterna magna (Dubový et al., 2018). The inhibitor of FPR2 (PBP10) or TLR9 (chloroquine) was dissolved in artificial cerebrospinal fluid (ACSF; Hylden and Wilcox, 1980). Ten microliter of ACSF was injected in two control rats. All operated rats were left to survive for 3 days.

Immunofluorescence Staining of Activated Schwann Cells Distal to Nerve Injury

After the period of survival, the animals were deeply anesthetized with a lethal dose of sodium pentobarbital (70 mg/kg body weight, i.p.) and perfused transcardially with 500 ml PBS (10 mM sodium phosphate buffer, pH 7.4, containing 0.15 M NaCl) followed by 500 ml of Zamboni's fixative (Zamboni and Demartin, 1967). The right ulnar nerves of sham-operated rats, distal stumps of transected and crushed ulnar nerves were removed and immersed in Zamboni's fixative overnight. After washing with 10% sucrose in PBS, longitudinal cryostat sections of 10 μ m thickness were cut.

The sections were washed with PBS containing 0.05% Tween 20 (PBS-T) and 1% BSA for 10 min, treated with 5% normal donkey serum in PBS-T for 30 min and immunostained. The longitudinal sections prepared from nerve segments of sham-operated animals and nerve segments distal to nerve transection were incubated under the same conditions with rabbit polyclonal anti-FPR2 (1:100; Novusbio) or anti-TLR9 (1:500; Acris) primary antibodies and TRITC-conjugated

and affinity-purified donkey anti-rabbit secondary antibody (1:100; Millipore). One portion of the sections was double immunostained for GFAP and FPR2 or TLR9 to detect these receptor proteins in activated Schwann cells. Briefly, the sections were incubated with rabbit polyclonal anti-FPR2 or anti-TLR9 antibodies and then with chicken polyclonal anti-GFAP antibody (1:500; Abcam), in each primary antibody overnight. To visualize the immunoreaction, the sections were incubated with TRITC-conjugated and affinity-purified donkey anti-rabbit secondary antibody, while FITC-conjugated donkey anti-chicken secondary antibody (both 1:100; Millipore) was used for development of GFAP immunostaining. Control sections were incubated without primary antibodies as well as with rabbit or chicken polyclonal antibodies and treated with FITC-conjugated donkey anti-chicken or TRITC-conjugated donkey anti-rabbit secondary antibodies, respectively. No immunofluorescence staining was observed in the control sections (data not shown).

To visualize activated Schwann cells close to growing axons, the longitudinal sections distal to ulnar nerve crush were double immunostained with mouse monoclonal anti-GAP43 (1:500; Sigma) and chicken polyclonal anti-GFAP antibodies. The immunostaining was visualized with FITC-conjugated donkey anti-mouse and TRITC-conjugated donkey anti-chicken secondary antibodies.

For evidence of FPR2 or TLR9 immunopositivity in cells close to growing axons, the sections were incubated with mouse monoclonal anti-GAP43 (1:500; Sigma) and rabbit polyclonal anti-FPR2 (1:100; Novusbio) or anti-TLR9 (1:500; Acris) antibodies. Moreover, double immunostaining with rabbit polyclonal anti-FPR2 and mouse monoclonal anti-phosphorylated p38 MAPK (1:100; Santa Cruz) antibodies as well as mouse monoclonal anti-TLR9 (1:100; Novusbio) and rabbit monoclonal anti-pNFkB(p65) (1:100; Cell Signaling) antibodies was used to determine downstream signaling pathways of FPR2 and TLR9. The nerve sections of ACSF- and PGP10- or chloroquine-treated rats were double immunostained under the same conditions. Double immunofluorescence was developed with corresponding FITC- and TRITC-conjugated affinity-purified donkey anti-mouse and anti-rabbit secondary antibodies (1:100; Millipore). Control sections were incubated without primary antibody.

All sections were stained with Hoechst 33342 to detect cell nuclei, mounted in aqueous mounting medium (Vectashield; Vector Laboratories, Burlingame, CA, USA) and analyzed using an epifluorescence microscope (Nikon Eclipse NI-E Motorized Microscope System) equipped with a Nikon DS-Ri1 camera (Nikon, Prague, Czechia).

RESULTS

Quantitative Analysis of Cytoplasmic Processes in RT4 Cells Induced by fMLP or CpG

To investigate whether the potential mtDAMPs fMLP or CpG can induce outgrowth of Schwann cells processes, RT4 cells were cultured *in vitro* with 100 nM, 10 μ M and 50 μ M

concentrations of fMLP or 1 μ M CpG ODN for 1, 6 and 24 h. Representative pictures illustrating changes of cytoplasmic processes in RT4 cells after treatment with fMLP and CpG in comparison to controls as well as following pretreatment with the FPR2 inhibitor PBP10 or INH ODN are shown in **Figure 1**.

Because fMLP was dissolved in DMSO, it was necessary to compare values of cytoplasmic processes measured in RT4 cells after fMLP treatment to control values obtained in RT4 cells cultivated with the corresponding concentration of DMSO used to dissolve fMLP. fMLP influenced the formation of RT4 cell processes very differently under different concentrations and treatment durations (**Figure 1G**). No effect on the number of cell processes was demonstrated in low concentrations of fMLP (100 nM and 10 μ M) after 1 h and 6 h, whereas a higher concentration of fMLP (50 μ M) for the same duration resulted in a significant increase in the number of cytoplasmic processes per cell (1 h: 6.2 ± 1.7 vs. 7.4 ± 1.8 , $p < 0.05$; 6 h: 6.7 ± 2.7 vs. 10.0 ± 2.2 , $p < 0.001$). Nevertheless, after 24 h, 100 nM fMLP resulted in a significantly increased number of cytoplasmic processes per cell (6.7 ± 2.4 vs. 8.4 ± 2.6 , $p < 0.05$), but higher concentrations (10 μ M and 50 μ M) reduced the number of the processes when compared to controls (**Figure 1G**). Because the greatest increase in the number of cytoplasmic processes was induced by 50 μ M fMLP treatment for 6 h, these conditions were used to test the effect of FPR2 inhibition. A 20 min preincubation with 1 μ M PBP10 as an FPR2 inhibitor before 50 μ M fMLP treatment resulted in a significant reduction of cytoplasmic process outgrowth when compared with the standard treatment for 6 h (6.9 ± 2.3 vs. 10.0 ± 2.2 , $p < 0.001$; see also **Figure 1C**).

CpG ODN treatment for 6 and 24 h induced a significantly increased number of cytoplasmic processes compared to control cells (6 h: 7.8 ± 2.5 vs. 6.1 ± 1.5 , $p < 0.05$; 8.8 ± 2.7 vs. 6.9 ± 2.0 , $p < 0.001$). However, CpG ODN treatment for 1 h did not significantly affect the number of cytoplasmic processes (**Figure 1H**). A pre-treatment with 1 or 10 μ M INH ODN before 1 or 24 h CpG ODN stimulation unexpectedly resulted in significantly increased outgrowth of cytoplasmic processes when compared to control cells or cells treated only with CpG ODN (**Figures 1F,H**). In contrast, pre-treatment with 1 or 10 μ M INH ODN and subsequent stimulation with CpG ODN for 6 h caused the expected inhibitory effect and the mean number of cell processes was reduced when compared with only CpG ODN treatment (**Figure 1H**).

Immunohistochemical Detection of FPR2, TLR9 and Analysis of Activated Paxillin in RT4 Cells

To prove that fMLP and CpG can induce changes of cytoplasmic processes in RT4 cells via the corresponding receptors, we detected FPR2 and TLR9 expression in control and treated cells. RT4 cells cultured in medium with fMLP (50 μ M) for 6 h displayed increased intensity of FPR2 immunofluorescence in contrast to control cells cultivated in medium only with

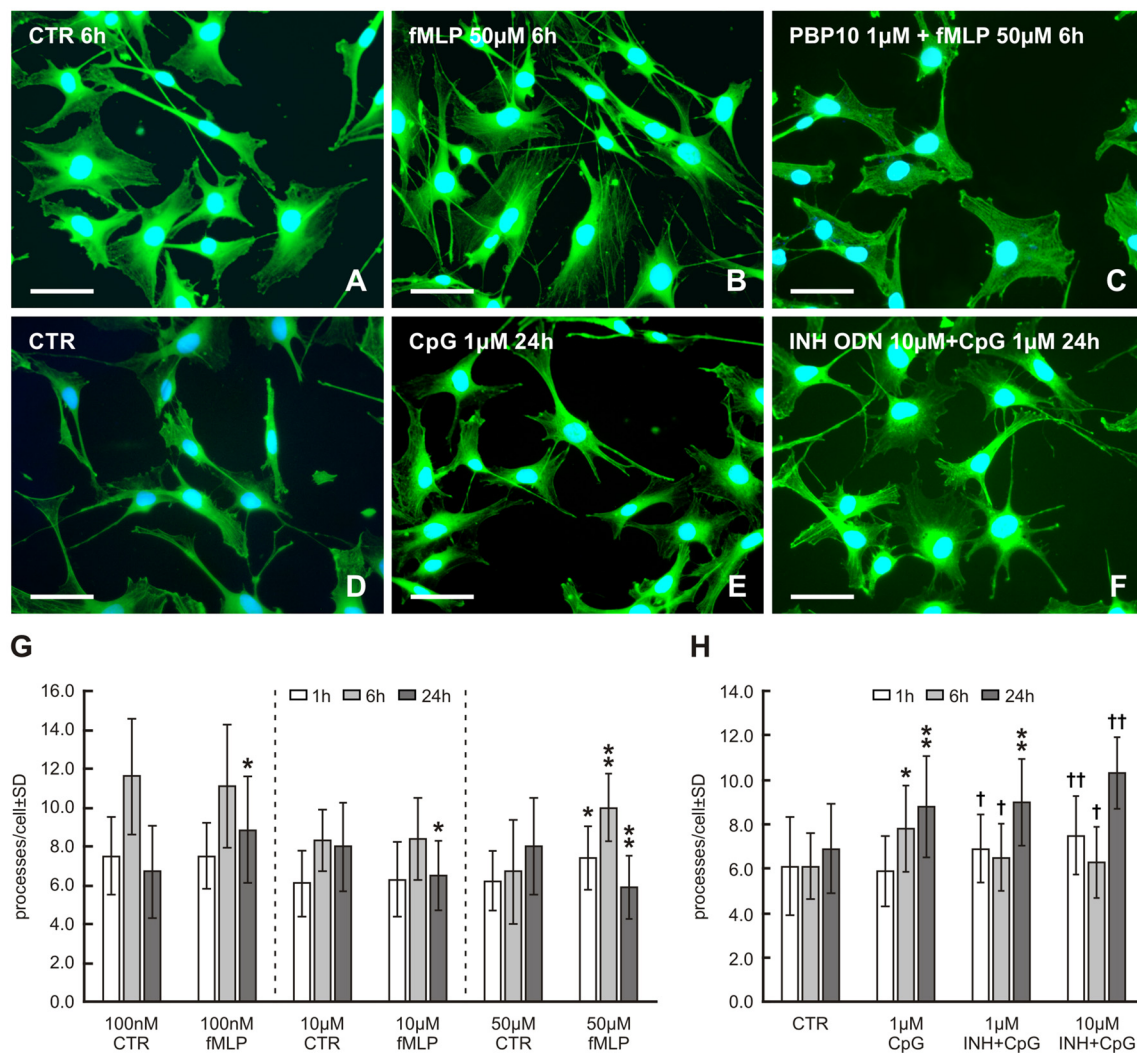


FIGURE 1 | Representative pictures of RT4-D6P2T cells cultivated in control medium (**A,D**) and medium with 50 μ M formyl-L-methionyl-L-leucyl-phenylalanine (fMLP) (**B**) for 6 h or 1 μ M cytosine-phospho-guanine oligodeoxynucleotide (CpG ODN) (**E**) for 24 h showing an increased number of cytoplasmic processes. Preincubation of RT4 cells with the formylpeptide receptor 2 (FPR2) inhibitor PBP10 (1 μ M) resulted in a noticeable reduction of cytoplasmic processes in comparison to only fMLP treatment (**C**). An additive effect of 10 μ M of inhibitory ODN (INH ODN) pre-treatment for 30 min before 1 μ M CpG ODN for 24 h on the development of cytoplasmic processes is shown in (**F**). After *in vitro* cultivation and treatment, the cells were fixed and immunostained with rabbit monoclonal anti- β -actin antibody and FITC-conjugated donkey anti-rabbit secondary antibody. Cell nuclei were stained with Hoechst 33342. Scale bars = 50 μ m. (**G**) The graph illustrates mean number of cytoplasmic processes per cell of the RT4-D6P2T cell line cultivated for different time periods (1, 6 and 24 h) with fMLP at 100 nM, 10 μ M and 50 μ M concentrations and controls (CTR) containing the appropriate volume of dissolved in dimethyl sulfoxide (DMSO). * p < 0.05 when compared with DMSO control, ** p < 0.001 when compared with DMSO control. (**H**) The graph illustrates mean number of cytoplasmic processes per cell of the RT4-D6P2T cell line cultivated for different time periods (1, 6 and 24 h) with control medium (CTR), 1 μ M CpG ODN (CpG) and cells pre-treated with 1 μ M or 10 μ M of INH ODN (INH) for 30 min before treating with CpG ODN. * p < 0.05 compared with control, ** p < 0.001 compared with control, † p < 0.05 INH ODN pre-treatment compared with CpG ODN, †† p < 0.001 INH ODN pre-treatment compared with CpG ODN.

the corresponding concentration of DMSO (Figures 2A,B). Similarly, untreated control RT4 cells displayed a weak TLR9 immunofluorescence whereas those cultivated in medium with CpG (1 μ M) for 24 h showed a more intense immunofluorescence (Figures 2C,D).

We also detected phosphorylated paxillin in RT4 cells. Dot-like immunofluorescence was observed in both control and treated cells with a marked increase of immunofluorescence in RT4 cells treated with 50 μ M fMLP for 6 h (Figures 3A,B)

or with 1 μ M CpG for 6 h (Figures 3C,D). Increased levels of phosphorylated paxillin in RT4 cells after treatment with 50 μ M fMLP or 1 μ M CpG for 6 h as well as decreased levels after FPR2 inhibition by PBP10 or inhibitory effect of INH ODN were demonstrated by western blot analysis (Figure 3E). These altered levels of phosphorylated paxillin corresponded to changes in numbers of cytoplasmic processes analyzed at the same conditions (Figures 1G,H).

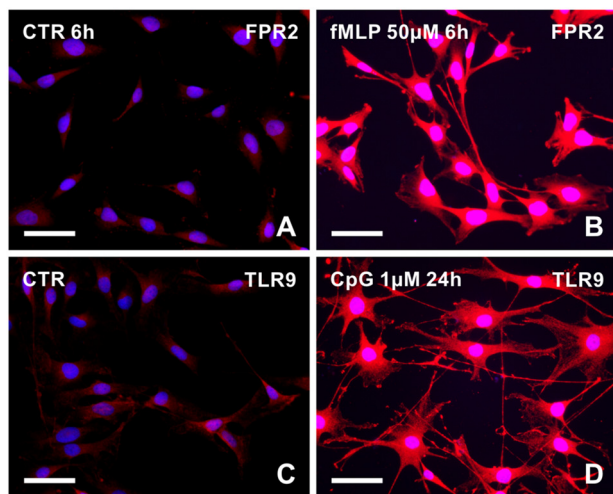


FIGURE 2 | Representative pictures illustrating FPR2 or toll-like receptor 9 (TLR9) immunostaining in RT4-D6P2T cells cultivated in control medium (A,C, respectively) and increased immunofluorescence intensity after treatment with 50 μ M fMLP for 6 h (B) or 1 μ M CpG ODN for 24 h (D). Both control and treated cells were immunostained under the same conditions with rabbit polyclonal anti-FPR2 or anti-TLR9 antibody and TRITC-conjugated donkey anti-rabbit secondary antibody. Cell nuclei were stained with Hoechst 33342. Scale bars = 50 μ m.

FPR2 and TLR9 Immunostaining Distal to Nerve Injury

Longitudinal cryostat sections through the ulnar nerves from sham-operated rats displayed very low intensity of FPR2 and TLR9 immunofluorescence (Figures 4A,B). In contrast, increased intensity of TLR9 and FPR2 immunostaining was detected in sections cut distal to the nerve transection (Figures 4C,F). FPR2 or TLR9 immunopositivity was present in spindle-shaped cells and their processes that also displayed GFAP immunostaining indicating their Schwann cell origin (Figures 4D,E,G,H). Double immunodetection showed p-p38 MAPK immunostaining in FPR2 immunopositive Schwann-like cells distal to the ulnar nerve crush and intrathecal administration of ACSF. In contrast, intrathecal application of PBP10, an inhibitor of FPR2, reduced markedly immunofluorescence for both FPR2 and p-p38 MAPK (Figures 5A–F). Double immunostaining also revealed perinuclear pNFkB(p65) immunofluorescence in TLR9 immunopositive Schwann-like cells after ACSF administration, while the nerve sections from rats treated with chloroquine displayed significantly decreased intensity of both TLR9 and NFkB immunofluorescence (Figures 5G–L).

Activated GFAP-immunopositive Schwann cells were found close to regenerated axons and their growth cones distal to ulnar nerve crush (Figures 6A–C). Moreover, Schwann-like cells with FPR2 or TLR9 immunopositivity were frequently observed near the regenerated axons and their growth cones as visualized by GAP43 immunostaining. Primarily, we could demonstrate increased FPR2 and TLR9 expression in activated Schwann cells and their cytoplasmic process close to regenerated axons. Surprisingly,

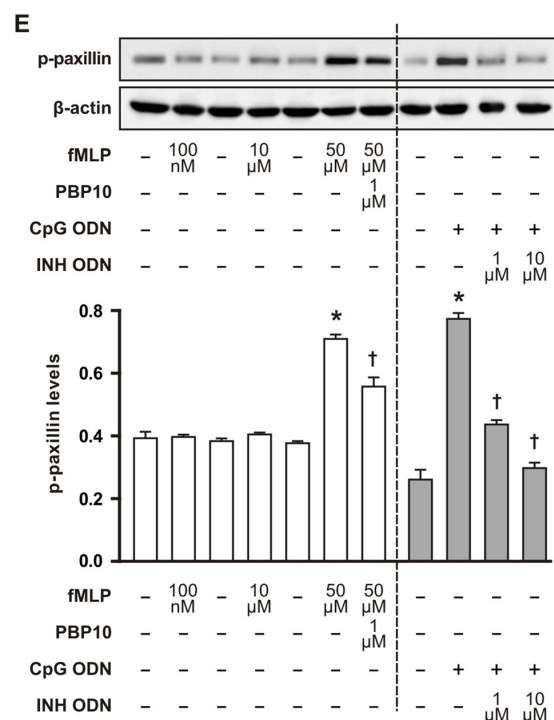
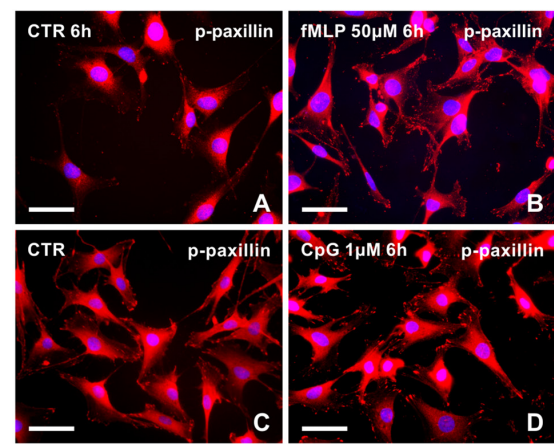


FIGURE 3 | Representative pictures of RT4-D6P2T cells cultivated in control medium displayed low immunofluorescence intensity for phosphorylated paxillin (A,C) in comparison to increased immunofluorescence intensity after treatment with 50 μ M fMLP (B) for 6 h or 1 μ M CpG ODN for 6 h (D). The cells were immunostained with mouse monoclonal antibody recognizing paxillin phosphorylated in tyrosine positions and TRITC-conjugated donkey anti-mouse secondary antibody. Cell nuclei were stained with Hoechst 33342. Scale bars = 50 μ m. (E) Upper panel shows a representative western blot of phosphorylated paxillin (p-paxillin) protein analyzed in RT4-D6P2T cells cultivated in control medium (–) and the cells after treatment with fMLP (100 nM, 10 μ M and 50 μ M) for 6 h or with 1 μ M PBP10 preincubation and treatment with 50 μ M fMLP for 6 h. Right-sided set shows a representative western blot of phosphorylated paxillin (p-paxillin) protein in RT4-D6P2T cells cultivated in control medium (–) and after 1 μ M CpG ODN (+) treatment for 6 h or pre-treatment with INH ODN (1 μ M, 10 μ M). The graph below illustrates mean values \pm SD of p-paxillin protein density relative to values of untreated cells from three independent experiments. * p < 0.05 when compared to fMLP or CpG ODN stimulation control, † p < 0.05 when compared to fMLP or CpG treatment.

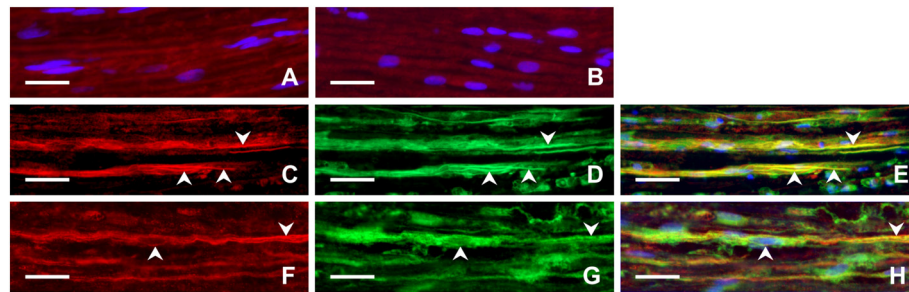


FIGURE 4 | Representative longitudinal sections of the ulnar nerve removed from sham-operated rats (**A,B**) and distal to the ulnar nerve 3 days after transection (**C–H**). The sections were immunostained with rabbit polyclonal anti-FPR2 (**A**) or anti-TLR9 (**B**) antibodies as well as double immunostained for FPR2 (**C**) or TLR9 (**F**) and then with chicken polyclonal anti-GFAP antibody (**D,G**). Immunostaining was visualized with TRITC-conjugated donkey anti-rabbit (**A,B,C,F**) and FITC-conjugated anti-chicken secondary antibodies (**D,G**). Merged pictures showed that GFAP+ activated Schwann cells and their cytoplasmic processes (arrowheads) displayed immunostaining for FPR2 (**E**) or TLR9 (**H**). Cell nuclei were stained with Hoechst 33342. Scale bars = 40 μm .

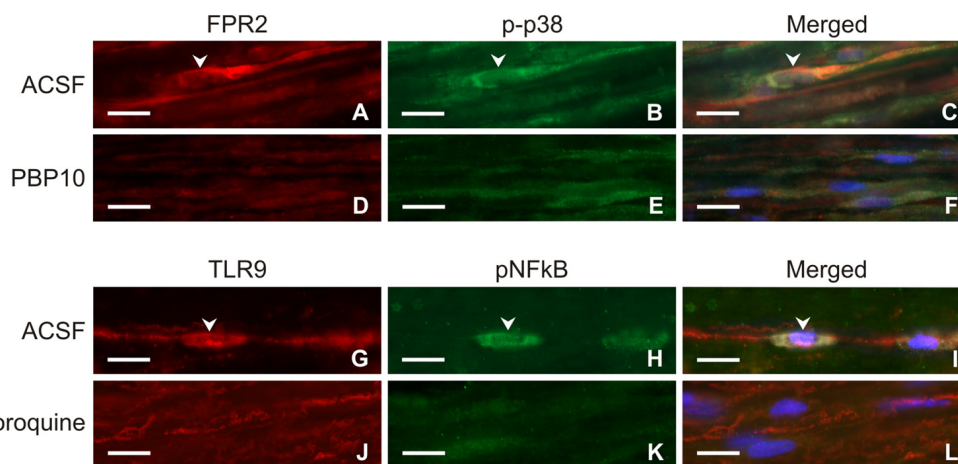


FIGURE 5 | Representative longitudinal sections of the ulnar nerve distal to nerve crush after 3 days and intrathecal injection of artificial cerebrospinal fluid (ACSF; **A–C, G–I**), 1 μM PBP10 (**D–F**) or 50 μM chloroquine (**J–L**). The sections were double immunostained for FPR2 (**A,D**) and p-p38 (**B,E**) or TLR9 (**G,J**) and pNFkB (**H,K**) under the same condition. Merged pictures revealed co-localization of p-p38 immunostaining in FPR2 immunopositive (**C**) and pNFkB immunofluorescence in TLR9 immunopositive (**I**) Schwann-like cells of rats with ACSF administration (arrowheads). Intrathecal injection of PBP10 or chloroquine significantly reduced FPR2/p-p38 (**D–F**) and TLR9/pNFkB (**J–L**) double immunostaining, respectively. Cell nuclei were stained with Hoechst 33342. Scale bars = 40 μm .

FPR2 or TLR9 immunostaining was also found in regenerated axons and mainly in their growth cones including filopodia (**Figures 6D–I**).

DISCUSSION

Schwann cells play a critical role in axon regeneration following peripheral nerve injury. Nerve injury-induced activation of Schwann cells is associated with extension of their cytoplasmic processes that promote axon growth and guidance of regenerated axons (Son and Thompson, 1995b; Gomez-Sanchez et al., 2017). Moreover, elaboration of cytoplasmic processes by Schwann cells is the main prerequisite for their migration to form a bridge spanning the gap between the distal and proximal stumps of severed nerves (Deumens et al., 2010) or other types of peripheral nerve lesions that then leads to nerve regeneration (Dubový and Svízenská, 1994; Liu et al., 2016).

Efficient axonal degeneration is essential for subsequent regeneration and functional recovery after nerve damage (Scheib and Höeke, 2013). Axonal degeneration of injured peripheral nerves involves granular degeneration of most axonal structures including mitochondria (Coleman, 2005; Park et al., 2013). Peripheral nerve axons contain a huge number of mitochondria which are a potent source of mtDAMPs as a result of their disintegration (Krysko et al., 2011). These include formylated peptides and mtDNA that can induce innate and inflammatory reactions after tissue damage (Zhang et al., 2010; Monlun et al., 2017).

fMLP and CpG were chosen as prototypic mtDAMPs for analyzing their effect on cytoplasmic process formation in RT4 schwannoma cells cultivated *in vitro*. Treatment with fMLP or CpG induced quantitative changes in cytoplasmic process extension in RT4 cells. The results indicated that formylated peptides and mtDNA released from mitochondria are involved,

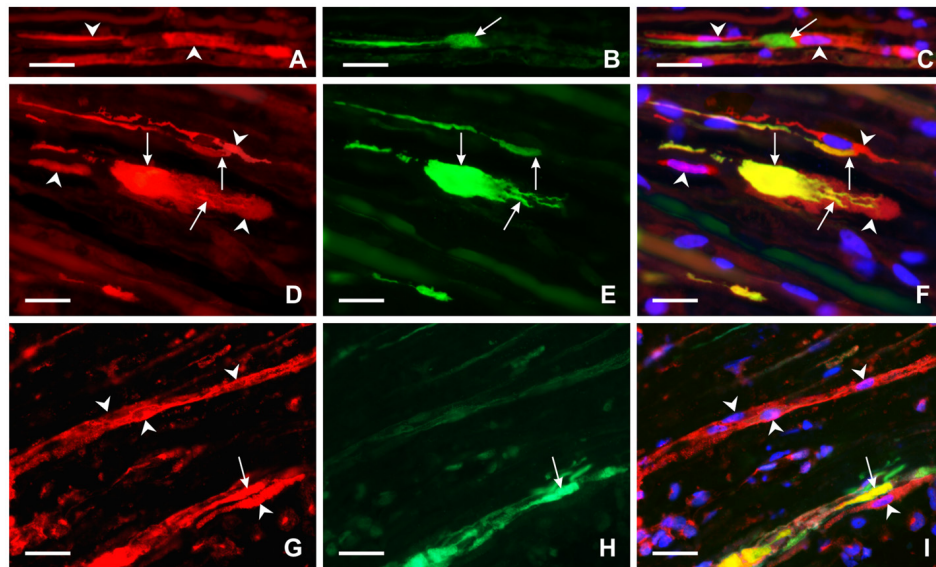


FIGURE 6 | Representative longitudinal sections of the ulnar nerve distal to nerve crush after 3 days. Longitudinal section of the distal ulnar segment was double immunostained with chicken polyclonal anti-GFAP (A) and mouse monoclonal anti-GAP43 (B) antibodies. Immunoreaction was visualized with TRITC-conjugated anti-chicken (A) and FITC-conjugated anti-mouse secondary antibodies (B). Cell nuclei were stained with Hoechst 33342. GFAP immunostained Schwann cells and their cytoplasmic processes (arrowheads) (A,C) were located close to the GAP43 immunopositive growth cone (arrow) (B,C). Other longitudinal sections were double immunostained with rabbit polyclonal anti-FPR2 (D) or anti-TLR9 (G) antibodies and mouse monoclonal anti-GAP43 antibody (E,H). Immunoreaction visualized with TRITC-conjugated donkey anti-rabbit (D,G) and FITC-conjugated donkey anti-mouse (E,H) secondary antibodies revealed that both FPR2 and TLR9 are present not only in cells close to (arrowheads) but also in growth cones and their processes (arrows) as shown in merged pictures (F,I). Cell nuclei were stained with Hoechst 33342. Scale bars = 40 μ m.

at the very least, in the initiation of cytoplasmic process extension by Schwann cells distal to nerve injury. This is in line with published evidence that mtDNA released by degenerating motor terminals can activate terminal Schwann cells and stimulate reinnervation of the neuromuscular junction through the MAPK pathway (Duregotti et al., 2015). In addition to mtDNA, terminal Schwann cells of degenerated motor terminals can be also activated by H_2O_2 triggering specific RNAs (Negro et al., 2018).

Our *in vitro* results revealed differences in the elaboration of cytoplasmic processes by various concentrations and durations of fMLP treatment. A higher concentration of fMLP (50 μ M) was required to increase the number of cytoplasmic processes with a 1 and 6 h treatment, while a lower concentration (100 nM) was enough with longer exposure (24 h). In contrast, extended (24 h) exposure to high concentrations of fMLP (10 μ M and 50 μ M) had an inhibitory effect on elaboration of RT4 cell processes. These results suggest that a higher concentration of formylated peptides is needed for early initiation of cytoplasmic processes, but low concentration is enough to stimulate the formation of Schwann cell processes during prolonged exposure. The sort of fMLP dynamics revealed *in vitro* affecting the formation of cytoplasmic processes, may be close to the *in vivo* situation during activation of Schwann cells by formylated peptides during WD.

In contrast to fMLP, 1 μ M CpG ODN induced a greater elaboration of cytoplasmic processes after 6 and 24 h treatment, while a shorter exposure for 1 h had no effect on the

outgrowth of cytoplasmic processes in RT4 cells. Surprisingly, the inhibitory effect of INH ODN pre-treatment was found only after subsequent exposure with CpG ODN for 6 h, but 1 h and 24 h CpG ODN treatment following INH ODN pre-treatment had a synergistic effect on the formation of cytoplasmic extensions of RT4 cells. This synergistic effect of INH ODN pre-treatment on cytoplasmic extensions cannot yet be fully explained and further experiments are indicated.

Paxillin is an approximately 68 kDa cytoskeletal adaptor protein required for cell adhesion and outgrowth of cytoplasmic processes related to cell migration (Vindis et al., 2004; Achuthan et al., 2006; Romanova and Mushinski, 2011; López-Colomé et al., 2017). We detected significantly increased levels of phosphorylated paxillin in RT4 cells after treatment with 50 μ M fMLP and 1 μ M CpG ODN for 6 h compared to control cells. In addition, phosphorylated paxillin protein levels were reduced by preincubation of RT4 cells with PBP10 or INH ODN in experimental sets for 6 h corresponding with inhibitory effects on cytoplasmic process development. Our immunohistochemistry and western blot results revealed that both fMLP and CpG treatments for 6 h lead to increased phosphorylated paxillin levels concomitantly with increased formation of cytoplasmic processes. This is in agreement with enhanced phosphorylation of paxillin associated with cytoplasmic processes induced by fMLP or CpG in other cell types (Leventhal et al., 1997; Weiner et al., 2001; VanCompernelle et al., 2003; Vindis et al., 2004; Achuthan et al., 2006; Miyamoto et al., 2012). Moreover, fMLP is a known chemoattractant stimulating

cell movement involving cytoplasmic processes (Xu et al., 2003).

Mitochondrial DAMPs produced by disintegrated mitochondria can be recognized by pattern-recognition receptors (PRRs) that include TLRs, FPR2, NOD-like receptors (NLRs), RIG-I-like receptors (RLRs) and purinergic receptors (Walsh et al., 2013; Wenceslau et al., 2013). Our results show that increased immunostaining for FPR2 and TLR9 was induced in RT4 cells treated with fMLP or CpG as prototypical ligands of these receptors, respectively. In addition, activated Schwann cells and their processes distal to nerve injury also displayed increased levels of both FPR2 and TLR9 indicating that these peripheral glial cells can react to mtDAMPs such as formylated peptides and mtDNA released from disintegrated axonal mitochondria during WD. Schwann cells and their processes positive for FPR2 and TLR9 immunostaining were frequently found close to growth cones of regenerated axons after nerve crush. Surprisingly, a distinct immunoreaction for these receptors was also observed in the growth cones indicating that these critical structures of regenerated axons can also react to formylated peptides and mtDNA present distal to nerve injury. The immunodetection of FPR2 and TLR9 in RT4 cells, activated Schwann cells and axonal growth cones indicates the involvement of both mtDAMP receptors in the overall mechanism of cell process formation.

It was demonstrated that FPR2 and TLR9 signaling pathway in glial cells contains activation of p38 MAPK and NFκB, respectively (Cattaneo et al., 2010; Lacagnina et al., 2018). To determine signaling events associated with FPR2 and TLR9 expression in activated Schwann cells after nerve injury, we used double immunostaining of these receptors with p-p38 MAPK and pNFκB(p65) in nerve segment distal to nerve crush after intrathecal administration of vehiculum (ACSF) in comparison to PBP10 or chloroquine as FPR2 and TLR9 inhibitors, respectively (Takeshita et al., 2004; Ho et al., 2018).

Our first observation of FPR2 localization in growth cones—thus, suggesting involvement of FPR2 signaling in axonal growth following nerve injury—is confirmed by the reduction of axon and dendrite outgrowth in developing hippocampal neurons after *in vitro* FPR2 inhibition (Ho et al., 2018). Moreover, FPR2 activation can promote axonal growth through F-actin polymerization—an important component of growth cones (Pacheco and Gallo, 2016; Wang et al., 2016). Besides formylated peptides, activation of FPR2 in growth cones may also be mediated by lipoxin A4 (LXA4) produced by myelin degradation during WD (Edström et al., 1996; De et al., 2003). For example, LXA4 binding to FPR2 can induce axonal or dendritic outgrowth as was revealed by treating primary hippocampal neurons with the FPR2 inhibitor PBP10, resulting in reduced axon and dendrite lengths (Ho et al., 2018). A role for TLR9 activation in the regenerating axon is suggested by a significant increase in both mRNA and protein levels of TLR9 in the developing mouse brain (Kaul et al., 2012). In contrast to FPR2, direct evidence for this TLR9 function is not yet available.

The *in vitro* results revealed a potentiated effect of INH ODN pre-treatment on the increased outgrowth of cytoplasmic processes of RT4 cells mainly following a 24 h CpG ODN treatment. Surprisingly, an inhibitory effect of INH ODN pre-treatment was observed on the extension of cytoplasmic processes at both concentrations used (1 μM, 10 μM), but only after CpG ODN stimulation of RT4 cells for 6 h. INH ODNs (e.g., TCCTGGCGGGGAAGT) selectively interfere with TLR9-mediated immunoactivation by competing with CpG ODN for binding to the C-terminal region of TLR9 (Avalos and Ploegh, 2011). Our results of the different efficacy of INH ODN pre-treatment on the induction of cytoplasmic processes in RT4 cells following various CpG ODN treatment times may reflect varying competition between INH ODN and CpG ODN.

CONCLUSION

We proved that fMLP and CpG ODN act as prototypic mtDAMPs and modulate the outgrowth of cytoplasmic processes of RT4 schwannoma cells in association with increased levels of phosphorylated paxillin. fMLP and CpG ODN affected formation of RT4 cell cytoplasmic processes in a dose- and time-dependent fashion. RT4 cells displayed increased immunostaining for FPR2 and TLR9 following treatments with fMLP or CpG, the ligands of these receptors, respectively. FPR2 and TLR9 immunofluorescence staining was also found in Schwann cells and their processes distal to nerve injury and close to growth cones suggesting a possible activation of the glial cells by mtDAMPs released after nerve injury. In addition to Schwann cells, both FPR2 and TLR9 were observed also in growth cones suggesting their involvement in axon regeneration. The results indicate the involvement of both FPR2 and TLR9 activation in the general mechanisms of cell process formation.

AUTHOR CONTRIBUTIONS

AK designed the experiments, ensured *in vitro* cells, conducted western blot analyses, participated in acquiring and analyzing the presented data and wrote the manuscript. IK, IH-S and MJ designed and performed the *in vivo* experiments. PD conceived, designed, coordinated the experiments and wrote the manuscript. All authors have approved the final version for publication.

FUNDING

This work was supported by grant No. 16-08508S of The Czech Science Foundation and grant No. ROZV/24/LF/2018 of the Masaryk University, Faculty of Medicine.

ACKNOWLEDGMENTS

We thank Ms. Dana Kutějová, Ms. Marta Lněničková, Ms. Jitka Mikulášková, Mgr. Jana Vachová and Mr. Lumír Trenčanský for their skillful technical assistance.

REFERENCES

- Achuthan, A., Elsegood, C., Masendycz, P., Hamilton, J. A., and Scholz, G. M. (2006). CpG DNA enhances macrophage cell spreading by promoting the Src-family kinase-mediated phosphorylation of paxillin. *Cell. Signal.* 18, 2252–2261. doi: 10.1016/j.cellsig.2006.05.007
- Avalos, A. M., and Ploegh, H. L. (2011). Competition by inhibitory oligonucleotides prevents binding of CpG to C-terminal TLR9. *Eur. J. Immunol.* 41, 2820–2827. doi: 10.1002/eji.201141563
- Boerboom, A., Dion, V., Chariot, A., and Franzen, R. (2016). Molecular mechanisms involved in Schwann cell plasticity. *Front. Mol. Neurosci.* 10:38. doi: 10.3389/fnmol.2017.00038
- Boivin, A., Pineau, I., Barrette, B., Filali, M., Vallières, N., Rivest, S., et al. (2007). Toll-like receptor signaling is critical for Wallerian degeneration and functional recovery after peripheral nerve injury. *J. Neurosci.* 27, 12565–12576. doi: 10.1523/JNEUROSCI.3027-07.2007
- Cattaneo, F., Guerra, G., and Ammendola, R. (2010). Expression and signaling of formyl-peptide receptors in the brain. *Neurochem. Res.* 35, 2018–2026. doi: 10.1007/s11064-010-0301-5
- Chen, J. J., Nag, S., Vidi, P. A., and Irudayaraj, J. (2011). Single molecule *in vivo* analysis of toll-like receptor 9 and CpG DNA interaction. *PLoS One* 6:e17991. doi: 10.1371/journal.pone.0017991
- Coleman, M. (2005). Axon degeneration mechanisms: commonality amid diversity. *Nat. Rev. Neurosci.* 6, 889–898. doi: 10.1038/nrn1788
- De, S., Trigueros, M. A., Kalyvas, A., and David, S. (2003). Phospholipase A₂ plays an important role in myelin breakdown and phagocytosis during Wallerian degeneration. *Mol. Cell. Neurosci.* 24, 753–765. doi: 10.1016/s1044-7431(03)00241-0
- Deumens, R., Bozkurt, A., Meek, M. F., Marcus, M. A. E., Joosten, E. A. J., Weis, J., et al. (2010). Repairing injured peripheral nerves: bridging the gap. *Progr. Neurobiol.* 92, 245–276. doi: 10.1016/j.pneurobio.2010.10.002
- Dubový, P. (2017). “Cytokines and their implication in axon degeneration and regeneration following peripheral nerve injury,” in *Cytokine Effector Functions in Tissues*, eds M. Foti and M. Locati (Cambridge, MA: Academic Press), 139–148.
- Dubový, P., Brázda, V., Klusáková, I., and Hradilová-Svíženská, I. (2013). Bilateral elevation of interleukin-6 protein and mRNA in both lumbar and cervical dorsal root ganglia following unilateral chronic compression injury of the sciatic nerve. *J. Neuroinflammation* 10:55. doi: 10.1186/1742-2094-10-55
- Dubový, P., Hradilová-Svíženská, I., Klusáková, I., Kokošová, V., Brázda, V., and Joukal, M. (2018). Bilateral activation of STAT3 by phosphorylation at the tyrosine-705 (Y705) and serine-727 (S727) positions and its nuclear translocation in primary sensory neurons following unilateral sciatic nerve injury. *Histochem. Cell Biol.* 150, 37–47. doi: 10.1007/s00418-018-1656-y
- Dubový, P., and Svízenská, I. (1994). Denervated skeletal-muscle stimulates migration of Schwann-cells from the distal stump of transected peripheral-nerve: an *in vivo* study. *Glia* 12, 99–107. doi: 10.1002/glia.440120203
- Duregotti, E., Negro, S., Scorsetto, M., Zornetta, I., Dickinson, B. C., Chang, C. J., et al. (2015). Mitochondrial alarmins released by degenerating motor axon terminals activate perisynaptic Schwann cells. *Proc. Nat. Acad. Sci. U S A* 112, E497–E505. doi: 10.1073/pnas.1417108112
- Edström, A., Briggman, M., and Ekström, P. A. R. (1996). Phospholipase A₂ activity is required for regeneration of sensory axons in cultured adult sciatic nerves. *J. Neurosci. Res.* 43, 183–189. doi: 10.1002/(sici)1097-4547(19960115)43:2<183::aid-jnr6>3.0.co;2-c
- Forsman, H., Andréasson, E., Karlsson, J., Boulay, F., Rabiet, M. J., and Dahlgren, C. (2012). Structural characterization and inhibitory profile of formyl peptide receptor 2 selective peptides descending from a PIP₂-binding domain of gelsolin. *J. Immunol.* 189, 629–637. doi: 10.4049/jimmunol.1101616
- Gaudet, A. D., Popovich, P. G., and Ramer, M. S. (2011). Wallerian degeneration: gaining perspective on inflammatory events after peripheral nerve injury. *J. Neuroinflammation* 8:110. doi: 10.1186/1742-2094-8-110
- Goethals, S., Ydens, E., Timmerman, V., and Janssens, S. (2010). Toll-Like Receptor expression in the peripheral nerve. *Glia* 58, 1701–1709. doi: 10.1002/glia.21041
- Gomez-Sanchez, J. A., Pilch, K. S., van der Lans, M., Fazal, S. V., Benito, C., Wagstaff, L. J., et al. (2017). After nerve injury, lineage tracing shows that myelin and remak Schwann cells elongate extensively and branch to form repair Schwann cells, which shorten radically on remyelination. *J. Neurosci.* 37, 9086–9099. doi: 10.1523/JNEUROSCI.1453-17.2017
- Ho, C. F. Y., Ismail, N. B., Koh, J. K. Z., Gunaseelan, S., Low, Y. H., Ng, Y. K., et al. (2018). Localisation of formyl-peptide receptor 2 in the rat central nervous system and its role in axonal and dendritic outgrowth. *Neurochem. Res.* 43, 1587–1598. doi: 10.1007/s11064-018-2573-0
- Hylden, J. L. K., and Wilcox, G. L. (1980). Intrathecal morphine in mice: a new technique. *Eur. J. Pharmacol.* 67, 313–316. doi: 10.1016/0014-2999(80)90515-4
- Karanth, S., Yang, G., Yeh, J., and Richardson, P. M. (2006). Nature of signals that initiate the immune response during Wallerian degeneration of peripheral nerves. *Exp. Neurol.* 202, 161–166. doi: 10.1016/j.expneurol.2006.05.024
- Kato, J., and Svensson, C. I. (2015). “Role of extracellular damage-associated molecular pattern molecules (DAMPs) as mediators of persistent pain,” in *Molecular and Cell Biology of Pain*, eds T. J. Price and G. Dussor (Elsevier: Academic Press Inc.), 251–279.
- Kaul, D., Habel, P., Derkow, K., Krüger, C., Franzoni, E., Wulczyn, F. G., et al. (2012). Expression of toll-like receptors in the developing brain. *PLoS One* 7:e37767. doi: 10.1371/journal.pone.0037767
- Krysko, D. V., Agostinis, P., Krysko, O., Garg, A. D., Bachert, C., Lambrecht, B. N., et al. (2011). Emerging role of damage-associated molecular patterns derived from mitochondria in inflammation. *Trends Immunol.* 32, 157–164. doi: 10.1016/j.it.2011.01.005
- Lacagnina, M. J., Watkins, L. R., and Grace, P. M. (2018). Toll-like receptors and their role in persistent pain. *Pharmacol. Ther.* 184, 145–158. doi: 10.1016/j.pharmthera.2017.10.006
- Le, Y. Y., Murphy, P. M., and Wang, J. M. (2002). Formyl-peptide receptors revisited. *Trends Immunol.* 23, 541–548. doi: 10.1016/s1471-4906(02)02316-5
- Lemieux, J. M., Wu, G., Morgan, J. A., and Kacena, M. A. (2011). DMSO regulates osteoclast development *in vitro*. *In Vitro Cell. Dev. Biol. Anim.* 47, 260–267. doi: 10.1007/s11626-011-9385-8
- Leventhal, P. S., Shelden, E. A., Kim, B., and Feldman, E. L. (1997). Tyrosine phosphorylation of paxillin and focal adhesion kinase during insulin-like growth factor-I-stimulated lamellipodial advance. *J. Biol. Chem.* 272, 5214–5218. doi: 10.1074/jbc.272.8.5214
- Liu, C., Kray, J., Toomajian, V., and Chan, C. (2016). Schwann cells migration on patterned polydimethylsiloxane microgrooved surface. *Tissue Eng. Part C Methods* 22, 644–651. doi: 10.1089/ten.tec.2015.0539
- López-Colomé, A. M., Lee-Rivera, I., Benavides-Hidalgo, R., and López, E. (2017). Paxillin: a crossroad in pathological cell migration. *J. Hematol. Oncol.* 10:50. doi: 10.1186/s13045-017-0418-y
- Miyamoto, Y., Torii, T., Yamamori, N., Eguchi, T., Nagao, M., Nakamura, K., et al. (2012). Paxillin is the target of c-Jun N-terminal kinase in Schwann cells and regulates migration. *Cell. Signal.* 24, 2061–2069. doi: 10.1016/j.cellsig.2012.06.013
- Monlun, M., Hyernard, C., Blanco, P., Lartigue, L., and Faustin, B. (2017). Mitochondria as molecular platforms integrating multiple innate immune signaling. *J. Mol. Biol.* 429, 1–13. doi: 10.1016/j.jmb.2016.10.028
- Negro, S., Stazi, M., Marchioretto, M., Tebaldi, T., Rodella, U., Duregotti, E., et al. (2018). Hydrogen peroxide is a neuronal alarmin that triggers specific RNAs, local translation of Annexin A2, and cytoskeletal remodeling in Schwann cells. *RNA* 24, 915–925. doi: 10.1261/rna.064816.117
- Pacheco, A., and Gallo, G. (2016). Actin filament-microtubule interactions in axon initiation and branching. *Brain Res. Bull.* 126, 300–310. doi: 10.1016/j.brainresbull.2016.07.013
- Park, J. Y., Jang, S. Y., Shin, Y. K., Koh, H., Suh, D. J., Shinji, T., et al. (2013). Mitochondrial swelling and microtubule depolymerization are associated with energy depletion in axon degeneration. *Neuroscience* 238, 258–269. doi: 10.1016/j.neuroscience.2013.02.033
- Romanova, L. Y., and Mushinski, J. F. (2011). Central role of paxillin phosphorylation in regulation of LFA-1 integrins activity and lymphocyte migration. *Cell Adhes. Migr.* 5, 457–462. doi: 10.4161/cam.5.6.18219
- Ronchi, G., Raimondo, S., Varejão, A. S. P., Tos, P., Perroteau, I., and Geuna, S. (2010). Standardized crush injury of the mouse median nerve. *J. Neurosci. Methods* 188, 71–75. doi: 10.1016/j.jneumeth.2010.01.024
- Scheib, J., and Höke, A. (2013). Advances in peripheral nerve regeneration. *Nat. Rev. Neurol.* 9, 668–676. doi: 10.1038/nrneurol.2013.227

- Son, Y. J., and Thompson, W. J. (1995a). Nerve sprouting in muscle is induced and guided by processes extended by Schwann-cells. *Neuron* 14, 133–141. doi: 10.1016/0896-6273(95)90247-3
- Son, Y. J., and Thompson, W. J. (1995b). Schwann-cell processes guide regeneration of peripheral axons. *Neuron* 14, 125–132. doi: 10.1016/0896-6273(95)90246-5
- Stoll, G., Jander, S., and Myers, R. R. (2002). Degeneration and regeneration of the peripheral nervous system: from Augustus Waller's observations to neuroinflammation. *J. Peripher. Nerv. Syst.* 7, 13–27. doi: 10.1046/j.1529-8027.2002.02002.x
- Takeshita, F., Gursel, I., Ishii, K. J., Suzuki, K., Gursel, M., and Klinman, D. M. (2004). Signal transduction pathways mediated by the interaction of CpG DNA with Toll-like receptor 9. *Sem. Immunol.* 16, 17–22. doi: 10.1016/j.smim.2003.10.009
- VanCompernelle, S. E., Clark, K. L., Rummel, K. A., and Todd, S. C. (2003). Expression and function of formyl peptide receptors on human fibroblast cells. *J. Immunol.* 171, 2050–2056. doi: 10.4049/jimmunol.171.4.2050
- Vindis, C., Teli, T., Cerretti, D. P., Turner, C. E., and Huynh-Do, U. (2004). EphB1-mediated cell migration requires the phosphorylation of paxillin at Tyr-31/Tyr-118. *J. Biol. Chem.* 279, 27965–27970. doi: 10.1074/jbc.M401295200
- Walsh, D., McCarthy, J., O'Driscoll, C., and Melgar, S. (2013). Pattern recognition receptors—molecular orchestrators of inflammation in inflammatory bowel disease. *Cytokine Growth Factor Rev.* 24, 91–104. doi: 10.1016/j.cytogfr.2012.09.003
- Wang, G., Zhang, L., Chen, X. X., Xue, X., Guo, Q. N., Liu, M. Y., et al. (2016). Formylpeptide receptors promote the migration and differentiation of rat neural stem cells. *Sci. Rep.* 6:25946. doi: 10.1038/srep25946
- Weiner, J. A., Fukushima, N., Contos, J. J., Scherer, S. S., and Chun, J. (2001). Regulation of Schwann cell morphology and adhesion by receptor-mediated lysophosphatidic acid signaling. *J. Neurosci.* 21, 7069–7078. doi: 10.1523/JNEUROSCI.21-18-07069.2001
- Wenceslau, C. F., McCarthy, C. G., Gouloupoulou, S., Szasz, T., NeSmith, E. G., and Webb, R. C. (2013). Mitochondrial-derived N-formyl peptides: novel links between trauma, vascular collapse and sepsis. *Med. Hypoth.* 81, 532–535. doi: 10.1016/j.mehy.2013.06.026
- Xu, J., Wang, F., Van Keymeulen, A., Herzmark, P., Straight, A., Kelly, K., et al. (2003). Divergent signals and cytoskeletal assemblies regulate self-organizing polarity in neutrophils. *Cell* 114, 201–214. doi: 10.1016/S0092-8674(03)00555-5
- Zamboni, L., and Demartin, C. (1967). Buffered picric acid-formaldehyde: a new rapid fixative for electron microscopy. *J. Cell Biol.* 35:A148.
- Zhang, Q., Raoof, M., Chen, Y., Sumi, Y., Sursal, T., Junger, W., et al. (2010). Circulating mitochondrial DAMPs cause inflammatory responses to injury. *Nature* 464, 104–115. doi: 10.1038/nature08780

Conflict of Interest Statement: The authors declare that the research was conducted in the absence of any commercial or financial relationships that could be construed as a potential conflict of interest.

Copyright © 2018 Korimová, Klusáková, Hradilová-Svřinská, Kohoutková, Joukal and Dubový. This is an open-access article distributed under the terms of the Creative Commons Attribution License (CC BY). The use, distribution or reproduction in other forums is permitted, provided the original author(s) and the copyright owner(s) are credited and that the original publication in this journal is cited, in accordance with accepted academic practice. No use, distribution or reproduction is permitted which does not comply with these terms.



In vivo Evaluation of Nanostructured Fibrin-Agarose Hydrogels With Mesenchymal Stem Cells for Peripheral Nerve Repair

Jesús Chato-Astrain^{1,2}, Fernando Campos^{1,3*}, Olga Roda^{3,4}, Esther Miralles⁵, Daniel Durand-Herrera¹, José Antonio Sáez-Moreno⁵, Salomé García-García⁵, Miguel Alaminos^{1,3}, Antonio Campos^{1,3} and Víctor Carriel^{1,3*}

¹ Department of Histology, Tissue Engineering Group, Faculty of Medicine, University of Granada, Granada, Spain, ² Doctoral Program in Biomedicine, Faculty of Medicine, University of Granada, Granada, Spain, ³ Instituto de Investigación Biosanitaria Ibs. GRANADA, Granada, Spain, ⁴ Department of Anatomy and Embryology, Faculty of Medicine, University of Granada, Granada, Spain, ⁵ Division of Clinical Neurophysiology, University Hospital San Cecilio, Granada, Spain

OPEN ACCESS

Edited by:

Stefania Raimondo,
Università di Torino, Italy

Reviewed by:

Chiara Tonda-Turo,
Politecnico di Torino, Italy
Ana Colette Mauricio,
Universidade do Porto, Portugal

*Correspondence:

Fernando Campos
fcampos@ugr.es
Víctor Carriel
vcarriel@ugr.es

Received: 28 September 2018

Accepted: 04 December 2018

Published: 18 December 2018

Citation:

Chato-Astrain J, Campos F, Roda O, Miralles E, Durand-Herrera D, Sáez-Moreno JA, García-García S, Alaminos M, Campos A and Carriel V (2018) *In vivo* Evaluation of Nanostructured Fibrin-Agarose Hydrogels With Mesenchymal Stem Cells for Peripheral Nerve Repair. *Front. Cell. Neurosci.* 12:501. doi: 10.3389/fncel.2018.00501

The regenerative capability of peripheral nerves is very limited, and several strategies have been proposed to increase nerve regeneration. In the present work, we have analyzed the *in vivo* usefulness of a novel nanostructured fibrin-agarose bio-artificial nerve substitute (Nano) used alone or in combination with NeuraGen® collagen type I conduits (Coll-Nano) in laboratory rats with a 10-mm sciatic nerve defect. Control animals were subjected to the gold-standard autograft technique (Auto). Results first demonstrated that the percentage of self-amputations was lower in Nano and Coll-Nano groups as compared to the Auto group. Neurotrophic ulcers were more abundant in the Auto group (60%, with 66.6% of them being >2-mm) than Nano and Coll-Nano groups (0%) at 4 weeks, although Nano showed more ulcers after 12 weeks. Foot length was significantly altered in Auto animals due to neurogenic retraction, but not in Nano and Coll-Nano groups after 12 weeks. At the functional level, all animals showed a partial sensory recovery as determined by the pinch test, especially in Nano and Auto groups, but did not reach the levels of native animals. Toe-spread test revealed a partial motor function recovery only in Nano animals at 4 weeks and Auto and Nano at 12 weeks. Electromyography showed clear denervation signs in all experimental groups, with few differences between Auto and Nano animals. After 12 weeks, an important denervation decrease and an increase of the reinnervation process was found in Auto and Nano groups, with no differences between these groups. Histological analyses demonstrated an active peripheral nerve regeneration process with newly formed peripheral nerve fascicles showing S-100, GAP-43 and myelin in all experimental groups. The peripheral nerve regeneration process was more abundant in Auto group, followed by Nano group, and both were better than Coll-Nano group. Muscle histology confirmed the electromyography results and showed some atrophy and fibrosis signs and an important weight and volume loss in all groups, especially in the Coll-Nano group (56.8% weight and 60.4% volume loss). All these results suggest that the novel Nano substitutes used in *in vivo* were able to contribute to bridge a 10-mm peripheral nerve defect in rats.

Keywords: peripheral nerve repair, neural tissue engineering, fibrin-agarose hydrogels, *in vivo*, histology, mesenchymal stem cells

INTRODUCTION

Peripheral nerves (PNs) are delicate organs which form a highly complex network throughout the body connecting the central nervous system with distal target organs (Topp and Boyd, 2006; Carriel et al., 2014a). Histologically, PNs are composed by the nerve tissue or parenchyma and three specialized connective tissue layers or stroma (Geuna et al., 2009; Carriel et al., 2014a). The parenchyma is organized in conductive units called peripheral nerve fibers (PNFs) internally formed by neuronal axons surrounded by Schwann cells (SCs) and a thin external basal lamina. PNFs can be myelinated (in which SCs form a lipid-rich multilayered myelin sheath) or unmyelinated (Carriel et al., 2017a). About the stroma, PNs are externally covered by a collagen-rich and vascularized connective tissue layer, the epineurium. Internally, the parenchyma is organized forming fascicles which are surrounded by the perineurium. Finally, at the intrafascicular level, each PNF is surrounded by a loose connective tissue, the endoneurium (Topp and Boyd, 2006; Geuna et al., 2009; Carriel et al., 2014a, 2017a).

The structure and function of PNs can be affected by several pathological conditions, neoplasm and traumatic injuries (Dahlin, 2008; Moore et al., 2009; Carriel et al., 2014a). Following structural damage, PNs have a limited capability to regenerate their components to reestablish the motor, sensory and vegetative functions. Neoplasm removal and traumatic injuries could severely affect the PNs structure and function with a negative impact in the quality of life of patients worldwide. Incomplete or complete transections of PNs, without loss of substance, are directly repaired by neuroorrhaphy in order to re-establish the nerve trunk and fascicles continuity with acceptable functional recovery (Dahlin, 2008; Carriel et al., 2014a). To repair nerve injuries with loss of substance, the use of nerve grafts (autograft or allograft) is needed (Campbell, 2008; Dahlin, 2008; Kehoe et al., 2012; Carriel et al., 2014a,b). Currently, the nerve autograft is the gold standard treatment to repair critical nerve gaps (>3-cm of length). This method provides an adequate ECM, functional SCs and growth factors which promote an efficient PN regeneration in approximately 50% of these cases (Pabari et al., 2010; Daly W. et al., 2012; Carriel et al., 2014a). However, the nerve autograft and especially the nerve allograft, have several well-known disadvantages (e.g., donor site morbidity, lack of graft material, possibility of painful neuroma, scarring, sensory loss, etc.) and their use should be limited to repair nerve gaps of approximately 5-cm length (Kehoe et al., 2012; Carriel et al., 2014a).

In this context, the tubulization technique emerged as a potential alternative for PN repair. The first generations of hollow nerve conduits, composed by natural or synthetic biomaterials, showed promising experimental results (Daly W. et al., 2012; Kehoe et al., 2012; Carriel et al., 2014a). However, once they started to be used to treat critical nerve gaps in human, failure results started to be published (Moore et al., 2009; Liadaki et al., 2013; Carriel et al., 2014a). Tubulization failure can be related to several factors, but in critical nerve defects, a reduction of growth factors diffusion occurs with the consequent failure of the regeneration process (Webber and Zochodne, 2010; Carriel et al.,

2014a). Currently, tubulization is considered a safe treatment in the repair of non-critical (<3-cm) sensory nerve gaps (Moore et al., 2009; Wangenstein and Kallianen, 2010; Boeckstyns et al., 2013; Carriel et al., 2014a). Due to the limitations and unsatisfactory results obtained with the nerve grafts and conduits, current research is focused on the generation of novel tissue engineering (TE) strategies for PN repair.

Tissue engineering combines cells with biomaterials and specific growth factors to elaborate tissue-like substitutes for the replacement or repair of damaged tissues or organs (Sanchez-Quevedo et al., 2007; Carriel et al., 2014a). In the case of the peripheral nerve TE (PNTE), the aim is to develop biological substitutes to promote and/or accelerate the intrinsic regeneration capability of damaged PNs (Geuna et al., 2010; Daly W. et al., 2012; Carriel et al., 2014a). Over the recent years, a wide range of promising TE strategies have been described (see reviews, Daly W. et al., 2012; Carriel et al., 2014a; Wieringa et al., 2018). From a physical and structural point of view, important advances were obtained by the incorporation of aligned biomaterials or nanofibers to the regenerative microenvironment (Gu et al., 2014; Pedrosa et al., 2017). From the biological perspective, authors demonstrated a significant increase of PNs regeneration through the use of functionalized and biologically active biomaterials, the incorporation of growth factors and gene-based therapies and, especially, by the incorporation of biomaterials containing different cells sources (Zheng and Cui, 2010; Ladak et al., 2011; Lopatina et al., 2011; McGrath et al., 2012; Carriel et al., 2013, 2017c; Georgiou et al., 2015). These advances suggest that the closer we get to the biomimetic regenerative microenvironment and structure, the better results we obtain (Carriel et al., 2014a; Wieringa et al., 2018).

In the field of TE, our research group developed a natural and biodegradable hybrid hydrogel composed by human fibrin and agarose type VII (Alaminos et al., 2006). This fibrin-agarose hydrogel (FAH) was successfully used to develop bioengineered cornea (Alaminos et al., 2006), oral mucosa (Sanchez-Quevedo et al., 2007), skin (Carriel et al., 2012), cartilage (Garcia-Martinez et al., 2017), PNs substitutes (Carriel et al., 2013, 2017c) and other tissue-like structures (Campos et al., 2016, 2017). Regarding the use of FAH in PNTE, these biomaterials were used alone and in combination with adipose-derived mesenchymal stem cells (ADMSCs) as intraluminal fillers of biodegradable NeuraGen® conduits to repair 10-mm nerve gap in rats (Carriel et al., 2013, 2017c). These studies demonstrated that the incorporation of acellular FAH hydrogels and, especially, FAH containing ADMSCs, provided a suitable regenerative microenvironment which resulted in a significant improvement of the clinical, functional, electromyographic and histological profiles (Carriel et al., 2013, 2017c). These studies suggest that NeuraGen® conduits and cellular FAH contributed synergistically to the PN regeneration process and reinnervation of distal target organs. Despite these positive results, FAH does not have the adequate biomechanical properties to be directly used in PN reconstruction. In this context, it was recently demonstrated that the biomechanical and structural properties of FAH can be significantly improved in a controlled manner with the nanostructuration technique (Campos et al., 2016, 2017).

This methodology promotes nanoscale molecular interactions among the biomaterial fibers, and it was recently applied to generate novel nanostructured fibrin-agarose bio-artificial nerve substitutes (NFABNS) (Carriel et al., 2017d). This fabrication process allowed to successfully recreate the size and shape of PNs with promising structural and biomechanical properties (Carriel et al., 2017d). In addition, *ex vivo* characterization demonstrated that NFABNS were cytocompatible, supporting human ADMSCs viability, proliferation and function over the time (Carriel et al., 2017d). However, the potential clinical usefulness of NFABNS has not been studied yet.

Due to the promising structural and biological properties offered by novel NFABNS for PN reconstruction, and in view of the putative synergetic effects of FAH and NeuraGen® collagen conduits, we have carried out an *in vivo* study to determine the usefulness of these devices in PN repair. For these reasons, the aim of this study was to evaluate the possibility to bridge 10-mm nerve gaps in rats by using NFABNS and NFABNS as intraluminal fillers of NeuraGen® conduits. Furthermore, the PN regeneration profile was determined through the use of clinical, functional, electromyography, histological, and ultrastructural studies.

MATERIALS AND METHODS

Laboratory Animals

In this study, 20 male 13-week-old Wistar rats weighing 250–300 g (at the beginning) were obtained from JANVIER LABS® and kept under veterinary and technical supervision in the animal facility of the University Hospital *Virgen de las Nieves, Granada, Spain*. Animals were housed in a light and temperature-controlled room (~21°C and 12 h light/dark) with *ad libitum* access to standard rat chow and tap water. In this study, 15 animals were subjected to surgical procedures using general anesthesia by intraperitoneal injection of a mixture of acepromazine -Calmo-Neosan® 0.001 mg per g of weight of the animal-, ketamine -Imalgene 1000® 0.15 mg per g of weight- and atropine –0.05 µg of per g of weight-. At the beginning of the study, we harvested a small biopsy (~1-cm³) from the inguinal pad fat for isolation of autologous ADMSCs. Once enough amounts of ADMSCs were obtained, PNs substitutes were generated. In addition, five healthy animals were used as control native (CTR-Native). At the end of this study, all animals were euthanatized by overdose of anesthesia. All procedures were performed according to the European Union and Spanish Government guidelines for the ethical care of animals (EU Directive No. 63/2010, RD 53/2013) and the research projects were approved by the ethical and experimentation committee of Granada (FIS PI14/01343 and FIS PI17/0393).

Adipose-Derived Mesenchymal Stem Cells Isolation and Culture

The autologous ADMSCs were isolated and cultured following previously described protocols (Carriel et al., 2013, 2017d). Concisely, adipose tissue biopsies were mechanically fragmented into small pieces and digested with 0.3% type I collagenase solution (Gibco BRL Life Technologies) for 8 h at 37°C. Once

the ECM was digested, the cells were isolated by centrifugation and then cultured in basal medium [Dulbecco's modified Eagle's medium (DMEM)] supplemented with 10% fetal bovine serum (FBS; Sigma-Aldrich) and antibiotic-antimycotics cocktail solution (100 U/ml penicillin G, 100 µg/ml streptomycin, and 0.25 µg/ml amphotericin B, Sigma-Aldrich, Steinheim, Germany). Cells were kept under standard culture conditions (37°C and 5% CO₂), the culture media was renewed every 3 days and cells expanded until passage 4.

The stemness profile of the rat ADMSCs used was determined by flow cytometry and immunofluorescence as previously reported (Sun et al., 2011; Lotfy et al., 2014). Flow cytometry was performed using a NovoCyte® 1000 Flow Cytometer (ACEA, Biosciences Inc., United States) and cells demonstrated to be positive for CD 90 (99.43%) and CD 29 (99.67%) and negative for CD 45 (0.07%) markers. Immunofluorescence representative images and the technical information of the antibodies used can be found in **Figure 1** and **Table 1**, respectively.

Fabrication of NFABNS

First, FAHs containing ADMSCs were elaborated following previously described protocols (Carriel et al., 2013, 2017d). Briefly, to prepare 10 ml of FAH a mixture composed by 7.6 ml human plasma, 0.15 ml tranexamic acid (Amchafibrin, Fides-Ecofarma, Valencia, Spain) and 1.25 ml of basal medium containing ADMSCs (5×10^4 cells/ml) was prepared. This solution was mixed and 1 ml of 2% CaCl₂ and 0.5 ml of melted 2% type VII agarose were added, carefully mixed, placed in 60-mm petri dishes and kept under standard culture condition until complete gelation (~1 h). This procedure resulted in the generation of 10 ml of uniform FAH containing ADMSCs with specific dimensions (5-mm of thickness and 6-mm of diameter). After gelation, 5 ml of basal medium was added to each construct and they were kept in culture for 24 h and then used for the fabrication of NFABNS.

To generate the NFABNS, we followed a well-described protocol, which allowed us to produce customized substitutes with specific biomechanical properties and dimensions ensuring the cellular viability and functionality (Carriel et al., 2017d). Briefly, to fabricate these NFABNS, FAHs were carefully harvested from the petri dishes and then nanostructured. Hydrogels were cut symmetrically (3-cm × 3-cm × 3-cm) and then placed between a couple of nylon filters membranes (0.22 µm) and Whatman 3-mm absorbent papers below a flat glass surface. Immediately, a uniform and homogeneously distributed mechanical pressure (500 g) was applied for 2.5 min obtaining a highly dense nanostructured FAH (NFAH) of 50–60 µm thickness (Scionti et al., 2014; Carriel et al., 2017d) (**Figure 1**). At this point, it was possible to fabricate NFABNS with specific dimensions (length and/or diameter) or number of fascicles (uni-fascicular or multi-fascicular) (*see examples of each in Figure 1*). Here, unifascicular NFABNS composed by multilayered NFAH of 1-cm long and ~1.5-mm or 1-mm diameter were generated based on the dimensions of the adult rat sciatic nerve, and according to the length of the nerve gap created (10-mm).

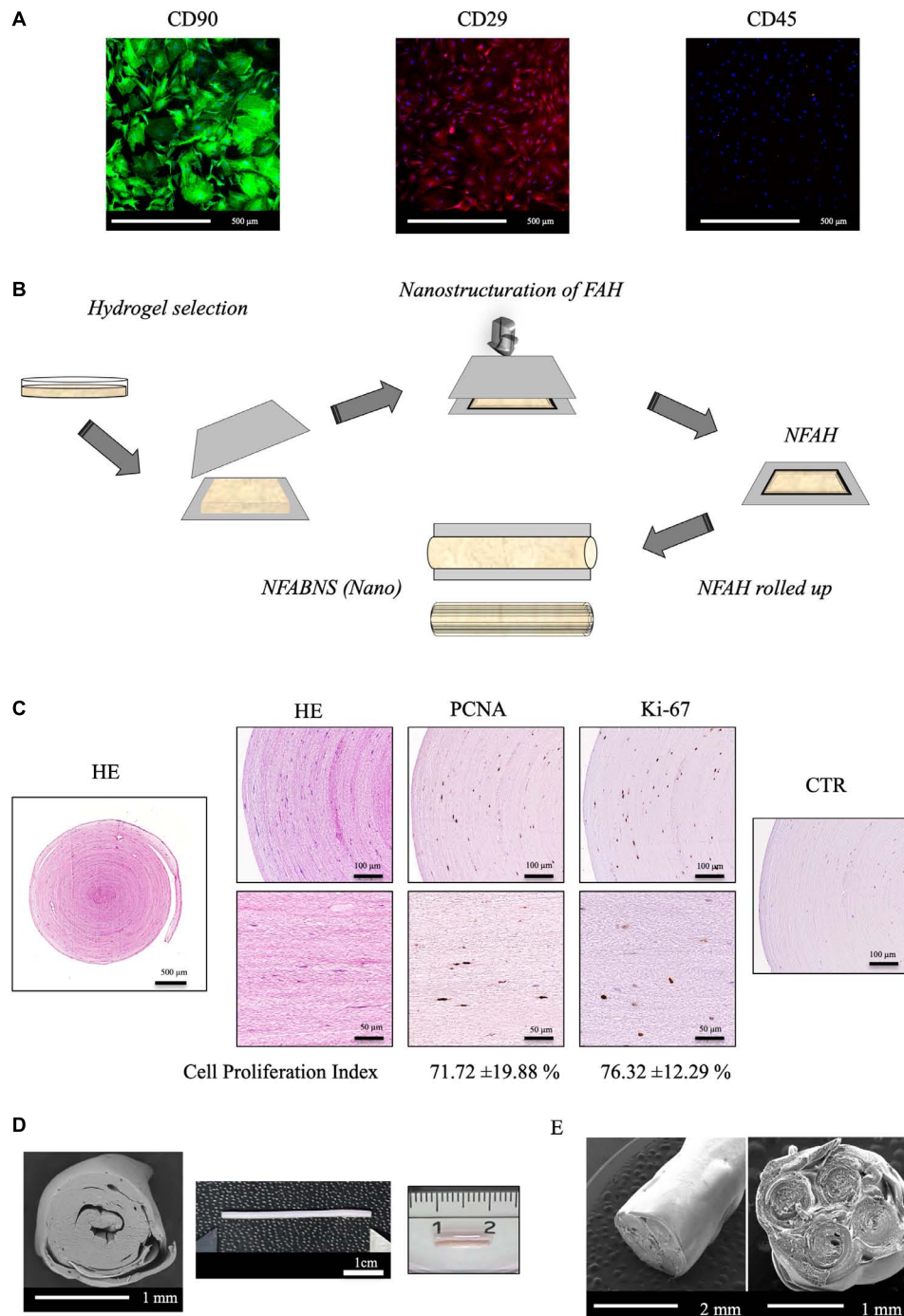


FIGURE 1 | ADMSCs characterization and NFABNS generation. **(A)** Shows representative images of the immunostaining pattern of stemness markers of the rat ADMSCs. **(B)** Shows how from a square uncompressed FAH it is possible to fabricate a cylindrical multilayered NFABNS of desire dimensions. **(C)** Exhibit the histological pattern of NFABNS, ADMSCs distribution with HE and the presence and percentages of proliferating cells (cell proliferation index) detected by immunohistochemistry for PCNA and Ki-67 markers, respectively. **(D)** Shows the macroscopic and scanning electron microscopy aspect of the NFABNS used to repair the nerve defect in this study. In **(E)** scanning electron microscopy images show examples of multifasciculated NFABNS that can be generated with this methodology if needed.

This methodology allowed us to generate NFABNS with 0.30 ± 0.04 MPa of Young's Modulus, 0.42 ± 0.03 MPa of stress at fracture and $169.6 \pm 9.85\%$ strain at fracture

(deformation) mean values, as previously characterized (Carriel et al., 2017d). Furthermore, to ensure the viability of the ADMSCs contained in the NFABNS, cell proliferation was

TABLE 1 | Antibodies used for flow cytometry and immunostaining.

Antibody	Dilution	Pretreatment	Application	Cat. No.
FITC/Mouse monoclonal anti-CD90 (Clone OX-7)	1:300 1:200	–	FC IF	BioLegend, San Diego, CA, United States cat. no. 202503
PerCP/Cy5.5/Hamster anti-CD-29	1:75 1:50	–	FC IF	BioLegend, San Diego, CA, United States cat. no. 102227
PE/Mouse monoclonal anti-CD-45	1:100	–	FC/IF	BioLegend, San Diego, CA, United States cat. no. 202207
Mouse monoclonal anti-PCNA (clone PC10)	1:1000	Citrate buffer, pH 6, 95°C for 25 min	IHC	Sigma-Aldrich, Steinheim, Germany cat. no. P8825
Rabbit monoclonal anti-Ki67	–	EDTA buffer pH 9, 95°C for 25 min	IHC	Master Diagnostica, Granada, Spain cat. no. MAD-000310QD
Rabbit polyclonal anti-S100	1:400	Citrate buffer, pH 6, 95°C for 25 min	IHC	Dako Cytomation, Glostrup, Denmark cat. no. Z0311
Rabbit polyclonal anti-GAP-43 (ab-41)	1:50	EDTA buffer, pH 9, 95°C for 25 min	IHC	Sigma-Aldrich, Steinheim, Germany cat. no. Sab4300525
Horse anti-mouse/rabbit IgG (peroxidase)	–	–	IHC	Vector Laboratories, CA, United States cat. no. MP-7500

FC, flow cytometry; IF, immunofluorescence; IHC, immunohistochemistry.

determined by immunohistochemistry for PCNA and Ki-67 after 48 h of culture (**Figure 1**) as described previously (Carriel et al., 2017d). In this sense, the cell proliferation index of the ADMSCs was 71.72% for PCNA and 76.32% for Ki-67. The technical information of the antibodies used is summarized in the **Table 1**.

Surgical Procedures and Experimental Study Groups

Initially, 15 animals were subjected to general anesthesia (as described above) and then a segment of 10-mm was removed from the left sciatic nerve. The right hind leg was used as non-operated control in all cases (CTR). Animals were then randomly assigned to the following experimental groups ($n = 5$ in each):

- Autograft control group (Auto), where the removed fragment of the nerve was rotated 180° and used to bridge the nerve gap.
- Nano group (Nano), in which the nerve gap was microsurgically bridged by using 10-mm NFABNS of ~1.5-mm diameter.
- Collagen Nano group (Coll-Nano), where the nerve defects were repaired with NeuraGen® collagen type I conduits (Integra® Life Sciences Corp., Plainsboro, NJ, United States) filled with an NFABNS of 10-mm of ~1-mm diameter.
- Control native (CTR-Native), where healthy animals were used for comparisons.

For all surgical procedures 7/0 Prolene (polypropylene, blue monofilament) suture material was used. After the nerve microsurgical repair and wound closure, all animals were housed as mentioned above and each one received analgesic treatment (metamizole) in the drinking water for 48 h. In this study, animals were subjected to a two-time clinical assessment and electromyography (EMG) at 4 and 12 weeks after surgery, respectively. The analyses at 4 weeks were performed to confirm

the clinical and functional impact of nerve injury, whereas the aim of the 12 weeks evaluation was to accurately determine differences among groups during an active regeneration and partial functional recovery, as recommended in the literature (Geuna, 2015). Following the second EMG, animals were housed for other 14 days and then euthanized. This period was used to favor muscle healing (hemorrhage and inflammation due to the EMG) for further morphometric and histological analyses. Therefore, all histological analyses were performed at 14 weeks after surgery.

The NeuraGen® conduits were chosen due to their well-known positive impact on PNs regeneration when combined with FAH and ADMSCs (Carriel et al., 2013, 2017c). Furthermore, these conduits are FDA approved and they are currently one of the most frequently used nerve guides in the clinical practice (Wangenstein and Kalliainen, 2010; Krarup et al., 2017).

Clinical Assessment

In order to determine the sensory and motor function profile after PN repair, animals were subjected to a series of well-known tests at 4 and 12 weeks after surgery (Vleggeert-Lankamp, 2007; Siemionow et al., 2011; Carriel et al., 2013). In this regard, the following analyses were performed: evaluation of toes self-amputations in the operated leg; the percentage and size of plantar neurotrophic ulcers (≤ 2 -mm/ > 2 -mm); the foot length (in mm), as indicator of the neurogenic retraction of the muscles innervated by the sciatic nerve; the pinch test of sensory recovery; and the toe-spread test.

For the pinch test, a mild pinching stimulus was applied to the skin of the operated leg from the toe to the knee joint, until a withdrawal reaction was observed. This reaction was graded on a four-point scale as follows: 0 = no withdrawal response, 1 = response to stimulus above the ankle, 2 = response to distal stimulation to the ankle in the heel/plantar region and

3 = response to stimulation in the metatarsal region as previously described (Siemionow et al., 2011; Carriel et al., 2013).

The toe-spread test consisted in the evaluation of the extension and abduction reaction of the toes during tail-suspension. These results were graded on a four-point scale as follows: 0 = no toe movement, 1 = some sign of toe movement, 2 = toe abduction, and 3 = toe abduction with extension (Vleggeert-Lankamp, 2007; Siemionow et al., 2011; Carriel et al., 2013).

For foot length, the rat's hind feet were dipped in a blue ink, and the animals were permitted to walk down the walking pathway on a Plexiglas® device (1-m length, 10-cm width and 15-cm height) covered with white paper, leaving its hind footprints on the paper. The foot length was measured as the distance from the heel to the third toe.

Electromyography

All animals were subjected to EMG tests 4 and 12 weeks after the surgical procedure as previously described (Carriel et al., 2013). Briefly, animals were mildly anesthetized (1/10 of the doses used for general anesthesia) with ketamine and acepromazine to study the muscle function at rest. Furthermore, the spontaneous electrical activity of the gastrocnemius (lateral and medial) and tibialis anterior muscles was determined. These muscles were analyzed using concentric-needles and a Topas 4-channel electromyograph (Schwarzer GmbH R, Munich, Germany) with band-pass filter settings of 5–5,000 Hz. Each muscle was subjected to three measurements in three different areas. Denervation and reinnervation results were scored using a four-point scale as follows: 0 = absent (no signs in any of the three muscle areas); 1 = mild (signs in one of the three areas); 2 = moderate (signs in two areas), or 3 = severe (signs in all three areas). These analyses were carried out and interpreted by three independent experts (EM, SGG, JAS) blinded to the experimental groups. The percentage of animals with specific denervation or reinnervation degrees was calculated for each study group. The right leg of each operated animal (CTR) and both legs of independent unoperated animals (CTR-Native) were also analyzed as controls.

Muscle Morphometric Evaluation

In order to assess the degree of atrophy of the muscles innervated by the operated left sciatic nerve, the weight (w) and volume (v) of the whole lower leg was measured at 14 weeks after surgery. Lower legs were harvested after the intracardiac perfusion (see details below). The lower legs [which contain several muscles exclusively innervated by the sciatic nerve trunk (Greene, 1968)] were exposed and then disjointed from the knee and ankle. For the w assessment, the dissected legs were removed from the fixative, dried in absorbent paper and weighed in a digital weighing machine (Sartorius BP 121S, precision: 0.1 mg, Sigma-Aldrich). For the v assessment, dissected legs were immersed in test tube (50 ml) containing 30 ml of PBS and the increase of this volume represented the lower legs volume. In this study, the percentage of w and v loss was calculated between the operated and the contralateral-side leg from each animal, including healthy

animals (CTR-Native), and these values were used for statistical comparisons.

Macroscopy, Histological, and Ultrastructural Analyses

First, animals under general anesthesia received an intraperitoneal heparin injection and then were euthanized by anesthesia overdose. After that, animals were perfused with 500 ml of saline solution followed by 500 ml of 4% neutral buffered paraformaldehyde. Perfused animals were used to evaluate the macroscopic aspect of the repaired nerves and then nerves, implants and muscle were harvested for histology.

Macroscopic analysis was aimed to evaluate nerve continuity, uniformity, adhesions, or inflammatory reactions. For the histological analyses, healthy PNs and implants were carefully harvested, sectioned transversally and the central portion was obtained for light and transmission electron microscopy (TEM) analyses. For light microscopy, samples were immersed in fixative for another 24 h. In the case of muscles, following the morphometric evaluation (described above), the tibialis anterior and gastrocnemius muscles were dissected from both legs. Muscles were immersed in fixative for 24 h, sectioned transversely and then fixed for another 24 h (a total of 48 h of chemical fixation). All fixed tissues were placed in histological cassettes embedded in paraffin and sectioned at 5 μ m of thickness (Carriel et al., 2017a,b).

In this study, all sections were stained with Hematoxylin and eosin (HE) for general histology. In addition, the MCOLL histochemical method was used to evaluate the general histology during the remyelination and collagen fibers reorganization processes in PNs and implants as described previously (Carriel V. et al., 2011; Carriel et al., 2013, 2014b, 2017a). The presence of SCs and newly formed axonal sprouts were evaluated by indirect immunohistochemistry for S-100 protein and GAP-43, respectively, as previously described (Carriel et al., 2013, 2014b, 2017c).

In order to determine the degree of muscle atrophy and fibrotic stromal reaction due to PN repair, the transversal sections of the tibialis anterior and gastrocnemius muscles were stained with picrosirius (PS) and Masson trichrome (MST) methods (Carriel V.S. et al., 2011; Philips et al., 2018b). Furthermore, histological sections from healthy muscles were used as native control.

For TEM analysis small tissue samples were obtained immediately after intracardiac perfusion and postfixed with 2.5% neutral buffered glutaraldehyde followed by 2% osmium tetroxide (Carriel et al., 2017d). Fixed samples were dehydrated, embedded in epoxy resin. Ultrathin sections were stained with uracil acetate and lead citrate, transferred to mesh grids and analyzed in a JEOL JEM 1200 EX II or a Carl Zeiss SMT LIBRA® 120 PLUS transmission electron microscopes.

Statistical Analyses

All quantitative data obtained from clinical assessments and muscle morphometry were analyzed using the Shapiro–Wilk test of normality. All non-normally distributed variables

(toe spread, pinch test, volume loss, weight loss, electromyogram results) were compared with the Mann–Whitney non-parametric test. In the case of ulcers and amputations, variables which were expressed in percentage, the Fisher exact test was used for statistical comparisons. In all cases, $p < 0.05$ values were considered statistically significant in two-tailed tests. All data and statistical comparisons were calculated with the SPSS 16.0 software.

RESULTS

Implantation and Macroscopic Postsurgical Aspect

In this study, one of the aims was to determine if, from the structural and surgical perspective, the NFABNS (Nano) and the NFABNS used as intraluminal fillers of collagen conduits (Coll-Nano) were suitable alternatives to bridge a 10-mm sciatic nerve gap in rats. The methodology used allowed to generate NFABNS with comparable size (length and diameter), shape and consistency than the target nerves. From the surgical point of view, NFABNS were easy to handle during implantation process and allowed us to repair the nerve gaps in a comparable time and technique than nerve autograft (Figure 2). Regarding the Coll-Nano group, the NFABNS were easily incorporated as intraluminal fillers of collagen conduits during surgery, and the defects were repaired by using the conventional tubulization technique without any technical inconvenience. After 14 weeks of *in vivo* implantation the Auto group showed a complete

repair of the defects without any sign of structural damage, although a loose connective tissue was observed covering the repaired area (Figure 2). In the case of the Nano group, the macroscopic analysis revealed that NFABNS allowed to bridge the nerve defects successfully without signs of adhesions or local adenopathies (Figure 2). Similarly, the postsurgical analysis confirmed that collagen conduits with NFABNS were able to successfully bridge the gap and the collagen conduits remained in the surface without any adherence, compression or conduit deformation (Figure 2).

Clinical Results

In this study, clinical and functional parameters were evaluated at 4 and 12 weeks after PN repair, and results are shown in Table 2. The percentages of self-amputations at 4 weeks were higher in Auto group (80%) as compared to Nano and Coll-Nano groups (20% each). However, differences were not statistically significant between experimental groups, except for the comparison between Auto vs. CTR-native group ($p < 0.05$, Table 2). Interestingly, the percentage of self-amputations increased in the Nano and Coll-Nano groups (reaching to 60% and 40%, respectively), and differences were only significant for comparisons between CTR-Native group vs. Auto and Nano groups ($p < 0.05$, Table 2).

Assessment of plantar neurotrophic ulcers after 4 weeks revealed that only animals from Auto groups developed these injuries (60% of animals), being these values significantly higher ($p < 0.05$) than Nano and Coll-Nano groups, where these injuries did not occur. In addition, the 66.6% of these ulcers

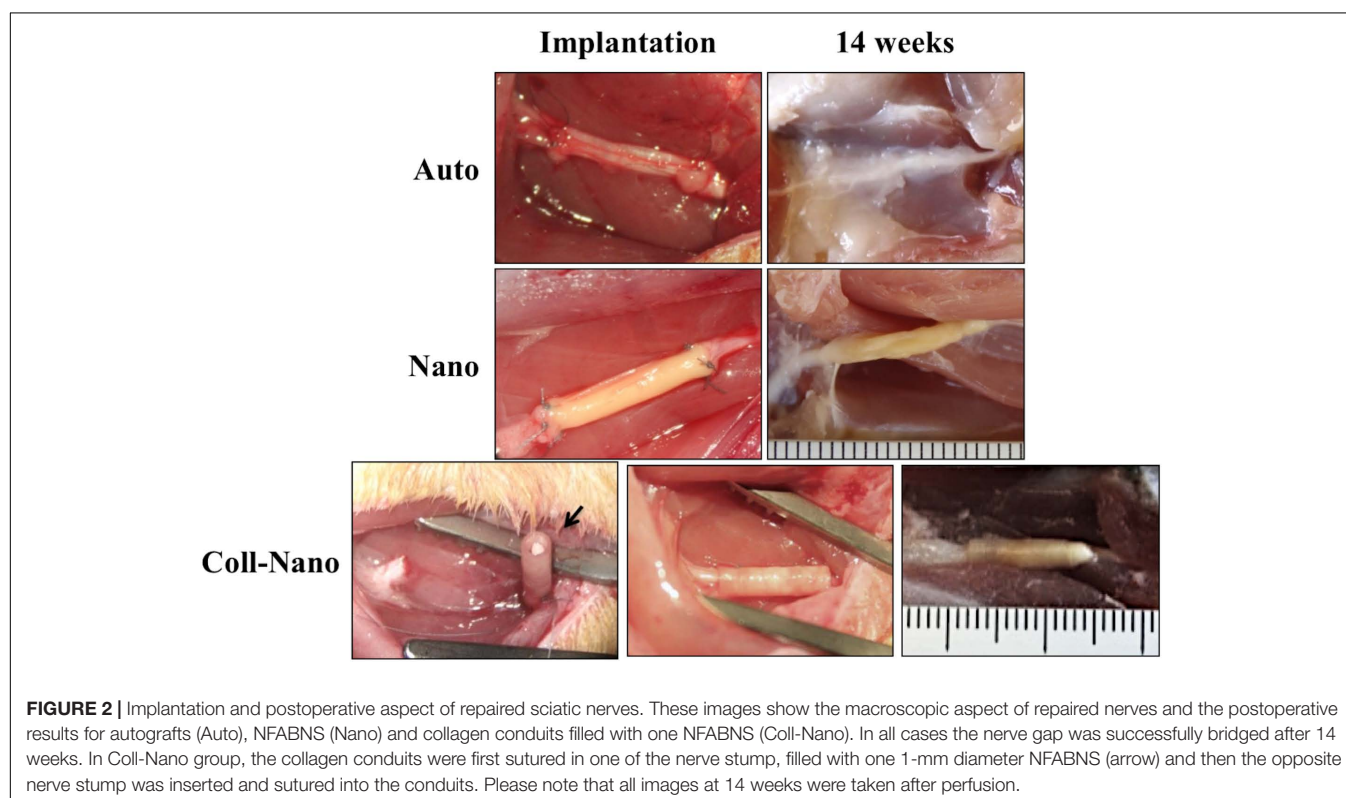


TABLE 2 | Quantitative clinical and functional recovery results.

Groups <i>n</i> = 5 each	% Self-amputations	% Neurotrophic ulcers	% Neurotrophic ulcers (> 2 mm)	Foot length (mm)	Pinch test	Toe spread test
4 weeks postsurgical analyses						
CTR-native	0.00	0.00	0.00	–	3.00 ± 0.00	3.00 ± 0.00
Auto	80.00 ^a	60.00 ^{a,b,d,e}	66.67 ^{a,b,d,e}	–	1.60 ± 0.55 ^{a,e}	0.00 ± 0.00 ^a
Nano	20.00 ^e	0.00 ^{b,e}	0.00 ^b	–	2.00 ± 0.71 ^{a,c,e}	0.40 ± 0.55 ^a
Coll-Nano	20.00 ^e	0.00 ^d	0.00 ^d	–	0.80 ± 0.84 ^{a,c}	0.00 ± 0.00 ^a
12 weeks postsurgical analyses						
CTR-native	0.00	0.00	0.00	39.17 ± 2.04	3.00 ± 0.00	3.00 ± 0.00
Auto	80.00 ^a	20.00 ^e	100.00 ^{a,b,d,e}	34.01 ± 2.47 ^{a,d}	1.00 ± 0.71 ^{a,e}	0.20 ± 0.45 ^a
Nano	60.00 ^{a,e}	40.00 ^e	50.00 ^{b,e}	37.39 ± 2.57	1.6 ± 0.55 ^{a,e}	1.00 ± 0.71 ^{a,c}
Coll-Nano	40.00 ^e	0.00	0.00 ^d	40.04 ± 1.67 ^d	1.40 ± 0.55 ^a	0.00 ± 0.00 ^{a,c}

The table shows all quantitative results conducted at 4 and 12 weeks followed peripheral nerve repair. Self-amputations and neurotrophic ulcers results are expressed in percentage, while the foot length, pinch and toe spread tests results are shown as mean ± standard deviation values. In this study, $p < 0.05$ values were considered statistically significant in two tailed tests. Significant differences are indicated as follows: ^aSignificant differences with CTR group. ^bSignificant differences between Auto vs. Nano group. ^cSignificant differences between Nano vs. Coll-Nano group. ^dSignificant differences between Auto vs Coll-Nano group. ^eSignificant differences between 4 weeks vs 12 weeks for each condition.

(Auto group) were higher than 2-mm (Table 2). The analysis after 12 weeks showed a decrease of the presence of ulcers in the Auto group (from 60 to 20%) and an increase in the Nano group (from 0 to 40%), while in Coll-Nano group values were not altered (0%). However, differences among groups were not statistically significant (Table 2). Curiously, 100% of ulcers of Auto group and the 50% of Nano group were higher than 2-mm, being the differences between Auto vs. Nano and Coll-Nano groups statistically significant ($p < 0.05$, Table 2).

Evaluation of neurogenic retraction of the muscles innervated by the sciatic nerve was evaluated through the measurement of foot length at 12 weeks. This analysis revealed lower foot length values, meaning neurogenic retraction, in Auto group (34.01-mm), followed by the Nano Group (37.39-mm) and then the Coll-Nano group (40-mm). Differences were only significant for comparisons between CTR-Native group vs. Auto group and for Auto vs. Coll-Nano group ($p < 0.05$, Table 2).

The pinch test of sensory recovery after 4 weeks showed higher values, better sensory recovery, in Nano group (2/3), than the Auto (1.6/3) and Coll-Nano (0.8/3) groups. Although signs of sensory recovery were observed, especially in Nano group, these values were significantly lower ($p < 0.05$) than the sensory reaction observed in healthy animals (CTR-Native group) (3/3). In addition, when we compared these values between experimental groups differences between Auto vs. Nano group were not significant ($p > 0.05$), but differences were statistically significant when we compared Nano vs. Coll-Nano groups values ($p < 0.05$, Table 2). The pinch test of sensory recovery after 12 weeks showed a slight decreased of these values in the Auto (from 1.6/3 to 1/3) and Nano (from 2/3 to 1.6/3) groups and a slight increase in Coll-Nano group (from 0.8/3 to 1.4). Differences among these groups were not statistically significant ($p > 0.05$, Table 2), and all operated animals showed significantly lower values than the CTR-native group ($p < 0.05$, Table 2).

Finally, assessment of the motor function of digital muscle with the toe spread test revealed that all operated animals were far to be comparable to the motor response of healthy animals at 4 and 12 weeks, and differences were statistically significant ($p < 0.05$, Table 2). Interestingly, after 4 weeks slight signs of motor function were only observed in Nano group (0.4/3), but these values were not significantly higher ($p > 0.05$) than the values observed in Auto and Coll-Nano groups (Table 2). When motor function was evaluated after 12 weeks these values were increased in the Nano group (from 0.4/3 to 1/3) and slight increase in the Auto group (from 0/3 to 0.2/3), but no signs of motor function recovery were observed in Coll-Nano group (0/3), which was significantly lower than Nano group ($p < 0.05$, Table 2).

Electromyography Results

First, the analysis of the right leg of each operated animal (CTR) and both legs of independent animals not subjected to surgery (CTR-Native group) revealed a normal recruitment pattern with normal motor unit potentials and no spontaneous activity at rest. In contrast, the EMG analysis of the experimental groups showed a wide variation of denervation and reinnervation signs (Table 3).

At a follow-up period of 4 weeks, most experimental groups showed clear signs of denervation (Table 3). The percentage of muscle denervation (gastrocnemius and tibialis anterior) was more severe in the Coll-Nano group (100% of tibialis anterior and gastrocnemius medial muscles were severely denervated) followed by Nano and Auto group, respectively (Table 3). Differences were statistically significant for the comparison of Coll-Nano group vs. Auto group for all analyzed muscles ($p < 0.05$) and for the gastrocnemius muscle for the comparison of Nano vs. Auto groups ($p < 0.05$). Curiously, some signs of reinnervation in the gastrocnemius and tibialis anterior muscles were observed in Auto group at this stage (Table 3).

TABLE 3 | Electromyography profile of muscles innervated by repaired sciatic nerves.

Groups <i>n</i> = 5 each	Muscles	% Denervation				% Reinnervation			
		0	1	2	3	0	1	2	3
Electromyography after 4 weeks of peripheral nerve repair									
Auto	Gastrocnemius lateral	40	40	20	0	0	67	33	0
	Gastrocnemius medial ^c	0	80	20	0	0	100	0	0
	Tibialis anterior ^c	0	20	80	0	0	100	0	0
Nano	Gastrocnemius lateral ^{a,f}	0	20	40	40	100	0	0	0
	Gastrocnemius medial ^{d,f}	20	0	40	40	100	0	0	0
	Tibialis anterior ^{d,f}	0	20	0	80	100	0	0	0
Coll-Nano	Gastrocnemius lateral ^a	0	0	20	80	100	0	0	0
	Gastrocnemius medial ^{a,c,d}	0	0	0	100	100	0	0	0
	Tibialis anterior ^{a,c,d}	0	0	0	100	100	0	0	0
Electromyography after 12 weeks of peripheral nerve repair									
Auto	Gastrocnemius lateral	100	0	0	0	0	60	40	0
	Gastrocnemius medial ^c	0	100	0	0	20	40	40	0
	Tibialis anterior ^c	100	0	0	0	20	60	20	0
Nano	Gastrocnemius lateral ^{a,b,f}	0	60	40	0	0	60	40	0
	Gastrocnemius medial ^{b,f}	20	40	40	0	0	80	20	0
	Tibialis anterior ^{a,f}	0	20	80	0	0	80	20	0
Coll-Nano	Gastrocnemius lateral ^{a,b,d}	0	0	60	40	60	40	0	0
	Gastrocnemius medial ^{a,b,c}	0	20	20	60	80	20	0	0
	Tibialis anterior ^{a,c}	0	20	60	20	60	40	0	0

Results are shown as the percentage of animals of each experimental group with specific denervation or reinnervation signs in the gastrocnemius (lateral and medial) and tibialis anterior muscles at 4 and 12 weeks after surgery. Each muscle was subjected to three measurements in three different areas, and the results were scored as follows: 0 = absent (no signs in any of the three muscle areas); 1 = mild (signs in one of the three areas); 2 = moderate (signs in two areas), or 3 = severe (signs in all three areas). In this study, $p < 0.05$ values were considered statistically significant in two-tailed tests. Significant differences are indicated as follows: ^aSignificant differences in denervation results with Auto group for each time. ^bSignificant differences in denervation between Nano group vs. Coll-Nano group for each time. ^cSignificant differences in denervation between 4 weeks vs. 12 weeks for each group. ^dSignificant differences in reinnervation results with Auto group for each time. ^eSignificant differences in reinnervation between Nano group vs. Coll-Nano group for each time. ^fSignificant differences in reinnervation between 4 weeks vs. 12 weeks for each group.

Analysis of animals after 12 weeks after the surgical procedure revealed significant changes in the percentage of denervation and, specially, in the reinnervation profile of all experimental groups (Table 3). In the Auto group, a significant decrease of the muscle denervation percentage was observed for all muscles, and none of the animals showed denervation signs for the gastrocnemius medial and tibialis anterior muscles at this time. These values were accompanied by a slight, but not statistically significant ($p > 0.05$, Table 3), increase of the reinnervation profile in this Auto group. The EMG profile of the Nano group revealed a slight non-significant decrease of the denervation profile, with none of the muscles being severely denervated after 12 weeks. In this group of animals, we found a significant improvement ($p < 0.05$) of the reinnervation profile of all muscles at 12 weeks of follow-up, and the reinnervation profile of the gastrocnemius lateral muscle was comparable to the Auto group at this time (Table 3). Although differences were non-significant ($p > 0.05$), the reinnervation profiles of gastrocnemius medial and tibialis anterior were slightly superior in Nano group as compared to the Auto group (Table 3). Finally, the analysis of the Coll-Nano animals at 12 weeks demonstrated a slight non-significant improvement ($p > 0.05$) of the denervation profile found after 4 weeks. However, none of the muscles showed reinnervation signs and did not differ from results found at the previous stage (Table 3).

Peripheral Nerve Regeneration Histology and Ultrastructure

The histological analysis carried out with HE staining at 14 weeks of the middle portion of repaired nerves confirmed an active regeneration process in all experimental groups. In the case of nerve gaps repaired with autograft technique (Auto group), the regeneration process was observed mainly at the intrafascicular level, but also in the epineurial connective tissue of the graft. In this group, the process was characterized by the presence of relatively small newly formed nerve fascicles containing PNFs. Furthermore, no sign of inflammatory reaction was found in any animals (Figures 3A,B). Interestingly, it was often observed a variable number of regenerating fascicles between the surrounding rhabdomyocytes confirming some degree of dispersion of the PN regeneration process (Figure 3B, inset). The HE analysis of the implanted NFABNS (Nano group) confirmed that these novel substitutes supported an active and abundant PNs regeneration process (Figures 3A,B). Regeneration took place through the connective tissue covering the implanted substitutes with a similar histological pattern than the observed in the auto group, meaning the presence of newly formed nerve fascicles and PNFs. In addition, like in Auto group, some degree of PN regeneration was also observed associated to the surrounding muscle tissues (Figure 3B, inset). Concerning the implanted

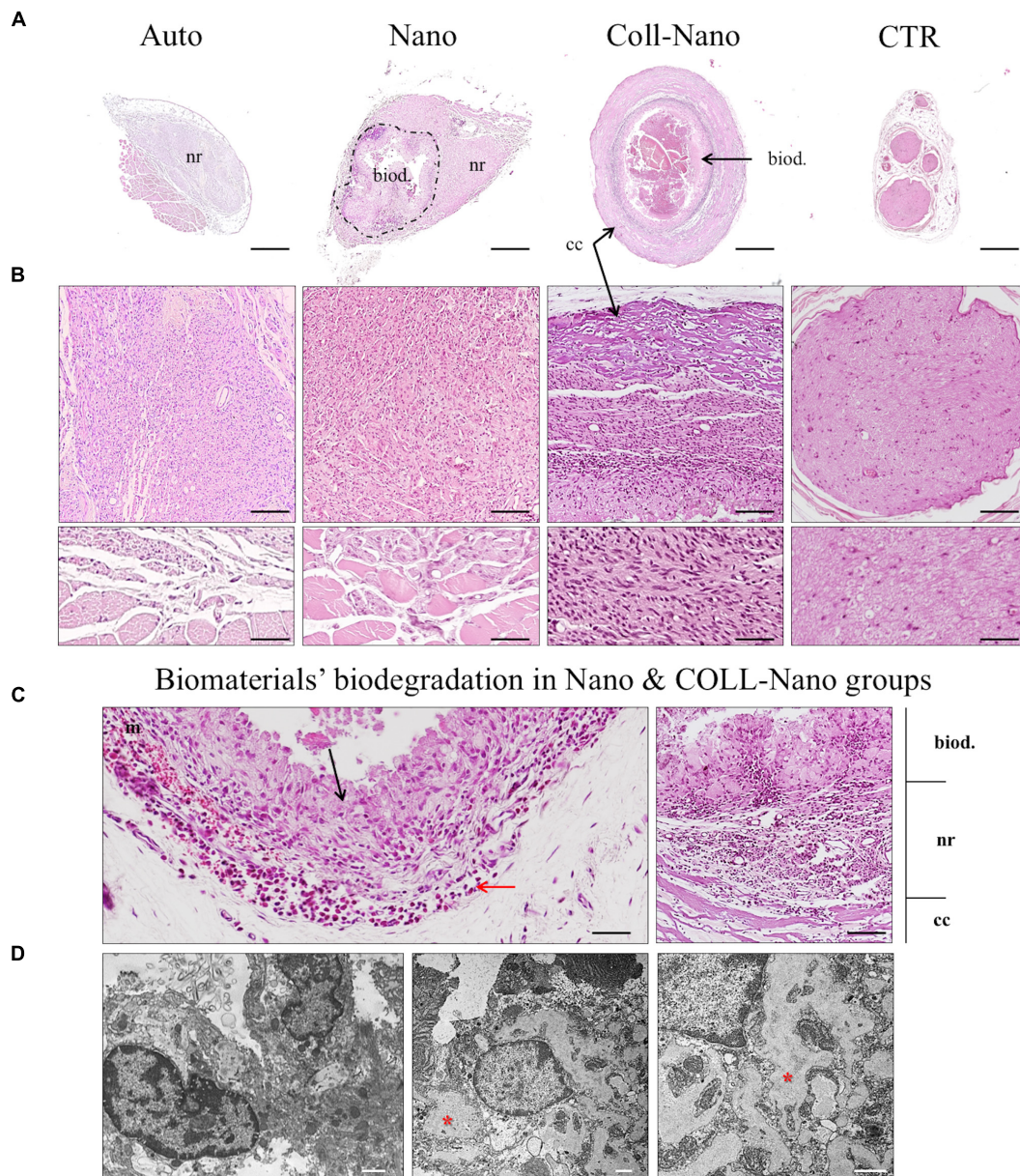


FIGURE 3 | Microscopic results of peripheral nerve regeneration and biomaterials biodegradation. Figures show HE cross-section staining at low (**A**) and middle magnifications (**B,C**) from the central portion of repaired nerves by autografts (Auto), NFABNS (Nano) and collagen conduits filled with NFABNS (Coll-Nano). In addition, a representative transversal histological section of a healthy nerve (CTR) was included. In (**A**) a general overview of the regeneration process is provided, where nerve regeneration is indicated as (nr) in all groups. In Nano and Coll-Nano groups the active biodegradation of FAH is indicated with (biod.) whereas the collagen conduit in Coll-Nano with (cc). Images in (**B**) show with moderate magnification the histological pattern of peripheral nerve regeneration in each group and also the native control. In Auto and Nano groups some disperse regenerating nerve fascicles were found associated to the surrounding skeletal muscle (insets). Figures in (**C**) show representative images of the biodegradation of the FAH [in Nano (left) and Coll-Nano (right) groups] and collagen conduit (Coll-Nano group) by host macrophages (black arrows). In association to the macrophages, it was also observed a variable amount of mononuclear cells (red arrows). In right image corresponding to Coll-Nano group the three well differentiated zones are indicated, the biodegradation of FAH (biod.), peripheral nerve regeneration zone (nr) and the biodegradation of the collagen conduit (cc). TEM images in (**D**) confirmed the presence of active macrophages in Nano (left) and Coll-Nano (middle and right) groups, where large phagosomes are indicated by red asterisks. Scale bar = 500 μ m in (**A**), 100 μ m and 50 μ m (insets) in (**B**), 50 μ m (left) and 100 μ m (right) in (**C**) and 1 μ m in (**D**).

substitutes, they were mostly biodegraded after 14 weeks. The biodegradation process was restricted to the biomaterial surface and composed by a well delimited inflammatory reaction

composed by well-organized mononuclear macrophages and some perivascular white blood cells (**Figures 3A,C**). In the case of PN defects repaired by collagen conduits filled with

NFABNS (Coll-Nano group), histology revealed a less abundant regenerating nerve tissue than in Auto and Nano groups. In this group, the regeneration was restricted to the ECM area between the collagen conduit wall and the internal biodegradation process of the NFABNS. The regenerating tissue was composed by poorly organized newly formed fascicles. Concerning the biomaterials, the collagen conduits were well-preserved with an associated biodegradation process by giant multinuclear cells and some mononuclear infiltration. The intraluminal NFABNS showed the same biodegradation process than the one observed in Nano groups, although the structure was more preserved (**Figures 3A,C**). Finally, TEM analysis confirmed that the NFABNS in Nano and Coll-Nano groups was actively degraded by mononuclear macrophages (**Figure 3D**).

The analyses of myelin and collagen fibers content carried out with MCOLL histochemical method demonstrated that the PN regeneration process was accompanied by certain degree of myelination and collagen extracellular matrix reorganization (**Figure 4A**). The analysis of Auto group revealed a high amount of myelinated newly formed PNFs immersed in a loose collagen extracellular matrix (**Figure 4A**). Similarly, in Nano

group abundant myelinated newly formed PNFs were observed in the regenerating tissue, but the ECM collagen resulted to be more abundant, especially around the newly formed nerve fascicles (**Figure 4A**). In the case of Coll-Nano group, evident histochemical reaction for myelin was not observed, although an important amount of collagen was detected accompanying the PN regeneration process (**Figure 4A**). Finally, TEM analysis confirmed the presence of newly formed PNFs with a well-formed myelin sheath as well as unmyelinated ones in both Auto and Nano groups. Interestingly, TEM analysis confirmed the presence of unmyelinated and myelinated PNFs in the Coll-Nano group, but the myelin sheath was considerably thinner and less organized than the myelin sheath observed in the other experimental groups (**Figure 4B**). Despite the high degree of myelination observed in Auto and Nano groups, light and electron microscopy findings were not comparable to the PNFs thickness and regularity observed in the control (**Figures 4A,B**).

In order to confirm the PN regeneration process, the SCs and newly formed axons were immunohistochemically identified by using antibodies against S-100 and GAP-43 proteins, respectively (**Figure 5**). The immunohistochemical analysis of Auto group

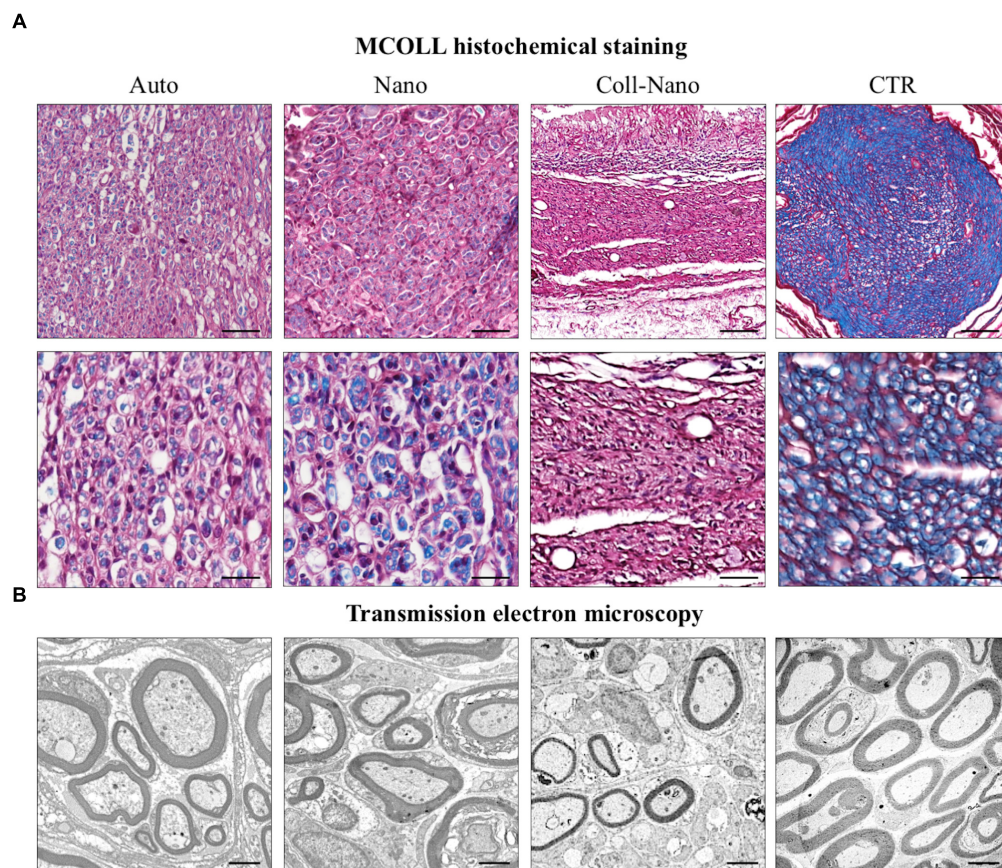


FIGURE 4 | Histochemical and ultrastructural analysis of peripheral nerve regeneration and myelination. Figures in **(A)** shows the peripheral nerve regeneration pattern, degree of myelination (blue histochemical reaction) and collagen reorganization (red) with MCOLL histochemical staining at moderate and higher magnification in each experimental condition (Auto, Nano, and Coll-Nano) and native control (CTR). TEM images in **(B)** confirm the presence of myelinated peripheral nerve fibers in all experimental groups and CTR. Scale bar = 100 μ m (upper images) and 50 μ m (lower images) in **(A)** and 2 μ m in **(B)**.

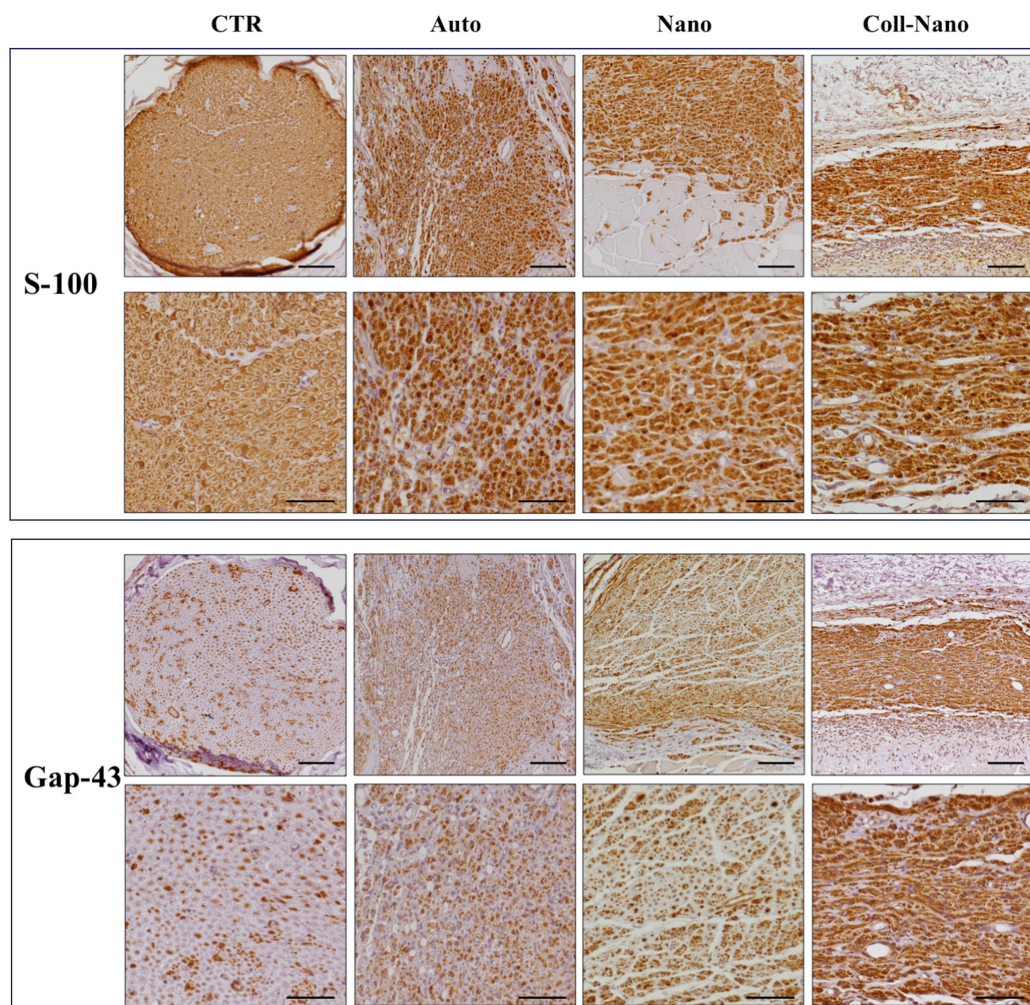


FIGURE 5 | Immunohistochemical evaluation of Schwann cells and regenerating axons. The immunohistochemical staining (brown reaction) of S-100 was used to reveal the presence and distribution of Schwann cells whereas Gap-43 was used as a marker of newly formed regenerating axons. Both immunostaining were performed in each experimental group (Auto, Nano, and Coll-Nano) and native control (CTR). Scale bar = 100 μ m in lower magnifications and 50 μ m higher magnification images.

revealed an abundant and consistent immunoreaction for S-100 and GAP-43 at the intrafascicular and interfascicular levels, confirming the presence of an active PN regeneration process as previously observed by the histological, histochemical and ultrastructural analyses (**Figure 5**). In the Nano group, an abundant immunoreaction for S-100 and GAP-43 was found associated with the regenerating tissue with a similar pattern than the one observed in the Auto group (**Figure 5**). The immunohistochemical study of Coll-Nano group confirmed the presence of an active PN regeneration process, but it was not comparable to the pattern and amount observed in Nano and Auto groups (**Figure 5**).

Results of Muscle Morphometry and Histology

Muscle atrophy is a well-known consequence that takes place after PN damage, and this process is an acceptable and

informative indicator of the degree of muscle reinnervation following PN repair and regeneration (Vleggeert-Lankamp, 2007; Siemionow et al., 2011). The quantitative analysis of lower leg muscles innervated by the repaired sciatic nerves after 14 weeks revealed an important w and v loss as compared to right control legs in each group (**Figure 6**). In general, healthy legs weight ranged between 7.8 and 7.1 g (mean 7.5 ± 0.2 g) and the volume from 8 to 6.6 ml (mean 7.1 ± 0.5 ml), while operated legs ranged from 3.3 to 4.7 g (mean 3.8 ± 0.6 g) and 2.7 to 4.6 ml (mean 3.5 ± 0.8 ml) (**Figure 6**). When comparing the percentage of weight and volume loss a slight difference in the CTR-Native group was found (0.94% and 3.1%, respectively). Concerning the operated animals, the lower percentage loss was found in Auto group, where animals lost 32.67% of the weight and 29.6% of the volume (**Figure 6**). When animals were repaired with bio-artificial nerve substitutes the percentages of weight and volume loss were significantly higher in Nano (54.4% of weight and 54.5% of volume) and especially in Coll-Nano

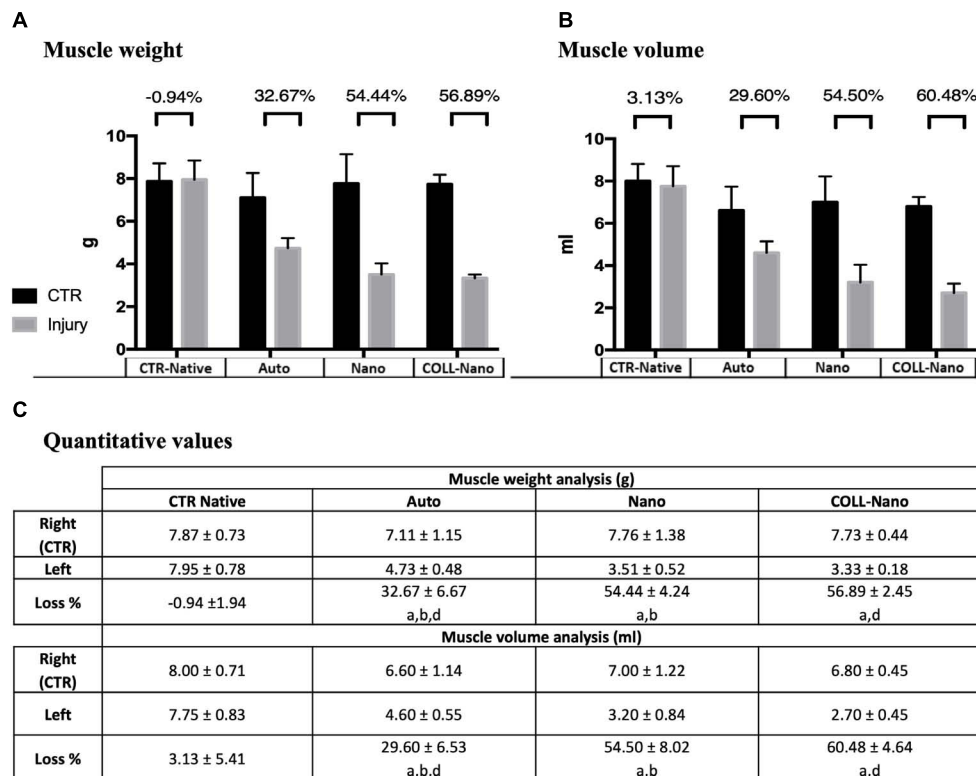


FIGURE 6 | Quantitative results of muscle's weight and volume loss. Graphics (A,B) show the muscle weight and volume quantitative results of the injured (gray) and right leg control (black) of the operated animals of each experimental condition (Auto, Nano, and Coll-Nano) and native control (CTR). Table in (C) shows the weight and volume mean \pm standard deviation values in grams (g) and milliliters (ml), respectively. Furthermore, the muscle atrophy is indicated by the % of loss between the CTR and injured leg of each animal. In this study, significant differences are indicated as follows: ^aSignificant differences with CTR group. ^bSignificant differences between Auto vs. Nano group. ^cSignificant differences between Nano vs. Coll-Nano group. ^dSignificant differences between Auto vs. Coll-Nano group. $p < 0.05$ values were considered statistically significant in two-tailed tests.

(56.8% of weight and 60.4% of volume) groups as compared to animals from CTR-Native and Auto group (Figure 6). Although the percentage of loss was higher in animals from Coll-Nano group than Nano group, these differences were not statistically significant ($p = 0.251$ for weight and $p = 0.281$ for volume).

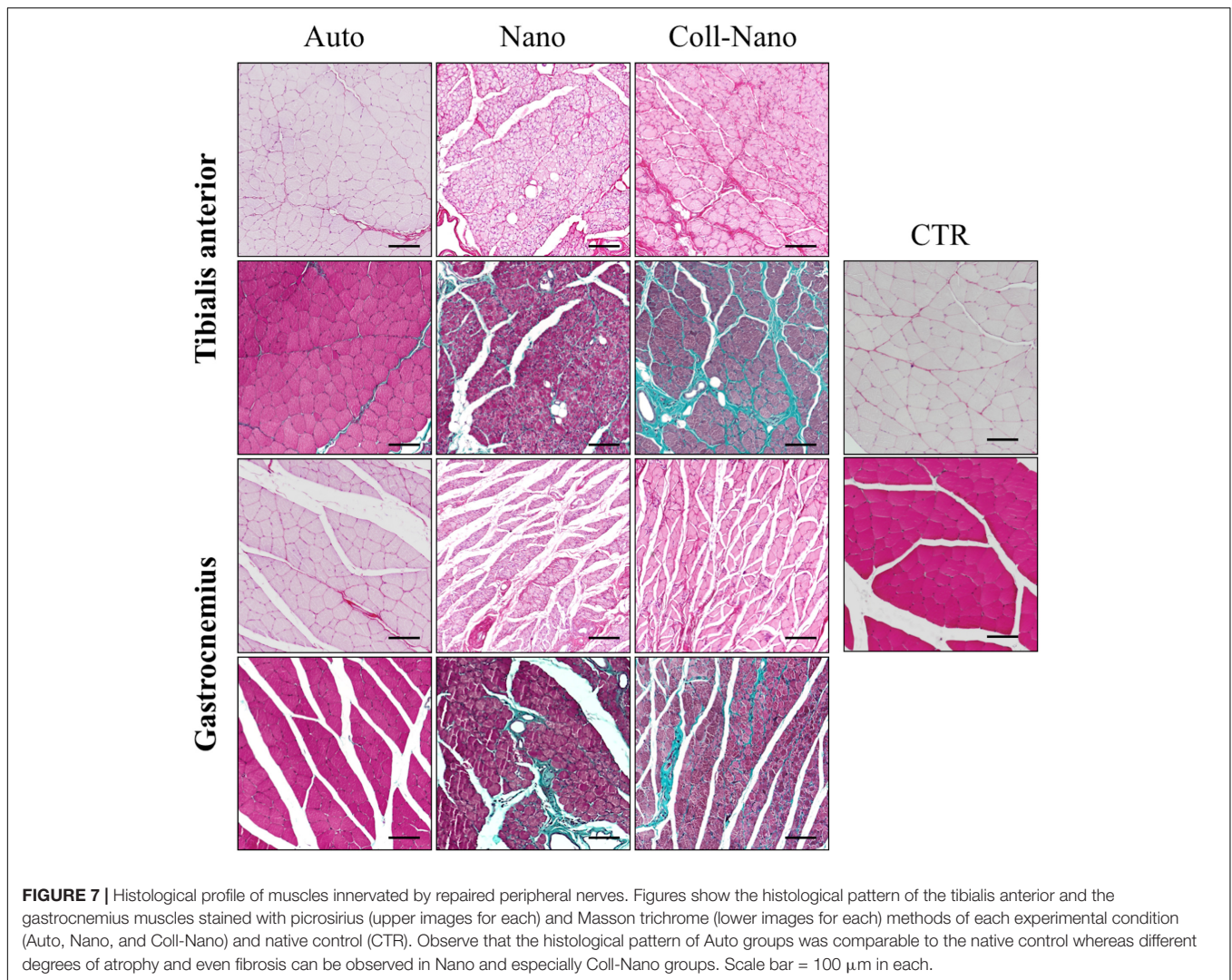
The histochemical analyses of the transversal sections of the tibialis anterior and gastrocnemius muscles confirmed the EMG findings and especially the different degree of atrophy observed by the morphometric evaluation among the experimental groups (Figure 7). In Auto group, histology revealed slight signs of atrophy in both muscles analyzed. The histological pattern was characterized by the presence of randomly distributed well-delimited rhabdomyocytes with certain signs of atrophy, such as nuclear internalization and cell size reduction. In addition, we did not observe signs of fibrosis or adipose tissue infiltration with PS and MST methods (Figure 7). In general, muscles in this group showed a similar histological pattern than healthy muscles used as controls (Figure 7). In the Nano group, the degree of atrophy in both muscles was more evident than in Auto group. In this case, a grouped atrophy was observed, which was characterized by the presence of groups of small and angular rhabdomyocytes. Concerning the ECM, histochemistry revealed a slight increase of the collagen content as well as the presence

of some adipocytes (Figure 7). The degree of atrophy observed in Coll-Nano group was considerably higher than in Auto and Nano groups. In this group, both muscles were mostly atrophic, composed by small muscle fascicles containing moderately to severely atrophied rhabdomyocytes. Furthermore, a considerable increase of collagen fibers and some occasional adipocytes were observed (Figure 7). Muscle histological analyses confirmed the morphometric and EMG results.

DISCUSSION

Here, we report an *in vivo* preclinical evaluation of two novel tissue engineering approaches for the repair of a 10-mm nerve gap in the sciatic nerve of rats: a multilayered NFABNS and the NFABNS used as intraluminal fillers of NeuraGen® conduits. The PN's regeneration process and functional recovery were assessed by using clinical, functional and histological analyses.

In PNTE, bioartificial substitutes must have adequate structural, physical and biological properties to successfully repair nerve defects supporting, and ideally increasing, the regeneration process and functional recovery (Daly W. et al., 2012; Carriel et al., 2014a; Wieringa et al., 2018). From the



surgical perspective, it is important that nerve substitutes may respond to specific anatomical requirements (e.g., length, diameter, number of fascicles), should be easy to handle and to suture to ensure an adequate tension-free PN repair, and should be available for use in a reasonable period of time (Carriel et al., 2014a; Gu et al., 2014; Pedrosa et al., 2017). In this regard, the current gold standard technique, the nerve autografts, effectively provides adequate biological and physical properties with an acceptable functional recovery. However, the use of sensory donor nerves to repair motor ones rarely respond to the anatomical needs (Brenner et al., 2006) and the well-known limitations of nerve autograft, and specially allografts, urge researchers to find more efficient alternatives (Daly W. et al., 2012; Carriel et al., 2014a). Although promising, most currently available PNTE strategies cannot be manufactured in an opportune range of time or, as it is the case of FDA-approved commercial devices, they are available with a pre-established range of dimensions and may hardly fulfill the anatomical demands.

In this study, we show the suitability of two natural biomaterial-based TE strategies for PN repair, which were generated following a previously described controlled and highly reproducible procedure (Carriel et al., 2017d). On the one hand, with our NFABNS, it was possible to successfully recreate the shape, diameter and length of the PNs to be repaired, thus demonstrating that the NFABNS can respond to specific anatomical needs. On the other hand, the NFABNS demonstrated to be suitable for use as intraluminal filler of NeuraGen® conduits. Concerning the design of the NFABNS, they were generated by rolling thin layers of NFAH to generate consistent multilayered rods containing viable, proliferating (positive for Ki-67 and PCNA) and functional ADMSCs (Carriel et al., 2017d). In addition, this simple, fast and economic procedure has the advantage that it could be programmed some hours before the surgery, which may fulfill the time requirements for an opportune PN repair (Pedrosa et al., 2017; Zhang and Rosen, 2018). Moreover, the NFABNS has been demonstrated to be surgically easy to handle with adequate mechanical stability and flexibility, which allowed a tension-free repair just like nerve

autografts. Interestingly, despite these advantages, tensile test demonstrated that our NFABNS were not fully comparable to the biomechanical response of native rat sciatic nerves (e.g., 0.30 ± 0.04 MPa vs. 8.5 ± 2.48 MPa Young's Modulus mean values, respectively) (Carriel et al., 2017d; Philips et al., 2018a,b). Nonetheless, here we demonstrated that, independently of these biomechanical differences, our NFABNS were consistent enough to successfully repair all defects ensuring the nerve continuity after 14 weeks. The potential suitability of the use of NFABNS in PN repair is supported by previous studies, in which natural biomaterial-based substitutes with comparable multilayered 3D design were successfully used *in vivo*. In this context, plastic compressed, multilayered, and even multifasciculated, collagen-based rods containing different cell sources were previously used to bridge 8-mm (Schuh et al., 2018) and 1.5-mm defects in rat sciatic nerves (Georgiou et al., 2013, 2015). Similarly, the use of multilayered acellular small intestinal submucosa coated with SC supported tissue regeneration in a 7-mm sciatic nerve defect in rats (Hadlock et al., 2001). Unfortunately, none of these reports provided information concerning the biomechanical properties of these promising engineered substitutes, and therefore these aspects as compared to our NFABNS remain unknown.

Concerning the use of NeuraGen® conduits filled with NFABNS in PN repair, this strategy allowed us to efficiently repair all nerve defects after 14 weeks without macroscopic complications. Technically, this strategy was considerably faster and easier than the use of NFABNS alone or nerve autografts because repair was done following the conventional tubulization technique. Regarding the suitability of this combined strategy in PNs repair, it is well-accepted that the use of conduits containing intraluminal fillers, especially those containing cells, is able to enrich the regenerative microenvironment with the consequent enhance of PN regeneration and functional recovery (Pedrosa et al., 2017; Gonzalez-Perez et al., 2018; Ronchi et al., 2018; Tajdaran et al., 2018; Wieringa et al., 2018). In this study, the incorporation of NFABNS into NeuraGen® conduits prevented the deformation or compression of these commercial devices during the period analyzed. Deformation, compression and early reabsorption of some hollow conduits has been described associated to this technique or to the use of vein grafts in PNs reconstruction (Moore et al., 2009; Hernandez-Cortes et al., 2010; Wangenstein and Kalliainen, 2010; Daly W. et al., 2012; Liodaki et al., 2013; Papalia et al., 2013; Carriel et al., 2014a; Krarup et al., 2017). In this regard, engineered neural tissue-like substitutes based on cellular self-aligned and plastic compressed collagen hydrogels were covered by NeuraWrap™ (Integra, United States) devices and successfully used to repair a critical nerve gap of 15-mm in rats (Georgiou et al., 2013). Furthermore, the use of NFABNS to fill NeuraGen® conduits is especially supported by our previous studies in which these conduits filled with uncompressed FAH containing ADMSCs successfully repaired 10-mm nerve gaps in rats, supporting tissue regeneration and functional recovery after 12 weeks (Carriel et al., 2013, 2017c). Finally, all these previous studies support the potential surgical usefulness of the use of NFABNS alone or as intraluminal filler of nerve conduits in PNs repair.

Clinical and functional assessments are needed to determine the degree of functional recovery following PN repair (Vleggeert-Lankamp, 2007; Siemionow et al., 2011; Carriel et al., 2014b; Navarro, 2016). This time-course study demonstrated that the created injury severely compromised clinical and functional parameters of all animals after 4 weeks, followed by a partial recovery after 12 weeks. Clinically, all operated animals had self-amputations over the time, but they were consistently higher in the autograft group, although differences were not statistically significant. Concerning the presence of neurotrophic ulcers, which are associated to an impairment of the sensitive and motor functions (den Dunnen and Meek, 2001; Vleggeert-Lankamp, 2007; Carriel et al., 2013), they were surprisingly absent in animals treated with NeuraGen® conduits filled with NFABNS over the time. However, ulcers were found in animals that received autograft (20%) and NFABNS (40%), without significant differences after 12 weeks, being these findings in agreement with previous studies (Meek et al., 1999; den Dunnen and Meek, 2001). In addition to these parameters, experimentally induced sciatic nerve injuries are associated to muscle dysfunction and neurogenic muscle retraction, which can be reflected by foot length alterations (Kim et al., 2007; Carriel et al., 2013; Kappos et al., 2015). In this study, a higher degree of neurogenic muscle retraction was observed in animals treated with autograft, while engineered strategies (NFABNS and filled conduits) were associated to better results. The development of these injuries at the foot level can be explained by a partial recovery of the sensitive and motor functions assessed by pinch and toe-spread tests. Our results were especially favorable with the use of NFABNS as compared to the autograft, being less favorable when nerves were repaired with filled conduits. However, these results were not comparable to the normal function observed in healthy animals. These results are in line with previous studies. For example, the use of fibrin conduits containing different kinds of ADMSCs demonstrated comparable functional recovery than autografts in the repair of 10-mm gaps in rats after 12 weeks (Kappos et al., 2015). In addition, a recent study demonstrated successful functional recovery through the use of chitosan conduits filled with cellular self-aligned collagen hydrogels in the repair of a critical size defect of 15-mm in rats (Gonzalez-Perez et al., 2018).

In order to accurately determine the degree of muscle denervation and reinnervation, EMG studies of gastrocnemius and tibialis anterior muscles were conducted as previously recommended (Vleggeert-Lankamp, 2007; Carriel et al., 2013, 2014b; Navarro, 2016). These analyses confirmed a high degree of muscle denervation at 4 weeks in all animals, as expected. Interestingly, after 12 weeks, a decrease of muscle denervation and an increase of muscle reinnervation were demonstrated in animals treated with NFABNS and autografts. However, certain degree of denervation was still present in the NFABNS group, especially when filled conduits were used. Interestingly, the EMG profile of animals treated with NFABNS resulted to be more favorable than the results previously obtained with the use of NeuraGen® conduits filled with cellular and acellular uncompressed FAH in the same animal model and period of analysis (Carriel et al., 2013). Furthermore, our EMG results are

in accordance with the percentage of w and v loss results. In fact, higher percentages of w and v loss were obtained with the use of filled conduits, followed by the use of NFABNS, being these results significantly higher than the obtained with autograft technique. These findings were later confirmed by the muscle histochemical analyses which clearly revealed slight, moderate and severe rhabdomyocytes atrophy in autograft, NFABNS and filled conduits groups, respectively. Finally, our results suggest that the use of NFABNS in PN repair promote an acceptable, and in some aspect equivalent clinical and functional recovery profile than the use autograft technique in the repair of 10-mm nerve gap in rats, being these results supported by comparable studies and engineered models (Georgiou et al., 2013, 2015; Jesuraj et al., 2014; Kappos et al., 2015; Pedrosa et al., 2017; Schuh et al., 2018; Wang and Sakiyama-Elbert, 2018).

Histological analyses are useful tools in PN regeneration research being an essential complement to the clinical, functional and electrophysiological investigation techniques (Vleggeert-Lankamp, 2007; Carriel et al., 2014b; Geuna, 2015). In this study, light microscopy and TEM histology were crucial to demonstrate an active PN regeneration process at the middle portion of all substitutes. However, differences in the amount, regenerative tissue distribution pattern and host tissue response to the implanted grafts were detected. Autograft group histology confirmed the presence of newly formed PN fascicles with moderate myelination (MCOLL and TEM results) along the connective tissue layers and especially, at the intrafascicular level. A comparable regeneration process was observed in NFABNS groups, although it was restricted to the connective tissue covering the implanted substitutes and not through the substitute layers. Surprisingly, tissue regeneration in filled conduits was considerably less abundant and poorly myelinated than the in autograft and NFABNS groups. In fact, the nerve tissue regeneration was restricted to the intraluminal area just around the intraluminal surface of the NFABNS. In summary, histology demonstrated that NFABNS – used alone or as intraluminal filler – did not promote nerve tissue regeneration through its biomaterials layers. Nevertheless, the direct use of NFABNS in PN repair resulted to be an efficient physical platform to keep both nerve stumps connected, supporting and guiding nerve tissue regeneration through its surrounding connective tissue, thus reaffirming the clinical, functional and EMG results. Therefore, our histological findings are in accordance with the active nerve tissue regeneration obtained by the use of comparable strategies (Hadlock et al., 2001; Georgiou et al., 2013, 2015; Ronchi et al., 2018; Schuh et al., 2018). In relation to the less favorable results obtained with filled NeuraGen® conduits, our histological analyses suggest that this finding could be related to physical factors (Daly W. et al., 2012; Carriel et al., 2014a). It is well accepted that nerve conduits provide a close and controlled protective microenvironment that guide and support nerve tissue regeneration in non-critical nerve gaps (Daly W. et al., 2012; Carriel et al., 2013, 2014a; Krarup et al., 2017; Pedrosa et al., 2017; Ronchi et al., 2018). In this regard, we hypothesize that the combined use of an external conduit filled with a highly dense NFABNS may reduce the area needed for an optimal tissue regeneration, and this would explain the poor functional

and electrophysiological recovery observed with this strategy. In fact, it was experimentally demonstrated that low-density intraluminal fillers enhance regeneration process and functional recovery (Daly W. et al., 2012; Daly W.T. et al., 2012; Lee et al., 2012; Carriel et al., 2013, 2014a, 2017c; Gu et al., 2014; Wieringa et al., 2018). On the other hand, highly dense and slowly degrading intraluminal fillers can reduce the area available for tissue regeneration, thus delaying or even inhibiting tissue regeneration (Labrador et al., 1998; Yao et al., 2010; Daly W. et al., 2012; Daly W.T. et al., 2012; Carriel et al., 2014a).

In relation to the host response to our biomaterials, histological analyses confirmed that NFABNS, used alone or as intraluminal fillers, were progressively biodegraded by a local inflammatory host response mainly consisting of macrophages. These findings are in agreement with previous studies where FAH-based substitutes were reabsorbed by a comparable biodegradation process in some weeks (Carriel et al., 2012, 2013; Fernandez-Valades-Gamez et al., 2016; Martin-Piedra et al., 2017). Besides, histology also confirmed that NeuraGen® conduits protect the intraluminal NFABNS from host tissue biodegradation. This could reduce the intraluminal area needed for an optimal tissue regeneration and would reaffirm the hypothesis discussed above.

Finally, the use of cellular systems in PN repair demonstrated to be an efficient alternative to increase regeneration and functional recovery (Carriel et al., 2013, 2014a, 2017c; Kappos et al., 2015; Gonzalez-Perez et al., 2018; Zhang and Rosen, 2018). In this study, autologous undifferentiated ADMSCs were used to functionalize the NFABNS due to their well-demonstrated positive impact on PN repair (Kalbermatten et al., 2008; Lopatina et al., 2011; Gu et al., 2014; Faroni et al., 2016; Carriel et al., 2017b). In this study, acceptable PN regeneration and functional recovery profiles were obtained with the direct use of NFABNS in PN repair. However, due to technical reasons, it was not possible to identify the cells implanted within the NFABNS. Therefore, we cannot directly attribute to the cells the positive effect on PN regeneration obtained with our NFABNS. Therefore, the fate and potential role of these cells following *in vivo* implantation remains unknown and should be determined in future studies. In this regard, previous studies suggested that ADMSCs could contribute to the regeneration process through their differentiation to a SCs-like phenotype, releasing essential neurotrophic factors and collaborating with the synthesis of an essential ECM (Salgado et al., 2010; Tomita et al., 2012; Carriel et al., 2013; Kappos et al., 2015; Faroni et al., 2016; Zhang and Rosen, 2018).

CONCLUSION

In conclusion, the present study suggests that NFABNS support a closely comparable functional recovery and tissue regeneration than autograft technique. Overall results suggest that NFABNS may have potential clinical usefulness in future clinical trials in humans. However, further research should confirm their positive impact on the reconstruction of critical nerve defects and should improve the properties of these bioartificial tissue substitutes.

AUTHOR CONTRIBUTIONS

VC, MA, and AC designed the experiments. VC, JC-A, and FC wrote the article. VC, JC-A, FC, OR, and DD-H performed the laboratory analyses. VC, JC-A, EM, JS-M, SG-G, and OR performed the functional and clinical analyses. VC, JC-A, FC, MA, and EM analyzed the results.

FUNDING

This study was supported by the Spanish “Plan Nacional de Investigación Científica, Desarrollo e Innovación Tecnológica,” from the National Ministry of Economy and Competitiveness

(Instituto de Salud Carlos III), Grants Nos FIS PI14-1343 and FIS PI17-0393, co-financed by “Fondo Europeo de Desarrollo Regional (FEDER),” European Union.

ACKNOWLEDGMENTS

The authors are grateful to Dr. Ariane Ruyffelaert (Faculty of Philosophy and Letters, University of Granada) for her proofreading service. The authors are grateful for the technical assistance of Amalia de la Rosa Romero, Concepción López Rodríguez, Dr. Víctor Domingo Roa (Experimental Unit of the University Hospital Virgen de las Nieves, Granada, Spain) and Leen Pieters (Ghent University, Belgium).

REFERENCES

- Alaminos, M., Del Carmen Sanchez-Quevedo, M., Munoz-Avila, J. I., Serrano, D., Medialdea, S., Carreras, I., et al. (2006). Construction of a complete rabbit cornea substitute using a fibrin-agarose scaffold. *Invest. Ophthalmol. Vis. Sci.* 47, 3311–3317. doi: 10.1167/iops.05-1647
- Boeckstyns, M. E., Sorensen, A. I., Vineta, J. F., Rosen, B., Navarro, X., Archibald, S. J., et al. (2013). Collagen conduit versus microsurgical neurotaphy: 2-year follow-up of a prospective, blinded clinical and electrophysiological multicenter randomized, controlled trial. *J. Hand Surg.* 38, 2405–2411. doi: 10.1016/j.jhsa.2013.09.038
- Brenner, M. J., Hess, J. R., Mykатыn, T. M., Hayashi, A., Hunter, D. A., and Mackinnon, S. E. (2006). Repair of motor nerve gaps with sensory nerve inhibits regeneration in rats. *Laryngoscope* 116, 1685–1692. doi: 10.1097/01.mlg.0000229469.31749.91
- Campbell, W. W. (2008). Evaluation and management of peripheral nerve injury. *Clin. Neurophysiol.* 119, 1951–1965. doi: 10.1016/j.clinph.2008.03.018
- Campos, F., Bonhame-Espinosa, A. B., Vizcaino, G., Rodriguez, I. A., Durand-Herrera, D., Lopez-Lopez, M. T., et al. (2017). Generation of genipin cross-linked fibrin-agarose hydrogels tissue-like models for tissue engineering applications. *Biomed. Mater.* doi: 10.1088/1748-605X/aa9ad2 [Epub ahead of print].
- Campos, F., Bonhome-Espinosa, A. B., Garcia-Martinez, L., Duran, J. D., Lopez-Lopez, M. T., Alaminos, M., et al. (2016). Ex vivo characterization of a novel tissue-like cross-linked fibrin-agarose hydrogel for tissue engineering applications. *Biomed. Mater.* 11:055004. doi: 10.1088/1748-6041/11/5/055004
- Carriel, V., Alaminos, M., Garzon, I., Campos, A., and Cornelissen, M. (2014a). Tissue engineering of the peripheral nervous system. *Expert Rev. Neurother.* 14, 301–318. doi: 10.1586/14737175.2014.887444
- Carriel, V., Garzon, I., Alaminos, M., and Cornelissen, M. (2014b). Histological assessment in peripheral nerve tissue engineering. *Neural Regen. Res.* 9, 1657–1660. doi: 10.4103/1673-5374.141798
- Carriel, V., Campos, A., Alaminos, M., Raimondo, S., and Geuna, S. (2017a). Staining methods for normal and regenerative myelin in the nervous system. *Methods Mol. Biol.* 1560, 207–218. doi: 10.1007/978-1-4939-6788-9_15
- Carriel, V., Campos, F., Aneiros-Fernandez, J., and Kiernan, J. A. (2017b). Tissue fixation and processing for the histological identification of lipids. *Methods Mol. Biol.* 1560, 197–206. doi: 10.1007/978-1-4939-6788-9_14
- Carriel, V., Garzon, I., Campos, A., Cornelissen, M., and Alaminos, M. (2017c). Differential expression of GAP-43 and neurofilament during peripheral nerve regeneration through bio-artificial conduits. *J. Tissue Eng. Regen. Med.* 11, 553–563. doi: 10.1002/term.1949
- Carriel, V., Scionti, G., Campos, F., Roda, O., Castro, B., Cornelissen, M., et al. (2017d). In vitro characterization of a nanostructured fibrin agarose bio-artificial nerve substitute. *J. Tissue Eng. Regen. Med.* 11, 1412–1426. doi: 10.1002/term.2039
- Carriel, V., Garrido-Gomez, J., Hernandez-Cortes, P., Garzon, I., Garcia-Garcia, S., Saez-Moreno, J. A., et al. (2013). Combination of fibrin-agarose hydrogels and adipose-derived mesenchymal stem cells for peripheral nerve regeneration. *J. Neural Eng.* 10:026022. doi: 10.1088/1741-2560/10/2/026022
- Carriel, V., Garzon, I., Alaminos, M., and Campos, A. (2011). Evaluation of myelin sheath and collagen reorganization pattern in a model of peripheral nerve regeneration using an integrated histochemical approach. *Histochem. Cell Biol.* 136, 709–717. doi: 10.1007/s00418-011-0874-3
- Carriel, V. S., Aneiros-Fernandez, J., Arias-Santiago, S., Garzon, I. J., Alaminos, M., and Campos, A. (2011). A novel histochemical method for a simultaneous staining of melanin and collagen fibers. *J. Histochem. Cytochem.* 59, 270–277. doi: 10.1369/0022155410398001
- Carriel, V., Garzon, I., Jimenez, J. M., Oliveira, A. C., Arias-Santiago, S., Campos, A., et al. (2012). Epithelial and stromal developmental patterns in a novel substitute of the human skin generated with fibrin-agarose biomaterials. *Cells Tissues Organs* 196, 1–12. doi: 10.1159/000330682
- Dahlin, L. B. (2008). Techniques of peripheral nerve repair. *Scand. J. Surg.* 97, 310–316. doi: 10.1177/145749690809700407
- Daly, W., Yao, L., Zeugolis, D., Windebank, A., and Pandit, A. (2012). A biomaterials approach to peripheral nerve regeneration: bridging the peripheral nerve gap and enhancing functional recovery. *J. R. Soc. Interface* 9, 202–221. doi: 10.1098/rsif.2011.0438
- Daly, W. T., Yao, L., Abu-rub, M. T., O’Connell, C., Zeugolis, D. I., Windebank, A. J., et al. (2012). The effect of intraluminal contact mediated guidance signals on axonal mismatch during peripheral nerve repair. *Biomaterials* 33, 6660–6671. doi: 10.1016/j.biomaterials.2012.06.002
- den Dunnen, W. F., and Meek, M. F. (2001). Sensory nerve function and auto-mutilation after reconstruction of various gap lengths with nerve guides and autologous nerve grafts. *Biomaterials* 22, 1171–1176. doi: 10.1016/S0142-9612(00)00339-2
- Faroni, A., Smith, R. J., Lu, L., and Reid, A. J. (2016). Human Schwann-like cells derived from adipose-derived mesenchymal stem cells rapidly de-differentiate in the absence of stimulating medium. *Eur. J. Neurosci.* 43, 417–430. doi: 10.1111/ejn.13055
- Fernandez-Valades-Gamez, R., Garzon, I., Licerias-Licerias, E., Espana-Lopez, A., Carriel, V., Martin-Piedra, M. A., et al. (2016). Usefulness of a bioengineered oral mucosa model for preventing palate bone alterations in rabbits with a mucoperiosteal defect. *Biomed. Mater.* 11:015015. doi: 10.1088/1748-6041/11/1/015015
- Garcia-Martinez, L., Campos, F., Godoy-Guzman, C., Del Carmen Sanchez-Quevedo, M., Garzon, I., Alaminos, M., et al. (2017). Encapsulation of human elastic cartilage-derived chondrocytes in nanostructured fibrin-agarose hydrogels. *Histochem. Cell Biol.* 147, 83–95. doi: 10.1007/s00418-016-1485-9
- Georgiou, M., Bunting, S. C., Davies, H. A., Loughlin, A. J., Golding, J. P., and Phillips, J. B. (2013). Engineered neural tissue for peripheral nerve repair. *Biomaterials* 34, 7335–7343. doi: 10.1016/j.biomaterials.2013.06.025
- Georgiou, M., Golding, J. P., Loughlin, A. J., Kingham, P. J., and Phillips, J. B. (2015). Engineered neural tissue with aligned, differentiated adipose-derived stem cells promotes peripheral nerve regeneration across a critical sized defect in rat sciatic nerve. *Biomaterials* 37, 242–251. doi: 10.1016/j.biomaterials.2014.10.009

- Geuna, S. (2015). The sciatic nerve injury model in pre-clinical research. *J. Neurosci. Methods* 243, 39–46. doi: 10.1016/j.jneumeth.2015.01.021
- Geuna, S., Fornaro, M., Raimondo, S., and Giacobini-Robecchi, M. G. (2010). Plasticity and regeneration in the peripheral nervous system. *Ital. J. Anat. Embryol.* 115, 91–94.
- Geuna, S., Raimondo, S., Ronchi, G., Di Scipio, F., Tos, P., Czaja, K., et al. (2009). Chapter 3: histology of the peripheral nerve and changes occurring during nerve regeneration. *Int. Rev. Neurobiol.* 87, 27–46. doi: 10.1016/S0074-7742(09)87003-7
- Gonzalez-Perez, F., Hernandez, J., Heimann, C., Phillips, J. B., Udina, E., and Navarro, X. (2018). Schwann cells and mesenchymal stem cells in laminin- or fibronectin-aligned matrices and regeneration across a critical size defect of 15 mm in the rat sciatic nerve. *J. Neurosurg. Spine* 28, 109–118. doi: 10.3171/2017.5.SPINE161100
- Greene, E. C. (1968). *Anatomy of the Rat. Transactions of the American Philosophical Society*, reprinted Edn, Vol. 27. New York, NY: Hafner Publishing.
- Gu, X., Ding, F., and Williams, D. F. (2014). Neural tissue engineering options for peripheral nerve regeneration. *Biomaterials* 35, 6143–6156. doi: 10.1016/j.biomaterials.2014.04.064
- Hadlock, T. A., Sundback, C. A., Hunter, D. A., Vacanti, J. P., and Cheney, M. L. (2001). A new artificial nerve graft containing rolled Schwann cell monolayers. *Microsurgery* 21, 96–101. doi: 10.1002/micr.1016
- Hernandez-Cortes, P., Garrido, J., Camara, M., and Ravassa, F. O. (2010). Failed digital nerve reconstruction by foreign body reaction to Neurolac nerve conduit. *Microsurgery* 30, 414–416. doi: 10.1002/micr.20730
- Jesuraj, N. J., Santosa, K. B., Macewan, M. R., Moore, A. M., Kasurkuthi, R., Ray, W. Z., et al. (2014). Schwann cells seeded in acellular nerve grafts improve functional recovery. *Muscle Nerve* 49, 267–276. doi: 10.1002/mus.23885
- Kalbermatten, D. F., Kingham, P. J., Mahay, D., Mantovani, C., Pettersson, J., Raffoul, W., et al. (2008). Fibrin matrix for suspension of regenerative cells in an artificial nerve conduit. *J. Plast. Reconstr. Aesthet. Surg.* 61, 669–675. doi: 10.1016/j.bjps.2007.12.015
- Kappos, E. A., Engels, P. E., Tremp, M., Meyer zu Schwabedissen, M., di Summa, P., Fischmann, A., et al. (2015). Peripheral nerve repair: multimodal comparison of the long-term regenerative potential of adipose tissue-derived cells in a biodegradable conduit. *Stem Cells Dev.* 24, 2127–2141. doi: 10.1089/scd.2014.0424
- Kehoe, S., Zhang, X. F., and Boyd, D. (2012). FDA approved guidance conduits and wraps for peripheral nerve injury: a review of materials and efficacy. *Injury* 43, 553–572. doi: 10.1016/j.injury.2010.12.030
- Kim, S. M., Lee, S. K., and Lee, J. H. (2007). Peripheral nerve regeneration using a three dimensionally cultured Schwann cell conduit. *J. Craniofac. Surg.* 18, 475–488. doi: 10.1097/01.scs.0000249362.41170.f3
- Krarup, C., Rosen, B., Boeckstyns, M., Ibsen Sorensen, A., Lundborg, G., Moldovan, M., et al. (2017). Sensation, mechanoreceptor, and nerve fiber function after nerve regeneration. *Ann. Neurol.* 82, 940–950. doi: 10.1002/ana.25102
- Labrador, R. O., Buti, M., and Navarro, X. (1998). Influence of collagen and laminin gels concentration on nerve regeneration after resection and tube repair. *Exp. Neurol.* 149, 243–252. doi: 10.1006/exnr.1997.6650
- Ladak, A., Olson, J., Tredget, E. E., and Gordon, T. (2011). Differentiation of mesenchymal stem cells to support peripheral nerve regeneration in a rat model. *Exp. Neurol.* 228, 242–252. doi: 10.1016/j.expneurol.2011.01.013
- Lee, J. Y., Giusti, G., Friedrich, P. F., Archibald, S. J., Kemnitzer, J. E., Patel, J., et al. (2012). The effect of collagen nerve conduits filled with collagen-glycosaminoglycan matrix on peripheral motor nerve regeneration in a rat model. *J. Bone Joint Surg. Am.* 94, 2084–2091. doi: 10.2106/JBJS.K.00658
- Liodaki, E., Bos, I., Lohmeyer, J. A., Senyaman, O., Mauss, K. L., Siemers, F., et al. (2013). Removal of collagen nerve conduits (NeuraGen®) after unsuccessful implantation: focus on histological findings. *J. Reconstr. Microsurg.* 29, 517–522. doi: 10.1055/s-0033-1348033
- Lopatina, T., Kalinina, N., Karagyaur, M., Stambolsky, D., Rubina, K., Revischin, A., et al. (2011). Adipose-derived stem cells stimulate regeneration of peripheral nerves: BDNF secreted by these cells promotes nerve healing and axon growth de novo. *PLoS One* 6:e17899. doi: 10.1371/journal.pone.0017899
- Lotfy, A., Salama, M., Zahran, F., Jones, E., Badawy, A., and Sobh, M. (2014). Characterization of mesenchymal stem cells derived from rat bone marrow and adipose tissue: a comparative study. *Int. J. Stem Cells* 7, 135–142. doi: 10.15283/ijsc.2014.7.2.135
- Martin-Piedra, M. A., Garzon, I., Gomez-Sotelo, A., Garcia-Abril, E., Jaimes-Parra, B. D., Lopez-Cantarero, M., et al. (2017). Generation and evaluation of novel stromal cell-containing tissue engineered artificial stromas for the surgical repair of abdominal defects. *Biotechnol. J.* 12:1700078. doi: 10.1002/biot.201700078
- McGrath, A. M., Brohlin, M., Kingham, P. J., Novikov, L. N., Wiberg, M., and Novikova, L. N. (2012). Fibrin conduit supplemented with human mesenchymal stem cells and immunosuppressive treatment enhances regeneration after peripheral nerve injury. *Neurosci. Lett.* 516, 171–176. doi: 10.1016/j.neulet.2012.03.041
- Meek, M. F., Den Dunnen, W. F., Schakenraad, J. M., and Robinson, P. H. (1999). Long-term evaluation of functional nerve recovery after reconstruction with a thin-walled biodegradable poly (DL-lactide-epsilon-caprolactone) nerve guide, using walking track analysis and electrostimulation tests. *Microsurgery* 19, 247–253. doi: 10.1002/(SICI)1098-2752(1999)19:5<247::AID-MICR7>3.0.CO;2-E
- Moore, A. M., Kasurkuthi, R., Magill, C. K., Farhadi, H. F., Borschel, G. H., and Mackinnon, S. E. (2009). Limitations of conduits in peripheral nerve repairs. *Hand* 4, 180–186. doi: 10.1007/s11552-008-9158-3
- Navarro, X. (2016). Functional evaluation of peripheral nerve regeneration and target reinnervation in animal models: a critical overview. *Eur. J. Neurosci.* 43, 271–286. doi: 10.1111/ejn.13033
- Pabari, A., Yang, S. Y., Seifalian, A. M., and Mosahebi, A. (2010). Modern surgical management of peripheral nerve gap. *J. Plast. Reconstr. Aesthet. Surg.* 63, 1941–1948. doi: 10.1016/j.bjps.2009.12.010
- Papalia, I., Raimondo, S., Ronchi, G., Magaouda, L., Giacobini-Robecchi, M. G., and Geuna, S. (2013). Repairing nerve gaps by vein conduits filled with lipoaspirate-derived entire adipose tissue hinders nerve regeneration. *Ann. Anat.* 195, 225–230. doi: 10.1016/j.aanat.2012.10.012
- Pedrosa, S. S., Caseiro, A. R., Santos, J. D., and Maurício, A. C. (2017). “Scaffolds for peripheral nerve regeneration, the importance of in vitro and in vivo studies for the development of cell-based therapies and biomaterials: state of the art,” in *Scaffolds in Tissue Engineering-Materials, Technologies and Clinical Applications*, ed. F. Bairo (London: InTech). doi: 10.5772/intechopen.69540
- Philips, C., Campos, F., Roosens, A., Sanchez-Quevedo, M. D. C., Declercq, H., and Carriell, V. (2018a). Qualitative and quantitative evaluation of a novel detergent-based method for decellularization of peripheral nerves. *Ann. Biomed. Eng.* 46, 1921–1937. doi: 10.1007/s10439-018-2082-y
- Philips, C., Cornelissen, M., and Carriell, V. (2018b). Evaluation methods as quality control in the generation of decellularized peripheral nerve allografts. *J. Neural Eng.* 15:021003. doi: 10.1088/1741-2552/aaa21a
- Ronchi, G., Fornasari, B. E., Crosio, A., Budau, C. A., Tos, P., Perroteau, I., et al. (2018). Chitosan tubes enriched with fresh skeletal muscle fibers for primary nerve repair. *Biomed. Res. Int.* 2018:9175248. doi: 10.1155/2018/9175248
- Salgado, A. J., Reis, R. L., Sousa, N. J., and Gimble, J. M. (2010). Adipose tissue derived stem cells secretome: soluble factors and their roles in regenerative medicine. *Curr. Stem Cell Res. Ther.* 5, 103–110. doi: 10.2174/157488810791268564
- Sanchez-Quevedo, M. C., Alaminos, M., Capitan, L. M., Moreu, G., Garzon, I., Crespo, P. V., et al. (2007). Histological and histochemical evaluation of human oral mucosa constructs developed by tissue engineering. *Histol. Histopathol.* 22, 631–640. doi: 10.14670/HH-22.631
- Schuh, C., Day, A. G. E., Redl, H., and Phillips, J. (2018). An optimized collagen-fibrin blend engineered neural tissue promotes peripheral nerve repair. *Tissue Eng. Part A* 24, 1332–1340. doi: 10.1089/ten.TEA.2017.0457
- Scionti, G., Moral, M., Toledano, M., Osorio, R., Duran, J. D., Alaminos, M., et al. (2014). Effect of the hydration on the biomechanical properties in a fibrin-agarose tissue-like model. *J. Biomed. Mater. Res. A* 102, 2573–2582. doi: 10.1002/jbm.a.34929
- Siemonow, M., Duggan, W., Brzezicki, G., Klimczak, A., Grykien, C., Gatherwright, J., et al. (2011). Peripheral nerve defect repair with epineural tubes supported with bone marrow stromal cells: a preliminary report. *Ann. Plast. Surg.* 67, 73–84. doi: 10.1097/SAP.0b013e318223c2db
- Sun, C. K., Yen, C. H., Lin, Y. C., Tsai, T. H., Chang, L. T., Kao, Y. H., et al. (2011). Autologous transplantation of adipose-derived mesenchymal stem cells

- markedly reduced acute ischemia-reperfusion lung injury in a rodent model. *J. Transl. Med.* 9:118. doi: 10.1186/1479-5876-9-118
- Tajdaran, K., Chan, K., Gordon, T., and Borschel, G. H. (2018). Matrices, scaffolds, and carriers for protein and molecule delivery in peripheral nerve regeneration. *Exp. Neurol.* doi: 10.1016/j.expneurol.2018.08.014 [Epub ahead of print].
- Tomita, K., Madura, T., Mantovani, C., and Terenghi, G. (2012). Differentiated adipose-derived stem cells promote myelination and enhance functional recovery in a rat model of chronic denervation. *J. Neurosci. Res.* 90, 1392–1402. doi: 10.1002/jnr.23002
- Topp, K. S., and Boyd, B. S. (2006). Structure and biomechanics of peripheral nerves: nerve responses to physical stresses and implications for physical therapist practice. *Phys. Ther.* 86, 92–109. doi: 10.1093/ptj/86.1.92
- Vleggeert-Lankamp, C. L. (2007). The role of evaluation methods in the assessment of peripheral nerve regeneration through synthetic conduits: a systematic review. Laboratory investigation. *J. Neurosurg.* 107, 1168–1189. doi: 10.3171/JNS-07/12/1168
- Wang, Z. Z., and Sakiyama-Elbert, S. E. (2018). Matrices, scaffolds & carriers for cell delivery in nerve regeneration. *Exp. Neurol.* doi: 10.1016/j.expneurol.2018.09.020 [Epub ahead of print].
- Wangenstein, K. J., and Kalliainen, L. K. (2010). Collagen tube conduits in peripheral nerve repair: a retrospective analysis. *Hand* 5, 273–277. doi: 10.1007/s11552-009-9245-0
- Webber, C., and Zochodne, D. (2010). The nerve regenerative microenvironment: early behavior and partnership of axons and Schwann cells. *Exp. Neurol.* 223, 51–59. doi: 10.1016/j.expneurol.2009.05.037
- Wieringa, P. A., Goncalves de Pinho, A. R., Micera, S., van Wezel, R. J. A., and Moroni, L. (2018). Biomimetic architectures for peripheral nerve repair: a review of biofabrication strategies. *Adv. Healthc. Mater.* 7:e1701164. doi: 10.1002/adhm.201701164
- Yao, L., de Ruiter, G. C., Wang, H., Knight, A. M., Spinner, R. J., Yaszemski, M. J., et al. (2010). Controlling dispersion of axonal regeneration using a multichannel collagen nerve conduit. *Biomaterials* 31, 5789–5797. doi: 10.1016/j.biomaterials.2010.03.081
- Zhang, R., and Rosen, J. M. (2018). The role of undifferentiated adipose-derived stem cells in peripheral nerve repair. *Neural Regen. Res.* 13, 757–763. doi: 10.4103/1673-5374.232457
- Zheng, L., and Cui, H. F. (2010). Use of chitosan conduit combined with bone marrow mesenchymal stem cells for promoting peripheral nerve regeneration. *J. Mater. Sci. Mater. Med.* 21, 1713–1720. doi: 10.1007/s10856-010-4003-y

Conflict of Interest Statement: The authors declare that the research was conducted in the absence of any commercial or financial relationships that could be construed as a potential conflict of interest.

The handling Editor declared a past co-authorship with several of the authors VC, AC, and MA.

Copyright © 2018 Chato-Astrain, Campos, Roda, Miralles, Durand-Herrera, Sáez-Moreno, García-García, Alaminos, Campos and Carriel. This is an open-access article distributed under the terms of the Creative Commons Attribution License (CC BY). The use, distribution or reproduction in other forums is permitted, provided the original author(s) and the copyright owner(s) are credited and that the original publication in this journal is cited, in accordance with accepted academic practice. No use, distribution or reproduction is permitted which does not comply with these terms.



Long-Term Denervated Rat Schwann Cells Retain Their Capacity to Proliferate and to Myelinate Axons *in vitro*

Tessa Gordon^{1*}, Patrick Wood² and Olawale A. R. Sulaiman³

¹Division of Neuroscience, Faculty of Medicine, University of Alberta, Edmonton, AB, Canada, ²The Miami Project to Cure Paralysis/Department of Neurological Surgery, University of Miami School of Medicine, Miami, FL, United States,

³Department of Neurosurgery, Ochsner Medical Center, New Orleans, LA, United States

OPEN ACCESS

Edited by:

Giovanna Gambarotta,
Università di Torino, Italy

Reviewed by:

Xavier Navarro,
Autonomous University of Barcelona,
Spain

Valerio Magnaghi,
University of Milan, Italy

*Correspondence:

Tessa Gordon
tessat.gordon@gmail.com

Received: 18 September 2018

Accepted: 10 December 2018

Published: 07 January 2019

Citation:

Gordon T, Wood P and
Sulaiman OAR (2019) Long-Term
Denervated Rat Schwann Cells
Retain Their Capacity to Proliferate
and to Myelinate Axons *in vitro*.
Front. Cell. Neurosci. 12:511.
doi: 10.3389/fncel.2018.00511

Functional recovery is poor after peripheral nerve injury and delayed surgical repair or when nerves must regenerate over long distances to reinnervate distant targets. A reduced capacity of Schwann cells (SCs) in chronically denervated distal nerve stumps to support and interact with regenerating axons may account for the poor outcome. In an *in vitro* system, we examined the capacity of adult, long-term denervated rat SCs to proliferate and to myelinate neurites in co-cultures with fetal dorsal root ganglion (DRG) neurons. Non-neuronal cells were counted immediately after their isolation from the distal sciatic nerve stumps that were subjected to acute denervation of 7 days or chronic denervation of either 7 weeks or 17 months. Thereafter, equal numbers of the non-neural cells were co-cultured with purified dissociated DRG neurons for 5 days. The co-cultures were then treated with ³H-Thymidine for 24 h to quantitate SC proliferation with S100 immunostaining and autoradiography. After a 24-day period of co-culture, Sudan Black staining was used to visualize and count myelin segments that were elaborated around DRG neurites by the SCs. Isolated non-neural cells from 7-week chronically denervated nerve stumps increased 2.5-fold in number compared to ~2 million in 7 day acutely denervated stumps. There were only <0.2 million cells in the 17-week chronically denervated stumps. Nonetheless, these chronically denervated SCs maintained their proliferative capacity although the capacity was reduced to 30% in the 17-month chronically denervated distal nerve stumps. Moreover, the chronically denervated SCs retained their capacity to myelinate DRG neurites: there was extensive myelination of the neurites by the acutely and chronically denervated SCs after 24 days co-culture. There were no significant differences in the extent of myelination. We conclude that the low numbers of surviving SCs in chronically denervated distal nerve stumps retain their ability to respond to axonal signals to divide and to elaborate myelin. However, their low numbers consequent to their poor survival and their reduced capacity to proliferate account, at least in part, for the poor functional recovery after delayed surgical repair of injured nerve and/or the repair of injured nerves far from their target organs.

Keywords: Schwann cells, nerve transection, myelination, SC proliferation, neurites, nerve injury

INTRODUCTION

The Schwann cells (SCs) in the peripheral nervous system support nerve regeneration after nerve injury in contrast to the oligodendrocytes in the central nervous system that do not (Cajal, 1928; Bunge, 1994; Fenrich and Gordon, 2004; Toy and Namgung, 2013). Yet, functional recovery is suboptimal after peripheral nerve injuries in patients who have sustained injury to large nerve trunks such as the brachial plexus (Sunderland, 1978; Kline and Hudson, 1995). The prevailing view is that this failure in recovery is due to the irreversible degeneration of chronically denervated muscles and their replacement with fat during nerve regeneration (Sunderland, 1978; Kline and Hudson, 1995). This is despite the early conclusions by Holmes and Young (1942) that there are “various factors, in addition to atrophy of the end-organs, which are likely to reduce the effectiveness of recovery when suture is made after a long delay” and the later conclusion that “Most likely, multiple mechanisms contribute to this phenomenon” (of diminished recovery of muscle mass and integrated motor function), “which is sometimes referred to as ‘irreversible denervation atrophy’” (Kobayashi et al., 1997). Peripheral nerves regenerate at 1–3 mm/day, resulting in delays of months and, in humans, even years before regenerating nerves reach their denervated targets (Fu and Gordon, 1997). Gutmann and Young (1944) reported that denervated rat neuromuscular junctions progressively deteriorate after delayed nerve surgery. The authors attributed poor functional recovery after such a delay to an irreversible inability of regenerating nerves to reinnervate chronically denervated neuromuscular junctions. However, more recent studies have demonstrated that the progressive failure of even freshly injured (axotomized) neurons to successfully regenerate their axons through chronically denervated distal nerve stumps is the major factor accounting for progressive decline in functional recovery (Fu and Gordon, 1995a; Vuorinen et al., 1995; Sulaiman and Gordon, 2000; Gordon et al., 2003, 2011) and the recovery of denervated muscle mass (Kobayashi et al., 1997). Chronically denervated muscles do accept reinnervation despite their declining satellite population and the consequent incomplete recovery of reinnervated muscle fiber size and muscle wet weight (Fu and Gordon, 1995a; Kobayashi et al., 1997; Sulaiman and Gordon, 2000; Jejuri et al., 2002; Gordon et al., 2011). Hence, changes in the microenvironment of the chronically denervated nerve stumps provide, at least in part, the explanation for the progressive failure of axonal regeneration through the nerve stumps and to the denervated muscles.

The specific changes in the microenvironment of the denervated distal nerve stump accounting for poor axonal regeneration, are not understood. Regeneration is fostered in acutely injured peripheral nerves by the functional, structural, and molecular changes occurring in the denervated SCs in the distal stumps. Denervated SCs take an active role in the phagocytosis of myelin, a role that is taken over by macrophages that infiltrate the denervated nerve stump after 3 days (Gibson, 1979; Avellino et al., 1995; reviewed by Gordon,

2015). The SCs proliferate and extend long processes across the injury site within the first 10 days after injury (Salonen et al., 1988; Son and Thompson, 1995; Witzel et al., 2005). They also participate in the development of reversible and organized endoneurial structures that include the synthesis and positioning of collagen fibrils close to the laminin-containing basal lamina of the SCs and the formation of fascicle-like structures by the endoneurial cells (Salonen et al., 1987a,b, 1988).

The early changes in the denervated SCs include the switch in their phenotype from myelinating to a growth supportive one, the SCs downregulating genes that transcribe myelin associated proteins and glycoproteins and upregulating hundreds of growth-supportive genes reciprocally (De Leon et al., 1991; El Soury et al., 2018). The latter include genes that are responsible for ribonuclear RNA metabolic processes which contribute to the synthesis and production of new proteins and molecules required for Wallerian degeneration and nerve regeneration (El Soury et al., 2018). The many growth associated genes include those that transcribe transcription factors, c-jun and Notch, neurotrophic factors (reviewed by Jessen and Mirsky, 2016; Gordon and Borschel, 2017), soluble neuregulin 1 (NRG1) type I and type II isoforms, the NRG1 receptor ErbB2/3 (Carroll et al., 1997; Audisio et al., 2008; Gambarotta et al., 2013; Ronchi et al., 2016), and Erbin, an Erb2 interacting protein required for remyelination (Liang et al., 2012). The neurotrophic factors include nerve growth factor (NGF), brain- and glial-derived neurotrophic factors, and pleiotrophin and the receptors include p75 and truncated trk receptors for the neurotrophic factors (Meyer et al., 1992; Funakoshi et al., 1993; Naveilhan et al., 1997; Hoke et al., 2002, 2006; Mi et al., 2007; Brushart et al., 2013). These early changes in the denervated SC phenotype are important in promoting axonal regeneration (Fu and Gordon, 1997; Boyd and Gordon, 2003; El Soury et al., 2018).

The decline in the capacity of chronically denervated SCs to support nerve regeneration is, at least in part, explained by the transient nature of neurotrophic factor and receptor upregulation (Boyd and Gordon, 2003; Gordon, 2015). Their upregulated gene expression declines within a month of denervation (Fu and Gordon, 1997; You et al., 1997; Hoke et al., 2002, 2006; Brushart et al., 2013), as does the upregulation of the erbB2/3 receptors (Li et al., 1997; Hall, 1999) required for the proliferation of denervated SCs (Carroll et al., 1997; Gambarotta et al., 2013). Importantly, the chronically denervated SCs atrophy and decline in numbers: progressive SC atrophy and loss with disruption of their basement membranes and shrinkage of their columns, have been reported in rat and rabbit hindlimb nerves over periods of 1 to 26 months (Weinberg and Spencer, 1978; Salonen et al., 1987a,b; Røyttä and Salonen, 1988; You et al., 1997; Bradley et al., 1998). SC numbers identified with S-100 immunoreactivity, declined from a peak of ~3.5 times that of normal nerves at 4 weeks to the relatively low levels seen in intact nerves by 30 and 50 weeks after chronic sciatic nerve stump denervation in adult Wistar rats (Salonen et al., 1988).

In the present study, we evaluated the long-term survival of chronically denervated SCs and their capacities for proliferation and for myelination in response to contact with neurites. We provide the first quantitative evaluation of survival of very long-term (17 months) survival of chronically denervated SCs and demonstrate their sustained capacity to proliferate and to myelinate axons.

MATERIALS AND METHODS

Ethical Approval

All surgical procedures and perioperative care measures were performed with strict accordance with the National Institutes of Health guidelines. All the procedures were reviewed and approved by the University of Alberta animal care committee following the Canadian Council of Animal Care (CCAC) guidelines. Rat embryos from pregnant females were removed on the 15th day of gestation for dissection of dorsal root ganglia (DRGs) for isolation of the DRG sensory neurons. All the procedures of removal and isolation of DRG neurons were carried out in Miami and were reviewed and approved by the Miami Animal Care and Use Committee.

Animals

Adult female Sprague-Dawley rats (180–200 g body weight, $n = 20$) were used in the experiments in which hindlimb nerves were transected and ligated *in vivo* prior to removal of the denervated distal nerve stumps. Pregnant rats ($n = 2$) were used to remove 8–14 embryos each on the 15th day of gestation.

Materials

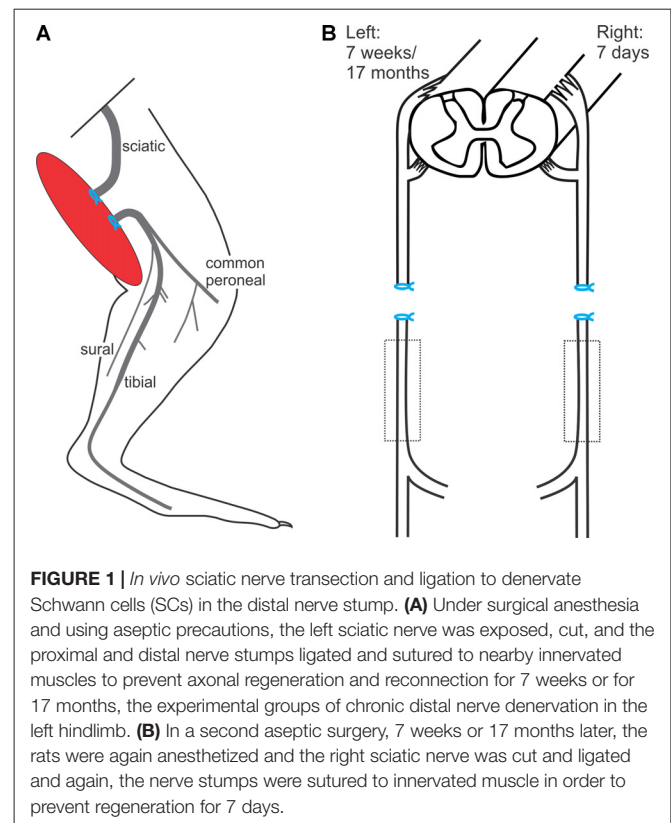
Cell culture reagents were purchased: Dulbecco's Modified Eagle Medium (DMEM) and Neurobasal medium and B27 supplement from Gibco, 0.05% collagenase from Worthington, 0.25% dispase from Boehringer-Mannheim, fetal bovine serum (FBS) from Hyclone, partially purified NGF from ProspectBio, trypsin from Worthington, TRL3, NTB2 emulsion from Kodak, mouse laminin from Collaborative Research, Inc., and rabbit anti-S100 antibody from Dako Corporation.

Anesthetic Protocols, Nerve Surgeries and Monitoring

All surgical procedures of sciatic nerve transection and ligation and the dissection of DRGs were made under anesthesia and using sterile surgical technique. Surgical anesthesia of the rats was induced with an intraperitoneal injection of sodium pentobarbital (30 mg/kg).

In vivo Sciatic Nerve Transection of the Sciatic Nerves and Ligation of the Nerve Stumps

The left hindlimb was shaved and a lateral skin incision was made. The intermuscular septum between the biceps femoris and the vastus lateralis muscles was divided and the sciatic nerve identified. The sciatic nerve was freed using blunt dissection in order to cut the nerve sharply with scissors. The proximal and distal nerve stumps were ligated with 4.0 silk and sutured



to nearby innervated muscles in order to prevent reconnection and subsequent axonal regeneration (**Figure 1**), as previously described (Fu and Gordon, 1995a,b; Sulaiman and Gordon, 2000; Gordon et al., 2011). The overlying muscle was closed and the skin incision on the thigh was closed in layers. The rats were placed under heat lamps and their recovery monitored.

In a second aseptic surgery, 7 weeks or 17 months later, the rats were again anesthetized, and the contralateral right sciatic nerve was cut and ligated. Again, the nerve stumps were sutured to innervated muscle in order to prevent regeneration for 7 days (**Figure 1B**).

Monitoring for Evidence of Nerve Regeneration

In a third aseptic surgical procedure, the skin was shaved on both hindlimbs and then opened to expose, bilaterally, the sciatic nerve and its tibial (TIB), common peroneal (CP) and sural nerve branches. An aseptic bipolar electrode attached to a Grass stimulator was used to deliver supramaximal stimuli at 10 Hz to the proximal sciatic nerve stump, followed by the distal stumps of the sciatic nerve and its branches to ensure that nerve regeneration had not occurred. No muscle contractions were observed in any of the rats confirming that the distal nerve stumps of the sciatic nerves were acutely denervated for 7 days and chronically denervated for 7 weeks and 17 months.

Surgical Removal of Sciatic, TIB, CP, and Sural Distal Nerve Stumps

In the same third surgical procedure, the chronically denervated (experimental) and the contralateral acutely denervated (control)

distal stumps of the sciatic nerve and its branches in the left and right hindlimbs, respectively, were removed and placed in Belzer's solution at 4°C for shipment to Miami for nerve dissociation, isolation of SCs, and preparation of co-cultures with DRG neurons.

Dissection of Dorsal Root Ganglia (DRGs) From Rat Embryos

Pregnant rats were deeply anesthetized with ether to allow surgery to remove embryos on the 15th day of gestation as previously described in detail (Kleitman et al., 1988). The DRGs from each of the 8–14 embryos were carefully dissected free and dissociated to establish DRG sensory neuron cultures (see below). The mothers were euthanized by exsanguination.

In vitro Cellular Dissociations and Co-culture

Non-neuronal Cells From Denervated Nerve Stumps

Using sterile procedure, the epineurium was removed from the dissected distal nerve stumps of the sciatic nerve and the CP, TIB and sural nerve branches which had been chronically denervated for 7 weeks and 17 months (in the left experimental hindlimb or acutely denervated in the right control hindlimb for 7 days. Because the chronically denervated nerves were shrunken, especially those after the lengthy 17-month period of chronic denervation, the nerves for each of the three periods of nerve stump denervation were pooled for dissociation of their denervated non-neuronal cells, i.e., 10 nerves each were pooled after 7 weeks and 17 months of chronic distal nerve stump denervation and 20 nerves were pooled after 7 days of acute distal nerve stump denervation.

The nerves were incubated in culture medium containing 0.05% collagenase, 0.25% dispase solution in DMEM, and 10% FBS (Medium 1), for 18 h at 35–37°C. The fascicles were rinsed free of collagenase/dispase with DMEM + 10% FBS. They were then dissociated into a single cell suspension by gentle trituration, using a glass micropipette with a tip diameter of 0.3–0.5 mm. The non-neuronal cells were harvested and re-suspended in Neurobasal medium with 2% B27 supplement and partially purified NGF at 50 units/ml (hereafter referred to as Medium 2). The cells were then counted and thereafter, their capacities to proliferate and to myelinate isolated DRG neurons were determined.

DRG Neurons From Rat Embryos

DRGs dissected from rat embryos on the 15th day of gestation were sequentially: (1) incubated with 0.25% trypsin in calcium and magnesium—free Hank's Balanced Salt Solution (Medium 3) for 1 h at 35–37°C on a slowly rotating shaker; (2) rinsed free of trypsin with L-15 medium containing 10% heat-inactivated FBS; and (3) dissociated by gentle trituration using a glass pipette with a tip diameter of 0.3–0.5 mm. The dissociated DRG cells were then harvested and re-suspended in Medium 2. The DRG cell suspension was plated at a density of 20,000 cells in a volume of two drops onto collagen-coated clear coverslips, 22 mm in diameter (Kleitman et al., 1988) and placed into 25 mm clear

mini-dishes that were incubated in a 5% CO₂ atmosphere at 37°C.

A day after plating, the DRG neuron cultures were flooded with 10 drops of the Medium 2 that was supplemented with fluorodeoxyuridine (FdU) and uridine, both at a concentration of 10 μ M (antimitotic Medium 2). This antimitotic treatment was repeated on days 8 and 15 of culture. Thereafter, the antimitotic agents were excluded from the culture medium (Medium 2), the Medium 2 (without FdU and uridine) being used to wash out the antimitotic agents (on days 19, 21, 26, 28, and 33, and 42). This washing ensured the depletion of antimitotic agents from the culture environment of the DRG neurons prior to their co-culture with non-neuronal cells from the acutely and chronically denervated distal nerve stumps.

Co-culture of DRG Neurons and Non-neuronal Cells From Denervated Nerve Stumps

The DRG neurons in each mini-dish were plated with 100,000 non-neuronal cells on the same day as the dissociation of the non-neuronal cells from the chronically (7 weeks and 17 months) and acutely (7 days) denervated distal nerve stumps.

Experiments

Cellular Counts

Small aliquots of non-neuronal cell suspensions, prepared in Medium 2 of each of the 7-week and 17-month chronically denervated nerve stumps and from the 7-day acutely denervated distal nerve stumps, were fixed in 4% paraformaldehyde in 0.05 M sodium phosphate buffer, pH 7.4 for 15 min at room temperature and stained with Hoechst 33342 dye (10 μ M). The cells were visualized by fluorescence microscopy, counted in a hemocytometer, and the total cell numbers calculated. The resulting bright staining of cell nuclei allowed the unambiguous recognition of the cells even when the suspensions were heavily laden with myelin debris.

Cellular Proliferation Assay

The non-neuronal cell suspensions were diluted with Medium 2 to 100,000 cells/ml and plated onto cultures of isolated DRG neurons at 1.0 ml per culture. Control neuronal cultures received 1.0 ml of Medium 2 without suspended cells. For maintenance, the co-cultures were re-fed three times each week with Medium 2.

After 5 days of co-culture, the non-neuronal cells in each of four cultures from the 7-day acutely denervated control group and the 7-week and 17-month chronic denervation experimental groups were labeled for 24 h with ³H-thymidine (0.5 μ Ci/ml) in Medium 2. The cultures were then rinsed and fixed with 4% paraformaldehyde in 0.1 M sodium phosphate buffer, pH 7.4 for 10 min at room temperature, permeabilized with 0.2% Triton X-100 in the fixative for another 10 min at room temperature, and prepared for immunostaining by blocking (30 s at room temperature) in a solution of 50% heat-inactivated goat serum in L-15 medium. The co-cultures were treated with rabbit anti-S100 antibody at 1:100 dilution in L-15/10% heat-inactivated goat serum for 30 min at room temperature, rinsed, and treated with fluorescein-conjugated goat anti-rabbit secondary antibody at 1:100 dilution in L-15/10% heat-inactivated goat serum for an additional 30 min at room temperature. The cultures

were rinsed with buffer, distilled water and ethanol, dried and mounted on glass slides, cell side up, with DPX mountant. The slides were dipped in NTB2 emulsion and processed for autoradiography (Wood and Bunge, 1975). The counts of the S-100 positive cells were made directly under microscopic view and not made on photographic images with their possible distortions. A proliferation index was defined as the number of the S-100 positive SCs that were labeled with ^3H -thymidine expressed as a percentage of the total number of S-100 positive SCs.

Myelination Assay

Six co-cultures per group of DRG neurons and non-neuronal cells isolated from the chronically denervated sciatic, TIB, CP, and sural nerve stumps, were maintained for 24 days in Medium 2 that was supplemented with 10 ng/ml of mouse laminin. Control cultures of DRG neurons without added non-neuronal cells were kept in parallel. All cultures were fixed overnight in FIX at 4°C, osmicated for 1 h in 0.1% osmium tetroxide in 0.1 M sodium phosphate buffer, pH 7.4, dehydrated to 70% ethanol in water and stained for 1 h in 0.7% Sudan Black in 70% ethanol in water (Kleitman et al., 1988). The cultures were rehydrated and mounted in glycerin jelly on glass slides. A quantitative measurement of myelination in each culture was made by counting the number of myelin segments crossing the equator of the cultures, using an eyepiece containing a single line horizontally bisecting the field of view at 200× magnification.

Statistics

Statistical analysis was conducted using an ANOVA with the Tukey's *post hoc* test (confidence interval = 95%). Comparisons were made between the experimental chronically denervated (7 weeks and 17 months) distal nerve stump of the cut and ligated left sciatic nerve and the control acutely denervated (7 day) distal nerve stump of the cut and ligated right sciatic nerve (Figure 1).

RESULTS

The Number of Non-neuronal Cells in Peripheral Nerve Stumps Decline With Time After Chronic Denervation

The nuclei of the non-neuronal cells in suspension were unambiguously identified with Hoechst stain and their numbers counted in a hemocytometer to calculate their total cell numbers. The bright staining of cell nuclei allowed the unambiguous recognition of cells even when the suspensions were heavily laden with myelin debris.

The total numbers of non-neuronal cells from the experimental 7-week denervated distal nerve stump from the left hindlimb were $>4 \times 10^6$ cells as compared to $<2 \times 10^6$ cells in the acutely 7 day denervated distal stump from the right hindlimb in each rat (Figure 2). This increase was not sustained, the numbers after 17 months chronic nerve stump denervation falling to ~10% of those numbers enumerated in the control 7-day acutely denervated distal nerve stumps. The increase of non-neuronal cells after chronic denervation at 7 weeks as compared to the numbers after acute denervation at 7 days, likely

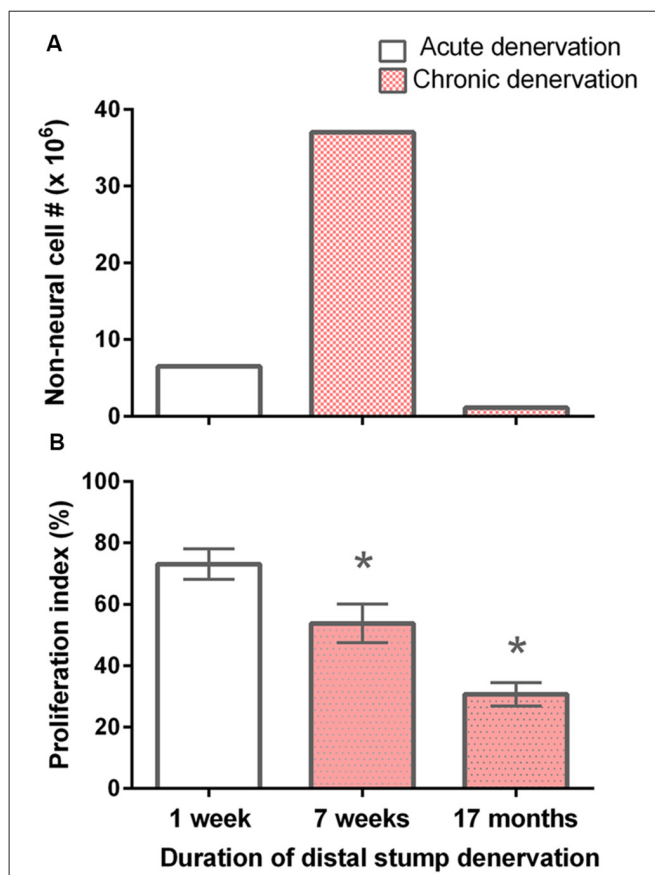


FIGURE 2 | Decline in the number of non-neuronal cells and the proliferative capacity of S-100 positive SCs with chronic denervation. **(A)** Non-neuronal cells isolated from acutely (7 days) and chronically (7 weeks and 17 months) denervated distal nerve stumps of the sciatic nerve and its tibial (TIB), common peroneal (CP), and sural nerve branches, namely control acute and experimental chronically denervated distal nerve stump from the right and left hindlimbs, respectively. The cells were counted in small aliquots of single cell suspensions. **(B)** The mean (\pm SE) of the proliferation index. The index is the number of S-100 positive SCs that, in co-cultures with isolated dorsal root ganglion (DRG) neurons for 5 days, were labeled with ^3H -thymidine and hence were dividing, expressed as a percentage of the total number of S-100 positive SCs. The proliferation indices at 7 days, 7 weeks and 17 months were significantly different from one another as indicated by *'s ($p < 0.025$).

include fibroblast-like and mast cells that also accumulate in the denervated nerve stump (Salonen et al., 1988; Ronchi et al., 2017) in addition to proliferating SCs in the nerve stumps during the Wallerian degeneration period of ~4 weeks (Salonen et al., 1988; You et al., 1997). The chronic denervation of the distal nerve stumps was controlled for the age and weight of the rats because the acutely and chronically denervated non-neuronal cells were dissociated from left and right hindlimbs, respectively, from the same rats.

Chronically Denervated Schwann Cells Retain Their Capacity to Proliferate, Albeit at a Reduced Rate

It is known that denervated SCs proliferate a second time when regenerating axons make contact with the SCs in the denervated

distal nerve stump (Pellegrino and Spencer, 1985). Five days after co-culture of denervated SCs with isolated DRG neurons and a 24-h exposure to ^3H -thymidine, most of the 7-day acutely denervated S-100 positive SCs were labeled with ^3H -thymidine and hence, had entered into the cell cycle (Figures 3A,D). Some of these SCs are identified in the phase-contrast autoradiograph with an arrowhead (Figure 3A) whilst those that were not dividing are identified by an arrow (Figure 3D). The proportion of mitotic SCs in the co-cultures of DRG neurons and SCs from the acutely denervated nerves was high, the ratio of the numbers of ^3H -thymidine labeled and unlabeled SCs, expressed as a percentage, the proliferative index in Figure 2B, being $\sim 75\%$.

The chronically denervated SCs from the left experimental hindlimb were also found to proliferate as shown in Figures 3B–F and quantitated in Figure 2B. However, the numbers of these ^3H -thymidine positive SCs undergoing proliferation in the co-culture with DRG neurons declined significantly after chronic denervation (Figures 3B–F) with $\sim 50\%$ and $\sim 30\%$ of the SCs proliferating in the 7-week and 17-month chronically denervated nerves, respectively, the indices declining significantly with chronic denervation

($p < 0.05$; Figure 2B). The differences in proliferative indices for the SCs from the control 1 week and experimental 7 weeks and 17 months were all significant ($p < 0.05$). Note that the S-100 immunostaining of the SCs in Figure 3 revealed that the SCs were closely associated with and aligned along the neurites of the DRG neurons, irrespective of the duration of prior SC denervation *in vivo*.

Chronically Denervated Schwann Cells Retain Their Capacity to Myelinate Axons

DRG neurons (without non-neuronal cells) were cultured for 24 days with and without non-neuronal cells that were freshly isolated from denervated nerve stumps of the sciatic nerve and its branches after acute (7 days) and chronic (7 weeks, 17 months) denervation in the right and left hindlimbs, respectively. In the absence of added non-neuronal cells, the DRG neurons exhibited extensive axon bundles that were not stained with Sudan Black (Figures 4A,B), a lipid stain widely used for detecting and distinguishing lipid-rich myelin sheaths in tissue culture (Eldridge et al., 1987). This result clearly indicates that myelin was not formed by any residual SCs that might not have been detected in the pure neuron cultures (Figures 4A,B). In contrast, in the cultures of DRG neurons to which non-neuronal cells (isolated from acute or chronically denervated sciatic nerve stumps) were added, many elongated Sudan black-positive

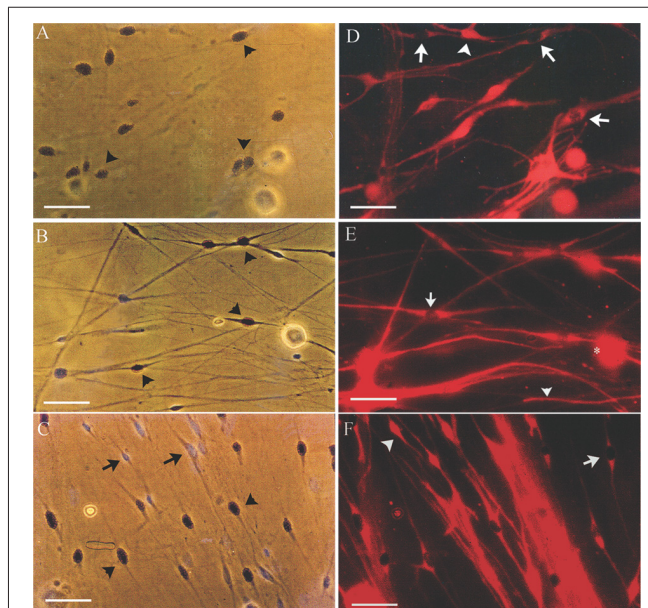


FIGURE 3 | Many SCs in the nerve stump distal to the site of sciatic nerve transection and ligation are in an active proliferative state after acute as well as after chronic denervation, at least for up to 7 weeks. Phase-contrast autoradiographs of isolated acutely (A,D: 7 days) and chronically (B,E: 7 weeks and C,F: 17 months) denervated SCs from right and left hindlimbs, respectively. (A–C) Phase-contrast of the SCs that were exposed to ^3H -thymidine for 24 h to identify dividing cells, 5 days after co-culture with DRG neurons. Many of the SCs incorporated ^3H -thymidine (arrowhead) demonstrating SCs in an active proliferative state in the acute phase of denervation (A) and up to 7 weeks (B). There are visibly more ^3H -Thymidine positive SCs than those that were not dividing (^3H -Thymidine—negative cells shown by arrows) after 7 weeks (B) as compared to 7 days (A). (C,D) Immunostaining of SCs with S-100 identifies the dividing SCs (^3H -thymidine positive SCs—arrows) and those that do not (^3H -thymidine—negative cells shown by arrowheads). The proliferating S-100 positive SCs (arrows) are in close contact with the neurites of the DRG neurons. Scale bars = 30 μm .

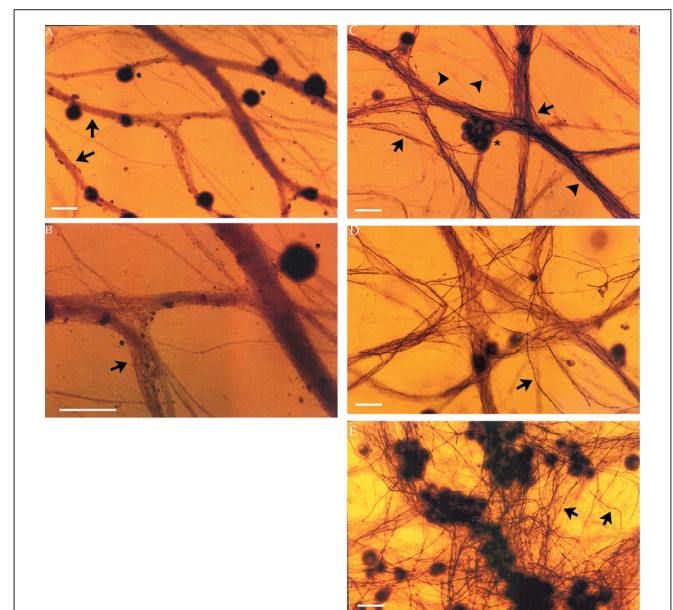


FIGURE 4 | Neurites extended from DRG sensory neurons *in vitro* become myelinated in co-cultures with chronically denervated SCs. Myelination of the axons is not evident in the absence of SCs but it proceeds normally in SC-DRG sensory neuronal co-cultures, even after chronic SC denervation. (A,B) DRG neurons (*) maintained in culture for 24 days without SCs, were not myelinated as indicated by the arrows and seen by absence of Sudan Black staining in the unmyelinated axon bundles. Magnification was 20 \times (A) and 40 \times (B). (C–E) DRG axons were myelinated when DRG neurons were co-cultured with SCs whether or not the SCs were acutely denervated (C: 7 days) or chronically for 7 weeks (D,E) or 17 months by transecting and ligating the sciatic nerve *in vivo* in the right and left hindlimbs, respectively, prior to co-culture. Scale bar = 30 μm .

profiles were observed (Figures 4C–E). These profiles exhibited the well characterized structure of myelin sheaths. These findings demonstrate that the SCs that remain in chronically denervated nerve stumps retain their capacity to form myelin sheaths around neurites.

Neurite myelination was quantitated by counting the myelin segments formed at 24 days after the co-culture of DRG neurons with the acutely and chronically denervated non-neuronal cells (see “Materials and Methods” section). In the assay, the non-neuronal cells that were isolated from chronically denervated sciatic nerve stumps from the left hindlimbs (i.e., the 7-week and 17-month groups) and co-cultured with DRG neurons, elaborated as many myelin segments as was elaborated by those cells isolated from the 7-day (acutely denervated) nerves from the right hindlimbs. The mean values (\pm standard deviations) were not significantly different ($p > 0.05$; Figure 5).

DISCUSSION

This study demonstrated that first, SCs do survive in hindlimb nerve stumps that were chronically denervated for periods of up to 17 months. However, their numbers diminish dramatically. Second, the chronically denervated and atrophic SCs retain their abilities to associate with and to proliferate in response to contact with the neurites that extend from co-cultured DRG neurons. However, the rate at which the SCs re-enter the cell cycle is lower after a long period of denervation. Third, the chronically denervated SCs also sustain their capacity to myelinate the neurites extended in co-cultures of the cells with DRG neurons.

Chronically Denervated SCs Atrophy and Many Die

Regeneration of injured peripheral nerves requires the presence of viable SCs in the denervated nerve stump (Hall, 1986).

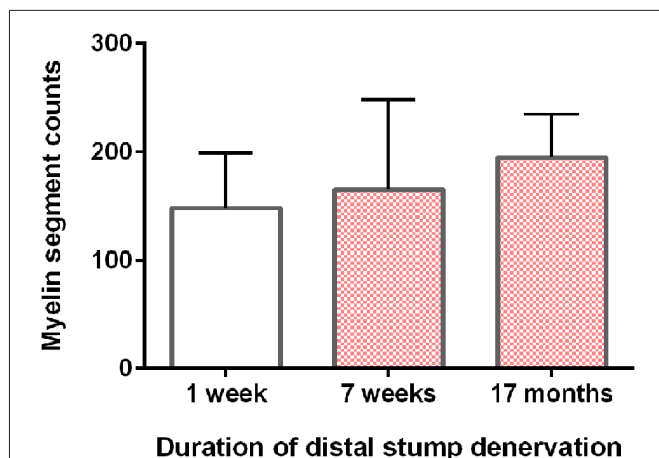


FIGURE 5 | DRG sensory neurites *in vitro* become myelinated irrespective of the duration of SC denervation *in vivo*. The mean (\pm standard deviation) counts of myelin segments in SC-DRG co-cultures. There was no statistical difference in the counts when the co-cultures were performed with SCs that were acutely (7 days) or chronically denervated (7 weeks and 17 months) in the right and left hindlimbs, respectively ($p > 0.05$).

Orphaned SCs normally proliferate in response to the mitogenic factor(s) provided by ingrowing axons (Wood and Bunge, 1975; Salzer and Bunge, 1980; Salzer et al., 1980a,b; Sabue et al., 1984; Pellegrino and Spencer, 1985; Stewart et al., 1991; Morrissey et al., 1995). When SCs are chronically denervated for extended periods of time, the SCs undergo atrophy and decline in number (Weinberg and Spencer, 1978; R  ytt   and Salonen, 1988; Salonen et al., 1988; You et al., 1997; Bradley et al., 1998; Dedkov et al., 2002; Jonsson et al., 2013; Kumar et al., 2016). There is a concomitant decline in the capacity of injured neurons, both motor and sensory, to regenerate their axons (Fu and Gordon, 1995a; Gordon et al., 2011; Jonsson et al., 2013), and in the numbers of regenerated nerve fibers (Jonsson et al., 2013). In our present study, the numbers of non-neuronal cells doubled 7 weeks after chronic distal nerve stump denervation in the experimental left hindlimb as compared to the number in the control right hindlimb (Figure 2A) but the cells likely included mast cells and fibroblasts that accumulate in the denervated stump (Salonen et al., 1988; Ronchi et al., 2017) which, in turn, complete their phagocytic activities within 6–8 weeks prior to withdrawing their processes (R  ytt   and Salonen, 1988). SC nuclei in the distal nerve stump increase \sim 8-fold 25 days after a crush injury (Abercrombie and Johnson, 1946; Abercrombie and Santler, 1957) and to decline thereafter (Bradley and Asbury, 1970). Four weeks after chronic denervation, Salonen et al. (1988) reported an increase of 3.5-fold in SC number, suggesting that the number of proliferating SCs had already declined by 7 weeks. The macrophages that enter into distal nerve stumps within 3 days of denervation decline to low levels within a month (Gibson, 1979; Avellino et al., 1995) and therefore, are not likely to contribute to the non-neuronal cells that were enumerated after chronic denervation in the experimental nerves in the left hindlimbs (Figure 2A) nerve stumps in this study. That several non-neuronal cells enumerated after chronic denervation were likely to be SCs is supported by their S100 immunostaining (Figures 3D–F) after their co-culture with DRG neurons and hence, their exposure to endogenous mitogens on the surface of their neurites (Wood and Bunge, 1975; Salzer and Bunge, 1980; Salzer et al., 1980a,b; Sabue et al., 1984). These SCs demonstrated processes that were closely associated with and aligned along the neurites of the DRG neurons, irrespective of the duration of prior SC denervation *in vivo*.

The apparent discrepancy between the elevated non-neuronal cell numbers, of which most are likely to be SCs, and the reduced neuronal regenerative capacity at 7 weeks (Fu and Gordon, 1995a; Gordon et al., 2011) is likely due to the regression of the SCs to a non-supportive phenotype in which upregulated neurotrophic factors, including brain derived neurotrophic and glial derived neurotrophic factors, their p75 and GFR α -1 and GFR α -2 receptors, respectively, and soluble neuregulin 1 (Type I/II) and its Erb3/4 receptors, have declined back to low baseline values (Hoke et al., 2002, 2006; Boyd and Gordon, 2003; Gordon, 2015; Ronchi et al., 2017).

The non-neural cell numbers of >5 million at 7 days of acute nerve stump denervation in the right control hindlimb is dramatically lower, <2 million, in the right experimental hindlimb after 17 months of chronic stump denervation

(**Figure 2A**), consistent with the progressive decline in numbers of viable SCs that were counted in rat hindlimb nerves after 3 and 6 months chronic denervation followed by 13 weeks nerve regeneration (Jonsson et al., 2013) and with the observed decline with light and electron microscopy, in 1–26-month chronically denervated rabbit nerves (Bradley et al., 1998), and 3–58-week chronically denervated rat nerves (Weinberg and Spencer, 1978). Microscopic observations demonstrated progressive Wallerian degeneration over the course of 7 weeks of chronic nerve stump denervation (You et al., 1997) with progressive disappearance of lipid-laden cells and residual myelin debris with cells of perineurial type (not fibroblasts) encircling small groups of denervated SC columns and progressive increase in the mass of collagen and elastin (Weinberg and Spencer, 1978; Bradley et al., 1998; see also Holmes and Young, 1942; Salonen et al., 1987a,b). The SC basement membranes progressively fragment, the shorter fragments dispersing throughout the endoneurium (Giannini and Dyck, 1990). It is likely that death of non-neuronal cells within chronically denervated nerve stumps explains the dramatic decline in their numbers. The nature of the death pathway is currently unknown and remains to be addressed.

Chronically Denervated SCs Proliferate but Less so Than Acutely Denervated SCs

Despite high number of non-neuronal cells in the 7-week chronically denervated distal nerve stumps in the experimental left hindlimb, the S-100 positive SCs were less able than acutely denervated SCs in the control right hindlimb to proliferate in response to endogenous mitogens released by 5-day co-cultured DRG neurons (**Figure 2B**). Reduced capacity of p75-positive SCs to proliferate was reported by Kumar et al. (2016). At 1 week, ~75% of the acutely denervated SCs proliferated (**Figure 2B**), after which the proliferative capacity fell to ~50% and ~30% 7 weeks and 17 months after chronic denervation, respectively.

These findings of reduced proliferative capacity of chronically denervated SCs in the left hindlimbs contrast with earlier findings that SC proliferation was not altered by prior chronic denervation when the proliferation was evaluated in reinnervated nerve stumps, 13 weeks after surgical repair of 1–6-month chronically injured sciatic nerve stumps via an autograft (Jonsson et al., 2013). It must be recognized though, that, once the epineurium was removed from the excised distal nerve stump in that study, the ~1 mm cut nerve pieces were incubated in a SC growth medium for 2 weeks and that the medium was supplemented by the exogenous mitogens of forskolin and neuregulin NRG1 prior to the isolation and incubation of the SCs for 7 days (see also Kumar et al., 2016). That the proliferative capacity of the SCs within the 13-week reinnervated nerve stumps was the same after this procedure, irrespective of the period of acute or chronic SC denervation that preceded the 13 weeks of nerve regeneration (Jonsson et al., 2013), likely reflected a renewed capacity of the SCs contained within the distal stump to proliferate normally in response to regenerating axons. The demonstration by Casella et al. (1996) of significantly enhanced proliferation of isolated human SCs after their exposure to the same mitogens immediately after

their isolation, as compared to that of the SCs isolated from untreated control nerves, provides further evidence that the proliferative properties of isolated SCs are altered after isolation and culture in media containing exogenous mitogens. In our experiments, proliferation of the SCs was analyzed only after the cells were exposed to the specific SC mitogens that are present on the surface of DRG neurites in the 5-day SC-DRG co-cultures (Wood and Bunge, 1975; Salzer and Bunge, 1980; Salzer et al., 1980a,b).

In the proliferation assay that we used, the isolated non-neuronal cells were labeled for 24 h with ^3H -thymidine after SC-DRG co-culture for 5 days. The cells were then fixed and the dividing SCs identified as p75 immunoreactive (**Figure 3**). Therefore, the proliferation index measures the occurrence of new DNA synthesis and thereby, determines the capacity of the denervated SCs to enter into the cell cycle in response to the endogenous mitogens on the DRG neurons. SCs, whether immediately reinnervated or after a delay of 1–6 months, require time to re-enter the G1 phase of proliferation because significantly more reinnervated SCs proliferated at 5 as compared to 3 days after a 2-week period of incubation (Jonsson et al., 2013). Nonetheless, the reduced proliferation of chronically denervated SCs during the early phase of proliferation argue that the slower rate is unlikely to account for the findings.

The vigorous proliferation that we observed in acutely denervated SCs from the control right hindlimbs (**Figure 2B**) is consistent with the spontaneous upregulation of their erbB receptors following nerve transection (Carroll et al., 1997; Fricker and Bennett, 2011; Fricker et al., 2011; Chang et al., 2013) whilst their reduced proliferation with chronic denervation is likely linked to their downregulation of erbB2/erbB3 receptors (Li et al., 1997; Hall, 1999; Jonsson et al., 2013; Ronchi et al., 2017). The retained, albeit reduced, capacity of chronically denervated SCs to proliferate *in vitro* (**Figure 2B**) and for 5%–10% of freshly injured neurons to regenerate their axons through chronically denervated nerve stumps (Fu and Gordon, 1995a; Sulaiman and Gordon, 2000; Gordon et al., 2011), elaborate normal myelin sheaths, and to recover their normal size once target contacts are remade (Sulaiman and Gordon, 2000), demonstrate that the proliferative quiescence of the chronically denervated SCs from the experimental left hindlimbs is reversible: the dormant SCs re-enter the cell cycle and proliferate (**Figures 2B, 3**), albeit at a more sluggish initial rate.

Chronically Denervated SCs Remyelinate Neurites

Sudan Black staining of the SCs isolated from chronically denervated distal nerve stumps of the experimental left hindlimbs and co-cultured with DRG neurons for 24 days, demonstrated normal capacity to remyelinate the neurites elaborated by the neurons (**Figures 4, 5**). Sudan Black staining of the lipid-rich membranes of compacted myelin sheaths was chosen to demonstrate remyelination of neurites rather than immunostaining because SC immunostaining without Sudan Black staining reveals SCs that are making myelin proteins but are not necessarily making myelin sheaths. SC immunostaining thereby, could give the erroneous impression

that the SCs were making myelin sheaths when they were not. The *in vitro* findings of neurite myelination reported here, corroborate our *in vivo* findings of the remyelination of the low numbers of axons that injured neurons regenerate into chronically denervated nerve stumps (Sulaiman and Gordon, 2000). There were no significant differences in the extent of myelination by acutely or chronically denervated SCs derived from the right and left hindlimbs, respectively, whether the duration of chronic denervation was 7 weeks or 17 months (Figure 5). 1% to 5% of the DRG neurites were well myelinated, irrespective of the duration of the SC denervation *in vivo* prior to their co-culture, the remaining neurites being <1 μ m in diameter and hence, unmyelinated. This “normal” myelinating capacity of chronically denervated SCs contrasts with the “severe impairment” of the myelination of the neurites of DRG neurons by 56-day denervated SCs after the non-neural passaging in the presence of mitogens and subsequent cell sorting (Kumar et al., 2016). This reported “severe impairment” however, does not correspond with the capacity of chronically denervated SCs to myelinate regenerated axons with restoration of the normal proportional relationship between myelin thickness and the size of the myelinated nerves (Sulaiman and Gordon, 2000).

Summary

The survival and sustained capacity of chronically denervated SCs to re-enter the cell cycle together with the sustained capacity for these SCs to form myelin around neurites *in vitro* and regenerating axons *in vivo* indicates that surviving SCs may be stimulated to divide and support axon regeneration and re-myelination after chronic nerve injuries. Overall our results

suggest that failure of axons to regenerate into long denervated nerve trunks is not due to lack of ability of the SCs to interact or respond to the axons. Rather, it is more likely to result from the reduced numbers of chronically injured neurons to regenerate their axons (Fu and Gordon, 1995b) and the extremely small number of SCs available to support and remyelinate the few regenerating axons in chronically denervated nerve stumps that and support nerve regeneration (Fu and Gordon, 1995a; Sulaiman and Gordon, 2000; Gordon et al., 2011). As such, cellular therapy may be a clinically viable option for patients who have sustained injuries to large nerve trunks.

AUTHOR CONTRIBUTIONS

All authors made equal contributions to the data interpretation and writing of the manuscript. PW and OS made the major contributions to the experimental execution.

FUNDING

We are grateful for funding from the Canadian Institutes of Health Research (CIHR).

ACKNOWLEDGMENTS

Our thanks to our colleague Ernesto Felipe-Cuervo for his help with the experiments in Dr. Patrick Wood's laboratory. We are also very grateful to the late Dr. Richard Bunge for his contribution to this manuscript as well as to his many articles during his imminent scientific career. Our thanks to Dr. Doan Nguyen for his assistance with the figures for the manuscript.

REFERENCES

- Abercrombie, M., and Johnson, M. L. (1946). Quantitative histology of Wallerian degeneration; nuclear population in rabbit sciatic nerve. *J. Anat.* 80, 37–50.
- Abercrombie, M., and Santler, J. E. (1957). An analysis of growth in nuclear population during Wallerian degeneration. *J. Cell. Comp. Physiol.* 50, 429–450. doi: 10.1002/jcp.1030500308
- Audisio, C., Nicolino, S., Scevola, A., Tos, P., Geuna, S., Battiston, B., et al. (2008). ErbB receptors modulation in different types of peripheral nerve regeneration. *Neuroreport* 19, 1605–1609. doi: 10.1097/wnr.0b013e32831313ef
- Avellino, A. M., Hart, D., Dailey, A. T., MacKinnon, M., Ellegala, D., and Klot, M. (1995). Differential macrophage responses in the peripheral and central nervous system during Wallerian degeneration of axons. *Exp. Neurol.* 136, 183–198. doi: 10.1006/exnr.1995.1095
- Boyd, J. G., and Gordon, T. (2003). Neurotrophic factors and their receptors in axonal regeneration and functional recovery after peripheral nerve injury. *Mol. Neurobiol.* 27, 277–324. doi: 10.1385/mn:27:3:277
- Bradley, J. L., Abernethy, D. A., King, R. H. M., Muddle, J. R., and Thomas, P. K. (1998). Neural architecture I transected rabbit sciatic nerve after prolonged nonreinnervation. *J. Anat.* 192, 529–538. doi: 10.1046/j.1469-7580.1998.19240529.x
- Bradley, W. G., and Asbury, A. K. (1970). Duration of synthesis phase in neurilemma cells in mouse sciatic nerve during degeneration. *Exp. Neurol.* 26, 275–282. doi: 10.1016/0014-4886(70)90125-1
- Brushart, T. M., Aspalter, M., Griffin, J. W., Redett, R., Hameed, H., Zhou, C., et al. (2013). Schwann cell phenotype is regulated by axon modality and central-peripheral location and persists *in vitro*. *Exp. Neurol.* 247, 272–281. doi: 10.1016/j.expneurol.2013.05.007
- Bunge, M. B. (1994). Transplantation of purified populations of Schwann cells into lesioned adult rat spinal cord. *J. Neurol.* 242, S36–S39. doi: 10.1007/bf00939240
- Cajal, S. R. (1928). *Degeneration and Regeneration of the Nervous System*. London: Oxford University Press (Reedited by DeFelipe J. and Jones E. G.).
- Carroll, S. L., Miller, M. L., Frohnert, P. W., Kim, S. S., and Corbett, J. A. (1997). Expression of neuregulins and their putative receptors, ErbB2 and ErbB3, is induced during Wallerian degeneration. *J. Neurosci.* 17, 1642–1659. doi: 10.1523/jneurosci.17-05-01642.1997
- Casella, G. T., Bunge, R. P., and Wood, P. M. (1996). Improved method for harvesting human Schwann cells from mature peripheral nerve and expansion *in vitro*. *Glia* 17, 327–338. doi: 10.1002/(SICI)1098-1136(199608)17:4<327::AID-GLIA7>3.0.CO;2-W
- Chang, H. M., Shyu, M. K., Tseng, G. F., Liu, C. H., Chang, H. S., Lan, C. T., et al. (2013). Neuregulin facilitates nerve regeneration by speeding Schwann cell migration via ErbB2/3-dependent FAK pathway. *PLoS One* 8:e53444. doi: 10.1371/journal.pone.0053444
- Dedkov, E. I., Kostrominova, T. Y., Borisov, A. B., and Carlson, B. M. (2002). Survival of Schwann cells in chronically denervated skeletal muscles. *Acta Neuropathol.* 103, 565–574. doi: 10.1007/s00401-001-0504-6
- De Leon, M., Welcher, A. A., Suter, U., and Shooter, E. M. (1991). Identification of transcriptionally regulated genes after sciatic nerve injury. *J. Neurosci. Res.* 29, 437–448. doi: 10.1002/jnr.490290404
- Eldridge, C. F., Bunge, M. B., Bunge, R. P., and Wood, P. M. (1987). Differentiation of axon-related Schwann cells *in vitro*. I. Ascorbic acid regulates basal lamina assembly and myelin formation. *J. Cell Biol.* 105, 1023–1034. doi: 10.1083/jcb.105.2.1023
- El Soury, M., Fornasari, B., Morano, M., Grazio, E., Ronchi, G., Incarnato, D., et al. (2018). Soluble Neuregulin1 down-regulates myelination genes in

- schwann cells. *Front. Mol. Neurosci.* 11:157. doi: 10.3389/fnmol.2018.00157
- Fenrich, K., and Gordon, T. (2004). Canadian association of neuroscience review: axonal regeneration in the peripheral and central nervous systems—current issues and advances. *Can. J. Neurol. Sci.* 31, 142–156. doi: 10.1017/s0317167100053798
- Fricker, F. R., and Bennett, D. L. (2011). The role of neuregulin-1 in the response to nerve injury. *Future Neurol.* 6, 809–822. doi: 10.2217/fnl.11.45
- Fricker, F. R., Lago, N., Balarajah, S., Tsantoulas, C., Tanna, S., Zhu, N., et al. (2011). Axonally derived neuregulin-1 is required for remyelination and regeneration after nerve injury in adulthood. *J. Neurosci.* 31, 3225–3233. doi: 10.1523/jneurosci.2568-10.2011
- Fu, S. Y., and Gordon, T. (1995a). Contributing factors to poor functional recovery after delayed nerve repair: prolonged denervation. *J. Neurosci.* 15, 3886–3895. doi: 10.1523/jneurosci.15-05-03886.1995
- Fu, S. Y., and Gordon, T. (1995b). Contributing factors to poor functional recovery after delayed nerve repair: prolonged axotomy. *J. Neurosci.* 15, 3876–3885. doi: 10.1523/jneurosci.15-05-03876.1995
- Fu, S. Y., and Gordon, T. (1997). The cellular and molecular basis of peripheral nerve regeneration. *Mol. Neurobiol.* 14, 67–116. doi: 10.1007/bf02740621
- Funakoshi, H., Frisén, J., Barbany, G., Timmusk, T., Zachrisson, O., Verge, V. M., et al. (1993). Differential expression of mRNAs for neurotrophins and their receptors after axotomy of the sciatic nerve. *J. Cell Biol.* 123, 455–465. doi: 10.1083/jcb.123.2.455
- Gambarotta, G., Fregnan, F., Gnani, S., and Perroteau, I. (2013). Neuregulin 1 role in Schwann cell regulation and potential applications to promote peripheral nerve regeneration. *Int. Rev. Neurobiol.* 108, 223–256. doi: 10.1016/b978-0-12-410499-0.00009-5
- Giannini, C., and Dyck, P. J. (1990). The fate of Schwann cell basement membranes in permanently transected nerves. *J. Neuropathol. Exp. Neurol.* 49, 550–563. doi: 10.1097/00005072-199011000-00002
- Gibson, J. D. (1979). The origin of the neural macrophage: a quantitative ultrastructural study of cell population changes during Wallerian degeneration. *J. Anat.* 129, 1–19.
- Gordon, T. (2015). “The biology, limits and promotion of peripheral nerve regeneration in rats and human,” in *Nerves and Nerve Injuries*, eds R. S. Tubbs, M. Shojia, M. Loukas and R. J. Spinner (New York, NY: Elsevier), 903–1019.
- Gordon, T., and Borschel, G. H. (2017). The use of the rat as a model for studying peripheral nerve regeneration and sprouting after complete and partial nerve injuries. *Exp. Neurol.* 287, 331–347. doi: 10.1016/j.expneurol.2016.01.014
- Gordon, T., Sulaiman, O. A. R., and Boyd, J. G. (2003). Experimental strategies to promote functional recovery after peripheral nerve injuries. *J. Peripher. Nerv. Syst.* 8, 236–250. doi: 10.1111/j.1085-9489.2003.03029.x
- Gordon, T., Tyreman, N., and Raji, M. A. (2011). The basis for diminished functional recovery after delayed peripheral nerve repair. *J. Neurosci.* 31, 5325–5334. doi: 10.1523/jneurosci.6156-10.2011
- Gutmann, E., and Young, J. Z. (1944). The re-innervation of muscle after various periods of atrophy. *J. Anat.* 78, 15–44.
- Hall, S. M. (1986). Regeneration in cellular and acellular autografts in the peripheral nervous system. *Neuropathol. Appl. Neurobiol.* 12, 27–46. doi: 10.1111/j.1365-2990.1986.tb00679.x
- Hall, S. M. (1999). The biology of chronically denervated Schwann cells. *Ann. N Y Acad. Sci.* 883, 215–233. doi: 10.1111/j.1749-6632.1999.tb08584.x
- Hoke, A., Gordon, T., Zochodne, D. W., and Sulaiman, O. A. R. (2002). A decline in glial cell-line-derived neurotrophic factor expression is associated with impaired regeneration after long-term Schwann cell denervation. *Exp. Neurol.* 173, 77–85. doi: 10.1006/exnr.2001.7826
- Hoke, A., Redett, R., Hameed, H., Jari, R., Zhou, C., Li, Z. B., et al. (2006). Schwann cells express motor and sensory phenotypes that regulate axon regeneration. *J. Neurosci.* 26, 9646–9655. doi: 10.1523/jneurosci.1620-06.2006
- Holmes, W., and Young, J. Z. (1942). Nerve regeneration after immediate and delayed suture. *J. Anat.* 77, 63–108.
- Jejurikar, S. S., Marcelo, C. L., and Kuzon, W. M. Jr. (2002). Skeletal muscle denervation increases satellite cell susceptibility to apoptosis. *Plast. Reconstr. Surg.* 110, 160–168. doi: 10.1097/00006534-200207000-00027
- Jessen, K. R., and Mirsky, R. (2016). The repair Schwann cell and its function in regenerating nerves. *J. Physiol.* 594, 3521–3531. doi: 10.1113/jp270874
- Jonsson, S., Wiberg, R., McGrath, A. M., Novikov, L. N., Wiberg, M., Novikova, L. N., et al. (2013). Effect of delayed peripheral nerve repair on nerve regeneration, Schwann cell function and target muscle recovery. *PLoS One* 8:e56484. doi: 10.1371/journal.pone.0056484
- Kleitman, N., Wood, P., Johnson, M. I., and Bunge, R. P. (1988). Schwann cell surfaces but not extracellular matrix organized by Schwann cells support neurite outgrowth from embryonic rat retina. *J. Neurosci.* 8, 653–663. doi: 10.1523/jneurosci.08-02-00653.1988
- Kline, D. G., and Hudson, A. R. (1995). *Nerve Injuries: Operative Results for Major Nerve Injuries, Entrapments and Tumors*. Philadelphia: W.B. Sanders.
- Kobayashi, J., Mackinnon, S. E., Watanabe, O., Ball, D. J., Gu, X. M., Hunter, D. A., et al. (1997). The effect of duration of muscle denervation on functional recovery in the rat model. *Muscle Nerve* 20, 858–866. doi: 10.1002/(sici)1097-4598(199707)20:7<858::aid-mus10>3.0.co;2-o
- Kumar, R., Sinha, S., Hagner, A., Stykel, M., Raharjo, E., Singh, K. K., et al. (2016). Adult skin-derived precursor Schwann cells exhibit superior myelination and regeneration supportive properties compared to chronically denervated nerve-derived Schwann cells. *Exp. Neurol.* 278, 127–142. doi: 10.1016/j.expneurol.2016.02.006
- Li, H., Terenghi, G., and Hall, S. M. (1997). Effects of delayed re-innervation on the expression of c-erbB receptors by chronically denervated rat Schwann cells *in vivo*. *Glia* 20, 333–347. doi: 10.1002/(SICI)1098-1136(199708)20:4<333::AID-GLIA6>3.0.CO;2-6
- Liang, C., Tao, Y., Shen, C., Tan, Z., Xiong, W. C., and Mei, L. (2012). Erbin is required for myelination in regenerated axons after injury. *J. Neurosci.* 32, 15169–15180. doi: 10.1523/jneurosci.2466-12.2012
- Meyer, M., Matsuoka, I., Wetmore, C., Olson, L., and Thoenen, H. (1992). Enhanced synthesis of brain-derived neurotrophic factor in the lesioned peripheral nerve: different mechanisms are responsible for the regulation of BDNF and NGF mRNA. *J. Cell Biol.* 119, 45–54. doi: 10.1083/jcb.119.1.45
- Mi, R., Chen, W., and Hoke, A. (2007). Pleiotrophin is a neurotrophic factor for spinal motor neurons. *Proc. Natl. Acad. Sci. U S A* 104, 4664–4669. doi: 10.1073/pnas.0603243104
- Morrissey, T. K., Levi, A. D., Nuijens, A., Sliwkowski, M. X., and Bunge, R. P. (1995). Axon-induced mitogenesis of human Schwann cells involves heregulin and p185erbB2. *Proc. Natl. Acad. Sci. U S A* 92, 1431–1435. doi: 10.1073/pnas.92.5.1431
- Naveilhan, P., ElShamy, W. M., and Ernfors, P. (1997). Differential regulation of mRNAs for GDNF and its receptors Ret and GDNFR α after sciatic nerve lesion in the mouse. *Eur. J. Neurosci.* 9, 1450–1460. doi: 10.1111/j.1460-9568.1997.tb01499.x
- Pellegrino, R. G., and Spencer, P. S. (1985). Schwann cell mitosis in response to regenerating peripheral axons *in vivo*. *Brain Res.* 341, 16–25. doi: 10.1016/0006-8993(85)91467-2
- Ronchi, G., Cillino, M., Gambarotta, G., Fornasari, B. E., Raomondo, S., Pugliese, P., et al. (2017). Irreversible changes occurring in long-term denervated Schwann cells after delayed nerve repair. *J. Neurosurg.* 127, 843–856. doi: 10.3171/2016.9.jns.16140
- Ronchi, G., Haastert-Talini, K., Fornasari, B. E., Perroteau, I., Geuna, S., Gambarotta, G., et al. (2016). The Neuregulin1/ErbB system is selectively regulated during peripheral nerve degeneration and regeneration. *Eur. J. Neurosci.* 43, 351–364. doi: 10.1111/ejn.12974
- Röyttä, M., and Salonen, V. (1988). Long-term endoneurial changes after nerve transection. *Acta Neuropathol.* 76, 35–45. doi: 10.1007/bf00687678
- Sabue, G., Brown, M. J., Kim, S. U., and Pleasure, D. (1984). Axolemma is a mitogen for human Schwann cells. *Ann. Neurol.* 15, 449–452. doi: 10.1002/ana.410150508
- Salonen, V., Aho, H., Röyttä, M., and Peltonen, J. (1988). Quantitation of Schwann cells and endoneurial fibroblast-like cells after experimental nerve trauma. *Acta Neuropathol.* 75, 331–336. doi: 10.1007/bf00687785
- Salonen, V., Peltonen, J., Röyttä, M., and Virtanen, I. (1987a). Laminin in traumatized peripheral nerve: basement membrane changes during degeneration and regeneration. *J. Neurocytol.* 16, 713–720. doi: 10.1007/bf01637662
- Salonen, V., Röyttä, M., and Peltonen, J. (1987b). The effects of nerve transection on the endoneurial collagen fibril sheaths. *Acta Neuropathol.* 74, 13–21. doi: 10.1007/bf00688333

- Salzer, J. L., and Bunge, R. P. (1980). Studies of Schwann cell proliferation. I. An analysis of tissue culture of proliferation during development, Wallerian degeneration and direct injury. *J. Cell Biol.* 84, 739–752. doi: 10.1083/jcb.84.3.739
- Salzer, J. L., Bunge, R. P., and Glaser, L. (1980a). Studies of Schwann cell proliferation. III. Evidence for the surface localization of the neurite mitogen. *J. Cell Biol.* 84, 767–778. doi: 10.1083/jcb.84.3.767
- Salzer, J. L., Williams, A. K., Glaser, L., and Bunge, R. P. (1980b). Studies of Schwann cell proliferation. II. Characterization of the stimulation and specificity of the response to a neurite membrane fraction. *J. Cell Biol.* 84, 753–766. doi: 10.1083/jcb.84.3.753
- Son, Y.-J., and Thompson, W. J. (1995). Schwann cell processes guide regeneration of peripheral axons. *Neuron* 14, 125–132. doi: 10.1016/0896-6273(95)90246-5
- Stewart, H. J., Eccleston, P. A., Jessen, K. R., and Mirsky, R. (1991). Interaction between cAMP elevation, identified growth factors, and serum components in regulating Schwann cell growth. *J. Neurosci. Res.* 30, 346–352. doi: 10.1002/jnr.490300210
- Sulaiman, O. A. R., and Gordon, T. (2000). Effects of short- and long-term Schwann cell denervation on peripheral nerve regeneration, myelination and size. *Glia* 32, 234–246. doi: 10.1002/1098-1136(200012)32:3<234::aid-glia40>3.0.co;2-3
- Sunderland, S. (1978). *Nerve and Nerve Injuries*. Edinburgh: Churchill Livingstone.
- Toy, D., and Namgung, U. (2013). Role of glial cells in axonal regeneration. *Exp. Neurobiol.* 22, 68–76. doi: 10.5607/en.2013.22.2.68
- Vuorinen, V., Siironen, J., and Røyttä, M. (1995). Axonal regeneration into chronically denervated distal stump. 1. Electron microscope studies. *Acta Neuropathol.* 89, 209–218. doi: 10.1007/bf00309336
- Weinberg, H. J., and Spencer, P. S. (1978). The fate of Schwann cells isolated from axonal contact. *J. Neurocytol.* 7, 555–569. doi: 10.1007/bf01260889
- Witzel, C., Rohde, C., and Brushart, T. M. (2005). Pathway sampling by regenerating peripheral axons. *J. Comp. Neurol.* 485, 183–190. doi: 10.1002/cne.20436
- Wood, P. M., and Bunge, R. P. (1975). Evidence that sensory axons are mitogenic for Schwann cells. *Nature* 256, 662–664. doi: 10.1038/256662a0
- You, S., Petrov, T., Chung, P. H., and Gordon, T. (1997). The expression of the low affinity nerve growth factor receptor in long-term denervated Schwann cells. *Glia* 20, 87–100. doi: 10.1002/(sici)1098-1136(199706)20:2<87::aid-glia1>3.0.co;2-1

Conflict of Interest Statement: The authors declare that the research was conducted in the absence of any commercial or financial relationships that could be construed as a potential conflict of interest.

Copyright © 2019 Gordon, Wood and Sulaiman. This is an open-access article distributed under the terms of the Creative Commons Attribution License (CC BY). The use, distribution or reproduction in other forums is permitted, provided the original author(s) and the copyright owner(s) are credited and that the original publication in this journal is cited, in accordance with accepted academic practice. No use, distribution or reproduction is permitted which does not comply with these terms.



The Role of BDNF in Peripheral Nerve Regeneration: Activity-Dependent Treatments and Val66Met

Claire Emma McGregor* and Arthur W. English

Department of Cell Biology, Emory University School of Medicine, Atlanta, GA, United States

Despite the ability of peripheral nerves to spontaneously regenerate after injury, recovery is generally very poor. The neurotrophins have emerged as an important modulator of axon regeneration, particularly brain derived neurotrophic factor (BDNF). BDNF regulation and signaling, as well as its role in activity-dependent treatments including electrical stimulation, exercise, and optogenetic stimulation are discussed here. The importance of a single nucleotide polymorphism in the *BDNF* gene, Val66Met, which is present in 30% of the human population and may hinder the efficacy of these treatments in enhancing regeneration after injury is considered. Preliminary data are presented on the effectiveness of one such activity-dependent treatment, electrical stimulation, in enhancing axon regeneration in mice expressing the met allele of the Val66Met polymorphism.

Keywords: peripheral nerve injury, BDNF, Val66Met, trkB, electrical stimulation, exercise, optogenetics

OPEN ACCESS

Edited by:

Esther Udina,
Autonomous University of Barcelona,
Spain

Reviewed by:

Doychin N. Angelov,
Medizinische Fakultät, Universität zu
Köln, Germany
Guilherme Lucas,
University of São Paulo, Brazil

*Correspondence:

Claire Emma McGregor
clairekmcgregor@gmail.com

Received: 26 September 2018

Accepted: 14 December 2018

Published: 11 January 2019

Citation:

McGregor CE and English AW (2019)
The Role of BDNF in Peripheral Nerve
Regeneration: Activity-Dependent
Treatments and Val66Met.
Front. Cell. Neurosci. 12:522.
doi: 10.3389/fncel.2018.00522

PERIPHERAL NERVE INJURY

Despite the ability of axons in peripheral nerves to regenerate, recovery is generally very poor (Portincasa et al., 2007; Scholz et al., 2009). The cellular changes that occur after an injury often cannot sustain axon regeneration for the duration required to reinnervate target organs (Fu and Gordon, 1995a,b). The neurotrophins have emerged as an important modulator of axon regeneration, particularly brain derived neurotrophic factor (BDNF). Here, we will review BDNF and its role in activity-dependent treatments to enhance regeneration. Then we will discuss a single nucleotide polymorphism in the *bdnf* gene, Val66Met, which is present in 30% of the human population and may hinder the efficacy of these treatments (Egan et al., 2003; Shimizu et al., 2004). Finally, we will present preliminary data on the effectiveness of one such activity-dependent treatment, electrical stimulation (ES), in enhancing axon regeneration in mice expressing the met allele of the Val66Met polymorphism.

BRAIN DERIVED NEUROTROPHIC FACTOR

BDNF is a member of the neurotrophin family, which also includes nerve growth factor (NGF), neurotrophin 3 (NT3), and neurotrophin 4/5 (NT4/5). BDNF is required for normal development—BDNF knockout (KO) is embryonic lethal (Jones et al., 1994; Schwartz et al., 1997). In adulthood, BDNF is involved in synaptic plasticity, long term potentiation (LTP), learning and memory as well as hippocampal neurogenesis and regeneration after injury (Lindsay, 1988; Lewin and Barde, 1996; Lu et al., 2014; Richner et al., 2014). In the subsequent paragraphs, we review

how BDNF is regulated at the level of mRNA transcripts, protein trafficking, and receptor binding, following with its role in peripheral nerve regeneration.

Regulation of BDNF Transcripts

The human *BDNF* gene resides on the short arm of the 11th chromosome (Maisonpierre et al., 1991). It consists of 9 exons—eight 5' untranslated exons and one protein coding 3' exon (Figure 1) (Liu et al., 2006; Aid et al., 2007; Pruunsild et al., 2007). Through alternative splicing, 17 distinct mRNA transcripts for BDNF have been identified in humans and 11 in rodents (Pruunsild et al., 2007). Additionally, the 3'UTR of the gene contains two polyadenylation sites, resulting in both a long 3'UTR and a short 3'UTR, doubling the possible splice variants. The entire protein-coding region resides on exon IX, so the mature BDNF protein synthesized is identical regardless of mRNA splicing. Splice variants allow for spatial and temporal control of the BDNF transcript.

Spatial control of the 5'UTRs can be seen in exon expression throughout the body. BDNF transcripts containing exons I, II, and III are found exclusively in the brain, and transcripts containing exon IV are predominantly found peripherally in the lung and heart, but can also be found in brain tissue (Timmusk et al., 1993). Even within brain tissue, different promoters can be found in different cell types. For example, exon IV transcripts are required for proper GABAergic interneuron function in the prefrontal cortex (Sakata et al., 2009).

Many different stimuli exert temporal control over BDNF transcription. In cultured cortical neurons, Ca^{2+} influx results predominantly in transcription of exon IV-containing mRNA (Tao et al., 1998). This promoter contains a cAMP/ Ca^{2+} -response element-like element (CaRE3/CRE) that is required for activity-dependent transcription (Tao et al., 1998; Hong et al., 2008). The transcription factor CREB binds this element, is phosphorylated by calcium-regulated kinase cascades, and recruits transcriptional machinery resulting in Ca^{2+} dependent transcription of exon IV-containing BDNF mRNA (West et al., 2001; Lonze and Ginty, 2002). Other stimuli have been identified in modulating BDNF expression. In motoneurons, exon VI

transcripts are androgen sensitive, despite no known androgen response element on the *bdnf* gene (Ottem et al., 2010; Sabatier and English, 2015). There is, however, an estrogen response element (Sohrabji et al., 1995). SRY-box containing gene 11 (Sox11), a transcription factor involved in neuronal survival, axon growth, and regeneration after injury, increases exon I containing BDNF mRNA transcripts specifically in peripheral DRG neurons, but not in CNS neurons (Jankowski et al., 2006; Salerno et al., 2012; Struebing et al., 2017). Exons II and VI are sensitive to tricyclic and atypical antidepressants (Vaghi et al., 2014).

A further role for 5' promoter exons regulating BDNF mRNA may lie in mRNA trafficking. In both cortical and hippocampal neurons, BDNF mRNA is found in dendrites and activity induces trafficking of BDNF mRNA to distal dendrites (Tongiorgi et al., 1997; Capsoni et al., 1999; Chiaruttini et al., 2008, 2009). Interestingly, only certain splice variants are found in dendrites—those containing exons IIB, IIC, and VI (Pattabiraman et al., 2005; Chiaruttini et al., 2008). Transcripts containing exons I, III, and IV are restricted to the cell body.

Further spatial and temporal translational control of BDNF mRNA may come via the 3'UTR. The *bdnf* 3' UTR contains two polyadenylation sites. This allows for both a long 3'UTR and a short 3'UTR to be transcribed (Timmusk et al., 1993; Aid et al., 2007; Pruunsild et al., 2007). These different 3'UTRs are thought to determine mRNA trafficking within the cell. Both the long and short 3'UTR transcripts can be found in the dendrites under different conditions (Vicario et al., 2015). However, in general, the long 3'UTR transcripts are trafficked to the dendrites, where local BDNF synthesis can regulate pruning and enlargement of synapses, whereas the short 3'UTR transcripts stay in the cell body (An et al., 2008). Both depolarization of the neuron as well as BDNF itself increase the number of BDNF mRNA transcripts targeted to the dendrites (Tongiorgi et al., 1997; Righi et al., 2000). Remarkably, the short 3'UTR transcripts account for the majority of BDNF translation, whereas the long 3'UTR transcripts are translationally repressed by RNA binding proteins which stabilize the mRNA until neural activity elicits rapid local translation (Lau et al., 2010; Allen et al., 2013; Vaghi et al., 2014). Calcium influx associated with neuronal activity

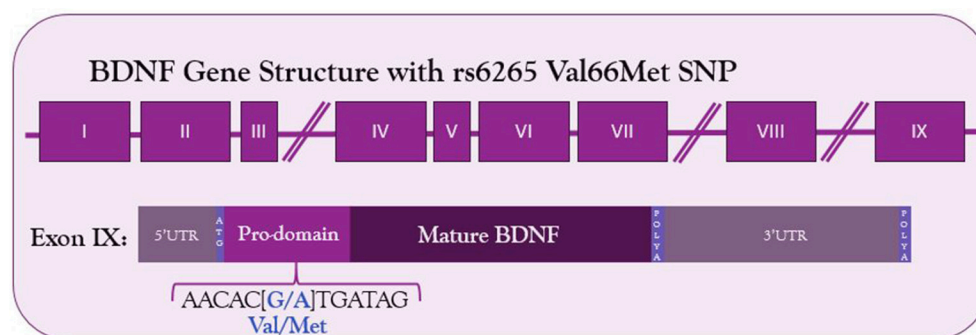


FIGURE 1 | Structure of BDNF gene and location of Val66Met SNP in the coding exon IX. The G to A substitution in the prodomain results in a valine to methionine substitution and decreased Ca^{2+} -dependent release of BDNF.

also results in increased stabilization of BDNF mRNA (Fukuchi and Tsuda, 2010). Conversely, the 3'UTR also contains regions which interact with microRNAs, which are short, non-coding RNA strands that complement mRNA transcripts and result in transcript degradation (Bartel, 2004). Numerous microRNAs have been identified as regulators of BDNF, and microRNA access to binding sites depends on the presence of the long or short 3'UTR (Mellios et al., 2008; Varendi et al., 2014).

BDNF Trafficking and Secretion

BDNF, like the other neurotrophins, is synthesized as a pre-proprotein. The pre-domain functions as a signaling peptide that directs synthesis to the endoplasmic reticulum (ER) for future packaging as a secretory protein. It is immediately cleaved to form proBDNF upon sequestration in the ER (Lessmann et al., 2003). Within the ER, proBDNF forms homodimers (Kolbeck et al., 1994). Both proBDNF and a further cleaved form, mature BDNF, can be packaged into vesicles and secreted. ProBDNF is approximately 29 kDa, and once cleaved, mature BDNF is approximately 14 kDa (Seidah et al., 1996a). Intracellularly, cleavage can occur within the trans-Golgi network or secretory vesicles by furin, a protease, and proprotein convertases PCSK6 and PC5-6b. Extracellularly, cleavage is executed by tissue plasminogen activator or matrix metalloproteinases, which are secreted in an activity-dependent manner (Krystosek and Seeds, 1981; Gualandris et al., 1996; Seidah et al., 1996a,b; Lee et al., 2001; Mowla et al., 2001; Hwang et al., 2005; Keifer et al., 2009; Nagappan et al., 2009; Yang et al., 2009). Once cleaved, the prodomain is not immediately degraded, and can be secreted with mature BDNF (Anastasia et al., 2013).

From the trans-Golgi network, BDNF is directed to two different secretory pathways: a constitutive pathway and a regulated, Ca^{2+} dependent pathway (Mowla et al., 1999; Lessmann et al., 2003; Kuczewski et al., 2009). The constitutive pathway consists of small granules (50–100 nm diameter) that fuse with the cell membrane near the neuronal somata and proximal processes. The regulated secretory pathway consists of larger granules (300 nm diameter) that fuse in distal processes and axon terminals (Conner et al., 1997; Kohara et al., 2001; Brigadski et al., 2005; Dieni et al., 2012). The dual pathway for release is distinctive of BDNF. The other neurotrophins are preferentially secreted through a constitutive pathway. Under normal conditions, most neuronal BDNF is packaged into the regulated pathway (Lu et al., 2014).

Two important interactions have been identified in the sorting of BDNF into the regulatory pathway. The first to be discovered was the interaction between the sorting receptor carboxipeptidase E (CPE) and a three-dimensional motif on the mature domain of BDNF (Lou et al., 2005). Knocking out CPE in cortical neurons blocks activity-dependent release of BDNF and increases constitutive release. Similarly, adding this motif to NGF redirected its release to the regulated secretory pathway (Lou et al., 2005). The second interaction is between the prodomain and the protein sortilin (Chen et al., 2005). Sortilin is localized predominantly to the Golgi apparatus and interacts with the BDNF prodomain to direct it to the regulated secretory pathway (Nielsen et al., 2001; Chen et al., 2005). When sortilin

is unable to interact with the prodomain of BDNF, regulated release is decreased, but there is no compensatory increase in constitutive release (Chen et al., 2005; Lu et al., 2005). This has led to the hypothesis that the interaction between sortilin and the prodomain of BDNF is necessary for proper protein folding, which allows CPE to interact with the mature domain and sort BDNF into one of the two pathways (Lu et al., 2005). When NT-4/5, which is secreted constitutively, is modified to contain the BDNF prodomain, it is trafficked to the regulated secretory pathway (Brigadski et al., 2005). Similarly, blocking the cleavage of the prodomain of NGF, which is also released constitutively, results in its sorting into regulated secretory pathways (Mowla et al., 1999).

BDNF Receptors

Once secreted, BDNF can bind to one of two receptors—tropomyosin receptor kinase B (trkB) or the common neurotrophin receptor, p75^{NTR}. Mature BDNF preferentially binds trkB, resulting in pro-growth signaling, whereas proBDNF (as well as the other proneurotrophins) preferentially binds p75^{NTR}, resulting in antigrowth signaling (Lee et al., 2001). BDNF is primarily secreted as proBDNF (Mowla et al., 1999, 2001; Chen et al., 2004). Thus the availability of proteins that cleave the prodomain may regulate which receptor is activated by BDNF release, providing another mechanism for control of BDNF signaling.

The trkB receptor is a typical tyrosine kinase. When ligand is bound, it dimerizes and autophosphorylates. In addition to BDNF, trkB can also bind NT-4/5. Several isoforms of trkB have been discovered, including isoforms that change its sensitivity to NT-4/5, as well as a truncated form that lacks an intracellular kinase domain (Eide et al., 1996). The truncated form acts as a dominant negative receptor, forming heterodimers with full length trkB receptors and blocking neurotrophin signaling (Eide et al., 1996; Fryer et al., 1997). Another possible role for truncated trkB on astrocytes and Schwann cells may be to act to control the pool of available neurotrophins, preventing them from degrading or signaling until released into the extracellular space (Alderson et al., 2000). In its full-length form, trkB has several intracellular tyrosine residues that can be phosphorylated (Huang and Reichardt, 2003). Three possible signaling cascades are then activated: phospholipase C gamma (PLC γ); phosphatidylinositol-3 kinase (PI3K); and mitogen activated protein kinase/extracellular receptor kinase (MAPK/ERK) (Reichardt, 2006).

The phosphorylation of residue Y490 creates a binding site for adaptor protein Shc (Patapoutian and Reichardt, 2001). Shc binding trkB allows for activation of Ras and further activation of the MAPK/ERK pathway. Downstream of this pathway is mechanistic target of rapamycin (mTOR). Shc binding residue Y490 also results in the recruitment of PI3K and activation of protein kinase B (Akt) (Reichardt, 2006). The phosphorylation of residue Y785 creates a binding site for PLC γ , which is then phosphorylated by trkB (Patapoutian and Reichardt, 2001). This phosphorylation activates PLC γ , which then hydrolyzes phosphatidylinositides to generate diacylglycerol (DAG), which activates protein kinase C (PKC), and inositol 1,4,5 triphosphate

(IP₃), which results in an influx of intracellular Ca²⁺ stores from the ER. These signaling cascades all converge at the level of the nucleus, where transcription is affected through CREB and other transcription factors (Minichiello, 2009).

Once bound to ligand, trkB is endocytosed to form a signaling endosome (Delcroix et al., 2003; Reichardt, 2006). Both ligand and receptor are contained within the endosome, allowing trkB to continue signaling as it is trafficked through the cell. In this way, trkB can be moved closer to the nucleus, where it can affect gene transcription, as well as brought into closer proximity to signaling effectors (Delcroix et al., 2003). However, not all actions of trkB happen at the level of the soma—BDNF-trkB activation has been shown to affect local protein synthesis in the growth cone as well (Yao et al., 2006).

The second receptor for BDNF is the pan-neurotrophin receptor, p75^{NTR} (Rodríguez-Tébar et al., 1992). Generally thought of as a pro-death receptor, p75^{NTR} is a member of the tumor necrosis factor receptor super family and contains a cytosolic death domain (Liepinsh et al., 1997; Locksley et al., 2001). It is expressed primarily during development, but sensory neurons and spinal motoneurons maintain low expression through adulthood (Ernfors et al., 1989; Heuer et al., 1990; Wyatt et al., 1990; Ibáñez and Simi, 2012). Its cytosolic domain is non-enzymatic, so its actions depend entirely on associations with cytoplasmic proteins (Nagata, 1997). Despite its canonical role, p75^{NTR} can mediate both pro-death and pro-survival signals depending on its cytosolic partners. For example, p75^{NTR} is required during development for normal neuron growth and ramification (Yamashita et al., 1999). Multiple adaptor complexes interact with its cytosolic domain to mediate downstream effects (Dechant and Barde, 2002).

Additionally, p75^{NTR} has multiple membrane-bound and extracellular binding partners which can alter whether its signaling is pro-survival or pro-death. Through extracellular pairing with sortilin, p75^{NTR} is able to bind the proneurotrophins (Nykjaer et al., 2004; Teng et al., 2005), resulting in pro-death or anti-growth signaling through downstream JNK activation or caspase activation (Reichardt, 2006). However, neurotrophin binding to p75^{NTR} can also result in NFκB activity, which is a pro-survival signal (Carter et al., 1996; Hamanoue et al., 1999; Middleton et al., 2000). One key protein regulated by p75^{NTR} is RhoA, a small GTPase that regulates the actin cytoskeleton and inhibits axon elongation (Walsh et al., 1999; Schmidt and Hall, 2002). Through such interactions with the so-called death domain of p75^{NTR}, neurotrophin binding inhibits Rho (Yamashita et al., 1999; Roux and Barker, 2002). Through forming a receptor complex with the Nogo receptor, NgR1, p75^{NTR} can act as a receptor for myelin-associated glycoprotein (MAG) (Wang et al., 2002), which enhances Rho activation and results in neurite collapse (Mi et al., 2004). Curiously, p75^{NTR} can act as a binding partner for the trks, including trkB, and increases affinity and selectivity of binding and thus enhancing trk signaling (Bibel et al., 1999).

Like trkB, truncated forms of p75^{NTR} have been identified. One short p75^{NTR} isoform lacks an extracellular ligand binding domain, but contains its intracellular machinery (Roux and Barker, 2002). This form is unable to bind the neurotrophins

(Dechant and Barde, 1997). The extracellular domain of p75^{NTR} can also be cleaved by extracellular metalloproteinases (Roux and Barker, 2002). These isoforms could act as modulators of neurotrophin signaling.

The two receptors for BDNF are generally thought to have opposing roles and may mediate a balance between growth and death. trkB has a higher affinity for mBDNF, but as levels of neurotrophin increase, p75^{NTR} will also bind mBDNF and activate signals in direct opposition to trkB. Because of the different affinities for pro- and mature BDNF, cleavage of BDNF becomes another mechanism to control its downstream signaling effects (Lee et al., 2001). Depolarization of a neuron, which results in secretion of BDNF, also results in secretion of tissue plasminogen activator which cleaves proBDNF to create mature BDNF (Gualandris et al., 1996). BDNF-trkB signaling increases expression of matrix metalloproteinase 9, which also cleaves BDNF (Kuzniwska et al., 2013).

ROLE OF BDNF IN PERIPHERAL NERVE INJURY

In peripheral nerves, BDNF is synthesized by motoneurons, a subset of DRG neurons, and Schwann cells (Apfel et al., 1996; Cho et al., 1997; Michael et al., 1997). After nerve crush or complete transection, BDNF mRNA increases in all three cell types, including in trkB- and trkC-expressing DRG neurons not found previously to express BDNF (Meyer et al., 1992; Funakoshi et al., 1993; Kobayashi et al., 1996; Michael et al., 1999; Al Majed et al., 2000a; English et al., 2007). BDNF mRNA can be found in low levels in the sciatic nerve, and after injury, that expression is upregulated. This upregulation is sustained over the course of weeks and can be attributed to both neuronal and non-neuronal sources (Meyer et al., 1992; Funakoshi et al., 1993). In facial nerve injury, upregulation of BDNF is correlated with enhanced functional outcome (Grosheva et al., 2016).

Following sciatic nerve injury, a transient increase in both BDNF and full length trkB mRNA is found in motoneurons (Kobayashi et al., 1996; Al Majed et al., 2000a). Unlike sensory neurons, NGF and trkA are not expressed by motoneurons, nor are they upregulated after injury (Funakoshi et al., 1993; Escandon et al., 1994). There is a small and short-lived upregulation of NT3 and NT4/5 in motoneurons (Funakoshi et al., 1993). TrkC is expressed by adult motoneurons, but it is not upregulated after injury (Johnson et al., 1999). Thus, the rapid upregulation of BDNF and trkB make it likely that BDNF is the main neurotrophin mediating early motoneuron response to nerve injury (Boyd and Gordon, 2003).

Schwann cells express only the truncated form of trkB, which has the potential to act as a dominant negative receptor for BDNF and NT4/5. Schwann cell truncated trkB mRNA levels decrease significantly after sciatic nerve injury (Frisén et al., 1993). This could be viewed as pro-regenerative, enabling available BDNF to bind to trkB receptors on regenerating neurites and enhance their growth. Conversely, after injury, Schwann cells upregulate p75^{NTR}, which has been suggested to result in sequestration of

neurotrophins and inhibit regeneration (Taniuchi et al., 1986; Bibel et al., 1999; Scott and Ramer, 2010).

trkB in Peripheral Nerve Injury

Axons regenerate through the formation of growth cones, which need cytoskeletal proteins, such as actin and tubulin, to extend and stabilize the new growth. Beta actin mRNA is localized to peripheral axons, and peripheral nerve injury triggers actin mRNA to be transported down the axon for local protein synthesis (Koenig et al., 2000; Sotelo-Silveira et al., 2008; Willis et al., 2011). BDNF/trkB signaling triggers local translation of transported mRNAs through a Ca^{2+} -dependent mechanism, and this is required for bidirectional turning toward BDNF (Yao et al., 2006). BDNF application to injured axons increases the number of actin waves (transport of actin filaments and associated proteins toward the growth cone) per hour (Difato et al., 2011; Inagaki and Katsuno, 2017). Neurotrophins also stimulate growth cone sprouting and actin accumulation in the sprouts (Gallo and Letourneau, 1998). Both of these processes are mediated through the PIP3/PI3K signaling pathway described above (Asano et al., 2008). When an actin wave reaches the growth cone, the growth cone enlarges, branches, and undergoes forward expansion (Flynn et al., 2009). Application of BDNF to growth cones results in microtubule reorganization to form lamellipodial as well as filopodial elongation (Gibney and Zheng, 2003).

In addition to local protein synthesis, trkB signaling has effects on cyclic AMP (cAMP) production, which may be important for the initial extension of growth cones across the site of injury. The MAPK/ERK pathway of BDNF/trkB signaling results in inhibition of phosphodiesterases (PDE) which normally degrade cAMP (Gao et al., 2003). As such, BDNF/trkB signaling results in increased levels of cAMP (Souness et al., 2000; Gao et al., 2003). This pathway has been shown to be necessary to overcome inhibition by MAG, and therefore PDE inhibition has been most thoroughly studied in models of spinal cord injury, where MAG inhibition of axon growth creates a substantial barrier to regeneration (Cai et al., 1999; Gao et al., 2003; Batty et al., 2017). Although injured peripheral nerves do not suffer inhibition by MAG to the same extent as that seen in the central nervous system, early in the regeneration process, inhibitory proteoglycans and myelin debris form an impermissible environment for axon regeneration (Shen et al., 1998). Increasing cAMP through PDE inhibition enhances peripheral regeneration after injury, and it is likely that trkB activation contributes to this cAMP-mediated effect on regeneration (Gordon et al., 2009; Udina et al., 2010).

The different neurotrophin signaling pathways activated through trk receptors converge at the level of transcription in the nucleus. CREB, resulting from trkB-generated PI3K-Akt activation, increases sensory neurite outgrowth (White et al., 2000). Inhibiting phosphatase and tensin homolog (PTEN), an endogenous inhibitor of the PI3K pathway, through genetic knock out or pharmacology, enhances peripheral nerve regeneration *in vivo* and neurite outgrowth *in vitro* (Park et al., 2008; Christie et al., 2010). Numerous other transcription factors downstream of MAPK/ERK signaling, such as c-jun, STAT3, and

ATF-3, have all been associated with changes in gene expression after injury that enhance survival and regeneration (Makwana and Raivich, 2005). mTOR, also downstream of MAPK/ERK signaling and repressed by PTEN, regulates protein synthesis and is also beneficial for DRG regeneration after injury (Park et al., 2008; Abe et al., 2010).

p75^{NTR} in Peripheral Nerve Injury

Because of its roles in both pro-death and pro-survival signaling, it is not surprising that the role of p75^{NTR} in regeneration after injury has been controversial. Although generally considered an anti-growth signal, its role is far more complex as evidenced by conflicting results using p75^{NTR} knock-out mice.

Although expression is high during development, mature Schwann cells do not express p75^{NTR}. Schwann cell expression of p75^{NTR} increases after injury (Taniuchi et al., 1986; Heumann et al., 1987a,b). Deletion of p75^{NTR} in Schwann cells mediates improved regeneration in DRG neurons (Scott and Ramer, 2010). Conversely, for motoneurons, Schwann cell p75^{NTR} deletion results in diminished functional recovery and axonal growth (Tomita et al., 2007). Expression of p75^{NTR} is thought to mediate remyelination through a BDNF-dependent mechanism. Disruption of endogenous BDNF signaling impairs myelination (Cosgaya et al., 2002; Zhang et al., 2008), as does p75^{NTR} knockout from Schwann cells (Cosgaya et al., 2002; Song et al., 2006; Tomita et al., 2007).

In motoneurons, p75^{NTR} levels rise dramatically after injury, returning to baseline levels by 30 days (Raivich and Kreutzberg, 1987; Yan and Johnson, 1988; Ernfors et al., 1989; Koliatsos et al., 1991; Saika et al., 1991; Rende et al., 1995; Gschwendtner et al., 2003). This upregulation in p75^{NTR} does not result in motoneuron cell death, however (Bueker and Meyers, 1951; Kuzis et al., 1999). Treating injured motoneurons with low-levels of recombinant human BDNF enhances their regeneration. Higher doses, however, result in failure to regenerate, which can be reversed by p75^{NTR} blockade (Boyd and Gordon, 2002). There is currently no motoneuron-specific p75^{NTR} knockout model, but conflicting results have been found with regard to motoneuron regeneration in p75^{NTR} pan-knockout mice. Boyd and Gordon found improved motor axon regeneration in knockout mice after peroneal nerve transection (Boyd and Gordon, 2001). Gschwendtner et al. found no effect of knocking out p75^{NTR} on facial nerve axon regeneration (Gschwendtner et al., 2003). Ferri et al. found worse axon regeneration but improved functional recovery after facial nerve crush (Ferri et al., 1998). Song et al. found fewer regenerating axons in p75^{NTR} knockout mice using both sciatic nerve and facial nerve crush injuries (Song et al., 2009). Most recently, Zhang et al. found worse axonal regeneration among p75^{NTR} knockout mice using a facial nerve crush model (Zhang et al., 2010). Using cell-type specific knockout of p75^{NTR} or targeting the binding partners of p75^{NTR} that result in different signaling could provide clarity to these conflicting results in how p75^{NTR} is affecting motoneuron regeneration.

Sensory neurons decrease expression of p75^{NTR} after injury (Zhou et al., 1996). Unlike adult motoneurons, there is significant cell death of DRG neurons after an injury, but this is restricted

to small-diameter, mainly cutaneous afferent neurons (Welin et al., 2008; Wiberg et al., 2018). Cell death in these smaller DRG neurons can be blocked by application of NGF (Rich et al., 1987; Ljungberg et al., 1999). Likewise, in injured DRG neurons, BDNF acts in an autocrine loop to prevent cell death, and disruption in BDNF expression increases cell death (Acheson et al., 1995). A decrease in expression of p75^{NTR} could act as a survival signal, such that the endogenous increased neurotrophin secretion would be more likely to bind trk receptors and result in pro-survival signaling. In support of this hypothesis, in cultures of DRG neurons in which p75^{NTR} has been rendered inactive, cell survival is higher, and increased neurotrophin concentration does not result in increased cell death (Zhou et al., 2005). Similarly, disrupting the NT binding domain of p75^{NTR} results in increased sprouting after injury in DRG neurons (Scott et al., 2005).

Despite the upregulation of BDNF and its receptors after injury, neither BDNF nor the other neurotrophins (NGF, NT3, and NT4/5), is required for spontaneous regeneration of peripheral neurons (Diamond et al., 1987, 1992; Streppel et al., 2002; Wilhelm et al., 2012). However, application of exogenous BDNF enhances axonal regeneration, functional recovery and decreases synaptic stripping (Lewin et al., 1997; Boyd and Gordon, 2002, 2003; Davis-Lopez de Carrizosa et al., 2009). Recently, small molecule trkB agonists have been developed, and these also enhance regeneration after injury (English et al., 2013).

ACTIVITY DEPENDENT TREATMENTS ENHANCE REGENERATION

The first published report using activity-dependent treatments to enhance peripheral nerve regeneration was from Hines in 1942. He tested both electrical stimulation (ES) and different exercise paradigms in enhancing functional outcome in rats with tibial nerve transections (Hines, 1942). Since then, there has been great interest in treatments which activate injured neurons, collectively known as activity-dependent treatments, to enhance nerve regeneration (Udina et al., 2011a). These treatments include ES (Table 1), exercise (Tables 2–4), and more recently, optogenetic stimulation (Table 5). One benefit of activity-dependent treatments is the potential for easy translation from bench to bedside—using ES and exercise in human patients would require meeting far fewer regulatory requirements than the use of an experimental drug. Moreover, for nerve injuries that require surgical intervention, ES could be performed easily at the time of surgical repair of the nerve, as has already begun with clinical trials for patients undergoing surgery for carpal tunnel release and complete digital nerve transection (Gordon et al., 2010; Wong et al., 2015). Exercise has the advantage of being low cost and allowing patients to take control of their recovery. However, in the case of extensive injuries, exercise may not be an option for a recovering patient. For this reason, finding treatments that mimic the effects of exercise, such as optogenetic stimulation, may be advantageous in treating patients. To accomplish such a goal, an understanding of the biological

basis for the enhancement seen with these treatments is necessary.

Electrical Stimulation

Immediately after a peripheral nerve injury, a calcium wave propagates along the cut axons toward their cell bodies. Blocking this calcium wave through inhibition of voltage gated calcium channels or inhibition of calcium release from the neuronal endoplasmic reticulum blocks regeneration (Ghosh-Roy et al., 2010). It has been proposed that ES mimics the retrograde calcium wave that propagates at the time of injury in order to elicit cell-autonomous mechanisms that initiate regeneration (Mar et al., 2014). This hypothesis is supported by evidence that ES enhances early regeneration by accelerating the process of axons crossing the site of injury to enter endoneurial tubes in the segment of the nerve distal to the injury (Brushart et al., 2002). ES results in a doubling of the number of motoneurons crossing the site of injury into the distal nerve at 1 week after nerve injury (Brushart et al., 2002). Without treatment, axons can take as long as 4 weeks to cross the site of injury, but by 3 weeks after injury, Al Majed et al. found all electrically stimulated motoneurons had already regenerated to their target muscle compared to 8 weeks for untreated controls (Al Majed et al., 2000b; Brushart et al., 2002).

The first applications of ES focused on the functional recovery of the affected muscles. In 1983; Nix and Hopf described that as early as 2 weeks after injury, treatment with 4 Hz stimulation 24 h daily increased twitch force, tetanic tension, and muscle action potentials (Nix and Hopf, 1983). In 1985; Pockett and Gavin found earlier return of the plantar extensor reflex with just 15–60 min of 20 Hz stimulation (Pockett and Gavin, 1985). Al Majed et al. chose their 20Hz regimen based on the mean physiological frequency of motoneuron discharge and tried numerous stimulation regimens, stimulating continuously for 1 h, 1 day, 1 week, and 2 weeks. They were the first to examine the effect of ES on the regenerating axons (Loeb et al., 1987; Al Majed et al., 2000b). Just 1 h of 20 Hz stimulation resulted in long-lasting enhancement of peripheral nerve regeneration. Following publication of this paper, 20 Hz stimulation became the standard for studying ES (Table 1).

Without treatment, axon regeneration into motor or sensory pathways in the distal segment of a cut nerve is random for the first 2 weeks following injury (Brushart, 1993). Motoneurons whose axons have entered only sensory pathways (endoneurial tubes previously occupied by cutaneous axons) remain permanently mistargeted (Brushart, 1993). Enhancing the speed of regeneration but increasing mistargeting could result in poorer functional recovery. However, ES has been shown to increase the sensorimotor specificity of regenerating axons after peripheral nerve injury. More motoneurons regenerate exclusively into motor pathways in rats treated with ES (Al Majed et al., 2000b). Fewer than 40% of injured DRG neurons reinnervated sensory pathways in controls compared to 75% in ES-treated animals (Brushart et al., 2005). However, innervating a motor endoneurial tube does not necessitate reaching the appropriate muscle target. Indeed, topographic analysis of motoneuron regeneration after ES revealed *increased*

TABLE 1 | Effect of electrical stimulation on peripheral nerve regeneration.

Regimen		Model	Result		References
Unspecified	3 min/day	Rat tibial nerve crush	Functional recovery	↑	Hines, 1942
4 Hz	24 h/4 weeks	Rabbit soleus nerve crush	Functional recovery	↑	Nix and Hopf, 1983
20 Hz	15–60 min	Rat sciatic nerve crush	Functional recovery	↑	Pockett and Gavin, 1985
20 Hz	60 min, 24 h, 1 week, 2 weeks	Rat femoral nerve transection	Axonal growth	↑	Al Majeed et al., 2000b
20 Hz	8 h/day/4 weeks	Rat sciatic nerve avulsion	Functional Recovery	↓	Tam et al., 2001
100 Hz	10 pulses/2 min	Cultured rat retinal ganglion cell	Neurite outgrowth		Goldberg et al., 2002
20 Hz	1 h	Rat femoral nerve transection	Axonal growth	↑	Brushart et al., 2002
20 Hz	1 h	Rat femoral nerve transection	Axonal growth	↑	Brushart et al., 2005
20 Hz	1 h	Thy1-H-YFP mouse fibular nerve transection	Axonal growth	↑	English et al., 2007
20 Hz	1 h, 3 h, 24 h, 1 week, 2 weeks	Rat femoral nerve transection	1 hr-Axonal growth Others—no change	↑	Geremia et al., 2007
20 Hz	1 h	Mouse femoral nerve transection	Functional recovery	↑	Ahlborn et al., 2007
?	30 min/day until recovery	Rat facial nerve transection	Functional recovery	↑	Lal et al., 2008
20 Hz	1 h	Rat sciatic nerve transection	Functional Recovery Axonal growth	↑	Vivo et al., 2008
20 Hz	1 h	Human carpal tunnel syndrome release surgery	Functional recovery	↑	Gordon et al., 2010
20 Hz	3 days	Rat adult cultured DRG neurons	Neurite outgrowth	↓	Enes et al., 2010
20 Hz	1 h	Rat sciatic nerve crush	Myelination and myelin thickness	↑	Wan et al., 2010
20 Hz	1 h	Thy1-H-YFP mouse sciatic nerve transection	Axonal growth	↑	Singh et al., 2012
20 Hz	1 h	Rat cultured DRG neurons	Neurite outgrowth		Singh et al., 2012
20 Hz	30 min/day 1–7 days	Rat facial nerve crush	Functional recovery	↑	Foecking et al., 2012
20 Hz	20 min	Rat sciatic nerve Delayed repair 2 h–24 weeks	Axonal growth Functional recovery	↑	Huang et al., 2013
20 Hz	1 h	Human digital nerve transection	Functional sensory recovery	↑	Wong et al., 2015
20 Hz	1 h	Rat common peroneal nerve transection Delayed repair 3 months	Axonal growth	↑	Elzinga et al., 2015

Regimen specifies stimulation paradigm. Model specifies which animal and injury model was used. Result specifies what outcome measure was analyzed. ↑ Denotes improvement in outcome measured, ↓ denotes worse outcome.

misdirection of regenerating motor axons to functionally inappropriate targets by over 500% (English, 2005). This misdirection resulted in motoneurons previously innervating extensor muscles reinnervating antagonistic flexor muscles.

Appropriate pathway innervation may rely on Schwann cells secreting specific growth factors for motor and sensory tubes. Schwann cells in the cutaneous nerves express high levels of NGF after injury, whereas Schwann cells in ventral roots express

high levels of glial cell line-derived neurotrophic factor (GDNF) (Hoke et al., 2006; Brushart et al., 2013). This difference in growth factor expression has been proposed to be the mechanism through which preferential motor reinnervation occurs, with DRG neurons choosing paths with high NGF, and motoneurons entering paths with high GDNF. With no treatment, in rodents, neurotrophin expression peaks 15 days after injury and declines back to baseline by day 30. The day 15 peak coincides with the

TABLE 2 | Effects of treadmill training on peripheral nerve regeneration.

Regimen	Duration	Delay	Model	Result		References
6.5–27 m/min 10–40 min/day	1–2/day	2–3 weeks	Rat sciatic nerve crush ♀	Functional recovery	↓	Herbison et al., 1980a
27 m/min 1–2/day 5 days/week	3–4 weeks	2–3 weeks	Rat sciatic nerve crush ♀	No change		Herbison et al., 1980b
1 h/day 26.8 m/min	10 weeks	Prior to injury	Rat L4 root transection ♀	Increased sprouting		Gardiner et al., 1984
10 m/min 30 min/twice/day	21 days	None	Rat sciatic nerve crush ♂	Functional recovery	↓	van Meeteren et al., 1998
10 m/min 1.5 h/twice/day 5 days/week	10 weeks	1 week	Rat peroneal nerve transection ♀	Functional recovery	↑	Marqueste et al., 2004
18 m/min 30 min/twice/day	2 weeks	12 h	Rat sciatic nerve crush ♂	Axonal growth	↑	Seo et al., 2006
10 m/min*1 h/day 20 m/min Or 2 min*4/day 5 days/week	2 weeks	3 days	Thy1-H-YFP mouse sciatic nerve transection	Axonal growth	↑	Sabatier et al., 2008
8 m/min 30 min/twice/day	2 weeks	12 h	Rat sciatic nerve crush ♂ DRG culture ♂	Axonal growth Neurite length	↑	Seo et al., 2009
10 m/min*1 h/day 20 m/min 2 min*4/day 5 days/week	2 weeks	3 days	Mouse sciatic nerve transection	Axonal growth	↑	English et al., 2009
20 Hz 1 h ES + 5 m/min 2h/day	4 weeks	5 days	Rat sciatic nerve transection ♀	Axonal growth	↑	Asensio-Pinilla et al., 2009
20 cm/s-54 cm/s 60 min/day 5 days/week	5 or 52 days	3 days	Mouse sciatic nerve chronic constriction injury ♂	Functional recovery	↑	Cobianchi et al., 2010
4.6 m/min 30min/twice/day	4 weeks	5 days	Rat sciatic nerve transection ♀	Functional Recovery Axonal growth	↑	Udina et al., 2011b
1.8–3 m/min 20 min/day	3 weeks	7 days	Rat ulnar nerve crush ♂	Functional recovery	↑	Pagnussat et al., 2012
10 m/min 1 h/5 days/week	2 weeks	3 days	Rat sciatic nerve transection ♀	Functional recovery	↑	Boeltz et al., 2013
10 m/min 1 h/5 days/week	2 weeks	3 days	Mouse sciatic nerve transection ♀ ♂	Synaptic stripping	↑	Liu et al., 2014
10 m/min 1 h/5 days/week	6 weeks	3 days	Mouse median nerve transection ♂	Functional recovery	↑	Park and Höke, 2014
20 m/min 2 min*4/day 5 days/week	2 weeks	3 days	SLICK::BDNF ^{f/f} mouse sciatic nerve transection ♀	Synaptic stripping	↑	Krakiwicz et al., 2015

Regimen is the speed of running and for how long each day. Duration is how many days TT was performed. Delay refers to how long after injury before exercise was performed. Model specifies what type of injury and in what animal. Sex of animals is specified by ♀ or ♂. If this is not listed, it was not specified. Result specifies what outcome measure was analyzed.

↑ Denotes improvement in outcome measured, ↓ denotes worse outcome. No arrow denotes no effect.

onset of pathway preference for regenerating axons (Gordon, 2015). ES, however, dramatically increases NGF secretion from Schwann cells for 3 days following stimulation (Koppes et al.,

2014), possibly providing an earlier signal to regenerating sensory axons as to which pathways to take, and thus improving pathway targeting.

TABLE 3 | Effect of swimming exercise on peripheral nerve regeneration.

Regimen	Delay	Model	Result		References
1 h/day	Unspecified	Rat tibial nerve transection	Functional recovery	↑	Hines, 1942
10 min/day 10 days	4, 11, 18 days	Rabbit sciatic nerve crush	Myelination	↑	Sarikcioglu and Oguz, 2001
30 min/day 2 weeks	None 2 weeks	Rat sciatic nerve crush ♂	Decreased sprouting		Teodori et al., 2011
10–30 min/day 3 days/week 3 weeks	7 days	Rat sciatic nerve transection	No change		Liao et al., 2017

Regimen specifies how long swimming exercise lasted each day and how many days swimming was performed. Delay refers to how long after injury before exercise was performed. Model specifies what type of injury and in what animal. Sex of animals is specified by ♀ or ♂. If this is not listed, it was not specified. Result specifies what outcome measure was analyzed. ↑ Denotes improvement in outcome measured, ↓ denotes worse outcome. No arrow denotes no effect.

Exercise Treatment

For years, the evidence for exercise enhancing regeneration was not as clear as the evidence for ES. Many different types of exercise with varying intensities applied at different times prior to or after injury have resulted in conflicting results. It was hypothesized that increased neuronal activity through exercise would enhance regeneration as early as 1979, but early studies utilizing treadmill training, voluntary wheel running, and swimming found unfavorable results (Hoffer et al., 1979; Herbison et al., 1980a; Gardiner et al., 1984; Badke et al., 1989; van Meeteren et al., 1998; Tam et al., 2001). These experiments largely focused on the effect of exercise on muscle fiber alterations and muscle function, and did not probe the effect of exercise on axon regeneration.

The change in emphasis from the effect of exercise on denervated muscle to the effect of exercise on injured spinal motoneurons and DRG neurons encouraged scientists to continue researching exercise, despite previous underwhelming results. In 2008, English and colleagues tested the efficacy of interval training (short high-speed sprints followed by periods of rest) in enhancing regeneration as a model that resembles how mice voluntarily run (De Bono et al., 2006; Sabatier et al., 2008). They found the surprising result that this regimen was effective only in female mice, and in fact the more commonly used training regimen of slow continuous treadmill walking was effective only in males (Wood et al., 2012). This previously unknown sex difference could have affected outcomes in numerous exercise experiments. For example, Seo et al. treated intact male rats with either high or low intensity treadmill training before culturing their DRGs and found only low intensity treadmill training increased neurite outgrowth (Seo et al., 2009). Their treadmill training regimen was very similar to the one used by Wood et al. that proved effective only in male mice, and the results of this experiment could have been different had females been included. Many of the prior experiments mentioned used animals of only one sex, and this could explain some of the variability in the effects of exercise (Tables 2–4).

There are a few advantages to exercise over ES. For example, while ES may increase misdirection of motoneurons reaching target muscles, treadmill training enhances motoneuron regeneration without decreasing topographic specificity (English

et al., 2009). The mechanism of ES is to accelerate crossing the site of injury by regenerative sprouts; exercise does the same but also sustains pro-growth signaling throughout the process of regeneration (Gordon and English, 2016). There is also evidence that the enhancing effects of 2 weeks of exercise are more robust than that of a single bout of ES (Sabatier et al., 2008; Wood et al., 2012; Gordon and English, 2016). In 2009, Asensio-Pinilla et al. combined treadmill training with a single bout of ES given at the time of injury, and found greater enhancement of muscle reinnervation in the initial phase of recovery compared to either treatment alone (Asensio-Pinilla et al., 2009). Thus, after inauspicious beginnings, exercise has shown great promise as a treatment in the field of peripheral nerve regeneration.

Optogenetic Stimulation

The advent of optogenetics enabled cell-specific neuronal activation with the use of the light-sensitive cation channel, Channelrhodopsin (ChR2) (Krook-Magnuson et al., 2014). Whereas ES stimulates all cells within the nerve (including Schwann cells and various immune cells) and exercise likely affects cells throughout the entire body, specific neuronal activation can be achieved using optogenetics by expressing ChR2 only in neurons. Park et al. were the first to demonstrate the efficacy of light stimulation in enhancing regeneration by replicating the common ES protocol using light stimulation of 20 Hz for 1 h on explanted neonatal DRGs (Park et al., 2015). Although they tested a number of different stimulation regimens, the 1 h of 20 Hz stimulation provided the largest effect on neurite outgrowth. Ward et al. recapitulated this *in vivo*, finding that 1 h of 20 Hz light stimulation of light-sensitive neurons enhanced axon regeneration only in the light-sensitive cells (Ward et al., 2016, 2018).

MECHANISMS

Neurotrophins

Activity-dependent treatments require neuronal neurotrophin production. ES increases neurotrophin expression in Schwann cells, DRG neurons, and motoneurons (Al Majed et al., 2000a; English et al., 2007; Wan et al., 2010; Koppes et al., 2014).

TABLE 4 | Effect of other exercise paradigms on peripheral nerve regeneration.

Exercise	Regimen	Delay	Model	Result		References
Forced Wheel Running	2 h/day	Unspecified	Rat tibial nerve transection	Functional Recovery	↑	Hines, 1942
Overwork	Chronic	None	Rat sciatic nerve crush ♀	Functional recovery	↑	Herbison et al., 1973
Voluntary wheel running	4 weeks	None	Mouse tibial nerve transection	Functional recovery Axonal growth	↑	Badke et al., 1989
				Axonal growth	↓	
Stretch Training	24 days	None	Rat sciatic nerve crush ♀	Functional recovery	↑	van Meeteren et al., 1997
Voluntary wheel running	8 h/day	None	L4 and L5 avulsion ♀	Axonal growth Functional Recovery	↓	Tam et al., 2001
				Functional Recovery	↓	
Voluntary wheel running	3 or 7 days	Prior to injury	Rat DRG culture Rat sciatic nerve crush	Neurite outgrowth Axonal growth	↑	Molteni et al., 2004
Manual Whisker Stimulation	5 min/day 5 days/week 2 months	1 day	Rat facial nerve transection ♀	Functional Recovery	↑	Angelov et al., 2007
Manual Muscle Stimulation	5 min/day 5 days/week 2 months	1 day	Rat hypoglossal transection ♀	Functional Recovery	↑	Guntinas-Lichius et al., 2007
Manual Whisker Stimulation	5 min/day 5 days/week 2 months	1 day	Rat hypoglossal transection ♀	Functional Recovery	↑	Evgenieva et al., 2008
Manual Muscle Stimulation	5 min/day 5 days/week 2 months	1 day	Rat facial nerve transection ♀	Functional Recovery	↑	Bischoff et al., 2009
Manual Whisker Stimulation	5 min/day 5 days/week 2 months	1 day	BDNF ^{+/-} or trkB ^{+/-} rat facial nerve transection ♀	Functional Recovery	↑	Sohnchen et al., 2010
Passive bicycle training	45 rpm 30 min/twice/day 4 weeks	5 days	Rat sciatic nerve transection ♀	Functional Recovery Axonal growth	↑	Udina et al., 2011b
Skilled Motor Task	20 min/day 3 weeks	7 days	Rat ulnar nerve crush ♂	Functional recovery	↑	Pagnussat et al., 2012




Exercise refers to what type of paradigm was used. Regimen specifies how long exercise lasted each day and how many days exercise was performed. Delay refers to how long after injury before exercise was performed. Model specifies what type of injury and in what animal. Sex of animals is specified by ♀ or ♂. If this is not listed, it was not specified. Result specifies what outcome measure was analyzed. ↑ Denotes improvement in outcome measured, ↓ denotes worse outcome. No arrow denotes no effect.



Electrically stimulating Schwann cells increases their secretion of NGF specifically, and not BDNF (Koppes et al., 2014). While Schwann cell NGF is sufficient to promote axon growth, the study of axon regeneration through nerve grafts made acellular by repeated freezing and thawing has demonstrated that stimulation of Schwann cells (and other cell types) is not required for the efficacy of ES to enhance axon regeneration (English et al., 2007; Koppes et al., 2014). Moreover, the use of optogenetics to stimulate neurons selectively has shown that specific neuronal activation is sufficient to enhance regeneration (Ward et al., 2016). ES is also effective in promoting regeneration in nerves that have been repaired months after injury, when Schwann cells have stopped secreting neurotrophins and have started to die

off (Sulaiman and Gordon, 2000; Hoke et al., 2006; Brushhart et al., 2013; Huang et al., 2013; Elzinga et al., 2015). Thus, while activity-dependent treatments may increase Schwann cell neurotrophin secretion, this is not required for their enhancing effects.

Unlike non-neuronal cells, neuronal neurotrophin secretion is required for the efficacy of activity-dependent treatments. Genetically deleting NT4/5 or BDNF from Schwann cells does not alter the efficacy of ES or treadmill training in enhancing axon growth, but deleting these neurotrophins from neurons abolishes the effectiveness of these activity-dependent treatments (English et al., 2007; Wilhelm et al., 2012). Both exercise and ES have been shown to increase neuronal BDNF and its receptor,

TABLE 5 | Effect of optogenetic stimulation on peripheral nerve regeneration.

Regimen	Mouse	Model	Result	References
1 h 20 Hz 5 ms pulse	Thy1ChR2	Neonate DRG explant	Neurite outgrowth 	Park et al., 2015
1 h 20 Hz 1 ms pulse	Thy1ChR2	Sciatic nerve transection	Axonal outgrowth 	Ward et al., 2016
1–2 h 10–20 Hz (72 k pulse total) 1 ms pulse	Avil-Cre::ChR2-YFP ^{f/f} Chat-ChR2-YFP	Sciatic nerve transection	Axonal outgrowth 	Ward et al., 2018

Regimen specifies stimulation paradigm. Mouse specifies what transgenic mouse model was used. Result specifies what outcome measure was analyzed.  Denotes improvement in outcome measured,  denotes worse outcome.

trkB (Al Majed et al., 2000a; Gomez-Pinilla et al., 2002; English et al., 2007; Park and Höke, 2014; Park et al., 2015). Through co-culturing light-sensitive DRG explants with wild type DRGs, Park et al. demonstrated that the BDNF secreted in response to light stimulation was sufficient to increase neurite outgrowth not only from cells in a light-sensitive (ChR2-expressing) DRG, but also in neighboring ganglia derived from wild type mice. Protein analysis of the media revealed increased BDNF and NGF secretion in response to optical stimulation from the light-sensitive DRGs only (Park et al., 2015).

There is a dose-dependence in activity-dependent treatments for enhancing nerve regeneration. Whereas 1 h of 20 Hz stimulation has been shown to enhance DRG regeneration after injury, an increase to just 3 h of ES decreased sensory neuron regeneration, and was associated with a downregulation in expression of the regeneration associated gene, GAP-43 (Geremia et al., 2007). *In vitro*, neurites from DRG explants containing ChR2 had higher rates of growth with stimulation paradigms resulting in 72k pulses of light (1 h 20 Hz, 2 h 10 Hz, 4 h 5 Hz) than stimulation paradigms that resulted in a higher number of pulses (20 Hz for 1–3 days) or much lower number of pulses (20 Hz for 15 min) (Park et al., 2015). Three days of continuous depolarization through ES or high concentrations of KCl results in complete failure of dissociated DRG neurons to grow neurites in culture (Enes et al., 2010). For motoneurons, high intensity exercise or repeated bouts of ES result in decreased sprouting and fewer synaptic contacts at neuromuscular junctions (Tam et al., 2001). Application of 1 h of 20 Hz ES every third day for 2 weeks after sciatic nerve transection and repair did not enhance the regeneration of motor axons in mice (Park et al., under review). Interestingly, exogenous application of BDNF resulted in a dose-dependent enhancement of axon regeneration as well (Boyd and Gordon, 2002). Low to modest doses produced enhanced axon regeneration, but higher doses inhibited regeneration. Treatments with high doses of BDNF caused p75^{NTR} activation, which prevented DRG neurite outgrowth (Boyd and Gordon, 2002).

Neuronal Activity

The success of activity-dependent treatments in promoting axon regeneration requires activation of the injured neurons. Treating the neurons proximal to the stimulation site with tetrodotoxin (TTX) to block their ability to conduct antidromic action potentials abolishes the effect of ES, despite the continued orthodromic firing of distal axons and muscle fibers (Al Majed et al., 2000b). Similarly, inhibition of motoneuron activity during treadmill training, using bioluminescent optogenetics (BL-OG), abolishes the enhancing effect of exercise on motoneuron regeneration (Jaiswal et al., 2017). Whether the increased activation needed to promote axon regeneration requires action potential generation is not entirely clear. Enhancement of regeneration of axons of many more motoneurons than are likely to be brought into full activity is found after treatments with exercise at a slow treadmill speed (Gordon and English, 2016). Simply increasing the excitability of injured neurons using chemogenetics could be sufficient to enhance regeneration (Jaiswal et al., 2018).

Although Park et al. found that BDNF secretion from neighbors can stimulate regeneration in neurons that were not activated *in vitro*, optogenetic stimulation *in vivo* of only motoneuron axons did not enhance DRG axon regeneration, nor vice versa (Ward et al., 2018). When BDNF is knocked out in only a subset of neurons, those specific neurons do not benefit from exercise treatment (Wilhelm et al., 2012). Thus, it appears neuronal BDNF is acting as an autocrine signal facilitating enhanced regeneration (English et al., 2014; Gordon, 2016).

Androgens

The sex difference found in response to different exercise regimens led to the hypothesis that androgen receptor signaling was involved in activity-dependent treatments. The effect of androgens in enhancing peripheral nerve regeneration had already been thoroughly explored several years prior (Fargo et al., 2009). All motoneurons contain androgen receptors, though testosterone is not required for spontaneous regeneration—treating animals of both sexes with the androgen receptor

blocker flutamide does not inhibit regeneration, nor does castration of males (Freeman et al., 1995; Thompson et al., 2013). Application of exogenous androgens in males and females, however, enhances axon regeneration in both cranial and spinal nerve injuries (Kujawa et al., 1989, 1991; Jones, 1993; Freeman et al., 1995; Tanzer and Jones, 1997; Brown et al., 1999). This effect is androgen receptor-dependent, and blocking the androgen receptor with flutamide prevents testosterone-induced enhanced regeneration (Kujawa et al., 1995). In females, treating mice with anastrozole, an aromatase inhibitor which blocks the conversion of testosterone into estradiol, also dramatically enhanced axon regeneration, without increasing serum androgen levels (Thompson et al., 2013).

The sex difference in response to exercise regimens was evidence that androgen receptor signaling and activity-dependent treatments were linked. Slow, continuous treadmill training resulted in an increase in serum testosterone levels in males, though no similar increase was found for females with interval training (Wood et al., 2012). Castrating males prior to treadmill training abolishes its enhancing effect, which cannot be rescued with interval training (Wood et al., 2012). Treating both sexes with flutamide before appropriate exercise regimens abolishes the effectiveness of this treatment in enhancing peripheral nerve regeneration (Thompson et al., 2013). Testosterone is also necessary for the beneficial effects of ES—castrated rats treated with ES have poorer regeneration compared to littermates who are treated with exogenous testosterone (Hetzler et al., 2008; Sharma et al., 2009). As with exercise, flutamide blocks the enhancing effects of ES in both males and females (Thompson et al., 2013). Conversely, combined exogenous androgen treatment with ES enhances facial nerve regeneration in gonadally intact rats (Sharma et al., 2010b).

Androgens regulate BDNF and its receptor, *trkB*, in motoneurons (Osborne et al., 2007; Ottem et al., 2010; Sharma et al., 2010a; Verhovshek et al., 2010). Exercise elicits an upregulation of testosterone that is sustained and could result in an increased duration of BDNF and *trkB* expression (Thompson et al., 2013; English et al., 2014). ES elicits an early increase in BDNF expression, whereas exogenous androgen application results in a later and longer-duration increase in expression. Combining the two treatments results in an additive upregulation of BDNF and could explain the improved recovery over either treatment alone (Sharma et al., 2010a).

SYNAPTIC REARRANGEMENTS

After peripheral nerve injury both excitatory and inhibitory synaptic inputs onto injured motoneurons are withdrawn (Blinzinger and Kreutzberg, 1968; Brannstrom and Kellerth, 1998; Linda et al., 2000; Oliveira et al., 2004). If motor axons regenerate and reinnervate muscle targets, many of these inputs are restored but, for those expressing the vesicular glutamate transporter 1 (VGLUT1) and arising from muscle spindles, a gradual withdrawal of their central axonal processes from the ventral horn follows, resulting in a permanent loss of these

synaptic inputs (Alvarez et al., 2011; Rotterman et al., 2014). In animals treated with exercise during the first few days following sciatic nerve transection and repair, the extent of synaptic contacts between these important sources of proprioceptive feedback and motoneurons is not reduced (English et al., 2011; Liu et al., 2014; Krakowiak et al., 2015). This robust connectivity by VGLUT1+ inputs is retained at least 12 weeks later. No similar effect is found if the onset of the exercise treatment is delayed (Brandt et al., 2015). Application of 1 h of 20 Hz ES had no effect on synaptic coverage after nerve injury, but repeated applications every third day for 2 weeks resulted in an effect similar to that observed using exercise (Park et al., under review). It is not clear whether this effect of these activity-dependent therapies is the prevention of the original synaptic withdrawal, a stimulation of new synapse formation to replace the withdrawn inputs, or some combination of both. More studies are needed.

It is clear that BDNF plays a role in maintaining and preserving synaptic inputs on motoneurons. Without exercise, axotomized motoneurons lose approximately 35% of their overall synaptic coverage (Krakowiak et al., 2015). This effect is BDNF-dependent—knocking out BDNF in a subset of motoneurons reduces synaptic coverage in those specific cells in intact animals, and this synapse loss cannot be rescued with exercise (Krakowiak et al., 2015). Wild-type motoneurons within an animal maintain their synaptic contacts after nerve injury with exercise, but those in which BDNF has been knocked out do not (Krakowiak et al., 2015).

BDNF VAL66MET POLYMORPHISM

Given the relationship between activity-dependent treatments and BDNF, any genetic mutations altering BDNF signaling among the human population could affect the success of these treatments. Such a mutation exists—a common single nucleotide polymorphism in the *BDNF* gene. The G to A mutation at site 196 results in a Valine to Methionine substitution in the 66th codon (**Figure 1**). This polymorphism was first described by Egan et al. in 2003 and was quickly identified as incredibly common—the met allele of the *BDNF* gene is present in 25% of the American population and up to 50% of East Asian populations (Egan et al., 2003; Shimizu et al., 2004). Carrying the met allele was originally described as a risk factor for schizophrenia (Egan et al., 2003). It has since been linked to numerous other disorders and diseases, including Alzheimer's disease, obsessive compulsive disorder, anorexia nervosa, and bipolar disorder (Neves-Pereira et al., 2002; Sklar et al., 2002; Egan et al., 2003; Hall et al., 2003; Ribases et al., 2003; Notaras et al., 2015). Physiologically, Met-carriers have been found to have decreased hippocampal volume, and cells transfected with the Met allele have altered activity-dependent secretion of BDNF (Egan et al., 2003).

Testing for deficient activity-dependent secretion of BDNF in humans can be tricky. Generally, BDNF secretion is measured through serum as an indirect measure of neuronal BDNF, and exercise is a reliable method to increase serum BDNF levels (Berchtold et al., 2005; Elfving et al., 2010; Klein et al., 2011; Szuhany et al., 2015). Although one study has found that healthy

adult Met-carriers did have increased serum BDNF after exercise (Helm et al., 2017), others have found serum levels of BDNF did not increase after high intensity exercise in elderly (Nascimento et al., 2015), spinal cord injured (Leech and Hornby, 2017), or healthy Met-carriers (Lemos et al., 2015). In mice expressing the met allele, exercise results in deficient mRNA production as well as decreased protein expression of BDNF (Ieraci et al., 2016). These deficiencies in exercise-induced BDNF secretion mirror the findings in cultured neurons expressing the Met allele, and the use of cells transfected with the met allele *in vitro* as well as the development of a transgenic mouse have allowed researchers to elucidate the mechanism behind this deficient secretion (Egan et al., 2003; Chen et al., 2004, 2006).

The valine to methionine substitution in this SNP occurs in the prodomain of the BDNF protein (Egan et al., 2003). Although it does not affect the ability of mBDNF to bind its receptor, this substitution results in disorganized folding of the prodomain, resulting in abnormal interactions with sortilin (see above) (Chen et al., 2004; Anastasia et al., 2013). BDNF_{Met} is thus packaged inefficiently into calcium-sensitive secretory vesicles, accounting for the deficient activity-dependent secretion that has been reported (Chen et al., 2004). Being heterozygous for the met allele does not protect from this deficient BDNF secretion—BDNF forms homodimers, and in cells heterozygous for the met allele, BDNF_{Met} dimerizes with BDNF_{Val} and prevents its packaging into Ca²⁺-regulated secretory vesicles (Kolbeck et al., 1994; Chen et al., 2004). Analysis of activity-induced BDNF secretion from cultured hippocampal cells bears this out—those cells heterozygous for the Met allele have deficient activity-dependent secretion despite the presence of one copy of the BDNF_{Val} allele (Chen et al., 2006). Furthermore, once secreted, BDNF availability may be affected by binding with the cleaved prodomain. The prodomain binds BDNF with high affinity, and the met allele results in enhanced BDNF binding and slower dissociation once bound (Uegaki et al., 2017). This could limit the availability of BDNF to bind its receptors.

Activity-dependent secretion of BDNF relies not only on packaging into calcium-sensitive vesicles, but also on the spatial targeting of mRNA into distal processes where BDNF can be locally translated (Chiaruttini et al., 2008). This targeting is achieved through binding of BDNF mRNA with translin, a DNA/RNA binding protein involved in dendritic trafficking of mRNAs (Li et al., 2008). The G to A mutation at site 196 disrupts translin binding of BDNF mRNA, and thus Met-carriers have deficient trafficking of BDNF mRNA to distal processes (Chiaruttini et al., 2009). Moreover, the transcripts containing exon VI, which is upregulated by exercise, and exon IV, which is calcium-sensitive, are found in reduced levels in the hippocampus of mice homozygous for the met allele (Tao et al., 1998; Baj et al., 2012; Mallei et al., 2015). These transcripts, along with those containing exon II, are generally trafficked to distal processes (Baj et al., 2011).

In addition to deficient activity-dependent BDNF secretion, the met allele may result in increased p75^{NTR} activation. Unlike BDNF_{Val}, when the prodomain is cleaved from BDNF_{Met}, it is bioactive and able to activate p75^{NTR} with the help of SorCS2, a member of the sortilin family of receptors (Deinhardt et al.,

2011; Anastasia et al., 2013). *In vitro*, application of exogenous prodomain protein results in growth cone collapse and dendritic spine disassembly (Anastasia et al., 2013; Giza et al., 2018). Stimulating cells with high KCl concentration results in activity-dependent secretion of both Val and Met proddomains, though secretion is deficient in Met-carriers (Anastasia et al., 2013). Although endogenous secretion of the Met prodomain has yet to be linked to alterations in dendrites, decreased arborization has been found in hippocampal and cortical neurons (Chen et al., 2006; Liu et al., 2012).

The deficit in activity-dependent release of BDNF led to the hypothesis that activity-dependent treatments to enhance axon regeneration after peripheral nerve injury would be ineffective in this population. Using a mouse model of this polymorphism which recapitulates certain phenotypic aspects of the human population such as decreased hippocampal volume and increased anxiety-like behavior (Chen et al., 2006), we tested the efficacy of treadmill training on motor axon regeneration 4 weeks after complete sciatic nerve transection and repair in mice both heterozygous and homozygous for the met allele of the *Bdnf* gene (McGregor et al., under review). Exercise was completely ineffective in enhancing axon regeneration in the Met-carriers. However, peripheral axon regeneration in Met-carriers was surprisingly enhanced without any treatment (McGregor et al., under review). One possibility for the failure of exercise to enhance regeneration in Met-carriers is a ceiling effect—exercise was not able to further enhance an already accelerated regeneration. The question of *why* regeneration is accelerated remains to be explored. The enhanced regeneration was found both *in vivo* and in cultured DRG neurons, indicating that enhanced axon outgrowth is a neuronal trait in Met-carriers. This unanticipated result is some of the first good news regarding what is a maligned SNP, although others have reported the met allele may also be protective in stroke and traumatic brain injury (Krueger et al., 2011; Rostami et al., 2011; Qin et al., 2014; Failla et al., 2015). Thus, in human populations there may be striking differences in response to peripheral nerve injury dependent on individual gene expression. Enhanced regeneration associated with the Val66Met polymorphism may explain the persistence of the mutation within the human population.

CONCLUSION

The suboptimal regeneration of peripheral nerves presents a challenge in medical care. Neurotrophins, particularly BDNF, have been studied for their pro-growth properties, and treatments that stimulate endogenous release of neurotrophins have been successful in enhancing regeneration in animal models. These treatments are currently being tested to enhance peripheral nerve regeneration in patients with some success (Gordon et al., 2010; Wong et al., 2015). The existence of genetic polymorphisms in the *bdnf* gene, however, will affect the outcome of these experiments, and preliminary investigations as to the efficacy of activity-dependent treatments in individuals with the met allele will hopefully spur the field toward personalized medicine. Activity-dependent treatments can be a

powerful tool for those responsive to them, and for the rest, new therapies that do not rely on endogenous BDNF-signaling must be developed.

AUTHOR CONTRIBUTIONS

All authors listed have made a substantial, direct and intellectual contribution to the work, and approved it for publication.

REFERENCES

- Abe, N., Borson, S. H., Gambello, M. J., Wang, F., and Cavalli, V. (2010). Mammalian target of rapamycin (mTOR) activation increases axonal growth capacity of injured peripheral nerves. *J. Biol. Chem.* 285, 28034–28043. doi: 10.1074/jbc.M110.125336
- Acheson, A., Conover, J. C., Fandl, J. P., Dechiara, T. M., Russell, M., Thadani, A., et al. (1995). A BDNF autocrine loop in adult sensory neurons prevents cell death. *Nature* 374, 450–453. doi: 10.1038/374450a0
- Ahlborn, P., Schachner, M., and Irintchev, A. (2007). One hour electrical stimulation accelerates functional recovery after femoral nerve repair. *Exp. Neurol.* 208, 137–144. doi: 10.1016/j.expneurol.2007.08.005
- Aid, T., Kazantseva, A., Piirsoo, M., Palm, K., and Timmusk, T. (2007). Mouse and rat BDNF gene structure and expression revisited. *J. Neurosci. Res.* 85, 525–535. doi: 10.1002/jnr.21139
- Al Majed, A., Brushart, T., and Gordon, T. (2000a). Electrical stimulation accelerates and increases expression of BDNF and trkB mRNA in regenerating rat femoral motoneurons. *Eur. J. Neurosci.* 12, 4381–4390. doi: 10.1046/j.1460-9568.2000.01341.x
- Al Majed, A., Neumann, C., Brushart, T., and Gordon, T. (2000b). Brief electrical stimulation promotes the speed and accuracy of motor axonal regeneration. *J. Neurosci.* 20, 2602–2608. doi: 10.1523/JNEUROSCI.20-07-02602.2000
- Alderson, R. F., Curtis, R., Alterman, A. L., Lindsay, R. M., and Distefano, P. S. (2000). Truncated TrkB mediates the endocytosis and release of BDNF and neurotrophin-4/5 by rat astrocytes and Schwann cells *in vitro*. *Brain Res.* 871, 210–222. doi: 10.1016/S0006-8993(00)02428-8
- Allen, M., Bird, C., Feng, W., Liu, G., Li, W., Perrone-Bizzozero, N. I., et al. (2013). HuD promotes BDNF expression in brain neurons via selective stabilization of the BDNF long 3'UTR mRNA. *PLoS ONE* 8:e55718. doi: 10.1371/journal.pone.0055718
- Alvarez, F. J., Titus-Mitchell, H. E., Bullinger, K. L., Kraszpulski, M., Nardelli, P., and Cope, T. C. (2011). Permanent central synaptic disconnection of proprioceptors after nerve injury and regeneration. I. Loss of VGLUT1/IA synapses on motoneurons. *J. Neurophysiol.* 106, 2450–2470. doi: 10.1152/jn.01095.2010
- An, J. J., Gharami, K., Liao, G. Y., Woo, N. H., Lau, A. G., Vanevski, F., et al. (2008). Distinct role of long 3' Utr Bdnf Mrna in spine morphology and synaptic plasticity in hippocampal neurons. *Cell* 134, 175–187. doi: 10.1016/j.cell.2008.05.045
- Anastasia, A., Deinhardt, K., Chao, M., Will, N., Irmady, K., Lee, F., et al. (2013). Val66Met polymorphism of BDNF alters prodomain structure to induce neuronal growth cone retraction. *Nat. Commun.* 4:2490. doi: 10.1038/ncomms3490
- Angelov, D. N., Ceynowa, M., Guntinas-Lichius, O., Streppel, M., Grosheva, M., Kiryakova, S. I., et al. (2007). Mechanical stimulation of paralyzed vibrissal muscles following facial nerve injury in adult rat promotes full recovery of whisking. *Neurobiol. Dis.* 26, 229–242. doi: 10.1016/j.nbd.2006.12.016
- Apfel, S. C., Wright, D. E., Wiideman, A. M., Dormia, C., Snider, W. D., and Kessler, J. A. (1996). Nerve growth factor regulates the expression of brain-derived neurotrophic factor mRNA in the peripheral nervous system. *Mol. Cell. Neurosci.* 7, 134–142. doi: 10.1006/mcne.1996.0010
- Asano, Y., Nagasaki, A., and Uyeda, T. Q. (2008). Correlated waves of actin filaments and PIP3 in Dictyostelium cells. *Cell Motil. Cytoskeleton* 65, 923–934. doi: 10.1002/cm.20314

ACKNOWLEDGMENTS

Support provided by grant NS057190 to AE from the USPHS. Many thanks to Dr. Francis Lee for the gift of the Val66Met mouse. The manuscript is based in part on a thesis for the Ph.D. degree in Neuroscience from The Laney Graduate School of Emory University (McGregor, 2018).

- Asensio-Pinilla, E., Udina, E., Jaramillo, J., and Navarro, X. (2009). Electrical stimulation combined with exercise increase axonal regeneration after peripheral nerve injury. *Exp. Neurol.* 219, 258–265. doi: 10.1016/j.expneurol.2009.05.034
- Badke, A., Irintchev, A. P., and Wernig, A. (1989). Maturation of transmission in reinnervated mouse soleus muscle. *Muscle Nerve* 12, 580–586. doi: 10.1002/mus.880120709
- Baj, G., D'alessandro, V., Musazzi, L., Mallei, A., Sartori, C. R., Sciancalepore, M., et al. (2012). Physical exercise and antidepressants enhance BDNF targeting in hippocampal CA3 dendrites: further evidence of a spatial code for BDNF splice variants. *Neuropsychopharmacology* 37, 1600–1611. doi: 10.1038/npp.2012.5
- Baj, G., Leone, E., Chao, M. V., and Tongiorgi, E. (2011). Spatial segregation of BDNF transcripts enables BDNF to differentially shape distinct dendritic compartments. *Proc. Natl. Acad. Sci. U.S.A.* 108, 16813–16818. doi: 10.1073/pnas.1014168108
- Bartel, D. P. (2004). MicroRNAs: genomics, biogenesis, mechanism, and function. *Cell* 116, 281–297. doi: 10.1016/S0092-8674(04)00045-5
- Batty, N. J., Fenrich, K. K., and Fouad, K. (2017). The role of cAMP and its downstream targets in neurite growth in the adult nervous system. *Neurosci. Lett.* 652, 56–63. doi: 10.1016/j.neulet.2016.12.033
- Berchtold, N. C., Chinn, G., Chou, M., Kesslak, J. P., and Cotman, C. W. (2005). Exercise primes a molecular memory for brain-derived neurotrophic factor protein induction in the rat hippocampus. *Neuroscience* 133, 853–861. doi: 10.1016/j.neuroscience.2005.03.026
- Bibel, M., Hoppe, E., and Barde, Y. A. (1999). Biochemical and functional interactions between the neurotrophin receptors trk and p75NTR. *EMBO J.* 18, 616–622. doi: 10.1093/emboj/18.3.616
- Bischoff, A., Grosheva, M., Irintchev, A., Skouras, E., Kaidoglou, K., Michael, J., et al. (2009). Manual stimulation of the orbicularis oculi muscle improves eyelid closure after facial nerve injury in adult rats. *Muscle Nerve* 39, 197–205. doi: 10.1002/mus.21126
- Blinzinger, K., and Kreutzberg, G. (1968). Displacement of synaptic terminals from regenerating motoneurons by microglial cells. *Z. Zellforsch. Mikrosk. Anat.* 85, 145–157. doi: 10.1007/BF00325030
- Boeltz, T., Ireland, M., Mathis, K., Nicolini, J., Poplavski, K., Rose, S., et al. (2013). Effects of treadmill training on functional recovery following peripheral nerve injury in rats. *J. Neurophysiol.* 109, 2645–2657. doi: 10.1152/jn.00946.2012
- Boyd, J. G., and Gordon, T. (2001). The neurotrophin receptors, trkB and p75, differentially regulate motor axonal regeneration. *J. Neurobiol.* 49, 314–325. doi: 10.1002/neu.10013
- Boyd, J. G., and Gordon, T. (2002). A dose-dependent facilitation and inhibition of peripheral nerve regeneration by brain-derived neurotrophic factor. *Eur. J. Neurosci.* 15, 613–626. doi: 10.1046/j.1460-9568.2002.01891.x
- Boyd, J. G., and Gordon, T. (2003). Neurotrophic factors and their receptors in axonal regeneration and functional recovery after peripheral nerve injury. *Mol. Neurobiol.* 27, 277–324. doi: 10.1385/MN:27:3:277
- Brandt, J., Evans, J. T., Mildenhall, T., Mulligan, A., Konieczny, A., Rose, S. J., et al. (2015). Delaying the onset of treadmill exercise following peripheral nerve injury has different effects on axon regeneration and motoneuron synaptic plasticity. *J. Neurophysiol.* 113, 2390–2399. doi: 10.1152/jn.00892.2014
- Brannstrom, T., and Kellerth, J. O. (1998). Changes in synaptology of adult cat spinal alpha-motoneurons after axotomy. *Exp. Brain Res.* 118, 1–13. doi: 10.1007/s002210050249
- Brigadski, T., Hartmann, M., and Lessmann, V. (2005). Differential vesicular targeting and time course of synaptic secretion of

- the mammalian neurotrophins. *J. Neurosci.* 25, 7601–7614. doi: 10.1523/JNEUROSCI.1776-05.2005
- Brown, T. J., Khan, T., and Jones, K. J. (1999). Androgen induced acceleration of functional recovery after rat sciatic nerve injury. *Restor. Neurol. Neurosci.* 15, 289–295.
- Brushart, T. M. (1993). Motor axons preferentially reinnervate motor pathways. *J. Neurosci.* 13, 2730–2738. doi: 10.1523/JNEUROSCI.13-06-02730.1993
- Brushart, T. M., Aspalter, M., Griffin, J. W., Redett, R., Hameed, H., Zhou, C., et al. (2013). Schwann cell phenotype is regulated by axon modality and central-peripheral location, and persists *in vitro*. *Exp. Neurol.* 247, 272–281. doi: 10.1016/j.expneurol.2013.05.007
- Brushart, T. M., Hoffman, P. N., Royall, R. M., Murinson, B. B., Witzel, C., and Gordon, T. (2002). Electrical stimulation promotes motoneuron regeneration without increasing its speed or conditioning the neuron. *J. Neurosci.* 22, 6631–6638. doi: 10.1523/JNEUROSCI.22-15-06631.2002
- Brushart, T. M., Jari, R., Verge, V., Rohde, C., and Gordon, T. (2005). Electrical stimulation restores the specificity of sensory axon regeneration. *Exp. Neurol.* 194, 221–229. doi: 10.1016/j.expneurol.2005.02.007
- Bueker, E. D., and Meyers, C. E. (1951). The maturity of peripheral nerves at the time of injury as a factor in nerve regeneration. *Anat. Rec.* 109, 723–743. doi: 10.1002/ar.1091090409
- Cai, D., Shen, Y., De Bellard, M., Tang, S., and Filbin, M. T. (1999). Prior exposure to neurotrophins blocks inhibition of axonal regeneration by MAG and Myelin via a cAMP-dependent mechanism. *Neuron* 22, 89–101. doi: 10.1016/S0896-6273(00)80681-9
- Capsoni, S., Tongiorgi, E., Cattaneo, A., and Domenici, L. (1999). Dark rearing blocks the developmental down-regulation of brain-derived neurotrophic factor messenger RNA expression in layers IV and V of the rat visual cortex. *Neuroscience* 88, 393–403. doi: 10.1016/S0306-4522(98)00250-4
- Carter, B. D., Kaltschmidt, C., Kaltschmidt, B., Offenhauser, N., Bohm-Matthaei, R., Baeuerle, P. A., et al. (1996). Selective activation of NF-kappa B by nerve growth factor through the neurotrophin receptor p75. *Science* 272, 542–545. doi: 10.1126/science.272.5261.542
- Chen, Z., Jing, D., Bath, K., Ieraci, A., Khan, T., Siao, C., et al. (2006). Genetic variant BDNF (Val66Met) polymorphism alters anxiety-related behavior. *Science* 314, 140–143. doi: 10.1126/science.1129663
- Chen, Z., Patel, P., Sant, G., Meng, C., Teng, K., Hempstead, B., et al. (2004). Variant brain-derived neurotrophic factor (BDNF) (Met66) alters the intracellular trafficking and activity-dependent secretion of wild-type BDNF in neurosecretory cells and cortical neurons. *J. Neurosci.* 24, 4401–4411. doi: 10.1523/JNEUROSCI.0348-04.2004
- Chen, Z. Y., Ieraci, A., Teng, H., Dall, H., Meng, C. X., Herrera, D. G., et al. (2005). Sortilin controls intracellular sorting of brain-derived neurotrophic factor to the regulated secretory pathway. *J. Neurosci.* 25, 6156–6166. doi: 10.1523/JNEUROSCI.1017-05.2005
- Chiaruttini, C., Sonogo, M., Baj, G., Simonato, M., and Tongiorgi, E. (2008). Bdnf mRNA splice variants display activity-dependent targeting to distinct hippocampal laminae. *Mol. Cell. Neurosci.* 37, 11–19. doi: 10.1016/j.mcn.2007.08.011
- Chiaruttini, C., Vicario, A., Li, Z., Baj, G., Braiuca, P., Wu, Y., et al. (2009). Dendritic trafficking of BDNF mRNA is mediated by translin and blocked by the G196A (Val66Met) mutation. *Proc. Natl. Acad. Sci. U.S.A.* 106, 16481–16486. doi: 10.1073/pnas.0902833106
- Cho, H. J., Kim, S. Y., Park, M. J., Kim, D. S., Kim, J. K., and Chu, M. Y. (1997). Expression of mRNA for brain-derived neurotrophic factor in the dorsal root ganglion following peripheral inflammation. *Brain Res.* 749, 358–362. doi: 10.1016/S0006-8993(97)00048-6
- Christie, K. J., Webber, C. A., Martinez, J. A., Singh, B., and Zochodne, D. W. (2010). PTEN inhibition to facilitate intrinsic regenerative outgrowth of adult peripheral axons. *J. Neurosci.* 30, 9306–9315. doi: 10.1523/JNEUROSCI.6271-09.2010
- Cobianchi, S., Marinelli, S., Florenzano, F., Pavone, F., and Luvisetto, S. (2010). Short- but not long-lasting treadmill running reduces allodynia and improves functional recovery after peripheral nerve injury. *Neuroscience* 168, 273–287. doi: 10.1016/j.neuroscience.2010.03.035
- Conner, J. M., Lauterborn, J. C., Yan, Q., Gall, C. M., and Varon, S. (1997). Distribution of Brain-Derived Neurotrophic Factor (BDNF) protein and mRNA in the normal adult rat CNS: evidence for anterograde axonal transport. *J. Neurosci.* 17, 2295–2313. doi: 10.1523/JNEUROSCI.17-07-02295.1997
- Cosgaya, J. M., Chan, J. R., and Shooter, E. M. (2002). The neurotrophin receptor p75NTR as a positive modulator of myelination. *Science* 298, 1245–1248. doi: 10.1126/science.1076595
- Davis-Lopez de Carrizosa, M. A., Morado-Diaz, C. J., Tena, J. J., Benitez-Temino, B., Pecero, M. L., Morcuende, S. R., et al. (2009). Complementary actions of BDNF and neurotrophin-3 on the firing patterns and synaptic composition of motoneurons. *J. Neurosci.* 29, 575–587. doi: 10.1523/JNEUROSCI.5312-08.2009
- De Bono, J. P., Adlam, D., Paterson, D. J., and Channon, K. M. (2006). Novel quantitative phenotypes of exercise training in mouse models. *Am. J. Physiol. Regul. Integr. Comp. Physiol.* 290, R926–R934. doi: 10.1152/ajpregu.00694.2005
- Dechant, G., and Barde, Y.-A. (1997). Signalling through the neurotrophin receptor p75NTR. *Curr. Opin. Neurobiol.* 7, 413–418. doi: 10.1016/S0959-4388(97)80071-2
- Dechant, G., and Barde, Y. A. (2002). The neurotrophin receptor p75(NTR): novel functions and implications for diseases of the nervous system. *Nat. Neurosci.* 5, 1131–1136. doi: 10.1038/nn1102-1131
- Deinhardt, K., Kim, T., Spellman, D. S., Mains, R. E., Eipper, B. A., Neubert, T. A., et al. (2011). Neuronal growth cone retraction relies on proneurotrophin receptor signaling through Rac. *Sci. Signal* 4:ra82. doi: 10.1126/scisignal.2002060
- Delcroix, J.-D., Valletta, J. S., Wu, C., Hunt, S. J., Kowal, A. S., and Mobley, W. C. (2003). NGF signaling in sensory neurons: evidence that early endosomes carry NGF retrograde signals. *Neuron* 39, 69–84. doi: 10.1016/S0896-6273(03)00397-0
- Diamond, J., Coughlin, M., Macintyre, L., Holmes, M., and Visheau, B. (1987). Evidence that endogenous beta nerve growth factor is responsible for the collateral sprouting, but not the regeneration, of nociceptive axons in adult rats. *Proc. Natl. Acad. Sci. U.S.A.* 84, 6596–6600. doi: 10.1073/pnas.84.18.6596
- Diamond, J., Foerster, A., Holmes, M., and Coughlin, M. (1992). Sensory nerves in adult rats regenerate and restore sensory function to the skin independently of endogenous NGF. *J. Neurosci.* 12, 1467–1476. doi: 10.1523/JNEUROSCI.12-04-01467.1992
- Dieni, S., Matsumoto, T., Dekkers, M., Rauskolb, S., Ionescu, M. S., Deogracias, R., et al. (2012). BDNF and its pro-peptide are stored in presynaptic dense core vesicles in brain neurons. *J. Cell Biol.* 196, 775–788. doi: 10.1083/jcb.201201038
- Difato, F., Tsushima, H., Pesce, M., Benfenati, F., Blau, A., and Chieriegiatti, E. (2011). The formation of actin waves during regeneration after axonal lesion is enhanced by BDNF. *Sci. Rep.* 1:183. doi: 10.1038/srep00183
- Egan, M., Kojima, M., Callicott, J., Goldberg, T., Kolachana, B., Bertolino, A., et al. (2003). The BDNF val66met polymorphism affects activity-dependent secretion of BDNF and human memory and hippocampal function. *Cell* 112, 257–269. doi: 10.1016/S0092-8674(03)00035-7
- Eide, F. F., Vining, E. R., Eide, B. L., Zang, K., Wang, X. Y., and Reichardt, L. F. (1996). Naturally occurring truncated trkB receptors have dominant inhibitory effects on brain-derived neurotrophic factor signaling. *J. Neurosci.* 16, 3123–3129. doi: 10.1523/JNEUROSCI.16-10-03123.1996
- Elfving, B., Plougmann, P. H., and Wegener, G. (2010). Detection of brain-derived neurotrophic factor (BDNF) in rat blood and brain preparations using ELISA: Pitfalls and solutions. *J. Neurosci. Methods* 187, 73–77. doi: 10.1016/j.jneumeth.2009.12.017
- Elzinga, K., Tyreman, N., Ladak, A., Savaryn, B., Olson, J., and Gordon, T. (2015). Brief electrical stimulation improves nerve regeneration after delayed repair in Sprague Dawley rats. *Exp. Neurol.* 269, 142–153. doi: 10.1016/j.expneurol.2015.03.022
- Enes, J., Langwieser, N., Ruschel, J., Carballosa-Gonzalez, M. M., Klug, A., Traut, M. H., et al. (2010). Electrical activity suppresses axon growth through Cav1.2 channels in adult primary sensory neurons. *Curr. Biol.* 20, 1154–1164. doi: 10.1016/j.cub.2010.05.055
- English, A. (2005). Enhancing axon regeneration in peripheral nerves also increases functionally inappropriate reinnervation of targets. *J. Comp. Neurol.* 490, 427–441. doi: 10.1002/cne.20678
- English, A., Cucoranu, D., Mulligan, A., and Sabatier, M. (2009). Treadmill training enhances axon regeneration in injured mouse peripheral nerves without increased loss of topographic specificity. *J. Comp. Neurol.* 517, 245–255. doi: 10.1002/cne.22149

- English, A., Liu, K., Nicolini, J., Mulligan, A., and Ye, K. (2013). Small-molecule trkB agonists promote axon regeneration in cut peripheral nerves. *Proc. Natl. Acad. Sci. U.S.A.* 110, 16217–16222. doi: 10.1073/pnas.1303646110
- English, A., Schartz, G., Meador, W., Sabatier, M., and Mulligan, A. (2007). Electrical stimulation promotes peripheral axon regeneration by enhanced neuronal neurotrophin signaling. *Dev. Neurobiol.* 67, 158–172. doi: 10.1002/dneu.20339
- English, A., Wilhelm, J., and Sabatier, M. (2011). Enhancing recovery from peripheral nerve injury using treadmill training. *Ann. Anat.* 193, 354–361. doi: 10.1016/j.aanat.2011.02.013
- English, A. W., Wilhelm, J. C., and Ward, P. J. (2014). Exercise, neurotrophins, and axon regeneration in the PNS. *Physiology* 29, 437–445. doi: 10.1152/physiol.00028.2014
- Ernfors, P., Henschen, A., Olson, L., and Persson, H. (1989). Expression of nerve growth factor receptor mRNA is developmentally regulated and increased after axotomy in rat spinal cord motoneurons. *Neuron* 2, 1605–1613. doi: 10.1016/0896-6273(89)90049-4
- Escandon, E., Soppet, D., Rosenthal, A., Mendoza-Ramirez, J., Szonyi, E., Burton, L., et al. (1994). Regulation of neurotrophin receptor expression during embryonic and postnatal development. *J. Neurosci.* 14, 2054–2068. doi: 10.1523/JNEUROSCI.14-04-02054.1994
- Evgenieva, E., Schweigert, P., Guntinas-Lichius, O., Pavlov, S., Grosheva, M., Angelova, S., et al. (2008). Manual stimulation of the suprahyoid-sublingual region diminishes polynervation of the motor endplates and improves recovery of function after hypoglossal nerve injury in rats. *Neurorehabil. Neural Repair* 22, 754–768. doi: 10.1177/1545968308316387
- Failla, M. D., Kumar, R., Peitzman, A., Conley, Y. P., Ferrell, R. E., and Wagner, A. K. (2015). Variation in the BDNF gene interacts with age to predict mortality in a prospective, longitudinal cohort with severe TBI. *Neurorehabil. Neural Repair* 29, 234–246. doi: 10.1177/1545968314542617
- Fargo, K. N., Foecking, E. M., Jones, K. J., and Sengelaub, D. R. (2009). Neuroprotective actions of androgens on motoneurons. *Front. Neuroendocrinol.* 30:141. doi: 10.1016/j.yfrne.2009.04.005
- Ferri, C. C., Moore, F. A., and Bisby, M. A. (1998). Effects of facial nerve injury on mouse motoneurons lacking the p75 low-affinity neurotrophin receptor. *J. Neurobiol.* 34, 1–9. doi: 10.1002/(SICI)1097-4695(199801)34:1<1::AID-NEU1>3.0.CO;2-C
- Flynn, K. C., Pak, C. W., Shaw, A. E., Bradke, F., and Bamberg, J. R. (2009). Growth cone-like waves transport actin and promote axonogenesis and neurite branching. *Dev. Neurobiol.* 69, 761–779. doi: 10.1002/dneu.20734
- Foecking, E. M., Fargo, K. N., Coughlin, L. M., Kim, J. T., Marzo, S. J., and Jones, K. J. (2012). Single session of brief electrical stimulation immediately following crush injury enhances functional recovery of rat facial nerve. *J. Rehabil. Res. Dev.* 49, 451–458. doi: 10.1682/JRRD.2011.03.0033
- Freeman, L. M., Padgett, B. A., Prins, G. S., and Breedlove, S. M. (1995). Distribution of androgen receptor immunoreactivity in the spinal cord of wild-type, androgen-insensitive and gonadectomized male rats. *J. Neurobiol.* 27, 51–59. doi: 10.1002/neu.480270106
- Frisén, J., Verge, V. M., Fried, K., Risling, M., Persson, H., Trotter, J., et al. (1993). Characterization of glial trkB receptors: differential response to injury in the central and peripheral nervous systems. *Proc. Natl. Acad. Sci. U.S.A.* 90, 4971–4975. doi: 10.1073/pnas.90.11.4971
- Fryer, R. H., Kaplan, D. R., and Kromer, L. F. (1997). Truncated trkB receptors on nonneuronal cells inhibit BDNF-induced neurite outgrowth *in vitro*. *Exp. Neurol.* 148, 616–627. doi: 10.1006/exnr.1997.6699
- Fu, S. Y., and Gordon, T. (1995a). Contributing factors to poor functional recovery after delayed nerve repair: prolonged axotomy. *J. Neurosci.* 15, 3876–3885. doi: 10.1523/JNEUROSCI.15-05-03876.1995
- Fu, S. Y., and Gordon, T. (1995b). Contributing factors to poor functional recovery after delayed nerve repair: prolonged denervation. *J. Neurosci.* 15, 3886–3895. doi: 10.1523/JNEUROSCI.15-05-03886.1995
- Fukuchi, M., and Tsuda, M. (2010). Involvement of the 3'-untranslated region of the brain-derived neurotrophic factor gene in activity-dependent mRNA stabilization. *J. Neurochem.* 115, 1222–1233. doi: 10.1111/j.1471-4159.2010.07016.x
- Funakoshi, H., Frisen, J., Barbany, G., Timmusk, T., Zachrisson, O., Verge, V. M., et al. (1993). Differential expression of mRNAs for neurotrophins and their receptors after axotomy of the sciatic nerve. *J. Cell Biol.* 123, 455–465. doi: 10.1083/jcb.123.2.455
- Gallo, G., and Letourneau, P. C. (1998). Localized sources of neurotrophins initiate axon collateral sprouting. *J. Neurosci.* 18, 5403–5414. doi: 10.1523/JNEUROSCI.18-14-05403.1998
- Gao, Y., Nikulina, E., Mellado, W., and Filbin, M. T. (2003). Neurotrophins elevate cAMP to reach a threshold required to overcome inhibition by MAG through extracellular signal-regulated kinase-dependent inhibition of phosphodiesterase. *J. Neurosci.* 23, 11770–11777. doi: 10.1523/JNEUROSCI.23-37-11770.2003
- Gardiner, P. F., Michel, R., and Iadeluca, G. (1984). Previous exercise training influences functional sprouting of rat hindlimb motoneurons in response to partial denervation. *Neurosci. Lett.* 45, 123–127. doi: 10.1016/0304-3940(84)90086-7
- Geremia, N., Gordon, T., Brushart, T., Al Majed, A., and Verge, V. (2007). Electrical stimulation promotes sensory neuron regeneration and growth-associated gene expression. *Exp. Neurol.* 205, 347–359. doi: 10.1016/j.expneurol.2007.01.040
- Ghosh-Roy, A., Wu, Z., Goncharov, A., Jin, Y., and Chisholm, A. D. (2010). Calcium and cyclic AMP promote axonal regeneration in *Caenorhabditis elegans* and require DLK-1 kinase. *J. Neurosci.* 30, 3175–3183. doi: 10.1523/JNEUROSCI.5464-09.2010
- Gibney, J., and Zheng, J. Q. (2003). Cytoskeletal dynamics underlying collateral membrane protrusions induced by neurotrophins in cultured *Xenopus* embryonic neurons. *J. Neurobiol.* 54, 393–405. doi: 10.1002/neu.10149
- Giza, J. I., Kim, J., Meyer, H. C., Anastasia, A., Dincheva, I., Zheng, C. I., et al. (2018). The BDNF Val66Met prodomain disassembles dendritic spines altering fear extinction circuitry and behavior. *Neuron* 99, 163–178.e6. doi: 10.1016/j.neuron.2018.05.024
- Goldberg, J. L., Espinosa, J. S., Xu, Y., Davidson, N., Kovacs, G. T., and Barres, B. A. (2002). Retinal ganglion cells do not extend axons by default: promotion by neurotrophic signaling and electrical activity. *Neuron* 33, 689–702. doi: 10.1016/S0896-6273(02)00602-5
- Gomez-Pinilla, F., Ying, Z., Roy, R. R., Molteni, R., and Edgerton, V. R. (2002). Voluntary exercise induces a BDNF-mediated mechanism that promotes neuroplasticity. *J. Neurophysiol.* 88, 2187–2195. doi: 10.1152/jn.00152.2002
- Gordon, T. (2015). “Chapter 61 - The biology, limits, and promotion of peripheral nerve regeneration in rats and humans” in *Nerves and Nerve Injuries*, eds R. S. Tubbs, E. Rizk, M. M. Shoja, M. Loukas, N. Barbaro, and R. J. Spinner (San Diego, CA: Academic Press), 993–1019.
- Gordon, T. (2016). Electrical stimulation to enhance axon regeneration after peripheral nerve injuries in animal models and humans. *Neurotherapeutics* 13, 295–310. doi: 10.1007/s13311-015-0415-1
- Gordon, T., Amirjani, N., Edwards, D. C., and Chan, K. M. (2010). Brief post-surgical electrical stimulation accelerates axon regeneration and muscle reinnervation without affecting the functional measures in carpal tunnel syndrome patients. *Exp. Neurol.* 223, 192–202. doi: 10.1016/j.expneurol.2009.09.020
- Gordon, T., Chan, K. M., Sulaiman, O. A. R., Udina, E., Amirjani, N., and Brushart, T. M. (2009). Accelerating axon growth to overcome limitations in functional recovery after peripheral nerve injury *Neurosurgery* 65, A132–A144. doi: 10.1227/01.NEU.0000335650.09473.D3
- Gordon, T., and English, A. W. (2016). Strategies to promote peripheral nerve regeneration: electrical stimulation and/or exercise. *Eur. J. Neurosci.* 43, 336–350. doi: 10.1111/ejn.13005
- Grosheva, M., Nohroudi, K., Schwarz, A., Rink, S., Bendella, H., Sarikcioglu, L., et al. (2016). Comparison of trophic factors' expression between paralyzed and recovering muscles after facial nerve injury. A quantitative analysis in time course. *Exp. Neurol.* 279, 137–148. doi: 10.1016/j.expneurol.2016.02.020
- Gschwendtner, A., Liu, Z., Hucho, T., Bohatschek, M., Kalla, R., Dechant, G., et al. (2003). Regulation, cellular localization, and function of the p75 neurotrophin receptor (p75NTR) during the regeneration of facial motoneurons. *Mol. Cell. Neurosci.* 24, 307–322. doi: 10.1016/S1044-7431(03)00167-2
- Gualandris, A., Jones, T. E., Strickland, S., and Tsirka, S. E. (1996). Membrane depolarization induces calcium-dependent secretion of tissue plasminogen activator. *J. Neurosci.* 16, 2220–2225.

- Guntinas-Lichius, O., Hundeshagen, G., Paling, T., Streppel, M., Grosheva, M., Irintchev, A., et al. (2007). Manual stimulation of facial muscles improves functional recovery after hypoglossal-facial anastomosis and interpositional nerve grafting of the facial nerve in adult rats. *Neurobiol. Dis.* 28, 101–112. doi: 10.1016/j.nbd.2007.07.006
- Hall, D., Dhill, A., Charalambous, A., Gogos, J. A., and Karayiorgou, M. (2003). Sequence variants of the brain-derived neurotrophic factor (BDNF) gene are strongly associated with obsessive-compulsive disorder. *Am. J. Hum. Genet.* 73, 370–376. doi: 10.1086/377003
- Hamanoue, M., Middleton, G., Wyatt, S., Jaffray, E., Hay, R. T., and Davies, A. M. (1999). p75-mediated NF-kappaB activation enhances the survival response of developing sensory neurons to nerve growth factor. *Mol. Cell. Neurosci.* 14, 28–40. doi: 10.1006/mcne.1999.0770
- Helm, E. E., Matt, K. S., Kirschner, K. F., Pohlig, R. T., Kohl, D., and Reisman, D. S. (2017). The influence of high intensity exercise and the Val66Met polymorphism on circulating BDNF and locomotor learning. *Neurobiol. Learn. Mem.* 144, 77–85. doi: 10.1016/j.nlm.2017.06.003
- Herbison, G. J., Jaweed, M. M., and Ditunno, J. F. (1980a). Effect of activity and inactivity on reinnervating rat skeletal muscle contractility. *Exp. Neurol.* 70, 498–506. doi: 10.1016/0014-4886(80)90176-4
- Herbison, G. J., Jaweed, M. M., and Ditunno, J. F. (1980b). Histochemical fiber type alterations secondary to exercise training of reinnervating adult rat muscle. *Arch. Phys. Med. Rehabil.* 61, 255–257.
- Herbison, G. J., Jaweed, M. M., Ditunno, J. F., and Scott, C. M. (1973). Effect of overwork during reinnervation of rat muscle. *Exp. Neurol.* 41, 1–14. doi: 10.1016/0014-4886(73)90176-3
- Hetzler, L. E. T., Sharma, N., Tanzer, L., Wurster, R. D., Leonetti, J., Marzo, S. J., et al. (2008). Accelerating functional recovery after rat facial nerve injury: effects of gonadal steroids and electrical stimulation. *Otolaryngol. Head Neck Surg.* 139, 62–67. doi: 10.1016/j.otohns.2008.02.006
- Heuer, J. G., Fatemie-Nainie, S., Wheeler, E. F., and Bothwell, M. (1990). Structure and developmental expression of the chicken NGF receptor. *Dev. Biol.* 137, 287–304. doi: 10.1016/0012-1606(90)90255-H
- Heumann, R., Korsching, S., Bandtlow, C., and Thoenen, H. (1987a). Changes of nerve growth factor synthesis in nonneuronal cells in response to sciatic nerve transection. *J. Cell Biol.* 104, 1623–1631. doi: 10.1083/jcb.104.6.1623
- Heumann, R., Lindholm, D., Bandtlow, C., Meyer, M., Radeke, M. J., Misko, T. P., et al. (1987b). Differential regulation of mRNA encoding nerve growth factor and its receptor in rat sciatic nerve during development, degeneration, and regeneration: role of macrophages. *Proc. Natl. Acad. Sci. U.S.A.* 84, 8735–8739. doi: 10.1073/pnas.84.23.8735
- Hines, H. M. (1942). Effects of immobilization and activity on neuromuscular regeneration. *JAMA* 120, 515–517. doi: 10.1001/jama.1942.02830420023006
- Hoffer, J. A., Stein, R. B., and Gordon, T. (1979). Differential atrophy of sensory and motor fibers following section of cat peripheral nerves. *Brain Res.* 178, 347–361. doi: 10.1016/0006-8993(79)90698-X
- Hoke, A., Redett, R., Hameed, H., Jari, R., Zhou, C., Li, Z. B., et al. (2006). Schwann cells express motor and sensory phenotypes that regulate axon regeneration. *J. Neurosci.* 26, 9646–9655. doi: 10.1523/JNEUROSCI.1620-06.2006
- Hong, E. J., McCord, A. E., and Greenberg, M. E. (2008). A biological function for the neuronal activity-dependent component of Bdnf transcription in the development of cortical inhibition. *Neuron* 60, 610–624. doi: 10.1016/j.neuron.2008.09.024
- Huang, E. J., and Reichardt, L. F. (2003). Trk receptors: roles in neuronal signal transduction. *Annu. Rev. Biochem.* 72, 609–642. doi: 10.1146/annurev.biochem.72.121801.161629
- Huang, J., Zhang, Y., Lu, X., Hu, X., and Luo, Z. (2013). Electrical stimulation accelerates nerve regeneration and functional recovery in delayed peripheral nerve injury in rats. *Eur. J. Neurosci.* 38, 3691–3701. doi: 10.1111/ejn.12370
- Hwang, J. J., Park, M. H., Choi, S. Y., and Koh, J. Y. (2005). Activation of the Trk signaling pathway by extracellular zinc. Role of metalloproteinases. *J. Biol. Chem.* 280, 11995–12001. doi: 10.1074/jbc.M403172200
- Ibáñez, C., and Simi, A. (2012). p75 neurotrophin receptor signaling in nervous system injury and degeneration: paradox and opportunity. *Trends Neurosci.* 35, 431–440. doi: 10.1016/j.tins.2012.03.007
- Ieraci, A., Madaio, A. I., Mallei, A., Lee, F. S., and Popoli, M. (2016). Brain-derived neurotrophic factor Val66Met human polymorphism impairs the beneficial exercise-induced neurobiological changes in mice. 41:3070–3079. *Neuropsychopharmacology* 41, 3070–3079. doi: 10.1038/npp.2016.120
- Inagaki, N., and Katsuno, H. (2017). Actin waves: origin of cell polarization and migration? *Trends Cell Biol.* 27, 515–526. doi: 10.1016/j.tcb.2017.02.003
- Jaiswal, P. B., Mistretta, O. C., Ward, P. J., and English, A. W. (2018). Chemogenetic enhancement of axon regeneration following peripheral nerve injury in the SLICK-A mouse. *Brain Sci.* 8:93. doi: 10.3390/brainsci8050093
- Jaiswal, P. B., Tung, J. K., Gross, R. E., and English, A. W. (2017). Motoneuron activity is required for enhancements in functional recovery after peripheral nerve injury in exercised female mice. *J. Neurosci. Res.* doi: 10.1002/jnr.24109. [Epub ahead of print].
- Jankowski, M. P., Cornuet, P. K., McIlwraith, S., Koerber, H. R., and Albers, K. M. (2006). SRY-box containing gene 11 (Sox11) transcription factor is required for neuron survival and neurite growth. *Neuroscience* 143, 501–514. doi: 10.1016/j.neuroscience.2006.09.010
- Johnson, H., Hokfelt, T., and Ulfhake, B. (1999). Expression of p75(NTR), trkB and trkC in nonmanipulated and axotomized motoneurons of aged rats. *Brain Res. Mol. Brain Res.* 69, 21–34. doi: 10.1016/S0169-328X(99)00068-6
- Jones, K. J. (1993). Recovery from facial paralysis following crush injury of the facial nerve in hamsters: differential effects of gender and androgen exposure. *Exp. Neurol.* 121, 133–138. doi: 10.1006/exnr.1993.1079
- Jones, K. R., Farinas, I., Backus, C., and Reichardt, L. F. (1994). Targeted disruption of the BDNF gene perturbs brain and sensory neuron development but not motor neuron development. *Cell* 76, 989–999. doi: 10.1016/0092-8674(94)90377-8
- Keifer, J., Sabirzhanov, B. E., Zheng, Z., Li, W., and Clark, T. G. (2009). Cleavage of proBDNF by a tolloid-like metalloproteinase (tTLL) is required for acquisition of *in vitro* eyeblink classical conditioning. *J. Neurosci.* 29, 14956–14964. doi: 10.1523/JNEUROSCI.3649-09.2009
- Klein, A. B., Williamson, R., Santini, M. A., Clemmensen, C., Ettrup, A., Rios, M., et al. (2011). Blood BDNF concentrations reflect brain-tissue BDNF levels across species. *Int. J. Neuropsychopharmacol.* 14, 347–353. doi: 10.1017/S1461145710000738
- Kobayashi, N. R., Bedard, A. M., Hincke, M. T., and Tetzlaff, W. (1996). Increased expression of BDNF and trkB mRNA in rat facial motoneurons after axotomy. *Eur. J. Neurosci.* 8, 1018–1029. doi: 10.1111/j.1460-9568.1996.tb01588.x
- Koenig, E., Martin, R., Titmus, M., and Sotelo-Silveira, J. R. (2000). Cryptic peripheral ribosomal domains distributed intermittently along mammalian myelinated axons. *J. Neurosci.* 20, 8390–8400. doi: 10.1523/JNEUROSCI.20-22-08390.2000
- Kohara, K., Kitamura, A., Morishima, M., and Tsumoto, T. (2001). Activity-dependent transfer of brain-derived neurotrophic factor to postsynaptic neurons. *Science* 291, 2419–2423. doi: 10.1126/science.1057415
- Kolbeck, R., Jungbluth, S., and Barde, Y. A. (1994). Characterisation of neurotrophin dimers and monomers. *Eur. J. Biochem.* 225, 995–1003. doi: 10.1111/j.1432-1033.1994.0995b.x
- Koliatsos, V., Crawford, T., and Price, D. (1991). Axotomy induces nerve growth factor receptor immunoreactivity in spinal motor neurons. *Brain Res.* 549, 297–304. doi: 10.1016/0006-8993(91)90471-7
- Koppes, A. N., Nordberg, A. L., Paolillo, G. M., Goodsell, N. M., Darwish, H. A., Zhang, L., et al. (2014). Electrical stimulation of schwann cells promotes sustained increases in neurite outgrowth. *Tissue Eng. Part A* 20, 494–506. doi: 10.1089/ten.TEA.2013.0012
- Krakowiak, J., Liu, C., Papudesu, C., Ward, P. J., Wilhelm, J. C., and English, A. W. (2015). Neuronal BDNF signaling is necessary for the effects of treadmill exercise on synaptic stripping of axotomized motoneurons. *Neural Plast.* 2015:392591. doi: 10.1155/2015/392591
- Krook-Magnuson, E., Ledri, M., Soltesz, I., and Kokaia, M. (2014). How might novel technologies such as optogenetics lead to better treatments in epilepsy? *Adv. Exp. Med. Biol.* 813, 319–336. doi: 10.1007/978-94-017-8914-1_26
- Krueger, F., Pardini, M., Huey, E. D., Rayment, V., Solomon, J., Lipsky, R. H., et al. (2011). The role of the Met66 brain-derived neurotrophic factor allele in the recovery of executive functioning after combat-related traumatic brain injury. *J. Neurosci.* 31, 598–606. doi: 10.1523/JNEUROSCI.1399-20.2011
- Krystosek, A., and Seeds, N. W. (1981). Plasminogen activator release at the neuronal growth cone. *Science* 213, 1532–1534. doi: 10.1126/science.7197054

- Kuczewski, N., Porcher, C., Lessmann, V., Medina, I., and Gaiarsa, J. L. (2009). Activity-dependent dendritic release of BDNF and biological consequences. *Mol. Neurobiol.* 39, 37–49. doi: 10.1007/s12035-009-8050-7
- Kujawa, K. A., Emeric, E., and Jones, K. J. (1991). Testosterone differentially regulates the regenerative properties of injured hamster facial motoneurons. *J. Neurosci.* 11, 3898–3906. doi: 10.1523/JNEUROSCI.11-12-03898.1991
- Kujawa, K. A., Kinderman, N. B., and Jones, K. J. (1989). Testosterone-induced acceleration of recovery from facial paralysis following crush axotomy of the facial nerve in male hamsters. *Exp. Neurol.* 105, 80–85. doi: 10.1016/0014-4886(89)90174-X
- Kujawa, K. A., Tanzer, L., and Jones, K. J. (1995). Inhibition of the accelerative effects of testosterone on hamster facial nerve regeneration by the antiandrogen flutamide. *Exp. Neurol.* 133, 138–143. doi: 10.1006/exnr.1995.1016
- Kuzis, K., Coffin, J. D., and Eckenstein, F. P. (1999). Time course and age dependence of motor neuron death following facial nerve crush injury: role of fibroblast growth factor. *Exp. Neurol.* 157, 77–87. doi: 10.1006/exnr.1999.7014
- Kuzniewska, B., Rejmak, E., Malik, A. R., Jaworski, J., Kaczmarek, L., and Kalita, K. (2013). Brain-derived neurotrophic factor induces matrix metalloproteinase 9 expression in neurons via the serum response factor/c-Fos pathway. *Mol. Cell. Biol.* 33, 2149–2162. doi: 10.1128/MCB.00008-13
- Lal, D., Hetzler, L. T., Sharma, N., Wurster, R. D., Marzo, S. J., Jones, K. J., et al. (2008). Electrical stimulation facilitates rat facial nerve recovery from a crush injury. *Otolaryngol. Head Neck Surg.* 139, 68–73. doi: 10.1016/j.otohns.2008.04.030
- Lau, A. G., Irier, H. A., Gu, J., Tian, D., Ku, L., Liu, G., et al. (2010). Distinct 3'UTRs differentially regulate activity-dependent translation of brain-derived neurotrophic factor (BDNF). *Proc. Natl. Acad. Sci. U.S.A.* 107, 15945–15950. doi: 10.1073/pnas.1002929107
- Lee, R., Kerami, P., Teng, K. K., and Hempstead, B. L. (2001). Regulation of cell survival by secreted Proneurotrophins. *Science* 294, 1945–1948. doi: 10.1126/science.1065057
- Leech, K. A., and Hornby, T. G. (2017). High-intensity locomotor exercise increases brain-derived neurotrophic factor in individuals with incomplete spinal cord injury. *J. Neurotrauma* 34, 1240–1248. doi: 10.1089/neu.2016.4532
- Lemos, J. R., Alves, C. R., De Souza, S. B. C., Marsiglia, J. D. C., Silva, M. S. M., Pereira, A. C., et al. (2015). Peripheral vascular reactivity and serum BDNF responses to aerobic training are impaired by the BDNF Val66Met polymorphism. *Physiol. Genomics* 48, 116–123. doi: 10.1152/physiolgenomics.00086.2015
- Lessmann, V., Gottmann, K., and Malsangio, M. (2003). Neurotrophin secretion: current facts and future prospects. *Prog. Neurobiol.* 69, 341–374. doi: 10.1016/S0304-0082(03)00019-4
- Lewin, G. R., and Barde, Y. A. (1996). Physiology of the neurotrophins. *Annu. Rev. Neurosci.* 19, 289–317. doi: 10.1146/annurev.ne.19.030196.001445
- Lewin, S. L., Utley, D. S., Cheng, E. T., Verity, A. N., and Terris, D. J. (1997). Simultaneous treatment with BDNF and CNTF after peripheral nerve transection and repair enhances rate of functional recovery compared with BDNF treatment alone. *Laryngoscope* 107, 992–999. doi: 10.1097/00005537-199707000-00029
- Li, Z., Wu, Y., and Baraban, J. M. (2008). The Translin/Trax RNA binding complex: clues to function in the nervous system. *Biochim. Biophys. Acta* 1779, 479–485. doi: 10.1016/j.bbagr.2008.03.008
- Liao, C.-F., Yang, T.-Y., Chen, Y.-H., Yao, C.-H., Way, T.-D., and Chen, Y.-S. (2017). Effects of swimming exercise on nerve regeneration in a rat sciatic nerve transection model. *Biomedicine* 7:3. doi: 10.1051/bmdcn/2017070103
- Liepinsh, E., Ilag, L. L., Otting, G., and Ibáñez, C. F. (1997). NMR structure of the death domain of the p75 neurotrophin receptor. *EMBO J.* 16, 4999–5005. doi: 10.1093/emboj/16.16.4999
- Linda, H., Shupliakov, O., Ornung, G., Ottersen, O. P., Storm-Mathisen, J., Risling, M., et al. (2000). Ultrastructural evidence for a preferential elimination of glutamate-immunoreactive synaptic terminals from spinal motoneurons after intramedullary axotomy. *J. Comp. Neurol.* 425, 10–23. doi: 10.1002/1096-9861(20000911)425:13.3.CO;2-R
- Lindsay, R. M. (1988). Nerve growth factors (NGF, BDNF) enhance axonal regeneration but are not required for survival of adult sensory neurons. *J. Neurosci.* 8, 2394–2405. doi: 10.1523/JNEUROSCI.08-07-02394.1988
- Liu, C., Ward, P. J., and English, A. W. (2014). The effects of exercise on synaptic stripping require androgen receptor signaling. *PLoS ONE* 9:e98633. doi: 10.1371/journal.pone.0098633
- Liu, Q. R., Lu, L., Zhu, X. G., Gong, J. P., Shaham, Y., and Uhl, G. R. (2006). Rodent BDNF genes, novel promoters, novel splice variants, and regulation by cocaine. *Brain Res.* 1067, 1–12. doi: 10.1016/j.brainres.2005.10.004
- Liu, R.-J., Lee, F. S., Li, X.-Y., Bambico, F., Duman, R. S., and Aghajanian, G. K. (2012). Brain-derived neurotrophic factor Val66Met allele impairs basal and ketamine-stimulated synaptogenesis in prefrontal cortex. *Biol. Psychiatry* 71, 996–1005. doi: 10.1016/j.biopsych.2011.09.030
- Ljungberg, C., Novikov, L., Kellerth, J. O., Ebendal, T., and Wiberg, M. (1999). The neurotrophins NGF and NT-3 reduce sensory neuronal loss in adult rat after peripheral nerve lesion. *Neurosci. Lett.* 262, 29–32. doi: 10.1016/S0304-3940(99)00040-3
- Locksley, R. M., Killeen, N., and Lenardo, M. J. (2001). The TNF and TNF receptor superfamilies: integrating mammalian biology. *Cell* 104, 487–501. doi: 10.1016/S0092-8674(01)00237-9
- Loeb, G. E., Marks, W. B., and Hoffer, J. A. (1987). Cat hindlimb motoneurons during locomotion. IV. Participation in cutaneous reflexes. *J. Neurophysiol.* 57, 563–573. doi: 10.1152/jn.1987.57.2.563
- Lonze, B. E., and Ginty, D. D. (2002). Function and regulation of creb family transcription factors in the nervous system. *Neuron* 35, 605–623. doi: 10.1016/S0896-6273(02)00828-0
- Lou, H., Kim, S. K., Zaitsev, E., Snell, C. R., Lu, B., and Loh, Y. P. (2005). Sorting and activity-dependent secretion of BDNF require interaction of a specific motif with the sorting receptor carboxypeptidase e. *Neuron* 45, 245–255. doi: 10.1016/j.neuron.2004.12.037
- Lu, B., Nagappan, G., and Lu, Y. (2014). “BDNF and synaptic plasticity, cognitive function, and dysfunction,” in: *Neurotrophic Factors*, G. R. Lewin and B. D. Carter. Heidelberg: Springer Berlin Heidelberg.
- Lu, B., Pang, P. T., and Woo, N. H. (2005). The yin and yang of neurotrophin action. *Nat. Rev. Neurosci.* 6, 603–614. doi: 10.1038/nrn1726
- Maisonpierre, P. C., Le Beau, M. M., Espinosa, R. III, Ip, N. Y., Belluscio, L., De La Monte, S. M., et al. (1991). Human and rat brain-derived neurotrophic factor and neurotrophin-3: gene structures, distributions, and chromosomal localizations. *Genomics* 10, 558–568. doi: 10.1016/0888-7543(91)90436-1
- Makwana, M., and Raivich, G. (2005). Molecular mechanisms in successful peripheral regeneration. *FEBS J.* 272, 2628–2638. doi: 10.1111/j.1742-4658.2005.04699.x
- Mallei, A., Baj, G., Ieraci, A., Corna, S., Musazzi, L., Lee, F. S., et al. (2015). Expression and dendritic trafficking of BDNF-6 splice variant are impaired in knock-in mice carrying human BDNF Val66Met polymorphism. *Int. J. Neuropsychopharmacol.* 18:pyv069. doi: 10.1093/ijnp/pyv069
- Mar, F. M., Bonni, A., and Sousa, M. M. (2014). Cell intrinsic control of axon regeneration. *EMBO Rep.* 15, 254–263. doi: 10.1002/embr.201337723
- Marqueste, T., Alliez, J.-R., Alluin, O., Jammes, Y., and Decherchi, P. (2004). Neuromuscular rehabilitation by treadmill running or electrical stimulation after peripheral nerve injury and repair. *J. Appl. Physiol.* 96, 1988–1995. doi: 10.1152/japplphysiol.00775.2003
- McGregor, C. (2018). *The Effect of the Val66Met BDNF Polymorphism on Axon Regeneration After Peripheral Nerve Injury*. Ph.D. Emory University.
- Mellios, N., Huang, H.-S., Grigorenko, A., Rogae, E., and Akbarian, S. (2008). A set of differentially expressed miRNAs, including miR-30a-5p, act as post-transcriptional inhibitors of BDNF in prefrontal cortex. *Hum. Mol. Genet.* 17, 3030–3042. doi: 10.1093/hmg/ddn201
- Meyer, M., Matsuoka, I., Wetmore, C., Olson, L., and Thoenen, H. (1992). Enhanced synthesis of brain-derived neurotrophic factor in the lesioned peripheral nerve: different mechanisms are responsible for the regulation of BDNF and NGF mRNA. *J. Cell Biol.* 119, 45–54. doi: 10.1083/jcb.119.1.45
- Mi, S., Lee, X., Shao, Z., Thill, G., Ji, B., Relton, J., et al. (2004). LINGO-1 is a component of the Nogo-66 receptor/p75 signaling complex. *Nat. Neurosci.* 7, 221–228. doi: 10.1038/nn1188
- Michael, G. J., Averill, S., Nitkunan, A., Rattray, M., Bennett, D. L., Yan, Q., et al. (1997). Nerve growth factor treatment increases brain-derived neurotrophic factor selectively in TrkA-expressing dorsal root ganglion cells and in their central terminations within the spinal cord. *J. Neurosci.* 17, 8476–8490. doi: 10.1523/JNEUROSCI.17-21-08476.1997

- Michael, G. J., Averill, S., Shortland, P. J., Yan, Q., and Priestley, J. V. (1999). Axotomy results in major changes in BDNF expression by dorsal root ganglion cells: BDNF expression in large trkB and trkC cells, in pericellular baskets, and in projections to deep dorsal horn and dorsal column nuclei. *Eur. J. Neurosci.* 11, 3539–3551. doi: 10.1046/j.1460-9568.1999.00767.x
- Middleton, G., Hamanoue, M., Enokido, Y., Wyatt, S., Pennica, D., Jaffray, E., et al. (2000). Cytokine-induced nuclear factor kappa B activation promotes the survival of developing neurons. *J. Cell Biol.* 148, 325–332. doi: 10.1083/jcb.148.2.325
- Minichiello, L. (2009). TrkB signalling pathways in LTP and learning. *Nat. Rev. Neurosci.* 10, 850–860. doi: 10.1038/nrn2738
- Molteni, R., Zheng, J.-Q., Ying, Z., Gómez-Pinilla, F., and Twiss, J. L. (2004). Voluntary exercise increases axonal regeneration from sensory neurons. *Proc. Natl. Acad. Sci. U.S.A.* 101, 8473–8478. doi: 10.1073/pnas.0401443101
- Mowla, S. J., Farhadi, H. F., Pareek, S., Atwal, J. K., Morris, S. J., Seidah, N. G., et al. (2001). Biosynthesis and post-translational processing of the precursor to brain-derived neurotrophic factor. *J. Biol. Chem.* 276, 12660–12666. doi: 10.1074/jbc.M008104200
- Mowla, S. J., Pareek, S., Farhadi, H. F., Petrecca, K., Fawcett, J. P., Seidah, N. G., et al. (1999). Differential sorting of nerve growth factor and brain-derived neurotrophic factor in hippocampal neurons. *J. Neurosci.* 19, 2069–2080. doi: 10.1523/JNEUROSCI.19-06.02069.1999
- Nagappan, G., Zaitsev, E., Senatorov, V. V., Yang, J., Hempstead, B. L., and Lu, B. (2009). Control of extracellular cleavage of ProBDNF by high frequency neuronal activity. *Proc. Natl. Acad. Sci. U.S.A.* 106, 1267–1272. doi: 10.1073/pnas.0807322106
- Nagata, S. (1997). Apoptosis by death factor. *Cell* 88, 355–365. doi: 10.1016/S0092-8674(00)81874-7
- Nascimento, C., Pereira, J., Pires De Andrade, L., Garuffi, M., Ayan, C., Kerr, D., et al. (2015). Physical exercise improves peripheral BDNF levels and cognitive functions in elderly mild cognitive impairment individuals with Different BDNF Val66Met Genotypes. *J. Alzheimers. Dis.* 43, 81–91. doi: 10.3233/JAD-140576
- Neves-Pereira, M., Mundo, E., Muglia, P., King, N., Macciardi, F., and Kennedy, J. L. (2002). The brain-derived neurotrophic factor gene confers susceptibility to bipolar disorder: evidence from a family-based association study. *Am. J. Hum. Genet.* 71, 651–655. doi: 10.1086/342288
- Nielsen, M. S., Madsen, P., Christensen, E. I., Nykjaer, A., Gliemann, J., Kasper, D., et al. (2001). The sortilin cytoplasmic tail conveys Golgi-endosome transport and binds the VHS domain of the GGA2 sorting protein. *EMBO J.* 20, 2180–2190. doi: 10.1093/emboj/20.9.2180
- Nix, W. A., and Hopf, H. C. (1983). Electrical stimulation of regenerating nerve and its effect on motor recovery. *Brain Res.* 272, 21–25. doi: 10.1016/0006-8993(83)90360-8
- Notaras, M., Hill, R., and Van Den Buuse, M. (2015). The BDNF gene Val66Met polymorphism as a modifier of psychiatric disorder susceptibility: progress and controversy. *Mol. Psychiatry* 20, 916–930. doi: 10.1038/mp.2015.27
- Nykjaer, A., Lee, R., Teng, K. K., Jansen, P., Madsen, P., Nielsen, M. S., et al. (2004). Sortilin is essential for proNGF-induced neuronal cell death. *Nature* 427, 843–848. doi: 10.1038/nature02319
- Oliveira, A. L. R., Thams, S., Lidman, O., Piehl, F., Hökfelt, T., Kärre, K., et al. (2004). A role for MHC class I molecules in synaptic plasticity and regeneration of neurons after axotomy. *Proc. Natl. Acad. Sci. U.S.A.* 101, 17843–17848. doi: 10.1073/pnas.0408154101
- Osborne, M. C., Verhovshek, T., and Sengelaub, D. R. (2007). Androgen regulates trkB immunolabeling in spinal motoneurons. *J. Neurosci. Res.* 85, 303–309. doi: 10.1002/jnr.21122
- Ottem, E. N., Poort, J. E., Wang, H., Jordan, C. L., and Breedlove, S. M. (2010). Differential expression and regulation of brain-derived neurotrophic factor (BDNF) mRNA isoforms in androgen-sensitive motoneurons of the rat lumbar spinal cord. *Mol. Cell. Endocrinol.* 328, 40–46. doi: 10.1016/j.mce.2010.07.001
- Pagnussat, A. S., Michaelsen, S. M., Achaval, M., Ilha, J., Hermel, E. E. S., Back, F. P., et al. (2012). Effect of skilled and unskilled training on nerve regeneration and functional recovery. *Braz. J. Med. Biol. Res.* 45, 753–762. doi: 10.1590/S0100-879X2012007500084
- Park, J.-S., and Höke, A. (2014). Treadmill exercise induced functional recovery after peripheral nerve repair is associated with increased levels of neurotrophic factors. *PLoS ONE* 9:e90245. doi: 10.1371/journal.pone.0090245
- Park, K. K., Liu, K., Hu, Y., Smith, P. D., Wang, C., Cai, B., et al. (2008). Promoting axon regeneration in the adult CNS by modulation of the PTEN/mTOR pathway. *Science* 322, 963–966. doi: 10.1126/science.1161566
- Park, S., Koppes, R. A., Froriep, U. P., Jia, X., Achyuta, A. K. H., McLaughlin, B. L., et al. (2015). Optogenetic control of nerve growth. *Sci. Rep.* 5:9669. doi: 10.1038/srep09669
- Patapoutian, A., and Reichardt, L. F. (2001). Trk receptors: mediators of neurotrophin action. *Curr. Opin. Neurobiol.* 11, 272–280. doi: 10.1016/S0959-4388(00)00208-7
- Pattabiraman, P. P., Tropea, D., Chiaruttini, C., Tongiorgi, E., Cattaneo, A., and Domenici, L. (2005). Neuronal activity regulates the developmental expression and subcellular localization of cortical BDNF mRNA isoforms *in vivo*. *Mol. Cell. Neurosci.* 28, 556–570. doi: 10.1016/j.mcn.2004.11.010
- Pockett, S., and Gavin, R. M. (1985). Acceleration of peripheral nerve regeneration after crush injury in rat. *Neurosci. Lett.* 59, 221–224. doi: 10.1016/0304-3940(85)90203-4
- Portincasa, A., Gozto, G., Parisi, D., Annacontini, L., Campanale, A., Basso, G., et al. (2007). Microsurgical treatment of injury to peripheral nerves in upper and lower limbs: a critical review of the last 8 years. *Microsurgery* 27, 455–462. doi: 10.1002/micr.20382
- Pruunsild, P., Kazantseva, A., Aid, T., Palm, K., and Timmusk, T. (2007). Dissecting the human BDNF locus: bidirectional transcription, complex splicing, and multiple promoters. *Genomics* 90, 397–406. doi: 10.1016/j.ygeno.2007.05.004
- Qin, L., Jing, D., Parada, S., Carmel, J., Ratan, R. R., Lee, F. S., et al. (2014). An adaptive role for BDNF Val66Met polymorphism in motor recovery in chronic stroke. *J. Neurosci.* 34, 2493–2502. doi: 10.1523/JNEUROSCI.4140-13.2014
- Raivich, G., and Kreutzberg, G. W. (1987). Expression of growth factor receptors in injured nervous tissue. I. Axotomy leads to a shift in the cellular distribution of specific beta-nerve growth factor binding in the injured and regenerating PNS. *J. Neurocytol.* 16, 689–700. doi: 10.1007/BF01637660
- Reichardt, L. F. (2006). Neurotrophin-regulated signalling pathways. *Philos. Trans. R. Soc. Lond. B Biol. Sci.* 361, 1545–1564. doi: 10.1098/rstb.2006.1894
- Rende, M., Giambanco, I., Buratta, M., and Tonalì, P. (1995). Axotomy induces a different modulation of both low-affinity nerve growth factor receptor and choline acetyltransferase between adult rat spinal and brainstem motoneurons. *J. Comp. Neurol.* 363, 249–263. doi: 10.1002/cne.903630207
- Ribases, M., Gratacos, M., Armengol, L., De Cid, R., Badia, A., Jimenez, L., et al. (2003). Met66 in the brain-derived neurotrophic factor (BDNF) precursor is associated with anorexia nervosa restrictive type. *Mol. Psychiatry* 8, 745–751. doi: 10.1038/sj.mp.4001281
- Rich, K. M., Luszczynski, J. R., Osborne, P. A., and Johnson, E. M. Jr. (1987). Nerve growth factor protects adult sensory neurons from cell death and atrophy caused by nerve injury. *J. Neurocytol.* 16, 261–268. doi: 10.1007/BF01795309
- Richner, M., Ulrichsen, M., Elmagaard, S. L., Dieu, R., Pallesen, L. T., and Vaegter, C. B. (2014). Peripheral nerve injury modulates neurotrophin signaling in the peripheral and central nervous system. *Mol. Neurobiol.* 50, 945–970. doi: 10.1007/s12035-014-8706-9
- Righi, M., Tongiorgi, E., and Cattaneo, A. (2000). Brain-derived neurotrophic factor (BDNF) induces dendritic targeting of BDNF and tyrosine kinase B mRNAs in hippocampal neurons through a phosphatidylinositol-3 kinase-dependent pathway. *J. Neurosci.* 20, 3165–3174. doi: 10.1523/JNEUROSCI.20-09.03165.2000
- Rodríguez-Tébar, A., Dechant, G., Götz, R., and Barde, Y. A. (1992). Binding of neurotrophin-3 to its neuronal receptors and interactions with nerve growth factor and brain-derived neurotrophic factor. *EMBO J.* 11, 917–922. doi: 10.1002/j.1460-2075.1992.tb05130.x
- Rostami, E., Krueger, F., Zoubak, S., Dal Monte, O., Raymont, V., Pardini, M., et al. (2011). BDNF polymorphism predicts general intelligence after penetrating traumatic brain injury. *PLoS ONE* 6:e27389. doi: 10.1371/journal.pone.0027389
- Rotterman, T. M., Nardelli, P., Cope, T. C., and Alvarez, F. J. (2014). Normal distribution of VGLUT1 synapses on spinal motoneuron dendrites and their reorganization after nerve injury. *J. Neurosci.* 34, 3475–3492. doi: 10.1523/JNEUROSCI.4768-13.2014
- Roux, P. P., and Barker, P. A. (2002). Neurotrophin signaling through the p75 neurotrophin receptor. *Prog. Neurobiol.* 67, 203–233. doi: 10.1016/S0304-0082(02)00016-3

- Sabatier, M. J., and English, A. W. (2015). Pathways mediating activity-induced enhancement of recovery from peripheral nerve injury. *Exerc. Sport Sci. Rev.* 43, 163–171. doi: 10.1249/JES.0000000000000047
- Sabatier, M. J., Redmon, N., Schwartz, G., and English, A. W. (2008). Treadmill training promotes axon regeneration in injured peripheral nerves. *Exp. Neurol.* 211, 489–493. doi: 10.1016/j.expneurol.2008.02.013
- Saika, T., Senba, E., Noguchi, K., Sato, M., Yoshida, S., Kubo, T., et al. (1991). Effects of nerve crush and transection on mRNA levels for nerve growth factor receptor in the rat facial motoneurons. *Brain Res. Mol. Brain Res.* 9, 157–160. doi: 10.1016/0169-328X(91)90142-K
- Sakata, K., Woo, N. H., Martinowich, K., Greene, J. S., Schloesser, R. J., Shen, L., et al. (2009). Critical role of promoter IV-driven BDNF transcription in GABAergic transmission and synaptic plasticity in the prefrontal cortex. *Proc. Natl. Acad. Sci. U.S.A.* 106, 5942–5947. doi: 10.1073/pnas.0811431106
- Salerno, K. M., Jing, X., Diges, C. M., Cornuet, P. K., Glorioso, J. C., and Albers, K. M. (2012). Sox11 modulates brain-derived neurotrophic factor expression in an exon promoter-specific manner. *J. Neurosci. Res.* 90, 1011–1019. doi: 10.1002/jnr.23010
- Sarikcioglu, L., and Oguz, N. (2001). Exercise training and axonal regeneration after sciatic nerve injury. *Int. J. Neurosci.* 109, 173–177. doi: 10.3109/00207450108986533
- Schmidt, A., and Hall, A. (2002). Guanine nucleotide exchange factors for Rho Gtpases: turning on the switch. *Genes Dev.* 16, 1587–1609. doi: 10.1101/gad.1003302
- Scholz, T., Krichevsky, A., Sumarto, A., Jaffurs, D., Wirth, G. A., Paydar, K., et al. (2009). Peripheral nerve injuries: an international survey of current treatments and future perspectives. *J. Reconstr. Microsurg.* 25, 339–344. doi: 10.1055/s-0029-1215529
- Schwartz, P. M., Borghesani, P. R., Levy, R. L., Pomeroy, S. L., and Segal, R. A. (1997). Abnormal cerebellar development and foliation in BDNF^{-/-} mice reveals a role for neurotrophins in CNS patterning. *Neuron* 19, 269–281. doi: 10.1016/S0896-6273(00)80938-1
- Scott, A. L., Borisoff, J. F., and Ramer, M. S. (2005). Deafferentation and neurotrophin-mediated intraspinal sprouting: a central role for the p75 neurotrophin receptor. *Eur. J. Neurosci.* 21, 81–92. doi: 10.1111/j.1460-9568.2004.03838.x
- Scott, A. L., and Ramer, M. S. (2010). Schwann cell p75NTR prevents spontaneous sensory reinnervation of the adult spinal cord. *Brain* 133, 421–432. doi: 10.1093/brain/awp316
- Seidah, N., Benjannet, S., Pareek, S., Chrétien, M., and Murphy, R. (1996a). Cellular processing of the neurotrophin precursors of NT3 and BDNF by the mammalian proprotein convertases. *FEBS Lett.* 379, 247–250. doi: 10.1016/0014-5793(95)01520-5
- Seidah, N. G., Benjannet, S., Pareek, S., Savaria, D., Hamelin, J., Goulet, B., et al. (1996b). Cellular processing of the nerve growth factor precursor by the mammalian pro-protein convertases. *Biochem. J.* 314, 951–960. doi: 10.1042/bj3140951
- Seo, T. B., Han, I. S., Yoon, J. H., Hong, K. E., Yoon, S. J., and Namgung, U. (2006). Involvement of Cdc2 in axonal regeneration enhanced by exercise training in rats. *Med. Sci. Sports Exerc.* 38, 1267–1276. doi: 10.1249/01.mss.0000227311.00976.68
- Seo, T. B., Oh, M. J., You, B. G., Kwon, K. B., Chang, I. A., Yoon, J. H., et al. (2009). ERK1/2-mediated Schwann cell proliferation in the regenerating sciatic nerve by treadmill training. *J. Neurotrauma* 26, 1733–1744. doi: 10.1089/neu.2008.0711
- Sharma, N., Coughlin, L., Porter, R., Tanzer, L., Wurster, R., Marzo, S., et al. (2009). Effects of electrical stimulation and gonadal steroids on rat facial nerve regenerative properties. *Restor. Neurol. Neurosci.* 27, 633–644. doi: 10.3233/RNN-2009-0489
- Sharma, N., Marzo, S. J., Jones, K. J., and Foecking, E. M. (2010a). Electrical stimulation and testosterone differentially enhance expression of regeneration-associated genes. *Exp. Neurol.* 223, 183–191. doi: 10.1016/j.expneurol.2009.04.031
- Sharma, N., Moeller, C. W., Marzo, S. J., Jones, K. J., and Foecking, E. M. (2010b). Combinatorial treatments enhance recovery following facial nerve crush. *Laryngoscope* 120, 1523–1530. doi: 10.1002/lary.20997
- Shen, Y. J., Debellard, M. E., Salzer, J. L., Roder, J., and Filbin, M. T. (1998). Myelin-associated glycoprotein in myelin and expressed by Schwann cells inhibits axonal regeneration and branching. *Mol. Cell. Neurosci.* 12, 79–91. doi: 10.1006/mcne.1998.0700
- Shimizu, E., Hashimoto, K., and Iyo, M. (2004). Ethnic difference of the BDNF 196G/A (val66met) polymorphism frequencies: the possibility to explain ethnic mental traits. *Am. J. Med. Genet. B Neuropsychiatr. Genet.* 126b, 122–123. doi: 10.1002/ajmg.b.20118
- Singh, B., Xu, Q. G., Franz, C. K., Zhang, R., Dalton, C., Gordon, T., et al. (2012). Accelerated axon outgrowth, guidance, and target reinnervation across nerve transection gaps following a brief electrical stimulation paradigm. *J. Neurosurg.* 116, 498–512. doi: 10.3171/2011.10.JNS11612
- Sklar, P., Gabriel, S. B., McInnis, M. G., Bennett, P., Lim, Y., Tsan, G., et al. (2002). Family-based association study of 76 candidate genes in bipolar disorder: BDNF is a potential risk locus. Brain-derived neurotrophic factor. *Mol. Psychiatry* 7, 579–593. doi: 10.1038/sj.mp.4001058
- Sohnchen, J., Grosheva, M., Kiryakova, S., Hubbers, C. U., Sinis, N., Skouras, E., et al. (2010). Recovery of whisking function after manual stimulation of denervated vibrissal muscles requires brain-derived neurotrophic factor and its receptor tyrosine kinase B. *Neuroscience* 170, 372–380. doi: 10.1016/j.neuroscience.2010.06.053
- Sohrabji, F., Miranda, R. C., and Toran-Allerand, C. D. (1995). Identification of a putative estrogen response element in the gene encoding brain-derived neurotrophic factor. *Proc. Natl. Acad. Sci. U.S.A.* 92, 11110–11114. doi: 10.1073/pnas.92.24.11110
- Song, X. Y., Zhang, F. H., Zhou, F. H., Zhong, J., and Zhou, X. F. (2009). Deletion of p75NTR impairs regeneration of peripheral nerves in mice. *Life Sci.* 84, 61–68. doi: 10.1016/j.lfs.2008.10.013
- Song, X. Y., Zhou, F. H., Zhong, J. H., Wu, L. L., and Zhou, X. F. (2006). Knockout of p75(NTR) impairs re-myelination of injured sciatic nerve in mice. *J. Neurochem.* 96, 833–842. doi: 10.1111/j.1471-4159.2005.03564.x
- Sotelo-Silveira, J., Crispino, M., Puppo, A., Sotelo, J. R., and Koenig, E. (2008). Myelinated axons contain beta-actin mRNA and ZBP-1 in periaxoplasmic ribosomal plaques and depend on cyclic AMP and F-actin integrity for *in vitro* translation. *J. Neurochem.* 104, 545–557. doi: 10.1111/j.1471-4159.2007.04999.x
- Souness, J. E., Aldous, D., and Sargent, C. (2000). Immunosuppressive and anti-inflammatory effects of cyclic AMP phosphodiesterase (PDE) type 4 inhibitors. *Immunopharmacology* 47, 127–162. doi: 10.1016/S0162-3109(00)00185-5
- Streppel, M., Azzolin, N., Dohm, S., Guntinas-Lichius, O., Haas, C., Grothe, C., et al. (2002). Focal application of neutralizing antibodies to soluble neurotrophic factors reduces collateral axonal branching after peripheral nerve lesion. *Eur. J. Neurosci.* 15, 1327–1342. doi: 10.1046/j.1460-9568.2002.01971.x
- Struebing, F. L., Wang, J., Li, Y., King, R., Mistretta, O. C., English, A. W., et al. (2017). Differential expression of Sox11 and Bdnf mRNA isoforms in the injured and regenerating nervous systems. *Front. Mol. Neurosci.* 10:354. doi: 10.3389/fnmol.2017.00354
- Sulaiman, O. A., and Gordon, T. (2000). Effects of short- and long-term Schwann cell denervation on peripheral nerve regeneration, myelination, and size. *Glia* 32, 234–246. doi: 10.1002/1098-1136(200012)32:3<234::AID-GLIA40>3.0.CO;2-3
- Szuhany, K. L., Bugatti, M., and Otto, M. W. (2015). A meta-analytic review of the effects of exercise on brain-derived neurotrophic factor. *J. Psychiatr. Res.* 60, 56–64. doi: 10.1016/j.jpsychires.2014.10.003
- Tam, S. L., Archibald, V., Jassar, B., Tyreman, N., and Gordon, T. (2001). Increased neuromuscular activity reduces sprouting in partially denervated muscles. *J. Neurosci.* 21, 654–667. doi: 10.1523/JNEUROSCI.21-02-00654.2001
- Taniuchi, M., Clark, H. B., and Johnson, E. M. (1986). Induction of nerve growth factor receptor in Schwann cells after axotomy. *Proc. Natl. Acad. Sci. U.S.A.* 83, 4094–4098. doi: 10.1073/pnas.83.11.4094
- Tanzer, L., and Jones, K. J. (1997). Gonadal steroid regulation of hamster facial nerve regeneration: effects of dihydrotestosterone and estradiol. *Exp. Neurol.* 146, 258–264. doi: 10.1006/exnr.1997.6529
- Tao, X., Finkbeiner, S., Arnold, D. B., Shaywitz, A. J., and Greenberg, M. E. (1998). Ca²⁺ influx regulates BDNF transcription by a CREB family transcription factor-dependent mechanism. *Neuron* 20, 709–726. doi: 10.1016/S0896-6273(00)81010-7

- Teng, H. K., Teng, K. K., Lee, R., Wright, S., Tevar, S., Almeida, R. D., et al. (2005). ProBDNF induces neuronal apoptosis via activation of a receptor complex of p75NTR and sortilin. *J. Neurosci.* 25, 5455–5463. doi: 10.1523/JNEUROSCI.5123-04.2005
- Teodori, R. M., Betini, J., De Oliveira, L. S., Sobral, L. L., Takeda, S. Y. M., and Montebelo, M. I. D. L. (2011). Swimming exercise in the acute or late phase after sciatic nerve crush accelerates nerve regeneration. *Neural Plast.* 2011:783901. doi: 10.1155/2011/783901
- Thompson, N. J., Sengelaub, D. R., and English, A. W. (2013). Enhancement of peripheral nerve regeneration due to treadmill training and electrical stimulation is dependent on androgen receptor signaling. *Dev. Neurobiol.* 74, 531–540. doi: 10.1002/dneu.22147
- Timmusk, T., Palm, K., Metsis, M., Reintam, T., Paalme, V., Saarma, M., et al. (1993). Multiple promoters direct tissue-specific expression of the rat BDNF gene. *Neuron* 10, 475–489. doi: 10.1016/0896-6273(93)90335-O
- Tomita, K., Kubo, T., Matsuda, K., Fujiwara, T., Yano, K., Winograd, J. M., et al. (2007). The neurotrophin receptor p75NTR in Schwann cells is implicated in remyelination and motor recovery after peripheral nerve injury. *Glia* 55, 1199–1208. doi: 10.1002/glia.20533
- Tongiorgi, E., Righi, M., and Cattaneo, A. (1997). Activity-Dependent dendritic targeting of BDNF and TrkB mRNAs in hippocampal neurons. *J. Neurosci.* 17, 9492–9505. doi: 10.1523/JNEUROSCI.17-24-09492.1997
- Udina, E., Cobiánchi, S., Allodi, I., and Navarro, X. (2011a). Effects of activity-dependent strategies on regeneration and plasticity after peripheral nerve injuries. *Ann. Anat.* 193, 347–353. doi: 10.1016/j.aanat.2011.02.012
- Udina, E., Ladak, A., Furey, M., Brushart, T., Tyreman, N., and Gordon, T. (2010). Roliapram-induced elevation of cAMP or chondroitinase ABC breakdown of inhibitory proteoglycans in the extracellular matrix promotes peripheral nerve regeneration. *Exp. Neurol.* 223, 143–152. doi: 10.1016/j.expneurol.2009.08.026
- Udina, E., Puigdemasa, A., and Navarro, X. (2011b). Passive and active exercise improve regeneration and muscle reinnervation after peripheral nerve injury in the rat. *Muscle Nerve* 43, 500–509. doi: 10.1002/mus.21912
- Uegaki, K., Kumanogoh, H., Mizui, T., Hirokawa, T., Ishikawa, Y., and Kojima, M. (2017). Bdnf binds its pro-peptide with high affinity and the common Val66Met polymorphism attenuates the interaction. *Int. J. Mol. Sci.* 18:E1042. doi: 10.3390/ijms18051042
- Vaghi, V., Polacchini, A., Baj, G., Pinheiro, V. L. M., Vicario, A., and Tongiorgi, E. (2014). Pharmacological profile of brain-derived neurotrophic factor (BDNF) splice variant translation using a novel drug screening assay: a “quantitative code”. *J. Biol. Chem.* 289, 27702–27713. doi: 10.1074/jbc.M114.586719
- van Meeteren, N. L., Brakkee, J. H., Hamers, F. P., Helden, P. J., and Gispén, W. H. (1997). Exercise training improves functional recovery and motor nerve conduction velocity after sciatic nerve crush lesion in the rat. *Arch. Phys. Med. Rehabil.* 78, 70–77. doi: 10.1016/S0003-9993(97)90013-7
- van Meeteren, N. L., Brakkee, J. H., Helden, P. J., and Gispén, W. H. (1998). The effect of exercise training on functional recovery after sciatic nerve crush in the rat. *J. Peripher. Nerv. Syst.* 3, 277–282.
- Varendi, K., Kumar, A., Härmä, M.-A., and Andressoo, J.-O. (2014). miR-1, miR-10b, miR-155, and miR-191 are novel regulators of BDNF. *Cell. Mol. Life Sci.* 71, 4443–4456. doi: 10.1007/s00018-014-1628-x
- Verhovshek, T., Cai, Y., Osborne, M. C., and Sengelaub, D. R. (2010). Androgen regulates brain-derived neurotrophic factor in spinal motoneurons and their target musculature. *Endocrinology* 151, 253–261. doi: 10.1210/en.2009-1036
- Vicario, A., Colliva, A., Ratti, A., Davidovic, L., Baj, G., Gricman, L., et al. (2015). Dendritic targeting of short and long 3' UTR BDNF mRNA is regulated by BDNF or NT-3 and distinct sets of RNA-binding proteins. *Front. Mol. Neurosci.* 8:62. doi: 10.3389/fnmol.2015.00062
- Vivo, M., Puigdemasa, A., Casals, L., Asensio, E., Udina, E., and Navarro, X. (2008). Immediate electrical stimulation enhances regeneration and reinnervation and modulates spinal plastic changes after sciatic nerve injury and repair. *Exp. Neurol.* 211, 180–193. doi: 10.1016/j.expneurol.2008.01.020
- Walsh, G. S., Krol, K. M., Crutcher, K. A., and Kawaja, M. D. (1999). Enhanced neurotrophin-induced axon growth in myelinated portions of the CNS in mice lacking the p75 neurotrophin receptor. *J. Neurosci.* 19, 4155–4168. doi: 10.1523/JNEUROSCI.19-10-04155.1999
- Wan, L., Xia, R., and Ding, W. (2010). Short-term low-frequency electrical stimulation enhanced remyelination of injured peripheral nerves by inducing the promyelination effect of brain-derived neurotrophic factor on Schwann cell polarization. *J. Neurosci. Res.* 88, 2578–2587. doi: 10.1002/jnr.22426
- Wang, K. C., Kim, J. A., Sivasankaran, R., Segal, R., and He, Z. (2002). P75 interacts with the Nogo receptor as a co-receptor for Nogo, MAG and OMgp. *Nature* 420, 74–78. doi: 10.1038/nature01176
- Ward, P. J., Clanton, S. L., and English, A. W. (2018). Optogenetically enhanced axon regeneration: motor versus sensory neuron-specific stimulation. *Eur. J. Neurosci.* 47, 294–304. doi: 10.1111/ejn.13836
- Ward, P. J., Jones, L. N., Mulligan, A., Goolsby, W., Wilhelm, J. C., and English, A. W. (2016). Optically-induced neuronal activity is sufficient to promote functional motor axon regeneration *in vivo*. *PLoS ONE* 11:e0154243. doi: 10.1371/journal.pone.0154243
- Welin, D., Novikova, L. N., Wiberg, M., Kellerth, J. O., and Novikov, L. N. (2008). Survival and regeneration of cutaneous and muscular afferent neurons after peripheral nerve injury in adult rats. *Exp. Brain Res.* 186, 315–323. doi: 10.1007/s00221-007-1232-5
- West, A. E., Chen, W. G., Dalva, M. B., Dolmetsch, R. E., Kornhauser, J. M., Shaywitz, A. J., et al. (2001). Calcium regulation of neuronal gene expression. *Proc. Natl. Acad. Sci. U.S.A.* 98, 11024–11031. doi: 10.1073/pnas.191352298
- White, D. M., Walker, S., Brenneman, D. E., and Gozes, I. (2000). CREB contributes to the increased neurite outgrowth of sensory neurons induced by vasoactive intestinal polypeptide and activity-dependent neurotrophic factor. *Brain Res.* 868, 31–38. doi: 10.1016/S0006-8993(00)02259-9
- Wiberg, R., Novikova, L. N., and Kingham, P. J. (2018). Evaluation of apoptotic pathways in dorsal root ganglion neurons following peripheral nerve injury. *Neuroreport* 29, 779–785. doi: 10.1097/WNR.00000000000010131
- Wilhelm, J., Xu, M., Cucoranu, D., Chmielewski, S., Holmes, T., Lau, K., et al. (2012). Cooperative roles of BDNF expression in neurons and Schwann cells are modulated by exercise to facilitate nerve regeneration. *J. Neurosci.* 32, 5002–5009. doi: 10.1523/JNEUROSCI.1411-11.2012
- Willis, D. E., Xu, M., Donnelly, C. J., Tep, C., Kendall, M., Erenstheyn, M., et al. (2011). Axonal localization of transgene mRNA in mature PNS and CNS neurons. *J. Neurosci.* 31, 14481–14487. doi: 10.1523/JNEUROSCI.2950-11.2011
- Wong, J. N., Olson, J. L., Morhart, M. J., and Chan, K. M. (2015). Electrical stimulation enhances sensory recovery: a randomized controlled trial. *Ann. Neurol.* 77, 996–1006. doi: 10.1002/ana.24397
- Wood, K., Wilhelm, J., Sabatier, M., Liu, K., Gu, J., and English, A. (2012). Sex differences in the effectiveness of treadmill training in enhancing axon regeneration in injured peripheral nerves. *Dev. Neurobiol.* 72, 688–698. doi: 10.1002/dneu.20960
- Wyatt, S., Shooter, E. M., and Davies, A. M. (1990). Expression of the NGF receptor gene in sensory neurons and their cutaneous targets prior to and during innervation. *Neuron* 4, 421–427. doi: 10.1016/0896-6273(90)90054-J
- Yamashita, T., Tucker, K. L., and Barde, Y. A. (1999). Neurotrophin binding to the p75 receptor modulates Rho activity and axonal outgrowth. *Neuron* 24, 585–593. doi: 10.1016/S0896-6273(00)81114-9
- Yan, Q., and Johnson, E. (1988). An immunohistochemical study of the nerve growth factor receptor in developing rats. *J. Neurosci.* 8, 3481–3498. doi: 10.1523/JNEUROSCI.08-09-03481.1988
- Yang, F., Je, H. S., Ji, Y., Nagappan, G., Hempstead, B., and Lu, B. (2009). Pro-BDNF-induced synaptic depression and retraction at developing neuromuscular synapses. *J. Cell Biol.* 185, 727–741. doi: 10.1083/jcb.200811147
- Yao, J., Sasaki, Y., Wen, Z., Bassell, G. J., and Zheng, J. Q. (2006). An essential role for β -actin mRNA localization and translation in Ca^{2+} -dependent growth cone guidance. *Nat. Neurosci.* 9, 1265–1273. doi: 10.1038/n1773

- Zhang, F. H., Huang, P., Yang, P. S., and Zhang, X. (2010). Influence of p75 neurotrophin receptor knockout on the regeneration of facial nerves after crush injury in mouse. *Hua Xi Kou Qiang Yi Xue Za Zhi* 28, 95–98.
- Zhang, J. Y., Luo, X. G., Xian Cory, J., Liu, Z. H., and Zhou, X. F. (2008). Endogenous BDNF is required for myelination and regeneration of injured sciatic nerve in rodents. *Eur. J. Neurosci.* 12, 4171–4180. doi: 10.1111/j.1460-9568.2000.01312.x
- Zhou, X. F., Li, W. P., Zhou, F. H., Zhong, J. H., Mi, J. X., Wu, L. L., et al. (2005). Differential effects of endogenous brain-derived neurotrophic factor on the survival of axotomized sensory neurons in dorsal root ganglia: a possible role for the p75 neurotrophin receptor. *Neuroscience* 132, 591–603. doi: 10.1016/j.neuroscience.2004.12.034
- Zhou, X. F., Rush, R. A., and McLachlan, E. M. (1996). Differential expression of the p75 nerve growth factor receptor in glia and neurons of the rat dorsal root ganglia after peripheral nerve transection. *J. Neurosci.* 16, 2901–2911. doi: 10.1523/JNEUROSCI.16-09-02901.1996
- Conflict of Interest Statement:** The authors declare that the research was conducted in the absence of any commercial or financial relationships that could be construed as a potential conflict of interest.

Copyright © 2019 McGregor and English. This is an open-access article distributed under the terms of the Creative Commons Attribution License (CC BY). The use, distribution or reproduction in other forums is permitted, provided the original author(s) and the copyright owner(s) are credited and that the original publication in this journal is cited, in accordance with accepted academic practice. No use, distribution or reproduction is permitted which does not comply with these terms.



The Success and Failure of the Schwann Cell Response to Nerve Injury

Kristjan R. Jessen* and Rhona Mirsky

Department of Cell and Developmental Biology, University College London, London, United Kingdom

The remarkable plasticity of Schwann cells allows them to adopt the Remak (non-myelin) and myelin phenotypes, which are specialized to meet the needs of small and large diameter axons, and differ markedly from each other. It also enables Schwann cells initially to mount a strikingly adaptive response to nerve injury and to promote regeneration by converting to a repair-promoting phenotype. These repair cells activate a sequence of supportive functions that engineer myelin clearance, prevent neuronal death, and help axon growth and guidance. Eventually, this response runs out of steam, however, because in the long run the phenotype of repair cells is unstable and their survival is compromised. The re-programming of Remak and myelin cells to repair cells, together with the injury-induced switch of peripheral neurons to a growth mode, gives peripheral nerves their strong regenerative potential. But it remains a challenge to harness this potential and devise effective treatments that maintain the initial repair capacity of peripheral nerves for the extended periods typically required for nerve repair in humans.

OPEN ACCESS

Edited by:

Esther Udina,
Autonomous University of Barcelona,
Spain

Reviewed by:

Valerio Magnaghi,
University of Milan, Italy
Edgar Richard Kramer,
Plymouth University, United Kingdom

*Correspondence:

Kristjan R. Jessen
k.jessen@ucl.ac.uk

Received: 03 October 2018

Accepted: 22 January 2019

Published: 11 February 2019

Citation:

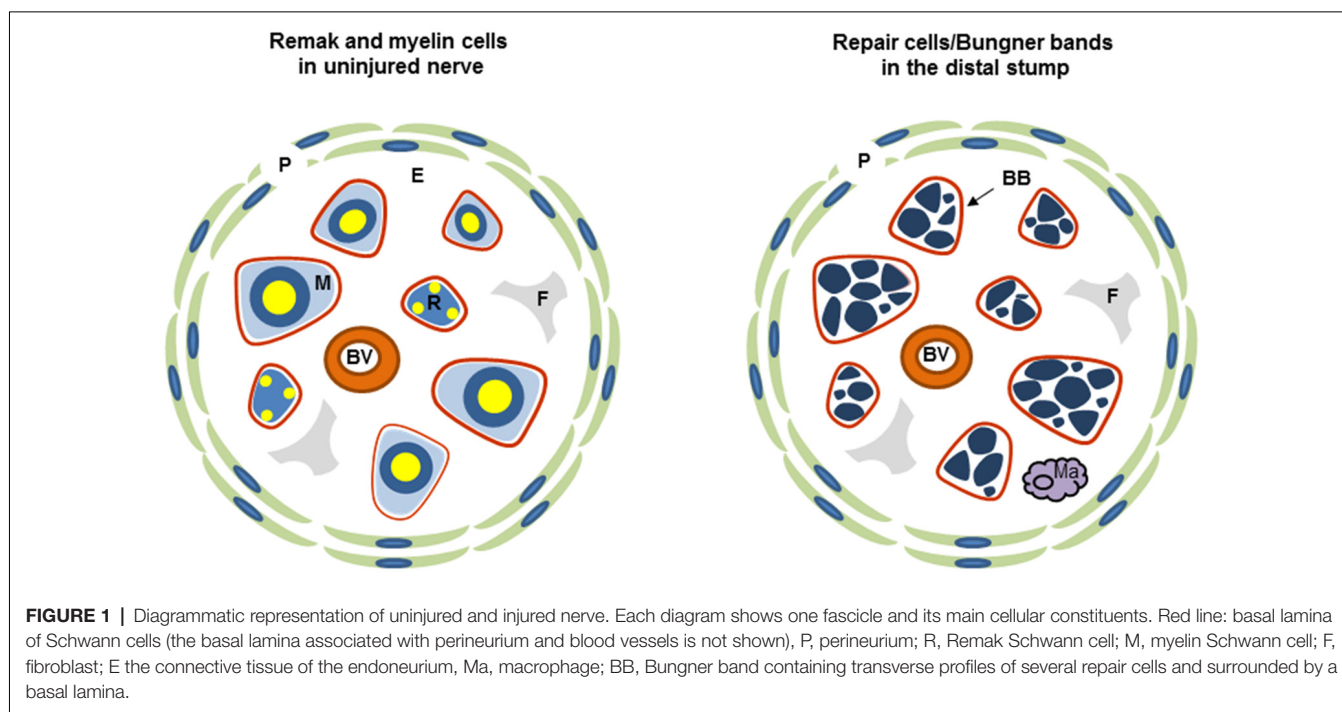
Jessen KR and Mirsky R (2019) The
Success and Failure of the Schwann
Cell Response to Nerve Injury.
Front. Cell. Neurosci. 13:33.
doi: 10.3389/fncel.2019.00033

Keywords: PNS, repair cell, nerve injury, regeneration, c-Jun, re-programming, Schwann cell

INTRODUCTION: OVERVIEW OF SCHWANN CELLS AND NERVE INJURY

Examination of the Schwann cells in uninjured nerves shows two surprisingly different cell types. One of them is the rather inconspicuous Remak cell, or non-myelin Schwann cell. These cells envelop all the small diameter axons, including many sensory axons and the all-important axons of the autonomic nervous system. The axons lie in troughs along the cell surface, and in rodents each cell generally ensheaths several axons, although in human nerves, one axon per Remak cell is common. The larger axons, including some sensory axons and the axons of motor neurons, are wrapped by myelin Schwann cells. They are 2–3 times longer than Remak cells and much bulkier, containing the myelin sheath, which is formed by the Schwann cell membrane wrapping multiple times around the axon and condensing to form a compact myelin cuff around the axon.

Both Remak and myelin cells are coated by a basal lamina, outside of which lies the connective tissue, the endoneurium, which contains fibroblasts, blood vessels and a few macrophages and is ultimately surrounded by a multi-layered cellular tube, the perineurium (**Figure 1**). This assembly is termed a fascicle. Small nerves are uni-fascicular, while large nerves contain many fascicles bound together by connective tissue, the epineurium.



While both Schwann cells are thought to provide axons with metabolic and trophic support, only the myelin cells have the key role of accelerating nerve impulse conduction. Remak and myelin cells also express some common proteins, such as S100, a classical Schwann cell marker, while at the same time each cell possesses a characteristic molecular profile (reviewed in Jessen and Mirsky, 2005, 2016; Glenn and Talbot, 2013; Brosius Lutz and Barres, 2014; Monk et al., 2015). Thus, Remak cells express several markers also found on developing Schwann cells, such as neural cell adhesion molecule (NCAM), p75 neurotrophin receptor (p75NTR) and glial fibrillary acidic protein (GFAP), and L1 NCAM. The myelin cells on the other hand express a large range of molecules that relate to the synthesis, maintenance or structure of the myelin sheath. This includes the major pro-myelin transcription factor *Egr2* (*Krox20*), high levels of the enzymes that control cholesterol synthesis, structural proteins such as myelin protein zero (MPZ) and myelin basic protein (MBP), and membrane associated proteins like myelin associated glycoprotein (MAG), PMP22, and periaxin.

As different as Remak and myelin cells appear, these cells nevertheless originate developmentally from a common cell, the immature Schwann cell, present in rodent nerves in the perinatal period (Figure 2). These cells, in turn, derive from a distinct glial cell of embryonic nerves, the Schwann cell precursor. The conversion of Schwann cell precursors to Schwann cells is controlled by transcription factors such as *AP2α*, *Zeb2*, and *Notch*, and extracellular signals including endothelin and axon-associated neuregulin, which is essential for precursor survival (reviewed in Jessen and Mirsky, 2005; Jessen et al., 2015b; Quintes and Brinkmann, 2017).

Schwann cell precursors unambiguously exhibit a glial phenotype, expressing characteristic glial features, such as

ensheathing axons within nerves and expressing Schwann cell associated mRNAs, such as those encoding for the major myelin protein MPZ and desert hedgehog (*Dhh*). It is interesting, however, that these cells also retain one notable feature of the neural crest cells from which they originate, namely they have a broad developmental potential. Thus, Schwann cell precursors give rise to cells such as melanocytes, endoneurial fibroblasts and neurons, in addition to Schwann cells, during embryonic development (reviewed in Jessen et al., 2015b; Kastriiti and Adameyko, 2017).

One of the most interesting biological properties of Schwann cells is their plasticity (reviewed in Boerboom et al., 2017; Castelnovo et al., 2017; Jacob, 2017; Ma and Svaren, 2018). The phenotype adopted by Schwann cells, such as the Remak or myelin phenotypes described above, is strikingly dependent on signals in the cellular environment. Thus, all the evidence indicates that if a Remak cell was placed in contact with large diameter axon it would adopt the myelin phenotype and conversely, a myelin cell would convert to a Remak cell if associated with small diameter axons. This phenotypic instability may pre-dispose Schwann cells to demyelinating disease, since myelin Schwann cells may regress from myelin maintenance relatively easily in response to mutations that disturb cellular homeostasis. After nerve damage, Schwann cell plasticity and the ready response to environmental signals initially helps to provide nerves with strong regenerative potential, but at later times after injury, these features contribute to regenerative failure, as repair supportive Schwann cells are not sustained during the long times required for nerve repair in humans.

After nerve injury, the Schwann cells distal to the damaged area lose contact with axons as they degenerate. This represents

Main transitions in the Schwann cell precursor lineage during development and in the adult

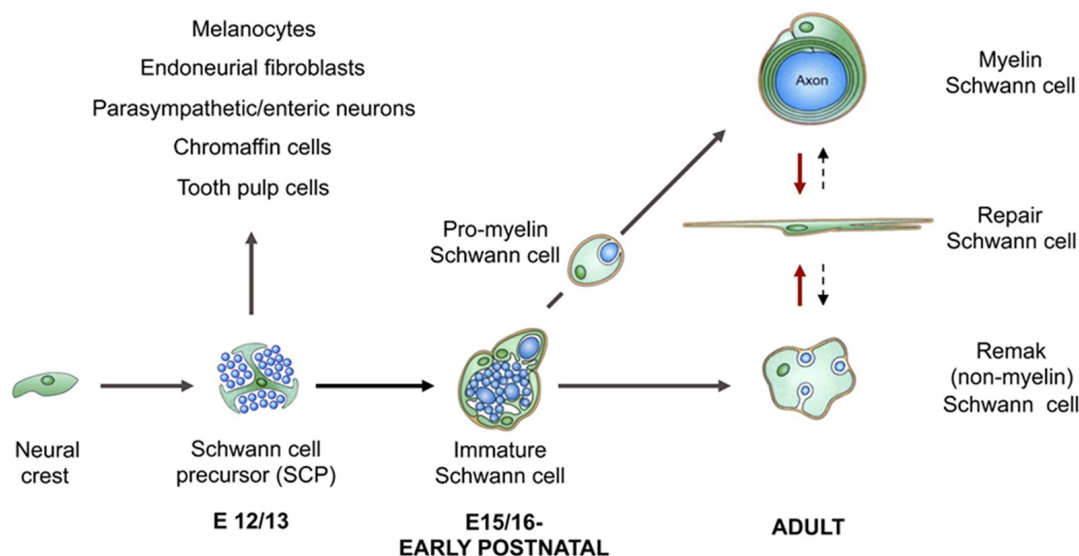


FIGURE 2 | The main transitions in the Schwann cell lineage during development and after injury. Black uninterrupted arrows show normal development. Red arrows show the Schwann cell injury response. Black stippled arrows show post-repair reformation of Remak and myelin cells (with permission from Jessen et al., 2015b).

a radical change in the signaling environment, because key signals for the control Schwann cell phenotype come from axons. Subsequently, further change is provided by a cocktail of bioactive factors secreted by macrophages, which invade injured nerves in large numbers. In response to these perturbations, Schwann cells show a remarkably fortunate response. This is the conversion of Remak and myelin cells, within their original basal lamina tubes, to a Schwann cell phenotype, the repair Schwann cell, which is specialized to encourage regeneration (reviewed in Jessen and Mirsky, 2016; **Figure 2**). These cells execute a repair program, a partly overlapping sequence of phenotypic changes involving myelin autophagy, expression of cytokines that call in macrophages for later stages of myelin clearance, activation of trophic factor expression and cellular elongation and branching to form regeneration tracks, called Bungner Bands. In this way, repair cells clear myelin, support the survival of injured neurons, axon regeneration and target innervation. These are the cells present in the distal stump of injured nerves along which regenerating axons navigate after injury, often for months or even years in humans due to the slow rate of axon growth.

One of the main problems in human nerve repair is that the phenotype of repair cells is not stable, but fades with time as the cells fail to maintain expression of trophic factors that promote axonal growth, likely due to gradual changes in the signaling environment within the chronically denervated distal stump (reviewed in Höke, 2006b; Sulaiman and Gordon, 2009). Furthermore, the repair cell population is not stable, their

number eventually declining to very low levels. The reasons for the deterioration of repair cells are poorly understood, although the transcription factors STAT3 and c-Jun have been implicated in this process.

Importantly, PNS neurons also respond to axonal damage by activating an extensive gene program that facilitates axonal regeneration, a response classically referred to as the cell body response or the signaling to growth mode switch (Allodi et al., 2012; Blesch et al., 2012; reviewed in Fu and Gordon, 1997; Doron-Mandel et al., 2015).

Therefore, in response to damage, both neurons and Schwann cells convert to cell states that are specialized to deal with injury and promote healing. Comparable reprogramming of differentiated cells in response to injury can also be seen in other systems. This includes the conversion of fibroblasts to myofibroblasts during wound healing, and of pigmented epithelial cells to lens cells in the eye, the conversions of supportive cells to hair cells in the ear, hepatocytes to biliary epithelial cells in the liver, and of endocrine α to β cells in the pancreatic isles. In all of these cases, differentiated cells change identity in order to promote tissue homeostasis and repair. This type of change has therefore been termed adaptive cellular reprogramming (reviewed in Jessen et al., 2015a).

Eventually, axons that have successfully regenerated induce ensheathing repair cells to adopt again the Remak and myelin phenotypes, thereby restoring the nerve to its functional state. The repair Schwann cells are therefore a transient population, which exists only while they are needed.

We will now discuss some of the issues aired above in more detail.

THE SCHWANN CELL INJURY RESPONSE: THE GENERATION OF REPAIR CELLS

Unfortunately, in humans most nerve injuries involve nerve transection rather than the more easily repaired nerve crush. After a nerve crush, the basal lamina around each axon/Schwann cell unit remains intact and an axon stays within its basal lamina tube as it grows across the injury site to reach the distal stump. It therefore has a favorable possibility to reconnect with its original target tissue and restore function.

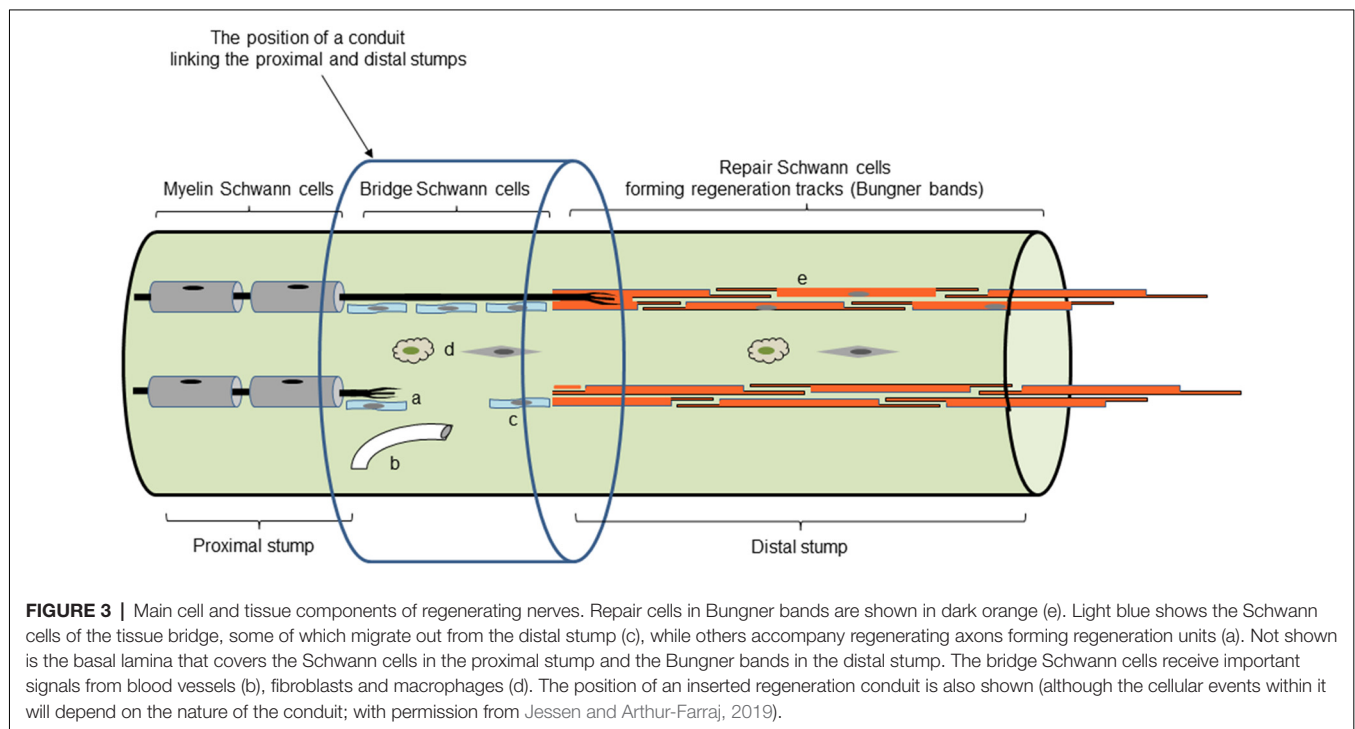
In contrast, after cut, the connective tissue and basal lamina tubes are disrupted. Regeneration units consisting of axons accompanied by Schwann cells grow through a tissue bridge that forms between the proximal and distal nerve stumps. As a result of complex signaling between axons, Schwann cells and macrophages, involving factors such as Sox2, ephrin-B/EphB2 and TGF β , and guidance by fibroblasts and blood vessels, axons regenerate across the bridge to meet the Schwann cells that grow from the transected end of the distal stump (Parrinello et al., 2010; Cattin et al., 2015; Clements et al., 2017; reviewed in Cattin and Lloyd, 2016). Thus in cut nerves, continuity between the proximal stump and the target is broken, and axons are much less likely to find their way into their original basal lamina tubes and their target tissues, compromising proper restoration of function (Morris et al., 1972; Friede and Bischhausen, 1980; Meller, 1987; Barrette et al., 2008). The standard clinical treatment is to re-attach the proximal and distal nerve stumps. Although this leaves only a microscopic gap to be

filled by a bridge, the problem of axons finding their original basal lamina tubes remains (Witzel et al., 2005). This problem is amplified when extensive injuries are repaired by the insertion of a nerve graft or an artificial insert (Figure 3). The interesting and intricate cellular interactions in the bridge region will not be discussed here in detail (for review see Cattin and Lloyd, 2016).

It does not matter whether axons are interrupted by crush or cut, in the distal stump the response of Schwann cells to injury is similar. In both cases, it converts Remak and myelin cells to repair supportive Schwann cells. The Schwann cell injury response has two principal components and will be discussed in terms of myelin Schwann cells only although similar principles are likely to apply to the response of Remak cells. The reversal of myelin differentiation represents one component. Genes coding for Egr2 (Krox20), cholesterol-related enzymes and the myelin-related proteins MPZ, MBP, MAG and periaxin are down-regulated. Conversely, molecules that characterize developing Schwann cells and adult Remak cells including, NCAM, p75NTR, GFAP and L1 are up-regulated (reviewed in Chen et al., 2007; Jessen and Mirsky, 2008; Martinez et al., 2015; Boerboom et al., 2017).

The second important part of the injury response is the appearance of a set of repair-supportive characteristics that are not seen, or seen in a muted form, in Schwann cells in normal mature nerves or in Schwann cells in developing nerves. This repair component of the response includes a number of elements (reviewed in Jessen and Mirsky, 2016).

1. Factors that promote the survival of injured neurons and axonal elongation are up-regulated. These include neurotrophic factors and surface molecules such as glial cell



line-derived neurotrophic factor (GDNF), artemin, brain-derived neurotrophic factor (BDNF), neurotrophin-3 (NT3), nerve growth factor (NGF), vascular endothelial growth factor (VEGF), erythropoietin, FGFs, pleiotrophin, N-cadherin and p75NTR (Grothe et al., 2006; Fontana et al., 2012; Brushart et al., 2013; reviewed in Boyd and Gordon, 2003; Chen et al., 2007; Scheib and Höke, 2013; Wood and Mackinnon, 2015).

2. An innate immune response is activated. This involves the upregulation of cytokines including tumor necrosis factor α (TNF α), interleukin-1 α (IL-1 α), IL-1 β , leukemia inhibitory factor (LIF), monocyte chemotactic protein-1 (MCP-1) and toll-like receptors by the Schwann cells in the distal stump (reviewed in Martini et al., 2008; Rotshenker, 2011). This allows repair Schwann cells to recruit macrophages and other immune system cells such as neutrophils to the nerve, promoting nerve regeneration in several ways. Cytokines including IL-6 and LIF attract macrophages to the nerve but also act directly on neurons to promote axon growth (Hirota et al., 1996; Cafferty et al., 2001; reviewed in Bauer et al., 2007). An additional sustained source of cytokines are macrophages that invade nerves and ganglia. They also promote vascularization of the nerve bridge between the proximal and distal stumps (Barrette et al., 2008; Niemi et al., 2013; Cattin et al., 2015). Macrophages also co-operate with Schwann cells to degrade myelin debris (see further below; reviewed in Hirata and Kawabuchi, 2002; Rotshenker, 2011).
3. Schwann cells proliferate and then undergo a striking about three-fold elongation as they form the regeneration tracks, Bungner bands, which are essential for guiding axons back to their target areas (see further below). These structural changes are a component of the tissue remodeling which transforms the distal stump into a collection of regeneration tracks (Gomez-Sanchez et al., 2017).
4. Repair cells activate mTOR-independent autophagy, myelinophagy, to break down their myelin sheaths, which are redundant after axonal degeneration (Gomez-Sanchez et al., 2015; Suzuki et al., 2015; Jang et al., 2016; Brosius Lutz et al., 2017).

THE PROPERTIES OF REPAIR CELLS

Repair Schwann Cells Show a Distinct Molecular Profile

At least two genes, *Olig 1*, *Shh*, differentiate repair cells from myelin and Remak cells, and also from immature Schwann cells, and Schwann cell precursors in embryonic nerves. These genes are highly up-regulated by c-Jun in Schwann cells of injured nerves. These genes are distinctive markers of repair Schwann cells because they are expressed de novo after injury. This applies also to *GDNF*, with the exception that this gene is down-regulated before birth (Lu et al., 2000; Zhou et al., 2000; Piirsoo et al., 2010; Arthur-Farraj et al., 2012; Fontana et al., 2012; Lin et al., 2015).

In addition, a gene expression screen found over a hundred genes that were significantly up- or down-regulated in the

distal stump after damage, although they were not regulated during development, since they were present at similar levels in developing and adult uninjured nerves. The majority of these genes were up-regulated by injury. This reveals a substantial group of genes that are specifically activated in injured nerves, and which are therefore candidate markers for repair cells (Bosse et al., 2006).

Timing and the Repair Program

The different components of the repair program are not switched on synchronously. Instead, each of them reaches peak expression at different times after injury. For instance, protein levels of cytokines such as IL-1 β and TNF α , peak within 1 day of injury, but are sharply lower at 3 days (Rotshenker, 2011), autophagy is high at 5 days and reduced thereafter (Gomez-Sanchez et al., 2015), GDNF protein levels peak at about 1 week after injury and BDNF is maximally expressed after 2–3 weeks (Eggers et al., 2010). The transcription factor c-Jun which is an important regulator of the repair program (see below), is activated within hours of injury, but c-Jun protein levels continue to increase for at least 7–10 days and cellular elongation continues for at least 4 weeks after injury (Gomez-Sanchez et al., 2017). The repair program therefore represents a temporal sequence of events that overlap and co-operate to support repair.

The Elongation and Branching of Repair Cells

One of the cardinal features of Schwann cells is their extended morphology, a feature that is often associated with the requirement to stretch out to cover the elongated axons. However, Schwann cells which lose contact with degenerating axons in the distal stump do not shorten. Rather, lineage tracing studies have shown that loss of axonal contact triggers a striking cellular elongation (Gomez-Sanchez et al., 2017). One week after nerve transection without regeneration, Remak cells have doubled in length, and 4 weeks after injury they are three-fold longer than Remak cells in intact nerves. Similarly, myelin cells have doubled in length by 4 weeks after injury. Loss of axonal contact also induces the cells to branch. About 50% and 30% of repair cells derived from Remak and myelin cells, respectively, form branches, which are often long and lie parallel to the main axis of the cell (Gomez-Sanchez et al., 2017; **Figure 4**).

This study also addressed two long-standing assumptions about Schwann cells. First, that Remak and myelin cells generate the cells found in the Bungner bands of injured nerves, and second, that the Bungner band cells, in turn, generate the myelin cells found in regenerated nerves. These fundamental presumptions were confirmed directly using lineage tracing methods (Gomez-Sanchez et al., 2017). This allowed repair cells from Remak cells and myelin cells to be studied separately, and made it possible to identify the progeny of myelin cell-derived repair cells among the cells that re-myelinate nerves after regeneration. This revealed that re-myelination involves a remarkable about seven-fold cell shortening, as the elongated repair cells wrap axons to generate the typically short myelin internodes of regenerated nerves.

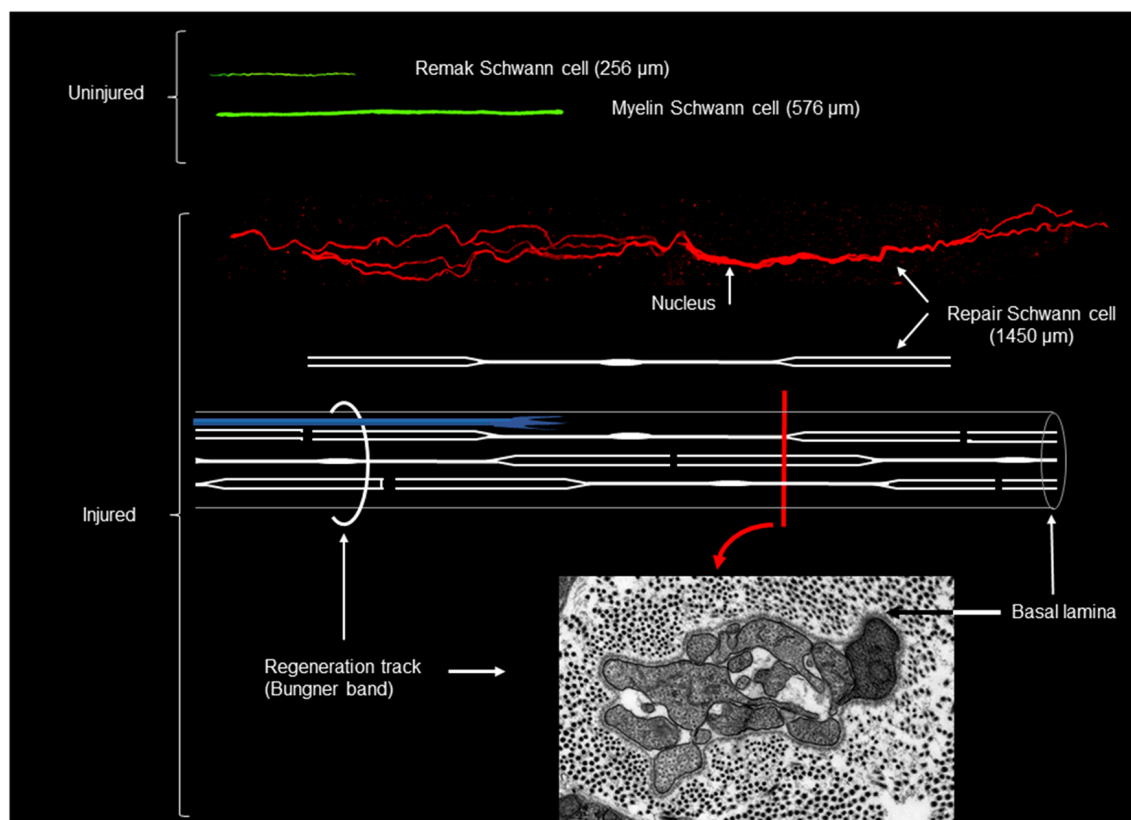


FIGURE 4 | Myelin, Remak and repair Schwann cells after genetic labeling *in vivo*. Shown in green are myelin and Remak cells of average length as they appear in uninjured nerve. In red is an example of a long, branched repair cell (generated from a myelin cell), in 4 week cut nerve without reinnervation. All cells are shown to scale. Shown also is a schematic diagram of a repair cell and the assembly of these cells to form a Bungner band enclosed by a basal lamina and containing a regenerating axon (in blue). The electron micrograph shows a transverse section of a Bungner band (red image printed with permission from Gomez-Sanchez et al., 2017). Scale bar: 1 μm .

Although Remak and myelin cells have sharply different structure, they generate repair cells with broadly similar morphology. The extremely elongated and branched structure of these cells differentiates repair cells from other cells in the Schwann cell lineage. This morphology also promotes the generation of uninterrupted and robust regeneration tracks by maximizing cell-cell overlap within each Bungner band.

Myelin Clearance

Unlike the CNS, peripheral nerves are able to clear redundant myelin after axonal degeneration, a feature that is widely believed to facilitate regeneration because of the growth-inhibitory nature of myelin (Kang and Lichtman, 2013; reviewed in Hirata and Kawabuchi, 2002; Rotshenker, 2011). Nerves clear myelin by two distinct mechanisms. First, Schwann cells switch from myelin maintenance to actively breaking down their own myelin sheaths through the mechanism of myelin autophagy (Gomez-Sanchez et al., 2015; Suzuki et al., 2015; Jang et al., 2016; Brosius Lutz et al., 2017). This process delivers myelin to Schwann cell lysosomes for degradation, following internalization of myelin in the form of myelin ovoids (Jung et al., 2011), and the formation of smaller

cytoplasmic myelin fragments. About 50% of total myelin is thought to be broken down by Schwann cells (Perry et al., 1995). Second, myelin debris is phagocytosed and degraded Schwann cells and in particular by macrophages, which gradually invade injured nerves, recruited by the repair cell cytokine expression referred to above.

CONTROL OF REPAIR CELL GENERATION

Repair Schwann Cells Are Controlled by Dedicated Signaling Mechanisms

A number of mechanisms take part in regulating the Schwann cell injury response. Importantly, it has become clear that this includes regulatory mechanisms that operate selectively in repair cells, and have only a minor or undetectable function in developing Schwann cells. This applies to the transcription factors c-Jun and STAT3, which will be discussed in subsequent sections. Regulation of histone H3K27 trimethylation represents another selective mechanism, which appears not to be significantly involved in control of Schwann cell development (Ma et al., 2016). In response to injury, however, the activation of several injury-related genes is promoted by

removal of the repressive histone mark H3K27 trimethylation at their promoter regions, combined with the gain of the active histone mark H3K4 methylation. At the same time, the active histone mark H3K27 acetylation is lost from the enhancers of myelin genes as their expression fades (Hung et al., 2015; Ma et al., 2016). An important, selective role in repair cells is also played by the tumor suppressor protein Merlin. Schwann cell specific inactivation of Merlin has major adverse effects on repair cell function, axonal regeneration and re-myelination, but only minor effects on Schwann cell development (Mindos et al., 2017). Together with the c-Jun and STAT3, these histone methylation events described above, and merlin, represent gene regulatory mechanisms, which selectively control repair cells, and appear unimportant in developing Schwann cells.

Other Signals That Control the Schwann Cell Injury Response

Positive regulators of repair cell generation or function include Notch (Woodhoo et al., 2009), Sox2 (Parrinello et al., 2010; Roberts et al., 2017), *gpr126* (Mogha et al., 2016), TGF β (Morgan et al., 1994; Stewart et al., 1995; Cattin et al., 2015; Clements et al., 2017) and ERK1/2, although its function is complex, since its ERK1/2 activation is also required for myelin synthesis (Harrisingh et al., 2004; Fischer et al., 2008; Newbern et al., 2011; Napoli et al., 2012; Sheean et al., 2014; Cervellini et al., 2018; reviewed in Monk et al., 2015; Jessen and Mirsky, 2016; Boerboom et al., 2017). The transcription factor Zeb2 is required for normal re-myelination after injury, but appears not to be important for the generation of repair cells (Quintes et al., 2016; Wu et al., 2016). Toll-like receptors are involved in up-regulation of cytokines, macrophage recruitment and myelin clearance after injury, while the mTORC1 pathway is also involved in myelin clearance and is needed for effective expression of c-Jun and other repair cell genes after injury (Boivin et al., 2007; Norrmén et al., 2018). The significance of these proteins for axonal regeneration is not clear.

Negative regulation of repair cells is exerted by histone deacetylase 2 (HDAC2), which is activated after injury acts to suppress c-Jun and delay the generation of repair cells. Inhibition of HDAC2 therefore represents a potential route to improve regeneration, because regeneration is accelerated when HDAC2 is inactivated, although re-myelination is impaired (Brügger et al., 2017; Jacob, 2017).

Considerable attention has been paid to the potential role of neuregulin in nerve injury. Schwann cells in transected nerves elevate expression of ErbB2/3 receptors and neuregulin-1 I/II isoforms (Carroll et al., 1997; Stassart et al., 2013; Ronchi et al., 2016). Surprisingly, however, neuregulin-1 is not involved in injury-induced Schwann cell proliferation, and macrophage recruitment, and myelin breakdown appears normal in nerves without neuregulin (Atanasoski et al., 2006; Fricker et al., 2013). Another unexpected finding is that even after removal of neuregulin-1 from both Schwann cells and axons, re-myelination of regenerated nerves after injury is eventually normal after a substantial delay (Fricker et al., 2013; Stassart et al., 2013).

This contrasts with development, since neuregulin-1, expressed by axons, is necessary for myelination by developing Schwann cells (Birchmeier and Nave, 2008). In another deviation from development, repair Schwann cell-derived neuregulin-1 has a significant role in accelerating re-myelination after injury, most likely working through an autocrine signaling loop, while Schwann cell-derived neuregulin-1 is not important for developmental myelination (Stassart et al., 2013). The involvement of neuregulin-1 in the control of myelination therefore differs between repair Schwann cells and developing cells.

Inactivation of neuregulin-1 in axons and Schwann cells results in slow axonal regeneration after injury. This suggests that endogenous neuregulin signaling through ErbB2/3 receptors in repair cells promotes the repair phenotype and enhances the capacity of these cells to support axon growth, but direct evidence for this mechanism of action is missing. Nevertheless, pharmacologically enhancing neuregulin signaling might serve as a tool for promoting nerve repair, because enforced Schwann cell ErbB2 expression, and exogenously applied neuregulin increase axonal regeneration *in vivo* (Ronchi et al., 2013; Han et al., 2017; reviewed in Gambarotta et al., 2013).

The Function of c-Jun in Repair Cells

The transcription factor c-Jun plays a crucial role in the Schwann cell injury response (Jessen and Mirsky, 2016). c-Jun levels are low in uninjured nerves, but are rapidly and strongly elevated by injury (De Felipe and Hunt, 1994; Shy et al., 1996). When this is prevented, by selective inactivation of c-Jun in Schwann cells in transgenic mice (c-Jun cKO mice) regeneration of axons and recovery of function after injury are strikingly compromised. Uninjured nerves in these mice are essentially normal. This indicates that c-Jun is not essential for Schwann cell development, and that the role of this transcription factor is restricted to controlling the response of Schwann cells to nerve damage (Arthur-Farraj et al., 2012).

The regeneration failure in c-Jun cKO mice is due to the important function of c-Jun in injury-induced Schwann cell reprogramming. c-Jun directly or indirectly affects the expression levels of at least 172 genes of the ~4,000 genes that change expression in Schwann cells after injury. This gives c-Jun significant control over both parts of the Schwann cell injury response, de-differentiation of myelin cells and activation of the repair program (Arthur-Farraj et al., 2012, 2017). c-Jun helps de-differentiation, because it is needed for the normal down-regulation of myelin genes after injury. Among these are the genes encoding the transcription factor *Egr2* (*Krox20*), a master regulator of the myelin program, and the *MPZ* and *MBP* genes. The negative gene regulation by c-Jun and its cross-antagonistic relationship with *Egr2* (*Krox20*) had been studied before its importance for regeneration was revealed and helped give rise to the idea that c-Jun, in combination with a group of other transcriptional regulators, including Notch, Sox2, Id2 and Pax3, functioned as negative regulators of myelination (Kioussi et al., 1995; Parkinson et al., 2004, 2008; Le et al., 2005; Doddrell et al., 2012; Fazal et al.,

2017; Florio et al., 2018; reviewed in Jessen and Mirsky, 2008). Although these genes may be important for modifying the rate or onset of myelination in developing nerves, a key role for c-Jun-mediated gene down-regulation *in vivo* appears to be that of helping to suppress myelin gene expression in adult nerves after injury.

c-Jun also promotes the normal activation of the repair program, which it controls in several important ways (Arthur-Farraj et al., 2012; Fontana et al., 2012). First, in the absence of Schwann cell c-Jun (c-Jun cKO mice), important trophic factors and cell surface proteins that support survival and axon growth fail to be normally upregulated. This includes GDNF, artemin and BDNF, p75NTR and N-cadherin. Two of these, GDNF and artemin, have been shown to be direct c-Jun targets and have been implicated in sensory neuron death after injury (Fontana et al., 2012). Normally some dorsal root ganglion (DRG) sensory neurons and facial motoneurons die after sciatic and facial nerve injury, respectively, and in humans DRG neuron death is considered a major reason for poor outcomes of nerve regeneration (Faroni et al., 2015). Death of DRG neurons and facial motoneurons is greatly increased in c-Jun cKO mice. This shows that a key function for repair Schwann cells and c-Jun signaling is to support the

survival of injured neurons. Second, the regeneration tracks formed by denervated Schwann cells without c-Jun have a disorganized structure (Figure 5). In culture, c-Jun is needed for the typical narrow, bi/tripolar Schwann cell morphology, since c-Jun-negative cells tend to be flat and sheet-forming. Similarly, *in vivo*, the repair Schwann cells within the regeneration tracks show grossly abnormal morphology when viewed in transverse electron micrograph sections. c-Jun appears to be necessary for the conversion of the complex and sheath-like structure of the myelin cells to the narrow, rod-like and branched structure of repair cells that is required for the formation of normal regeneration tracks. Third, c-Jun promotes myelinophagy, and c-Jun cKO nerves show a substantial delay in breakdown of myelin (Arthur-Farraj et al., 2012; Gomez-Sanchez et al., 2017).

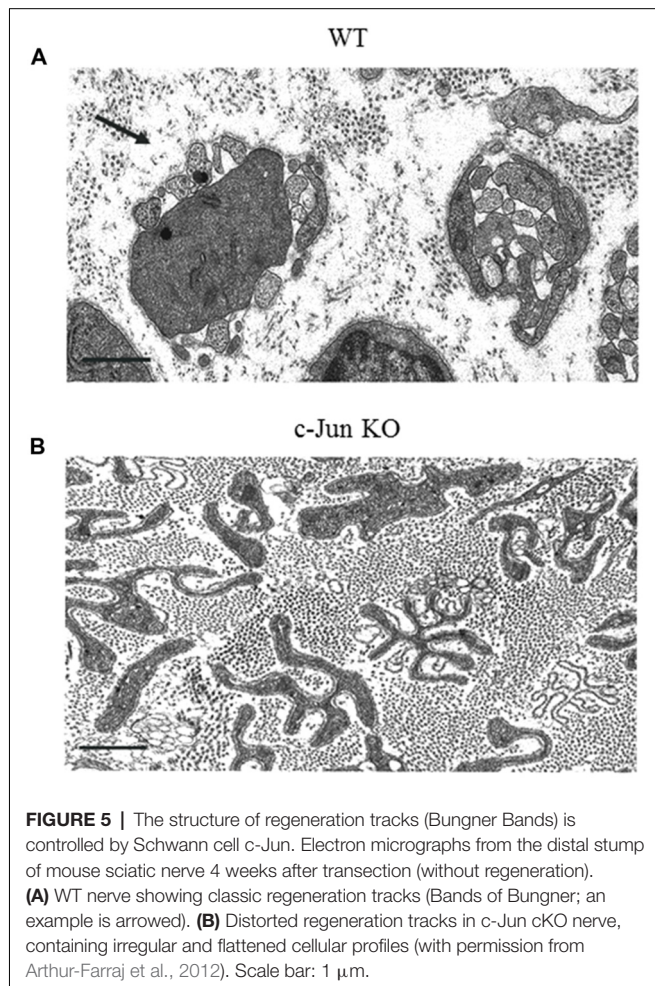
Thus, c-Jun exerts a broad control over the Schwann cell injury response, and thereby neuronal survival and regeneration. It is therefore of interest that in two important situations where repair cells fail, namely chronic denervation and aging, c-Jun levels in these cells are reduced. This is discussed in “Nerve Injury Activates Epithelial Mesenchymal Transition (EMT) Genes” section below.

NERVE INJURY ACTIVATES EPITHELIAL MESENCHYMAL TRANSITION (EMT) GENES

Recent gene screen studies suggest that the generation of repair cells involves the activation of a process related to epithelial mesenchymal transitions (EMTs; Arthur-Farraj et al., 2017; Clements et al., 2017). RNA-Seq of distal nerve stumps 7 days after injury show enrichment for EMT mRNAs and miRNAs. This includes down-regulation of RNAs that are linked to mesenchymal-epithelial transition (MET), and up-regulation of RNAs associated with EMT. Enrichment for EMT genes was also shown in more detailed experiments using FACs to sort td-tomato labeled Schwann cells from injured nerves (Clements et al., 2017). This study also showed that EMT activation was strongest in the Schwann cells the tissue bridge, where arguably tissue remodeling is more radical than in the distal stump.

Typically, EMT-like processes involve also an increase in stemness, namely the activation of genes associated with stem cells (Fabregat et al., 2016; Liao and Yang, 2017). This is also seen in injured nerves, where the generation of repair cells is accompanied by activation of the Myc stemness and Core pluripotency modules and suppression of polycomb-related factors (Clements et al., 2017).

In many tissues, the combined activation of EMT and stemness is associated with increased cellular motility, proliferation, morphological flexibility, tissue remodeling, and the loosening up of differentiation states (Nieto et al., 2016; Forte et al., 2017). These events are key features of the response of many tissues to injury. Not surprisingly, therefore, the activation of EMT and stemness programs have now been established as a key physiological response to injury in various tissues.



The demonstration of EMT/stemness activation in Schwann cells of injured nerves brings the nerve injury response in line with injury responses in many other systems. It adds an important new component to our understanding of the injury response. In particular, the loosening of differentiation states associated with increased stemness is consistent with the notion that nerve injury triggers a shift in Schwann cell differentiation state from myelin and Remak phenotypes to a Schwann cell state specialized to promote repair.

WHY DOES REGENERATION FAIL?

In the light of the radical, adaptive injury response of neurons and Schwann cells, which in many types of rodent experiments results in effective nerve repair, why is it that the clinical outcome after nerve injury in humans is generally poor? This paradox of PNS repair can be explained by a number of factors, including the hindrance to axon growth provided by the injury site and the difficulty of getting large numbers of axons from the proximal to the distal stump, misrouting of axons resulting in re-innervation errors, and the presence of growth-inhibiting extracellular matrix. Perhaps the most difficult problems arise from the relatively slow growth of axons. Because of this, most human nerve injuries involve chronic denervation of the more distal parts of damaged nerves and of the target tissues such as muscle. This results in target atrophy, while neurons gradually die and surviving neurons may fail to sustain their capacity to regenerate axons during the extended period required for repair (Höke, 2006a; Sulaiman and Gordon, 2013; Patel et al., 2018).

Here, we will consider another major issue in regeneration failure. This is the fact that the nerve stump distal to transection gradually loses the ability to support the growth of regenerating axons during chronic denervation. This has been shown in a number of studies, most of which represent cross-suturing, typically involving the suturing of acutely transected tibial nerve to the distal stump of the common peroneal nerve, which had been transected either acutely, the control condition, or at different times up to 6 months previously. Other experiments for addressing the same question have studied regeneration through nerve grafts, where the graft is obtained from nerves that have been denervated previously for various lengths of time. All of the experiments agree that transected nerve stumps retain full or only mildly reduced capacity for supporting regeneration for about 1 month (Li et al., 1997; Sulaiman and Gordon, 2000; Kou et al., 2011; Jonsson et al., 2013). By 2 months, regeneration support remains unchanged in some studies (Li et al., 1997), although other reports show it reduced by about 40%–50% (Sulaiman and Gordon, 2000; Kou et al., 2011). At 3 months regeneration support is further diminished and reduced to very low levels by 6 months (Li et al., 1997; Sulaiman and Gordon, 2002; Gordon et al., 2011; Jonsson et al., 2013; see however Rönkkö et al., 2011).

While these experiments were carried out on rats, we find that also in mice, the capacity of distal stumps to support regeneration is reduced by about 50% after 2.5 months of chronic denervation (Wagstaff et al., 2017).

IS THE FAILURE OF DISTAL STUMPS TO SUPPORT GROWTH DUE TO LACK OF SCHWANN CELLS?

The deterioration in the capacity of chronically denervated stumps to support regeneration could result from two separate factors: gradual reduction in Schwann cell numbers, or the fading of the repair phenotype of cells still present in the nerve. Both of these factors could in turn be influenced by signals from macrophages that invade injured nerves and are initially present in large numbers that decline with time. The question of whether Schwann cell number is a key factor raises two additional ones. First, what is known about Schwann cell numbers in chronically transected nerves? Second, are variations in Schwann cell numbers within the range seen in cut nerves likely to affect regeneration?

While it is long established that nerve injury triggers a wave of Schwann cell proliferation, there is surprisingly little quantitative information on Schwann cell numbers in cut nerves after injury. Cell counts using electron microscopy show that 2 weeks after cut the number of Schwann cells in mouse sciatic nerve has risen about 2.5-fold compared to uninjured nerves and remains similar at 1 and 1.5 months (Wagstaff et al., 2017). Using S100 to identify Schwann cells in the cut sciatic nerve of rats show 3–4-fold increase at 1–2 weeks with little change at 1.5 months (Siironen et al., 1994). These workers also report a sharp drop between 1.5 and 2 months, but since S100 is present at reduced levels after injury, these figures might overestimate the reduction in Schwann cell number (Siironen et al., 1994). Another study also using S100 indicates that Schwann cell numbers at 2.5 months remains 2–3-fold that in uncut nerves (Salonen et al., 1988). Our data from mouse nerves show a drop of about 30% between 2 weeks and 2.5 months (Wagstaff et al., 2017).

A study employing a more indirect method involving counting of the number of cells obtained by enzymatic dissociation of nerves at different times after nerve cut without innervation, concluded that the number of Schwann cells drops by about 30% between 1 and 2 months with little change at 3 and 4 months (Li et al., 1998). The number of cells that can be isolated from nerves after 6 months of chronic denervation is only 10%–15% of that obtained at 4 weeks (Li et al., 1998; Jonsson et al., 2013).

Although the data are limited and not always consistent, the above suggests that 2–3 months after chronic denervation, a time when growth support by the distal stump is significantly reduced, the number of Schwann cells has dropped at most by about 30%–50% from the high cell number seen 1–4 weeks after injury. This would mean that the number of cells at 2–3 months remains substantially higher than the number in uninjured nerves.

Is it likely that this fall from peak cell numbers accounts for the reduction in regenerative support during chronic denervation? The answer to this question depends on the weight is put on the reports discussed below that imply that regeneration remains normal in nerves where injury-induced increase in Schwann cell numbers is prevented, and cell numbers in the

distal stump therefore remain similar to those in uninjured nerves.

DOES NERVE REGENERATION DEPEND ON SCHWANN CELL PROLIFERATION?

It is a common view that Schwann cell proliferation and expansion in Schwann cell numbers in injured nerves is required for regeneration (Hall and Gregson, 1977; Hall, 2005). Recent genetic approaches to specifically inhibit Schwann cell proliferation suggest, however, that this may not be the case. Injury-induced Schwann cell proliferation depends on cyclin D1, although this protein is not important for proliferation during development. Nerves in D1^{-/-} mice therefore develop normally, but Schwann cell proliferation after injury is blocked. Perhaps surprisingly, regeneration appears not to be markedly affected in these mice (Kim et al., 2000; Atanasoski et al., 2001; Yang et al., 2008).

DETERIORATION OF REPAIR CELLS: AN IMPORTANT REASON FOR REGENERATION FAILURES

Since Schwann cell numbers after 2–3 months of chronic denervation are likely to remain at least double that in uninjured nerves, and in view of the experiments on cyclin1^{-/-} mice outlined above, it seems that lack of Schwann cells is unlikely to be the major reason for the reduction in growth support provided by 2–3 month chronically denervated stumps, although at later times ongoing reduction in cell number will eventually be significant. This suggests that the deterioration of repair cells is a two-stage process involving, first, surviving cells gradually down-regulating their repair phenotype, followed by death of cells that have by that time lost most of their regeneration-supportive properties. There is in fact ample evidence for such fading of the repair cell phenotype, manifest in reduced expression of neuron-supportive trophic factors during chronic denervation, including GDNF, BDNF, NT3 and NGF (Eggers et al., 2010; reviewed in Boyd and Gordon, 2003; Höke and Brushart, 2010).

Thus, the fading of the repair phenotype, combined in the long run with dwindling cell numbers, are likely to be the twin reasons for reduced growth support provided by chronically denervated stumps. It is therefore important to identify factors that control the long-term maintenance of repair cells, sustain the expression of repair supportive genes and support cell survival.

SIGNALS THAT MAINTAIN REPAIR CELLS

While there are as yet surprisingly few studies on this important topic, two transcription factors, STAT3 and c-Jun have recently been shown to have a role in repair cell maintenance (Benito et al., 2017; Wagstaff et al., 2017). Activation of Schwann cell STAT3 is triggered by injury, and largely sustained in long-term denervated repair cells (Sheu et al., 2000). Genetic inactivation of STAT3 in these cells results in decreased autocrine Schwann cell survival signaling and a striking loss of Schwann

cells from chronically denervated stumps. Loss of STAT3 also reduces the expression of repair cell markers, including GDNF, BDNF and Shh, during long-term denervation (Benito et al., 2017). Inactivation of Schwann cell STAT3 does, however, not significantly affect nerve development. The important role of STAT3, therefore, is to act as a brake on the deterioration of repair cells in chronically denervated adult nerves.

Unlike STAT3, c-Jun levels in Schwann cells decline significantly during long-term denervation, in tandem with the fading of the repair phenotype, reduced cell numbers, and reduced capacity to support regeneration. Significantly, the ability of long-term denervated repair cells to support regeneration can be restored to control levels by genetically enhancing c-Jun expression in these cells to levels similar to those in short-term denervated nerve stumps (Fazal et al., 2017; Wagstaff et al., 2017). This raises the possibility that the deterioration of chronically denervated repair cells is to a significant extent caused by a failure to sustain high c-Jun levels.

Aging, like chronic denervation, is accompanied by a marked reduction in the rate of nerve regeneration (Verdú et al., 2000; Painter, 2017). Using rodent models, this has been traced primarily to age-related deterioration of repair Schwann cells, since repair cells from older animals show reduced expression of repair cell markers and reduced ability to support axon growth (Painter et al., 2014). Many of the abnormally expressed genes are c-Jun regulated, and c-Jun activation after injury is also significantly reduced in older animals. These observations have implicated dysregulation of Schwann cell c-Jun in the age-related deterioration of nerve repair (Painter et al., 2014; Wagstaff et al., 2017). A support for this suggestion comes from experiments on transgenic animals in which c-Jun expression in injured old nerves has been elevated to levels similar to those of injured young nerves. This correction of Schwann cell c-Jun levels is sufficient to correct the age-related regeneration deficit, and accelerate the rate of axonal regeneration to that seen in young animals (Wagstaff et al., 2017). Therefore, the inability of repair Schwann cells in older animals to elevate c-Jun to high levels may be a significant factor in the age-related failure of nerve repair.

CONCLUSIONS

The key driver of nerve regeneration, apart from the neurons themselves, are the denervated Schwann cells that make up the regeneration tracks, Bungner bands, that occupy nerves distal to the injury site. These repair Schwann cells are adapted to meet the particular needs that arise in injured adult nerves. They differ from other Schwann cells, having separate transcriptional and epigenetic mechanisms, distinct morphology and molecular profile, in addition to carrying out a set of functions, comprising the repair program, which support nerve regeneration.

The realization that these cells possess distinct properties and cell-type specific control mechanisms is a useful step forward. It will help to focus future work on learning how to manipulate these particular cells, how to amplify their repair-supportive

functions, and how prevent their deterioration in older age and during the prolonged periods required for axonal regeneration in human nerves.

AUTHOR CONTRIBUTIONS

Both authors contributed equally to the writing and editing of the manuscript.

REFERENCES

- Allodi, I., Udina, E., and Navarro, X. (2012). Specificity of peripheral nerve regeneration: interactions at the axon level. *Prog. Neurobiol.* 98, 16–37. doi: 10.1016/j.pneurobio.2012.05.005
- Arthur-Farraj, P. J., Latouche, M., Wilton, D. K., Quintes, S., Chabrol, E., Banerjee, A., et al. (2012). c-Jun reprograms Schwann cells of injured nerves to generate a repair cell essential for regeneration. *Neuron* 75, 633–647. doi: 10.1016/j.neuron.2012.06.021
- Arthur-Farraj, P. J., Morgan, C. C., Adamowicz, M., Gomez-Sanchez, J. A., Fazal, S. V., Beucher, A., et al. (2017). Changes in the coding and non-coding transcriptome and DNA methylome that define the Schwann Cell repair phenotype after nerve injury. *Cell Rep.* 20, 2719–2734. doi: 10.1016/j.celrep.2017.08.064
- Atanasoski, S., Scherer, S. S., Sirkowski, E., Leone, D., Garratt, A. N., Birchmeier, C., et al. (2006). ErbB2 signaling in Schwann cells is mostly dispensable for maintenance of myelinated peripheral nerves and proliferation of adult Schwann cells after injury. *J. Neurosci.* 26, 2124–2131. doi: 10.1523/JNEUROSCI.4594-05.2006
- Atanasoski, S., Shumas, S., Dickson, C., Scherer, S. S., and Suter, U. (2001). Differential cyclin D1 requirements of proliferating Schwann cells during development and after injury. *Mol. Cell. Neurosci.* 18, 581–592. doi: 10.1006/mcne.2001.1055
- Barrette, B., Hébert, M. A., Filali, M., Lafortune, K., Vallières, N., Gowing, G., et al. (2008). Requirement of myeloid cells for axon regeneration. *J. Neurosci.* 28, 9363–9376. doi: 10.1523/jneurosci.1447-08.2008
- Bauer, S., Kerr, B. J., and Patterson, P. H. (2007). The neuropoietic cytokine family in development, plasticity, disease and injury. *Nat. Rev. Neurosci.* 8, 221–232. doi: 10.1038/nrn2054
- Benito, C., Davis, C. M., Gomez-Sanchez, J. A., Turmaine, M., Meijer, D., Poli, V., et al. (2017). STAT3 controls the long-term survival and phenotype of repair schwann cells during nerve regeneration. *J. Neurosci.* 37, 4255–4269. doi: 10.1523/jneurosci.3481-16.2017
- Birchmeier, C., and Nave, K. A. (2008). Neuregulin-1, a key axonal signal that drives Schwann cell growth and differentiation. *Glia* 56, 1491–1497. doi: 10.1002/glia.20753
- Blesch, A., Lu, P., Tsukada, S., Alto, L. T., Roet, K., Coppola, G., et al. (2012). Conditioning lesions before or after spinal cord injury recruit broad genetic mechanisms that sustain axonal regeneration: superiority to cAMP-mediated effects. *Exp. Neurol.* 235, 162–173. doi: 10.1016/j.expneurol.2011.12.037
- Boerboom, A., Dion, V., Chariot, A., and Franzen, R. (2017). Molecular mechanisms involved in schwann cell plasticity. *Front. Mol. Neurosci.* 10:38. doi: 10.3389/fnmol.2017.00038
- Boivin, A., Pineau, I., Barrette, B., Filali, M., Vallières, N., Rivest, S., et al. (2007). Toll-like receptor signaling is critical for Wallerian degeneration and functional recovery after peripheral nerve injury. *J. Neurosci.* 27, 12565–12576. doi: 10.1523/jneurosci.3027-07.2007
- Bosse, F., Hasenpusch-Theil, K., Küry, P., and Müller, H. W. (2006). Gene expression profiling reveals that peripheral nerve regeneration is a consequence of both novel injury-dependent and reactivated developmental processes. *J. Neurochem.* 96, 1441–1457. doi: 10.1111/j.1471-4159.2005.03635.x
- Boyd, J. G., and Gordon, T. (2003). Neurotrophic factors and their receptors in axonal regeneration and functional recovery after peripheral nerve injury. *Mol. Neurobiol.* 27, 277–324. doi: 10.1385/mn:27:3:277
- Brosius Lutz, A., and Barres, B. A. (2014). Contrasting the glial response to axon injury in the central and peripheral nervous systems. *Dev. Cell* 28, 7–17. doi: 10.1016/j.devcel.2013.12.002

FUNDING

The work from the authors laboratory discussed in this article was supported by the Wellcome Trust (Programme Grant 074665 to KJ and RM), the Medical Research Council (Project Grant G0600967 to KJ and RM), and the FP7 Ideas: European Research Council Community (Grant HEALTH-F2-2008-201535 from FP7/2007-3013).

- Brosius Lutz, A., Chung, W. S., Sloan, S. A., Carson, G. A., Zhou, L., Lovelett, E., et al. (2017). Schwann cells use TAM receptor-mediated phagocytosis in addition to autophagy to clear myelin in a mouse model of nerve injury. *Proc. Natl. Acad. Sci. U S A* 114, E8072–E8080. doi: 10.1073/pnas.1710566114
- Brügger, V., Duman, M., Bochud, M., Mürger, E., Heller, M., Ruff, S., et al. (2017). Delaying histone deacetylase response to injury accelerates conversion into repair Schwann cells and nerve regeneration. *Nat. Commun.* 8:14272. doi: 10.1038/ncomms14272
- Brushart, T. M., Aspalter, M., Griffin, J. W., Redett, R., Hameed, H., Zhou, C., et al. (2013). Schwann cell phenotype is regulated by axon modality and central-peripheral location and persists *in vitro*. *Exp. Neurol.* 247, 272–281. doi: 10.1016/j.expneurol.2013.05.007
- Cafferty, W. B., Gardiner, N. J., Gavazzi, I., Powell, J., McMahon, S. B., Heath, J. K., et al. (2001). Leukemia inhibitory factor determines the growth status of injured adult sensory neurons. *J. Neurosci.* 21, 7161–7170. doi: 10.1523/jneurosci.21-18-07161.2001
- Carroll, S. L., Miller, M. L., Frohnert, P. W., Kim, S. S., and Corbett, J. A. (1997). Expression of neuregulins and their putative receptors, ErbB2 and ErbB3, is induced during Wallerian degeneration. *J. Neurosci.* 17, 1642–1659. doi: 10.1523/jneurosci.17-05-01642.1997
- Castelnovo, L. F., Bonalume, V., Melfi, S., Ballabio, M., Colleoni, D., and Magnaghi, V. (2017). Schwann cell development, maturation and regeneration: a focus on classic and emerging intracellular signaling pathways. *Neural Regen. Res.* 12, 1013–1023. doi: 10.4103/1673-5374.211172
- Cattin, A. L., Burden, J. J., Van Emmenis, L., Mackenzie, F. E., Hoving, J. J., Garcia Calavia, N., et al. (2015). Macrophage-induced blood vessels guide schwann cell-mediated regeneration of peripheral nerves. *Cell* 162, 1127–1139. doi: 10.1016/j.cell.2015.07.021
- Cattin, A. L., and Lloyd, A. C. (2016). The multicellular complexity of peripheral nerve regeneration. *Curr. Opin. Neurobiol.* 39, 38–46. doi: 10.1016/j.conb.2016.04.005
- Cervellini, I., Galino, J., Zhu, N., Allen, S., Birchmeier, C., and Bennett, D. L. (2018). Sustained MAPK/ERK activation in adult schwann cells impairs nerve repair. *J. Neurosci.* 38, 679–690. doi: 10.1523/jneurosci.2255-17.2017
- Chen, Z. L., Yu, W. M., and Strickland, S. (2007). Peripheral regeneration. *Annu. Rev. Neurosci.* 30, 209–233. doi: 10.1146/annurev.neuro.30.051606.094337
- Clements, M. P., Byrne, E., Camarillo Guerrero, L. F., Cattin, A. L., Zakka, L., Ashraf, A., et al. (2017). The wound microenvironment reprograms schwann cells to invasive mesenchymal-like cells to drive peripheral nerve regeneration. *Neuron* 96, 98.e7–114.e7. doi: 10.1016/j.neuron.2017.09.008
- De Felipe, C., and Hunt, S. P. (1994). The differential control of c-jun expression in regenerating sensory neurons and their associated glial cells. *J. Neurosci.* 14, 2911–2923. doi: 10.1523/jneurosci.14-05-02911.1994
- Doddrell, R. D., Dun, X. P., Moate, R. M., Jessen, K. R., Mirsky, R., and Parkinson, D. B. (2012). Regulation of Schwann cell differentiation and proliferation by the Pax-3 transcription factor. *Glia* 60, 1269–1278. doi: 10.1002/glia.22346
- Doron-Mandel, E., Fainzilber, M., and Terenzio, M. (2015). Growth control mechanisms in neuronal regeneration. *FEBS Lett.* 589, 1669–1677. doi: 10.1016/j.febslet.2015.04.046
- Eggers, R., Tannemaat, M. R., Ehlert, E. M., and Verhaagen, J. (2010). A spatio-temporal analysis of motoneuron survival, axonal regeneration and neurotrophic factor expression after lumbar ventral root avulsion and implantation. *Exp. Neurol.* 223, 207–220. doi: 10.1016/j.expneurol.2009.07.021
- Fabregat, I., Malfettone, A., and Soukupova, J. (2016). New insights into the crossroads between EMT and stemness in the context of cancer. *J. Clin. Med* 5:E37. doi: 10.3390/jcm5030037

- Faroni, A., Mobasser, S. A., Kingham, P. J., and Reid, A. J. (2015). Peripheral nerve regeneration: experimental strategies and future perspectives. *Adv. Drug Deliv. Rev.* 82–83, 160–167. doi: 10.1016/j.addr.2014.11.010
- Fazal, S. V., Gomez-Sanchez, J. A., Wagstaff, L. J., Musner, N., Otto, G., Janz, M., et al. (2017). Graded elevation of c-Jun in Schwann Cells *in vivo*: gene dosage determines effects on development, remyelination, tumorigenesis, and hypomyelination. *J. Neurosci.* 37, 12297–12313. doi: 10.1523/jneurosci.0986-17.2017
- Fischer, S., Weishaupt, A., Troppmair, J., and Martini, R. (2008). Increase of MCP-1 (CCL2) in myelin mutant Schwann cells is mediated by MEK-ERK signaling pathway. *Glia* 56, 836–843. doi: 10.1002/glia.20657
- Florito, F., Ferri, C., Scapin, C., Feltri, M. L., Wrabetz, L., and D'Antonio, M. (2018). Sustained expression of negative regulators of myelination protects Schwann cells from dysmyelination in a Charcot-Marie-Tooth 1B mouse model. *J. Neurosci.* 38, 4275–4287. doi: 10.1523/jneurosci.0201-18.2018
- Fontana, X., Hristova, M., Da Costa, C., Patodia, S., Thei, L., Makwana, M., et al. (2012). c-Jun in Schwann cells promotes axonal regeneration and motoneuron survival via paracrine signaling. *J. Cell Biol.* 198, 127–141. doi: 10.1083/jcb.201205025
- Forté, E., Chimenti, I., Rosa, P., Angelini, F., Pagano, F., Calogero, A., et al. (2017). EMT/MET at the crossroad of stemness, regeneration and oncogenesis: the ying-yang equilibrium recapitulated in cell spheroids. *Cancers* 9:E98. doi: 10.3390/cancers9080098
- Fricker, F. R., Antunes-Martins, A., Galino, J., Paramsothy, R., La Russa, F., Perkins, J., et al. (2013). Axonal neuregulin 1 is a rate limiting but not essential factor for nerve remyelination. *Brain* 136, 2279–2297. doi: 10.1093/brain/awt148
- Friede, R. L., and Bischhausen, R. (1980). The fine structure of stumps of transected nerve fibers in subserial sections. *J. Neurol. Sci.* 44, 181–203. doi: 10.1016/0022-510x(80)90126-4
- Fu, S. Y., and Gordon, T. (1997). The cellular and molecular basis of peripheral nerve regeneration. *Mol. Neurobiol.* 14, 67–116. doi: 10.1007/bf02740621
- Gambarotta, G., Fregnan, F., Gnani, S., and Perroteau, I. (2013). Neuregulin 1 role in Schwann cell regulation and potential applications to promote peripheral nerve regeneration. *Int. Rev. Neurobiol.* 108, 223–256. doi: 10.1016/b978-0-12-410499-0.00009-5
- Glenn, T. D., and Talbot, W. S. (2013). Signals regulating myelination in peripheral nerves and the Schwann cell response to injury. *Curr. Opin. Neurobiol.* 23, 1041–1048. doi: 10.1016/j.conb.2013.06.010
- Gomez-Sanchez, J. A., Carty, L., Iruarizaga-Lejarreta, M., Palomo-Irigoyen, M., Varela-Rey, M., Griffith, M., et al. (2015). Schwann cell autophagy, myelinophagy, initiates myelin clearance from injured nerves. *J. Cell Biol.* 210, 153–168. doi: 10.1083/jcb.201503019
- Gomez-Sanchez, J. A., Pilch, K. S., van der Lans, M., Fazal, S. V., Benito, C., Wagstaff, L. J., et al. (2017). After nerve injury, lineage tracing shows that myelin and remak schwann cells elongate extensively and branch to form repair schwann cells, which shorten radically on remyelination. *J. Neurosci.* 37, 9086–9099. doi: 10.1523/JNEUROSCI.1453-17.2017
- Gordon, T., Tyreman, N., and Raji, M. A. (2011). The basis for diminished functional recovery after delayed peripheral nerve repair. *J. Neurosci.* 31, 5325–5334. doi: 10.1523/jneurosci.6156-10.2011
- Grothe, C., Haastert, K., and Jungnickel, J. (2006). Physiological function and putative therapeutic impact of the FGF-2 system in peripheral nerve regeneration—lessons from *in vivo* studies in mice and rats. *Brain Res. Rev.* 51, 293–299. doi: 10.1016/j.brainresrev.2005.12.001
- Hall, S. M., and Gregson, N. A. (1977). The effects of mitomycin C on the process of regeneration in the mammalian peripheral nervous system. *Neuropathol. Appl. Neurobiol.* 3, 65–78. doi: 10.1111/j.1365-2990.1977.tb00570.x
- Hall, S. (2005). The response to injury in the peripheral nervous system. *J. Bone Joint Surg. Br.* 87, 1309–1319. doi: 10.1302/0301-620X.87B10.16700
- Han, S. B., Kim, H., Lee, H., Grove, M., Smith, G. M., and Son, Y. J. (2017). Postinjury induction of activated ErbB2 selectively hyperactivates denervated schwann cells and promotes robust dorsal root axon regeneration. *J. Neurosci.* 37, 10955–10970. doi: 10.1523/jneurosci.0903-17.2017
- Harrisingh, M. C., Perez-Nadales, E., Parkinson, D. B., Malcolm, D. S., Mudge, A. W., and Lloyd, A. C. (2004). The Ras/Raf/ERK signalling pathway drives Schwann cell dedifferentiation. *EMBO J.* 23, 3061–3071. doi: 10.1038/sj.emboj.7600309
- Hirata, K., and Kawabuchi, M. (2002). Myelin phagocytosis by macrophages and nonmacrophages during Wallerian degeneration. *Microsc. Res. Tech.* 57, 541–547. doi: 10.1002/jemt.10108
- Hirota, H., Kiyama, H., Kishimoto, T., and Taga, T. (1996). Accelerated nerve regeneration in mice by upregulated expression of interleukin (IL) 6 and IL-6 receptor after trauma. *J. Exp. Med.* 183, 2627–2634. doi: 10.1084/jem.183.6.2627
- Höke, A. (2006a). Mechanisms of disease: what factors limit the success of peripheral nerve regeneration in humans? *Nat. Clin. Pract. Neurol.* 2, 448–454. doi: 10.1038/ncpneuro0262
- Höke, A. (2006b). Neuroprotection in the peripheral nervous system: rationale for more effective therapies. *Arch. Neurol.* 63, 1681–1685. doi: 10.1001/archneur.63.12.1681
- Höke, A., and Brushart, T. (2010). Challenges and opportunities for regeneration in the peripheral nervous system. *Exp. Neurol.* 223, 1–4. doi: 10.1016/j.expneurol.2009.12.001
- Hung, H. A., Sun, G., Keles, S., and Svaren, J. (2015). Dynamic regulation of Schwann cell enhancers after peripheral nerve injury. *J. Biol. Chem.* 290, 6937–6950. doi: 10.1074/jbc.M114.622878
- Jacob, C. (2017). Chromatin-remodeling enzymes in control of Schwann cell development, maintenance and plasticity. *Curr. Opin. Neurobiol.* 47, 24–30. doi: 10.1016/j.conb.2017.08.007
- Jang, S. Y., Shin, Y. K., Park, S. Y., Park, J. Y., Lee, H. J., Yoo, Y. H., et al. (2016). Autophagic myelin destruction by Schwann cells during Wallerian degeneration and segmental demyelination. *Glia* 64, 730–742. doi: 10.1002/glia.22957
- Jessen, K. R., and Arthur-Farraj, P. (2019). Repair Schwann cell update: adaptive reprogramming, EMT and stemness in regenerating nerves. *Glia* doi: 10.1002/glia.23532 [Epub ahead of print].
- Jessen, K. R., and Mirsky, R. (2005). The origin and development of glial cells in peripheral nerves. *Nat. Rev. Neurosci.* 6, 671–682. doi: 10.1038/nrn1746
- Jessen, K. R., and Mirsky, R. (2008). Negative regulation of myelination: relevance for development, injury, and demyelinating disease. *Glia* 56, 1552–1565. doi: 10.1002/glia.20761
- Jessen, K. R., Mirsky, R., and Arthur-Farraj, P. (2015a). The role of cell plasticity in tissue repair: adaptive cellular reprogramming. *Dev. Cell* 34, 613–620. doi: 10.1016/j.devcel.2015.09.005
- Jessen, K. R., Mirsky, R., and Lloyd, A. C. (2015b). Schwann cells: development and role in nerve repair. *Cold Spring Harb. Perspect. Biol.* 7:a020487. doi: 10.1101/cshperspect.a020487
- Jessen, K. R., and Mirsky, R. (2016). The repair Schwann cell and its function in regenerating nerves. *J. Physiol.* 594, 3521–3531. doi: 10.1113/jp270874
- Jonsson, S., Wiberg, R., McGrath, A. M., Novikov, L. N., Wiberg, M., Novikova, L. N., et al. (2013). Effect of delayed peripheral nerve repair on nerve regeneration, Schwann cell function and target muscle recovery. *PLoS One* 8:e56484. doi: 10.1371/journal.pone.0056484
- Jung, J., Cai, W., Lee, H. K., Pellegatta, M., Shin, Y. K., Jang, S. Y., et al. (2011). Actin polymerization is essential for myelin sheath fragmentation during Wallerian degeneration. *J. Neurosci.* 31, 2009–2015. doi: 10.1523/jneurosci.4537-10.2011
- Kang, H., and Lichtman, J. W. (2013). Motor axon regeneration and muscle reinnervation in young adult and aged animals. *J. Neurosci.* 33, 19480–19491. doi: 10.1523/JNEUROSCI.4067-13.2013
- Kastriti, M. E., and Adameyko, I. (2017). Specification, plasticity and evolutionary origin of peripheral glial cells. *Curr. Opin. Neurobiol.* 47, 196–202. doi: 10.1016/j.conb.2017.11.004
- Kim, H. A., Pomeroy, S. L., Whoriskey, W., Pawlitzky, I., Benowitz, L. I., Sicinski, P., et al. (2000). A developmentally regulated switch directs regenerative growth of Schwann cells through cyclin D1. *Neuron* 26, 405–416. doi: 10.1016/s0896-6273(00)81173-3
- Kioussi, C., Gross, M. K., and Gruss, P. (1995). Pax3: a paired domain gene as a regulator in PNS myelination. *Neuron* 15, 553–562. doi: 10.1016/0896-6273(95)90144-2
- Kou, Y., Zhang, P., Yin, X., Wei, S., Wang, Y., Zhang, H., et al. (2011). Influence of different distal nerve degeneration period on peripheral nerve collateral sprouts regeneration. *Artif. Cells Blood Substit. Immobil. Biotechnol.* 39, 223–227. doi: 10.3109/10731199.2010.533127
- Le, N., Nagarajan, R., Wang, J. Y., Araki, T., Schmidt, R. E., and Milbrand, J. (2005). Analysis of congenital hypomyelinating Egr2Lo/Lo nerves identifies Sox2 as an

- inhibitor of schwann cell differentiation and myelination. *Proc. Natl. Acad. Sci. U S A* 102, 2596–2601. doi: 10.1073/pnas.0407836102
- Li, H., Terenghi, G., and Hall, S. M. (1997). Effects of delayed re-innervation on the expression of c-erbB receptors by chronically denervated rat Schwann cells *in vivo*. *Glia* 20, 333–347. doi: 10.1002/(sici)1098-1136(199708)20:4<333::aid-glia6>3.0.co;2-6
- Li, H., Wigley, C., and Hall, S. M. (1998). Chronically denervated rat Schwann cells respond to GGF *in vitro*. *Glia* 24, 290–303. doi: 10.1002/(sici)1098-1136(199811)24:3<290::aid-glia3>3.0.co;2-6
- Liao, T. T., and Yang, M. H. (2017). Revisiting epithelial-mesenchymal transition in cancer metastasis: the connection between epithelial plasticity and stemness. *Mol. Oncol.* 11, 792–804. doi: 10.1002/1878-0261.12096
- Lin, H.-P., Oksuz, I., Hurley, E., Wrabetz, L., and Awatramani, R. (2015). Microprocessor complex subunit digeorge Syndrome critical region gene 8 (Dgcr8) is required for schwann cell myelination and myelin maintenance. *J. Biol. Chem.* 290, 24294–24307. doi: 10.1074/jbc.m115.636407
- Lu, Q. R., Yuk, D., Alberta, J. A., Zhu, Z., Pawlitzky, I., Chan, J., et al. (2000). Sonic hedgehog-regulated oligodendrocyte lineage genes encoding bHLH proteins in the mammalian central nervous system. *Neuron* 25, 317–332. doi: 10.1016/s0896-6273(00)80897-1
- Ma, K. H., Hung, H. A., and Svaren, J. (2016). Epigenomic regulation of schwann cell reprogramming in peripheral nerve injury. *J. Neurosci.* 36, 9135–9147. doi: 10.1523/JNEUROSCI.1370-16.2016
- Ma, K. H., and Svaren, J. (2018). Epigenetic control of schwann cells. *Neuroscientist* 24, 627–638. doi: 10.1177/1073858417751112
- Martinez, J. A., Kobayashi, M., Krishnan, A., Webber, C., Christie, K., Guo, G., et al. (2015). Intrinsic facilitation of adult peripheral nerve regeneration by the Sonic hedgehog morphogen. *Exp. Neurol.* 271, 493–505. doi: 10.1016/j.expneurol.2015.07.018
- Martini, R., Fischer, S., López-Vales, R., and David, S. (2008). Interactions between Schwann cells and macrophages in injury and inherited demyelinating disease. *Glia* 56, 1566–1577. doi: 10.1002/glia.20766
- Meller, K. (1987). Early structural changes in the axoplasmic cytoskeleton after axotomy studied by cryofixation. *Cell Tiss. Res.* 250, 663–672. doi: 10.1007/bf00218961
- Mindos, T., Dun, X. P., North, K., Doddrell, R. D., Schulz, A., Edwards, P., et al. (2017). Merlin controls the repair capacity of Schwann cells after injury by regulating Hippo/YAP activity. *J. Cell Biol.* 216, 495–510. doi: 10.1083/jcb.201606052
- Mogha, A., Harty, B. L., Carlin, D., Joseph, J., Sanchez, N. E., Suter, U., et al. (2016). Gpr126/Adgrg6 Has schwann cell autonomous and nonautonomous functions in peripheral nerve injury and repair. *J. Neurosci.* 36, 12351–12367. doi: 10.1523/JNEUROSCI.3854-15.2016
- Monk, K. R., Feltri, M. L., and Taveggia, C. (2015). New insights on Schwann cell development. *Glia* 63, 1376–1393. doi: 10.1002/glia.22852
- Morgan, L., Jessen, K., and Mirsky, R. (1994). Negative regulation of the P0 gene in Schwann cells: suppression of P0 mRNA and protein induction in cultured Schwann cells by FGF2 and TGF β 1, TGF β 2 and TGF β 3. *Development* 120, 1399–1409.
- Morris, J. H., Hudson, A. R., and Weddell, G. (1972). A study of degeneration and regeneration in the divided rat sciatic nerve based on electron microscopy. II. The development of the “regenerating unit”. *Z. Zellforsch. Mikrosk. Anat.* 124, 103–130. doi: 10.1007/bf00981943
- Napoli, I., Noon, L. A., Ribeiro, S., Kerai, A. P., Parrinello, S., Rosenberg, L. H., et al. (2012). A central role for the ERK-signaling pathway in controlling Schwann cell plasticity and peripheral nerve regeneration *in vivo*. *Neuron* 73, 729–742. doi: 10.1016/j.neuron.2011.11.031
- Newbern, J. M., Li, X., Shoemaker, S. E., Zhou, J., Zhong, J., Wu, Y., et al. (2011). Specific functions for ERK/MAPK signaling during PNS development. *Neuron* 69, 91–105. doi: 10.1016/j.neuron.2010.12.003
- Niemi, J. P., DeFrancesco-Lisowitz, A., Roldán-Hernández, L., Lindborg, J. A., Mandell, D., and Zigmond, R. E. (2013). A critical role for macrophages near axotomized neuronal cell bodies in stimulating nerve regeneration. *J. Neurosci.* 33, 16236–16248. doi: 10.1523/JNEUROSCI.3319-12.2013
- Nieto, M. A., Huang, R. Y., Jackson, R. A., and Thiery, J. P. (2016). EMT: 2016. *Cell* 166, 21–45. doi: 10.1016/j.cell.2016.06.028
- Normén, C., Figlia, G., Pfister, P., Pereira, J. A., Bachofner, S., and Suter, U. (2018). mTORC1 is transiently reactivated in injured nerves to promote c-Jun elevation and Schwann cell dedifferentiation. *J. Neurosci.* 380, 4811–4828. doi: 10.1523/JNEUROSCI.3619-17.2018
- Painter, M. W. (2017). Aging Schwann cells: mechanisms, implications, future directions. *Curr. Opin. Neurobiol.* 47, 203–208. doi: 10.1016/j.conb.2017.10.022
- Painter, M. W., Brosius Lutz, A., Cheng, Y. C., Latremoliere, A., Duong, K., Miller, C. M., et al. (2014). Diminished Schwann cell repair responses underlie age-associated impaired axonal regeneration. *Neuron* 83, 331–343. doi: 10.1016/j.neuron.2014.06.016
- Parkinson, D. B., Bhaskaran, A., Arthur-Farraj, P., Noon, L. A., Woodhoo, A., Lloyd, A. C., et al. (2008). c-Jun is a negative regulator of myelination. *J. Cell Biol.* 181, 625–637. doi: 10.1083/jcb.200803013
- Parkinson, D. B., Bhaskaran, A., Droggiti, A., Dickinson, S., D’Antonio, M., Mirsky, R., et al. (2004). Krox-20 inhibits Jun-NH2-terminal kinase/c-Jun to control Schwann cell proliferation and death. *J. Cell Biol.* 164, 385–394. doi: 10.1083/jcb.200307132
- Parrinello, S., Napoli, I., Ribeiro, S., Wingfield Digby, P., Fedorova, M., Parkinson, D. B., et al. (2010). EphB signaling directs peripheral nerve regeneration through Sox2-dependent Schwann cell sorting. *Cell* 143, 145–155. doi: 10.1016/j.cell.2010.08.039
- Patel, N. P., Lyon, K. A., and Huang, J. H. (2018). An update-tissue engineered nerve grafts for the repair of peripheral nerve injuries. *Neural Regen. Res.* 13, 764–774. doi: 10.4103/1673-5374.232458
- Perry, V. H., Tsao, J. W., Fearn, S., and Brown, M. C. (1995). Radiation-induced reductions in macrophage recruitment have only slight effects on myelin degeneration in sectioned peripheral nerves of mice. *Eur. J. Neurosci.* 7, 271–280. doi: 10.1111/j.1460-9568.1995.tb01063.x
- Piirsoo, M., Kaljas, A., Tamm, K., and Timmus, T. (2010). Expression of NGF and GDNF family members and their receptors during peripheral nerve development and differentiation of Schwann cells *in vitro*. *Neurosci. Lett.* 469, 135–140. doi: 10.1016/j.neulet.2009.11.060
- Quintes, S., and Brinkmann, B. G. (2017). Transcriptional inhibition in Schwann cell development and nerve regeneration. *Neural Regen. Res.* 12, 1241–1246. doi: 10.4103/1673-5374.213537
- Quintes, S., Brinkmann, B. G., Ebert, M., Fröb, F., Kungl, T., Arlt, F. A., et al. (2016). Zeb2 is essential for Schwann cell differentiation, myelination and nerve repair. *Nat. Neurosci.* 19, 1050–1059. doi: 10.1038/nn.4321
- Roberts, S. L., Dun, X. P., Doddrell, R. D. S., Mindos, T., Drake, L. K., Onaitis, M. W., et al. (2017). Sox2 expression in Schwann cells inhibits myelination *in vivo* and induces influx of macrophages to the nerve. *Development* 144, 3114–3125. doi: 10.1242/dev.150656
- Ronchi, G., Gambarotta, G., Di Scipio, F., Salamone, P., Sprio, A. E., Cavallo, F., et al. (2013). ErbB2 receptor over-expression improves post-traumatic peripheral nerve regeneration in adult mice. *PLoS One* 8:e56282. doi: 10.1371/journal.pone.0056282
- Ronchi, G., Haastert-Talini, K., Fornasari, B. E., Perroteau, I., Geuna, S., and Gambarotta, G. (2016). The Neuregulin1/ErbB system is selectively regulated during peripheral nerve degeneration and regeneration. *Eur. J. Neurosci.* 43, 351–364. doi: 10.1111/ejn.12974
- Rönkkö, H., Göransson, H., Siironen, P., Taskinen, H. S., Vuorinen, V., and Rönkkö, M. (2011). The capacity of the distal stump of peripheral nerve to receive growing axons after two and six months denervation. *Scand. J. Surg.* 100, 223–229. doi: 10.1177/145749691110000315
- Rotshenker, S. (2011). Wallerian degeneration: the innate-immune response to traumatic nerve injury. *J. Neuroinflammation* 8:109. doi: 10.1186/1742-2094-8-109
- Salonen, V., Aho, H., Röttä, M., and Pelttonen, J. (1988). Quantitation of Schwann cells and endoneurial fibroblast-like cells after experimental nerve trauma. *Acta Neuropathol.* 75, 331–336. doi: 10.1007/bf00687785
- Scheib, J., and Höke, A. (2013). Advances in peripheral nerve regeneration. *Nat. Rev. Neurol.* 9, 668–676. doi: 10.1038/nrneurol.2013.227
- Sheehan, M. E., McShane, E., Cheret, C., Walcher, J., Müller, T., Wulf-Goldenberg, A., et al. (2014). Activation of MAPK overrides the termination of myelin growth and replaces Nrg1/ErbB3 signals during Schwann cell development and myelination. *Genes Dev.* 28, 290–303. doi: 10.1101/gad.230045.113
- Sheu, J. Y., Kulhanek, D. J., and Eckenstein, F. P. (2000). Differential patterns of ERK and STAT3 phosphorylation after sciatic nerve transection in the rat. *Exp. Neurol.* 166, 392–402. doi: 10.1006/exnr.2000.7508

- Shy, M. E., Shi, Y., Wrabetz, L., Kamholz, J., and Scherer, S. S. (1996). Axon-Schwann cell interactions regulate the expression of c-jun in Schwann cells. *J. Neurosci. Res.* 43, 511–525. doi: 10.1002/(sici)1097-4547(19960301)43:5<511::aid-jnr1>3.0.co;2-l
- Siironen, J., Collan, Y., and Röttä, M. (1994). Axonal reinnervation does not influence Schwann cell proliferation after rat sciatic nerve transection. *Brain Res.* 654, 303–311. doi: 10.1016/0006-8993(94)90492-8
- Stassart, R. M., Fledrich, R., Velanac, V., Brinkmann, B. G., Schwab, M. H., Meijer, D., et al. (2013). A role for Schwann cell-derived neuregulin-1 in remyelination. *Nat. Neurosci.* 16, 48–54. doi: 10.1038/nn.3281
- Stewart, H. J., Rougon, G., Dong, Z., Dean, C., Jessen, K. R., and Mirsky, R. (1995). TGF- β s upregulate NCAM and L1 expression in cultured Schwann cells, suppress cyclic AMP-induced expression of O4 and galactocerebroside, and are widely expressed in cells of the Schwann cell lineage *in vivo*. *Glia* 15, 419–436. doi: 10.1002/glia.440150406
- Sulaiman, O. A., and Gordon, T. (2002). Transforming growth factor- β and forskolin attenuate the adverse effects of long-term Schwann cell denervation on peripheral nerve regeneration *in vivo*. *Glia* 37, 206–218. doi: 10.1002/glia.10022
- Sulaiman, O. A., and Gordon, T. (2009). Role of chronic Schwann cell denervation in poor functional recovery after nerve injuries and experimental strategies to combat it. *Neurosurgery* 65, A105–A114. doi: 10.1227/01.neu.0000358537.30354.63
- Sulaiman, O. A., and Gordon, T. (2000). Effects of short- and long-term Schwann cell denervation on peripheral nerve regeneration, myelination, and size. *Glia* 32, 234–246. doi: 10.1002/1098-1136(200012)32:3<234::aid-glia40>3.0.co;2-3
- Sulaiman, W., and Gordon, T. (2013). Neurobiology of peripheral nerve injury, regeneration, and functional recovery: from bench top research to bedside application. *Ochsner J.* 13, 100–108.
- Suzuki, K., Lovera, M., Schmachtenberg, O., and Couve, E. (2015). Axonal degeneration in dental pulp precedes human primary teeth exfoliation. *J. Dent. Res.* 94, 1446–1453. doi: 10.1177/0022034515593055
- Verdú, E., Ceballos, D., Vilches, J. J., and Navarro, X. J. (2000). Influence of aging on peripheral nerve function and regeneration. *J. Peripher. Nerv. Syst.* 5, 191–208. doi: 10.1111/j.1529-8027.2000.00026.x
- Wagstaff, L., Gomez-Sanchez, J., Mirsky, R., and Jessen, K. R. (2017). The relationship between Schwann cell c-Jun and regeneration failures due to aging and long-term injury. *Glia* 65:E532.
- Witzel, C., Rohde, C., and Brushart, T. M. (2005). Pathway sampling by regenerating peripheral axons. *J. Comp. Neurol.* 485, 183–190. doi: 10.1002/cne.20436
- Wood, M. D., and Mackinnon, S. E. (2015). Pathways regulating modality-specific axonal regeneration in peripheral nerve. *Exp. Neurol.* 265, 171–175. doi: 10.1016/j.expneurol.2015.02.001
- Woodhoo, A., Alonso, M. B., Droggiti, A., Turmaine, M., D'Antonio, M., Parkinson, D. B., et al. (2009). Notch controls embryonic Schwann cell differentiation, postnatal myelination and adult plasticity. *Nat. Neurosci.* 12, 839–847. doi: 10.1038/nn.2323
- Wu, L. M., Wang, J., Conidi, A., Zhao, C., Wang, H., Ford, Z., et al. (2016). Zeb2 recruits HDAC-NuRD to inhibit Notch and controls Schwann cell differentiation and remyelination. *Nat. Neurosci.* 19, 1060–1072. doi: 10.1038/nn.4322
- Yang, D. P., Zhang, D. P., Mak, K. S., Bonder, D. E., Pomeroy, S. L., and Kim, H. A. (2008). Schwann cell proliferation during Wallerian degeneration is not necessary for regeneration and remyelination of the peripheral nerves: axon-dependent removal of newly generated Schwann cells by apoptosis. *Mol. Cell. Neurosci.* 38, 80–88. doi: 10.1016/j.mcn.2008.01.017
- Zhou, Q., Wang, S., and Anderson, D. J. (2000). Identification of a novel family of oligodendrocyte lineage-specific basic helix-loop-helix transcription factors. *Neuron* 25, 331–343. doi: 10.1016/s0896-6273(00)80898-3

Conflict of Interest Statement: The authors declare that the research was conducted in the absence of any commercial or financial relationships that could be construed as a potential conflict of interest.

Copyright © 2019 Jessen and Mirsky. This is an open-access article distributed under the terms of the Creative Commons Attribution License (CC BY). The use, distribution or reproduction in other forums is permitted, provided the original author(s) and the copyright owner(s) are credited and that the original publication in this journal is cited, in accordance with accepted academic practice. No use, distribution or reproduction is permitted which does not comply with these terms.



Cholesterol Depletion Regulates Axonal Growth and Enhances Central and Peripheral Nerve Regeneration

Cristina Roselló-Busquets^{1,2†}, Natalia de la Oliva^{2,3†}, Ramón Martínez-Mármol^{1,2†‡}, Marc Hernaiz-Llorens^{1,2}, Marta Pascual^{1,2,4}, Ashraf Muhaisen^{1,2,4}, Xavier Navarro^{2,3}, Jaume del Valle^{2,3*} and Eduardo Soriano^{1,2,4,5*}

¹ Department of Cell Biology, Physiology and Immunology, Faculty of Biology, Institute of Neurosciences, University of Barcelona, Barcelona, Spain, ² Centro de Investigación Biomédica en Red sobre Enfermedades Neurodegenerativas (CIBERNED), Instituto de Salud Carlos III, Madrid, Spain, ³ Department of Cell Biology, Physiology and Immunology, Institute of Neurosciences, Universitat Autònoma de Barcelona, Bellaterra, Spain, ⁴ Vall d'Hebron Research Institute (VHIR), Barcelona, Spain, ⁵ ICREA Academia, Barcelona, Spain

OPEN ACCESS

Edited by:

Stefania Raimondo,
University of Turin, Italy

Reviewed by:

Mehmet Emin Onger,
Ondokuz Mayıs University, Turkey
Petr Dubový,
Masaryk University, Czechia

*Correspondence:

Jaume del Valle
jaume.delvalle@gmail.com
Eduardo Soriano
esoriano@ub.edu

[†] These authors have contributed
equally to this work

‡Present address:

Ramón Martínez-Mármol,
Clem Jones Centre for Ageing
Dementia Research, Queensland
Brain Institute, The University
of Queensland, Brisbane,
QLD, Australia

Received: 05 October 2018

Accepted: 25 January 2019

Published: 12 February 2019

Citation:

Roselló-Busquets C,
de la Oliva N, Martínez-Mármol R,
Hernaiz-Llorens M, Pascual M,
Muhaisen A, Navarro X, del Valle J
and Soriano E (2019) Cholesterol
Depletion Regulates Axonal Growth
and Enhances Central and Peripheral
Nerve Regeneration.
Front. Cell. Neurosci. 13:40.
doi: 10.3389/fncel.2019.00040

Axonal growth during normal development and axonal regeneration rely on the action of many receptor signaling systems and complexes, most of them located in specialized raft membrane microdomains with a precise lipid composition. Cholesterol is a component of membrane rafts and the integrity of these structures depends on the concentrations present of this compound. Here we explored the effect of cholesterol depletion in both developing neurons and regenerating axons. First, we show that cholesterol depletion *in vitro* in developing neurons from the central and peripheral nervous systems increases the size of growth cones, the density of filopodium-like structures and the number of neurite branching points. Next, we demonstrate that cholesterol depletion enhances axonal regeneration after axotomy *in vitro* both in a microfluidic system using dissociated hippocampal neurons and in a slice-coculture organotypic model of axotomy and regeneration. Finally, using axotomy experiments in the sciatic nerve, we also show that cholesterol depletion favors axonal regeneration *in vivo*. Importantly, the enhanced regeneration observed in peripheral axons also correlated with earlier electrophysiological responses, thereby indicating functional recovery following the regeneration. Taken together, our results suggest that cholesterol depletion *per se* is able to promote axonal growth in developing axons and to increase axonal regeneration *in vitro* and *in vivo* both in the central and peripheral nervous systems.

Keywords: regeneration, cholesterol, lipid rafts, axon growth, growth cone, filopodia

INTRODUCTION

Axonal guidance during the development of the nervous system is thought to be highly regulated through interactions of transmembrane receptors with attractive, repulsive, and trophic cues. Similar mechanisms regulate axonal regeneration after injury. The transected axon undergoes morphological changes to form the growth cone, a highly dynamic structure that senses the environment and leads the regenerative growth (Allodi et al., 2012). Membrane receptors localized in the growth cone have an important role in axonal signaling (Guirland et al., 2004; Kamiguchi, 2006). The regenerative shift of axotomized neurons is promoted by injury-induced signals, which stimulate the transcription of various trophic factors,

adhesion molecules, growth-associated proteins and structural components needed for axonal regrowth and cell survival (Rishal and Fainzilber, 2014).

Many intrinsic and extrinsic signals can promote or inhibit axonal regeneration. Due to the importance of these signals during axonal degeneration and regeneration after peripheral nerve injury, microdomains in the membrane that cluster a range of proteins and molecules related to cellular signaling may play a key role in the regulation of these pathways. In particular, lipid rafts have been described as cholesterol-enriched cell membrane microdomains that compartmentalize lipids and protein to form signaling platforms (Golub et al., 2004).

Cholesterol is a major component of the nervous system, being essential for normal brain development. The brain is the most cholesterol-rich organ, containing about 20% of the body's total cholesterol (Bjorkhem and Meaney, 2004). Under normal physiological situations and because plasma lipoproteins do not cross the intact blood-brain barrier, nearly all cholesterol in the brain is synthesized *in situ* (Dietschy and Turley, 2001). Brain cholesterol is an important structural component of cellular membranes and myelin. It is also required for the synthesis of steroid hormones and for the organization of lipid rafts, which are involved in many aspects of brain function, such as growth factor signaling, synapse and dendritic formation (Goritz et al., 2005), and axon elongation and guidance (de Chaves et al., 1997).

Here we studied the effects of altered membrane integrity by reducing the cholesterol content in the axons of three neuronal systems, namely hippocampal and cerebellar external granular layer (EGL) cells as a Central Nervous System (CNS) example, and the dorsal root ganglion (DRG) neurons as a Peripheral Nervous System (PNS) example. We show that depletion of cholesterol leads to increased sizes of growth cones, filopodial extensions and neurite length. Moreover, we also demonstrate that cholesterol membrane and raft disruption increase the regenerative capacity of axons after axotomy both *in vitro* and *in vivo* and enhance muscle and sensory re-innervation of distal targets. On the basis of our findings, we propose that acute reduction of neuronal cholesterol emerges as a potential therapeutic strategy to improve regenerative outcomes after peripheral nerve lesion.

MATERIALS AND METHODS

Reagents and Antibodies

The following antibodies were used: anti-GFP (A11122, Invitrogen); anti-III β -tubulin (MMS-435P, Covance); anti-growth associated protein 43 (GAP43) (AB5220, Millipore); anti-myelin basic protein antibody (MBP) (ab7349, Abcam); anti-neurofilament H (NF-H) (AB5539, Millipore); Donkey anti-Mouse IgG (H+L) Highly Cross-Adsorbed Secondary Antibody Alexa Fluor 488 (A-21202, Thermo Fisher); Donkey anti-Rabbit IgG (H+L) Highly Cross-Adsorbed Secondary Antibody Alexa Fluor 488 (A-21206, Thermo Fisher); Goat anti-Chicken IgY (H+L) Alexa Fluor 488 (A-11039, Thermo Fisher), Biotinylated Horse anti-rabbit IgG (BA-1000, Vector); Biotinylated Goat anti-rat IgG (BA-9400, Vector), Streptavidin-Biotinylated HRP

Complex (RPN1051, GE Healthcare); and Streptavidin-Alexa Fluor 594 (S32356, Thermo Fisher).

The following drugs and reagents were used: poly-D-Lysine (P7280, Sigma); laminin (L2020, Sigma); Nystatin dihydrate (N4014, Sigma); Cholesterol Oxidase *Streptomyces* sp. (ChOx) (228250, Calbiochem); Methyl- β -cyclodextrin (M β CD) (C4555, Sigma); DMSO (D5879, Sigma); phalloidin – TRITC (P1951, Sigma); biocytin (B4261, Sigma); Cholera Toxin Subunit B (Recombinant) Alexa Fluor 594 (CTxB-594) (C34777, Life BioSciences).

Primary Cultures

Hippocampus

Primary cultures of mouse hippocampi were prepared from E16–E17. Pregnant CD1 mice were sacrificed by cervical dislocation, and the fetuses were collected in a PBS-glucose 0.3% solution and then decapitated. Hippocampi were isolated and trypsinized for 6 min at 37°C. Trypsin was then neutralized with FBS and incubated with DNase for 10 min at 37°C. Neurons were then centrifuged at 800 rpm for 5 min, resuspended and plated in pre-coated culture glasses with poly-D-lysine in medium containing Neurobasal (w/o L-glutamine, w/Phenol Red; GIBCO, 21103-049), 1% penicillin/streptomycin (GIBCO, 15140-122), 1% glutamine (GIBCO, 25030-024) and 2% B27 (GIBCO, 17504-044).

Cerebellum

Primary cultures of cerebellums were prepared from P4–P5 CD1 mice sacrificed by decapitation. Cerebellums were isolated, mechanically disaggregated and trypsinized as previously described. After centrifugation, neurons were resuspended in 2 mL of DMEM, and EGL were isolated by centrifugation in a percol gradient. After a wash centrifugation, EGL were plated in pre-coated culture glasses with poly-D-lysine in medium containing DMEM (GIBCO, 41966-029), 1% penicillin/streptomycin (GIBCO, 15140-122), 1% glutamine (GIBCO, 25030-024), 4.5% D-(+)-Glucose (Sigma, G-8769), 5% NHS (GIBCO, 26050-088), and 10% FBS (GIBCO, 16000-044) for 24 h, and then NHS and FBS were replaced by 2% B27 (GIBCO, 17504-044) and 1% N2 (GIBCO, 17502-048).

Dorsal Root Ganglion (DRG)

Primary cultures of DRG neurons were prepared from E13–E14 mice. Pregnant CD1 mice were sacrificed by cervical dislocation, and the fetuses were collected and decapitated. DRG neurons were isolated and trypsinized as previously described. After centrifugation, neurons were resuspended and plated in pre-coated culture glasses with poly-D-lysine and laminin in medium containing DMEM (GIBCO, 41966-029), 1% penicillin/streptomycin (GIBCO, 15140-122), 1% glutamine (GIBCO, 25030-024), 0.06% D-(+)-Glucose (Sigma, G-8769), 0.0045% NaHCO₃ (GIBCO, 25080-060), 2% B27 (GIBCO, 17504-044) and 5 μ g/ml NGF.

Organotypic entorhino-hippocampal slice cultures were obtained from P0 actin-GFP and WT mice sacrificed by decapitation. Horizontal sections 325 μ m thick containing both the entorhinal cortex (EC) and the hippocampus were

obtained by cutting tissue pieces in a chopper (McIlwain Tissue Chopper, Standard Table, 220V, Prod 10180-220). Slices were laid on a porous Millicell CM plate culture insert (Millipore, PICM03050) and incubated using the interface culture technique. The medium comprised 35.5% Neurobasal, 25% MEM powder, 25% NHS (GIBCO, 26050-088), 12.5% HBSS (w/Mg, w/Phenol Red, GIBCO, 24020-083), 0.5% D-(+)-glucose (Sigma, G-8769), 1% glutamine (GIBCO, 25030-024), 1% penicillin/streptomycin (GIBCO, 15140-122), 1.1% sodium pyruvate (Sigma, P2256-5G), 0.04% NaHCO₃ (GIBCO, 25080-060), 2% B27 (GIBCO, 17504-044) and 1% N2 (GIBCO, 17502-048). The medium was changed every 2 days. After 21 days *in vitro* (DIV), axotomy was performed between the EC and the hippocampus with a needle, and WT hippocampi were put with EC GFP. The cultures were treated for 10 days with Nystatin or control medium and fixed with 4% paraformaldehyde (PFA) for 1h. Cultures were cut into 60 μ m slices with a vibratome (Leica VT 1000 S) and cryopreserved at -20°C until immunohistochemistry was performed.

Drug Treatments *in vitro*

Growth Cone and Filopodium Experiments

Hippocampal and EGL primary cultures were treated after 3 DIV and DRG after 1 DIV with 2.5 $\mu\text{g/mL}$ Nystatin for 10 min, 0.5 mM M β CD for 10 min or 2U ChOx for 2 h. They were then incubated for an additional 30 min in culture media (Neurobasal or DMEM) and then fixed in 4% PFA.

Axon Extension and Branching Experiments in DRG Neurons

After 2 h in culture, 2.5 $\mu\text{g/mL}$ Nystatin and 2U ChOx were added to the media for 24 h and neurons were then fixed. After 22 h *in vitro*, and therefore 2 h before neurons were fixed, 0.5 mM M β CD was added to the media.

Axotomy Experiments

Axotomy in microfluidic chambers (AX50010TC, Millipore) was performed with a pipette connected to a vacuum pump. Complete axotomy was verified in the inverted microscope. Immediately after axotomy, 2.5 $\mu\text{g/mL}$ Nystatin was added and maintained in the culture for 3 days. In organotypic cultures, 5 $\mu\text{g/mL}$ Nystatin was added to the media just after axotomy and maintained for 10 days, changing the media every 2 days.

Animals and Surgical Procedures

To study the effect of cholesterol depletion on healthy mice, 10 OF1 female mice (20–25 g) were divided in two groups and treated with saline (vehicle) or M β CD 1000 mg/kg/week intraperitoneal (i.p.) during 1 month. To study the effect of lipid raft disruption on peripheral nerve regeneration, 13 female mice (25–30 g) were injured on the sciatic nerve and allowed to regenerate for 1 month while receiving saline ($n = 6$) or 1000 mg/kg/week M β CD ($n = 7$) i.p. treatment.

To perform the nerve injury, animals were anesthetized by i.p. injection of ketamine (90 mg/kg; Imalgene 500, Rhône-Merieux, Lyon, France) and xylazine (10 mg/kg; Rompun, Bayer, Leverkusen, Germany). The right sciatic nerve was surgically

exposed at the mid thigh and carefully freed from adherences to surrounding tissues. Afterwards, it was cut at 45 mm from the tip of the 3rd toe and immediately repaired using two epineurial sutures (10–0), maintaining the fascicular alignment of the sciatic branches. Finally, the wound was sutured in planes and disinfected. Animals were left to recover on a hot pad after being returned to their cages. The left paw was left uninjured as a control.

All the animals had food and water *ad libitum* and were kept at a standard temperature ($22 \pm 2^{\circ}\text{C}$) and under 12:12-h light-dark cycles (300 lux/0 lux). The experimental procedures followed the recommendations of the European Communities Council Directive 2010/63/EU for the care and use of laboratory animals and were approved by the Committee for Ethics on Experimental Animal and Human Research of the Universitat Autònoma de Barcelona.

Electrophysiology Tests

To test possible effects of M β CD on intact animals, electrophysiological tests were performed every 7 days after beginning of the treatment and for 4 weeks. To monitor peripheral nerve regeneration, electrophysiological tests were performed at 14, 21, 25, 28, and 33 days post-injury (dpi).

Animals were anesthetized with pentobarbital (10 mg/kg) and the sciatic nerve was stimulated using two needle electrodes inserted percutaneously at the sciatic notch, applying single rectangular pulses of 0.02 ms up to the voltage required to obtain a maximal evoked response. The compound muscle action potentials (CMAP, M wave) evoked by stimulation of motor nerve fibers were recorded from the tibialis anterior (TA) and plantar (PL) muscles with microneedle electrodes. All potentials were amplified and displayed on a digital oscilloscope (Tektronix 450S; Tektronix, Beaverton, OR, United States) at the appropriate settings for latency and amplitude measurements from the baseline to the maximal negative peak. During the tests, the animals were placed over a warmed flat coil controlled by a hot water circulating pump to maintain body skin temperature.

Locomotion Evaluation

The DigiGait system (Mouse Specifics, Boston, MA, United States) was used to assess locomotor performance of healthy animals treated with M β CD or vehicle at weekly intervals during treatment. The mice were forced to run over the transparent belt of a motorized treadmill and recorded with a high-speed video camera (80 frames/s) from below while running at a constant treadmill velocity of 20 cm/s. A minimum of 200 images were collected for each walking mouse containing more than eight strides for each run and each video was analyzed with the DigiGait software. The print length, and the toe spread distance between toes 1–5 and toes 2–4 were measured, and the sciatic functional index (SFI) between the right and the left paw was calculated (Navarro, 2016).

Mechanical Algesimetry

The algesimetry tests for mechanical stimuli were performed on both hindpaws every week along treatment in uninjured animals. Sensibility to a non-noxious mechanical stimulus was

measured by using an electronic Von Frey algesimeter (Bioseb, Chaville, France). Mice were placed on a wire net platform in plastic chambers 10 min before the experiment for habituation. The hindpaw plantar surface was stimulated from the bottom of the box by applying a 0.4 mm non-noxious pointed metal probe to the central area of the paw, and then slowly increasing the pressure until the mouse raised the paw, with a 35 g cut off force to avoid skin damage. The mechanical nociceptive threshold was taken as the mean of three measurements per paw and the threshold was expressed as the force (in grams) at which mice withdrew the paw in response to the stimulus (Cobianchi et al., 2014).

Pinprick Test

Progression of nociceptive reinnervation of the hindpaw was assessed at 14, 21, 25, 28, and 33 dpi by means of the pinprick test. Awake animals were gently wrapped in a cloth with the injured paw facing upward. The skin surface near C plantar pad and 4th toe (more distal) were stimulated with a blunt needle with enough intensity to indent the skin without damaging it (Cobianchi et al., 2014). Each site was stimulated twice and responses were recorded as positive only when clear pain reactions such as fast withdrawal or vocalization were triggered. Positive responses were taken as a sign of functional reinnervation of the skin.

Histology, Immunohistochemistry and Immunocytochemistry

Neurons were fixed with a solution of 4% PFA in PBS for 10 min. Subsequently, they were rinsed with PBS and permeabilized with a solution of triton 0.1% X-100 in PBS for 10 min. Afterwards, they were rinsed with PBS once more, and blocking solution (NHS 10% in PBS) was added for 1 h at room temperature. After blocking, the cells were incubated for 2 h with the respective primary antibodies diluted in blocking solution. Unbound primary antibodies were washed with PBS, and neurons were incubated with the respective secondary antibodies in blocking solution for 1 h at room temperature. For F-actin staining after permeabilization, phalloidin diluted in PBS was added and maintained for 30 min. Neurons were mounted using Mowiol.

Organotypic slices were rinsed with PBS with 0.5% Triton three times, and were incubated for 2 h at room temperature with blocking solution (10% NHS, 0.2M Glycine in PBS-Gelatin with 0.5% Triton). After blocking, the cells were incubated overnight at 4°C with the respective primary antibodies diluted in antibody solution (5% NHS in PBS-Gelatin with 0.5% Triton). Unbound primary antibodies were washed with PBS with 0.5% Triton, and slices were incubated with the respective secondary antibodies in antibody solution for 2 h at room temperature.

For the *in vivo* regeneration experiment, mice were transcardially perfused with 4% PFA in PBS (0.1 M, pH 7.4) 1 month after beginning the treatment. Subsequently, the sciatic nerve, spinal cord, L4 and L5 DRG neurons were removed, postfixed for 24 h with PFA and cryopreserved in PB containing 30% of sucrose for immunohistochemistry analysis. Samples were serially cut (15 µm) with a cryotome (Leica CM190) and stored at −20°C for further analysis.

For cholesterol depletion analysis, samples were defrosted for 30 min at room temperature and then rehydrated with PBS for 5 min. DRG neurons were then incubated for 3 h at room temperature with CTxB (1:200) in PBS. Slides were washed and mounted using Mowiol.

For immunohistochemistry, samples were defrosted at room temperature, blocked with PBS-specific animal serum, and incubated overnight at 4°C with the primary antibodies rabbit anti- GAP43 (1:100), rat anti- MBP (1:200) and chicken anti- NF-H (1:100). After washes, sections were incubated with the respective biotinylated secondary antibody (1:200) for GAP43 and MBP and then for 1 h at room temperature with conjugated Alexa Fluor streptavidin (1:200) or Alexa Fluor anti-chicken IgY. Finally, sections were mounted with Mowiol containing DAPI for nuclear staining.

Image Analysis

Images of primary cell cultures were taken in an epifluorescence microscope (Eclipse Nikon E1000) with a 60× oil-immersion objective. To take images from the *in vitro* axotomy experiments, we used an inverted microscope (Olympus ScanR) with a 20× objective. For images of the organotypic cultures, we used a confocal microscope (Leica TCS SP5) with a 20× objective and a 20× objective with 2× zoom to quantify axon regeneration. Images of the tibial nerve with MBP and NF-H immunostaining were taken 10 mm distally from the injury site with an epifluorescence microscope (Eclipse Ni, Nikon) attached to a digital camera (DS-Ri2, Nikon). Finally, we used a confocal fluorescent microscope (Zeiss LSM 700) to acquire the images from the SC and DRG tissue sections stained with GAP43, and images were analyzed with ImageJ (Schneider et al., 2012). Briefly, the area of the soma of at least 100 DRG neurons/animal and 10 motoneurons/animal were taken as ROI, and the integrated density (mean gray value × area) was obtained. The mean value obtained for each animal was used for comparison (Romeo-Guitart et al., 2018).

Statistical Analysis

All *in vitro* experiments were done three times independently. Data show means ± SEM. To analyze the statistics, we used GraphPad software and applied ANOVA test for multiple conditions or the Student's *t*-test for two conditions. *In vivo* results are presented as mean ± SEM and means were compared with two-tailed, unpaired Student's *t*-test, two-way ANOVA followed by Tukey's Multiple Comparison Test or Mantel-Cox test. Differences were considered significant at $p < 0.05$.

RESULTS

Cholesterol Depletion Increases Growth Cone Area and Number of Filopodia in Hippocampal and EGL Cerebellar Axons

Growth cones play a key role during axonal growth and guidance. First, we examined the effect of cholesterol depletion on the morphological features of growth cones. To this end,

we treated hippocampal and EGL neurons with two drugs that efficiently reduce cholesterol in the cell membrane (Nystatin and M β CD), and with ChOx, a cholesterol-depleting enzyme (**Figure 1**) (Bolard, 1986; Cahuzac et al., 2006; Zidovetzki and Levitan, 2007). Both neuron types were kept in culture for 3 DIV before being treated with the aforementioned drugs. In hippocampal neurons, depletion of cholesterol driven by the three drugs significantly increased the growth cone area identified by phalloidin staining (**Figures 1A,C**). However, only Nystatin increased this parameter in EGL neurons (**Figures 1B,D**). Overall, our results show that cholesterol depletion increases the growth cone area in hippocampal and EGL neurons in the CNS.

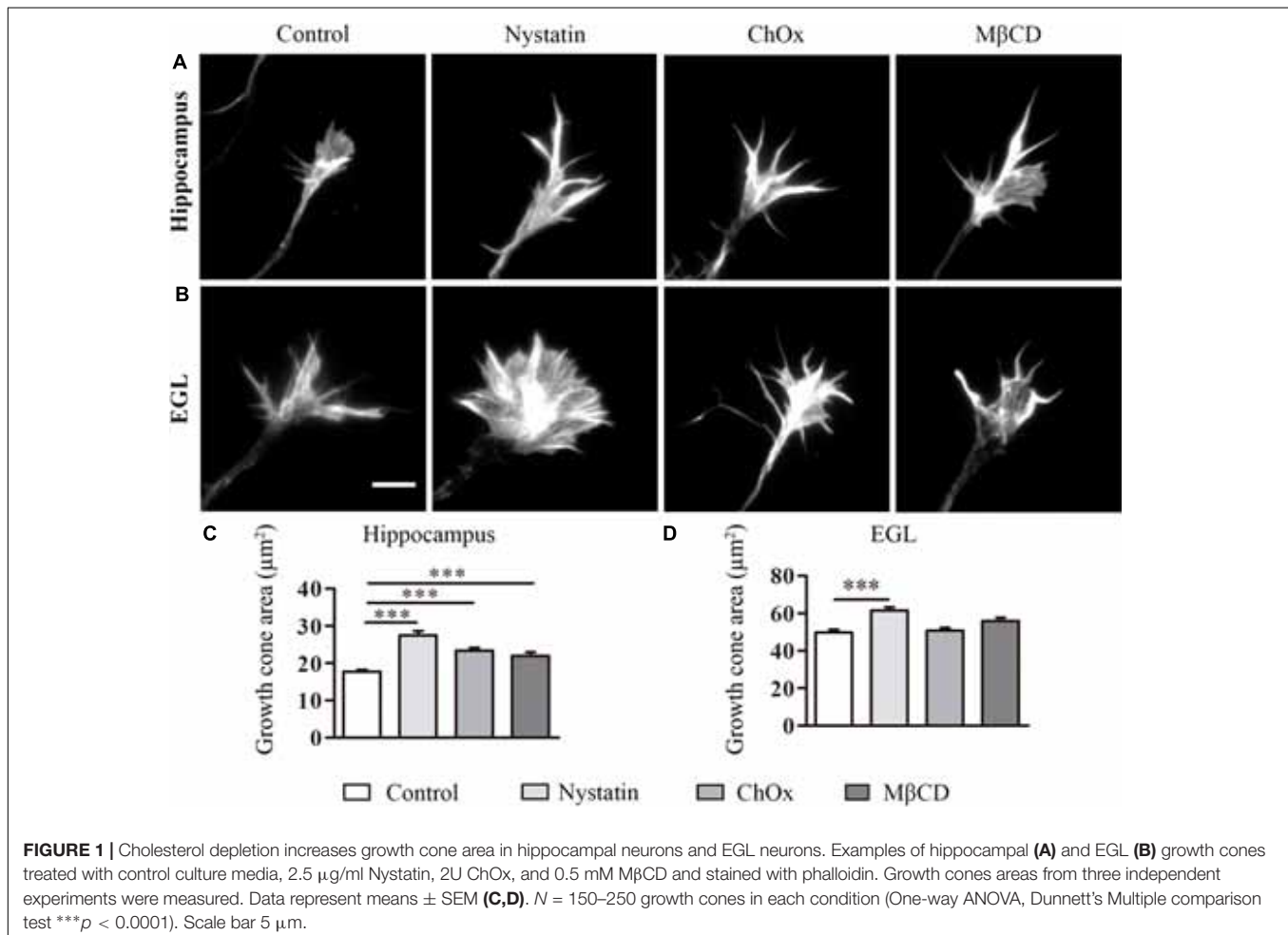
During the course of the experiments, we observed another effect of cholesterol depletion, namely the development of numerous filopodium-like extensions/branching points along neurites. Filopodia, dynamic membranous structures driven from the actin cytoskeleton, are necessary for axonal motility, guidance, branching and regeneration. To determine the importance of cholesterol in the formation of filopodium-like structures, we again treated hippocampal and EGL neurons with Nystatin, ChOx, and M β CD (**Figure 2**). The filopodium-like structures were counted in discrete segments of hippocampal and EGL axons (**Figures 2A,B**). Cholesterol

depletion induced by these drugs led to a significant increase in the number of filopodium-like structures in both types of neuron (**Figures 2C,D**).

These results indicate that a reduction in the cholesterol content of the cell membrane of both types of neuron promoted an increase in the number of filopodium-like structures and branching. In contrast to the effect of these drugs on growth cone area, these compounds enhanced the number of filopodia/branches in hippocampal and EGL neurons.

Cholesterol Depletion Affects Growth Cone Area, Number of Filopodia, and Neurite Extension in DRG Neurons

To determine whether the effects of cholesterol depletion observed in the CNS neurons can be extrapolated to the PNS, we performed the same experiments using DRG neurons (**Figure 3**). DRG neurons were isolated from mouse embryos at E13–14 and treated after 1 DIV with cholesterol removal agents. Treatment with Nystatin and ChOx led to an increase in growth cone area in DRG neurons (**Figures 3A,C**), and the removal of cholesterol with any of the three drugs enhanced the number of filopodia (**Figures 3B,D**).



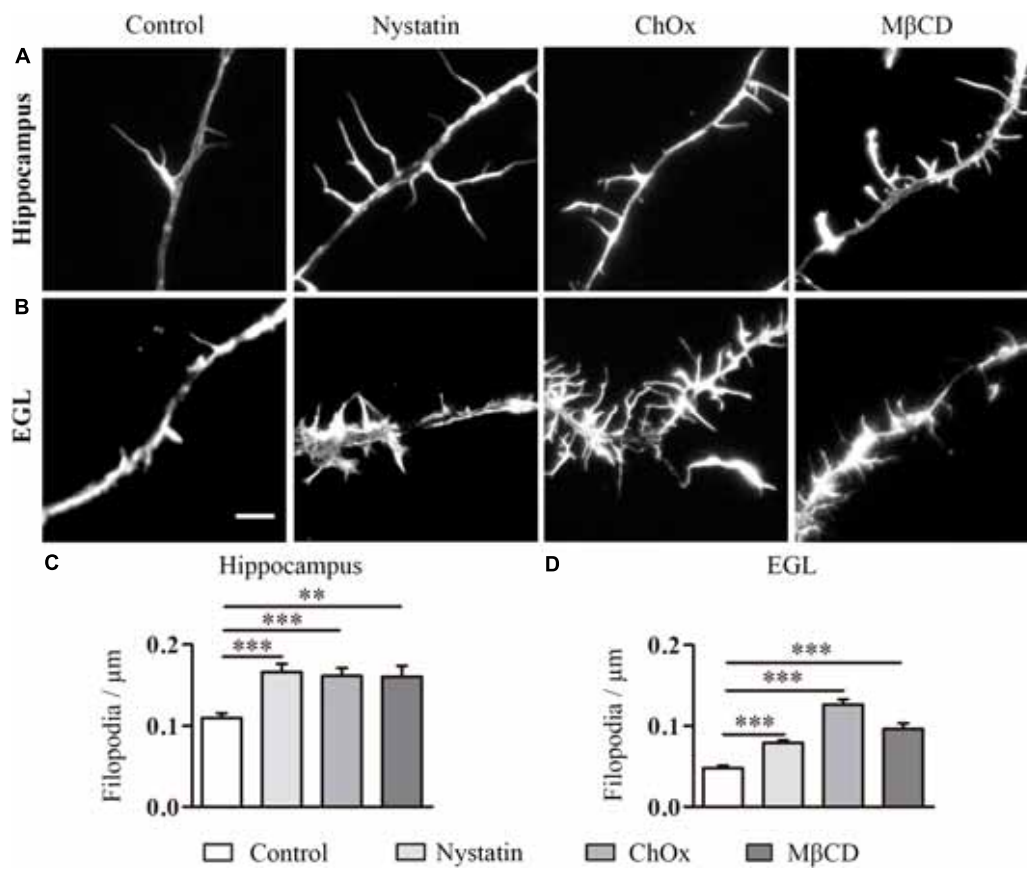


FIGURE 2 | Cholesterol depletion increases filopodium-like structures in hippocampal neurons and EGL neurons. Examples of hippocampal (A) and EGL (B) filopodium-like structures in axons treated with control culture media, 2.5 $\mu\text{g/ml}$ Nystatin, 2U ChOx, and 0.5 mM MβCD and stained with phalloidin. The density of filopodium-like structures was measured in discrete segments of axons in three independent experiments. Data represent means \pm SEM (C,D). $N = 150$ –250 neurons in each condition (One-way ANOVA, Dunnett's Multiple comparison test $**p < 0.01$, $***p < 0.0001$). Scale bar 5 μm .

We also quantified the effect of cholesterol depletion on neurite extension and branching (Figure 4). Treatments were performed for 24 h in the case of Nystatin and ChOx and for 2 h before fixation in the case of MβCD, as we observed increased cell death with longer incubations with this drug. Only the treatment with Nystatin increased the total length of DRG neurites while ChOx and MβCD did not affect this parameter (Figures 4A,B). We found that 24 h treatments with Nystatin and ChOx led to a significant increase in the number of branching points (Figures 4A,C).

These results suggest that pharmacological removal of cholesterol from the cell membrane has similar effects on CNS (hippocampal and cerebellar) and PNS (DRG) neurons. An acute decrease in cholesterol levels *per se* increases growth cone area and filopodia/branching point density in developing neurons.

Cholesterol Depletion Improves Axonal Regeneration After Axotomy *in vitro* and *ex vivo*

One of the hallmarks of CNS regeneration is the difficulty to achieve the regrowth of damaged axons. This difficulty is

attributed mainly to the generation of an axon blocking “milieu.” As we have shown that cholesterol depletion increases axonal growth cone area and axonal extension, we next addressed, using an *in vitro* and an *ex vivo* system, whether depletion of this lipid enhances axonal regeneration.

First, E16 hippocampal neurons were seeded in a microfluidic chamber (Figure 5) and neurons were axotomized. This chamber allowed us to differentially treat the axons, on one side with control medium and on the other with medium supplemented with Nystatin applied immediately after axotomy (Figure 5D). Axons treated with Nystatin showed a significant increase in length when compared with those cultured in basal control medium (Figures 5A–C).

These results suggest that the removal of cholesterol by means of Nystatin enhances axon regeneration after axotomy *in vitro*. We next used the *ex vivo* organotypic model of axotomy and regeneration (del Rio and Soriano, 2010). Slice co-cultures from P0 mouse hippocampi and the EC were isolated and kept in culture for 21 days (Figure 6). Some EC slices were obtained from actin-GFP transgenic mice. At 21 DIV, axotomy was performed sectioning the entorhino-hippocampal connection (EHP) using a needle, and mixed

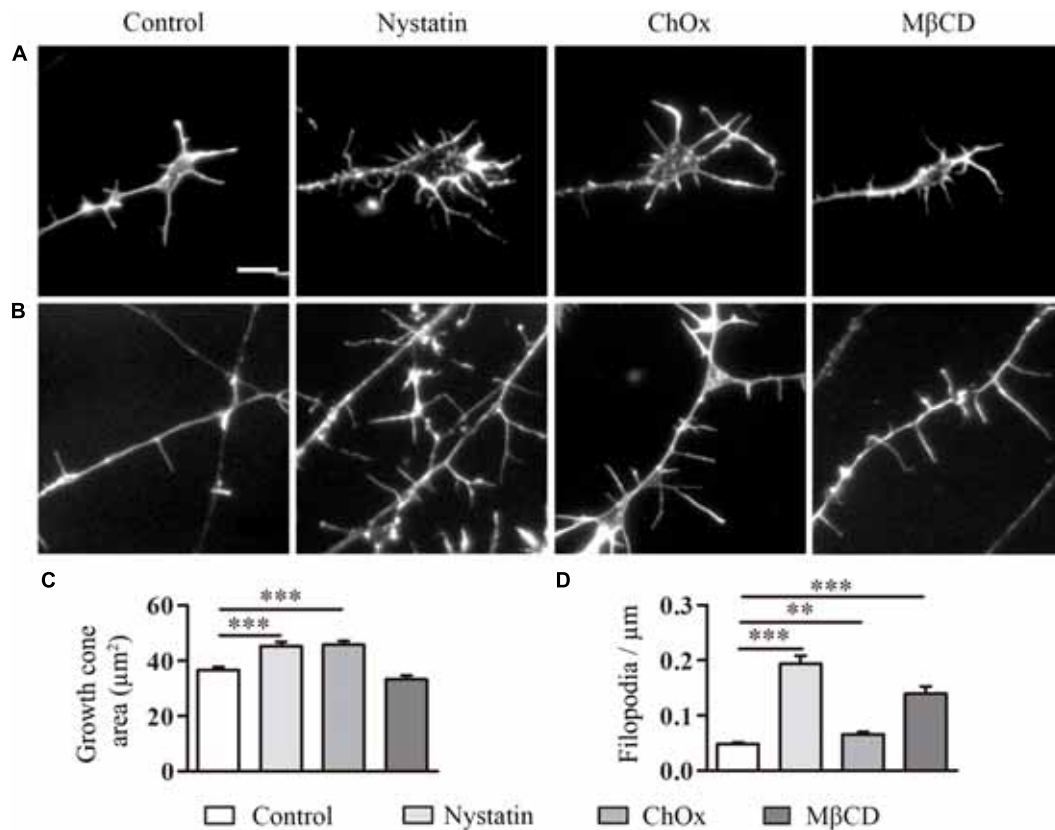


FIGURE 3 | Cholesterol depletion affects growth cone area and the density of filopodia in DRG neurons. Examples of DRG growth cones (A) and filopodia (B) incubated with control media, 2.5 μg/ml Nystatin, 2U ChOx, and 0.5 mM MβCD and stained with phalloidin. Growth cone areas and filopodia from three independent experiments were measured. Data represent means ± SEM (C,D). $N = 150$ –250 neurons in each condition (One-way ANOVA, Dunnett's Multiple comparison test $**p < 0.01$, $***p < 0.0001$). Scale bar 5 μm.

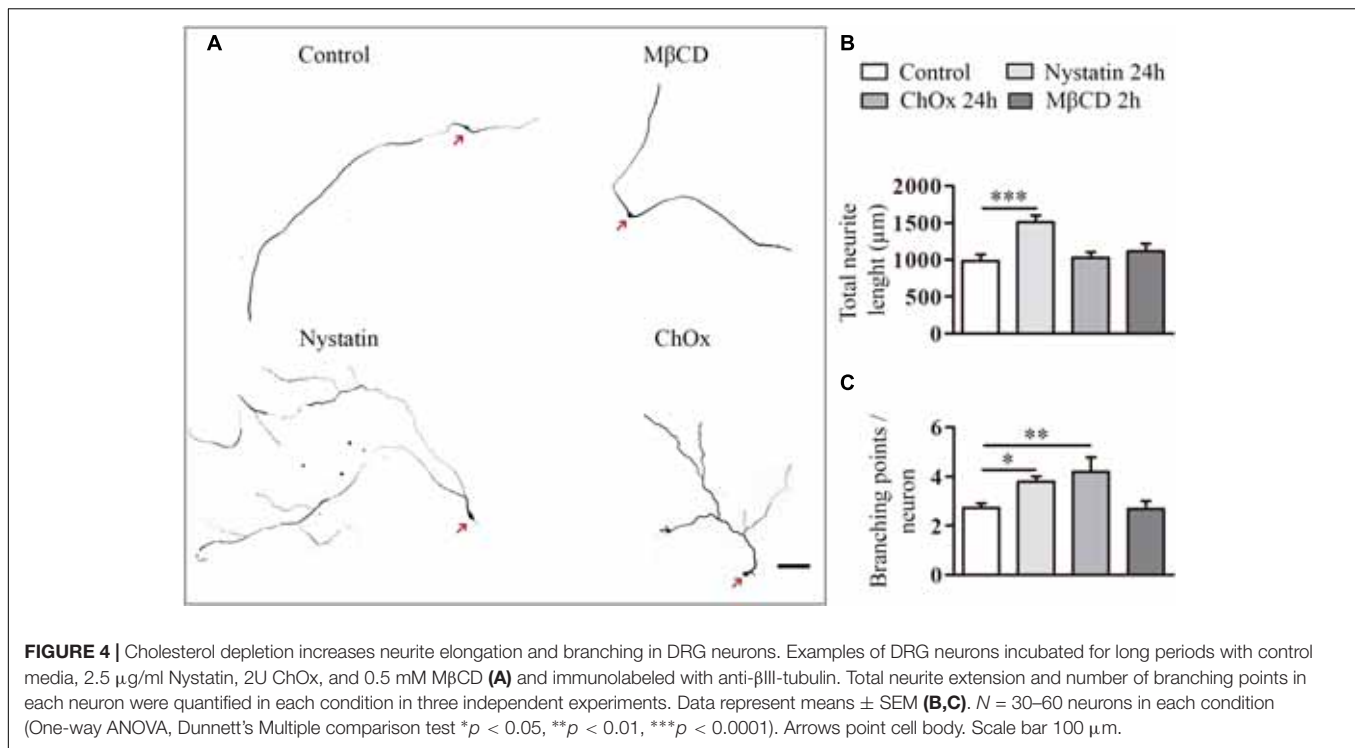
co-cultures were generated. The hippocampi from actin-GFP co-cultures were removed and replaced by hippocampi from WT mice organotypic cultures, thereby allowing the direct visualization of regenerating GFP-positive EC-hippocampal axons. Axotomized organotypic cocultures were treated with Nystatin for 10 additional days (Figure 6A). In axotomized co-cultures that were not treated with Nystatin, virtually no regenerating axons (or very few) were found in the SLM/ML layers, which are the layers of termination of the EHP pathway (Figures 6B,D). In contrast, after Nystatin treatment, we observed a 10-fold increase in the density of regenerating EC axons present in the SLM/ML layers (Figures 6C,D). Organotypic cultures treated with Nystatin showed a normal morphology and distribution, and no evidence of neuronal degeneration was appreciated (Figure 6C). In another set of experiments, WT EC slice-cocultures were generated and axotomized as described above (Figure 6A) and regenerating EC axons were visualized by Biocytin injections (del Rio and Soriano, 2010). Again, the number of regenerating EHP axons was markedly increased by the incubation with Nystatin. Together with the above results, the present findings indicate that cholesterol depletion favors axonal regeneration *in vitro* and *ex vivo*.

Treatment With MβCD Has No Effect on Healthy Mice

The results of motor electrophysiological tests performed showed that MβCD administration *in vivo* did not cause any impairment in the mice. The M wave amplitude (Supplementary Figures S1A,B) and latency (Supplementary Figures S1C,D) of TA and PL muscles did not present significant differences between MβCD treated and saline control groups. The walking track test yielded no differences in the SFI between groups (Supplementary Figure S1E). Finally, mechanical algometry was performed to evaluate possible changes in nociception in MβCD treated animals. Results showed no significant differences between control and treated animals in pain threshold along time (Supplementary Figure S1F).

Treatment With MβCD Alters the Integrity of the Lipid Raft by Reducing the Amount of Membrane Cholesterol

Our previous results suggest that cholesterol depletion is directly involved in promoting axonal regeneration. However, we next sought to determine the effect of acute reduction of cholesterol levels in the *in vivo* model of peripheral nerve lesion and



regeneration. Cholesterol is a major component of lipid rafts, which are specialized membrane microdomains that hold a multitude of signaling receptors. It has recently been shown that disruption of the raft by acute depletion of cholesterol promotes regeneration and functional recovery after spinal cord injury (Tassew et al., 2014). Thus, we first examined the integrity of raft structures in DRG nerves after acute depletion of cholesterol by treatment with MβCD. Contralateral DRG neurons of injured mice treated with MβCD or saline were incubated with the CTxB. This fraction of the toxin has a known affinity for ganglioside GM1, a lipid raft-associated molecule (Schnaar et al., 2014) widely used as a marker of the presence of cholesterol in the cellular membrane and of lipid raft integrity. Fluorescent staining showed clear CTxB labeling in the plasma membrane of DRG neurons from animals that received vehicle for 1 month (Figure 7A) in comparison with those treated with MβCD (Figure 7B).

Cholesterol Depletion Induced by MβCD Increases GAP43 in Sensory Neurons After Axotomy

To study the regenerative response in sensory (Figure 8A) and motor (Figure 8B) neurons after nerve section, the expression of the GAP43 was measured. GAP43 is expressed at high levels during development and axonal regeneration, and it is considered a crucial component of an effective regenerative response in the nervous system, being used as a marker of regeneration in injured axons. The results showed higher immunoreactivity for GAP43 in DRG neurons in injured animals treated with MβCD compared to those treated with vehicle (Figure 8C). This observation indicates that cholesterol depletion after sciatic injury enhances

the neuronal regenerative program. No significant difference was observed for motoneurons (Figure 8D). Moreover, myelin staining of the regenerated nerve was conducted to assess whether lipid raft disruption could affect axonal remyelination. Qualitative assessment of both saline- and MβCD-treated animals (Figure 8E) shows similar presence of myelin in nerve fibers of both groups, thus indicating that lipid raft disruption did not block remyelination after injury.

Cholesterol Depletion Induced by MβCD Improves Muscle Reinnervation and Sensory Responses in Mice

Electrophysiological tests performed to follow up nerve regeneration after sciatic nerve section and repair showed a progressive increase in the amplitude of the M wave of the two muscles in both groups, thereby indicating progressive reinnervation of the muscles by the regenerated axons. Although no differences were seen for the proximal TA muscle, MβCD-treated mice had significantly higher M wave amplitude of the PL muscle than control animals at 33 days (Figures 9A,B), indicative of greater reinnervation of the distal muscles. Values of M wave latency did not show significant differences between the two groups (Figures 9C,D).

No signs of autotomy, that could be indicative of neuropathic pain, were found in any studied mice. Recovery of sensitivity was studied by means of the pinprick test on areas of the paw from proximal to distal region of the sciatic nerve innervation territory (Cobianchi et al., 2014). In the C plantar pad, no animals showed positive response at 21 days, and with time more animals recovered sensory response without differences

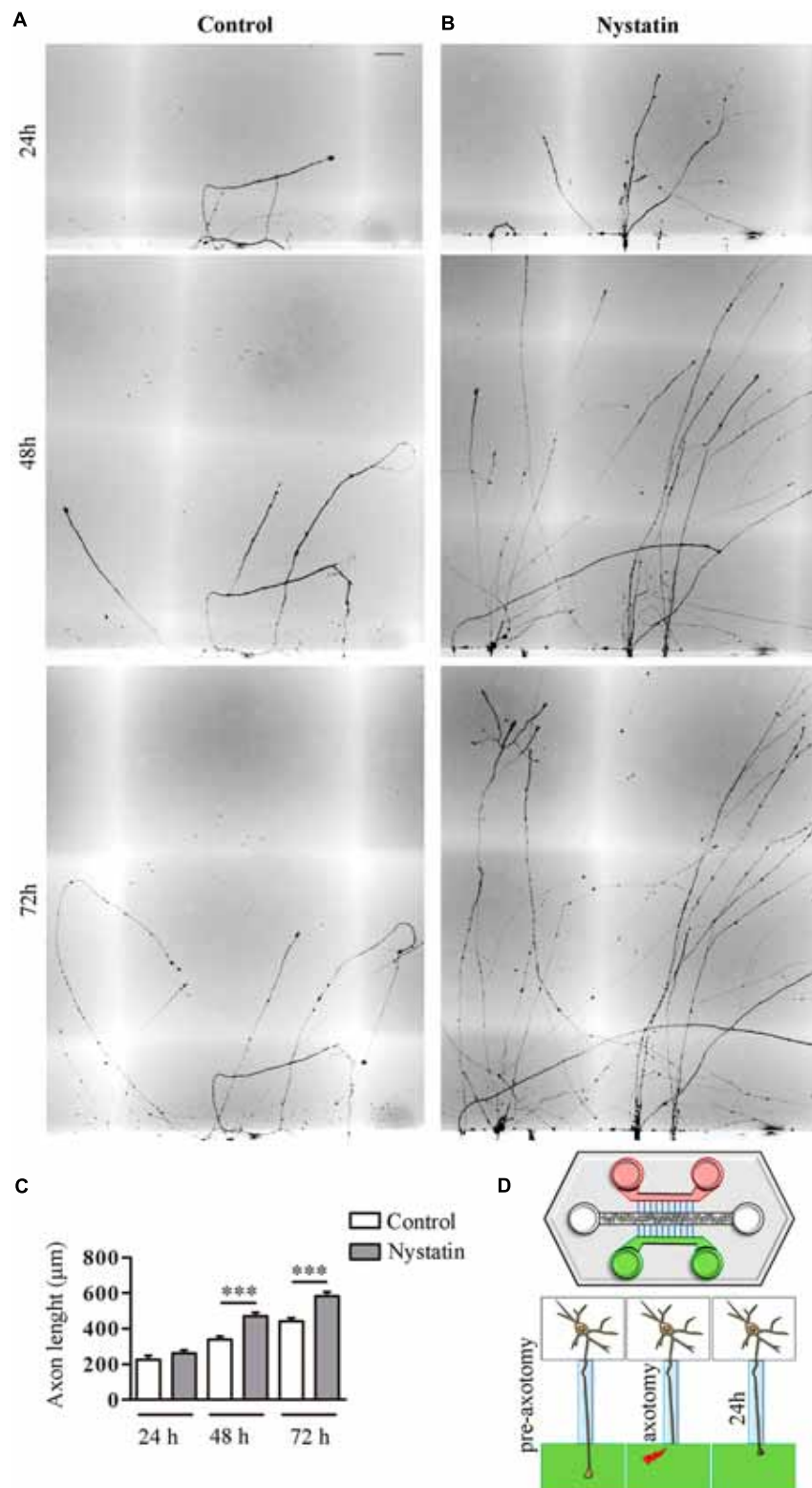
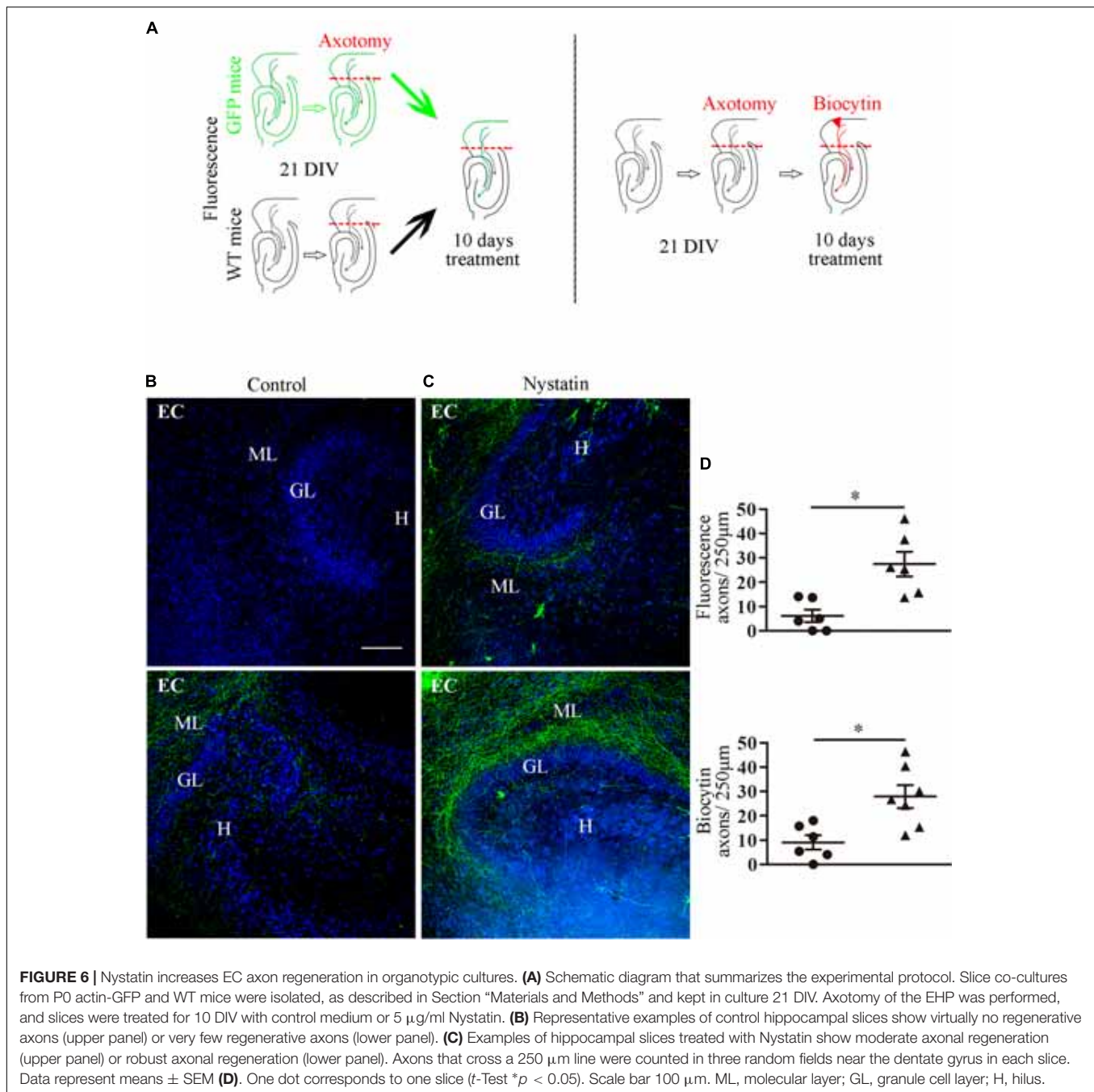


FIGURE 5 | Nystatin improves axon regeneration after axotomy *in vitro*. Examples of hippocampal axon regrowth at 24, 48, and 72 h after axotomy in control condition **(A)** and in response to treatment with 2.5 $\mu\text{g/ml}$ Nystatin **(B)**. Axon lengths were measured in each condition. Data represent means \pm SEM **(C)**. Schematic diagram of a microfluidic chamber **(D)**. Cell bodies are in the central channel (white), axon growth through microfluidic channels (blue) to both sides (green and red). After axotomy, control medium was applied on one side (red) and Nystatin on the other (green). $N = 3$ chambers (t -Test in each time point, *** $p < 0.0001$). Scale bar 50 μm .



between groups. However, in the 4th toe, which is the most distal area, cholesterol-depleted mice showed positive response earlier than injured controls, and at 33 dpi, 50% of the M β CD group showed positive responses whilst only 12.5% of the vehicle-treated animals did (Figures 9E,F).

DISCUSSION

Following axotomy, several metabolic changes occur in injured neurons to reinnervate denervated targets and thus

ensure survival and regeneration. Moreover, a growth cone is formed at the tip of growing axons, and this process requires morphological and biochemical changes in the plasma membrane, including membrane extension and remodeling. In this context, cholesterol-rich lipid rafts, also called membrane microdomains, play a key role as signaling platforms of both growth-promoting and growth-inhibiting molecules. With regard to the possible contribution of lipid rafts and cholesterol to nerve regeneration, conflicting views can be found in the literature. Some authors demonstrated that lipid rafts promote axonal regeneration (Santuccione et al., 2005; Zhang et al., 2013)

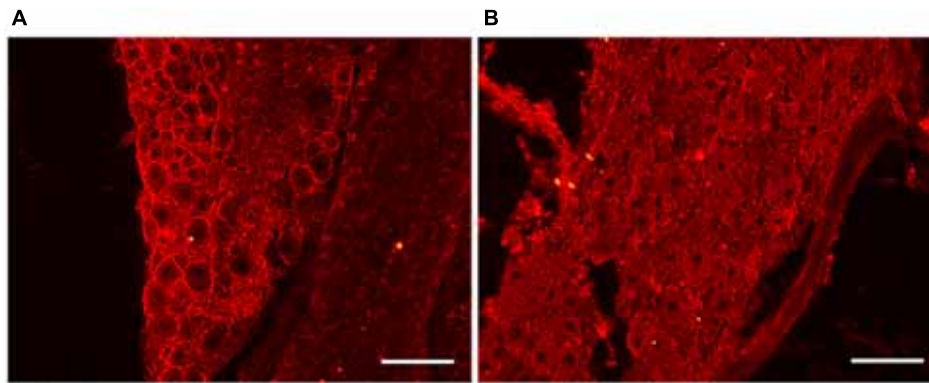


FIGURE 7 | M β CD disruption of lipid rafts in DRG neurons. **(A,B)** Representative images of the DRGs of animals treated with vehicle **(A)** and M β CD **(B)**. Note the absence of CTxB membrane staining in B after M β CD treatment, indicating lipid raft disruption. Scale bar: 100 μ m.

while others claim that they have an inhibitory role (Vinson et al., 2003; Hausott et al., 2011). These contradictions can be explained by the fact that, in addition to a variety of proteins and molecules that promote axonal regeneration, such as receptors of neurotrophic factors, lipid rafts also contain proteins and molecules that exert an inhibitory role, such as receptors of myelin-associated proteins (Kappagantula et al., 2014). On the other hand, there is also some discrepancy about the role of lipid rafts in cell apoptosis. It is described that pro-apoptotic receptors like Neogenin, FAS and its ligand, JNK, PKC, Src kinases and a wide variety of lymphocyte-related receptors are more functional when are localized in lipid rafts, inducing a line of investigation in which lipid rafts are targets for chemotherapy (George and Wu, 2012). However, receptors related with cell survival, like Akt cascade, also depend on lipid rafts (George and Wu, 2012). It has been shown that cholesterol depletion with M β CD protects cerebellar neurons from apoptosis (Zhou et al., 2012) and after spinal cord injury, lipid raft disruption promotes cell survival due to a loss of function of Neogenin (Tassew et al., 2014). In conclusion, some of these studies were performed *in vitro* and sought to address the cellular pathway or the signaling of a specific neurotrophin through lipid rafts, and did not take into account all the trophic factors and cell responses that occur *in vivo*, but instead focused on single pathways.

In the present study, we show that cholesterol depletion in juvenile cultured neurons increases the size of growth cones and enhances neurite and axonal extension and the marked formation of filopodium-like extensions in both central and peripheral neurons. Although we did not address the underlying molecular mechanisms, we believe that both the membrane fluidity induced by cholesterol depletion and partial lipid raft disruption may account for the effects observed, as extracellular matrix and adhesion receptors are also grouped in lipid rafts (Leitinger and Hogg, 2002; Decker and French-Constant, 2004; Head et al., 2014). In addition, the increased size of neurites suggests that cholesterol depletion might be involved in the positive regulation of the exocytotic machinery needed for neurite growth (Ros et al., 2015).

Next, we addressed whether cholesterol depletion increases the regrowth of axotomized neurons in two *in vitro* models: dissociated hippocampal cultures and axotomized EC-hippocampal slice cultures. In both cases, we found a marked increase in the regenerative potential of lesioned axons, again suggesting that cholesterol depletion not only increases axonal length in developing axons but also axonal regrowth and regeneration *in vitro*. In addition, the observation that regenerated EC-hippocampal axons were correctly targeted to the appropriate termination layers (SLM and ML) indicates that cholesterol depletion does not alter the molecular mechanisms involved in the guidance and targeting of these axons to the hippocampus.

Membrane extension during axon growth after axotomy requires the incorporation of new lipids to the tips of the regenerating axons. Incorporated cholesterol in the axons of peripheral neurons after axotomy comes from transported cholesterol synthesized in the cell bodies of lesioned neurons (de Chaves et al., 1997), and from recycled cholesterol from cellular and myelin debris originated during the injury (Goodrum, 1991; de Chaves et al., 1997). The existence of multiple complementary mechanism to incorporate cholesterol into the re-growing membranes suggest a redundancy in the process of cholesterol reutilization. Our results *in vitro* and *in vivo* suggest that acute and medium-term reduction of cholesterol levels have positive effects for axon elongation and regeneration after nerve injury. However, further studies are required to evaluate long-term effects of systemic cholesterol reduction. Secondary undesired effects associated with alteration of membrane cholesterol levels should also have to be considered. Previous reports have found that M β CD may alter crayfish neuromuscular junction functioning in cold conditions (14°C) but not at 21°C (Ormerod et al., 2012) and cholesterol depletion in *Caenorhabditis elegans* results in decreased motility (Merris et al., 2004). Moreover, reduction of membrane cholesterol alters ion channel activity in sensory peripheral neurons (Saghy et al., 2015), with direct consequences for their hypersensitivity (Pristera et al., 2012) and the development of neuropathic pain (Ferrari and Levine, 2015; Amsalem et al., 2018). As a

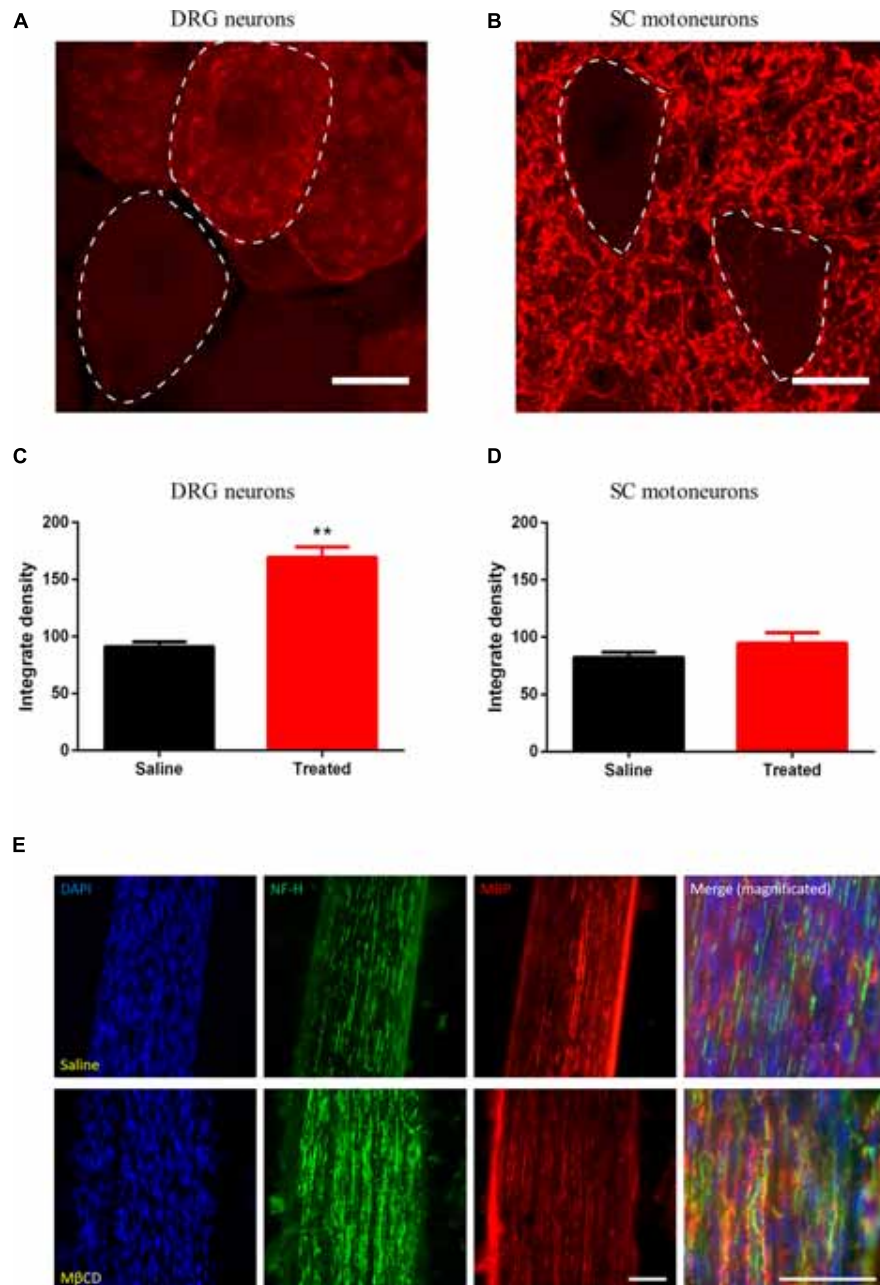


FIGURE 8 | MβCD increases GAP43 expression in injured DRG neurons. **(A,B)** Detail of DRG **(A)**, dashed line) and motoneurons **(B)**, dashed line) analyzed for GAP43 expression. **(C,D)** Quantification of GAP43 positivity in DRG neurons **(C)** and motoneurons **(D)** from animals treated with vehicle or MβCD vs. Saline. **(E)** Detail of a regenerated nerve stained for cell nuclei (blue), NF-H (green), and GAP43 (red) of saline- (top) and MβCD-treated (bottom) animals. Scale bar: 15 μm in **(A,B)**; 50 μm in **(E)**. Student's *t*-test, ***p* < 0.01.

consequence, electrophysiological tests, pain threshold tests and locomotion studies were performed on healthy animals to evaluate any possible effect derived from the systemic MβCD administration and the consequent membrane cholesterol depletion. Our results on healthy mice showed no significant differences between treated and control animals with reported values similar to those found in previous studies in the literature (Verdu et al., 1996; Bruna et al., 2010; Ale et al.,

2016). Of particular interest, the algesimetry results showed no indication of hyperalgesia in intact mice, and the absence of autotomy in mice in the regeneration experiment also points out that there was no increased pain sensitivity after lipid raft disruption (Casals-Diaz et al., 2009). Therefore, although some uncontrolled effect cannot be dismissed, 1 month of systemic MβCD administration and lipid raft disruption did not alter normal nervous system function in mice.

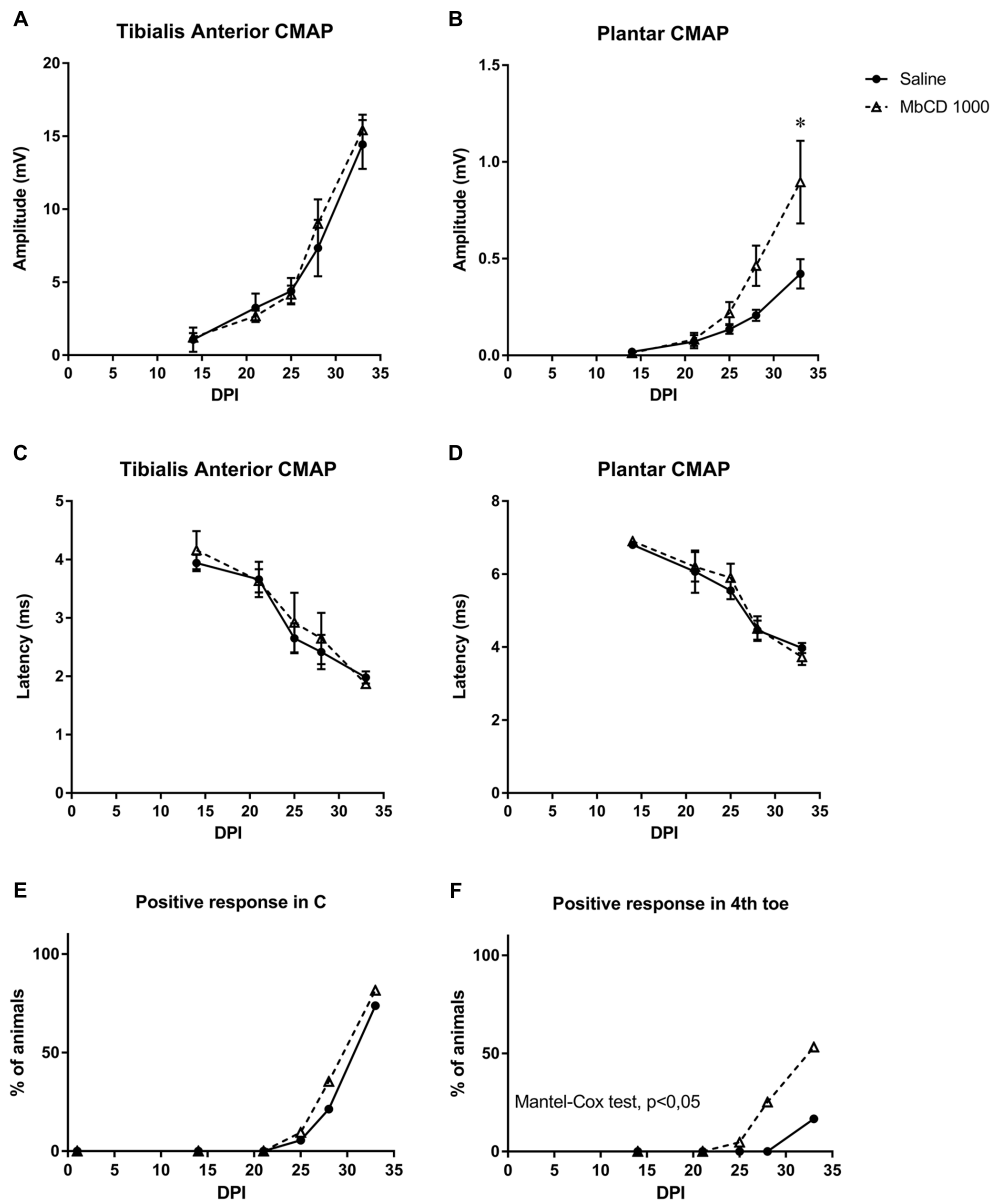


FIGURE 9 | MβCD treatment accelerates motor and sensory functional recovery following sciatic nerve injury. (A–D) Electrophysiological results after nerve injury in mice treated with vehicle or with MβCD. Results of CMAP amplitude (A,B) and latency (C,D) recorded in TA and PL at 14, 21, 25, 28, and 33 dpi. Data are shown as the mean and SEM (bars). * $p < 0.05$ with two-way Anova and Bonferroni test. (E,F) Pinprick test results to analyze sensory reinnervation in the hindpaw pad C (E) and 4th toe (F). Results show the percentage of animals with positive response in each area in the groups treated with vehicle or MβCD. $p < 0.05$ Mantel–Cox test indicate differences in the proportion of mice with reinnervation.

We then studied the effect of cholesterol depletion on peripheral nerve regeneration. To this end, we chose an *in vivo* model of peripheral nerve injury to avoid focusing on a single pathway or molecule, thus gaining a complete view of nerve regeneration. Cholesterol depletion and lipid raft disruption were achieved by means of treatment with MβCD (Zidovetzki and Levitan, 2007), a cyclic oligosaccharide that has been used as an antineoplastic (Grosse et al., 1998) and also as a complexing agent in pharmacological applications (Upadhyay et al., 2006). The latter use of MβCD is attributed to its

amphipathic properties, and molecules can be encapsulated inside the cavity of cyclodextrins. Thus, MβCD may act not only by extracting cholesterol from the plasma membrane and disrupting lipid rafts but also by catalyzing neurotrophic factors and favoring their uptake by neurons or glial cells that play a role in peripheral nerve regeneration. This could explain the increase in the number of GAP43-positive DRG neurons, an observation that indicates that, after MβCD treatment, there are more neurons able to regenerate or that have switched to a regenerative state sooner.

Our results indicate that lipid rafts are disrupted from the cell membrane after M β CD treatment, as shown by the loss of CTxB staining. CTxB has affinity for the GM1 ganglioside, a member of the complex ganglioside family, which also includes GD1 and GT1 (Schnaar et al., 2014), and it has been widely used as a marker of lipid raft integrity (Kalka et al., 2001). It has been reported that treatment with M β CD destabilizes the link between the axon and myelin as a result of the reduction of GD1 and GT1 in the membrane. These two gangliosides act as a myelin-associated glycoprotein receptors (Vyas et al., 2002) and, consequently, they mediate the inhibition of neurite outgrowth. With lipid raft disruption by M β CD, gangliosides are removed from the cell membrane and they cannot mediate the inhibition of neurite outgrowth. This situation may confer the axon with a greater capacity to regenerate. Thus, the increased motor and sensory reinnervation we observed after axotomy and treatment with M β CD is consistent with a reduction of GD1 and GT1 inhibition.

Moreover, other studies have reported that cholesterol removal affects various modes of endocytosis (Rodrigues et al., 2013). Endocytosis is a widely used mechanism for receptor internalization from the cell membrane, and it has been demonstrated that cholesterol and lipid rafts play key roles in clathrin-independent endocytic (Lamaze et al., 2001) and in clathrin-dependent endocytic mechanisms (Rodal et al., 1999). Thus, with lipid raft alteration, endocytosis might be impaired, thereby also remodeling the normal presence or removal of different receptors at the cell surface. With cholesterol depletion by M β CD, the endocytosis of neurotrophic factor receptors may be inhibited (Hausott et al., 2011). As the improvement in motor and sensory regeneration suggests, this inhibition would lead to increased cell receptor availability at cell surface, thus facilitating axon regeneration. On the other hand, M β CD treatment might interfere with myelin as it has a high lipid and cholesterol content. Indeed, deficient cholesterol biosynthesis in oligodendrocytes delays myelination (Saher et al., 2005) and the maximal brain cholesterol synthesis corresponds to the peak of myelination process (Korade and Kenworthy, 2008). However, our results indicate that M β CD treatment did not affect myelination of the regenerated nerve fibers in the adult mice. Nevertheless, a detailed histomorphometric quantification of the regenerated axons might be needed for a quantitative evaluation of the degree of remyelination after lipid raft disruption.

Finally, our results indicate that M β CD treatment accelerates nerve regeneration after complete nerve lesion. The positive effect was detected as faster and higher levels of reinnervation of distal targets, such as plantar muscles, which are the most discriminative for detecting differences in nerve regeneration rate. Whether these results would be more pronounced after a more severe nerve injury requires further attention.

The results of this study shed light on the role of lipid rafts in peripheral nerve regeneration, although more research is needed to elucidate the specific mechanisms affected by lipid raft disruption. As this study was performed from a functional perspective, a number of alterations may have been occurring. On the one hand, we may have accelerated regeneration due to an increase in myelin clearance and thus a decrease in

myelin-associated inhibitory agents. On the other, the beneficial effect might be due to an alteration of membrane ganglioside ratio or because lipid raft disruption promotes an environment that is favorable for neuron regeneration.

In conclusion, we have found that lipid raft disruption increases axonal growth in young neurons *in vitro*, enhances axonal regeneration in two *in vitro* models, and promotes peripheral nerve regeneration. Our results support the notion that these membrane microdomains play an important role in the signaling responsible for determining neural growth during development, as well as for nerve degeneration and regeneration after injury. This could be important because many pathways and molecules are involved in the processes that occur after nerve injury, and the environment plays a key role in the success or failure of nerve regeneration and functional recovery. However, caution should be taken before the translationability of our results. Considering the slow rate of nerve regeneration, in humans with considerable nerve length, target reinnervation may need several months to year. The possible effects of long-term lipid raft disruption treatment pointed above need to be investigated in preclinical models before any potential clinical application.

AUTHOR CONTRIBUTIONS

CR-B, RM-M, and MH-L designed, conducted, and analyzed the *in vitro* experiments. NO, JV, and XN designed, conducted, and analyzed the *in vivo* experiments. CR-B, RM-M, MH-L, and NO wrote the first draft of the manuscript. MP performed the organotypic experiments. AM did percoll gradients to isolated EGL neurons. RM-M, JV, XN, and ES designed the experiments, analyzed the data, and wrote the final version manuscript.

FUNDING

Research in our laboratories was supported by grants from the Spanish MINECO (SAF2016-76340R), CIBERNED, Spanish MECO (FPU14/02156 and BES-2014-067857), TERCEL (RD12/0019/0011) and ERDF funds. It was also supported by the European Union FPT-ICT projects NEBIAS (contract number FP7-611687), EPIONE (FP7-602547), and FP7-NMP MERIDIAN 280778.

SUPPLEMENTARY MATERIAL

The Supplementary Material for this article can be found online at: <https://www.frontiersin.org/articles/10.3389/fncel.2019.00040/full#supplementary-material>

FIGURE S1 | Electrophysiological, locomotion and algesimetry tests performed after vehicle or M β CD treatment in uninjured mice. **(A–D)** Electrophysiological results in mice. Results of CMAP amplitude **(A,B)** and latency **(C,D)** recorded in TA and PL muscles at 7, 14, 21, and 28 days after beginning of treatment. **(E)** Plot of the SFI obtained in walking track test. **(F)** Algesimetry test results during the 4 weeks of treatment.

REFERENCES

- Ale, A., Bruna, J., Calls, A., Karamita, M., Haralambous, S., Probert, L., et al. (2016). Inhibition of the neuronal NF κ B pathway attenuates bortezomib-induced neuropathy in a mouse model. *Neurotoxicology* 55, 58–64. doi: 10.1016/j.neuro.2016.05.004
- Allodi, I., Udina, E., and Navarro, X. (2012). Specificity of peripheral nerve regeneration: interactions at the axon level. *Prog. Neurobiol.* 98, 16–37. doi: 10.1016/j.pneurobio.2012.05.005
- Amsalem, M., Poilbout, C., Ferracci, G., Delmas, P., and Padilla, F. (2018). Membrane cholesterol depletion as a trigger of Nav1.9 channel-mediated inflammatory pain. *EMBO J.* 37:e97349. doi: 10.15252/embj.201797349
- Bjorkhem, I., and Meaney, S. (2004). Brain cholesterol: long secret life behind a barrier. *Arterioscler. Thromb. Vasc. Biol.* 24, 806–815. doi: 10.1161/01.ATV.0000120374.59826.1b
- Bolard, J. (1986). How do the polyene macrolide antibiotics affect the cellular membrane properties? *Biochim. Biophys. Acta* 864, 257–304. doi: 10.1016/0304-4157(86)90002-X
- Bruna, J., Udina, E., Ale, A., Vilches, J. J., Vynckier, A., Monbaliu, J., et al. (2010). Neurophysiological, histological and immunohistochemical characterization of bortezomib-induced neuropathy in mice. *Exp. Neurol.* 223, 599–608. doi: 10.1016/j.expneurol.2010.02.006
- Cahuzac, N., Baum, W., Kirkin, V., Conchonaud, F., Wawrezinieck, L., Marguet, D., et al. (2006). Fas ligand is localized to membrane rafts, where it displays increased cell death-inducing activity. *Blood* 107, 2384–2391. doi: 10.1182/blood-2005-07-2883
- Casals-Diaz, L., Vivo, M., and Navarro, X. (2009). Nociceptive responses and spinal plastic changes of afferent C-fibers in three neuropathic pain models induced by sciatic nerve injury in the rat. *Exp. Neurol.* 217, 84–95. doi: 10.1016/j.expneurol.2009.01.014
- Cobianchi, S., de Cruz, J., and Navarro, X. (2014). Assessment of sensory thresholds and nociceptive fiber growth after sciatic nerve injury reveals the differential contribution of collateral reinnervation and nerve regeneration to neuropathic pain. *Exp. Neurol.* 255, 1–11. doi: 10.1016/j.expneurol.2014.02.008
- de Chaves, E. I., Rusinol, A. E., Vance, D. E., Campenot, R. B., and Vance, J. E. (1997). Role of lipoproteins in the delivery of lipids to axons during axonal regeneration. *J. Biol. Chem.* 272, 30766–30773. doi: 10.1074/jbc.272.49.30766
- Decker, L., and ffrench-Constant, C. (2004). Lipid rafts and integrin activation regulate oligodendrocyte survival. *J. Neurosci.* 24, 3816–3825. doi: 10.1523/JNEUROSCI.5725-03.2004
- del Rio, J. A., and Soriano, E. (2010). Regenerating cortical connections in a dish: the entorhino-hippocampal organotypic slice co-culture as tool for pharmacological screening of molecules promoting axon regeneration. *Nat. Protoc.* 5, 217–226. doi: 10.1038/nprot.2009.202
- Dietschy, J. M., and Turley, S. D. (2001). Cholesterol metabolism in the brain. *Curr. Opin. Lipidol.* 12, 105–112. doi: 10.1097/00041433-200104000-00003
- Ferrari, L. F., and Levine, J. D. (2015). Plasma membrane mechanisms in a preclinical rat model of chronic pain. *J. Pain* 16, 60–66. doi: 10.1016/j.jpain.2014.10.007
- George, K. S., and Wu, S. (2012). Lipid raft: a floating island of death or survival. *Toxicol. Appl. Pharmacol.* 259, 311–319. doi: 10.1016/j.taap.2012.01.007
- Golub, T., Wacha, S., and Caroni, P. (2004). Spatial and temporal control of signaling through lipid rafts. *Curr. Opin. Neurobiol.* 14, 542–550. doi: 10.1016/j.conb.2004.08.003
- Goodrum, J. F. (1991). Cholesterol from degenerating nerve myelin becomes associated with lipoproteins containing apolipoprotein E. *J. Neurochem.* 56, 2082–2086. doi: 10.1111/j.1471-4159.1991.tb03469.x
- Goritz, C., Mauch, D. H., and Pfriger, F. W. (2005). Multiple mechanisms mediate cholesterol-induced synaptogenesis in a CNS neuron. *Mol. Cell. Neurosci.* 29, 190–201. doi: 10.1016/j.mcn.2005.02.006
- Grosse, P. Y., Bressolle, F., and Pinguet, F. (1998). Antiproliferative effect of methyl-beta-cyclodextrin in vitro and in human tumour xenografted athymic nude mice. *Br. J. Cancer* 78, 1165–1169. doi: 10.1038/bjc.1998.648
- Guirland, C., Suzuki, S., Kojima, M., Lu, B., and Zheng, J. Q. (2004). Lipid rafts mediate chemotropic guidance of nerve growth cones. *Neuron* 42, 51–62. doi: 10.1016/S0896-6273(04)00157-6
- Hausott, B., Rietzler, A., Vallant, N., Auer, M., Haller, I., Perkhofer, S., et al. (2011). Inhibition of fibroblast growth factor receptor 1 endocytosis promotes axonal branching of adult sensory neurons. *Neuroscience* 188, 13–22. doi: 10.1016/j.neuroscience.2011.04.064
- Head, B. P., Patel, H. H., and Insel, P. A. (2014). Interaction of membrane/lipid rafts with the cytoskeleton: impact on signaling and function: membrane/lipid rafts, mediators of cytoskeletal arrangement and cell signaling. *Biochim. Biophys. Acta* 1838, 532–545. doi: 10.1016/j.bbame.2013.07.018
- Kalka, D., von Reitzenstein, C., Kopitz, J., and Cantz, M. (2001). The plasma membrane ganglioside sialidase cofractionates with markers of lipid rafts. *Biochem. Biophys. Res. Commun.* 283, 989–993. doi: 10.1006/bbrc.2001.4864
- Kamiguchi, H. (2006). The region-specific activities of lipid rafts during axon growth and guidance. *J. Neurochem.* 98, 330–335. doi: 10.1111/j.1471-4159.2006.03888.x
- Kappagantula, S., Andrews, M. R., Cheah, M., Abad-Rodríguez, J., Dotti, C. G., and Fawcett, J. W. (2014). Neu3 sialidase-mediated ganglioside conversion is necessary for axon regeneration and is blocked in CNS axons. *J. Neurosci.* 34, 2477–2492. doi: 10.1523/JNEUROSCI.4432-13.2014
- Korade, Z., and Kenworthy, A. K. (2008). Lipid rafts, cholesterol, and the brain. *Neuropharmacology* 55, 1265–1273. doi: 10.1016/j.neuropharm.2008.02.019
- Lamaze, C., Dujeancourt, A., Baba, T., Lo, C. G., Benmerah, A., and Dautry-Varsat, A. (2001). Interleukin 2 receptors and detergent-resistant membrane domains define a clathrin-independent endocytic pathway. *Mol. Cell.* 7, 661–671. doi: 10.1016/S1097-2765(01)00212-X
- Leitinger, B., and Hogg, N. (2002). The involvement of lipid rafts in the regulation of integrin function. *J. Cell Sci.* 115(Pt 5), 963–972.
- Merris, M., Kraeft, J., Tint, G. S., and Lenard, J. (2004). Long-term effects of sterol depletion in elegans, C: sterol content of synchronized wild-type and mutant populations. *J. Lipid Res.* 45, 2044–2051. doi: 10.1194/jlr.M400100-JLR200
- Navarro, X. (2016). Functional evaluation of peripheral nerve regeneration and target reinnervation in animal models: a critical overview. *Eur. J. Neurosci.* 43, 271–286. doi: 10.1111/ejn.13033
- Ormerod, K. G., Rogasevskaja, T. P., Coorsen, J. R., and Mercier, A. J. (2012). Cholesterol-independent effects of methyl-beta-cyclodextrin on chemical synapses. *PLoS One* 7:e36395. doi: 10.1371/journal.pone.0036395
- Pristera, A., Baker, M. D., and Okuse, K. (2012). Association between tetrodotoxin resistant channels and lipid rafts regulates sensory neuron excitability. *PLoS One* 7:e40079. doi: 10.1371/journal.pone.0040079
- Rishal, I., and Fainzilber, M. (2014). Axon-soma communication in neuronal injury. *Nat. Rev. Neurosci.* 15, 32–42. doi: 10.1038/nrn3609
- Rodal, S. K., Skretting, G., Garred, O., Vilhardt, F., van Deurs, B., and Sandvig, K. (1999). Extraction of cholesterol with methyl-beta-cyclodextrin perturbs formation of clathrin-coated endocytic vesicles. *Mol. Biol. Cell* 10, 961–974. doi: 10.1091/mbc.10.4.961
- Rodrigues, H. A., Lima, R. F., Fonseca, C., Mde Amaral, E. A., Martinelli, P. M., Naves, L. A., et al. (2013). Membrane cholesterol regulates different modes of synaptic vesicle release and retrieval at the frog neuromuscular junction. *Eur. J. Neurosci.* 38, 2978–2987. doi: 10.1111/ejn.12300
- Romeo-Guitart, D., Fores, J., Herrando-Grabulosa, M., Valls, R., Leiva-Rodríguez, T., Galea, E., et al. (2018). Neuroprotective drug for nerve trauma revealed using artificial intelligence. *Sci. Rep.* 8:1879. doi: 10.1038/s41598-018-19767-3
- Ros, O., Cotrufo, T., Martínez-Marmol, R., and Soriano, E. (2015). Regulation of patterned dynamics of local exocytosis in growth cones by netrin-1. *J. Neurosci.* 35, 5156–5170. doi: 10.1523/JNEUROSCI.0124-14.2015
- Saghy, E., Szoke, E., Payrits, M., Helyes, Z., Borzsei, R., Erotyak, J., et al. (2015). Evidence for the role of lipid rafts and sphingomyelin in Ca²⁺-gating of transient receptor potential channels in trigeminal sensory neurons and peripheral nerve terminals. *Pharmacol. Res.* 100, 101–116. doi: 10.1016/j.phrs.2015.07.028
- Saher, G., Brugger, B., Lappe-Siefke, C., Mobius, W., Tozawa, R., Wehr, M. C., et al. (2005). High cholesterol level is essential for myelin membrane growth. *Nat. Neurosci.* 8, 468–475. doi: 10.1038/nn1426
- Santucci, A., Sytnyk, V., Leshchyn'ska, I., and Schachner, M. (2005). Prion protein recruits its neuronal receptor NCAM to lipid rafts to activate p59fyn and to enhance neurite outgrowth. *J. Cell Biol.* 169, 341–354. doi: 10.1083/jcb.200409127
- Schnaar, R. L., Gerardy-Schahn, R., and Hildebrandt, H. (2014). Sialic acids in the brain: gangliosides and polysialic acid in nervous system development,

- stability, disease, and regeneration. *Physiol. Rev.* 94, 461–518. doi: 10.1152/physrev.00033.2013
- Schneider, C. A., Rasband, W. S., and Eliceiri, K. W. (2012). NIH Image to ImageJ: 25 years of image analysis. *Nat. Methods* 9, 671–675. doi: 10.1038/nmeth.2089
- Tassew, N. G., Mothe, A. J., Shabanzadeh, A. P., Banerjee, P., Koeberle, P. D., Bremner, R., et al. (2014). Modifying lipid rafts promotes regeneration and functional recovery. *Cell Rep.* 8, 1146–1159. doi: 10.1016/j.celrep.2014.06.014
- Upadhyay, A. K., Singh, S., Chhipa, R. R., Vijayakumar, M. V., Ajay, A. K., and Bhat, M. K. (2006). Methyl-beta-cyclodextrin enhances the susceptibility of human breast cancer cells to carboplatin and 5-fluorouracil: involvement of Akt, NF-kappaB and Bcl-2. *Toxicol. Appl. Pharmacol.* 216, 177–185. doi: 10.1016/j.taap.2006.05.009
- Verdu, E., Buti, M., and Navarro, X. (1996). Functional changes of the peripheral nervous system with aging in the mouse. *Neurobiol. Aging* 17, 73–77. doi: 10.1016/0197-4580(95)02010-1
- Vinson, M., Rausch, O., Maycox, P. R., Prinjha, R. K., Chapman, D., Morrow, R., et al. (2003). Lipid rafts mediate the interaction between myelin-associated glycoprotein (MAG) on myelin and MAG-receptors on neurons. *Mol. Cell. Neurosci.* 22, 344–352. doi: 10.1016/S1044-7431(02)00031-3
- Vyas, A. A., Patel, H. V., Fromholt, S. E., Heffer-Laue, M., Vyas, K. A., Dang, J., et al. (2002). Gangliosides are functional nerve cell ligands for myelin-associated glycoprotein (MAG), an inhibitor of nerve regeneration. *Proc. Natl. Acad. Sci. U.S.A.* 99, 8412–8417. doi: 10.1073/pnas.072211699
- Zhang, Y. H., Khanna, R., and Nicol, G. D. (2013). Nerve growth factor/p75 neurotrophin receptor-mediated sensitization of rat sensory neurons depends on membrane cholesterol. *Neuroscience* 248, 562–570. doi: 10.1016/j.neuroscience.2013.06.039
- Zhou, M. H., Yang, G., Jiao, S., Hu, C. L., and Mei, Y. A. (2012). Cholesterol enhances neuron susceptibility to apoptotic stimuli via cAMP/PKA/CREB-dependent up-regulation of Kv2.1. *J. Neurochem.* 120, 502–514. doi: 10.1111/j.1471-4159.2011.07593.x
- Zidovetzki, R., and Levitan, I. (2007). Use of cyclodextrins to manipulate plasma membrane cholesterol content: evidence, misconceptions and control strategies. *Biochim. Biophys. Acta* 1768, 1311–1324. doi: 10.1016/j.bbamem.2007.03.026

Conflict of Interest Statement: The authors declare that the research was conducted in the absence of any commercial or financial relationships that could be construed as a potential conflict of interest.

Copyright © 2019 Roselló-Busquets, de la Oliva, Martínez-Mármol, Hernaiz-Llorens, Pascual, Muhaisen, Navarro, del Valle and Soriano. This is an open-access article distributed under the terms of the Creative Commons Attribution License (CC BY). The use, distribution or reproduction in other forums is permitted, provided the original author(s) and the copyright owner(s) are credited and that the original publication in this journal is cited, in accordance with accepted academic practice. No use, distribution or reproduction is permitted which does not comply with these terms.



Role of Noradrenergic Inputs From Locus Coeruleus on Changes Induced on Axotomized Motoneurons by Physical Exercise

Ariadna Arbat-Plana, Maria Puigdomenech, Xavier Navarro and Esther Udina*

Department of Cell Biology, Physiology and Immunology, Institute of Neurosciences, Centro de Investigación Biomédica en Red sobre Enfermedades Neurodegenerativas, Universitat Autònoma de Barcelona, Bellaterra, Spain

OPEN ACCESS

Edited by:

Qi Yuan,
Memorial University of Newfoundland,
Canada

Reviewed by:

Elena Vazey,
University of Massachusetts Amherst,
United States
Fani Moreira Neto,
Universidade do Porto, Portugal

*Correspondence:

Esther Udina
esther.udina@uab.cat

Received: 29 September 2018

Accepted: 11 February 2019

Published: 26 February 2019

Citation:

Arbat-Plana A, Puigdomenech M, Navarro X and Udina E (2019) Role of Noradrenergic Inputs From Locus Coeruleus on Changes Induced on Axotomized Motoneurons by Physical Exercise. *Front. Cell. Neurosci.* 13:65. doi: 10.3389/fncel.2019.00065

Physical rehabilitation is one of the cornerstones for the treatment of lesions of the nervous system. After peripheral nerve injuries, activity dependent therapies promote trophic support for the paralyzed muscles, enhance axonal growth and also modulate the maladaptive plastic changes induced by the injury at the spinal level. We have previously demonstrated that an intensive protocol of treadmill running (TR) in rats reduces synaptic stripping on axotomized motoneurons, preserves their perineuronal nets (PNN) and attenuates microglia reactivity. However, it is not clear through which mechanisms exercise is exerting these effects. Here we aimed to evaluate if activation of the locus coeruleus (LC), the noradrenergic center in the brain stem, plays a role in these effects. Since LC is strongly activated during stressful situations, as during intensive exercise, we selectively destroyed the LC by administering the neurotoxin DSP-4 before injuring the sciatic nerve of adult rats. Animals without LC had increased microglia reactivity around injured motoneurons. In these animals, an increasing intensity protocol of TR was not able to prevent synaptic stripping on axotomized motoneurons and the reduction in the thickness of their PNN. In contrast, TR was still able to attenuate microglia reactivity in DSP-4 treated animals, thus indicating that the noradrenergic projections are important for some but not all the effects that exercise induces on the spinal cord after peripheral nerve injury. Moreover, animals subjected to treadmill training showed delayed muscle reinnervation, more evident if treated with DSP-4. However, we did not find differences in treated animals regarding the H/M amplitude ratio, which increased during the first stages of regeneration in all injured groups.

Keywords: peripheral nerve injury, spinal circuitry, physical exercise, motoneuron, noradrenaline, locus coeruleus

INTRODUCTION

Peripheral nerve injury (PNI) results in a loss of motor, sensory and autonomic function in the denervated territory. Although peripheral axons have the ability to regenerate, this regenerative process is slow and functional recovery is often limited, mainly due to unspecific reinnervation of the target organs but also to alterations at the central level. The disconnection between the neurons and their target organs is accompanied by a disorganization of the central circuitry, in

part due to the massive stripping of central synapses that axotomized motoneurons suffer. The most affected ones are the proprioceptive afferents from the muscle spindle that never recover basal values (Alvarez et al., 2010).

There is extensive literature on the use of activity-dependent therapies to improve axonal regeneration (van Meeteren et al., 1997; Al-majed et al., 2000; Sabatier et al., 2008; Asensio-Pinilla et al., 2009), and muscle reinnervation after sciatic nerve injury in rats (Asensio-Pinilla et al., 2009; Udina et al., 2011a). In general, when initiated during the denervation phase, moderate exercise training results in accelerated functional recovery (Gutmann and Jokubek, 1963), whereas forced exercise or long-term hyperactivity tend to have a detrimental effect (Herbison et al., 1974; van Meeteren et al., 1997). Activity can also modulate the plastic changes observed after PNI, as neuropathic pain (Nam et al., 2001; Cobiañchi et al., 2010) and hyperreflexia (Vivó et al., 2008; Asensio-Pinilla et al., 2009; Udina et al., 2011a). Increased activity, by reducing excitability of sensory neurons and synaptic stripping of motoneurons, attenuates maladaptive plastic changes in the spinal cord and central pathways (Mòdol et al., 2014; Arbat-Plana et al., 2015).

Although it is well-known that exercise exerts positive effects on the nervous system through modulation of brain derived neurotrophic factor (BDNF) (Hutchinson et al., 2004; Molteni et al., 2004; Gomez-Pinilla et al., 2012; Cobiañchi et al., 2013), in a recent work we observed that pharmacological activation of TrkB, the specific receptor of BDNF, did not mimic all the effects of exercise on axotomized spinal motoneurons (Arbat-Plana et al., 2016). Moreover, we had previously shown that the integrity of sensory inputs from the injured limb is important for the maintenance of motoneuron perineuronal nets (PNN) induced by treadmill exercise (Arbat-Plana et al., 2015). PNN restrict plasticity and stabilize synapses (Kwok et al., 2011), and thus exercise, by activating proprioceptive and cutaneous receptors, facilitates preservation of central circuits after PNI. However, besides peripheral activation of muscles and sensory receptors, physical exercise is also activating a complex central circuitry related with locomotion and stress. Among it, the activation of noradrenergic neurons of the locus coeruleus (LC) may be important. Whereas ascending projections from this brain stem center, as part of the ascending reticular formation system, regulates arousal and attention (Berridge and Waterhouse, 2003), descending projections inhibit nociceptive transmission (Millan, 2002; Pertovaara, 2006) and modulate excitability of motoneurons (Heckman et al., 2003) in the spinal cord. In addition, noradrenaline release influences microglial function, by suppressing production of pro-inflammatory cytokines and promoting anti-inflammatory mediators (Heneka et al., 2010; Jandanhazi-Kurutz et al., 2011). Interestingly, an intensive protocol of treadmill exercise is able to attenuate the activation of microglia observed in the spinal cord after PNI (Cobiañchi et al., 2010). This anti-inflammatory effect may be related to the increased activation of the LC induced by physical activity. However, the role of the LC in the activity-dependent-modulation of the spinal changes observed after axotomy has not been addressed yet. The LC can be chemically destroyed by using the neurotoxin

N-(2-chloroethyl)-N-ethyl-2-bromobenzylamine (DSP-4), that selectively damages noradrenergic projections originating from the LC, inducing degeneration of noradrenergic terminals (Dooley et al., 1987; Dudley et al., 1990; Prieto and Giral, 2001; Scullion et al., 2009). Therefore, we evaluated the role of the LC on the modulation of physical exercise on the plastic changes that motoneurons suffer after axotomy by submitting to TR control rats and rats that previously had suffered chemical ablation of the LC.

MATERIALS AND METHODS

Experimental Design

Adult female Sprague Dawley rats (8 weeks old, 200–280 g) were housed with free access to food and water at room temperature of $22 \pm 2^\circ\text{C}$ under a 12:12-h light–dark cycle. All experimental procedures were approved by the ethics committee of Universitat Autònoma de Barcelona and followed the guidelines of the European Commission on Animal Care (EU Directive 2010/63/EU). For all surgical interventions, rats were anesthetized by intraperitoneal administration of ketamine (90 mg/kg, 0.9 ml/kg; Imalgen 2000) supplemented with xylazine (10 mg/kg, 0.5 ml/kg; Rompun 2%).

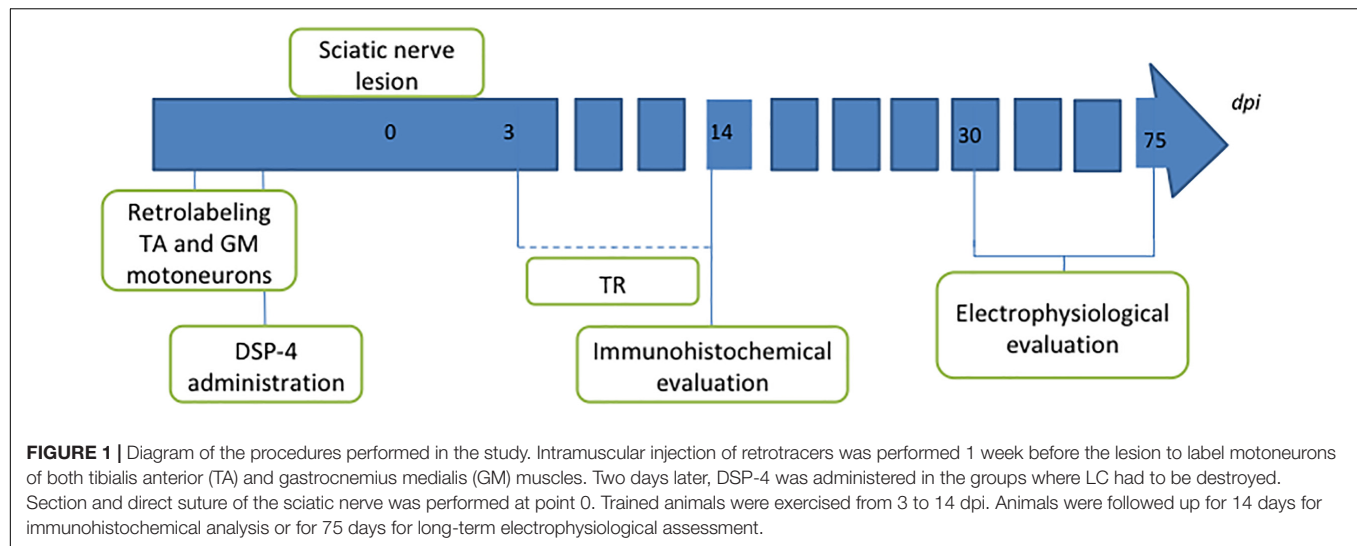
One group of animals was used as control group; these animals were only axotomized and did not receive any treatment (AX). Two groups of animals received DSP-4 before the surgery, as described below. Animals of one of these groups were subjected to exercise 3 days after the surgery (DSP-4+TR) whereas the other ones were not trained (DSP-4). A fourth group was subjected to the same protocol of exercise without receiving pharmacological treatment (TR). Each group was divided in two subgroups: one subgroup was euthanized 14 days after injury (short-term) to evaluate motoneurons changes and the other was euthanized 75 days after injury (long-term) in order to evaluate functional recovery (Figure 1 and Table 1). Contralateral side was used as control-intact side.

Retrograde Labeling

Retrograde tracing [True Blue Chloride (TB, Setareh Biotech) and Fluorogold (FG, Fluorochrome)] were bilaterally applied 1 week before intervention to identify motoneuron pools of both tibialis anterior (TA) and gastrocnemius medialis (GM) muscles. A small incision to the skin was made to expose the muscle, and then two injections (2.5 μl /injection) were distributed within the muscle with a glass pipette using a Picospritzer (Arbat-Plana et al., 2015). The area of application was rinsed with saline to clean any remnants of the tracer and the skin wound was sutured.

Surgical Procedure

Under anesthesia, the sciatic nerve was exposed at the mid-thigh and cut by using micro scissors. The proximal and distal stumps were rejoined with two epineural 10-0 sutures. Afterward, muscle and skin were sutured in layers, iodine povidone was applied to the wound, and the rats were allowed to recover in a warm environment under close observation.



Noradrenergic Depletion

DSP-4 (Sigma Aldrich) was dissolved in sterile NaCl 0.9% saline and delivered as a single i.p. dose of 50 mg/kg according to the work of Lyons et al. (1989) within 10 min of preparation. DSP-4 was administered 4 days before the injury to ensure LC destruction at the beginning of the treadmill protocol. Control animals received a single i.p. injection of saline solution. The doses of DSP-4 used were devoid of adverse effects, and therefore rats did not require special care during follow up.

Treadmill Training Protocol

To acclimatize the animals subject to training exercise in a motor-driven rodent treadmill (Treadmill LE 8706, LETICA, Spain), they were placed on the treadmill for 60 min twice a week prior to surgery. During these training sessions, previous to surgery, shock grid intensity was set at 0.4 mA to provide a mild negative stimulus. The TR protocol was started 3 days after surgery and was carried out during 2 weeks. TR consisted of one session of TR 5 days/week with duration and intensity being progressively increased; running started at a locomotion speed of 10 cm/s that was increased 2 cm/s every 5 min, until a maximum speed of 30 cm/s for 60 min was reached during the final training session (Cobianchi et al., 2013).

TABLE 1 | Description of the different experimental groups used in this study, the type of follow-up and the number of animals used.

Group	Follow-up	Study
(1) Control group (AX)	Short-term	Changes around soma ($n = 4$)
	Long-term	EMG ($n = 5$)
(2) DSP-4 administration group (DSP-4)	Short-term	Changes around soma ($n = 4$)
	Long-term	EMG ($n = 5$)
(3) DSP-4 + Treadmill running (DSP-4+TR)	Short-term	Changes around soma ($n = 4$)
	Long-term	EMG ($n = 5$)
(4) Treadmill running (TR)	Short-term	Changes around soma ($n = 4$)
	Long-term	EMG ($n = 5$)

Immunohistochemical Analysis of Locus Coeruleus and Spinal Cord

Fourteen days after sciatic nerve injury, deeply anesthetized animals were transcardially perfused with 4% paraformaldehyde in PBS. Brain and L3–L6 spinal cord segment were removed, post-fixed for 4 h, cryoprotected in 30% sucrose, and stored at 4°C until use. To localize the LC in the brain, we used an acrylic array of coronal brain matrix (Acrylic brain matrices Alto, for small rat coronal, 175–300 gr). Both brain and spinal cord samples were embedded in Tissue-Tek, serially cut (25 and 20 μ m thickness, respectively) with a cryostat, and collected onto gelatin-coated glass slides. All sections were first blocked with 10% normal bovine serum for 1 h, followed by overnight incubation at 4°C with anti-tyrosine hydroxylase (1:500, Sigma) for the brain sections or combinations of primary antibodies for the spinal cord sections: rabbit anti Synaptophysin (1:200, Covance), guinea pig anti VGlut1 (1:300, Millipore), guinea pig anti VGat (1:200, Synaptic Systems), Lectin from Wisteria Floribunda (1:100, Sigma), mouse anti GFAP (1:1000, Millipore), rabbit anti Iba1 (1:500, Wako). After washes, immunoreactive sites were revealed by species-specific secondary antibodies conjugated to 488 Alexa Fluor (1:200, Invitrogen), 538 Alexa Fluor (1:500, Invitrogen), Cy3 (1:200, Millipore), or Streptavidin 488 Alexa Fluor (1:200, Invitrogen). After 2 h incubation at room temperature, the sections were thoroughly washed, mounted on slides, and coverslipped with Fluoromount-G (SouthernBiotech). Back-labeled motoneurons were localized and images captured with a scanning confocal microscope (LSM 700 Axio Observer, Carl Zeiss 40 \times /1.3 Oil DIC M27). On the brain sections, LC was localized and images captured with an epifluorescence microscope (Nikon eclipse Ni DS-Ri2, 40 \times).

Image analysis, processing and regression analysis from motoneurons labeling quantification were performed by means of in-house software implemented in MATLAB R2012b (The Mathworks Inc., Natick, MA, United States). Firstly, back-labeled motoneurons were automatically selected and delineated and a constant threshold was used to segment and obtain an estimated

average density for each labeling. As a control for the background, the software checked for each analyzed neuron that the soma had no labeling for the set threshold. Immunoreactivity was evaluated in a perimeter of 5 μm thickness surrounding the motoneuron soma (Arbat-Plana et al., 2015). Since some variability between animals, samples and processing can occur, similar amount of motoneurons from both sides were analyzed in each slide. For each animal, 10 to 15 motoneurons of each pool and each side were analyzed.

Electrophysiology Tests

For the long term follow-up, motor reinnervation and H reflex were assessed by means of nerve conduction tests, performed at 30, 45, 60, and 75 days after surgery, using an electromyography apparatus (Synergy Medelec, Viasys HealthCare). Electrophysiological evaluation was performed under ketamine/xylazine anesthesia. During the test, the rat body temperature was kept constant between 34 and 36°C by means of a thermostated flat coil. The sciatic nerve was stimulated by two needle electrodes percutaneously inserted at the sciatic notch, applying single rectangular pulses of 0.1 ms duration up to the voltage required to obtain a maximal evoked response. The compound muscle action potentials (CMAP) were recorded from the TA, GM and plantar (PL) muscles with microneedle electrodes. Onset latency and amplitude from baseline to the maximal negative peak of the direct M wave and the reflex H wave were measured. The maximal H/M amplitude ratio was calculated for each muscle tested. The H wave (the electrophysiological equivalent of the stretch reflex) suffers a rate dependent depression (RDD) that is useful to corroborate that the recorded wave is truly the H wave. It is important to note that at early stages of regeneration, characterized by polyphasic CMAPs in the reinnervated muscles, the H wave can be masked. Thus, to ensure that the selected wave was the H wave, repeat stimulation was applied at increasing frequencies (0.3, 1, 3, 5, 10, 15, 20, and 30 pps) and at the threshold intensity for the H wave. The ratio between the amplitude of the last and the first H wave recorded for the different protocols was calculated, in order to evaluate the RDD. The different tests were performed also in the contralateral non-injured side to obtain control values for each animal.

Statistical Analysis

For the immunohistochemical analysis, quantitative variables were normality assessed by Shapiro-Wilk test (Royston, 1993). For variables with a normal distribution one-way ANOVA and *post hoc* analysis by Bonferroni test were used to test the significance of the difference between the lesion side and the contralateral side. For non-normal variables such analysis was performed by Kruskal-Wallis test. SPSS 20.0 (SPSS Inc., Chicago, IL, United States) was used for statistical analyses. A nested design ANOVA test was used in order to determine if the variability was due to differences between the different motoneurons or between animals in each group. The H/M ratio and RDD data were analyzed by two way ANOVA with Bonferroni *post hoc* correction.

RESULTS

DSP-4 was administrated to destroy the LC and thus, to evaluate the effects of this center on the spinal changes mediated by TR during 14 days following PNI. Firstly, we explored the state of LC after DSP-4 administration using Tyrosine Hydroxylase antibody (TH), which is a useful marker for dopaminergic and noradrenergic neurons. To localize the LC we used sections 9.16 to 10.04 mm caudal to Bregma, following the Rat Brain Atlas in stereotaxic coordinates (Paxinos and Watson, 1998).

In control animals, a group of TH+ neurons organized in a typical triangular shape was easily localized in each side of the 4th ventricle (**Figure 2A**). In contrast, in DSP-4 treated animals, few TH+ neurons were localized (**Figure 2B**). In some animals, isolated brightly stained neurons were observed in the region (**Figure 2C**).

Effects of DSP-4 Administration on Central Changes After Axotomy

Synaptophysin (Syn) immunolabeling, a general marker for synapses, showed that the number of synaptic coverage of motoneurons was reduced after sciatic nerve injury, whereas TR partially preserved that loss ($77 \pm 3 \text{ Syn}/\mu\text{m}^2$ and $97 \pm 3 \text{ Syn}/\mu\text{m}^2$ in AX animals vs. $89 \pm 2 \text{ Syn}/\mu\text{m}^2$ and $104 \pm 4 \text{ Syn}/\mu\text{m}^2$ in trained animals, in TA and GM, respectively, $p < 0.01$). No significant differences were found between animals treated with DSP-4 ($83 \pm 3 \text{ Syn}/\mu\text{m}^2$ in both TA and GM) compared to control injured animals. DSP-4 administration combined with TR induced a marked decrease of synapses labeling on injured motoneurons compared to AX ($63 \pm 5 \text{ Syn}/\mu\text{m}^2$ in TA and $71 \pm 10 \text{ Syn}/\mu\text{m}^2$ in GM, $p < 0.05$) (**Figures 3A, 4**).

Excitatory synapses were analyzed using VGlut1, a specific marker of proprioceptive afferents from the muscle spindle. Axotomized TA and GM motoneurons had a density of about 40 ± 2 per μm^2 , less than half than in intact motoneurons. After TR, the loss of excitatory synapses was also attenuated ($60 \pm 4 \text{ VGlut1}/\mu\text{m}^2$ in both TA and GM, $p < 0.01$). Animals treated with DSP-4 did not show significant differences compared to injured control animals ($42 \pm 5 \text{ VGlut1}/\mu\text{m}^2$). However, animals treated with DSP-4 subjected to TR showed a significant decrease of VGlut1 contacts on motoneurons in both TA and GM pools compared to AX and TR animals ($30 \pm 3 \text{ VGlut1}/\mu\text{m}^2$, $p < 0.01$) (**Figures 3B, 4**).

The reduction of excitatory VGlut1 synapses suffered by axotomized motoneurons was accompanied by an increase of VGat labeled inhibitory synapses ($67 \pm 1 \text{ VGat}/\mu\text{m}^2$ and $100 \pm 3 \text{ VGat}/\mu\text{m}^2$ in TA and GM, respectively). TR animals, showed a lower increase in inhibitory synapses after axotomy ($49 \pm 2 \text{ VGat}/\mu\text{m}^2$ and $85 \pm 2 \text{ VGat}/\mu\text{m}^2$ in TA and GM, $p < 0.01$) than controls. In this case, no significant differences were found between DSP-4 and DSP-4+TR animals compared to control animals (**Figures 3C, 4**).

Wisteria floribunda immunoreactivity was used to analyze PNN. Axotomized motoneurons had a reduction in the amount

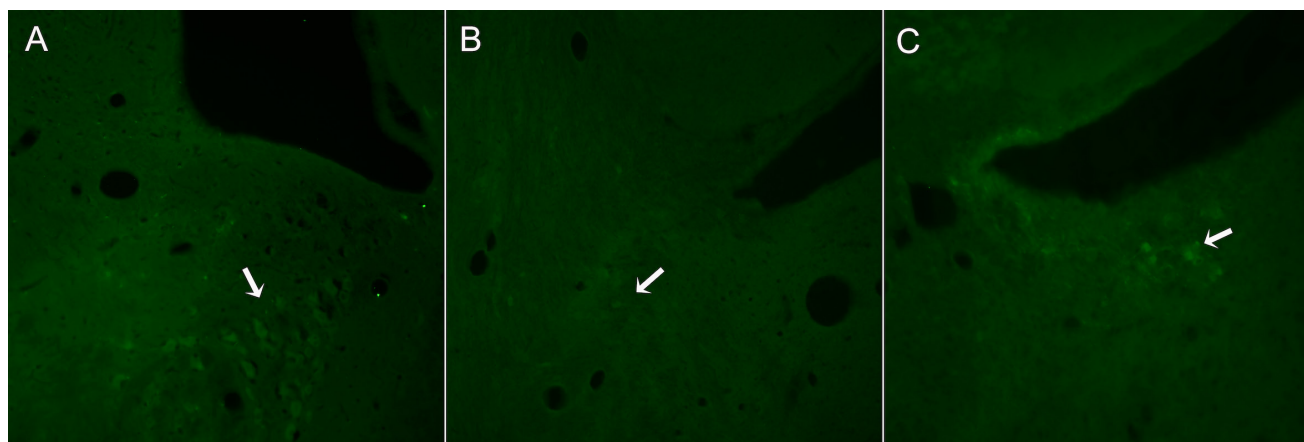


FIGURE 2 | Representative images from sections of the brain stem regions where LC is localized in animals non-treated (**A**) or treated with DSP-4 (**B,C**) and immunostained against TH. The characteristic triangular shape of the LC nucleus (**A**) is lost 14 days after DSP-4 treatment. Hardly any TH+ neuron can be seen in the region (arrow, **B**), being some isolated neurons highly stained (arrow, **C**).

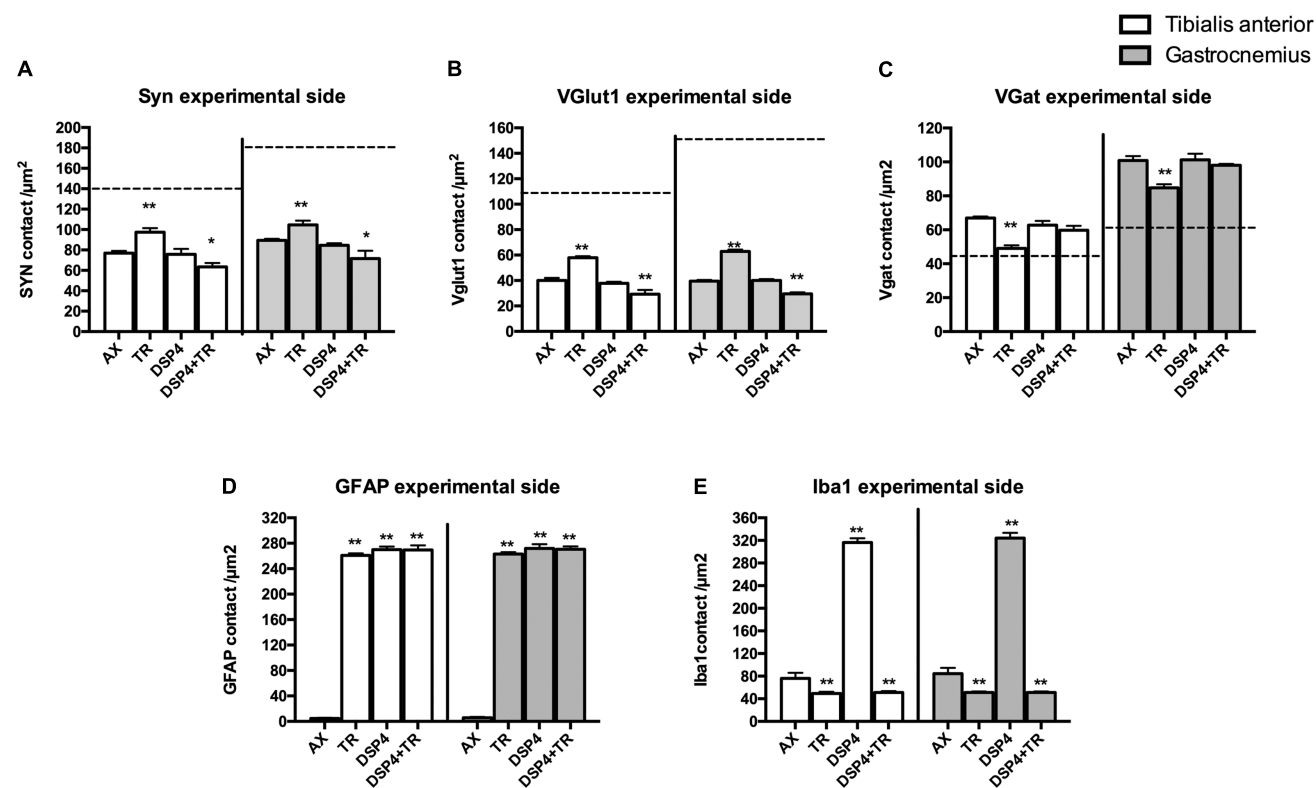


FIGURE 3 | Quantitative analysis of synaptic stripping and excitatory/inhibitory synapses after axotomy in the different groups of animals. Evaluation of Synaptophysin (**A**), Vglut1 (**B**), Vgat (**C**), GFAP (**D**), and Iba1 (**E**) in TA (white bars) and GM (gray bars) 15 days after sciatic nerve cut and suture in sedentary or trained animals, either treated with DSP-4 or untreated. Horizontal dotted lines indicate the average of motoneuron labeling in the non-injured side of both TA and GM motoneurons. Immunoreactivity for GFAP and Iba1 is so low in intact motoneurons that the horizontal dotted lines are missing in **D,E** graphs. Synaptophysin, Iba1 and GFAP values followed a normal distribution, whereas Vglut1 followed a non-normal one. Data are expressed as mean \pm SEM, * $p < 0.05$, ** $p < 0.01$, vs. AX group.

of PNN (52 ± 5 PNN/ μm^2 in AX group compared to 150 ± 21 PNN/ μm^2 in intact rats) that was partially prevented if animals were subjected to exercise (75 ± 4 PNN/ μm^2 ; $p < 0.01$

vs. AX group). We observed that PNN immunoreactivity in injured motoneurons was lower in rats receiving DSP-4 (35 ± 1 PNN/ μm^2 and 42 ± 2 PNN/ μm^2 in TA and GM, respectively)

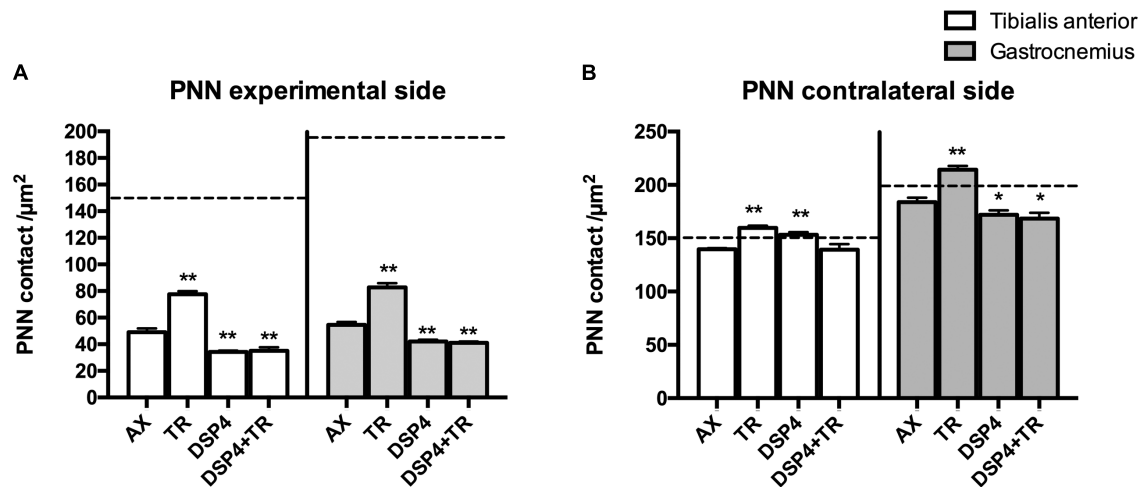


FIGURE 4 | Quantitative analysis of perineuronal nets (PNN) 15 days after axotomy in animals subjected to treadmill or left untrained, either treated with DSP-4 or untreated, in both experimental side (A) and contralateral side (B). Horizontal dotted lines indicate the mean of motoneuron labeling in the non-injured side of both TA and GM motoneurons. PNN values followed a non-normal distribution. Data are expressed as mean \pm SEM, * $p < 0.05$, ** $p < 0.01$, vs. AX group.

than in only injured animals ($p < 0.01$). DSP-4+TR animals had also a low density of PNN surrounding motoneurons (35 ± 5 PNN/ μm^2 in both TA and GM). Interestingly, in DSP-4 group, GM motoneurons at the contralateral side showed a reduced PNN density (172 ± 8 PNN/ μm^2) compared to those of AX animals (182 ± 6 PNN/ μm^2), whereas this reduction was not observed in PNN from TA motoneurons (145 ± 18 PNN/ μm^2 in DSP-4 group and 139 ± 2 PNN/ μm^2 in AX group) (Figures 4, 5).

Astroglial reactivity, estimated by measuring the density of GFAP immunolabeling surrounding motoneurons, was significantly increased in animals subjected to TR (261 ± 1 and 263 ± 1 GFAP/ μm^2 in TA and GM, respectively) compared to the control injured group (5 ± 1 and 6 ± 1 GFAP/ μm^2 , respectively, $p < 0.001$). Astroglial reactivity was also increased in both groups of animals treated with DSP-4 (around 271 ± 3 GFAP/ μm^2 for both muscles) similarly to TR only animals. Thus, administration of DSP-4 did not affect the modulation of astroglial reactivity induced by exercise (Figures 3, 5).

Iba1 immunostaining around axotomized motoneurons was used to evaluate microglial reactivity. Fourteen days after nerve injury, there was a marked increase of microglia labeling in control rats (76 ± 4 and 84 ± 5 Iba1/ μm^2 in TA and GM, respectively). DSP-4 administration significantly increased microglial reactivity (316 ± 4 and 324 ± 5 Iba1/ μm^2 in TA and GM, respectively, Figure 3) that also presented a phagocytic phenotype (Figure 5). Exercise drastically reduced microglia reactivity around injured motoneurons (49 ± 1 and 51 ± 1 Iba1/ μm^2 in TA and GM, respectively), and similar low activation of microglia was observed in animals treated with DSP-4 and also subjected to exercise (51 ± 1 Iba1/ μm^2 for both muscles), thus indicating that the modulation of microglia by exercise was not affected with the loss of LC.

Muscle Reinnervation

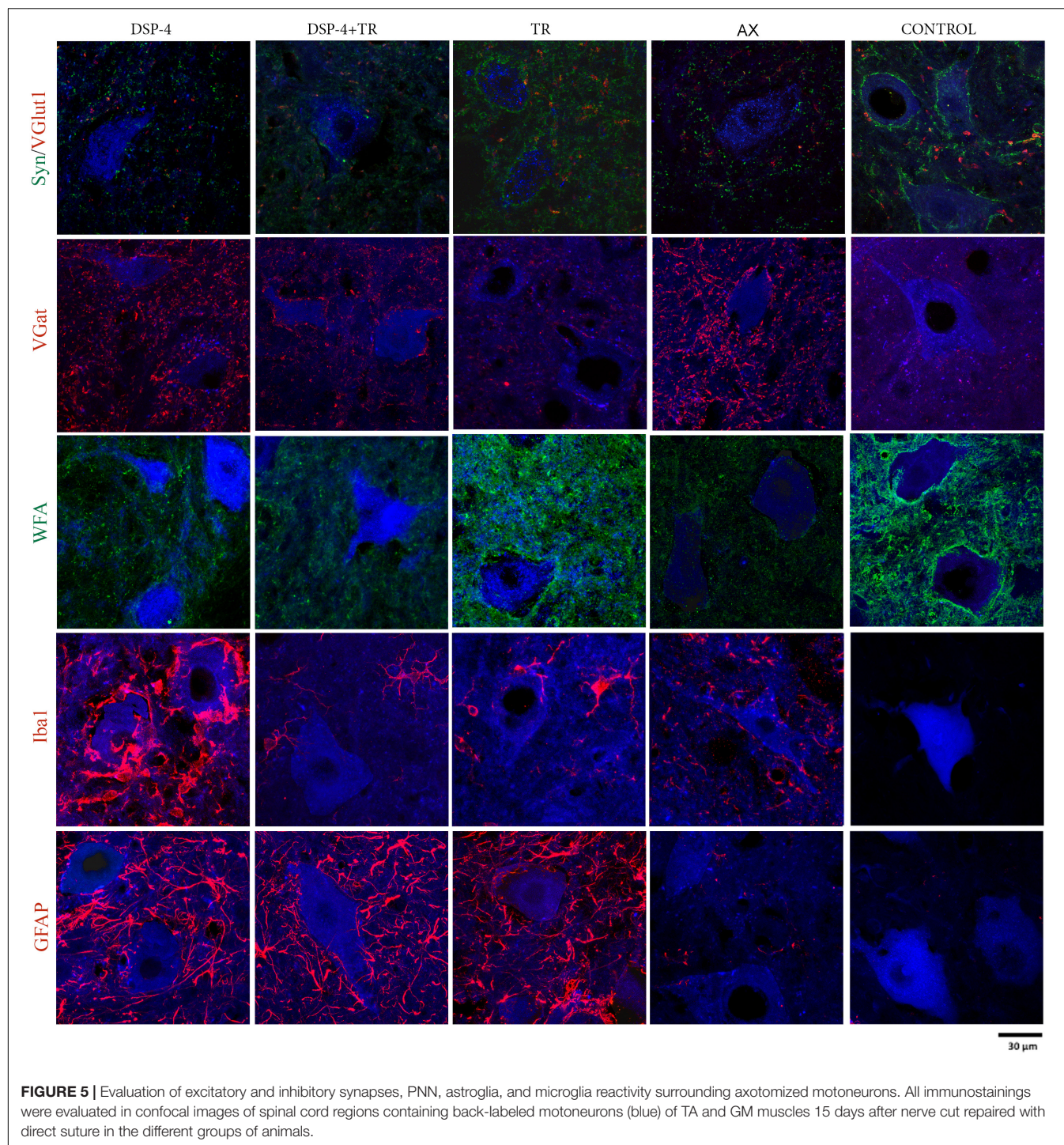
Electrophysiological studies were performed to evaluate motor reinnervation during 75 days after sciatic nerve injury. The M wave values of the muscles at the contralateral side were similar in all animals. At the injured side, all the groups showed an increase in the amplitude of the M wave of the muscles tested along time, but with different progression.

The groups of animals subjected to TR had lower M wave amplitude of the GM muscle at 45 and 60 days than the untreated group. However, at the end of follow up, the TR group achieved similar levels of reinnervation than the control, whereas the DSP-4+TR group remained with lower levels of reinnervation in both GM and TA muscles (Figures 6A,B). GM from DSP-4 group followed a similar progression of reinnervation than GM from control group. In contrast, at the end of follow-up, TA reinnervation in DSP-4 group was significantly higher than in AX group. Reinnervation of the PL muscles started in AX and DSP-4 groups at 45 dpi, and at 60 dpi in TR group. In contrast, in the DSP-4+TR group, we did not record M waves in the PL muscles at the end of follow up (data not shown), further indicating that motor regeneration was hampered by the combination of both treatments (Figures 6A,B).

Regarding the recovery of the H wave, there was an increase of the maximal H/M ratio after sciatic nerve injury, indicative of hyperreflexia, that followed a similar course to attain close to normal values at 75 days, without significant differences between groups (Figures 6C,D). In the injured side, the RDD rate was increased at all time points but again no differences between groups were observed.

DISCUSSION

The results of this study corroborate that a high intensity protocol of TR applied during 2 weeks after sciatic nerve



injury was able to attenuate synaptic stripping and PNN loss around axotomized motoneurons, as we had shown previously (Arbat-Plana et al., 2015). In this work we aimed to analyze if the noradrenergic neurons of the LC play a role in these effects. Since a previous work pointed different responses to exercise in male and female mice (Liu et al., 2015), and we had previously evaluated the effects of two protocol of TR in female rats, here we used the more successful

intensity of exercise to prevent central changes after PNI in female rats only.

The LC is strongly activated in stressful situations and besides its key role in arousal (Berridge and Waterhouse, 2003), it also plays an important role in modulating excitability of spinal motoneurons (Heckman et al., 2003) and nociceptive transmission (Millan, 2002; Pertovaara, 2006). It has recently demonstrated that contrasting modulation of pain-related

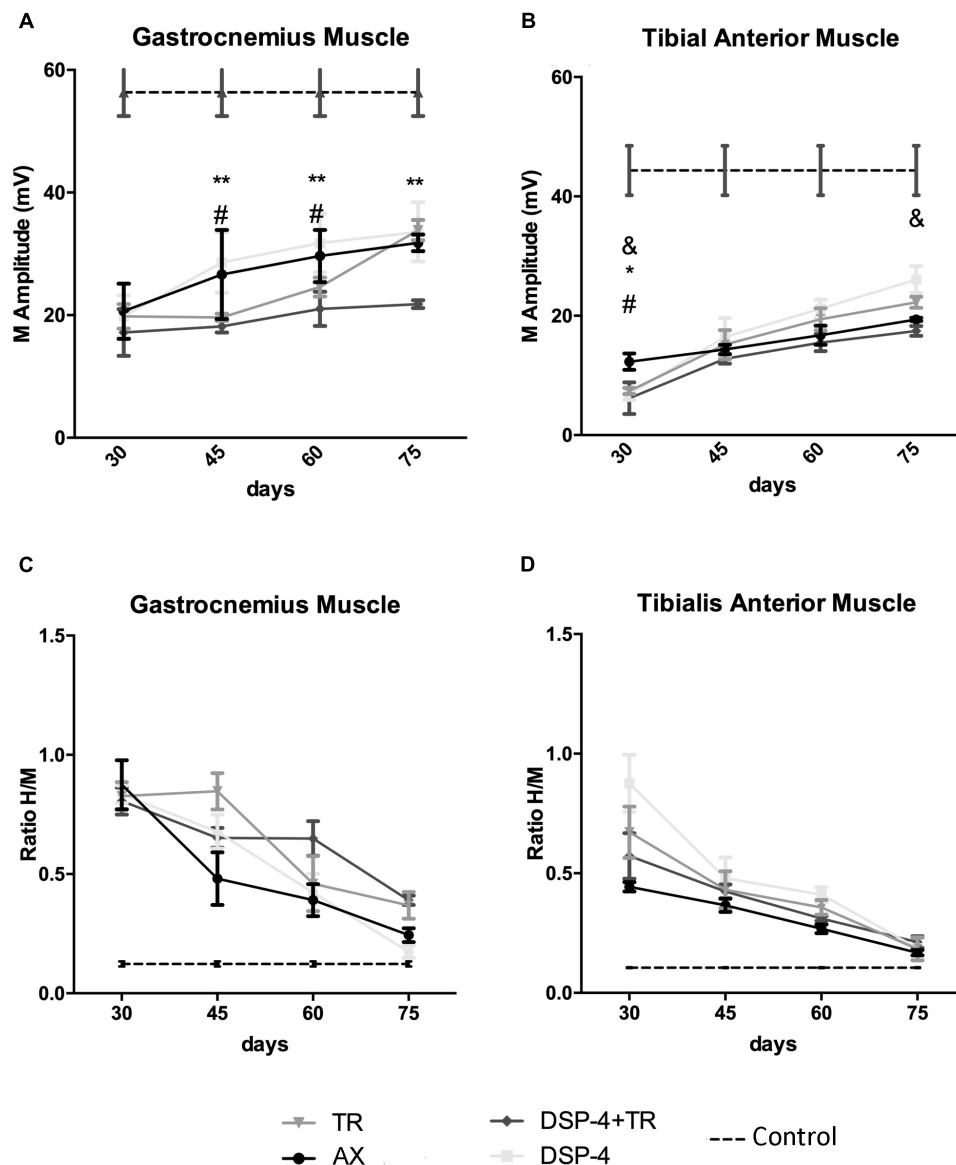


FIGURE 6 | Plots of the amplitude of the CMAPs (A,B) and of the H/M ratio (ratio between the amplitude of the H reflex wave and the amplitude of the direct M wave after electrical stimulation of the nerve) (C,D) from the electrophysiological tests performed in the different experimental groups. Results recorded in GM (A,C) and TA (B,D) muscles at 30, 45, 60, and 75 dpi. Horizontal dotted lines indicate the average of CMAP or H/M ratio in the non-injured side of both TA and GM muscles. Data are expressed as mean \pm SEM, * $p < 0.05$, ** $p < 0.01$, *AX vs. DSP-4+TR; #AX vs. TR; &AX vs. DSP-4.

behaviors is mediated with distinct noradrenergic neuronal populations, being the spinal-projections from the LC the ones related with analgesia (Hirschberg et al., 2017). Therefore, we disrupted the LC by administration of DSP-4 before performing a sciatic nerve injury in rats. DSP-4 is a neurotoxin that quite specifically destroys noradrenergic neurons of the LC, whereas respects similar neurons of other brain stem regions (Ross and Stenfors, 2015).

Destruction of LC did not affect synaptic stripping on axotomized spinal motoneurons. In contrast, when these animals were subjected to TR, the preventing effects of exercise on synaptic stripping were lost. In fact, they even showed more

marked synaptic stripping and larger loss of VGlut1 synaptic contacts than injured control rats. Loss of noradrenergic projections from the brain stem also blocked the ability of TR exercise to revert the reduction in PNN. These results support the hypothesis that the increasing intensity TR protocol promotes activation of the LC, which play a role on the maintenance of synapses in axotomized motoneurons. As stated before, ascending projections from the LC influence arousal and attention (Berridge and Waterhouse, 2003) and optimize also task-performance (Aston-jones and Cohen, 2005). Therefore, loss of these ascending projections could indirectly affect spinal motoneurons. However, since descending neurons project

directly onto the spinal cord, its logical to assume that are the descending neurons the ones mediating most of the effects we observed on DSP-4 treated animals. In fact, the LC is an important source of descending noradrenergic projections to the spinal cord (Grzanna and Fritschy, 1991), and thus its destruction would reduce the noradrenergic inputs that spinal motoneurons receive. Nevertheless, other brainstem noradrenergic nuclei, like A5 and A7, also send projections to the spinal cord. Since DSP-4 is a specific neurotoxin for LC neurons (Ross and Stenfors, 2015), we did not completely abolish all the NA projections that motoneurons receive and, therefore, stronger effects could be expected if all the spinal sources of NA had been ablated.

It is important to take into account that descending noradrenergic projections have a modulatory effect on the excitability of motoneurons, facilitating their activation when receiving other synaptic inputs (Heckman et al., 2008). Noradrenaline acts by facilitating persistent inward currents (PICs) in the dendrites (Hultborn et al., 2004; Perrier and Delgado-Lezama, 2005; Heckman et al., 2008, 2003). When activated, PICs amplify ionotropic synaptic inputs and are essential for normal repetitive firing (Lee and Heckman, 1999; Heckman et al., 2003), and thus for the production and facilitation of movement. Therefore, the loss of noradrenergic projections can reduce the effects of other synaptic inputs on motoneurons and limit the effects of increased activity induced by exercise. It is interesting to note that loss of noradrenergic projections also had effects on PNN of uninjured motoneurons, suggesting a widespread effect. After injury, animals that are not forced to run probably decrease their motor activity and thus, the loss of descendent noradrenergic projections does not potentiate the effects observed after the injury in motoneurons. In contrast, animals forced to run in a treadmill strongly activate these projections. It seems that in these situation, the lack of noradrenergic modulatory inputs in axotomized motoneurons is detrimental on the maintenance of the synaptic arbor and the PNN.

As we have already shown (Arbat-Plana et al., 2015), TR also affects the contralateral side, increasing the thickness of PNN around intact motoneurons, but it is unlikely that this increase has any relevant physiological effect in a context where plasticity is not triggered. In contrast, after a PNI, that lead to changes in the spinal circuitry, preservation of PNN could attenuate maladaptive plasticity and disorganization of the synaptic arbor of axotomized motoneurons, facilitating functional recovery.

Besides its ability to increase activity of the injured circuits and to preserve synapses and PNN in spinal motoneurons, TR exercise also modulates the inflammatory response observed in the spinal cord after PNI. Interestingly, noradrenaline has anti-inflammatory effects in the periphery (Kohm and Sanders, 1999; Sanders and Straub, 2002). Loss of the LC increased microglia reactivity around axotomized motoneurons in DSP-4 treated animals compared to controls. In contrast, animals forced to run in the treadmill downregulated microglia reactivity (Cobianchi et al., 2013). However, this anti-inflammatory effect of exercise at the spinal level seems independent of the LC noradrenergic system, since similar attenuation of microglia reactivity was observed in exercised animals after its depletion. Of course, NA

from other sources could compensate the loss of noradrenergic inputs from LC and thus, modulate this inflammatory response.

Recent works have shown that the inflammatory response is important to switch the peripheral sensory neurons from a neurotransmitter state to a pro-regenerative state (Liberto et al., 2004; Frey et al., 2008; Niemi et al., 2013). Similarly, reactive microglia might influence the regenerative program in axotomized motoneurons. Since noradrenaline is a known anti-inflammatory (Heneka et al., 2010), its reduction in the spinal cord due to LC ablation, by increasing microglia reactivity around motoneurons might facilitate faster axonal regeneration and thus, explain the increased motor reinnervation observed in the DSP-4 group. On the contrary, TR exercise by itself attenuated the inflammatory response and delayed muscle reinnervation, as suggested by the lower amplitude of CMAPs observed in exercised animals during the first 8 weeks. Indeed, the effects of exercise on regeneration and muscle reinnervation are variable, depending upon intensity and duration of the protocol, and the period during which it is applied after the injury (Udina et al., 2011b; Gordon and English, 2015). It has been hypothesized that moderate exercise training enhances functional sensorimotor recovery, whereas forced intense exercise, such as the increasing intensity TR protocol applied here, may have a detrimental effect. In our study we also observed that at later stages, several weeks after stopping TR training, reinnervation improved. However, in exercised animals treated with DSP-4 this late increase of reinnervation was not observed, indicating that LC noradrenergic pathways are somehow mediating the effects of exercise on nerve regeneration.

It is interesting to note that that low intensity TR protocols, although being more effective promoting nerve regeneration and muscle reinnervation (Udina et al., 2011a), have limited effects on the preservation of synapses and PNN on axotomized motoneurons (Arbat-Plana et al., 2015), thus indicating that the protocol that facilitates regeneration differs from the one that favors maintenance of spinal circuitry.

Since the lack of recovery of the functional stretch reflex can be due to the permanent loss of proprioceptive afferent/VGluT1 synapses onto injured motoneurons even when they reinnervate the muscle (Alvarez et al., 2010; Rotterman et al., 2014) we also evaluated the state of the stretch reflex circuit by means of its electrophysiological equivalent, the H wave. The H/M amplitude ratio has been extensively used in the literature to measure spinal excitability. When the spinal reflex response is facilitated, the H/M ratio increases (Burke et al., 1999). At early stages of muscle reinnervation there is an electrophysiological hyperexcitability and the H/M ratio increases; as muscle reinnervation is consolidated, it returns to normal values (Valero-Cabré and Navarro, 2001). In our study we observed the same changes along time, without differences between experimental groups. However, it is argued that the electrophysiological recovery of the H reflex after PNI does not guarantee the functionality of the stretch reflex (Cope et al., 1994; Haftel et al., 2005; Bullinger et al., 2011).

In fact, we previously found that a low intensity protocol of TR (Vivó et al., 2008; Asensio-Pinilla et al., 2009; Udina et al., 2011a) attenuated such hyperexcitability by means of a decreased H/M ratio. However, this protocol was less effective preserving

proprioceptive synapses on axotomized motoneurons than the high intensity TR protocol used here (Arbat-Plana et al., 2015). Therefore, evaluation of the functionality of stretch reflex is needed in order to fully understand the functional relevance of proprioceptive synaptic preservation by exercise after PNI.

In conclusion, LC seems to play a complex role on the effects of exercise on injured motoneurons. This center mediates the ability of physical exercise to activate motoneurons, and contribute to the maintenance of the normal synaptic inputs but does not participate in the anti-inflammatory effect of TR at the spinal level. Other sources of NA or either other monoamines like serotonin (Lopez-Alvarez et al., 2018) can also contribute to the effects of TR on the spinal cord. Interestingly, the sole elimination of LC in injured animals not subjected to exercise markedly increased microglia reactivity and improved early muscle reinnervation. In contrast, TR exercise, by reducing microglia reactivity, would delay motor regeneration and muscle reinnervation. However, this reduced microglia reactivity mediates other positive effects, such as attenuation of synaptic stripping and neuropathic pain (Cobianchi et al., 2010; López-Álvarez et al., 2015). Therefore, it seems that there is a delicate equilibrium between modulation of maladaptive plasticity and enhancement of regeneration. At this stage of research, exercise of moderate intensity seems more adequate than intensive protocols that can interfere with axonal regeneration. Use of combined protocols could also compensate the limitations of single therapeutic approaches.

REFERENCES

- Al-majed, A. A., Brushart, T. M., and Gordon, T. (2000). Electrical stimulation accelerates and increases expression of BDNF and trkB mRNA in regenerating rat femoral motoneurons. *Eur. J. Neurosci.* 12, 4381–4390. doi: 10.1111/j.1460-9568.2000.01341.x
- Alvarez, F. J., Bullinger, K. L., Titus, H. E., Nardelli, P., and Cope, T. C. (2010). Permanent reorganization of Ia afferent synapses on motoneurons after peripheral nerve injuries. *Ann. N. Y. Acad. Sci.* 1198, 231–241. doi: 10.1111/j.1749-6632.2010.05459.x
- Arbat-Plana, A. (2016). *Modulation of the Stretch Reflex Arc to Improve Functional Recovery After Peripheral Nerve Injury*. Ph.D. thesis, Universitat Autònoma de Barcelona, Bellaterra, Barcelona.
- Arbat-Plana, A., Cobianchi, S., Herrando-Grabulosa, M., and Uda, E. (2016). Endogenous modulation of Trkb signaling by treadmill exercise after peripheral nerve injury. *Neuroscience* 340, 188–200. doi: 10.1016/j.neuroscience.2016.10.057
- Arbat-Plana, A., Torres-Espín, E., Navarro, X., and Uda, E. (2015). Activity dependent therapies modulate the spinal changes that motoneurons suffer after a peripheral nerve injury. *Exp. Neurol.* 263, 293–305. doi: 10.1016/j.expneurol.2014.10.009
- Asensio-Pinilla, E., Uda, E., Jaramillo, J., and Navarro, X. (2009). Electrical stimulation combined with exercise increase axonal regeneration after peripheral nerve injury. *Exp. Neurol.* 219, 258–265. doi: 10.1016/j.expneurol.2009.05.034
- Aston-jones, G., and Cohen, J. D. (2005). An integrative theory of locus coeruleus-norepinephrine function: adaptive gain and optimal performance. *Annu. Rev. Neurosci.* 28, 403–450. doi: 10.1146/annurev.neuro.28.061604.135709
- Berridge, C. W., and Waterhouse, B. D. (2003). The locus coeruleus noradrenergic system?: modulation of behavioral state and state-dependent cognitive

AUTHOR CONTRIBUTIONS

AA-P contributed to the design of the experiments, performed all the experiments, analyzed the data, and wrote the manuscript. The work is part of her Ph.D. thesis dissertation. MP performed some of the experiments and collaborated in the writing of the manuscript. XN contributed to the design of the experiments and the writing of the manuscript. EU designed the experiments, performed some of the experiments, analyzed the data, and wrote the manuscript.

FUNDING

This study was supported by project grants TV3-201736 from the Fundació la Marató de TV3, PI11/00464, TERCEL (RD12/0019/0011) and CIBERNED (CB06/05/1105) funds from the Instituto de Salud Carlos III of Spain, the European Community's Seventh Framework Programme (FP7-HEALTH-2011) under grant agreement n° 278612 (BIOHYBRID), and FEDER funds. This work is part of the Ph.D. thesis dissertation of AA-P (Arbat-Plana, 2016), who had a four-year fellowship from the Universitat Autònoma de Barcelona as a Ph.D. student.

ACKNOWLEDGMENTS

We are grateful for the technical help of Jessica Jaramillo and Mónica Espejo.

- processes. *Brain Res. Brain Res. Rev.* 42, 33–84. doi: 10.1016/S0165-0173(03)00143-7
- Bullinger, K. L., Nardelli, P., Pinter, M. J., Alvarez, F. J., and Cope, T. C. (2011). Permanent central synaptic disconnection of proprioceptors after nerve injury and regeneration. II. Loss of functional connectivity with motoneurons. *J. Neurophysiol.* 106, 2471–2485. doi: 10.1152/jn.01097.2010
- Burke, D., Hallett, M., Fuhr, P., and Pierrot-Deseilligny, E. (1999). H reflexes from the tibial and median nerves. The international federation of clinical neurophysiology. *Electroencephalogr. Clin. Neurophysiol. Suppl.* 52, 259–262.
- Cobianchi, S., Casals-Diaz, L., Jaramillo, J., and Navarro, X. (2013). Differential effects of activity dependent treatments on axonal regeneration and neuropathic pain after peripheral nerve injury. *Exp. Neurol.* 240, 157–167. doi: 10.1016/j.expneurol.2012.11.023
- Cobianchi, S., Marinelli, S., Florenzano, F., Pavone, F., and Luvisetto, S. (2010). Short- but not long-lasting treadmill running reduces allodynia and improves functional recovery after peripheral nerve injury. *Neuroscience* 168, 273–287. doi: 10.1016/j.neuroscience.2010.03.035
- Cope, T. C., Bonasera, S. J., and Nichols, T. R. (1994). Reinnervated muscles fail to produce stretch reflexes. *J. Neurophysiol.* 71, 817–820. doi: 10.1152/jn.1994.71.2.817
- Dooley, D., Heal, D., and Goodwin, G. (1987). Repeated electroconvulsive shock prevents increased neocortical beta 1-adrenoceptor binding after DSP-4 treatment in rats. *Eur. J. Pharmacol.* 134, 333–337. doi: 10.1016/0014-2999(87)90365-7
- Dudley, M., Bruce, D., and Howard, C. (1990). The interaction of the beta-haloethyl benzylamines, xylamine, and DSP-4 with catecholaminergic neurons. *Annu. Rev. Pharmacol. Toxicol.* 30, 387–403. doi: 10.1146/annurev.pa.30.040190.002131
- Frey, E., Valakh, V., Katney-Grobe, Y., Shi, Y., Milbrandt, J., and DiAntonio, A. (2008). An in vitro assay to study induction of the regenerative state in

- sensory neurons. *Exp. Neurol.* 141, 520–529. doi: 10.1016/j.expneurol.2014.10.012
- Gomez-Pinilla, F., Zhuang, Y., Feng, J., Ying, Z., and Fan, G. (2012). Exercise impacts brain-derived neurotrophic factor plasticity by engaging mechanisms of epigenetic regulation. *Eur. J. Neurosci.* 33, 383–390. doi: 10.1111/j.1460-9568.2010.07508.x
- Gordon, T., and English, A. W. (2015). Strategies to promote peripheral nerve regeneration: electrical stimulation and/or exercise. *Eur. J. Neurosci.* 43, 336–350. doi: 10.1111/ejn.13005
- Grzanna, R., and Fritschy, J. M. (1991). Efferent projections of different subpopulations of central noradrenaline neurons. *Prog. Brain Res.* 88, 89–101. doi: 10.1016/S0079-6123(08)63801-7
- Gutmann, E., and Jokubek, B. (1963). Effect on increased motor activity on regeneration on the peripheral nerve in young rats. *Physiol. Bohemoslov.* 12, 463–468.
- Haftel, V. K., Bichler, E. K., Wang, Q.-B., Prather, J. F., Pinter, M. J., and Cope, T. C. (2005). Central suppression of regenerated proprioceptive afferents. *J. Neurosci.* 25, 4733–4742. doi: 10.1523/JNEUROSCI.4895-04.2005
- Heckman, C. J., Hyngstrom, A. S., and Johnson, M. D. (2008). Active properties of motoneurone dendrites: diffuse descending neuromodulation, focused local inhibition. *J. Physiol.* 586, 1225–1231. doi: 10.1113/jphysiol.2007.145078
- Heckman, C. J., Lee, R. H., and Brownstone, R. M. (2003). Hyperexcitable dendrites in motoneurons and their neuromodulatory control during motor behavior. *Trends Neurosci.* 26, 688–695. doi: 10.1016/j.tins.2003.10.002
- Heneka, M. T., Nadrigny, F., Regen, T., Martinez-Hernandez, A., Dumitrescu-Ozimek, L., Terwel, D., et al. (2010). Locus ceruleus controls alzheimer's disease pathology by modulating microglial functions through norepinephrine. *Proc. Natl. Acad. Sci. U.S.A.* 107, 6058–6063. doi: 10.1073/pnas.0909586107
- Herbison, G., Jaweed, M., and Ditunno, J. (1974). Effect of swimming on reinnervation of rat skeletal muscle. *J. Neurol. Neurosurg. Psychiatry* 37, 1247–1251. doi: 10.1136/jnnp.37.11.1247
- Hirschberg, S., Li, Y., Randall, A., Kremer, E. J., and Pickering, A. E. (2017). Functional dichotomy in spinal- vs prefrontal-projecting locus coeruleus modules splits descending noradrenergic analgesia from ascending aversion, and anxiety in rats. *eLife* 6:e29808. doi: 10.7554/eLife.29808
- Hultborn, H., Brownstone, R. B., Toth, T. I., and Gossard, J.-P. (2004). Key mechanisms for setting the input-output gain across the motoneuron pool. *Prog. Brain Res.* 143, 77–95. doi: 10.1016/S0079-6123(03)43008-2
- Hutchinson, K., Gómez-Pinilla, F., Crowe, M., Ying, Z., and Basso, D. (2004). Three exercise paradigms differentially improve sensory recovery after spinal cord contusion in rats. *Brain* 127, 1403–1414. doi: 10.1093/brain/awh160
- Jardanhazi-Kurutz, D., Kummer, M. P., Terwel, D., Vogel, K., Thiele, A., and Heneka, M. T. (2011). Distinct adrenergic system changes and neuroinflammation in response to induced locus ceruleus degeneration in APP/PS1 transgenic mice. *Neuroscience* 176, 396–407. doi: 10.1016/j.neuroscience.2010.11.052
- Kohm, A. P., and Sanders, V. M. (1999). Suppression of antigen-specific Th2 cell-dependent IgM and IgG1 production following norepinephrine depletion in vivo. *J. Immunol.* 162, 5299–5308.
- Kwok, J. C. F., Dick, G., Wang, D., and Fawcett, J. W. (2011). Extracellular matrix and perineuronal nets in CNS repair. *Dev. Neurobiol.* 71, 1073–1089. doi: 10.1002/dneu.20974
- Lee, R. H., and Heckman, C. J. (1999). Enhancement of bistability in spinal motoneurons in vivo by the noradrenergic alpha-1 agonist methoxamine. *Am. J. Physiol. Soc.* 81, 2164–2174.
- Liberto, C. M., Albrecht, P. J., Herx, L. M., Yong, V. W., and Levison, S. W. (2004). Pro-regenerative properties of cytokine-activated astrocytes. *J. Neurochem.* 89, 1092–1100. doi: 10.1111/j.1471-4159.2004.02420.x
- Liu, C., Ward, P. J., and English, A. W. (2015). The effects of exercise on synaptic stripping require androgen receptor signaling. *PLoS One* 9:e98633. doi: 10.1371/journal.pone.0098633
- López-Álvarez, V. M., Modol, L., Navarro, X., and Cobiañchi, S. (2015). Early increasing-intensity treadmill exercise reduces neuropathic pain by preventing nociceptor collateral sprouting and disruption of chloride cotransporters homeostasis after peripheral nerve injury. *Pain* 156, 1812–1825. doi: 10.1097/j.pain.0000000000000268
- Lopez-Alvarez, V. M., Puigdomenech, M., Navarro, X., and Cobiañchi, S. (2018). Monoaminergic descending pathways contribute to modulation of neuropathic pain by increasing-intensity treadmill exercise after peripheral nerve injury. *Exp. Neurol.* 299, 42–55. doi: 10.1016/j.expneurol.2017.10.007
- Lyons, W. E., Fritschy, J. M., and Grzanna, R. (1989). The noradrenergic neurotoxin DSP-4 eliminates the coeruleospinal projection but spares projections of the A5 and A7 groups to the ventral horn of the rat spinal cord. *J. Neurosci.* 9, 1481–1489. doi: 10.1523/JNEUROSCI.09-05-01481.1989
- Millan, M. J. (2002). Descending control of pain. *Prog. Neurobiol.* 66, 355–474. doi: 10.1016/S0304-0082(02)00009-6
- Módol, L., Cobiañchi, S., and Navarro, X. (2014). Prevention of NKCC1 phosphorylation avoids downregulation of KCC2 in central sensory pathways and reduces neuropathic pain after peripheral nerve injury. *Pain* 155, 1577–1590. doi: 10.1016/j.pain.2014.05.004
- Molteni, R., Zheng, J.-Q., Ying, Z., Gómez-Pinilla, F., and Twiss, J. L. (2004). Voluntary exercise increases axonal regeneration from sensory neurons. *Proc. Natl. Acad. Sci. U.S.A.* 101, 8473–8478. doi: 10.1073/pnas.0401443101
- Nam, T. S., Choi, Y., Yeon, D. S., Leem, J. W., and Paik, K. S. (2001). Differential antinociceptive effect of transcutaneous electrical stimulation on pain behavior sensitive or insensitive to phentolamine in neuropathic rats. *Neurosci. Lett.* 301, 17–20. doi: 10.1016/S0304-3940(01)01587-7
- Niemi, J. P., DeFrancesco-Lisowicz, A., Roldan-Hernandez, L., Lindborg, J. A., Mandell, D., and Zigmond, R. E. (2013). A Critical Role for Macrophages Near Axotomized Neuronal Cell Bodies in Stimulating Nerve Regeneration. *J. Neurosci.* 33, 16236–16248. doi: 10.1523/JNEUROSCI.3319-12.2013
- Paxinos, G., and Watson, C. (1998). *The Rat Brain in Stereotaxic Coordinates*, 4th Edn. San Diego, CA: Academic Press.
- Perrier, J., and Delgado-Lezama, R. (2005). Synaptic Release of Serotonin Induced by Stimulation of the Raphe Nucleus Promotes Plateau Potentials in Spinal Motoneurons of the Adult Turtle. *J. Neurosci.* 25, 7993–7999. doi: 10.1523/JNEUROSCI.1957-05.2005
- Pertovaara, A. (2006). Noradrenergic pain modulation. *Prog. Neurobiol.* 80, 53–83. doi: 10.1016/j.pneurobio.2006.08.001
- Prieto, M., and Giralt, M. T. (2001). Effects of N-(2-chloroethyl)-N-ethyl-2-bromobenzylamine (DSP4) on alpha2-adrenoceptors which regulate the synthesis and release of noradrenaline in the rat brain. *Pharmacol. Toxicol.* 88, 152–158. doi: 10.1034/j.1600-0773.2001.d01-97.x
- Ross, S. B., and Stenfors, C. (2015). DSP4, a selective neurotoxin for the locus coeruleus noradrenergic system: a review of its mode of action. *Neurotox. Res.* 27, 15–30. doi: 10.1007/s12640-014-9482-z
- Rotterman, T. M., Nardelli, P., Cope, T. C., and Alvarez, F. J. (2014). Normal distribution of VGLUT1 synapses on spinal motoneuron dendrites and their reorganization after nerve injury. *J. Neurosci.* 34, 3475–3492. doi: 10.1523/JNEUROSCI.4768-13.2014
- Royston, P. (1993). A pocket-calculator algorithm for the shapiro-francia test for non-normality: an application to medicine. *Stat. Med.* 12, 181–184. doi: 10.1002/sim.4780120209
- Sabatier, M. J., Redmon, N., Schwartz, G., and English, A. W. (2008). Treadmill training promotes axon regeneration in injured peripheral nerves. *Exp. Neurol.* 211, 489–493. doi: 10.1016/j.expneurol.2008.02.013
- Sanders, V. M., and Straub, R. H. (2002). Norepinephrine, the β -adrenergic receptor, and immunity. *Brain. Behav. Immun.* 16, 290–332. doi: 10.1006/brbi.2001.0639
- Scullion, G. A., Kendall, D. A., Sunter, D., Marsden, C. A., and Pardon, M. C. (2009). Central noradrenergic depletion by DSP-4 prevents stress-induced memory impairments in the object recognition task. *Neuroscience* 164, 415–423. doi: 10.1016/j.neuroscience.2009.08.046
- Udina, E., Cobiañchi, S., Allodi, I., and Navarro, X. (2011a). Effects of activity-dependent strategies on regeneration and plasticity after peripheral nerve injuries. *Ann. Anat.* 193, 347–353. doi: 10.1016/j.aanat.2011.02.012
- Udina, E., Puigdemasa, A., and Navarro, X. (2011b). Passive and active exercise improve regeneration and muscle reinnervation after peripheral nerve injury in the rat. *Muscle Nerve* 43, 500–509. doi: 10.1002/mus.21912

- Valero-Cabré, A., and Navarro, X. (2001). H reflex restitution and facilitation after different types of peripheral nerve injury and repair. *Brain Res.* 919, 302–312. doi: 10.1016/S0006-8993(01)03052-9
- van Meeteren, N. L., Brakkee, J. H., Hamers, F. P. T., Helders, P. J., and Gispén, W. H. (1997). Exercise training improves functional recovery and motor nerve conduction after sciatic nerve crush lesion in the rat. *Arch. Phys. Med. Rehabil.* 78, 70–77. doi: 10.1016/S0003-9993(97)90013-7
- Vivó, M., Puigdemasa, A., Casals, L., Asensio, E., Udina, E., and Navarro, X. (2008). Immediate electrical stimulation enhances regeneration and reinnervation and modulates spinal plastic changes after sciatic nerve injury and repair. *Exp. Neurol.* 211, 180–93. doi: 10.1016/j.expneurol.2008.01.020

Conflict of Interest Statement: The authors declare that the research was conducted in the absence of any commercial or financial relationships that could be construed as a potential conflict of interest.

Copyright © 2019 Arbat-Plana, Puigdomenech, Navarro and Udina. This is an open-access article distributed under the terms of the Creative Commons Attribution License (CC BY). The use, distribution or reproduction in other forums is permitted, provided the original author(s) and the copyright owner(s) are credited and that the original publication in this journal is cited, in accordance with accepted academic practice. No use, distribution or reproduction is permitted which does not comply with these terms.



The Complex Work of Proteases and Secretases in Wallerian Degeneration: Beyond Neuregulin-1

Marta Pellegatta* and Carla Taveggia*

Division of Neuroscience and INSPE at IRCCS San Raffaele Scientific Institute, Milan, Italy

After damage, axons in the peripheral nervous system (PNS) regenerate and regrow following a process termed Wallerian degeneration, but the regenerative process is often incomplete and usually the system does not reach full recovery. Key steps to the creation of a permissive environment for axonal regrowth are the trans-differentiation of Schwann cells and the remodeling of the extracellular matrix (ECM). In this review article, we will discuss how proteases and secretases promote effective regeneration and remyelination. We will detail how they control neuregulin-1 (NRG-1) activity at the post-translational level, as the concerted action of alpha, beta and gamma secretases cooperates to balance activating and inhibitory signals necessary for physiological myelination and remyelination. In addition, we will discuss the role of other proteases in nerve repair, among which A Disintegrin And Metalloproteinases (ADAMs) and gamma-secretases substrates. Moreover, we will present how matrix metalloproteinases (MMPs) and proteases of the blood coagulation cascade participate in forming newly synthesized myelin and in regulating axonal regeneration. Overall, we will highlight how a deeper comprehension of secretases and proteases mechanism of action in Wallerian degeneration might be useful to develop new therapies with the potential of readily and efficiently improve the regenerative process.

Keywords: wallerian degeneration, remyelination, secretases, matrix metalloproteinases, fibrinolysis

OPEN ACCESS

Edited by:

Giovanna Gambiarotta,
University of Turin, Italy

Reviewed by:

Douglas William Zochodne,
University of Alberta, Canada
Petr Dubový,
Masaryk University, Czechia

*Correspondence:

Marta Pellegatta
pellegatta.marta@hsr.it
Carla Taveggia
taveggia.carla@hsr.it

Received: 24 October 2018

Accepted: 26 February 2019

Published: 20 March 2019

Citation:

Pellegatta M and Taveggia C
(2019) The Complex Work of
Proteases and Secretases in
Wallerian Degeneration:
Beyond Neuregulin-1.
Front. Cell. Neurosci. 13:93.
doi: 10.3389/fncel.2019.00093

PERIPHERAL NERVE REGENERATION

In the peripheral nervous system (PNS), nerves can be damaged following various events such as traumatic injuries, metabolic alterations and genetic peripheral neuropathies. All these events significantly impact the quality of life of both patients and caregivers. Regardless of the nature of the triggering cause, after injury both Schwann cells and neurons are compromised as their reciprocal interdependence determines that damaging one cell type will eventually influence the other. Unlike the central nervous system, the PNS possesses the intrinsic capability to regenerate, as axons can regrow over long distances to reach their final target and Schwann cells are able to remyelinate them. Nonetheless, the regenerative process often remains incomplete, due to the inability of the repair machinery to maintain an extended growth promoting response (Gaudet et al., 2011).

After traumatic injury, PNS axons can regrow and remyelinate following a process termed Wallerian degeneration. The cascade of events leading to the axon regrow and the re-establishment of a functional myelinated axo-glia unit has been originally described by August Waller as the result of nerve axotomy (Waller and Owen, 1850), and might partially differ from those observed after crush injury (Stoll et al., 2002; Gaudet et al., 2011; Rotshenker, 2011).

In this review article, we will report the role of molecules and modifiers of the extracellular matrix (ECM) in the process of regeneration and remyelination. Since these molecules have been investigated in both models of crush injury and axotomy we will generally refer to their role in peripheral nerve injury.

During early Wallerian degeneration, axons degenerate and Schwann cells adopt a specific response to injury: the repair program (Gerds et al., 2016). Specifically, denervated Schwann cells lose their myelin sheath and downregulate the expression of myelin-associated genes, among which *Egr2/Krox20*, *MPZ*, *MBP*, *MAG* and *periaxin*. In addition, they start to proliferate and upregulate molecules characteristic of their immature stage such as *L1*, *NCAM*, *p75NTR* and *GFAP* (Jessen and Mirsky, 2008). However, after injury, Schwann cells do not simply revert their phenotype to an earlier developmental stage, but undergo a proper “trans-differentiation” phase in which they acquire unique characteristics, becoming true “repair cells” (Arthur-Farraj et al., 2012; Jessen et al., 2015). In particular, they upregulate neurotrophic factors supporting axon survival and elongation, a necessary step towards regeneration (Fontana et al., 2012; Brushart et al., 2013). In addition, they specifically activate a massive myelin-breakdown and play an early pivotal role in removing myelin debris, which represents a barrier to the regrowth of axons distal to the injury site (Brown et al., 1994; Perry et al., 1995; Hirata and Kawabuchi, 2002; Gomez-Sanchez et al., 2015; Jang et al., 2016). During the first week after injury, repair Schwann cells also produce cytokines that induce macrophages’ activation and recruitment from the bloodstream (Bolin et al., 1995; Kurek et al., 1996; Shamash et al., 2002; Tofaris et al., 2002; Roberts et al., 2017). In the following stages, indeed, macrophages assume a primary role in debris removal and growth factors production, supporting axons regeneration and Schwann cells migration through the distal nerve stump (Gaudet et al., 2011; Gerds et al., 2016). Within this complex pro-regenerative environment, repair Schwann cells adopt an elongated bipolar morphology and align to form regenerative tracks from the injury site to the nerve target, called “Bungner bands” (Gomez-Sanchez et al., 2017). These structures generate along the basal lamina that previously surrounded the Schwann cell-axon unit in intact nerves and support injured axons regrowth through the distal stump to reach their final target.

Axo-glial communication is essential for nerve repair: not only Schwann cells create a permissive environment for axons regrowth, but also axon-derived signals promote differentiation of repair cells (Fawcett and Keynes, 1990; Stassart et al., 2018). The re-establishment of the axo-glial unit during later phases of the regenerative process allows Schwann cells to re-differentiate and remyelinate the newly generated axon and to re-establish rapid saltatory conduction of the nerve impulse. Nonetheless, remyelinated axons have shorter internodes and thinner myelin sheaths as compared to uninjured nerves (Fancy et al., 2011; Stassart et al., 2018).

Given the inefficiency in the regenerative process, there is an evident need to envisage more effective therapeutic strategies allowing complete recovery. Recent advances in biomaterial

and biomedical engineering have provided new strategies to improve regenerative capabilities in injured nerves with synthetic conduits (Tajdaran et al., 2018). These scaffolds support the reconstruction of long nerve gaps, as they allow the application of exogenous agents with neurotrophic properties. Although not pertinent to this review, nerve-scaffolding techniques represent a strategic line of research in nerve regeneration.

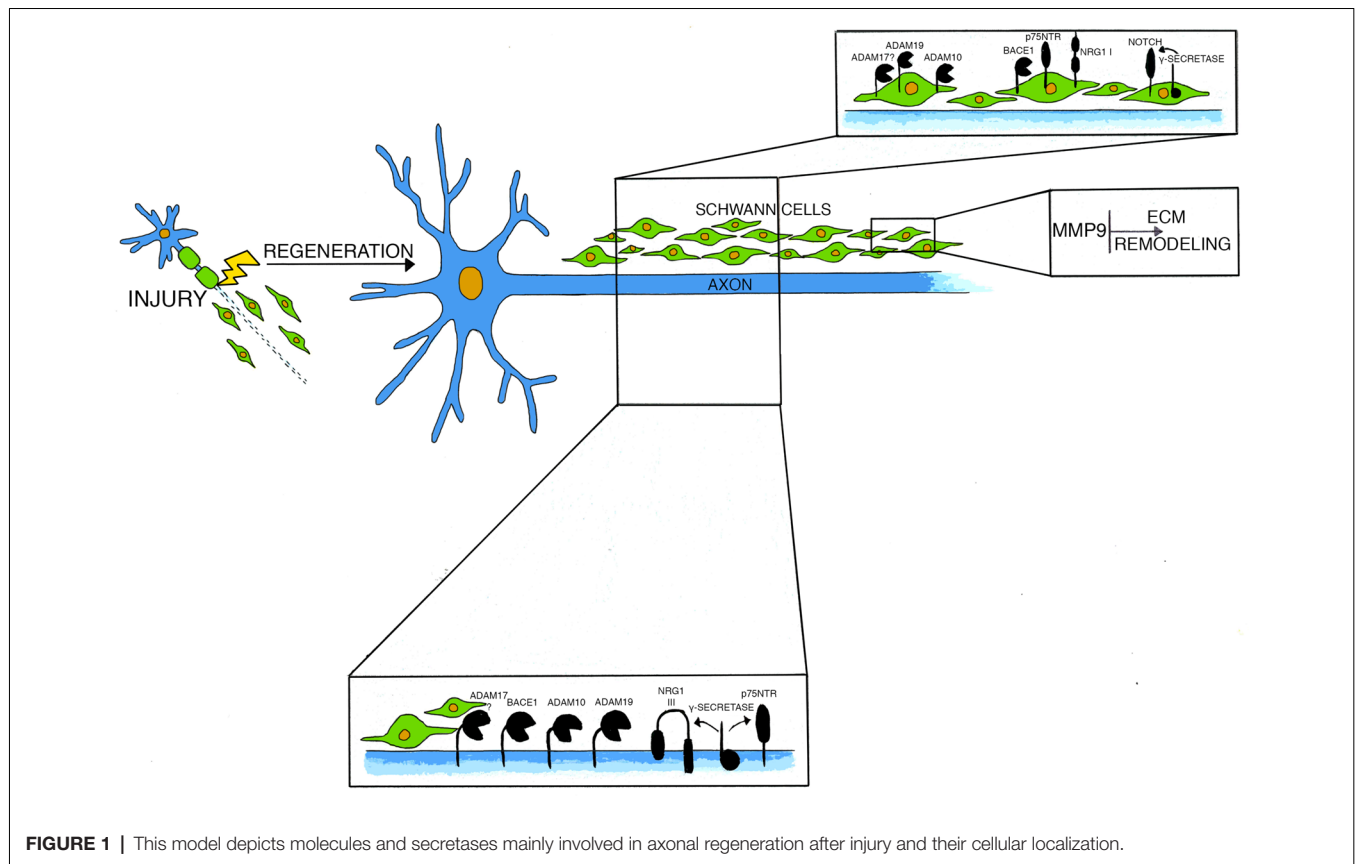
Finally, axonal loss and repeated attempts of nerve regeneration are key features also of several peripheral neuropathies, like Charcot Marie Tooth hereditary neuropathies (Stassart et al., 2018). Thus, the development of more adequate treatments to promote nerve repair could similarly benefit these pathologies for which there is no effective therapy.

NEUREGULIN-1

Neuregulins are transmembrane proteins belonging to the family of epidermal growth factor (EGF)-like growth factors (Falls, 2003). They signal by binding to the tyrosine kinase receptors of the ErbB family expressed on Schwann cells (Yarden and Sliwkowski, 2001), thereby activating different intracellular signal transduction pathways in glial cells (Yang et al., 2004; Gu et al., 2005). Neuregulin-1 (NRG-1) is the most important gene among the members of this family and it is also the best characterized. The *Nrg1* gene encodes for several isoforms, all containing an EGF-like domain, which is required to activate the ErbB receptors. All NRG1 isoforms differ mainly for the composition of their N-terminal end, on the base of which they have been classified into six different groups (Garratt et al., 2000; Buonanno and Fischbach, 2001; Mei and Nave, 2014). Distinct NRG1 isoforms use specific promoters to drive their expression in a tight spatio-temporal regulated pattern. Indeed, they are implicated in different cellular function, like migration, proliferation, morphogenesis and control of cell size (Buonanno and Fischbach, 2001; Esper et al., 2006; Britsch, 2007; Mei and Nave, 2014).

Among the various types of Neuregulins, we will focus on NRG1 type I and type III, which are the main isoforms thus far investigated in PNS development and regeneration. NRG1 type I is a single-pass membrane protein and presents an Immunoglobulin-like domain at the N-terminus, while NRG1 type III, in addition to the transmembrane domain, possesses a cysteine-rich domain in the N-terminal portion that further anchors the protein to the plasma membrane (Ho et al., 1995).

In the PNS, NRG1 type III is essentially expressed on axonal membranes (Figure 1). During nerve formation, NRG1 type III is required for Schwann cells proliferation and differentiation (Nave and Salzer, 2006). Indeed, in mutant mice lacking NRG1 type III expression, Schwann cells are absent, and this causes a severe cell death of dorsal root ganglia (DRG) and motor neurons (Wolpowitz et al., 2000). During development, NRG1 type III forces Schwann cells to choose between myelination and non-myelination (Taveggia et al., 2005). Of note, axonal levels of NRG1 type III also determine the thickness of the myelin sheath: mice overexpressing



axonal NRG1 type III are hypermyelinated, whereas mice haploinsufficient for NRG1 type III are hypomyelinated (Michailov et al., 2004; Taveggia et al., 2005). Binding of NRG1 to their cognate ErbB2/ErbB3 receptors, activates multiple signal transduction pathways in Schwann cells, including PI3K-AKT1, calcineurin and MAPK signaling pathways (Taveggia et al., 2005, 2010; Kao et al., 2009; Pereira et al., 2012). Of note, NRG1 type III activity is regulated by the extracellular cleavage of secretases (Willem, 2016). While the beta secretase β -site amyloid precursor protein-cleaving enzyme 1 (BACE1) activates NRG1 type III, enhancing myelination (Hu et al., 2006; Willem et al., 2006), cleavage of NRG1 type III by the α -secretase ADAM17 inhibits myelination (La Marca et al., 2011; Bolino et al., 2016). Accordingly, transgenic mice lacking BACE1 are hypomyelinated (Hu et al., 2006; Willem et al., 2006) and mice depleted of neuronal ADAM17 are hypermyelinated, with a phenotype that remarkably resembles NRG1 type III overexpressing mice (Michailov et al., 2004; La Marca et al., 2011).

Following traumatic nerve injury, the expression of several components of the NRG1 signaling machinery is dys-regulated (Birchmeier and Bennett, 2016; Morano et al., 2018). For example, ErbB2/ErbB3 receptors expression is increased after damage and their activation status is enhanced (Cohen et al., 1992; Carroll et al., 1997; Kwon et al., 1997; Guertin et al., 2005), although the effective role of ErbB receptors in peripheral

nerve injury is partly controversial (Atanasoski et al., 2006). Moreover, neuronal NRG1 type III expression decreases as soon as the Schwann cells-axon unit is destroyed but it is subsequently re-expressed during late phases of nerve regeneration, when axons re-innervate their target (Bermingham-McDonogh et al., 1997; Stassart et al., 2013).

Axonal NRG1 plays an important role in peripheral nerve repair, which, under many aspects, is different from that accomplished during nerve development (Birchmeier and Bennett, 2016). After an injury insult, axonal NRG1 is a driving force for regeneration and it controls the expression of genes involved in peripheral nerve injury (El Soury et al., 2018). Its juxtacrine interactions with Schwann cells, in fact, prompt both remyelination and normal re-innervation of neuromuscular junctions (Fricker et al., 2011). Accordingly, remyelination in mice lacking NRG1 expression in a subset of motor and sensory neurons is severely impaired (Fricker et al., 2011). Unexpectedly, these defects are transient, and axons in mutant nerves are efficiently remyelinated during late nerve regeneration (Fricker et al., 2013). NRG1 therefore is an important factor in regulating nerve repair following injury but, unlike development, it does not control the myelinating fate of axons.

While the above-mentioned studies suggest that axonal NRG1 is dispensable for long term remyelination, it has also been reported that neuronal overexpression of NRG1 type I and type III isoforms facilitates nerve repair and improves remyelination after injury (Stassart et al., 2013). Although these

findings seem contradictory, it is possible that gain and loss of function approaches are targeting different mechanisms. Lack of NRG1 after injury might in fact be compensated with time by other molecules, whereas its overexpression could promote Schwann cells re-differentiation and favor nerve regeneration through a distinct process.

Unlike NRG1 type III, NRG1 type I expression is potently induced in Schwann cells early after nerve damage, and although dispensable for developmental myelination, it is critical for remyelination (**Figure 1**; Loeb et al., 1999; Falls, 2003; Stassart et al., 2013). Indeed, mutant mice specifically lacking NRG1 type I expression in Schwann cells poorly remyelinate after injury, suggesting that Schwann cells require autocrine NRG1 type I signaling to support re-differentiation and repair (Stassart et al., 2013).

Interestingly, administration of exogenous NRG1 type III and NRG1 type I promotes neurite outgrowth and nerve regeneration (Mahanthappa et al., 1996; Cai et al., 2004). Moreover, modulation of NRG1 activity in animal models of CMT1A (Fledrich et al., 2014), CMT1B (Scapin et al., 2018) and Congenital Hypomyelinating Neuropathy (Belin et al., 2018), can ameliorate the peripheral hypomyelination observed in these diseases, prevent axonal loss and promote nerve functional recovery, the latter all features observed also after nerve injury. Nonetheless, it has also been recently reported that NRG1 is already highly expressed in nerves of CMT1A pre-clinical models, thus indicating that delivery of exogenous NRG1 should be carefully evaluated (Fornasari et al., 2018).

Collectively these studies suggest that after damage, Schwann cells might have developed new strategies to accomplish many of their cellular functions. Thus, a better understanding of the molecular mechanism underlying their extraordinary plasticity remains crucial towards the development of powerful therapies leading to complete regeneration.

BACE1

The beta secretase BACE1 is an aspartyl protease mostly involved in processing type I transmembrane proteins, which results in the generation of a cleaved, membrane-bound portion of the target molecule and in the release of a soluble fragment. BACE1 has been well characterized in the pathogenesis of Alzheimer's disease, since it is one of the main enzymes responsible for the processing of the amyloid precursor protein and for the generation of amyloid beta plaques, a pathological hallmark of the disease (Sinha and Lieberburg, 1999; Vassar et al., 1999; Yan et al., 1999; Cai et al., 2001; Luo et al., 2001; Roberds et al., 2001).

Besides the amyloid precursor protein, BACE1 cleaves a variety of substrates (Hemming et al., 2009). Among them, in the nervous system, there are voltage-gated sodium channels (Wong et al., 2005; Kim et al., 2007, 2011; Gersbacher et al., 2010), the potassium channel proteins KCNE1 and KCNE2 (Hitt et al., 2012; Sachse et al., 2013), the adhesion molecules L1 and close homolog of L1 (CHL1; Hitt et al., 2012; Kuhn et al., 2012; Zhou et al., 2012), contactin-2 (Kuhn et al., 2012) and Seizure-related gene 6 protein (Sez 6; Kuhn et al., 2012). Processing of these substrates by BACE1 perturbs several brain functions, as

these proteins are involved in different tasks. Indeed, BACE1 is crucial to generate axonal connections (Hitt et al., 2012), regulate axonal guidance (Kuhn et al., 2012; Zhou et al., 2012) and modulate neurite outgrowth and neural connectivity (Kuhn et al., 2012). Surprisingly, despite being implicated in processing many substrates, constitutive ablation of BACE1 in mice results in viable and fertile animals, with only moderate behavioral abnormalities (Cai et al., 2001; Luo et al., 2001; Roberds et al., 2001; Laird et al., 2005; Savonenko et al., 2008).

In the PNS, BACE1 is mainly expressed in motor neurons and in DRG sensory neurons (Willem et al., 2006) and its expression is highly similar to that of NRG1 type III. Nonetheless, BACE1 is present at very low levels also in Schwann cells in normal nerves and at higher levels in damaged nerves (Hu et al., 2015; **Figure 1**). Constitutive deletion of BACE1 results in severe myelination defects during development (Hu et al., 2006; Willem et al., 2006; Velanac et al., 2012). Interestingly, NRG1 cleavage is impaired in BACE1 null mice (Hu et al., 2006; Willem et al., 2006), and the hypomyelinating phenotype resembles that observed in NRG1 type III haploinsufficient mice (Michailov et al., 2004; Taveggia et al., 2005). Accordingly, in peripheral nerves, BACE1 directly cleaves axonal NRG1 type III, generating a membrane-tethered portion of the molecule that exposes the EGF-like domain allowing the activation of the ErbB2/ErbB3 receptors complex on Schwann cells, thereby promoting myelination (Hu et al., 2008; Velanac et al., 2012).

BACE1 is also implicated in peripheral nerve injury; specifically, in the absence of BACE1 remyelination is impaired. Accordingly, injured nerves of BACE1 null mice have thinner myelin sheath and increased number of un-myelinated axons (Hu et al., 2008). These defects have been ascribed to aberrant processing of axonal NRG1 type III, which impairs PI3K/AKT1 signaling pathway activity (Hu et al., 2008). More recently, also the contribution of glial BACE1, i.e., expressed in Schwann cells, has been investigated in nerve remyelination (Hu et al., 2015). Nerve graft experiments suggest that both axonal and Schwann cell-derived BACE1 activity are decisive for remyelination (Hu et al., 2015). Interestingly, since both BACE1 and NRG1 type I are induced in Schwann cells after injury (Hu et al., 2008, 2015; Stassart et al., 2013), it is likely that glial BACE1 contributes to nerve repair by promoting NRG1 type I cleavage (Hu et al., 2015), though this has never been formally demonstrated.

Other studies reported an opposite role for BACE1 in PNS remyelination. By analyzing early regenerative events, Farah et al. (2011) observed that BACE1 knockout mice present enhanced myelin and axonal debris clearance, an increased number of regenerated fibers and precocious re-innervation of neuromuscular junctions. These phenomena are likely due to neuronal BACE1, as overexpression of BACE1 in neurons determines a marked decrease in peripheral axons regeneration capacity (Tallon et al., 2017). These data suggest that neuronal BACE1 could act as a negative regulator of axonal regeneration in early events following injury, contradicting previous studies. To reconcile these conflicting results and to better clarify the role of BACE1 in nerve regeneration and remyelination, further studies in conditional knockout mice allowing ablation

in defined temporal windows are necessary. Moreover, since BACE1 processes many substrates, which are expressed in different cell types and at specific stages of the repair process, the study of its cell autonomous role could help in defining the effector(s) through which BACE1 regulates specific stages of axonal regeneration and remyelination.

Since BACE1 has a prominent role in the generation of amyloid beta plaques during AD pathogenesis, a lot of effort has been devoted in developing small molecules that could inhibit the enzyme's activity (Coimbra et al., 2018), however only one study has tested their efficacy in a model of nerve crush injury. A 7 days treatment with a BACE1 inhibitor starting immediately after damage increases regeneration and enhances myelin debris clearance (Farah et al., 2011), supporting the hypothesis that BACE1 inhibits early axonal regeneration (Farah et al., 2011; Tallon et al., 2017). Although the possibility of using BACE1 inhibitors to boost axonal regeneration is potentially promising, it is essential to better define their application, given the contradictory role of BACE1 after injury (Hu et al., 2008, 2015). Thus, further studies are required to exactly determine the efficacy of BACE1 inhibitor(s) in the resolution of PNS injury. Particularly relevant would be to define the exact time frame in which to administer these compounds to promote axonal growth without altering remyelination.

A DISINTEGRIN AND METALLOPROTEINASES

A Disintegrin And Metalloproteinases (ADAMs) are membrane-anchored metalloproteinases involved in the proteolytic processing of several transmembrane proteins and in the consequent regulation of the cleaved substrates' activity (Schlöndorff and Blobel, 1999). ADAM proteases have both proteolytic and disintegrin characteristics (Schlöndorff and Blobel, 1999). They present a conserved structure composed by distinct domains (Schlöndorff and Blobel, 1999; Primakoff and Myles, 2000) and have been implicated in the release of several molecules among which EGF receptor ligands, tumor necrosis factor family members, neuregulins and other transmembrane proteins (Black and White, 1998; Blobel, 2000). ADAM proteins participate in many biological functions such as cell migration, cell membrane fusion and cytokines and growth factors shedding. Moreover, members of this family cooperate in muscle development, fertilization, neurogenesis, angiogenesis and cell fate determination (Schlöndorff and Blobel, 1999; Primakoff and Myles, 2000; Horiuchi et al., 2003; Seals and Courtneidge, 2003). Pathologies like inflammation-related disorders and cancer also implicate ADAM proteins (Seals and Courtneidge, 2003; Blobel, 2005).

It is thus not surprising that ADAM secretases have a role also in PNS myelination. In particular, the α -secretase ADAM17 possesses an intrinsic proteolytic activity, which inhibits NRG1 type III and the process of myelination during development. Thus, only a fine balance between activating and inhibitory signals coming from the activity of BACE1 and ADAM17 could physiologically regulate the correct formation of the myelin sheath (La Marca et al., 2011).

Not only ADAM17, but also ADAM10 and ADAM19, play important roles in PNS functioning (**Figure 1**). In particular, ADAM10 is highly expressed in Schwann-cells DRG neuronal co-cultures during myelination and its chemical inhibition impairs axonal outgrowth *in vitro* (Jangouk et al., 2009). Nonetheless, *in vivo* studies have shown that ADAM10 is dispensable for developmental myelination. In fact, both overexpression of a dominant negative form of the protein (Freese et al., 2009) as well as its conditional inactivation in a transgenic model (Meyer zu Horste et al., 2015) do not alter myelination. Interestingly, ADAM10 promotes axonal sprouting, as its deficiency in motor neurons impairs the extent of axons growth *in vitro* (Meyer zu Horste et al., 2015). Moreover, this secretase is critical for axonal outgrowth during peripheral nerve regeneration as deletion of ADAM10 in motor neurons reduces the axonal density of small caliber fibers after crush injury. Thus, ADAM10 seems mainly implicated in the specific control of post-traumatic outgrowth of axons (Meyer zu Horste et al., 2015).

ADAM19 is highly expressed in developing PNS, and its expression pattern resembles that of NRG1 (Kurisaki et al., 1998; Shirakabe et al., 2001); both proteins are co-expressed in DRG and in motor neurons (Marchionni et al., 1993; Shirakabe et al., 2001). Of note, ADAM19 can cleave membrane-anchored NRG1 proteins in cultured neurons (Kurisaki et al., 1998; Shirakabe et al., 2001; Wakatsuki et al., 2004). *In vivo* studies have shown that while ADAM19 is dispensable for PNS development, remyelination after nerve injury is impaired in its absence (Wakatsuki et al., 2009). Further, after injury, ADAM19 regulates the re-differentiation of Schwann cells from a pro-myelinating stage to a fully myelinating one by activating the AKT pathway (Wakatsuki et al., 2009).

Although ADAM10 and ADAM19 participate in the progression of nerve regeneration, nerve repair is eventually achieved in both mutants. It is thus possible that compensatory mechanisms intervene to favor remyelination, likely carried out by other secretases. Since ADAM17 is fundamental in nerve development and NRG1 processing, it would be important to assess the role of this secretase during nerve regeneration.

GAMMA SECRETASES

Gamma secretases (γ -secretases) are a multi-subunit protease complex responsible for the intramembrane cleavage of transmembrane proteins, mostly known for the generation of the β -amyloid peptide in Alzheimer's disease (De Strooper et al., 1998; Wolfe et al., 1999). Beside the amyloid precursor protein, γ -secretases process several type I transmembrane proteins, among which the adhesion molecules N-cadherin and E-cadherin (Struhl and Adachi, 2000; Golde and Eckman, 2003), the neurotrophin receptor p75 (p75NTR; Jung et al., 2003), the β 2 subunit of voltage-gated sodium channel (Kim et al., 2005), the protein receptor Notch (De Strooper et al., 1999) and Neuregulins (Dejaegere et al., 2008; Trimarco et al., 2014). Although no direct functional role of the γ -secretase complex has been described in peripheral nerve regeneration, some of

its substrates are relevant for such process, in particular Notch and p75NTR.

Notch activity is regulated by a classical regulated intramembrane proteolysis (RIP) mechanism (**Figure 1**). After binding to its substrates, Notch is first cleaved in its extracellular domain (Pan and Rubin, 1997; Brou et al., 2000; Hartmann et al., 2002; van Tetering et al., 2009); this cleavage induces a subsequent process in the transmembrane domain, which is mediated by the γ -secretase complex (De Strooper et al., 1999; Struhl and Greenwald, 1999). Notch intracellular domain then translocates in the cell nucleus, where it regulates the transcription of genes important for cell development and differentiation (Kopan and Goate, 2000; Kopan and Ilagan, 2004; Louvi and Artavanis-Tsakonas, 2006). In peripheral nerves, Notch negatively regulates developmental myelination (Woodhoo et al., 2009). After injury, Notch is rapidly upregulated in peripheral nerves and, in a mouse model in which Notch is conditionally ablated in Schwann cells, the rate of Schwann cells dedifferentiation after axotomy is reduced (Woodhoo et al., 2009). This impairment relies on Notch intracellular domain, as a similar defect is found also in mice deficient in Schwann cells RBPJ (Recombination signal Binding Protein for Immunoglobulin Kappa J region), the key transcriptional mediator of canonical Notch intracellular signaling (Woodhoo et al., 2009).

p75NTR regulates a variety of cellular function in the nervous system, from programmed cell death, axonal growth and degeneration, to cell proliferation, myelination and synaptic plasticity (Kraemer et al., 2014; Meeker and Williams, 2015). This wide range of biological effects is due to the multiplicity of ligands and co-receptors which partner with p75NTR to regulate its signaling. In particular, p75NTR promotes cells survival through association with TRK receptors (Hempstead et al., 1991; Meeker and Williams, 2015; Pathak et al., 2018), inhibits axonal regeneration by interacting with Nogo receptor and Lingo (Wang et al., 2002; Wong et al., 2002; Mi et al., 2004) and induces apoptosis via high affinity binding with Sortilin (Friedman, 2000; Beattie et al., 2002; Nykjaer et al., 2004). Similarly to Notch, also p75NTR is regulated by RIP: upon ligand binding, the extracellular domain of the receptor is first cleaved by ADAM17 (Weskamp et al., 2004) and then processed by the γ -secretase complex, thereby releasing a small intracellular domain (Zampieri et al., 2005). p75NTR is highly expressed in Schwann cells and neurons during development, and its expression levels decline with age (Cosgaya et al., 2002). Both nerve crush injury and axotomy induce a strong upregulation of p75NTR in neurons and Schwann cells in distal nerve segments (Ernfors et al., 1989; Koliatsos et al., 1991; Saika et al., 1991; Syroid et al., 2000; Petratos et al., 2003; **Figure 1**). The role of p75NTR after injury is complex and partially contradictory (for a comprehensive review see Meeker and Williams, 2015), nonetheless, grafting of Schwann cells deficient for p75NTR impairs motor neuron survival after injury (Tomita et al., 2007). Moreover, remyelination is hampered in mice lacking p75NTR and nerve repair is delayed (Song et al., 2006; Chen et al., 2016). Thus, p75NTR likely has a pivotal role in supporting neuronal survival, nerve regeneration and remyelination after injury.

In addition to the above-described roles, p75NTR also regulates fibrinolysis. Upon nerve injury, fibrin accumulates in the nerves to promote axon degeneration and Schwann cells dedifferentiation. However, to achieve efficient regeneration, fibrin has to be degraded in a process called fibrinolysis (Akassoglou et al., 2002). In injured nerves, accumulation of p75NTR in Schwann cells inhibits fibrinolysis thus maintaining Schwann cells in a un-differentiated state (Akassoglou et al., 2002; Sachs et al., 2007). During nerve regeneration, fibrin is degraded, p75NTR is downregulated and Schwann cells can re-differentiate to initiate remyelination (Akassoglou et al., 2000; Sachs et al., 2007; **Figure 2**). Thus, the biological role of p75NTR in axonal regeneration and remyelination is complex and probably depends on the relative contribution of its function as a regulator of cell death/survival and as an inhibitor of fibrin degradation.

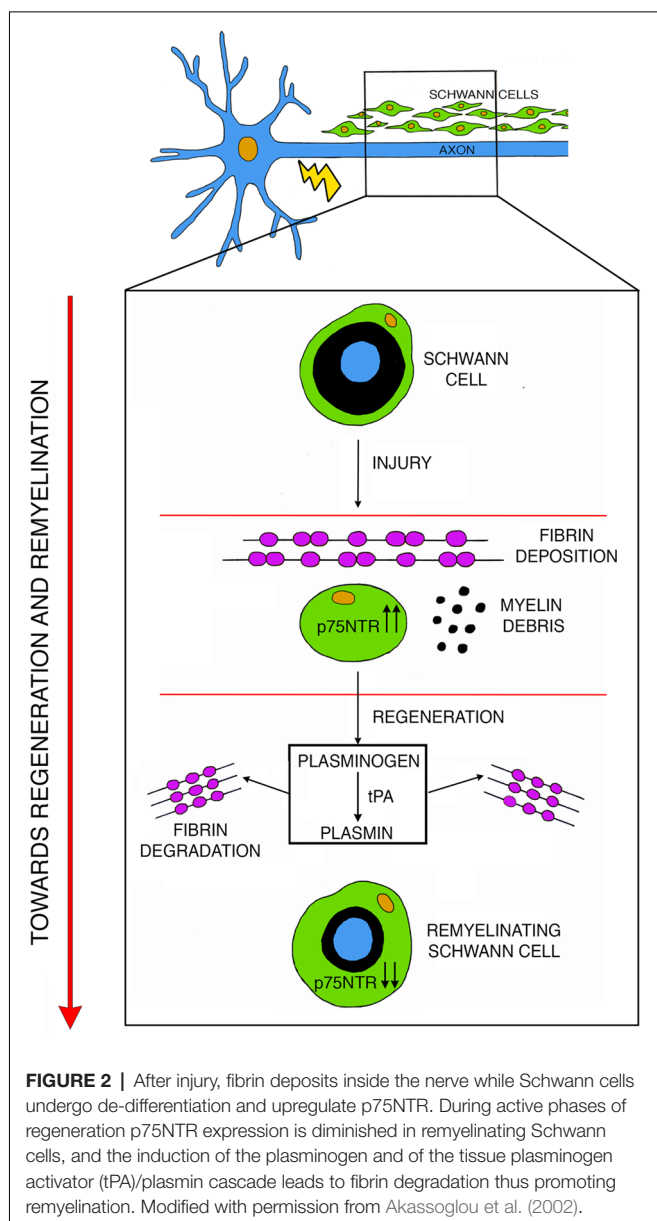
Of note, the γ -secretase complex processes also axonal NRG1 type III (Bao et al., 2003, 2004). As already described, the extracellular processing of NRG1 type III prompts a forward signaling to initiate myelination (Hu et al., 2006; Willem et al., 2006; La Marca et al., 2011). The γ -secretase intracellular cleavage of axonal NRG1 type III, instead, generates a NRG1-ICD intracellular fragment, which activates the transcription of the lipocalin-type prostaglandin-D synthase (L-Pgds) gene (Trimarco et al., 2014). L-PGDS further induces a pro-myelinating pathway in Schwann cells controlling formation and maintenance of the myelin sheath (Trimarco et al., 2014). Given the importance of NRG1 in nerve regeneration, additional studies to clarify the contribution of NRG1-ICD and L-PGDS after injury could contribute to the understanding of the processes involved in nerve repair.

MATRIX METALLOPROTEINASES

The matrix metalloproteinases (MMPs) are a family of zinc-dependent enzymes, which can degrade all components of the ECM (McCawley and Matrisian, 2001). At least 24 members, including collagenases, gelatinases, matrilysins, stromelysins and membrane-type MMPs belong to the MMPs family (Nagase et al., 2006). Proteolytic MMPs activity is necessary to regulate expression levels and function of ECM components and cell surface signaling receptors (Page-McCaw et al., 2007).

Among the various MMPs, MMP-2 and MMP-9 have been implicated in nerve development, and after injury (Platt et al., 2003). During development, MMP-2 and MMP-9 process dystroglycan to facilitate the formation of the dystroglycan receptor complex, a laminin receptor required for the correct formation of apposition and Cajal bands along myelinated fibers (Court et al., 2011).

Upon axotomy, MMP-9 mRNA levels are rapidly upregulated starting few hours after injury and peak at day 3 (La Fleur et al., 1996; Siebert et al., 2001; Hughes et al., 2002; Platt et al., 2003) while its activity increases already 12 h after axotomy, peaks around day 2 and returns to basal levels after 4 days (Siebert et al., 2001). In a model of crush nerve injury, MMP-9 localizes in myelinating Schwann cells, immune cells and endothelial cells (La Fleur et al., 1996;



Shubayev and Myers, 2000; Hughes et al., 2002; **Figure 1**). During nerve regeneration, MMP-9 negatively controls Schwann cells proliferation (Chattopadhyay et al., 2007). Accordingly, nerves of mice lacking MMP-9 have increased numbers of post-mitotic Schwann cells, together with shorter internodes and nodal abnormalities (Kim et al., 2012). *In vivo* studies in mutants lacking MMP-9 indicate that MMP-9 activity during axonal degeneration is crucial to promote myelin sheath collapse and to prompt the blood-nerve-barrier breakdown allowing the influx of immune cells into the nerve (Shubayev and Myers, 2000; Chattopadhyay et al., 2007; Kobayashi et al., 2008). More recent studies have implicated also MMP-9, together with MMP-7, in regulating claudin proteins expression at the tight junction in nerves after crush injury, suggesting that high levels of MMPs might alter nerve physical barriers (Wang et al., 2018). Further, MMP-9 stimulates the rearrangement of the basal

lamina (La Fleur et al., 1996; Hartung and Kieseier, 2000; Platt et al., 2003; Shubayev et al., 2006; Chattopadhyay et al., 2007; Kobayashi et al., 2008).

Interestingly, together with MMP-9, also its endogenous inhibitor TIMP-1 is upregulated in nerves early after injury (Kim et al., 2012); thus, it has been proposed that a fine balance between MMP-9 and TIMP-1 activity might regulate Schwann cells mitogenesis and maturation and control the molecular and structural assembly of myelin domains in remyelinated fibers to prompt a correct nerve repair (Kim et al., 2012). Thus, during early phases of axonal degeneration, a physiological inhibition of MMP-9 activity might be precisely coupled with its activation to coordinate an effective nerve repair.

PLASMINOGEN ACTIVATORS AND RELATED PROTEASES

The plasminogen activators (PAs), namely tissue PA (tPA) and urokinase PA (uPA), are key enzymes of the blood coagulation cascade implicated in several biological processes, including vascular and tissue remodeling, tumor development and progression (Mekawaty et al., 2014) and nervous system pathophysiology (Deryugina and Quigley, 2012; Thiebaut et al., 2018). These secreted proteases cleave the proenzyme plasminogen to turn it into its active form, plasmin (Collen, 1999; Rijken and Lijnen, 2009). Plasmin is a serine protease involved in processing a vast spectrum of molecules (Liotta et al., 1981), but its main substrate is fibrin (Bugge et al., 1996). Plasmin, in fact, degrades fibrin clots allowing scar resolution (Weisel and Litvinov, 2017). In addition, plasmin can activate other proteins, like MMPs (Keski-Oja et al., 1992; Murphy and Docherty, 1992; Zou et al., 2006) and growth factors (Saksela and Rifkin, 1990; Brauer and Yee, 1993; Munger et al., 1997). In the PNS, PAs activity is elevated during axonal outgrowth. PAs are secreted by primary neurons and Schwann cells in culture (Krystosek and Seeds, 1981, 1984) and their activity is localized in growth cones (Krystosek and Seeds, 1984). Moreover, the PA system is induced *in vivo* in embryonic DRG and motor neurons during axonal outgrowth (Seeds et al., 1992; Sumi et al., 1992). Interestingly, the PA system is potently induced also after peripheral nerve injury in mice (Siconolfi and Seeds, 2001a,b). Regeneration of peripheral nerves relies on the ability of axons to regrow in a very complex environment at the injury site, made of a structurally altered ECM, myelin and axon debris, surrounding tissues and infiltrating inflammatory cells. These adverse conditions represent an obstacle for axonal growth, thus regenerating neurites secrete PAs to dissolve cell-cell and cell-matrix adhesion. Accordingly, tPA and uPA mRNAs are promptly upregulated early after peripheral nerve injury in Schwann cells and neurons and their activity increases at the injury site up to 7 days post-crush (Akassoglou et al., 2000; Siconolfi and Seeds, 2001a; **Figure 2**). Moreover, recovery in knockout mice deficient for tPA, uPA and Plasminogen is significantly delayed after nerve injury, indicating that they are necessary for timely regeneration of peripheral nerves and the re-establishment of peripheral

sensitivity (Siconolfi and Seeds, 2001b). Plasmin is therefore protective for nerve injury (Akassoglou et al., 2000) and this effect is linked to the proteolytic activity plasmin exerts on fibrin (Figure 2). Accordingly, the vast axonal damage observed in tPA and plasminogen knockout nerves correlates with excessive accumulation of fibrin. Interestingly, genetic and pharmacological depletion of fibrinogen, the fibrin molecular precursor, enhances regeneration in these mutants (Akassoglou et al., 2000). Thus, fibrin deposition exacerbates axonal injury and the physiological induction of the tPA/plasmin cascade after injury prompts fibrin removal and stimulates repair (Figure 2). Of note, the important role of this cascade has been described also in humans, as there is a direct correlation between the extent of fibrinolytic activity and the degree of regeneration in patients with peripheral neuropathies (Previtali et al., 2008; Rivellini et al., 2012).

In addition to the PA system, thrombin, another key enzyme of the blood coagulation system, and its inhibitor Nexin-1, are potentially induced after sciatic nerve injury. In the blood coagulation cascade, thrombin converts fibrinogen into fibrin, its insoluble derivative (Weisel and Litvinov, 2017). Nexin-1, instead, a member of the large serpin superfamily, directly inhibits thrombin proteolytic activity (Cavanaugh et al., 1990; Gurwitz and Cunningham, 1990). In injured sciatic nerves, thrombin levels are elevated immediately after damage and reach their peak 1 day post-injury, declining after one week (Smirnova et al., 1996; Gera et al., 2016). On the contrary, upregulation of Nexin-1 in injured nerves occurs 6–9 days after thrombin induction (Meier et al., 1989; Smirnova et al., 1996) and is required to neutralize excessive thrombin proteolytic activity.

Collectively, these studies indicate that the proteases of the blood coagulation system and their regulators are essential to stimulate recovery in injured PNS and a precise balance between activation and inhibition of their proteolytic activity is required to correctly modulate nerve repair.

REFERENCES

- Akassoglou, K., Kombrinck, K. W., Degen, J. L., and Strickland, S. (2000). Tissue plasminogen activator-mediated fibrinolysis protects against axonal degeneration and demyelination after sciatic nerve injury. *J. Cell Biol.* 149, 1157–1166. doi: 10.1083/jcb.149.5.1157
- Akassoglou, K., Yu, W. M., Akpinar, P., and Strickland, S. (2002). Fibrin inhibits peripheral nerve remyelination by regulating Schwann cell differentiation. *Neuron* 33, 861–875. doi: 10.1016/s0896-6273(02)00617-7
- Arthur-Farraj, P. J., Latouche, M., Wilton, D. K., Quintes, S., Chabrol, E., Banerjee, A., et al. (2012). c-Jun reprograms Schwann cells of injured nerves to generate a repair cell essential for regeneration. *Neuron* 75, 633–647. doi: 10.1016/j.neuron.2012.06.021
- Atanasoski, S., Scherer, S. S., Sirkowski, E., Leone, D., Garratt, A. N., Birchmeier, C., et al. (2006). ErbB2 signaling in Schwann cells is mostly dispensable for maintenance of myelinated peripheral nerves and proliferation of adult Schwann cells after injury. *J. Neurosci.* 26, 2124–2131. doi: 10.1523/JNEUROSCI.4594-05.2006
- Bao, J., Lin, H., Ouyang, Y., Lei, D., Osman, A., Kim, T. W., et al. (2004). Activity-dependent transcription regulation of PSD-95 by neuregulin-1 and Eos. *Nat. Neurosci.* 7, 1250–1258. doi: 10.1038/nn1342
- Bao, J., Wolpowitz, D., Role, L. W., and Talmage, D. A. (2003). Back signaling by the Nrg-1 intracellular domain. *J. Cell Biol.* 161, 1133–1141. doi: 10.1083/jcb.200212085

CONCLUDING REMARKS

In the present review article, we presented a selected range of molecules and pathways involved in injured PNS. We specifically focused on extra cellular matrix and tissue modifiers and on growth factors' processing. Several studies have demonstrated how crucial is the role of these enzymes in tissue remodeling in response to damage. Nonetheless, despite the extensive studies conducted thus far, additional work is required to better define both the cell autonomy and the time frame in which these molecules and pathways are mostly active. We thus think that clarifying these aspects could be beneficial to define new therapeutic strategies that, together with the development of conduit devices, could efficiently improve the regenerative process and prompt full functional recovery.

AUTHOR CONTRIBUTIONS

MP and CT searched PubMed for articles published up until August 2018. Both MP and CT discussed the topics, decided the outline of the review and wrote the manuscript.

FUNDING

The studies from our laboratory are supported by grants from the Italian Ministry of Health (Ministero della Salute) RF PE 2013-02355206 (CT), Italy; Fondazione Telethon award number GPP 14040 and GGP 15012 (CT), Italy; the National Institutes of Health (NIH) NS099102-02, USA.

ACKNOWLEDGMENTS

We are indebted to Maria Grazia Forese for extensive discussions and suggestions. We apologize to colleagues whose relevant work could not be cited because of space limitations.

- Beattie, M. S., Harrington, A. W., Lee, R., Kim, J. Y., Boyce, S. L., Longo, F. M., et al. (2002). ProNGF induces p75-mediated death of oligodendrocytes following spinal cord injury. *Neuron* 36, 375–386. doi: 10.1016/s0896-6273(02)01005-x
- Belin, S., Ornaghi, F., Shackleford, G., Wang, J., Scapin, C., Lopez-Anido, C., et al. (2018). Neuregulin 1 type III improves peripheral nerve myelination in a mouse model of congenital hypomyelinating neuropathy. *Hum. Mol. Genet.* doi: 10.1093/hmg/ddy420 [Epub ahead of print].
- Bermingham-McDonogh, O., Xu, Y. T., Marchionni, M. A., and Scherer, S. S. (1997). Neuregulin expression in PNS neurons: isoforms and regulation by target interactions. *Mol. Cell. Neurosci.* 10, 184–195. doi: 10.1006/mcne.1997.0654
- Birchmeier, C., and Bennett, D. L. (2016). Neuregulin/ErbB signaling in developmental myelin formation and nerve repair. *Curr. Top. Dev. Biol.* 116, 45–64. doi: 10.1016/bs.ctdb.2015.11.009
- Black, R. A., and White, J. M. (1998). ADAMs: focus on the protease domain. *Curr. Opin. Cell Biol.* 10, 654–659. doi: 10.1016/s0955-0674(98)80042-2
- Blobel, C. P. (2000). Remarkable roles of proteolysis on and beyond the cell surface. *Curr. Opin. Cell Biol.* 12, 606–612. doi: 10.1016/s0955-0674(00)00139-3
- Blobel, C. P. (2005). ADAMs: key components in EGFR signalling and development. *Nat. Rev. Mol. Cell Biol.* 6, 32–43. doi: 10.1038/nrm1548
- Bolin, L. M., Verity, A. N., Silver, J. E., Shooter, E. M., and Abrams, J. S. (1995). Interleukin-6 production by Schwann cells and induction in sciatic nerve injury. *J. Neurochem.* 64, 850–858. doi: 10.1046/j.1471-4159.1995.64020850.x

- Bolino, A., Piguët, F., Alberizzi, V., Pellegatta, M., Rivellini, C., Guerrero-Valero, M., et al. (2016). Niacin-mediated Tace activation ameliorates CMT neuropathies with focal hypermyelination. *EMBO Mol. Med.* 8, 1438–1454. doi: 10.15252/emmm.201606349
- Brauer, P. R., and Yee, J. A. (1993). Cranial neural crest cells synthesize and secrete a latent form of transforming growth factor β that can be activated by neural crest cell proteolysis. *Dev. Biol.* 155, 281–285. doi: 10.1006/dbio.1993.1026
- Britsch, S. (2007). The neuregulin-1/ErbB signaling system in development and disease. *Adv. Anat. Embryol. Cell Biol.* 190, 1–65. doi: 10.1007/978-3-540-37107-6
- Brou, C., Logeat, F., Gupta, N., Bessia, C., Lebail, O., Doedens, J. R., et al. (2000). A novel proteolytic cleavage involved in Notch signaling: the role of the disintegrin-metalloprotease TACE. *Mol. Cell* 5, 207–216. doi: 10.1016/S1097-2765(00)80417-7
- Brown, M. C., Perry, V. H., Hunt, S. P., and Lapper, S. R. (1994). Further studies on motor and sensory nerve regeneration in mice with delayed Wallerian degeneration. *Eur. J. Neurosci.* 6, 420–428. doi: 10.1111/j.1460-9568.1994.tb00285.x
- Brushart, T. M., Aspalter, M., Griffin, J. W., Redett, R., Hameed, H., Zhou, C., et al. (2013). Schwann cell phenotype is regulated by axon modality and central-peripheral location and persists *in vitro*. *Exp. Neurol.* 247, 272–281. doi: 10.1016/j.expneurol.2013.05.007
- Bugge, T. H., Kombrinck, K. W., Flick, M. J., Daugherty, C. C., Danton, M. J., and Degen, J. L. (1996). Loss of fibrinogen rescues mice from the pleiotropic effects of plasminogen deficiency. *Cell* 87, 709–719. doi: 10.1016/s0092-8674(00)81390-2
- Buonanno, A., and Fischbach, G. D. (2001). Neuregulin and ErbB receptor signaling pathways in the nervous system. *Curr. Opin. Neurobiol.* 11, 287–296. doi: 10.1016/s0959-4388(00)00210-5
- Cai, J., Peng, X., Nelson, K. D., Eberhart, R., and Smith, G. M. (2004). Synergistic improvements in cell and axonal migration across sciatic nerve lesion gaps using bioresorbable filaments and heregulin- β 1. *J. Biomed. Mater. Res. A* 69, 247–258. doi: 10.1002/jbm.a.20119
- Cai, H., Wang, Y., McCarthy, D., Wen, H., Borchelt, D. R., Price, D. L., et al. (2001). BACE1 is the major β -secretase for generation of A β peptides by neurons. *Nat. Neurosci.* 4, 233–234. doi: 10.1038/85064
- Carroll, S. L., Miller, M. L., Frohnert, P. W., Kim, S. S., and Corbett, J. A. (1997). Expression of neuregulins and their putative receptors, ErbB2 and ErbB3, is induced during Wallerian degeneration. *J. Neurosci.* 17, 1642–1659. doi: 10.1523/JNEUROSCI.17-05-01642.1997
- Cavanaugh, K. P., Gurwitz, D., Cunningham, D. D., and Bradshaw, R. A. (1990). Reciprocal modulation of astrocyte stellation by thrombin and protease nexin-1. *J. Neurochem.* 54, 1735–1743. doi: 10.1111/j.1471-4159.1990.tb01228.x
- Chattopadhyay, S., Myers, R. R., Janes, J., and Shubayev, V. (2007). Cytokine regulation of MMP-9 in peripheral glia: implications for pathological processes and pain in injured nerve. *Brain Behav. Immun.* 21, 561–568. doi: 10.1016/j.bbi.2006.10.015
- Chen, X., Zhang, J., Wang, X., and Bi, J. (2016). Functional recovery from sciatic nerve crush injury is delayed because of increased distal atrophy in mice lacking the p75 receptor. *Neuroreport* 27, 940–947. doi: 10.1097/WNR.0000000000000635
- Cohen, J. A., Yachnis, A. T., Arai, M., Davis, J. G., and Scherer, S. S. (1992). Expression of the neu proto-oncogene by Schwann cells during peripheral nerve development and Wallerian degeneration. *J. Neurosci. Res.* 31, 622–634. doi: 10.1002/jnr.490310406
- Coimbra, J. R. M., Marques, D. F. F., Baptista, S. J., Pereira, C. M. F., Moreira, P. I., Dinis, T. C. P., et al. (2018). Highlights in BACE1 inhibitors for Alzheimer's disease treatment. *Front. Chem.* 6:178. doi: 10.3389/fchem.2018.00178
- Collen, D. (1999). The plasminogen (fibrinolytic) system. *Thromb. Haemost.* 82, 259–270. doi: 10.1055/s-0037-1615841
- Cosgaya, J. M., Chan, J. R., and Shooter, E. M. (2002). The neurotrophin receptor p75NTR as a positive modulator of myelination. *Science* 298, 1245–1248. doi: 10.1126/science.1076595
- Court, F. A., Zamboni, D., Pavoni, E., Colombelli, C., Baragli, C., Figlia, G., et al. (2011). MMP2-9 cleavage of dystroglycan alters the size and molecular composition of Schwann cell domains. *J. Neurosci.* 31, 12208–12217. doi: 10.1523/JNEUROSCI.0141-11.2011
- De Strooper, B., Annaert, W., Cupers, P., Saftig, P., Craessaerts, K., Mumm, J. S., et al. (1999). A presenilin-1-dependent γ -secretase-like protease mediates release of Notch intracellular domain. *Nature* 398, 518–522. doi: 10.1038/19083
- De Strooper, B., Saftig, P., Craessaerts, K., Vanderstichele, H., Guhde, G., Annaert, W., et al. (1998). Deficiency of presenilin-1 inhibits the normal cleavage of amyloid precursor protein. *Nature* 391, 387–390. doi: 10.1038/34910
- Dejaegere, T., Serneels, L., Schäfer, M. K., Van Biervliet, J., Horre, K., Depboylu, C., et al. (2008). Deficiency of Aph1B/C- γ -secretase disturbs Nrg1 cleavage and sensorimotor gating that can be reversed with antipsychotic treatment. *Proc. Natl. Acad. Sci. U S A* 105, 9775–9780. doi: 10.1073/pnas.0800507105
- Deryugina, E. I., and Quigley, J. P. (2012). Cell surface remodeling by plasmin: a new function for an old enzyme. *J. Biomed. Biotechnol.* 2012:564259. doi: 10.1155/2012/564259
- El Soury, M., Fornasari, B. E., Morano, M., Grazio, E., Ronchi, G., Incarnato, D., et al. (2018). Soluble neuregulin1 down-regulates myelination genes in schwann cells. *Front. Mol. Neurosci.* 11:157. doi: 10.3389/fnmol.2018.00157
- Ernfors, P., Henschen, A., Olson, L., and Persson, H. (1989). Expression of nerve growth factor receptor mRNA is developmentally regulated and increased after axotomy in rat spinal cord motoneurons. *Neuron* 2, 1605–1613. doi: 10.1016/0896-6273(89)90049-4
- Esper, R. M., Pankonin, M. S., and Loeb, J. A. (2006). Neuregulins: versatile growth and differentiation factors in nervous system development and human disease. *Brain Res. Rev.* 51, 161–175. doi: 10.1016/j.brainresrev.2005.11.006
- Falls, D. (2003). Neuregulins: functions, forms and signaling strategies. *Exp. Cell Res.* 284, 14–30. doi: 10.1016/s0014-4827(02)00102-7
- Fancy, S. P., Chan, J. R., Baranzini, S. E., Franklin, R. J., and Rowitch, D. H. (2011). Myelin regeneration: a recapitulation of development? *Annu. Rev. Neurosci.* 34, 21–43. doi: 10.1146/annurev-neuro-061010-113629
- Farah, M. H., Pan, B. H., Hoffman, P. N., Ferraris, D., Tsukamoto, T., Nguyen, T., et al. (2011). Reduced BACE1 activity enhances clearance of myelin debris and regeneration of axons in the injured peripheral nervous system. *J. Neurosci.* 31, 5744–5754. doi: 10.1523/JNEUROSCI.6810-10.2011
- Fawcett, J. W., and Keynes, R. J. (1990). Peripheral nerve regeneration. *Annu. Rev. Neurosci.* 13, 43–60. doi: 10.1146/annurev.ne.13.030190.000355
- Fledrich, R., Stassart, R. M., Klink, A., Rasch, L. M., Prukop, T., Haag, L., et al. (2014). Soluble neuregulin-1 modulates disease pathogenesis in rodent models of Charcot-Marie-Tooth disease 1A. *Nat. Med.* 20, 1055–1061. doi: 10.1038/nm.3664
- Fontana, X., Hristova, M., Da Costa, C., Patodia, S., Thei, L., Makwana, M., et al. (2012). c-Jun in Schwann cells promotes axonal regeneration and motoneuron survival via paracrine signaling. *J. Cell Biol.* 198, 127–141. doi: 10.1083/jcb.201205025
- Fornasari, B. E., Ronchi, G., Pascal, D., Visigalli, D., Capodivento, G., Nobbio, L., et al. (2018). Soluble Neuregulin1 is strongly up-regulated in the rat model of Charcot-Marie-Tooth 1A disease. *Exp. Biol. Med.* 243, 370–374. doi: 10.1177/1535370218754492
- Freese, C., Garratt, A. N., Fahrenholz, F., and Endres, K. (2009). The effects of α -secretase ADAM10 on the proteolysis of neuregulin-1. *FEBS J.* 276, 1568–1580. doi: 10.1111/j.1742-4658.2009.06889.x
- Fricker, F. R., Antunes-Martins, A., Galino, J., Paramsothy, R., La Russa, F., Perkins, J., et al. (2013). Axonal neuregulin 1 is a rate limiting but not essential factor for nerve remyelination. *Brain* 136, 2279–2297. doi: 10.1093/brain/awt148
- Fricker, F. R., Lago, N., Balarajah, S., Tsantoulas, C., Tanna, S., Zhu, N., et al. (2011). Axonally derived neuregulin-1 is required for remyelination and regeneration after nerve injury in adulthood. *J. Neurosci.* 31, 3225–3233. doi: 10.1523/JNEUROSCI.2568-10.2011
- Friedman, W. J. (2000). Neurotrophins induce death of hippocampal neurons via the p75 receptor. *J. Neurosci.* 20, 6340–6346. doi: 10.1523/JNEUROSCI.20-17-06340.2000
- Garratt, A. N., Britsch, S., and Birchmeier, C. (2000). Neuregulin, a factor with many functions in the life of a schwann cell. *Bioessays* 22, 987–996. doi: 10.1002/1521-1878(200011)22:11<987::aid-bies5>3.3.co;2-x
- Gaudet, A. D., Popovich, P. G., and Ramer, M. S. (2011). Wallerian degeneration: gaining perspective on inflammatory events after peripheral nerve injury. *J. Neuroinflammation* 8:110. doi: 10.1186/1742-2094-8-110

- Gera, O., Shavit-Stein, E., Bushi, D., Harnof, S., Shimon, M. B., Weiss, R., et al. (2016). Thrombin and protein C pathway in peripheral nerve Schwann cells. *Neuroscience* 339, 587–598. doi: 10.1016/j.neuroscience.2016.10.034
- Gerds, J., Summers, D. W., Milbrandt, J., and Diantonio, A. (2016). Axon self-destruction: new links among SARM1, MAPKs, and NAD⁺ Metabolism. *Neuron* 89, 449–460. doi: 10.1016/j.neuron.2015.12.023
- Gersbacher, M. T., Kim, D. Y., Bhattacharyya, R., and Kovacs, D. M. (2010). Identification of BACE1 cleavage sites in human voltage-gated sodium channel $\beta 2$ subunit. *Mol. Neurodegener.* 5:61. doi: 10.1186/1750-1326-5-61
- Golde, T. E., and Eckman, C. B. (2003). Physiologic and pathologic events mediated by intramembranous and juxtamembranous proteolysis. *Sci. STKE* 2003:RE4. doi: 10.1126/stke.2003.172.re4
- Gomez-Sanchez, J. A., Carty, L., Iruarrizaga-Lejarreta, M., Palomo-Irigoyen, M., Varela-Rey, M., Griffith, M., et al. (2015). Schwann cell autophagy, myelinophagy, initiates myelin clearance from injured nerves. *J. Cell Biol.* 210, 153–168. doi: 10.1083/jcb.201503019
- Gomez-Sanchez, J. A., Pilch, K. S., van der Lans, M., Fazal, S. V., Benito, C., Wagstaff, L. J., et al. (2017). After nerve injury, lineage tracing shows that myelin and remak schwann cells elongate extensively and branch to form repair schwann cells, which shorten radically on remyelination. *J. Neurosci.* 37, 9086–9099. doi: 10.1523/JNEUROSCI.1453-17.2017
- Gu, Z., Jiang, Q., Fu, A. K., Ip, N. Y., and Yan, Z. (2005). Regulation of NMDA receptors by neuregulin signaling in prefrontal cortex. *J. Neurosci.* 25, 4974–4984. doi: 10.1523/JNEUROSCI.1086-05.2005
- Guertin, A. D., Zhang, D. P., Mak, K. S., Alberta, J. A., and Kim, H. A. (2005). Microanatomy of axon/glia signaling during Wallerian degeneration. *J. Neurosci.* 25, 3478–3487. doi: 10.1523/JNEUROSCI.3766-04.2005
- Gurwitz, D., and Cunningham, D. D. (1990). Neurite outgrowth activity of protease nexin-1 on neuroblastoma cells requires thrombin inhibition. *J. Cell. Physiol.* 142, 155–162. doi: 10.1002/jcp.1041420119
- Hartmann, D., de Strooper, B., Serneels, L., Craessaerts, K., Herreman, A., Annaert, W., et al. (2002). The disintegrin/metalloprotease ADAM 10 is essential for Notch signalling but not for α -secretase activity in fibroblasts. *Hum. Mol. Genet.* 11, 2615–2624. doi: 10.1093/hmg/11.21.2615
- Hartung, H. P., and Kieseier, B. C. (2000). The role of matrix metalloproteinases in autoimmune damage to the central and peripheral nervous system. *J. Neuroimmunol.* 107, 140–147. doi: 10.1016/s0165-5728(00)00225-3
- Hemming, M. L., Elias, J. E., Gygi, S. P., and Selkoe, D. J. (2009). Identification of β -secretase (BACE1) substrates using quantitative proteomics. *PLoS One* 4:e8477. doi: 10.1371/journal.pone.0008477
- Hempstead, B. L., Martin-Zanca, D., Kaplan, D. R., Parada, L. F., and Chao, M. V. (1991). High-affinity NGF binding requires coexpression of the trk proto-oncogene and the low-affinity NGF receptor. *Nature* 350, 678–683. doi: 10.1038/350678a0
- Hirata, K., and Kawabuchi, M. (2002). Myelin phagocytosis by macrophages and nonmacrophages during Wallerian degeneration. *Microsc. Res. Tech.* 57, 541–547. doi: 10.1002/jemt.10108
- Hitt, B., Riordan, S. M., Kukreja, L., Eimer, W. A., Rajapaksha, T. W., and Vassar, R. (2012). β -site amyloid precursor protein (APP)-cleaving enzyme 1 (BACE1)-deficient mice exhibit a close homolog of L1 (CHL1) loss-of-function phenotype involving axon guidance defects. *J. Biol. Chem.* 287, 38408–38425. doi: 10.1074/jbc.M112.415505
- Ho, W. H., Armanini, M. P., Nuijens, A., Phillips, H. S., and Osheroff, P. L. (1995). Sensory and motor neuron-derived factor. A novel heregulin variant highly expressed in sensory and motor neurons. *J. Biol. Chem.* 270, 14523–14532. doi: 10.1074/jbc.270.24.14523
- Horiuchi, K., Weskamp, G., Lum, L., Hammes, H. P., Cai, H., Brodie, T. A., et al. (2003). Potential role for ADAM15 in pathological neovascularization in mice. *Mol. Cell. Biol.* 23, 5614–5624. doi: 10.1128/mcb.23.16.5614-5624.2003
- Hu, X., He, W., Diaconu, C., Tang, X., Kidd, G. J., Macklin, W. B., et al. (2008). Genetic deletion of BACE1 in mice affects remyelination of sciatic nerves. *FASEB J.* 22, 2970–2980. doi: 10.1096/fj.08-106666
- Hu, X., Hicks, C. W., He, W., Wong, P., Macklin, W. B., Trapp, B. D., et al. (2006). Bace1 modulates myelination in the central and peripheral nervous system. *Nat. Neurosci.* 9, 1520–1525. doi: 10.1038/nn1797
- Hu, X., Hu, J., Dai, L., Trapp, B., and Yan, R. (2015). Axonal and Schwann cell BACE1 is equally required for remyelination of peripheral nerves. *J. Neurosci.* 35, 3806–3814. doi: 10.1523/JNEUROSCI.5207-14.2015
- Hughes, P. M., Wells, G. M., Perry, V. H., Brown, M. C., and Miller, K. M. (2002). Comparison of matrix metalloproteinase expression during Wallerian degeneration in the central and peripheral nervous systems. *Neuroscience* 113, 273–287. doi: 10.1016/s0306-4522(02)00183-5
- Jang, S. Y., Shin, Y. K., Park, S. Y., Park, J. Y., Lee, H. J., Yoo, Y. H., et al. (2016). Autophagic myelin destruction by Schwann cells during Wallerian degeneration and segmental demyelination. *Glia* 64, 730–742. doi: 10.1002/glia.22957
- Jangouk, P., Dehmel, T., Meyer Zu Hörste, G., Ludwig, A., Lehmann, H. C., and Kieseier, B. C. (2009). Involvement of ADAM10 in axonal outgrowth and myelination of the peripheral nerve. *Glia* 57, 1765–1774. doi: 10.1002/glia.20889
- Jessen, K. R., and Mirsky, R. (2008). Negative regulation of myelination: relevance for development, injury and demyelinating disease. *Glia* 56, 1552–1565. doi: 10.1002/glia.20761
- Jessen, K. R., Mirsky, R., and Lloyd, A. C. (2015). Schwann cells: development and role in nerve repair. *Cold Spring Harb. Perspect. Biol.* 7:a020487. doi: 10.1101/cshperspect.a020487
- Jung, K. M., Tan, S., Landman, N., Petrova, K., Murray, S., Lewis, R., et al. (2003). Regulated intramembrane proteolysis of the p75 neurotrophin receptor modulates its association with the TrkA receptor. *J. Biol. Chem.* 278, 42161–42169. doi: 10.1074/jbc.M306028200
- Kao, S. C., Wu, H., Xie, J., Chang, C. P., Ranish, J. A., Graef, I. A., et al. (2009). Calcineurin/NFAT signaling is required for neuregulin-regulated Schwann cell differentiation. *Science* 323, 651–654. doi: 10.1126/science.1166562
- Keski-Oja, J., Lohi, J., Tuuttila, A., Tryggvason, K., and Vartio, T. (1992). Proteolytic processing of the 72,000-Da type IV collagenase by urokinase plasminogen activator. *Exp. Cell Res.* 202, 471–476. doi: 10.1016/0014-4827(92)90101-d
- Kim, D. Y., Carey, B. W., Wang, H., Ingano, L. A. M., Binshtok, A. M., Wertz, M. H., et al. (2007). BACE1 regulates voltage-gated sodium channels and neuronal activity. *Nat. Cell Biol.* 9, 755–764. doi: 10.1038/ncb1602
- Kim, D. Y., Gersbacher, M. T., Inquimbert, P., and Kovacs, D. M. (2011). Reduced sodium channel Na_v1.1 levels in BACE1-null mice. *J. Biol. Chem.* 286, 8106–8116. doi: 10.1074/jbc.M110.134692
- Kim, D. Y., Ingano, L. A., Carey, B. W., Pettingell, W. H., and Kovacs, D. M. (2005). Presenilin/ γ -secretase-mediated cleavage of the voltage-gated sodium channel $\beta 2$ -subunit regulates cell adhesion and migration. *J. Biol. Chem.* 280, 23251–23261. doi: 10.1074/jbc.M412938200
- Kim, Y., Remacle, A. G., Chernov, A. V., Liu, H., Shubayev, I., Lai, C., et al. (2012). The MMP-9/TIMP-1 axis controls the status of differentiation and function of myelin-forming Schwann cells in nerve regeneration. *PLoS One* 7:e33664. doi: 10.1371/journal.pone.0033664
- Kobayashi, H., Chattopadhyay, S., Kato, K., Dolkas, J., Kikuchi, S., Myers, R. R., et al. (2008). MMPs initiate Schwann cell-mediated MBP degradation and mechanical nociception after nerve damage. *Mol. Cell. Neurosci.* 39, 619–627. doi: 10.1016/j.mcn.2008.08.008
- Koliatsos, V. E., Crawford, T. O., and Price, D. L. (1991). Axotomy induces nerve growth factor receptor immunoreactivity in spinal motor neurons. *Brain Res.* 549, 297–304. doi: 10.1016/0006-8993(91)90471-7
- Kopan, R., and Goate, A. (2000). A common enzyme connects notch signaling and Alzheimer's disease. *Genes Dev.* 14, 2799–2806. doi: 10.1101/gad.836900
- Kopan, R., and Ilagan, M. X. (2004). γ -secretase: proteasome of the membrane? *Nat. Rev. Mol. Cell Biol.* 5, 499–504. doi: 10.1038/nrm1406
- Kraemer, B. R., Yoon, S. O., and Carter, B. D. (2014). The biological functions and signaling mechanisms of the p75 neurotrophin receptor. *Handb. Exp. Pharmacol.* 220, 121–164. doi: 10.1007/978-3-642-45106-5_6
- Krystosek, A., and Seeds, N. W. (1981). Plasminogen activator release at the neuronal growth cone. *Science* 213, 1532–1534. doi: 10.1126/science.7197054
- Krystosek, A., and Seeds, N. W. (1984). Peripheral neurons and Schwann cells secrete plasminogen activator. *J. Cell Biol.* 98, 773–776. doi: 10.1083/jcb.98.2.773
- Kuhn, P. H., Koroniak, K., Hög, S., Colombo, A., Zeitschel, U., Willem, M., et al. (2012). Secretome protein enrichment identifies physiological BACE1 protease substrates in neurons. *EMBO J.* 31, 3157–3168. doi: 10.1038/emboj.2012.173
- Kurek, J. B., Austin, L., Cheema, S. S., Bartlett, P. F., and Murphy, M. (1996). Up-regulation of leukaemia inhibitory factor and interleukin-6 in transected

- sciatic nerve and muscle following denervation. *Neuromuscul. Disord.* 6, 105–114. doi: 10.1016/0960-8966(95)00029-1
- Kurisaki, T., Masuda, A., Osumi, N., Nabeshima, Y., and Fujisawa-Sehara, A. (1998). Spatially- and temporally-restricted expression of meltrin α (ADAM12) and β (ADAM19) in mouse embryo. *Mech. Dev.* 73, 211–215. doi: 10.1016/s0925-4773(98)00043-4
- Kwon, Y. K., Bhattacharyya, A., Alberta, J. A., Giannobile, W. V., Cheon, K., Stiles, C. D., et al. (1997). Activation of ErbB2 during wallerian degeneration of sciatic nerve. *J. Neurosci.* 17, 8293–8299. doi: 10.1523/jneurosci.17-21-08293.1997
- La Fleur, M., Underwood, J. L., Rappolee, D. A., and Werb, Z. (1996). Basement membrane and repair of injury to peripheral nerve: defining a potential role for macrophages, matrix metalloproteinases, and tissue inhibitor of metalloproteinases-1. *J. Exp. Med.* 184, 2311–2326. doi: 10.1084/jem.184.6.2311
- La Marca, R., Cerri, F., Horiuchi, K., Bachi, A., Feltri, M. L., Wrabetz, L., et al. (2011). TACE (ADAM17) inhibits Schwann cell myelination. *Nat. Neurosci.* 14, 857–865. doi: 10.1038/nn.2849
- Laird, F. M., Cai, H., Savonenko, A. V., Farah, M. H., He, K., Melnikova, T., et al. (2005). BACE1, a major determinant of selective vulnerability of the brain to amyloid- β amyloidogenesis, is essential for cognitive, emotional, and synaptic functions. *J. Neurosci.* 25, 11693–11709. doi: 10.1523/jneurosci.2766-05.2005
- Liotta, L. A., Goldfarb, R. H., Brundage, R., Siegal, G. P., Terranova, V., and Garbisa, S. (1981). Effect of plasminogen activator (urokinase), plasmin, and thrombin on glycoprotein and collagenous components of basement membrane. *Cancer Res.* 41, 4629–4636.
- Loeb, J. A., Khurana, T. S., Robbins, J. T., Yee, A. G., and Fischbach, G. D. (1999). Expression patterns of transmembrane and released forms of neuregulin during spinal cord and neuromuscular synapse development. *Development* 126, 781–791.
- Louvi, A., and Artavanis-Tsakonas, S. (2006). Notch signalling in vertebrate neural development. *Nat. Rev. Neurosci.* 7, 93–102. doi: 10.1038/nrn1847
- Luo, Y., Bolon, B., Kahn, S., Bennett, B. D., Babu-Khan, S., Denis, P., et al. (2001). Mice deficient in BACE1, the Alzheimer's β -secretase, have normal phenotype and abolished β -amyloid generation. *Nat. Neurosci.* 4, 231–232. doi: 10.1038/85059
- Mahanthappa, N. K., Anton, E. S., and Matthew, W. D. (1996). Glial growth factor 2, a soluble neuregulin, directly increases Schwann cell motility and indirectly promotes neurite outgrowth. *J. Neurosci.* 16, 4673–4683. doi: 10.1523/jneurosci.16-15-04673.1996
- Marchionni, M. A., Goodearl, A. D., Chen, M. S., Bermingham-McDonogh, O., Kirk, C., Hendricks, M., et al. (1993). Glial growth factors are alternatively spliced erbB2 ligands expressed in the nervous system. *Nature* 362, 312–318. doi: 10.1038/362312a0
- McCawley, L. J., and Matrisian, L. M. (2001). Matrix metalloproteinases: they're not just for matrix anymore! *Curr. Opin. Cell Biol.* 13, 534–540. doi: 10.1016/s0955-0674(00)00248-9
- Meeker, R. B., and Williams, K. S. (2015). The p75 neurotrophin receptor: at the crossroad of neural repair and death. *Neural Regen. Res.* 10, 721–725. doi: 10.4103/1673-5374.156967
- Mei, L., and Nave, K. A. (2014). Neuregulin-ERBB signaling in the nervous system and neuropsychiatric diseases. *Neuron* 83, 27–49. doi: 10.1016/j.neuron.2014.06.007
- Meier, R., Spreyer, P., Ortmann, R., Harel, A., and Monard, D. (1989). Induction of glia-derived nexin after lesion of a peripheral nerve. *Nature* 342, 548–550. doi: 10.1038/342548a0
- Mekkawy, A. H., Pourgholami, M. H., and Morris, D. L. (2014). Involvement of urokinase-type plasminogen activator system in cancer: an overview. *Med. Res. Rev.* 34, 918–956. doi: 10.1002/med.21308
- Meyer zu Horste, G., Derksen, A., Stassart, R., Szezanowski, F., Thanos, M., Stettner, M., et al. (2015). Neuronal ADAM10 promotes outgrowth of small-caliber myelinated axons in the peripheral nervous system. *J. Neuropathol. Exp. Neurol.* 74, 1077–1085. doi: 10.1097/nen.0000000000000253
- Mi, S., Lee, X., Shao, Z., Thill, G., Ji, B., Relton, J., et al. (2004). LINGO-1 is a component of the Nogo-66 receptor/p75 signaling complex. *Nat. Neurosci.* 7, 221–228. doi: 10.1038/nn1188
- Michailov, G. V., Sereda, M. W., Brinkmann, B. G., Fischer, T. M., Haug, B., Birchmeier, C., et al. (2004). Axonal neuregulin-1 regulates myelin sheath thickness. *Science* 304, 700–703. doi: 10.1126/science.1095862
- Morano, M., Ronchi, G., Nicolo, V., Fornasari, B. E., Crosio, A., Perroteau, I., et al. (2018). Modulation of the Neuregulin 1/ErbB system after skeletal muscle denervation and reinnervation. *Sci. Rep.* 8:5047. doi: 10.1038/s41598-018-23454-8
- Munger, J. S., Harpel, J. G., Gleizes, P.-E., Mazzieri, R., Nunes, I., and Rifkin, D. B. (1997). Latent transforming growth factor- β : structural features and mechanisms of activation. *Kidney Int.* 51, 1376–1382. doi: 10.1038/ki.1997.188
- Murphy, G., and Docherty, A. J. (1992). The matrix metalloproteinases and their inhibitors. *Am. J. Respir. Cell Mol. Biol.* 7, 120–125. doi: 10.1165/ajrcmb/7.2.120
- Nagase, H., Visse, R., and Murphy, G. (2006). Structure and function of matrix metalloproteinases and TIMPs. *Cardiovasc. Res.* 69, 562–573. doi: 10.1016/j.cardiores.2005.12.002
- Nave, K. A., and Salzer, J. L. (2006). Axonal regulation of myelination by neuregulin 1. *Curr. Opin. Neurobiol.* 16, 492–500. doi: 10.1016/j.conb.2006.08.008
- Nykjaer, A., Lee, R., Teng, K. K., Jansen, P., Madsen, P., Nielsen, M. S., et al. (2004). Sortilin is essential for proNGF-induced neuronal cell death. *Nature* 427, 843–848. doi: 10.1038/nature02319
- Page-McCaw, A., Ewald, A. J., and Werb, Z. (2007). Matrix metalloproteinases and the regulation of tissue remodelling. *Nat. Rev. Mol. Cell Biol.* 8, 221–233. doi: 10.1038/nrm2125
- Pan, D., and Rubin, G. M. (1997). Kuzbanian controls proteolytic processing of Notch and mediates lateral inhibition during *Drosophila* and vertebrate neurogenesis. *Cell* 90, 271–280. doi: 10.1016/s0092-8674(00)80335-9
- Pathak, A., Stanley, E. M., Hickman, F. E., Wallace, N., Brewer, B., Li, D., et al. (2018). Retrograde degenerative signaling mediated by the p75 neurotrophin receptor requires p150(Glued) deacetylation by axonal HDAC1. *Dev. Cell* 46, 376.e7–387.e7. doi: 10.1016/j.devcel.2018.07.001
- Pereira, J. A., Lebrun-Julien, F., and Suter, U. (2012). Molecular mechanisms regulating myelination in the peripheral nervous system. *Trends Neurosci.* 35, 123–134. doi: 10.1016/j.tins.2011.11.006
- Perry, V. H., Tsao, J. W., Fearn, S., and Brown, M. C. (1995). Radiation-induced reductions in macrophage recruitment have only slight effects on myelin degeneration in sectioned peripheral nerves of mice. *Eur. J. Neurosci.* 7, 271–280. doi: 10.1111/j.1460-9568.1995.tb01063.x
- Petratos, S., Butzkueven, H., Shipham, K., Cooper, H., Buccì, T., Reid, K., et al. (2003). Schwann cell apoptosis in the postnatal axotomized sciatic nerve is mediated via NGF through the low-affinity neurotrophin receptor. *J. Neuropathol. Exp. Neurol.* 62, 398–411. doi: 10.1093/jnen/62.4.398
- Platt, C. I., Krekoski, C. A., Ward, R. V., Edwards, D. R., and Gavrilovic, J. (2003). Extracellular matrix and matrix metalloproteinases in sciatic nerve. *J. Neurosci. Res.* 74, 417–429. doi: 10.1002/jnr.10783
- Previtali, S. C., Malaguti, M. C., Riva, N., Scarlato, M., Dacci, P., Dina, G., et al. (2008). The extracellular matrix affects axonal regeneration in peripheral neuropathies. *Neurology* 71, 322–331. doi: 10.1212/01.wnl.0000319736.43628.04
- Primakoff, P., and Myles, D. G. (2000). The ADAM gene family: surface proteins with adhesion and protease activity. *Trends Genet.* 16, 83–87. doi: 10.1016/s0168-9525(99)01926-5
- Rijken, D. C., and Lijnen, H. R. (2009). New insights into the molecular mechanisms of the fibrinolytic system. *J. Thromb. Haemost.* 7, 4–13. doi: 10.1111/j.1538-7836.2008.03220.x
- Rivellini, C., Dina, G., Porrello, E., Cerri, F., Scarlato, M., Domi, T., et al. (2012). Urokinase plasminogen receptor and the fibrinolytic complex play a role in nerve repair after nerve crush in mice and in human neuropathies. *PLoS One* 7:e32059. doi: 10.1371/journal.pone.0032059
- Roberds, S. L., Anderson, J., Basi, G., Bienkowski, M. J., Branstetter, D. G., Chen, K. S., et al. (2001). BACE knockout mice are healthy despite lacking the primary β -secretase activity in brain: implications for Alzheimer's disease therapeutics. *Hum. Mol. Genet.* 10, 1317–1324. doi: 10.1093/hmg/10.12.1317
- Roberts, S. L., Dun, X. P., Doddrell, R. D. S., Mindos, T., Drake, L. K., Onaitis, M. W., et al. (2017). Sox2 expression in Schwann cells inhibits myelination *in vivo* and induces influx of macrophages to the nerve. *Development* 144, 3114–3125. doi: 10.1242/dev.150656
- Rotshenker, S. (2011). Wallerian degeneration: the innate-immune response to traumatic nerve injury. *J. Neuroinflammation* 8:109. doi: 10.1186/1742-2094-8-109

- Sachs, B. D., Baillie, G. S., McCall, J. R., Passino, M. A., Schachtrup, C., Wallace, D. A., et al. (2007). p75 neurotrophin receptor regulates tissue fibrosis through inhibition of plasminogen activation via a PDE4/cAMP/PKA pathway. *J. Cell Biol.* 177, 1119–1132. doi: 10.1083/jcb.200701040
- Sachse, C. C., Kim, Y. H., Agsten, M., Huth, T., Alzheimer, C., Kovacs, D. M., et al. (2013). BACE1 and presenilin-1/2 regulate proteolytic processing of KCNE1 and 2, auxiliary subunits of voltage-gated potassium channels. *FASEB J.* 27, 2458–2467. doi: 10.1096/fj.12-124056
- Saika, T., Senba, E., Noguchi, K., Sato, M., Yoshida, S., Kubo, T., et al. (1991). Effects of nerve crush and transection on mRNA levels for nerve growth factor receptor in the rat facial motoneurons. *Mol. Brain Res.* 9, 157–160. doi: 10.1016/0169-328x(91)90142-k
- Saksela, O., and Rifkin, D. B. (1990). Release of basic fibroblast growth factor-heparan sulfate complexes from endothelial cells by plasminogen activator-mediated proteolytic activity. *J. Cell Biol.* 110, 767–775. doi: 10.1083/jcb.110.3.767
- Savonenko, A. V., Melnikova, T., Laird, F. M., Stewart, K. A., Price, D. L., and Wong, P. C. (2008). Alteration of BACE1-dependent NRG1/ErbB4 signaling and schizophrenia-like phenotypes in BACE1-null mice. *Proc. Natl. Acad. Sci. U S A* 105, 5585–5590. doi: 10.1073/pnas.0710373105
- Scapin, C., Ferri, C., Pettinato, E., Zamboni, D., Bianchi, F., Del Carro, U., et al. (2018). Enhanced axonal neuregulin-1 type-III signaling ameliorates neurophysiology and hypomyelination in a charcot-marie-tooth type 1B mouse model. *Hum. Mol. Genet.* doi: 10.1093/hmg/ddy411 [Epub ahead of print].
- Schlöndorff, J., and Blobel, C. P. (1999). Metalloprotease-disintegrins: modular proteins capable of promoting cell-cell interactions and triggering signals by protein-ectodomain shedding. *J. Cell Sci.* 112, 3603–3617.
- Seals, D. F., and Courtneidge, S. A. (2003). The ADAMs family of metalloproteases: multidomain proteins with multiple functions. *Genes Dev.* 17, 7–30. doi: 10.1101/gad.1039703
- Seeds, N. W., Verrall, S., Friedman, G., Hayden, S., Gadotti, D., Haffke, S., et al. (1992). Plasminogen activators and plasminogen activator inhibitors in neural development. *Ann. N Y Acad. Sci.* 667, 32–40. doi: 10.1111/j.1749-6632.1992.tb51592.x
- Shamash, S., Reichert, F., and Rotshenker, S. (2002). The cytokine network of Wallerian degeneration: tumor necrosis factor- α , interleukin-1 α , and interleukin-1 β . *J. Neurosci.* 22, 3052–3060. doi: 10.1523/JNEUROSCI.22-08-03052.2002
- Shirakabe, K., Wakatsuki, S., Kurisaki, T., and Fujisawa-Sehara, A. (2001). Roles of Meltrin β /ADAM19 in the processing of neuregulin. *J. Biol. Chem.* 276, 9352–9358. doi: 10.1074/jbc.m007913200
- Shubayev, V. I., Angert, M., Dolkas, J., Campana, W. M., Palenscar, K., and Myers, R. R. (2006). TNF α -induced MMP-9 promotes macrophage recruitment into injured peripheral nerve. *Mol. Cell. Neurosci.* 31, 407–415. doi: 10.1016/j.mcn.2005.10.011
- Shubayev, V. I., and Myers, R. R. (2000). Upregulation and interaction of TNF α and gelatinases A and B in painful peripheral nerve injury. *Brain Res.* 855, 83–89. doi: 10.1016/s0006-8993(99)02321-5
- Siconolfi, L. B., and Seeds, N. W. (2001a). Induction of the plasminogen activator system accompanies peripheral nerve regeneration after sciatic nerve crush. *J. Neurosci.* 21, 4336–4347. doi: 10.1523/JNEUROSCI.21-12-04336.2001
- Siconolfi, L. B., and Seeds, N. W. (2001b). Mice lacking tPA, uPA, or plasminogen genes showed delayed functional recovery after sciatic nerve crush. *J. Neurosci.* 21, 4348–4355. doi: 10.1523/JNEUROSCI.21-12-04348.2001
- Siebert, H., Dippel, N., Mader, M., Weber, F., and Brück, W. (2001). Matrix metalloproteinase expression and inhibition after sciatic nerve axotomy. *J. Neuropathol. Exp. Neurol.* 60, 85–93. doi: 10.1093/jnen/60.1.85
- Sinha, S., and Lieberburg, I. (1999). Cellular mechanisms of β -amyloid production and secretion. *Proc. Natl. Acad. Sci. U S A* 96, 11049–11053. doi: 10.1073/pnas.96.20.11049
- Smirnova, I. V., Ma, J. Y., Citron, B. A., Ratzlaff, K. T., Gregory, E. J., Akaaboune, M., et al. (1996). Neural thrombin and protease nexin I kinetics after murine peripheral nerve injury. *J. Neurochem.* 67, 2188–2199. doi: 10.1046/j.1471-4159.1996.67052188.x
- Song, X. Y., Zhou, F. H., Zhong, J. H., Wu, L. L., and Zhou, X. F. (2006). Knockout of p75(NTR) impairs re-myelination of injured sciatic nerve in mice. *J. Neurochem.* 96, 833–842. doi: 10.1111/j.1471-4159.2005.03564.x
- Stassart, R. M., Fledrich, R., Velanac, V., Brinkmann, B. G., Schwab, M. H., Meijer, D., et al. (2013). A role for Schwann cell-derived neuregulin-1 in remyelination. *Nat. Neurosci.* 16, 48–54. doi: 10.1038/nn.3281
- Stassart, R. M., Möbius, W., Nave, K. A., and Edgar, J. M. (2018). The axon-myelin unit in development and degenerative disease. *Front. Neurosci.* 12:467. doi: 10.3389/fnins.2018.00467
- Stoll, G., Jander, S., and Myers, R. R. (2002). Degeneration and regeneration of the peripheral nervous system: from augustus waller's observations to neuroinflammation. *J. Peripher. Nerv. Syst.* 7, 13–27. doi: 10.1046/j.1529-8027.2002.02002.x
- Struhl, G., and Adachi, A. (2000). Requirements for presenilin-dependent cleavage of notch and other transmembrane proteins. *Mol. Cell* 6, 625–636. doi: 10.1016/s1097-2765(00)00061-7
- Struhl, G., and Greenwald, I. (1999). Presenilin is required for activity and nuclear access of Notch in *Drosophila*. *Nature* 398, 522–525. doi: 10.1038/19091
- Sumi, Y., Dent, M. A., Owen, D. E., Seeley, P. J., and Morris, R. J. (1992). The expression of tissue and urokinase-type plasminogen activators in neural development suggests different modes of proteolytic involvement in neuronal growth. *Development* 116, 625–637.
- Syroid, D. E., Maycox, P. J., Soilu-Hanninen, M., Petratos, S., Bucci, T., Burrola, P., et al. (2000). Induction of postnatal schwann cell death by the low-affinity neurotrophin receptor *in vitro* and after axotomy. *J. Neurosci.* 20, 5741–5747. doi: 10.1523/JNEUROSCI.20-15-05741.2000
- Tajdaran, K., Chan, K., Gordon, T., and Borschel, G. H. (2018). Matrices, scaffolds, and carriers for protein and molecule delivery in peripheral nerve regeneration. *Exp. Neurol.* doi: 10.1016/j.expneurol.2018.08.014 [Epub ahead of print].
- Tallon, C., Rockenstein, E., Masliah, E., and Farah, M. H. (2017). Increased BACE1 activity inhibits peripheral nerve regeneration after injury. *Neurobiol. Dis.* 106, 147–157. doi: 10.1016/j.nbd.2017.07.003
- Taveggia, C., Feltri, M. L., and Wrabetz, L. (2010). Signals to promote myelin formation and repair. *Nat. Rev. Neurol.* 6, 276–287. doi: 10.1038/nrnneurol.2010.37
- Taveggia, C., Zanazzi, G., Petrylak, A., Yano, H., Rosenbluth, J., Einheber, S., et al. (2005). Neuregulin-1 type III determines the ensheathment fate of axons. *Neuron* 47, 681–694. doi: 10.1016/j.neuron.2005.08.017
- Thiebaut, A. M., Gauberti, M., Ali, C., Martinez De Lizarrondo, S., Vivien, D., Yepes, M., et al. (2018). The role of plasminogen activators in stroke treatment: fibrinolysis and beyond. *Lancet Neurol.* 17, 1121–1132. doi: 10.1016/S1474-4422(18)30323-5
- Tofaris, G. K., Patterson, P. H., Jessen, K. R., and Mirsky, R. (2002). Denervated Schwann cells attract macrophages by secretion of leukemia inhibitory factor (LIF) and monocyte chemoattractant protein-1 in a process regulated by interleukin-6 and LIF. *J. Neurosci.* 22, 6696–6703. doi: 10.1523/JNEUROSCI.22-15-06696.2002
- Tomita, K., Kubo, T., Matsuda, K., Fujiwara, T., Yano, K., Winograd, J. M., et al. (2007). The neurotrophin receptor p75NTR in Schwann cells is implicated in remyelination and motor recovery after peripheral nerve injury. *Glia* 55, 1199–1208. doi: 10.1002/glia.20533
- Trimarco, A., Forese, M. G., Alfieri, V., Lucente, A., Brambilla, P., Dina, G., et al. (2014). Prostaglandin D2 synthase/GPR44: a signaling axis in PNS myelination. *Nat. Neurosci.* 17, 1682–1692. doi: 10.1038/nn.3857
- van Tetering, G., van Diest, P., Verlaan, I., van der Wall, E., Kopan, R., and Vooijs, M. (2009). Metalloprotease ADAM10 is required for Notch1 site 2 cleavage. *J. Biol. Chem.* 284, 31018–31027. doi: 10.1074/jbc.M109.006775
- Vassar, R., Bennett, B. D., Babu-Khan, S., Kahn, S., Mendiaz, E. A., Denis, P., et al. (1999). β -secretase cleavage of Alzheimer's amyloid precursor protein by the transmembrane aspartic protease BACE. *Science* 286, 735–741. doi: 10.1126/science.286.5440.735
- Velanac, V., Unterbarnscheidt, T., Hinrichs, W., Gummert, M. N., Fischer, T. M., Rossner, M. J., et al. (2012). Bace1 processing of NRG1 type III produces a myelin-inducing signal but is not essential for the stimulation of myelination. *Glia* 60, 203–217. doi: 10.1002/glia.21255
- Wakatsuki, S., Kurisaki, T., and Sehara-Fujisawa, A. (2004). Lipid rafts identified as locations of ectodomain shedding mediated by Meltrin β /ADAM19. *J. Neurochem.* 89, 119–123. doi: 10.1046/j.1471-4159.2003.02303.x
- Wakatsuki, S., Yumoto, N., Komatsu, K., Araki, T., and Sehara-Fujisawa, A. (2009). Roles of meltrin- β /ADAM19 in progression of Schwann cell

- differentiation and myelination during sciatic nerve regeneration. *J. Biol. Chem.* 284, 2957–2966. doi: 10.1074/jbc.m803191200
- Waller, V. A., and Owen, R. (1850). Experiments on the section of the glossopharyngeal and hypoglossal nerves of the frog and observations of the alterations produced thereby in the structure of their primitive fibres. *Philos. Trans. R. Soc. Lond.* 140, 423–429. doi: 10.1098/rstl.1850.0021
- Wang, K. C., Kim, J. A., Sivasankaran, R., Segal, R., and He, Z. (2002). P75 interacts with the Nogo receptor as a co-receptor for Nogo, MAG and OMgp. *Nature* 420, 74–78. doi: 10.1038/nature01176
- Wang, X., Miao, Y., Ni, J., Wang, Y., Qian, T., Yu, J., et al. (2018). Peripheral nerve injury induces dynamic changes of tight junction components. *Front. Physiol.* 9:1519. doi: 10.3389/fphys.2018.01519
- Weisel, J. W., and Litvinov, R. I. (2017). Fibrin formation, structure and properties. *Subcell. Biochem.* 82, 405–456. doi: 10.1007/978-3-319-49674-0_13
- Weskamp, G., Schlondorff, J., Lum, L., Becherer, J. D., Kim, T. W., Saftig, P., et al. (2004). Evidence for a critical role of the tumor necrosis factor α convertase (TACE) in ectodomain shedding of the p75 neurotrophin receptor (p75NTR). *J. Biol. Chem.* 279, 4241–4249. doi: 10.1074/jbc.M307974200
- Willem, M. (2016). Proteolytic processing of Neuregulin-1. *Brain Res. Bull.* 126, 178–182. doi: 10.1016/j.brainresbull.2016.07.003
- Willem, M., Garratt, A. N., Novak, B., Citron, M., Kaufmann, S., Rittger, A., et al. (2006). Control of peripheral nerve myelination by the β -secretase BACE1. *Science* 314, 664–666. doi: 10.1126/science.1132341
- Wolfe, M. S., De Los Angeles, J., Miller, D. D., Xia, W., and Selkoe, D. J. (1999). Are presenilins intramembrane-cleaving proteases? Implications for the molecular mechanism of Alzheimer's disease. *Biochemistry* 38, 11223–11230. doi: 10.1021/bi991080q
- Wolpowitz, D., Mason, T. B., Dietrich, P., Mendelsohn, M., Talmage, D. A., and Role, L. W. (2000). Cysteine-rich domain isoforms of the neuregulin-1 gene are required for maintenance of peripheral synapses. *Neuron* 25, 79–91. doi: 10.1016/s0896-6273(00)80873-9
- Wong, S. T., Henley, J. R., Kanning, K. C., Huang, K. H., Bothwell, M., and Poo, M. M. (2002). A p75(NTR) and Nogo receptor complex mediates repulsive signaling by myelin-associated glycoprotein. *Nat. Neurosci.* 5, 1302–1308. doi: 10.1038/nn975
- Wong, H. K., Sakurai, T., Oyama, F., Kaneko, K., Wada, K., Miyazaki, H., et al. (2005). β Subunits of voltage-gated sodium channels are novel substrates of β -site amyloid precursor protein-cleaving enzyme (BACE1) and γ -secretase. *J. Biol. Chem.* 280, 23009–23017. doi: 10.1074/jbc.m414648200
- Woodhoo, A., Alonso, M. B., Droggiti, A., Turmaine, M., D'Antonio, M., Parkinson, D. B., et al. (2009). Notch controls embryonic Schwann cell differentiation, postnatal myelination and adult plasticity. *Nat. Neurosci.* 12, 839–847. doi: 10.1038/nn.2323
- Yan, R., Bienkowski, M. J., Shuck, M. E., Miao, H., Tory, M. C., Pauley, A. M., et al. (1999). Membrane-anchored aspartyl protease with Alzheimer's disease β -secretase activity. *Nature* 402, 533–537. doi: 10.1038/990107
- Yang, X. L., Xiong, W. C., and Mei, L. (2004). Lipid rafts in neuregulin signaling at synapses. *Life Sci.* 75, 2495–2504. doi: 10.1016/j.lfs.2004.04.036
- Yarden, Y., and Slivkowski, M. X. (2001). Untangling the ErbB signalling network. *Nat. Rev. Mol. Cell Biol.* 2, 127–137. doi: 10.1038/35052073
- Zampieri, N., Xu, C. F., Neubert, T. A., and Chao, M. V. (2005). Cleavage of p75 neurotrophin receptor by α -secretase and γ -secretase requires specific receptor domains. *J. Biol. Chem.* 280, 14563–14571. doi: 10.1074/jbc.M412957200
- Zhou, L., Barão, S., Laga, M., Bockstael, K., Borgers, M., Gijzen, H., et al. (2012). The neural cell adhesion molecules L1 and CHL1 are cleaved by BACE1 protease *in vivo*. *J. Biol. Chem.* 287, 25927–25940. doi: 10.1074/jbc.M112.377465
- Zou, T., Ling, C., Xiao, Y., Tao, X., Ma, D., Chen, Z. L., et al. (2006). Exogenous tissue plasminogen activator enhances peripheral nerve regeneration and functional recovery after injury in mice. *J. Neuropathol. Exp. Neurol.* 65, 78–86. doi: 10.1097/01.jnen.0000195942.25163.f5

Conflict of Interest Statement: The authors declare that the research was conducted in the absence of any commercial or financial relationships that could be construed as a potential conflict of interest.

Copyright © 2019 Pellegatta and Taveggia. This is an open-access article distributed under the terms of the Creative Commons Attribution License (CC BY). The use, distribution or reproduction in other forums is permitted, provided the original author(s) and the copyright owner(s) are credited and that the original publication in this journal is cited, in accordance with accepted academic practice. No use, distribution or reproduction is permitted which does not comply with these terms.



Ascorbic Acid Facilitates Neural Regeneration After Sciatic Nerve Crush Injury

Lixia Li^{1,2,3†}, Yuanyuan Li^{1,2†}, Zhihao Fan^{1,2†}, Xianghai Wang^{1,2,3,4}, Zhenlin Li^{1,2}, Jinkun Wen^{1,2}, Junyao Deng^{1,2}, Dandan Tan^{1,2}, Mengjie Pan^{1,2}, Xiaofang Hu^{1,2,3}, Haowen Zhang^{1,2}, Muhua Lai^{1,2} and Jiasong Guo^{1,2,3,4*}

¹Guangdong Provincial Key Laboratory of Construction and Detection in Tissue Engineering, Southern Medical University, Guangzhou, China, ²Department of Histology and Embryology, Southern Medical University, Guangzhou, China, ³Guangzhou Regenerative Medicine and Health Guangdong Laboratory, Guangzhou, China, ⁴Key Laboratory of Mental Health of the Ministry of Education, Southern Medical University, Guangzhou, China

OPEN ACCESS

Edited by:

James Phillips,
University College London,
United Kingdom

Reviewed by:

Simone Di Giovanni,
Imperial College London,
United Kingdom
Xinpeng Dun,
University of Plymouth,
United Kingdom

*Correspondence:

Jiasong Guo
jiasongguo@aliyun.com

[†]These authors have contributed
equally to this work

Received: 24 November 2018

Accepted: 05 March 2019

Published: 21 March 2019

Citation:

Li L, Li Y, Fan Z, Wang X, Li Z, Wen J,
Deng J, Tan D, Pan M, Hu X,
Zhang H, Lai M and Guo J
(2019) Ascorbic Acid Facilitates
Neural Regeneration After Sciatic
Nerve Crush Injury.
Front. Cell. Neurosci. 13:108.
doi: 10.3389/fncel.2019.00108

Ascorbic acid (AA) is an essential micronutrient that has been safely used in the clinic for many years. The present study indicates that AA has an unexpected function in facilitating nerve regeneration. Using a mouse model of sciatic nerve crush injury, we found that AA can significantly accelerate axonal regrowth in the early stage [3 days post-injury (dpi)], a finding that was revealed by immunostaining and Western blotting for antibodies against GAP-43 and SCG10. On day 28 post-injury, histomorphometric assessments demonstrated that AA treatment increased the density, size, and remyelination of regenerated axons in the injured nerve and alleviated myoatrophy in the gastrocnemius. Moreover, the results from various behavioral tests and electrophysiological assays revealed that nerve injury-derived functional defects in motor and sensory behavior as well as in nerve conduction were significantly attenuated by treatment with AA. The potential mechanisms of AA in nerve regeneration were further explored by investigating the effects of AA on three types of cells involved in this process [neurons, Schwann cells (SCs) and macrophages] through a series of experiments. Overall, the data illustrated that AA treatment in cultured dorsal root ganglionic neurons resulted in increased neurite growth and lower expression of RhoA, which is an important inhibitory factor in neural regeneration. In SCs, proliferation, phagocytosis, and neurotrophin expression were all enhanced by AA. Meanwhile, AA treatment also improved proliferation, migration, phagocytosis, and anti-inflammatory polarization in macrophages. In conclusion, this study demonstrated that treatment with AA can promote the morphological and functional recovery of injured peripheral nerves and that this effect is potentially due to AA's bioeffects on neurons, SCs and macrophages, three of most important types of cells involved in nerve injury and regeneration.

Keywords: ascorbic acid, nerve regeneration, peripheral nerve injury, neuron, Schwann cell, macrophage

INTRODUCTION

Although the peripheral nervous system (PNS) has an intrinsic ability to repair and regenerate, this capability is limited, and spontaneous neural regeneration is notably slow. Functional recovery from peripheral nerve injury (PNI) is generally far from satisfactory. Due to the slow rate of axonal regeneration, irreversible damage to the structure and function of target

organs may occur before regenerated axons reinnervate these targets, which could have a profound and permanent impact on patients (Grinsell and Keating, 2014; Faroni et al., 2015). To alleviate the suffering of PNI patients, research on approaches to accelerate peripheral nerve regeneration is encouraged. In the present study, the effect of ascorbic acid (AA) on neural regeneration after PNI was assessed.

AA, or vitamin C, is a dietary essential micronutrient that plays key roles in many important biological processes (Granger and Eck, 2018). AA is not only considered an important daily nutrient for maintaining health but also has long been used safely in the clinic to protect against many diseases. Moreover, recent studies indicate that AA has many unexpected newly discovered biological functions. For example, AA can be used to promote stem cell reprogramming (Wang et al., 2011; Cimmino et al., 2018). It is essential for the development and physiological functions of nervous tissue (May, 2012; Granger and Eck, 2018) and has therapeutic effects in neurodegenerative diseases (Kocot et al., 2017; Moretti et al., 2017). Clinical studies and animal experiments have demonstrated that AA administration can improve functional recovery from spinal cord injury (Lamid, 1983; Robert et al., 2012; Yan et al., 2014; Guo et al., 2018). Existing data on PNI indicate that AA has antinociceptive effects on PNI animals, which may be achieved mainly through interactions with N-Methyl-D-aspartate (NMDA) receptors or through ROS activity (Lu et al., 2011; Saffarpour and Nasirinezhad, 2017). However, evidence regarding whether AA has an effect on the morphological and functional recovery of injured nerves is lacking. To address this issue, we developed a sciatic nerve crush injury mouse model of PNI to test the potential role of AA in peripheral nerve regeneration. Its potential mechanism was studied in neurons, Schwann cells (SCs) and macrophages, which are the most important cell types involved in nerve injury and regeneration.

MATERIALS AND METHODS

Ethics Statement

All procedures involving animals, including surgery, electrophysiological tests, behavior tests and tissue collection, were carried out with the approval of the Southern Medical University Animal Care and Use Committee in accordance with the guidelines for the ethical treatments of animals. All efforts were made to minimize the number of animals used and their suffering.

Sciatic Nerve Injury Model Preparation and Drug Administration

C57BL/6 mice ($n = 16$ per group, female, 6–8 weeks old, weighing 18–20 g, provided by the Animal Center of the Southern Medical University) were used for the sciatic nerve crush injury model as described in our previous report (Qian et al., 2018). Briefly, the mice were anesthetized with an intraperitoneal injection of 12 mg/ml tribromoethanol (180 mg/kg body weight). The sciatic nerve in the left leg was bluntly exposed after performing a lateral skin incision along the length of the femur. Then, wound closure without manipulation of the nerve was performed

(sham-surgery group), or the mice were subjected to a calibrated sciatic crush injury 0.5 cm distal to the sciatic notch. The nerves were crushed with a fine, smooth, straight hemoostat (tip width: 1 mm) for 2 min, and the crush site was marked with a 9–0 nylon suture as previously reported (Sheu et al., 2012). The mice that underwent nerve injury were randomly divided into the AA and saline groups. AA (purchased from Baiyunshan Pharmaceuticals Company, Guangzhou, China) was prepared in a suspension with saline at a concentration of 13.33 mg/ml. Immediately after surgery, the animals in the AA group received an intragastric administration (i.a.) of the AA solution (400 mg/kg) followed by daily i.a. of AA (200 mg/kg). The mice in the saline group received the same volume of saline as the volume of AA suspension administered to the AA group. The drug administration method strictly followed published protocols (Yagi et al., 2015; Liu et al., 2016). A solution of AA or saline was intragastrically administered *via* a customized probe through which the solution could be pushed forward into the stomach. All animals received routine postoperative care and were housed under standard laboratory conditions with a 12 h/12 h light-dark cycle and free access to food and water. At 3 days post-injury (dpi), six mice per group were sacrificed, and axonal regeneration in the injured nerve was detected by immunohistochemistry and Western blotting for antibodies against growth-associated protein 43 (GAP43) and superior cervical ganglion 10 (SCG10). At 28 dpi, 10 mice per group were subjected to behavioral tests and an electrophysiological assessment. Then, the sciatic nerves and gastrocnemius muscles were collected, and immunohistochemistry, electromicroscopy, and hemeatoxylin staining were performed as described in the following sections.

Behavioral Tests

The motor and sensory functional recovery of the injured hindlimb of mice receiving sciatic nerve crush injury was detected at 28 dpi by gait analysis, rotarod, and the hot plate test, which are widely used in sciatic nerve crush injury models (Jungnickel et al., 2010; Gallaher and Steward, 2018). Each mouse was allowed at least a 2-h break between testing sessions. All behavior tests were formally performed 28 dpi, but the mice were trained for 2 days before the final tests.

Gait Analysis

Motor function of the experimental mice was quantified using a gait analysis system (Mouse Specifics Inc., Quincy, MA, USA, DigiGait; Glajch et al., 2012). The mice were trained to walk on a motorized transparent treadmill belt, and their footprints were captured with a video camera set beneath the belt. Then, the sciatic functional index (SFI) was calculated with software following the protocol of the system (Jungnickel et al., 2010; Wang et al., 2018).

Rotarod Assay

Motor performance was also measured using a rotarod device (TSE Systems; Singh et al., 2017). Briefly, the mice were pretrained for 2 days on an automated 6-lane rotarod unit that could be set at a fixed or accelerating speed. During the training protocol, the mice were placed on the rod as it rotated at a

speed of 5 rotations per minute (RPM) for 60 s. During the testing phase, the mice were placed on the rod as it accelerated from 0 RPM to 40 RPM over a period of 20 s. The length of time that each mouse stayed on the rotating rod was measured and recorded.

Hot Plate Test

The recovery of sensory function of the injured nerve was assessed by a hind paw thermal withdrawal test using a hot-plate instrument (Muromachi Kikai, Tokyo, Japan) as previously described (Gallaher and Steward, 2018; Ibrahim et al., 2018). Before performing the test, each mouse was habituated twice to the hot plate set to room temperature. Then, each mouse was placed on the hot plate set to a temperature of $55 \pm 0.5^\circ\text{C}$. The withdrawal latency, manifested by the time (in seconds) until hind paw licking or jumping, was recorded.

Electrophysiological Assessment

Two hours after the final behavioral analyses, each mouse was anesthetized by an intraperitoneal injection of 12 mg/ml tribromoethanol (180 mg/kg body weight) and subjected to electrophysiological tests following a previously described protocol (Wang et al., 2014). Briefly, the sciatic nerve was re-exposed, a pair of stimulating electrodes (13 mm long, 0.5 mm in diameter) was inserted 3 mm proximal to the crushed site to stimulate the sciatic nerve, and a pair of needle electrodes (13 mm long, 0.5 mm in diameter) was inserted subcutaneously into the middle of the intrinsic foot muscle to record the compound muscle action potential (CMAP) with a set of electrophysiological recorders (Axon Digidata 1550 Digitizer, Molecular Devices). The amplitude and latency of each test were analyzed to determine the nerve conduction strength and nerve conduction speed, respectively.

Tissue Collection

Neural regeneration after nerve injury was detected at two time points. At 3 dpi, six mice per group were sacrificed by decapitation. Then, tissue was collected for Western blotting ($n = 3$ per group) or, following perfusion, for immunohistochemistry ($n = 3$ per group). At 28 dpi, immediately after the electrophysiological recordings were completed, the mice ($n = 10$ per group) were intracardially perfused with 0.1 M phosphate-buffered saline (PBS) for 10 min, followed by 4% paraformaldehyde (PFA, in 0.1 M PBS) for 30 min; then, the sciatic nerves and gastrocnemius muscles were harvested for further investigation.

Western Blotting

Three mice per group were decapitated at 3 dpi, and a 1-cm piece of the sciatic nerve was dissected from the injury site, frozen in liquid nitrogen for 30 s, minced and homogenized in RIPA lysis buffer (Sigma, St. Louis, MO, USA) containing 1% protease inhibitor cocktail (Cell Signaling). The cultured SCs and macrophages were also homogenized in RIPA lysis buffer (Sigma, St. Louis, MO, USA) containing 1% protease inhibitor cocktail (Cell Signaling). The proteins were separated on 10% sodium dodecyl sulfate-polyacrylamide gels and transferred to polyvinylidene difluoride membranes

(Bio-Rad, Hercules, CA, USA). After blocking with 5% bovine serum albumin (BSA) in Tris-buffered solution containing 0.5% Tween-20 for 2 h, the blots were probed overnight at 4°C with the following primary antibodies: rabbit anti-GAP43 (1:2,000; ab16053, Abcam), rabbit anti-SCG10 (1:1,000; NBP1-49461, Novusbio), rabbit anti-iNOS (1:1,000; ab178945, Abcam), rabbit anti-CD163 (1:1,000; ab213612, Abcam), rabbit anti-NGF (1:1,000; ab6199, Abcam), rabbit anti-NT-3 (1:500; sc-547, Santa Cruz), rabbit anti-GDNF (1:500; ab119473, Abcam), rabbit anti-BDNF (1:500; ab6201, Abcam), rabbit anti-laminin (1:500; ab7463, Abcam), rabbit anti- β -actin (1:1,000; ab008, Multisciences). After incubation with an HRP-conjugated secondary antibody (Molecular Probes) for 2 h at room temperature, the immunoreactive proteins were visualized by an enhanced chemiluminescence reaction, and the band density was calculated using Image-Pro Plus 6.0 software (Media Cybernetics).

Immunohistochemistry

The nerves dissected from the perfused animals (3 dpi, $n = 3$; 28 dpi, $n = 6$ per group) were post-fixed in 4% PFA for 24 h, cryoprotected in 30% sucrose overnight at 4°C , and then sectioned on a cryostat (Leica) at a thickness of 10 μm . The sciatic nerve samples collected at 3 dpi were longitudinally cut 1.5 cm distal to the injury site. The nerves collected at 28 dpi were transversely cut in the range of 5–6 mm distal to the injury site. All sections were mounted onto poly-lysine-coated glass slides and stored at -20°C for immunohistochemistry. Briefly, the sections were penetrated with 0.5% Triton X-100 (Sigma, St. Louis, MO, USA) for 30 min and incubated with blocking buffer [5% fish gelatine (Sigma, St. Louis, MO, USA) containing 0.3% Triton X-100] at room temperature for 1 h, followed by incubation with primary antibodies diluted in blocking buffer overnight at 4°C , incubation with Alexa Fluor 488 and/or 568 fluorescent-conjugated secondary antibodies (Molecular Probes) for 2 h at room temperature, and incubation with DAPI (1:5,000; Sigma, St. Louis, MO, USA) for 2 min to counterstain the nuclei. After immunohistochemistry, the sections were mounted using anti-fading mounting medium (Vector), and images were captured under a fluorescence microscope (Leica). The following primary antibodies were used for immunostaining of the longitudinal sections: rabbit anti-GAP43 (1:400; ab16053, Abcam), rabbit anti-SCG10 (1:500; NBP1-49461, Novusbio), rat anti-mouse f4/80 (1:400; CL89170AP, Cedarlane), rabbit anti-iNOS (1:1,000; ab178945, Abcam) and rabbit anti-CD163 (1:1,000; ab213612, Abcam). In addition, mouse anti-MBP (1:200; NE1018, Calbiochem) and rabbit anti-NF (1:800; N4142, Sigma, St. Louis, MO, USA) primary antibodies were used for double staining of the transverse sections. The number of S100-positive cells, f4/80-positive cells, iNOS-positive cells or CD163-positive cells in the longitudinal sections of each sciatic nerve was counted in a $250 \mu\text{m} \times 250 \mu\text{m}$ area 1 mm distal to the crush site. The number of NF-positive axons in the cross-sections of each sciatic nerve was counted with Photoshop 5.0 software (Adobe, USA) by an investigator blinded to the experimental groups (Schreiber et al., 2015).

Transmission Electron Microscopy

Partial sciatic nerves dissected at 28 dpi ($n = 4$ per group) were subjected to transmission electron microscopy (TEM). Briefly, 2-mm long segments from an area 5 mm distal to the injury site were post-fixed with 2.5% glutaraldehyde plus 2% PFA for 24 h followed by 1% OsO_4 for 2 h at 4°C, dehydrated stepwise in increasing concentrations of acetone and embedded in Spurr's resin (Sigma, St. Louis, MO, USA) for ultrathin transverse sectioning (70 nm). After staining with 2% uranyl acetate and lead citrate, ultrathin sections were observed under a transmission electron microscope (H-7500, Hitachi). Six images of each sample were randomly captured at a magnification of 3,500. Then, the diameter of each axon or whole nerve fiber and the area of each axon were measured with Image-Pro Plus 6.0 software (Media Cybernetics). Based on the collected data, the G-ratio and axon area distribution were calculated to reflect the myelin thickness and axon size, respectively. Briefly, the G-ratio was determined as the ratio of the axon diameter to the fiber diameter (Wen et al., 2017). The axon area distribution was determined by Penna's protocol (Penna et al., 2011) with minor revisions. Briefly, after the area of each axon was measured by Image-Pro Plus 6.0 software, the collected data were grouped in $5\text{-}\mu\text{m}^2$ increments (i.e., 0–5 μm^2 , 5–10 μm^2 , 10–15 μm^2 , etc.). Then, the percentage of the number of axons in each group compared with the total number of axons was determined as the axon area distribution (%).

Histomorphometry of the Gastrocnemius Muscle

Since the level of myoatrophy in target muscles is known to be an important index of nerve injury and regeneration, we performed histomorphometry of the gastrocnemius muscle at 28 dpi. Briefly, the midbellies of the gastrocnemius muscles from the perfused mice were trimmed and post-fixed with 4% PFA for 24 h at 4°C. Subsequently, the muscles were embedded with Tissue OCT-Freezing Medium and transversally cut into 10- μm sections. The sections were stained with 0.5% hemeatoxylin to show the outline of the myofibers, and the areas of the myofibers were calculated as described in our previous publications (Wang et al., 2014; Pan et al., 2017). Briefly, six random non-overlapping fields from five sections from each animal were captured, and the image analysis was performed using Image-Pro Plus 6.0 software to quantify the areas of the myofibers.

Primary Cell Culture

DRG Neuron Cultures

Based on the protocol described previously (Chang et al., 2016), the dorsal root ganglia (DRG) from neonatal 1-day-old SD rats were rapidly dissected and digested with 0.125% trypsin (Sigma, St. Louis, MO, USA) at 37°C for 30 min. The separated cells were cultured in Dulbecco's modified Eagle's medium/Ham's F-12 (DMEM/F-12) with 1% fetal bovine serum (FBS; Corning) and plated onto the Poly-L-lysine (PLL, Sigma-Aldrich, St. Louis, MO, USA)-treated coverslips in culture dishes. Medium for half of the cultures was supplemented with AA (200 μM , Sigma, St. Louis, MO, USA). After being cultured for 24 h, the cells were fixed with 4% PFA. Immunocytochemistry for a mouse anti-Tuj1

antibody (1:400; T8660, Sigma, St. Louis, MO, USA) or a mouse anti-RhoA antibody (1:200; sc-418, Santa Cruz) was performed following routine protocols.

Primary Schwann Cell Cultures

As described in our previous publication (Wen et al., 2017), SCs were isolated from the spinal nerves of SD rats at postnatal day 3. The collected nerves were dissociated with 0.25% trypsin-EDTA (Gibco) at 37°C for 30 min, and single cells suspended in DMEM/F12 (Corning) containing 10% FBS (Corning) were plated onto PLL-coated Petri dishes. After overnight incubation, the cultures were treated with cytosine arabinoside (10 μM , Sigma-Aldrich, St. Louis, MO, USA) for 48 h to eliminate fibroblasts. Then, the cells were routinely cultured with SC medium [DMEM/F12 containing 3% FBS, 3 μM forskolin (Sigma-Aldrich, St. Louis, MO, USA), 10 ng/ml heregulin (PeproTech) and 100 mg/ml penicillin-streptomycin (Gibco)] to expand the cells.

Primary Macrophage Cultures

Resident peritoneal macrophages were isolated from adult SD rats. Immediately after the rat was anesthetized by overdose with 80 mg/kg pentobarbital sodium, 10 ml of sterile Hank's Balanced Salt Solution (HBSS, Gibco) was gently injected into the caudal half of the peritoneal cavity, and then the HBSS containing the resident peritoneal cells was slowly withdrawn. The cells were resuspended in DMEM culture medium (Gibco) with 10% FBS and plated onto dishes at a density of 2×10^6 cells/ml. The medium was replaced twice every 2 h to remove the non-adherent cells. Thereafter, the adhered macrophages were cultured using a routine cell culture protocol (Yuan et al., 2017).

Cell Proliferation Assays

The proliferating capability of SCs and macrophages was measured by a WST-1 assay and a bromodeoxyuridine (BrdU) assay.

First, a WST-1 Cell Proliferation Assay Kit II (Abcam) was utilized to detect cell proliferation based on the manufacturer's instructions and previous literature (Wu et al., 2017). Briefly, primary SCs or macrophages were seeded in 96-well plates at a density of 1×10^4 cells/well in 100 μl of medium (SC medium for SCs and DMEM/F12 with 10% FBS for macrophages) with or without 200 μM AA. Following 36 h of routine incubation, WST working solution was added to the culture medium (10 μl /well) and maintained for another 3 h. Then, the absorbance was recorded at 450 nm with a Microplate Reader (Bio-Rad, Hercules, CA, USA). All experiments were performed in triplicate, and three independent experiments were performed.

For the BrdU assay, 1×10^5 SCs or macrophages in 1 ml of medium (SC medium for SCs and DMEM/F12 with 10% FBS for macrophages) with or without 200 μM AA were plated onto PLL-coated coverslips in 24-well plates. Twenty-four hours later, BrdU (10 μM , Sigma, St. Louis, MO, USA) was added to the medium, and the cells were further incubated for 36 h. Then, the cells were fixed with 4% PFA for 1 h, denatured with 2 N HCl at 37°C for 30 min and neutralized with 0.1 M borate buffer (pH = 8.5) for 15 min. Immunocytochemistry was performed as follows: after blocking with 1% BSA for

1 h, the cells were penetrated with 1% Triton X-100 for 1 h, incubated with a mouse anti-BrdU primary antibody (1:200; NA61, Sigma, St. Louis, MO, USA) followed by an Alexa Fluor 568-conjugated secondary antibody (Molecular Probe) and incubated with DAPI (1:5,000, Sigma, St. Louis, MO, USA) for 5 min to counterstain the nuclei of the cells. Five images of each coverslip (the center and four quadrants) were captured using a fluorescence microscope (Leica), and the percentage of cells that were positive for BrdU was quantified. All experiments were performed in triplicate, and three independent experiments were performed.

Migration Assay

The migration of the SCs and macrophages was assessed by a Transwell assay using 6.5-mm Transwell chambers (8- μ m pores, Corning Costar) as described previously (Wen et al., 2017). After the chambers were pretreated with 10 μ g/ml laminin solution or culture medium, 1×10^5 SCs or macrophages in 100 μ l of DMEM/F12 containing 1% FBS were seeded into the upper chamber, and the lower chamber was filled with 600 μ l DMEM/F12 containing 10% FBS without cells. The SCs and macrophages were allowed to migrate for 4 h and 24 h, respectively, and then fixed with 4% PFA for 20 min. After careful removal of the cells on the upper surface with a cotton swab, the cells adhered to the lower surface of the Transwell membrane were stained with 0.1% crystal violet (Beyotime) for 30 min. Then, five images of each membrane (the center and four quadrants) were captured under an inverted microscope (Leica) for quantification.

Phagocytic Capability Assay

Phagocytosis in SCs and macrophages was assessed by the ingestion of lumispheres. Briefly, 0.1 mg/ml fluorescent lumispheres (1- μ m diameter, BaseLine Chromtech, China) were added into the culture medium of SCs or macrophages for 6 h or 3 h, respectively. To accurately count the number of intracellular lumispheres, the lumisphere-treated cells were collected by trypsinization and then re-cultured on PLL-coated slides for 3 h after being rinsed three times with HBSS to remove the attached lumispheres from the cell surface. Finally, the cells were fixed with 4% PFA and stained with CNPase (1:400; BS3461, Bioword Technology, Inc., St. Louis Park, MN, USA) or ED1 (1:200; MAC341GA, AbD Serotec) to identify the outlines of the SCs and macrophages. With a fluorescence microscope (Leica), the number of lumispheres ingested by each cell was counted.

Statistical Analysis

Statistical analyses were performed using SPSS statistical software 20.0 (IBM). All values are presented as the mean \pm the standard error of the mean (SEM). In experiments with two groups, independent samples *t*-tests were used to analyze values between the two groups. In experiments with more than two groups, one-way analysis of variance (ANOVA) was used. A *p*-value <0.05 was considered statistically significant. For all graphs, *indicates $P < 0.05$ and N.D. indicates no significant difference.

RESULTS

AA Accelerates Axonal Regeneration in the Early Stage of Nerve Injury

GAP43 is a widely used marker of axonal regeneration after nerve injury (Ma et al., 2011). SCG10, which is expressed in adult sensory neurons, is an efficient and selective marker for regenerating sensory axons in the early stage of axonal regeneration (Shin et al., 2014). Both are barely detectable in intact adult nerves but are highly expressed in regenerating axons (Figures 1A–C,F–H). Figures 1B,C,F,G show that the GAP43- or SCG10-positive axons extending from the crush site to the distal trunk were significantly longer in the AA group than those in the saline group. This finding was verified by the quantification of Western blot analysis (Figures 1D,E or 1I,J). Significant differences among the groups were revealed by statistical analysis.

AA Increases the Number of Regenerated Axons and the Level of Remyelination in the Injured Nerve

As shown in Figure 2, many NF-positive axons were present in the distal portion of the injured nerves at 28 dpi, and most of these axons were wrapped with MBP-positive myelin. Compared those in the saline group (Figure 2B), the number of axons (Figure 2D) and the ratio of MBP/NF (Figure 2E) were dramatically increased in the nerves of the AA group (Figure 2C). However, the number of axons and the thickness of the myelin sheaths in the nerves of the AA group did not reach the levels observed in the nerves of the sham control group (Figure 2A).

To accurately quantify the size of the regenerated axons and the myelin, parts of the nerves ($n = 4$ per group) were examined by TEM (Figures 2F–H). Statistically, the G-ratio (the diameter of the axon/the diameter of the whole nerve fiber), a widely used myelin thickness index (Tateshita et al., 2018), in the AA group was significantly lower than that in the saline group (Figure 2I), indicating that AA administration enhanced myelination and increased the thickness of the myelin sheaths. However, the G-ratio in the nerves of the AA group did not reach the level observed in the nerves of the sham group. In addition, the axonal area observed in the AA group was greater than that observed in the saline group (Figure 2J). The axonal area distribution (Figure 2K) reveals that the predominance of axons in the saline group had an area in the range of 0–15 μ m². Almost no axons in this group had an area greater than 15 μ m². Most axons in the AA groups had an area in the range of 0–15 μ m², but the percentage of axons with an area between 10 and 15 μ m² was notably higher in the AA group compared with that in the saline group (20.1% vs. 6.7%). Moreover, some axon areas (5.2%) in the AA group reached the range of 15–20 μ m². Overall, these data indicate that AA treatment not only increased the number and size of the regenerated axons but also enhanced the thickness of the myelin.

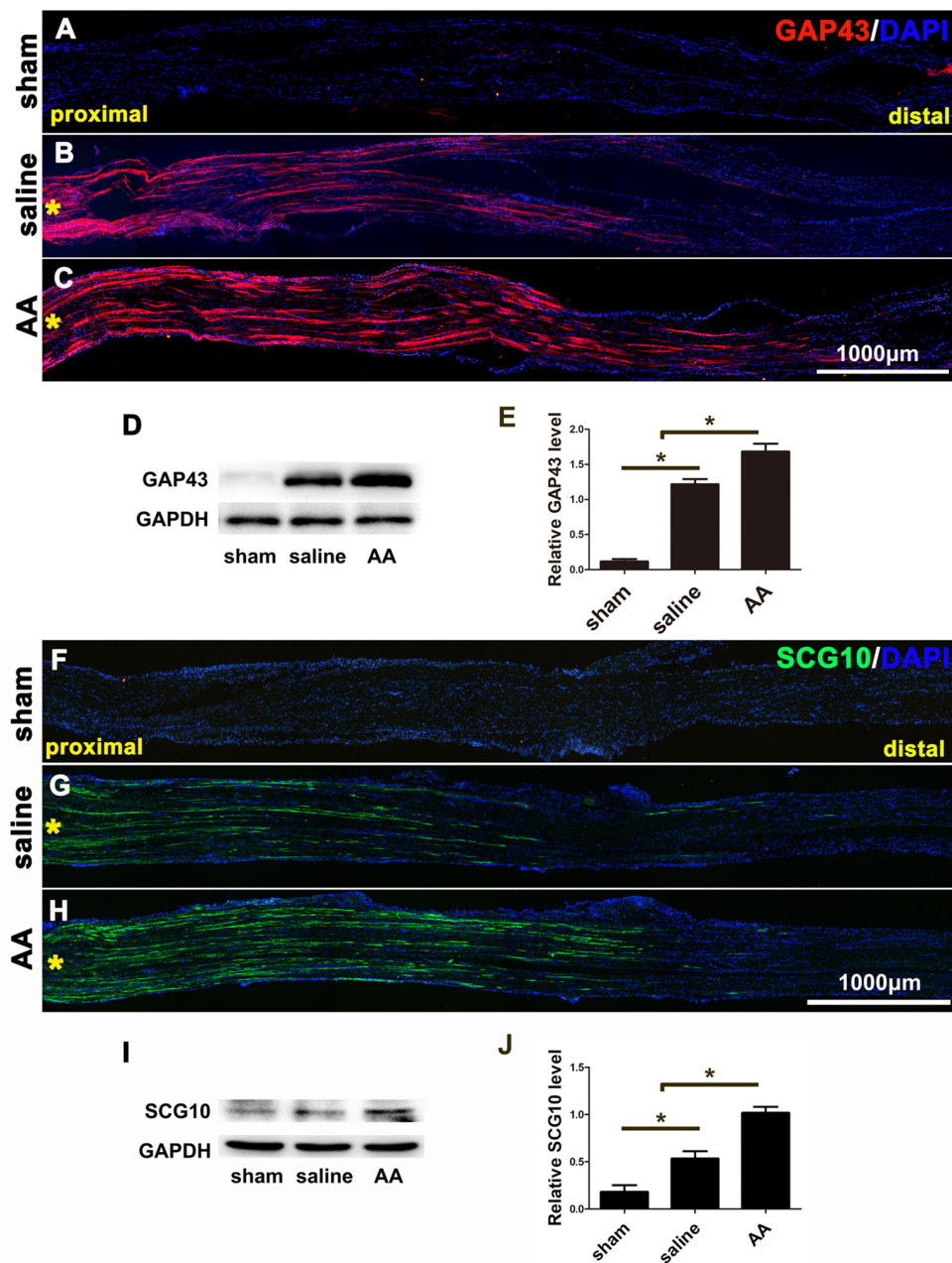


FIGURE 1 | GAP43 and SCG10 immunostaining and Western blotting show that ascorbic acid (AA) accelerates the regrowth of injured axons in the early stage after sciatic nerve crush injury. (A–C) Representative samples of GAP43-immunostained longitudinal sciatic nerve sections at 3 dpi from the sham group (A), saline group (B), and AA group (C). Asterisks represent the lesion site. (D,E) Western blots and schematic diagrams of the statistical analysis showing the protein level of GAP43 in the distal trunk of the injured sciatic nerves ($n = 3$, $*P < 0.05$). (F,G) Representative samples of SCG10-immunostained longitudinal sciatic nerve sections from the sham group (F), saline group (G), and AA group (H). Asterisks represent the lesion site. (I,J) Western blots and schematic diagrams of the statistical analysis showing the protein level of SCG10 in the distal trunk of the injured sciatic nerves ($n = 3$ for each test, $*P < 0.05$).

AA Attenuates Myoatrophy of the Gastrocnemius Muscle

The gastrocnemius muscle is one of the main target muscles of the sciatic nerve and is widely used to reflect functional recovery in injured sciatic nerves. Compared to those in the sham group, the myofibers in the groups that underwent

sciatic nerve injury (the saline group and the AA group) were notably smaller, which suggests dramatic myoatrophy. Nevertheless, the level of myoatrophy in the AA group was much less than that in the saline group (Figures 3A–C). This difference can be quantified by measurements and statistical analyses (Figure 3D).

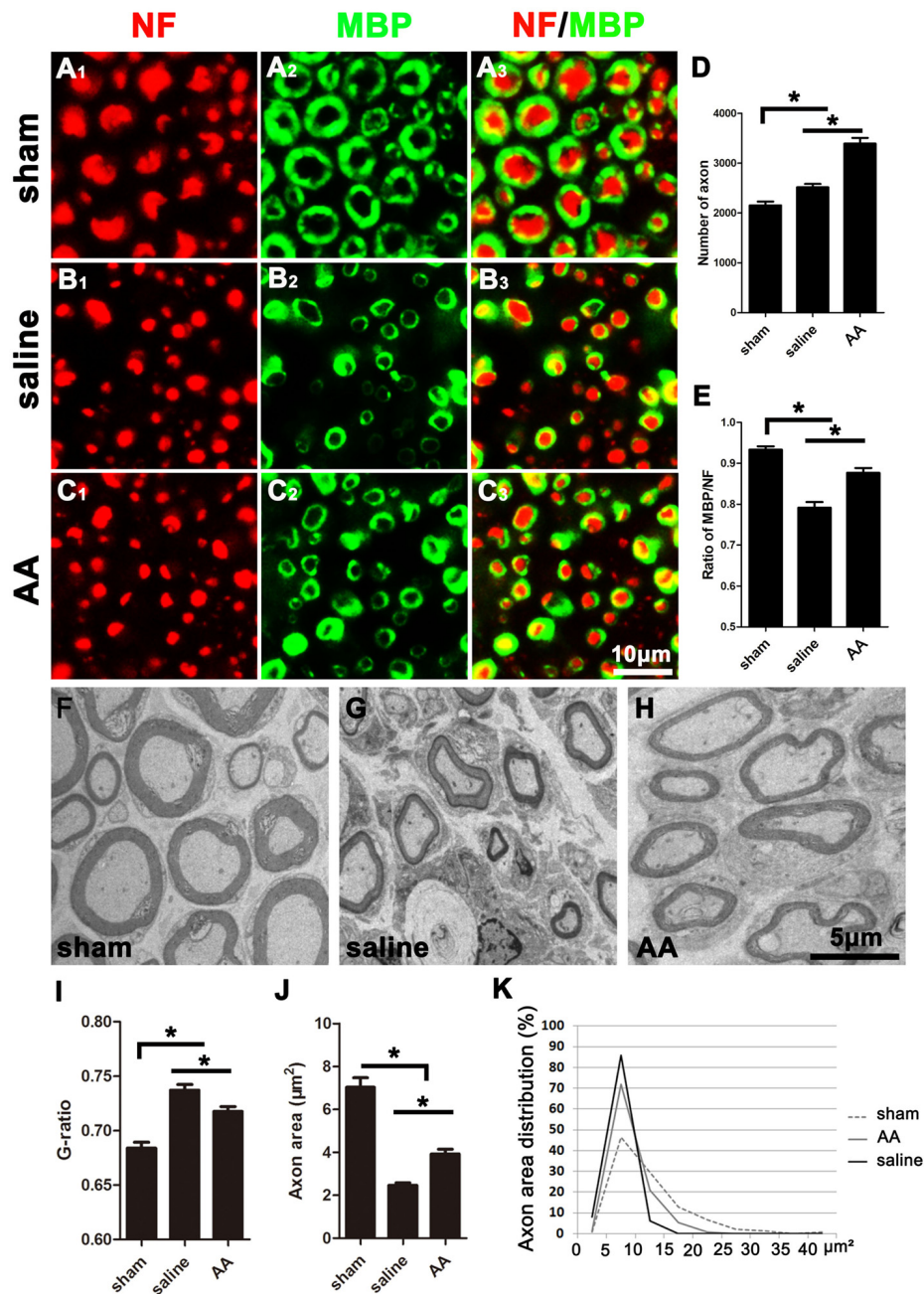


FIGURE 2 | NF (Neurofilament, red) and MBP (Myelin Basic Protein, green) double immunohistochemistry and transmission electron microscopy (TEM) illustrating that AA enhances axonal regeneration and remyelination in the distal portion of the injured sciatic nerve at 28 dpi. Representative samples from (A₁–A₃) the sham group, (B₁–B₃) saline group, and (C₁–C₃) AA group. (D) The number of NF-positive axons in the cross-sections of the nerves ($n = 6$, $*P < 0.05$). (E) The MBP/NF ratio of myelinated axons from each group ($n = 6$, $*P < 0.05$). (F–H) Representative TEM images showing the axons and their myelin sheaths. (I–K) Quantification of the G-ratio (I), the axonal area (J), and the axonal area distribution (K; $n = 4$, $*P < 0.05$).

AA Enhances Motor and Sensory Function Recovery

The SFI is among the most widely used parameters for measuring reflexive motor function after sciatic nerve injury. Compared to that in the sham group, the SFI value was significantly decreased in the PNI groups. However, this lower SFI was

dramatically reversed by AA treatment (Figure 4A). Motor coordination and balance were also measured by a rotarod test. The mice in the AA group remained on the rotating rod for a much longer duration than the mice in the saline group but for a shorter duration than the mice in the sham group (Figure 4B).

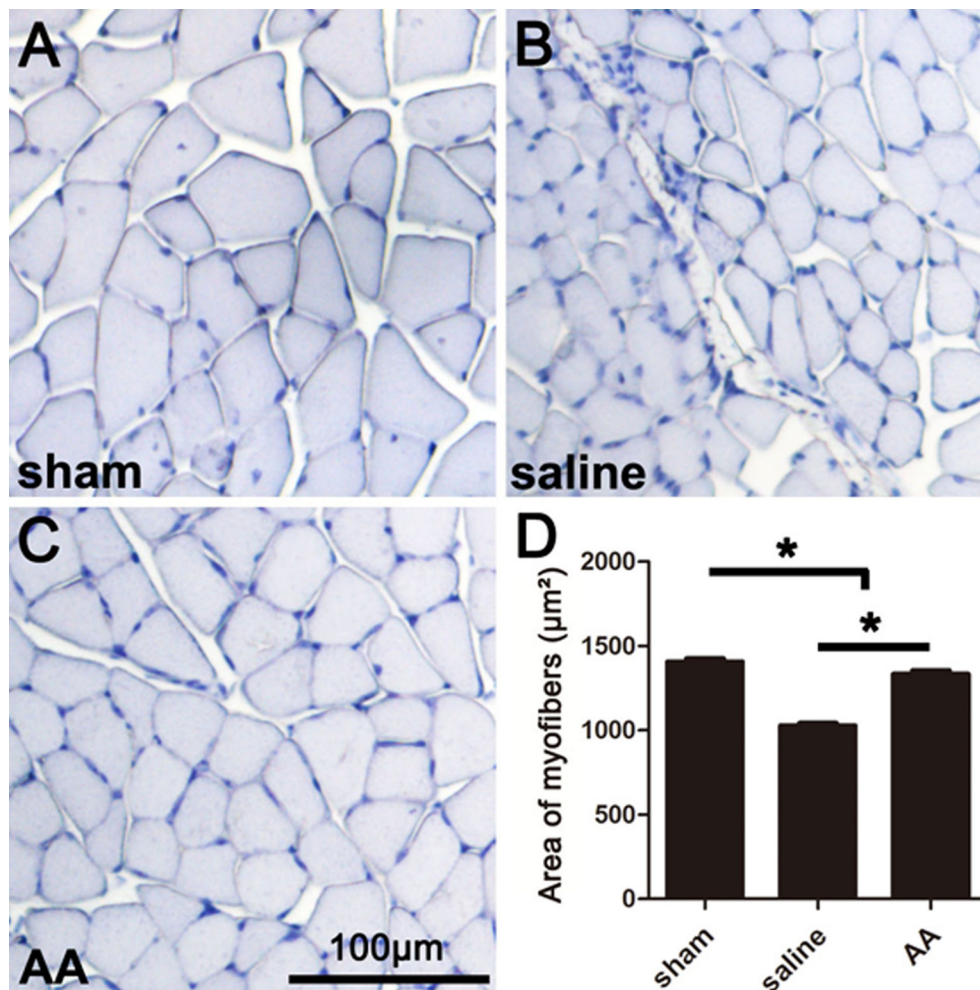


FIGURE 3 | Histomorphometry of gastrocnemius muscles showing that AA alleviates myoatrophy in the target muscle. **(A–C)** Representative images of hemeatoxylin-stained transverse sections of gastrocnemius muscles from each group collected at 28 dpi. **(D)** Quantification of the myofiber area for each group ($n = 10$, $*P < 0.05$).

Furthermore, sensory functional recovery was assessed with the hot plate test, in which longer latency reflexes suggest a sluggish sensory function in the tested foot. As expected, sciatic nerve injury caused the latency to significantly increase in the saline group compared to that in the sham group, but AA treatment shortened the latency (**Figure 4C**).

AA Facilitates Nerve Conduction Function Recovery

The amplitude and latency of the CMAP were measured by electrophysiology. A shorter latency corresponds to quicker nerve conduction, which may result from a higher level of nerve myelination. A higher amplitude indicates a greater number of regenerated axons and a higher level of reinnervation of the measured muscles (Park et al., 2018). Quantification analysis of the CMAP images (**Figures 4D–F**) revealed that the latency in the sham group $<$ AA group $<$ saline

group (**Figure 4G**) and that the amplitude in the sham group $>$ AA group $>$ saline group (**Figure 4H**). The differences among the groups were all statistically significant. Overall, the data from the above experiments indicate that PNI impairs nerve conduction, while the oral administration of AA significantly accelerates functional recovery, including the recovery of motor and sensory behavior and nerve conduction electrophysiology.

AA Promotes Neurite Outgrowth and Alleviates RhoA Expression in Cultured DRG Neurons

When the isolated DRG neurons were cultured in medium with a low concentration of serum (1% FBS), there were few neurites extending from the soma, and those that were present were short in length, as illustrated by Tuj1 immunostaining (**Figure 5A**). AA treatment dramatically increased the number

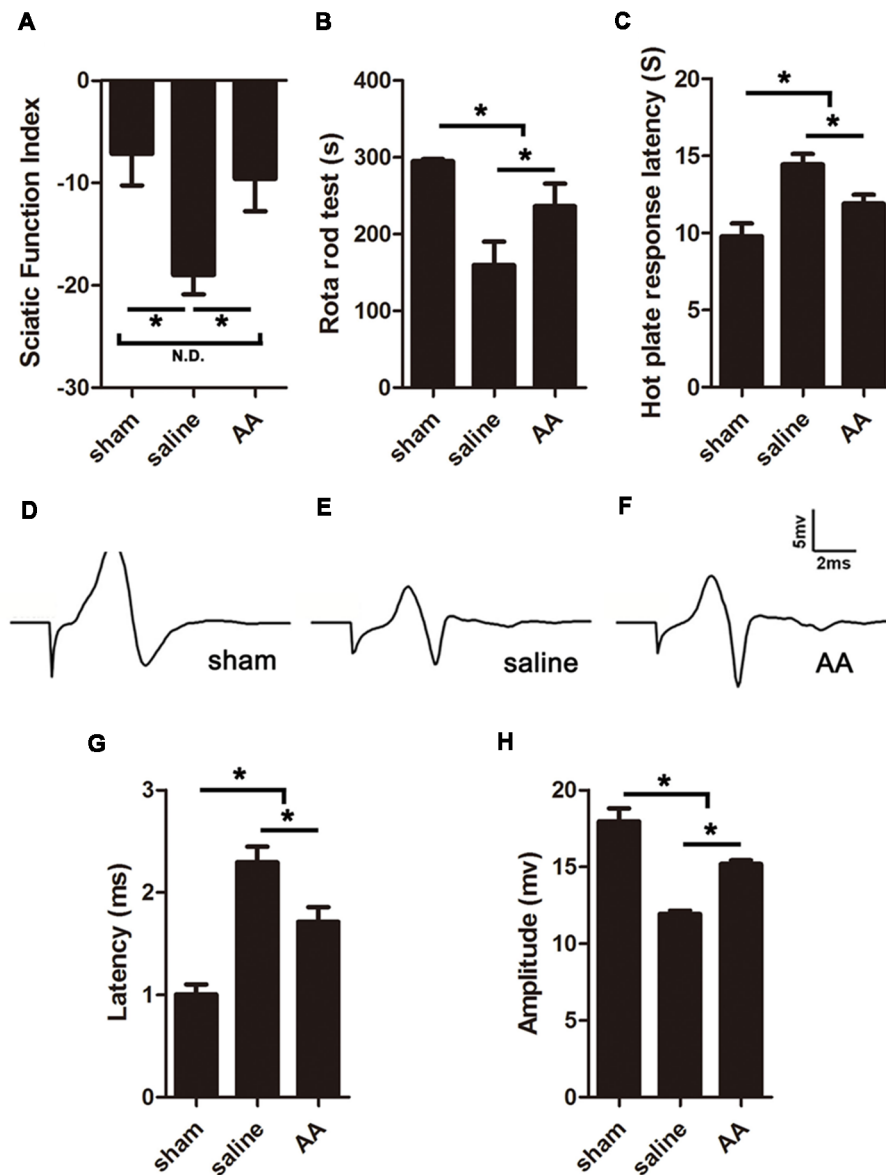


FIGURE 4 | AA enhances functional recovery after sciatic nerve injury at 28 dpi. **(A)** Gait analysis results indicating the sciatic functional index (SFI). **(B)** Rotarod assay results showing the amount of time the mice remained on the rotating rod. **(C)** Hot plate test results showing withdrawal latency from a hot plate. **(D–F)** Respective compound muscle action potential (CMAP) images of the three groups. **(G,H)** Quantification of latencies and amplitudes of the CMAPs ($n = 10$, $*P < 0.05$; N.D. indicates no significant difference).

and length of the neurites (Figures 5B–D). Moreover, immunostaining showed that RhoA immunoreactivity was concentrated in the neuronal soma and that the immune intensity was much higher in the control group than in the AA group (Figures 5E–G).

AA Promotes Proliferation, Phagocytosis and Neurotrophic Factor Secretion in SCs

In the present study, two methods were used to assess the capability for cell proliferation *in vitro*. Using a BrdU assay, we found that the ratio of BrdU-positive cells in the AA-treated

SCs was significantly higher than that in SCs from the control group (Figures 6A–C). The OD value determined by the WST-1 test in the AA group was also statistically higher than that in the control group (Figure 6D). The above data indicate that AA can increase the proliferation of SCs. To confirm the results obtained from the *in vitro* experiments, S100 and Ki67 double immunohistochemistry was performed on the longitudinal sections of the sciatic nerves collected at 3 dpi (Figures 7A–H). Quantitative analysis illustrated that both the number of S100-positive cells (Figure 7I) and the ratio of ki67/S100 (Figure 7J) in the AA group were higher

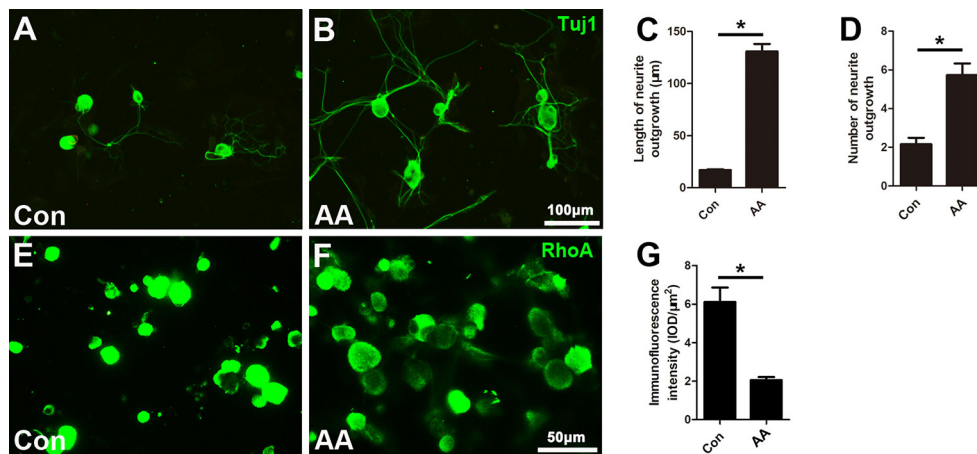


FIGURE 5 | AA promotes neurite outgrowth and alleviates RhoA expression in cultured dorsal root ganglia (DRG) neurons. **(A,B)** Representative images of cultured neurons immunostained for Tuj1 to show the neurites. **(C,D)** Comparison of neurite length and number between two groups is shown ($n = 3$, $*P < 0.05$). **(E-G)** Immunofluorescence and quantification analysis illustrated that the immunointensity of RhoA was significantly decreased in the AA group ($n = 3$, $*P < 0.05$).

than those in the saline group. However, the Transwell test indicated that the migration ability of the SCs was not affected by AA, as the number of migrated cells was not different between the AA group and the control group (Figures 6E–G). Since the lumispheres are considered foreign materials to the co-cultured cells, it is expected that some of them would be ingested by SCs (Figures 6H–M); thus, the number of lumispheres in each cell reflects the cell's phagocytic capability. Quantitative analysis illustrated that there were more ingested lumispheres in the AA-treated SCs than in SCs from the control group (Figure 6N). Finally, Western blotting indicated that the protein levels of NGF, NT-3, GDNF, BDNF, and laminin expressed by the SCs were all significantly increased by AA treatment (Figures 6O,P).

AA Increases the Proliferation, Migration, Phagocytic Capability and M2 Subtype Polarization of Macrophages

As described in the “Materials and Methods” section, the proliferation, migration and phagocytic capability of the cultured macrophages were detected using the same assays as those used in the SCs. Statistical data of the BrdU assay (Figures 8A–C) and the WST-1 test (Figure 8D) showed that the BrdU positive ratio and the WST-1 OD value were significantly higher in the AA group compared to those in the control group, which indicated that AA increases the proliferation of macrophages. Double immunohistochemistry with f4/80 and ki67 antibodies of the sciatic nerve longitudinal sections (Figures 9A–H) illustrated that both the number of f4/80-positive cells (Figure 9I) and the ratio of ki67/f4/80 (Figure 9J) in the AA group were higher than those in the saline group. Subsequently, the migration and phagocytic capability of the macrophages were detected by a Transwell assay and lumisphere ingestion test in the cultured cells. The number of macrophages on the lower surface of the Transwell membrane

was almost double that in the AA group (Figures 8E–G). This upregulation effect was also found in the phagocytic capability assay (Figures 8H–M). The number of lumispheres ingested by the macrophages was almost doubled by treatment with AA (Figure 8N).

Finally, macrophage polarization was assessed by immunocytochemistry with specific markers of a pro-inflammatory subtype (M1, iNOS) or an anti-inflammatory subtype (M2, CD163), both *in vitro* (Figures 8O–V) and *in vivo* (Figures 10A–L). Quantitative results illustrated that the number of iNOS-positive M1 macrophages (Figures 8R, 10M) decreased dramatically, while the number of CD163-positive M2 macrophages (Figures 8V, 10N) increased significantly in the AA group. The Western blot results (Figures 10O–Q) were consistent with the immunostaining data.

DISCUSSION

PNI is a common disease worldwide. Epidemiologic studies have indicated that PNI is involved in up to 2.8% of trauma cases (Noble et al., 1998). PNI has a marked impact on patient quality of life because the injury causes partial or complete loss of function in the target organs of the lesioned nerve. In contrast to the central nervous system (CNS), where damaged axons are usually unable to regenerate, axons in the PNS are capable of regeneration in cases where the injured nerve is properly surgically repaired (Gey et al., 2016; Wang et al., 2017). Nevertheless, the regeneration rate of peripheral nerves is slow, and functional recovery is generally far from satisfactory (Modrak et al., 2017). Thus, the effort to identify effective and safe drugs that can accelerate the neural regeneration rate has gained broad awareness.

To the best of our knowledge, this report is the first to provide solid evidence demonstrating that the oral administration of AA has significant efficacy in facilitating peripheral nerve

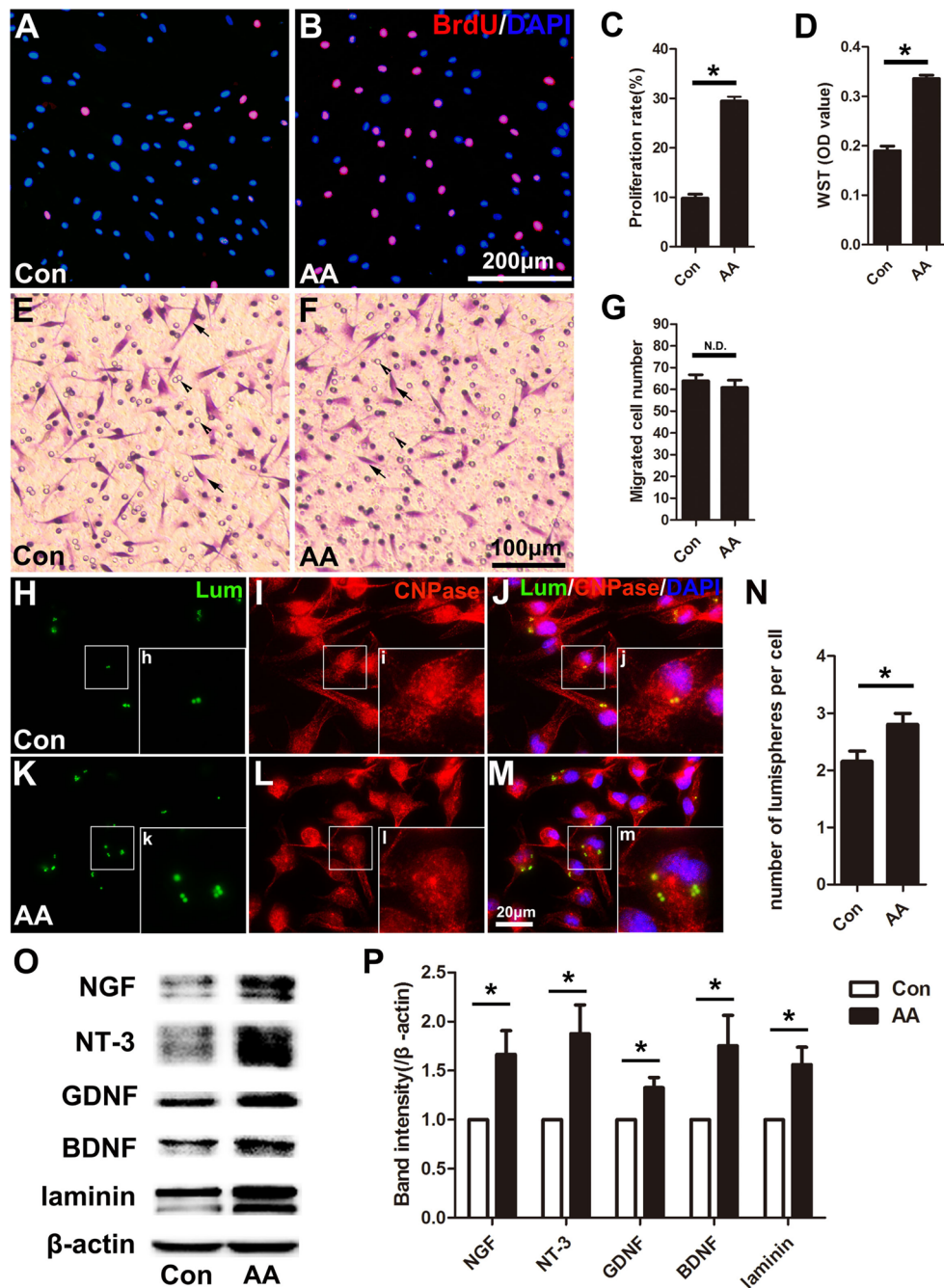


FIGURE 6 | AA promotes proliferation, phagocytosis and neurotrophic factor secretion in Schwann cells (SCs) but does not affect the migration of SCs *in vitro*. **(A,B)** Representative images of BrdU immunofluorescence staining from each group. The total cells were labeled with DAPI (blue). **(C,D)** Quantitative analysis of the BrdU and WST assays ($n = 3$, $*P < 0.05$). **(E,F)** Representative images showing migrated SCs (arrows) from each group (arrowheads indicate the micropores on the membrane). **(G)** Statistics showing there was no significant difference between the two groups ($n = 3$, N.D. indicates no significant difference). **(H–M)** Images showing the ingested lumispheres (green) within the cells. The SCs were identified with CNPase immunocytochemistry (red). **(N)** Quantitative analysis of the number of lumispheres per cell ($n = 3$, $*P < 0.05$). **(O)** Western blots and **(P)** their quantification indicate the expression level of neurotrophic factors ($n = 3$, $*P < 0.05$).

regeneration. Previously, some studies have reported using vitamins to treat peripheral nerve injuries, but these studies mainly focused on nerve injury-derived neuropathic pain, and the reported effects were mainly the results of interactions between the vitamins and pain-related receptors in the spinal

cord (Teixeira et al., 2002; Lu et al., 2011). In addition, many studies have demonstrated that AA plays a role in myelin formation, mainly myelination studies of SC/neuron coculture systems *in vitro* (Podratz et al., 2001; La Marca et al., 2011; Hyung et al., 2015), and observations of peripheral nerve demyelination

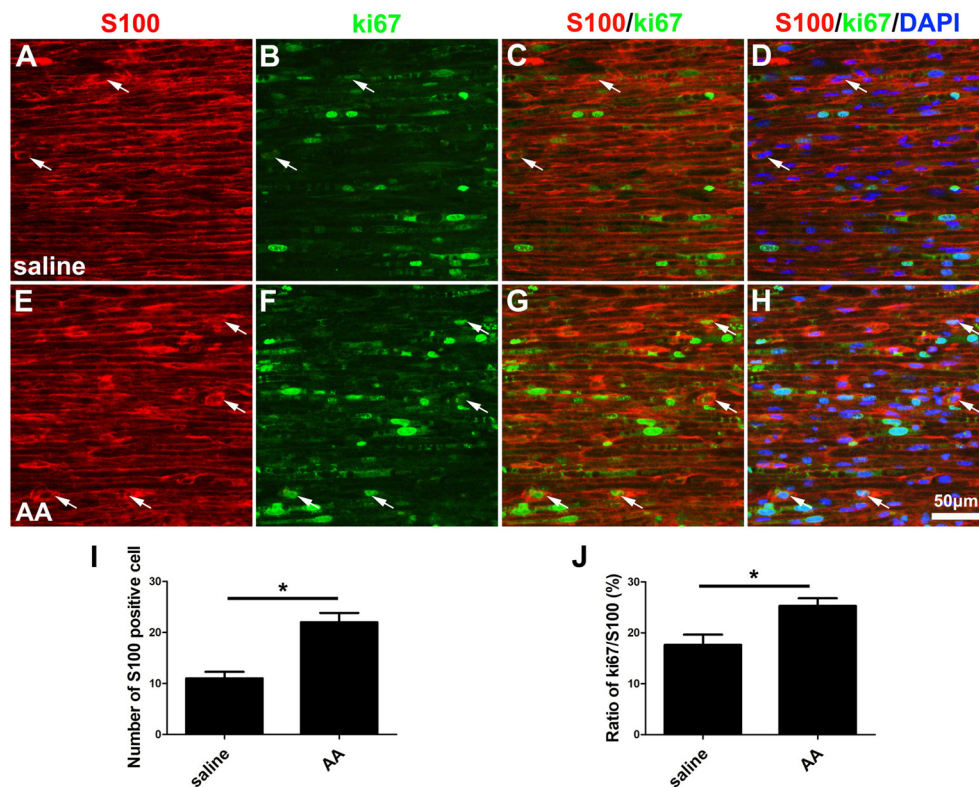


FIGURE 7 | AA promotes the proliferation of SCs *in vivo*. **(A–H)** Representative images of S100 (red) and ki67 (green) double immunostaining showing proliferating SCs (arrows) in each group. **(I)** Quantitative analysis of the number of S100-positive cells ($n = 3$, $*P < 0.05$). **(J)** The ratio of ki67/S100 in each group ($n = 3$, $*P < 0.05$).

in Charcot-Marie-Tooth disease (Passage et al., 2004; Gess et al., 2013). However, no data revealing the role of AA in axonal regeneration and remyelination after PNI are available.

The present data showed that at 3 dpi, GAP43- or SCG10-positive regenerating axons in lesioned nerves treated with AA were significantly longer than those in nerves from the control group, which indicates that AA can accelerate early axonal regeneration. In addition, axons in the distal stump and their myelin sheaths must be disintegrated after nerve injury. Subsequently, the axons regrow from the proximal end, extend to the distal trunk and become remyelinated by SCs. Thus, the axons and myelin sheaths detected in the distal portion of an injured nerve are the result of nerve regeneration. As shown in **Figure 2**, the number of NF-positive axons in the AA group was greater than that in the saline group and even greater than that in the sham group. Following nerve injury, a single proximal axon generates several lateral buds and then regenerates toward the distal trunk during nerve repair. These lateral buds noticeably outnumber the original axons in the nerve. This phenomenon is known as “multiple amplification” (Jiang et al., 2007; Deng et al., 2017). The present assessments by NF/MBP double immunostaining and TEM demonstrate that AA may increase the number and size of the regenerated axons and the myelin thickness.

It is well known that PNI-derived denervation leads to myoatrophy in the target muscles. Once regenerating axons reach and reinnervate the target muscles, myoatrophy can be reversed (Pak et al., 2016). Here, we performed histomorphometry on the gastrocnemius muscle and found larger myofibers in the AA-treated animals compared with those in the saline-treated control animals. This result combined with the behavior, electrophysiology and morphology results, leads us to believe that supplementation with AA is an efficient approach for facilitating nerve regeneration in PNI.

The most disastrous consequences of PNI are the loss of motor and sensory functions in the area innervated by the injured nerve. Here, we utilized three widely used behavior tests to evaluate functional nerve regeneration. The data shown in **Figure 4** demonstrate that all nerve injury-derived functional defects identified by comparing the saline group with the sham group were significantly alleviated in the AA group, which indicated that supplementation with AA can significantly improve both motor and sensory functional recovery. Then, the behavior profiles were confirmed by an electrophysiological assessment that showed that the AA treatment shortened the latency and increased the amplitude of CMAP in the injured sciatic nerves. CMAP is commonly used to measure nerve conduction properties. A shortened latency can reflect quicker nerve conduction, which is mainly related to the level and

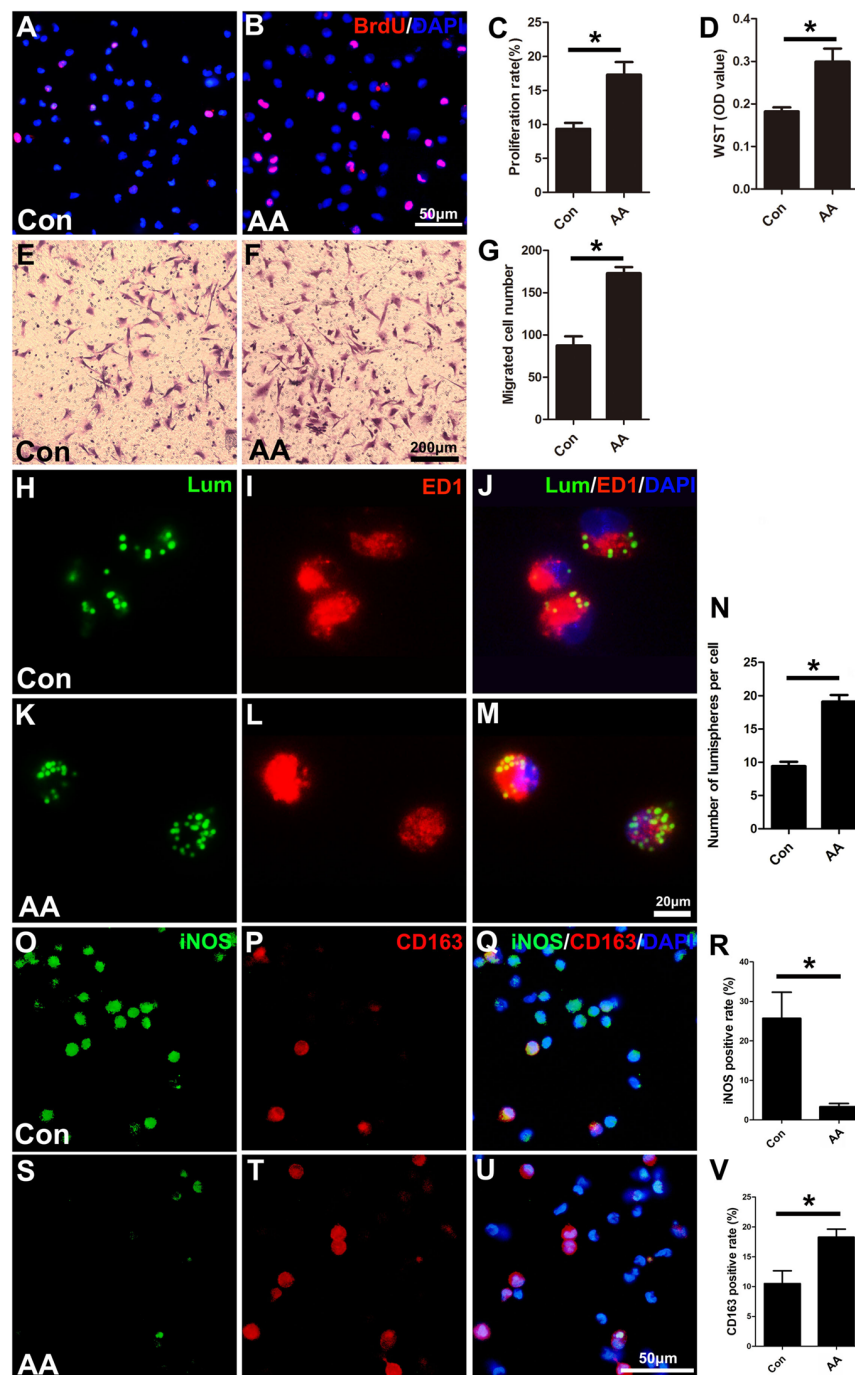


FIGURE 8 | AA promotes the proliferation, migration, phagocytic capability, and M2 polarization of macrophages but inhibits M1 polarization *in vitro*. **(A,B)** Images of immunofluorescence staining for BrdU (red). Cell nuclei were labeled with DAPI (blue). **(C,D)** Statistical analysis of the quantifications of the BrdU and WST assays ($n = 3$, $*P < 0.05$). **(E–G)** Images and quantification showing migrated macrophages in the two groups ($n = 3$, $*P < 0.05$). **(H–M)** Representative images of lumispheres ingested by macrophages (ED1 positive). **(N)** Quantitative analysis of the number of lumispheres per macrophage ($n = 3$, $*P < 0.05$). **(O–U)** Representative images and quantitative analysis illustrate that, compared with that in the control group, the number of M1-type macrophages in the AA group was reduced **(R)**, while the number of M2 macrophages in the AA-treated group was increased **(V)**; $n = 4$, $*P < 0.05$).

quality of myelin surrounding the nerve fibers. In addition, an increased amplitude suggests that a greater number of regenerated axons are present at the assessed time point (Wang

et al., 2015; Salehi et al., 2018). Overall, the data derived from this electrophysiological assessment illustrate that nerve conduction capability is improved by treatment with AA.

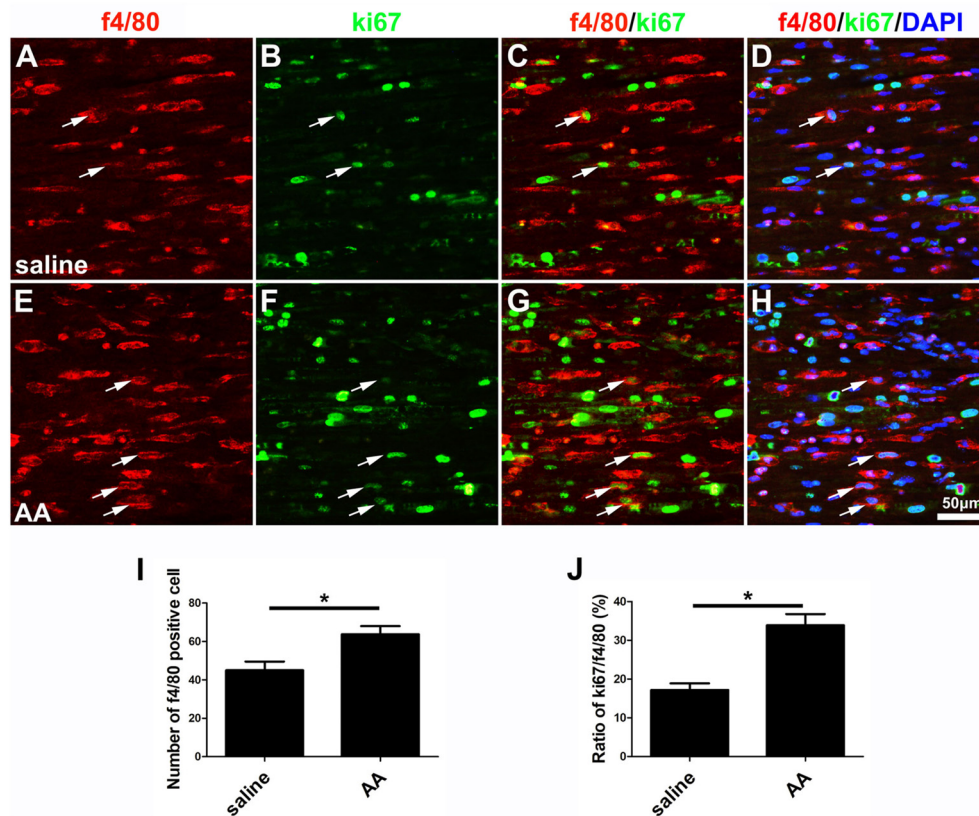


FIGURE 9 | AA promotes the proliferation of macrophages *in vivo*. (A–H) Representative images of f4/80 (red) and ki67 (green) double immunohistochemistry showing proliferating macrophages (arrow) in each group. (I) Quantitative analysis of the number of f4/80-positive cells ($n = 3$, $*P < 0.05$). (J) The ratio of ki67/f4/80 in each group ($n = 3$, $*P < 0.05$).

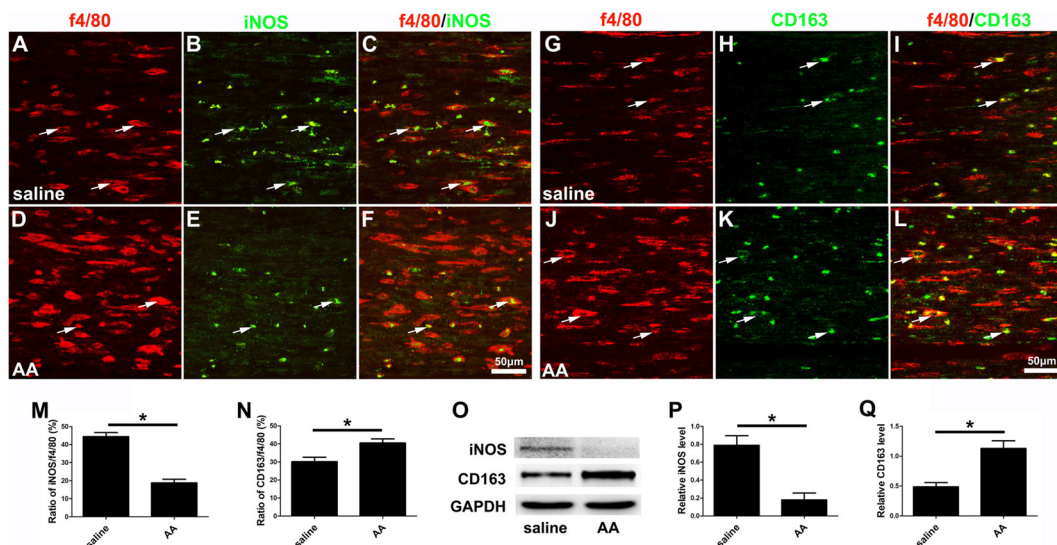


FIGURE 10 | AA inhibits the M1 polarization of macrophages but promotes M2 polarization *in vivo*. (A–F) Representative images of f4/80 (red) and iNOS (green) double immunohistochemistry in each group. (G–L) Representative images of f4/80 (red) and CD163 (green) double immunohistochemistry in each group. (M) The ratio of iNOS/f4/80 in each group ($n = 3$, $*P < 0.05$). (N) The ratio of CD163/f4/80 in each group ($n = 3$, $*P < 0.05$). (O–Q) Western blots and schematic diagrams of the statistical analysis showing the protein levels of iNOS and CD163 in the distal trunk of the injured sciatic nerves ($n = 3$, $*P < 0.05$).

Subsequently, three types of cells, including neurons, SCs and macrophages, which are involved in nerve injury and repair, were investigated to explore the potential role of AA in nerve regeneration. First, we isolated neurons from the DRG after axon removal, and the neurons were cultured in medium with a low concentration of FBS (1%) to mimic an unhealthy microenvironment. In these cultures, we found that AA significantly increased the number and length of regenerated neurites and decreased the expression of RhoA. RhoA is a crucial inhibiting factor for neuronal regeneration and is highly expressed in injured neurons (Devaux et al., 2017; Hu et al., 2017). Therefore, the downregulation of RhoA expression is beneficial to neurite outgrowth.

In addition to neuronal intrinsic capacity, environmental factors such as SC activation can contribute to axonal regeneration and remyelination. Adequate proliferation to produce a sufficient cell population and the migration of cells to the correct site are important processes in peripheral nerve regeneration even before the cells contribute to regeneration (Zhang et al., 2017). The present *in vitro* data from the BrdU assay and the WST-1 assay and the *in vivo* data from the double immunohistochemistry for S100 and ki67 demonstrated that AA can promote SC proliferation but has no statistical effect on SC migration. SCs are reported to participate in myelin phagocytosis in the early stage of Wallerian degeneration, prior to the recruitment of macrophages (Lutz et al., 2017). Using a lumisphere test, we found that many more lumispheres were ingested by AA-treated SCs than by naïve cells. These results indicate that AA can enhance the phagocytic capability of SCs and favor nerve regeneration by accelerating the elimination of debris from the injured nerve. Another important function of SCs is the secretion of neurotrophins and extracellular molecules (ECMs) to support and induce axonal regeneration. Herein, we detected the expression levels of laminin, a well-accepted component of the ECM that is essential for neuroregeneration, and NGF, NT-3, GDNF and BDNF, which are neurotrophins produced by SCs. Consistently, these proteins were all significantly upregulated by AA treatment. Overall, our data suggest that AA may affect the behavior of SCs and thereby enhance nerve regeneration.

Macrophage recruitment to the injured nerve is considered a key prerequisite for nerve regeneration by eliminating broken myelin and axonal debris. Our *in vitro* data also demonstrate that AA promotes the phagocytic and migration capabilities of macrophages. Furthermore, the present *in vitro* and *in vivo* data indicate that AA may significantly improve the proliferation and M2 polarization while decreasing the pro-inflammatory subtype (M1) polarization of macrophages. The anti-inflammatory subtype (M2) of macrophages is well accepted and has the capability to facilitate axonal regeneration

by secreting axonal regeneration-related factors, including ECM proteins, growth factors, cytokines and chemokines (Gaudet et al., 2011; Nadeau et al., 2011). In this view, our data are reasonable. However, post-injury inflammatory signals are also regarded as having a positive influence on axonal oxidative signaling for promoting axonal regeneration (Hervera et al., 2018). As inflammatory signals are mainly released by M1 macrophages, the present data cannot thoroughly explain the potential effect of the decreased number of M1 macrophages induced by treatment with AA in nerve regeneration. We hypothesize that an appropriate ratio of M1 vs. M2 macrophages may be important for nerve regeneration, and this hypothesis should be systematically studied in the future. In summary, the present experiments suggest that AA may have an effect on neurons, SCs and macrophages to facilitate nerve regeneration.

CONCLUSION

The current study is the first to provide experimental evidence demonstrating that supplementation with AA can sufficiently promote nerve regeneration in a model of moderate nerve injury and that this effect is related to the effect of AA on neurons, SCs and macrophages, which are key cells involved in nerve injury and repair. Given that AA is an essential nutrient in our diet and that it has been widely used as a dietary supplement and clinical drug (Chin and Ima-Nirwana, 2018; Granger and Eck, 2018), supplementation with AA may be a safe, affordable, convenient, and efficient strategy for accelerating peripheral nerve regeneration.

AUTHOR CONTRIBUTIONS

JG designed the study. LL, YL, ZF and XW performed the experiments. LL, YL, ZF, ZL, JW, JD, DT, MP and XH participated in collecting and analyzing experimental data. HZ, XH, and ML contributed to the double-blind analyzing data and statistics. The manuscript was written by JG, LL and reviewed by all authors.

FUNDING

This work was supported by the National Natural Science Foundation of China (81870982, 81571182 & 81371354); National Key Basic Research Program of China (2014CB542202); the Program for Changjiang Scholars and Innovative Research Team in University (IRT-16R37); Key Research & Development Program of Guangzhou Regenerative Medicine and Health Guangdong Laboratory (2018GZR110104008) and Natural Science Foundation of Guangdong Province (2017A030312009).

REFERENCES

- Chang, I. A., Lim, H. D., Kim, K. J., Shin, H., and Namgung, U. (2016). Enhanced axonal regeneration of the injured sciatic nerve by administration of Buyang Huanwu decoction. *J. Ethnopharmacol.* 194, 626–634. doi: 10.1016/j.jep.2016.10.053
- Chin, K. Y., and Ima-Nirwana, S. (2018). Vitamin C and bone health: evidence from cell, animal and human studies. *Curr. Drug Targets* 19, 439–450. doi: 10.2174/1389450116666150907100838
- Cimmino, L., Neel, B. G., and Aifantis, I. (2018). Vitamin C in stem cell reprogramming and cancer. *Trends Cell Biol.* 28, 698–708. doi: 10.1016/j.tcb.2018.04.001

- Deng, J. X., Zhang, D. Y., Li, M., Weng, J., Kou, Y. H., Zhang, P. X., et al. (2017). Autologous transplantation with fewer fibers repairs large peripheral nerve defects. *Neural. Regen. Res.* 12, 2077–2083. doi: 10.4103/1673-5374.221167
- Devaux, S., Cizkova, D., Mallah, K., Karnoub, M. A., Laouby, Z., Kobeissy, F., et al. (2017). RhoA inhibitor treatment at acute phase of spinal cord injury may induce neurite outgrowth and synaptogenesis. *Mol. Cell. Proteomics.* 16, 1394–1415. doi: 10.1074/mcp.m116.064881
- Faroni, A., Mobasser, S. A., Kingham, P. J., and Reid, A. J. (2015). Peripheral nerve regeneration: experimental strategies and future perspectives. *Adv. Drug Deliv. Rev.* 82–83, 160–167. doi: 10.1016/j.addr.2014.11.010
- Gallagher, Z. R., and Steward, O. (2018). Modest enhancement of sensory axon regeneration in the sciatic nerve with conditional co-deletion of PTEN and SOCS3 in the dorsal root ganglia of adult mice. *Exp. Neurol.* 303, 120–133. doi: 10.1016/j.expneurol.2018.02.012
- Gaudet, A. D., Popovich, P. G., and Ramer, M. S. (2011). Wallerian degeneration: gaining perspective on inflammatory events after peripheral nerve injury. *J. Neuroinflammation* 8:110. doi: 10.1186/1742-2094-8-110
- Gess, B., Röhr, D., and Young, P. (2013). Ascorbic acid and sodium-dependent vitamin C transporters in the peripheral nervous system: from basic science to clinical trials. *Antioxid. Redox Signal.* 19, 2105–2114. doi: 10.1089/ars.2013.5380
- Gey, M., Wanner, R., Schilling, C., Pedro, M. T., Sinske, D., and Knöll, B. (2016). Atf3 mutant mice show reduced axon regeneration and impaired regeneration-associated gene induction after peripheral nerve injury. *Open Biol.* 6:160091. doi: 10.1098/rsob.160091
- Glajch, K. E., Fleming, S. M., Surmeier, D. J., and Osten, P. (2012). Sensorimotor assessment of the unilateral 6-hydroxydopamine mouse model of Parkinson's disease. *Behav. Brain Res.* 230, 309–316. doi: 10.1016/j.bbr.2011.12.007
- Granger, M., and Eck, P. (2018). Dietary Vitamin C in human health. *Adv. Food Nutr. Res.* 83, 281–310. doi: 10.1016/b.s.afnr.2017.11.006
- Grinsell, D., and Keating, C. P. (2014). Peripheral nerve reconstruction after injury: a review of clinical and experimental therapies. *Biomed Res. Int.* 2014:698256. doi: 10.1155/2014/698256
- Guo, Y. E., Suo, N., Cui, X., Yuan, Q., and Xie, X. (2018). Vitamin C promotes oligodendrocytes generation and remyelination. *Glia* 66, 1302–1316. doi: 10.1002/glia.23306
- Hervera, A., De Virgiliis, F., Palmisano, I., Zhou, L., Tantardini, E., Kong, G., et al. (2018). Reactive oxygen species regulate axonal regeneration through the release of exosomal NADPH oxidase 2 complexes into injured axons. *Nat. Cell Biol.* 20, 307–319. doi: 10.1038/s41556-018-0063-x
- Hu, J., Zhang, G., Rodemer, W., Jin, L. Q., Shifman, M., and Selzer, M. E. (2017). The role of RhoA in retrograde neuronal death and axon regeneration after spinal cord injury. *Neurobiol. Dis.* 98, 25–35. doi: 10.1016/j.nbd.2016.11.006
- Hyung, S., Yoon Lee, B., Park, J. C., Kim, J., Hur, E. M., and Francis Suh, J. K. (2015). Coculture of primary motor neurons and schwann cells as a model for *in vitro* myelination. *Sci. Rep.* 5:15122. doi: 10.1038/srep15122
- Ibrahim, M. A., Abdelzaher, W. Y., Rofaail, R. R., and Abdelwahab, S. (2018). Efficacy and safety of combined low doses of either diclofenac or celecoxib with gabapentin versus their single high dose in treatment of neuropathic pain in rats. *Biomed. Pharmacother.* 100, 267–274. doi: 10.1016/j.biopha.2018.01.102
- Jiang, B. G., Yin, X. F., Zhang, D. Y., Fu, Z. G., and Zhang, H. B. (2007). Maximum number of collaterals developed by one axon during peripheral nerve regeneration and the influence of that number on reinnervation effects. *Eur. Neurol.* 58, 12–20. doi: 10.1159/000102161
- Jungnickel, J., Haastert, K., Grzybek, M., Thau, N., Lipokatic-Takacs, E., Ratzka, A., et al. (2010). Mice lacking basic fibroblast growth factor showed faster sensory recovery. *Exp. Neurol.* 223, 166–172. doi: 10.1016/j.expneurol.2009.06.003
- Kocot, J., Luchowska-Kocot, D., Kielczykowska, M., Musik, I., and Kurzepa, J. (2017). Does vitamin C influence neurodegenerative diseases and psychiatric disorders? *Nutrients* 9:E659. doi: 10.3390/nu9070659
- La Marca, R., Cerri, F., Horiuchi, K., Bachi, A., Feltri, M. L., Wrabetz, L., et al. (2011). TACE (ADAM17) inhibits Schwann cell myelination. *Nat. Neurosci.* 14, 857–865. doi: 10.1038/nn.2849
- Lamid, S. (1983). Ascorbic acid and methenamine mandelate on the urinary pH of spinal cord injury patients. *J. Urol.* 129, 845–846. doi: 10.1016/s0022-5347(17)52396-4
- Liu, G. M., Xu, K., Li, J., and Luo, Y. G. (2016). Curcumin upregulates S100 expression and improves regeneration of the sciatic nerve following its complete amputation in mice. *Neural Regen. Res.* 11, 1304–1311. doi: 10.4103/1673-5374.189196
- Lu, R., Kallenborn-Gerhardt, W., Geisslinger, G., and Schmidtke, A. (2011). Additive antinociceptive effects of a combination of vitamin C and vitamin E after peripheral nerve injury. *PLoS One.* 6:e29240. doi: 10.1371/journal.pone.0029240
- Lutz, A. B., Chung, W.-S., Sloan, S. A., Carson, G. A., Zhou, L., Lovelett, E., et al. (2017). Schwann cells use TAM receptor-mediated phagocytosis in addition to autophagy to clear myelin in a mouse model of nerve injury. *Proc. Natl. Acad. Sci. U S A.* 114, E8072–E8080. doi: 10.1073/pnas.1710566114
- Ma, C. H., Omura, T., Cobos, E. J., Latrémolière, A., Ghasemlou, N., Brenner, G. J., et al. (2011). Accelerating axonal growth promotes motor recovery after peripheral nerve injury in mice. *J. Clin. Invest.* 121, 4332–4347. doi: 10.1172/jci58675
- May, J. M. (2012). Vitamin C transport and its role in the central nervous system. *Subcell. Biochem.* 56, 85–103. doi: 10.1007/978-94-007-2199-9_6
- Modrak, M., Sundem, L., and Elfar, J. (2017). Erythropoietin enhanced recovery after peripheral nerve injury. *Neural Regen. Res.* 12, 1268–1269. doi: 10.4103/1673-5374.213544
- Moretti, M., Fraga, D. B., and Rodrigues, A. L. S. (2017). Preventive and therapeutic potential of ascorbic acid in neurodegenerative diseases. *CNS Neurosci. Ther.* 23, 921–929. doi: 10.1111/cns.12767
- Nadeau, S., Filali, M., Zhang, J., Kerr, B. J., Rivest, S., Soulet, D., et al. (2011). Functional recovery after peripheral nerve injury is dependent on the pro-inflammatory cytokines IL-1 β and TNF: implications for neuropathic pain. *J. Neurosci.* 31, 12533–12542. doi: 10.1523/jneurosci.2840-11.2011
- Noble, J., Munro, C. A., Prasad, V. S., and Midha, R. (1998). Analysis of upper and lower extremity peripheral nerve injuries in a population of patients with multiple injuries. *J. Trauma.* 45, 116–122. doi: 10.1097/00005373-199807000-00025
- Pak, K., Shin, M. J., Hwang, S. J., Shin, J. H., Shin, H. K., Kim, S. J., et al. (2016). Longitudinal changes in glucose metabolism of denervated muscle after complete peripheral nerve injury. *Mol. Imaging Biol.* 18, 741–747. doi: 10.1007/s11307-016-0948-7
- Pan, M., Wang, X., Chen, Y., Cao, S., Wen, J., Wu, G., et al. (2017). Tissue engineering with peripheral blood-derived mesenchymal stem cells promotes the regeneration of injured peripheral nerves. *Exp. Neurol.* 292, 92–101. doi: 10.1016/j.expneurol.2017.03.005
- Park, H. J., Shin, H. Y., Kim, S. H., Jeong, H. N., Choi, Y. C., Suh, B. C., et al. (2018). Partial conduction block as an early nerve conduction finding in neurolymphomatosis. *J. Clin. Neurol.* 14, 73–80. doi: 10.3988/jcn.2018.14.1.73
- Passage, E., Norreel, J. C., Noack-Fraissignes, P., Sanguedolce, V., Pizant, J., Thirion, X., et al. (2004). Ascorbic acid treatment corrects the phenotype of a mouse model of Charcot-Marie-Tooth disease. *Nat. Med.* 10, 396–401. doi: 10.1038/nm1023
- Penna, V., Munder, B., Stark, G. B., and Lang, E. M. (2011). An *in vivo* engineered nerve conduit-fabrication and experimental study in rats. *Microsurgery* 31, 395–400. doi: 10.1002/micr.20894
- Wang, Z., Yang, X., Zhang, W., Zhang, P., and Jiang, B. (2018). Tanshinone IIA attenuates nerve structural and functional damage induced by nerve crush injury in rats. *PLoS One* 13:e0202532. doi: 10.1371/journal.pone.0202532
- Podratz, J. L., Rodriguez, E., and Windebank, A. J. (2001). Role of the extracellular matrix in myelination of peripheral nerve. *Glia* 35, 35–40. doi: 10.1002/glia.1068
- Qian, C., Tan, D., Wang, X., Li, L., Wen, J., Pan, M., et al. (2018). Peripheral nerve injury-induced astrocyte activation in spinal ventral horn contributes to nerve regeneration. *Neural Plast.* 2018:8561704. doi: 10.1155/2018/8561704
- Robert, A. A., Zamzami, M., Sam, A. E., Al Jadid, M., and Al Mubarak, S. (2012). The efficacy of antioxidants in functional recovery of spinal cord injured rats: an experimental study. *Neurol. Sci.* 33, 785–791. doi: 10.1007/s10072-011-0829-4
- Saffarpour, S., and Nasirinezhad, F. (2017). Functional interaction between N-methyl-D-aspartate receptor and ascorbic acid during neuropathic pain induced by chronic constriction injury of the sciatic nerve. *J. Basic Clin. Physiol. Pharmacol.* 28, 601–608. doi: 10.1515/jbcpp-2017-0015

- Salehi, M., Naseri-Nosar, M., Ebrahimi-Barough, S., Nourani, M., Khojasteh, A., Farzamfar, S., et al. (2018). Polyurethane/gelatin nanofibrils neural guidance conduit containing platelet-rich plasma and melatonin for transplantation of schwann cells. *Cell. Mol. Neurobiol.* 38, 703–713. doi: 10.1007/s10571-017-0535-8
- Schreiber, J. J., Byun, D. J., Khair, M. M., Rosenblatt, L., Lee, S. K., and Wolfe, S. W. (2015). Optimal axon counts for brachial plexus nerve transfers to restore elbow flexion. *Plast. Reconstr. Surg.* 135, 135e–141e. doi: 10.1097/prs.0000000000000795
- Sheu, M. L., Cheng, F. C., Su, H. L., Chen, Y. J., Chen, C. J., Chiang, C. M., et al. (2012). Recruitment by SDF-1 α of CD34-positive cells involved in sciatic nerve regeneration. *J. Neurosurg.* 116, 432–444. doi: 10.3171/2011.3.jns101582
- Shin, J. E., Geisler, S., and DiAntonio, A. (2014). Dynamic regulation of SCG10 in regenerating axons after injury. *Exp. Neurol.* 252, 1–11. doi: 10.1016/j.expneurol.2013.11.007
- Singh, S., Jamwal, S., and Kumar, P. (2017). Neuroprotective potential of Quercetin in combination with piperine against 1-methyl-4-phenyl-1,2,3,6-tetrahydropyridine-induced neurotoxicity. *Neural Regen. Res.* 12, 1137–1144. doi: 10.4103/1673-5374.211194
- Tateshita, T., Ueda, K., and Kajikawa, A. (2018). End-to-end and end-to-side neurorrhaphy between thick donor nerves and thin recipient nerves: an axon regeneration study in a rat model. *Neural Regen. Res.* 13, 699–703. doi: 10.4103/1673-5374.230296
- Teixeira, F., Pollock, M., Karim, A., and Jiang, Y. (2002). Use of antioxidants for the prophylaxis of cold-induced peripheral nerve injury. *Mil. Med.* 167, 753–755. doi: 10.1093/milmed/167.9.753
- Wang, C., Lu, C. F., Peng, J., Hu, C. D., and Wang, Y. (2017). Roles of neural stem cells in the repair of peripheral nerve injury. *Neural Regen. Res.* 12, 2106–2112. doi: 10.4103/1673-5374.221171
- Wang, T., Chen, K., Zeng, X., Yang, J., Wu, Y., Shi, X., et al. (2011). The histone demethylases Jhdmla/1b enhance somatic cell reprogramming in a vitamin-C-dependent manner. *Cell Stem Cell* 9, 575–587. doi: 10.1016/j.stem.2011.10.005
- Wang, X., Pan, M., Wen, J., Tang, Y., Hamilton, A. D., Li, Y., et al. (2014). A novel artificial nerve graft for repairing long-distance sciatic nerve defects: a self-assembling peptide nanofiber scaffold-containing poly(lactic-co-glycolic acid) conduit. *Neural Regen. Res.* 9, 2132–2141. doi: 10.4103/1673-5374.147944
- Wang, Y., Wang, H., Mi, D., Gu, X., and Hu, W. (2015). Periodical assessment of electrophysiological recovery following sciatic nerve crush via surface stimulation in rats. *Neurol. Sci.* 36, 449–456. doi: 10.1007/s10072-014-2005-0
- Wen, J., Qian, C., Pan, M., Wang, X., Li, Y., Lu, Y., et al. (2017). Lentivirus-mediated RNA interference targeting RhoA slacks the migration, proliferation and myelin formation of schwann cells. *Mol. Neurobiol.* 54, 1229–1239. doi: 10.1007/s12035-016-9733-5
- Wu, J., Li, J., Ren, J., and Zhang, D. (2017). MicroRNA-485-5p represses melanoma cell invasion and proliferation by suppressing Frizzled7. *Biomed Pharmacother* 90, 303–310. doi: 10.1016/j.biopha.2017.03.064
- Yagi, H., Ohkawara, B., Nakashima, H., Ito, K., Tsushima, M., Ishii, H., et al. (2015). Zonisamide enhances neurite elongation of primary motor neurons and facilitates peripheral nerve regeneration *in vitro* and in a mouse model. *PLoS One*. 10:e0142786. doi: 10.1371/journal.pone.0142786
- Yan, M., Yang, M., Shao, W., Mao, X. G., Yuan, B., Chen, Y. F., et al. (2014). High-dose ascorbic acid administration improves functional recovery in rats with spinal cord contusion injury. *Spinal Cord.* 52, 803–808. doi: 10.1038/sc.2014.135
- Yuan, M., Li, D., An, M., Li, Q., Zhang, L., and Wang, G. (2017). Rediscovering peritoneal macrophages in a murine endometriosis model. *Hum. Reprod.* 32, 94–102. doi: 10.1093/humrep/dew274
- Zhang, X., Gong, X., Qiu, J., Zhang, Y., and Gong, F. (2017). MicroRNA-210 contributes to peripheral nerve regeneration through promoting the proliferation and migration of Schwann cells. *Exp. Ther. Med.* 14, 2809–2816. doi: 10.3892/etm.2017.4869

Conflict of Interest Statement: The authors declare that the research was conducted in the absence of any commercial or financial relationships that could be construed as a potential conflict of interest.

Copyright © 2019 Li, Li, Fan, Wang, Li, Wen, Deng, Tan, Pan, Hu, Zhang, Lai and Guo. This is an open-access article distributed under the terms of the Creative Commons Attribution License (CC BY). The use, distribution or reproduction in other forums is permitted, provided the original author(s) and the copyright owner(s) are credited and that the original publication in this journal is cited, in accordance with accepted academic practice. No use, distribution or reproduction is permitted which does not comply with these terms.



Relevance and Recent Developments of Chitosan in Peripheral Nerve Surgery

A. Boecker*, S. C. Daeschler, U. Kneser and L. Harhaus

¹ Department of Hand, Plastic and Reconstructive Surgery, Burn Center, BG Trauma Center Ludwigshafen, University of Heidelberg, Ludwigshafen, Germany

OPEN ACCESS

Edited by:

Stefania Raimondo,
University of Turin, Italy

Reviewed by:

Giovanni Vozzi,
University of Pisa, Italy
Federica Fregnan,
University of Turin, Italy

*Correspondence:

A. Boecker
arnehendrik.boecker@
bgu-ludwigshafen.de

Received: 28 October 2018

Accepted: 28 February 2019

Published: 04 April 2019

Citation:

Boecker A, Daeschler SC,
Kneser U and Harhaus L (2019)
Relevance and Recent Developments
of Chitosan in Peripheral
Nerve Surgery.
Front. Cell. Neurosci. 13:104.
doi: 10.3389/fncel.2019.00104

Developments in tissue engineering yield biomaterials with different supporting strategies to promote nerve regeneration. One promising material is the naturally occurring chitin derivate chitosan. Chitosan has become increasingly important in various tissue engineering approaches for peripheral nerve reconstruction, as it has demonstrated its potential to interact with regeneration associated cells and the neural microenvironment, leading to improved axonal regeneration and less neuroma formation. Moreover, the physiological properties of its polysaccharide structure provide safe biodegradation behavior in the absence of negative side effects or toxic metabolites. Beneficial interactions with Schwann cells (SC), inducing differentiation of mesenchymal stromal cells to SC-like cells or creating supportive conditions during axonal recovery are only a small part of the effects of chitosan. As a result, an extensive body of literature addresses a variety of experimental strategies for the different types of nerve lesions. The different concepts include chitosan nanofibers, hydrogels, hollow nerve tubes, nerve conduits with an inner chitosan layer as well as hybrid architectures containing collagen or polyglycolic acid nerve conduits. Furthermore, various cell seeding concepts have been introduced in the preclinical setting. First translational concepts with hollow tubes following nerve surgery already transferred the promising experimental approach into clinical practice. However, conclusive analyses of the available data and the proposed impact on the recovery process following nerve surgery are currently lacking. This review aims to give an overview on the physiologic properties of chitosan, to evaluate its effect on peripheral nerve regeneration and discuss the future translation into clinical practice.

Keywords: microsurgery, peripheral nerve injuries, nerve surgery, nerve regeneration, nerve reconstruction, chitosan, nerve growth factors

Abbreviations: BMSC, bone marrow mesenchymal stromal cells; CCL2, chemokine ligand 2; DOA, degree of acetylation; EGR2, early growth response protein 2; FGF-2, fibroblast growth factor-2; GDNF, glial cell line-derived growth factor; NCAM, neural cell adhesion molecule; NGF, nerve growth factor; PDGF, platelet-derived growth factor (PDGF); PGA, poly glycolic acid; PLA, polylactic acid; PLGA, poly(lactic-co-glycolic acid); PNI, peripheral nerve injury; SC, Schwann cells.

INTRODUCTION

Approximately 2.8% of all hospitalized trauma patients suffer from traumatic peripheral nerve injury (Noble et al., 1998). The related severe functional impairment, as well as the consequent socio-economic impact, led to continuous research efforts in this field (Nicholson and Verma, 2004). If a direct tension free approximation of the nerve stumps is possible, to this day, the epineural nerve suture represents the first line therapy. Alternatively, if tension free coaptation is not achievable, the autologous nerve transplantation (ANT) is the current gold standard (Deumens et al., 2010). However, given the limited availability of donor nerves and the associated donor site morbidity, new approaches are needed to support in peripheral nerve surgery. Ideally, nerve conduits could provide guidance for the regenerating axons toward the distal nerve stump in the absence of negative side effects like an extended foreign body reaction or an undirected axonal regeneration. Tissue engineering utilized a considerable diversity of materials, but basic techniques like the ANT, firstly described in the 1970's, are still up to date (Davis and Perret, 1946; Tarlov et al., 1946). Various materials have been tested for bridging peripheral nerve defects reaching from non-resorbable materials like silicon (Lundborg, 2004) to fully biodegradable materials such as Collagen or PGA (Inada et al., 2007; Bozkurt et al., 2012; Boecker et al., 2015). Today, it is a common consent that the material used to support the peripheral nerve regeneration should ideally base on a fully degradable matrix without negatively influencing the regeneration during biodegradation process (Schmidt and Leach, 2003). However, despite substantial developments in tissue engineering, there is still no material or bio-mimicking concept, which revealed superior results in peripheral nerve regeneration compared to the ANT as the current gold standard for bridging peripheral nerve defects (Deumens et al., 2010).

Besides the already established materials, Chitosan is a promising relatively novel material in the field of peripheral nerve regeneration. As it is based on the shell of arthropods it is universally available at low costs and provides a fully bioresorbable structure in the absence of toxic metabolites, potentially interfering the regeneration process (Freier et al., 2005b). Moreover, its specific physical and chemical properties enable to simulate the physiological multilayer architecture of peripheral nerves in artificial tissue engineered nerve conduits. This provides a wide field of potential applications in peripheral nerve surgery such as gap bridging, nerve suture protection or even neuroma prevention.

Previous preclinical and clinical studies investigated these conditions and demonstrated chitosan to support the axonal regeneration (Haastert-Talini et al., 2013; Stenberg et al., 2016), reduce extensive scarring, improve functional recovery (Neubrecht et al., 2018) and prevent neuroma formation following peripheral nerve injury (Marcol et al., 2011). These promising preclinical and early clinical experiences in diverse nerve injury models along with its physiologic features emphasize the future potential of chitosan-based matrices in reconstructive nerve surgery. This work aims to systematically review the current tissue engineering strategies and the current process of clinical implementation.

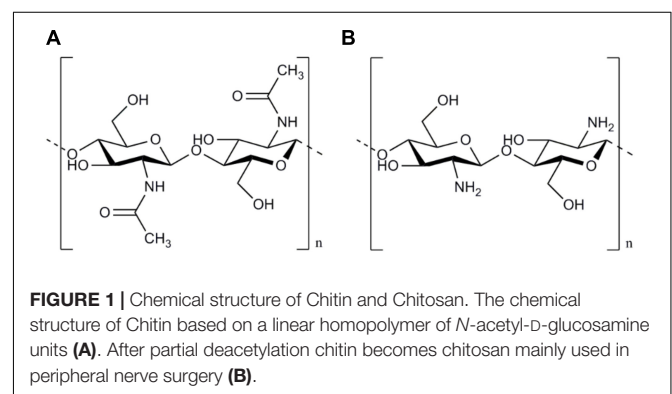
PROPERTIES OF CHITOSAN AND ITS IMPACT ON PERIPHERAL NERVE REGENERATION

The basic component of Chitosan is Chitin, a long-chain polymer of *N*-acetylglucosamine which is harvested by the exoskeletons of arthropods. After cellulose, Chitin is the second most abundant polysaccharide in nature and is aimed to be mainly used in its deacetylated modification (Chitosan) in the field of peripheral nerve surgery (Crompton et al., 2007). Chitin and chitosan can be classified into the family of the glycosaminoglycans, related to groups of chondroitin sulfates, hyaluronic acid, and heparins. However, glycosaminoglycans may be the only polysaccharides with bioactive capabilities (Struszczyk, 2002). Chitin consists of a linear homopolymer of *N*-acetyl-D-glucosamine units with β -(1-4)-linkages. After partial deacetylation, chitin becomes chitosan (see Figure 1). Thus it can be easily obtained at very low production costs for commercial purposes by alkaline hydrolysis of chitin (Freier et al., 2005b). Depending on the processing of the chitosan, the degree of acetylation (DOA) can be varied and thus influences the molar mass as well as solvent characteristics (Chatelet et al., 2001).

Moreover, the DOA has also been shown to be a relevant factor, influencing survival, proliferation and cell activity of regeneration supporting cells like SC (Carvalho et al., 2017). But, the exact adjustments of chitosan matrices remain challenging, because the mechanical stiffness, the biodegradation time, the geometric architecture as well as the sterilization method potentially influence the axonal regeneration process and thus need to be taken into account throughout the manufacturing process (Stöbel et al., 2018).

In tissue engineered nerve conduits, the biodegradation and physiologic replacement processes start immediately and thus present the central mechanisms of action which influence nerve recovery. In contrast to acid-based materials, like polyglycolic acid (PGA) or polylactide derivatives, which undergo a pH decrease during biodegradation or signs of inflammatory foreign body reaction (Meek and Coert, 2008), metabolites of chitosan demonstrated neuroprotective effects during peripheral nerve regeneration.

Here, a degradation product of Chitosan, the Chitoooligosaccharide (COS), has been found to promote cell proliferation and prevent apoptosis especially for SC, as the



vital cell for a sufficient axonal regeneration (Zhou et al., 2008; Huang et al., 2015). Furthermore, Wang et al. (2016) attributed these stimulating effects of COS to an accelerated cell cycle leading to increased SC proliferation.

Moreover, COS stimulate the CCL2 expression by down-regulating the miR-327 of the SC, resulting in enhanced macrophage migration to the injury site (Zhao et al., 2017). In line with this, Bin et al. analyzed the anti-apoptotic effects of carboxymethylated chitosan (CMC) on SC by decreasing caspase-3, -9 and Bax activities and increasing Bcl-2 activities in CMC treated SC. To prevent the SC against oxidative stress, COS led to a reduced activity of malondialdehyde as well as to increased activity of superoxide dismutase activities (SOD) (He et al., 2014). Further *in vivo* experiments demonstrated a significantly improved peripheral nerve regeneration following daily intravenous injection COS for 6 weeks in an axotomy rabbit animal model. Interestingly, the number of regenerated myelinated nerve fibers, the myelin sheath thickness, as well as the compound muscle action potential (CMAP) as the parameter for electrophysiological recovery, has been shown to be significantly superior in COS treated animals. Thus, Gong et al. (2009) sum up, that COS not only accelerate the peripheral nerve regeneration but also can be seen as a neuroprotective agent after PNI.

Furthermore, the beneficial effect on neural disorders by suppression of the β -amyloid formation and supporting the anti-neuroinflammatory activity underlines the tremendous potential of COS, and consequently of chitosan, in the field of neuropathologies (Pangestuti and Kim, 2010; Hao et al., 2017).

Focusing on the tissue engineered designs, in most publications, Chitosan is the main component for a new tissue-engineered nerve conduit to bridge peripheral nerve defects. Interestingly, there are some alternative geometric structures of chitosan to promote axonal regeneration or even prevent neuroma formation.

Xu et al. (2017) have recently published another concept in the tissue engineering of chitosan by presenting a chitosan-based hydrogel in combination with a poly 3,4-ethylenedioxythiophene. Supported cell adhesion, vitality, and proliferation of PC-12 cells underline the potential of chitosan hydrogel for further neural tissue engineering. Interestingly tissue engineered concepts based on chitosan focused not only on the treatment of PNI but also for neuroma prevention. Marcol et al. (2011) applied, microcrystalline chitosan to the proximal nerve stump after PNI and showed less autotomy behavior and minor axonal sprouting as a key ability for neuroma prevention in the future.

MECHANICAL PROPERTIES AND TOPOGRAPHIC STRATEGIES IN TISSUE ENGINEERING OF CHITOSAN

Mechanical Properties and Challenges

In a medical application, chitosan has already a long history due to its biocompatibility and to its non-toxic, biodegradable properties (Freier et al., 2005b).

Not only in the field of peripheral nerve surgery chitosan plays a crucial role, but also for wound healing or as a drug delivery system. Referring to the peripheral nerve, low mechanical strength has been a tremendous challenge in the early phase after implantation of chitosan and its derivatives. Matrices of chitosan showed decreased stability under physiological conditions (Madhally and Matthew, 1999; Itoh et al., 2003) and therefore make it not suitable for the translational application. Modifications have been made to improve mechanical stability by designing an internal architecture by puncturing the chitosan while molding procedures with needles (Wang et al., 2006). Alternatively, Ao et al. (2006) developed a new uni-directional temperature gradient leading to a chitosan scaffolds incorporated with longitudinal microfibers. Unfortunately, the scaffold presents an appropriate mechanical strength under *in vitro* conditions but fail to show stability under physiological *in vivo* circumstances. To improve the mechanical strength of chitosan, further adjustments like additional cross-linking by supplementation of chitin (Yang et al., 2004) or formaldehyde (Desai and Park, 2005) have been published. The mechanical stability of the chitosan is also affected by the degree of acetylation (DOA). Higher DOA has been reported to improve the stability of chitosan and lead to a superior keratinocytes cell adhesion (Chatelet et al., 2001). Referring to the neural cell lineage, acetylation rates of 0.5 and 11% showed more and longer neurites of regeneration of dorsal chick root ganglions neurons compared to other concentration. However, cell viability of 0.5% was approximately eight times higher compared to a DOA of 11%. Thus, surface modifications of chitosan films referring to the cell viability and cell adhesion can clearly be modified by the DOA (Freier et al., 2005a) and needs to be addressed in the future tissue engineering for chitosan materials. In line with this, supporting cells, like SC, also benefit from a low DOA by presenting a better cell spreading and proliferation (Wenling et al., 2005).

However, for translation applications, the mechanical strength of the material to prevent the collapse of the material is essential as well as the ability for an inner lining of regenerating axons. Exemplary, Wang et al. present a chitosan two-layer approach with an oriented inner layer of nanofibers and a random outer layer with superior stability compared to random fiber mesh tubes (Wang et al., 2008a,b).

Forms of Chitosan and Topographic Concepts

Several forms and techniques of chitosan have been published in literature reaching from hydrogels (Zheng et al., 2010; Rickett et al., 2011; Nawrotek et al., 2016b; Du et al., 2017), films (Pavinatto et al., 2010; Xiao et al., 2013; Meyer et al., 2016b), microspheres (Zeng et al., 2014) or tubes (Itoh et al., 2003; Wang et al., 2006; Shapira et al., 2016) in the field of peripheral nerve surgery.

Hydrogels

Hydrogels are a frequently applied form in the field of tissue engineering because of the similarity to the extracellular matrix, and the modest way of processing.

Freier et al. (2005b) presented, after the hydrolyzation of chitin, a hydrogel-based chitosan tube with superior mechanical

strength, measured by the transverse compressive test. Chitosan Hydrogel has also been used as an alternative to the fibrin glue or even to the epineural suture after peripheral nerve lesion (Rickett et al., 2011). Further *in vitro* studies combine chitosan hydrogels with hydroxyapatite as a source for calcium ions to modify mechanical and biological properties. Cytotoxic and pro-inflammatory tests could mark the biocompatibility of this hydrogel solution independently of the tested composition (Nawrotek et al., 2016a).

Interestingly, *in vivo* studies with a chitosan/glycerol-beta-phosphate disodium salt hydrogel presented an impaired peripheral nerve regeneration for 10 mm sciatic nerve defect compared to chitosan tubes filled with SC suspension or culture medium (Zheng et al., 2010). Hydrogels as an inner filling in combination with chitosan tubes tested under *in vivo* conditions led to further enhanced peripheral nerve regeneration.

As drug delivery system, chitosan hydrogels have also been explored by a continuous delivery of methylprednisolone. Functional recovery of the rat's facial (Chao et al., 2015) and sciatic nerve (Mehrshad et al., 2017) was accelerated for animals with a supplementary methylprednisolone delivery.

Hydrogels of other components, like Hyaluronic hydrogels (Meyer et al., 2016b) fibrin nanofiber hydrogels (Du et al., 2017) or simvastatin/Pluronic F-127 hydrogels (Guo et al., 2018) have been frequently combined with chitosan tubes. Axonal regeneration and motor functional recovery was improved by applying these hydrogels as inner filling for chitosan tubes.

Films

In the field of peripheral nerve surgery, chitosan films are applied directly for enhancing peripheral nerve regeneration but also as an inner architecture for nerve guides to bridge peripheral nerve defects. Mechanical stability and biocompatibility were proven for neural cells and peripheral nerves tissue engineering (Pavinatto et al., 2010).

Meyer et al. (2016a) combined a chitosan nerve tube with a supporting inner layer of a chitosan film over 15 mm long distance defects of a rat's sciatic nerve lesion and presented superior axonal regeneration as well functional recovery compared to hollow non-modified chitosan tubes.

Chitosan films have been modified with several other components by crosslinking or incorporation. Proanthocyanidin was crosslinked to chitosan films with gelatine and showed improved mechanical properties, a decreased biodegradation rate, superior cell adhesion as well as improved proliferation compared to non-crosslinked gelatin or chitosan alone (Kim et al., 2005). Similar results have been found by the crosslinking of chitosan and hyaluronic in a polyelectrolyte multilayer film (Schneider et al., 2007). Incorporation of polyethylene oxid with chitosan revealed a superior water permeability and a ratio-dependent antibacterial effects as well as improved mechanical strength compared to non-modified chitosan films (Zivanovic et al., 2007).

Microspheres

Chitosan can also be manufactured as microspheres or microparticles mainly used for drug delivery. Chitosan

microspheres loaded with NGF has been incorporated to collagen-chitosan scaffolds for a rat's sciatic nerve and led to promising results in functional outcome in combination with microchannels as inner lining (Zeng et al., 2014) as well as combined with a chitosan nerve guide conduit for reconstruction of facial nerve injuries (Liu et al., 2013). Further developments in tissue engineering enable an additional loading of cores-shell poly(lactide-co-glycolide)-chitosan microparticles as drug delivery system for continuous release of NGF (Zhang et al., 2017).

Tubes and Inner Architecture

Different strategies of the treatment of peripheral nerve injuries based on chitosan have been explored in the literature, reaching from chitosan filament mesh tubes to chitosan-based nerve conduits. Exemplary, chitosan tubes were described by Suzuki et al. (2003) coupled with synthesized laminin under *in vivo* conditions to bridge a 15 mm sciatic nerve lesion. Despite the modification with the laminin peptides YIGSR and IKVAV, no superior results compared to the ANT have been shown (Suzuki et al., 2003). Further developments of tissue engineering led to chitosan tubes with a triangular inner surface and an additional coating with hydroxyapatite as well as laminin and laminin-1 peptides. Histological findings presented the beneficial effects of a triangular inner architecture for peripheral nerve regeneration. However, despite histological regeneration is like the ANT, delayed functional recovery was shown after 12 weeks of regeneration (Itoh et al., 2003). Addressing the essential need for inner guidance to bridge long distance peripheral nerve defects, porous chitosan tubular scaffold with chitosan fiber-based yarns with interconnected micropores were created (Wang et al., 2006). Wang et al. (2008a) also published alternative strategies for an inner lining by combining chitosan film tube as an outer layer with a nano/microfiber mesh as inner guidance. Different degrees of deacetylation were tested and compared to an ANT. Histological finding presents a better cell migration and attachment as well as neurite outgrowth for scaffolds with deacetylation rate of 93% compared to scaffolds with 78% (Wang et al., 2008a).

Furthermore, an additional mobilization with polarized β -tricalcium phosphate particles led to superior results in histological findings compared to non-polarized mesh tubes and similar results to the ANT (Wang et al., 2010). Silva et al. (2014) followed another approach presenting nanostructured hollow tubes with an additional crosslinking of genipin. Biological performance of this modified hollow tubes was assessed focussing on cell adhesion, viability, and proliferation (Silva et al., 2014). Recently, chitosan flat membranes crosslinked with dibasic sodium phosphate alone and combined with γ -glycidoxypolytrimethoxysilan showed increased water stability and stiffness under *in vitro* conditions. For a 1 cm median nerve gap, chitosan conduits associated with γ -glycidoxypolytrimethoxysilan promoted nerve fiber regeneration and functional recovery similar to the autograft (Fregnan et al., 2016).

Chitosan can also be combined with autologous materials by utilizing a chitosan tube with fresh skeletal muscle fibers as an

inner layer to bridge nerve defects in the rat's median nerve. Interestingly, Neuregulin-1 is upregulated for chitosan tubes with internal muscle fibers but not for hollow tubes and may be crucial to further improve axonal nerve regeneration over long nerve lesions (Ronchi et al., 2018).

Biochemical Properties and Surface Modifications

Cell affinity for the neural cell lineage plays a crucial role to support neural regeneration. Therefore, chitosan is loaded with laminin or poly-lysine and led mainly to superior neurite outgrowth compared to the non-blended alternative (Haipeng et al., 2000). Cheng et al. (2004) applied PC12 cell culture to test cell affinity in poly-L-lysine different blended chitosan nerve tubes. Interestingly, the hydrophobicity of the poly-L-lysine in combination with the increased surface charge might be the reason for the increased cell attachment, growth, and differentiation (Cheng et al., 2004). Furthermore, increased concentration of poly-D-lysine not influence cell survival but can inhibit neurite outgrowth (Crompton et al., 2007).

Compositions of chitosan and gelatin have also been tested referring to the cell affinity and the potential to neurite outgrowth. Despite a decreased cell viability, chitosan blended with gelatine was able to show superior neurite outgrowth and in the first days of cell culture compared to PLL containing materials (Martín-López et al., 2012).

Alternative surface modification to promote peripheral nerve regeneration, are the YIGSR (Tyr-Ile-Gly-Ser-Arg) and IKVAV (Ile-Lys-Val-Ala-Val) sequences, which are known to modify receptor specific neural cell adhesion as well as to support neurite outgrowth. Itoh et al. (2005) were able to bond the YIGSR (Tyr-Ile-Gly-Ser-Arg) and IKVAV (Ile-Lys-Val-Ala-Val) peptides to molecular aligned chitosan. The peptides A3G75 and A3G83 of the laminin alpha chain LG4 modules promote neurite outgrowth. Conjugated peptides of the LG4 and LG5 modules to chitosan membranes presented improved cell attachment and neurite outgrowth for PC12 cells (Kato et al., 2002). A2G94 peptide is expressed by the Laminin alpha2 chain and led to a promoted alpha6beta1-mediated cell attachment as well as neurite outgrowth after conjugation in a chitosan tube (Urushibata et al., 2010).

Furthermore, Laminin-modified chitosan membranes significantly enhance SCs attachment and affinity for the guided peripheral nerve regeneration. Percentage of laminin incorporation is significantly higher by using the oxygen plasma technique compared to conventional chemical methods (Huang et al., 2007). Laminin has also been used to bond an additional glycine spacer to nano/microfiber mesh surface of the chitosan tube. SC affinity has been further improved by these surface modification (Huang et al., 2007). The combination of negatively charged heparin and positively charged γ -aminopropyltriethoxysilane (APTE) on porous chitosan scaffolds led to superior SC proliferation, attachment, and biological activity after seeding was shown under *in vitro* conditions (Li et al., 2015).

EXPERIMENTAL CHITOSAN-BASED HYBRID STRATEGIES TO PROMOTE PERIPHERAL NERVE REGENERATION UNDER EXPERIMENTAL CONDITIONS

The recent literature describes a variety of different types of hybrid strategies which aim to combine the advantages of chitosan with specific characteristics of other materials (see Table 1). The following section presents such chitosan hybrid strategies and discusses their potential role in reconstructive nerve surgery.

Collagen

Advantages of an adjustable biodegradation time as well as the relief of non-toxic components during biodegradation, make collagen a precious and well-investigated material supporting peripheral nerve healing (Deumens et al., 2010). Considering the accepted biomimicking concept for the treatment of peripheral nerve lesions, Nawrotek et al. (2016c) developed an epineurium-mimicking chitosan conduit by a chemical composition of collagen, chitosan, and hyaluronic acid. Testing on mHippoE-18 mouse hippocampal cells, cell stimulation without cytotoxicity has been shown. As an alternative geometric design, one of the first chitosan-collagen films presented by Wei et al. (2003) showed promising results in a functional recovery for bridging peripheral nerve lesion of 5–10 mm. Progress in tissue engineering further expanded the biomimicking approach for peripheral nerve reconstruction; thus Xiao combined a hybrid nerve guide based on collagen-chitosan and added an Arg-Gly-Asp (RGD) sequence, which is a well-known pattern and mostly used for supporting cell-adhesion abilities in tissue engineering. This led to superior results in histological and functional recovery compared to nerve conduits lacking an additional RGD sequence (Xiao et al., 2013). Recently, a collagen/chitosan nerve scaffold was introduced by Peng et al. (2018) fabricated by an “unidirectional freezing process” followed by further freeze-drying (Ding et al., 2010). On the basis of a collagen and chitosan suspension, this new scaffold was applied for bridging a peripheral nerve defect of 30 mm of the beagle's sciatic nerve. Based on the results of the electrophysiological assessment, retrograde tracing as well as histological evaluation, this collagen-chitosan nerve scaffold presented results equivalent to the ANT. If further experimental research confirms these identical recovery results via artificial conduits, such strategies will next be investigated in future clinical trials (Peng et al., 2018).

Polyglycolic Acid (PGA)

Polyglycolic acid has been widely used in the field of bridging peripheral nerve defects. Focusing on the reconstruction of extended-distance peripheral nerve defects PGA conduits filled with laminin-soaked collagen scaffolds or PGA-collagen fibers were found to promote axonal regeneration over a nerve lesion of up to 80 mm (Toba et al., 2002). Thus, it is reasonable to combine the beneficial effects of PGA with the potential of chitosan to further optimize the regeneration

TABLE 1 | Recently published chitosan-based hybrid models for peripheral nerve regeneration.

Nerve tube	Filler/Internal architecture/Conduit modification	Cells or growth factors	Nerve	Animal	Defect size (in mm)	Controls	Recovery Time in weeks	Methods	Outcome	Author
Chitosan-collagen film	–	–	Sciatic nerve	Rat	5–10	ANT	12	Electrophysiological measurements, Histological analysis	Chitosan-collagen tubes presented similar recovery for 5 mm and inferior recovery for 10 mm compared to ANT	Wei et al., 2003
Chitosan-collagen scaffold	RGD-Peptide	–	Sciatic nerve	Rat	15	ANT	8	Electrophysiological measurements, Retrograde tracing, Histological analysis, Immunohistochemistry	Chitosan-collagen scaffolds with RGD-Peptide modification showed superior results to non-modified scaffold but less recovery to ANT	Xiao et al., 2013
Chitosan-collagen scaffold	–	–	Sciatic nerve	beagle dog	30	ANT	12	Electrophysiological measurements, Retrograde tracing, Histological analysis, Immunohistochemistry	Chitosan-collagen scaffold revealed functional nerve recovery equivalent to the ANT without additional exogenous delivery or cell transplantation	Peng et al., 2018
Chitosan conduit	PGA filaments	–	Sciatic nerve	beagle dog	30	ANT	24	Electrophysiological measurements, Retrograde tracing, Histological analysis, Immunohistochemistry	Similar distribution patterns for myelinated axons were able to show for chitosan/PGA conduits	Wang et al., 2005
Chitosan/PGA conduit	–	–	Sciatic nerve	rat	10	ANT	12–24	Electrophysiological measurements, Retrograde tracing, Histological analysis	Even after maintained treatment after 3–6 months, chitosan/PGA conduits peripheral nerve regeneration is possible, however, an immediate repair presented superior functional results	
PLGA/chitosan nanofiber mesh tubes	Nanofibers	SC	Sciatic nerve	rat	10	PLGA/ chitosan nanofiber mesh tubes without additional cell seeding	12	Electrophysiological measurements, Histological analysis, Immunohistochemistry	PLGA/chitosan nanofiber mesh tubes seeded with SC led to superior results for functional recovery compared to non-seeded tubes	Zhao et al., 2014
PLGA/chitosan conduit	–	CNTF	tibial nerve	dog	25	ANT	12	Electrophysiological measurements, Histological analysis, Immunohistochemistry	PLGA/chitosan-CNTF presented slightly inferior recovery compared to ANT in the electrophysiological measurements and histological analysis, but better results than non-blended PLGA/chitosan	Shen et al., 2010
Chitosan- nanofiber conduit	Nanofibers with polyethylene glycol solution (PEG)	–	Sciatic nerve	rat	10	ANT	12	Histological analysis, Immunohistochemistry, Functional testing, Muscle Mass Measurement	Chitosan nanofiber conduit/PEG revealed superior results compared to chitosan nanofiber alone, but inferior recovery compared to ANT	Mokarizadeh et al., 2016

supporting conduit features. Therefore, Wang et al. (2005) developed a dual-component artificial nerve graft with an outer microporous conduit of chitosan and an inner layer of filaments PGA. In a beagle dog animal model with sciatic nerve lesion of 30 mm and a recovery interval of 6 months, the chitosan/PGA group showed a similar distribution pattern of myelinated fiber diameter compared to the ANT (Wang et al., 2005).

Poly(lactic Acid (PLA) and Poly(Lactic-Co-glycolic Acid) (PLGA)

The combination of chitosan and polylactide (CH-PLA) fibers presented a higher tensile strength and a lower tendency for swelling compared to chitosan fibers alone. The combination of a chitosan-based outer layer with an inner lining by (CH-PLA) fibers led to a guided axonal regeneration and thereby to the possibility to bridged long-distance peripheral nerve defects.

Furthermore, the CH-PLA fibers have been tested as a continuous release system of attached growth factors such as NGF and thereby induced a continuous outgrowth of PC12 cells as receptors for epidermal growth factor (EGF) both known to promote peripheral nerve regeneration (Huff and Guroff, 1979). Thus, CH-PLA fibers can be manufactured for gradient delivering not only for NGF but also other relevant growth factors by loading them into the alginate layers. Wu et al. emphasized the vast potential of these CH-PLA fibers, especially for a guided axonal regeneration for long-gap nerve repair (Wu et al., 2017). In line with this, Shen and colleagues bridged a peripheral nerve lesion of 25 mm of the canine tibial nerve in a dog animal model. Histological results illustrated that the PLGA/chitosan conduits were capable of providing peripheral nerve regeneration after 12 weeks. Results similar to the ANT can be reached by combining the PLGA/chitosan conduit with an additional coating of the ciliary neurotrophic factor (Shen et al., 2010). Moreover, the average maximum nerve fiber diameter and motor function have been improved by introducing dorsal root ganglion-derived SC to poly-(lactic-co-glycolic acid)/chitosan nerve scaffold for 10 mm sciatic nerve lesion in the rat (Zhao et al., 2014). However, materials based on PLA and PLGA suffer under a pH-decrease of the microenvironment during degradation and leading to an impaired of axonal regeneration (Deumens et al., 2010).

Polyethylene Glycol

Another promising hybrid approach is to combine chitosan-based nanofiber conduits with an additional filling of polyethylene glycol solution. In a 10 mm nerve defect of the rat's sciatic nerve, the superior functional outcome has been shown for animals treated with a substitute of the polyethylene solution. In contrast, functional recovery compared to the ANT showed clear inferior results for the experimental groups (Mokarizadeh et al., 2016). Furthermore, challenges of the chitosan in tissue engineering referring to the disadvantage in the processing of three-dimensional tubular forms without heating processing methods like extrusion or casting (Ao et al., 2006), were addressed by Nawrotek and colleagues by

developing a tubular chitosan-carbon nanotube through the electrodeposition method. This conduit provided an excellent cell-adhesion, cell-proliferation, and cell-viability as well as structural stability for 28 days under *in vivo* conditions (Nawrotek et al., 2016c).

To sum up, hybrid concepts with chitosan have been well explored in literature, mostly for bridging peripheral nerve defects and led to promising results in peripheral nerve regeneration. Interestingly, the hybrid approach mainly revealed superior results of axonal recovery compared to concepts with chitosan alone. However, an exact differentiation of the effects of chitosan and the added material in a hybrid approach is not possible. Furthermore, hybrids concepts present the possibility of a tailored biodegradation as well as the embedding of growth factors or additional cell seeding related to the needs of peripheral nerve regeneration.

ADDITIONAL CELL SEEDING COMBINED WITH CHITOSAN-BASED TREATMENT STRATEGIES

Nerve regeneration through chitosan-based nerve tubes can be promoted by conduit enrichment via supportive molecules like laminin or growth factors as well as additional cell seeding (see Table 2).

Additional Cell-Seeding With Schwann Cells (SC)

The proliferative effect of chitosan on SC and inhibiting effect on the fibroblast growth has already been shown by Kuang et al. (1998). Thereby, chitosan has the potential to support the axonal regeneration by increasing the number of SC and may prevent scar tissue formation after peripheral nerve lesion (Kuang et al., 1998). Further investigations regarding biocompatibility among SC chitosan scaffolds or fibers were conducted by Yuan et al. (2004), leading to the conclusion that chitosan has an excellent neuroglial cell affinity with the ability to be an excellent cell carrier system after implantation. Chitosan membranes or fibers showed almost no cell toxicity for SC considering the results in the MTT Assay (Yuan et al., 2004).

As mentioned above, the DOA of the chitosan is crucial for the solvent characteristics and molar mass. Carvalho has shown that acetylation of 5% results in higher cell proliferation and phenotypic expression of SC-like cells compared to chitosan membranes with acetylation rates of 1% or 2% (Carvalho et al., 2017). The combination of SC with a chitosan nerve conduit substituted with self-fibroin filamentous fillers showed superior regeneration results compared to non-seeded chitosan conduits regarding the histological and functional outcome (Zhu et al., 2017).

Additional Cell-Seeding With Bone Marrow Stromal Cells (BMSC)

Bone marrow stromal cells seeded nerve conduits, in general, have shown to be a successful concept for bridging peripheral nerve defects and promoting axonal regeneration (Mimura et al.,

TABLE 2 | Recently published incorporation advances of supportive cells or growth factors in the peripheral nerve system.

Nerve tube	Filler/Internal architecture/Conduit modification	Cells or growth factor	Nerve	Animal	Defect size (in mm)	Controls	Total recovery time in weeks	Methods	Outcome	Author
Chitosan conduit	Skin fibroin filamentous fillers	Skin-derived SC	Sciatic nerve	Rat	10	Acellular nerve graft	12	Electrophysiological measurements, Retrograde tracing, Histological analysis.	Histological and functional analysis were showed superior results compared to acellular nerve	Zhu et al., 2017
Laminin-modified multi-walled nerve tube	Inner layer laminin-modified chitosan; outer layer silicon	BMSC	Sciatic nerve	Rat	10	Empty silicon tube, physiological sciatic nerve	16	Immunohistochemistry, Muscle mass measurement, Histological analysis, Retrograde Tracing, Immunohistochemistry, Functional testing	Additional seeding with BMSC on the multi-walled nerve tube showed superior results in terms of regrowth, muscle mass of gastrocnemius, function recovery and retrograde tracing compared to empty silicon tubes	Hsu et al., 2013
Poly-3-hydroxybutyrate nerve conduit	Coating with chitosan	BMSC	Sciatic nerve	Rat	10	ANT	8	Electrophysiological measurements, Retrograde tracing, Histological analysis	Histological analysis revealed a beneficial effect of PHB/chitosan with supplementary seeding of BMSC compared to non-seeded nerve conduits. However, results still remain inferior compared to the ANT	Ozer et al., 2018
Chitosan film	Chitosan films placed around the nerve coaptation	BMSC	Sciatic nerve	Rat	–	Sciatic nerve transection and end-to-end suture	8	Electrophysiological measurements, Histological analysis, Immunohistochemistry, Functional testing	BMSC seeded chitosan films presented improved functional electrophysiological and histomorphometric recovery compared to non-seeded chitosan films. Results were also superior to the control group	
Chitosan/ poly(lactic glycolic acid) (PLGA)-based neural scaffold	Chitosan conduit combined with about 1000 longitudinal aligned PLGA fibers	BMSC	Sciatic nerve	Dog	50	ANT	24	Electrophysiological measurements, Retrograde tracing, Histological analysis, Muscle mass measurement	(PLGA)-based neural scaffolds seeded with BMSC indicate nerve recovery close to the ANT and better results to non-seeded nerve scaffolds, referring to the results of electrophysiological measurements and histological analysis	Ding et al., 2010
Chitosan poly(lactic-co-glycolic acid) (PLGA)-based neural scaffold	Chitosan conduit combined with about 1000 longitudinal aligned PLGA fibers	BMSC	Sciatic nerve	Dog	60	ANT	52	Retrograde Tracing, Histological analysis, Immunohistochemistry, Functional testing	The outcome of (PLGA)- based neural scaffolds seeded with BMSC is similar to the ANT and showed better recovery compared to non-seeded scaffold	Xue et al., 2012
Chitosan/silk fibroin nerve scaffold		Bone marrow nuclear cells	Sciatic nerve	Rat	10	ANT	12	Electrophysiological measurements, Histological analysis, Immunohistochemistry, Functional testing	Similar peripheral nerve regeneration of seeded chitosan/fibroin nerve scaffolds compared to the ANT and better recovery than non-seeded scaffolds	Yao et al., 2016

(Continued)

TABLE 2 | Continued

Nerve tube	Filler/Internal architecture/Conduit modification	Cells or growth factor	Nerve	Animal	Defect size (in mm)	Controls	Total recovery time in weeks	Methods	Outcome	Author
Autologous vein conduit combined with chitosan- β -glycerophosphate e-nerve growth factor (C/GP-NGF) hydrogel	Autologous vein graft filled with chitosan modified hydrogel	NGF	Buccal branch nerve	Rat	5	ANT	12	Electrophysiological measurements. Histological analysis. Functional testing	Autologous veins filled with C/GP-NGF hydrogel led to similar degree of functional and electrophysiological recovery like the ANT as well as to superior results to vein conduits blended with NGF solution	Chao et al., 2016
Chitosan conduit	NGF immobilization by Genipin cross linking	NGF	Sciatic nerve	Rat	10	ANT	24	Electrophysiological measurements. Histological analysis. Functional testing. Muscle Mass Measurements.	Considering the wet-weight ratio of the gastrocnemius muscle, the ANT presented superior results to the modified nerve conduit. Electrophysiological measurements and histological analysis revealed similar	Wang et al., 2012
GDNF- laminin blended chitosan nerve tube	Chitosan tubes blended with laminin and glial cell-line derived nerve growth	GDNF	Sciatic nerve	Rat	8	ANT	12	Functional testing. Muscle Mass Measurements	Especially sensory recovery is supported by the supplementation of GDNF to the chitosan nerve tube; Motoric recovery revealed similar in comparison to non-blended nerve tubes	Patel et al., 2007

2004; Keilhoff et al., 2006; Boecker et al., 2015). Consequently, strategies to enhance peripheral nerve regeneration by BMSC seeded chitosan-based nerve guides has also been described. Hsu et al. (2013) published a two-component nerve tube with an inner layer based on laminin-modified chitosan and a silicon-based outer layer with a supplementary seeding of BMSC. As the control group, non-seeded laminin modified-chitosan scaffolds and empty silicone tubes have been utilized. After a regeneration period of 16 weeks and following histological investigations, hyperplasia tissue enriched with eosinophils and macrophages has been found. In this context, the importance of the inflammation after PNI, induced by these cells, was emphasized by the author (Hsu et al., 2013). In line with this, a chitosan-coated poly-3-hydroxybutyrate nerve conduit has been seeded with BMSC to bridge a 10 mm sciatic nerve lesion and led to superior results in functional recovery compared to non-seeded control group. However, the ANT showed still the best results of functional recovery (Ozer et al., 2018). Similar results have been assessed through Moattari et al. (2018) by exhibiting significant superior effects in which group? in the electromyography, nerve fiber density and myelinated axon diameter (Moattari et al., 2018). For bridging long distance peripheral nerve injuries of 50 mm or even 60 mm, in a dog sciatic nerve, chitosan/poly(lactic-co-glycolic acid) (PLGA)-based neural scaffolds have been combined with BMSC and evaluated by electrophysiology, retrograde tracing, and histology after recovery of 6 or 12 months. The results led to a nearly similar degree of functional regeneration compared to the ANT (Ding et al., 2010; Xue et al., 2012). Interestingly, Yao et al. (2016) was able to show, that Bone Marrow Mononuclear Cells joined with a chitosan/silk fibroin scaffold survived at least 2 weeks under *in vivo* conditions associated with an improved axonal guidance. Nearly similar results for functional recovery was accomplished compared to the ANT in the CatWalk gait analysis after 12 weeks of recovery (Yao et al., 2016). However, SC harvested during nerve surgery need long cultivation times to reach sufficient cell numbers for reimplantation and are associated with a loss of function related to donor's nerve.

Alternatively, BMSC can be harvested through bone marrow biopsy and revealed cell plasticity that can be adapted to the conditions of peripheral nerve regeneration (Keilhoff et al., 2006). However, the operation procedure is associated with surgical risks, like infection, bleeding, etc. Furthermore, the stability of differentiation has to be taken into account, BMSC have the ability to differentiate to SC-like cells under *in vitro* conditions but also have the capacity to re-differentiate to stem cell under the absence of the required factors, which is associated with a higher malignancy degeneration rate (Gore et al., 2011).

Most current concepts of additional cell-seeding in peripheral nerve surgery remain as a proof principle because of the potential donor site morbidities, long lasting cultivation times before implantation and instability of cell differentiation (Boecker et al., 2015). Thereby, translational concepts with additional cell seeding based on chitosan are strongly restricted.

CHITOSAN-BASED DELIVERY SYSTEMS FOR GROWTH FACTORS

In tissue engineered delivery systems the release kinetics of growth factors play a crucial role for axonal regeneration. Recently, a variety of different concepts have been published using chitosan as a delivery system for growth factors while peripheral nerve regeneration (see **Table 2**).

Nerve Growth Factor (NGF)

Pfister et al. (2008) were able to show a continuous delivery of bioactive NGF in low nanogram doses for 15 days. A nerve conduits of polyelectrolyte alginate/chitosan was coated with layers of poly(lactide-co-glycolide) (PLGA) to control the delivery of embedded NGF (Pfister et al., 2008). Moreover, the relevance of continuous delivery of NGF by using chitosan as carrying material and its synergetic effects have been marked by Chao et al. (2016). The combination of vein conduits filled with a chitosan- β -glycerophosphate-NGF hydrogel presented superior histological, functional and electrophysiological recovery compared to non-filled vein conduits (Chao et al., 2016). This underlines the capacity of chitosan to be an excellent delivering system for growth factors related to the peripheral nerve regeneration.

Furthermore, chitosan nerve conduits with a supplementary immobilization of NGF via genipin cross-linking, were compared to the ANT for a 10 mm-long sciatic nerve gap with 24 weeks recovery time. The crosslinked nerve conduit was superior compared to a non-crosslinked control but not to the ANT and led to inferior results in the electrophysiology and axon density compared to the gold standard. Thus, the real potential of additional NGF-application is hard to evaluate in this study design (Wang et al., 2012). The indication of chitosan tubes is not only limited to the treatment of PNI but can also be extended for nerve compression syndromes. Zhang et al. (2017) developed a chitosan-sericin scaffold for a continuous delivering of NGF. After application, a better functional recovery, as well as superior histological results has been demonstrated, probably caused by the beneficial effects of degradation products and the corresponding inducement of mRNA levels of GDNF, EGR2, NCAM as well as down-regulation levels of inflammatory genes (Zhang et al., 2017).

Glial Cell Line-Derived Growth Factor (GDNF)

The beneficial effects of GDNF on the peripheral nerve regeneration, like the support of motoneuron regeneration, acceleration of axonal regeneration and the prevention of muscle atrophy are known in the literature (Chen et al., 2001; Jubran and Widenfalk, 2003). Further developments in tissue engineering led to chitosan conduits enriched with laminin and GDNF. Non-prepared laminin-loaded chitosan tubes were compared to laminin-loaded chitosan tubes with supplementation of GDNF and used to bridge a nerve lesion of 10 mm. An additional GDNF blending explicated a significant superior sensory recovery compared to unblended chitosan tubes (Patel et al., 2007).

Fibroblast Growth Factor-2 (FGF-2)

Fibroblast growth factor-2 is one of the 22-member of the fibroblast growth factor family. In association with heparin or heparin sulfate proteoglycan, a variety of different effects has been reported including potent effects on angiogenesis and cell differentiation in the central nervous system. Chitosan-nanoparticles have been utilized as drug delivery systems for FGF-2. The chitosan scaffolds with incorporated FGF-2 microspheres reviewed superior results in cell survival and growth of neural stem cells compared to non-incorporated chitosan scaffolds under *in vitro* conditions (Woodbury and Ikezu, 2014). In line with this, chitosan scaffolds cross-linked with heparin and FGF-2 were assessed for cytocompatibility, attachment, and survival of neural stem cells (Skop et al., 2013). Alternatively, FGF-2 concentration can be increased by overpressing SC seeded in a chitosan hydrogel as an inner filling for a chitosan tube. Neural and Vascular (NVR) gel as inner filling has the obstacle to impair axonal outgrowth in a rat's sciatic nerve model. However, this challenge could be overcome by consistent delivery of FGF-2 of overexpressing SC and led to a significant extent in neurite outgrowth compared to free FGF-2 delivery or non-modified Neonatal Rat SC (Meyer et al., 2016b).

Platelet-Derived Growth Factor (PDGF)

Platelet-derived growth factor (PDGF) has been shown to support the migration of bone marrow stromal cells. Chitosan scaffolds have been loaded with chitosan-encapsulated PDGF microspheres and investigated for the biocompatibility of neural progenitor cells. Directional migration and growth of these cells were shown for scaffolds with additional PDGF incorporation. Chitosan microspheres underline their potential as a drug delivery system by releasing 52% of the PDGF in 4 weeks under *in vitro* conditions without a burst release (Chen et al., 2018). The beneficial effect of PDGF on neural stem progenitor cells by promoting the cell survival and cell differentiation to oligodendrocytes is described in the literature (Delayed transplantation of adult neural precursor cells promotes remyelination and functional neurological recovery after spinal cord injury; Endogenous and exogenous CNS derived stem/progenitor cell approaches for neurotrauma). In combination with chitosan channels and a continuous release of PDGF osmotic pump, neural stem progenitor cells have been significantly enhanced in cell survival under *in vivo* conditions (Guo et al., 2012).

TRANSLATIONAL CONCEPTS OF CHITOSAN-BASED NERVE TUBES

Yet, the application of chitosan-based nerve conduits beneath experimental research as translational concepts has not been explored sophisticatedly. Only a few studies have already implemented chitosan tubes in clinical practice and evaluated the functional outcome after application.

In first clinical treatments, the combination of a chitosan-PGA nerve conduit was utilized to bridge a long-distance defect of 35 mm of the median nerve distal to the biceps aponeurosis.

During a 3-year follow-up period sensory and motor function recovered satisfactorily to M4 and S3+ levels in testing. However, this case report need to be amended by further clinical studies to prove the clinical value of this nerve conduit (Fan et al., 2008). Similar results have been found by Gu et al. (2011) after bridging a 30 mm nerve defect of the median nerve with the same nerve conduit 2 years later. In June 2014, the first unaccompanied chitosan-based nerve conduit, named Reaxon® has been launched by Medovent GmbH (Mainz, Germany). Reaxon® was developed in accordance with the international standard DIN EN ISO 13485 and can be manufactured in different sizes depending on the diameter of the nerve. Nerve defects with a size up to 26 mm can be bridged in the clinical setting (Neubrech et al., 2016b). Furthermore, Reaxon® cannot only be used as tubulization-technique for bridging the peripheral nerve defects but also as a protector for the nerve coaptation after a tension-free epineural suture (Neubrech et al., 2016a).

Thus, besides several studies investigated beneficial effects of chitosan and its derivatives in preclinical *in vitro* and *in vivo* models, the functional outcome after traumatic sensory nerve lesions can significantly be enhanced by a supplementary use of Reaxon® as protection for the epineural suture in daily clinical routine (see **Figure 2**). In a double-blinded, randomized, prospective clinical trial, after a 6-months follow-up, a 6.3 mm two-point-discrimination has been found for patients treated with the additional chitosan-based conduit compared to the control group with two-point

discrimination of 8 mm. This significant enhancement of the tactile gnosis is a relevant parameter for functional recovery of the hand (Neubrech et al., 2018). The capability of Reaxon® has been further investigated by Ronchi et al. by combining the chitosan tube with skeletal muscle fibers of the pectoralis muscle to bridge a 10 mm nerve lesion of the median nerve. Biomolecular analysis has shown an increased production and release of Neuregulin, as a key factor for SC survival and vitality. However, functional recovery and morphometric analyses presented no significant differences compared to hollow chitosan tubes. The author considered, beneficial effects of an inner lining by an additional muscle application is more indicated for nerve lesion of an extended distance than for a nerve lesion size of 10 mm in humans (Ronchi et al., 2018).

In the future, the possible clinical application of Chitosan in the field of peripheral nerve surgery is vast and can be used for bridging peripheral nerve lesion, protecting the epineural coaptation or even for neuroma prevention.

Referring to the findings of Marcol et al. (2011), new developments in material science led to chitosan-based nerve caps, which may have the capacity to limit neuroma formation by combining a mechanical obstacle with an additional material-related biochemical barrier for unguided axonal sprouting. Based on the material properties, recent material science concepts, such as chitosan gel, film or microcrystals, for an easier application of the material is also possible.

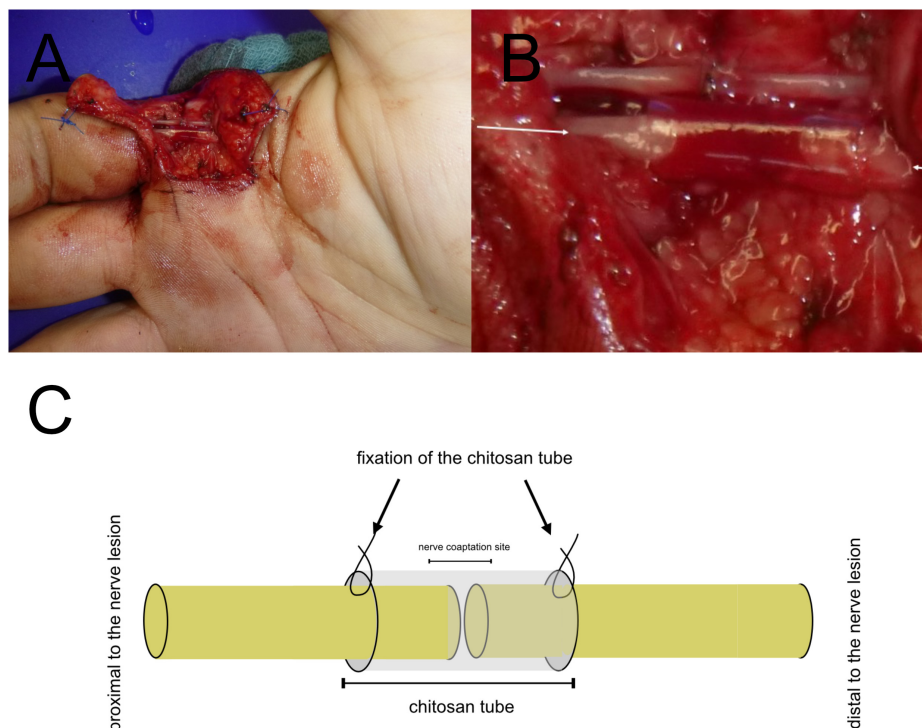


FIGURE 2 | Translational Concepts in daily clinical practice. Chitosan nerve tube protects the epineural nerve coaptation (A). Magnification of the chitosan-based nerve tube for covering the epineural suture of the third proper palmar digital (B). Protection of the epineural nerve coaptation by a chitosan-based nerve tube in a model (C). (A,B) has been taken during clinical routine care.

In conclusion, the capability of chitosan as a sophisticated partner in the peripheral nerve regeneration has been explored in several *in vitro* and *in vivo* experimental approaches. Not only the cell biocompatibility of chitosan on neural cells was shown but also beneficial effects on the differentiation and proliferation on SC as well as BMSC. Moreover, COS, as the metabolite of chitosan during biodegradation, is a neuroprotective agent during peripheral nerve regeneration and a direct stimulator for SC. Under *in vivo* conditions, chitosan was able to bridge peripheral nerve defects up to 60 mm in combination with a chitosan/poly(lactic-co-glycolic acid) (PLGA)-based neural scaffold combined with BMSC. First human trials in 2011 presented sensory recovery after chitosan tube implantation for a median nerve lesion. Recently, the first chitosan-based nerve guide was launched for clinical application and led to superior sensory recovery by using it as a biochemical protector for the site of the epineural nerve coaptation. However, given the only few human clinical trials investigating chitosan conduits, the effect on the outcome following all kinds of nerve surgery (decompression, defect reconstruction, and neuroma prevention) and thereby its potential value have to be evaluated. However, considering the first results of clinical trials and previous *in vitro* and *in vivo* experiments, chitosan has an immense potential to be a valuable partner for the peripheral nerve surgeon in the future.

CONCLUSION

The relevance and application of chitosan in the field of peripheral nerve surgery are tremendous and can principally be separated between the support axonal regeneration by giving mechanical guidance and stability (as chitosan tube, inner filling or epineural suture protector) or being used as drug delivery system.

Chitosan has good biocompatibility of the peripheral nervous system, and mechanical properties make custom-made biodegradation possible. To overcome mechanical instability in a variety of different approaches in tissue engineering reaching from chitosan microspheres to chitosan hydrogel have been explored. Especially hybrid-models based on chitosan can be tailored to the demands of nerve

recovery and showed promising results on all levels of peripheral nerve regeneration. In translational concepts, chitosan has been generally proven to support functional recovery, however, the clinical evidence is limited to a small number of studies yet. Future investigations should focus on the clinical outcome after application of chitosan as a drug delivery system or mechanical guidance/protection after peripheral nerve injury.

DISCLOSURES

Referring to Reaxon mentioned in this review, the study “Enhancing the Outcome of Traumatic Sensory Nerve Lesions of the Hand by Additional Use of a Chitosan Nerve Tube in Primary Nerve Repair: A Randomized Controlled Bicentric Trial” was sponsored by the Medovent. The study was conceived and designed before seeking financial support. Medovent was excluded from any aspect, conduct, analysis, write-up or publication of the trial. None of the authors has any personal financial related to Medovent. None of the authors has accepted compensations, fees, funding, or salary from Medovent.

AUTHOR CONTRIBUTIONS

AB contributed to the concept and design of the review, performed literature research, and involved in drafting and critically revising the manuscript. SD and UK involved in drafting and critically revising the manuscript. LH contributed to the concept and design of the review and involved in drafting and critically revising the manuscript. All authors read and approved the final manuscript.

FUNDING

We acknowledge financial support by Deutsche Forschungsgemeinschaft within the funding programme Open Access Publishing, by the Baden-Württemberg Ministry of Science, Research and the Arts and by Ruprecht-Karls-Universität Heidelberg.

REFERENCES

- Ao, Q., Wang, A., Cao, W., Zhang, L., Kong, L., He, Q., et al. (2006). Manufacture of multimicrotubule chitosan nerve conduits with novel molds and characterization in vitro. *J. Biomed. Mater. Res. A* 77, 11–18. doi: 10.1002/jbm.a.30593
- Boecker, A. H., van Neerven, S. G. A., Scheffel, J., Tank, J., Altinova, H., Seidensticker, K., et al. (2015). Pre-differentiation of mesenchymal stromal cells in combination with a microstructured nerve guide supports peripheral nerve regeneration in the rat sciatic nerve model. *Eur. J. Neurosci.* 43, 404–416. doi: 10.1111/ejn.13052
- Bozkurt, A., Lassner, F., O'Dey, D., Deumens, R., Böcker, A., Schwendt, T., et al. (2012). The role of microstructured and interconnected pore channels in a collagen-based nerve guide on axonal regeneration in peripheral nerves. *Biomaterials* 33, 1363–1375. doi: 10.1016/j.biomaterials.2011.10.069
- Carvalho, C. R., López-Cebral, R., Silva-Correia, J., Silva, J. M., Mano, J. F., Silva, T. H., et al. (2017). Investigation of cell adhesion in chitosan membranes for peripheral nerve regeneration. *Mater. Sci. Eng. C* 71, 1122–1134. doi: 10.1016/j.msec.2016.11.100
- Chao, X., Fan, Z., Han, Y., Wang, Y., Li, J., Chai, R., et al. (2015). Effects of local application of methylprednisolone delivered by the C/GP-hydrogel on the recovery of facial nerves. *Acta Otolaryngol.* 135, 1178–1184.
- Chao, X., Xu, L., Li, J., Han, Y., Li, X., Mao, Y., et al. (2016). Facilitation of facial nerve regeneration using chitosan- β -glycerophosphate-nerve growth factor hydrogel. *Acta Otolaryngol.* 136, 585–591. doi: 10.3109/00016489.2015.1136432
- Chatelet, C., Damour, O., and Domard, A. (2001). Influence of the degree of acetylation on some biological properties of chitosan films. *Biomaterials* 22, 261–268. doi: 10.1016/S0142-9612(00)00183-6
- Chen, X., Xu, M. L., Wang, C. N., Zhang, L. Z., Zhao, Y. H., Zhu, C. L., et al. (2018). A partition-type tubular scaffold loaded with PDGF-releasing microspheres

- for spinal cord repair facilitates the directional migration and growth of cells. *Neural Regen. Res.* 13, 1231–1240. doi: 10.4103/1673-5374.235061
- Chen, Z.-Y., Chai, Y.-F., Cao, L., Lu, C.-L., and He, C. (2001). Glial cell line-derived neurotrophic factor enhances axonal regeneration following sciatic nerve transection in adult rats. *Brain Res.* 902, 272–276. doi: 10.1016/S0006-8993(01)02395-2
- Cheng, M., Gong, K., Li, J., Gong, Y., Zhao, N., Zhang, X., et al. (2004). Surface modification and characterization of chitosan film blended with poly-L-lysine. *J. Biomater. Appl.* 19, 59–75. doi: 10.1177/0885328204043450
- Crompton, K. E., Goud, J. D., Bellamkonda, R. V., Gengenbach, T. R., Finkelstein, D. I., Horne, M. K., et al. (2007). Polylysine-functionalised thermoresponsive chitosan hydrogel for neural tissue engineering. *Biomaterials* 28, 441–449. doi: 10.1016/j.biomaterials.2006.08.044
- Davis, L., and Perret, G. (1946). Homogenous grafts in the repair of peripheral nerve lesions in man. *Proc. Inst. Med. Chic.* 16:167.
- Desai, K. G. H., and Park, H. J. (2005). Preparation of cross-linked chitosan microspheres by spray drying: effect of cross-linking agent on the properties of spray dried microspheres. *J. Microencapsul.* 22, 377–395. doi: 10.1080/02652040500100139
- Deumens, R., Bozkurt, A., Meek, M. F., Marcus, M. A., Joosten, E. A., Weis, J., et al. (2010). Repairing injured peripheral nerves: bridging the gap. *Prog. Neurobiol.* 92, 245–276. doi: 10.1016/j.pneurobio.2010.10.002
- Ding, F., Wu, J., Yang, Y., Hu, W., Zhu, Q., Tang, X., et al. (2010). Use of tissue-engineered nerve grafts consisting of a chitosan/poly(lactic-co-glycolic acid)-based scaffold included with bone marrow mesenchymal cells for bridging 50-mm dog sciatic nerve gaps. *Tissue Eng. Part A* 16, 3779–3790. doi: 10.1089/ten.tea.2010.0299
- Du, J., Liu, J., Yao, S., Mao, H., Peng, J., Sun, X., et al. (2017). Prompt peripheral nerve regeneration induced by a hierarchically aligned fibrin nanofiber hydrogel. *Acta Biomater.* 55, 296–309. doi: 10.1016/j.actbio.2017.04.010
- Fan, W., Gu, J., Hu, W., Deng, A., Ma, Y., Liu, J., et al. (2008). Repairing a 35-mm-long median nerve defect with a chitosan/PGA artificial nerve graft in the human: a case study. *Microsurgery* 28, 238–242. doi: 10.1002/micr.20488
- Fregnan, F., Ciglieri, E., Tos, P., Crosio, A., Ciardelli, G., Ruini, F., et al. (2016). Chitosan crosslinked flat scaffolds for peripheral nerve regeneration. *Biomed. Mater.* 11:045010. doi: 10.1088/1748-6041/11/4/045010
- Freier, T., Koh, H. S., Kazazian, K., and Shoichet, M. S. (2005a). Controlling cell adhesion and degradation of chitosan films by N-acetylation. *Biomaterials* 26, 5872–5878. doi: 10.1016/j.biomaterials.2005.02.033
- Freier, T., Montenegro, R., Shan Koh, H., and Shoichet, M. S. (2005b). Chitin-based tubes for tissue engineering in the nervous system. *Biomaterials* 26, 4624–4632. doi: 10.1016/j.biomaterials.2004.11.040
- Gong, Y., Gong, L., Gu, X., and Ding, F. (2009). Chito oligosaccharides promote peripheral nerve regeneration in a rabbit common peroneal nerve crush injury model. *Microsurgery* 29, 650–656. doi: 10.1002/micr.20686
- Gore, A., Li, Z., Fung, H.-L. L., Young, J. E., Agarwal, S., Antosiewicz-Bourget, J., et al. (2011). Somatic coding mutations in human induced pluripotent stem cells. *Nature* 470, 63–67. doi: 10.1038/nature09805
- Gu, X., Ding, F., Yang, Y., and Liu, J. (2011). Construction of tissue engineered nerve grafts and their application in peripheral nerve regeneration. *Prog. Neurobiol.* 93, 204–230. doi: 10.1016/j.pneurobio.2010.11.002
- Guo, Q., Liu, C., Hai, B., Ma, T., Zhang, W., Tan, J., et al. (2018). Chitosan conduits filled with simvastatin/Pluronic F-127 hydrogel promote peripheral nerve regeneration in rats. *J. Biomed. Mater. Res. Part B Appl. Biomater.* 106, 787–799. doi: 10.1002/jbm.b.33890
- Guo, X., Zahir, T., Mothe, A., Shoichet, M. S., Morshead, C. M., Katayama, Y., et al. (2012). The effect of growth factors and soluble Nogo-66 receptor protein on transplanted neural stem/progenitor survival and axonal regeneration after complete transection of rat spinal cord. *Cell Transplant.* 21, 1177–1197. doi: 10.3727/096368911X612503
- Haastert-Talini, K., Geuna, S., Dahlin, L. B., Meyer, C., Stenberg, L., Freier, T., et al. (2013). Chitosan tubes of varying degrees of acetylation for bridging peripheral nerve defects. *Biomaterials* 34, 9886–9904. doi: 10.1016/j.biomaterials.2013.08.074
- Haipeng, G., Yinghui, Z., Jianchun, L., Yandao, G., Nanming, Z., and Xiufang, Z. (2000). Studies on nerve cell affinity of chitosan-derived materials. *J. Biomed. Mater. Res.* 52, 285–295.
- Hao, C., Wang, W., Wang, S., Zhang, L., and Guo, Y. (2017). An overview of the protective effects of chitosan and acetylated chitosan oligosaccharides against neuronal disorders. *Mar. Drugs* 15:E89. doi: 10.3390/md15040089
- He, B., Tao, H.-Y., and Liu, S.-Q. (2014). Neuroprotective effects of carboxymethylated chitosan on hydrogen peroxide induced apoptosis in Schwann cells. *Eur. J. Pharmacol.* 740, 127–134. doi: 10.1016/j.ejphar.2014.07.008
- Hsu, S. H., Kuo, W. C., Chen, Y. T., Yen, C. T., Chen, Y. F., Chen, K. S., et al. (2013). New nerve regeneration strategy combining laminin-coated chitosan conduits and stem cell therapy. *Acta Biomater.* 9, 6606–6615. doi: 10.1016/j.actbio.2013.01.025
- Huang, H.-C., Hong, L., Chang, P., Zhang, J., Lu, S.-Y., Zheng, B.-W., et al. (2015). Chito oligosaccharides attenuate Cu²⁺-induced cellular oxidative damage and cell apoptosis involving Nrf2 activation. *Neurotox. Res.* 27, 411–420. doi: 10.1007/s12640-014-9512-x
- Huang, Y.-C., Huang, C.-C., Huang, Y.-Y., and Chen, K.-S. (2007). Surface modification and characterization of chitosan or PLGA membrane with laminin by chemical and oxygen plasma treatment for neural regeneration. *J. Biomed. Mater. Res. A* 82, 842–851. doi: 10.1002/jbm.a.31036
- Huff, K. R., and Guroff, G. (1979). Nerve growth factor-induced reduction in epidermal growth factor responsiveness and epidermal growth factor receptors in PC12 cells: an aspect of cell differentiation. *Biochem. Biophys. Res. Commun.* 89, 175–180. doi: 10.1016/0006-291X(79)90960-4
- Inada, Y., Hosoi, H., Yamashita, A., Morimoto, S., Tatsumi, H., Notazawa, S., et al. (2007). Regeneration of peripheral motor nerve gaps with a polyglycolic acid-collagen tube: technical case report. *Neurosurgery* 61, E1105–E1107. doi: 10.1227/01.neu.0000303210.45983.97
- Itoh, S., Matsuda, A., Kobayashi, H., Ichinose, S., Shinomiya, K., and Tanaka, J. (2005). Effects of a laminin peptide (YIGSR) immobilized on crab-tendon chitosan tubes on nerve regeneration. *J. Biomed. Mater. Res. B Appl. Biomater.* 73, 375–382. doi: 10.1002/jbm.b.30224
- Itoh, S., Suzuki, M., Yamaguchi, I., Takakuda, K., Kobayashi, H., Shinomiya, K., et al. (2003). Development of a nerve scaffold using a tendon chitosan tube. *Artif. Organs* 27, 1079–1088. doi: 10.1111/j.1525-1594.2003.07208.x
- Jubran, M., and Widenfalk, J. (2003). Repair of peripheral nerve transections with fibrin sealant containing neurotrophic factors. *Exp. Neurol.* 181, 204–212. doi: 10.1016/S0014-4886(03)00041-4
- Kato, K., Utani, A., Suzuki, N., Mochizuki, M., Yamada, M., Nishi, N., et al. (2002). Identification of neurite outgrowth promoting sites on the laminin alpha 3 chain G domain. *Biochemistry* 41, 10747–10753. doi: 10.1021/bi020180k
- Keilhoff, G., Goihl, A., Langnase, K., Fansa, H., Wolf, G., Langnase, K., et al. (2006). Transdifferentiation of mesenchymal stem cells into schwann cell-like myelinating cells. *Eur. J. Cell Biol.* 85, 11–24. doi: 10.1016/j.ejcb.2005.09.021
- Kim, S., Nimni, M. E., Yang, Z., and Han, B. (2005). Chitosan/gelatin-based films crosslinked by proanthocyanidin. *J. Biomed. Mater. Res. B Appl. Biomater.* 75, 442–450. doi: 10.1002/jbm.b.30324
- Kuang, Y., Hou, C., and Gou, S. (1998). [Experimental study of the effect on growth of Schwann cell from chitin and chitosan in vitro]. *Zhongguo Xiu Fu Chong Jian Wai Ke Za Zhi* 12, 90–93.
- Li, G., Zhang, L., and Yang, Y. (2015). Tailoring of chitosan scaffolds with heparin and gamma-aminopropyltriethoxysilane for promoting peripheral nerve regeneration. *Colloids Surf. B Biointerfaces* 134, 413–422. doi: 10.1016/j.colsurfb.2015.07.012
- Liu, H., Wen, W., Hu, M., Bi, W., Chen, L., Liu, S., et al. (2013). Chitosan conduits combined with nerve growth factor microspheres repair facial nerve defects. *Neural Regen. Res.* 8, 3139–3147. doi: 10.3969/j.issn.1673-5374.2013.33.008
- Lundborg, G. (2004). Alternatives to autologous nerve grafts. *Handchir. Mikrochir. Plast. Chir.* 36, 1–7. doi: 10.1055/s-2004-820870
- Madhally, S. V., and Matthew, H. W. (1999). Porous chitosan scaffolds for tissue engineering. *Biomaterials* 20, 1133–1142. doi: 10.1016/S0142-9612(99)00011-3
- Marcol, W., Larysz-Brysz, M., Kucharska, M., Niekaszewicz, A., Slusarczyk, W., Kotulska, K., et al. (2011). Reduction of post-traumatic neuroma and epineural scar formation in rat sciatic nerve by application of microcrystalline chitosan. *Microsurgery* 31, 642–649. doi: 10.1002/micr.20945
- Martín-López, E., Alonso, F. R., Nieto-Díaz, M., and Nieto-Sampedro, M. (2012). Chitosan, gelatin and poly(L-lysine) polyelectrolyte-based scaffolds and films

- for neural tissue engineering. *J. Biomater. Sci. Polym. Ed.* 23, 207–232. doi: 10.1163/092050610X546426
- Meek, M. F., and Coert, J. H. (2008). US Food and Drug Administration /Conformit Europe- approved absorbable nerve conduits for clinical repair of peripheral and cranial nerves. *Ann. Plast. Surg.* 60, 466–472. doi: 10.1097/SAP.0b013e31804d441c
- Mehrshad, A., Shahraki, M., and Ehteshamfar, S. (2017). Local administration of methylprednisolone laden hydrogel enhances functional recovery of transected sciatic nerve in rat. *Bull. Emerg. Trauma* 5, 231–239. doi: 10.18869/acadpub.beat.5.4.509
- Meyer, C., Stenberg, L., Gonzalez-Perez, F., Wrobel, S., Ronchi, G., Udina, E., et al. (2016a). Chitosan-film enhanced chitosan nerve guides for long-distance regeneration of peripheral nerves. *Biomaterials* 76, 33–51. doi: 10.1016/j.biomaterials.2015.10.040
- Meyer, C., Wrobel, S., Raimondo, S., Rochkind, S., Heimann, C., Shahar, A., et al. (2016b). Peripheral nerve regeneration through hydrogel-enriched chitosan conduits containing engineered schwann cells for drug delivery. *Cell Transplant.* 25, 159–182. doi: 10.3727/096368915X688010
- Mimura, T., Dezawa, M., Kanno, H., Sawada, H., and Yamamoto, I. (2004). Peripheral nerve regeneration by transplantation of bone marrow stromal cell-derived Schwann cells in adult rats. *J. Neurosurg.* 101, 806–812. doi: 10.3171/jns.2004.101.5.0806
- Moattari, M., Kouchesfehiani, H. M., Kaka, G., Sadraie, S. H., Naghdi, M., and Mansouri, K. (2018). Chitosan-film associated with mesenchymal stem cells enhanced regeneration of peripheral nerves: a rat sciatic nerve model. *J. Chem. Neuroanat.* 88, 46–54. doi: 10.1016/j.jchemneu.2017.10.003
- Mokarizadeh, A., Mehrshad, A., and Mohammadi, R. (2016). Local polyethylene glycol in combination with chitosan based hybrid nanofiber conduit accelerates transected peripheral nerve regeneration. *J. Invest. Surg.* 29, 167–174. doi: 10.3109/08941939.2015.1098758
- Nawrotek, K., Tylman, M., Decherchi, P., Marqueste, T., Rudnicka, K., Gatkowska, J., et al. (2016a). Assessment of degradation and biocompatibility of electrodeposited chitosan and chitosan-carbon nanotube tubular implants. *J. Biomed. Mater. Res. A* 104, 2701–2711. doi: 10.1002/jbm.a.35812
- Nawrotek, K., Tylman, M., Rudnicka, K., Balcerzak, J., and Kamiński, K. (2016b). Chitosan-based hydrogel implants enriched with calcium ions intended for peripheral nervous tissue regeneration. *Carbohydr. Polym.* 136, 764–771. doi: 10.1016/j.carbpol.2015.09.105
- Nawrotek, K., Tylman, M., Rudnicka, K., Gatkowska, J., and Wieczorek, M. (2016c). Epineurium-mimicking chitosan conduits for peripheral nervous tissue engineering. *Carbohydr. Polym.* 152, 119–128. doi: 10.1016/j.carbpol.2016.07.002
- Neubrech, F., Heider, S., Harhaus, L., Bickert, B., Kneser, U., and Kremer, T. (2016a). Chitosan nerve tube for primary repair of traumatic sensory nerve lesions of the hand without a gap: study protocol for a randomized controlled trial. *Trials* 17:48. doi: 10.1186/s13063-015-1148-5
- Neubrech, F., Heider, S., Otte, M., Hirche, C., Kneser, U., and Kremer, T. (2016b). Nerve tubes for the repair of traumatic sensory nerve lesions of the hand: review and planning study for a randomised controlled multicentre trial. *Handchir. Mikrochir. Plast. Chir.* 48, 148–154. doi: 10.1186/s13063-015-1148-5
- Neubrech, F., Sauerbier, M., Moll, W., Seegmüller, J., Heider, S., Harhaus, L., et al. (2018). Enhancing the outcome of traumatic sensory nerve lesions of the hand by additional use of a chitosan nerve tube in primary nerve repair. *Plast. Reconstr. Surg.* 142, 415–424. doi: 10.1097/PRS.0000000000004574
- Nicholson, B., and Verma, S. (2004). Comorbidities in chronic neuropathic pain. *Pain Med.* 5(Suppl. 1), S9–S27. doi: 10.1111/j.1526-4637.2004.04019.x
- Noble, J., Munro, C. A., Prasad, V. S., and Midha, R. (1998). Analysis of upper and lower extremity peripheral nerve injuries in a population of patients with multiple injuries. *J. Trauma* 45, 116–122. doi: 10.1097/00005373-199807000-00025
- Ozer, H., Bozkurt, H., Bozkurt, G., and Demirbilek, M. (2018). Regenerative potential of chitosan-coated poly-3-hydroxybutyrate conduits seeded with mesenchymal stem cells in a rat sciatic nerve injury model. *Int. J. Neurosci.* 128, 828–834. doi: 10.1080/00207454.2018.1435536
- Pangestuti, R., and Kim, S.-K. (2010). Neuroprotective properties of chitosan and its derivatives. *Mar. Drugs* 8, 2117–2128. doi: 10.3390/md8072117
- Patel, M., Mao, L., Wu, B., and VandeVord, P. J. (2007). GDNF–chitosan blended nerve guides: a functional study. *J. Tissue Eng. Regen. Med.* 1, 360–367. doi: 10.1002/term.44
- Pavinatto, F. J., Caseli, L., and Oliveira, O. N. (2010). Chitosan in nanostructured thin films. *Biomacromolecules* 11, 1897–1908. doi: 10.1021/bm1004838
- Peng, Y., Li, K.-Y. Y., Chen, Y.-F. F., Li, X.-J. J., Zhu, S., Zhang, Z.-Y. Y., et al. (2018). Beagle sciatic nerve regeneration across a 30 mm defect bridged by chitosan/PGA artificial nerve grafts. *Injury* 49, 1477–1484. doi: 10.1016/j.injury.2018.03.023
- Pfister, L. A., Alther, E., Papaloizos, M., Merkle, H. P., and Gander, B. (2008). Controlled nerve growth factor release from multi-ply alginate/chitosan-based nerve conduits. *Eur. J. Pharm. Biopharm.* 69, 563–572. doi: 10.1016/j.ejpb.2008.01.014
- Rickett, T. A., Amoozgar, Z., Tucheck, C. A., Park, J., Yeo, Y., and Shi, R. (2011). Rapidly photo-cross-linkable chitosan hydrogel for peripheral neurosurgeries. *Biomacromolecules* 12, 57–65. doi: 10.1021/bm101004r
- Ronchi, G., Fornasari, B. E., Crosio, A., Budau, C. A., Tos, P., Perroteau, I., et al. (2018). Chitosan tubes enriched with fresh skeletal muscle fibers for primary nerve repair. *Biomed. Res. Int.* 2018:9175248. doi: 10.1155/2018/9175248
- Schmidt, C. E., and Leach, J. B. (2003). Neural tissue engineering: strategies for repair and regeneration. *Annu. Rev. Biomed. Eng.* 5, 293–347. doi: 10.1146/annurev.bioeng.5.011303.120731
- Schneider, A., Vodouhe, C., Richert, L., Francius, G., Le Guen, E., Schaaf, P., et al. (2007). Multifunctional polyelectrolyte multilayer films: combining mechanical resistance, biodegradability, and bioactivity. *Biomacromolecules* 8, 139–145. doi: 10.1021/bm060765k
- Shapira, Y., Tolmasov, M., Nissan, M., Reider, E., Koren, A., Biron, T., et al. (2016). Comparison of results between chitosan hollow tube and autologous nerve graft in reconstruction of peripheral nerve defect: an experimental study. *Microsurgery* 36, 664–671. doi: 10.1002/micr.22418
- Shen, H., Shen, Z.-L., Zhang, P.-H., Chen, N.-L., Wang, Y.-C., Zhang, Z.-F., et al. (2010). Ciliary neurotrophic factor-coated polylactic-polyglycolic acid chitosan nerve conduit promotes peripheral nerve regeneration in canine tibial nerve defect repair. *J. Biomed. Mater. Res. B Appl. Biomater.* 95, 161–170. doi: 10.1002/jbm.b.31696
- Silva, J. M., Duarte, A. R. C., Custódio, C. A., Sher, P., Neto, A. I., Pinho, A. C. M., et al. (2014). Nanostructured hollow tubes based on chitosan and alginate multilayers. *Adv. Healthc. Mater.* 3, 433–440. doi: 10.1002/adhm.201300265
- Skop, N. B., Calderon, F., Levison, S. W., Gandhi, C. D., and Cho, C. H. (2013). Heparin crosslinked chitosan microspheres for the delivery of neural stem cells and growth factors for central nervous system repair. *Acta Biomater.* 9, 6834–6843. doi: 10.1016/j.actbio.2013.02.043
- Stenberg, L., Kodama, A., Lindwall-Blom, C., and Dahlin, L. B. (2016). Nerve regeneration in chitosan conduits and in autologous nerve grafts in healthy and in type 2 diabetic Goto-Kakizaki rats. *Eur. J. Neurosci.* 43, 463–473. doi: 10.1111/ejn.13068
- Stöfel, M., Wildhagen, V. M., Helmecke, O., Metzen, J., Pfund, C. B., Freier, T., et al. (2018). Comparative evaluation of chitosan nerve guides with regular or increased bendability for acute and delayed peripheral nerve repair: a comprehensive comparison with autologous nerve grafts and muscle-in-vein grafts. *Anat. Rec.* 301, 1697–1713. doi: 10.1002/ar.23847
- Struszczyk, M. H. (2002). Chitin and chitosan: part III. Some aspects of biodegradation and bioactivity. *Polimery* 47, 619–629. doi: 10.14314/polimery.2002.619
- Suzuki, M., Itoh, S., Yamaguchi, I., Takakuda, K., Kobayashi, H., Shinomiya, K., et al. (2003). Tendon chitosan tubes covalently coupled with synthesized laminin peptides facilitate nerve regeneration in vivo. *J. Neurosci. Res.* 72, 646–659. doi: 10.1002/jnr.10589
- Tarlov, I. M., Hoffman, W., and Hayner, J. C. (1946). Source of nerve autografts in clinical surgery. *Am. J. Surg.* 72, 700–710. doi: 10.1016/0002-9610(46)90346-7
- Toba, T., Nakamura, T., Lynn, A. K., Matsumoto, K., Fukuda, S., Yoshitani, M., et al. (2002). Evaluation of peripheral nerve regeneration across an 80-mm gap using a polyglycolic acid (PGA)–collagen nerve conduit filled with laminin-soaked collagen sponge in dogs. *Int. J. Artif. Organs* 25, 230–237. doi: 10.1177/039139880202500310

- Urushibata, S., Hozumi, K., Ishikawa, M., Katagiri, F., Kikkawa, Y., and Nomizu, M. (2010). Identification of biologically active sequences in the laminin $\alpha 2$ chain G domain. *Arch. Biochem. Biophys.* 497, 43–54. doi: 10.1016/j.abb.2010.03.006
- Wang, A., Ao, Q., Cao, W., Yu, M., He, Q., Kong, L., et al. (2006). Porous chitosan tubular scaffolds with knitted outer wall and controllable inner structure for nerve tissue engineering. *J. Biomed. Mater. Res. A* 79, 36–46. doi: 10.1002/jbm.a.30683
- Wang, H., Zhao, Q., Zhao, W., Liu, Q., Gu, X., and Yang, Y. (2012). Repairing rat sciatic nerve injury by a nerve-growth-factor-loaded, chitosan-based nerve conduit. *Biotechnol. Appl. Biochem.* 59, 388–394. doi: 10.1002/bab.1031
- Wang, W., Itoh, S., Matsuda, A., Aizawa, T., Demura, M., Ichinose, S., et al. (2008a). Enhanced nerve regeneration through a bilayered chitosan tube: the effect of introduction of glycine spacer into the CYIGSR sequence. *J. Biomed. Mater. Res. A* 85, 919–928. doi: 10.1002/jbm.a.31522
- Wang, W., Itoh, S., Matsuda, A., Ichinose, S., Shinomiya, K., Hata, Y., et al. (2008b). Influences of mechanical properties and permeability on chitosan nano/microfiber mesh tubes as a scaffold for nerve regeneration. *J. Biomed. Mater. Res. A* 84, 557–566. doi: 10.1002/jbm.a.31536
- Wang, W., Itoh, S., Yamamoto, N., Okawa, A., Nagai, A., and Yamashita, K. (2010). Enhancement of nerve regeneration along a chitosan nanofiber mesh tube on which electrically polarized β -tricalcium phosphate particles are immobilized. *Acta Biomater.* 6, 4027–4033. doi: 10.1016/j.actbio.2010.04.027
- Wang, X., Hu, W., Cao, Y., Yao, J., Wu, J., and Gu, X. (2005). Dog sciatic nerve regeneration across a 30-mm defect bridged by a chitosan/PGA artificial nerve graft. *Brain* 128, 1897–1910. doi: 10.1093/brain/awh517
- Wang, Y., Zhao, Y., Sun, C., Hu, W., Zhao, J., Li, G., et al. (2016). Chitosan degradation products promote nerve regeneration by stimulating schwann cell proliferation via miR-27a/FOXO1 axis. *Mol. Neurobiol.* 53, 28–39. doi: 10.1007/s12035-014-8968-2
- Wei, X., Lao, J., and Gu, Y. (2003). Bridging peripheral nerve defect with chitosan-collagen film. *Chin. J. Traumatol.* 6, 131–134.
- Wenling, C., Duohui, J., Jiamou, L., Yandao, G., Nanming, Z., and Xiufang, Z. (2005). Effects of the degree of deacetylation on the physicochemical properties and Schwann cell affinity of chitosan films. *J. Biomater. Appl.* 20, 157–177. doi: 10.1177/0885328205049897
- Woodbury, M. E., and Ikezu, T. (2014). Fibroblast growth factor-2 signaling in neurogenesis and neurodegeneration. *J. Neuroimmune Pharmacol.* 9, 92–101. doi: 10.1007/s11481-013-9501-5
- Wu, H., Liu, J., Fang, Q., Xiao, B., and Wan, Y. (2017). Establishment of nerve growth factor gradients on aligned chitosan-poly(lactide /alginate fibers for neural tissue engineering applications. *Colloids Surf. B Biointerfaces* 160, 598–609. doi: 10.1016/j.colsurfb.2017.10.017
- Xiao, W., Hu, X. Y., Zeng, W., Huang, J. H., Zhang, Y. G., and Luo, Z. J. (2013). Rapid sciatic nerve regeneration of rats by a surface modified collagen-chitosan scaffold. *Injury* 44, 941–946. doi: 10.1016/j.injury.2013.03.029
- Xu, C., Guan, S., Wang, S., Gong, W., Liu, T., Ma, X., et al. (2017). Biodegradable and electroconductive poly(3,4-ethylenedioxythiophene)/carboxymethyl chitosan hydrogels for neural tissue engineering. *Mater. Sci. Eng. C* 84, 32–43. doi: 10.1016/j.msec.2017.11.032
- Xue, C., Hu, N., Gu, Y., Yang, Y., Liu, Y., Liu, J., et al. (2012). Joint use of a chitosan/PLGA scaffold and MSCs to bridge an extra large gap in dog sciatic nerve. *Neurorehabil. Neural Repair* 26, 96–106. doi: 10.1177/1545968311420444
- Yang, Y., Gu, X., Tan, R., Hu, W., Wang, X., Zhang, P., et al. (2004). Fabrication and properties of a porous chitin/chitosan conduit for nerve regeneration. *Biotechnol. Lett.* 26, 1793–1797. doi: 10.1007/s10529-004-4611-z
- Yao, M., Zhou, Y., Xue, C., Ren, H., Wang, S., Zhu, H., et al. (2016). Repair of rat sciatic nerve defects by using allogeneic bone marrow mononuclear cells combined with chitosan/silk fibroin scaffold. *Cell Transplant.* 25, 983–993. doi: 10.3727/096368916X690494
- Yuan, Y., Zhang, P., Yang, Y., Wang, X., and Gu, X. (2004). The interaction of Schwann cells with chitosan membranes and fibers in vitro. *Biomaterials* 25, 4273–4278. doi: 10.1016/j.biomaterials.2003.11.029
- Zeng, W., Rong, M., Hu, X., Xiao, W., Qi, F., Huang, J., et al. (2014). Incorporation of chitosan microspheres into collagen-chitosan scaffolds for the controlled release of nerve growth factor. *PLoS One* 9:e101300. doi: 10.1371/journal.pone.0101300
- Zhang, L., Yang, W., Tao, K., Song, Y., Xie, H., Wang, J., et al. (2017). Sustained local release of NGF from a chitosan-sericin composite scaffold for treating chronic nerve compression. *ACS Appl. Mater. Interfaces* 9, 3432–3444. doi: 10.1021/acsami.6b14691
- Zhao, L., Qu, W., Wu, Y., Ma, H., and Jiang, H. (2014). Dorsal root ganglion-derived Schwann cells combined with poly(lactic-co-glycolic acid)/chitosan conduits for the repair of sciatic nerve defects in rats. *Neural Regen. Res.* 9, 1961–1967. doi: 10.4103/1673-5374.145374
- Zhao, Y., Wang, Y. Y., Gong, J., Yang, L., Niu, C., Ni, X., et al. (2017). Chitosan degradation products facilitate peripheral nerve regeneration by improving macrophage-constructed microenvironments. *Biomaterials* 134, 64–77. doi: 10.1016/j.biomaterials.2017.02.026
- Zheng, L., Ao, Q., Han, H., Zhang, X., and Gong, Y. (2010). Evaluation of the chitosan/glycerol- β -phosphate disodium salt hydrogel application in peripheral nerve regeneration. *Biomed. Mater.* 5:035003. doi: 10.1088/1748-6041/5/3/035003
- Zhou, S., Yang, Y., Gu, X., and Ding, F. (2008). Chitoooligosaccharides protect cultured hippocampal neurons against glutamate-induced neurotoxicity. *Neurosci. Lett.* 444, 270–274. doi: 10.1016/j.neulet.2008.08.040
- Zhu, C., Huang, J., Xue, C., Wang, Y., Wang, S., Bao, S., et al. (2017). Skin derived precursor Schwann cell-generated acellular matrix modified chitosan/silk scaffolds for bridging rat sciatic nerve gap. *Neurosci. Res.* 135, 21–31. doi: 10.1016/j.neures.2017.12.007
- Zivanovic, S., Li, J., Davidson, P. M., and Kit, K. (2007). Physical, mechanical, and antibacterial properties of chitosan/PEO blend films. *Biomacromolecules* 8, 1505–1510. doi: 10.1021/bm061140p

Conflict of Interest Statement: The authors declare that the research was conducted in the absence of any commercial or financial relationships that could be construed as a potential conflict of interest.

Copyright © 2019 Boecker, Daeschler, Kneser and Harhaus. This is an open-access article distributed under the terms of the Creative Commons Attribution License (CC BY). The use, distribution or reproduction in other forums is permitted, provided the original author(s) and the copyright owner(s) are credited and that the original publication in this journal is cited, in accordance with accepted academic practice. No use, distribution or reproduction is permitted which does not comply with these terms.



Beyond Trophic Factors: Exploiting the Intrinsic Regenerative Properties of Adult Neurons

Arul Duraikannu, Anand Krishnan, Ambika Chandrasekhar and Douglas W. Zochodne*

Division of Neurology, Department of Medicine, and Neuroscience and Mental Health Institute, University of Alberta, Edmonton, AB, Canada

OPEN ACCESS

Edited by:

Giovanna Gambarotta,
University of Turin, Italy

Reviewed by:

Valerio Magnaghi,
University of Milan, Italy
Ertugrul Kilic,
Istanbul Medipol University, Turkey

*Correspondence:

Douglas W. Zochodne
zochodne@ualberta.ca

Received: 03 December 2018

Accepted: 14 March 2019

Published: 05 April 2019

Citation:

Duraikannu A, Krishnan A, Chandrasekhar A and Zochodne DW (2019) Beyond Trophic Factors: Exploiting the Intrinsic Regenerative Properties of Adult Neurons. *Front. Cell. Neurosci.* 13:128. doi: 10.3389/fncel.2019.00128

Injuries and diseases of the peripheral nervous system (PNS) are common but frequently irreversible. It is often but mistakenly assumed that peripheral neuron regeneration is robust without a need to be improved or supported. However, axonal lesions, especially those involving proximal nerves rarely recover fully and injuries generally are complicated by slow and incomplete regeneration. Strategies to enhance the intrinsic growth properties of reluctant adult neurons offer an alternative approach to consider during regeneration. Since axons rarely regrow without an intimately partnered Schwann cell (SC), approaches to enhance SC plasticity carry along benefits to their axon partners. Direct targeting of molecules that inhibit growth cone plasticity can inform important regenerative strategies. A newer approach, a focus of our laboratory, exploits tumor suppressor molecules that normally dampen unconstrained growth. However several are also prominently expressed in stable adult neurons. During regeneration their ongoing expression “brakes” growth, whereas their inhibition and knockdown may enhance regrowth. Examples have included phosphatase and tensin homolog deleted on chromosome ten (PTEN), a tumor suppressor that inhibits PI3K/pAkt signaling, Rb1, the protein involved in retinoblastoma development, and adenomatous polyposis coli (APC), a tumor suppressor that inhibits β -Catenin transcriptional signaling and its translocation to the nucleus. The identification of several new targets to manipulate the plasticity of regenerating adult peripheral neurons is exciting. How they fit with canonical regeneration strategies and their feasibility require additional work. Newer forms of nonviral siRNA delivery may be approaches for molecular manipulation to improve regeneration.

Keywords: peripheral nerve, RhoA, Netrin/Unc5H, PTEN, RB1, BRCA1, APC/ β -catenin

INTRODUCTION

Favorable outgrowth of peripheral nervous system (PNS) axons after injury is often considered in comparison with that of the central nervous system (CNS) where severe barriers, even for limited outgrowth occur. In the clinical context, however, there is striking evidence for its inadequacy. Functional recovery from trauma or disease to the PNS is slow, incomplete and complicated by neuropathic pain. Long target distances, gaps from nerve transection and delayed regrowth into distal nerve territories add substantial and additional barriers to regrowth (Zochodne, 2012). Patients with severe, nominally reversible peripheral nerve disorders such as Guillain-Barre syndrome or vasculitis have prolonged, if not permanent deficits. Similarly, large proximal nerve

lesions such as those at the brachial plexus or high sciatic nerve rarely recover completely. There are both intrinsic and extrinsic factors that act as barriers to the successful regrowth of neurons.

Following acute axonal injury to peripheral nerves, a series of active molecular events that degrade the distal axon develop. “Wallerian” degeneration refers to these degenerative events in distal nerve stumps strictly after transection whereas “axonal degeneration (AxD)” (or “Wallerian-like degeneration”), is a broader term that encompasses all forms of irreversible axon injury. While AxD is initiated immediately after axon injury, a series of morphological changes soon follow. There is fragmentation of axons, dissolution of their neurofilament scaffolds, proliferation and activation of Schwann cells (SCs), recruitment of inflammatory cells including macrophages, and dissolution then clearance of the myelin sheath and axon debris (Waller, 1850; Ide, 1996; Burnett and Zager, 2004; Chen et al., 2007; Zochodne, 2008; **Figure 1**). Following axonal degeneration, proliferating SCs organize themselves into bands of Bungner. These are tubular collections of both SC and basement membrane that serve as both guideposts and channels for newly sprouting axons. These peripheral events accompany changes in neuron perikarya and associated satellite glial cells. For example perineuronal satellite cells which surround nerve cell bodies in sensory and autonomic ganglia, begin to proliferate within a 2–3 days after peripheral axon injury accompanied by local proliferation of resident macrophages, both constituting a population of dorsal root ganglia (DRG) recycling cells (DRCCs) (Wong and Mattox, 1991; Sulaiman and Gordon, 2000; McKay Hart et al., 2002; Zochodne, 2008; Krishnan et al., 2018a).

At most steps during regeneration, there is unexpected axon hesitation. For example, axon regrowth from proximal nerve stumps after transection is delayed, slow and staggered. “Pioneer” axons, which resemble those of development are the first to emerge, but almost always follow leading SCs and their processes (Chen et al., 2005; McDonald et al., 2006). Navigation of axons across gaps that form between the proximal and distal stump is challenging and it is estimated that only one in 10 axons traverse it (Witzel et al., 2005). Distal nerve stumps over time also become inhospitable to hosting regrowing axons. This is contributed to by loss or atrophy of SCs, declines in their elaboration of SC-derived growth factors and declines in the local vascular supply (Sulaiman and Gordon, 2000; Hoke et al., 2001, 2002).

Here, we discuss why peripheral neurons do not grow as robustly as assumed. We begin with a discussion of growth factors that support the PNS, but shift our emphasis to intrinsic controls of growth within neurons and the potential to manipulate novel molecular pathways to enhance growth after injury (**Table 1**).

EXTRINSIC SUPPORT OF REGENERATION THROUGH GROWTH FACTORS

The discovery over the past 50 years that extrinsic molecules can influence the behavior of neurons, either during development

or during adulthood was a remarkable advance. The prototypic growth factor was nerve growth factor (NGF) discovered in mouse submaxillary glands and snake venom that supported robust outgrowth of branches from sympathetic neurons. For its discovery, the Nobel prize in Medicine and Physiology was awarded to Drs Levi-Montalcini and Cohen in 1986. NGF was the first of a family of extrinsic growth factors termed neurotrophins. Several of these are discussed below (**Table 1**). Beyond this family, an expanded repertoire of growth factors is now available for improving the outcome of peripheral nerve trunk injury but their practical application remains problematic. Each axon subtype has a limited receptor deployment available to a given growth factor, requiring cocktails to support all classes of fibers in a nerve trunk. There also remain issues with access, timing of such delivery, where to administer them and their overall stability (Kemp et al., 2007).

Neurotrophin Family Members

Nerve Growth Factor

NGF supports the survival and subsequent differentiation of sensory and sympathetic neurons of the PNS (Levi-Montalcini, 1950, 1987). In the CNS, NGF plays a role in the neurodevelopment and ongoing maintenance of basal forebrain cholinergic neurons (Dreyfus, 1989), septo-hippocampal pathways, hippocampal neurons and cortical neurons (Zhang et al., 1993; Culmsee et al., 1999a,b; Kume et al., 2000). NGF mediates its trophic effect by binding to specific receptors, tropomyosin-receptor kinase A (TrkA) and p75 neurotrophin receptor (p75^{NTR}) (Hempstead et al., 1991; Chao, 2003; Huang and Reichardt, 2003). When p75^{NTR} is activated in the absence of Trk ligation, however, it promotes apoptosis of neurons. In the presence of Trks, p75^{NTR} enhances neurotrophin responses (Kaplan and Miller, 1997). After sciatic nerve injury, NGF receptor expression increased in motor neurons at spinal levels L4-L6 where it reached a maximum level between 1 and 7 days, and normalized to baseline by day 30 (Rende et al., 1992a; DiStefano and Curtis, 1994). NGF is also increased in injured distal nerve stumps (Richardson and Ebendal, 1982; Heumann et al., 1987) and it probably protects adult rat DRG neurons from retrograde cell atrophy and death following axotomy injury (Rich et al., 1987). NGF treatment to pre-injured sensory neurons *in vitro*, derived from young (3 months) and old (26 months) mice supports neurite outgrowth (Horie et al., 1991). Similarly, delayed administration of NGF to the sciatic nerve 3 weeks after transection restores high-affinity NGF receptor density and partially restores neuronal volume (Verge et al., 1989). Topical application of NGF (1 µg) into a nerve crush site increases motor nerve conduction velocity (MNCV), and numbers of regenerating myelinated fibers (RMFs) in rat sciatic nerves (Chen and Wang, 1995). Similar benefits accrue when NGF is given by silicone chamber to injured nerves (Derby et al., 1993; Santos et al., 2017) although gradients are difficult to establish (Kemp et al., 2007).

Brain Derived Neurotrophic Factor

Perhaps the best characterized and most promising neurotrophin family member is brain derived neurotrophic factor (BDNF).

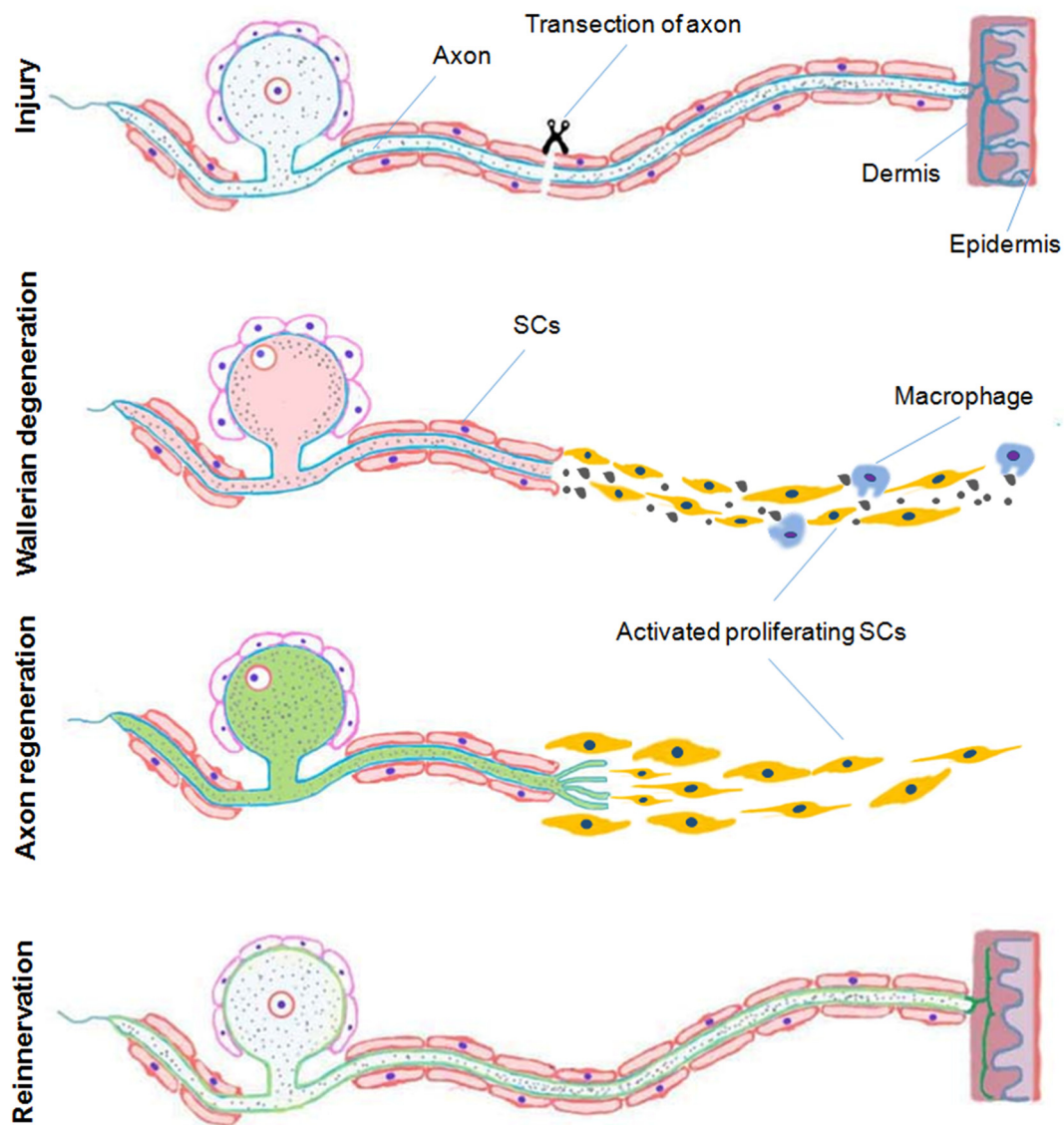


FIGURE 1 | A schematic representation of Wallerian degeneration and regeneration after peripheral nervous system (PNS) injury. In the peripheral nerve following and acute transection axonal injury, Wallerian degeneration, which takes place during few days after injury, is characterized by proliferation and activation of Schwann cells (SCs), recruitment of inflammatory cells including macrophages and dissolution and clearance of the myelin sheath and debris. Proliferating SCs respond by organizing themselves providing a pathway for newly sprouting axons during regeneration and later remyelination associated with reinnervation of the distal target tissue (Duraikannu, original illustration).

BDNF has essential roles in neuronal survival, growth and differentiation during development, and synaptic plasticity in adult peripheral neurons (Thoenen, 1995; Huang and Reichardt, 2001). As such, BDNF has been a potential candidate to promote nerve regeneration. After injury, the BDNF mRNA expression is increased in DRG, SCs and muscle fibers (Zhang et al., 2000; Fukuoka et al., 2001; Kobayashi et al., 2008). Enhanced BDNF protein expression has also been identified in DRG neurons after spinal dorsal horn injury (Fukuoka et al., 2001; Miletic and Miletic, 2002; Geng et al., 2010). More importantly, BDNF and its receptor TrkB (affinity tyrosine kinase receptor B) are robustly expressed in both

DRG sensory, and spinal motor neurons (Foster et al., 1994; Hammarberg et al., 2000) after sciatic nerve injury. Specifically, BDNF was expressed prominently in both small and medium size DRG neurons following nerve injury (Cho et al., 1998; Kashiba and Senba, 1999). Sensory-neuron derived BDNF is also transported in the anterograde direction, appearing at the injured nerve site. The levels of BDNF decline over weeks following the injury (Zhou and Rush, 1996; Tonra et al., 1998). Furthermore, BDNF and TrkB receptors are expressed in different muscles to coordinate muscle innervation and the functional differentiation of neuromuscular junctions (Chevrel et al., 2006). In contrast, following nerve injury deprivation

TABLE 1 | A selected listing of approaches discussed in this review that promote axonal regeneration.**Neurotrophic factors**

Nerve growth factor (NGF)
 Brain derived neurotrophic factor (BDNF)
 Neurotrophin-3 (NT-3) and neurotrophin-4/5 (NT-4/5)
 Ciliary neurotrophic factor (CNTF)
 Leukemia inhibitory factor (LIF)
 Oncostatin M (OSM)
 Glial cell line-derived neurotrophic factor (GDNF)
 Hepatocyte growth factor (HGF)
 Cardiotrophin-1 (CT-1)
 Neurturin (NRTN)
 Artemin (ARTN)
 Persephin (PSP)
 Bone morphogenetic proteins (BMPs)
 Epidermal growth factor (EGF)
 Fibroblast growth factor (FGF)
 Osteopontin (OPN)
 Insulin

Electrical stimulation**Developmental molecules in regeneration**

Unc5H inhibition

Growth cone manipulation

Inhibition of RHOA-ROK

Influence of tumor suppressor pathways during regeneration

Phosphatase and tensin homolog (PTEN)
 Retinoblastoma 1 (Rb1)
 APC- β -catenin pathway

of endogenous BDNF showed attenuated axon outgrowth, and reduced myelinated axon repopulation and regeneration (Song et al., 2008). Treatment with exogenous BDNF to peripheral nerves is transganglionically transported within the spinal cord (Curtis et al., 1998) and as expected, increased recovery after spinal cord injury (Song et al., 2008). In addition, single intrathecal injections of BDNF effectively produce long-lasting thermal hyperalgesia and tactile allodynia in normal mice and may play an important role in chronic pain syndromes (Yajima et al., 2002; Nijs et al., 2015; Sikandar et al., 2018). Delivery of BDNF to the hindpaw or sciatic nerve improves locomotion recovery after contusion injury (Song et al., 2008). Therefore, given these data, there is a reason to believe that BDNF may offer therapeutic benefits for peripheral nerve regeneration.

Neurotrophins-3 and 4/5

Neurotrophin-3 (NT-3) and neurotrophin-4/5 (NT-4/5), additional members of neurotrophin family, support nervous system development, survival, differentiation, and repair (Yamamoto et al., 1996). In the CNS, NT-3 prevents degeneration of noradrenergic (Arenas and Persson, 1994) and dopaminergic neurons (Hyman et al., 1994). NT-3 with or without BDNF improves axonal regeneration after spinal cord injury (Schnell et al., 1994; Xu et al., 1995; Ramer et al., 2001; Liu et al., 2016; Keefe et al., 2017). NT-4/5 stimulates axonal branching from regenerating retinal ganglion cells (RGCs; Sawai et al., 1996). In the PNS, NT-3 promotes neurite outgrowth and survival in peripheral sensory, motor and sympathetic neurons (Rosenthal et al., 1990; Henderson et al., 1993). NT-3 binds to the TrkC receptor (Katoh-Semba et al., 1996) mainly

in large sensory neurons (Zhou and Rush, 1993). NT-4 at the site of sciatic nerve injury increases axon numbers, axonal diameter, myelin thickness and sciatic function index (Yin et al., 2001). NT-4/5 prevents the cell death of embryonic rat spinal motor neurons *in vitro* (Henderson et al., 1993). NT-3 and NT-5 stimulate functional reinnervation of skeletal muscle (Braun et al., 1996).

Other Extrinsic Growth Factors**Ciliary Neurotrophic Factor**

Ciliary neurotrophic factor (CNTF) is derived from parasympathetic cholinergic neurons and is highly expressed in embryonic chick eye (Helfand et al., 1976; Adler et al., 1979; Barbin et al., 1984), adult rat peripheral nerve axons, SCs and spinal nerve roots (Williams et al., 1984; Manthorpe et al., 1986; Millaruelo et al., 1986; Rende et al., 1992b). In the CNS, CNTF is expressed in the optic nerve, mainly in astrocytes (Stöckli et al., 1991). Intravitreal injection of recombinant CNTF increased RGC survival and axon regeneration (Müller et al., 2009). In nerve, CNTF expression appears to be downregulated in the distal stump after injury site but recovered within SCs during regeneration (Williams et al., 1984; Sendtner et al., 1992). CNTF was detected in both small and large subpopulation neurons and regenerating neurites *in vitro* (Sango et al., 2007). Exogenous CNTF prevents degeneration of motor neurons after facial nerve lesions in neonatal rats (Sendtner et al., 1990). In addition, injured nerve sites exposed to recombinant human CNTF had greater numbers of regrowing axons in the distal stumps after injury (Sahenk et al., 1994). Topical application of CNTF to injured sciatic nerves resulted in higher MNCV indicating larger, more mature axons and higher compound muscle action potential amplitudes of the anterior tibial muscle (Zhang et al., 2004b). Likewise, CNTF null (-/-) mutant mice have reductions in axon diameter, had myelin sheath disruption, and demonstrated loss of axon-SC cell architecture at nodes of Ranvier (Gatzinsky et al., 2003). Exposure to CNTF enhanced neurite outgrowth of dissociated adult sensory neurons *in vitro* (Saleh et al., 2013). Finally, CNTF treatment improved sensory nerve regeneration after crush injury in diabetic rats (Mizisin et al., 2004).

Leukemia Inhibitory Factor

Leukemia inhibitory factor (LIF) supports the neurodevelopment of sensory neurons from the neural crest (Murphy et al., 1991). In the mouse DRG (embryos), LIF supports the survival of NGF non-responsive neurons and regulates sensory development *in vivo* (Murphy et al., 1993). LIF supports the survival of sensory neurons after sciatic nerve injury in rat pup. Interestingly, sciatic nerve injury induced LIF expression in the distal and proximal stumps and in denervated muscle fibers (Curtis et al., 1994; Kurek et al., 1996). Injured sciatic nerves treated with a silicone cuff containing LIF increased the recovery of muscle contraction, conduction velocity, myelinated fiber number and diameter (Tham et al., 1997). LIF deleted nerve segments were less supportive of axonal outgrowth (Ekström et al., 2000) and LIF knockdown mouse had impaired muscle regeneration (Kurek et al., 1997). In the CNS, deletion of LIF expression

was associated with impaired axon sprouting of cultured RGC neurons *in vitro* and delayed recovery after optic nerve injury *in vivo* (Ogai et al., 2014).

Oncostatin M

Oncostatin M (OSM), a neuroprotective cytokine of the interleukin-6 family (Taga and Kishimoto, 1997; Heinrich et al., 1998; Senaldi et al., 1999) attenuates neuronal neuron death (Weiss et al., 2006). OSM induces signals through glycoprotein 130 (gp130) and the OSM-specific β subunit receptor complex (Mosley et al., 1996). In the PNS, OSMR beta was expressed in small caliber non-peptidergic neurons of the dorsal root and trigeminal ganglia (Tamura et al., 2003; Morikawa et al., 2004; Morikawa, 2005). OSM mRNA expression in the nerve increased rapidly up to 14 days following injury (Ito et al., 2000). Interestingly, subcutaneous injection of OSM into the hind paw of C57BL6J wild type mice was associated with a reduction of paw withdrawal latencies to heat stimulation (Langeslag et al., 2011), indicating support for axon repair (Ito et al., 2000).

Glial Cell Line-Derived Neurotrophic Factor

Glial cell line-derived neurotrophic factor (GDNF), belongs to the transforming growth factor- β (TGF- β) superfamily (Tomas et al., 1995), and enhances the survival and morphological differentiation of midbrain dopaminergic neurons (Lin et al., 1993). Recombinant GDNF promotes the survival of motor neurons (Chen et al., 2000), sympathetic neurons and enhanced neurite outgrowth in embryonic chick sympathetic neurons (Trupp et al., 1995). Local application of GDNF to the injured neonatal facial nerve prevented retrograde motor neuron loss and atrophy (Yan et al., 1995). After injury, GDNF and its receptor, GFR α -1, mRNA levels increased in sciatic nerve (Trupp et al., 1995) distal stumps. Interestingly, GFR α -1 was also increased in the DRG ipsilateral to the nerve injury (Hoke et al., 2000). GDNF mRNA and protein expression was upregulated in SCs 48 h after injury and declined to basal levels by 6 months of denervation. GFR α -1 and GFR α -2 mRNAs were increased only after GDNF upregulation and remained elevated as late as 6 months (Hoke et al., 2002). Pre-conditioning injury of cultured DRG neurons *in vitro* treated with exogenous GDNF increased neurite outgrowth (Mills et al., 2007). In addition, GDNF induced neurite outgrowth and upregulation of galectin-1 (GAL-1) through the RET/PI3K pathway in DRG sensory neurons *in vitro* (Takaku et al., 2013). GDNF also induced directional turning of adult neuron growth cones but only did so in the company of hepatocyte growth factor (HGF) or a phosphatase and tensin homolog (PTEN) inhibitor (Guo et al., 2014). GDNF also influences SC function (Zhang et al., 2009). In contrast, lentiviral vector-mediated GDNF overexpression for 16 weeks increased GDNF expression at regenerating sites but impaired long-distance nerve regeneration (Eggers et al., 2008; Tannemaat et al., 2008; Ortmann and Hellenbrand, 2018). Finally, GDNF may offer analgesia in animal models of neuropathic pain (Boucher et al., 2000).

Hepatocyte Growth Factor

HGF, was initially identified as a mitogen for hepatocytes (Nakamura et al., 1984, 1989). HGF interacts with c-Met receptor

tyrosine kinase (Bottaro et al., 1991). In normal DRG, c-Met receptor was expressed in small and medium-size neurons and to a lesser extent in large-size neurons. However, following sciatic nerve ligation (SNL) c-Met expression increased after injury (Zheng et al., 2010). Mutations in the HGF receptor (Met tyrosine kinase), show abnormal limb innervation correlated with reductions of muscle fibers of mouse embryos (Maina et al., 1997). In normal DRG, HGF is expressed mainly in medium and large diameter neurons. Following SNL, HGF expression decreased in L4-L5 DRG neurons (Zheng et al., 2010). HGF in combination with BDNF and NT3, had no impact on DRG sensory neurite outgrowth *in vitro*. In contrast, HGF cooperated with NGF to enhance axonal outgrowth (Maina et al., 1997). Similarly, HGF also cooperates with CNTF positive neurons in supporting the survival and growth of parasympathetic and proprioceptive neurons (Davey et al., 2000). Repeated intramuscular injection of human HGF gene to a crush injured rat showed increased expression of HGF protein and mRNA level in DRGs associated with improvements in function and structure of the crushed nerve (Kato et al., 2005; Boldyreva et al., 2018; Ko et al., 2018).

Cardiotrophin-1

Cardiotrophin-1 (CT-1) supports the survival of developing motor neurons *in vivo* and *in vitro* (Pennica et al., 1996; Oppenheim et al., 2001). CT-1 signals by activating the leukemia inhibitory factor, gp130 (LIFR β /gp130) and the CT-1 α receptor subunit (CT-1R α) receptor complex (Pennica et al., 1995; Robledo et al., 1997). CT-1 protects animals from progressive motor neuronopathy (PMN), a condition in which mice suffer from motor neuronal degeneration of facial motoneurons and phrenic nerve myelinated axons (Bordet et al., 1999). CT-1 also prevents deterioration in wobbler mice motor neuron disease (MND): paw position, walking pattern abnormalities, intramuscular axonal sprouting and large myelinated motor axons (Mitsumoto et al., 2001), indicating CT-1 may have therapeutic benefits in patients with MND.

Neurturin

Neurturin (NRTN) supports embryonic and adult rat midbrain dopaminergic neurons (Horger et al., 1998; Reyes-Corona et al., 2017). NRTN signaling activates Ret tyrosine kinase together with a glycosylphosphatidylinositol (GPI)-linked coreceptor (either GFR α 1 or GFR β 2) (Kotzbauer et al., 1996; Golden et al., 1999). NTN $^{-/-}$ mice had loss of GFR α 2-expressing neurons from DRG and trigeminal sensory ganglia (Heuckeroth et al., 1999). Neurturin and activated GFR α 2 receptor are important for parasympathetic innervation of mucosae (Wanigasekara et al., 2004). NRTN has been shown to upregulate B1 (bradykinin) receptors expressed in isolated nociceptive neurons in mice, indicating a possible influence on pain and inflammation pathways (Vellani et al., 2004).

Artemin

Artemin (ARTN) supports the dopaminergic neurons in the rat embryonic ventral midbrain (Baloh et al., 1998b). ARTN operates through GDNF family receptor GFR α 3, together with RET tyrosine kinase receptor (Baloh et al., 1998b). After optic

nerve injury, ARTN receptor GFR α 3 mRNA and protein levels increased within the first week. ARTN and its receptor (GFR α 3), offered neuroprotection of injured RGCs through the PI3K-AKT signaling pathway and enhanced optic nerve regeneration in rats (Omodaka et al., 2014). In the PNS, ARTN is expressed in both immature and mature myelinating SCs. After injury, ARTN was highly expressed in the distal nerve segment, indicating that it influences both developing and regenerating peripheral neurons (Baloh et al., 1998b; Ikeda-Miyagawa et al., 2015). In neonatal rat neuron cultures *in vitro*, ARTN supported the survival of sensory neurons derived from the DRG and the trigeminal ganglion (TG) and visceral sensory neurons of the nodose ganglion (NG; Baloh et al., 1998b). *In vivo*, ARTN is expressed in both large and small sensory neurons before and after injury (Baloh et al., 1998b; Wang et al., 2014). Treatment of injured peripheral nerves with ARTN enhanced motor, sensory axon regeneration including functional recovery (Jeong et al., 2008; Wang et al., 2008, 2014; Widenfalk et al., 2009; Zhou et al., 2009; Wong L. E. et al., 2015).

Persephin

Persephin (PSP) supports midbrain dopaminergic neuron survival (Milbrandt et al., 1998) in a manner similar to other neurotrophic factors like GDNF and NRN (Baloh et al., 1998a; Milbrandt et al., 1998; Leitner et al., 1999). However, PSP binds efficiently only to GFR α -4 receptors (Enokido et al., 1998). Recent work has suggested that PSP has a neuroprotective effect in animal models of Parkinson's disease (Yin et al., 2015). In the PNS, PSP supports the survival of motor neurons but not autonomic neurons in the superior cervical ganglion (SCG), sensory neurons, or enteric neurons (Milbrandt et al., 1998).

Bone Morphogenetic Proteins

Bone morphogenetic proteins (BMPs) belong to the TGF- β superfamily. BMPs signal using serine/threonine kinases type I and type II receptors (Ebendal et al., 1998). BMP-2 is expressed in normal sciatic nerve. After injury, BMP-2 was localized at both distal and proximal stumps (Tsujii et al., 2009). BMP-2 improved regeneration of facial nerves and acted as a potential neurotrophic factor (Wang et al., 2007). In contrast, treatment of E10 (mouse embryos) trigeminal neurons with BMP4 *in vitro* resulted in neuronal death, indicating responsiveness of the neurons to BMP4 (Guha et al., 2004). However, BMP-4 promotes the survival of motor neurons and protects neurons from glutamate-induced toxicity (Chou et al., 2013). Treatment with BMP-7 improved recovery in spinal cord injured rats (Chen et al., 2018). In double-ligated sciatic nerves, BMP4 protein was expressed at both the proximal and distal portion of motor axons, indicating BMP-4 proteins were anterogradely and retrogradely transported (Chou et al., 2013). During Wallerian degeneration, BMP-7 expression was increased within proximal and distal injured nerve stumps (Tsujii et al., 2009).

Epidermal Growth Factor

Epidermal growth factor (EGF) promotes the proliferation of fibroblast and epithelial cells (Carpenter and Cohen, 1979; Plata-Salamán, 1991; Wong and Guillaud, 2004). EGF-induced neurotrophic action is mediated by activation of EGF receptor

(EGFr) and plays a vital role during the development of mouse and rat brain (Yamada et al., 1997; Wong and Guillaud, 2004; Yang et al., 2018). In the adult normal human DRG, Epidermal growth factor receptor (EGFR) is strongly expressed in the small, intermediate size neurons, satellite glial cells and SCs (Huerta et al., 1996). In the sciatic nerve, EGFr mRNA and protein are expressed mainly in both SCs and fibroblasts in rats. After transection injury, EGFr mRNA and protein levels increased in both proximal and distal nerve stumps (Toma et al., 1992). During development, EGF limited the neurite branching in DRG (Explant and dissociated) neurons *in vitro* (Maklad et al., 2009). Interestingly, ablation of EGFr was associated with disorganized sensory innervation in dorsal skin, indicating that EGFr is required for proper cutaneous innervations of the skin (Maklad et al., 2009).

Fibroblast Growth Factor (FGF)

Basic fibroblast growth factor (bFGF or FGF2), is a potent growth factor for mesoderm derived cells and acts as a neurotrophic factor to various neural cells. It has been found to enhance hippocampal, cerebral cortical, granule, ciliary ganglion and spinal cord neuron survival. bFGF also promotes neurite extension (Gospodarowicz, 1979; Gospodarowicz et al., 1984; Morrison et al., 1986; Walicke et al., 1986; Unsicker et al., 1987; Hatten et al., 1988; Fujimoto et al., 1997). FGF mainly mediates its trophic action by binding to membrane-bound receptors (FGF receptors) that possess tyrosine kinase activity to generate downstream signal transduction (Imamura et al., 1988; Walicke et al., 1989; Ornitz and Itoh, 2015). In the PNS, both acidic and basic fibroblast factors (aFGF, bFGF) mRNA levels were expressed in small and medium-size DRG neurons (Ji et al., 1995; Acosta et al., 2001). After 3 days of sciatic nerve injury, aFGF(FGF1) mRNA levels increase in DRG neurons but bFGF mRNA levels were upregulated in most DRG neurons but declined after 1 week (Ji et al., 1995). In addition, FGF 2 and 7 were also increased in lumbar DRG neurons but FGF 13 levels decreased after injury (Li et al., 2002). In the sciatic nerve, FGF 2 and FGF receptor (FGFR1-3) mRNA expression increased after injury (Grothe et al., 2001). Local treatment with bFGF after injury increased the number of regenerating axons. FGF receptor expression increased in the proximal and distal segments (Fujimoto et al., 1997; Archer et al., 1999; Grothe and Nikkhah, 2001; Namaka et al., 2001). Interestingly, FGF-2 overexpression generated SC proliferation, doubled the number of regenerating axons and enhanced remyelination after sciatic crush in mice (Jungnickel et al., 2006). Treatment with recombinant human FGF-2 (rhFGF-2) to a mental nerve crush injured rats had improved regeneration and sensory functional recovery (Lee et al., 2017).

Osteopontin

Osteopontin (OPN) is a secreted phosphoprotein that interacts with receptor $\alpha_v\beta_3$ integrin (Liaw et al., 1995). OPN plays an important role in rat brain development (Shin et al., 1999; Lee et al., 2001). Furthermore, OPN expression was increased in pyramidal neurons in Alzheimer's disease (AD) brain in comparison to age-matched controls (Wung et al., 2007). In the PNS, OPN is expressed mainly in the larger sized DRG

and TG neurons (Ichikawa et al., 2000). After injury, OPN was expressed in the degenerating distal nerve stump during the first day but was downregulated at day 14. Later stage after axotomy, SC-OPN was re-expressed in regenerating crushed nerves but not in permanently transected nerves (Jander et al., 2002; Wright et al., 2014).

Insulin

Insulin acts as a growth factor that supports the survival and synaptic plasticity of neurons (FERNYHOUGH et al., 1993; Toth et al., 2006; Hoybergs and Meert, 2007; McNay et al., 2010; Singh et al., 2012b). Insulin receptor (IR) mRNA is regulated during postnatal peripheral nerve development (Shettar and Muttagi, 2012). In dissociated neurons *in vitro*, insulin signaling regulates neurite outgrowth (FERNYHOUGH et al., 1989, 1993; Govind et al., 2001; Choi et al., 2005; Singh et al., 2012b). Neurons may also have the capacity to synthesize insulin (Devaskar et al., 1994; Rulifson et al., 2002). In adult DRG neurons, IR mRNA and protein levels were higher in small caliber neurons and sciatic nerves (Sugimoto et al., 2000, 2002). Similarly, insulin receptor subunit β (IR β) expression was increased in sensory neurons after sciatic nerve crush injury (Xu et al., 2004) and has been identified in dermal fibers of mouse foot pads (Guo et al., 2011). In injured sciatic nerves, systemic insulin administration enhanced reinnervation of foot interosseous endplates associated with enhanced functional recovery (Xu et al., 2004). Intrathecal insulin increased calcitonin gene related peptide (CGRP) expression in DRG neurons, enhanced functional recovery of sensation and increased axon regrowth rate identified by the pinch test following sural nerve crush (Toth et al., 2006). In diabetic rats, near sciatic nerve insulin treatment enhanced local motor conduction velocities but also increased the percentage of small ($\leq 9.0 \mu\text{m}$ diameter) myelinated fibers within nerves exposed to it (Singhal et al., 1997). Local sub-hypoglycemic insulin has had additional impacts in diabetic models including reversal of axon atrophy after intrathecal injection, enhanced epidermal axon regrowth following local injection and improvements in neuropathy from intranasal injection (Brussee et al., 2004; Guo et al., 2011; De la Hoz et al., 2017).

ELECTRICAL STIMULATION AND AXON REGENERATION

One of the most robust empiric approaches, now with evidence of efficacy in humans, has been post-injury exogenous electrical stimulation. In work pioneered by Brushart, Gordon, Verge, Chan and others (Brushart et al., 2002; Geremia et al., 2007; Gordon et al., 2008, 2010; McLean et al., 2014; Wong J. N. et al., 2015), brief post-injury electrical stimulation enhanced the regrowth of motor and sensory axons (Al-Majed et al., 2000a; Gordon et al., 2007). While its full capabilities and exact mechanisms are not fully characterized, they include a retrograde ramp-up of regeneration-associated genes and the action of BDNF.

Work by Gordon et al. established that post-injury stimulation at 20 Hz for 1 h offered an impressive impact

on regeneration. Interestingly this is a very specific outcome limited to a well-circumscribed paradigm but not effective with other tested forms of Electrical stimulation (ES). For this review, most of the citations here refer to this specific approach. ES increased the speed and accuracy of axonal regeneration and re-innervation (Al-Majed et al., 2000b; Brushart et al., 2002; English et al., 2007) and benefitted both sensory and motor re-innervation (Al-Majed et al., 2000b; Brushart et al., 2002; Geremia et al., 2007; Gordon et al., 2009; Singh et al., 2012a). In adult DRG neurons *in vitro* plated over stimulating microelectrodes, ES accelerated early neurite outgrowth (Singh et al., 2012a). Brief electrical stimulation then applied *in vivo* to the proximal injured site in mice enhanced regrowth of axons across transection sites (Singh et al., 2012a). ES accelerated the return of reflex foot withdrawal and contractile force in re-innervated leg muscles (Nix and Hopf, 1983; Pockett and Gavin, 1985). ES also increased the numbers of regenerated axon density and diameter after 8 weeks of surgery (Haastert et al., 2011), enhanced myelination and angiogenesis (Lu et al., 2008; Deng et al., 2018). In post-surgical patients that had sustained complete digital nerve transection there were greater improvements in sensory re-innervation following ES (Wong J. N. et al., 2015).

ES facilitates myelination through impacts on SC polarization and BDNF (Wan et al., 2010). Along these lines, delayed brief ES increased expression of myelin basic protein (MBP) and promoted re-organization of the node of Ranvier coinciding with the early reappearance of re-myelinated axons (McLean et al., 2014). ES also accelerated the removal of myelin debris and promoted more vigorous clearance of activated macrophages from the demyelination zone (McLean et al., 2014).

In sensory neurons, enhanced BDNF immunoreactivity expression was identified after ES (Alrashdan et al., 2010). Al-Majed et al. (2000a) demonstrated that 7 days after femoral nerve transection and stimulation the mRNA expression of BDNF and its receptor TrkB level had a two-fold rise within rat femoral motor neurons. In additional work, ES promoted the release of NGF from cultured SCs through calcium influx (Huang et al., 2010). ES is associated with rises in neuronal calcium content (Singh et al., 2012b) a change that might correlate with additional mechanisms of the ES response such as rises in regeneration related molecules including tubulin, Sonic hedgehog (Shh) and GAP43 mRNA (Singh et al., 2015).

RESURRECTION OF DEVELOPMENTAL MOLECULES IN REGENERATION

An important regeneration theme is the redeployment of developmental related molecules for new roles during regrowth. The netrin-Deleted in Colorectal Cancer (DCC)-Unc5H interactions are an important example.

Netrins belong to an evolutionarily conserved and developmentally important family of laminin-related proteins (Sun et al., 2011). Netrin-1 receptors include two main families: DCC, comprising DCC and neogenin, and the uncoordinated gene 5 (UNC-5) proteins (Keino-Masu et al., 1996; Ackerman et al., 1997; Leonardo et al., 1997). Ligation of

DCC and UNC4H2 receptors by extracellular netrin-1 inhibited apoptosis. DCC and UNC5H2 are also called “dependence receptors” that trigger either survival or apoptotic signals depending on whether netrin-1 is respectively present or absent (Mehlen and Mazelin, 2003; Mehlen and Tauszig-Delamasure, 2014). Netrin-1 up-regulation is important for neuronal navigation (Jiang et al., 2003; Cirulli and Yebra, 2007; Mehlen et al., 2011). Netrin-1 and DCC have specifically been linked to neural crest cell migration (Jiang et al., 2003).

Netrin-1 and its receptor proteins are involved in axonal guidance in *C. elegans* (Serafini et al., 1994; Leonardo et al., 1997) and act as a cue that is bifunctional and attracts or repels different axons. It attracts commissural axons using the DCC receptor and repels others through Unc5 receptors (Kennedy et al., 1994; Moore et al., 2007; Briançon-Marjollet et al., 2008). Moreover, its repulsive guidance may specifically be involved in DRG sensory axon fate during development (Watanabe et al., 2006; Masuda et al., 2008). In the CNS, netrin-1 is also expressed by oligodendrocytes and inhibits regeneration of adult CNS neurons that express Unc5H2 (Manitt et al., 2009). Netrin-1 may also have direct impacts on axon growth and branching (Dun and Parkinson, 2017; Boyer and Gupton, 2018). For example, netrin guides RGC axons as they navigate the visual pathway (Deiner and Sretavan, 1999) but also targets arborization of mature RGC axons. This involves DCC-dependent increases in presynaptic differentiation and dynamic branching (Manitt et al., 2009).

In the PNS, netrin-1 receptors are expressed in sensory and motor neurons, SCs and axons both intact or after injury (Park et al., 2007). DCC receptors and Unc5H2 receptor are expressed in glial cells, particularly in proximal nerve stumps following peripheral nerve injury (Webber et al., 2011). Knockdown of DCC locally, using an siRNA approach directed at the proximal stump of a transected nerve trunk impaired SC activation and outgrowing migration, and was associated with secondarily attenuated regeneration. In contrast, similar local knockdown of Unc5H2 receptors enhanced SC outgrowth and follow on axon regeneration. The overall findings indicated that the netrin-DCC receptor interaction is redeployed from development for use during adult axon regeneration. There were, however, differences between development and adult regeneration. In the former, the specific attractive netrin-DCC and repulsive netrin-Unc5H2 interactions are among growing neurons. In the adult, this machinery is subsumed by reactive SCs but with the same direction of impact. Since axon-SC interactions are intimate and essential for overall nerve regrowth, knockdown of the Unc5H2 “brake” ultimately benefitted axon regrowth, following along outgrowing SCs. Interestingly, injury itself upregulated DCC receptors and down-regulated Unc5H2 receptors providing facilitation for regrowth. Similarly, knockdown of DCC upregulated its reciprocal Unc5H2 receptor. Taken together, not only was there acquisition of attractive and repellant developmental neuronal molecules by SCs in the adult, their relationship also remained reciprocal. Exogenous netrin-1 peptides added to neurons *in vitro* or sciatic nerves *in vivo* did not impact regeneration, likely indicating sufficient endogenous levels to activate these receptors (Webber et al., 2011). However, higher

concentrations of exogenous netrin-1 in adult DRG explants and dissociated DRG culture may inhibit neurite outgrowth (Park et al., 2007).

GROWTH CONE GTPases: RhoA AND Rac1

Local growth cone molecules may be the final arbiters over whether extension or advancement of axons occurs or whether they retract and withdraw. Among these molecules, a prominent role for the Rho family GTPases exists. RhoA GTPase and its downstream effector Rho-kinase (ROCK) signal an inhibitory pathway involved in cellular growth, differentiation, migration and survival (Mueller et al., 2005). RhoA is activated by GTP binding. RhoA/ROCK activation is involved in growth cone collapse and reduced axonal outgrowth in CNS neurons (Lehmann et al., 1999). Moreover, RhoA/ROCK activation has been detected in both spinal cord and optic nerve injury (Lehmann et al., 1999; Fu et al., 2016). After spinal cord injury, expression of RhoA was increased in neurons, astrocytes and oligodendrocytes (Dubreuil et al., 2003), indicating an important role in the inhibition of CNS regeneration (Hu and Selzer, 2017). Thus, the ROCK inhibitor, Y27632 administered after spinal cord injury was associated with new axon sprouts in the gray matter distal to injury and improved functional recovery (Chan et al., 2005).

RhoA/ROCK impacts PNS axon regeneration. In the PNS, RhoA and ROCK1 mRNA and proteins are expressed in the dorsal root ganglion (DRG) neurons, axons and SCs of the sciatic nerve and upregulated after injury (Terashima et al., 2001; Cheng et al., 2008). Moreover activated RhoA GTPase was upregulated in proximal stumps of transected nerve trunks (Cheng et al., 2008). RhoA protein was also increased in motor neurons after mouse sciatic nerve injury (Hiraga et al., 2006; Joshi et al., 2015). Pharmacological inhibition of RhoA-ROCK, using the small molecule inhibitor HA1077 promoted neurite and axonal outgrowth of DRG neurons *in vitro*. Furthermore, when the ROCK inhibitor was applied to the tip of the sciatic nerve injury site, the number of outgrowing axons and associated SCs was enhanced (Cheng et al., 2008). RhoA GTPase also is involved in growth cone behaviour of PNS neurons. Specifically, application of a ROCK inhibitor induced growth in sensory neuron growth cones (Guo et al., 2014). Hiraga et al. (2006), noted that the ROCK inhibitor (fasudil) increased amplitudes of distally evoked compound muscle action potentials after axonal injury. Along with these physiological benefits, the agent increased numbers and caliber of regenerating axons indicating a role in promoting axon maturation through ROCK inhibition.

A ROLE FOR TUMOR SUPPRESSORS IN NEURONS: PTEN IS AN INTRINSIC BLOCKER OF AXON REGROWTH

PTEN is a tumor suppressor that converts phosphatidylinositol (3,4,5)-triphosphate (PIP3) into phosphatidylinositol (4,5)-biphosphate (PIP2). On inactivation of PTEN, PIP3 accumulates, thereby phosphorylation activating Akt whereas pAkt

subsequently inhibits GSK3 β , itself an inhibitor of axon growth. Knockdown of PTEN and activating the PIP3/Akt pathway is closely linked to proliferation, cell survival, increased cell size and epithelial polarity. Mutations in PTEN are found in malignant glial brain tumors (Ali et al., 1999; Broderick et al., 2004). Loss of heterozygosity of PTEN is observed in human malignancies especially endometrial and ovarian cancer, late-stage metastatic tumors and others (Li and Sun, 1997). Inactivation of a single PTEN allele increases cell proliferation and cell survival and reduces apoptosis (Di Cristofano et al., 1999; Podsypanina et al., 1999). Accordingly, PTEN has many roles in the nervous system during development and adulthood (Kath et al., 2018). Recent studies have demonstrated that neurotrophin-related growth and differentiation is specifically inhibited by PTEN overexpression (Musatov et al., 2004). Conditional deletion of PTEN in the developing hippocampus and cortex is associated with neuronal hypertrophy and behavioral alterations that model human autism (Kwon et al., 2006). On the other hand, PI3K activation regulates neuronal differentiation, survival migration, extension and guidance (Brunet et al., 2001; Rodgers and Theibert, 2002; Arimura and Kaibuchi, 2005; Chang et al., 2006).

PI3K/Akt signals are expressed and activated during axon regeneration. For example, knockdown of PTEN by siRNA increased neuronal polarity and axonal outgrowth in hippocampal neurons *in vitro* (Jiang et al., 2005). PTEN deleted mice had increased RGC survival and extended robust long-distance axon regeneration after 14 days of optic nerve injury. Inactivation of PTEN leads to activation of PI3K, pAkt and mammalian target of rapamycin (mTOR) signaling in CNS neurons. Studies from several models (*C. elegans* to mammalian neurons) have identified a role for PI3K in asymmetric signaling and its impact on orienting polarized outgrowth during axonogenesis (Yoshimura et al., 2005; Adler et al., 2006). PTEN knockdown through enhanced mTOR activity increased RGC survival and axon regeneration whereas rapamycin blocked mTOR activity and attenuated regeneration. Further, axotomy in RGCs markedly reduced pS6 levels possibly accounting for the limited CNS regeneration after crush injury (Park et al., 2008). S6 ribosomal kinase 1 is targeted by the mTOR pathway, and its phosphorylation is indicative of mTOR activity (Kim et al., 2016). Similarly, PTEN deleted mice had improved repair of the corticospinal tract (CST) of spinal cord injury mice (Geoffroy et al., 2016). Inhibition of PTEN improves outcome in experimental spinal cord injuries, with lesser motor neuron death, greater tissue sparing and smaller cavity formation (Walker et al., 2012).

PTEN knockdown is associated with substantial benefits following peripheral nerve injury. PTEN is expressed widely in sensory and motor neurons but there is intense expression among small caliber IB4 nonpeptidergic DRG neurons. Paradoxically its levels rise after nerve injury. PTEN is also expressed in SC and in regrowing injured axons (Christie et al., 2010). Local inhibition using either the pharmacological inhibitor BpV(pic) or siRNA knockdown enhances axon

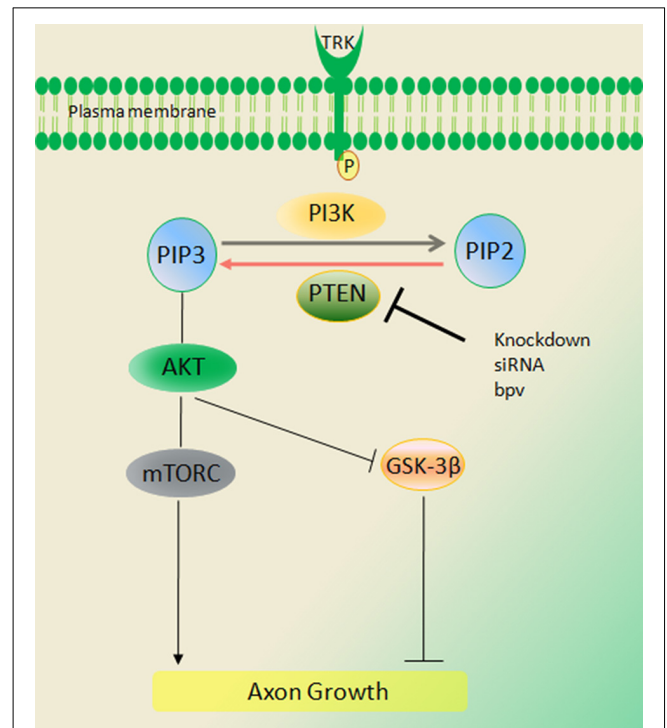


FIGURE 2 | Signaling of the phosphatase and tensin homolog deleted on chromosome ten (PTEN)/PI3K/Akt pathway. PTEN converts phosphatidylinositol (3,4,5)-triphosphate (PIP3) into phosphatidylinositol (4,5)-bisphosphate (PIP2), thus inhibiting Akt activation and peripheral nerve regeneration. Activation of PI3K and Akt signals through deletion of PTEN [BPV (pic) or siRNA] increases regeneration of axons in injury. These impacts appear to be independent of mammalian target of rapamycin (mTOR) but require the activity of PI3K and Akt (Duraikannu, original illustration).

outgrowth as evaluated in both *in vitro* and *in vivo* analysis (Figure 2; Christie et al., 2010). PTEN knockdown using siRNA was accomplished without a viral vector. In the PNS these impacts appear to be independent of mTOR but require the activity of PI3K and Akt.

PTEN may influence distal regenerative events within growing axons through central rather than peripheral modulation of cellular machinery. For example, local exposure of adult growth cones to gradients of the PTEN inhibitor, BpV (pic) did not have significant impacts on growth cone turning, unless combined with a local growth factor. However, when inhibitory gradients were instead directed at the perikarya of *in vitro* adult sensory neurons, there was a striking rise of distal outgrowth in distal branches growing in directions unrelated to the inhibitory gradient. These data suggest that PTEN modulation is a central deterministic signal that instructs distal growth cone behavior (Christie et al., 2010).

In a mouse spinal muscular atrophy (SMA) model, knockdown of PTEN rescued defects in axon length, growth cone structure and overall survival (Ning et al., 2010). In a chronic diabetic neuropathy model, with documented regenerative failure, PTEN levels in motor and sensory neurons were upregulated (Singh et al., 2014). In keeping with this finding, PTEN knockdown rescued the regenerative deficit.

A FURTHER TUMOR SUPPRESSOR AND ITS IMPACT ON ADULT NEURONS: RETINOBLASTOMA 1

The retinoblastoma tumor suppressor Retinoblastoma 1 (Rb1) operates at the core of the cell cycle pathway. Its mutations are associated with childhood retinoblastoma tumors. Rb1 is linked to neuronal fate, regulating proliferation and migration of neuronal progenitors during brain development (Slack et al., 1998; Ferguson et al., 2002, 2005; McClellan et al., 2007; Andrusiak et al., 2010). In the canonical pathway, Rb1 regulates cell cycle progression by binding and signaling through the E2F family of transcription factors. The operational status of Rb1 protein depends on its phosphorylation status, in turn mediated by the cyclin/cyclin-dependent kinase (CDK) complex (Giacinti and Giordano, 2006).

Deletion of Rb1 is a frequent and early molecular hallmark of cancer. Specifically, individuals with germ-line Rb1 mutations are at risk of developing trilateral retinoblastoma, a pediatric intracranial neuroblastic tumor (Jakobiec et al., 1977; Marcus et al., 1998). Rb null mice die as embryos by E15 from hematopoietic and neurological abnormalities linked to the failure of cells to permanently withdraw from the cell cycle (Clarke et al., 1992; Jacks et al., 1992; Lee et al., 1992). Conditional deletion of Rb1 in the embryonic retina display ectopic division and apoptosis of developing retinal transition cells (MacPherson et al., 2004; Zhang et al., 2004a). Rb1 functions within RGC axons, such that its absence is associated with retinal and midline pathfinding errors, leading to aberrant tectal innervation. In sensory ganglia, extensive loss of sensory neurons and expression of TrkA, B neurotrophin receptors was associated with Rb1 deletion during development (Lee et al., 1992).

Rb deletion induces cell cycle re-entry in several systems (Sage, 2012), including mouse embryonic fibroblasts (MEFs; Sage et al., 2003), mammalian muscle cells (Zacksenhaus et al., 1996; Pajcini et al., 2010) and adult cortical neurons (Andrusiak et al., 2012). In contrast, loss of Rb is capable of driving mutated SC growth through a signaling pathway distinct from PI3-AKT-mTOR and using an E2F-independent mechanism (Collins et al., 2012).

As discussed, previous studies indicate that the PI3K/Akt signaling pathway influences axon outgrowth and neuronal plasticity and that these roles overlap with protection and survival. In postmitotic adult injured neurons, Rb1 may influence the downstream PI3K-Akt pathway on growth, a pattern resembling the impact of PTEN (Christie et al., 2014). Following sciatic nerve injury, Rb was robustly expressed in neurofilament labeled DRG neurons and axons, despite its role as an inhibitor of sensory neuron growth after injury. Like PTEN, the Rb1 protein paradoxically rises following injury and may also operate downstream of Raf-MEK and the PI3K-Akt pathway. *In vitro* knockdown of Rb using siRNA increased neurite outgrowth and length in dissociated adult sensory neurons (Christie et al., 2014). As in the PTEN knockdown studies and subsequent adenomatous polyposis coli (APC) work described below, the approach used nonviral methods to achieve

knockdown. In addition, silencing of Rb protein enhanced neurite branching in both uninjured and injured DRG neurons. These actions were abrogated with concurrent knockdown of the Rb1 effector, E2F1. E2F1 operates as a divergent transcription factor and stimulates transcription and neuronal plasticity. In adult neurons, knockdown of Rb1 was not associated with cell death with no impact on the expression of activated caspase-3 or DNA damage markers (phosphohistone H2A.X). *In vivo* local knockdown at a nerve crush site enhanced regeneration of axons and promoted functional recovery in injured mice (Christie et al., 2014).

BRCA1 PROTECTS REGENERATING NEURONS

Breast cancer susceptibility protein 1 (BRCA1), a tumor suppressor, plays a critical role in DNA repair and CNS development (Miki et al., 1994). BRCA1 is expressed in proliferating embryonic and adult neural stem cells (Korhonen et al., 2003). Deleting BRCA1 in the CNS, results in various abnormalities in brain development and overall brain volume is severely reduced, apparent in the neocortex, cerebellum, and olfactory bulbs (Gowen et al., 1996; Pulvers and Huttner, 2009; Pao et al., 2014). BRCA1 is also involved in rat RGC neuron survival and DNA repair after exposure to ionizing radiation *in vitro* (Wang et al., 2018). In spinal cord injury, BRCA1 is highly expressed in spinal microglia (Noristani et al., 2017). In the PNS, BRCA1 is expressed in DRG, sciatic nerve and SCs in adult rat and after injury, is expressed at high levels in both proximal and distal nerve. BRCA1 expression was identified in injured SCs, neuronal satellite cells and axons and it translocated to neuronal nuclei. Interestingly, BRCA1 supported the regenerative phenotype in neurons such that its knockdown was associated with a decrease in neurite outgrowth and reduced branch length of injured sensory neurons *in vitro* (Krishnan et al., 2018b). In SCs BRCA1 depletion impaired SC proliferation. BRCA1 modulates oxidative stress in injured sensory neurons and SCs (Krishnan et al., 2018b). It appears critical in modulating DNA repair by preserving DNA integrity in neurons, particularly after injury through its nuclear enrichment. The role of BRCA1 in sensory neurons has taught us that DNA repair may be an intrinsic element of their acquisition of a regenerative phenotype. In addition to BRCA1, adult peripheral neurons constitutively express additional DNA repair molecules, such as 53BP1, important for their ongoing wellbeing.

APC AND ITS β -CATENIN PARTNER

The parallel but thus far largely unconnected impact of two critical tumor suppressor pathways, PTEN and Rb1, on post-mitotic adult sensory neurons was remarkable. BRCA1 appears to have a different operational mandate in neurons. Given all of these findings, however, we hypothesized that exploitation of a range of tumor-related pathways might be a general property of regenerating adult neurons. Along these lines, we chose to study yet an additional tumor suppressor pathway, APC and

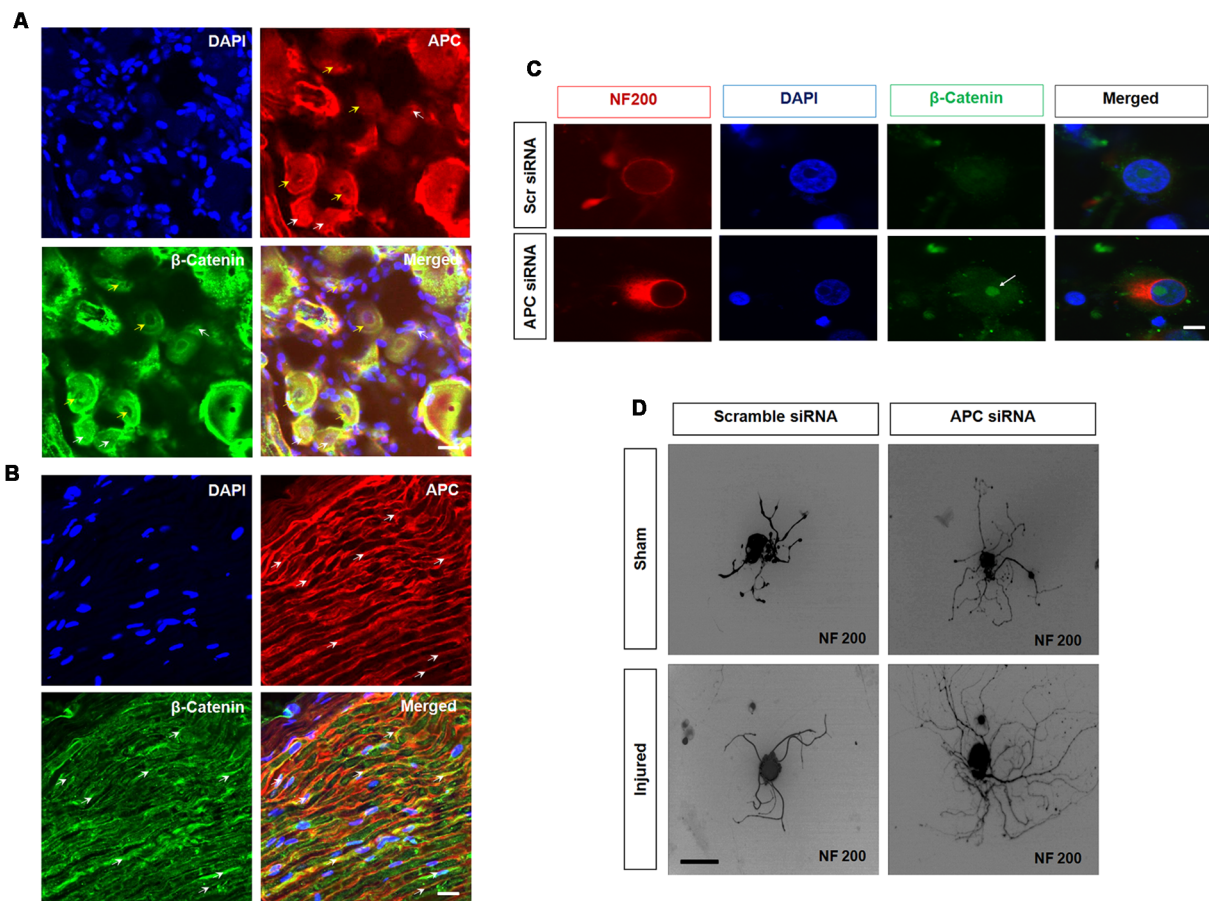


FIGURE 3 | Adenomatous polyposis coli (APC) and β -Catenin in sensory neurons. **(A,B)** APC and β -Catenin co-localize in the dorsal root ganglia (DRG) and sciatic nerve. **(A)** APC is expressed in β -catenin positive DRG neurons. Importantly, APC is prominently co-localized with β -Catenin in a subset of small (white arrow) and medium size (yellow arrow) uninjured DRG neurons. **(B)** Longitudinal section of uninjured sciatic nerve. APC (red, white arrow) and β -catenin (green, white arrow) showing colocalization. **(C)** Z stacks confocal picture demonstrate the nuclear localization of β -catenin in cultured DRG neurons with APC knockdown when compared to those exposed to scrambled control siRNA *in vitro*. Scale bar = 50 μ m. **(D)** Silencing APC by siRNA increased neurite outgrowth in cultured DRG neurons when compared to scrambled siRNA in both sham sciatic injury and sciatic axotomy pre-conditioning injury. Scale bar = 50 μ m (Duraikannu, original illustration).

its β -catenin pathway, important culprits in the development of colorectal tumors.

Wnt/ β -catenin signaling plays a significant role in neurodevelopment and neuronal plasticity (Tawak et al., 2011). The Wnt/ β -catenin pathway contributes toward oligodendrocyte and SC myelination; the expression of myelin genes, SC migration, and their proliferation in the PNS (Tawak et al., 2011). In Wnt signaling, β -catenin is an important multifunctional transcriptional protein, binding to APC and GSK3 β . A remarkable feature of β -catenin protein is that it promotes cell proliferation and resistance to apoptosis (Clevers, 2006; Shelton et al., 2006). APC is a binding partner to β -catenin that results in a destruction complex involving proteasomal degradation and transcriptional inhibition (Kimelman and Xu, 2006). Through this interaction, APC is involved in proliferation, apoptosis, cell adhesion, and migration (Hanson and Miller, 2005). APC activities also play a vital role in both the developing as well as adult nervous system (Bhat et al., 1994). APC is

expressed in neurites of neuroblastoma cells and cortical neurons (Morrison et al., 1997a,b). Loss of APC enhances β -catenin accumulation in the nucleus with its transcriptional partner T cell factor/lymphoid enhancer factor (TCF/LEF).

β -catenin expression influences neural proliferation and neuronal differentiation (Patapoutian and Reichardt, 2000) and it is involved in hippocampal neurogenesis (Peng et al., 2009). Furthermore, β -catenin phosphorylation at residue Y654 and Y142 and its nuclear localization increases axon growth and branching in hippocampal neurons through TCF4/ β dependent transcription (David et al., 2008). In post-mitotic neurons, it is involved in dendritogenesis, synaptogenesis and synaptic formation (Peng et al., 2009). Both Wnt and β -catenin combined regulate synaptic plasticity and axonal growth. In CNS neurons, N and C-terminal domains of β -catenin are involved in cell-cell adhesion and promotion of axonal branching (Elul et al., 2003). Increased expression of β -catenin and Wnt were observed after spinal transection in adult zebrafish and

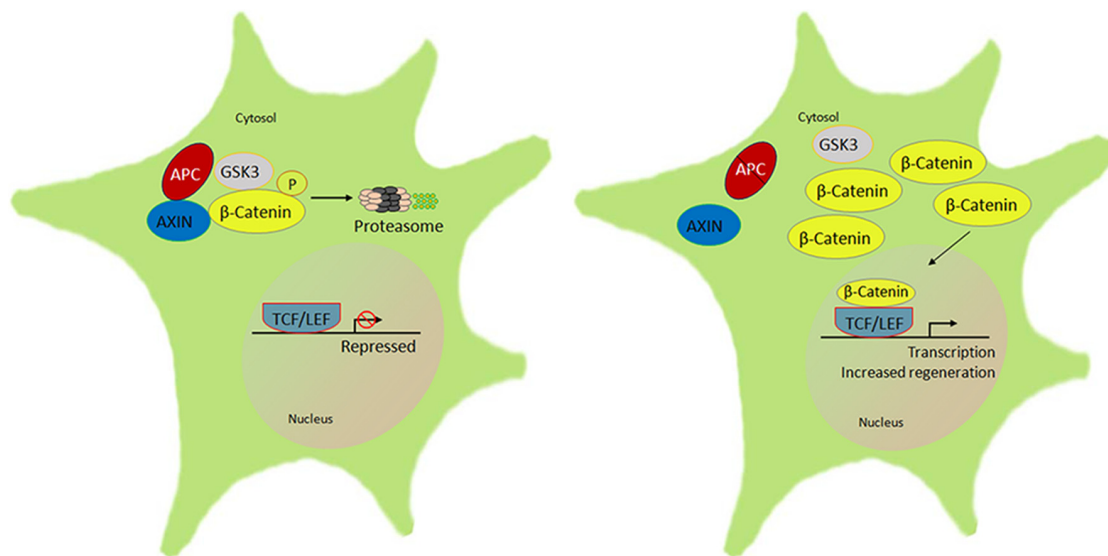


FIGURE 4 | Schematic of the β -catenin-lymphoid enhancer-binding factor/T cell factor (LEF/TCF) signal pathway that regulates peripheral neuron regeneration by APC knockdown. There is normally interaction of APC with AXIN and GSK3 that phosphorylates β -catenin to be rapidly degraded by the ubiquitin proteasome. In the absence or knockdown of APC signal with an altered AXIN-GSK3 β complex, β -catenin accumulates and forms a complex with LEF/TCF in the nucleus, which initiates transcription of downstream target genes, in turn to promote regeneration (Duraikannu, original illustration).

correlated with axonal regeneration and improved functional recovery (Strand et al., 2016). With spinal cord lesions, Wnt/ β -catenin signaling also regulates collagen type XII alpha 1 chain (col12a1) transcription and synthesis of Collagen XII by non-neuronal cells such as fibroblasts for the extracellular matrix (ECM). These actions promoted axon regeneration and functional recovery (Wehner et al., 2017). Knockdown of β -catenin showed a delay in axonal sorting whereas gain-of-function of β -catenin mutations resulted in accelerated sorting (Grigoryan et al., 2013).

In adult DRG sensory neurons, β -catenin was expressed widely among all sensory neurons including neuronal nuclei, and cytoplasm and was also identified in perineurial satellite cells. Axonal injury results in reduced β -catenin expression in neuronal nuclei, satellite cells and sciatic nerves. In contrast, its binding partner APC was reciprocally increased following axotomy injury. Notably, after injury, expression of APC was prominent within slower growing small nonpeptidergic IB4 DRG neurons and SCs, in a remarkable similarity to PTEN expression. Furthermore, the intensity of APC expression increased in motor neurons and regenerating axons. The rises of APC, considering its role to inactivate transcriptional-related targets, indicated that it might act as a regenerative “brake” on neurons. Indeed, both the APC and β -catenin partners are combinatorially expressed in DRG neurons and their axon branches (Figure 3). Overexpression of APC interacts with β -catenin to enhance proteasomal degradation and attenuate transcription. In sensory neurons, knockdown of APC increased β -catenin nuclear accumulation, was associated with upregulation TCF and lymphoid enhancing binding factor (LEF) transcription factors (Figure 4). In addition, knockdown of APC in adult DRG neurons increased neurite outgrowth of both uninjured and

preconditioned neurons (Duraikannu et al., 2018). Narciso et al. (2009), showed that β -catenin expression increased in Galectin-3 knockout mice associated with enhanced neuronal survival and axon regeneration after traumatic nerve lesions. Furthermore, interactions between β -catenin and TCF3 were required for SC myelination *in vivo* (Tawk et al., 2011). Inhibition of β -catenin and TCF activity impaired neurite outgrowth in DRG neurons *in vitro* (Duraikannu et al., 2018). *In vivo*, local knockdown of APC following nerve trunk crush injury using siRNA increased the repopulation of myelinated axons and was associated with improved indices of functional recovery. In keeping with the reciprocal actions of these partners, knockdown of APC led axons and SCs to express higher levels of β -catenin *in vivo*. Moreover, β -catenin appears to be required for SC proliferation *in vitro*, a critical partnering step in nerve regeneration (Narciso et al., 2009).

Overall, manipulation of the APC- β -catenin pathway has provided yet another example of how plasticity molecules are expressed in apparently stable and hard-wired neural systems. However, after injury, they play a role in supporting the plasticity essential for regeneration. In the case of APC, knockdown of its inhibitory impact releases β -catenin transcriptional activation required to support repair and outgrowth. Like PTEN and Rb1, APC is a new and important tumor suppressor in neurons that normally suppresses their growth. Whether this approach offers synergy with other tumor suppressor pathways is unclear at this time.

CONCLUSIONS

The primary goal of many endpoints in the clinical treatment of nerve injury and neuropathies is to identify improved functional

recovery. Here, we identify how that may be accomplished through the actions of neuronal growth factors but more recently by manipulating the intrinsic growth properties of adult neurons. These approaches operate downstream of growth factors, that have the potential for off-target actions and that have impacts limited to specific subtypes of neurons. Exogenous ES activates neuronal regenerative progress through a “brute force” reset of intrinsic neuron properties that recapitulates their injury response. By doing so, the approach exploits the known property of previously injured neurons to ramp up their regenerative machinery, the “preconditioning” response. Resurrection of developmental pathways to enhance regeneration in adults likely has more room for investigation. Recognition that the array of receptors and expression patterns of neurons differs between development and adulthood is essential toward further understanding of their potential role. Re-appropriation of pathways used by neurons in development by glial cells, as described with netrin-DCC-Unc5h, is an important example of this.

Here, we focus most of this review on novel intrinsic pathways that have remarkable impacts on regrowth, downstream from growth factor receptors. That all three pathways described here influence the development of neoplasms should not be seen as a disincentive for further consideration. It is unlikely that anatomically restricted administration and temporary use of knockdown during regeneration would replicate the complex and multistage prolonged processes required for oncogenesis. In the case of BRCA1, ongoing DNA repair during neuron reprogramming toward a regenerative state may be essential. Further work is required over how the growth pathways presented here, and very likely additional neuron growth pathways interact. It is not known whether they

operate synergistically with a downstream common impact on PI3K-pAkt signaling, an unequivocal and critical pathway that supports regrowth. It is also yet to be determined whether manipulation of intrinsic growth pathways might be coupled with added growth factors. Finally, the use of nonviral siRNA delivery has been an important part of regenerative studies using *in vivo* models. The elimination of viral delivery constructs will prove to be a major advantage to its use in humans and builds on the recognition that there is considerable extracellular trafficking capability in using siRNA. We have, for example, shown that siRNAs are routinely taken up by distal axons and retrogradely transported to their perikarya to knockdown “central” cellular gene expression. Improved approaches to enhance the stability of applied siRNAs and their access to penetrate the blood-brain barrier will be very welcomed.

AUTHOR CONTRIBUTIONS

AD: collated background literature, prepared the figures and wrote initial and revised versions of the manuscript prior to submission. DZ: the scope of the review article, wrote portions of the manuscript, and edited all versions prior to submission, including the final submitted version. AK and AC: contributed to the experimental work reviewed in this article, reviewed the intellectual content of the article and edited the final version.

ACKNOWLEDGMENTS

The review is based on work funded by the Canadian Institutes of Health Research. The authors are members of the Neuroscience and Mental Health Institute, University of Alberta.

REFERENCES

- Ackerman, S. L., Kozak, L. P., Przyborski, S. A., Rund, L. A., Boyer, B. B., and Knowles, B. B. (1997). The mouse rostral cerebellar malformation gene encodes an UNC-5-like protein. *Nature* 386, 838–842. doi: 10.1038/386838a0
- Acosta, C. G., Fábrega, A. R., Mascó, D. H., and López, H. S. (2001). A sensory neuron subpopulation with unique sequential survival dependence on nerve growth factor and basic fibroblast growth factor during development. *J. Neurosci.* 21, 8873–8885. doi: 10.1523/jneurosci.21-22-08873.2001
- Adler, C. E., Fetter, R. D., and Bargmann, C. I. (2006). UNC-6/Netrin induces neuronal asymmetry and defines the site of axon formation. *Nat. Neurosci.* 9, 511–518. doi: 10.1038/nn1666
- Adler, R., Landa, K. B., Manthorpe, M., and Varon, S. (1979). Cholinergic neuronotrophic factors: intraocular distribution of trophic activity for ciliary neurons. *Science* 204, 1434–1436. doi: 10.1126/science.451576
- Ali, I. U., Schriml, L. M., and Dean, M. (1999). Mutational spectra of PTEN/MMAC1 gene: a tumor suppressor with lipid phosphatase activity. *J. Natl. Cancer Inst.* 91, 1922–1932. doi: 10.1093/jnci/91.22.1922
- Al-Majed, A. A., Brushart, T. M., and Gordon, T. (2000a). Electrical stimulation accelerates and increases expression of BDNF and trkB mRNA in regenerating rat femoral motoneurons. *Eur. J. Neurosci.* 12, 4381–4390. doi: 10.1111/j.1460-9568.2000.01341.x
- Al-Majed, A. A., Neumann, C. M., Brushart, T. M., and Gordon, T. (2000b). Brief electrical stimulation promotes the speed and accuracy of motor axonal regeneration. *J. Neurosci.* 20, 2602–2608. doi: 10.1523/jneurosci.20-07-02602.2000
- Alrashdan, M. S., Park, J. C., Sung, M. A., Yoo, S. B., Jahng, J. W., Lee, T. H., et al. (2010). Thirty minutes of low intensity electrical stimulation promotes nerve regeneration after sciatic nerve crush injury in a rat model. *Acta Neurol. Belg.* 110, 168–179.
- Andrusiak, M. G., McClellan, K. A., Dugal-Tessier, D., Julian, L. M., Rodrigues, S. P., Park, D. S., et al. (2010). Rb/E2F regulates expression of neogenin during neuronal migration. *Mol. Cell Biol.* 31, 238–247. doi: 10.1128/MCB.00378-10
- Andrusiak, M. G., Vandenbosch, R., Park, D. S., and Slack, R. S. (2012). Therenoblastoma protein is essential for survival of postmitotic neurons. *J. Neurosci.* 32, 14809–14814. doi: 10.1523/JNEUROSCI.1912-12.2012
- Archer, F. R., Doherty, P., Collins, D., and Bolsover, S. R. (1999). CAMs and FGF cause a local submembrane calcium signal promoting axon outgrowth without a rise in bulk calcium concentration. *Eur. J. Neurosci.* 11, 3565–3573. doi: 10.1046/j.1460-9568.1999.00773.x
- Arenas, E., and Persson, H. (1994). Neurotrophin-3 prevents the death of adult central noradrenergic neurons *in vivo*. *Nature* 367, 368–371. doi: 10.1038/367368a0
- Arimura, N., and Kaibuchi, K. (2005). Key regulators in neuronal polarity. *Neuron* 48, 881–884. doi: 10.1016/j.neuron.2005.11.007
- Baloh, R. H., Gorodinsky, A., Golden, J. P., Tansey, M. G., Keck, C. L., Popescu, N. C., et al. (1998a). GFR α 3 is an orphan member of the GDNF/neurturin/persephin receptor family. *Proc. Natl. Acad. Sci. U S A* 95, 5801–5806. doi: 10.1073/pnas.95.10.5801
- Baloh, R. H., Tansey, M. G., Lampe, P. A., Fahrner, T. J., Enomoto, H., Simburger, K. S., et al. (1998b). Artemin, a novel member of the GDNF ligand family, supports peripheral and central neurons and signals through the GFR α 3-RET receptor complex. *Neuron* 21, 1291–1302. doi: 10.1016/s0896-6273(00)80649-2

- Barbin, G., Manthorpe, M., and Varon, S. (1984). Purification of the chick eye ciliary neuronotrophic factor. *J. Neurochem.* 43, 1468–1478. doi: 10.1111/j.1471-4159.1984.tb05410.x
- Bhat, R. V., Baraban, J. M., Johnson, R. C., Eipper, B. A., and Mains, R. E. (1994). High levels of expression of the tumor suppressor gene APC during development of the rat central nervous system. *J. Neurosci.* 14, 3059–3071. doi: 10.1523/jneurosci.14-05-03059.1994
- Boldyreva, M. A., Bondar, I. V., Stafeev, I. S., Makarevich, P. I., Beloglazova, I. B., Zubkova, E. S., et al. (2018). Plasmid-based gene therapy with hepatocyte growth factor stimulates peripheral nerve regeneration after traumatic injury. *Biomed. Pharmacother.* 101, 682–690. doi: 10.1016/j.biopha.2018.02.138
- Bordet, T., Schmalbruch, H., Pettmann, B., Hagege, A., Castelnau-Ptakhine, L., Kahn, A., et al. (1999). Adenoviral cardiotrophin-1 gene transfer protects pmn mice from progressive motor neuronopathy. *J. Clin. Invest.* 104, 1077–1085. doi: 10.1172/jci6265
- Bottaro, D. P., Rubin, J. S., Faletto, D. L., Chan, A. M., Kmiecik, T. E., Vande Woude, G. F., et al. (1991). Identification of the hepatocyte growth factor receptor as the c-met proto-oncogene product. *Science* 251, 802–804. doi: 10.1126/science.1846706
- Boucher, T. J., Okuse, K., Bennett, D. L., Munson, J. B., Wood, J. N., and McMahon, S. B. (2000). Potent analgesic effects of GDNF in neuropathic pain states. *Science* 290, 124–127. doi: 10.1126/science.290.5489.124
- Boyer, N. P., and Gupton, S. L. (2018). Revisiting Netrin-1: one who guides (axons). *Front. Cell. Neurosci.* 12:221. doi: 10.3389/fncel.2018.00221
- Braun, S., Croizat, B., Lagrange, M. C., Warter, J. M., and Poindron, P. (1996). Neurotrophins increase motoneurons' ability to innervate skeletal muscle fibers in rat spinal cord–human muscle cocultures. *J. Neurol. Sci.* 136, 17–23. doi: 10.1016/0022-510x(95)00315-s
- Briançon-Marjollet, A., Ghogha, A., Nawabi, H., Triki, I., Auziol, C., Fromont, S., et al. (2008). Trio mediates netrin-1-induced Rac1 activation in axon outgrowth and guidance. *Mol. Cell. Biol.* 28, 2314–2323. doi: 10.1128/MCB.00998-07
- Broderick, D. K., Di, C., Parrett, T. J., Samuels, Y. R., Cummins, J. M., McLendon, R. E., et al. (2004). Mutations of PIK3CA in anaplastic oligodendrogliomas, high-grade astrocytomas and medulloblastomas. *Cancer Res.* 64, 5048–5050. doi: 10.1158/0008-5472.CAN-04-1170
- Brunet, A., Datta, S. R., and Greenberg, M. E. (2001). Transcription-dependent and -independent control of neuronal survival by the PI3K-Akt signaling pathway. *Curr. Opin. Neurobiol.* 11, 297–305. doi: 10.1016/s0959-4388(00)00211-7
- Brushart, T. M., Hoffman, P. N., Royall, R. M., Murinson, B. B., Witzel, C., and Gordon, T. (2002). Electrical stimulation promotes motoneuron regeneration without increasing its speed or conditioning the neuron. *J. Neurosci.* 22, 6631–6638. doi: 10.1523/jneurosci.22-15-06631.2002
- Brussee, V., Cunningham, F. A., and Zochodne, D. W. (2004). Direct insulin signaling of neurons reverses diabetic neuropathy. *Diabetes* 53, 1824–1830. doi: 10.2337/diabetes.53.7.1824
- Burnett, M. G., and Zager, E. L. (2004). Pathophysiology of peripheral nerve injury: a brief review. *Neurosurg. Focus* 16:E1. doi: 10.3171/foc.2004.16.5.2
- Carpenter, G., and Cohen, S. (1979). Epidermal growth factor. *Annu. Rev. Biochem.* 48, 193–216. doi: 10.1146/annurev.bi.48.070179.001205
- Chan, C. C., Khodarahmi, K., Liu, J., Sutherland, D., Oshchepok, L. W., Steeves, J. D., et al. (2005). Dose-dependent beneficial and detrimental effects of ROCK inhibitor Y27632 on axonal sprouting and functional recovery after rat spinal cord injury. *Exp. Neurol.* 196, 352–364. doi: 10.1016/j.expneurol.2005.08.011
- Chang, C., Adler, C. E., Krause, M., Clark, S. G., Gertler, F. B., Tessier-Lavigne, M., et al. (2006). MIG-10/lamellipodin and AGE-1/PI3K promote axon guidance and outgrowth in response to slit and netrin. *Curr. Biol.* 16, 854–862. doi: 10.1016/j.cub.2006.03.083
- Chao, M. V. (2003). Neurotrophins and their receptors: a convergence point for many signalling pathways. *Nat. Rev. Neurosci.* 4, 299–309. doi: 10.1038/nrn1078
- Chen, C., Bai, G. C., Jin, H. L., Lei, K., and Li, K. X. (2018). Local injection of bone morphogenetic protein 7 promotes neuronal regeneration and motor function recovery after acute spinal cord injury. *Neural Regen. Res.* 13, 1054–1060. doi: 10.4103/1673-5374.233449
- Chen, Z. Y., He, Z. Y., He, C., Lu, C. L., and Wu, X. F. (2000). Human glial cell-line-derived neurotrophic factor: a structure-function analysis. *Biochem. Biophys. Res. Commun.* 268, 692–696. doi: 10.1006/bbrc.2000.2196
- Chen, Y. Y., McDonald, D., Cheng, C., Magnowski, B., Durand, J., and Zochodne, D. W. (2005). Axon and Schwann cell partnership during nerve regrowth. *J. Neuropathol. Exp. Neurol.* 64, 613–622. doi: 10.1097/01.jnen.0000171650.94341.46
- Chen, Z. L., Yu, W. M., and Strickland, S. (2007). Peripheral regeneration. *Annu. Rev. Neurosci.* 30, 209–233. doi: 10.1146/annurev.neuro.30.051606.094337
- Chen, Z. W., and Wang, M. S. (1995). Effects of nerve growth factor on crushed sciatic nerve regeneration in rats. *Microsurgery* 16, 547–551. doi: 10.1002/micr.1920160808
- Cheng, C., Webber, C. A., Wang, J., Xu, Y., Martinez, J. A., Liu, W. Q., et al. (2008). Activated RHOA and peripheral axon regeneration. *Exp. Neurol.* 212, 358–369. doi: 10.1016/j.expneurol.2008.04.023
- Chevrel, G., Hohlfeld, R., and Sendtner, M. (2006). The role of neurotrophins in muscle under physiological and pathological conditions. *Muscle Nerve* 33, 462–476. doi: 10.1002/mus.20444
- Cho, H. J., Kim, J. K., Park, H. C., Kim, J. K., Kim, D. S., Ha, S. O., et al. (1998). Changes in brain-derived neurotrophic factor immunoreactivity in rat dorsal root ganglia, spinal cord, and gracile nuclei following cut or crush injuries. *Exp. Neurol.* 154, 224–230. doi: 10.1006/exnr.1998.6936
- Choi, J., Ko, J., Racz, B., Burette, A., Lee, J. R., Kim, S., et al. (2005). Regulation of dendritic spine morphogenesis by insulin receptor substrate 53, a downstream effector of Rac1 and Cdc42 small GTPases. *J. Neurosci.* 25, 869–879. doi: 10.1523/JNEUROSCI.3212-04.2005
- Chou, H. J., Lai, D. M., Huang, C. W., McLennan, I. S., Wang, H. D., and Wang, P. Y. (2013). BMP4 is a peripherally-derived factor for motor neurons and attenuates glutamate-induced excitotoxicity *in vitro*. *PLoS One* 8:e58441. doi: 10.1371/journal.pone.0058441
- Christie, K. J., Krishnan, A., Martinez, J. A., Purdy, K., Singh, B., Eaton, S., et al. (2014). Enhancing adult nerve regeneration through the knockdown of retinoblastoma protein. *Nat. Commun.* 5:3670. doi: 10.1038/ncomms4670
- Christie, K. J., Webber, C. A., Martinez, J. A., Singh, B., and Zochodne, D. W. (2010). PTEN inhibition to facilitate intrinsic regenerative outgrowth of adult peripheral axons. *J. Neurosci.* 30, 9306–9315. doi: 10.1523/JNEUROSCI.6271-09.2010
- Cirulli, V., and Yebra, M. (2007). Netrins: beyond the brain. *Nat. Rev. Mol. Cell Biol.* 8, 296–306. doi: 10.1038/nrm2142
- Clarke, A. R., Maandag, E. R., van Roon, M., van der Lugt, N. M., van der Valk, M., Hooper, M. L., et al. (1992). Requirement for a functional Rb-1 gene in murine development. *Nature* 359, 328–330. doi: 10.1038/359328a0
- Clevers, H. (2006). Wnt/ β -catenin signaling in development and disease. *Cell* 127, 469–480. doi: 10.1016/j.cell.2006.10.018
- Collins, M. J., Napoli, I., Ribeiro, S., Roberts, S., and Lloyd, A. C. (2012). Loss of Rb cooperates with Ras to drive oncogenic growth in mammalian cells. *Curr. Biol.* 22, 1765–1773. doi: 10.1016/j.cub.2012.07.040
- Culmsee, C., Stumm, R. K., Schäfer, M. K., Weihe, E., and Kriegstein, J. (1999a). “Neuroprotection by drug-induced growth factors,” in *Pharmacology of Cerebral Ischemia* 1998, ed. J. Kriegstein (Stuttgart, Germany: Medpharm Scientific), 333–348.
- Culmsee, C., Stumm, R. K., Schäfer, M. K., Weihe, E., and Kriegstein, J. (1999b). Clenbuterol induces growth factor mRNA, activates astrocytes and protects rat brain tissue against ischemic damage. *Eur. J. Pharmacol.* 379, 33–45. doi: 10.1016/s0014-2999(99)00452-5
- Curtis, R., Scherer, S. S., Somogyi, R., Adryan, K. M., Ip, N. Y., Zhu, Y., et al. (1994). Retrograde axonal transport of LIF is increased by peripheral nerve injury: correlation with increased LIF expression in distal nerve. *Neuron* 12, 191–204. doi: 10.1016/0896-6273(94)90163-5
- Curtis, R., Tonra, J. R., Stark, J. L., Adryan, K. M., Park, J. S., Cliffer, K. D., et al. (1998). Neuronal injury increases retrograde axonal transport of the neurotrophins to spinal sensory neurons and motor neurons via multiple receptor mechanisms. *Mol. Cell. Neurosci.* 12, 105–118. doi: 10.1006/mcne.1998.0704
- Davey, F., Hilton, M., and Davies, A. M. (2000). Cooperation between HGF and CNTF in promoting the survival and growth of sensory and parasympathetic neurons. *Mol. Cell. Neurosci.* 15, 79–87. doi: 10.1006/mcne.1999.0803
- David, M. D., Yeramian, A., Duñach, M., Llovera, M., Cantí, C., de Herreros, A. G., et al. (2008). Signalling by neurotrophins and hepatocyte growth factor regulates axon morphogenesis by differential β -catenin phosphorylation. *J. Cell Sci.* 121, 2718–2730. doi: 10.1242/jcs.029660

- Deiner, M. S., and Sretavan, D. W. (1999). Altered midline axon pathways and ectopic neurons in the developing hypothalamus of netrin-1- and DCC-deficient mice. *J. Neurosci.* 19, 9900–9912. doi: 10.1523/JNEUROSCI.19-22-09900.1999
- De la Hoz, C. L., Cheng, C., Fernyhough, P., and Zochodne, D. W. (2017). A model of chronic diabetic polyneuropathy: benefits from intranasal insulin are modified by sex and RAGE deletion. *Am. J. Physiol. Endocrinol. Metab.* 312, E407–E419. doi: 10.1152/ajpendo.00444.2016
- Deng, Y., Xu, Y., Liu, H., Peng, H., Tao, Q., Liu, H., et al. (2018). Electrical stimulation promotes regeneration and re-myelination of axons of injured facial nerve in rats. *Neurol. Res.* 40, 231–238. doi: 10.1080/01616412.2018.1428390
- Derby, A., Engleman, V. W., Frierich, G. E., Neises, G., Rapp, S. R., and Roufa, D. G. (1993). Nerve growth factor facilitates regeneration across nerve gaps: morphological and behavioral studies in rat sciatic nerve. *Exp. Neurol.* 119, 176–191. doi: 10.1006/exnr.1993.1019
- Devaskar, S. U., Giddings, S. J., Rajakumar, P. A., Carnaghi, L. R., Menon, R. K., and Zahm, D. S. (1994). Insulin gene expression and insulin synthesis in mammalian neuronal cells. *J. Biol. Chem.* 269, 8445–8454.
- Di Cristofano, A., Kotsi, P., Peng, Y. F., Cordon-Cardo, C., Elkon, K. B., and Pandolfi, P. P. (1999). Impaired Fas response and autoimmunity in Pten^{+/-} mice. *Science* 285, 2122–2125. doi: 10.1126/science.285.5436.2122
- DiStefano, P. S., and Curtis, R. (1994). Receptor mediated retrograde axonal transport of neurotrophic factors is increased after peripheral nerve injury. *Prog. Brain Res.* 103, 35–42. doi: 10.1016/s0079-6123(08)61124-3
- Dreyfus, C. F. (1989). Effects of nerve growth factor on cholinergic brain neurons. *Trends Pharmacol. Sci.* 10, 145–149. doi: 10.1016/0165-6147(89)90166-1
- Dubreuil, C. I., Winton, M. J., and McKerracher, L. (2003). Rho activation patterns after spinal cord injury and the role of activated Rho in apoptosis in the central nervous system. *J. Cell Biol.* 162, 233–243. doi: 10.1083/jcb.200301080
- Dun, X. P., and Parkinson, D. B. (2017). Role of netrin-1 signaling in nerve regeneration. *Int. J. Mol. Sci.* 18:E491. doi: 10.3390/ijms18030491
- Duraikannu, A., Martinez, J. A., Chandrasekhar, A., and Zochodne, D. W. (2018). Expression and manipulation of the APC- β -catenin pathway during peripheral neuron regeneration. *Sci. Rep.* 8:13197. doi: 10.1038/s41598-018-31167-1
- Ebendal, T., Bengtsson, H., and Söderström, S. (1998). Bone morphogenetic proteins and their receptors: potential functions in the brain. *J. Neurosci. Res.* 51, 139–146. doi: 10.1002/(sici)1097-4547(19980115)51:2<139::aid-jnr2>3.0.co;2-e
- Eggers, R., Hendriks, W. T., Tannemaat, M. R., van Heerikhuizen, J. J., Pool, C. W., Carlstedt, T. P., et al. (2008). Neuroregenerative effects of lentiviral vector-mediated GDNF expression in reimplanted ventral roots. *Mol. Cell Neurosci.* 39, 105–117. doi: 10.1016/j.mcn.2008.05.018
- Ekström, P. A., Kerekes, N., and Hökfelt, T. (2000). Leukemia inhibitory factor null mice: unhampered *in vitro* outgrowth of sensory axons but reduced stimulatory potential by nerve segments. *Neurosci. Lett.* 281, 107–110. doi: 10.1016/s0304-3940(00)00816-8
- Elul, T. M., Kimes, N. E., Kohwi, M., and Reichardt, L. F. (2003). N- and C-Terminal domains of β -catenin, respectively, are required to initiate and shape axon arbors of retinal ganglion cells *in vivo*. *J. Neurosci.* 23, 6567–6575. doi: 10.1523/JNEUROSCI.23-16-06567.2003
- English, A. W., Schwartz, G., Meador, W., Sabatier, M. J., and Mulligan, A. (2007). Electrical stimulation promotes peripheral axon regeneration by enhanced neuronal neurotrophin signaling. *Dev. Neurobiol.* 67, 158–172. doi: 10.1002/dneu.20339
- Enokido, Y., de Sauvage, F., Hongo, J. A., Ninkina, N., Rosenthal, A., Buchman, V. L., et al. (1998). GFR α -4 and the tyrosine kinase Ret form a functional receptor complex for persephin. *Curr. Biol.* 8, 1019–1022. doi: 10.1016/s0960-9822(07)00422-8
- Ferguson, K. L., McClellan, K. A., Vanderluit, J. L., McIntosh, W. C., Schuurmans, C., Polleux, F., et al. (2005). A cell-autonomous requirement for the cell cycle regulatory protein, Rb, in neuronal migration. *EMBO J.* 24, 4381–4391. doi: 10.1038/sj.emboj.7600887
- Ferguson, K. L., Vanderluit, J. L., Hébert, J. M., McIntosh, W. C., Tibbo, E., MacLaurin, J. G., et al. (2002). Telencephalon-specific Rb knockouts reveal enhanced neurogenesis, survival and abnormal cortical development. *EMBO J.* 21, 3337–3346. doi: 10.1093/emboj/cdf338
- Fernyhough, P., Mill, J. F., Roberts, J. L., and Ishii, D. N. (1989). Stabilization of tubulin mRNAs by insulin and insulin-like growth factor I during neurite formation. *Mol. Brain Res.* 6, 109–120. doi: 10.1016/0169-328x(89)90044-2
- Fernyhough, P., Willars, G. B., Lindsay, R. M., and Tomlinson, D. R. (1993). Insulin and insulin-like growth factor I enhance regeneration in cultured adult rat sensory neurones. *Brain Res.* 607, 117–124. doi: 10.1016/0006-8993(93)91496-f
- Foster, E., Robertson, B., and Fried, K. (1994). trkB-like immunoreactivity in rat dorsal root ganglia following sciatic nerve injury. *Brain Res.* 659, 267–271. doi: 10.1016/0006-8993(94)90891-5
- Fu, P. C., Tang, R. H., Wan, Y., Xie, M. J., Wang, W., Luo, X., et al. (2016). ROCK inhibition with fasudil promotes early functional recovery of spinal cord injury in rats by enhancing microglia phagocytosis. *J. Huazhong Univ. Sci. Technol. Med. Sci.* 36, 31–36. doi: 10.1007/s11596-016-1537-3
- Fujimoto, E., Mizoguchi, A., Hanada, K., Yajima, M., and Ide, C. (1997). Basic fibroblast growth factor promotes extension of regenerating axons of peripheral nerve. *In vivo* experiments using a Schwann cell basal lamina tube model. *J. Neurocytol.* 26, 511–528. doi: 10.1023/A:1015410203132
- Fukuoka, T., Kondo, E., Dai, Y., Hashimoto, N., and Noguchi, K. (2001). Brain-derived neurotrophic factor increases in the uninjured dorsal root ganglion neurons in selective spinal nerve ligation model. *J. Neurosci.* 21, 4891–4900. doi: 10.1523/JNEUROSCI.21-13-04891.2001
- Gatzinsky, K. P., Holtmann, B., Daraie, B., Berthold, C. H., and Sendtner, M. (2003). Early onset of degenerative changes at nodes of Ranvier in α -motor axons of Cntf null ($-/-$) mutant mice. *Glia.* 42, 340–349. doi: 10.1002/glia.10221
- Geng, S. J., Liao, F. F., Dang, W. H., Ding, X., Liu, X. D., Cai, J., et al. (2010). Contribution of the spinal cord BDNF to the development of neuropathic pain by activation of the NR2B-containing NMDA receptors in rats with spinal nerve ligation. *Exp. Neurol.* 222, 256–266. doi: 10.1016/j.expneurol.2010.01.003
- Geoffroy, C. G., Hilton, B. J., Tetzlaff, W., and Zheng, B. (2016). Evidence for an age-dependent decline in axon regeneration in the adult mammalian central nervous system. *Cell Rep.* 15, 238–246. doi: 10.1016/j.celrep.2016.03.028
- Geremia, N. M., Gordon, T., Brushart, T. M., Al-Majed, A. A., and Verge, V. M. (2007). Electrical stimulation promotes sensory neuron regeneration and growth-associated gene expression. *Exp. Neurol.* 205, 347–359. doi: 10.1016/j.expneurol.2007.01.040
- Giacinti, C., and Giordano, A. (2006). RB and cell cycle progression. *Oncogene* 25, 5220–5227. doi: 10.1038/sj.onc.1209615
- Golden, J. P., DeMaro, J. A., Osborne, P. A., Milbrandt, J., and Johnson, E. M. Jr. (1999). Expression of neurturin, GDNF, and GDNF family-receptor mRNA in the developing and mature mouse. *Exp. Neurol.* 158, 504–528. doi: 10.1006/exnr.1999.7127
- Gordon, T., Amirjani, N., Edwards, D. C., and Chan, K. M. (2010). Brief post-surgical electrical stimulation accelerates axon regeneration and muscle reinnervation without affecting the functional measures in carpal tunnel syndrome patients. *Exp. Neurol.* 223, 192–202. doi: 10.1016/j.expneurol.2009.09.020
- Gordon, T., Brushart, T. M., Amirjani, N., and Chan, K. M. (2007). The potential of electrical stimulation to promote functional recovery after peripheral nerve injury—comparisons between rats and humans. *Acta Neurochir.* 100, 3–11. doi: 10.1007/978-3-211-72958-8_1
- Gordon, T., Brushart, T. M., and Chan, K. M. (2008). Augmenting nerve regeneration with electrical stimulation. *Neurol. Res.* 30, 1012–1022. doi: 10.1179/174313208x362488
- Gordon, T., Chan, K. M., Sulaiman, O. A., Udina, E., Amirjani, N., and Brushart, T. M. (2009). Accelerating axon growth to overcome limitations in functional recovery after peripheral nerve injury. *Neurosurgery* 65, A132–A144. doi: 10.1227/01.neu.0000335650.09473.d3
- Gospodarowicz, D. (1979). Fibroblast and epidermal growth factors: their uses *in vivo* and *in vitro* in studies on cell functions and cell transplantation. *Mol. Cell. Biochem.* 25, 79–110. doi: 10.1007/bf00228991
- Gospodarowicz, D., Cheng, J., Lui, G. M., Baird, A., and Böhlent, P. (1984). Isolation of brain fibroblast growth factor by heparin-Sepharose affinity

- chromatography: identity with pituitary fibroblast growth factor. *Proc. Natl. Acad. Sci. U S A* 81, 6963–6967. doi: 10.1073/pnas.81.22.6963
- Govind, S., Kozma, R., Monfries, C., Lim, L., and Ahmed, S. (2001). Cdc42Hs facilitates cytoskeletal reorganization and neurite outgrowth by localizing the 58-kD insulin receptor substrate to filamentous actin. *J. Cell Biol.* 152, 579–594. doi: 10.1083/jcb.152.3.579
- Gowen, L. C., Johnson, B. L., Latour, A. M., Sulik, K. K., and Koller, B. H. (1996). Brca1 deficiency results in early embryonic lethality characterized by neuroepithelial abnormalities. *Nat. Genet.* 12, 191–194. doi: 10.1038/ng0296-191
- Grigoryan, T., Stein, S., Qi, J., Wende, H., Garratt, A. N., Nave, K. A., et al. (2013). Wnt/Rspondin/ β -catenin signals control axonal sorting and lineage progression in Schwann cell development. *Proc. Natl. Acad. Sci. U S A* 110, 18174–18179. doi: 10.1073/pnas.1310490110
- Grothe, C., Meisinger, C., and Claus, P. (2001). *In vivo* expression and localization of the fibroblast growth factor system in the intact and lesioned rat peripheral nerve and spinal ganglia. *J. Comp. Neurol.* 434, 342–357. doi: 10.1002/cne.1181
- Grothe, C., and Nikkiah, G. (2001). The role of basic fibroblast growth factor in peripheral nerve regeneration. *Anat. Embryol.* 204, 171–177. doi: 10.1007/s004290100205
- Guha, U., Gomes, W. A., Samanta, J., Gupta, M., Rice, F. L., and Kessler, J. A. (2004). Target-derived BMP signaling limits sensory neuron number and the extent of peripheral innervation *in vivo*. *Development* 131, 1175–1186. doi: 10.1242/dev.01013
- Guo, G., Kan, M., Martinez, J. A., and Zochodne, D. W. (2011). Local insulin and the rapid regrowth of diabetic epidermal axons. *Neurobiol. Dis.* 43, 414–421. doi: 10.1016/j.nbd.2011.04.012
- Guo, G., Singh, V., and Zochodne, D. W. (2014). Growth and turning properties of adult glial cell-derived neurotrophic factor coreceptor $\alpha 1$ nonpeptidergic sensory neurons. *J. Neuropathol. Exp. Neurol.* 73, 820–836. doi: 10.1097/NEN.0000000000000101
- Haastert, T. K., Schmitte, R., Korte, N., Klode, D., Ratzka, A., and Grothe, C. (2011). Electrical stimulation accelerates axonal and functional peripheral nerve regeneration across long gaps. *J. Neurotrauma*. 28, 661–674. doi: 10.1089/neu.2010.1637
- Hammarberg, H., Piehl, F., Risling, M., and Cullheim, S. (2000). Differential regulation of trophic factor receptor mRNAs in spinal motoneurons after sciatic nerve transection and ventral root avulsion in the rat. *J. Comp. Neurol.* 426, 587–601. doi: 10.1002/1096-9861(20001030)426:4<587::aid-cne7>3.0.co;2-r
- Hanson, C. A., and Miller, J. R. (2005). Non-traditional roles for the adenomatous polyposis coli (APC) tumor suppressor protein. *Gene* 361, 1–12. doi: 10.1016/j.gene.2005.07.024
- Hatten, M. E., Lynch, M., Rydel, R. E., Sanchez, J., Joseph-Silverstein, J., Moscatelli, D., et al. (1988). *in vitro* neurite extension by granule neurons is dependent upon astroglial-derived fibroblast growth factor. *Dev. Biol.* 125, 280–289. doi: 10.1016/0012-1606(88)90211-4
- Heinrich, P. C., Behrmann, I., Müller-Newen, G., Schaper, F., and Graeve, L. (1998). Interleukin-6-type cytokine signalling through the gp130/Jak/STAT pathway. *Biochem. J.* 334, 297–314. doi: 10.1042/bj3340297
- Helfand, S. L., Smith, G. A., and Wessells, N. K. (1976). Survival and development in culture of dissociated parasympathetic neurons from ciliary ganglia. *Dev. Biol.* 50, 541–547. doi: 10.1016/0012-1606(76)90174-3
- Hempstead, B. L., Martin-Zanca, D., Kaplan, D. R., Parada, L. F., and Chao, M. V. (1991). High-affinity NGF binding requires coexpression of the trk proto-oncogene and the low-affinity NGF receptor. *Nature* 350, 678–683. doi: 10.1038/350678a0
- Henderson, C. E., Camu, W., Mettling, C., Gouin, A., Poulsen, K., Karihaloo, M., et al. (1993). Neurotrophins promote motor neuron survival and are present in embryonic limb bud. *Nature* 363, 266–270. doi: 10.1038/363266a0
- Heuckeroth, R. O., Enomoto, H., Grider, J. R., Golden, J. P., Hanke, J. A., Jackman, A., et al. (1999). Gene targeting reveals a critical role for neurturin in the development and maintenance of enteric, sensory, and parasympathetic neurons. *Neuron* 22, 253–263. doi: 10.1016/s0896-6273(00)81087-9
- Heumann, R., Korsching, S., Bandtlow, C., and Thoenen, H. (1987). Changes of nerve growth factor synthesis in nonneuronal cells in response to sciatic nerve transection. *J. Cell Biol.* 104, 1623–1631. doi: 10.1083/jcb.104.6.1623
- Hiraga, A., Kuwabara, S., Doya, H., Kanai, K., Fujitani, M., Taniguchi, J., et al. (2006). Rho-kinase inhibition enhances axonal regeneration after peripheral nerve injury. *J. Peripher. Nerv. Syst.* 11, 217–224. doi: 10.1111/j.1529-8027.2006.00091.x
- Hoke, A., Cheng, C., and Zochodne, D. W. (2000). Expression of glial cell line-derived neurotrophic factor family of growth factors in peripheral nerve injury in rats. *Neuroreport* 11, 1651–1654. doi: 10.1097/00001756-200006050-00011
- Hoke, A., Gordon, T., Zochodne, D. W., and Sulaiman, O. A. (2002). A decline in glial cell-line-derived neurotrophic factor expression is associated with impaired regeneration after long-term Schwann cell denervation. *Exp. Neurol.* 173, 77–85. doi: 10.1006/exnr.2001.7826
- Hoke, A., Sun, H., Gordon, T., and Zochodne, D. W. (2001). Do denervated peripheral nerve trunks become ischemic? The impact of chronic denervation on vasa nervorum. *Exp. Neurol.* 172, 398–406. doi: 10.1006/exnr.2001.7808
- Horger, B. A., Nishimura, M. C., Armanini, M. P., Wang, L. C., Poulsen, K. T., Rosenblad, C., et al. (1998). Neurturin exerts potent actions on survival and function of midbrain dopaminergic neurons. *J. Neurosci.* 18, 4929–4937. doi: 10.1523/JNEUROSCI.18-13-04929.1998
- Horie, H., Bando, Y., Chi, H., and Takenaka, T. (1991). NGF enhances neurite regeneration from nerve-transected terminals of young adult and aged mouse dorsal root ganglia *in vitro*. *Neurosci. Lett.* 121, 125–128. doi: 10.1016/0304-3940(91)90665-g
- Hoybergs, Y. M., and Meert, T. F. (2007). The effect of low-dose insulin on mechanical sensitivity and allodynia in type I diabetes neuropathy. *Neurosci. Lett.* 417, 149–154. doi: 10.1016/j.neulet.2007.02.087
- Hu, J., and Selzer, M. E. (2017). RhoA as a target to promote neuronal survival and axon regeneration. *Neural Regen Res.* 12, 525–528. doi: 10.4103/1673-5374.205080
- Huang, E. J., and Reichardt, L. F. (2001). Neurotrophins: roles in neuronal development and function. *Annu. Rev. Neurosci.* 24, 677–736. doi: 10.1146/annurev.neuro.24.1.677
- Huang, E. J., and Reichardt, L. F. (2003). Trk receptors: roles in neuronal signal transduction. *Annu. Rev. Biochem.* 72, 609–642. doi: 10.1146/annurev.biochem.72.121801.161629
- Huang, J., Ye, Z., Hu, X., Lu, L., and Luo, Z. (2010). Electrical stimulation induces calcium-dependent release of NGF from cultured Schwann cells. *Glia* 58, 622–631. doi: 10.1002/glia.20951
- Huerta, J. J., Diaz-Trelles, R., Naves, F. J., Llamas, M. M., Del Valle, M. E., and Vega, J. A. (1996). Epidermal growth factor receptor in adult human dorsal root ganglia. *Anat. Embryol.* 194, 253–257. doi: 10.1007/bf00187136
- Hyman, C., Juhasz, M., Jackson, C., Wright, P., Ip, N. Y., and Lindsay, R. M. (1994). Overlapping and distinct actions of the neurotrophins BDNF, NT-3, and NT-4/5 on cultured dopaminergic and GABAergic neurons of the ventral mesencephalon. *J. Neurosci.* 14, 335–347. doi: 10.1523/JNEUROSCI.14-01-00335.1994
- Ichikawa, H., Itota, T., Nishitani, Y., Torii, Y., Inoue, K., and Sugimoto, T. (2000). Osteopontin-immunoreactive primary sensory neurons in the rat spinal and trigeminal nervous systems. *Brain Res.* 863, 276–281. doi: 10.1016/s0006-8993(00)02126-0
- Ide, C. (1996). Peripheral nerve regeneration. *Neurosci. Res.* 25, 101–121. doi: 10.1016/0168-0102(96)01042-5
- Ikeda-Miyagawa, Y., Kobayashi, K., Yamanaka, H., Okubo, M., Wang, S., Dai, Y., et al. (2015). Peripherally increased artemin is a key regulator of TRPA1/V1 expression in primary afferent neurons. *Mol. Pain* 11:8. doi: 10.1186/s12990-015-0004-7
- Imamura, T., Tokita, Y., and Mitsui, Y. (1988). Purification of basic FGF receptors from rat brain. *Biochem. Biophys. Res. Commun.* 55, 583–590. doi: 10.1016/s0006-291x(88)80534-5
- Ito, Y., Yamamoto, M., Li, M., Mitsuma, N., Tanaka, F., Doyu, M., et al. (2000). Temporal expression of mRNAs for neurotrophic cytokines, interleukin-11 (IL-11), oncostatin M (OSM), cardiotrophin-1 (CT-1) and their receptors (IL-11R α and OSMR β) in peripheral nerve injury. *Neurochem. Res.* 25, 1113–1118. doi: 10.1023/A:1007674113440
- Jacks, T., Fazeli, A., Schmitt, E. M., Bronson, R. T., Goodell, M. A., and Weinberg, R. A. (1992). Effects of an Rb mutation in the mouse. *Nature* 359, 295–300. doi: 10.1038/359295a0

- Jakobiec, F. A., Tso, M. O., Zimmerman, L. E., and Danis, P. (1977). Retinoblastoma and intracranial malignancy. *Cancer* 39, 2048–2058. doi: 10.1002/1097-0142(197705)39:5<2048::aid-cnrcr2820390522>3.0.co;2-9
- Jander, S., Bussini, S., Neuen-Jacob, E., Bosse, F., Menge, T., Müller, H. W., et al. (2002). Osteopontin: a novel axon-regulated Schwann cell gene. *J. Neurosci. Res.* 67, 156–166. doi: 10.1002/jnr.10099
- Jeong, D. G., Park, W. K., and Park, S. (2008). Artemin activates axonal growth via SFK and ERK-dependent signalling pathways in mature dorsal root ganglia neurons. *Cell Biochem. Funct.* 26, 210–220. doi: 10.1002/cbf.1436
- Ji, R. R., Zhang, Q., Zhang, X., Piehl, F., Reilly, T., Pettersson, R. F., et al. (1995). Prominent expression of bFGF in dorsal root ganglia after axotomy. *Eur. J. Neurosci.* 7, 2458–2468. doi: 10.1111/j.1460-9568.1995.tb01044.x
- Jiang, H., Guo, W., Liang, X., and Rao, Y. (2005). Both the establishment and the maintenance of neuronal polarity require active mechanisms: critical roles of GSK-3 β and its upstream regulators. *Cell* 120, 123–135. doi: 10.1016/s0092-8674(04)01258-9
- Jiang, Y., Min-tai, L., and Gershon, M. D. (2003). Netrins and DCC in the guidance of migrating neural crest-derived cells in the developing bowel and pancreas. *Dev. Biol.* 258, 364–384. doi: 10.1016/s0012-1606(03)00136-2
- Joshi, A. R., Bobylev, I., Zhang, G., Sheikh, K. A., and Lehmann, H. C. (2015). Inhibition of Rho-kinase differentially affects axon regeneration of peripheral motor and sensory nerves. *Exp. Neurol.* 263, 28–38. doi: 10.1016/j.expneurol.2014.09.012
- Jungnickel, J., Haase, K., Konitzer, J., Timmer, M., and Grothe, C. (2006). Faster nerve regeneration after sciatic nerve injury in mice over-expressing basic fibroblast growth factor. *J. Neurobiol.* 66, 940–948. doi: 10.1002/neu.20265
- Kaplan, D. R., and Miller, F. D. (1997). Signal transduction by the neurotrophin receptors. *Curr. Opin. Cell Biol.* 9, 213–221. doi: 10.1016/S0955-0674(97)80065-8
- Kashiba, H., and Senba, E. (1999). Up and down-regulation of BDNF mRNA in distinct subgroups of rat sensory neurons after axotomy. *Neuro. Report.* 10, 3561–3565. doi: 10.1097/00001756-19991260-00018
- Kath, C., Goni-Oliver, P., Müller, R., Schultz, C., Haucke, V., Eickholt, B., et al. (2018). PTEN suppresses axon outgrowth by down-regulating the level of dytrosinated microtubules. *PLoS One* 13:e0193257. doi: 10.1371/journal.pone.0193257
- Kato, N., Nemoto, K., Nakanishi, K., Morishita, R., Kaneda, Y., Uenoyama, M., et al. (2005). Nonviral HVJ (hemagglutinating virus of Japan) liposome-mediated retrograde gene transfer of human hepatocyte growth factor into rat nervous system promotes functional and histological recovery of the crushed nerve. *Neurosci Res.* 52, 299–310. doi: 10.1016/j.neures.2005.04.004
- Katoh-Semba, R., Kaisho, Y., Shintani, A., Nagahama, M., and Kato, K. (1996). Tissue distribution and immunocytochemical localization of neurotrophin-3 in the brain and peripheral tissues of rats. *J. Neurochem.* 66, 330–337. doi: 10.1046/j.1471-4159.1996.66010330.x
- Keefe, K. M., Sheikh, I. S., and Smith, G. M. (2017). Targeting neurotrophins to specific populations of neurons: NGF, BDNF and NT-3 and their relevance for treatment of spinal cord injury. *Int. J. Mol. Sci.* 18:E548. doi: 10.3390/ijms18030548
- Keino-Masu, K., Masu, M., Hinck, L., Leonardo, E. D., Chan, S. S., Culotti, J. G., et al. (1996). Deleted in colorectal cancer (DCC) encodes a netrin receptor. *Cell* 87, 175–185. doi: 10.1016/s0092-8674(00)81336-7
- Kemp, S. W., Walsh, S. K., Zochodne, D. W., and Midha, R. (2007). A novel method for establishing daily *in vivo* concentration gradients of soluble nerve growth factor (NGF). *J. Neurosci. Methods* 165, 83–88. doi: 10.1016/j.jneumeth.2007.05.032
- Kennedy, T. E., Serafini, T., de la Torre, J. R., and Tessier-Lavigne, M. (1994). Netrins are diffusible chemotropic factors for commissural axons in the embryonic spinal cord. *Cell* 78, 425–435. doi: 10.1016/0092-8674(94)90421-9
- Kim, M. S., El-Fiqi, A., Kim, J. W., Ahn, H. S., Kim, H., Son, Y. J., et al. (2016). Nanotherapeutics of PTEN inhibitor with mesoporous silica nanocarrier effective for axonal outgrowth of adult neurons. *ACS Appl. Mater. Interfaces* 8, 18741–18753. doi: 10.1021/acsami.6b06889
- Kimelman, D., and Xu, W. (2006). β -catenin destruction complex: insights and questions from a structural perspective. *Oncogene* 25, 7482–7491. doi: 10.1038/sj.onc.1210055
- Ko, K. R., Lee, J., Lee, D., Nho, B., and Kim, S. (2018). Hepatocyte growth factor (HGF) promotes peripheral nerve regeneration by activating repair schwann cells. *Sci. Rep.* 8:8316. doi: 10.1038/s41598-018-26704-x
- Kobayashi, H., Yokoyama, M., Matsuoka, Y., Omori, M., Itano, Y., Kaku, R., et al. (2008). Expression changes of multiple brain-derived neurotrophic factor transcripts in selective spinal nerve ligation model and complete Freund's adjuvant model. *Brain Res.* 1206, 13–19. doi: 10.1016/j.brainres.2007.12.004
- Korhonen, L., Brännvall, K., Skoglösa, Y., and Lindholm, D. (2003). Tumor suppressor gene BRCA-1 is expressed by embryonic and adult neural stem cells and involved in cell proliferation. *J. Neurosci. Res.* 71, 769–776. doi: 10.1002/jnr.10546
- Kotzbauer, P. T., Lampe, P. A., Heuckeroth, R. O., Golden, J. P., Creedon, D. J., Johnson, E. M. Jr., et al. (1996). Neurturin, a relative of glial-cell-line-derived neurotrophic factor. *Nature* 384, 467–470. doi: 10.1038/384467a0
- Krishnan, A., Bhavanam, S., and Zochodne, D. (2018a). An intimate role for adult dorsal root ganglia resident cycling cells in the generation of local macrophages and satellite glial cells. *J. Neuropathol. Exp. Neurol.* 77, 929–941. doi: 10.1093/jnen/nly072
- Krishnan, A., Purdy, K., Chandrasekhar, A., Martinez, J., Cheng, C., and Zochodne, D. W. (2018b). A BRCA1-dependent DNA damage response in the regenerating adult peripheral nerve milieu. *Mol. Neurobiol.* 55, 4051–4067. doi: 10.1007/s12035-017-0574-7
- Kume, T., Nishikawa, H., Tomioka, H., Katsuki, H., Akaike, A., Kaneko, S., et al. (2000). p75-mediated neuroprotection by NGF against glutamate cytotoxicity in cortical cultures. *Brain Res.* 852, 279–289. doi: 10.1016/s0006-8993(99)02226-x
- Kurek, J. B., Austin, L., Cheema, S. S., Bartlett, P. F., and Murphy, M. (1996). Up-regulation of leukaemia inhibitory factor and interleukin-6 in transected sciatic nerve and muscle following denervation. *Neuromuscul. Disord.* 6, 105–114. doi: 10.1016/0960-8966(95)00029-1
- Kurek, J. B., Bower, J. J., Romanella, M., Koentgen, F., Murphy, M., and Austin, L. (1997). The role of leukemia inhibitory factor in skeletal muscle regeneration. *Muscle Nerve* 20, 815–822. doi: 10.1002/(sici)1097-4598(199707)20:7<815::aid-mus5>3.0.co;2-a
- Kwon, C. H., Luikart, B. W., Powell, C. M., Zhou, J., Matheny, S. A., Zhang, W., et al. (2006). Pten regulates neuronal arborization and social interaction in mice. *Neuron* 50, 377–388. doi: 10.1016/j.neuron.2006.03.023
- Langeslag, M., Constantin, C. E., Andratsch, M., Quarta, S., Mair, N., and Kress, M. (2011). Oncostatin M induces heat hypersensitivity by gp130-dependent sensitization of TRPV1 in sensory neurons. *Mol. Pain* 7:102. doi: 10.1186/1744-8069-7-102
- Lee, E. Y., Chang, C. Y., Hu, N., Wang, Y. C., Lai, C. C., Herrup, K., et al. (1992). Mice deficient for Rb are nonviable and show defects in neurogenesis and haematopoiesis. *Nature* 359, 288–294. doi: 10.1038/359288a0
- Lee, M. Y., Choi, J. S., Lim, S. W., Cha, J. H., Chun, M. H., and Chung, J. W. (2001). Expression of osteopontin mRNA in developing rat brainstem and cerebellum. *Cell Tissue Res.* 306, 179–185. doi: 10.1007/s004410100456
- Lee, S. H., Jin, W. P., Seo, N. R., Pang, K. M., Kim, B., Kim, S. M., et al. (2017). Recombinant human fibroblast growth factor-2 promotes nerve regeneration and functional recovery after mental nerve crush injury. *Neural Regen. Res.* 12, 629–636. doi: 10.4103/1673-5374.205104
- Lehmann, M., Fournier, A., Selles-Navarro, I., Dergham, P., Sebok, A., Leclerc, N., et al. (1999). Inactivation of Rho signaling pathway promotes CNS axon regeneration. *J. Neurosci.* 19, 7537–7547. doi: 10.1523/JNEUROSCI.19-17-07537.1999
- Leitner, M. L., Molliver, D. C., Osborne, P. A., Vejsada, R., Golden, J. P., Lampe, P. A., et al. (1999). Analysis of the retrograde transport of glial cell line-derived neurotrophic factor (GDNF), neurturin, and persephin suggests that *in vivo* signaling for the GDNF family is GFR α coreceptor-specific. *J. Neurosci.* 19, 9322–9331. doi: 10.1523/JNEUROSCI.19-21-09322.1999
- Leonardo, E. D., Hinck, L., Masu, M., Keino-Masu, K., Ackerman, S. L., and Tessier-Lavigne, M. (1997). Vertebrate homologues of *C. elegans* UNC-5 are candidate netrin receptors. *Nature* 386, 833–838. doi: 10.1038/386833a0
- Levi-Montalcini, R. (1987). The nerve growth factor: thirty-five years later. *EMBO J.* 6, 1145–1154. doi: 10.1002/j.1460-2075.1987.tb02347.x
- Levi-Montalcini, R. (1950). The origin and development of the visceral system in the spinal cord or chick embryo. *Dev. Biol.* 86, 253–284. doi: 10.1002/jmor.1050860203

- Li, D. M., and Sun, H. (1997). TEP1, encoded by a candidate tumor suppressor locus, is a novel protein tyrosine phosphatase regulated by transforming growth factor β . *Cancer Res.* 57, 2124–2129.
- Li, G. D., Wo, Y., Zhong, M. F., Zhang, F. X., Bao, L., Lu, Y. J., et al. (2002). Expression of fibroblast growth factors in rat dorsal root ganglion neurons and regulation after peripheral nerve injury. *Neuroreport* 13, 1903–1907. doi: 10.1097/00001756-200210280-00014
- Liaw, L., Skinner, M. P., Raines, E. W., Ross, R., Cheresch, D. A., Schwartz, S. M., et al. (1995). The adhesive and migratory effects of osteopontin are mediated via distinct cell surface integrins. Role of α v β 3 in smooth muscle cell migration to osteopontin *in vitro*. *J. Clin. Invest.* 95, 713–724. doi: 10.1172/jci117718
- Lin, L. F., Doherty, D. H., Lile, J. D., Bektesh, S., and Collins, F. (1993). GDNF: a glial cell line-derived neurotrophic factor for midbrain dopaminergic neurons. *Science* 260, 1130–1132. doi: 10.1126/science.8493557
- Liu, Y., Kelamangalath, L., Kim, H., Han, S. B., Tang, X., Zhai, J., et al. (2016). NT-3 promotes proprioceptive axon regeneration when combined with activation of the mTor intrinsic growth pathway but not with reduction of myelin extrinsic inhibitors. *Exp. Neurol.* 283, 73–84. doi: 10.1016/j.expneurol.2016.05.021
- Lu, M. C., Ho, C. Y., Hsu, S. F., Lee, H. C., Lin, J. H., Yao, C. H., et al. (2008). Effects of electrical stimulation at different frequencies on regeneration of transected peripheral nerve. *Neurorehabil. Neural Repair* 22, 367–373. doi: 10.1177/1545968307313507
- MacPherson, D., Sage, J., Kim, T., Ho, D., McLaughlin, M. E., and Jacks, T. (2004). Cell typespecific effects of Rb deletion in the murine retina. *Genes Dev.* 18, 1681–1694. doi: 10.1101/gad.1203304
- Maina, F., Hilton, M. C., Ponzetto, C., Davies, A. M., and Klein, R. (1997). Met receptor signaling is required for sensory nerve development and HGF promotes axonal growth and survival of sensory neurons. *Genes Dev.* 11, 3341–3350. doi: 10.1101/gad.11.24.3341
- Maklad, A., Nicolai, J. R., Bichsel, K. J., Evenson, J. E., Lee, T. C., Threadgill, D. W., et al. (2009). The EGFR is required for proper innervation to the skin. *J. Invest. Dermatol.* 129, 690–698. doi: 10.1038/jid.2008.281
- Manitt, C., Nikolakopoulou, A. M., Almaro, D. R., Nguyen, S. A., and Cohen-Cory, S. (2009). Netrin participates in the development of retinotectal synaptic connectivity by modulating axon arborization and synapse formation in the developing brain. *J. Neurosci.* 29, 11065–11077. doi: 10.1523/JNEUROSCI.0947-09.2009
- Manthorpe, M., Skaper, S. D., Williams, L. R., and Varon, S. (1986). Purification of adult rat sciatic nerve ciliary neuronotrophic factor. *Brain Res.* 367, 282–286. doi: 10.1016/0006-8993(86)91603-3
- Marcus, D. M., Brooks, S. E., Leff, G., McCormick, R., Thompson, T., Anfinson, S., et al. (1998). Trilateral retinoblastoma: insights into histogenesis and management. *Surv. Ophthalmol.* 43, 59–70. doi: 10.1016/S0039-6257(98)00019-8
- Masuda, T., Watanabe, K., Sakuma, C., Ikenaka, K., Ono, K., and Yaginuma, H. (2008). Netrin-1 acts as a repulsive guidance cue for sensory axonal projections toward the spinal cord. *J. Neurosci.* 28, 10380–10385. doi: 10.1523/JNEUROSCI.1926-08.2008
- McClellan, K. A., Ruzhynsky, V. A., Douda, D. N., Vanderluit, J. L., Ferguson, K. L., Chen, D., et al. (2007). Unique requirement for Rb/E2F3 in neuronal migration: evidence for cell cycle-independent functions. *Mol. Cell. Biol.* 27, 4825–4843. doi: 10.1128/mcb.02100-06
- McDonald, D., Cheng, C., Chen, Y., and Zochodne, D. (2006). Early events of peripheral nerve regeneration. *Neuron Glia Biol.* 2, 139–147. doi: 10.1017/S1740925X05000347
- McKay Hart, A., Brannstrom, T., Wiberg, M., and Terenghi, G. (2002). Primary sensory neurons and satellite cells after peripheral axotomy in the adult rat: timecourse of cell death and elimination. *Exp. Brain Res.* 142, 308–318. doi: 10.1007/s00221-001-0929-0
- McLean, N. A., Popescu, B. F., Gordon, T., Zochodne, D. W., and Verge, V. M. (2014). Delayed nerve stimulation promotes axon-protective neurofilament phosphorylation, accelerates immune cell clearance and enhances remyelination *in vivo* in focally demyelinated nerves. *PLoS One* 9:e110174. doi: 10.1371/journal.pone.0110174
- McNay, E. C., Ong, C. T., McCrimmon, R. J., Cresswell, J., Bogan, J. S., and Sherwin, R. S. (2010). Hippocampal memory processes are modulated by insulin and high-fat-induced insulin resistance. *Neurobiol. Learn. Mem.* 93, 546–553. doi: 10.1016/j.nlm.2010.02.002
- Mehlen, P., Delloye-Bourgeois, C., and Chedotal, A. (2011). Novel roles for Slits and netrins: axon guidance cues as anticancer targets? *Nat. Rev. Cancer* 11, 188–197. doi: 10.1038/nrc3005
- Mehlen, P., and Mazelin, L. (2003). The dependence receptors DCC and UNC5H as a link between neuronal guidance and survival. *Biol. Cell.* 95, 425–436. doi: 10.1016/s0248-4900(03)00072-8
- Mehlen, P., and Tauszig-Delamasure, S. (2014). Dependence receptors and colorectal cancer. *Gut* 63, 1821–1829. doi: 10.1136/gutjnl-2013-306704
- Miki, Y., Swensen, J., Shattuck-Eidens, D., Futreal, P. A., Harshman, K., Tavtigian, S., et al. (1994). A strong candidate for the breast and ovarian cancer susceptibility gene BRCA1. *Science* 266, 66–71. doi: 10.1126/science.7545954
- Milbrandt, J., de Sauvage, F. J., Fahrner, T. J., Baloh, R. H., Leitner, M. L., Tansey, M. G., et al. (1998). Persephin, a novel neurotrophic factor related to GDNF and neurturin. *Neuron* 20, 245–253. doi: 10.1016/s0896-6273(00)80453-5
- Miletic, G., and Miletic, V. (2002). Increases in the concentration of brain derived neurotrophic factor in the lumbar spinal dorsal horn are associated with pain behavior following chronic constriction injury in rats. *Neurosci. Lett.* 319, 137–140. doi: 10.1016/s0304-3940(01)02576-9
- Millaruelo, A. I., Nieto-Sampedro, M., Yu, J., and Cotman, C. W. (1986). Neurotrophic activity in the central and peripheral nervous systems of the cat. Effects of injury. *Brain Res.* 374, 12–20. doi: 10.1016/0006-8993(86)90389-6
- Mills, C. D., Allchorne, A. J., Griffin, R. S., Woolf, C. J., and Costigan, M. (2007). GDNF selectively promotes regeneration of injury-primed sensory neurons in the lesioned spinal cord. *Mol. Cell. Neurosci.* 36, 185–194. doi: 10.1016/j.mcn.2007.06.011
- Mitsumoto, H., Klinkosz, B., Pioro, E. P., Tsuzaka, K., Ishiyama, T., O'Leary, R. M., et al. (2001). Effects of ciliary neurotrophic factor (CNTF) in a mouse motor neuron disease. *Muscle Nerve* 24, 769–777. doi: 10.1002/mus.1068
- Mizisin, A. P., Vu, Y., Shuff, M., and Calcutt, N. A. (2004). Ciliary neurotrophic factor improves nerve conduction and ameliorates regeneration deficits in diabetic rats. *Diabetes* 53, 1807–1812. doi: 10.2337/diabetes.53.7.1807
- Moore, S. W., Tessier-Lavigne, M., and Kennedy, T. E. (2007). Netrins and their receptors. *Adv. Exp. Med. Biol.* 621, 17–31. doi: 10.1007/978-0-387-76715-4_2
- Morikawa, Y. (2005). Oncostatin M in the development of the nervous system. *Anat. Sci. Int.* 80, 53–59. doi: 10.1111/j.1447-073x.2005.00100.x
- Morikawa, Y., Tamura, S., Minehata, K., Donovan, P. J., Miyajima, A., and Senba, E. (2004). Essential function of oncostatin m in nociceptive neurons of dorsal root ganglia. *J. Neurosci.* 24, 1941–1947. doi: 10.1523/JNEUROSCI.4975-03.2004
- Morrison, E. E., Askham, J., Clissold, P., Markham, A. F., and Meredith, D. M. (1997a). Expression of β -catenin and the adenomatous polyposis coli tumour suppressor protein in mouse neocortical cells *in vitro*. *Neurosci. Lett.* 235, 129–132. doi: 10.1016/s0304-3940(97)00739-8
- Morrison, E. E., Askham, J., Clissold, P., Markham, A. F., and Meredith, D. M. (1997b). The cellular distribution of the adenomatous polyposis coli tumour suppressor protein in neuroblastoma cells is regulated by microtubule dynamics. *Neuroscience* 81, 553–563. doi: 10.1016/s0306-4522(97)00099-7
- Morrison, R. S., Sharma, A., de Vellis, J., and Bradshaw, R. A. (1986). Basic fibroblast growth factor supports the survival of cerebral cortical neurons in primary culture. *Proc. Natl. Acad. Sci. U S A* 83, 7537–7541. doi: 10.1073/pnas.83.19.7537
- Mosley, B., De Imus, C., Friend, D., Boiani, N., Thoma, B., Park, L. S., et al. (1996). Dual oncostatin M (OSM) receptors. Cloning and characterization of an alternative signaling subunit conferring OSM-specific receptor activation. *J. Biol. Chem.* 271, 32635–32643. doi: 10.1074/jbc.271.51.32635
- Mueller, B. K., Mack, H., and Teusch, N. (2005). Rho kinase, a promising drug target for neurological disorders. *Nat. Rev. Drug Discov.* 4, 387–398. doi: 10.1038/nrd1719
- Müller, A., Hauk, T. G., Leibinger, M., Marienfeld, R., and Fischer, D. (2009). Exogenous CNTF stimulates axon regeneration of retinal ganglion cells partially via endogenous CNTF. *Mol. Cell. Neurosci.* 41, 233–246. doi: 10.1016/j.mcn.2009.03.002

- Murphy, M., Reid, K., Brown, M. A., and Bartlett, P. F. (1993). Involvement of leukemia inhibitory factor and nerve growth factor in the development of dorsal root ganglion neurons. *Development* 117, 1173–1182.
- Murphy, M., Reid, K., Hilton, D. J., and Bartlett, P. F. (1991). Generation of sensory neurons is stimulated by leukemia inhibitory factor. *Proc. Natl. Acad. Sci. U S A* 88, 3498–3501. doi: 10.1073/pnas.88.8.3498
- Musatov, S., Roberts, J., Brooks, A. I., Pena, J., Betchen, S., Pfaff, D. W., et al. (2004). Inhibition of neuronal phenotype by PTEN in PC12 cells. *Proc. Natl. Acad. Sci. U S A* 101, 3627–3631. doi: 10.1073/pnas.0308289101
- Nakamura, T., Nishizawa, T., Hagiya, M., Seki, T., Shimonishi, M., Sugimura, A., et al. (1989). Molecular cloning and expression of human hepatocyte growth factor. *Nature* 342, 440–443. doi: 10.1038/342440a0
- Nakamura, T., Teramoto, H., Tomita, Y., and Ichihara, A. (1984). L-proline is an essential amino acid for hepatocyte growth in culture. *Biochem. Biophys. Res. Commun.* 122, 884–891. doi: 10.1016/0006-291x(84)91173-2
- Namaka, M. P., Sawchuk, M., MacDonald, S. C., Jordan, L. M., and Hochman, S. (2001). Neurogenesis in postnatal mouse dorsal root ganglia. *Exp. Neurol.* 172, 60–69. doi: 10.1006/exnr.2001.7761
- Narciso, M. S., Mietto Bde, S., Marques, S. A., Soares, C. P., Mermelstein Cdos, S., El-Cheikh, M. C., et al. (2009). Sciatic nerve regeneration is accelerated in galectin-3 knockout mice. *Exp. Neurol.* 217, 7–15. doi: 10.1016/j.expneurol.2009.01.008
- Nijs, J., Meeus, M., Versijpt, J., Moens, M., Bos, I., Knaepen, K., et al. (2015). Brain-derived neurotrophic factor as a driving force behind neuroplasticity in neuropathic and central sensitization pain: a new therapeutic target? *Expert Opin. Ther. Targets* 19, 565–576. doi: 10.1517/14728222.2014.994506
- Ning, K., Drepper, C., Valori, C. F., Ahsan, M., Wyles, M., Higginbottom, A., et al. (2010). PTEN depletion rescues axonal growth defect and improves survival in SMN-deficient motor neurons. *Hum. Mol. Genet.* 19, 3159–3168. doi: 10.1093/hmg/ddq226
- Nix, W. A., and Hopf, H. C. (1983). Electrical stimulation of regenerating nerve and its effect on motor recovery. *Brain Res.* 272, 21–25. doi: 10.1016/0006-8993(83)90360-8
- Noristani, H. N., Gerber, Y. N., Sabourin, J. C., Le Corre, M., Lonjon, N., Mestre-Frances, N., et al. (2017). RNA-seq analysis of microglia reveals time-dependent activation of specific genetic programs following spinal cord injury. *Front. Mol. Neurosci.* 10:90. doi: 10.3389/fnmol.2017.00090
- Ogai, K., Kuwana, A., Hisano, S., Nagashima, M., Koriyama, Y., Sugitani, K., et al. (2014). Upregulation of leukemia inhibitory factor (LIF) during the early stage of optic nerve regeneration in zebrafish. *PLoS One* 9:e106010. doi: 10.1371/journal.pone.0106010
- Omodaka, K., Kurimoto, T., Nakamura, O., Sato, K., Yasuda, M., Tanaka, Y., et al. (2014). Artemin augments survival and axon regeneration in axotomized retinal ganglion cells. *J. Neurosci. Res.* 92, 1637–1646. doi: 10.1002/jnr.23449
- Oppenheim, R. W., Wiese, S., Prevette, D., Armanini, M., Wang, S., Houenou, L. J., et al. (2001). Cardiotrophin-1, a muscle-derived cytokine, is required for the survival of subpopulations of developing motoneurons. *J. Neurosci.* 21, 1283–1291. doi: 10.1523/JNEUROSCI.21-04-01283.2001
- Ornitz, D. M., and Itoh, N. (2015). The fibroblast growth factor signaling pathway. *Wiley Interdiscip. Rev. Dev. Biol.* 4, 215–266. doi: 10.1002/wdev.176
- Ortmann, S. D., and Hellenbrand, D. J. (2018). Glial cell line-derived neurotrophic factor as a treatment after spinal cord injury. *Neural Regen. Res.* 13, 1733–1734. doi: 10.4103/1673-5374.238610
- Pajcini, K. V., Corbel, S. Y., Sage, J., Pomerantz, J. H., and Blau, H. M. (2010). Transient inactivation of Rb and ARF yields regenerative cells from postmitotic mammalian muscle. *Cell Stem Cell* 7, 198–213. doi: 10.1016/j.stem.2010.05.022
- Pao, G. M., Zhu, Q., Perez-Garcia, C. G., Chou, S. J., Suh, H., Gage, F. H., et al. (2014). Role of BRCA1 in brain development. *Proc. Natl. Acad. Sci. U S A* 111, E1240–E1248. doi: 10.1073/pnas.1400783111
- Park, J. I., Seo, I. A., Lee, H. K., Park, H. T., Shin, S. W., Park, Y. M., et al. (2007). Netrin inhibits regenerative axon growth of adult dorsal root ganglion neurons *in vitro*. *J. Korean Med. Sci.* 22, 641–645. doi: 10.3346/jkms.2007.22.4.641
- Park, K. K., Liu, K., Hu, Y., Smith, P. D., Wang, C., Cai, B., et al. (2008). Promoting axon regeneration in the adult CNS by modulation of the PTEN/mTOR pathway. *Science* 322, 963–966. doi: 10.1126/science.1161566
- Patapoutian, A., and Reichardt, L. F. (2000). Roles of Wnt proteins in neural development and maintenance. *Curr. Opin. Neurobiol.* 10, 392–399. doi: 10.1016/s0959-4388(00)00100-8
- Peng, Y. R., He, S., Marie, H., Zeng, S. Y., Ma, J., Tan, Z. J., et al. (2009). Coordinated changes in dendritic arborization and synaptic strength during neural circuit development. *Neuron* 61, 71–84. doi: 10.1016/j.neuron.2008.11.015
- Pennica, D., Arce, V., Swanson, T. A., Vejsada, R., Pollock, R. A., Armanini, M., et al. (1996). Cardiotrophin-1, a cytokine present in embryonic muscle, supports long-term survival of spinal motoneurons. *Neuron* 17, 63–74. doi: 10.1016/s0896-6273(00)80281-0
- Pennica, D., Shaw, K. J., Swanson, T. A., Moore, M. W., Shelton, D. L., Zioncheck, K. A., et al. (1995). Cardiotrophin-1. Biological activities and binding to the leukemia inhibitory factor receptor/gp130 signaling complex. *J. Biol. Chem.* 270, 10915–10922. doi: 10.1074/jbc.270.18.10915
- Plata-Salamán, C. R. (1991). Epidermal growth factor and the nervous system. *Peptides* 12, 653–663. doi: 10.1016/0196-9781(91)90115-6
- Pockett, S., and Gavin, R. M. (1985). Acceleration of peripheral nerve regeneration after crush injury in rat. *Neurosci. Lett.* 59, 221–224. doi: 10.1016/0304-3940(85)90203-4
- Podsypanina, K., Ellenson, L. H., Nemes, A., Gu, J., Tamura, M., Yamada, K. M., et al. (1999). Mutation of Pten/Mmac1 in mice causes neoplasia in multiple organ systems. *Proc. Natl. Acad. Sci. U S A* 96, 1563–1568. doi: 10.1073/pnas.96.4.1563
- Pulvers, J. N., and Huttner, W. B. (2009). Brca1 is required for embryonic development of the mouse cerebral cortex to normal size by preventing apoptosis of early neural progenitors. *Development* 136, 1859–1868. doi: 10.1242/dev.033498
- Ramer, M. S., Duraisingam, I., Priestley, J. V., and McMahon, S. B. (2001). Two-tiered inhibition of axon regeneration at the dorsal root entry zone. *J. Neurosci.* 21, 2651–2660. doi: 10.1523/JNEUROSCI.21-08-02651.2001
- Rende, M., Hagg, T., Manthorpe, M., and Varon, S. (1992a). Nerve growth factor receptor immunoreactivity in neurons of the normal adult rat spinal cord and its modulation after peripheral nerve lesions. *J. Comp. Neurol.* 319, 285–298. doi: 10.1002/cne.903190208
- Rende, M., Muir, D., Ruoslahti, E., Hagg, T., Varon, S., and Manthorpe, M. (1992b). Immunolocalization of ciliary neurotrophic factor in adult rat sciatic nerve. *Glia* 5, 25–32. doi: 10.1002/glia.440050105
- Reyes-Corona, D., Vázquez-Hernández, N., Escobedo, L., Orozco-Barrios, C. E., Ayala-Davila, J., Moreno, M. G., et al. (2017). Neurturin overexpression in dopaminergic neurons induces presynaptic and postsynaptic structural changes in rats with chronic 6-hydroxydopamine lesion. *PLoS One* 12:e0188239. doi: 10.1371/journal.pone.0188239
- Rich, K. M., Luszczynski, J. R., Osborne, P. A., and Johnson, E. M. Jr. (1987). Nerve growth factor protects adult sensory neurons from cell death and atrophy caused by nerve injury. *J. Neurocytol.* 16, 261–268. doi: 10.1007/bf01795309
- Richardson, P. M., and Ebendal, T. (1982). Nerve growth activities in rat peripheral nerve. *Brain Res.* 246, 57–64. doi: 10.1016/0006-8993(82)90141-x
- Robledo, O., Fourcin, M., Chevalier, S., Guillet, C., Auguste, P., Pouplard-Barthelax, A., et al. (1997). Signaling of the cardiotrophin-1 receptor. Evidence for a third receptor component. *J. Biol. Chem.* 272, 4855–4863. doi: 10.1074/jbc.272.8.4855
- Rodgers, E. E., and Theibert, A. B. (2002). Functions of PI 3-kinase in development of the nervous system. *Int. J. Dev. Neurosci.* 20, 187–197. doi: 10.1016/s0736-5748(02)00047-3
- Rosenthal, A., Goeddel, D. V., Nguyen, T., Lewis, M., Shih, A., Laramée, G. R., et al. (1990). Primary structure and biological activity of a novel human neurotrophic factor. *Neuron* 4, 767–773. doi: 10.1016/0896-6273(90)90203-r
- Rulifson, E. J., Kim, S. K., and Nusse, R. (2002). Ablation of insulin-producing neurons in flies: growth and diabetic phenotypes. *Science* 296, 1118–1120. doi: 10.1126/science.1070058
- Sage, J. (2012). The retinoblastoma tumor suppressor and stem cell biology. *Genes Dev.* 26, 1409–1420. doi: 10.1101/gad.193730.112
- Sage, J., Miller, A. L., Pérez-Mancera, P. A., Wysocki, J. M., and Jacks, T. (2003). Acute mutation of retinoblastoma gene function is sufficient for cell cycle re-entry. *Nature* 424, 223–228. doi: 10.1038/nature01764
- Sahenk, Z., Seharaseyon, J., and Mendell, J. R. (1994). CNTF potentiates peripheral nerve regeneration. *Brain Res.* 655, 246–250. doi: 10.1016/0006-8993(94)91621-7
- Saleh, A., Roy Chowdhury, S. K., Smith, D. R., Balakrishnan, S., Tessler, L., Martens, C., et al. (2013). Ciliary neurotrophic factor activates NF-κB to

- enhance mitochondrial bioenergetics and prevent neuropathy in sensory neurons of streptozotocin-induced diabetic rodents. *Neuropharmacology* 65, 65–73. doi: 10.1016/j.neuropharm.2012.09.015
- Sango, K., Yanagisawa, H., and Takaku, S. (2007). Expression and histochemical localization of ciliary neurotrophic factor in cultured adult rat dorsal root ganglion neurons. *Histochem. Cell Biol.* 128, 35–43. doi: 10.1007/s00418-007-0290-x
- Santos, D., González-Pérez, F., Giudetti, G., Micera, S., Udina, E., Del Valle, J., et al. (2017). Preferential enhancement of sensory and motor axon regeneration by combining extracellular matrix components with neurotrophic factors. *Int. J. Mol. Sci.* 18:E65. doi: 10.3390/ijms18010065
- Sawai, H., Clarke, D. B., Kittlerova, P., Bray, G. M., and Aguayo, A. J. (1996). Brain-derived neurotrophic factor and neurotrophin-4/5 stimulate growth of axonal branches from regenerating retinal ganglion cells. *J. Neurosci.* 16, 3887–3894. doi: 10.1523/JNEUROSCI.16-12-03887.1996
- Schnell, L., Schneider, R., Kolbeck, R., Barde, Y. A., and Schwab, M. E. (1994). Neurotrophin-3 enhances sprouting of corticospinal tract during development and after adult spinal cord lesion. *Nature* 367, 170–173. doi: 10.1038/367170a0
- Senaldi, G., Varnum, B. C., Sarmiento, U., Starnes, C., Lile, J., Scully, S., et al. (1999). Novel neurotrophin-1/B cell-stimulating factor-3: a cytokine of the IL-6 family. *Proc. Natl. Acad. Sci. U S A* 96, 11458–11463. doi: 10.1073/pnas.96.20.11458
- Sendtner, M., Kreutzberg, G. W., and Thoenen, H. (1990). Ciliary neurotrophic factor prevents the degeneration of motor neurons after axotomy. *Nature* 345, 440–441. doi: 10.1038/345440a0
- Sendtner, M., Stöckli, K. A., and Thoenen, H. (1992). Synthesis and localization of ciliary neurotrophic factor in the sciatic nerve of the adult rat after lesion and during regeneration. *J. Cell Biol.* 118, 139–148. doi: 10.1083/jcb.118.1.139
- Serafini, T., Kennedy, T. E., Galko, M. J., Mirzayan, C., Jessell, T. M., and Tessier-Lavigne, M. (1994). The netrins define a family of axon outgrowth-promoting proteins homologous to *C. elegans* UNC-6. *Cell* 78, 409–424. doi: 10.1016/0092-8674(94)90420-0
- Shelton, D. N., Sandoval, I. T., Eisinger, A., Chidester, S., Ratnayake, A., Ireland, C. M., et al. (2006). Up-regulation of CYP26A1 in adenomatous polyposis coli-deficient vertebrates via a WNT-dependent mechanism: implications for intestinal cell differentiation and colon tumor development. *Cancer Res.* 66, 7571–7577. doi: 10.1158/0008-5472.can-06-1067
- Shettar, A., and Muttagi, G. (2012). Developmental regulation of insulin receptor gene in sciatic nerves and role of insulin on glycoprotein P0 in the Schwann cells. *Peptides* 36, 46–53. doi: 10.1016/j.peptides.2012.04.012
- Shin, S. L., Cha, J. H., Chun, M. H., Chung, J. W., and Lee, M. Y. (1999). Expression of osteopontin mRNA in the adult rat brain. *Neurosci. Lett.* 273, 73–76. doi: 10.1016/s0304-3940(99)00516-9
- Sikandar, S., Minett, M. S., Millet, Q., Santana-Varela, S., Lau, J., Wood, J. N., et al. (2018). Brain-derived neurotrophic factor derived from sensory neurons plays a critical role in chronic pain. *Brain* 141, 1028–1039. doi: 10.1093/brain/awy009
- Singh, B., Krishnan, A., Micu, I., Koshy, K., Singh, V., Martinez, J. A., et al. (2015). Peripheral neuron plasticity is enhanced by brief electrical stimulation and overrides attenuated regrowth in experimental diabetes. *Neurobiol. Dis.* 83, 134–151. doi: 10.1016/j.nbd.2015.08.009
- Singh, B., Singh, V., Krishnan, A., Koshy, K., Martinez, J. A., Cheng, C., et al. (2014). Regeneration of diabetic axons is enhanced by selective knockdown of the PTEN gene. *Brain* 137, 1051–1067. doi: 10.1093/brain/awu031
- Singh, B., Xu, Q. G., Franz, C. K., Zhang, R., Dalton, C., Gordon, T., et al. (2012a). Accelerated axon outgrowth, guidance, and target reinnervation across nerve transection gaps following a brief electrical stimulation paradigm. *J. Neurosurg.* 116, 498–512. doi: 10.3171/2011.10.jns.11612
- Singh, B., Xu, Y., McLaughlin, T., Singh, V., Martinez, J. A., Krishnan, A., et al. (2012b). Resistance to trophic neurite outgrowth of sensory neurons exposed to insulin. *J. Neurochem.* 121, 263–276. doi: 10.1111/j.1471-4159.2012.07681.x
- Singhal, A., Cheng, C., Sun, H., and Zochodne, D. W. (1997). Near nerve local insulin prevents conduction slowing in experimental diabetes. *Brain Res.* 763, 209–214. doi: 10.1016/s0006-8993(97)00412-5
- Slack, R. S., El-Bizri, H., Wong, J., Belliveau, D. J., and Miller, F. D. (1998). A critical temporal requirement for the retinoblastoma protein family during neuronal determination. *J. Cell Biol.* 140, 1497–1509. doi: 10.1083/jcb.140.6.1497
- Song, X. Y., Li, F., Zhang, F. H., Zhong, J. H., and Zhou, X. F. (2008). Peripherally-derived bdnf promotes regeneration of ascending sensory neurons after spinal cord injury. *PLoS One* 3:e1707. doi: 10.1371/journal.pone.0001707
- Stöckli, K. A., Lillien, L. E., Näher-Noé, M., Breitfeld, G., Hughes, R. A., Raff, M. C., et al. (1991). Regional distribution, developmental changes, and cellular localization of CNTF-mRNA and protein in the rat brain. *J. Cell Biol.* 115, 447–459. doi: 10.1083/jcb.115.2.447
- Strand, N. S., Hoi, K. K., Phan, T. M. T., Ray, C. A., Berndt, J. D., and Moon, R. T. (2016). Wnt/ β -catenin signaling promotes regeneration after adult zebrafish spinal cord injury. *Biochem. Biophys. Res. Commun.* 477, 952–956. doi: 10.1016/j.bbrc.2016.07.006
- Sugimoto, K., Murakawa, Y., and Sima, A. A. (2002). Expression and localization of insulin receptor in rat dorsal root ganglion and spinal cord. *J. Peripher. Nerv. Syst.* 7, 44–53. doi: 10.1046/j.1529-8027.2002.02005.x
- Sugimoto, K., Murakawa, Y., Zhang, W., Xu, G., and Sima, A. A. (2000). Insulin receptor in rat peripheral nerve: its localization and alternatively spliced isoforms. *Diabetes Metab. Res. Rev.* 16, 354–363. doi: 10.1002/1520-7560(200009/10)16:5<354::aid-dmrr149>3.0.co;2-h
- Sulaiman, O. A., and Gordon, T. (2000). Effects of short- and long-term schwann cell denervation on peripheral nerve regeneration, myelination, and size. *Glia* 32, 234–246. doi: 10.1002/1098-1136(200012)32:3<234::aid-glia40>3.0.co;2-3
- Sun, K. L. W., Correia, J. P., and Kennedy, T. E. (2011). Netrins: versatile extracellular cues with diverse functions. *Development* 138, 2153–2169. doi: 10.1242/dev.044529
- Taga, T., and Kishimoto, T. (1997). Gp130 and the interleukin-6 family of cytokines. *Annu. Rev. Immunol.* 15, 797–819. doi: 10.1146/annurev.immunol.15.1.797
- Takaku, S., Yanagisawa, H., Watabe, K., Horie, H., Kadoya, T., Sakumi, K., et al. (2013). GDNF promotes neurite outgrowth and upregulates galectin-1 through the RET/PI3K signaling in cultured adult rat dorsal root ganglion neurons. *Neurochem. Int.* 62, 330–339. doi: 10.1016/j.neuint.2013.01.008
- Tamura, S., Morikawa, Y., Miyajima, A., and Senba, E. (2003). Expression of oncostatin M receptor β in a specific subset of nociceptive sensory neurons. *Eur. J. Neurosci.* 17, 2287–2298. doi: 10.1046/j.1460-9568.2003.02681.x
- Tannemaat, M. R., Eggers, R., Hendriks, W. T., de Ruiter, G. C., van Heerikhuizen, J. J., Pool, C. W., et al. (2008). Differential effects of lentiviral vector-mediated overexpression of nerve growth factor and glial cell line-derived neurotrophic factor on regenerating sensory and motor axons in the transected peripheral nerve. *Eur. J. Neurosci.* 28, 1467–1479. doi: 10.1111/j.1460-9568.2008.06452.x
- Tawk, M., Makoukji, J., Belle, M., Fonte, C., Trousson, A., Hawkins, T., et al. (2011). Wnt/ β -catenin signaling is an essential and direct driver of myelin gene expression and myelinogenesis. *J. Neurosci.* 31, 3729–3742. doi: 10.1523/JNEUROSCI.4270-10.2011
- Terashima, T., Yasuda, H., Terada, M., Kogawa, S., Maeda, K., Haneda, M., et al. (2001). Expression of Rho-family GTPases (Rac, cdc42, RhoA) and their association with p-21 activated kinase in adult rat peripheral nerve. *J. Neurochem.* 77, 986–993. doi: 10.1046/j.1471-4159.2001.00336.x
- Tham, S., Dowsing, B., Finkelstein, D., Donato, R., Cheema, S. S., Bartlett, P. F., et al. (1997). Leukemia inhibitory factor enhances the regeneration of transected rat sciatic nerve and the function of reinnervated muscle. *J. Neurosci. Res.* 47, 208–215. doi: 10.1002/(sici)1097-4547(19970115)47:2<208::aid-jnr9>3.0.co;2-j
- Thoenen, H. (1995). Neurotrophins and neuronal plasticity. *Science* 270, 593–598. doi: 10.1126/science.270.5236.593
- Toma, J. G., Pareek, S., Barker, P., Mathew, T. C., Murphy, R. A., Acheson, A., et al. (1992). Spatiotemporal increases in epidermal growth factor receptors following peripheral nerve injury. *J. Neurosci.* 12, 2504–2515. doi: 10.1523/JNEUROSCI.12-07-02504.1992
- Tomac, A., Lindqvist, E., Lin, L. F., Ogren, S. O., Young, D., Hoffer, B. J., et al. (1995). Protection and repair of the nigrostriatal dopaminergic system by GDNF in vivo. *Nature* 373, 335–339. doi: 10.1038/373335a0
- Tonra, J. R., Curtis, R., Wong, V., Cliffer, K. D., Park, J. S., Timmes, A., et al. (1998). Axotomy upregulates the anterograde transport and expression of brain-derived neurotrophic factor by sensory neurons. *J. Neurosci.* 18, 4374–4383. doi: 10.1523/JNEUROSCI.18-11-04374.1998
- Toth, C., Brussee, V., Martinez, J. A., McDonald, D., Cunningham, F. A., and Zochodne, D. W. (2006). Rescue and regeneration of injured peripheral

- nerve axons by intrathecal insulin. *Neuroscience* 139, 429–449. doi: 10.1016/j.neuroscience.2005.11.065
- Trupp, M., Rydén, M., Jörnval, H., Funakoshi, H., Timmusk, T., Arenas, E., et al. (1995). Peripheral expression and biological activities of GDNF, a new neurotrophic factor for avian and mammalian peripheral neurons. *J. Cell Biol.* 130, 137–148. doi: 10.1083/jcb.130.1.137
- Tsuji, M., Akeda, K., Iino, T., and Uchida, A. (2009). Are BMPs involved in normal nerve and following transection?: a pilot study. *Clin. Orthop. Relat. Res.* 467, 3183–3189. doi: 10.1007/s11999-009-1009-1
- Unsicker, K., Reichert-Preibsch, H., Schmidt, R., Pettmann, B., Labourette, G., and Sensenbrenner, M. (1987). Astroglial and fibroblast growth factors have neurotrophic functions for cultured peripheral and central nervous system neurons. *Proc. Natl. Acad. Sci. U S A* 84, 5459–5463. doi: 10.1073/pnas.84.15.5459
- Vellani, V., Zachrisson, O., and McNaughton, P. A. (2004). Functional bradykinin B1 receptors are expressed in nociceptive neurones and are upregulated by the neurotrophin GDNF. *J. Physiol.* 560, 391–401. doi: 10.1113/jphysiol.2004.067462
- Verge, V. M., Riopelle, R. J., and Richardson, P. M. (1989). Nerve growth factor receptors on normal and injured sensory neurons. *J. Neurosci.* 9, 914–922. doi: 10.1523/JNEUROSCI.09-03-00914.1989
- Walicke, P., Cowan, W. M., Ueno, N., Baird, A., and Guillemin, R. (1986). Fibroblast growth factor promotes survival of dissociated hippocampal neurons and enhances neurite extension. *Proc. Natl. Acad. Sci. U S A* 83, 3012–3016. doi: 10.1073/pnas.83.9.3012
- Walicke, P. A., Feige, J. J., and Baird, A. (1989). Characterization of the neuronal receptor for basic fibroblast growth factor and comparison to receptors on mesenchymal cells. *J. Biol. Chem.* 264, 4120–4126.
- Walker, C. L., Walker, M. J., Liu, N. K., Risberg, E. C., Gao, X., Chen, J., et al. (2012). Systemic bisperoxovanadium activates Akt/mTOR, reduces autophagy and enhances recovery following cervical spinal cord injury. *PLoS One* 7:e30012. doi: 10.1371/journal.pone.0030012
- Waller, A. (1850). Experiments on the section of the glossopharyngeal and hypoglossal nerves of the frog and observations of the alterations produced thereby in the structure of their primitive fibres. *Philos. Trans. R. Soc. Lond.* 140, 423–429. doi: 10.1098/rstl.1850.0021
- Wan, L., Xia, R., and Ding, W. (2010). Short-term low-frequency electrical stimulation enhanced remyelination of injured peripheral nerves by inducing the promyelination effect of brain-derived neurotrophic factor on Schwann cell polarization. *J. Neurosci. Res.* 88, 2578–2587. doi: 10.1002/jnr.22426
- Wang, R., King, T., Ossipov, M. H., Rossomando, A. J., Vanderah, T. W., Harvey, P., et al. (2008). Persistent restoration of sensory function by immediate or delayed systemic artemin after dorsal root injury. *Nat. Neurosci.* 11, 488–496. doi: 10.1038/nn2069
- Wang, R., Rossomando, A., Sah, D. W., Ossipov, M. H., King, T., and Porreca, F. (2014). Artemin induced functional recovery and reinnervation after partial nerve injury. *Pain* 155, 476–484. doi: 10.1016/j.pain.2013.11.007
- Wang, Y. L., Wang, D. Z., Nie, X., Lei, D. L., Liu, Y. P., Zhang, Y. J., et al. (2007). The role of bone morphogenetic protein-2 *in vivo* in regeneration of peripheral nerves. *Br. J. Oral Maxillofac. Surg.* 45, 197–202. doi: 10.1016/j.bjoms.2006.06.003
- Wang, Q., Xu, L., Chen, P., Xu, Z., Qiu, J., Ge, J., et al. (2018). Brcal is upregulated by 5-Aza-CdR and promotes DNA repair and cell survival and inhibits neurite outgrowth in rat retinal neurons. *Int. J. Mol. Sci.* 19:E1214. doi: 10.3390/ijms19041214
- Wanigasekara, Y., Airaksinen, M. S., Heuckeroth, R. O., Milbrandt, J., and Keast, J. R. (2004). Neurturin signalling via GFR α 2 is essential for innervation of glandular but not muscle targets of sacral parasympathetic ganglion neurons. *Mol. Cell Neurosci.* 25, 288–300. doi: 10.1016/j.mcn.2003.10.019
- Watanabe, K., Tamamaki, N., Furuta, T., Ackerman, S. L., Ikenaka, K., and Ono, K. (2006). Dorsally derived netrin 1 provides an inhibitory cue and elaborates the ‘waiting period’ for primary sensory axons in the developing spinal cord. *Development* 133, 1379–1387. doi: 10.1242/dev.02312
- Webber, C. A., Christie, K. J., Cheng, C., Martinez, J. A., Singh, B., Singh, V., et al. (2011). Schwann cells direct peripheral nerve regeneration through the Netrin-1 receptors, DCC and Unc5H2. *Glia* 59, 1503–1517. doi: 10.1002/glia.21194
- Wehner, D., Tsarouchas, T. M., Michael, A., Haase, C., Weidinger, G., Reimer, M. M., et al. (2017). Wnt signaling controls pro-regenerative Collagen XII in functional spinal cord regeneration in zebrafish. *Nat. Commun.* 8:126. doi: 10.1038/s41467-017-00143-0
- Weiss, T. W., Samson, A. L., Niego, B., Daniel, P. B., and Medcalf, R. L. (2006). Oncostatin M is a neuroprotective cytokine that inhibits excitotoxic injury *in vitro* and *in vivo*. *FASEB J.* 20, 2369–2371. doi: 10.1096/fj.06-5850fje
- Widenfalk, J., Wu, W., Hao, J., Person, J. K., Wiesenfeldt-Hallin, Z., and Risling, M. (2009). Treatment of transected peripheral nerves with artemin improved motor neuron regeneration, but did not reduce nerve injury-induced pain behaviour. *Scand. J. Plast. Reconstr. Surg. Hand. Surg.* 43, 245–250. doi: 10.3109/02844310903259082
- Williams, L. R., Manthorpe, M., Barbin, G., Nieto-Sampedro, M., Cotman, C. W., and Varon, S. (1984). High ciliary neurotrophic specific activity in rat peripheral nerve. *Int. J. Dev. Neurosci.* 2, 177–180. doi: 10.1016/0736-5748(84)90009-1
- Witzel, C., Rohde, C., and Brushart, T. M. (2005). Pathway sampling by regenerating peripheral axons. *J. Comp. Neurol.* 485, 183–190. doi: 10.1002/cne.20436
- Wong, L. E., Gibson, M. E., Arnold, H. M., Pepinsky, B., and Frank, E. (2015). Artemin promotes functional long-distance axonal regeneration to the brainstem after dorsal root crush. *Proc. Natl. Acad. Sci. U S A* 112, 6170–6175. doi: 10.1073/pnas.1502057112
- Wong, R. W., and Guillaud, L. (2004). The role of epidermal growth factor and its receptors in mammalian CNS. *Cytokine Growth Factor Rev.* 15, 147–156. doi: 10.1016/j.cytogfr.2004.01.004
- Wong, B. J., and Mattox, D. E. (1991). Experimental nerve regeneration: a review. *Otolaryngol. Clin. North Am.* 24, 739–752.
- Wong, J. N., Olson, J. L., Morhart, M. J., and Chan, K. M. (2015). Electrical stimulation enhances sensory recovery: a randomized controlled trial. *Ann. Neurol.* 77, 996–1006. doi: 10.1002/ana.24397
- Wright, M. C., Mi, R., Connor, E., Reed, N., Vyas, A., Alspalter, M., et al. (2014). Novel roles for osteopontin and clusterin in peripheral motor and sensory axon regeneration. *J. Neurosci.* 34, 1689–1700. doi: 10.1523/JNEUROSCI.3822-13.2014
- Wung, J. K., Perry, G., Kowalski, A., Harris, P. L., Bishop, G. M., Trivedi, M. A., et al. (2007). Increased expression of the remodeling- and tumorigenic-associated factor osteopontin in pyramidal neurons of the Alzheimer’s disease brain. *Curr. Alzheimer Res.* 4, 67–72. doi: 10.2174/156720507779939869
- Xu, X. M., Guénard, V., Kleitman, N., Aebischer, P., and Bunge, M. B. (1995). A combination of BDNF and NT-3 promotes supraspinal axonal regeneration into Schwann cell grafts in adult rat thoracic spinal cord. *Exp. Neurol.* 134, 261–272. doi: 10.1006/exnr.1995.1056
- Xu, Q. G., Li, X. Q., Kotecha, S. A., Cheng, C., Sun, H. S., and Zochodne, D. W. (2004). Insulin as an *in vivo* growth factor. *Exp. Neurol.* 188, 43–51. doi: 10.1016/j.expneurol.2004.03.008
- Yajima, Y., Narita, M., Narita, M., Matsumoto, N., and Suzuki, T. (2002). Involvement of a spinal brain-derived neurotrophic factor/full-length TrkB pathway in the development of nerve injury-induced thermal hyperalgesia in mice. *Brain Res.* 958, 338–346. doi: 10.1016/s0006-8993(02)03666-1
- Yamada, M., Ikeuchi, T., and Hatanaka, H. (1997). The neurotrophic action and signalling of epidermal growth factor. *Prog. Neurobiol.* 51, 19–37. doi: 10.1016/s0304-0082(96)00046-9
- Yamamoto, M., Sobue, G., Yamamoto, K., Terao, S., and Mitsuma, T. (1996). Expression of mRNAs for neurotrophic factors (NGF, BDNF, NT-3 and GDNF) and their receptors (p75NGFR, trkA, trkB, and trkC) in the adult human peripheral nervous system and nonneural tissues. *Neurochem. Res.* 21, 929–938. doi: 10.1007/bf02532343
- Yan, Q., Matheson, C., and Lopez, O. T. (1995). *In vivo* neurotrophic effects of GDNF on neonatal and adult facial motor neurons. *Nature* 373, 341–344. doi: 10.1038/373341a0
- Yang, Q., Peng, L., Wu, Y., Li, Y., Wang, L., Luo, J. H., et al. (2018). Endocytic adaptor protein HIP1R controls intracellular trafficking of epidermal growth factor receptor in neuronal dendritic development. *Front. Mol. Neurosci.* 11:447. doi: 10.3389/fnmol.2018.00447

- Yin, Q., Kemp, G. J., Yu, L. G., Wagstaff, S. C., and Frostick, S. P. (2001). Neurotrophin-4 delivered by fibrin glue promotes peripheral nerve regeneration. *Muscle Nerve* 24, 345–351. doi: 10.1002/1097-4598(200103)24:3<345::aid-mus1004>3.0.co;2-p
- Yin, X. F., Xu, H. M., Jiang, Y. X., Zhi, Y. L., Liu, Y. X., Xiang, H. W., et al. (2015). Lentivirus-mediated Persephin over-expression in Parkinson's disease rats. *Neural Regen Res.* 10, 1814–1818. doi: 10.4103/1673-5374.170309
- Yoshimura, T., Kawano, Y., Arimura, N., Kawabata, S., Kikuchi, A., and Kaibuchi, K. (2005). GSK-3 β regulates phosphorylation of CRMP-2 and neuronal polarity. *Cell* 120, 137–149. doi: 10.1016/j.cell.2004.11.012
- Zacksenhaus, E., Jiang, Z., Chung, D., Marth, J. D., Phillips, R. A., and Gallie, B. L. (1996). pRb controls proliferation, differentiation, and death of skeletal muscle cells and other lineages during embryogenesis. *Genes Dev.* 10, 3051–3064. doi: 10.1101/gad.10.23.3051
- Zhang, J., Gray, J., Wu, L., Leone, G., Rowan, S., Cepko, C. L., et al. (2004a). Rb regulates proliferation and rod photoreceptor development in the mouse retina. *Nat. Genet.* 36, 351–360. doi: 10.1038/ng1318
- Zhang, J., Lineaweaver, W. C., Oswald, T., Chen, Z., Chen, Z., and Zhang, F. (2004b). Ciliary neurotrophic factor for acceleration of peripheral nerve regeneration: an experimental study. *J. Reconstr. Microsurg.* 20, 323–327. doi: 10.1055/s-2004-824891
- Zhang, J. Y., Luo, X. G., Xian, C. J., Liu, Z. H., and Zhou, X. F. (2000). Endogenous BDNF is required for myelination and regeneration of injured sciatic nerve in rodents. *Eur. J. Neurosci.* 12, 4171–4180. doi: 10.1111/j.1460-9568.2000.01312.x
- Zhang, L., Ma, Z., Smith, G. M., Wen, X., Pressman, Y., Wood, P. M., et al. (2009). GDNF-enhanced axonal regeneration and myelination following spinal cord injury is mediated by primary effects on neurons. *Glia* 57, 1178–1191. doi: 10.1002/glia.20840
- Zhang, Y., Tatsuno, T., Carney, J. M., and Mattson, M. P. (1993). Basic FGF, NGF, and IGFs protect hippocampal and cortical neurons against iron-induced degeneration. *J. Cereb. Blood Flow Metab.* 13, 378–388. doi: 10.1038/jcbfm.1993.51
- Zheng, L. F., Wang, R., Yu, Q. P., Wang, H., Yi, X. N., Wang, Q. B., et al. (2010). Expression of HGF/c-Met is dynamically regulated in the dorsal root ganglions and spinal cord of adult rats following sciatic nerve ligation. *Neurosignals* 18, 49–56. doi: 10.1159/000320715
- Zhou, Z., Peng, X., Fink, D. J., and Mata, M. (2009). HSV-mediated transfer of artemin overcomes myelin inhibition to improve outcome after spinal cord injury. *Mol. Ther.* 17, 1173–1179. doi: 10.1038/mt.2009.52
- Zhou, X. F., and Rush, R. A. (1993). Localization of neurotrophin-3-like immunoreactivity in peripheral tissues of the rat. *Brain Res.* 621, 189–199. doi: 10.1016/0006-8993(93)90106-w
- Zhou, X. F., and Rush, R. A. (1996). Endogenous brain-derived neurotrophic factor is anterogradely transported in primary sensory neurons. *Neuroscience* 74, 945–951. doi: 10.1016/0306-4522(96)00237-0
- Zochodne, D. W. (2008). *Neurobiology of Peripheral Nerve Regeneration*. New York, NY: Cambridge University Press.
- Zochodne, D. W. (2012). The challenges and beauty of peripheral nerve regrowth. *J. Peripher. Nerv. Syst.* 17, 1–18. doi: 10.1111/j.1529-8027.2012.00378.x

Conflict of Interest Statement: The authors declare that the research was conducted in the absence of any commercial or financial relationships that could be construed as a potential conflict of interest.

Copyright © 2019 Duraikannu, Krishnan, Chandrasekhar and Zochodne. This is an open-access article distributed under the terms of the Creative Commons Attribution License (CC BY). The use, distribution or reproduction in other forums is permitted, provided the original author(s) and the copyright owner(s) are credited and that the original publication in this journal is cited, in accordance with accepted academic practice. No use, distribution or reproduction is permitted which does not comply with these terms.



Spatiotemporal Differences in Gene Expression Between Motor and Sensory Autografts and Their Effect on Femoral Nerve Regeneration in the Rat

David Hercher^{1,2*}, Markus Kerbl^{1,2}, Christina M. A. P. Schuh^{1,2,3}, Johannes Heinzel^{1,2}, László Gal⁴, Michaela Stainer^{1,2}, Robert Schmidhammer^{1,2}, Thomas Hausner^{1,2}, Heinz Redl^{1,2}, Antal Nógrádi^{1,2,4†} and Ara Hacobian^{1,2†}

¹ Ludwig Boltzmann Institute for Experimental and Clinical Traumatology, Vienna, Austria, ² Austrian Cluster for Tissue Regeneration, Vienna, Austria, ³ Centro de Medicina Regenerativa, Facultad de Medicina Clínica Alemana-Universidad del Desarrollo, Santiago, Chile, ⁴ Department of Anatomy, Histology and Embryology, University of Szeged, Szeged, Hungary

OPEN ACCESS

Edited by:

Esther Udina,
Autonomous University of Barcelona,
Spain

Reviewed by:

Ahmet Hoke,
Johns Hopkins University,
United States
Rajiv Midha,
University of Calgary, Canada

*Correspondence:

David Hercher
david.hercher@trauma.lbg.ac.at

†Co-last authors

Specialty section:

This article was submitted to
Cellular Neurophysiology,
a section of the journal
Frontiers in Cellular Neuroscience

Received: 02 February 2019

Accepted: 12 April 2019

Published: 08 May 2019

Citation:

Hercher D, Kerbl M, Schuh CMAP, Heinzel J, Gal L, Stainer M, Schmidhammer R, Hausner T, Redl H, Nógrádi A and Hacobian A (2019) Spatiotemporal Differences in Gene Expression Between Motor and Sensory Autografts and Their Effect on Femoral Nerve Regeneration in the Rat. *Front. Cell. Neurosci.* 13:182. doi: 10.3389/fncel.2019.00182

To improve the outcome after autologous nerve grafting in the clinic, it is important to understand the limiting variables such as distinct phenotypes of motor and sensory Schwann cells. This study investigated the properties of phenotypically different autografts in a 6 mm femoral nerve defect model in the rat, where the respective femoral branches distally of the inguinal bifurcation served as homotopic, or heterotopic autografts. Axonal regeneration and target reinnervation was analyzed by gait analysis, electrophysiology, and wet muscle mass analysis. We evaluated regeneration-associated gene expression between 5 days and 10 weeks after repair, in the autografts as well as the proximal, and distal segments of the femoral nerve using qRT-PCR. Furthermore we investigated expression patterns of phenotypically pure ventral and dorsal roots. We identified highly significant differences in gene expression of a variety of regeneration-associated genes along the central – peripheral axis in healthy femoral nerves. Phenotypically mismatched grafting resulted in altered spatiotemporal expression of neurotrophic factor BDNF, GDNF receptor GFR α 1, cell adhesion molecules Cadm3, Cadm4, L1CAM, and proliferation associated Ki67. Although significantly higher quadriceps muscle mass following homotopic nerve grafting was measured, we did not observe differences in gait analysis, and electrophysiological parameters between treatment paradigms. Our study provides evidence for phenotypic commitment of autologous nerve grafts after injury and gives a conclusive overview of temporal expression of several important regeneration-associated genes after repair with sensory or motor graft.

Keywords: femoral nerve, Schwann cell, phenotype, gene expression, neurotrophic factor, cell adhesion molecule, peripheral nerve regeneration

INTRODUCTION

Injuries to the upper extremities are amongst the most common work-, sports- and traffic related injuries. These injuries may result in peripheral nerve damages with loss of nerve continuity and subsequent loss of motor and sensory function. They require long rehabilitation phases and have a major impact on the quality of life of the patient. The clinical gold standard to bridge a

nerve injury with segmental loss is the autologous nerve transplant. In clinical cases, a sensory nerve is harvested and used as a transplant to bridge the defect in order to restore essential motor functions. However, functional outcome after nerve grafting is very often not satisfactory, especially after nerve injury with profound tissue loss (Meek et al., 2005; Secer et al., 2008; Yang et al., 2011). A reason could be the presence of phenotypically mismatched Schwann cells in the purely sensory nerve grafts. Several groups have provided evidence that there are phenotypical differences between Schwann cells from sensory and motor nerves regarding the expression of neurotrophic factors and their receptors (Höke et al., 2006; Chu et al., 2008; He et al., 2012b; Jesuraj et al., 2012, 2014). Furthermore, sensory and motor branches of the femoral nerve differ in architecture, thereby influencing regeneration of axons after injury (Moradzadeh et al., 2008). The majority of publications investigating the effect of sensory nerve grafts suggests a negative impact of sensory phenotype on motor axon regeneration when compared to a motor graft (Sulaiman et al., 2002; Brenner et al., 2006; Abdullah et al., 2013). However, a comprehensive study investigating the effect of phenotypically different grafting including functional outcome, gene expression patterns and histology has not been published yet. We hypothesized that there are differences in the gene expression patterns in sensory Schwann cells when compared to Schwann cells derived from motor nerves and that this phenotypical commitment has an effect on the regenerative capacity of axons. First, we investigated the baseline gene expression levels along the central-peripheral axis in uninjured femoral nerves with emphasis on phenotypical differences. Second, we determined the influence of a phenotypically different environment on the regenerative capacity of motor and sensory axons, thereby establishing a characteristic expression profile along the phenotypical mixed, motor (carrying afferent and efferent fibers from/to the muscle) and purely sensory nerves. For this study we used a preclinical *in vivo* model, which reflects the clinical situations (i.e., the use of autologous sensory nerve graft to support axonal regeneration and restore motor function). Therefore we performed homotopic as well as heterotopic nerve autografting in a femoral nerve defect model. Taken together, this study evaluated the spatiotemporal expression of key regeneration-associated genes and their influence on functional reinnervation. We aim to add insight into regenerative processes in phenotypically mismatched environments to allow future development of strategies to improve functional outcome after nerve grafting surgeries.

MATERIALS AND METHODS

Experimental Model

To analyze the spatiotemporal gene expression changes during nerve regeneration the establishment of an appropriate animal model was mandatory for this study. We adapted the rat femoral nerve model, described earlier to the present study, as it bifurcates into a mixed motor, and a purely sensory branch at the inguinal region (Brushart, 1990; Jesuraj et al., 2012; He et al., 2016).

A power analysis was performed using StatMate 2.0 (GraphPad) in order to evaluate appropriate sample size and power. A total of 99 male *Sprague Dawley* rats (Charles River, Sulzfeld, Germany) weighing 300–350 g were randomly assigned to treatment groups. Group sizes were as follows: gene expression analysis ($n = 8$ –10), histological evaluation ($n = 3$ –5), and retrograde labeling ($n = 2$ –3). Animals were subdivided in 4 different observation time groups: 5 days, 2 weeks, 6 and 10 weeks (**Figure 1E** and **Table 1**).

Animals were kept pairwise in appropriate cages according to internal standard operating procedures, including food (Sniff, Soest, Germany), and water *ad libitum*. Animals were allowed to accustomize for 7 days prior to any experimental handling.

Surgical Procedure

All procedures were performed under aseptical conditions according to Austrian law and the guide for the care and use of laboratory animals, and were approved by the City Government of Vienna (Animal use permit: MA58 149539/2012/5). Under general anesthesia (110 mg/kg Ketamin, 12 mg/kg Xylazin; inhalation of 1–2 Vol% Isofluran-Oxygen mix) and analgesia (1× daily 1.25 mg/kg Butorphanol s.c. and 1× daily 0.15 mg/kg Meloxicam for 4 days starting on the day of surgery) a longitudinal 3–4 cm groin incision was applied in order to expose the right femoral neurovascular bundle. Blunt exploration was performed until the bifurcation of the femoral nerve was exposed. The exposed motor and sensory branches were sharply transected distal to the bifurcation resulting in a 6 mm gap and a 6 mm graft of each branch, respectively (**Figure 1B**). Elastic retraction of nerves was negligible and tension-free suturing was carried out. According to the assigned treatment group the gaps were repaired with either a homotopic graft (motor graft in motor branch and sensory graft in sensory branch) (**Figure 1C**) or a heterotopic graft (motor graft in sensory branch and sensory graft in motor branch) (**Figure 1D**) using 2 epineural sutures per coaptation site (Ethilon 11-0; Ethicon, Somerville, NJ, United States). Postoperative analgesia was given once a day for 4 days.

Catwalk Automated Gait Analysis

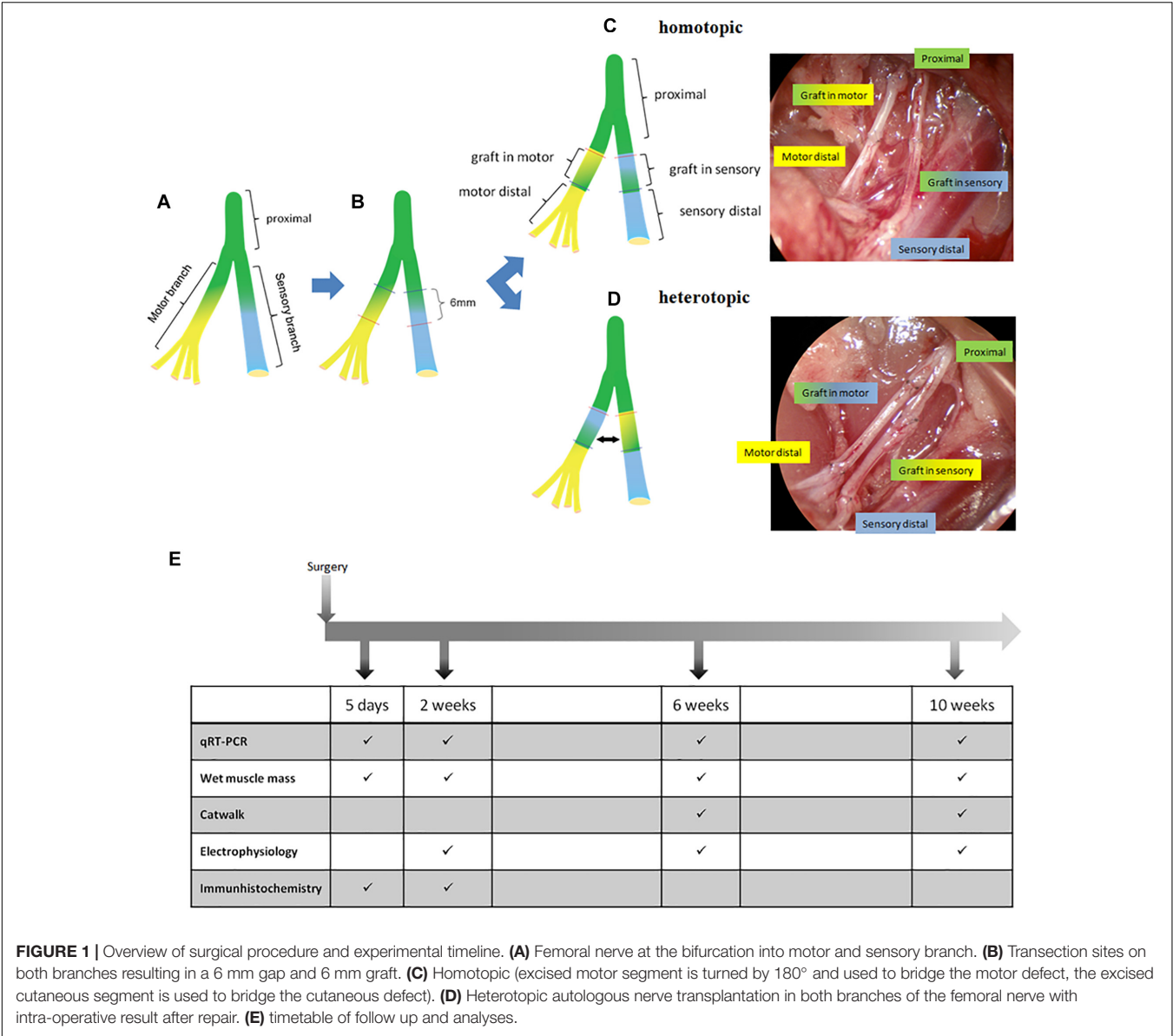
Functional analysis was performed with the CatWalk XT (Version 10.6) automated gait analysis system (Noldus Information System, Wageningen, Netherlands). (Pena and Baron, 1988; Hamers et al., 2001; Vrinten and Hamers, 2003; Koopmans et al., 2007; Bozkurt et al., 2008, 2011, 2012; Hausner et al., 2012; Huang et al., 2012; Li et al., 2014; Kappos et al., 2017).

Animals were pre-trained to use the CatWalk daily, for 1 week prior to surgery. Data was collected according to the recommendations made in the literature (Deumens et al., 2014). Parameters assessed were print area, swing time, and duty cycle.

Data was obtained from 37 animals in total, which were subdivided into the following groups:

Homotopic nerve graft ($n = 19$, observed 6 weeks: $n = 9$, observed 10 weeks: $n = 10$).

Heterotopic nerve graft ($n = 18$, observed 6 weeks: $n = 10$, observed 10 weeks: $n = 8$).



We collected 3 runs per trial at baseline and from then every week, ending data collection either 6 weeks ($n = 19$) or 10 weeks ($n = 18$) after surgery.

Since strong emphasis has been placed on crossing time or crossing speed as crucial factors to control for proper analysis of data we collected 3 runs per trial, within the exact same velocity ranges as defined by Koopmans et al. (2007). Additionally, only those runs were recorded which contained at least 3 step cycles per paw.

Each of the three parameters (Print Area, Swing Time and Duty Cycle) was assessed for both hind paws and for each one a ratio was calculated by dividing the right side's value (transection) by the left side's (control). This ratio (Print Area ratio, Swing Time ratio, Duty Cycle ratio) was then compared to the ratio at baseline for each postoperative time point and the result given in percent.

Electrophysiology and Quadriceps Muscle Mass

In order to evaluate successful reinnervation of the quadriceps muscle, compound muscle action potential (CMAP), and peak amplitude of voltage signal was measured at the end of the observation time at 2, 6, and 10 weeks. The femoral nerve was explored and for stimulation of the motor branch a bipolar stimulation electrode was placed proximal to the bifurcation using a micro manipulator. Two needle electrodes were placed into the quadriceps muscle approximately 10 mm apart for recording, whereas the grounding electrode was placed in the surrounding tissue. A Neuromax EMG device (Natus, WI, United States) was used for stimulation and recording. The contralateral healthy femoral nerve and quadriceps muscle served as an internal control. Core temperature of the animal was measured rectally and used for normalization.

TABLE 1 | Nerve segments used for qRT-PCR.

Excised nerve samples for qRT-PCR analysis	
Healthy contralateral	Injured ipsilateral
Dorsal roots (DR) L2 and L3	
Ventral roots (VR) L2 and L3	
Femoral nerve proximal of bifurcation	Femoral nerve proximal of bifurcation
Cutaneous branch of femoral nerve	Graft in cutaneous branch
	Cutaneous branch distal of graft
Motor branch of femoral nerve	Graft in motor branch
	Motor branch distal of graft

Baseline expression was evaluated using the contralateral, healthy nerves. Effect of injury and graft phenotype was evaluated by comparing the nerve segments from the injured side to their contralateral counter part in the same animal.

(Muscle) Mass Evaluation

At all endpoints quadriceps muscles were excised bilaterally and weighed to evaluate atrophy and regeneration. Muscle weight was set in to relation of total weight of the animal.

(Immuno)-Histological Evaluation

For immunohistological evaluation, femoral nerves were harvested 5 days and 2 weeks after surgery and fixated in 4% buffered formaldehyde (VWR, Radnor, PA, United States) overnight. Subsequently, nerves were washed (distilled water) and transferred into 30% sucrose in phosphate buffered saline (PBS). 25 μ m thick longitudinal sections were cut using a cryostat and mounted on gelatine-coated glass slides.

In order to evaluate axonal reinnervation, sections were blocked with 5% skim milk and subsequently stained with anti-Neurofilament (rabbit monoclonal; Abcam, United Kingdom) overnight at 4°C. After washing with PBS, sections were incubated with secondary antibody (anti-rabbit Alexa Fluor 488 Life Technologies, MA, United States) mounted for microscopical evaluation using glycerol.

Cresyl violet staining was performed as follows: cryosections were rinsed in distilled water and stained with 1% w/v Cresyl Violet solution pH 4 (Sigma-Aldrich) for 5–10 min. Samples were mounted with DPX mounting media (Sigma-Aldrich).

Quantitative Real Time Reverse Transcription Polymerase Chain Reaction (qRT-PCR)

For gene expression analysis, nerve fragments were harvested from all observation time groups 5 days, 2, 6, and 10 weeks ($n = 8-10$), according to **Table 1**. Samples were immediately snap frozen in liquid N₂ and stored on -80°C . RNA was isolated using peqGOLD TriFast according to manufacturer's instructions (VWR, United States) and used for subsequent cDNA synthesis (EasyScriptTM RTase, ABM, CAN). Analysis of mRNA levels were performed by qRT-PCR using 18 ng cDNA, primer according to **Table 2**, and KAPA SYBR (KAPA SYBR, Peqlab/PerfeCTa SYBR, VWR, United States) on a Bio-Rad CFX 96 cycloer (Bio-Rad, CA, United States) (for detailed protocol see **Supplementary Data**).

We focused our investigation on three groups of targets: First, neurotrophins and their receptors, as they play crucial roles in regeneration and maintenance of the peripheral nervous system. Second, cell adhesion molecules, with special emphasis on Schwann cell – axon interactions. Third, a group of genes, which give us information about the cell status, again with emphasis on Schwann cells.

We tested several reference genes including beta-actin (β -Actin) and ankyrin repeat domain-containing protein 27 (Ankrd27) (Gambarotta et al., 2014) in a subset of samples, however, we did not detect a significant influence of central-peripheral axis and phenotype as well as injury on the expression levels between HPRT and others (**Supplementary Figure 1**). Data were normalized to Hypoxanthine-guanine phosphoribosyltransferase (HPRT) mRNA level in the same sample.

Statistical Analysis

Statistical analysis was performed using GraphPad Prism 6.0 (GraphPad Software Inc., San Diego, CA, United States). The data was tested for normal distribution using the Kolmogorov–Smirnov test. Data was statistically analyzed using either Student's *t*-test (two groups to compare), multiple *t*-tests using Holm-Sidak correction for multiple comparison or one-way ANOVA, and Tukey's multiple comparison *post hoc* test. To compare various experimental groups among different time points, two-way ANOVA with Tukey's multiple comparison *post hoc* tests was used. Results are expressed as means with standard error of the mean (SEM). *P*-value of <0.05 was considered as statistically significant.

RESULTS

Functional Reinnervation Is Comparable After Homotopic and Heterotopic Autografting

Gait Analysis Is a Feasible but Limited Functional Testing Method in Femoral Nerve Defect Models

Several gait parameters showed overall significant changes after autografting surgery. Mean hind paw print area was reduced to 33.6 ± 8.75 and $35.6 \pm 9.83\%$ (homotopic vs. heterotopic group) with no significant differences found between the two setup paradigms 1 week after injury. At the same time point duty cycle was reduced to 64.77 ± 10.6 and $69.09 \pm 6.8\%$ (homotopic vs. heterotopic groups) compared to the contralateral side. Swing time extended to $234.59 \pm 55.6\%$ (homotopic) and $225.96 \pm 36\%$ (heterotopic). Restoration of all three parameters to pre-injury levels was observed between postoperative weeks 7 and 10 with no significant differences between homotopic and heterotopic grafting (**Figure 2**). Furthermore, counting of retrograde labeled motoneurons innervating the femoral motor branch indicated similar numbers of reinnervating motoraxons (**Supplementary Figure 2** and see **Supplementary Data** for methods).

TABLE 2 | Primer sequence, annealing- and melting temperature, and detected transcript variants.

Target name	Primer sequence	Annealing temp. (exp)	Melting temp. (exp)	Transcript variants
BDNF NM_012513.4	s: TGA G AGA C G CAC AGG A as: AGA GGT A GTG TAG G GGA C	59.0°C	77.5°C	1-10 X1
GDNF NM_019139.1	s: G TAG G GCT C G TGA C as: CCA GGG TCA GAT ACA TCC AC	60.0°C	82.0°C	X1–X4
L1CAM (He et al., 2012a) NM_017345.1	s: GCCTCAGCCTCTATGTG as: GCCAGTGCCATTAGTCTTC	60.0°C	80.0°C	X1–X4
HPRT NM_012583.2	s: AGT CCC AGC GTC GTG ATT AG as: TGG CCT CCC ATC TCC TTC AT	63.5°C	78.0°C	HPRT, HPRT1
Fibronectin (Yoshida et al., 2002) NM_019143.2	s: GTGGCTGCCTTCCTTCTC as: GTGGGTTGCACCTTCT	58.0°C	80.0°C	X1–X10
Ankrd27 (Gambiarotta et al., 2014) NM_001271264.1	s: CCCAGGATCCGAGAGGTGCTGTC as: CAGAGCCATATGGACTTCAGGGGG	62.0°C	79.0°C	X1, X6
GFAP (Tanga et al., 2004) NM_017009.2	s: TGG CCA CCA GTA ACA TGC as: CAGTTGCGCGCGATAGTCAT	62.0°C	83.0°C	GFAP
TrkB (Kondo et al., 2010) NM_012731.2	s: CACACACAGGGCTCCTTA as: AGTGGTGGTCTGAGGTTGG	63.0°C	80.0°C	X1–X5
Itga5 NM_001108118.1	s: GTTTACACATGCCCTCTCAC as: GATTCCCTTTACAGCTCCA	59.0°C	80.0°C	Itga5
Itgb1 NM_017022.2	s: A CAG T C AGA ACA GTC C as: AGG ATC G T CTC ACA ATG G	56.0°C	81.0°C	X1
MKi-67 NM_001271366.1	s: ACT GTA T T ATT GCC TGT GCT as: CCC ACC A CAT TTA C TGC T	60.0°C	78.0°C	X1
GFRα1 NM_012959.1	s: CTG TCT TTC TGA TAG TGA TTT CGG as: GTG A CTG CTT CTC C GG	56.0°C	83.5°C	X1,X2
Cadm3 NM_001047103.1	s: CTCTCTGTCCGACCCT as: TTTGTGCCGGATCATAGTG	60.0°C	80.5°C	X1
Cadm4 NM_001047107.1	s: CAG TAT GAT GGG TCT ATA GTC GT as: GGA GCC ACT G ACA GTG AG	64.0°C	85.5°C	Cadm4
LIFR NM_031048.1	s: CATCTACTGGCCTTTACC as: TCTCTGCTTTGTGTGTGGA	59.0°C	78.5°C	X1–X3
p75 NM_012610.2	s: CTG T GCG G AGA TCC CT as: G ATG GAG C TAG ACA GGA	60.0°C	85.0°C	X1,X2
HSP70 NM_212546.4, NM_031971.2, NM_212504.1	s: GGTGCTGATCCAGGTGTACGAGG as: GATGTCGGGTACCTCGATCTGG	55.0°C	85.0°C	Hspa1a, Hspa1b, Hspa1l
β-Actin (Kondo et al., 2010) NM_031144.3	s: CCTGTATGCCTCTGGTCGTA as: CCATCTCTTGCTCGGTCT	55.0°C	85.5°C	Actb

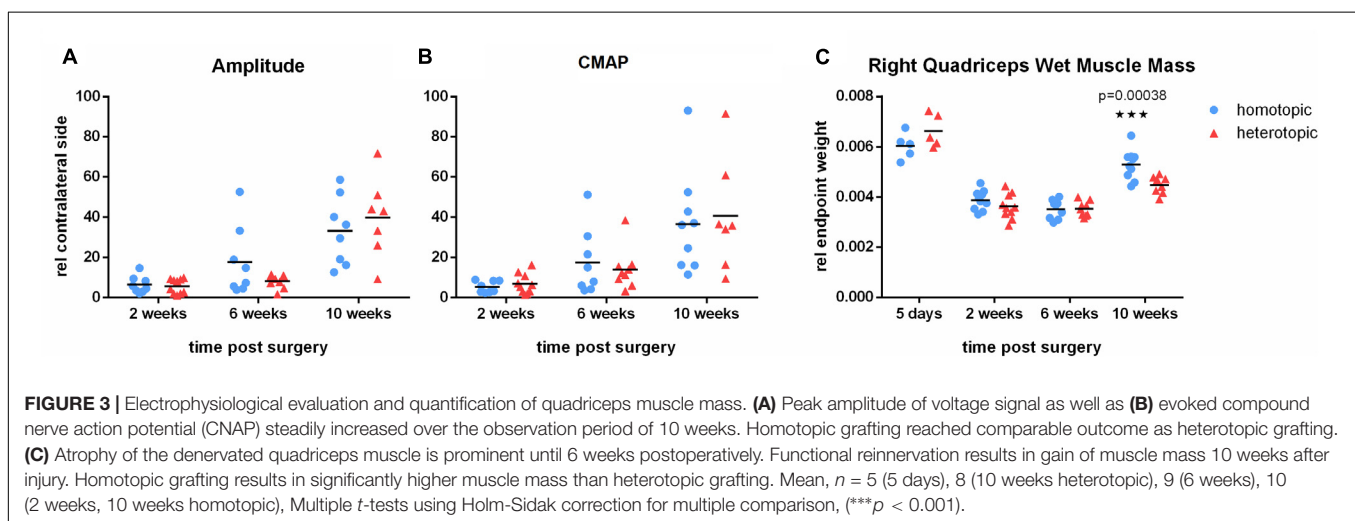
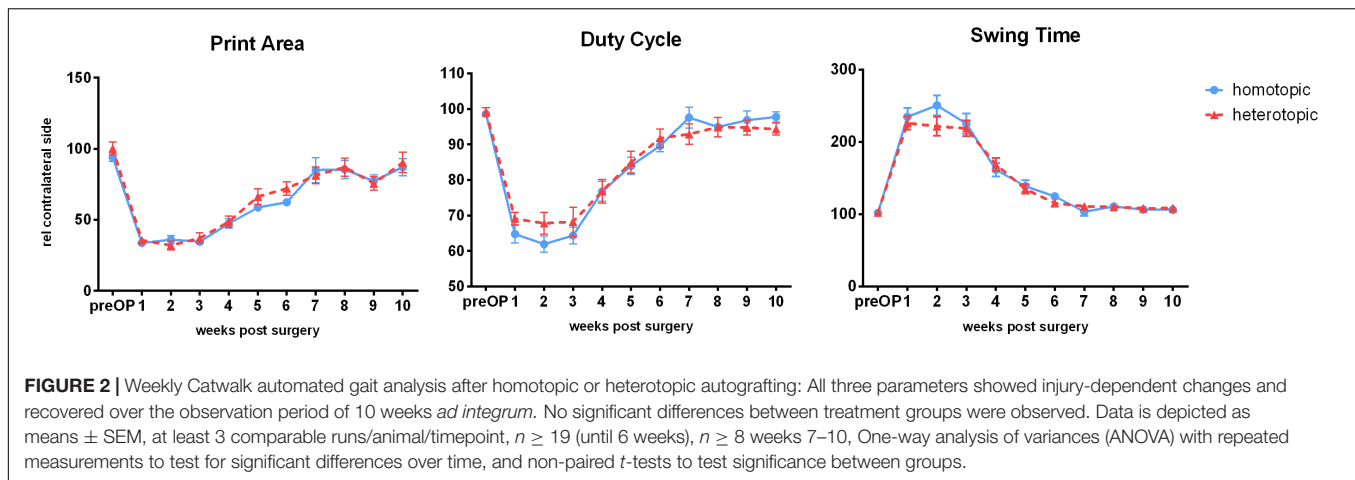
Homotopic Grafting Results in Increased Wet Muscle Mass but Not in Improved Electrophysiological Parameters

In order to further evaluate axonal regeneration through the phenotypically different autografts and reinnervation of the quadriceps muscle, we performed electrophysiological testing at 2, 6 and 10 weeks after homotopic or heterotopic femoral nerve autografting. Evoked CMAP and peak amplitude increased steadily over time indicating functional regeneration of motor axons and reinnervation of the denervated quadriceps muscle. As peak amplitude correlates well with the number of regenerated large ($A\alpha\beta$) myelinated fibers (Navarro, 2016), this demonstrates functional regeneration in both grafting groups over the time course of 10 weeks. However, both repair groups did not show full recovery of electrophysiological parameters (**Figures 3A,B**) during the observation period. Wet muscle mass of the quadriceps muscle evaluated 5 days, 2, 6 and 10 weeks after repair, demonstrated strong atrophy after femoral nerve defect in

both autografting paradigms. Atrophy remained prominent until 6 weeks postoperatively. This was followed by increase in muscle mass on week 10. Interestingly, homotopic autografting of the femoral motor branch resulted in significantly higher quadriceps muscle mass recovery than heterotopic grafting (**Figure 3C**).

Staggered Regeneration of Axons Occurs Independently of Pathway Modality and Graft Phenotype

To evaluate overall integrity of the grafts and axonal regeneration of the femoral motor and cutaneous branches, cresyl violet as well as neurofilament (NF) stainings were performed 5 days and 2 weeks after nerve repair. Representative images of macroscopical evaluation as well as cresyl violet staining showed intact suture sites in all excised samples (**Figure 4**). NF staining revealed the axonal regeneration front to be staggered at the proximal coaptation sites at 5 days. However, 2 weeks



postoperatively, regenerated axons were visible in the distal parts of the motor and cutaneous branches regardless of homotopic or heterotopic grafting.

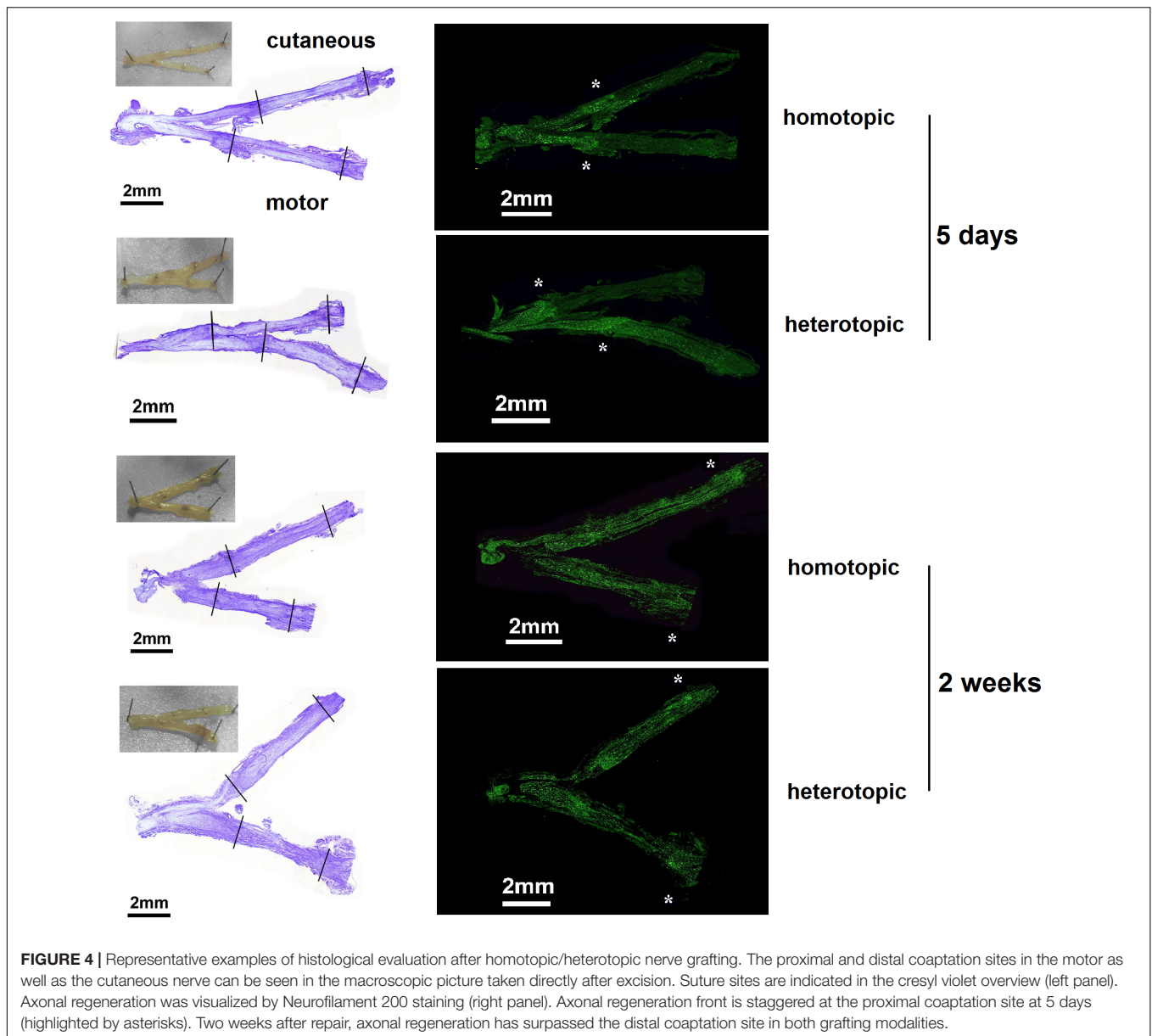
Quantification of Baseline Gene Expression Analysis in Healthy Nerves

Quantitative reverse transcription PCR was used to evaluate expression profiles of 15 target genes over the motor and cutaneous central-peripheral axis of the femoral nerve. L2 and L3 dorsal (DR) and ventral roots (VR), the motor and cutaneous branches and a 10 mm piece of the proximal part of the healthy, contralateral femoral nerve were excised. Targets constitute of two well-described neurotrophic factors (BDNF and GDNF) and three of their receptors (Low affinity neurotrophic receptor – p75, Tropomyosin kinase receptor B – TrkB and GDNF receptor $\alpha 1$ – GFR $\alpha 1$), additionally we included the receptor of leukemia inhibitory factor (LIFR) as LIF is a known autocrine survival factor for Schwann cells (Ito et al., 1998; Dowsing et al., 1999). Furthermore, cell adhesion molecules, involved in axonal pathfinding (Fibronectin and its receptor integrin $\alpha 5\beta 1$) and

in (re-)myelination processes (Cadm3, Cadm4, and L1CAM) were investigated. Finally Schwann cell specific glial fibrillary acidic protein (GFAP), proliferation associated protein Ki-67 and stress-responsive heat shock protein 70 (HSP70) were chosen to provide a more general overview of cell-status in the analyzed nerve samples. Comparison of expression levels of three different reference genes: HPRT, β -Actin, and Ankrd27, was performed on a subset of samples. Expression levels of all three reference genes were proven to be unaffected by phenotypical and central-peripheral origin of nerve samples (**Supplementary Figure 1**). All subsequent data were normalized to HPRT.

Nerve Phenotype and Central-Peripheral Axis Do Not Affect Neurotrophic Factor Expression Whereas Their Receptors Are Strongly Affected

Due to their potent effect on regeneration we evaluated the baseline mRNA levels of neurotrophic factors and their receptors (**Figure 5**). Brain derived neurotrophic factor (BDNF) as well as glial cell line-derived neurotrophic factor (GDNF) showed similar expression levels in dorsal, ventral roots as well as the peripheral mixed (proximal), motor, and cutaneous nerves.



However, expression of the BDNF receptor tyrosine receptor kinase B (TrkB) was strongly increased in the cutaneous branch, when compared to other parts of the femoral nerve. The low-affinity neurotrophic factor receptor p75, as well as the GDNF receptor GFR α 1, displayed central-peripheral commitment as both receptors showed significantly higher expression in the central L2, and L3 roots regardless of their phenotype. In contrast, LIFR demonstrated reduced expression in central parts of the femoral nerve.

Central-Peripheral Axis Strongly Affects Expression Levels of Cell Adhesion-Associated Genes

Fibronectin and its neuronal integrin receptor α 5 β 1 play crucial roles in Schwann cell migration after peripheral nerve injury (de Luca et al., 2014). Also Cadm4, Cadm3, and the

L1 cell adhesion molecule (L1CAM) are prominent factors in cell migration, axon pathfinding, and (re)-myelination processes. Therefore we evaluated differences in baseline expression of these factors along the different parts of the femoral nerve (**Figure 6**). All excised peripheral parts of the femoral nerve (proximal, cutaneous, and motor branch) showed higher expression of Fibronectin and Integrin α 5 than the dorsal and ventral roots. However, expression levels of Integrin β 1, Cadm4, and Cadm3 were reduced in these samples when compared to the dorsal and ventral roots. L1CAM expression displayed a strong phenotypical/central discrepancy as the motor branch of the femoral nerve expressed significantly lower levels of L1CAM mRNA than the central roots and the proximal as well as cutaneous parts of the femoral nerve.

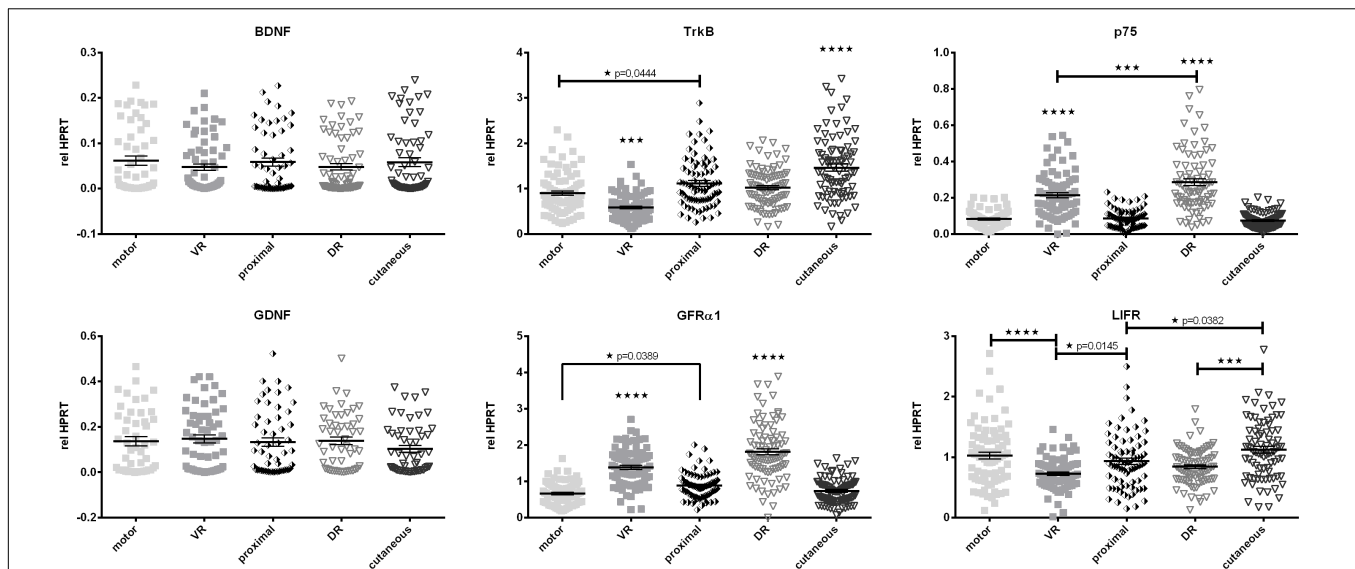


FIGURE 5 | Comparison of baseline mRNA expression of neurotrophic factors and their receptors relative to HPRT in Schwann cells of the femoral nerve constituents. In contrast to BDNF and GDNF, expression levels of neurotrophic factor receptors display significant discrepancies along the central-peripheral axis. motor, femoral nerve motor branch; cutaneous, femoral nerve cutaneous branch; proximal, mixed femoral nerve segment proximal to bifurcation; VR, ventral root; DR, dorsal root. Data are presented as mean \pm SEM, $n \geq 57$, One-way analysis of variances (ANOVA) with Tukey's multiple comparison. (* $p < 0.05$, *** $p < 0.001$, **** $p < 0.0001$).

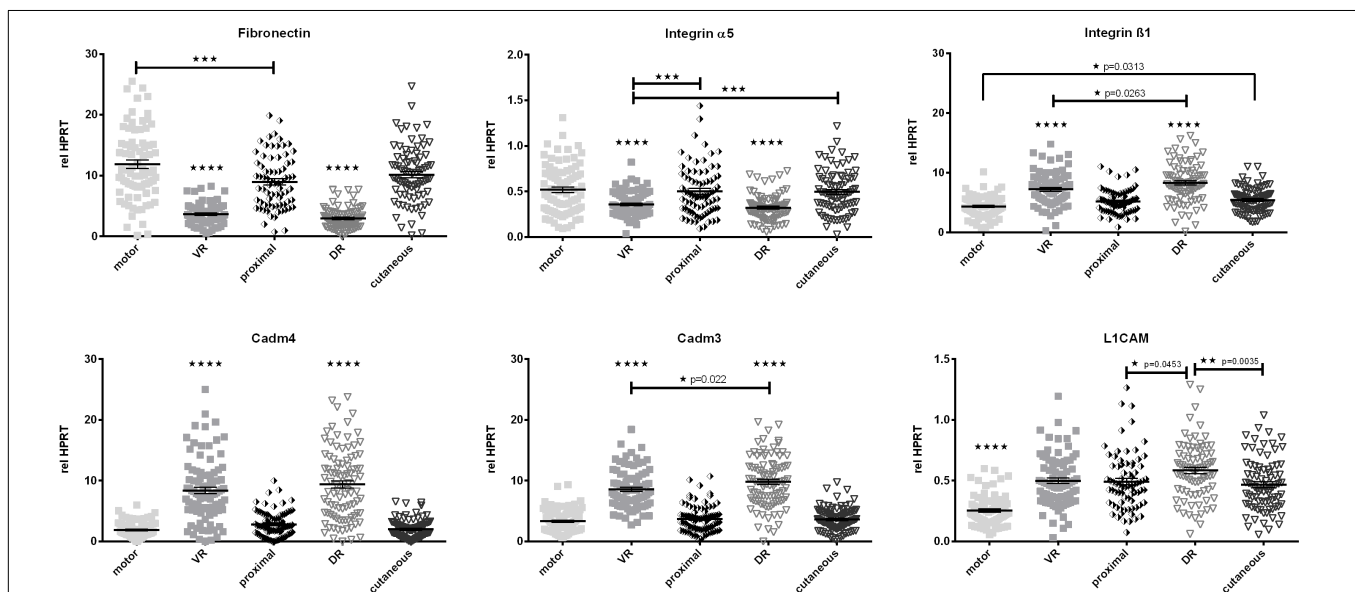
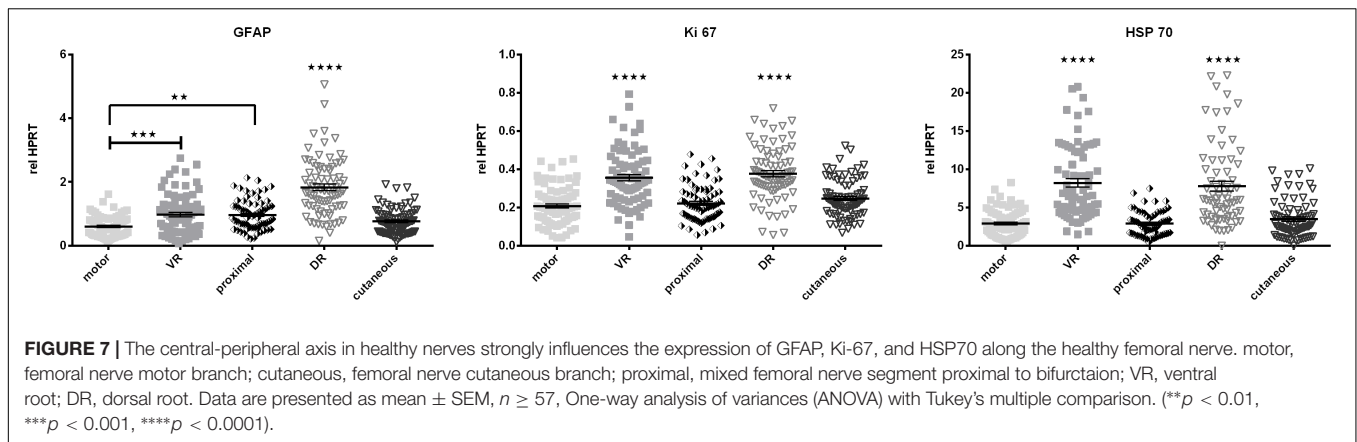


FIGURE 6 | Quantification of baseline expression of cell adhesion molecules along the central-peripheral axis in healthy nerves. A strong spatial influence on expression of cell adhesion molecules was measured. Additionally the L1CAM mRNA levels in the femoral motor branch were significantly lower than in the central, proximal and cutaneous nerve segments. motor, femoral nerve motor branch; cutaneous, femoral nerve cutaneous branch; proximal, mixed femoral nerve segment proximal to bifurcation; VR, ventral root; DR, dorsal root. Data are presented as mean \pm SEM, $n \geq 57$, One-way analysis of variances (ANOVA) with Tukey's multiple comparison. (* $p < 0.05$, ** $p < 0.01$, *** $p < 0.001$, **** $p < 0.0001$).

Cell Proliferation and Survival – Associated Genes Are Differentially Expressed Along the Central-Peripheral Axis

Cell proliferation-associated Ki-67 as well as stress responsive heat shock protein 70 (HSP70) show expression patterns similar

to Cadm3 and Cadm4 as well as Integrin $\beta 1$, GFR $\alpha 1$, and p75 as they exhibit higher mRNA levels in ventral and dorsal roots. Levels of Schwann cell specific cytoskeleton constituent, GFAP mRNA were highest in the L2 and L3 dorsal roots, and lowest in the motor branch of the femoral nerve (**Figure 7**).



Spatiotemporal Expression Patterns After Homotopic and Heterotopic Autografting

We used qRT-PCR to evaluate the expression patterns of 15 regeneration-associated genes in a femoral nerve defect model. Target mRNAs were chosen upon literature research and include several mRNAs investigated in previous studies (see **Table 2**). Besides the investigation of expression of neurotrophic factors and their receptors we decided to include several cell adhesion molecules as well as proliferation and damage response – associated proteins. We evaluated gene expression patterns 5 days, 2, 6, and 10 weeks after nerve repair. The expression of these targets is first compared to the reference gene HPRT and then set into relation to the healthy contralateral corresponding femoral nerve part. We hypothesize that this broad spectrum of targets provides an intelligible overview of the cellular responses after nerve injury and repair with an either phenotypically matched or mismatched autologous nerve graft.

Expression Levels of BDNF and GDNF as Well as Their Receptors Are Strongly Affected by Injury and Axonal Regeneration

As neurotrophic factors and their signaling play crucial roles in axonal path finding and regeneration, Schwann cell proliferation as well as (re-) myelination, we investigated mRNA levels over time. The neurotrophic factors BDNF and GDNF were highly up regulated in the grafts, bridging the motor and cutaneous defects as well as the distal compartments of the respective branches (**Figure 8**). Two weeks after repair, expression of both factors reached a peak followed by normalization of mRNA levels at 6 and 10 weeks. Grafting of a purely sensory autologous transplant resulted in a significantly higher BDNF expression 2 weeks postoperatively in the graft bridging the motor defect as well as the distal motor branch, when compared to homotopic grafting. The phenotypical mismatch of a motor graft to bridge the defect of the cutaneous nerve did however, not influence BDNF expression. The phenotypically mixed femoral nerve fragment proximal to the injury displayed no up regulation of either neurotrophic factor at any timepoint.

Accordingly to previous studies (Boyd and Gordon, 2003a), we observed significant up regulation of the low affinity neurotrophic receptor p75 as soon as 5 days after nerve injury. Here a strong trend indicates higher expression in sensory derived graft in the motor defect than the phenotypically matched motor graft. We observed up regulation of p75 mRNA with peak expression at 2 weeks followed by normalization of p75 mRNA levels at later timepoints in all nerve samples distal to the injury. In contrast, the high affinity BDNF receptor TrkB is strongly down regulated after injury in motor as well as cutaneous pathways. Analogous to the preferential expression of BDNF in cutaneous nerves, the expression of TrkB is increased after heterotopic grafting in the motor branch on week 10.

The spatiotemporal expression pattern of GFR α 1 closely resembles the GDNF expression pattern, with a peak expression at 2 weeks. However, in the denervated cutaneous branch the motor phenotype graft demonstrated significantly lower GFR α 1 expression at 5 days than the phenotypically matched cutaneous graft. Similar to the neurotrophic factors and p75, the mRNA levels of GFR α 1 reduced to contralateral, healthy levels over the time course of 6–10 weeks.

We were able to show a reduced expression of LIFR, 5 days, and 2 weeks after femoral nerve defect repair, with a steady increase to contralateral expression levels at 6 and 10 weeks. It is noteworthy, that at 10 weeks the motor derived graft in the cutaneous graft displayed higher levels of LIFR than the sensory derived autograft.

Expression of Fibronectin and Its Receptor Integrin α 5 β 1 Was Not Influenced by Autologous Nerve Grafting in Contrast to Cell Adhesion Molecules Cadm3, Cadm4, and L1CAM

We investigated the expression levels of Fibronectin mRNA as well as the spatiotemporal expression of integrins α 5 and β 1, which form one of the major Fibronectin receptors. We did not observe any significant differences in either of the three mRNAs at any timepoint investigated. The levels in the injured nerves were similar to the contralateral side (**Figure 9**).

Schwann cell specific cell adhesion molecule Cadm4, as well as its heterophilic axonal counterpart Cadm3 were strongly down regulated 5 days after nerve grafting surgery in the

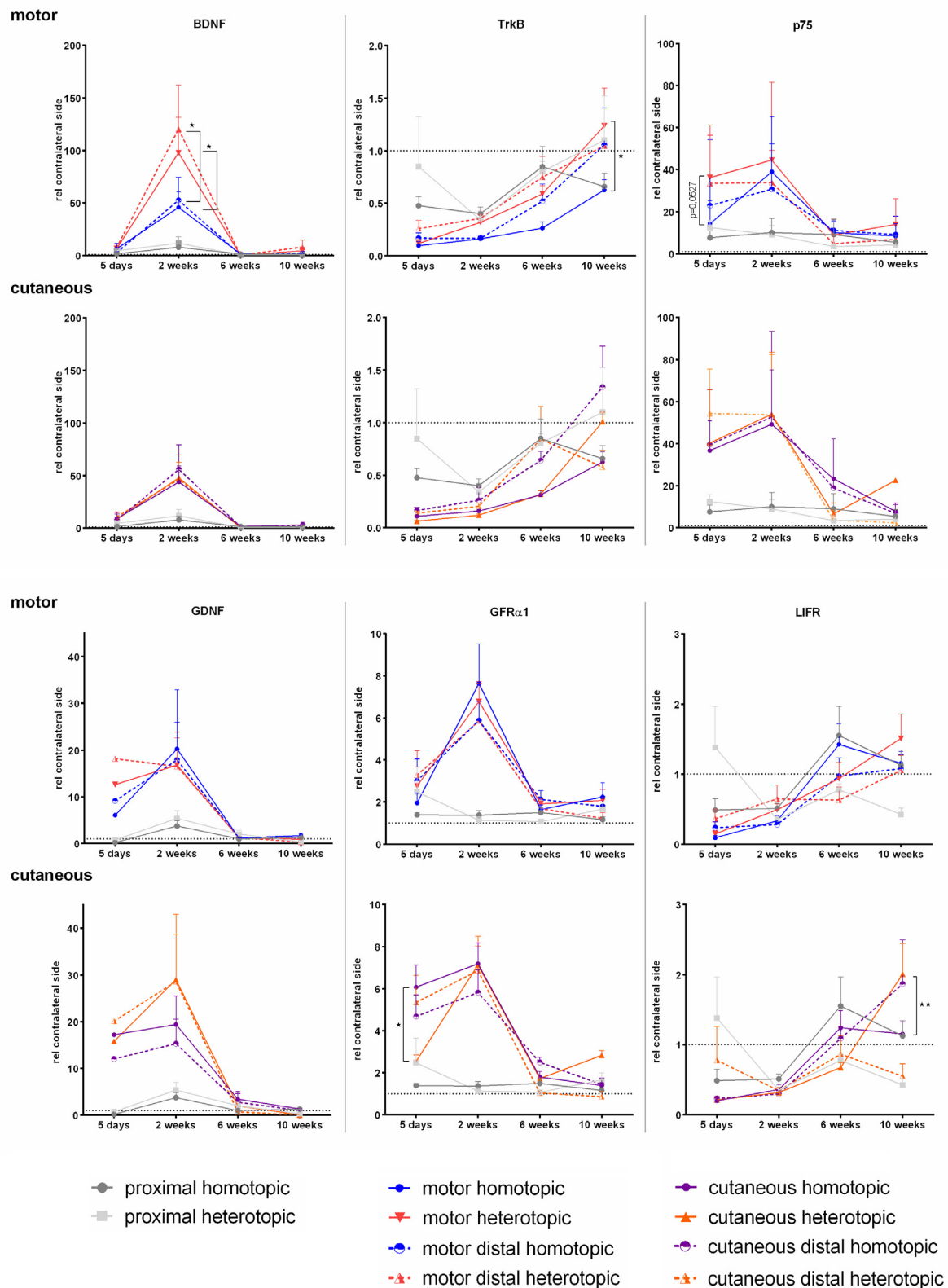


FIGURE 8 | Normalized mRNA levels of neurotrophic factors and receptors after homotopic or heterotopic autografting relative to contralateral side. Data are presented as mean \pm SEM, Two-way ANOVA with Tukey's multiple comparison test. (* $p < 0.05$, ** $p < 0.01$).

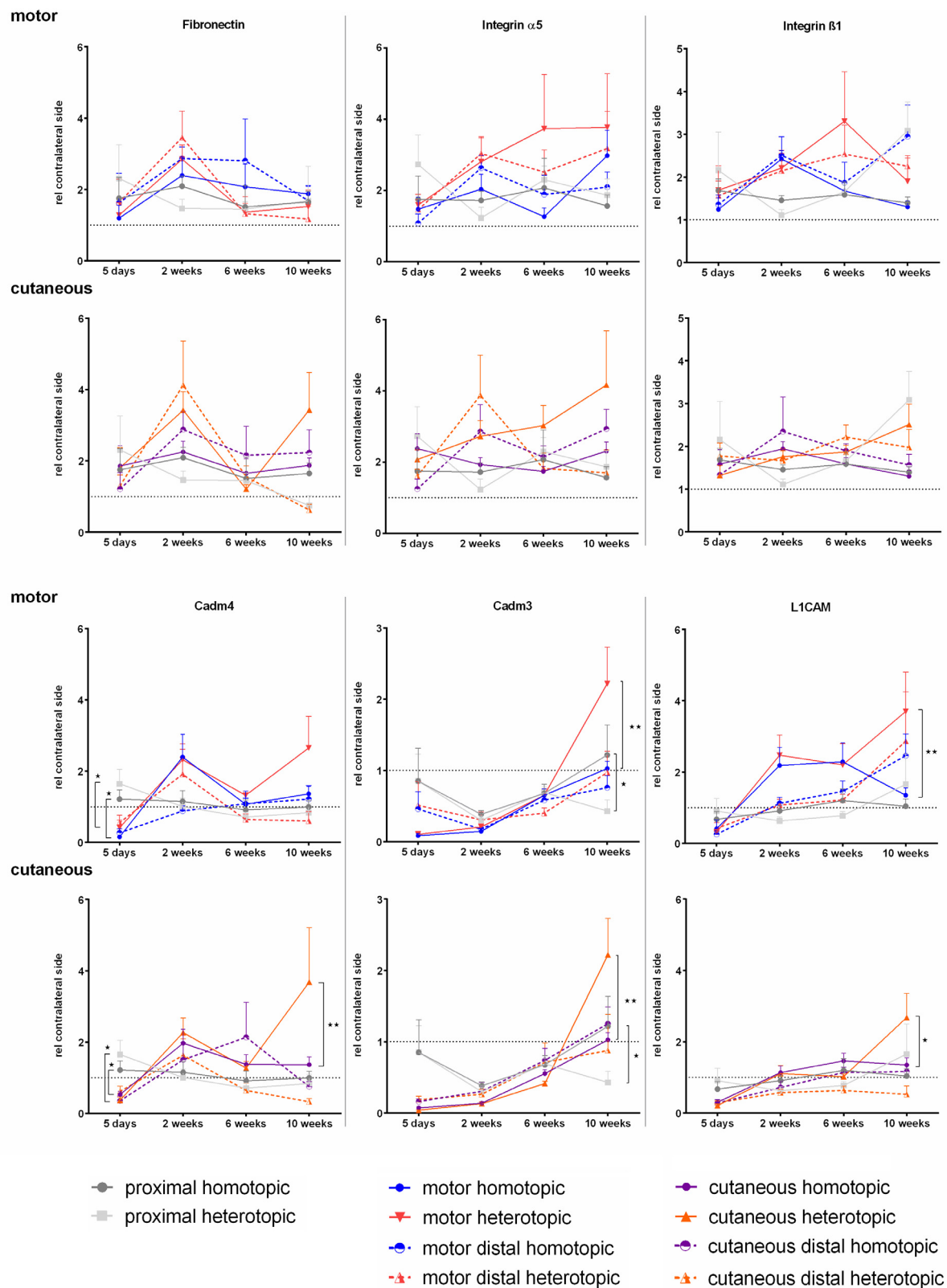


FIGURE 9 | Normalized mRNA levels of cell adhesion molecules after homotopic and heterotopic autografting relative to contralateral side. Data are presented as mean \pm SEM, Two-way ANOVA with Tukey's multiple comparison test. (* $p < 0.05$, ** $p < 0.01$).

repaired branches of the femoral nerve. This was followed by an up regulation of *Cadm4* in the cutaneous and motor branch at 2 weeks. In contrast to *Cadm4*, *Cadm3* mRNA levels stayed reduced for at least 2 weeks with a slow increase to contralateral levels at 10 weeks. Phenotypically mismatched grafting resulted in higher *Cadm3* expression at 10 weeks in the respective grafts in the motor and the cutaneous femoral nerve.

Five days after nerve repair, both femoral nerve branches demonstrated reduced expression of *L1CAM*, whereas at 2 weeks, the mRNA levels normalized in all investigated nerve samples except for the grafts in the motor branch. Here an increase in expression was observed as well as higher expression of *L1CAM* in the grafted nerve segments at 10 weeks after heterotopic grafting compared to homotopic grafting.

Influence of Homotopic or Heterotopic Grafting on Expression of GFAP, Ki-67, and HSP70

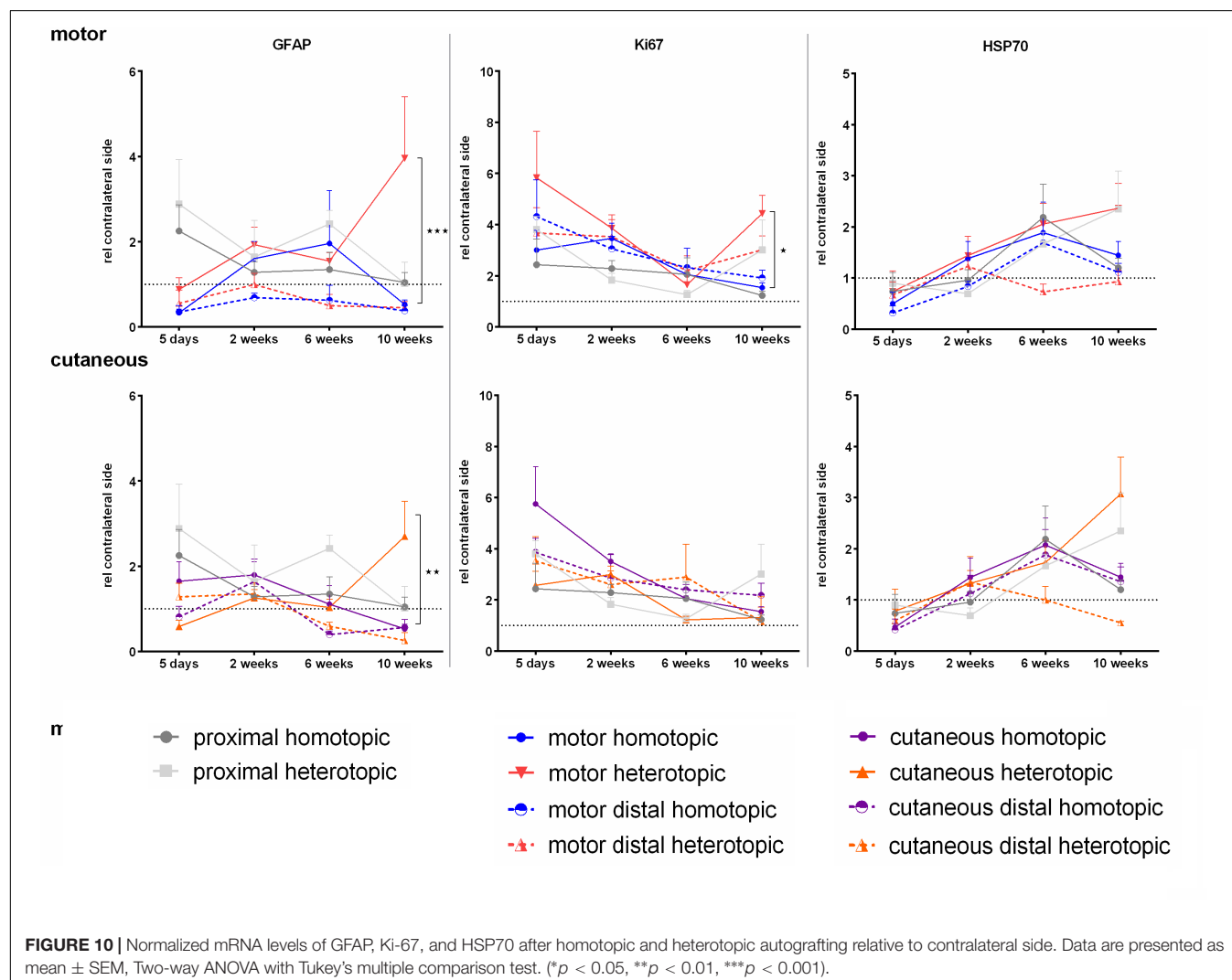
In contrast to previously published data, we were not able to detect significant up regulation of GFAP in neither the

motor nor the cutaneous branch after injury, except for a late increase in GFAP mRNA levels in the respective heterotopic grafts at 10 weeks (**Figure 10**). However, significantly enhanced expression of the proliferation-associated gene Ki-67 was observed at 5 days. The sensory graft demonstrated highest Ki-67 expression levels in both the cutaneous as well as the motor branch, indicating enhanced proliferation of Schwann cells of a sensory phenotype. Finally the chaperone HSP70 displayed a slight increase in expression over the time course of 10 weeks after injury, although no significant changes were determined.

DISCUSSION

Experimental Model

We chose the femoral nerve model for our investigations, as it has been used to investigate phenotypical differences between motor and cutaneous pathways before (Brushart, 1990; Höke et al., 2006; Kawamura et al., 2010; Jesuraj et al., 2012; Brushart



et al., 2013; Gordon and Borschel, 2017). Motor and cutaneous femoral branches are similar in size, fiber width and nerve cross sectional area (Brenner et al., 2006). Previous studies used ventral root isografts as phenotypically pure motor nerve grafts (Höke et al., 2006) or femoral nerve isografts from other animals (Moradzadeh et al., 2008; Kawamura et al., 2010). However, we adapted the model by performing homotopic and heterotopic autografting techniques for the repair of the motor and cutaneous branch (**Figure 1**). We used the femoral motor branch in contrast to the purely motor ventral root, as this more closely reflects the situation in other experimental autologous nerve transplantation models (i.e., the sciatic nerve defect model). Although a mixed nerve, a previous study by Marquardt and Sakiyama-Elbert proved motor phenotypical commitment of Schwann cells derived from the motor branch of the femoral nerve (Marquardt and Sakiyama-Elbert, 2015), deeming it a suitable graft for our purposes. Furthermore we performed autografting instead of isografting to represent clinical cases more accurately. Brushart et al. investigated the mRNA expression patterns of a variety of growth factors in cutaneous and motor nerves with differing denervation times ranging from 5 to 30 days (Brushart et al., 2013). Accordingly, we aimed to investigate the spatiotemporal gene expression pattern in denervated cutaneous and motor pathways, repaired with either phenotypically matched, or mismatched grafts.

Functional Evaluation

So far, functional regeneration after injury to the femoral nerve was performed using single-frame motion analysis (SFMA) (Irintchev et al., 2005; Ahlborn et al., 2007). We identified three parameters directly correlating to de- and reinnervation of femoral nerve using gait analysis: Print area, swing time and duty cycle. Knee extension and bending are impaired after defect to the femoral nerve, as the quadriceps muscle is solely innervated by the femoral motor branch (Irintchev et al., 2005). The resulting abnormal bending of the knee joint results in abnormal plantar flexion and lifting of the heel, which decreases print area of the paw. The dynamic parameters swing time and duty cycle were also affected significantly by denervation of the quadriceps muscle, which is in accordance with findings after sciatic nerve injury in rats (Bozkurt et al., 2008), probably due to injury to the cutaneous branch of the femoral nerve (Puigdel·lvols-Sánchez et al., 2000; Kambiz et al., 2014). To the best of our knowledge this is the first study using catwalk automated gait analysis to evaluate regeneration in a femoral nerve defect model. Homotopic and heterotopic grafting resulted in comparable outcome regarding all three parameters. However, we consider the possibility that this evaluation method is lacking sensitivity due to the superior regenerative capacity of rodents combined with the short defect (6 mm) as well as the proximity to the target muscle and the provision of activated Schwann cells in both treatment paradigms.

Similarly, it was not possible to observe significant differences between the treatment groups in electrophysiological evaluations of the femoral motor branch. A general increase in CMAP and peak amplitude over time was determined. However, a large dispersion of values was apparent. The short defect of 6 mm in

combination with high variability in the chosen functional tests is very likely hindering detection of differences between treatment groups. Previous studies claimed no difference after isografting of a femoral nerve defect with either a sensory or motor graft regarding histomorphometrical evaluations (Kawamura et al., 2010). Extended atrophy of the quadriceps muscle was measured until 6 weeks after injury, followed by an increase of muscle mass at 10 weeks in both treatment groups. Increase in muscle mass is only possible after successful reinnervation and reversal of atrophic processes of the quadriceps muscle. Interestingly, we measured significantly larger quadriceps muscle mass gain at 10 weeks after homotopic grafting than after heterotopic grafting (**Figure 3C**). This could indicate a superior capability of a phenotypically matched motor graft to regenerate motor axons when compared to a sensory graft, in accordance with data by Brenner et al. (2006) indicating inferior motor axonal regeneration through sensory grafts than size-matched motor grafts. As a growing body of literature has shown in numerous *in vitro* as well as *in vivo* studies, these effects could be explained by the phenotypical commitment of Schwann cells (Nichols et al., 2004; Höke et al., 2006; Moradzadeh et al., 2008; Jesuraj et al., 2012).

Axonal Regeneration

In order to correlate functional regeneration and spatiotemporal gene expression patterns, we performed immunohistological evaluations of the repaired femoral nerves. NF staining revealed that 5 days after injury the main axonal regeneration front is still at the proximal coaptation site (**Figure 4**). Amongst other factors, the presence of a proximal suture site and ongoing clearance of residual myelin debris by macrophages hinder axonal reinnervation of the grafts in motor as well as cutaneous branches at this early timepoint (Fex Svennigsen and Dahlin, 2013). When confronted with a suture site, axons show staggered regeneration as a result of misalignment of Schwann cells in the fragmented extracellular matrix and asynchronous outgrowth of axons (Witzel et al., 2005). At 2 weeks we observed axonal reinnervation of all distal nerve stumps in both treatment groups, proving the capacity of phenotypically different Schwann cells to support axonal regeneration. Interestingly, Kawamura et al. (2010) observed no reinnervation of the distal branches 5 weeks after isografting of 10 mm nerve grafts in the same model, indicating a far slower regeneration of axons through isografts.

Schwann Cell Phenotype and the Central-Peripheral Axis

Schwann cells are the glial cells of the peripheral nervous system and their phenotype is mainly associated with their functions as myelinating or non-myelinating cells, ensheathing Remak cells (Jessen and Mirsky, 2002). Schwann cells provide metabolic support for axons and are essential for axonal integrity (Nave, 2010; Harty and Monk, 2017). Over the last two decades, studies additionally revealed phenotypes of motor and sensory Schwann cells with distinct expression profiles for a variety of growth factors (Höke et al., 2006; He et al., 2012b; Jesuraj et al., 2012). We combined the expression profile data of more than 56 animals

to investigate phenotypical commitment in healthy, contralateral nerves further. We focused on three sets of mRNAs: neurotrophic factors and their receptors, cell adhesion molecules and cell status-defining mRNAs, giving us insight into a broad spectrum of cellular responses.

Neurotrophic factors and their receptors play essential roles during development of the peripheral nervous system in axonal guidance, myelination and neuronal survival (Zhang et al., 2000; Wiese et al., 2001). The effects of neurotrophic factors and their receptors have been investigated intensively *in vitro* as well as *in vivo*. However, data on their baseline expression in healthy peripheral nerves is scarce. In contrast to Brushart et al. (2013) we did not observe significantly higher expression of neurotrophic factors BDNF or GDNF in L2 and L3 dorsal and ventral roots when compared to the peripheral motor, cutaneous or proximal segments of the healthy femoral nerve. The reason could be the use of HPRT instead of glyceraldehyde-3-phosphat dehydrogenase (GAPDH) as a reference gene in the present study, as GAPDH is more highly expressed, resulting in generally very low relative expression levels in the studies by Höke et al. (2006), (Brushart et al., 2013). Furthermore higher variances were observed in the present study, as no pooling of samples was performed prior to qRT-PCR. In addition, we used a BDNF primer set, detecting all splicing variants of BDNF as expression of different splicing variants of BDNF is highly tissue dependent (Aid et al., 2007). Also, regarding BDNF expression our results are in line with data from Jesuraj et al. (2012), indicating no preferential expression along the central-peripheral axis nor in healthy phenotypically different Schwann cells. In stark contrast to neurotrophin expression levels, all investigated neurotrophin receptors showed large differences in expression along the central-peripheral axis in the healthy nerve.

We determined significantly increased TrkB expression in the cutaneous femoral branch and a very low relative expression of TrkB in ventral roots L2 and L3. This may indicate increased dependency of distal sensory Schwann cells on BDNF signaling including PI3K and the ras/ERK pathway (Boyd and Gordon, 2003b) or enhanced signaling of BDNF via the TrkB receptor rather than via p75. The low affinity neurotrophic factor p75 as well GFR α 1 on the other hand were more highly expressed in dorsal and ventral roots, which could explain the responsiveness of motoneurons and their axons to introduced BDNF, and GDNF after ventral root avulsion (Pajenda et al., 2014). Additionally, a low expression is known in motoneurons and sensory neurons in adulthood (Ernfors et al., 1989; Wyatt et al., 1990). As p75 expression is correlating with proliferation (Provenzano et al., 2011), it was not surprising that Ki67 expression is also higher in central parts of the femoral nerve. However, the reason underlying the higher mitotic activity of dorsal and ventral root cells compared to peripheral segments remains target of further studies.

Schwann cells have the intrinsic capacity to produce not only LIF but also LIFR resulting in strong autocrine survival signaling. The lower expression of LIFR in central segments of the femoral nerve could be explained by the reduced relative numbers of non-neuronal cells in ventral and dorsal roots. This

may also be the reason for our observation of lower expression of Fibronectin and integrin subunit α 5 in ventral and dorsal roots. A close coregulation of Integrin α 5 with Fibronectin can be expected, as the only binding partner for integrin α 5 is Fibronectin. The interactions of neural crest cells and peripheral neurons with Fibronectin are mediated by integrins containing the β 1 subunit (Bronner-Fraser, 1985; Thiery and Duband, 1986; Plantman, 2013), which has numerous heterodimeric partners including vimentin, laminin, and L1CAM. Therefore an increased expression in proximity to neuronal cell bodies is not surprising. Dorsal root ganglions as well as motoneurons express especially high levels of integrin β 1 as reviewed by Plantman (Plantman, 2013). Furthermore, He et al. (2012b) demonstrated, that integrin β 1 is more highly expressed in sensory nerves, which is in line with our observation, that dorsal roots express significantly higher levels of β 1 than ventral roots. The same holds true for the cutaneous femoral branch exhibits higher expression than the motor branch. Another class of cell adhesion molecules, also known as nectin-like molecules are Cadm4 and Cadm3. Cadm4 is mainly expressed in Schwann cells and builds strong heterophilic interactions with Cadm3, which is expressed by axons (Maurel et al., 2007). In the healthy nerve both molecules are clustered at the periaxonal membrane and at the internodes and Schmidt-Lanterman incisures of myelinated axons (Maurel et al., 2007; Perlin and Talbot, 2007; Spiegel et al., 2007). Cadm4 and Cadm3 are essential for myelination, therefore the increased central expression observed in this study can be explained by the high numbers of myelinated axons in L2 and L3 ventral roots (Biscoe et al., 1982) and the substantial expression in dorsal root ganglions (Chen et al., 2016).

The neuronal cell adhesion molecule L1CAM is part of the Ig superfamily of cell adhesion molecules and displays homophilic as well as heterophilic (i.e., NCAM) interactions. We detected less pronounced expression levels of L1CAM in the motor femoral branch in healthy nerves than in the cutaneous branch. This is in accordance with other studies, where sensory Schwann cells exhibit higher levels of L1CAM than motor Schwann cells *in vitro* (He et al., 2012a) and *in vivo* (Jesuraj et al., 2012). However, this phenomenon is restricted to the peripheral nerve segments, as we observed similar expression levels of L1CAM in purely motor ventral roots, and dorsal roots. GFAP is known to be mainly expressed in non-myelinating or repair Schwann cells, explaining the low expression in femoral motor nerve branch. The higher expression in ventral and dorsal roots could be due to a higher proportion of undifferentiated, proliferating Schwann cells in these segments, as we also detected enhanced expression of proliferation-associated Ki67 and stress responsive HSP70 levels in ventral and dorsal roots. Additionally the significantly higher expression of GFAP in dorsal roots is expected, as they contain a high number of non-myelinating Schwann cells. HSP70 is one of the earliest up regulated proteins after nerve injury in zebrafish (Nagashima et al., 2011). This might occur because ventral and dorsal roots are more prone to experience stress-inducing traction and compression even in healthy animals, as they do not possess a protective connective tissue layer.

Spatiotemporal Expression Patterns After Homotopic and Heterotopic Grafting

Brain derived neurotrophic factor is a potent survival factor for motoneurons after proximal axotomy (Kishino et al., 1997; Pajenda et al., 2014). Furthermore, its expression is necessary for remyelination (Zhang et al., 2000) and as a guidance molecule for axonal regeneration (Boyd and Gordon, 2003a). In our study, grafting of a purely sensory autologous transplant resulted in a significantly higher BDNF expression 2 weeks postoperatively in the graft bridging the motor defect as well as the distal motor branch, when compared to homotopic grafting. This indicates not only that Schwann cells of a sensory phenotype express higher levels of BDNF when they encounter motor axons, but also influence expression levels in the distal motor branch. Sensory Schwann cells enhance expression of BDNF, probably to overcome their reduced capacity to support motor axonal regeneration. Sensory axons are less susceptible to phenotypical mismatch than motor axons, therefore no compensation in the cutaneous graft was observed (Marquardt and Sakiyama-Elbert, 2015). BDNF signals via two receptors, TrkB and p75.

Denervation of motor and sensory branches of the femoral nerve resulted in a marked decrease of TrkB, which is consistent with data provided by Funakoshi et al. (1993). Over the time course of 6–10 weeks normalization of TrkB expression was observed, which allows normal remyelination of regenerated axons (Cosgaya et al., 2002). We observed up regulation of p75 mRNA with peak expression at 2 weeks followed by normalization of p75 mRNA levels at later timepoints in all nerve samples distal to the injury. This is consistent with data from previous work which indicate a role in pre-myelination (Cosgaya et al., 2002). Although the general up regulation of p75 after injury is well described (Boyd and Gordon, 2003b; Cragolini and Friedman, 2008; Jessen and Mirsky, 2016), the exact spatiotemporal expression pattern in phenotypically different, injured nerves has not been described earlier. Timeline of expression levels closely resembles the BDNF mRNA expression pattern indicating co-regulation of BDNF and its low affinity receptor p75. Binding of BDNF to p75 results in activation of the Ras/ERK pathway and activation of c-Jun, which in turn activates BDNF as well as GDNF transcription (Arthur-Farraj et al., 2012; Jessen and Mirsky, 2016).

GDNF is produced by myelinating and non-myelinating Schwann cells (Xu et al., 2013) and in our setup, exhibited a close resemblance in expression pattern to its high affinity receptor GFR α 1, with a peak expression at 2 weeks. GDNF signaling may occur in a ret-dependent and ret-independent way. Both signaling modalities promote cell survival and, as Schwann cells are the main producers of GDNF, it is thought that the elevated levels of GDNF in the denervated parts of the femoral nerve branches induce strong pro-survival cues via GFR α 1 in an autocrine way. Interestingly, homotopic grafting in the cutaneous branch resulted in a delayed up regulation of GFR α 1 mRNA.

Leukemia inhibitory factor receptor (LIFR) mRNA is known to be reduced after crush and transection injury, however, the expression pattern after autologous nerve grafting as well as the influence of phenotypically mismatched Schwann cells has not been investigated. As LIF expression is up regulated after peripheral nerve injury (Banner and Patterson, 1994), observed down regulation of LIFR for at least 2 weeks may prevent non-neuronal cells from undesired consumption of LIF (Ito et al., 1998). In contrast to previously published data we did not observe a significant increase in mRNA levels of neither Fibronectin nor its heterodimeric integrin receptor α 5 β 1. A possible explanation could be post-transcriptional regulation of these molecules.

Cell adhesion molecules Cadm4, which is mainly expressed on Schwann cells as well as its heterophilic axonal counterpart Cadm3, were strongly down regulated 5 days after nerve grafting surgery in the repaired branches of the femoral nerve (Figure 9). In contrast to Zelano et al. (2009) we did not observe Cadm4 up regulation 5 days after injury, which might originate from the different animal model used, as they investigated a sciatic nerve defect without repair. However, we observed up regulation of Cadm4 in the cutaneous and motor branch at 2 weeks, the time point at which axonal reinnervation of the nerve grafts and even the distal segments is taking place. This is in line with the role Cadm4 plays in remyelination processes. It is required for myelination and its expression is increased by axonal contact (Perlin and Talbot, 2007; Spiegel et al., 2007). More precisely, Cadm4 induces clustering of Cadm3 on axons to enable efficient heterophilic interaction between regrown axons and resident Schwann cells. This also explains the spatiotemporal expression of Cadm3, which is reaching normal levels between 6 and 10 weeks after injury. The significantly higher expression of Cadm3 in sensory-derived grafts in both branches indicates ongoing reorganization processes of myelination in phenotypically mismatched grafts. As uninjured Schwann cells also express Cadm3 another explanation could be the re-established expression of Cadm3 by Schwann cells at this late timepoint after injury (Zelano et al., 2009). Finally, Cadm3 has been shown to inhibit myelination via activation of PI3 Kinase/Akt signaling. This may result in less myelination of regenerated axons in these grafts (Chen et al., 2016).

The neuronal cell adhesion molecule L1CAM plays a role in early myelination and its expression coincides with a decrease in proliferation (Guseva et al., 2009; Lutz et al., 2016). L1CAM signaling results in activation of the ERK pathway and induces axonal growth (Maness and Schachner, 2007). The restoration of L1CAM expression 2 weeks after injury and the observed axonal regeneration at this timepoint confirms this observation. In accordance with Qian-ru et al we measured higher L1CAM mRNA levels in the grafts bridging the motor defect than in the cutaneous defect. An increase in L1CAM to induce axonal growth in the motor branch is to be expected, considering that the baseline expression of L1CAM in motor nerves is lower than in cutaneous nerves (Jesuraj et al., 2012; He et al., 2016). We did not observe significant influences of phenotypical mismatch at early stages after nerve grafting.

Furthermore we discovered a decrease of GFAP mRNA in the denervated motor branch 5 days after injury, which indicates regulation of GFAP expression on the protein level, as other groups provided evidence for enhanced levels of GFAP after nerve defect (Triolo, 2006; Wang et al., 2010). Heterotopic grafting however, resulted in increased levels of GFAP in the respective grafts at late stages of regeneration, indicating higher numbers of non-myelinating Schwann cells in phenotypically mismatched grafts (Yang and Wang, 2015). Proliferation of denervated Schwann cells is a hallmark of the repair phenotype (Jessen and Mirsky, 2016). We observed slightly increased expression of Ki67 in sensory derived grafts, providing further evidence for a higher proliferative capacity of cutaneous Schwann cells (Jesuraj et al., 2014).

We summarized spatiotemporal expression patterns in a comprehensive overview of all investigated genes in motor as well as sensory grafts in **Figure 11**.

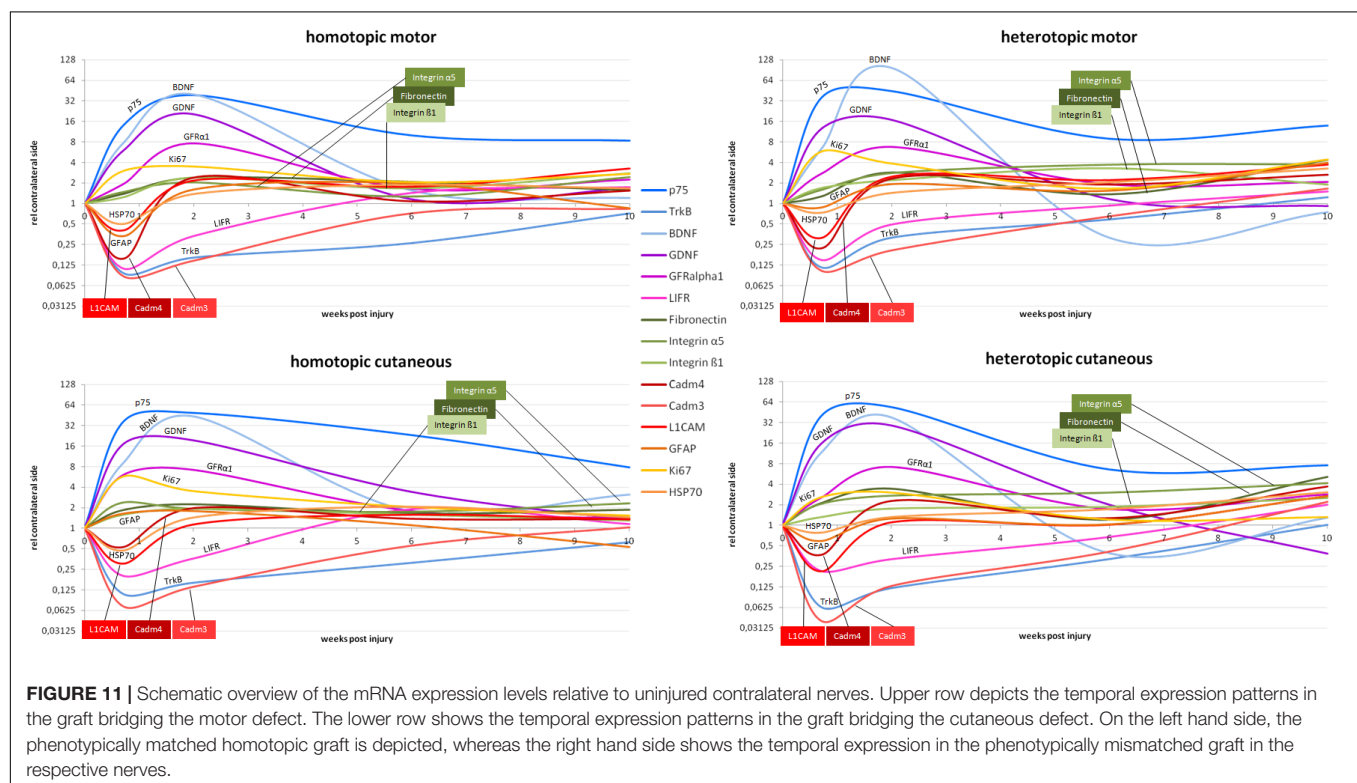
CONCLUSION

Sensory nerve autografts are the clinical gold standard to bridge peripheral nerve defects. However, functional outcome after autologous nerve transplantation is often unsatisfying (Meek et al., 2005; Secer et al., 2008; Yang et al., 2011). In this study we investigated the effect of phenotypical commitment of peripheral motor and sensory nerve grafts on axonal regeneration in a rat femoral nerve defect model. Furthermore, we examined the influence of motor and sensory phenotype on the expression level of several regeneration-associated genes in healthy and injured

femoral nerves. We uncovered highly significant differences in gene expression along the central-peripheral axis and between motor and sensory constituents of the healthy femoral nerve. A significant influence of phenotypical mismatch on the spatiotemporal expression of several investigated mRNAs in regenerating motor and cutaneous nerves was evident. Overall, we observed similar but not identical spatiotemporal expression of a variety of regeneration-associated genes in motor (mixed) and cutaneous grafts. Furthermore, we elucidated that phenotypical mismatched grafting can influence expression patterns of distal nerve segments, thereby potentially influencing axonal regeneration, and target reinnervation. This study shows that in a small 6 mm femoral nerve defect the graft phenotype has only a minor influence on functional regeneration. Success of axonal regeneration after nerve defect repair is highly dependent on a tightly regulated spatiotemporal profile of genes. The differences observed in our study might prove to be crucial in large nerve defects, where mismatched Schwann cell phenotype may interfere with correct path finding of motor and sensory nerves to their respective end organs. However, the effect of phenotypically mismatched long grafts on axonal regeneration and functional recovery -especially after delayed repair- remains to be elucidated.

ETHICS STATEMENT

This study was carried out according to Austrian law and the guide for the care and use of laboratory animals, and was approved by the City Government of Vienna.



AUTHOR CONTRIBUTIONS

DH contributed to conception and all evaluations as well as the analyses and wrote the manuscript. MK performed the surgeries. JH performed the gait analysis. CS contributed to critical revision of data and manuscript. MS contributed in establishment of qRT-PCR protocols. LG performed the histological evaluations. RS and TH contributed to conception. HR, AN, and AH contributed to conception and critically reviewed the manuscript.

FUNDING

This study was supported by Lorenz Böhler Fonds, DH received an AUVF Forschungskonto.

REFERENCES

- Abdullah, M., O'Daly, A., Vyas, A., Rohde, C., and Brushart, T. M. (2013). Adult motor axons preferentially reinnervate predegenerated muscle nerve. *Exp. Neurol.* 249, 1–7. doi: 10.1016/j.expneurol.2013.07.019
- Ahlborn, P., Schachner, M., and Irintchev, A. (2007). One hour electrical stimulation accelerates functional recovery after femoral nerve repair. *Exp. Neurol.* 208, 137–144. doi: 10.1016/j.expneurol.2007.08.005
- Aid, T., Kazantseva, A., Piirsoo, M., Palm, K., and Timmusk, T. (2007). Mouse and rat BDNF gene structure and expression revisited. *J. Neurosci. Res.* 85, 525–535. doi: 10.1002/jnr.21139
- Arthur-Farraj, P. J., Latouche, M., Wilton, D. K., Quintes, S., Chabrol, E., Banerjee, A., et al. (2012). c-Jun reprograms schwann cells of injured nerves to generate a repair cell essential for regeneration. *Neuron* 75, 633–647. doi: 10.1016/j.neuron.2012.06.021
- Banner, L. R., and Patterson, P. H. (1994). Major changes in the expression of the mRNAs for cholinergic differentiation factor/leukemia inhibitory factor and its receptor after injury to adult peripheral nerves and ganglia. *Proc. Natl. Acad. Sci. U.S.A.* 91, 7109–7113. doi: 10.1073/pnas.91.15.7109
- Biscoe, T. J., Nickels, S. M., and Stirling, C. A. (1982). Numbers and sizes of nerve fibres in mouse spinal roots. *Q. J. Exp. Physiol.* 67, 473–494. doi: 10.1113/expphysiol.1982.sp002663
- Boyd, J. G., and Gordon, T. (2003a). Glial cell line-derived neurotrophic factor and brain-derived neurotrophic factor sustain the axonal regeneration of chronically axotomized motoneurons in vivo. *Exp. Neurol.* 183, 610–619. doi: 10.1016/S0014-4886(03)00183-3
- Boyd, J. G., and Gordon, T. (2003b). Neurotrophic factors and their receptors in axonal regeneration and functional recovery after peripheral nerve injury. *Mol. Neurobiol.* 27, 277–324. doi: 10.1385/mn:27:3:277
- Bozkurt, A., Deumens, R., Scheffel, J., O'Dey, D. M., Weis, J., Joosten, E. A., et al. (2008). CatWalk gait analysis in assessment of functional recovery after sciatic nerve injury. *J. Neurosci. Methods* 173, 91–98. doi: 10.1016/j.jneumeth.2008.05.020
- Bozkurt, A., Lassner, F., O'Dey, D., Deumens, R., Böcker, A., Schwendt, T., et al. (2012). The role of microstructured and interconnected pore channels in a collagen-based nerve guide on axonal regeneration in peripheral nerves. *Biomaterials* 33, 1363–1375. doi: 10.1016/j.biomaterials.2011.10.069
- Bozkurt, A., Scheffel, J., Brook, G. A., Joosten, E. A., Suschek, C. V., O'Dey, D. M., et al. (2011). Aspects of static and dynamic motor function in peripheral nerve regeneration: SSI and CatWalk gait analysis. *Behav. Brain Res.* 219, 55–62. doi: 10.1016/j.bbr.2010.12.018
- Brenner, M. J., Hess, J. R., Myckatyn, T. M., Hayashi, A., Hunter, D. A., and Mackinnon, S. E. (2006). Repair of motor nerve gaps with sensory nerve inhibits regeneration in rats. *Laryngoscope* 116, 1685–1692. doi: 10.1097/01.mlg.0000229469.31749.91

ACKNOWLEDGMENTS

The authors would like to acknowledge the valuable aid by Georg Feichtinger, James Ferguson, Karin Brenner, Claudia Keibl, Rudolf Hopf, Shorena Mosia, Karl Schneider, and the Department of Molecular Biology at the LBI Trauma.

SUPPLEMENTARY MATERIAL

The Supplementary Material for this article can be found online at: <https://www.frontiersin.org/articles/10.3389/fncel.2019.00182/full#supplementary-material>

- Bronner-Fraser, M. (1985). Alterations in neural crest migration by a monoclonal antibody that affects cell adhesion. *J. Cell Biol.* 101, 610–617. doi: 10.1083/jcb.101.2.610
- Brushart, T. M. (1990). Preferential motor reinnervation: a sequential double-labeling study. *Restor. Neurol. Neurosci.* 1, 281–287. doi: 10.3233/RNN-1990-13416
- Brushart, T. M., Aspalter, M., Griffin, J. W., Redett, R., Hameed, H., Zhou, C., et al. (2013). Schwann cell phenotype is regulated by axon modality and central-peripheral location, and persists in vitro. *Exp. Neurol.* 247, 272–281. doi: 10.1016/j.expneurol.2013.05.007
- Chen, M. S., Kim, H., Jagot-Lacoussiere, L., and Maurel, P. (2016). Cadm3 (Nect-1) interferes with the activation of the PI3 kinase/Akt signaling cascade and inhibits Schwann cell myelination in vitro. *Glia* 64, 2247–2262. doi: 10.1002/glia.23072
- Chu, T. H., Du, Y., and Wu, W. (2008). Motor nerve graft is better than sensory nerve graft for survival and regeneration of motoneurons after spinal root avulsion in adult rats. *Exp. Neurol.* 212, 562–565. doi: 10.1016/j.expneurol.2008.05.001
- Cosgaya, J. M., Chan, J. R., and Shooter, E. M. (2002). The neurotrophin receptor p75NTR as a positive modulator of myelination. *Science* 298, 1245–1248. doi: 10.1126/science.1076595
- Cragg, A. B., and Friedman, W. J. (2008). The function of p75NTR in glia. *Trends Neurosci.* 31, 99–104. doi: 10.1016/j.tins.2007.11.005
- de Luca, A. C., Lacour, S. P., Raffoul, W., and di Summa, P. G. (2014). Extracellular matrix components in peripheral nerve repair: how to affect neural cellular response and nerve regeneration? *Neural Regen. Res.* 9, 1943–1948. doi: 10.4103/1673-5374.145366
- Deumens, R., Marinangeli, C., Bozkurt, A., and Brook, G. A. (2014). Assessing motor outcome and functional recovery following nerve injury. *Methods Mol. Biol.* 1162, 179–188. doi: 10.1007/978-1-4939-0777-9_15
- Dowsing, B. J., Morrison, W. A., Nicola, N. A., Starkey, G. P., Bucci, T., and Kilpatrick, T. J. (1999). Leukemia inhibitory factor is an autocrine survival factor for Schwann cells. *J. Neurochem.* 73, 96–104. doi: 10.1046/j.1471-4159.1999.0730096.x
- Ernfors, P., Henschen, A., Olson, L., and Persson, H. (1989). Expression of nerve growth factor receptor mRNA is developmentally regulated and increased after axotomy in rat spinal cord motoneurons. *Neuron* 2, 1605–1613. doi: 10.1016/0896-6273(89)90049-4
- Fex Svenngissen, Å., and Dahlin, L. B. (2013). Repair of the peripheral nerve-remyelination that works. *Brain Sci.* 3, 1182–1197. doi: 10.3390/brainsci3031182
- Funakoshi, H., Frisén, J., Barbany, G., Timmusk, T., Zachrisson, O., Verge, V. M. K., et al. (1993). Differential expression of mRNAs for neurotrophins and their receptors after axotomy of the sciatic nerve. *J. Cell Biol.* 123, 455–465. doi: 10.1083/jcb.123.2.455
- Gambarotta, G., Ronchi, G., Friard, O., Galletta, P., Perroteau, I., and Geuna, S. (2014). Identification and validation of suitable housekeeping genes for

- normalizing quantitative real-time PCR assays in injured peripheral nerves. *PLoS One* 9:e105601. doi: 10.1371/journal.pone.0105601
- Gordon, T., and Borschel, G. H. (2017). The use of the rat as a model for studying peripheral nerve regeneration and sprouting after complete and partial nerve injuries. *Exp. Neurol.* 287, 331–347. doi: 10.1016/j.expneurol.2016.01.014
- Guseva, D., Angelov, D. N., Irintchev, A., and Schachner, M. (2009). Ablation of adhesion molecule L1 in mice favours Schwann cell proliferation and functional recovery after peripheral nerve injury. *Brain* 132, 2180–2195. doi: 10.1093/brain/awp160
- Hamers, F. P. T., Lankhorst, A. J., van Laar, T. J., Veldhuis, W. B., and Gispens, W. H. (2001). Automated quantitative gait analysis during overground locomotion in the rat: its application to spinal cord contusion and transection injuries. *J. Neurotrauma* 18, 187–201. doi: 10.1089/08977150150502613
- Harty, B. L., and Monk, K. R. (2017). Unwrapping the unappreciated: recent progress in Remak Schwann cell biology. *Curr. Opin. Neurobiol.* 47, 131–137. doi: 10.1016/j.conb.2017.10.003
- Hausner, T., Pajer, K., Halat, G., Hopf, R., Schmidhammer, R., Redl, H., et al. (2012). Improved rate of peripheral nerve regeneration induced by extracorporeal shock wave treatment in the rat. *Exp. Neurol.* 236, 363–370. doi: 10.1016/j.expneurol.2012.04.019
- He, Q., Man, L., Ji, Y., and Ding, F. (2012a). Comparison in the biological characteristics between primary cultured sensory and motor Schwann cells. *Neurosci. Lett.* 521, 57–61. doi: 10.1016/j.neulet.2012.05.059
- He, Q., Man, L., Ji, Y., Zhang, S., Jiang, M., Ding, F., et al. (2012b). Comparative proteomic analysis of differentially expressed proteins between peripheral sensory and motor nerves. *J. Proteome Res.* 11, 3077–3089. doi: 10.1021/pr300186t
- He, Q.-R., Cong, M., Chen, Q.-Z., Sheng, Y.-F., Li, J., Zhang, Q., et al. (2016). Expression changes of nerve cell adhesion molecules L1 and semaphorin 3A after peripheral nerve injury. *Neural Regen. Res.* 11, 2025–2030. doi: 10.4103/1673-5374.197148
- Höke, A., Redett, R., Hameed, H., Jari, R., Zhou, C., Li, Z. B., et al. (2006). Schwann cells express motor and sensory phenotypes that regulate axon regeneration. *J. Neurosci.* 26, 9646–9655. doi: 10.1523/jneurosci.1620-06.2006
- Huang, W., Begum, R., Barber, T., Ibba, V., Tee, N. C. H., Hussain, M., et al. (2012). Regenerative potential of silk conduits in repair of peripheral nerve injury in adult rats. *Biomaterials* 33, 59–71. doi: 10.1016/j.biomaterials.2011.09.030
- Irintchev, A., Simova, O., Eberhardt, K. A., Morellini, F., and Schachner, M. (2005). Impacts of lesion severity and tyrosine kinase receptor B deficiency on functional outcome of femoral nerve injury assessed by a novel single-frame motion analysis in mice. *Eur. J. Neurosci.* 22, 802–808. doi: 10.1111/j.1460-9568.2005.04274.x
- Ito, Y., Yamamoto, M., Li, M., Doyu, M., Tanaka, F., Mutch, T., et al. (1998). Differential temporal expression of mRNAs for ciliary neurotrophic factor (CNTF), leukemia inhibitory factor (LIF), interleukin-6 (IL-6), and their receptors (CNTFR alpha, LIFR beta, IL-6R alpha and gp130) in injured peripheral nerves. *Brain Res.* 793, 321–327. doi: 10.1016/s0006-8993(98)00242-x
- Jessen, K. R., and Mirsky, R. (2002). Signals that determine Schwann cell identity. *J. Anat.* 200, 367–376. doi: 10.1046/j.1469-7580.2002.00046.x
- Jessen, K. R., and Mirsky, R. (2016). The repair Schwann cell and its function in regenerating nerves: repair Schwann cell and its function in regenerating nerves. *J. Physiol.* 594, 3521–3531. doi: 10.1113/JP270874
- Jesuraj, N. J., Marquardt, L. M., Kwasa, J. A., and Sakiyama-Elbert, S. E. (2014). Glial cell line-derived neurotrophic factor promotes increased phenotypic marker expression in femoral sensory and motor-derived Schwann cell cultures. *Exp. Neurol.* 257, 10–18. doi: 10.1016/j.expneurol.2014.04.005
- Jesuraj, N. J., Nguyen, P. K., Wood, M. D., Moore, A. M., Borschel, G. H., Mackinnon, S. E., et al. (2012). Differential gene expression in motor and sensory Schwann cells in the rat femoral nerve. *J. Neurosci. Res.* 90, 96–104. doi: 10.1002/jnr.22752
- Kambiz, S., Baas, M., Duraku, L. S., Kerver, A. L., Koning, A. H. J., Walbeehm, E. T., et al. (2014). Innervation mapping of the hind paw of the rat using Evans blue extravasation, optical surface mapping and CASAM. *J. Neurosci. Methods* 229, 15–27. doi: 10.1016/j.jneumeth.2014.03.015
- Kappos, E. A., Sieber, P. K., Engels, P. E., Mariolo, A. V., D'Arpa, S., Schaefer, D. J., et al. (2017). Validity and reliability of the CatWalk system as a static and dynamic gait analysis tool for the assessment of functional nerve recovery in small animal models. *Brain Behav.* 7:e00723. doi: 10.1002/brb3.723
- Kawamura, D. H., Johnson, P. J., Moore, A. M., Magill, C. K., Hunter, D. A., Ray, W. Z., et al. (2010). Matching of motor-sensory modality in the rodent femoral nerve model shows no enhanced effect on peripheral nerve regeneration. *Exp. Neurol.* 223, 496–504. doi: 10.1016/j.expneurol.2010.01.016
- Kishino, A., Ishige, Y., Tatsuno, T., Nakayama, C., and Noguchi, H. (1997). BDNF prevents and reverses adult rat motor neuron degeneration and induces axonal outgrowth. *Exp. Neurol.* 144, 273–286. doi: 10.1006/exnr.1996.6367
- Kondo, Y., Saruta, J., To, M., Shiiki, N., Sato, C., and Tsukinoki, K. (2010). Expression and role of the BDNF receptor-TrkB in rat adrenal gland under acute immobilization stress. *Acta Histochem. Cytochem.* 43, 139–147. doi: 10.1267/ahc.10027
- Koopmans, G. C., Deumens, R., Brook, G., Gerver, J., Honig, W. M. M., Hamers, F. P. T., et al. (2007). Strain and locomotor speed affect over-ground locomotion in intact rats. *Physiol. Behav.* 92, 993–1001. doi: 10.1016/j.physbeh.2007.07.018
- Li, M. T. A., Willett, N. J., Uhrig, B. A., Guldberg, R. E., and Warren, G. L. (2014). Functional analysis of limb recovery following autograft treatment of volumetric muscle loss in the quadriceps femoris. *J. Biomech.* 47, 2013–2021. doi: 10.1016/j.jbiomech.2013.10.057
- Lutz, D., Kataria, H., Kleene, R., Loers, G., Chaudhary, H., Guseva, D., et al. (2016). Myelin basic protein cleaves cell adhesion molecule L1 and improves regeneration after injury. *Mol. Neurobiol.* 53, 3360–3376. doi: 10.1007/s12035-015-9277-0
- Maness, P. F., and Schachner, M. (2007). Neural recognition molecules of the immunoglobulin superfamily: signaling transducers of axon guidance and neuronal migration. *Nat. Neurosci.* 10, 19–26. doi: 10.1038/nn1827
- Marquardt, L. M., and Sakiyama-Elbert, S. E. (2015). GDNF preconditioning can overcome Schwann cell phenotypic memory. *Exp. Neurol.* 265, 1–7. doi: 10.1016/j.expneurol.2014.12.003
- Maurel, P., Einheber, S., Galinska, J., Thaker, P., Lam, I., Rubin, M. B., et al. (2007). Nectin-like proteins mediate axon-Schwann cell interactions along the internode and are essential for myelination. *J. Cell Biol.* 178, 861–874. doi: 10.1083/jcb.200705132
- Meek, M. F., Coert, J. H., and Robinson, P. H. (2005). Poor results after nerve grafting in the upper extremity: Quo vadis? *Microsurgery* 25, 396–402. doi: 10.1002/micr.20137
- Moradzadeh, A., Borschel, G. H., Luciano, J. P., Whitlock, E. L., Hayashi, A., Hunter, D. A., et al. (2008). The impact of motor and sensory nerve architecture on nerve regeneration. *Exp. Neurol.* 212, 370–376. doi: 10.1016/j.expneurol.2008.04.012
- Nagashima, M., Fujikawa, C., Mawatari, K., Mori, Y., and Kato, S. (2011). HSP70, the earliest-induced gene in the zebrafish retina during optic nerve regeneration: its role in cell survival. *Neurochem. Int.* 58, 888–895. doi: 10.1016/j.neuint.2011.02.017
- Navarro, X. (2016). Functional evaluation of peripheral nerve regeneration and target reinnervation in animal models: a critical overview. *Eur. J. Neurosci.* 43, 271–286. doi: 10.1111/ejn.13033
- Nave, K. A. (2010). Myelination and support of axonal integrity by glia. *Nature* 468, 244–252. doi: 10.1038/nature09614
- Nichols, C. M., Brenner, M. J., Fox, I. K., Tung, T. H., Hunter, D. A., Rickman, S. R., et al. (2004). Effects of motor versus sensory nerve grafts on peripheral nerve regeneration. *Exp. Neurol.* 190, 347–355. doi: 10.1016/j.expneurol.2004.08.003
- Pajenda, G., Hercher, D., Márton, G., Pajer, K., Feichtinger, G., Maléth, J., et al. (2014). Spatiotemporally limited BDNF and GDNF overexpression rescues motoneurons destined to die and induces elongative axon growth. *Exp. Neurol.* 261, 367–376. doi: 10.1016/j.expneurol.2014.05.019
- Pena, M. C., and Baron, J. (1988). Femoral nerve and rectus femoris muscle of the rat: a study in anatomy, histology, and histoenzymes. *Ann. Plast. Surg.* 20, 527–532. doi: 10.1097/0000637-198806000-00005
- Perlin, J. R., and Talbot, W. S. (2007). Putting the glue in glia: neclns mediate Schwann cell-axon adhesion. *J. Cell Biol.* 178, 721–723. doi: 10.1083/jcb.200708019
- Plantman, S. (2013). Proneurogenic properties of ECM molecules. *Biomed Res. Int.* 2013:981695. doi: 10.1155/2013/981695
- Provenzano, M. J., Minner, S. A., Zander, K., Clark, J. J., Kane, C. J., Green, S. H., et al. (2011). P75NTR expression and nuclear localization of p75NTR intracellular domain in spiral ganglion Schwann cells following

- deafness correlate with cell proliferation. *Mol. Cell. Neurosci.* 47, 306–315. doi: 10.1016/j.mcn.2011.05.010
- Puigdemívol-Sánchez, A., Forcada-Calvet, P., Prats-Galino, A., and Molander, C. (2000). Contribution of femoral and proximal sciatic nerve branches to the sensory innervation of hindlimb digits in the rat. *Anat. Rec.* 260, 180–188. doi: 10.1002/1097-0185(20001001)260:2<180::aid-ar70>3.0.co;2-e
- Secer, H. I., Daneyemez, M., Tehli, O., Gonul, E., and Izci, Y. (2008). The clinical, electrophysiologic, and surgical characteristics of peripheral nerve injuries caused by gunshot wounds in adults: a 40-year experience. *Surg. Neurol.* 69, 143–152. doi: 10.1016/j.surneu.2007.01.032
- Spiegel, I., Adamsky, K., Eshed, Y., Milo, R., Sabanay, H., Sarig-Nadir, O., et al. (2007). A central role for *Necl4* (SynCAM4) in Schwann cell-axon interaction and myelination. *Nat. Neurosci.* 10, 861–869. doi: 10.1038/nn1915
- Sulaiman, O. A. R., Midha, R., Munro, C. A., Matsuyama, T., Al-Majed, A., Gordon, T., et al. (2002). Chronic Schwann cell denervation and the presence of a sensory nerve reduce motor axonal regeneration. *Exp. Neurol.* 176, 342–354. doi: 10.1006/exnr.2002.7928
- Tanga, F. Y., Raghavendra, V., and DeLeo, J. A. (2004). Quantitative real-time RT-PCR assessment of spinal microglial and astrocytic activation markers in a rat model of neuropathic pain. *Neurochem. Int.* 45, 397–407. doi: 10.1016/s0197-0186(03)00302-4
- Thiery, J. P., and Duband, J. L. (1986). Role of tissue environment and fibronectin in the patterning of neural crest derivatives. *Trends Neurosci.* 9, 565–570. doi: 10.1016/0166-2236(86)90178-5
- Triolo, D. (2006). Loss of glial fibrillary acidic protein (GFAP) impairs Schwann cell proliferation and delays nerve regeneration after damage. *J. Cell Sci.* 119, 3981–3993. doi: 10.1242/jcs.03168
- Vrinten, D. H., and Hamers, F. F. T. (2003). 'CatWalk' automated quantitative gait analysis as a novel method to assess mechanical allodynia in the rat; a comparison with von Frey testing. *Pain* 102, 203–209. doi: 10.1016/s0304-3959(02)00382-2
- Wang, J., Zhang, P., Wang, Y., Kou, Y., Zhang, H., and Jiang, B. (2010). The observation of phenotypic changes of Schwann cells after rat sciatic nerve injury. *Artif. Cells Blood Substit. Biotechnol.* 38, 24–28. doi: 10.3109/10731190903495736
- Wiese, S., Pei, G., Karch, C., Troppmair, J., Holtmann, B., Rapp, U. R., et al. (2001). Specific function of B-Raf in mediating survival of embryonic motoneurons and sensory neurons. *Nat. Neurosci.* 4, 137–142. doi: 10.1038/83960
- Witzel, C., Rohde, C., and Brushart, T. M. (2005). Pathway sampling by regenerating peripheral axons. *J. Comp. Neurol.* 485, 183–190. doi: 10.1002/cne.20436
- Wyatt, S., Shooter, E. M., and Davies, A. M. (1990). Expression of the NGF receptor gene in sensory neurons and their cutaneous targets prior to and during innervation. *Neuron* 4, 421–427. doi: 10.1016/0896-6273(90)90054-j
- Xu, P., Rosen, K. M., Hedstrom, K., Rey, O., Guha, S., Hart, C., et al. (2013). Nerve injury induces glial cell line-derived neurotrophic factor (GDNF) expression in schwann cells through purinergic signaling and the PKC-PKD pathway. *Glia* 61, 1029–1040. doi: 10.1002/glia.22491
- Yang, M., Rawson, J. L., Zhang, E. W., Arnold, P. B., Lineaweaver, W., and Zhang, F. (2011). Comparisons of outcomes from repair of median nerve and ulnar nerve defect with nerve graft and tubulization: a meta-analysis. *J. Reconstr. Microsurg.* 27, 451–460. doi: 10.1055/s-0031-1281526
- Yang, Z., and Wang, K. K. W. (2015). Glial fibrillary acidic protein: from intermediate filament assembly and gliosis to neurobiomarker. *Trends Neurosci.* 38, 364–374. doi: 10.1016/j.tins.2015.04.003
- Yoshida, T., Kurella, M., Beato, F., Min, H., Ingelfinger, J. R., Stears, R. L., et al. (2002). Monitoring changes in gene expression in renal ischemia-reperfusion in the rat. *Kidney Int.* 61, 1646–1654. doi: 10.1046/j.1523-1755.2002.00341.x
- Zelano, J., Plantman, S., Hailer, N. P., and Cullheim, S. (2009). Altered expression of nectin-like adhesion molecules in the peripheral nerve after sciatic nerve transection. *Neurosci. Lett.* 449, 28–33. doi: 10.1016/j.neulet.2008.10.061
- Zhang, J. Y., Luo, X. G., Xian, C. J., Liu, Z. H., and Zhou, X. F. (2000). Endogenous BDNF is required for myelination and regeneration of injured sciatic nerve in rodents. *Eur. J. Neurosci.* 12, 4171–4180. doi: 10.1111/j.1460-9568.2000.01312.x

Conflict of Interest Statement: The authors declare that the research was conducted in the absence of any commercial or financial relationships that could be construed as a potential conflict of interest.

Copyright © 2019 Hercher, Kerbl, Schuh, Heinzl, Gal, Stainer, Schmidhammer, Hausner, Redl, Nógrádi and Hacobian. This is an open-access article distributed under the terms of the Creative Commons Attribution License (CC BY). The use, distribution or reproduction in other forums is permitted, provided the original author(s) and the copyright owner(s) are credited and that the original publication in this journal is cited, in accordance with accepted academic practice. No use, distribution or reproduction is permitted which does not comply with these terms.



Two-Chambered Chitosan Nerve Guides With Increased Bendability Support Recovery of Skilled Forelimb Reaching Similar to Autologous Nerve Grafts in the Rat 10 mm Median Nerve Injury and Repair Model

OPEN ACCESS

Edited by:

Tycho Hoogland,
Erasmus University Rotterdam,
Netherlands

Reviewed by:

Lorenzo Di Cesare Mannelli,
University of Florence, Italy
De-Lai Qiu,
Yanbian University, China

*Correspondence:

Kirsten Haastert-Talini
haastert-talini.kirsten@
mh-hannover.de

† These authors have contributed
equally to this work

Specialty section:

This article was submitted to
Cellular Neuropathology,
a section of the journal
Frontiers in Cellular Neuroscience

Received: 14 November 2018

Accepted: 08 April 2019

Published: 10 May 2019

Citation:

Dietzmeier N, Förthmann M,
Leonhard J, Helmecke O,
Brandenberger C, Freier T and
Haastert-Talini K (2019)
Two-Chambered Chitosan Nerve
Guides With Increased Bendability
Support Recovery of Skilled Forelimb
Reaching Similar to Autologous Nerve
Grafts in the Rat 10 mm Median
Nerve Injury and Repair Model.
Front. Cell. Neurosci. 13:149.
doi: 10.3389/fncel.2019.00149

**Nina Dietzmeier^{1,2†}, Maria Förthmann^{1,2†}, Julia Leonhard¹, Olaf Helmecke³,
Christina Brandenberger⁴, Thomas Freier³ and Kirsten Haastert-Talini^{1,2*}**

¹ Institute of Neuroanatomy and Cell Biology, Hannover Medical School, Hanover, Germany, ² Center for Systems Neuroscience (ZSN) Hannover, Hanover, Germany, ³ Medovent GmbH, Mainz, Germany, ⁴ Institute of Functional and Applied Anatomy, Hannover Medical School, Hanover, Germany

Tension-free surgical reconstruction of transected digital nerves in humans is regularly performed using autologous nerve grafts (ANGs) or bioartificial nerve grafts. Nerve grafts with increased bendability are needed to protect regenerating nerves in highly mobile extremity parts. We have recently demonstrated increased bendability and regeneration supporting properties of chitosan nerve guides with a corrugated outer wall (corrCNGs) in the common rat sciatic nerve model (model of low mobility). Here, we further modified the hollow corrCNGs into two-chambered nerve guides by inserting a perforated longitudinal chitosan-film (corrCNG[F]s) and comprehensively monitored functional recovery in the advanced rat median nerve model. In 16 adult female Lewis rats, we bilaterally reconstructed 10 mm median nerve gaps with either ANGs, standard chitosan nerve guides (CNGs), CNGs (CNG[F]s), or corrCNG[F]s ($n = 8$, per group). Over 16 weeks, functional recovery of each forelimb was separately surveyed using the grasping test (reflex-based motor task), the staircase test (skilled forelimb reaching task), and non-invasive electrophysiological recordings from the thenar muscles. Finally, regenerated tissue harvested from the distal part of the nerve grafts was paraffin-embedded and cross-sections were analyzed regarding the number of Neurofilament 200-immunopositive axons and the area of newly formed blood vessels. Nerve tissue harvested distal to the grafts was epon-embedded and semi-thin cross-sections underwent morphometrical analyses (e.g., number of myelinated axons, axon and fiber diameters, and myelin thicknesses). Functional recovery was fastest and most complete in the ANG group (100% recovery rate regarding all parameters), but corrCNG[F]s accelerated the recovery of all functions evaluated in comparison to the other nerve

guides investigated. Furthermore, corrCNG[F]s supported recovery of reflex-based grasping (87.5%) and skilled forelimb reaching (100%) to eventually significantly higher rates than the other nerve guides (grasping test: CNGs: 75%, CNG[F]s: 62.5%; staircase test: CNGs: 66.7%, CNG[F]s: 83.3%). Histological and nerve morphometrical evaluations, in accordance to the functional results, demonstrated best outcome in the ANG group and highest myelin thicknesses in the corrCNG[F] group compared to the CNG and CNG[F] groups. We thus clearly demonstrate that corrCNG[F]s represent promising innovative nerve grafts for nerve repair in mobile body parts such as digits.

Keywords: bendable nerve guides, chitosan, rat median nerve, functional recovery, nerve histomorphometry

INTRODUCTION

Traumatic injuries of peripheral nerves represent a frequent reason for morbidity and life-long physical restrictions. Worldwide, about 2.8% of all trauma patients suffer from peripheral nerve injuries (Noble et al., 1998). In many cases, these injuries lead to life-long dependency on aid and substantial reduction of quality of life (Noble et al., 1998). Around the world, more than 1 million people are affected per year (Asplund et al., 2009). Recovery of peripheral nerve injuries often remains incomplete and progresses slowly. Additionally, only less than 50% of the patients regain good to excellent motor functions (Grinsell and Keating, 2014). In clinical routine, peripheral nerve injuries most often affect the upper limbs (Kouyoumdjian, 2006; Deumens et al., 2010) and in 6.4% of all hand injuries, the joint-crossing digital nerves are affected (Renner et al., 2004).

When nerve ends cannot be surgically reconnected by tension-free end-to-end-suture, insertion of autologous nerve grafts (ANGs) still represents the gold standard therapy. However, the usage of ANGs comes along with several downsides such as donor side morbidity, limited availability of donor tissue, and prolonged surgery time followed by increased surgery costs (Hallgren et al., 2013; Faroni et al., 2015).

To circumvent these downsides, we have previously contributed to the development of bioartificial nerve guidance conduits made out of chitosan (Haastert-Talini et al., 2013). In 2015, these nerve guides have been made available for the reconstruction of peripheral nerve gaps in human patients with a maximum distance of 2.6 cm (Reaxon[®] Nerve Guides; Medovent GmbH, Germany). In animal studies, the suitability of those chitosan nerve guides (CNGs) to support peripheral nerve regeneration across limited and critical gap lengths have been proven not only for acute (Haastert-Talini et al., 2013; Gonzalez-Perez et al., 2015; Shapira et al., 2015; Meyer et al., 2016b), but also for delayed (Stenberg et al., 2017) repair of rat sciatic nerves. The rat sciatic nerve injury and repair model is most commonly used to evaluate new developments for peripheral nerve guidance and regeneration support (Angius et al., 2012; Geuna, 2015). When using this model, however, nerve reconstruction is usually performed in an extremity region with minimized mobility, e.g., along the femur bone. In order to address the need for nerve grafts with increased flexibility/bendability in connection with preserved collapse stability for nerve reconstruction in highly mobile regions such as digital joints, we recently modified the

original standard CNGs into CNGs with a wavy wall structure at the outside, the so-called corrugated chitosan nerve guide (corrCNG). These corrCNGs have demonstrated similar support as standard hollow CNGs with regard to axonal and functional peripheral nerve regeneration in 15 mm rat sciatic nerve gaps, both after acute and delayed repair (Stöbel et al., 2018b). We have previously shown that longitudinal insertion of a perforated chitosan film into hollow CNGs and applying such two-chambered nerve guides (CNG[F]s) for 15 mm rat sciatic nerve gap reconstruction could significantly increase recovery of motor function. However, ANG implantation still resulted in best recovery rates (Meyer et al., 2016a). To further increase the regeneration support given by corrCNGs, we also enhanced them into two-chambered nerve guides by inserting a perforated longitudinal chitosan film (corrCNG[F]) in the current study.

Using the recently advanced rat median nerve injury and repair model (Stöbel et al., 2017), we here investigated the regeneration supporting properties of corrCNG[F]s in comparison to ANGs, CNGs, and CNG[F]s after reconstruction of 10 mm nerve gaps. While implantation of ANGs still showed fast and most complete functional recovery, we clearly demonstrate that corrCNG[F]s accelerated and for some skilled-forelimb reaching also significantly increased the recovery of all functions evaluated in comparison to the other bioartificial nerve guides investigated. Results from immunohistological and histomorphometrical evaluation of the distal graft and nerve distal to it underline the superiority of corrCNG[F]s compared to the other artificial nerve guidance channels tested here.

MATERIALS AND METHODS

Experimental Design

In this study, we bilaterally reconstructed 10 mm median nerve gaps of 16 female Lewis rats with either gold standard ANGs (control group; $n = 8$), standard hollow CNGs ($n = 8$), two-chambered chitosan-film enhanced chitosan nerve grafts (CNG[F]s; $n = 8$), or two-chambered corrugated chitosan-film enhanced CNGs (corrCNG[F]s; $n = 8$). This procedure resulted in a 50% reduction of animal numbers for the study, because two reconstruction conditions could be studied in one animal. During 16 weeks of investigation, functional recovery of each paw was separately surveyed using the grasping test (every second week), the staircase test and non-invasive electrophysiological

recordings from the thenar muscles (every fourth week). Evaluation was finalized by histomorphometrical analyses of the regenerated nerve tissue within the grafts and distal to it at 16 weeks post-surgery.

Manufacturing of Classic, Corrugated, and Corrugated Chitosan-Film Enhanced Chitosan Nerve Guides

Medical grade chitosan derived from *Pandalus borealis* shrimp shells was processed by Chitinor AS (Norway). All types of CNGs were manufactured by Medovent GmbH (Germany) under ISO 13485 regulations using a patented extrusion process with either standard tubular molds or molds with a corrugated design. All nerve guides were prepared in a length of 14 mm, an inner diameter of 1.6 mm, and a final degree of acetylation (DA) of ~5%. A DA of ~5% has previously been proven to be most supportive for peripheral nerve regeneration in the rat sciatic nerve model (Haastert-Talini et al., 2013). Chitosan-films for CNG[F]s and for corrCNG[F]s were manually produced as described earlier (Meyer et al., 2016a). Briefly, rectangular pieces (length 10 mm, width: 5 mm) of chitosan-films were perforated (along the midline of the longer axis, diameter of perforation: 0.3 mm, distance in between: 2 mm) and subsequently Z-shape-folded (opposite kinked edges, width of outer edges: 1.7 mm) before they were inserted into the lumen of hollow standard CNGs or corrCNGs leading to 2 mm spaces on each side of the tubes.

Sterilization of all types of CNGs was performed by beta irradiation (11 kGy, 10 MeV) by BGS Beta-Gamma-Service GmbH & Co. KG (Wiehl, Germany) (Stößel et al., 2018a). All CNGs used for median nerve repair were rinsed in 0.9% sodium chloride solution (NaCl 0.9%, B. Braun Melsungen GmbH, Germany) for at least 20 min prior to implantation.

Animals and Surgical Procedure

This study was carried out in accordance with the principles of the Basel Declaration and recommendations of Directive 2010/63/EU: TierSchG 13.07.2013, BGBl I Nr. 36 12.07.2013, p. 2182 + TierSchVersV. The protocol was approved by the animal care committee of Lower-Saxony, Germany (approval code: 33.12-42502-04-15/1761; approval date: April 10, 2015).

Sixteen young adult female Lewis rats (LEW/OrlRj, mean body weight at the day of surgery: 217.8 ± 1.73 g) were obtained from Janvier Labs SAS [Genest Saint Isle (Le), France] at an age of 13 weeks and housed in groups of four under standardized housing conditions (22.2°C; humidity 55.5%; light/dark cycle 14 h/10 h). Food and water was provided *ad libitum* except during staircase test phases, when animals were fed restrictively with 12 g food per animal and day. As earlier described (Stößel et al., 2017) body weight was controlled every other day (tolerable weight loss up to 15%). A time interval of 72 h was kept between the end of restrictive feeding and eventual anesthesia. Female rats were used because they are generally smaller than male rats (weight difference 100–150 g) and in order to guarantee only minimal size increase during the 16 weeks observation time. Weight increase in Lewis rats follows a flatter curve

in female than in male individuals and is already reaching the plateau at an age of 12 weeks in female animals when male rats are still growing. The use of female animals in this study therefore ensured easy handling for the grasping test, when animals were grasped around their trunk with one hand pending to be quickly held only on their tail during the test procedure. The flatter growth curve of female rats further ensured that while already being optimally sized at training onset for the staircase test (not able to turn around or grab pellets with the contralateral paw), tentative weight gain was limited during the observation period. Thus, the staircase test apparatuses did not become too narrow for the still slightly growing young adult animals.

Animals were habituated to the functional testing procedures (grasping test and staircase test) 3 weeks prior to surgery and pre-surgically healthy baseline reference values of all animals were recorded as described in the related sections below.

All surgeries (performed on rats with an age of 19 weeks) and electrodiagnostic recordings were performed under deep anesthesia (intraperitoneal injection of chloral hydrate, 370 mg/kg, Sigma-Aldrich Chemie GmbH, Germany) and aseptic conditions. To minimize the decrease of body temperature animals were placed on a heating pad and rectal body temperature was measured before and after surgery in order to ensure that it did not fall below 36.5°C. After surgery the animals were blanketed with several layers of tissue paper in order to avoid further cooling. Sufficient analgesia during surgery/electrodiagnostic evaluation and the two following days was induced by subcutaneous injection of Butorphanol (0.5 mg/kg, Turbogesic®; Pfizer GmbH, Germany).

For nerve transection surgery, a 1 cm incision was performed parallel to the humerus in the axillary region to approach the median nerve. In addition to general anesthesia (see above), drops of bupivacaine (0.25%, Carbostesin®; AstraZeneca GmbH, Germany) and lidocaine (2%, Xylocain®; AstraZeneca GmbH, Germany) were locally applied on the prospective transection sites of the exposed nerve some minutes before nerve transection in order to ensure sufficient analgesia.

In case of ANG repair, the median nerve was first transected at the distal location (proximal to the point where the median nerve is crossed by the brachial artery), followed by the second transection 10 mm proximal to this point. The nerve piece was then reversed and rotated 180° before suturing it between the two nerve ends. Each end was sutured by two epineural 9–0 stitches. In CNG, CNG[F], and corrCNG[F] groups, the second transection was performed 7 mm proximal to the distal transection with removal of the nerve piece and its further procession for histomorphometrical analyses (healthy control). After application of either nerve guide, both nerve ends were introduced into the nerve graft and sutured with one epineural 9–0 stitch generating an overlap of 2 mm at each nerve end and a 10 mm median nerve gap.

Wound closure was performed by using first three to four resorbable sutures on the muscle layers (3–0 Polysorb, UL-215, Syneture, United States) followed by three to four non-resorbable mattress sutures (4–0 Ethilon™ II, EH7791H, Ethicon, United Kingdom) for skin suture.

Grasping Test – Evaluation of Reflex-Based Paw-Usage Ability

To evaluate the recovery of finger flexion progressing to restoration of grip force, reflex-based movement (Tupper and Wallace, 1980) was assessed every second week from the fourth week post-surgery onward.

Briefly, the paw-usage ability was video recorded and grip force was measured as described previously (Stöbel et al., 2017).

During testing the animals were carefully grasped around their trunk to support them while bringing them close to the test apparatus. For the concrete test procedure the hand around the trunk was removed and the animals were held only by their tail root (1–1.5 cm from the fur) for 5–15 s. Test periods >5 s were only needed when finger flexion was not possible and the experimenter had to take some more time for deciding to end the trial.

For scoring, three categories of grasping behavior were set: Category 1 – no finger flexion while touching the grasping bar; Category 2 – ability to grasp the bar (closing digits around it) but not able to hold it while being slowly withdrawn; and Category 3 – ability to grasp and pull the bar with a detectable force (gross motor skills). Since the scoring was performed in accordance to our previous open access report we kindly refer the reader to it for an illustration (Stöbel et al., 2017).

Staircase Test – Evaluation of Skilled Forelimb Reaching Ability

Prior to surgery (for the recording of healthy baseline reference values) and at pre-defined time points after surgery, the animals were (re-)habituated to the testing procedure and restrictively fed for 7 consecutive days. Therefore, food was restricted to 12 g per animal and day and body weight was controlled every other day. The tolerable weight loss was up to 15%.

On the next 3 days (for pre-surgery values) or on the last 3 days (for post-surgical values), the mean maximum number of pellets retrieved per animal/paw was determined for each individual paw (Stöbel et al., 2017). Therefore, the rats sat within the staircase apparatuses on the plinth in the middle not being able to turn around and only reaching the left/right stairs with the respective paw. Each of the stairs is composed of seven steps, and was equipped with three sugar pellets each (AIN-76A Rodent Tablet 45 mg IRR, Lot number: 12SEP17RTD1, TestDiet™, United States). After a 15 min testing period, remaining sugar pellets on the stairs and also sugar pellets on the ground (representing failed attempts) were summed up. Post-surgically, the test was performed at 4, 8, 12, and 16 weeks.

Forelimbs were classified as successfully participating as soon as more than three pellets were retrieved, because over time and with further slightly increasing body size, the animals could reach three pellets on the first step with their tongue and mouth.

Non-invasive Electrophysiological Recordings – Evaluation of Thenar Muscle Reinnervation

Healthy baseline reference values of non-invasive electrophysiological measurements were recorded from the anesthetized

animals, right before surgery. Post-surgical recordings were performed every fourth week.

Under deep anesthesia (body temperature was controlled and approximately $36.6 \pm 0.3^\circ\text{C}$), animals were placed in supine position and single stimulating electric impulses (100 μs , 1 Hz) were induced by transcutaneous monopolar needle electrodes. Stimulation intensity was constantly increased up to 30% supramaximal level. The reconstructed median nerve was either stimulated proximal to the injury site in the axillary region or distal to the graft at the elbow. Evocable compound muscle action potentials (CMAPs) were recorded transcutaneously from the thenar muscles (Stöbel et al., 2017). Despite possible co-stimulation of the ulnar nerve in the axillary region, CMAP recordings from the thenar muscles only result from the median nerve stimulation, because of the anatomical situation and trajectory of the median nerve (Stöbel et al., 2017).

Semi-automated evaluation of the amplitudes caused by the evocable CMAPs (manual setting of baseline to negative peak of M-wave) was performed by using a Dantec® Keypoint® Focus device (Natus Europe GmbH, Germany). If no evocable CMAP or CMAPs with no clear negative M-wave peak could be detected, a zero value was included into the statistical analysis.

Nerve Immunohistochemistry in the Distal Nerve Grafts – Quantification of Axonal Profiles

At 16 weeks post-surgery, all animals were sacrificed in deep anesthesia in carbon dioxide atmosphere followed by cervical dislocation. The regenerated nerve tissue was removed from the lumen of the nerve guides, together with the central chitosan-film, in case of chitosan-film enhanced nerve guides. The tissue was fixed overnight [4% paraformaldehyde in phosphate-buffered saline (PBS, Dulbecco, Biochrom GmbH, Germany), 4°C , Sigma-Aldrich Chemie GmbH, Germany] before paraffin-embedding was performed.

From the distal portion of ANG grafts or at 3.7 mm proximal to the distal suture of tissue harvested from the nerve guides, series of 80 blind-coded cross-sections (7 μm) were prepared. Selected sections were Hematoxylin and Eosin (HE) stained in order to generate an overview of the composition of the regenerated tissue and to quantify median blood vessel areas (see the section “Quantification of median blood vessel area in the distal nerve grafts”). Consecutive sections were stained for neurofilament 200 (NF200) (Meyer et al., 2016a; Stenberg et al., 2017). For anti-NF200 staining, sections were incubated in blocking solution [3% milk powder (Bio Magermilch Pulver, Heirler Cenovis GmbH, Germany), 0.5% Triton-X 100 (Roche Diagnostics GmbH, Germany) in PBS] prior to incubation with primary rabbit anti-NF200 antibody (against phosphorylated NFeH, N4142, 1:500, Sigma-Aldrich GmbH, Germany, 4°C overnight) followed by incubation with Alexa-488-conjugated secondary goat anti-rabbit antibody (A11034, 1:1000, Invitrogen AG, Germany, 1 h at room temperature). The antibodies were diluted in blocking solution and the incubation steps separated by three-times washing in PBS. After nuclear counter staining with 4',6-diamidin-2-phenylindol (DAPI, 1:2000 in PBS,

Sigma-Aldrich GmbH), sections were mounted using Mowiol (Calbiochem GmbH, Germany).

Representative photomicrographs of NF200-stained as well as HE-stained sections were created as multiple image alignments (MIA) using a BX51 microscope (Olympus GmbH, Germany).

Neurofilament 200-immunopositive axonal profiles were quantified with the help of ImageJ version 1.48 (National Institutes of Health, United States). Therefore, areas containing NF200-immunopositive axons were used to determine the regions of interest (ROI), which were needed to quantify the particle number later. By using a threshold strategy, NF200-photomicrographs were converted to binary images. Threshold pixel values reached from minimum 71 to maximum 172. This allowed distinguishing between individual nerve fibers. Afterwards NF200-immunopositive axonal profiles within the ROI were detected by using the particle analysis function of ImageJ. To avoid the detection of background noises, only particles with a size bigger than 0.001 Pixel^2 were counted.

Quantification of Median Blood Vessel Area in the Distal Nerve Grafts

Virtual slides of HE-stained sections were created with the help of macroscopic tissue slide scanner (Axio Scan.Z1, Carl Zeiss Microscopy GmbH, Germany). Tissue sections were scanned at $40\times$ magnification. Cross sectional areas (μm^2) of blood vessels within complete sections were quantified with the help of ZEN Imaging Software version 2.5, blue edition (Carl Zeiss Microscopy GmbH, Germany). Therefore, blood vessels within HE-photomicrographs were identified and their inner border, meaning the endothelial layer adjacent to the lumen, was contoured by using the Graphics tool and its area was quantified. Only blood vessels with visible erythrocytes within their lumen or, if no erythrocytes could be detected, with an intact endothelial layer were included into the evaluation.

Nerve Histomorphometry Distal to the Nerve Grafts

Segments of the nerve, which were harvested directly distal to the nerve grafts, were fixed in Karnovsky solution, flushed in sucrose-sodium cacodylate buffer. Post-fixation was performed in 1% osmium tetroxide for 1.5 h before myelin sheaths were stained with 1% potassium dichromate and hematoxylin (Korte et al., 2011). Afterwards the samples were embedded into Epon and semi-thin cross-sections ($1 \mu\text{m}$) were prepared. To enhance the myelin staining a toluidine blue staining was performed. Finally, sections were mounted by using Mowiol.

Histomorphometrical evaluation was performed as described before (Stöbel et al., 2017). Two sections of each reconstructed median nerve ($n = 8$ per group) were randomly selected and were evaluated at light microscopic level (BX50 microscope Olympus GmbH, Germany; $100\times$ magnification) equipped with a prior controller (MBF Bioscience, United States). Total fiber numbers were determined using a two-dimensional procedure (optical fractionator; grid size: $150 \times 150 \mu\text{m}^2$; counting frame size $30 \times 30 \mu\text{m}^2$) by means of Stereo Investigator version 11.04 (MBF Bioscience). Therefore, systematic random sampling

(Geuna, 2000) was applied to pick 12–16 sampling fields, depending on the size of the cross sectional area. In each of these sampling fields a two-dimensional dissector procedure was performed. Here, only the “tops” of fibers, meaning the first part of the fiber’s border that touched the edge of the counting frame, were counted to overcome the “edge effect” (Geuna, 2000).

In four photomicrographs ($100\times$ magnification) of each section, which were randomly selected, assessment of axon and fiber diameters and myelin thicknesses (G-ratio plug-in¹, ImageJ version 1.48, National Institutes of Health, United States) was performed in, with an examination of 10 axons per picture, 80 axons per specimen, and 640 axons per group. Axon and fiber diameter were calculated based on the assumption of a circular shape.

Statistical Analysis

Statistical analyses were applied to the data obtained in this study by using GraphPad Prism version 6.07 (GraphPad Software, United States). To detect significant differences, we resorted to two-way ANOVA followed by Tukey’s multiple comparisons and Kruskal–Wallis test followed by Dunn’s multiple comparisons. For statistical analysis of the qualitative outcome of the functional evaluation, we calculated the proportion of animals per group displaying evocable CMAPs or successful participation in either the grasping or the staircase test as percentages (0–100%) and compared them pair-wise with the Chi-square test. The p -value was set to $p < 0.05$ as significance level. All results are displayed as mean \pm SEM or median \pm range as indicated.

RESULTS

Overall Qualitative Assessment of Functional Recovery

For full clarity, it needs to be stressed again that in this study 10 mm median nerve gaps were bilaterally reconstructed in 16 female Lewis rats and that the numbers given for specimen analyzed per group consequently refer to median nerves repaired with the respective approach ($n = 8$ for each group) instead of the number of animals studied.

Table 1 summarizes the qualitative results from the functional evaluation performed. For each evaluated parameter a more detailed description of the obtained results follows.

Forelimbs were evaluated as successfully participating in the grasping test when displaying recovery of function of category 3 (ability to grasp and pull the bar with detectable force, see also **Figure 1**). Forelimbs were evaluated as successfully participating in the staircase test when they retrieved more than three pellets, because the three pellets initially placed on the first step could be reached with their tongue and mouth. With regard to electrodiagnostic measurements forelimbs were evaluated as successful, when evocable CMAPs, recorded from the thenar muscle, were detected.

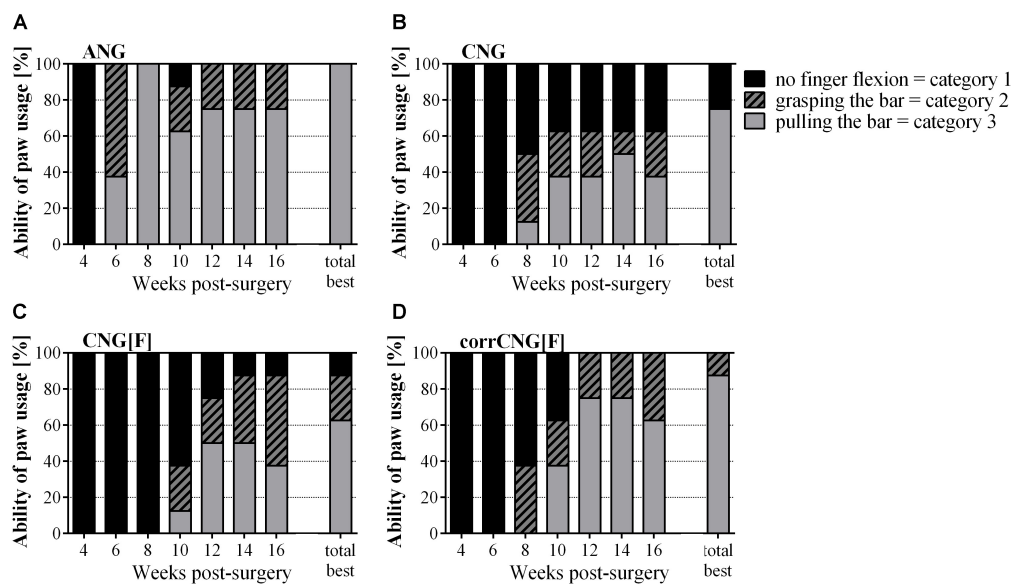
As depicted in **Table 1**, the electrodiagnostic measurements showed similar results for the ANG and corrCNG[F] group as

¹<http://gratio.efil.de/>

TABLE 1 | Summary of functional recovery based on successful participation in the grasping and the staircase test and on evocable CMAPs recorded from the thenar muscle upon electric stimulation of the reconstructed median nerve.

		4 Weeks post-surgery		8 Weeks post-surgery		12 Weeks post-surgery		16 Weeks post-surgery		Total best	
		Forelimbs/ group	[%]	Forelimbs/ group	[%]	Forelimbs/ group	[%]	Forelimbs/ group	[%]	Forelimbs/ group	[%]
Grasping test ^a	ANG	0/8	0.0	8/8	100.0*	6/8	75.0 ^{#,♦}	6/8	75.0 ^{#,♦}	8/8	100.0*
	CNG	0/8	0.0	1/8	12.5 ^{♦,*}	3/8	37.5	3/8	37.5	6/8	75.0
	CNG[F]	0/8	0.0	0/8	0.0	4/8	50.0	3/8	37.5	5/8	62.5
	corrCNG[F]	0/8	0.0	0/8	0.0	6/8	75.0 ^{#,♦}	5/8	62.5 ^{#,♦}	7/8	87.5 [♦]
Staircase test ^b	ANG	1/6	16.7*	6/6	100.0*	6/6	100.0 ^{#,♦}	6/6	100.0 ^{#,♦}	6/6	100.0 ^{#,♦}
	CNG	0/6	0.0	1/6	16.7	4/6	66.7 [♦]	4/6	66.7	4/6	66.7
	CNG[F]	0/6	0.0	1/6	16.7	3/6	50.0	5/6	83.3 [#]	5/6	83.3 [#]
	corrCNG[F]	0/6	0.0	1/6	16.7	6/6	100.0 ^{#,♦}	6/6	100.0 ^{#,♦}	6/6	100.0 ^{#,♦}
Electro-diagnostic recordings ^c	ANG	8/8	100.0 ^{♦,*}	8/8	100.0 ^{#,♦}	8/8	100.0	8/8	100.0	8/8	100.0
	CNG	8/8	100.0 ^{♦,*}	7/8	87.5	8/8	100.0	8/8	100.0	8/8	100.0
	CNG[F]	5/8	62.5	7/8	87.5	8/8	100.0	8/8	100.0	8/8	100.0
	corrCNG[F]	6/8	75.0	8/8	100.0 ^{#,♦}	8/8	100.0	8/8	100.0	8/8	100.0

The process of recovery started with evocable CMAPs upon electrodiagnostic measurements, followed by participation in the staircase test and at latest participation in the grasping test was detected. At the end of the study, all animals showed recordable CMAPs. Full recovery of gross motor function (grasping test) in 100% of the tested forelimbs was only achieved by the ANG group, while full recovery of fine motor skills (staircase test) in all tested forelimbs was present in the ANG and corrCNG[F] groups. ANG, autologous nerve graft; CNG, chitosan nerve guide; CNG[F], chitosan-film enhanced chitosan nerve guide; corrCNG[F], corrugated chitosan-film enhanced chitosan nerve guide. Values are given as total numbers (forelimbs successfully participating per group) as well as percentages (%). ^aForelimbs were evaluated as successfully participating when displaying recovery of function of Category 3 (ability to grasp and pull the bar with a detectable force). ^bForelimbs were evaluated as successfully participating, when they retrieved more than three pellets because three pellets on the first step could be reached with their tongue and mouth. ^cForelimbs were evaluated as successfully, when evocable CMAPs recorded from the thenar muscle were detected. Statistical differences were calculated with the Chi-square test between single group pairs at the same time point (* $p < 0.05$ ANG vs. all nerve guide groups, [#] $p < 0.05$ vs. CNG, [♦] $p < 0.05$ vs. CNG[F], * $p < 0.05$ vs. corrCNG[F]).

**FIGURE 1 |** Percentage of the individual paw usage abilities based on video-recorded reflex-based grasping test performed every 2 weeks over 16 weeks post-surgery. Pulling the bar with a force is the most complete ability to be recovered (Category 3). This recovery of gross motor function is achieved by all forelimbs of the ANG group (A). Among the artificial nerve guides corrCNG[F]s (D) led to the highest recovery rate. No statistical evaluation was applied. Values are given as percentages in relation to all evaluated forelimbs per group. (A) ANG, autologous nerve graft; (B) CNG, chitosan nerve guide; (C) CNG[F], chitosan-film enhanced chitosan nerve guide; (D) corrCNG[F], corrugated chitosan-film enhanced chitosan nerve guide; $n = 8$.

early as 8 weeks post-surgery, while performance in the other groups was still significantly inferior ($p < 0.05$, Chi-square test). At 12 weeks post-surgery ANG and corrCNG[F] reconstructed

forelimb groups showed the same level of performance in the grasping and the staircase test which was again significantly superior to the performance of the other groups evaluated

($p < 0.05$, Chi-square test). The total best performance could be ranked number 1 for ANG reconstructed forelimbs (100% in all three tests applied), number 2 for corrCNG[F] (100% in electrodiagnostic testing and skilled fore-limb reaching test, 87.5% in reflexed-based motor task), and number 3 for CNG and CNG[F].

Grasping Test – Evaluation of Reflex-Based Paw-Usage Ability

The reflex-based grasping test (Figure 1) was categorized as described above [Category 1 – no finger flexion while touching the grasping bar; Category 2 – ability to grasp the bar (closing digits around the bar) but not to hold it while being slowly withdrawn; Category 3 – ability to grasp and pull the bar with a detectable force (gross motor skills)].

Generally, recovery of gross motor function was fastest in the ANG group achieving 100% recovery 8 weeks post-surgery. At 4 weeks post-surgery, no ANG-treated forelimb showed finger flexion while 2 weeks later all animals were able to grab the bar. At this time point, three out of eight forelimbs in the ANG group were able to apply a certain force to the grasping frame. At 8 weeks post-surgery, all ANG group forelimbs regained their gross motor function. Finger flexion (Category 2) was possible in week 8 by 37.5% (3/8) of forelimbs of the CNG and corrCNG[F] groups, while the first 12.5% (2/8) of forelimbs of the CNG[F] group showed finger flexion at 10 weeks post-surgery. At 12 weeks after surgical intervention, 37.5% of forelimbs in the CNG group, 50% (4/8) in the CNG[F], and 75% (6/8) of the forelimbs that received median nerve reconstruction with corrCNG[F] had recovered the ability to encompass the grasping bar, to close the digits around it and to pull it with some force (Category 3).

Over time, the animals showed less motivation to participate in this test, which induced little fluctuations in the performances from 8 weeks post-surgery onward. Therefore, the total best performance of each animal was considered additionally (Figure 1, see also Table 1).

Looking at the total best performances, none of the nerve guide groups achieved recovery of gross motor skills in all forelimbs in contrast to the ANG group. The ability to grasp and pull the bar with a recordable force (Category 3) recovered in 75% of the CNG group, whereby the residual 25% remained without finger flexion (Category 1). 62.5% of the CNG[F]-reconstructed forelimbs regained gross motor function. 25% of this group had the ability for finger flexion (Category 2), while one reconstructed forelimb (12.5%) remained without finger flexion (Category 1). Among the artificial nerve guide groups regeneration was most complete in the corrCNG[F] group (87.5%, Category 3). The residual 12.5% were able to flex their fingers (Category 2).

Staircase Test – Evaluation of Skilled Forelimb Reaching Ability

Healthy baseline reference values for each individual paw, which were calculated as mean maximum number of pellets retrieved in the last 3 days of training, display that animals were able to retrieve a median of 7.84 pellets per paw at the end of the training

period (data not shown). Eight forelimbs of five animals (left and right forelimbs of three animals, left forelimbs of two animals) had to be excluded from evaluation, since these animals only achieved a median of 0.84 retrieved pellets pre-surgically and their participation in the test did not improve post-surgically due to lack of motivation. This resulted in a number of $n = 6$ animals per group evaluated in the staircase test.

To exclude individual paw preference and behavioral influences, post-surgical outcomes are presented as percentages from healthy individual reference values, which were calculated as 100% (Figure 2).

At 4 weeks post-surgery two ANG-reconstructed forelimbs participated in the test, but only one of the two ANG-treated forelimbs participated successfully (retrieving more than three pellets, see also Table 1). At 8 weeks post-surgery one forelimb of each nerve guide group performed successfully (see also Table 1), whereby three additional forelimbs in the corrCNG[F] group started to participate. At this time point, all ANG-reconstructed forelimbs participated successfully (retrieving more than three pellets, individual success rates reached from 84.3 to 399.4%, median success rate: 105.5% of the maximum pellets retrieved in healthy state). At 12 weeks post-surgery, four forelimbs of the CNG group and three forelimbs of the CNG[F] group participated successfully and two additional animals of the CNG[F] group evidently started to participate. At the same time, all forelimbs of the corrCNG[F] group (median individual success rate: 128.1%) showed successful participation. While the number of paws that successfully participated in the staircase test did not further increase in the CNG group (4/6 forelimbs), one animal of the CNG[F] group was not able to reliably regain fine motor skills until 16 weeks after surgery. After 16 weeks of observation the median maximum number of pellets retrieved vs. healthy state exceeded the 100% healthy baseline in the ANG, CNG, and corrCNG[F] groups (ANG: 131.35; CNG: 118.25; corrCNG[F]: 132.10). Animals of the CNG group reached a median maximum number of 98.00% of healthy values. Despite the pre-surgical performance of the animals had reached a plateau after the 7 days training period, the finding, that healthy baseline reference values were far exceeded in part, can be attributed to the fact, that the process of learning was still ongoing during the observation period and not completed pre-surgically (Stöbel et al., 2017). Also it cannot be excluded that the lesion and use of the temporarily impaired limb did recapitulate the learning process toward a better performance after recovery.

Non-invasive Electrodiagnostic Recordings – Evaluation of Thenar Muscle Reinnervation

Compound muscle action potential amplitude areas resulting from stimulation distal to the graft were recorded in order to estimate the number of axons participating in thenar muscle reinnervation (Figure 3). Healthy baseline reference values for each paw were determined right before surgery (healthy mean: 4.595 ± 0.267 ms * mV).

At 4 weeks, most reconstructed forelimbs of all groups showed evocable signals (ANG: 8/8, CNG: 8/8, CNG[F]: 5/8,

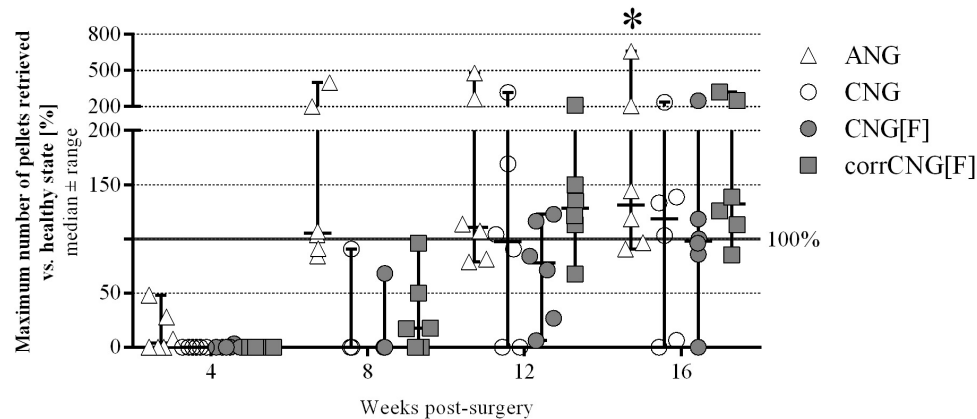


FIGURE 2 | Quantitative results of the staircase test showing recovery of skilled forelimb reaching revealed by individual success rates in pellet retrieval over 16 weeks post-surgery. The success rates of ANG-reconstructed forelimbs significantly increased 16 weeks after reconstruction when compared to the 4-week time point. CorrCNG[F]-reconstructed forelimbs recovered to the same extend as forelimbs of the ANG group, while not all forelimbs of the CNG and CNG[F] groups achieved pre-surgical performance levels. Two-way ANOVA showed an effect of the parameters 4 vs. 16 weeks post-surgery [$F(3,80) = 12.9, p < 0.0001$] and groups [$F(3,80) = 5.59, p = 0.0016$] but there was no interaction. Tukey's multiple comparisons were applied to detect significant differences ($*p < 0.05$ vs. 4 weeks post-surgery within the same group). Values are displayed as median \pm range and displayed as percentages in relation to pre-surgical healthy nerve mean values shown as baseline at 100%. ANG, autologous nerve graft; CNG, chitosan nerve guide; CNG[F], chitosan-film enhanced chitosan nerve guide; corrCNG[F], corrugated chitosan-film enhanced chitosan nerve guide; $n = 6$).

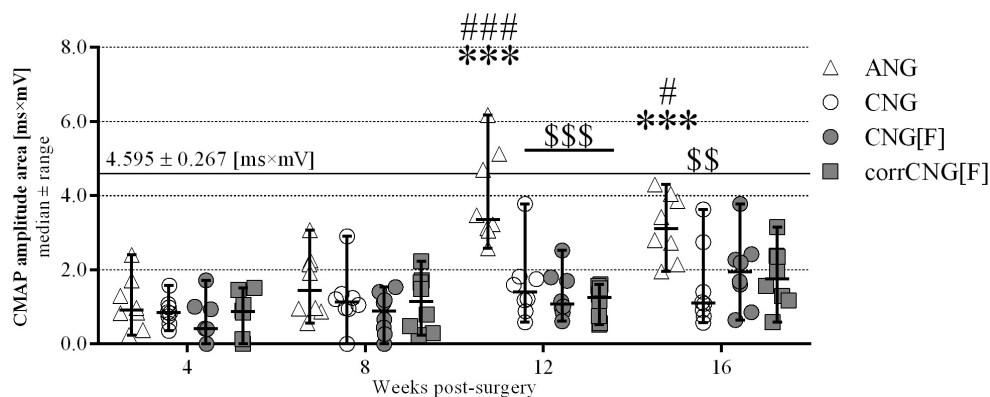
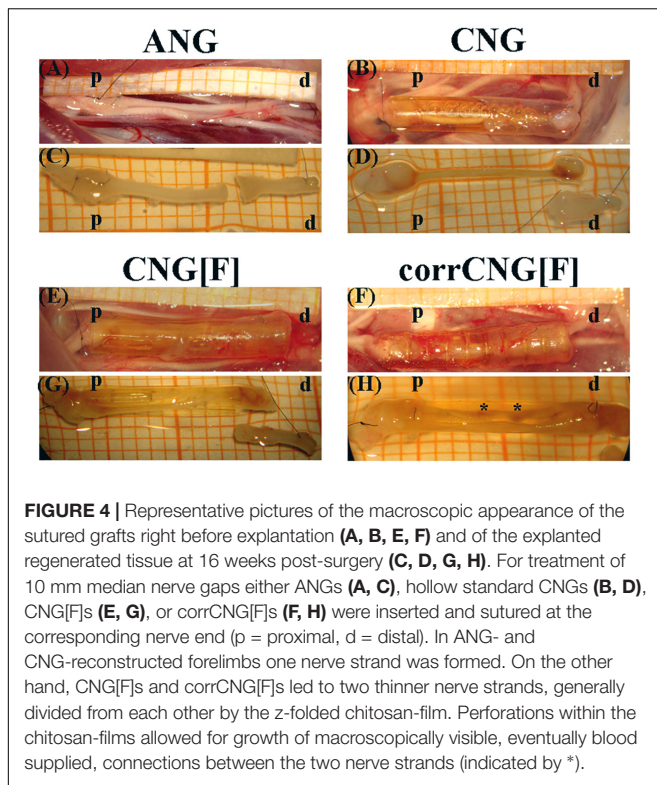


FIGURE 3 | Evocable CMAPs amplitude areas as evaluated during electrodiagnostic recordings from the thenar muscle over 16 weeks observation period. ANG-reconstructed forelimbs showed significant improvement after 12 weeks post-surgery and significantly higher amplitudes compared to the nerve guide groups. Among the artificial nerve guide groups, no significant increase could be detected after the 16-week observation period. CNG-reconstructed forelimbs, however, revealed a significantly lower amplitude area in comparison to ANG. The continuous horizontal line displays the pre-surgically recorded healthy nerve mean value ($n = 32$ forelimbs). Two-way ANOVA showed an effect of the parameters 12 vs. 4 and 8, as well as 16 vs. 4 and 8 weeks post-surgery [$F(3, 112) = 19.35, p < 0.0001$], groups [$F(3,112) = 18.54, p < 0.0001$], and the interaction between both parameters [$F(9,12) = 3.534, p = 0.0007$]. Tukey's multiple comparisons were applied to detect significant differences ($***p < 0.001$ vs. 4 weeks post-surgery within the same group; $#p < 0.05$, $###p < 0.001$ vs. 8 weeks post-surgery within the same group; $$$$p < 0.01$, $$$$p < 0.001$ vs. ANG). Values are given as median \pm range ($n = 8$). ANG, autologous nerve graft; CNG, chitosan nerve guide; CNG[F], chitosan-film enhanced chitosan nerve guide; corrCNG[F], corrugated chitosan-film enhanced chitosan nerve guide.

corrCNG[F]: 6/8, see also **Table 1**). There were no significant differences in the CMAP amplitude areas when comparing all groups (two-way ANOVA). While CMAP amplitude area in the ANG group was highest (1.085 ms * mV) it was smallest in the CNG[F] group (0.561 ms * mV). In comparison to the 4-week time point, medians only slightly increased within the next 4 weeks in all groups (ANG: 1.595 ms * mV, CNG: 1.208 ms * mV, CNG[F]: 0.826 ms * mV, corrCNG[F]: 1.111 ms * mV). At that time point, stimulation in only one forelimb each in the CNG as well as in the CNG[F] group did not result in a recordable

CMAP. In the ANG group, CMAP amplitude areas significantly increased at 12 weeks post-surgery (3.931 ms * mV) when compared to 4 and 8 weeks post-surgery ($p < 0.001$, two-way ANOVA). At this time point, ANG reconstructed forelimbs delivered significantly higher CMAP amplitude areas than the artificial nerve guide groups (CNG: 1.601 ms * mV, CNG[F]: 1.328 ms * mV, corrCNG[F]: 1.123 ms * mV) with none of the forelimbs remaining unresponsive to stimulation ($p < 0.001$, two-way ANOVA). Sixteen weeks after surgical intervention, CMAP amplitude areas of the CNG[F] and the corrCNG[F]



group further increased while CNG reconstructed forelimbs still performed significantly less compared to the ANG group ($p < 0.01$, two-way ANOVA).

Macroscopic Evaluation of the Regenerated Tissue Upon Explantation

To generate an overview of tissue regeneration between the proximal and the distal nerve end, ANGs as well as regrown tissue inside the diverse nerve guides were first surveyed macroscopically at 16 weeks post-surgery (**Figure 4**). Reconstruction of the nerves with ANGs and corrCNG[F]s resulted in full-distance regenerated tissue in all animals of the group. Two reconstructed median nerves of the CNG group revealed no connections between the nerve ends and in one graft only a very thin connection was detectable, which was too thin for paraffin embedding. For the latter sample the nerve distal to the graft was, however, processed for nerve morphometry (see the section “Quantification of blood vessel area in the distal chitosan nerve grafts”). Also, implantation of CNG[F]s led to one forelimb without any regenerated tissue.

While reconstruction with ANGs and CNGs, respectively, led to one thick connection between the proximal and distal nerve ends, reconstruction with either type of CNG[F]s or corrCNG[F] resulted in the formation of two thinner tissue cables, one on each side of the film, connecting the two nerve ends. At the level of chitosan-film perforations, tissue which grew through the perforations could be detected. These tissue bridges formed a connection between the two regenerated tissue cables.

Nerve Immunohistochemistry in the Distal Nerve Grafts – Quantification of Axon Profiles

For histological evaluation of the regenerated tissue within the nerve grafts, not all samples could be used. This was related to very thin or even missing connections between the proximal and distal nerve ends, so that no tissue could be processed for immunocytochemistry. Therefore, regenerated tissue from $n = 8$ ANG- and corrCNG[F]-treated forelimbs, $n = 5$ CNG-treated forelimbs, and $n = 7$ CNG[F]-treated forelimbs were incorporated into the evaluation. Cross-sections were prepared at the distal end of the ANG grafts and at 3.7 mm proximal to the distal suture site within the nerve grafts. These cross-sections were stained for HE to demonstrate the composition of the regenerated tissue (**Figures 5B,D,F**) and to analyze the area of blood vessel within the regenerated tissue inside the nerve guides (see the section “Nerve immunohistochemistry in the distal nerve grafts – quantification of axon profiles”).

Hematoxylin and Eosin-stained cross-sections show single strands of regenerated tissue in the ANG and CNG (**Figure 5B**) groups, while two strands, one at each side of the chitosan-film, were formed in the CNG[F] (**Figure 5D**) and corrCNG[F] (**Figure 5E**) groups. HE stained sections eventually also illustrated, that film-perforations contained regrown tissue as well (**Figure 5F**, indicated by arrow). Consecutive sections of those, that underwent HE staining, were stained for NF200 and counter-stained with DAPI. This enabled the immunodetection of regenerated axonal profiles in the distal nerve grafts. Representative photomicrographs (**Figures 5A,C,E**) show the presence of NF200-immunopositive axons within the regenerated tissue strands. In chitosan-film enhanced nerve guides, axonal profiles were detectable at both sides of the chitosan-film (**Figures 5C,D**, indicated by *), but eventually also in tissue bridges connecting the two nerve strands (**Figure 5C**, indicated by #). As ANGs and CNGs led to regeneration of thicker tissue cables, we further investigated if this was associated with a higher number of regrown axons within the distal graft in comparison to CNG[F]s and corrCNG[F]s. Therefore, quantification of NF200-immunopositive axonal profiles was performed (**Figure 6**). Median nerve reconstruction with ANGs revealed the highest number of NF200-immunopositive axonal profiles (3981 ± 393.9). Numbers of NF200-immunopositive axonal profiles were smaller in the distal CNGs (2139.1 ± 165.5), CNG[F]s (1993.4 ± 185.4), and corrCNG[F]s (2285.2 ± 425.2), but no significant differences could be detected between all groups (Kruskal–Wallis test). Among the bioartificial nerve guide groups, the highest number of NF200-immunopositive axonal profiles was detected in distal nerve graft samples from corrCNG[F] reconstructed forelimbs.

Quantification of Blood Vessel Area in the Distal Chitosan Nerve Grafts

In previous studies we have postulated that introducing the chitosan-films into the CNGs may increase the vascularization of the regenerated tissue (Stenberg et al., 2017; Stöbel et al., 2018b). To analyze this in some more detail, we quantified the

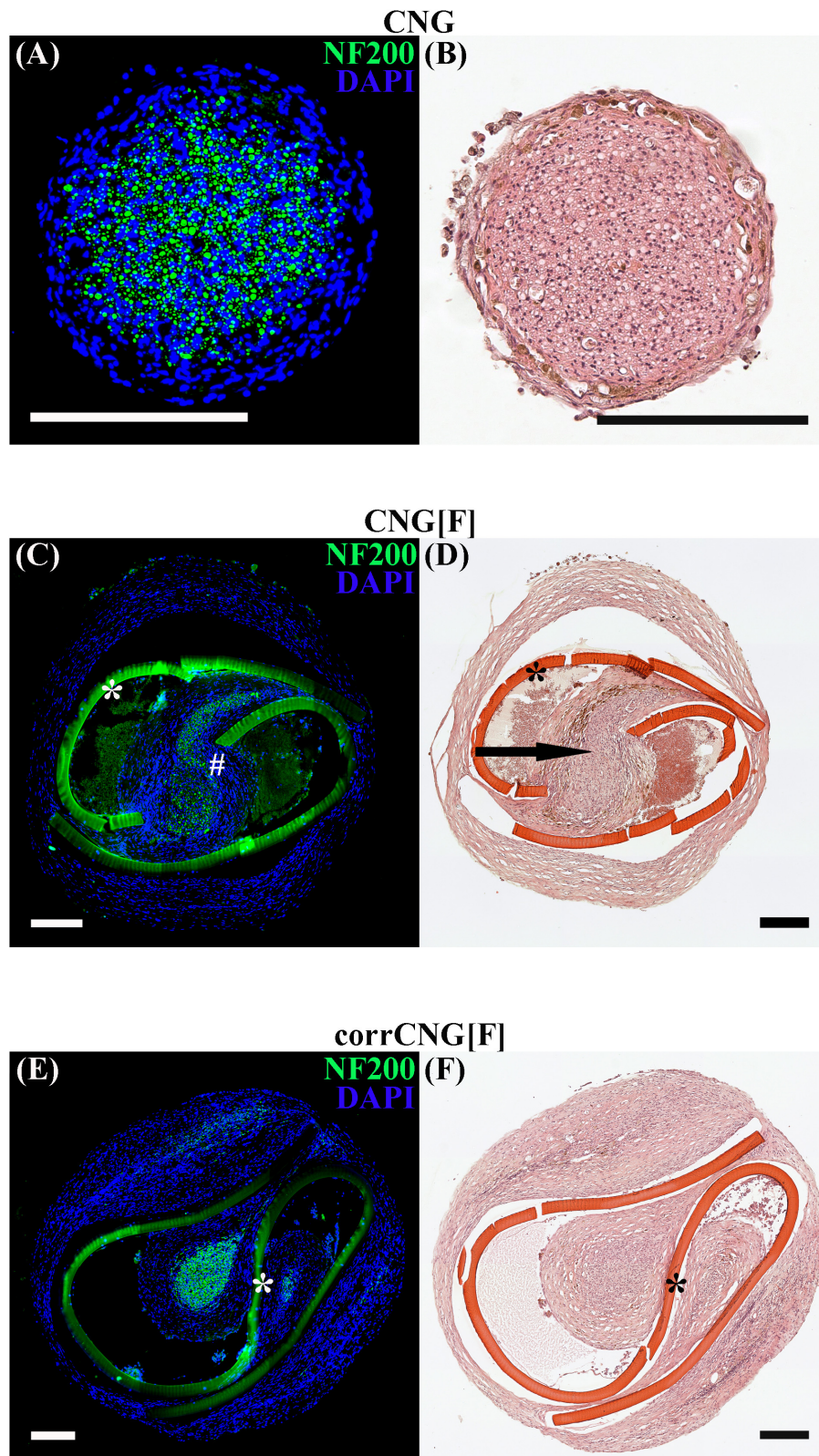


FIGURE 5 | Representative photomicrographs of consecutive cross-sections through the regenerated tissue within the distal nerve graft at 16 weeks post-surgery. Immunohistological staining (A, C, E) against NF200 (green) and DAPI nuclear counter staining (blue) display immunodetection of all regenerated axonal profiles.

(Continued)

FIGURE 5 | Continued

HE staining (**B, D, F**) displays an overview of the composition of the regenerated tissue. Thicker and single-strand tissue connections between proximal and distal nerve ends were found in the ANG and CNG groups. Axonal staining proved that on each side of the chitosan-film the regenerated tissue contained NF200-positive axons. Arrow is indicating the tissue bridge, which was formed inside the chitosan-film perforation and connected the two nerve cables (chitosan-film indicated by *, NF200-positive axonal profiles within the tissue bridge indicated by #). CNG, standard chitosan nerve guide; CNG[F], chitosan-film enhanced CNG; corrCNG[F], corrugated chitosan-film enhanced chitosan nerve guide.

mean area of clearly identifiable blood vessels in the HE sections obtained from the CNG groups ($n = 5$ CNG, $n = 7$ CNG[F], and $n = 8$ corrCNG[F]). As depicted in **Figure 7**, the evaluation of the mean blood vessel area did not reveal any significant differences between the experimental groups (Kruskal–Wallis test). The data point out, however, that larger mean blood vessel

areas (e.g., $>100 \mu\text{m}^2$) have a higher probability to be formed when CNGs contain a chitosan-film.

Nerve Histomorphometry Distal to the Nerve Grafts

For stereological and morphometrical assessment of regenerated myelinated axons, semi-thin cross-sections were prepared from distal nerve segments of reconstructed median nerves at 16 weeks post-surgery (**Figure 8**). Two samples of the CNG group with no evident regrown tissue detected during macroscopic inspection (see the section “Non-invasive electrodiagnostic recordings – evaluation of thenar muscle reinnervation”) were excluded from evaluation ($n = 6$). In the CNG[F] group also one sample was excluded due to lack of regeneration ($n = 7$).

Regarding the numbers of myelinated fibers (**Figure 9A**), axon diameters (**Figure 9B**), fiber diameters (**Figure 9C**), and myelin thicknesses (**Figure 9D**), samples resulting from ANG reconstructed forelimbs were superior over all bioartificial nerve guide groups tested. While no significant differences could be detected when comparing numbers of myelinated fibers of ANGs with CNGs and corrCNG[F]s, CNG[F]s revealed significantly lower numbers of myelinated fibers ($p < 0.05$, Kruskal–Wallis test). When looking at the axon diameters and fiber diameters, CNG(F)s and corrCNG[F]s showed significantly smaller diameters in both parameters when compared to the ANG group ($p < 0.05$ for axon diameter of CNG[F], corrCNG[F], and fiber diameter of corrCNG[F], $p < 0.01$ for fiber diameter of CNG[F], Kruskal–Wallis test). However, only CNG[F]s showed significantly thinner myelin sheaths when compared to ANGs ($p < 0.01$, Kruskal–Wallis test), whereas reconstruction with corrCNG[F]s revealed the thickest myelin sheaths among the nerve guide groups. Major variations or significant differences in g-ratio values (data not shown), however, were not detected among all groups (ANG: 0.67 ± 0.01 ; CNG: 0.68 ± 0.03 ; CNG[F]: 0.68 ± 0.02 ; corrCNG[F]: 0.66 ± 0.01).

DISCUSSION

In connection with peripheral nerve injuries the application of ANGs still represents the gold standard (Daly et al., 2012). As this method goes along with various downsides (Siemionow et al., 2010; Hallgren et al., 2013; Kuffler, 2014), researchers still try to substitute or replace the use of ANGs by alternative bioartificial nerve guide-based treatment strategies (Gu et al., 2014; Faroni et al., 2015).

For studying the properties of novel bioartificial nerve grafts, nerve transection models are commonly used. Complete nerve transection injuries are characterized by structural changes,

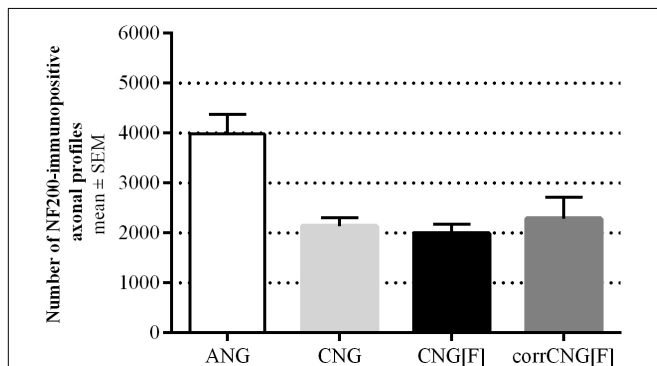


FIGURE 6 | Quantification of NF200-immunopositive axonal profiles at midgraft-level at 16 weeks post-surgery. ANG reconstructions revealed the highest numbers of NF200-positive axonal profiles among all tested implants. CorrCNG[F]s showed slightly increased numbers of immunopositive axonal profiles, when compared to the other artificial nerve guides tested. Kruskal–Wallis test [$H(3, N = 28) = 7.74, p = 0.0517$] followed by Dunn’s multiple comparisons were applied. No significant differences were detected. Values are given as mean \pm SEM. ANG, autologous nerve graft; corrCNG[F], corrugated chitosan-film enhanced chitosan nerve guide; $n = 8$; CNG, chitosan nerve guide; $n = 5$; CNG[F], chitosan-film enhanced chitosan nerve guide; $n = 7$.

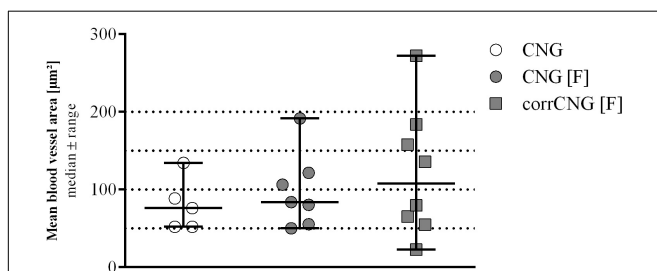


FIGURE 7 | Quantitative results of the mean blood vessel area within the distal nerve graft at 16 weeks post-surgery. No significant differences could be detected among the experimental groups. Kruskal–Wallis test [$H(2, N = 20) = 0.929, p = 0.6456$] followed by Dunn’s multiple comparisons were applied to detect significant differences. Values are given as median \pm range. CNG, chitosan nerve guide; $n = 5$; CNG[F], chitosan-film enhanced chitosan nerve guide; $n = 7$; corrCNG[F], corrugated chitosan-film enhanced chitosan nerve guide; $n = 8$.

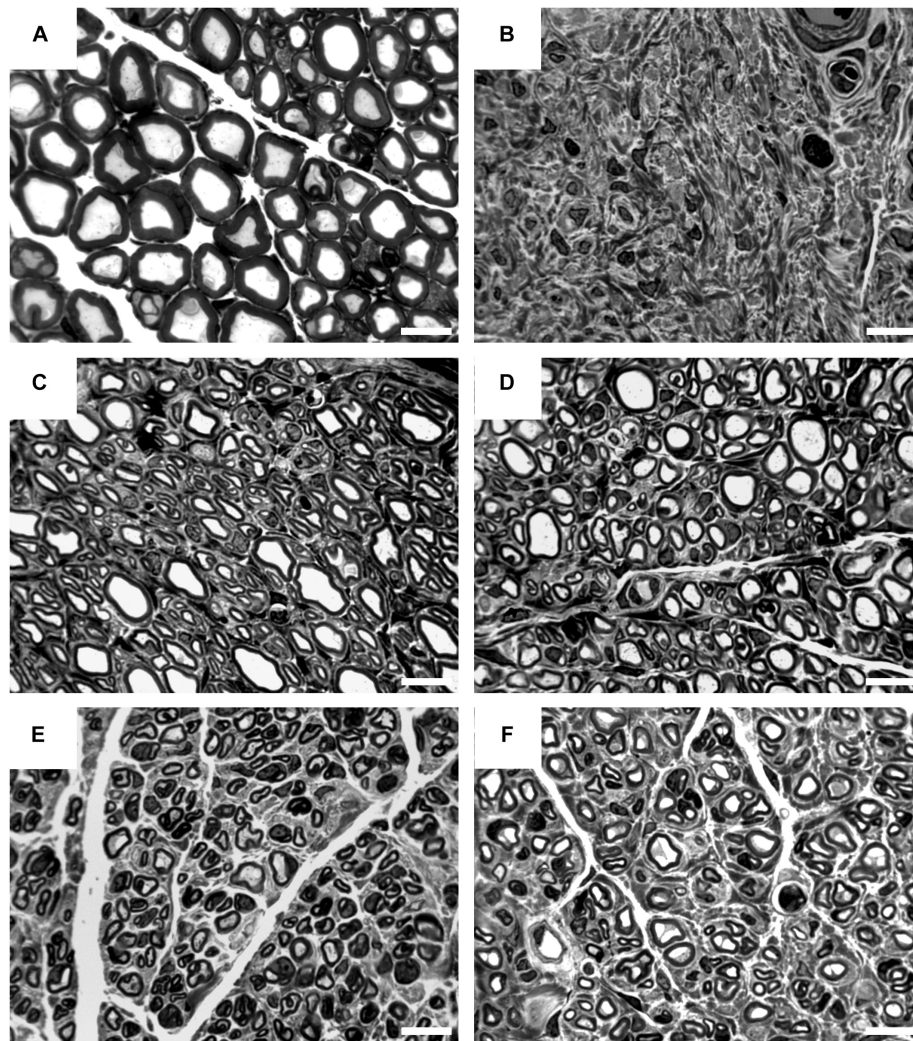


FIGURE 8 | Representative pictures of toluidine blue-stained semi-thin cross-sections of distal nerve segments at 16 weeks post-surgery. Images show healthy nerve segments (A) serving as control compared to distal nerve segments of reconstructed median nerves (B–F). (B) Example of no axonal regeneration from the CNG[F] group. Examples of regenerated nerve samples from the ANG group (C), CNG group (D), CNG[F] group (E), and corrCNG[F] group (F). White scale bars display 10 μ m.

including axonal and myelin breakdown (Deumens et al., 2010). As such the model has distinct differences to other peripheral nerve injury models, e.g., loose ligation models of the rat sciatic nerve. Nerve ligation models are studied in the context of the development of neuropathic pain in which early events at the lesion sites are characterized by edema and inflammatory infiltration (e.g., Pacini et al., 2010; Di Cesare Mannelli et al., 2016). One leading event after nerve transection injury, besides axonal and myelin breakdown, is also recruitment of macrophages that help in myelin clearance during Wallerian degeneration over 3–6 weeks after the injury (Gaudet et al., 2011; Faroni et al., 2015; Jessen and Mirsky, 2016). Since morphological changes after median nerve transection injury have been described elsewhere before (e.g., Ronchi et al., 2016), we were not focusing on these events in the current study. Here, besides thorough functional analyses, we focused on

end-point histological analysis of the regenerated nerve tissue after 16 weeks post-surgery. At this late time point, edema or continued inflammatory infiltrations would only be expected in case of immune responses against the artificial nerve grafts or their degradation products. This was, however, never detected in other studies evaluating chitosan-based nerve guides before (e.g., Haastert-Talini et al., 2013; Stöbel et al., 2018a,b). We further did not study effects of any complementary treatment to protect peripheral nerve arrangement and to prevent development of neuropathic pain, like, e.g., daily oral administration of rosemary extracts (Pacini et al., 2010; Di Cesare Mannelli et al., 2016), because the rat median nerve transection and repair model has not been reported before to induce neuropathic pain.

In this study we compared ANGs and three different types of chitosan-based nerve guide grafts with regard to their support for peripheral nerve regeneration after acute repair of 10 mm median

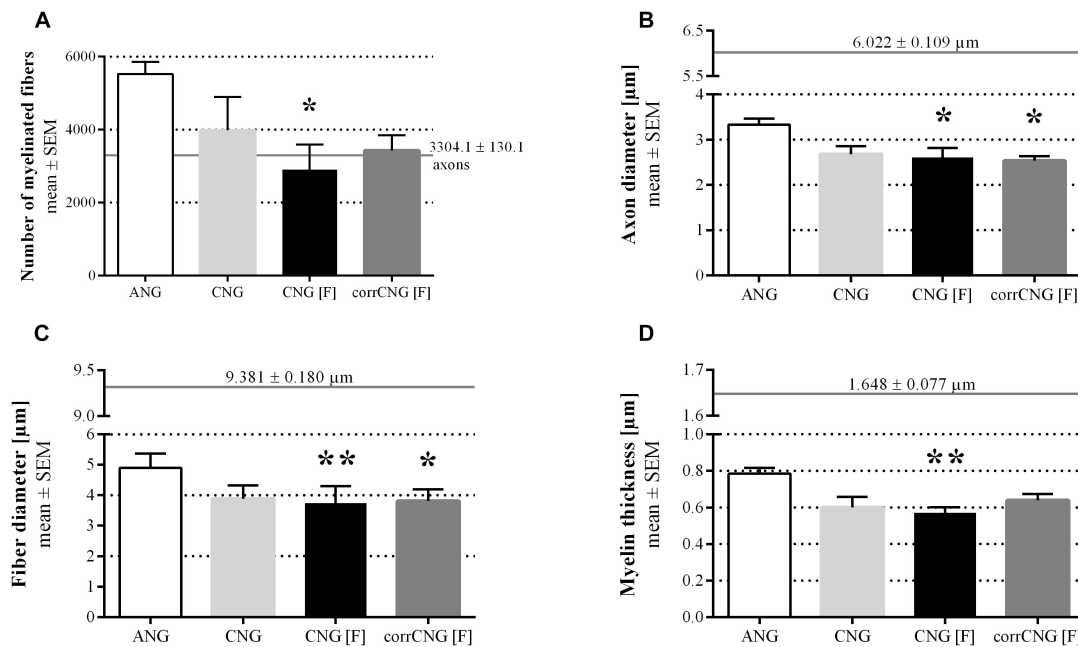


FIGURE 9 | Quantitative results of the nerve morphometrical analyses of distal nerve segments of reconstructed median nerves at 16 weeks post-surgery. Bar graphs are representing the total numbers of myelinated fibers **(A)**, axon diameters **(B)**, fiber diameters **(C)**, and myelin thicknesses **(D)**. Samples from ANG-reconstructed forelimbs were superior to the artificial nerve guides concerning all tested parameters. Only single events of statistically significant differences could be detected. CNG[F]s and corrCNG[F]s led to significantly lower axon diameters when compared to the ANG group. Additionally, CNG[F]s led to significantly thinner nerve fibers and myelin sheaths when compared to samples from ANG-reconstructed forelimbs. Horizontal continuous lines display healthy nerve mean values ($n = 6$). Kruskal–Wallis test [(A) $H(3, N = 29) = 10.19$; (B) $H(3, N = 29) = 11.24$; (C) $H(3, N = 29) = 15.03$; (D) $H(3, N = 29) = 12.34$] with Dunn's multiple comparisons were applied to detect significant differences (* $p < 0.05$, ** $p < 0.01$ vs. ANG at the same time point). Values are given as mean \pm SEM. ANG, autologous nerve graft; corrCNG[F], corrugated chitosan-film enhanced chitosan nerve guide; $n = 8$; CNG, chitosan nerve guide; $n = 6$; CNG[F], chitosan-film enhanced chitosan nerve guide; $n = 7$.

nerve defects. The nerve guides evaluated consisted of standard hollow CNGs (Haastert-Talini et al., 2013), CNG[F]s (Meyer et al., 2016a), or corrCNG[F]s. The corrugated structure of the outer wall of hollow CNGs is thought to make them most suitable for bridging peripheral nerve gaps in highly mobile locations (Stöbel et al., 2018b). Highly mobile locations are for example human digits, in which digital nerves, originating from the median nerve, are even traveling across joints. Previous studies have demonstrated that by inserting a z-folded chitosan-film and creating a two-chambered chitosan nerve guide (CNG[F]), the support of functional recovery after immediate and delayed critical defect length rat sciatic nerve repair could even be increased in comparison to standard CNGs (Meyer et al., 2016a; Stenberg et al., 2017). Consequently, in this current study, we have evaluated corrCNG[F]s for their regeneration supporting properties in the rat median nerve model. We suppose the rat median nerve model to be more translational than the classic rat sciatic nerve model (Stöbel et al., 2018b) with regard to the repair of human digital nerve injuries, which are displaying the majority of clinically relevant peripheral nerve injuries (McAllister et al., 1996; Renner et al., 2004).

Clinically most important for patients suffering from peripheral nerve injury is the recovery of fine and gross motor function (Fugleholm et al., 2000; Valero-Cabre et al., 2001), which can still not be guaranteed even after nerve reconstruction

with the use of ANGs (Deumens et al., 2010; Isaacs, 2010). The median nerve model used in the current study allows to define rather precisely the onset of different level motor functional recovery and to evaluate the final recovery level of the different motor functions (Stöbel et al., 2017). For a good comparison of results and like in many other studies in the field and in accordance to our previous work (Stöbel et al., 2017) we used female young adult rats (15 weeks at beginning of adaptation to test conditions) in the current study.

Our results demonstrate that median nerve reconstruction in the rat with corrCNG[F]s achieved functional results comparable to the results obtained after reconstruction with ANGs. Even though the functional recovery was fastest and most complete (100% recovery rate) in the ANG group already 8 weeks post-surgery, corrCNG[F]s significantly accelerated the recovery of fine and gross motor functions when compared to CNGs and CNG[F]s. Final recovery levels for skilled forelimb reaching ability were even significantly superior in the corrCNG[F] group when compared to the two other nerve guide groups evaluated.

While this overall conclusion could easily be drawn from the results presented, this discussion will focus on a more detailed analysis of the evaluation methods used and the particular results they provided.

The reflex-based grasping test, which is used to analyze the recovery of gross motor function (Tupper and Wallace, 1980),

was performed every second week in the current study. This is the simplest test in our test battery and certainly the less stress-full for the animals, because it does not require any specific preparation and is performed with the awaken animal. Therefore, in our preceding study (Stöbel et al., 2017), the grasping test was performed weekly and was found to thereby discover rather precisely the onset of reflex-based gross motor functional recovery. But the weekly testing procedure also resulted in a reduced motivation of the animals to participate in the test (Stöbel et al., 2017). This observation has also been described before (Bertelli and Mira, 1995), and therefore, to keep motivation to participate, we decided to perform the test only every second week in the current study. Still we were facing minor undulation in the recovery rate of gross motor function (ANG group between 8 and 10 weeks post-surgery; and either nerve guide groups between 14 and 16 weeks post-surgery), but were also able to detect differences in the recovery time and recovery rates among the groups. The grasping test confirmed that ANG reconstruction was most supportive for recovery of gross motor function, since exclusively the ANG group showed a 100% recovery rate in this test. Comparing the total best results among the nerve guide groups, use of corrCNG[F]s for reconstruction led to the highest percentage of forelimbs (87.5%) being able to apply a certain force to the bar (Category 3), which is the most complete ability to be recovered (Stöbel et al., 2017). Notably, superiority of the corrCNG[F] grafts over the other nerve guides is also indicated by the observation, that none of the corrCNG[F] reconstructed forelimbs remained without ability of finger flexion (Category 2) in contrast to the CNG group (two animals without finger flexion) and the CNG[F] group (one animal without finger flexion).

The staircase test was performed for comprehensive evaluation of recovery of fine motor skills (Montoya et al., 1991). The test requires a preparatory period of restrictive feeding and can therefore only be applied on a monthly basis. The power of this test is again highly affected by the motivation of the animals to participate (Nikkhah et al., 1998; Galtrey and Fawcett, 2007). While in our previous study only 1 out of 16 animals demonstrated un-willingness to participate already during the pre-surgical habituation and training period (Stöbel et al., 2017), in the current study, three animals were not at all sufficiently participating and two additional animals were only participating with their right forelimb. This situation was reducing the power of the test since it reduced the evaluated group size from initially eight to only six animals. Lewis rats had been described before to probably display less motivation to participate, but to also provide a potentially reduced learning ability (Nikkhah et al., 1998; Galtrey and Fawcett, 2007). On the other hand, some of the remaining animals in all evaluated groups achieved success rates highly above their pre-surgical values during the recovery period. Thus, this displays an ongoing process of learning after pre-surgical training and during the post-surgical observation period (Stöbel et al., 2017). Although there is certainly more to consider when applying the staircase test paradigm for median nerve injury and repair studies, we again found it useful in depicting another type of motor functional recovery than the grasping test and in elucidating

differences among our evaluated groups. Complete recovery of fine motor skills (100% recovery rate) was achieved in the ANG as well as by the corrCNG[F] group, while not all forelimbs of the CNG and CNG[F] groups achieved pre-surgical performance levels and some of them did not recover skilled forelimb reaching abilities at all.

When assembling the overall motor abilities recovered as assessed by us in the advanced rat median nerve model, one could even detect some striking results in single animals that need a more reflected view on the underlying axonal regeneration. One of the ANG-reconstructed forelimbs successfully participated in the staircase test already 4 weeks post-surgery (retrieving more than three pellets), while demonstrating no finger flexion in the grasping test at the same time. The same phenomenon also occurred in one animal of the CNG[F] group at 8 weeks post-surgery. Looking at these results one should assume that axons were correctly directed to the target muscles, since fine motor skills require accurate reinnervation (Galtrey and Fawcett, 2007). Furthermore, successful pellet retrieval requires the ability for finger flexion, resulting in the assumption that the absence of finger flexion in the grasping test may be again explained by a lack of motivation of the animals (Nikkhah et al., 1998; Galtrey and Fawcett, 2007). This observation can obviously not be related to the nerve graft applied for reconstruction and has therefore negatively biased the results from the grasping test. One should also consider that even a certain number of misdirected axons would lead to the ability for reflexed-based gross motor grasping function, because for this the amount of reinnervating axons is more important than the accuracy of reinnervation (Galtrey and Fawcett, 2007).

The previous considerations lead over to the discussion of the electrodiagnostic measurements applied in the current study. Similar to the staircase test, these measurements were performed on a monthly basis, because we have been experiencing low tolerability of repetitive anesthesia in a previous study (Korte et al., 2011). Also, the obtainable data by recording and analyzing evocable CMAP amplitude areas are providing a quantitative estimation on the degree of motor reinnervation, but no indication on its consequences on forelimb usage abilities. In our previous study we demonstrated that electrodiagnostic recordings from the thenar muscles are a valuable tool to elucidate the early onset of motor axon regeneration, which is somehow predictive for the time period needed until motor skills will also start to return (Stöbel et al., 2017). We had a similar observation in the current study. At 4 weeks post-surgery, evoked CMAPs were recordable in 100% of ANG and CNG reconstructed forelimbs when still no finger flexion was detected with the grasping test and only one ANG-forelimb and none CNG-forelimb successfully participated in the staircase test. The same findings could be detected in the two other groups where the majority of the reconstructed nerves (CNG[F]: 62.5%; corrCNG[F]: 75.0%) transmitted evocable CMAPs to the thenar muscles, but none of the forelimbs achieved Category 2 (ability for finger flexion) in the grasping test or successfully participated in the staircase test. Occurrence of 100% of reconstructed forelimbs showing evocable thenar muscle CMAPs revealed a timeline among the groups with the ANG-group and CNG-group

being the first (4 weeks post-surgery), the corrCNG[F] group the second (8 weeks post-surgery), and the CNG[F] group followed 12 weeks post-surgery.

Electrodiagnostic recordings provide a twofold estimation of functional recovery. First, the pure evidence of muscle reinnervation as detected by recording of evoked CMAPs, and second, the estimation of the quality of reinnervation as it can be retrieved from analyzing the CMAP amplitude area. The CMAP amplitude area correlates with the number of functioning axons (Cuddon, 2002). Although, in the current study, the CNG group showed the earliest onset of motor reinnervation among the bioartificial nerve guide groups, the CMAP amplitude area was still significantly smaller after 16 weeks post-surgery when compared to the ANG group, which achieved the overall highest median amplitude area among all nerve grafts tested. At this time point median CMAP amplitude areas were not anymore significantly different to the ANG values in the CNG[F] and corrCNG[F] groups.

Extrapolating these results now to usage abilities and evidently recovered motor skills is, however, also not fully possible. Although the median CMAP amplitude area recorded in the CNG[F]s ranged slightly above that one recorded from the corrCNG[F] reconstructed forelimbs, motor skills returned to a higher rate in the second group. This indicates again that CMAP amplitude recovery is not necessarily accompanied by precise regeneration of all motor axons (Archibald et al., 1991; Fugleholm et al., 2000; Valero-Cabre et al., 2001; Navarro and Udina, 2009; Pfister et al., 2011). Additionally, it demonstrates that also stimulation of finally misdirected axons contributes to the value of CMAP amplitude areas and these axons do not compulsorily lead to regeneration of especially fine motor skills (Galtrey and Fawcett, 2007).

Those electrodiagnostic measurements, as performed in our current study, should only be one tool to evaluate functional recovery of the rat median nerve, as must also be concluded from the macroscopic inspection of the nerve grafts upon explantation and the subsequent histomorphometrical analysis. The latter is also irreplaceable for a comprehensive evaluation of nerve repair approaches.

Upon explantation of the nerve grafts, we could macroscopically detect visible tissue connections between the proximal and the distal nerve end in all ANG and corrCNG[F] grafts, while surprisingly two nerve guides from the CNG group and one from the CNG[F] group did not contain sufficient amount of tissue. Although during establishment of the advanced median nerve model we did not find evidences that false positive recordings could occur from electrodiagnostic measurements (Stöbel et al., 2017), we need to reconsider this possibility. In the current study, all forelimbs of the CNG and the CNG[F] group presented with evocable CMAPs in electrodiagnostic evaluation. Analysis of CMAP amplitude areas could again be judged to be of major value, since we at least detected that the false positive CMAPs displayed an area below the group median and histomorphometric analysis of distal nerve segments did not detect regrown axons.

Histomorphometrical analysis finally serves not only to reveal more quantitative data indicative also for the quality of

axonal regeneration, but could also provide insight into tissue compositions related to good functional recovery.

As observed in previous studies (Meyer et al., 2016a; Stenberg et al., 2017), tissue regeneration through CNG[F]s results in growth of two nerve strands separated by the chitosan-film. As we have shown previously and here again, these nerve strands are eventually connected via tissue bridges that have formed within the perforations in the film. In the current study we were even able to detect NF200-immunopositive axons inside these tissue bridges.

Quantification of the number of NF200-immunopositive axonal profiles within the distal grafts revealed no significant differences within the groups, although the highest mean value was detected in the ANG group and the corrCNG[F] group showed slightly higher values than the two other nerve guide groups. These findings already correlate to our results from the motor skills analyses. We have previously postulated that chitosan-film enhanced nerve guides would attract a higher degree of neovascularization and that this may directly correlate to better functional outcome (Meyer et al., 2016a; Stenberg et al., 2017). Early revascularization is an important factor for successful regeneration as it is supposed to prevent apoptosis of Schwann cells, fibrosis, and failure of regeneration (Penkert et al., 1988). In addition, blood-derived macrophages are known to support peripheral nerve regeneration by producing growth factors and adhesion molecules (Fansa et al., 2001; Haastert-Talini et al., 2013; Mokarram et al., 2017; Stenberg et al., 2017). In the current study we determined the median blood vessel area in the distal nerve guides in order to elucidate potential differences in neovascularization among the different nerve guide types. And indeed, although not significant again, in the corrCNG[F] group, with the best functional outcome among the nerve guide groups, we found in 50% of the samples mean blood vessel areas above the group mean, while in the CNG[F] group and CNG group these are only 43 and 40%, respectively.

It is noteworthy that immunohistological evaluation of the number of NF200-immunopositive axonal profiles in the distal grafts resulted in reduced numbers of detected axons in comparison to the histomorphometrical analysis performed distal to the grafts. Among all investigated groups, more regenerated and myelinated nerve fibers were detected in the nerve specimen distal to the grafts than within the grafts. This could be found to be in contradiction to the assumption that not all nerve fibers that sprout proximally should reach their distal target and that the number of detectable axons will therefore get smaller at more distal locations. One should, however, consider that immunohistological staining and quantification in fluorescence microscopy may miss a certain amount especially of small regenerated axons, due to thresholds that have to be set manually. Therefore, a more reliable axon count will always result from nerve morphometrical analysis.

Nerve morphometry finally performed in specimen harvested distal to the grafts revealed that less axons regenerated in the nerve guide groups than in the ANG group, with CNG[F] samples showing significantly less axons. As shown before (Sinis et al., 2005; Haastert-Talini et al., 2013; Ronchi et al., 2017; Stöbel et al., 2017), ANG reconstruction results in higher numbers of

myelinated fibers in comparison to the artificial nerve guides and even compared to the healthy nerve. Healthy nerve values for numbers of myelinated fibers were exceeded by the ANG, CNG, and corrCNG[F] group, a phenomenon that has been described before in different models (Meyer et al., 2016a; Stenberg et al., 2017; Stöbel et al., 2017). Probably the second most indicative nerve morphometrical parameter for functional recovery, which has been analyzed in the current study, is the myelin thickness. The myelin thickness determines the nerve conduction velocity (Valero-Cabre and Navarro, 2002; Korte et al., 2011) and could therefore have a direct impact on fine motor reaching skills. Axons from CNG[F] group samples displayed significantly thinner myelin sheaths than those from the ANG group, while the other nerve guide groups showed no significant differences. Samples from the corrCNG[F] group displayed slightly thicker myelin sheaths of their axons among the bioartificial nerve graft groups. These findings underline that corrCNG[F] supported functional regeneration of the reconstructed median nerve to a higher extend than the other CNGs evaluated.

In conclusion, we demonstrated that the use of corrCNG[F]s represents a promising approach for reconstruction of small nerves in a mobile extremity location. The results of the current study are translational for the repair of digital nerves in humans since different nerve guides were comprehensively tested against the gold standard ANG and the clinically approved classic hollow CNG.

ETHICS STATEMENT

This study was conducted in accordance with the German animal protection law and with the European Communities Council Directive 2010/63/EU for the protection of animals used for experimental purposes. All experiments were approved by the Local Institutional Animal Care and Research Advisory

Committee and permitted by the local authority (Lower Saxony State Office for Consumer Protection, Food Safety, and Animal Welfare Service, 33.12-42502-04-15/1761).

AUTHOR CONTRIBUTIONS

KH-T and TF contributed conception and design of the study. MF and KH-T conducted the experiments. OH produced the CNGs. MF and ND evaluated the functional recovery. MF organized the respective data presentation and performed the statistical data analysis. ND and JL performed the histomorphometrical evaluation, organized the respective data presentation, and performed the statistical data analysis. ND, MF, and KH-T wrote the first draft of the manuscript. All authors contributed to manuscript revision, read, and approved the submitted version.

FUNDING

Financial support was provided (1) by the Federal Ministry for Economic Affairs and Energy based on a decision by the German Bundestag, ZiM-AiF project EPINUR to KH-T (KF3188602SB3) and TF (KF2192804SB3); (2) For finalizing the histomorphometrical analyses, ND was provided with a 3-Months Scholarship by the Internationale Stiftung Neurobionik Hannover.

ACKNOWLEDGMENTS

For their excellent technical assistance, we thank Jennifer Metzen, Silke Fischer, and Natascha Heidrich from the Institute of Neuroanatomy and Cell Biology.

REFERENCES

- Angius, D., Wang, H., Spinner, R. J., Gutierrez-Cotto, Y., Yaszemski, M. J., and Windebank, A. J. (2012). A systematic review of animal models used to study nerve regeneration in tissue-engineered scaffolds. *Biomaterials* 33, 8034–8039. doi: 10.1016/j.biomaterials.2012.07.056
- Archibald, S. J., Krarup, C., Shefner, J., Li, S. T., and Madison, R. D. (1991). A collagen-based nerve guide conduit for peripheral nerve repair: an electrophysiological study of nerve regeneration in rodents and nonhuman primates. *J. Comp. Neurol.* 306, 685–696.
- Asplund, M., Nilsson, M., Jacobsson, A., and von Holst, H. (2009). Incidence of traumatic peripheral nerve injuries and amputations in Sweden between 1998 and 2006. *Neuroepidemiology* 32, 217–228. doi: 10.1159/000197900
- Bertelli, J. A., and Mira, J. C. (1995). The grasping test: a simple behavioral method for objective quantitative assessment of peripheral nerve regeneration in the rat. *J. Neurosci. Methods* 58, 151–155.
- Cuddon, P. A. (2002). Electrophysiology in neuromuscular disease. *Vet. Clin. North Am. Small Anim. Pract.* 32, 31–62.
- Daly, W., Yao, L., Zeugolis, D., Windebank, A., and Pandit, A. (2012). A biomaterials approach to peripheral nerve regeneration: bridging the peripheral nerve gap and enhancing functional recovery. *J. R. Soc. Interface* 9, 202–221. doi: 10.1098/rsif.2011.0438
- Deumens, R., Bozkurt, A., Meek, M. F., Marcus, M. A., Joosten, E. A., Weis, J., et al. (2010). Repairing injured peripheral nerves: bridging the gap. *Prog. Neurobiol.* 92, 245–276. doi: 10.1016/j.pneurobio.2010.10.002
- Di Cesare Mannelli, L., Micheli, L., Maresca, M., Cravotto, G., Bellumori, M., Innocenti, M., et al. (2016). Anti-neuropathic effects of *Rosmarinus officinalis* L. terpenoid fraction: relevance of nicotinic receptors. *Sci. Rep.* 6:34832. doi: 10.1038/srep34832
- Fansa, H., Keilhoff, G., Wolf, G., Schneider, W., and Gold, B. G. (2001). Tissue engineering of peripheral nerves: a comparison of venous and acellular muscle grafts with cultured schwann cells. *Plast. Reconstr. Surg.* 107, 495–496.
- Faroni, A., Mobasser, S. A., Kingham, P. J., and Reid, A. J. (2015). Peripheral nerve regeneration: experimental strategies and future perspectives. *Adv. Drug Deliv. Rev.* 8, 160–167. doi: 10.1016/j.addr.2014.11.010
- Fugleholm, K., Schmalbruch, H., and Krarup, C. (2000). Post reinnervation maturation of myelinated nerve fibers in the cat tibial nerve: chronic electrophysiological and morphometric studies. *J. Peripher. Nerv. Syst.* 5, 82–95.
- Galtrey, C. M., and Fawcett, G. J. W. (2007). Characterization of tests of functional recovery after median and ulnar nerve injury and repair in the rat forelimb. *J. Peripher. Nerv. Syst.* 12, 11–27. doi: 10.1111/j.1529-8027.2007.00113.x
- Gaudet, A. D., Popovich, P. G., and Ramer, M. S. (2011). Wallerian degeneration: gaining perspective on inflammatory events after peripheral nerve injury. *J. Neuroinflammation* 8:110. doi: 10.1186/1742-2094-8-110

- Geuna, S. (2000). Appreciating the difference between design-based and model-based sampling strategies in quantitative morphology of the nervous system. *J. Comp. Neurol.* 427, 333–339.
- Geuna, S. (2015). The sciatic nerve injury model in pre-clinical research. *J. Neurosci. Methods* 243, 39–46. doi: 10.1016/j.jneumeth.2015.01.021
- Gonzalez-Perez, F., Cobiánchi, S., Geuna, S., Barwig, C., Freier, T., Udina, E., et al. (2015). Tubulization with chitosan guides for the repair of long gap peripheral nerve injury in the rat. *Microsurgery* 35, 300–308. doi: 10.1002/micr.22362
- Grinsell, D., and Keating, C. P. (2014). Peripheral nerve reconstruction after injury: a review of clinical and experimental therapies. *Biomed. Res. Int.* 2014:698256. doi: 10.1155/2014/698256
- Gu, X., Ding, F., and Williams, D. F. (2014). Neural tissue engineering options for peripheral nerve regeneration. *Biomaterials* 35, 6143–6156. doi: 10.1016/j.biomaterials.2014.04.064
- Haastert-Talini, K., Geuna, S., Dahlin, L. B., Meyer, C., Stenberg, L., Freier, T., et al. (2013). Chitosan tubes of varying degrees of acetylation for bridging peripheral nerve defects. *Biomaterials* 34, 9886–9904. doi: 10.1016/j.biomaterials.2013.08.074
- Hallgren, A., Bjorkman, A., Chemnitz, A., and Dahlin, L. B. (2013). Subjective outcome related to donor site morbidity after sural nerve graft harvesting: a survey in 41 patients. *BMC Surg.* 13:39. doi: 10.1186/1471-2482-13-39
- Isaacs, J. (2010). Treatment of acute peripheral nerve injuries: current concepts. *J. Hand Sur. Am.* 35a, 491–497. doi: 10.1016/j.jhsa.2009.12.009
- Jessen, K. R., and Mirsky, R. (2016). The repair Schwann cell and its function in regenerating nerves. *J. Physiol.* 594, 3521–3531. doi: 10.1113/JP270874
- Korte, N., Schenk, H. C., Grothe, C., Tipold, A., and Haastert-Talini, K. (2011). Evaluation of periodic electrodiagnostic measurements to monitor motor recovery after different peripheral nerve lesions in the rat. *Muscle Nerve* 44, 63–73. doi: 10.1002/mus.22023
- Kouyoumdjian, J. A. (2006). Peripheral nerve injuries: a retrospective survey of 456 cases. *Muscle Nerve* 34, 785–788. doi: 10.1002/mus.20624
- Kuffler, D. P. (2014). An assessment of current techniques for inducing axon regeneration and neurological recovery following peripheral nerve trauma. *Prog. Neurobiol.* 116, 1–12. doi: 10.1016/j.pneurobio.2013.12.004
- McAllister, R. M., Gilbert, S. E., Calder, J. S., and Smith, P. J. (1996). The epidemiology and management of upper limb peripheral nerve injuries in modern practice. *J. Hand Surg. Br.* 21, 4–13.
- Meyer, C., Stenberg, L., Gonzalez-Perez, F., Wrobel, S., Ronchi, G., Udina, E., et al. (2016a). Chitosan-film enhanced chitosan nerve guides for long-distance regeneration of peripheral nerves. *Biomaterials* 76, 33–51. doi: 10.1016/j.biomaterials.2015.10.040
- Meyer, C., Wrobel, S., Raimondo, S., Rochkind, S., Heimann, C., Shahar, A., et al. (2016b). Peripheral nerve regeneration through hydrogel-enriched chitosan conduits containing engineered schwann cells for drug delivery. *Cell Transp.* 25, 159–182. doi: 10.3727/096368915X688010
- Mokarram, N., Dymanus, K., Srinivasan, A., Lyon, J. G., Tipton, J., Chu, J., et al. (2017). Immunoengineering nerve repair. *Proc. Natl. Acad. Sci. U.S.A.* 114, E5077–E5084. doi: 10.1073/pnas.1705757114
- Montoya, C. P., Campbell-Hope, L. J., Pemberton, K. D., and Dunnett, S. B. (1991). The "staircase test": a measure of independent forelimb reaching and grasping abilities in rats. *J. Neurosci. Methods* 36, 219–228.
- Navarro, X., and Udina, E. (2009). Chapter 6: methods and protocols in peripheral nerve regeneration experimental research: part III-electrophysiological evaluation. *Int. Rev. Neurobiol.* 87, 105–126. doi: 10.1016/S0074-7742(09)87006-2
- Nikkhah, G., Rosenthal, C., Hedrich, H. J., and Samii, M. (1998). Differences in acquisition and full performance in skilled forelimb use as measured by the 'staircase test' in five rat strains. *Behav. Brain Res.* 92, 85–95.
- Noble, J., Munro, C. A., Prasad, V. S., and Midha, R. (1998). Analysis of upper and lower extremity peripheral nerve injuries in a population of patients with multiple injuries. *J. Trauma* 45, 116–122.
- Pacini, A., Di Cesare Mannelli, L., Bonaccini, L., Ronzoni, S., Bartolini, A., and Ghelardini, C. (2010). Protective effect of alpha7 nAChR: behavioural and morphological features on neuropathy. *Pain* 150, 542–549. doi: 10.1016/j.pain.2010.06.014
- Penkert, G., Bini, W., and Samii, M. (1988). Revascularization of nerve grafts: an experimental study. *J. Reconstr. Microsurg.* 4, 319–325.
- Pfister, B. J., Gordon, T., Loverde, J. R., Kochar, A. S., Mackinnon, S. E., and Cullen, D. K. (2011). Biomedical engineering strategies for peripheral nerve repair: surgical applications, state of the art, and future challenges. *Crit. Rev. Biomed. Eng.* 39, 81–124.
- Renner, A., Cserkúti, F., and Hankiss, J. (2004). [Late results after nerve transplantation on the upper extremities]. *Handchir. Mikrochir. Plast. Chir.* 36, 13–18.
- Ronchi, G., Cillino, M., Gambarotta, G., Fornasari, B. E., Raimondo, S., Pugliese, P., et al. (2017). Irreversible changes occurring in long-term denervated Schwann cells affect delayed nerve repair. *J. Neurosurg.* 127, 843–856. doi: 10.3171/2016.9.JNS16140
- Ronchi, G., Haastert-Talini, K., Fornasari, B. E., Perroteau, I., Geuna, S., and Gambarotta, G. (2016). The Neuregulin1/ErbB system is selectively regulated during peripheral nerve degeneration and regeneration. *Eur. J. Neurosci.* 43, 351–364. doi: 10.1111/ejn.12974
- Shapira, Y., Tolmasov, M., Nissan, M., Reider, E., Koren, A., Biron, T., et al. (2015). Comparison of results between chitosan hollow tube and autologous nerve graft in reconstruction of peripheral nerve defect: an experimental study. *Microsurgery* 36, 664–671. doi: 10.1002/micr.22418
- Siemionow, M., Bozkurt, M., and Zor, F. (2010). Regeneration and repair of peripheral nerves with different biomaterials: review. *Microsurgery* 30, 574–588. doi: 10.1002/micr.20799
- Sinis, N., Schaller, H. E., Schulte-Eversum, C., Schlosshauer, B., Doser, M., Dietz, K., et al. (2005). Nerve regeneration across a 2-cm gap in the rat median nerve using a resorbable nerve conduit filled with Schwann cells. *J. Neurosurg.* 103, 1067–1076.
- Stenberg, L., Stöfel, M., Ronchi, G., Geuna, S., Yin, Y., Mommert, S., et al. (2017). Regeneration of long-distance peripheral nerve defects after delayed reconstruction in healthy and diabetic rats is supported by immunomodulatory chitosan nerve guides. *BMC Neurosci.* 18:53. doi: 10.1186/s12868-017-0374-z
- Stöfel, M., Metzen, J., Wildhagen, V. M., Helmecke, O., Rehra, L., Freier, T., et al. (2018a). Long-term in vivo evaluation of chitosan nerve guide properties with respect to two different sterilization methods. *Biomed. Res. Int.* 2018:6982738. doi: 10.1155/2018/6982738
- Stöfel, M., Wildhagen, V. M., Helmecke, O., Metzen, J., Pfund, C. B., Freier, T., et al. (2018b). Comparative evaluation of chitosan nerve guides with regular or increased bendability for acute and delayed peripheral nerve repair: a comprehensive comparison with autologous nerve grafts and muscle-in-vein grafts. *Anat. Rec.* 301, 1697–1713. doi: 10.1002/ar.23847
- Stöfel, M., Rehra, L., and Haastert-Talini, K. (2017). Reflex-based grasping, skilled forelimb reaching, and electrodiagnostic evaluation for comprehensive analysis of functional recovery – the 7 mm rat median nerve gap repair model revisited. *Brain Behav.* 2017, e00813. doi: 10.1002/brb3.813
- Topper, D. E., and Wallace, R. B. (1980). Utility of the neurological examination in rats. *Acta Neurobiol. Exp.* 40, 999–1003.
- Valero-Cabre, A., and Navarro, X. (2002). Changes in crossed spinal reflexes after peripheral nerve injury and repair. *J. Neurophysiol.* 87, 1763–1771. doi: 10.1152/jn.00305.2001
- Valero-Cabre, A., Tsironis, K., Skouras, E., Perego, G., Navarro, X., and Neiss, W. F. (2001). Superior muscle reinnervation after autologous nerve graft or poly-L-lactide-epsilon-caprolactone (PLC) tube implantation in comparison to silicone tube repair. *J. Neurosci. Res.* 63, 214–223.

Conflict of Interest Statement: OH and TF were employed by Medovent GmbH, Mainz, Germany. No benefit of any kind will be received either directly or indirectly by the authors.

The remaining authors declare that the research was conducted in the absence of any commercial or financial relationships that could be construed as a potential conflict of interest.

Copyright © 2019 Dietzmeyer, Förthmann, Leonhard, Helmecke, Brandenberger, Freier and Haastert-Talini. This is an open-access article distributed under the terms of the Creative Commons Attribution License (CC BY). The use, distribution or reproduction in other forums is permitted, provided the original author(s) and the copyright owner(s) are credited and that the original publication in this journal is cited, in accordance with accepted academic practice. No use, distribution or reproduction is permitted which does not comply with these terms.



The Effects of Surgical Antiseptics and Time Delays on RNA Isolated From Human and Rodent Peripheral Nerves

Matthew Wilcox^{1,2,3}, Tom J. Quick^{1,2,3} and James B. Phillips^{2,3*}

¹ Peripheral Nerve Injury Research Unit, Royal National Orthopaedic Hospital, Stanmore, United Kingdom, ² Department of Pharmacology, UCL School of Pharmacy, University College London, London, United Kingdom, ³ UCL Centre for Nerve Engineering, University College London, London, United Kingdom

OPEN ACCESS

Edited by:

Kirsten Haastert-Talini,
Hannover Medical School, Germany

Reviewed by:

Joost Verhaagen,
Netherlands Institute for
Neuroscience, Netherlands
Erik Walbeehm,
Radboud University Nijmegen Medical
Centre, Netherlands

*Correspondence:

James B. Phillips
jb.phillips@ucl.ac.uk

Specialty section:

This article was submitted to
Cellular Neuropathology,
a section of the journal
Frontiers in Cellular Neuroscience

Received: 30 October 2018

Accepted: 12 April 2019

Published: 22 May 2019

Citation:

Wilcox M, Quick TJ and
Phillips JB (2019) The Effects
of Surgical Antiseptics and Time
Delays on RNA Isolated From Human
and Rodent Peripheral Nerves.
Front. Cell. Neurosci. 13:189.
doi: 10.3389/fncel.2019.00189

Peripheral Nerve Injury (PNI) is common following blunt or penetrating trauma with an estimated prevalence of 2% among the trauma population. The resulting economic and societal impacts are significant. Nerve regeneration is a key biological process in those recovering from neural trauma. Real Time-quantitative Polymerase Chain Reaction (RT-qPCR) and RNA sequencing (RNA seq) are investigative methods that are often deployed by researchers to characterize the cellular and molecular mechanisms that underpin this process. However, the ethical and practical challenges associated with studying human nerve injury have meant that studies of nerve injury have largely been limited to rodent models of reinnervation. In some circumstances it is possible to liberate human nerve tissue for study, for example during reconstructive nerve repair. This complex surgical environment affords numerous challenges for optimizing the yield of RNA in sufficient quantity and quality for downstream RT-qPCR and/or RNA seq applications. This study characterized the effect of: (1) Time delays between surgical liberation and cryopreservation and (2) contact with antiseptic surgical reagents, on the quantity and quality of RNA isolated from human and rodent nerve samples. It was found that time delays of greater than 3 min between surgical liberation and cryopreservation of human nerve samples significantly decreased RNA concentrations to be sub-optimal for downstream RT-qPCR/RNA seq applications (<5 ng/ μ l). Minimizing the exposure of human nerve samples to antiseptic surgical reagents significantly increased yield of RNA isolated from samples. The detrimental effect of antiseptic reagents on RNA yield was further confirmed in a rodent model where RNA yield was 8.3-fold lower compared to non-exposed samples. In summary, this study has shown that changes to the surgical tissue collection protocol can have significant effects on the yield of RNA isolated from nerve samples. This will enable the optimisation of protocols in future studies, facilitating characterisation of the cellular and molecular mechanisms that underpin the regenerative capacity of the human peripheral nervous system.

Keywords: peripheral nerve regeneration/repair, RNA isolation and purification, RT-qPCR, RNA seq, surgery, cellular and molecular biology, human tissue, surgical antiseptics

INTRODUCTION

Peripheral nerve injury (PNI) is a common outcome following blunt or penetrating trauma with an estimated prevalence of 2% among the trauma population (Brattain, 2013). The resulting economic and societal ramifications are significant (Taylor et al., 2008). Nerve regeneration is a key biological process in those recovering from neural trauma. The cellular and molecular mechanisms that underpin this process have been well characterized in rodent models of PNI and have been central to therapeutic advancements made in this field of regenerative neuroscience (Kaplan et al., 2015; Jessen and Mirsky, 2016). Investigative methods such as RNA seq (RNA sequencing) and/or Real Time-quantitative Polymerase Chain Reaction (RT-qPCR) are often deployed in studies to characterize these mechanisms (Bosse et al., 2001; Jiang et al., 2014; Clements et al., 2017; Yi et al., 2017). However, the ethical and practical challenges associated with studying human nerve injury have meant that studies of nerve injury have largely been limited to rodent models of damage and renervation. For example, it is challenging to liberate human nerve samples without worsening patient morbidity. Moreover, traumatic nerve injuries represent a highly heterogeneous cohort and a standardized model in which human nerve regeneration can be studied is awaited.

In some circumstances it is possible to liberate human nerve tissue for study, for example during reconstructive nerve repair. Samples that can be extracted are often finite and are exposed to the complex surgical environment, which includes chemical and physical environmental factors, time pressures and other priorities which are not present when sampling animal tissues in a laboratory setting. This affords numerous challenges when optimizing protocols for the extraction of RNA with sufficient quantity and quality for quantitative analysis, therefore this study is dedicated to exploring these challenges.

The extraction of RNA in sufficient quantity and quality is a critical step toward obtaining valid RT-qPCR/RNA seq results (Atz et al., 2007; Popova et al., 2008; Abasolo et al., 2011). A minimum concentration of 5 ng/ μ l is often used for the synthesis of single stranded complementary DNA (cDNA) (Fox et al., 2012; França et al., 2012) and in the quantitative and qualitative assessments of RNA yields; a critical step toward valid RT-qPCR and/or RNA seq results (Bastard et al., 2002; Fleige and Pfaffl, 2006; Wilkes et al., 2010). The quality of RNA can be determined using quantitative and qualitative assays; 260/280 ratios and electropherograms respectively (Mee et al., 2011; Yockteng et al., 2013; Samadani et al., 2015; Walker et al., 2016). When optimizing RNA extraction protocols to attain yields sufficient for RT-qPCR assays, it is necessary to consider the tissue that is being processed; a review of the literature highlights differentials in the yield of RNA isolated from different tissues (Ruettgger et al., 2010; Walker et al., 2016; Grinstein et al., 2018).

Based on experiences within our research unit and others, there appears to be a differential between the RNA extraction ratio [mean total RNA (μ g) divided by initial tissue sample mass (mg)] of healthy and denervated nerve liberated from rats. Typical values range from 0.09 μ g/mg for healthy sciatic nerve to 0.27 μ g/mg for denervated sciatic nerve (Yamamoto et al., 2012;

Weng et al., 2018). This differential is perhaps attributable to the presence of higher numbers of proliferating cells in denervated tissue. Moreover, the degradation of connective tissue during Wallerian degeneration is likely to make denervated tissue more amenable to complete lysis. In comparing peripheral nerve to other tissues, the reported RNA extraction ratios are considerably lower than those reported for RNA isolated from other tissues such as liver, kidney and spleen which have mean extraction ratios of 1.56 μ g/mg, 0.50 μ g/mg, and 0.41 μ g/mg respectively (Yamamoto et al., 2012). The lower RNA yields reported from nerve samples are at least partially attributable to the fact that nerves are invested by fibrous connective tissue particularly in the epineurium (Thomas, 1963). The biomechanical properties of this tissue are antagonistic to total cellular disruption and lysis of nerve tissue which is an imperative step in RNA isolation (Bastard et al., 2002; Guan and Yang, 2008). This is an indication for the application of specialist RNA extraction kits which include a broad spectrum serine protease such as Proteinase K to facilitate optimal digestion of tissue and lysis of cells (Yockteng et al., 2013; Peeters et al., 2016; Amini et al., 2017).

Accepting that the concentration of RNA that can be isolated from peripheral nerve tissue is likely to be lower than other tissues, it is pertinent to optimize surgical protocols in order to conserve whatever RNA is available. One variable that has been shown to be predictive of the quality and quantity of RNA extracted from samples is the time interval between sample liberation and cryopreservation (Borgan et al., 2011; Hatzis et al., 2011; Caboux et al., 2013); a variable that is difficult to control in the surgical environment due to intra-operative priorities and handling limitations. It has been shown that delays of hours between sample liberation and cryopreservation impairs RNA isolated from cancerous samples (Borgan et al., 2011; Hatzis et al., 2011; Caboux et al., 2013). However, corresponding time frames using human nerve samples have not been reported.

While a number of past studies of other surgically liberated tissues for qPCR analysis have been optimized by manipulating variables such as time delays and RNA extraction protocols (Berglund et al., 2007; Borgan et al., 2011; Hatzis et al., 2011; Caboux et al., 2013), the exploration of other peri-operative variables that could impact on RNA yields, such as the chemical environment, have not been reported. The liberal application of antiseptic compounds in a surgical setting may influence RNA yields although this has not been reported previously. The most common constituents of these reagents globally are chlorhexidine and iodine (Hirsch et al., 2010). Despite *in vitro* experimental evidence demonstrating chlorhexidine and iodine based surgical antiseptic reagents can be cytotoxic to human SH-SY5Y neuroblastoma cells and rat RSC96 Schwann cell populations (Doan et al., 2012), their effects on RNA yield and quality have not been well characterized.

Protocols that detail how human nerve samples should be handled to optimize RNA yields for subsequent RT-qPCR and RNA seq analysis are not documented. This study aimed to explore the time course of RNA degradation in nerve tissue in order to establish an ideal time frame for the liberation of human nerve samples and cryopreservation (snap-freezing in liquid nitrogen). Additionally, this study aimed to investigate for

the first time the effect of exposure of human nerve samples to surgical antiseptic reagents.

MATERIALS AND METHODS

Optimizing the Human Surgical Environment for RNA Isolation

A total of 12 denervated human nerve samples were harvested from 12 different patients who underwent reconstructive surgery at the Peripheral Nerve Injury Unit, Royal National Orthopaedic Hospital after informed consent for the therapeutic procedure and for tissue donation (**Table 1**). Informed consent was obtained using the guidelines detailed in the UK Human Tissue Act (Human Tissue Act, 2004). Ethical approval for this project was provided by the UCL Biobank Research Committee (REC 15.15).

In all cases the site of operation was prepared with chlorhexidine or iodine based antiseptic reagents in concordance with standard surgical protocol (Digison, 2007). The demographic of the study subjects and details of the nerve samples harvested are documented in **Table 1**.

Samples harvested were often heterogeneous in size, morphology and innervation, so they were dissected into sections measuring 0.5 ± 0.2 cm in the longitudinal orientation. The dimensions of the samples were chosen to allow comparisons with other RT-qPCR studies of rodent nerve samples which used similar dimensions (Jiang et al., 2014). Additionally, samples were characterized as denervated using intra-operative neurophysiological monitoring to record compound nerve action potentials (CNAPs) (Simp, 2000; Herrera-Perez et al., 2015). The nerve was assumed to be denervated if a CNAP was absent and no muscle twitch was observed. Innervated samples were harvested from sites external to the site of injury (sural, intercostal and supraclavicular nerve samples) for the purpose of surgical nerve repair.

Nerve samples were stratified into 3 experimental groups (shown in **Table 1**):

- Group 1:** Samples whereby the time between sample liberation and cryopreservation was less than 3 min.
- Group 2:** Samples where the time interval between surgical liberation of the nerve sample and cryopreservation was greater than 3 min ranging up to 20 min. Since RNA yields from nerve samples remained lower than that reported in rodent studies following optimisation of handling times, the exploration of other peri-operative variables was necessitated. This informed the development of a third experimental group to explore the effect of minimizing the exposure of nerve samples to antiseptic reagents.
- Group 3:** Samples liberated and cryopreserved within 3 min but utilizing a “clean change” of surgical gloves and surgical equipment for harvest and handling of the sample to minimize exposure to antiseptic reagents. This group included healthy nerve samples in addition to denervated nerves.

Isolating the Effects of Antiseptic Reagents on RNA Yield Using a Rodent Model of Peripheral Nerve Liberation

Standard international operating protocols dictate that iodine and/or chlorhexidine based antiseptic reagents should be used to prepare the site of surgical incision as detailed by the World Health Organization (WHO Surgical Site Infection Prevention Guidelines, 2016). In order to investigate the effects of these reagents on RNA, a rodent model of surgical nerve liberation was utilized in an environment that was otherwise absent of antiseptic reagents. All animal use was performed according to the UK Animal Scientific Procedures Act 1986 / the European Communities Council Directives (86/609/EEC) and approved by the UCL Animal Welfare and Ethics Review Board. A total of 9 Sprague Dawley rats (6 female and 3 male) were culled using CO₂ inhalation and had their sciatic nerves excised. The nerves were then sharply dissected into 0.5 cm sections (to reflect the size of samples harvested from human patients). The sections were then randomized into 2 groups:

Control group: Samples were processed before any of the experimental samples to minimize the risk of contamination of the experimental environment.

Experimental group: 100 µl of one of the following commonly used surgical antiseptic reagents were applied by pipette: 10% iodine/water, 10% iodine/EtOH (Ethanol) or 2% chlorhexidine gluconate. Within 30 s of the nerve samples being excised, the nerve sample and antiseptic reagent was allowed to stand for 30 s and then immediately snap-frozen.

RNA Extraction Protocol

All materials used in this process of RNA isolation were treated with RNase Zap (Invitrogen). Rodent and human nerves were placed into a 5 ml tube and snap frozen in liquid nitrogen. The time between tissue isolation and freezing was monitored as well as the interaction of samples with antiseptic surgical reagents. RNA was isolated from all nerve samples using the Qiagen RNeasy® Fibrous Tissue Mini Kit. The total volume of eluted RNA for each sample was 40 µl.

The quantity of RNA was determined using a Tecan™ Infinite 200 PRO multimode reader. Quality of RNA was measured using a NanoDrop™ spectrophotometer to ascertain 260/280 ratios for each sample. Samples were also analyzed using Bio-rad Experion™ RNA analysis kits to assess Ribosomal Integrity Number (RIN), and obtain electropherogram data and automated agarose gel readings from samples using the Experion™ Automated Electrophoresis System.

RESULTS

Optimisation of the Surgical Environment for RNA Extraction

The effect of time between tissue extraction and freezing on the yield of RNA isolated from human nerve samples

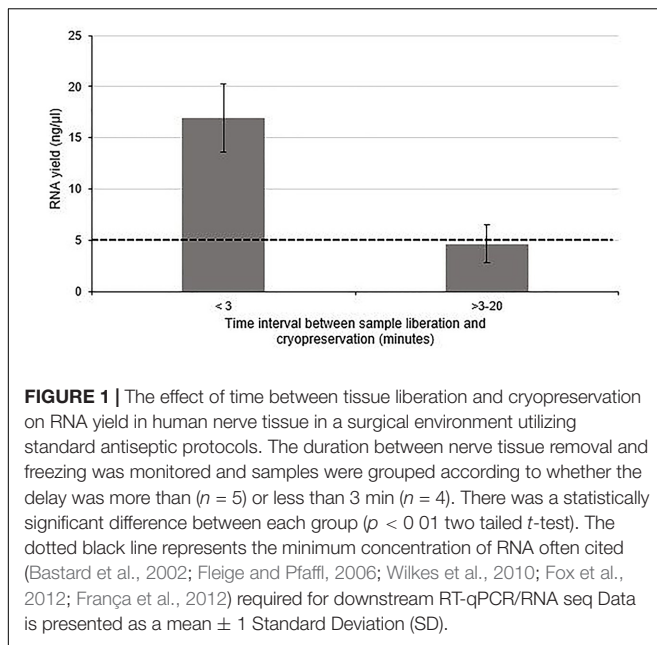
TABLE 1 | Demographic of patients and samples included in this study.

Mechanism of injury	Intra-operative findings	Details of surgery	Nerve assessed	Denervated/Innervated	Approximate time delay between surgical liberation and cryopreservation (min)
Experimental group 1					
Motorbike accident	Axonotmesis of the tibial nerve	Below the knee amputation	Tibial	Denervated	3
Motorbike accident	Right C5/6 Avulsion	Oberlin's nerve transfer	Biceps branch of musculocutaneous	Denervated	3
Fall on to sharp cast iron railing	Axonotmesis of superficial peroneal nerve	Excision of nerve	Superficial common peroneal nerve	Denervated	3
Motorbike accident	Left C6-T1 root avulsion	Somsak's nerve transfer	Medial head of triceps branch of the radial nerve	Denervated	3
Experimental group 2					
Iatrogenic nerve injury secondary to humeral fracture repair	Neurotmesis of the axillary nerve	Somsak's nerve transfer	Axillary	Denervated	5
Car v Tree	Right C4 - T1 avulsion	Intercostal nerve transfer to musculocutaneous nerve	Biceps branch of musculocutaneous	Denervated	10
Motorbike accident	Right C5/6 Avulsion	Oberlin's nerve transfer	Biceps branch of musculocutaneous	Denervated	15
Car v Lorry	Axonotmesis of the accessory nerve	Fascicle of C7 transfer to accessory nerve	Fascicle of C7 to pectoralis muscles to accessory nerve	Denervated	15
Motorbike accident	C5/6/7 Avulsion	Double Oberlin's nerve transfer	Biceps branch of musculocutaneous	Denervated	20
Experimental group 3					
Iatrogenic nerve injury secondary to left neck lymph node biopsy	Neurotmesis of the spinal accessory nerve	Supraclavicular nerve transfer to spinal accessory	Supraclavicular and Spinal accessory	Supraclavicular (innervated) and Spinal accessory (denervated)	3
Trampoline accident	Neurotmesis of the ulnar nerve	Sural nerve autograft to ulnar	Ulnar and Sural	Ulnar (denervated), Sural (innervated)	3
Moped v Lamppost	C5-8 Avulsion	Intercostal nerve transfer to triceps division of radial nerve	Radial and Intercostal	Intercostal (innervated), Radial (denervated)	3

was investigated (Group 1 and Group 2). **Figure 1** demonstrates that the optimal yield of RNA isolated from samples cryopreserved within 3 min of surgical liberation (Group 1) is approximately 3.6-fold higher than that from samples frozen after more than 3 min (Group 2) ($p < 0.01$). Importantly, the latter group had an RNA yield approximately equivalent to the minimum threshold value required for acceptable analysis and cDNA synthesis (Bastard et al., 2002; Fleige and Pfaffl, 2006; Wilkes et al., 2010; Fox et al., 2012; França et al., 2012).

The quality of RNA extracted from these nerve samples was concurrently determined quantitatively using 260/280 absorbance ratios (**Figure 2**) and semi-quantitatively by analyzing the ratio of ribosomal RNA bands in agarose gels and

changes in electropherogram morphology (**Figure 2**). Nucleic acids have an absorbance maxima at 260 nm. The ratio of this to the absorbance at 280 nm is used to determine the purity of DNA and RNA. A ratio of 1.8–2.2 is predictive of high quality RNA (Desjardins and Conklin, 2010). The distribution of 260/280 ratios assessed for samples cryopreserved within 3 min (Group 1) is shown in **Figure 2**, all of which fall within the optimal range (1.8–2.2). In addition, two distinct ribosomal RNA bands at 28S and 18S with a ratio of around 2.0 can be seen in the agarose gels (**Figure 2**) indicating high quality RNA isolated from samples processed within 3 min. **Figure 2** demonstrates how this ratio is lost in samples exposed to time delays of up to 20 min (Group 2 samples). An electropherogram was also assessed to illustrate the overall size of the ribosomal peaks and to further characterize the



differential in RNA quality between samples processed within 3 min and those exposed to time delays (Figure 2).

Using the data from the electropherogram reports, a RIN ranging from 1 to 10 (with 10 being predictive of high quality RNA) was assigned to each sample. RIN is generated using an algorithm that selects features from the electropherograms and constructs regression models based on Bayesian learning techniques. This assessment has been validated in a number of studies and has been shown to be highly predictive of RNA quality (Mueller et al., 2004; Imbeaud et al., 2005; Schroeder et al., 2006). It was found that all samples with 260/280 ratios between 1.8 and 2.2 (considered optimal) had RIN of between 7 and 10. Moreover, samples that did not have a ratio of between 1.8 and 2.2 had a RIN lower than 7. This provides further evidence that this RNA is of high quality and suitable for RT-qPCR and/or RNA seq analysis.

Since RNA yields from human denervated tissue remained lower than that reported from rodent studies (Yamamoto et al., 2012; Weng et al., 2018), this necessitated further exploration of peri-operative variables. Specifically, the effect of surgical antiseptics on RNA yield. Figure 3 suggests that samples liberated using the “clean change” surgical protocol (Group 3) yielded RNA in concentrations 2.8 times higher than those extracted under standard conditions ($p < 0.01$) (Groups 1 and 2). In comparing denervated tissue to healthy nerve samples, the concentration of RNA isolated from healthy nerve samples was significantly lower than that from denervated tissue ($p < 0.05$) (Figure 3). Assessments of RNA quality (260/280 absorbance ratios, ratio of ribosomal RNA bands in agarose gels and changes in electropherogram morphology) suggested that the RNA was of high quality (Figure 2) similar to the quality of RNA from nerve samples cryopreserved within 3 min (Figure 2).

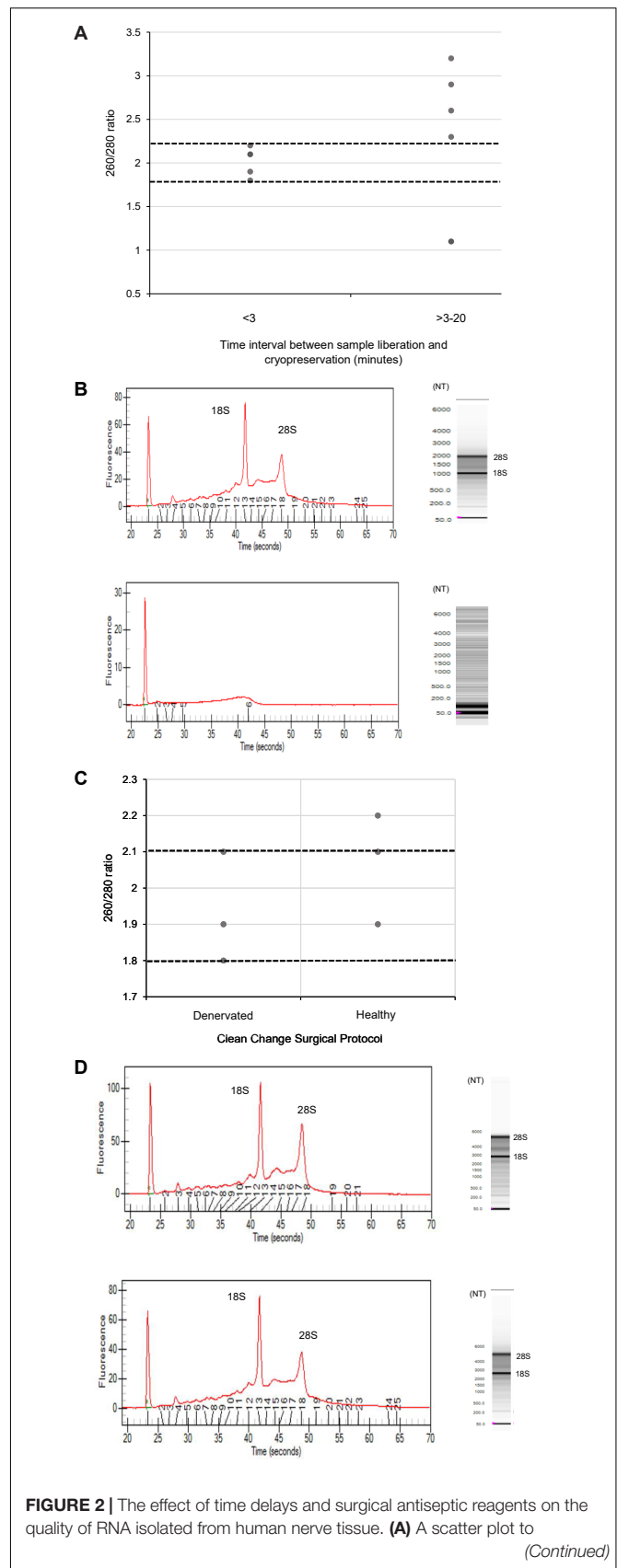


FIGURE 2 | Continued

demonstrate the distribution of 260/280 ratios yielded from RNA isolated from denervated human nerve samples surgically liberated and cryopreserved within 3 min (experimental Group 1) compared to those that were not cryopreserved within this timeframe (experimental Group 2). The two dotted black lines represent the range of 260/280 ratios that is predictive of high quality RNA (1.8–2.2). **(B)** Electropherograms (left) and agarose gels (right) digitally produced by the Experon™ Automated Electrophoresis System to assess quality of RNA isolated from denervated human nerve samples. The electropherogram is displayed with fluorescence on the y-axis and time of the fragment on the x-axis. The upper electropherogram/agarose gel represents a denervated sample cryopreserved within 3 min (Group 1) and the lower electropherogram/agarose gel represents a denervated sample that was exposed to a time delay of 20 min (Group 2). **(C)** A scatter plot to represent the 260/280 ratios yielded from healthy and denervate samples liberated under a “clean change” surgical protocol (Group 3). **(D)** Electropherogram (left) and agarose gels (right) to assess the quality of RNA isolated from healthy and denervated samples liberated under a “clean change” surgical protocol. The upper electropherogram/agarose gel represents a denervated sample (Group 3) and the lower electropherogram/agarose gel represents sural nerve (Group 3). All samples that yielded 260/280 ratios of between 1.8 and 2.2 were assessed to have Ribosomal Integrity Numbers (RIN) of between 7 and 10 (predictive of high quality RNA).

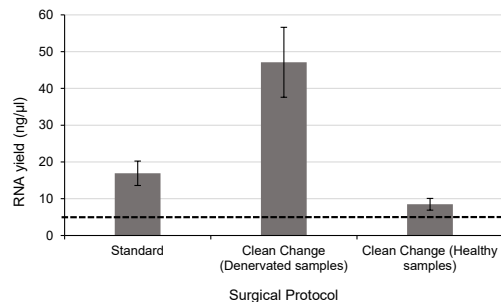


FIGURE 3 | Even when the time delay is minimized/equivalent between samples there is still a large differential in RNA yield due to exposure to surgical antiseptics. Denervated samples were liberated under a standard ($n = 4$) and “clean change” ($n = 3$) surgical protocol. Samples liberated in a surgical environment where the “clean change” surgical protocol was implemented yielded RNA concentrations significantly higher than those liberated under standard conditions ($p < 0.01$, two tailed t -test). Healthy nerve samples were also liberated under a “clean change” protocol ($n = 3$) which yielded significantly lower concentrations of RNA compared to denervated samples ($p < 0.001$ two tailed t -test). The dotted black line represents the minimum concentration of RNA often required for downstream RT-qPCR/RNA seq. Data are means \pm 1 SD.

Using nerve tissue freshly harvested from rats under carefully controlled environmental conditions enabled the effects of antiseptic reagents to be studied in isolation. A significant decrease in the yield of RNA (approximately 8.3 fold lower in exposed nerves compared to the untreated group) ($p < 0.01$) was detected following exposure of rodent nerve samples to each of the different antiseptic reagents (Figure 4).

DISCUSSION

In order to establish a protocol for the reliable extraction of RNA from human nerve samples, this study set out to characterize peri-operative variables predictive of RNA yield. The effect on

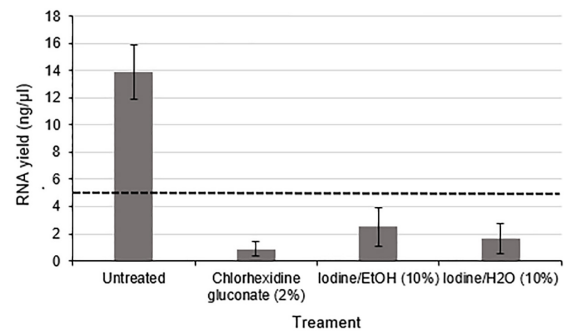


FIGURE 4 | RNA yield from rodent nerves is reduced following exposure to surgical antiseptic reagents. There was a statistically significant difference between the untreated ($n = 8$) and each of the treated groups (2% Chlorhexidine gluconate ($n = 6$), 10% Iodine/EtOH ($n = 6$), 10% Iodine/H₂O ($n = 6$)) as assessed by a one way ANOVA and Dunnett's test ($p < 0.01$ between each treatment group and the untreated group). Data are means \pm 1 SD. The black dotted line at 5 ng/μl represents the minimum concentration of RNA required for downstream RT-qPCR and RNA seq applications.

RNA yield of time delays between liberation of the nerve sample and snap freezing was investigated and results suggested that nerve samples should be snap frozen within 3 min to preserve RNA quantity and quality. This time interval is considerably shorter than that cited in other studies that have extracted RNA from surgical specimens which have shown that time delays of several hours between surgical liberation of a sample and cryopreservation is detrimental to RNA quantity and quality (Mee et al., 2011; Samadani et al., 2015; Patel et al., 2017). Studies of surgically harvested tissue have largely been limited to the study of non-fibrous cancerous tissues such as breast and prostate (Mee et al., 2011; Samadani et al., 2015; Patel et al., 2017). These studies achieved optimal yields of RNA (sufficient for RT-qPCR and RNA seq analysis) largely through the optimisation of RNA extraction protocols alone. This is perhaps attributable to the fact that the cancerous tissues explored in these studies have higher cellular densities than nerve tissue and thus more RNA that can be isolated, perhaps diminishing the impact of time delays and/or exposure of samples to antiseptic reagents on the quantity and quality of isolated RNA. Another major difference between nerve samples and other organs is that the nerve trunk contains bundles of axons, together with Schwann cells, fibroblasts, endothelial cells, perineurial cells and other associated cells, but the cell bodies of the neurons are not present since they are located within the CNS or adjacent ganglia. Therefore the RNA which is obtained from excised nerve samples will be predominantly derived from Schwann cells and other non-neuronal cells rather than neurons.

Even when delay was minimized, RNA yields from human nerves in this study remained lower than those reported in rodent studies of denervated nerve tissue (Yamamoto et al., 2012; Weng et al., 2018). Therefore the exploration of other peri-operative variables such as the interaction of samples with antiseptic surgical reagents such as chlorhexidine and iodine was necessitated. This study showed for the first time that exposure of nerves to surgical antiseptic reagents had detrimental

effects on the quantity of RNA that was isolated from the samples. Chlorhexidine and povidone-iodine based antiseptic reagents are cytotoxic to prokaryotic and eukaryotic cells. Chlorhexidine works by binding to the cell membrane causing it to rupture. On the other hand, povidone-iodine has a broader spectrum of antimicrobial activity. It works by crossing the cell membrane and destroying microbial proteins as well as DNA. It follows that these reagents may have acute cytotoxic effects within the nerve samples thus impairing RNA yield.

It was evident that healthy nerve samples yielded significantly lower quantities of RNA than that from denervated tissue, which concurs with rodent studies (Yamamoto et al., 2012; Weng et al., 2018) even when the exposure of nerve samples to antiseptic reagents was minimized and the time delay was limited to 3 min. The differential observed in both species is likely to be due to the biological mechanisms that underpin nerve regeneration. Evidence from rodent and human models of nerve injury have shown that Wallerian degeneration starts soon after nerve injury, involving a complex cascade of events including degradation of the fibrous connective tissue (Rotshenker, 2011). This may make denervated tissue more amenable to lysis and cellular disruption leading to higher yields of RNA compared with intact healthy nerve tissue. Furthermore, Wallerian degeneration involves proliferation of Schwann cells as well as infiltration and proliferation of other non-neuronal cells (such as macrophages and other immune system cells) (Rotshenker, 2011), potentially contributing to increased RNA content in denervated nerve tissue. This finding highlights the pertinence of considering the innervation status of nerve tissue in order to optimize RNA yield.

In order to isolate and further investigate the effects of exposure to antiseptic reagents, this study used a rodent model of peripheral nerve liberation which showed that these antiseptic reagents reduced RNA yields significantly. Chlorhexidine and iodine based reagents can be found in abundance in operating theaters around the world where they are often deployed for preoperative skin preparation. This finding, together with experimental evidence that has shown iodine and chlorhexidine based reagents to have cytotoxic effects on *in vitro* populations of human neuronal cells and rodent Schwann cells (Doan et al., 2012), necessitates further work to characterize the effect of these reagents on the regenerative capacity of the peripheral nervous system. This could potentially inform the modification and development of surgical tissue handling protocols more generally, beyond just the focus here on obtaining nerve tissue RNA for research.

In addition to influencing RNA extraction, iodine and chlorhexidine based reagents may have downstream effects on qPCR assays. These reagents have been shown to inactivate the Human Immunodeficiency Virus through a mechanism thought

to be at least partially attributable to the ability of these reagents to manipulate the viral DNA reverse transcriptase (Harbison and Hammer, 1989; Sattar and Springthorpe, 1991). This enzyme is analogous to the RNA to cDNA reverse transcriptase step used in RT-qPCR and RNA seq assays, providing an additional reason to avoid the contamination of samples intended for downstream qPCR and RNA seq assays.

In summary, this study reports new experimental evidence from human and animal studies that reveals the effects of time delays and surgical antiseptics on the RNA yield obtained from nerve tissue. This information can help to inform the development of improved methodology, specifically limiting time delay between sample liberation and cryopreservation to less than 3 min whilst utilizing a “clean change” surgical protocol to reduce antiseptic exposure. These findings provide new information about the response of fresh nerve tissue following isolation, including differences between healthy and denervated samples. This understanding will enable more effective use to be made of valuable human nerve tissue samples, addressing the knowledge gaps that currently exist in studying cellular and molecular mechanisms that underpin human nerve regeneration.

ETHICS STATEMENT

This study was carried out in accordance with the recommendations of ‘HTA guidelines, Biobank Ethical Review Committee’ with written informed consent from all subjects. All subjects gave written informed consent in accordance with the Declaration of Helsinki. The protocol was approved by the UCL Biobank Ethical Review Committee.

AUTHOR CONTRIBUTIONS

MW designed the concept and experimental methods used to assess quality and quantity of RNA yields, executed the experiments, performed analysis, and wrote the manuscript. TQ contributed to experimental design and clinical data detailed in the manuscript, made comments on the manuscript, and involved in writing up. JP contributed to experimental design and data analysis and informed the writing of the manuscript.

FUNDING

This work was supported by the UCL Graduate Research Scholarship, England Golf Trust, and Royal National Orthopaedic Hospital Charitable Trust.

REFERENCES

- Abasolo, N., Torrell, H., Roig, B., Moyano, S., Vilella, E., and Martorell, L. (2011). RT-qPCR study on post-mortem brain samples from patients with major psychiatric disorders: reference genes and specimen characteristics. *J. Psychiatr. Res.* 45, 1411–1418. doi: 10.1016/j.jpsychires.2011.06.001
- Amini, P., Ettlin, J., Opitz, L., Clementi, E., Malbon, A., and Markkanen, E. (2017). An optimised protocol for isolation of RNA from small sections of laser-capture microdissected FFPE tissue amenable for next-generation sequencing. *BMC Mol. Biol.* 18:22. doi: 10.1186/s12867-017-0099-7
- Atz, M., Walsh, D., Cartagena, P., Li, J., Evans, S., Choudary, P., et al. (2007). Methodological considerations for gene expression profiling of human brain. *J. Neurosci. Methods* 163, 295–309. doi: 10.1016/j.jneumeth.2007.03.022

- Bastard, J. P., Chambert, S., Ceppa, F., Coude, M., Grapez, E., Loric, S., et al. (2002). RNA isolation and purification methods. *Ann. Biol. Clin.* 60, 513–523.
- Berglund, S. R., Schwietert, C. W., Jones, A. A., Stern, R. L., Lehmann, J., and Goldberg, Z. (2007). Optimized methodology for sequential extraction of RNA and protein from small human skin biopsies. *J. Invest. Dermatol.* 127, 349–353. doi: 10.1038/sj.jid.5700557
- Borgan, E., Navon, R., Vollan, H. K. M., Schlichting, E., Sauer, T., Yakhini, Z., et al. (2011). Ischemia caused by time to freezing induces systematic microRNA and mRNA responses in cancer tissue. *Mol. Oncol.* 5, 564–576. doi: 10.1016/j.molonc.2011.08.004
- Bosse, F., Kury, P., and Muller, H. W. (2001). Gene expression profiling and molecular aspects in peripheral nerve regeneration. *Restor. Neurol. Neurosci.* 19, 5–18.
- Brattain, K. (2013). *Analysis of the Peripheral Nerve Repair Market in the US*. Minneapolis, MN: Magellan Medical Technology Consultants, Inc.
- Caboux, E., Paciencia, M., Durand, G., Robinot, N., Wozniak, M. B., Galateau-Salle, F., et al. (2013). Impact of delay to cryopreservation on RNA integrity and genome-wide expression profiles in resected tumor samples. *PLoS One* 8:e79826. doi: 10.1371/journal.pone.0079826
- Clements, M. P., Byrne, E., Camarillo Guerrero, L. F., Cattin, A.-L., Zakka, L., Ashraf, A., et al. (2017). The wound microenvironment reprograms schwann cells to invasive mesenchymal-like cells to drive peripheral nerve regeneration. *Neuron* 96, 98.e7–114.e7. doi: 10.1016/j.neuron.2017.09.008
- Desjardins, P., and Conklin, D. (2010). NanoDrop microvolume quantitation of nucleic acids. *J. Vis. Exp.* 22, pii:2565. doi: 10.3791/2565
- Digison, M. B. (2007). A review of anti-septic agents for pre-operative skin preparation. *Plast. Surg. Nurs.* 27, 181–185. doi: 10.1097/01.PSN.0000306182.50071.e2
- Doan, L., Piskoun, B., Rosenberg, A. D., Blanck, T. J. J., Phillips, M. S., and Xu, F. (2012). In vitro antiseptic effects on viability of neuronal and Schwann cells. *Reg. Anesth. Pain Med.* 37, 131–138. doi: 10.1097/AAP.0b013e31823cdd96
- Fleige, S., and Pfaffl, M. W. (2006). RNA integrity and the effect on the real-time qRT-PCR performance. *Mol. Aspects Med.* 27, 126–139. doi: 10.1016/j.mam.2005.12.003
- Fox, B. C., Devonshire, A. S., Baradez, M.-O., Marshall, D., and Foy, C. A. (2012). Comparison of reverse transcription-quantitative polymerase chain reaction methods and platforms for single cell gene expression analysis. *Anal. Biochem.* 427, 178–186. doi: 10.1016/j.ab.2012.05.010
- França, A., Freitas, A. I., Henriques, A. F., and Cerca, N. (2012). Optimizing a qPCR gene expression quantification assay for *s. epidermidis* biofilms: a comparison between commercial kits and a customized protocol. *PLoS One* 7:e37480. doi: 10.1371/journal.pone.0037480
- Grinstein, M., Dingwall, H. L., Shah, R. R., Capellini, T. D., and Galloway, J. L. (2018). A robust method for RNA extraction and purification from a single adult mouse tendon. *PeerJ* 6:e4664. doi: 10.7717/peerj.4664
- Guan, H., and Yang, K. (2008). RNA isolation and real-time quantitative RT-PCR. *Methods Mol. Biol.* 456, 259–270. doi: 10.1007/978-1-59745-245-8_19
- Harbison, M. A., and Hammer, S. M. (1989). Inactivation of human immunodeficiency virus by betadine products and chlorhexidine. *J. Acquir. Immune Defic. Syndr.* 2, 16–20.
- Hatzis, C., Sun, H., Yao, H., Hubbard, R. E., Meric-Bernstam, F., Babiera, G. V., et al. (2011). Effects of tissue handling on RNA integrity and microarray measurements from resected breast cancers. *J. Natl. Cancer Inst.* 103, 1871–1883. doi: 10.1093/jnci/djr438
- Herrera-Perez, M., Oller-Boix, A., Perez-Lorensu, P. J., de Bergua-Domingo, J., Gonzalez-Casamayor, S., Marquez-Marfil, F., et al. (2015). Intraoperative neurophysiological monitoring in peripheral nerve surgery: technical description and experience in a centre. *Rev. Esp. Cir. Ortop. Traumatol.* 59, 266–274. doi: 10.1016/j.recot.2014.11.004
- Hirsch, T., Koerber, A., Jacobsen, F., Dissemmond, J., Steinau, H.-U., Gattermann, S., et al. (2010). Evaluation of toxic side effects of clinically used skin antiseptics in vitro. *J. Surg. Res.* 164, 344–350. doi: 10.1016/j.jss.2009.04.029
- Human Tissue Act (2004). *Human Tissue Act*. Available at: <http://www.legislation.gov.uk/ukpga/2004/30/contents> (accessed January 12, 2019).
- Imbeaud, S., Graudens, E., Boulanger, V., Barlet, X., Zaborski, P., Eveno, E., et al. (2005). Towards standardization of RNA quality assessment using user-independent classifiers of microcapillary electrophoresis traces. *Nucleic Acids Res.* 33:e56. doi: 10.1093/nar/gni054
- Jessen, K. R., and Mirsky, R. (2016). The repair Schwann cell and its function in regenerating nerves. *J. Physiol.* 594, 3521–3531. doi: 10.1113/JP270874
- Jiang, N., Li, H., Sun, Y., Yin, D., Zhao, Q., Cui, S., et al. (2014). Differential gene expression in proximal and distal nerve segments of rats with sciatic nerve injury during Wallerian degeneration. *Neural Regen. Res.* 9, 1186–1194.
- Kaplan, H. M., Mishra, P., and Kohn, J. (2015). The overwhelming use of rat models in nerve regeneration research may compromise designs of nerve guidance conduits for humans. *J. Mater. Sci. Mater. Med.* 26:226. doi: 10.1007/s10856-015-5558-4
- Mee, B. C., Carroll, P., Donatello, S., Connolly, E., Griffin, M., Dunne, B., et al. (2011). Maintaining breast cancer specimen integrity and individual or simultaneous extraction of quality DNA, RNA, and proteins from allprotect-stabilized and nonstabilized tissue samples. *Biopreserv. Biobank.* 9, 389–398. doi: 10.1089/bio.2011.0034
- Mueller, O., Lightfoot, S., and Schroeder, A. (2004). *RNA Integrity Number (RIN)—Standardization of RNA Quality Control Tech Rep 5989-1165EN*. Santa Clara: Agilent Technologies.
- Patel, P. G., Selvarajah, S., Guérard, K.-P., Bartlett, J. M. S., Lapointe, J., Berman, D. M., et al. (2017). Reliability and performance of commercial RNA and DNA extraction kits for FFPE tissue cores. *PLoS One* 12:e0179732. doi: 10.1371/journal.pone.0179732
- Peeters, M., Huang, C. L., Vonk, L. A., Lu, Z. F., Bank, R. A., Helder, M. N., et al. (2016). Optimisation of high-quality total ribonucleic acid isolation from cartilaginous tissues for real-time polymerase chain reaction analysis. *Bone Joint Res.* 5, 560–568. doi: 10.1302/2046-3758.511.BJR-2016-0033.R3p
- Popova, T., Mennerich, D., Weith, A., and Quast, K. (2008). Effect of RNA quality on transcript intensity levels in microarray analysis of human post-mortem brain tissues. *BMC Genomics* 9:91. doi: 10.1186/1471-2164-9-91
- Rotshenker, S. (2011). Wallerian degeneration: the innate-immune response to traumatic nerve injury. *Neuroinflamm.* 8:109. doi: 10.1186/1742-2094-8-109
- Ruettger, A., Neumann, S., Wiederanders, B., and Huber, R. (2010). Comparison of different methods for preparation and characterization of total RNA from cartilage samples to uncover osteoarthritis in vivo. *BMC Res. Notes* 3:7. doi: 10.1186/1756-0500-3-7
- Samadani, A. A., Nikbakhsh, N., Fattahi, S., Pourbagher, R., Aghajani-pour Mir, S. M., Mousavi Kani, N., et al. (2015). RNA extraction from animal and human's cancerous tissues: does tissue matter? *Int. J. Mol. Cell. Med.* 4, 54–59.
- Sattar, S. A., and Springthorpe, V. S. (1991). Survival and disinfectant inactivation of the human immunodeficiency virus: a critical review. *Rev. Infect. Dis.* 13, 430–447. doi: 10.1093/clinids/13.3.430
- Schroeder, A., Mueller, O., Stocker, S., Salowsky, R., Leiber, M., Gassmann, M., et al. (2006). The RIN: an RNA integrity number for assigning integrity values to RNA measurements. *BMC Mol. Biol.* 7:3. doi: 10.1186/1471-2199-7-3
- Slimp, J. C. (2000). Intraoperative monitoring of nerve repairs. *Hand. Clin.* 16, 25–36.
- Taylor, C. A., Braza, D., Rice, J. B., and Dillingham, T. (2008). The incidence of peripheral nerve injury in extremity trauma. *Am. J. Phys. Med. Rehabil.* 87, 381–385. doi: 10.1097/PHM.0b013e31815e6370
- Thomas, P. K. (1963). The connective tissue of peripheral nerve: an electron microscope study. *J. Anat.* 97(Pt 1), 35–44.
- Walker, D. G., Whetzel, A. M., Serrano, G., Sue, L. I., Lue, L.-F., and Beach, T. G. (2016). Characterization of RNA isolated from eighteen different human tissues: results from a rapid human autopsy program. *Cell Tissue Bank.* 17, 361–375. doi: 10.1007/s10561-016-9555-8
- Weng, J., Zhang, P., Yin, X., and Jiang, B. (2018). The whole transcriptome involved in denervated muscle atrophy following peripheral nerve injury. *Front. Mol. Neurosci.* 11:69. doi: 10.3389/fnmol.2018.00069
- WHO Surgical Site Infection Prevention Guidelines (2016). *WHO Surgical Site Infection Prevention Guidelines*. Available at: <https://www.who.int/gpsc/appendix8.pdf> (accessed August 26, 2018).
- Wilkes, T. M., Devonshire, A. S., Ellison, S. L. R., and Foy, C. A. (2010). Evaluation of a novel approach for the measurement of RNA quality. *BMC Res. Notes* 3:89. doi: 10.1186/1756-0500-3-89

- Yamamoto, T., Nakashima, K., Maruta, Y., Kiriya, T., Sasaki, M., Sugiyama, S., et al. (2012). Improved RNA extraction method using the BioMasher and BioMasher power-plus. *J. Vet. Med. Sci.* 74, 1561–1567. doi: 10.1292/jvms.12-0213
- Yi, S., Tang, X., Yu, J., Liu, J., Ding, F., and Gu, X. (2017). Microarray and qPCR analyses of wallerian degeneration in rat sciatic nerves. *Front. Cell. Neurosci.* 11:22. doi: 10.3389/fncel.2017.00022
- Yockteng, R., Almeida, A. M. R., Yee, S., Andre, T., Hill, C., and Specht, C. D. (2013). A method for extracting high-quality RNA from diverse plants for next-generation sequencing and gene expression analyses. *Appl. Plant Sci.* 1:apps.1300070. doi: 10.3732/apps.1300070

Conflict of Interest Statement: The authors declare that the research was conducted in the absence of any commercial or financial relationships that could be construed as a potential conflict of interest.

The handling Editor is currently co-organizing a Research Topic with one of the authors JP, and confirms the absence of any other collaboration.

Copyright © 2019 Wilcox, Quick and Phillips. This is an open-access article distributed under the terms of the Creative Commons Attribution License (CC BY). The use, distribution or reproduction in other forums is permitted, provided the original author(s) and the copyright owner(s) are credited and that the original publication in this journal is cited, in accordance with accepted academic practice. No use, distribution or reproduction is permitted which does not comply with these terms.



Peripheral Nerve Regeneration Is Independent From Schwann Cell p75^{NTR} Expression

Nádia P. Gonçalves^{1,2}, Simin Mohseni³, Marwa El Soury⁴, Maj Ulrichsen¹, Mette Richner¹, Junhua Xiao⁵, Rhiannon J. Wood⁵, Olav M. Andersen¹, Elizabeth J. Coulson⁶, Stefania Raimondo⁵, Simon S. Murray⁵ and Christian B. Vægter^{1,2*}

¹ Danish Research Institute of Translational Neuroscience – DANDRITE, Nordic-EMBL Partnership for Molecular Medicine, Department of Biomedicine, Aarhus University, Aarhus, Denmark, ² The International Diabetic Neuropathy Consortium, Aarhus University Hospital, Aarhus, Denmark, ³ Division of Cell Biology, Department of Clinical and Experimental Medicine, Linköping University, Linköping, Sweden, ⁴ Department of Clinical and Biological Sciences, Neuroscience Institute Cavalieri Ottolenghi, University of Turin, Turin, Italy, ⁵ Department of Anatomy and Neuroscience, School of Biomedical Science, Faculty of Medicine, Dentistry and Health Sciences, The University of Melbourne, Parkville, VIC, Australia, ⁶ School of Biomedical Sciences, Faculty of Medicine, Queensland Brain Institute, The University of Queensland, Brisbane, QLD, Australia

OPEN ACCESS

Edited by:

Thomas Fath,
Macquarie University, Australia

Reviewed by:

Se-Young Choi,
Seoul National University,
South Korea
Simone Di Giovanni,
Imperial College London,
United Kingdom

*Correspondence:

Christian B. Vægter
cv@biomed.au.dk

Specialty section:

This article was submitted to
Cellular Neuropathology,
a section of the journal
Frontiers in Cellular Neuroscience

Received: 07 February 2019

Accepted: 09 May 2019

Published: 29 May 2019

Citation:

Gonçalves NP, Mohseni S,
El Soury M, Ulrichsen M, Richner M,
Xiao J, Wood RJ, Andersen OM,
Coulson EJ, Raimondo S, Murray SS
and Vægter CB (2019) Peripheral
Nerve Regeneration Is Independent
From Schwann Cell p75^{NTR}
Expression.
Front. Cell. Neurosci. 13:235.
doi: 10.3389/fncel.2019.00235

Schwann cell reprogramming and differentiation are crucial prerequisites for neuronal regeneration and re-myelination to occur following injury to peripheral nerves. The neurotrophin receptor p75^{NTR} has been identified as a positive modulator for Schwann cell myelination during development and implicated in promoting nerve regeneration after injury. However, most studies base this conclusion on results obtained from complete p75^{NTR} knockout mouse models and cannot dissect the specific role of p75^{NTR} expressed by Schwann cells. In this present study, a conditional knockout model selectively deleting p75^{NTR} expression in Schwann cells was generated, where p75^{NTR} expression is replaced with that of an mCherry reporter. Silencing of Schwann cell p75^{NTR} expression was confirmed in the sciatic nerve *in vivo* and *in vitro*, without altering axonal expression of p75^{NTR}. No difference in sciatic nerve myelination during development or following sciatic nerve crush injury was observed, as determined by quantification of both myelinated and unmyelinated nerve fiber densities, myelinated axonal diameter and myelin thickness. However, the absence of Schwann cell p75^{NTR} reduced motor nerve conduction velocity after crush injury. Our data indicate that the absence of Schwann cell p75^{NTR} expression *in vivo* is not critical for axonal regrowth or remyelination following sciatic nerve crush injury, but does play a key role in functional recovery. Overall, this represents the first step in redefining the role of p75^{NTR} in the peripheral nervous system, suggesting that the Schwann cell-axon unit functions as a syncytium, with the previous published involvement of p75^{NTR} in remyelination most likely depending on axonal/neuronal p75^{NTR} and/or mutual glial-axonal interactions.

Keywords: Schwann cells, p75^{NTR}, myelination, regeneration, nerve injury

INTRODUCTION

Schwann cells are axon-ensheathing glial cells of the peripheral nervous system (PNS) and are essential in maintaining normal nerve function as well as facilitating nerve repair following injury. Two subtypes of Schwann cells exist in the adult PNS, either myelinating or non-myelinating. The myelinating Schwann cells form a multi-layered myelin sheath around a segment of a single large-caliber axon, spirally wrapping its plasma membrane around the axon. In contrast, non-myelinating Schwann cells surround and segregate groups of several small-diameter nociceptive axons, in a structure called Remak bundles. The development of the PNS into these organized structures has been extensively studied and the identification of essential molecules and signaling pathways established (Jessen and Mirsky, 2005; Richner et al., 2014; Gonçalves et al., 2017). An important group in this context is the family of neurotrophins consisting of nerve growth factor (NGF), brain derived neurotrophic factor (BDNF), neurotrophin-3 (NT-3) and neurotrophin-4/5 (NT-4/5), which binds to two structurally unrelated receptors: the p75 neurotrophin receptor (p75^{NTR}) and the tropomyosin receptor kinases (TrkA, -B, and -C). It is generally well accepted that binding of neurotrophins to the Trk receptors mediate survival and differentiation, but the specific functions of p75^{NTR} in the PNS remains elusive. The controversy may partly be attributed to the fact that p75^{NTR} is expressed by both neuronal and glial cell types and furthermore may have very different and even contradictory roles depending on cell type and temporal expression pattern, including survival signaling, cytoskeletal organization as well as the induction of cell death (Chao, 2003; Reichardt, 2006; Meeker and Williams, 2015), providing substantial cellular and molecular diversity of this receptor.

Damage to adult peripheral nerves causes axonal degeneration, myelin degradation and Schwann cell dedifferentiation distal to the injury site in the process of Wallerian degeneration. Interestingly, such injury also induces mechanisms at the cellular level resembling those active during development, including increased neurotrophin synthesis in neurons and Schwann cells which, which is important for guiding and supporting axonal regeneration (Richner et al., 2014). It is well established that p75^{NTR} is expressed by Schwann cells during development and following peripheral nerve injury (Taniuchi et al., 1986; Johnson et al., 1988), where a high expression level is maintained until contact between the (re)growing axons and Schwann cells have been established and (re)myelination initiated (Johnson et al., 1988). In line with this, studies using complete p75^{NTR} knockout (KO) mouse models have found that the lack of p75^{NTR} results in reduced PNS myelination (Cosgaya et al., 2002). However, the mechanism by which p75^{NTR} affects nerve regeneration following injury is unclear. p75^{NTR} has been reported to inhibit motor axonal regeneration (Boyd and Gordon, 2001), be indispensable for motor axonal regrowth (Gschwendtner et al., 2003), to be important for regeneration and remyelination of motor neurons (Tomita et al., 2007), and important for both the number and regrowth of axons in a mixed nerve (Song et al., 2006, 2009). A central tool for the majority of previous studies investigating the role of p75^{NTR} in the PNS has been the

complete p75^{NTR} KO mouse models, the exon III deletion (Lee et al., 1992) and the subsequent exon IV model (von Schack et al., 2001). These KO models demonstrate a dramatic PNS phenotype, with an approximately 40–50% reduction in DRG neurons and myelinated axon numbers as well as impaired levels of myelination (Cosgaya et al., 2002). Importantly, these models exhibit loss of p75^{NTR} in Schwann cells, DRG- and motor neurons and the use of such models cannot therefore clarify whether the observed phenotypes result from loss of p75^{NTR} in the Schwann cells, a neuronal subpopulation or both. To complicate matters further, it has subsequently been determined that both models are not complete KOs but retain the expression of an alternative active splice variant (exon III model) or results in a pro-apoptotic fragment (exon IV model) (von Schack et al., 2001; Murray et al., 2003; Paul et al., 2004). In this study, to dissect the role of p75^{NTR} signaling in Schwann cells in the process of nerve regeneration and remyelination following nerve crush injury, we have developed a conditional KO model selectively deleting p75^{NTR} expression in Schwann cells. Our results show that p75^{NTR} deletion in Schwann cells does not affect the structure of the uninjured myelinated or unmyelinated fibers. In response to injury, although axonal regeneration and remyelination appeared unaffected in Schwann cell p75^{NTR} deficient animals, these mice nonetheless exhibited reduced recovery of motor nerve conduction velocity.

MATERIALS AND METHODS

Mouse Model Generation

To generate mice with conditional deletion of p75^{NTR} in Schwann cells, p75^{fl/fl} mice (Boskovic et al., 2014) were crossed to transgenic mice containing the myelin protein zero promoter driving expression of Cre recombinase (Mpz-cre) (sourced from the Jackson Laboratory strain #017927) (Feltri et al., 1999). Upon recombination, the p75^{NTR} genomic DNA flanked by the loxP sites is inverted and, in p75^{in/in} cells, expression of p75^{NTR} is replaced by expression of mCherry (Boskovic et al., 2014). The resulting knockout mice were termed p75^{in/in} Mpz-cre (referred to as SC-p75^{NTR}-KO throughout this manuscript). All mice were on a C57BL/6 background and housed in specific pathogen-free conditions at the Melbourne Brain Centre Animal Facility (The Royal Melbourne Hospital, Australia). Animal breeding procedures were approved by The Florey Institute for Neuroscience and Mental Health Animal Ethics Committee and followed the Australian Code of Practice for the Care and Use of Animals for Scientific Purposes.

Mouse Surgery

For the mouse model of injury, 8–10-week-old female SC-p75^{NTR}-KO and p75^{NTR}^{fl/fl} Cre- (control littermates) were used. By this age, the PNS is already mature and injury effects will not be misinterpreted by the developmental process. Anesthesia was induced with isoflurane and a subcutaneous injection of buprenorphine and ampicillin administered prior to surgery, to minimize pain and post-surgical distress. The thigh and legs were shaved, eyes protected from drying and the sciatic nerve

exposed at the mid-thigh level by separating the biceps femoris and the gluteus superficialis. After carefully clearing surrounding connective tissue, the left sciatic nerve was crushed with a non-serrated clamp, twice for 15 s. A sham operation was performed similarly at the contralateral side, where the sciatic nerve was exposed and the skin closed immediately after. In both situations, the musculature was prepared with minimum tissue damage to guarantee the ideal conditions for functional recovery.

Mice were cared for in a pathogen-free environment, in a 12 h light/dark cycle and with water and food *ad libitum*. One group of animals was euthanized at post-injured day 15 ($n = 4$ littermates, $n = 6$ SC-p75^{NTR}-KO) while the other group was sacrificed 29 days after injury ($n = 8$ littermates, $n = 6$ SC-p75^{NTR}-KO). Animals were handled according to the European Union Council Directive and National rules.

Sensorimotor Analysis

Sensorimotor behavior was analyzed before (0) and 1, 5, 7, 14, and 28 days after injury.

Mechanical allodynia was assessed with the application of a set of calibrated Von Frey filaments (Touch-Test[®] Sensory Evaluators, North Coast Medical, CA, United States) into the midplantar side of the hind paw until the filament was just bent (bending forces from 0.2 to 2 g). Mice were placed in a Plexiglas cage with mesh flooring and allowed to acclimate for 1 h. The stimulus was repeated five times with each filament and a positive response in three out of five repetitive stimulations stated as the pain threshold. The withdrawal threshold is expressed in grams.

The Hargreaves test was used to measure paw withdrawal latency to a noxious thermal stimulus using a Heat Flow I.R. Radiometer (Hargreaves Apparatus, Cat. #37370, Ugo Basile, Gemonio, Italy). The radiant heat source was kept at 50% (190 mW/cm²) in all tested animals that were let to acclimatize for 1 h before the procedure. Hind paws were tested alternately with 5 min between consecutive tests, and five measurements were obtained for each side, that were averaged for a final result. A cut-off of 20 s was established to avoid potential burn injury.

Walking tract analysis was performed to access locomotor functional recovery. Briefly, the mice hind feet were pressed onto a non-toxic ink pad and animals were then allowed to walk through a dark corridor over an A3 white printer paper. The obtained footprints were then measured to calculate the sciatic functional index (SFI) using the empirical equation adapted for mice by Inserra et al. (1998): $SFI = 118.9 \times [(ETS-CTS)/CTS] - 51.2 \times [(EPL-CPL)/CPL] - 7.5$, where ETS represents operated experimental toe spread (distance between the first and fifth toes), CTS stands for control toe spread, EPL for operated experimental print length and CPL for control print length (Inserra et al., 1998). Footmarks made at the beginning of the trial were excluded and three analyzable walks were evaluated from each run, for individual step parameter calculation. The pre-injured SFI values (time point = 0) were used as control for comparison. The SFI scores that we processed ranged from 0 to -130, with 0 representing normal or completely recovered nerve function and -100 or more, a non-functional nerve; thus, mice that dragged their toes were arbitrarily assigned a value of -100.

Nerve Conduction Velocities

Motor (sciatic) and sensory (sural) nerve conduction velocities (NCV) were performed in naïve mice and 29 days injured ones, according to (Oh et al., 2010) using a Viking Quest apparatus (Natus Neurology Incorporated, United States). Briefly, for sural nerve, recording electrodes were placed in the dorsal part of the foot, with supramaximal stimulation at the ankle. Sural sensory NCV (m/s) was calculated by dividing the distance between the recording and stimulating electrodes (mm) by the onset latency (ms) of the sensory nerve action potential after supramaximal antidromic stimulation. Sciatic-tibial motor NCV was recorded by placing electrodes dorsally in the foot and orthodromically stimulating first at the ankle, then at the sciatic notch. The distance between the two sites of stimulation (mm) was then divided by the difference between the two onset latencies (ankle distance and notch distance, ms) to calculate the final sciatic-tibial motor NCV (m/s).

Immunohistochemistry and Microscopy

Naïve P11 mice were perfused transcardially with 4% paraformaldehyde (PFA), sciatic nerves isolated, frozen and 10 µm cryosections collected. For tissue imaging, frozen sections were incubated with primary antibodies directed against p75^{NTR} (G323A, Promega), βIII-tubulin (G7121, Promega) and contactin-associated protein 1 (Caspr, a kind gift from Professor Elior Peles, Weizmann Institute of Science, Israel), diluted in blocking buffer containing 10% FBS and 0.3% Triton X100 in PBS. Incubation with proper fluorophore-conjugated secondary antibodies (Invitrogen) was followed. PBS was then used to wash the sections that were finally mounted in DAKO mounting medium containing DAPI. Three animals per group were evaluated, and images captured by confocal microscopy (LSM 780, Carl Zeiss, Germany).

Western Blot Analysis

Sciatic nerves from adult control littermates ($n = 6$) and SC-p75^{NTR}-KO ($n = 6$) mice were dissociated in lysis buffer (2 mM CaCl₂, 1 mM MgCl₂, 10 mM HEPES, 140 mM NaCl and 1% Triton X-100, pH 7.8, with protease inhibitors from Roche) and centrifuged at $10,000 \times g$ for 10 min at 4°C. Total protein concentration was determined using the Bicinchoninic Acid kit from Sigma. Protein lysates were run on 12% SDS-PAGE (20 µg/lane) and electro-blotted for 1.5 h onto polyvinylidenedifluoride (PVDF) filters (Amersham) in 192 mM glycine, 25 mM Tris-HCl, pH 8.0. Membranes were then blocked and incubated overnight at 4°C with the primary antibodies: rabbit anti-p75^{NTR} (1:500, Promega, Cat. #G323A) and mouse anti-β-actin (1:5000, Sigma, Cat. #A5441). Following a washing step, membranes were incubated with horseradish peroxidase (HRP)-conjugated secondary antibodies (1:1000, swine anti-rabbit, Dako, Cat. # P0217; rabbit anti-mouse, Dako # P0260) and blots visualized with the Amersham ECL plus western blotting detection reagents (GE Healthcare) and Fuji film LAS1000. Densitometry was performed with QuantityOne software (Bio-Rad).

Morphological and Morphometric Analysis

Nerve samples were processed for morphological and morphometrical analysis of myelinated and unmyelinated nerve fibers. Fixation of nerve samples was carried out using 2.5% purified glutaraldehyde and 0.5% sucrose in 0.1M Sorensen phosphate buffer for 2–4 h. Samples were subsequently post-fixed in 2% osmium tetroxide for 2 h at 4°C and dehydrated in a sequence of ethanol from 30 to 100%. After being cleared in propylene oxide, samples were embedded in Glauerts' embedding mixture of resins containing equal parts of Araldite M and Araldite Harter, HY 964 (Merck, Darmstadt, Germany), including 0.5% of the plasticizer dibutyl phthalate and 1–2% of the accelerator 964, DY 064 (Merck). For high-resolution light microscopy, semi-thin transverse sections (2.5 µm) were cut in a Leica Ultracut UCT ultramicrotome (Leica Microsystems, Wetzlar, Germany) and stained with Toluidine blue. Stereology was performed in a DM4000B microscope equipped with a DFC320 digital camera and an IM50 image manager system (Leica Microsystems, Wetzlar, Germany). Systematic random sampling and D-dissector were adopted using a protocol previously described (Geuna et al., 2000, 2004). Total number of myelinated fibers, axon and fiber size, myelin thickness and g-ratio were then determined.

For electron microscopy, ultrathin sections (70 nm thickness) were cut by using an ultramicrotome Leica EM UC7 (Leica, Wien, Austria). Sections were collected onto formvar-coated slot grids and counterstained with uranyl acetate and lead citrate. A 100 kV transmission electron microscope (EM JEM 1230, JEOL Ltd., Tokyo, Japan) was used for qualitative and quantitative examination of the samples. For C-fiber counting, we started at one corner of the fascicle and acquired images of every third microscopic field with 15,000× magnification until 35 images were photographed. C-fibers in the images were counted and their density calculated.

Schwann Cell Cultures Derived From Sciatic Nerves of Adult Mice

Schwann cell cultures from adult mouse sciatic nerves were prepared as described by Wang and colleagues (Wang et al., 2013), with some alterations to the protocol. In brief, $n = 16$ littermates and $n = 16$ SC-p75^{NTR}-KO mice were sacrificed by cervical dislocation prior to sciatic nerve dissection into L-15 medium. The dissected nerves were rinsed in PBS and incubated in Schwann cell culture medium [SCCM; DMEM supplemented with 10% FBS, 2 µM forskolin (Sigma, Cat. #F6886), 10 ng/mL human heregulin-β1 (R&D Systems, Cat. #396-HB) and 50 ng/mL b-FGF (PeproTech, Cat. #100-18B)] for 1 week at 37°C and 5% CO₂. The media was changed every 2 days. Nerves were then cut into approximately 2 mm and digested for 40 min with a mixture of 0.2% collagenase NB4 Standard Grade (Nordmark Biochemicals, Cat. #S1745402) and 0.2% dispase (Sigma, Cat. #D4693) at 37°C and subsequently triturated and plated onto poly-L-lysine coated 60 mm dishes and incubated for 2 days in SCCM. The mixed cultures where

then trypsinized and plated on coverslips at a density of 100,000 cells/coverslip and cultured for additional 2 days before fixation in 4% PFA for further processing.

Immunocytochemistry and Microscopy of Schwann Cell Cultures

The fixed Schwann cell cultures were permeabilized with PBS containing 0.1% Triton-X 100 for three times 10 min and subsequently incubated in PBS containing 5% donkey serum and 1% BSA to block unspecific binding of the antibodies. The cells were incubated with rabbit anti-p75^{NTR} [1:1500, (Huber and Chao, 1995), Cat. #9651] diluted in PBS containing 1% BSA overnight at 4°C. The samples were incubated 1 h at room temperature the following day before three times 10 min wash in PBS and 4 h incubation with AlexaFluor488 donkey anti-rabbit IgG (H+L) (1:300, Life Technologies, #A21206) diluted in PBS containing 1% BSA. After three times 10 min washing, Hoechst 33258 was used for nuclear staining (1:10,000, Sigma). Sections were then mounted with Dako Fluorescent mounting medium and sealed with nail polish. Images were acquired with a ZEISS Axio Imager 2 microscope (Carl Zeiss, Germany) equipped with a Hamamatsu digital camera (ORCA-flash4.0 digital camera, model C11440-22CU, Hamamatsu Photonics Deutschland GmbH, Germany) and subsequent image analysis performed with ImageJ.

Statistical Analysis

Statistical comparison of data was accomplished using the Student *t*-test or One/Two-way ANOVA followed by Bonferroni post-test, with Graph Pad Prism software. Quantitative data is reported as mean ± SEM. Statistical significance was established for $p^* < 0.05$, $p^{**} < 0.01$, $p^{***} < 0.001$.

RESULTS

Targeted Disruption of p75^{NTR} in Schwann Cells

To generate an *in vivo* model appropriate for investigating the involvement of Schwann cell-expressed p75^{NTR} in peripheral myelination, we developed mice with selective deletion of p75^{NTR} in Schwann cells. For this purpose, mice harboring *loxP* recognition sites in the *Ngfr* gene (Boskovic et al., 2014) were crossed with transgenic mice in which *Cre* recombinase is expressed under the control of the Myelin Protein Zero (P0) promoter (Feltri et al., 1999), to finally produce SC-p75^{NTR}-KO mice. The P0 promoter becomes active in Schwann cell precursors at embryonic day 13.5–14.5, which includes cells that develop into both myelinating and non-myelinating Schwann cells but excludes other glial cells and dorsal root ganglion neurons (Feltri et al., 1999, 2002). Therefore, upon introduction of *Cre* recombinase (as heterozygote *Cre*^{+/−}), the *Ngfr* genomic DNA flanked by *loxP* sites is inverted and expression of p75^{NTR} in Schwann cells is replaced with that of mCherry, while *Cre*-negative (*Cre*^{−/−}) littermate controls have unchanged p75^{NTR} expression (Figure 1A). Immunofluorescent

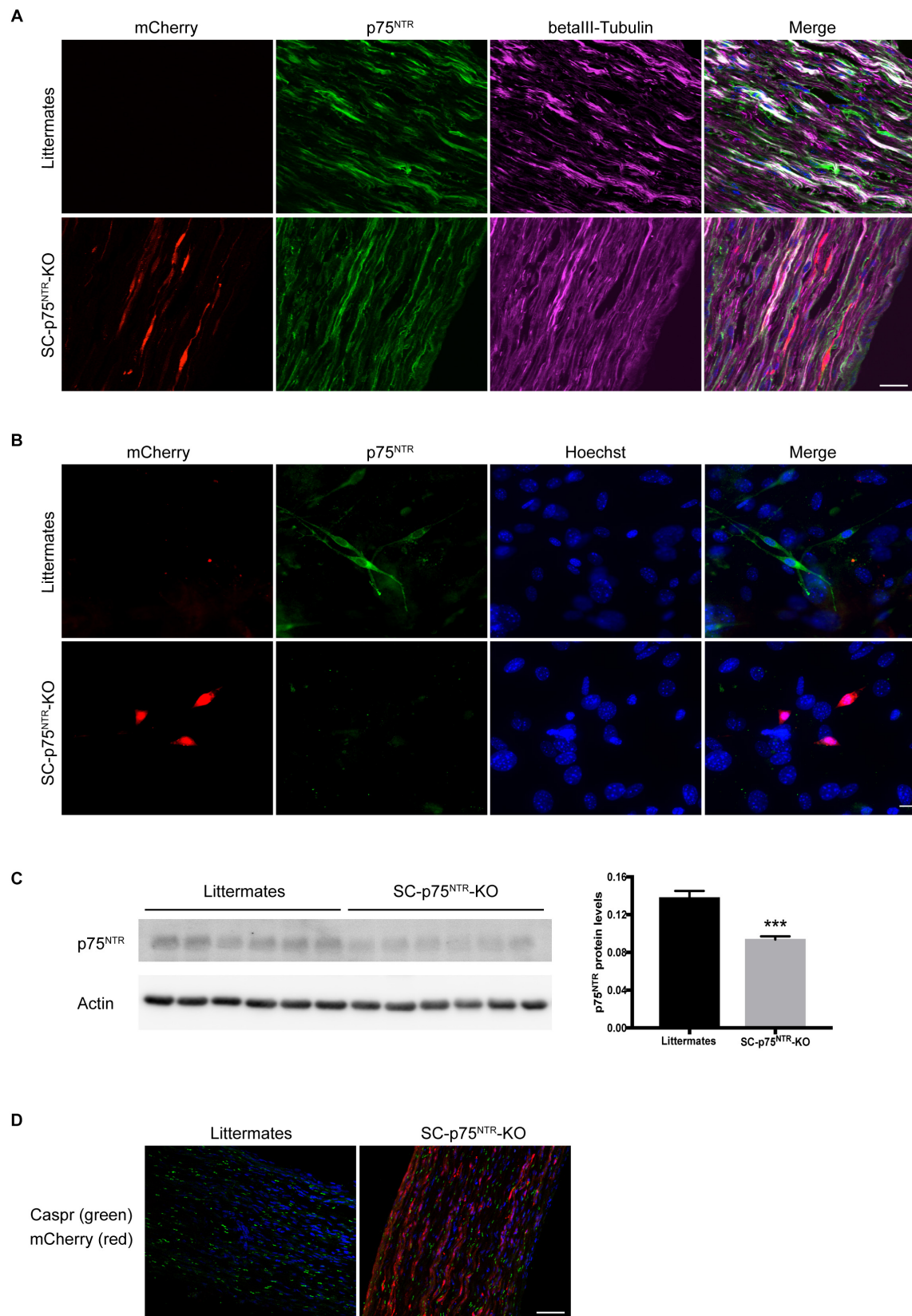


FIGURE 1 | Continued

FIGURE 1 | P75^{NTR} inactivation in Schwann cells. **(A)** Double-label immunofluorescence microscopy of p75^{NTR} (green) and β III-tubulin (pink) in P11 sciatic nerve of SC-p75^{NTR}-KO and WT littermates. mCherry emitting fluorescence was identified in channel 568. Nuclei are labeled with Hoechst (blue). The overlap of tubulin and p75^{NTR} reflects axonal p75^{NTR} (white). Note that in the WT, there is a noticeable amount of p75^{NTR} staining that does not overlap with tubulin (green color in the merge), possibly due to p75^{NTR} expression in Schwann cells. Images represent $n = 4$ mice/group; scale bar 25 μ m. **(B)** Fluorescence images of cells that were primary cultured from adult mice sciatic nerves, fixed and stained with an antibody against p75^{NTR} (green). mCherry 568 fluorescence was observed in Schwann cells from SC-p75^{NTR}-KO but not WT littermates. In the merge panel, it is clear that p75^{NTR} was only present in Schwann cells and not fibroblasts from the WT nerves (cells with bigger nuclei displayed with Hoechst, blue), being completely absent in the SC-p75^{NTR}-KO. Scale bar 10 μ m; $n = 16$ mice/group. **(C)** P75^{NTR} was determined by immunoblot analysis in extracts of sciatic nerves isolated from adult mice. Quantification of p75^{NTR} ratios by densitometry against levels of β -actin. Data represent the mean \pm SEM for six mice/genotype (** $p < 0.001$ compared with littermate controls). **(D)** Immunofluorescence microscopy of Caspr (green) in naïve P11 sciatic nerves. Note similar intensity and distribution of immunoreactivity throughout the tissue in both genotypes. Nuclei are identified with DAPI (blue) and mCherry visualized in the red channel in SC-p75^{NTR}-KO mice. Scale bar, 50 μ m; $n = 4$ mice/group.

staining of sciatic nerves demonstrated a significant amount of p75^{NTR} immunostaining in axons of both SC-p75^{NTR}-KO or littermate controls (**Figure 1A**), confirming that SC-p75^{NTR}-KO mice continuously express p75^{NTR} in peripheral neurons/axons. To further substantiate that the inversion strategy resulted in loss of p75^{NTR} protein in Schwann cells, we prepared Schwann cell primary cultures from adult mice. Our results clearly confirmed that SC-p75^{NTR}-KO derived Schwann cells presented red mCherry fluorescent signal and no p75^{NTR} immunostaining, with contrary observations in Schwann cells isolated from the littermate controls (**Figure 1B**). Western blot analysis of lysates isolated from whole sciatic nerves demonstrated an approximately 30% reduction of p75^{NTR} expression in SC-p75^{NTR}-KO nerves relative to littermate control nerves (**Figure 1C**), revealing that the majority of p75^{NTR} protein in adult mouse sciatic nerves is expressed by other cell types, primarily neurons (axons). We did not detect any evidence of altered Mendelian ratios of the SC-p75^{NTR}-KO mice relative to littermate controls, and deviation in size or weight was not found between adult mice of different genotypes (data not shown). Finally, there were no indication of any overt neurological abnormalities in the SC-p75^{NTR}-KO mice, and Caspr immunostaining in developing nerve (at P11) did not reveal any differences between paranodal junctions in myelinated fibers between genotypes (**Figure 1D**).

SC-p75^{NTR}-KO Mice Exhibit Mild Behavioral Defects After Nerve Injury

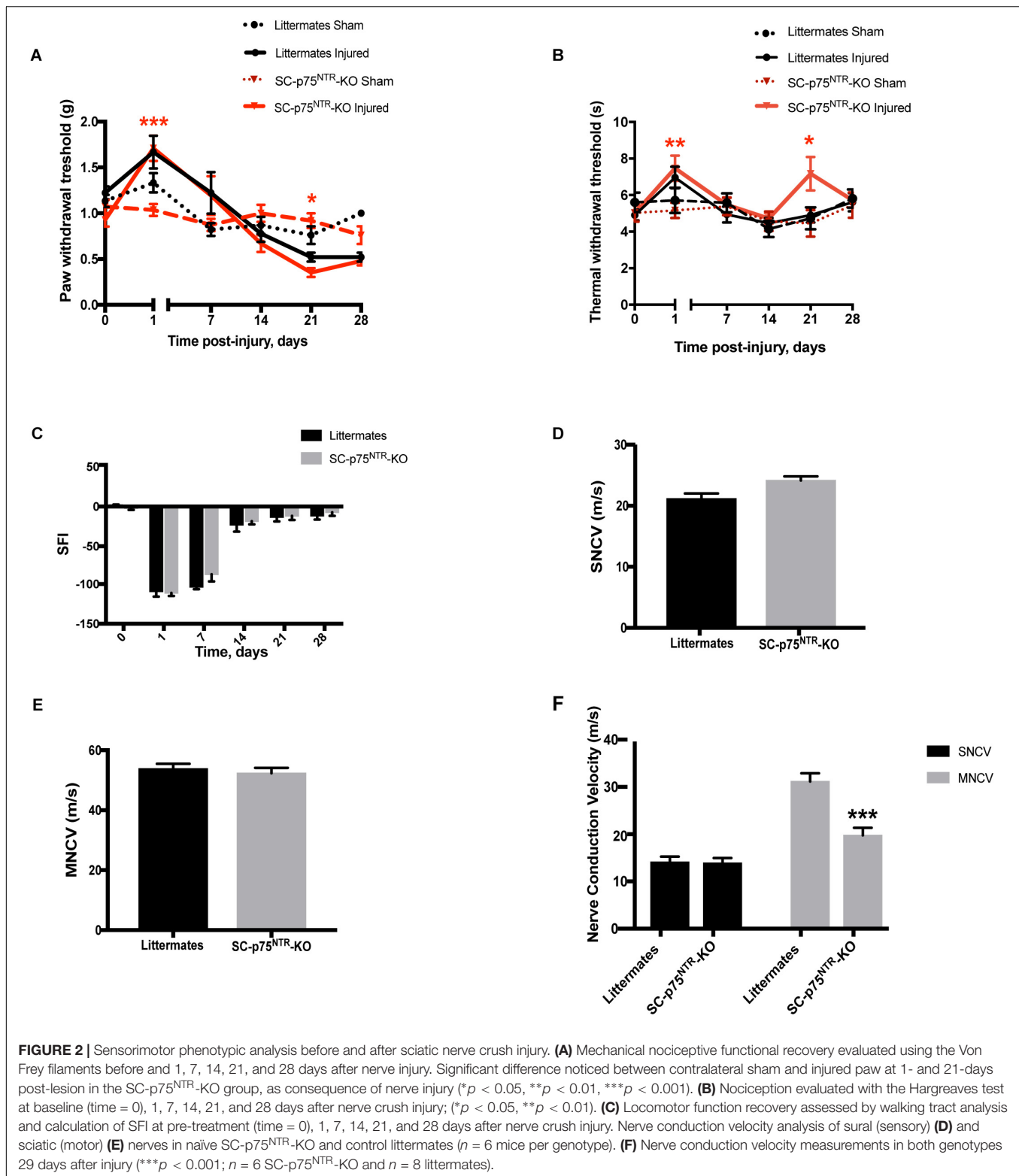
To investigate the sensorimotor phenotype of SC-p75^{NTR}-KO mice, we initially evaluated sensory profiles by von Frey filaments (mechanical sensitivity) and Hargreaves test (thermal/heat sensitivity), as well as motor recovery by walking tract analysis. Tests were performed as pre-injury baseline (time point = 0) and at 1, 7, 14, 21, and 28 days following sciatic crush injury. Baseline levels were equivalent between sham-operated SC-p75^{NTR}-KO and littermate controls for both Von Frey and Hargreaves tests (**Figures 2A,B**). As expected, both genotypes demonstrated reduced sensitivity from day 1 post-injury, confirming destruction of sensory axons by the crush procedure. Mechanical sensitivity increased over the following period for both genotypes, likely reflecting axonal regeneration and accompanying reinnervation of target tissues. The recovery profile was largely identical for the two genotypes, reaching baseline levels at day 14 and with a non-significant tendency

of increased sensitivity in the injured paw. For the SC-p75^{NTR}-KO we observed a small but significant transient decrease in mechanical threshold at day 21 (relative to the contralateral uninjured paw), however, this effect was absent at day 28 (**Figure 2A**). Hargreaves test demonstrated a pattern largely identical to that of the von Frey test; 1-day after injury, both SC-p75^{NTR}-KO mice and littermate controls experienced reduced sensitivity to heat-induced noxious stimulus that recovered to baseline levels by day 7. We again observed a transient reduction in sensitivity 21 days following nerve crush in the SC-p75^{NTR}-KO mice, which was absent by day 28 (**Figure 2B**). Recovery of motor function was determined by assessing the SFI at the same time points as for the sensory tests. No differences were found at day 0 or any other time point after sciatic nerve crush injury among the two mice groups (**Figure 2C**).

Electrophysiological properties of the sciatic nerves were evaluated by measurements of sensory and motor nerve conduction velocity (SNCV and MNCV, respectively) at 29 days post nerve damage, as a terminal endpoint. Nerves from naïve SC-p75^{NTR}-KO mice and littermate controls displayed identical SNCV (**Figure 2D**) and MNCV (**Figure 2E**). As expected, SNCV and MNCV were significantly reduced following the injury. However, although we did not detect any difference in post-injury SNCV between SC-p75^{NTR}-KO mice and littermate controls, SC-p75^{NTR}-KO mice exhibited a further 36% reduction of post-injury MNCV relative to littermate controls (**Figure 2F**), pointing toward ion leakage or/and structural defects in the largest myelinated axons.

Conditional Deletion of p75^{NTR} in Schwann Cells Has No Impact on Peripheral Myelination or Axon Regeneration Following Nerve Injury

The observation of decreased MNCV in the injured SC-p75^{NTR}-KO mouse model could be due to variation in Schwann cell remyelination of the damaged axons since appropriate re-myelination after peripheral nerve injury has previously been attributed to p75^{NTR} (Song et al., 2006; Tomita et al., 2007). We therefore evaluated nerve fiber morphology in semi-thin cross-sections of sciatic nerves using light microscopy. Representative images of sciatic nerves from SC-p75^{NTR}-KO and littermate controls, 15 and 29 days after injury, together with respective non-lesioned nerves (contralateral sham) are illustrated in **Figure 3A**.



Naïve sciatic nerves from SC-p75^{NTR}-KO mice appeared normal, with axons of various diameters present in proportions that appeared similar to those observed in littermate controls and with similar total numbers of myelinated axons (Figures 3A,B).

Features of myelinated axonal degeneration consistent with axonal loss were observed in both SC-p75^{NTR}-KO and littermate controls after injury, with a similar decrease in axon number (Figure 3B) in mice of both genotypes, however, only statistically

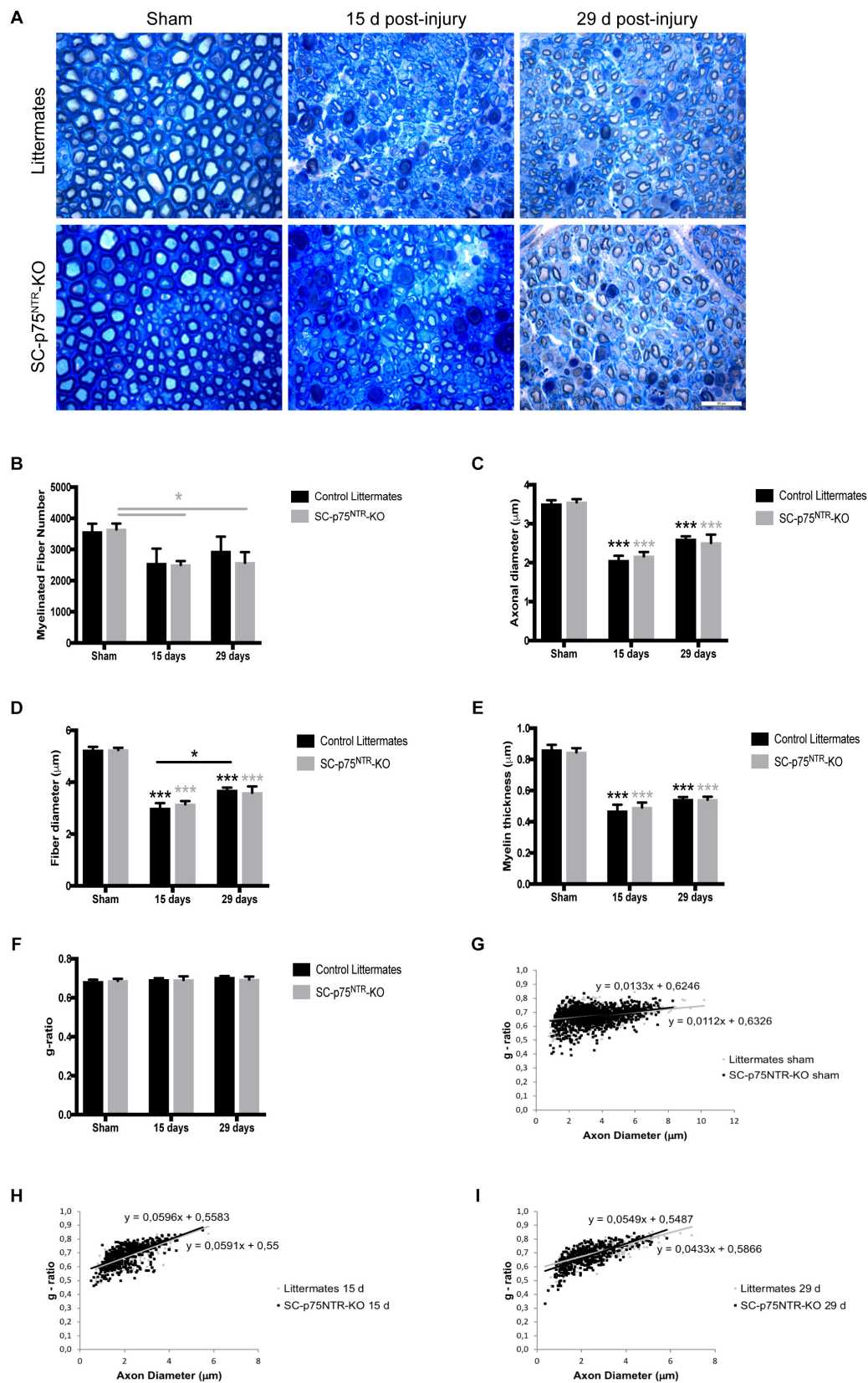


FIGURE 3 | Continued

FIGURE 3 | Ablation of p75^{NTR} in Schwann cells has no impact on re-myelination after nerve injury. **(A)** Representative light microscopy images of toluidine-blue stained semithin transverse sections of sham contralateral and distal stumps from crush injured nerves, 15- and 29-days post-lesion. Scale bar 20 μ m. **(B–G)** Histograms obtained from the morphometrical analysis of the myelinated fibers. **(B)** Total number of myelinated fibers, **(C)** axon diameter, **(D)** fiber diameter, **(E)** myelin thickness, and **(F)** g-ratio. Scatter plots showing g-ratio of individual myelinated axons as a function of axon diameter in contralateral shams **(G)** or injured nerves at time points of 15 **(H)** and 29 days post lesion **(I)**. Numbers for quantifications were as follows: $n = 11$ sham, $n = 6$ at 15 days, and $n = 6$ at 29 days for SC-p75^{NTR}-KO; $n = 9$ sham, $n = 3$ at 15 days, and $n = 6$ at 29 days for littermates.

different in the SC-p75^{NTR}-KO mice. Mean of axonal diameter (**Figure 3C**), fiber diameter (**Figure 3D**) or myelin thickness (**Figure 3E**) were unchanged between genotypes both before and following crush injury, but with an injury effect over time, compared with the respective shams, as expected. Quantification of acquired light microscopy images (with about 100 fibers analyzed per animal) revealed no differences in averaged g-ratios (**Figure 3F**) or in g-ratios of individual fibers vs. axon diameters, as illustrated by scatter plots of sham and injured nerves, 15 or 29 days after damage (**Figures 3G–I**).

Proceeding with ultrastructural EM analysis of sciatic nerve transverse sections, we found that the uninjured contralateral nerve of both SC-p75^{NTR}-KO and control mice was dominated by large and medium-sized myelinated axons. Unmyelinated axons (C-fibers) occurred in large groups embedded in Schwann cells, forming Remak bundles (**Figure 4A**, left panel). The endoneurium contained several blood vessels, fibroblasts, and a few mast cells and macrophages. No variance in C-fiber density was observed between the two mice cohorts (**Figure 4B**). Pathology was evident in the injured ipsilateral side of mice of both genotypes 15 days after crush, with most large myelinated axons being absent and several medium-sized remyelinated axons present in the endoneurium (**Figure 4C**). At days 15 and 29 post injury we observed myelin debris, multi-vesicular bodies (MVB) and osmophilic and osmophobic fat droplets in the perineurium, endoneurium, Schwann cells, macrophages, fibroblasts and pericytes in all injured nerves. Segmental demyelination of the internodal length and paranode (**Figure 4D**) was a prominent feature of injured nerves from both WT and SC-p75^{NTR}-KO mice. Unmyelinated axons were very sparse and predominantly appeared solitary rather than in high numbers in Remak bundles in the Schwann cell cytoplasm (**Figure 4A**, right panel). No obvious morphological differences were found between control littermates and SC-p75^{NTR}-KO mice; however, although not statistically significant, the mean C-fiber density in SC-p75^{NTR}-KO mice tended to be slightly decreased compared to that of littermate controls, 29 days after injury (**Figure 4B**). This result suggests that lack of p75^{NTR} expression in Schwann cells can possibly alter their molecular signaling profile, affecting glial-axon communication and slowing down the C-fiber regenerative process.

DISCUSSION

In this study, to elucidate the *in vivo* function of p75^{NTR} in Schwann cells during re-myelination and regeneration after peripheral nerve injury, we generated a new mouse model for the conditional deletion of p75^{NTR} in Schwann cells.

Through functional testing, morphological and morphometrical analyses of SC-p75^{NTR}-KO mice, we found that ablation of p75^{NTR} in Schwann cells correlated with a reduced motor nerve conduction velocity but had no impact regarding remyelination or axonal growth after sciatic nerve crush injury.

p75^{NTR} is widely expressed in the nervous system during development and has even been considered as a neural crest marker (Wislet et al., 2018). Although p75^{NTR}, also called NGF receptor, has no intrinsic catalytic activity, it interacts and modulates the function of TrkA, TrkB, and TrkC, providing substantial cellular and molecular diversity for regulation of neuron survival, neurogenesis, immune responses and processes that support neural function (McGregor and English, 2019). In Schwann cells, p75^{NTR} is expressed by the immature type during development and remains being expressed by the mature non-myelinating Schwann cells in the adult. In contrast, myelinating Schwann cells are not immunoreactive for p75^{NTR} (Jessen and Mirsky, 2005). Because p75^{NTR} is highly down-regulated as the nervous system matures, a powerful tool to induce expression of this receptor is the dedifferentiation of Schwann cells by induced nerve injury. Several reports demonstrated dramatic upregulation of p75^{NTR} in response to injury or disease, in both the PNS and CNS (Meeker and Williams, 2015). However, these previous studies focusing on the roles of p75^{NTR} in development and nerve regeneration have utilized the complete p75^{NTR} KO mouse model, resulting in loss of p75^{NTR} in both Schwann cells as well as in a DRG neuron subpopulation (Lee et al., 1992; von Schack et al., 2001).

Two complete p75^{NTR} KO models have been developed, both of which demonstrate a dramatic PNS phenotype with approximately 50% reduction in neuron/myelinated axon number as well as reduced myelination of the remaining axons. The first model was constructed by deleting exon III of the *Ngfr* gene (Lee et al., 1992), however, it later turned out that this model produces an alternatively spliced isoform of p75^{NTR} (s-p75^{NTR}), producing a protein that lacks the portion of the extracellular domain responsible for neurotrophin binding but with its intracellular death-signaling moiety intact (Murray et al., 2003). Complicating the picture, it appears that the genetic background of the mouse also impacts on the phenotype as expression of the s-p75^{NTR} splice variant demonstrated a strain dependent expression level (Naumann et al., 2002). This finding triggered the development of another KO model, the exon IV KO model (p75^{NTR}ExonIV) which does not express the s-p75^{NTR} variant. The p75^{NTR}ExonIV mice display a more severe phenotype than the previous p75^{NTR}exonIII mutants, including a larger reduction in the number of DRG neurons and Schwann cells, vascular system defects, and approximately 40% of p75^{NTR}ExonIV mice do not survive beyond the perinatal

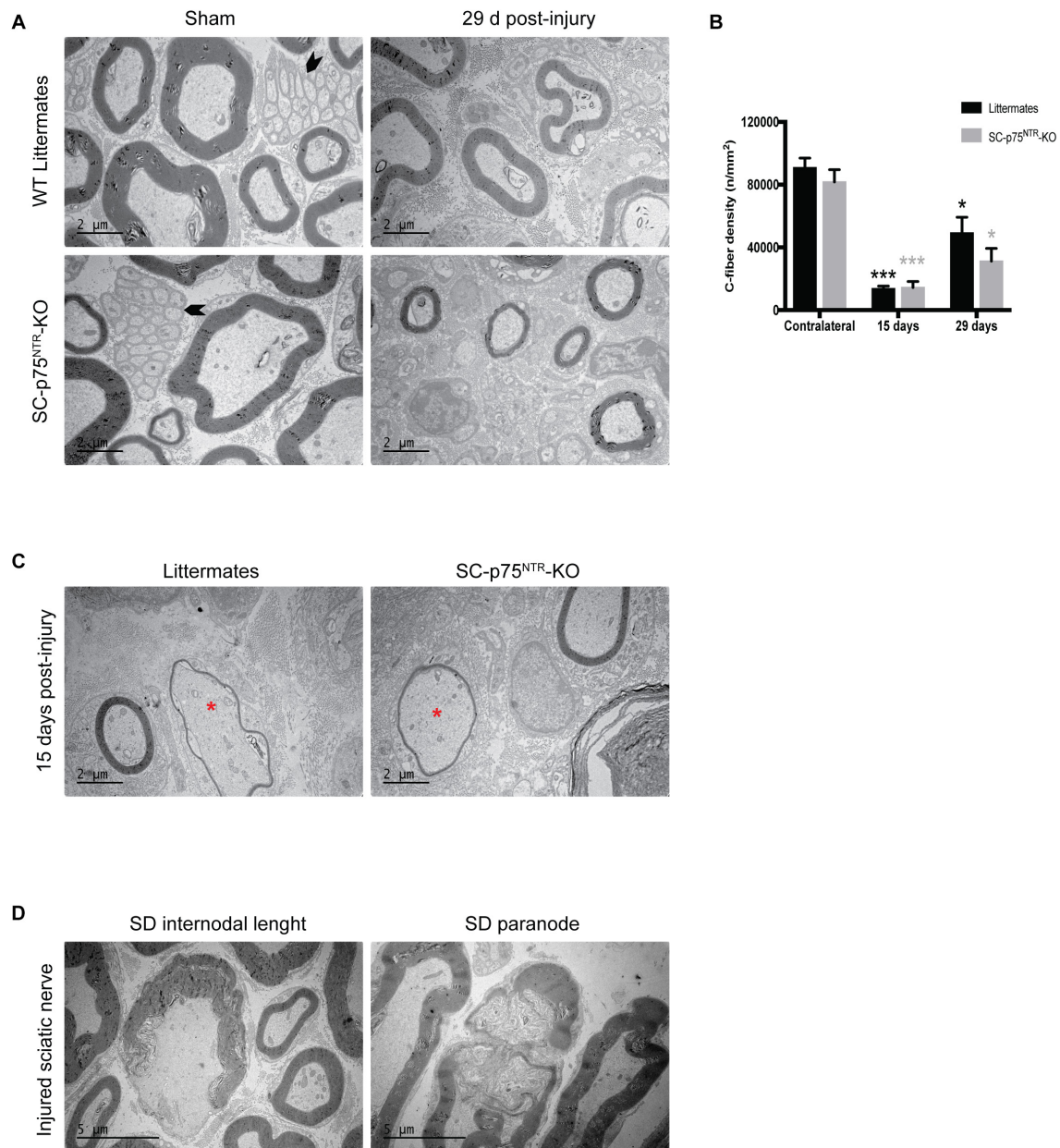


FIGURE 4 | Trend toward decreased C-fiber density in injured nerves from mice lacking Schwann cell p75^{NTR} expression. **(A)** Representative images of ultrathin transverse sciatic nerve sections from sham contralateral nerves (left panel) and 29 days post injury distal stumps (right panel) of the two experimental groups. Arrowheads identify C-fibers. Scale bar 2 μ m. **(B)** Density of C-fibers expressed as number of unmyelinated axons per square millimeter (n/mm²). Numbers for quantifications were as follows: $n = 12$ sham, $n = 6$ at 15 days, and $n = 4$ at 29 days for SC-p75^{NTR}-KO; $n = 9$ sham, $n = 3$ at 15 days, and $n = 4$ at 29 days for littermates. **(C)** Electron micrographs showing re-myelinated fibers (asterisk) in both SC-p75^{NTR}-KO and control WT littermates, 15 days after sciatic nerve crush injury. **(D)** Representative pictures of segmental demyelination observed in both strains after sciatic nerve injury, both at internodal and paranodal regions. Scale bar 5 μ m.

period (von Schack et al., 2001). It was, however, soon determined that the p75^{NTR}ExonIV model express a p75^{NTR} gene product encoding a truncated protein with an apparent molecular weight of 26 kDa (Paul et al., 2004). The utilization of mouse models with a general targeting profile (including both neurons and Schwann cells) combined with the incomplete nature of the p75^{NTR} deletions and the difficulties in delineating the impact of

the genetic background, all complicates a rigorous interpretation of previous findings on the role of p75^{NTR} in specific PNS cell subpopulations.

In the present study, the conditional deletion of p75^{NTR} in Schwann cells is driven by the P0 promotor, expressed in Schwann cell precursors early in development (around E14), thus silencing p75^{NTR} expression in both myelinating and

non-myelinating Schwann cells types (Feltri et al., 1999). Several studies support a key role for p75^{NTR} in the myelination process (Chan et al., 2001; Cosgaya et al., 2002; Tolwani et al., 2004). Surprisingly, our present results demonstrate that depleting the myelinating Schwann cell subpopulation of p75^{NTR} during the myelination process does not compromise myelin sheet formation nor motor function in the adult naïve SC-p75^{NTR}-KO mice.

Boskovic et al. (2014) have not detected any splice variant at the transcriptional or protein levels when developing the p75^{in/in} mouse line used in our study. The fact that we see no neuronal phenotype (reduction in axon number) supports that the model is “clean” from the splice variants found in the p75^{NTR}ExonIII and p75^{NTR}ExonIV models (which display dramatic PNS phenotypes). Besides neurons and Schwann cells, other cells types have been reported to express p75^{NTR} such as macrophages (Wong et al., 2010), endothelial cells (Tanaka et al., 2004), white fatty tissue (Peeraully et al., 2004), and fibroblasts (Palazzo et al., 2011). Whether such cell types in the sciatic nerve also express p75^{NTR} remains to be determined but this (along with continued axonal expression) may explain the remaining expression of p75^{NTR} in the sciatic nerve upon deletion of Schwann cell p75^{NTR}. Our *in vitro* cultures of mouse Schwann cells reveal that these cells are indeed devoid of p75^{NTR} (and positive for mCherry, confirming Cre-activity in these cells).

Due to the pleiotropic roles of p75^{NTR}, it is not surprising that its role in regeneration following nerve injury has been controversial. While Song et al. observed reduced regeneration in the p75^{NTR} KO model, work from Scott and Ramer reported that p75^{NTR} expressed by Schwann cells is actually deleterious for nerve regeneration. The mechanism suggested was that increased Schwann cell p75^{NTR} expression might sequester endogenous neurotrophins and thus reduce their availability for axonal Trk signaling (Scott and Ramer, 2009); a notion supported by the enhanced regeneration of injured peripheral motor axons in mice lacking the neurotrophin-binding domain of p75^{NTR} (Boyd and Gordon, 2001). In contrast with this observation, another study using transplantation of p75^{NTR}-deficient Schwann cells to injured nerves from nude mice found that a lack of glial p75^{NTR} had a negative impact in the regeneration of motor neurons (Tomita et al., 2007). This model is closer to ours in terms of Schwann cell selectivity, however, the fact that they used nude mice may complicate comparisons since other mechanisms might have been activated by the inhibited immune system, which consequently altered the Schwann cell-axon signaling profile. Nevertheless, like in our study, no difference in the total number of myelinated fibers and fiber density was observed, but a significant decrease in motor nerve conduction velocity was detected (Tomita et al., 2007). Myelin affects nerve conduction velocity and in contrast with our observations, p75^{NTR} null Schwann cell-grafted mice displayed a significant decrease in myelin thickness (Tomita et al., 2007), which could explain the altered motor nerve conduction profile. Yet, this is not always the case; for example, in mouse models of diabetic neuropathy, decreased nerve conduction velocity is often not accompanied by demyelination or fiber loss (Hinder et al., 2017). The reason why this happens is not really understood, but

several factors are known to alter nerve conduction velocity in addition to motor axon loss or decreased myelin thickness, such as length of nodal gap (Arancibia-Cárcamo et al., 2017), nodal axonal hydropic swelling (Kolaric et al., 2013), distribution of sodium channels, defects in the Na⁺/K⁺ ATPase (Freeman et al., 2016), impaired Schwann cell exocytosis (Chen et al., 2012), mitochondrial fiber deficiency (Viader et al., 2011; Bala et al., 2018) or reduced endoneurial nutritive blood flow (Coppey et al., 2001). We speculate that in our model, the segmental demyelination of the internodal length and paranode in the SC-p75^{NTR}-KO injured nerves leads to leakage of ions from the axons culminating with slower motor nerve conduction velocities, throughout a mechanism that still needs further clarification but that might involve alterations in axonal sodium channels, molecular signaling or composition, and differential regulation of myelin production and repair (Taveggia et al., 2010). Thus, it is fair to speculate that p75^{NTR} might have a role in internode length and/or nodal composition after injury. In line with this, the regulation of neuronal form and function by Schwann cells has been found to be mediated by different forms of intercellular communication (Orellana et al., 2012; Samara et al., 2013), and recent findings suggest the occurrence of lateral molecular cargo transfer to axons mediated by exosomes secreted from Schwann cells (Lopez-Verrilli and Court, 2012). This mechanism has been poorly explored to date, but recent papers have described Schwann cell secreted exosomes being incorporated into axons and increasing neurite sprouting (Court et al., 2008; Lopez-Verrilli et al., 2013). These findings open a new dimension to the degree of intercellular interactions and the idea of a functional nerve syncytium. Deletion of p75^{NTR} in Schwann cells had no apparent effect on basic sciatic nerve structure (developmental effects) including the number or density of myelinated and unmyelinated axons, myelination (g-ratio), nor on regeneration upon crush injury. This is somewhat surprising, considering the observations that p75^{NTR} is highly expressed in Schwann cells during development and the regenerative process. It is now accepted that neurons can synthesize proteins locally in axons and dendrites, and that this localized translation is required for neuronal homeostasis (Jung et al., 2012). Perhaps neurons/axons develop compensatory mechanisms to balance and counteract the absence of p75^{NTR} Schwann cell expression, altering e.g., vesicle cargo and the glial-axon communication process?

A mouse line carrying a conditional knockout allele for p75^{NTR} (p75^{NTR}ExonIV–VI) was previously generated to investigate its functions in DRG neurons *in vivo* (Bogenmann et al., 2011). The allele was designed such that a complete and conditional knockout could be achieved without the molecular complexities observed in mice with either the p75^{NTR}ExonIII (von Schack et al., 2001) or the p75^{NTR}ExonIV allele (Paul et al., 2004). While otherwise normal in size (contrasting the ExonIV model), p75^{NTR}ExonIV–VI mice displayed an abnormal hind limb “clenching” phenotype similar to that seen in p75^{NTR}ExonIII and p75^{NTR}ExonIV mice, suggesting that this common neuropathic phenotype was at least in part due to the impaired function of p75^{NTR} specifically in neural crest cells. In addition, there were far fewer small (unmyelinated and lightly myelinated) diameter axon bundles in the mutant nerves

(Bogenmann et al., 2011). Another study using stereological counting demonstrated that p75^{NTR}ExonIII mice display a 52% loss of DRG neurons, with the loss of small nociceptors being larger than the loss of large proprioceptors (57 vs. 39%, respectively), and these data were supported by similar results obtained by nerve fiber counts of unmyelinated vs. myelinated axons (Gjerstad et al., 2002). This could either reflect that p75^{NTR} expression occurs predominantly in small nociceptors or that it is most important for non-myelinating Schwann cells to support axon survival, homeostasis and growth. The fact that non-myelinating Schwann cells express p75^{NTR} in adult mice in contrast to the myelinating type also fits well within this observation. Recently, one study indicated that neuron-specific deletion of p75^{NTR} at E12.5 was insufficient to impact on neuronal survival during embryogenesis whereas 20% of DRG neurons were lost in adult mice, suggesting that neuronal p75^{NTR} functions only postnatally in sensory neuron diversification (Chen et al., 2017). In our Schwann cell conditional p75^{NTR} KO mouse model, we found a trend for reduced preservation of unmyelinated fibers in the sciatic nerve 29 days after injury. The crush injury model is a model of axonotmesis, in which axons are disrupted but the connective tissue and the Schwann cell basal lamina remains intact. When this crush model is applied in rodents, axonal regeneration is remarkably efficient and function is restored in 3–4 weeks (Jessen et al., 2015). Thus, it would be predictable that potential early or late differences regarding remyelination and axon regeneration would be detected by evaluation of nerve morphology and morphometry at both 15- and 29-days post-crush injury. Nevertheless, whether different outcomes could have been found at even earlier time points after nerve injury remains to be investigated.

In summary, the influence that p75^{NTR} exerts upon the regenerative and remyelination processes in the PNS remain controversial, with conflicting findings in DRG- and motor neurons (Tomita et al., 2007; Scott and Ramer, 2009) and a lack of clarity around Schwann cell and neuronal influences. Through utilization of a Schwann cell specific p75^{NTR} knockout strategy, we demonstrate that Schwann cell expression of p75^{NTR} is not important for either sciatic nerve regeneration and remyelination

following crush injury, but does exert important influences upon recovery of motor nerve function.

ETHICS STATEMENT

This study was carried out in accordance with the recommendations of The Florey Institute for Neuroscience and Mental Health Animal Ethics Committee and Danish regulations. The protocol was approved by the Australian Code of Practice for the Care and Use of Animals for Scientific Purposes and the Danish Animal Experiments Inspectorate under the Ministry of Environment and Food.

AUTHOR CONTRIBUTIONS

NG, SSM, and CV designed the experiments. NG, SM, MS, MU, MR, and RW performed the experiments. NG, SM, JX, OA, EC, SR, SSM, and CV interpreted the results, contributed with reagents, materials, and analysis tools. NG, MU, and CV wrote the manuscript. All authors read and helped to complete the manuscript.

FUNDING

This work was supported by Aarhus University Research Foundation (AUFF-E-2015-FLS-8-4), a challenge grant from the Novo Nordisk Foundation (NNF14OC0011633), Dagmar Marshall's Fund, and the Australian National Health and Medical Research Council Project Grant #APP1058647.

ACKNOWLEDGMENTS

We thank Maria Ntzouni at EM lab of Core Facility, Linköping University, Sweden for sectioning and counter staining of electron microscopy samples.

REFERENCES

- Arancibia-Cárcamo, I. L., Ford, M. C., Cossell, L., Ishida, K., Tohyama, K., and Attwell, D. (2017). Node of Ranvier length as a potential regulator of myelinated axon conduction speed. *Elife* 6:521. doi: 10.7554/eLife.23329
- Bala, U., Leong, M. P.-Y., Lim, C. L., Shahar, H. K., Othman, F., Lai, M.-I., et al. (2018). Defects in nerve conduction velocity and different muscle fibre-type specificity contribute to muscle weakness in Ts1Cje Down syndrome mouse model. *PLoS One* 13:e0197711. doi: 10.1371/journal.pone.0197711
- Bogenmann, E., Thomas, P. S., Li, Q., Kim, J., Yang, L.-T., Pierchala, B., et al. (2011). Generation of mice with a conditional allele for the p75^{NTR} neurotrophin receptor gene. *Genesis* 49, 862–869. doi: 10.1002/dvg.20747
- Boskovic, Z., Alfonsi, F., Rumballe, B. A., Fonseka, S., Windels, F., and Coulson, E. J. (2014). The role of p75^{NTR} in cholinergic basal forebrain structure and function. *J. Neurosci.* 34, 13033–13038. doi: 10.1523/JNEUROSCI.2364-14.2014
- Boyd, J. G., and Gordon, T. (2001). The neurotrophin receptors, trkB and p75, differentially regulate motor axonal regeneration. *J. Neurobiol.* 49, 314–325.
- Chan, J. R., Cosgaya, J. M., Wu, Y. J., and Shooter, E. M. (2001). Neurotrophins are key mediators of the myelination program in the peripheral nervous system. *Proc. Natl. Acad. Sci. U.S.A.* 98, 14661–14668. doi: 10.1073/pnas.251543398
- Chao, M. V. (2003). Neurotrophins and their receptors: a convergence point for many signalling pathways. *Nat. Rev. Neurosci.* 4, 299–309. doi: 10.1038/nrn1078
- Chen, G., Zhang, Z., Wei, Z., Cheng, Q., Li, X., Li, W., et al. (2012). Lysosomal exocytosis in Schwann cells contributes to axon remyelination. *Glia* 60, 295–305. doi: 10.1002/glia.21263
- Chen, Z., Donnelly, C. R., Dominguez, B., Harada, Y., Lin, W., Halim, A. S., et al. (2017). p75 is required for the establishment of postnatal sensory neuron diversity by potentiating ret signaling. *Cell Rep.* 21, 707–720. doi: 10.1016/j.celrep.2017.09.037
- Coppey, L. J., Gallett, J. S., Davidson, E. P., Dunlap, J. A., Lund, D. D., and Yorek, M. A. (2001). Effect of antioxidant treatment of streptozotocin-induced diabetic rats on endoneurial blood flow, motor nerve conduction velocity, and vascular reactivity of epineurial arterioles of the sciatic nerve. *Diabetes* 50, 1927–1937.

- Cosgaya, J. M., Chan, J. R., and Shooter, E. M. (2002). The neurotrophin receptor p75^{NTR} as a positive modulator of myelination. *Science* 298, 1245–1248. doi: 10.1126/science.1076595
- Court, F. A., Hendriks, W. T. J., MacGillivray, H. D., Alvarez, J., and van Minnen, J. (2008). Schwann cell to axon transfer of ribosomes: toward a novel understanding of the role of glia in the nervous system. *J. Neurosci.* 28, 11024–11029. doi: 10.1523/JNEUROSCI.2429-08.2008
- Feltri, M. L., D'Antonio, M., Previtali, S., Fasolini, M., Messing, A., and Wrabetz, L. (1999). P0-Cre transgenic mice for inactivation of adhesion molecules in schwann cells. *Ann. N. Y. Acad. Sci.* 883, 116–123. doi: 10.1111/j.1749-6632.1999.tb08574.x
- Feltri, M. L., Porta, D. G., Previtali, S. C., Nodari, A., Migliavacca, B., Cassetti, A., et al. (2002). Conditional disruption of $\beta 1$ integrin in Schwann cells impedes interactions with axons. *J. Cell Biol.* 156, 199–209. doi: 10.1083/jcb.200109021
- Freeman, S. A., Desmazières, A., Fricker, D., Lubetzki, C., and Sol-Foulon, N. (2016). Mechanisms of sodium channel clustering and its influence on axonal impulse conduction. *Cell. Mol. Life Sci.* 73, 723–735. doi: 10.1007/s00018-015-2081-1
- Geuna, S., Gigo-Benato, D., and Rodrigues, A. de C. (2004). On sampling and sampling errors in histomorphometry of peripheral nerve fibers. *Microsurgery* 24, 72–76. doi: 10.1002/micr.10199
- Geuna, S., Tos, P., Battiston, B., and Guglielmone, R. (2000). Verification of the two-dimensional disector, a method for the unbiased estimation of density and number of myelinated nerve fibers in peripheral nerves. *Ann. Anat.* 182, 23–34. doi: 10.1016/S0940-9602(00)80117-X
- Gjerstad, M. D., Tandrup, T., Koltzenburg, M., and Jakobsen, J. (2002). Predominant neuronal B-cell loss in L5 DRG of p75 receptor-deficient mice. *J. Anat.* 200, 81–87.
- Gonçalves, N. P., Vægter, C. B., Andersen, H., Østergaard, L., Calcutt, N. A., and Jensen, T. S. (2017). Schwann cell interactions with axons and microvessels in diabetic neuropathy. *Nat. Rev. Neurol.* 13, 135–147. doi: 10.1038/nrneurol.2016.201
- Gschwendtner, A., Liu, Z., Hucho, T., Bohatschek, M., Kalla, R., Dechant, G., et al. (2003). Regulation, cellular localization, and function of the p75 neurotrophin receptor (p75^{NTR}) during the regeneration of facial motoneurons. *Mol. Cell. Neurosci.* 24, 307–322. doi: 10.1016/S1044-7431(03)00167-2
- Hinder, L. M., O'Brien, P. D., Hayes, J. M., Backus, C., Solway, A. P., Sims-Robinson, C., et al. (2017). Dietary reversal of neuropathy in a murine model of prediabetes and metabolic syndrome. *Dis. Models Mech.* 10, 717–725. doi: 10.1242/dmm.028530
- Huber, L. J., and Chao, M. V. (1995). Mesenchymal and neuronal cell expression of the p75 neurotrophin receptor gene occur by different mechanisms. *Dev. Biol.* 167, 227–238. doi: 10.1006/dbio.1995.1019
- Insera, M. M., Bloch, D. A., and Terris, D. J. (1998). Functional indices for sciatic, peroneal, and posterior tibial nerve lesions in the mouse. *Microsurgery* 18, 119–124. doi: 10.1002/(SICI)1098-2752(1998)18:2<119::AID-MICR10>3.3.CO;2-Z
- Jessen, K. R., and Mirsky, R. (2005). The origin and development of glial cells in peripheral nerves. *Nat. Rev. Neurosci.* 6, 671–682. doi: 10.1038/nrn1746
- Jessen, K. R., Mirsky, R., and Lloyd, A. C. (2015). Schwann cells: development and role in nerve repair. *Cold Spring Harb. Perspect. Biol.* 7:a020487. doi: 10.1101/cshperspect.a020487
- Johnson, E. M. Jr., Taniuchi, M., and DiStefano, P. S. (1988). Expression and possible function of nerve growth factor receptors on Schwann cells. *Trends Neurosci.* 11, 299–304. doi: 10.1016/0166-2236(88)90090-2
- Jung, H., Yoon, B. C., and Holt, C. E. (2012). Axonal mRNA localization and local protein synthesis in nervous system assembly, maintenance and repair. *Nat. Rev. Neurosci.* 13, 308–324. doi: 10.1038/nrn3210
- Kolaric, K. V., Thomson, G., Edgar, J. M., and Brown, A. M. (2013). Focal axonal swellings and associated ultrastructural changes attenuate conduction velocity in central nervous system axons: a computer modeling study. *Physiol. Rep.* 1:e00059. doi: 10.1002/phy2.59
- Lee, K. F., Li, E., Huber, L. J., Landis, S. C., Sharpe, A. H., Chao, M. V., et al. (1992). Targeted mutation of the gene encoding the low affinity NGF receptor p75 leads to deficits in the peripheral sensory nervous system. *Cell* 69, 737–749.
- Lopez-Verrilli, M. A., and Court, F. A. (2012). Transfer of vesicles from schwann cells to axons: a novel mechanism of communication in the peripheral nervous system. *Front. Physiol.* 3:205. doi: 10.3389/fphys.2012.00205
- Lopez-Verrilli, M. A., Picou, F., and Court, F. A. (2013). Schwann cell-derived exosomes enhance axonal regeneration in the peripheral nervous system. *Glia* 61, 1795–1806. doi: 10.1002/glia.22558
- McGregor, C. E., and English, A. W. (2019). The role of BDNF in peripheral nerve regeneration: activity-dependent treatments and Val6Met. *Front. Cell. Neurosci.* 12:28034. doi: 10.3389/fncel.2018.00522
- Meeker, R. B., and Williams, K. S. (2015). The p75 neurotrophin receptor: at the crossroad of neural repair and death. *Neural Regen. Res.* 10, 721–725. doi: 10.4103/1673-5374.156967
- Murray, S. S., Bartlett, P. F., Lopes, E. C., Coulson, E. J., Greferath, U., and Cheema, S. S. (2003). Low-affinity neurotrophin receptor with targeted mutation of exon 3 is capable of mediating the death of axotomized neurons. *Clin. Exp. Pharmacol. Physiol.* 30, 217–222.
- Naumann, T., Casademunt, E., Hollerbach, E., Hofmann, J., Dechant, G., Frotscher, M., et al. (2002). Complete deletion of the neurotrophin receptor p75^{NTR} leads to long-lasting increases in the number of basal forebrain cholinergic neurons. *J. Neurosci.* 22, 2409–2418. doi: 10.1523/JNEUROSCI.22-07-02409.2002
- Oh, S. S., Hayes, J. M., Sims-Robinson, C., Sullivan, K. A., and Feldman, E. L. (2010). The effects of anesthesia on measures of nerve conduction velocity in male C57Bl6/J mice. *Neurosci. Lett.* 483, 127–131. doi: 10.1016/j.neulet.2010.07.076
- Orellana, J. A., Sánchez, H. A., Schalper, K. A., Figueroa, V., and Sáez, J. C. (2012). Regulation of intercellular calcium signaling through calcium interactions with connexin-based channels. *Adv. Exp. Med. Biol.* 740, 777–794. doi: 10.1007/978-94-007-2888-2_34
- Palazzo, E., Marconi, A., Truzzi, F., Dallaglio, K., Petrachi, T., Humbert, P., et al. (2011). Role of neurotrophins on dermal fibroblast survival and differentiation. *J. Cell Physiol.* 227, 1017–1025. doi: 10.1002/jcp.22811
- Paul, C. E., Paul, C. E., Vereker, E., Dickson, K. M., and Barker, P. A. (2004). A pro-apoptotic fragment of the p75 neurotrophin receptor is expressed in p75^{NTR}ExonIV null mice. *J. Neurosci.* 24, 1917–1923. doi: 10.1523/JNEUROSCI.5397-03.2004
- Peeraully, M. R., Jenkins, J. R., and Trayhurn, P. (2004). NGF gene expression and secretion in white adipose tissue: regulation in 3T3-L1 adipocytes by hormones and inflammatory cytokines. *Am. J. Physiol. Endocrinol. Metab.* 287, E331–E339. doi: 10.1152/ajpendo.00076.2004
- Reichardt, L. F. (2006). Neurotrophin-regulated signalling pathways. *Philos. Trans. R. Soc. Lond. B Biol. Sci.* 361, 1545–1564. doi: 10.1098/rstb.2006.1894
- Richner, M., Ulrichsen, M., Elmegaard, S. L., Dieu, R., Pallesen, L. T., and Vaegter, C. B. (2014). Peripheral nerve injury modulates neurotrophin signaling in the peripheral and central nervous system. *Mol. Neurobiol.* 50, 945–970. doi: 10.1007/s12035-014-8706-9
- Samara, C., Poirot, O., Doménech-Estévez, E., and Chrast, R. (2013). Neuronal activity in the hub of extrasynaptic Schwann cell-axon interactions. *Front. Cell. Neurosci.* 7:228. doi: 10.3389/fncel.2013.00228
- Scott, A. L. M., and Ramer, M. S. (2009). Schwann cell p75^{NTR} prevents spontaneous sensory reinnervation of the adult spinal cord. *Brain* 133, 421–432. doi: 10.1093/brain/awp316
- Song, X.-Y., Zhang, F.-H., Zhou, F. H., Zhong, J., and Zhou, X.-F. (2009). Deletion of p75^{NTR} impairs regeneration of peripheral nerves in mice. *Life Sci.* 84, 61–68. doi: 10.1016/j.lfs.2008.10.013
- Song, X.-Y., Zhou, F. H.-H., Zhong, J.-H., Wu, L. L. Y., and Zhou, X.-F. (2006). Knockout of p75^{NTR} impairs re-myelination of injured sciatic nerve in mice. *J. Neurochem.* 96, 833–842. doi: 10.1111/j.1471-4159.2005.03564.x
- Tanaka, A., Wakita, U., Kambe, N., Iwasaki, T., and Matsuda, H. (2004). An autocrine function of nerve growth factor for cell cycle regulation of vascular endothelial cells. *Biochem. Biophys. Res. Commun.* 313, 1009–1014. doi: 10.1016/j.bbrc.2003.12.036
- Taniuchi, M., Clark, H. B., and Johnson, E. M. Jr. (1986). Induction of nerve growth factor receptor in Schwann cells after axotomy. *Proc. Natl. Acad. Sci. U.S.A.* 83, 4094–4098. doi: 10.1073/pnas.83.11.4094
- Taveggia, C., Feltri, M. L., and Wrabetz, L. (2010). Signals to promote myelin formation and repair. *Nat. Rev. Neurol.* 6, 276–287. doi: 10.1038/nrneurol.2010.37
- Tolwani, R. J., Cosgaya, J. M., Varma, S., Jacob, R., Kuo, L. E., and Shooter, E. M. (2004). BDNF overexpression produces a long-term increase in myelin formation in the peripheral nervous system. *J. Neurosci. Res.* 77, 662–669. doi: 10.1002/jnr.20181

- Tomita, K., Kubo, T., Matsuda, K., Fujiwara, T., Yano, K., Winograd, J. M., et al. (2007). The neurotrophin receptor p75^{NTR} in Schwann cells is implicated in remyelination and motor recovery after peripheral nerve injury. *Glia* 55, 1199–1208. doi: 10.1002/glia.20533
- Viader, A., Golden, J. P., Baloh, R. H., Schmidt, R. E., Hunter, D. A., and Milbrandt, J. (2011). Schwann cell mitochondrial metabolism supports long-term axonal survival and peripheral nerve function. *J. Neurosci.* 31, 10128–10140. doi: 10.1523/JNEUROSCI.0884-11.2011
- von Schack, D., Casademunt, E., Schweigreiter, R., Meyer, M., Bibel, M., and Dechant, G. (2001). Complete ablation of the neurotrophin receptor p75^{NTR} causes defects both in the nervous and the vascular system. *Nat. Neurosci.* 4, 977–978. doi: 10.1038/nn730
- Wang, H.-B., Wang, X.-P., Zhong, S.-Z., and Shen, Z.-L. (2013). Novel method for culturing Schwann cells from adult mouse sciatic nerve in vitro. *Mol. Med. Rep.* 7, 449–453. doi: 10.3892/mmr.2012.1177
- Wislet, S., Vandervelden, G., and Rogister, B. (2018). From neural crest development to cancer and vice versa: how p75^{NTR} and (Pro)neurotrophins could act on cell migration and invasion? *Front. Mol. Neurosci.* 11:244. doi: 10.3389/fnmol.2018.00244
- Wong, I., Liao, H., Bai, X., Zaknic, A., Zhong, J., Guan, Y., et al. (2010). ProBDNF inhibits infiltration of ED1+ macrophages after spinal cord injury. *Brain Behav. Immun.* 24, 585–597. doi: 10.1016/j.bbi.2010.01.001

Conflict of Interest Statement: The authors declare that the research was conducted in the absence of any commercial or financial relationships that could be construed as a potential conflict of interest.

Copyright © 2019 Gonçalves, Mohseni, El Soury, Ulrichsen, Richner, Xiao, Wood, Andersen, Coulson, Raimondo, Murray and Vægter. This is an open-access article distributed under the terms of the Creative Commons Attribution License (CC BY). The use, distribution or reproduction in other forums is permitted, provided the original author(s) and the copyright owner(s) are credited and that the original publication in this journal is cited, in accordance with accepted academic practice. No use, distribution or reproduction is permitted which does not comply with these terms.



The Median Nerve Injury Model in Pre-clinical Research – A Critical Review on Benefits and Limitations

Giulia Ronchi^{1,2*}, Michela Morano^{1,2}, Federica Fregnan^{1,2}, Pierfrancesco Pugliese³, Alessandro Crosio⁴, Pierluigi Tos⁴, Stefano Geuna^{1,2}, Kirsten Haastert-Talini^{5,6} and Giovanna Gambarotta¹

¹ Department of Clinical and Biological Sciences, University of Turin, Turin, Italy, ² Neuroscience Institute Cavalieri Ottolenghi Foundation (NICO), University of Turin, Turin, Italy, ³ Dipartimento di Chirurgia Generale e Specialistica, Azienda Ospedaliera Universitaria, Ancona, Italy, ⁴ UO Microchirurgia e Chirurgia della Mano, Ospedale Gaetano Pini, Milan, Italy, ⁵ Institute of Neuroanatomy and Cell Biology, Hannover Medical School, Hanover, Germany, ⁶ Center for Systems Neuroscience (ZSN) Hannover, Hanover, Germany

OPEN ACCESS

Edited by:

Esther Udina,
Autonomous University of Barcelona,
Spain

Reviewed by:

Arthur W. English,
Emory University, United States
Guilherme Lucas,
University of São Paulo, Brazil

*Correspondence:

Giulia Ronchi
giulia.ronchi@unito.it

Specialty section:

This article was submitted to
Cellular Neuropathology,
a section of the journal
Frontiers in Cellular Neuroscience

Received: 08 January 2019

Accepted: 13 June 2019

Published: 28 June 2019

Citation:

Ronchi G, Morano M, Fregnan F, Pugliese P, Crosio A, Tos P, Geuna S, Haastert-Talini K and Gambarotta G (2019) The Median Nerve Injury Model in Pre-clinical Research – A Critical Review on Benefits and Limitations. *Front. Cell. Neurosci.* 13:288. doi: 10.3389/fncel.2019.00288

The successful introduction of innovative treatment strategies into clinical practise strongly depends on the availability of effective experimental models and their reliable pre-clinical assessment. Considering pre-clinical research for peripheral nerve repair and reconstruction, the far most used nerve regeneration model in the last decades is the sciatic nerve injury and repair model. More recently, the use of the median nerve injury and repair model has gained increasing attention due to some significant advantages it provides compared to sciatic nerve injury. Outstanding advantages are the availability of reliable behavioural tests for assessing posttraumatic voluntary motor recovery and a much lower impact on the animal wellbeing. In this article, the potential application of the median nerve injury and repair model in pre-clinical research is reviewed. In addition, we provide a synthetic overview of a variety of methods that can be applied in this model for nerve regeneration assessment. This article is aimed at helping researchers in adequately adopting this *in vivo* model for pre-clinical evaluation of peripheral nerve reconstruction as well as for interpreting the results in a translational perspective.

Keywords: median nerve, injury, animal experimental model, repair, regeneration, translational research

INTRODUCTION

Peripheral nerve injuries are commonly caused by motor vehicle, domestic, work or sport accidents or during surgeries (iatrogenic nerve injuries) (Jones et al., 2016). Nerve injuries can lead to motor and sensory deficits that may result in disabilities permanently compromising the patients' quality of life.

The general ability of peripheral nerves to regenerate has been recognised more than a century ago, but until today functional recovery outcome after severe nerve injury and reconstructive surgery is often still poor in many patients. Nowadays, the “gold standard” reconstructive technique for bridging a nerve gap is autologous nerve grafting. This technique, however, is accompanied by important drawbacks such as the donor site morbidity, the need of additional surgery and the limited availability of graft material for extended repair (Konofaos and Ver Halen, 2013; Faroni et al., 2015).

Over the past decades, substantial effort has been made to identify new strategies to improve peripheral nerve regeneration after grafting and to substitute the autologous nerve graft. Advancements in biomedical methods, the tissue-engineered technology, gene therapy approaches, nanotechnology, biology, and microsurgical skills have opened new research fields in the nerve reconstruction area. Indeed, there is an exponential increase in the number of publications dealing with experimental nerve regeneration research over the years: a literature search with the PubMed search string (“Nerve-Regeneration”[Mesh] OR nerve-regenerat* OR nerve-repair*) AND (rat* OR mouse OR mice OR rabbit* OR sheep), delivered 26 results in 1970 and 479 in 2018.

In the context of pre-clinical peripheral nerve regeneration research, the choice of the experimental animal model is of fundamental importance. When a researcher moves on to test a novel attempt *in vivo*, the animal model should be chosen according to the study aims [e.g., for studying the involvement of a specific molecule in the biological process of nerve regeneration, the most appropriate choice will most likely be different to the model chosen for evaluating the effectiveness of a nerve conduit for long gap (>50 mm) repair]. Obviously, the pros and cons of the different available options must also be taken into careful consideration.

The choice of the appropriate experimental nerve injury model is usually guided by several factors. For nerve repair studies, in particular, the size (diameter and length) of the model nerve is certainly one of the main aspects considered. Indeed, most nerve repair studies are conducted on the sciatic nerve especially because of its big dimension that facilitates experimental microsurgery (Varejao et al., 2004; Bozkurt et al., 2011; Sinis et al., 2011a). The sciatic nerve is the biggest nerve in the body and the choice among mouse, rat, rabbit, dog, or sheep already provides variability in nerve gap lengths to be applied (Angius et al., 2012).

Different downsides resulting from experimental injury to the sciatic nerve have, however, led to increasing interest in the median nerve as alternative model nerve (Bertelli et al., 2004). At first, injury to the sciatic nerve results in a paralysis of the hind limb and, often, in automutilation behaviour, such as biting and self-amputation of denervated toes and paw areas by the subjected animal. Longer lasting paralysis (>4 weeks in the rat) often leads to joint contractures and stiffness. Automutilation behaviour and joint contractures reduce the reliability of functional tests, such as estimation of the sciatic function index or, in severe cases, will lead to exclusion of the respective animal from a study for ethical and animal welfare reasons. Furthermore, possibilities for evaluation functional recovery of motor skills after sciatic nerve lesion in the awaken animal are rather limited or need considerable efforts to be realised (Navarro, 2016).

In the recent years employment of the median nerve injury and repair model in the experimental research has increased (Papalia et al., 2003b; Ronchi et al., 2009) because of several advantages. Transection injury of the rodent median nerve,

results in only partial impairment of the upper limb function (Bertelli et al., 1995). Incidence of automutilation is significantly lower in comparison to the sciatic nerve model, ulcerations are fewer and no joint contractures can be seen. This milder phenotype results from the fact that after median nerve injury, the ulnar and radial nerves still preserve sensitivity and motor function in the forearm (Sinis et al., 2006). An additional advantage of the rodent median nerve injury and repair model is that positively evaluated attempts are more likely to be translated into clinical practise, since surgical interventions for the repair of a damaged human nerve are very often performed at the upper limb level. In addition, the hand functions require a fine finger movement that is quite similar between rodents and humans (Whishaw et al., 1992). From this perspective, the possibility to apply specific and precise functional tests for motor recovery evaluation following median nerve reconstruction is a further pro of this model in pre-clinical research.

This review provides an overview on the use of the median nerve injury and repair experimental model in pre-clinical research. The different animal species (not only mouse and rat but also larger animals such as rabbit, sheep, and monkey) are taken into account as are the different options these species provide with regard to comprehensive analysis of the regeneration outcome.

THE PRE-CLINICAL MEDIAN NERVE INJURY AND REPAIR MODEL IN DIFFERENT ANIMAL SPECIES

The use of the median nerve injury and repair model as pre-clinical model has progressively increased in the last years, but the sciatic nerve injury and repair model is still more often employed [in PubMed a research on (median-nerv*) AND (regenerat* OR repair) yielded 1002 papers, while (sciatic-nerv*) yielded 6612 papers].

Information from our literature search is presented in **Tables 1–5**. The tables summarise peripheral nerve regeneration studies after median nerve injury and repair in the different animal models. In addition to the specific reference, the tables list animal strain and sex, type of injury/gap, follow up periods and type of analyses conducted. We took our best efforts to include all articles available until end of 2018; nevertheless, inadvertently, we could have missed some papers and apologise in advance with their authors.

In the following paragraph specificities of the different models listed in the tables will be reviewed in more detail.

Mouse Model

Since most of the available transgenic animal models are mice, they are often used for studying the role of specific genes in the peripheral nerve regeneration process. For this purpose, genes of interest are knocked-out, mutated or over-expressed. Moreover, mice – especially wild type strains – are economical in their keeping, simple to handle and to care for and can therefore

TABLE 1 | Mouse model.

References	Strain	Sex	Type of injury/gap	Follow up	Analysis
Jager et al., 2014	–	F	Crush injury ($n = 5$); Contralateral nerves used as control (uninjured) nerves	25 days	Functional analysis (grasping test), histological analysis, TEM, morphometry
Park and Hoke, 2014	C57Bl/6J	M	Nerve repair (microsurgical 10/0 suture) without Exercise ($n = 8$); Nerve repair (microsurgical 10/0 suture) with Exercise ($n = 8$); Control group ($n = 8$)	6 weeks	Functional test, Electrophysiology, morphometry, Immunohistochemistry, ELISA assay (serum sample)
Speck et al., 2014	Swiss mice	M	Crush injury ($n = 12$); Control group ($n = 12$)	21 days	Functional test (IBB – Irvine, Beatties, and Bresnahan – Forelimb Scale), Histology
Jamiset et al., 2013b	CD1 and C57BL/6	M	Immediate microsurgical repair using 12/0 sutures ($n = 48$ WT); Immediate microsurgical repair using 12/0 sutures ($n = 8$ WT); Control ($n = 8$ WT) Immediate microsurgical repair using 12/0 sutures ($n = 8$ heterozygous Netrin-1(+/-); Control ($n = 8$ heterozygous Netrin-1(+/-))	0, 7, 14, 21, and 50 days	Real-time PCR, Western Blot, TEM, morphometry, functional analysis (grasping test)
Jamiset et al., 2013a	C57BL/6	–	Immediate microsurgical repair using 12/0 sutures ($n = 24$ WT); Immediate microsurgical repair using 12/0 sutures ($n = 12$ WT); Control ($n = 12$ WT) Immediate microsurgical repair using 12/0 sutures ($n = 12$ UNC5b ^{+/-} heterozygous); Control ($n = 12$ UNC5b ^{+/-} heterozygous)	0, 7, 14, 21, and 50 days	Western Blot, TEM, morphometry, functional analysis (grasping test)
Ronchi et al., 2013	BALB/c	M	Crush injury ($n = 16$ BALB-neuT); Crush injury ($n = 16$ WT); Contralateral nerves used as control (uninjured) nerves	2 and 28 days	Functional analysis, immunohistochemistry, histology, stereological analyses, TEM, western blot, real-time PCR
Oliveira et al., 2010	C57/Black6	–	Nerve lesion followed by tubulization [polycaprolactone (PCL) conduits] with DMEM ($n = 10$), 3-mm gap; Nerve lesion followed by tubulization (PCL conduits) with MSC in DMEM ($n = 11$), 3-mm gap Control ($n = 10$)	4, 8, and 12 weeks	SEM, TEM, histomorphometry analysis, immunohistochemistry, functional analysis
Ronchi et al., 2010	FVB	M	Crush injury (5 animals); Microsurgical 12/0 suture (end-to-end neurorrhaphy) ($n = 6$) and controls ($n = 6$) from Tos et al. (2008)	25 days	Functional analysis, histology, stereological analyses
Tos et al., 2008	FVB	M	Microsurgical 12/0 suture (end-to-end neurorrhaphy) ($n = 6$); Controls ($n = 6$)	75 days	Functional, histology, stereological analyses, TEM

be studied in large groups. Mice nerves can be subjected to different types of injury and repair and analysed with all kinds of functional, morphological and biomolecular assays. The most simple crush injury can be easily used and standardised. On the other hand, peripheral nerves in mice are rather small and experimental *in vivo* work employing more complex surgeries on them, such as end-to-end repair, requires advanced microsurgical skills. These skills are provided by many clinical researchers from disciplines routinely performing nerve surgeries but are less prevalent in the basic researcher community. Furthermore, when it comes to studies evaluating new developments for bio-artificial nerve guides, the much smaller diameter of mouse peripheral nerves is not fitting the larger one of nerve guides that are primarily commonly designed to fit human digital nerves.

Rat Model

Among rodents, rats are the most commonly used *in vivo* model in peripheral nerve regeneration research. This relates

mainly to the dimension of their nerves. Surgery on rat peripheral nerves requires less microsurgical skills than needed for mouse models and rat limbs and nerves are long enough to allow 1.5–2 cm gap repair to be studied at least in the sciatic nerve. Moreover, rats can be investigated in large groups because their keeping is economical, and they are mostly simple to handle and to care for. Transgenic rat models are, however, less available than mouse transgenic models and also the availability of rat specific antibodies for molecular and histological examination is rather limited. But due to their prevalent employment, functional tests for evaluating motor or sensory recovery in rats are more standardised (Navarro, 2016) and comparable among different research groups. Rat nerves can be subjected to different types of injury and repair and analysed in most comprehensive functional, morphological and biomolecular assays (Ronchi et al., 2009; Navarro, 2016; Ronchi et al., 2016). Different rat strains can be utilised, for which varying willingness to enrol in specific functional tests is

TABLE 2 | Rat model.

References	Strain	Sex	Type of injury/gap	Follow up	Analysis
Casal et al., 2018	Wistar	F	Control ($n = 17$) Excision ($n = 17$) 10 mm autograft ($n = 19$); Conventional flap ($n = 19$); Arterialised venous nerve flap ($n = 15$); Prefabricate nerve flap ($n = 8$)	100 days	Grasping test; nociception evaluation; running velocity; walking track analysis, retrograde labelling, infra-red thermography, electroneuromyography, immunohistochemistry
Chen et al., 2018	Sprague-Dawley	M	Control ($n = 6$); Nerve constriction with four loose ligatures for 1 ($n = 6$), 2 ($n = 4$), 3 ($n = 4$), and 4 weeks ($n = 4$); Median nerve transection ($n = 5$), 1 week intraplantar administration of saline, M871 (a GalR2 antagonist), or AR-M1896 (a GalR2 agonist)	1, 2, 3, and 4 weeks	Immunocytochemistry, von Frey filaments test
Gao et al., 2018	Sprague-Dawley	F	Entire contralateral C7 root was transected and transferred to the median nerve ($n = 18$); Only the posterior division of the contralateral C7 root was transected and transferred to the median nerve ($n = 18$); The entire contralateral C7 root was transected but only the posterior division was transferred to the median nerve ($n = 18$)	8, 12, and 16 weeks	Electrophysiological examination, Muscle tetanic contraction force test, Muscle fibre cross-sectional area, histological and morphometrical analysis
Gluck et al., 2018	Sprague-Dawley	F	Control ($n = 10$); Low strain injury (strain of 14% elongation) ($n = 5$ /time point); High strain injury (strain of 20% elongation) ($n = 5$ /time point)	0, 1, 3, 8, and 12 weeks	Second Harmonic Generation (SHG) microscopy, histology, and Immunohistochemistry
Marchesini et al., 2018	Wistar	M	Autograft – 1.5 cm gap ($n = 6$) 1.5 cm median nerve gap repaired with amnion muscle combined graft (AMCG) conduits ($n = 8$)	90 days	Grasping test, histological and morphometrical analysis
Marcioli et al., 2018	Wistar	M	Neural compression without treatment ($n = 6$); Neural compression and treated with neural mobilisation for 1 min ($n = 6$); then 6 sessions on alternate days of mobilisation; Neural compression and treated with neural mobilisation for 3 min ($n = 6$); then 6 sessions on alternate days of mobilisation	14 days	Histology and morphometric analysis, PCR
Muratori et al., 2018	Wistar	F	Control ($n = 6$); Crush injury ($n = 3$ /time point + 3 for histology); End-to-end repair ($n = 3$ /time point); Degenerating nerve ($n = 3$ /time point)	1, 3, 7, 15, and 30 days	Real time PCR, western blot, immunohistochemistry
Ronchi et al., 2018	Wistar	F	Nerve repaired with chitosan conduit (10 mm long) ($n = 5$ for each time point); Nerve repaired with chitosan conduit (10 mm long) filled with fresh muscle fibres ($n = 5$ for each time point); Autograft ($n = 5$ for each time point)	1, 7, 14, and 28 days and 12 weeks	Grasping test, histological analysis, morphometrical analysis,
Meyers et al., 2017	Sprague-Dawley	F	End-to-end repair of the median nerve distal to the elbow ($n = 6$); End-to-end repair of the median and ulnar nerves proximal to the elbow ($n = 6$); Repair of the median and ulnar nerves with a 7-mm polyurethane tube (gap 5 mm) proximal to the elbow ($n = 9$)	Up to 13 weeks	Evaluation of volitional forelimb strength
Ronchi et al., 2017	Wistar	F	Immediate, 3 and 6 months delayed nerve repair with a cross suture between the degenerated median nerve distal stump and the freshly axotomised ulnar proximal stump ($n = 7$ /group); Controls: healthy nerve ($n = 5$); 9-month degenerated nerve ($n = 5$); 3-month regenerated end-to-end-repaired median nerves ($n = 5$)	6 months	Grasping test, histological analysis, morphometrical analysis, gene expression analysis, protein analysis
Stossel et al., 2017	Lewis	F	7 mm-long nerve repaired with muscle-in vein graft ($n = 8$); Control: autologous nerve graft ($n = 8$)	1, 2, and 3 months	Electrophysiology, grasping test, staircase test, histological analysis, morphometrical analysis
Coradini et al., 2015	Wistar	M	Healthy nerve in obese rat model (8 rats); Crush nerve injury in obese rat model (8 rats); Crush nerve injury and physical exercise (swimming) in obese rat model (8 rats); Controls: healthy nerve (8 rats); crush nerve injury (8 rats); crush nerve injury plus physical exercise (8 rats)	3, 7, 14, and 21 days	Nociception threshold, histological analysis, protein analysis

(Continued)

TABLE 2 | Continued

References	Strain	Sex	Type of injury/gap	Follow up	Analysis
Fregnan et al., 2016	Wistar	F	10 mm-nerve gap repaired with two different types of chitosan membrane based conduit ($n = 4$ /group); Control: autograft ($n = 4$)	3 months	Grasping test, histological analysis, morphometrical analysis
Huang and Tsai, 2016	Sprague–Dawley	M	Control ($n = 12$); Median nerve compression with four loose ligatures ($n = 12$ /time point) with delivery of the JNK inhibitor at different doses [20 ($n = 6$), 40 ($n = 6$), or 80 nmol ($n = 6$), or with vehicle ($n = 6$); Animals were given vehicle ($n = 18$) or DHA at doses of 100 ($n = 18$), 250 ($n = 18$), or 500 nmol/kg ($n = 18$)	5 h, 1, 3, 5, 7, 14, and 21 days	Immunohistochemistry, double-immunofluorescence labelling and Western blotting, Enzyme-linked immunosorbent assay, Behavioural testing
Papalia et al., 2016	Wistar	F	10 mm-nerve gap repaired with end-to-side neurorrhaphy with or without epineurial window, using ulnar nerve fixed by applying cyanoacrylate solution ($n = 7$ /group); Control: healthy nerve ($n = 5$)	9 months	Grasping test, histological analysis, morphometrical analysis
Ronchi et al., 2016	Wistar	F	Crush nerve injury ($n = 15$); Nerve transection and immediately repair with end-to-end technique ($n = 15$); Nerve transection followed by no repair ($n = 15$); Control: healthy nerve ($n = 7$)	1, 3, 7, 14, and 28 days	Histological analysis, gene expression analysis, protein analysis
Shaikh et al., 2016	Long Evans	F	Nerve transection and nerve wrapping with a strip of Rose Bengal chitosan adhesive followed by laser irradiation ($n = 10$); Nerve transection repaired with end-to-end neurorrhaphy ($n = 10$); Control: nerve wrapping with a strip of Rose Bengal chitosan adhesive followed by laser irradiation ($n = 10$)	3 months	Cold and warm plate test, withdrawal threshold tests
Gambarotta et al., 2015	Wistar	F	Transected nerve repaired with 10 mm-long muscle-in-vein graft with muscle fibres expressing AAV2-LacZ or AAV2-ecto-ErbB4 ($n = 5$ /group); Control: 10 mm-long nerve graft ($n = 5$)	3 months	Grasping test, histological analysis, morphometrical analysis
Beck-Broichsitter et al., 2014b	Wistar	F	Nerve transection repaired with direct coaptation plus pulsed magnetic therapy ($n = 12$); Controls: nerve transection repaired with direct coaptation ($n = 12$)	3 months	Grasping test, histological analysis, morphometrical analysis
Beck-Broichsitter et al., 2014a	Wistar	F	6 weeks delayed nerve repair with autograft ($n = 10$); Nerve injury with sensory protection and 6 weeks delayed repair with autograft ($n = 10$)	15 weeks	Grasping test, muscle weight, histological analysis, morphometrical analysis
Li et al., 2014	Sprague–Dawley	–	Acute group (immediately after injury, $n = 18$) and subacute (2 weeks after injury, $n = 18$) group, each divided in three subgroups: Nerve transected without repair; Nerve transected and repaired immediately; Healthy control	Immediately and 2 weeks after injury	fMRI/fcMRI
Manoli et al., 2014	Wistar	F	Direct suture ($n = 3$); Direct suture plus vein-graft wrapping ($n = 4$); Direct suture plus vein-graft wrapping filled with Perineurin vehicle ($n = 2$); Direct suture plus vein-graft wrapping filled with Perineurin ($n = 6$); Direct suture ($n = 5$) FloSeal application to the nerve stumps and direct suture ($n = 6$); Electrocoagulation of the nerve stumps and direct suture ($n = 5$)	12 weeks	Electrophysiological and histomorphological analysis
Oliveira et al., 2014	Wistar	M	Nerve transection (4 mm gap) repaired with polycaprolactone conduit, with an injection of cell medium alone ($n = 3$) or containing bone marrow-derived mesenchymal stem cell ($n = 3$); Control: healthy nerve ($n = 4$)	10 weeks	Histological analysis, morphometrical analysis, electrophysiological cortical mapping of the somatosensory representation
Ronchi et al., 2014	Wistar	F	Control ($n = 5$); Crush injury ($n = 5$); Autograft ($n = 5$)	12 weeks	Histological and morphometrical analysis (at light and electron microscopy)

(Continued)

TABLE 2 | Continued

References	Strain	Sex	Type of injury/gap	Follow up	Analysis
Ghizoni et al., 2013	Sprague-Dawley	F	40 mm nerve gap repaired with autograft (contralateral median nerve) and nandrolone treatment ($n = 20$) 40 mm nerve gap repaired with autograft (contralateral median nerve) ($n = 20$); Control: non-grafted animals ($n = 20$)	6 months	Electrophysiology, grasping test, muscle weight, nociceptive sensation recovery
Ho et al., 2013	Sprague-Dawley		Nerve repaired with silicone rubber tubes (gap 5 mm) and subjected to acupuncture and electroacupuncture at two different intensities ($n = 7$ /group); Control: nerve repaired with silicone rubber tubes (gap 5 mm); no stimulation	5 weeks	Electrophysiology, Histology, Grasping test
Marcioli et al., 2013	Wistar	M	Nerve compression and treatment with neural mobilisation for 1 or 3 min ($n = 6$ /group); Control: nerve compression without mobilisation ($n = 6$)	3, 5, 7, 11, and 13 days, 2 weeks	Nociception evaluation, histological Analysis, morphometrical analysis
Moimas et al., 2013	Wistar	F	Transected nerve repaired using 10 mm-long muscle-in-vein graft with muscular fibres expressing AAV2-LacZ or AAV2-VEGF ($n = 7$ /group). Control: healthy nerve ($n = 5$)	3 months	Grasping test, histological analysis and morphometrical analysis of both nerve and muscle, muscle immunochemistry
Papalia et al., 2013	Wistar	F	10 mm-long defect repaired with adipose tissue-in-vein conduit ($n = 5$) or muscle-in-vein conduit ($n = 5$); Control: autologous nerve graft ($n = 5$)	6 months	Grasping test, histological analysis, morphometrical analysis
Lanza et al., 2012	Wistar	F	Nerve transection immediately repaired with end-to-side neurorrhaphy ($n = 10$); 2 mm-long nerve segment exported and not repaired ($n = 10$)	6 and 12 days	Histological analysis, gene expression analysis
Muratori et al., 2012	Wistar	F	Crush injury ($n = 5$); Control: healthy nerve ($n = 5$)	8 and 24 weeks	Histological analysis, morphometrical analysis
Moges et al., 2011	Sprague Dawley	F	7 mm-long nerve gap repaired with autograft (sural nerve) with/without light therapy ($n = 12$ /group). Control: sham operated group without injury and repair; Control: sham operated group ($n = 12$)	4 months	Grasping test, muscle action potential measurements, histological analysis, morphometrical analysis
Nabian et al., 2011	Wistar	M	Right sciatic nerve and both median nerves (1 week later) were excised ($n = 10$); Both median nerves were excised, and the sciatic nerves were left intact ($n = 10$); Control: no surgical intervention ($n = 10$)	17 days	Sciatic functional index
Sinis et al., 2011b	Wistar	F	Floreal application to nerve stumps before nerve repair with end-to-end neurorrhaphy ($n = 12$); Electrocoagulation of nerve stumps before end-to-end neurorrhaphy ($n = 12$); Control: nerve repaired with end-to-end neurorrhaphy ($n = 12$)	3 months	Grasping test, muscle weight, histological analysis, morphometrical analysis
Chiono et al., 2009	Wistar	F	Repair of a 1.5 cm gap with PCL guides (2 cm long); Cross chest median/median nerve (5 cm PCL guides; 4.5 cm gap)	6 and 8 months, respectively	Grasping test, histological and immunohistochemical analysis
Nicolino et al., 2009	Wistar	F	10 mm-long nerve gap repaired with muscle-in-vein graft ($n = 16$); Nerve transection with no repair ($n = 16$)	5, 15, and 30 days	Histological analysis, expression analysis in muscle
Ronchi et al., 2009	Wistar	F	Crush injury ($n = 14$); Control (no injury) ($n = 6$)		Grasping test, histology, morphometrical analysis, TEM
Sinis et al., 2009	Wistar	F	Nerve repaired with end-to-end neurorrhaphy, with a wrapping by external jugular vein segment, filled with iron chelator DFO; Control: nerve repaired with end-to-end neurorrhaphy, with a wrapping by empty external jugular vein segment	3 months	Grasping test, muscle weight, histological analysis, morphometrical analysis, immunochemistry
Werdin et al., 2009	Wistar	F	Control group ($n = 9$); End-to-end nerve repair ($n = 18$) 2-cm autograft ($n = 27$)	12 weeks	Electrophysiological analysis
Audisio et al., 2008	Wistar	F	Nerve transection and repair with end-to-end neurorrhaphy ($n = 10$); Nerve transection and repair with end-to-side neurorrhaphy (distal stump sutured to the ulnar nerve) ($n = 10$); Control: healthy nerve ($n = 10$)	1, 2, and 3 weeks	Gene expression analysis

(Continued)

TABLE 2 | Continued

References	Strain	Sex	Type of injury/gap	Follow up	Analysis
Ozalp and Masquelet, 2008	Wistar albino	M	5-mm gap repaired with silicon tube; after 5 weeks, the implant was removed and a nerve graft was anastomosed inside the neo-formed biological membrane ($n = 10$) 5-mm gap repaired with autograft ($n = 10$)	12 weeks	Grasping test
Geuna et al., 2007a	Wistar	F	Median nerve repaired with muscle-vein-combined conduit ($n = 3$ /time point)	0 (2 h after preparation), 5, 15, and 30 days	IHC, Electron Microscopy, PCR
Geuna et al., 2007b	Wistar	F	End-to-side neurorrhaphy on the intact ulnar with a perineurial window; Tubulization by muscle-vein-combined guides Y-shaped muscle-vein-combined guides to repair both median and ulnar nerves	5 and 30 days	Grasping test, histological analysis (light, confocal and electron microscopy), PCR, muscle weight
Lee et al., 2007	Wistar	F	Controls ($n = 4$); End-to-end (median-to-median) ($n = 4$); End-to end (ulnar-to-ulnar) ($n = 4$); Median and ulnar nerve repaired with a 14-mm Y-shaped muscle-in-vein conduit ($n = 4$)	10 months	Grasping test, histological and morphometrical analysis
Papalia et al., 2007	Wistar	F	Median nerve repaired with end-to-side neurorrhaphy after epineurotomy on the radial nerve ($n = 10$)	30 weeks	Grasping test, histological, morphometrical and electrophysiological analysis
Sinis et al., 2007	Lewis	F	Control ($n = 22$); Autologous nerve graft ($n = 22$); Empty TMC/CL conduit ($n = 16$); TMC/CL conduit and SC ($n = 22$)	9 months	Grasping test, electrophysiological and histological analysis; muscle weight
Tos et al., 2007	Wistar	F	10-mm-long nerve defect repaired with muscle-in-vein conduit (15 mm long) using fresh muscle ($n = 12$); 10-mm-long nerve defect repaired with muscle-in-vein conduit (15 mm long) using freeze-thawed muscle ($n = 12$)	5 days, 1 month	Histological analysis, morphometrical analysis, gene expression analysis
Sinis et al., 2006	Lewis		Cross-chest (a gap of 40 mm was repaired with the two ulnar nerves) ($n = 12$); Control (healthy) ($n = 12$)	12 months	Grasping test, histological and morphological analysis
Bontioti et al., 2005	Wistar	F	End-to-side neurorrhaphy median/ulnar nerves to the musculocutaneous nerve ($n = 11$); End-to-side neurorrhaphy radial nerve to the musculocutaneous nerve ($n = 11$)	7 days and 6 months	Pawprints test, retrograde labelling, histological and morphometrical analysis, tetanic muscle force and muscle weight
Sinis et al., 2005	Lewis	F	Nerve defect of 2 cm repaired with resorbable hollow nerve conduit ($n = 16$); Nerve defect of 2 cm repaired with nerve conduit containing Schwann cells suspended in matrigel ($n = 16$); Nerve defect of 2 cm repaired with autograft ($n = 22$); Control: healthy nerve ($n = 22$)	9 months	Electrophysiology, grasping test, histological analysis, muscle weight
Gigo-Benato et al., 2004	Wistar	F	Complete nerve transection (15 mm gap) repaired with end-to-side neurorrhaphy on the ulnar nerve plus laser therapy (laser used: continuous, pulsed and a combination of the two) ($n = 4$ /group). Nerve transection repaired with end-to-side neurorrhaphy on the ulnar nerve ($n = 4$); Controls: nerve transection without repair ($n = 4$), healthy nerve ($n = 5$)	4 months	Grasping test, muscle weight, histological analysis, morphometrical analysis
Tos et al., 2004	Wistar	F	Controls ($n = 5$); Median and ulnar nerve repaired with a 14-mm Y-shaped muscle-in-vein conduit ($n = 5$)	8 months	Grasping test, histological and morphometrical analysis
Papalia et al., 2003a	Wistar	F	10 mm-long nerve defect repaired with end-to-side neurorrhaphy, through an epineurial window on the ulnar nerve ($n = 20$)	7 months	Grasping test, electrophysiology, muscle weight, histological analysis, morphometrical analysis
Papalia et al., 2003b	Wistar	F	End-to-side neurorrhaphy ($n = 6$)	16 weeks	Grasping test
Accioli De Vaconcellos et al., 1999	Sprague-Dawley	F	Control group ($n = 8$); Fresh autograft 20 mm long ($n = 12$); Frozen acellular autograft 20 mm long ($n = 12$); Fresh xenograft 20 mm long ($n = 12$); Frozen acellular xenograft 20 mm long ($n = 12$)	3, 6, 9, and 12 months	Grasping test, Retrograde labelling of neurons, Histological and histochemistry studies

(Continued)

TABLE 2 | Continued

References	Strain	Sex	Type of injury/gap	Follow up	Analysis
Bertelli and Mira, 1995	Sprague-Dawley	F	Median and ulnar nerve bilateral dissection ($n = 15$); Left median nerve crush ($n = 10$); Left median nerve crush and right median nerve transection ($n = 10$); Left median nerve transection ($n = 10$); Left median and ulnar nerve transection ($n = 10$)	14 days, 3, 4, and 5 weeks	Grasping test, muscle weight

reported (Nikkhah et al., 1998; Galtrey and Fawcett, 2007), but so no comparative studies investigating differences in their ability to regenerate have been published.

When using rodents (mice and rats) as animal models for peripheral nerve regeneration, researchers must finally be aware of the following immanent differences to mankind: (1) gaps that can be produced are shorter than those commonly found in human nerve lesions; (2) axonal regeneration rate is faster than in humans; (3) recovery is often complete, while in humans it is often incomplete (Kaplan et al., 2015).

Rabbit Model

In peripheral nerve regeneration research, rabbits offer the possibility to study regeneration across gap lengths of up to 6 cm. Rabbits are, however, expensive to purchase and maintain, and difficult to care for. Rabbits are more delicate and less resilient than rats and mice, and their occurrence as pet animals probably creates ethical problems for animal care takers and researchers. Also, there are almost no valid functional assays that can be applied in rabbit models, besides electrodiagnostic evaluation. Finally, very few specific antibodies are available to be used on rabbit tissue samples, so that conclusions on the regeneration outcome can mainly only be based on nerve morphometry studies.

Sheep Model

The sheep as an animal model is useful when nerve regeneration across very long gaps should be evaluated. An ethical advantage of this animal is provided by the fact that a median nerve transection injury does not result in serious impairment of the limb usage ability and functional read-outs have been described in the recent years. To establish the model and to provide adequate housing conditions is, however, a considerable challenge, and research in this model will often only be realised through collaborative work.

Monkey Model

Although non-human primates could be useful to test safety and efficacy of synthetic nerve conduits – because of the similarity of non-human primates with human beings – their use is considerably limited for ethical reasons. Monkeys are considered as animal models mainly to study neuronal plasticity occurring in the brain following peripheral nerve injury and repair. Again, studies in this model will mainly be subject of collaborative work and not appropriate for early stage pre-clinical research.

Other Animals

Other large animals can be used as models to study median nerve injury and regeneration, such as pigs (Ochoa and Marotte, 1973;

Marotte, 1974), dogs (Lee et al., 1999), and cats (Murray et al., 1997), but their use is limited for three main reasons: (1) animal care for large species is considerably expensive; (2) for some species the possibilities for functional testing are limited or require complex training, therefore, nerve regeneration may only be assessed with nerve morphometry; (3) dogs and cats are domestic animals, and their use in research is more restricted for ethical reasons.

METHODOLOGICAL CONSIDERATIONS – APPROACHES FOR THE TREATMENT OF NERVE INJURIES

The following criteria should be considered for selecting the most suitable animal model for pre-clinical research on peripheral nerve regeneration: (1) costs to purchase and house the animals; (2) ease of handling, such as tolerance to captivity; (3) tolerance for surgery and eventual repetitive anaesthesia, as well as resistance to infection; (4) compliance with national policies and with ethical principles; (5) inter-animal uniformity, life span of the species, biological information and available tools; (6) overall experimental plan (Angius et al., 2012). With regard to the latter, especially when several time-points are to be analysed, rodents represent the best choice. On the contrary, rodent life span is short, therefore for long experiments (> 1–1.5 years), it becomes necessary to use larger animals as model organism.

In the last years, several approaches have been developed and tested in pre-clinical animal models to improve peripheral nerve regeneration. All these approaches can be applied on different nerves and are not median-nerve specific. In this paragraph we will present an overview of different techniques, including the use of different conduits to guide regenerating axons, the use of stem cell transplantation, the application of physical therapies and optogenetics, all of which have been demonstrating variable positive effects on nerve regeneration irrespectively of the model they were investigated in.

Nerve Guidance Conduits

The major disadvantage of the autologous nerve graft technique is the remarkable sensitivity loss (mainly sural nerve grafts are harvested for this) and the limited availability of donor tissue (Ray and Mackinnon, 2010). Reconstruction of a nerve with artificial or non-artificial nerve conduit grafts is particularly indicated in case of extensive nerve tissue loss. Nerve guidance conduits made of several materials, artificial or of natural origin, are available; most common and FDA approved for clinical use

TABLE 3 | Rabbit model.

References	Strain	Sex	Type of injury/gap	Follow up	Analysis
Sun et al., 2012	New Zealand rabbits	M/F	<i>In situ</i> anastomosis of the median nerves was made in parallel to the surrounding elbow veins, the transplanted epineurium and the adventitia were sutured with nerve anastomosis line ($n = 30$). Gap: 3 cm <i>In situ</i> anastomosis (control group); ($n = 30$). Gap: 3 cm	1, 2, 4, 8, and 12 weeks	Electrophysiological testing, and histopathology observation, TEM
Yin et al., 2011	New Zealand rabbits	–	Groups 2 and 3: Proximal median/ulnar nerve segment was served as father nerve to repair the distal nerve stump (Dor–Dor) ($n = 6$ /group) Group 4: Serving as a donor nerve, the proximal 1/2 median nerve was fixed to the distal stumps of 1/2 median and ulnar nerve simultaneously, using biodegradable chitin conduits with a gap of 1 mm. (1/2 Dor – 1/2 Dor + Rec) ($n = 6$) Group 1: Control group ($n = 6$)	4 months	Electrophysiology, histology and morphometry
Kim et al., 2011	New Zealand rabbits	M	The ulnar nerve was transected and the distal end sutured to the median nerve 3 cm above the elbow ($n = 30$); The ulnar nerve was transected and the distal end sutured to the median 3 cm below the elbow joint ($n = 30$)	1, 2, 3, 4, 5, and 6 weeks	Morphometric analysis and immunohistochemistry.
Wang et al., 2009	New Zealand rabbits	–	Proximal nerve segment as donor nerve ($n = 6$) Intermediate nerve segment as donor nerve ($n = 6$); Distal nerve segment as donor nerve ($n = 6$); Right side nerves as control	3 months	Electrophysiology, histology and stereology; muscle weights
Zhang et al., 2006	New Zealand rabbits	–	End-to-side nerve coaptation performed immediately ($n = 12$); End-to-side nerve coaptation performed after nerve degeneration ($n = 12$); Control ($n = 12$)	3 and 6 months	Electrophysiology, Histomorphometry, Muscle weight
Baoguo et al., 2004	Japanese white rabbits	–	Study 1: the median nerve was elongated for 10 days ($n = 6$), for 15 days ($n = 7$) and for 20 days ($n = 6$). Study 2: Right arm: the proximal segment of an injured median nerve was elongated for 10 days ($n = 10$) and for 15 days ($n = 10$). Left arm: a 10- for 15-mm segment of the median nerve was removed, and a 10- for 15-mm segment, respectively, of the tibial nerve was grafted in its place.	4 months	Electrophysiology, Histomorphometry
Ruch et al., 2004	New Zealand rabbits	M	Group 1: nerve repaired with a tension-free medial antebrachial cutaneous graft ($n = 11$); Group 2: end-to-end repair without distraction ($n = 13$); Group 3: end-to-end repair with gradual distraction) ($n = 12$)	3 and 6 months	Electrophysiology, Histomorphometry, Muscle weight
Gui et al., 1997	–	–	The injured median nerve regenerated through degenerative latissimus dorsi muscle; The injured median nerve regenerated through the brachial triceps muscle	7, 14, 28, 45, 60, and 180 days	Histology
Shibata et al., 1991	–	–	Median nerve immediately repaired with the contralateral ulnar nerve graft (gap: 3-cm); Median nerve repaired with the contralateral ulnar nerve graft (gap: 3-cm) after resection of scar and coaptation at the distal site done 10 weeks later.	24 and 62 weeks	Electrophysiology, Histomorphometry, Muscle weight
Kawai et al., 1990	–	–	Nerve repaired with vascularised median nerve graft; Nerve repaired with non-vascularised median nerve graft. Length of the grafts: 2, 4, or 6 cm.	8 and 24 weeks	Histomorphometry
de la Monte et al., 1988	–	–	$n = 34$ total; Axonal regeneration across allografts (fresh or predegenerated) or autograft in cyclosporin A-treated/non-treated animals	–	Histology

TABLE 4 | Sheep model.

References	Strain	Sex	Type of injury/gap	Follow up	Analysis
Kettle et al., 2013	–	–	Median-to-ulnar nerve end-to-side neurorrhaphy ($n = 12$); Conventional method of nerve repair ($n = 18$); Control ($n = 8$)	12 months	Electrophysiology and histology; Physiology of the muscle
Forden et al., 2011	Suffolk ewes	–	Defect of 5 cm repaired with 7 cm of radial sensory nerve ($n = 12$); Control ($n = 1$)	6 and 9 months	Electrophysiology, histology, immunohistochemistry, and morphometric analyses
Jeans L.A. et al., 2007	–	–	Microsurgical epineurial repair using 10/0 polyamide ($n = 12$); CRG-wrap and 6/0 polyglactin ($n = 12$); CRG-wrap and fibrin glue ($n = 12$)	7 months	Measure of transcutaneous stimulated jitter (TSJ), maximum conduction velocity (CVmax), wet muscle mass and morphometric measurements.
Jeans L. et al., 2007	–	–	Epineurial suture repair using 9/0 polyamide; CRG-wrap secured by Tisseel glue; CRG-wrap secured by polycaprolactone glue; Wrap secured by suturing (6/0 polyamide)	7 months	Electromyography, nerve conduction studies, wet muscle mass measurements, and morphometry
Kelleher et al., 2006a	–	–	Entubulation within a biodegradable glass tube (CRG tubes) ($n = 6$); Gap: 4/5 cm; Small magnets were applied to the sides of the biodegradable glass tube before the median nerve was repaired ($n = 6$); Gap: 4/5 cm Control ($n = 6$);	10 months	Morphometry electrophysiology and isometric tension assessment
Kelleher et al., 2006b	–	–	Median nerve repaired using an epineurial suture technique. CNTF was supplied into the CSF at the level of C6 by an implanted osmotic pump ($n = 5$). Median nerve repaired using an epineurial suture technique. Physiological saline was placed in the osmotic pump ($n = 5$); Control ($n = 5$);	6 months	Electrophysiological, morphometric and isometric tension experiments; muscle mass.
Matsuyama et al., 2000	–	–	Autograft (right side) and allograft (left side); immunosuppression with Cyclosporine A; 5-cm gap repaired with two cables of the radial sensory nerve (8-cm) ($n = 4$); Autograft (right side) and allograft (left side); (control $n = 4$)	between 35 and 47 days	Histology, Morphometry
Fullarton et al., 1998	Scottish black-faced sheep	F	Nerve immediately repaired with freeze-thawed muscle autografts ($n = 5$); gap 3 cm; Nerve repaired 30 days after injury with freeze-thawed muscle autografts ($n = 5$); gap 3 cm.	6 months	Electrophysiology and morphometry. Blood flow
Glasby et al., 1998	Scottish, black-faced sheep	F	Nerve immediately repaired with freeze-thawed muscle autografts ($n = 5$); gap 3 cm; Nerve repaired 4 weeks after injury with freeze-thawed muscle autografts ($n = 5$); gap 3 cm.	6 months	Electrophysiology and morphometry. Blood flow
Lawson and Glasby, 1998	Scottish, black-faced sheep	F	Nerve repaired with fascicular cable graft ($n = 5$); Nerve repaired with freeze-thawed muscle grafts ($n = 5$)	6 months	Nerve blood flow, nerve conduction velocity and morphological indices
Glasby et al., 1998	Scottish, black-faced sheep	F	Nerve immediately repaired with freeze-thawed muscle autografts ($n = 6$); gap 3 cm; Nerve repaired 30 days after injury with freeze-thawed muscle autografts ($n = 6$); gap 3 cm.	6 months	Electrophysiology and morphometry. Blood flow
Strasberg et al., 1996	–	–	Fresh nerve autograft ($n = 5$); Fresh nerve allograft ($n = 5$); Cold-preserved nerve ($n = 5$); Cold-preserved nerve allograft ($n = 5$)	6 and 10 months	Histological, morphometric, and electrophysiologic analyses.
Lawson and Glasby, 1995	Scottish, black-faced sheep	F	Nerve immediately repaired with freeze-thawed muscle autografts ($n = 5$); gap 3 cm; Nerve repaired 30 days after injury with freeze-thawed muscle autografts ($n = 5$); gap 3 cm.	6 months	Electrophysiology and morphometry. Blood flow

TABLE 5 | Monkey model.

References	Strain	Sex	Type of injury/gap	Follow up	Analysis
Pace et al., 2014	Macaca fascicularis monkeys	F	Nerve repaired with bovine collagen I nerve conduit (NeuraGen) filled with keratin hydrogel ($n = 8$) (gap: 1 cm); Nerve repaired with bovine collagen I nerve conduit (NeuraGen) filled with sterile saline ($n = 6$) (gap: 1 cm)	12 months	Electrophysiology, nerve histology and morphometry, muscle histology and morphometry, antibody titer
Hu et al., 2013	Rhesus monkeys	–	Nerve defect (50 mm) repaired with: Autograft ($n = 3$); Chitosan/PLGA scaffold, followed by injection of autologous MSCs ($n = 3$); Chitosan/PLGA scaffold alone ($n = 3$); Nerve defect left untreated (control) ($n = 3$)	12 months	Locomotive activity observation, electrophysiological assessments, FG retrograde tracing tests, histological and morphometric analyses, blood test and histopathological examination
Hara et al., 2012	Macaca fascicularis	–	20-mm-long-segment was resected and repaired with: Lengthening of both nerve stumps ($n = 3$); Autograft with the sural nerve ($n = 3$);	16 weeks	Electrophysiological, histological, and functional recovery
Zhang et al., 2009	Rhesus monkeys	M	Right sides: small gap (2 mm) repaired with chitin conduit (length 10 mm); Left sides: traditional epineurium suture ($n = 8$)	6 months	Histology
Krarp et al., 2002	Macaca fascicularis	M	Nerve gap distances of 5, 20, or 50 mm were repaired with nerve grafts or collagen-based nerve guide tubes (total of 46 median nerve lesion). Control: direct repair	3–4 years	Electrophysiology
Florence et al., 2001	Macaca radiata	–	Median nerve was cut and sutured prenatally ($n = 1$); sensory enrichment of the nerve-injured hand; Median nerve was cut and sutured after birth ($n = 5$); 4 animals received sensory enrichment of the nerve-injured hand	3.5 months	Electrophysiological mapping studies (3b somatosensory cortex)
Florence et al., 1996	Macaque monkeys (immature)	–	Median nerve was cut and sutured prenatally ($n = 2$); Median nerve was cut and sutured after birth ($n = 2$)	10–18 months of age	Retrograde labelling to study the dorsal horn and cuneate nucleus; Electrophysiological mapping studies (3b somatosensory cortex)
Archibald et al., 1995	Macaca fascicularis	–	Autograft (gap 5 mm) in one side; In the contralateral wrist, the 5 mm nerve gap was bridged with a collagen nerve guide ($n = 4$); Direct suture (positive controls) ($n = 4$); Nerve gaps of mm bridged by polylactate nerve guides ($n = 1$). After 630–679 d the nerve guide was removed and the resulting gap of 15 mm was bridged by a collagen nerve guide.	Average of 1,342 d after surgery	Electrophysiology, motor conduction studies, sensory conduction studies, responses evoked by tactile stimulation, morphometric analyses.
Florence et al., 1994	Macaque monkeys	–	Median nerve was cut and sutured ($n = 3$)	7–13 months	Retrograde labelling to study the dorsal horn and cuneate nucleus; Electrophysiology to study the 3b of somatosensory cortex
Tountas et al., 1993	–	–	Median nerve repaired by microsurgical suture or tubulization with a non-woven, bioabsorbable, polyglycolic acid device (n tot = 30)	6 and 12 months	Electrophysiology and histology
Archibald et al., 1991	Macaca fascicularis	M	Nerve transected and repaired with: 4 mm nerve autograft ($n = 3$); Collagen-based nerve guide conduit (gap 4 mm) ($n = 3$)	760 days	Electrophysiology

(Continued)

TABLE 5 | Continued

References	Strain	Sex	Type of injury/gap	Follow up	Analysis
Badalamente et al., 1989	Capuchin monkeys (<i>C. apella</i>)	-	Epineural repair (nerve stumps and thenar muscles were first bathed/injected with leupeptin) ($n = 5$); Epineural repair (nerve stumps were bathed with saline solution) ($n = 5$)	6 and 8 weeks, 3, 6 months	Electrophysiology, histology
Wall et al., 1986	Aotus trivirgatus	-	Nerves reconnected with 10/0 epineural sutures ($n = 5$)	From 76 to 322 days	Neurophysiological recording (cortical areas 3b and 1)
Grabb, 1968	Rhesus monkeys	F	Nerves were cut and sutured primarily (4 h after nerve injury, $n = 30$), or secondarily (about 3 weeks after injury, $n = 30$).	9 months	Electromyographic examination

are conduits made of collagen, chitosan, or poly (DL-lactide- ϵ -caprolactone) (Kornfeld et al., 2018). All devices currently on the market and FDA-approved have proven good support for the promotion of peripheral nerve regeneration in pre-clinical models. Good clinical results, however, are obtained only for lesions with a substance loss inferior to 3 cm in length, while severe and enlarged injuries remain a critical condition (Kaplan et al., 2015). For this reason, research in the field of novel nerve conduit functionalisation strategies is still highly vivid.

Application of Stem Cells and Their Secretome

In regenerative medicine and tissue engineering, the use of Stem Cells and their secretome is fast expanding with the aim to develop innovative therapeutic strategies for the treatment of peripheral nerve injuries (Caplan, 2015; Caseiro et al., 2016; Busuttill et al., 2017; Sayad-Fathi et al., 2019). In particular, Mesenchymal Stem Cells (MSCs) present relevant key features: they can be easily expanded, they can differentiate into different cell types, they are immune-privileged and immune-modulatory, they show preferential homing to injured sites (Frausin et al., 2015; Sullivan et al., 2016; Jiang et al., 2017). Moreover, the MSC secretome contains trophic mediators (Meirelles Lda et al., 2009; Fu et al., 2017), modulating the function of several tissues, including the skeletal muscle (Pereira et al., 2014) and the peripheral nervous system (Lopatina et al., 2011; Gartner et al., 2012, 2014).

The most widely source of MSCs for therapeutic purposes is the bone marrow; as good alternative other sources are: the umbilical cord blood, the stromal tissue of the umbilical cord, the dental pulp, the adipose tissue (Jin et al., 2013).

Transgenic Models to Promote Peripheral Nerve Regeneration

To study the biology of peripheral nerve regeneration, different transgenic models can be used (Magill et al., 2008). Most of the available transgenic animals are mice and they represent a powerful tool to study the influence of over-expression or depletion or mutation of a specific gene in a specific cell type, using inducible systems, but it must be kept in mind that mice are difficult subjects for microsurgical models due to the small size of their nerves, as discussed above.

To investigate the function of specific genes in nerve regeneration discriminating between motor and sensitive neurons, transgenic mice over-expressing the gene of interest in postnatal motoneurons or dorsal root ganglion neurons can be obtained using Thy1 or NSE (neuron specific enolase) promoters (Michailov et al., 2004; Gomez-Sanchez et al., 2009; Velanac et al., 2012).

To obtain tissue specific expression or depletion of specific proteins, the inducible cre-lox system can be applied: transgenic mice driving motor neuron specific expression of cre recombinase with the promoter of Mnx1 (motor neuron and pancreas homeobox 1) gene can be used to specifically in/activate the expression of floxed genes in motor neurons, while specific in/activation in Schwann cells can be obtained using the promoter of Mpz (myelin protein zero) gene (La Marca et al., 2011).

Transgenic animals can also be developed as advanced experimental models to study genetic diseases giving rise to peripheral neuropathies (Hoke, 2012; Juneja et al., 2018), and they can be studied to investigate their ability to regenerate injured peripheral nerves.

Finally, the expression of neurotrophic factors or other potentially therapeutic proteins in Schwann cells or in neurons can be obtained through the use of different viral vectors (Tannemaat et al., 2008).

Physical Therapies

The efficacy of brief Electric Stimulation (ES) of the proximal stump of an injured nerve in promoting nerve regeneration in animal models has been verified in several independent studies reviewed by Gordon (2016) and Gordon and English (2016). In particular, a 14 days period of ES was chosen (Al-Majed et al., 2000) to accelerate the regenerative process and the effect was dramatic: preferential motor reinnervation of motor pathways was evident at 21 days rather than at 42 days, and, importantly, all of the motoneurons had regenerated into the motor nerve branch.

Another interesting study was aiming at evaluating the value of electromagnetic stimulation for the neural regenerative process of the rat median nerve after transection and end-to-end repair (Beck-Broichsitter et al., 2014b). From the 1st day after surgery a pulsed magnetic therapy was daily applied in the experimental group. Magnetic stimulation was positively influencing the

functional regeneration in terms of grasping force and reduced muscular atrophy.

Optogenetics

Axonal regeneration and functional recovery are enhanced by activity-related therapies, such as exercise and electrical stimulation (Gordon, 2016). Unlike electrical stimulation, optogenetics allows to selectively activate or inactivate specific neurons: for example, selective expression of the light-sensitive cation channel channelrhodopsin-2 (ChR2), that is maximally activated by blue light, can be used to depolarise neurons, thereby driving action potentials. Conversely, selective expression of the light-sensitive inward chloride pump halorhodopsin (Halo), that is maximally activated by amber light, can be used to obtain neuron hyperpolarisation, thereby inhibiting action potentials (Montgomery et al., 2016). Optically induced neuronal activity has been shown to be sufficient to promote functional motor axon regeneration *in vivo* (Ward et al., 2016). Moreover, through the selective expression of opsins in sensory neurons or motoneurons, it was possible to investigate the effect of system-specific neuronal activation on axonal regeneration, thus demonstrating that acute activation is sufficient to enhance regeneration of both motor and sensory axons (Ward et al., 2018).

Until now, in the peripheral nervous system, optogenetics has been applied mainly to sciatic nerves in transgenic mice expressing different opsins, but given its therapeutic potential it will be certainly applied also to median nerves and in other animal models, by injection of optogenetic constructs to transduce opsin expression in peripheral nerves in the future.

Immunomodulation

The early inflammatory reactions undergoing in the course of Wallerian Degeneration of the distal nerve, comprise the activation of the complement system, arachidonic acid metabolites, and inflammatory mediators involved in myelin fragmentation and activation of repair Schwann cells. Fine-tuned upregulation of the cytokine/chemokine network by repair Schwann cells activates resident and hematogenous macrophages to complete the clearance of axonal and myelin debris and stimulate regrowth of axonal sprouts (Yona and Jung, 2010; Cortez-Retamozo et al., 2012; Dubovy et al., 2013; Jessen and Mirsky, 2016). An innovative approach in the field of peripheral nerve regeneration is exploiting the endogenous capacity of the body to repair itself through immune cells. In very promising studies, starting from the known different pro-inflammatory and pro-regenerative macrophage phenotypes, they were modulated through their response to different IFN- γ or IL-4 cytokines and studied in their ability to influence nerve regeneration in a critically sized, 15 mm rat sciatic nerve gap. The results of this research have shown that the administration of IL-4 at the injury site increased the pro-regenerative effect and therefore that the regenerative outcomes appeared to be influenced not only by the macrophage presence, but by their specific phenotype at the site of injury (Mokarram et al., 2012). A similar approach was conducted later by the same authors, through early stage administration of fractalkine, a chemokine able to

control the phenotype in monocyte recruitment and to increase the regenerative potential. The pharmaceutical approach was evaluated from a morphological and functional point of view (Mokarram et al., 2017).

METHODOLOGICAL CONSIDERATIONS – TECHNIQUES TO INVESTIGATE PERIPHERAL NERVE REGENERATION

A number of different techniques have been developed to investigate the degree and the accuracy of nerve regeneration. While functional tests must be nerve-specific, all other methods can be applied to all types of peripheral nerves. In this paragraph we describe in detail different functional tests that are used to study the functional recovery of the median nerve and, in addition, we present an overview of other methods used for the investigation of nerve regeneration, including morphological and morphometrical analysis, gene expression analysis and fluorescent transgenic animal models.

Functional Evaluation

Several functional tests are available for rodents, both rats and mice (Galtrey and Fawcett, 2007). Some have been designated *ad hoc* to evaluate functional recovery following median nerve repair (e.g., grasping test), others have been adapted from tests normally used following other lesion types (injuries to the spinal cord or sciatic nerves).

The tests described below refer to the rat, but most of them are adaptable also to mice.

- The *grasping test* is a simple method to assess the flexor function, first introduced by Bertelli and Mira (1995). The modified method (Papalia et al., 2003a) consists in presenting a small tower with only three bars forming a triangle on its top instead of a grid for grasping. With this modification the tendency to walk on the grid is avoided and the presence of a band put just below the three bars avoids that the rat employs the wrist flexion to hold the bars. This device is connected to a precision dynamometer. The animal is held by its tail and allowed to grasp the grid. Then, the animal is pulled upward until it loses its grip. The balance records the maximum weight that the animal managed to hold before losing the grip.
- The *staircase test* is a functional test which assesses skilled forepaw reaching and grasping (Montoya et al., 1991). Two/three food pellets are placed on each step of two staircases located one on either side of a central platform. Both stairs are composed of seven steps. The animal is placed in a box and can only reach the pellets from the left staircase with its left paw and those from the right staircase with its right paw. The rat can grasp, lift, and retrieve food pellets from the steps of the staircase. The number of pellets completely removed from the staircase box provides a quantifiable measure of the

distance and efficiency of fine motor reaching skills. Rats need to be pre-trained in the staircase test before surgery, put on restrictive diet before testing and need to be accommodated again to the test conditions for some days before the following evaluation. Therefore, this test is more complex to be applied than the grasping test described above.

- The *walking track analysis* is used to evaluate forelimb motor recovery (Ozmen et al., 2002; Galtrey and Fawcett, 2007). The rat forepaw is dipped in an ink solution and the animal is allowed to walk down the track upon a strip of white or graph paper. The prints by the ink are left to dry and then analysed. Different parameters can be analysed (longest length and widest width of the paw impression, widest width between the second and third fingers, distance between homologous points of sequential paw impressions on a given side, perpendicular distance between the central portion of the paw impression and the direction of movement). Moreover, walking track analysis can be performed by 2D digital video motion analysis, which allows also to quantify the movement of the wrist and the metacarpophalangeal joint (Wang et al., 2008).
- The *Von Frey filament test* is used to evaluate mechanical allodynia (Galtrey and Fawcett, 2007). The animal is placed in a box on a wire mesh floor. Von Frey filaments of different bending forces are used to examine the mechanical threshold of the rat forepaws. The test starts with the smallest bending force and continues in increasing order. Each filament is inserted through the mesh and applied in the medial surface of the forepaw. To perform the test, the rat must be stationary and standing on the four paws. The first filament in the series that evoked withdrawal three times is regarded as the paw withdrawal threshold.
- The *Irvine, Beattie, and Bresnahan (IBB) scale test* (Irvine et al., 2014) is used for the assessment of fine control of the forelimb and digit movements. Spherical- and donut-shaped pieces of cereal are given to the rat. The forelimb behaviour (joint position, object support, wrist and digit movement, and grasping method) used while eating both cereal shapes is analysed. An IBB score is assigned using the 10-point (0–9) ordinal scale for each shape, and the highest score reflects the greatest amount of forelimb recovery.
- The *ladder rung walking test* is used to assess forelimb strength, stepping, placing, and co-ordination during skilled locomotion (Metz and Whishaw, 2002; Galtrey and Fawcett, 2007). The apparatus consists of two side walls with rungs inserted into the walls to create a ladder. The ladder is elevated and can also be inclined. The animal is conditioned to run on the ladder on several training sessions. Performance is scored (successful steps/total steps).
- The *Randall-Selitto test* is used to assess the nociceptive withdrawal threshold (Galtrey and Fawcett, 2007). The test consists in the application of an increasing mechanical force with the tip of an algesimeter on the medial portion of the forepaw until a withdrawal response results.
- For the *cold sensory test* an ice probe is made by freezing water in a 1.5-ml tube (Lindsey et al., 2000; Galtrey and Fawcett, 2007). When the rat is drinking from the water bottle, the ice probe is applied to the glabrous skin of the forepaw. The withdrawal latency is measured. At least 1 min between trials is needed to allow the skin to return to body temperature and prevent sensitisation. If the rat does not withdraw the paw after 10 s, the probe is removed.
- The *cold and hot plate test* is used to assess temperature sensation. The rat is placed in a Plexiglas chamber where the metal base temperature is 25°C. For cold plate testing, the temperature is rapidly lowered and the animal behaviour is observed for signs of pain-like behaviour (avoiding contact with the cold plate, suspension of the affected forelimb, licking of the paw, lack of grooming and exploration vocalisation, or freezing behaviour). Once pain-like behaviour is observed, the temperature is increased to a higher temperature. For hot plate testing, the temperature is raised and the behaviour is assessed as described above (Shaikh et al., 2016).
- The *CatWalk* automated quantitative gait analysis is a computer-assisted method that can simultaneously measure dynamic as well as static gait parameters, including duration of different phases of the step cycle and pressure applied during locomotion (Bozkurt et al., 2008). The animal is placed in the CatWalk walkway, which is comprised of a glass plate with two Plexiglas walls, a high-speed colour camera, and recording and analysis software. The animal walks voluntarily from one side of the glass plate to the other. Its footprints are captured. The intensity of the signal depends on the degree of paw floor contact and increases with pressure applied. The more pressure is exerted, the larger the total area of skin–floor contact and thus the brighter the pixel. An appropriate software visualises the prints and calculates statistics related to print dimensions and the time and distance relationships between footfalls (Chen et al., 2012a,b).
- *Electrophysiology* is often used in rat, while in the mouse model it is less used probably for the small size. The maximum amplitude and latency of evoked compound muscle action potentials recorded from the thenar muscles are usually evaluated (Werdin et al., 2009).

In conclusion, the list provided above clearly demonstrates that a large variety of tests can be used to evaluate the functional recovery after median nerve transection and repair in rodents.

From a translational point of view, tests should be selected in way to model as closely as possible the course of functional recovery as it is observed in human patients. Recently, the combination of electrodiagnostic evaluation, with the commonly used grasping test (reflex-based gross motor function) and the

staircase test (skilled forelimb reaching) has been described to produce results with high translatability (Stossel et al., 2017).

A final comment needs to be put on the fact that different rat strains have been described to demonstrate different motivation degrees to participate in more complex tasks, like, e.g., the staircase test. Especially, Lewis rats have been described to be less motivated and also to eventually be less capable of learning how to perform more complex motor tasks (Nikkhah et al., 1998; Galtrey and Fawcett, 2007).

In the other animals, the functional recovery is assessed mainly by electrophysiology. Indeed, while in rats and mice the fingers do a fine movement quite similar to humans and their functionality can be assessed by different suitable and specific tests, the other animals can do gross movements only.

Morphology and Morphometry (Stereology)

Regardless of the animal model used, nerve regeneration assessment must necessarily have an accurate morphological and morphometrical evaluation (Geuna and Herrera-Rincon, 2015). Among the techniques that allow this type of analysis, immunohistochemistry offers the possibility to specifically identify the different structures of the regenerating nerve, such as Schwann cells, motor or sensory axons, blood vessels, and other cell types, including macrophages, fibroblast-like cells, perineurial cells, endothelial cells (Carriel et al., 2014b). Moreover, immunofluorescence or immunohistochemical techniques allow to accurately quantify the fraction area and the intensity of the expression of specific proteins which are correlated with regenerative processes. For example, the expression of markers such as Neurofilament in neurons or S-100 in Schwann cells are indicative of an excellent regenerative process, when these levels reach the values of the control nerves (Carriel et al., 2014a).

To quantify the number of sensitive and motor neurons which were able to regenerate axons across a nerve gap, the retrograde-labelling technique can be applied. A dye will be applied into the distal nerve and taken up by regenerated axons and retrogradely transported into the neuronal soma of sensory neurons in the dorsal root ganglia or motor-neurons in the ventral horn of the spinal cord (Hayashi et al., 2007; Kemp et al., 2017).

Together with functional assessment, quantitative estimation of regenerated nerve fibres is a key investigation tool in nerve regeneration research (Kanaya et al., 1996; Geuna et al., 2004). The toluidine blue staining of resin-embedded semithin sections allows to clearly identify most of the myelinated axons and their myelin organisation thanks to the post-fixation with OsO₄ (Raimondo et al., 2009). Usually, morpho-quantitative analysis is performed on one randomly selected toluidine blue semi-thin transverse nerve section. The total cross-sectional area of the nerve is measured. Then, an adequate number of fields of interest (according to the size of the nerve) is randomly selected following a systematic random protocol and analysed (Raimondo et al., 2009). The parameters used as nerve regeneration indicators are myelinated fibre number and density, fibre and axon diameter,

myelin thickness and *g-ratio* (axon-diameter/fibre-diameter) (Geuna, 2000, 2005).

In order to compare results obtained by different research groups, different potential sources of bias should be considered.

First of all, the strain, the gender and the age of experimental animals, that can affect the quantification outcome.

The second aspect that can influence the results of a stereological analysis is the level at which it is conducted and, obviously, the different investigation time points. The analysed parameters can vary significantly depending on the distance from the lesion point, especially in the early time points after injury, considering that a nerve can grow approximately 1 mm/day (Santos et al., 2007). Therefore, only quantitative data taken at the same location along the nerves can actually be compared (e.g., 5 mm distal to the lesion site). Obviously, also the time point analysed gives different results and should always be considered (with the same lesion type, a 3-month regenerated nerve will be different from a 6-month regenerated nerve). Finally, it must possibly be considered to analyse all branches of a nerve. The portion of the median nerve that is usually injured and repaired in experimental studies goes from the axillary region to the elbow. In this tract, the median nerve is unifascicular, but for more distal investigation sites the anatomy of the nerve needs to be considered. The median nerve gives off three palmar digital branches more distally, at the level of the carpal bones, that in turn bifurcate between the 1st, 2nd, and 3rd digit (Barton et al., 2016). Other nerves (i.e., the sciatic nerve) release branches in the tract that is commonly investigated. Therefore, if the morphological/morphometrical analysis requires the nerve cross section (for example to estimate the total number of nerve fibres), all branches must be analysed.

The third aspect is represented by the chosen method for measuring the selected size parameters (computerised or manual analysis). It is important to note how computers can certainly make quantitative morphology easier and faster (Williams and Rakic, 1988; Dolapchieva et al., 2000), but a comparison of the performance of automated cell detection revealed that a manual approach is still the most appropriate method for stereological counting (Schmitz et al., 2014).

Gene Expression Analysis

Injured median nerve gene expression analysis can be carried out both at mRNA and protein level. To reduce the number of animals and comply with the 3R' Principle (Replace, Reduce, and Refine) (Tannenbaum and Bennett, 2015) a good strategy is to extract from the same nerve sample both total RNA and proteins, using commercially available kits.

The first point that should be considered when analysing a nerve sample is that protein extraction involves all nerve components, neuronal axons and peripheral cells (Schwann cells, fibroblasts, macrophages, and so on). RNA extraction mostly encloses peripheral cells, because neuronal RNA is mainly localised in the cell bodies of sensory neurons (in the dorsal root ganglia) or motor neurons (in the ventral horn of the spinal cord), with only few mRNAs locally translated in the axon after nerve injury (Terenzio et al., 2018).

The second point that should be carefully considered is the portion of the injured nerve to be analysed and the time window for the analysis. Indeed, in the 1st days after injury, regenerating axons start to colonise the proximal portion of the repaired nerve, while in the distal portion axons are still undergoing Wallerian degeneration (Girouard et al., 2018). In the following days, regeneration occurs also in the distal stump. Therefore, gene expression analysis will give information about regeneration or Wallerian degeneration taking place according to the region and the time point analysed: for gene expression analysis, like previously discussed for morphology and morphometry, the region and the time point analysed must be the same for all samples and for comparison with other studies.

For mRNA analysis, quantitative real time PCR can be carried under paying attention to the housekeeping genes used for normalisation: indeed, it is really important to normalise data to genes whose expression is not affected by nerve injury (Vandesompele et al., 2002). To this aim, stable housekeeping genes suitable for gene expression analysis were identified (Gambardella et al., 2014; Wang et al., 2017). To avoid amplification of contaminant genomic DNA, a good strategy is to design primers on different exons, possibly separated by introns larger than 1,000 bp, or straddling two contiguous exons. For protein analysis, western blots can be carried out using the stain-free technology, which is a good strategy, because protein expression is normalised to the total protein content, bypassing the problem of the choice of suitable housekeeping genes (Gurtler et al., 2013).

Transgenic Models to Evaluate Peripheral Nerve Regeneration

A transgenic model that can be used for evaluating and monitoring peripheral nerve regeneration in mice and rats is Thy1-GFP, in which Thy1 promoter drives neuron specific expression of GFP, allowing imaging of nerve regeneration following nerve injuries (Porrero et al., 2010; Moore et al., 2012; Kemp et al., 2013).

REFERENCES

- Accioli De Vaconcellos, Z. A., Duchossoy, Y., Kassas-Duchossoy, L., and Mira, J. C. (1999). Experimental median nerve repair by fresh or frozen nerve autografts and xenografts. *Ann. Chir. Main Memb. Super* 18, 74–84. doi: 10.1016/s0753-9053(99)80059-3
- Al-Majed, A. A., Brushart, T. M., and Gordon, T. (2000). Electrical stimulation accelerates and increases expression of BDNF and trkB mRNA in regenerating rat femoral motoneurons. *Eur. J. Neurosci.* 12, 4381–4390. doi: 10.1111/j.1460-9568.2000.01341.x
- Angius, D., Wang, H., Spinner, R. J., Gutierrez-Cotto, Y., Yaszemski, M. J., and Windebank, A. J. (2012). A systematic review of animal models used to study nerve regeneration in tissue-engineered scaffolds. *Biomaterials* 33, 8034–8039. doi: 10.1016/j.biomaterials.2012.07.056
- Archibald, S. J., Krarup, C., Shefner, J., Li, S. T., and Madison, R. D. (1991). A collagen-based nerve guide conduit for peripheral nerve repair: an electrophysiological study of nerve regeneration in rodents and nonhuman primates. *J. Comp. Neurol.* 306, 685–696. doi: 10.1002/cne.903060410
- Archibald, S. J., Shefner, J., Krarup, C., and Madison, R. D. (1995). Monkey median nerve repaired by nerve graft or collagen nerve guide tube. *J. Neurosci.* 15(5 Pt 2), 4109–4123. doi: 10.1523/jneurosci.15-05-04109.1995

CONCLUSION

In this review we emphasised the use of the median nerve as pre-clinical experimental model to study nerve regeneration *in vivo*. Accordingly, in the last years the median nerve model is increasingly used due to different reasons, including a better animal well-being, and availability of different functional tests which, specifically in rodents, allow testing the digital fine movement, making the results obtained with this model more translatable into the clinic.

With regard to the animal choice, the rat definitely represents the easiest and more translatable model, especially for studies evaluating regeneration across short nerve gaps, while for large nerve gaps the use of other, larger, animals would be recommended. In case large animal facilities are not available, an alternative and very interesting approach might be the cross-chest median nerve transfer in the rat animal model (Sinis et al., 2006). Indeed, this method would allow the use of rodents, which are less expensive and easier to handle compared to large animals, but at the same time would allow studying nerve regeneration across long gaps (up to 40 mm).

AUTHOR CONTRIBUTIONS

GR, GG, SG, and KH-T organised the manuscript. GR, GG, and MM prepared all the tables. GR, GG, MM, FF, SG, and KH-T wrote different sections of the manuscript. All authors contributed to manuscript revision, and read and approved the submitted version.

FUNDING

This study was supported by the European Community's Seventh Framework Programme (FP7-HEALTH-2011) (Grant No. 278612; BIOHYBRID).

- Audisio, C., Nicolino, S., Scevola, A., Tos, P., Geuna, S., Battiston, B., et al. (2008). ErbB receptors modulation in different types of peripheral nerve regeneration. *Neuroreport* 19, 1605–1609. doi: 10.1097/WNR.0b013e32831313ef00001756-200810290-00010
- Badalamente, M. A., Hurst, L. C., and Stracher, A. (1989). Neuromuscular recovery using calcium protease inhibition after median nerve repair in primates. *Proc. Natl. Acad. Sci. U.S.A.* 86, 5983–5987. doi: 10.1073/pnas.86.15.5983
- Baoguo, J., Shibata, M., Matsuzaki, H., and Takahashi, H. E. (2004). Proximal nerve elongation vs nerve grafting in repairing segmental nerve defects in rabbits. *Microsurgery* 24, 213–217. doi: 10.1002/micr.20039
- Barton, M. J., StJohn, J., Tatian, A., Riches, J. D., Mograby, O., and Mahns, D. A. (2016). Morphological and morphometric analysis of the distal branches of the rat brachial plexus. *Italian J. Anat. Embryol.* 121, 13. doi: 10.13128/IJAE-20273
- Beck-Broichsitter, B. E., Becker, S. T., Lamia, A., Fregnan, F., Geuna, S., and Sinis, N. (2014a). Sensoric protection after median nerve injury: babysitter-procedure prevents muscular atrophy and improves neuronal recovery. *Biomed. Res. Int.* 2014:724197. doi: 10.1155/2014/724197
- Beck-Broichsitter, B. E., Lamia, A., Geuna, S., Fregnan, F., Smeets, R., Becker, S. T., et al. (2014b). Does pulsed magnetic field therapy influence nerve regeneration in the median nerve model of the rat? *Biomed. Res. Int.* 2014:401760. doi: 10.1155/2014/401760

- Bertelli, J. A., dos Santos, A. R., Taleb, M., Calixto, J. B., Mira, J. C., and Ghizoni, M. F. (2004). Long interpositional nerve graft consistently induces incomplete motor and sensory recovery in the rat. An experimental model to test nerve repair. *J. Neurosci. Methods* 134, 75–80. doi: 10.1016/j.jneumeth.2003.11.002
- Bertelli, J. A., and Mira, J. C. (1995). The grasping test: a simple behavioral method for objective quantitative assessment of peripheral nerve regeneration in the rat. *J. Neurosci. Methods* 58, 151–155. doi: 10.1016/0165-0270(94)00169-h
- Bertelli, J. A., Taleb, M., Saadi, A., Mira, J. C., and Pecot-Dechavassine, M. (1995). The rat brachial plexus and its terminal branches: an experimental model for the study of peripheral nerve regeneration. *Microsurgery* 16, 77–85. doi: 10.1002/micr.1920160207
- Bontioti, E., Kanje, M., Lundborg, G., and Dahlin, L. B. (2005). End-to-side nerve repair in the upper extremity of rat. *J. Peripher. Nerv. Syst.* 10, 58–68. doi: 10.1111/j.1085-9489.2005.10109.x
- Bozkurt, A., Deumens, R., Scheffel, J., O'Dey, D. M., Weis, J., Joosten, E. A., et al. (2008). CatWalk gait analysis in assessment of functional recovery after sciatic nerve injury. *J. Neurosci. Methods* 173, 91–98. doi: 10.1016/j.jneumeth.2008.05.020
- Bozkurt, A., Scheffel, J., Brook, G. A., Joosten, E. A., Suschek, C. V., O'Dey, D. M., et al. (2011). Aspects of static and dynamic motor function in peripheral nerve regeneration: SSI and CatWalk gait analysis. *Behav. Brain Res.* 219, 55–62. doi: 10.1016/j.bbr.2010.12.018
- Busuttill, F., Rahim, A. A., and Phillips, J. B. (2017). Combining gene and stem cell therapy for peripheral nerve tissue engineering. *Stem Cells Dev.* 26, 231–238. doi: 10.1089/scd.2016.0188
- Caplan, A. I. (2015). Adult mesenchymal stem cells: when, where, and how. *Stem Cells Int.* 2015:628767. doi: 10.1155/2015/628767
- Carriel, V., Alaminos, M., Garzon, I., Campos, A., and Cornelissen, M. (2014a). Tissue engineering of the peripheral nervous system. *Expert Rev. Neurother.* 14, 301–318. doi: 10.1586/14737175.2014.887444
- Carriel, V., Garzon, I., Alaminos, M., and Cornelissen, M. (2014b). Histological assessment in peripheral nerve tissue engineering. *Neural Regen. Res.* 9, 1657–1660. doi: 10.4103/1673-5374.141798
- Casal, D., Mota-Silva, E., Iria, I., Alves, S., Farinho, A., Pen, C., et al. (2018). Reconstruction of a 10-mm-long median nerve gap in an ischemic environment using autologous conduits with different patterns of blood supply: a comparative study in the rat. *PLoS One* 13:e0195692. doi: 10.1371/journal.pone.0195692
- Caseiro, A. R., Pereira, T., Ivanova, G., Luis, A. L., and Mauricio, A. C. (2016). Neuromuscular regeneration: perspective on the application of mesenchymal stem cells and their secretion products. *Stem Cells Int.* 2016:9756973. doi: 10.1155/2016/9756973
- Chen, S. H., Lue, J. H., Hsiao, Y. J., Lai, S. M., Wang, H. Y., Lin, C. T., et al. (2018). Elevated galanin receptor type 2 primarily contributes to mechanical hypersensitivity after median nerve injury. *PLoS One* 13:e0199512. doi: 10.1371/journal.pone.0199512
- Chen, S. H., Tsai, Y. J., Lin, C. T., Wang, H. Y., Li, S. F., and Lue, J. H. (2012a). Changes in GABA and GABA(B) receptor expressions are involved in neuropathy in the rat cuneate nucleus following median nerve transection. *Synapse* 66, 561–572. doi: 10.1002/syn.21539
- Chen, S. H., Tsai, Y. J., Wang, H. Y., Lin, C. T., Li, S. F., and Lue, J. H. (2012b). Decreases of glycine receptor expression induced by median nerve injury in the rat cuneate nucleus contribute to NPY release and c-Fos expression. *Life Sci.* 90, 278–288. doi: 10.1016/j.lfs.2011.11.014
- Chiono, V., Vozzi, G., Vozzi, F., Salvadori, C., Dini, F., Carlucci, F., et al. (2009). Melt-extruded guides for peripheral nerve regeneration. Part I: poly(epsilon-caprolactone). *Biomed. Microdev.* 11, 1037–1050. doi: 10.1007/s10544-009-9321-9329
- Coradini, J. G., Kunz, R. I., Kakihata, C. M., Errero, T. K., Bonfleur, M. L., Ribeiro Lde, F., et al. (2015). Swimming does not alter nociception threshold in obese rats submitted to median nerve compression. *Neurol. Res.* 37, 1118–1124. doi: 10.1080/01616412.2015.1114742
- Cortez-Retamozo, V., Etzrodt, M., and Pittet, M. J. (2012). Regulation of macrophage and dendritic cell responses by their lineage precursors. *J. Innate Immun.* 4, 411–423. doi: 10.1159/000335733
- de la Monte, S. M., Bour, C., Radhakrishnan, V. V., Jupiter, J. B., Smith, R. J., and Hedley-Whyte, E. T. (1988). Effects of cyclosporin A and predegeneration on survival and regeneration of peripheral nerve allografts in rabbits. *Surg. Neurol.* 29, 95–100. doi: 10.1016/0090-3019(88)90064-x
- Dolapchieva, S., Eggers, R., and Kuhnel, W. (2000). Automatic image analysis of the postnatal growth of axons and myelin sheaths in the tibial and peroneal nerves of the rabbit. *Ann. Anat.* 182, 133–142. doi: 10.1016/s0940-9602(00)80072-80072
- Dubovy, P., Jancalek, R., and Kubek, T. (2013). Role of inflammation and cytokines in peripheral nerve regeneration. *Int. Rev. Neurobiol.* 108, 173–206. doi: 10.1016/b978-0-12-410499-0.00007-1
- Faroni, A., Mobasser, S. A., Kingham, P. J., and Reid, A. J. (2015). Peripheral nerve regeneration: experimental strategies and future perspectives. *Adv. Drug Deliv. Rev.* 82–83, 160–167. doi: 10.1016/j.addr.2014.11.010
- Florence, S. L., Boydston, L. A., Hackett, T. A., Lachoff, H. T., Strata, F., and Niblock, M. M. (2001). Sensory enrichment after peripheral nerve injury restores cortical, not thalamic, receptive field organization. *Eur. J. Neurosci.* 13, 1755–1766. doi: 10.1046/j.0953-816x.2001.01555.x
- Florence, S. L., Garraghty, P. E., Wall, J. T., and Kaas, J. H. (1994). Sensory afferent projections and area 3b somatotopy following median nerve cut and repair in macaque monkeys. *Cereb. Cortex* 4, 391–407. doi: 10.1093/cercor/4.4.391
- Florence, S. L., Jain, N., Pospichal, M. W., Beck, P. D., Sly, D. L., and Kaas, J. H. (1996). Central reorganization of sensory pathways following peripheral nerve regeneration in fetal monkeys. *Nature* 381, 69–71. doi: 10.1038/381069a0
- Forden, J., Xu, Q. G., Khu, K. J., and Midha, R. (2011). A long peripheral nerve autograft model in the sheep forelimb. *Neurosurgery* 68, 1354–1362. doi: 10.1227/NEU.0b013e31820c08de
- Frausin, S., Viventi, S., Verga Falzacappa, L., Quattromani, M. J., Leanza, G., Tommasini, A., et al. (2015). Wharton's jelly derived mesenchymal stromal cells: biological properties, induction of neuronal phenotype and current applications in neurodegeneration research. *Acta Histochem.* 117, 329–338. doi: 10.1016/j.acthis.2015.02.005
- Fregnan, F., Ciglieri, E., Tos, P., Crosio, A., Ciardelli, G., Ruini, F., et al. (2016). Chitosan crosslinked flat scaffolds for peripheral nerve regeneration. *Biomed. Mater.* 11:045010. doi: 10.1088/1748-6041/11/4/045010
- Fu, Y., Karbaat, L., Wu, L., Leijten, J., Both, S. K., and Karperien, M. (2017). Trophic effects of mesenchymal stem cells in tissue regeneration. *Tissue Eng. Part B Rev.* 23, 515–528. doi: 10.1089/ten.TEB.2016.0365
- Fullarton, A. C., Glasby, M. A., and Lawson, G. M. (1998). Immediate and delayed nerve repair using freeze-thawed muscle allografts. associated long-bone fracture. *J. Hand. Surg. Br.* 23, 360–364. doi: 10.1016/s0266-7681(98)80058-2
- Galtrey, C. M., and Fawcett, J. W. (2007). Characterization of tests of functional recovery after median and ulnar nerve injury and repair in the rat forelimb. *J. Peripher. Nerv. Syst.* 12, 11–27. doi: 10.1111/j.1529-8027.2007.00113.x
- Gambarotta, G., Pascal, D., Ronchi, G., Morano, M., Jager, S. B., Moimas, S., et al. (2015). Local delivery of the neuregulin1 receptor ecto-domain (ecto-ErbB4) has a positive effect on regenerated nerve fiber maturation. *Gene Ther.* 22, 901–907. doi: 10.1038/gt.2015.46gt201546
- Gambarotta, G., Ronchi, G., Friard, O., Galletta, P., Perroteau, I., and Geuna, S. (2014). Identification and validation of suitable housekeeping genes for normalizing quantitative real-time PCR assays in injured peripheral nerves. *PLoS One* 9:e105601. doi: 10.1371/journal.pone.0105601PONE-D-14-24896
- Gao, K. M., Lao, J., Guan, W. J., and Hu, J. J. (2018). Is it necessary to use the entire root as a donor when transferring contralateral C7 nerve to repair median nerve? *Neural Regen. Res.* 13, 94–99. doi: 10.4103/1673-5374.224376
- Gartner, A., Pereira, T., Alves, M. G., Armada-da-Silva, P. A., Amorim, I., Gomes, R., et al. (2012). Use of poly(DL-lactide-epsilon-caprolactone) membranes and mesenchymal stem cells from the Wharton's jelly of the umbilical cord for promoting nerve regeneration in axonotmesis: in vitro and in vivo analysis. *Differentiation* 84, 355–365. doi: 10.1016/j.diff.2012.10.001
- Gartner, A., Pereira, T., Armada-da-Silva, P., Amado, S., Veloso, A., Amorim, I., et al. (2014). Effects of umbilical cord tissue mesenchymal stem cells (UCX(R)) on rat sciatic nerve regeneration after neurotmesis injuries. *J. Stem Cells Regen. Med.* 10, 14–26.
- Geuna, S. (2000). Appreciating the difference between design-based and model-based sampling strategies in quantitative morphology of the nervous system. *J. Comp. Neurol.* 427, 333–339. doi: 10.1002/1096-9861(20001120)427:3<333::aid-cne1>3.3.co;2-k

- Geuna, S. (2005). The revolution of counting "tops": two decades of the disector principle in morphological research. *Microsc. Res. Tech.* 66, 270–274. doi: 10.1002/jemt.20167
- Geuna, S., Gigo-Benato, D., and Rodrigues Ade, C. (2004). On sampling and sampling errors in histomorphometry of peripheral nerve fibers. *Microsurgery* 24, 72–76. doi: 10.1002/micr.10199
- Geuna, S., and Herrera-Rincon, C. (2015). Update on stereology for light microscopy. *Cell Tissue Res.* 360, 5–12. doi: 10.1007/s00441-015-2143-2146
- Geuna, S., Nicolino, S., Raimondo, S., Gambarotta, G., Battiston, B., Tos, P., et al. (2007a). Nerve regeneration along bioengineered scaffolds. *Microsurgery* 27, 429–438. doi: 10.1002/micr.20383
- Geuna, S., Tos, P., Raimondo, S., Lee, J. M., Gambarotta, G., Nicolino, S., et al. (2007b). Functional, morphological and biomolecular assessment of posttraumatic neuro-muscular recovery in the rat forelimb model. *Acta Neurochir. Suppl.* 100, 173–177. doi: 10.1007/978-3-211-72958-8_36
- Ghizoni, M. F., Bertelli, J. A., Grala, C. G., and da Silva, R. M. (2013). The anabolic steroid nandrolone enhances motor and sensory functional recovery in rat median nerve repair with long interpositional nerve grafts. *Neurorehabil. Neural. Repair* 27, 269–276. doi: 10.1177/1545968312465190
- Gigo-Benato, D., Geuna, S., de Castro Rodrigues, A., Tos, P., Fornaro, M., Boux, E., et al. (2004). Low-power laser biostimulation enhances nerve repair after end-to-side neurorrhaphy: a double-blind randomized study in the rat median nerve model. *Lasers Med. Sci.* 19, 57–65. doi: 10.1007/s10103-004-0300-303
- Girouard, M. P., Bueno, M., Julian, V., Drake, S., Byrne, A. B., and Fournier, A. E. (2018). The molecular interplay between axon degeneration and regeneration. *Dev. Neurobiol.* 78, 978–990. doi: 10.1002/dneu.22627
- Glasby, M. A., Fullerton, A. C., and Lawson, G. M. (1998). Immediate and delayed nerve repair using freeze-thawed muscle autografts in complex nerve injuries. associated arterial injury. *J. Hand. Surg. Br.* 23, 354–359. doi: 10.1016/s0266-7681(98)80057-0
- Gluck, M. J., Vijayaraghavan, S., Sinclair, E. B., Ashraf, A., Hausman, M. R., and Cagle, P. J. (2018). Detecting structural and inflammatory response after in vivo stretch injury in the rat median nerve via second harmonic generation. *J. Neurosci. Methods* 303, 68–80. doi: 10.1016/j.jneumeth.2018.02.006
- Gomez-Sanchez, J. A., Lopez de Armentia, M., Lujan, R., Kessaris, N., Richardson, W. D., and Cabedo, H. (2009). Sustained axon-glia signaling induces Schwann cell hyperproliferation, remak bundle myelination, and tumorigenesis. *J. Neurosci.* 29, 11304–11315. doi: 10.1523/JNEUROSCI.1753-09.2009
- Gordon, T. (2016). Electrical stimulation to enhance axon regeneration after peripheral nerve injuries in animal models and humans. *Neurotherapeutics* 13, 295–310. doi: 10.1007/s13311-015-0415-411
- Gordon, T., and English, A. W. (2016). Strategies to promote peripheral nerve regeneration: electrical stimulation and/or exercise. *Eur. J. Neurosci.* 43, 336–350. doi: 10.1111/ejn.13005
- Grabb, W. C. (1968). Median and ulnar nerve suture. An experimental study comparing primary and secondary repair in monkeys. *J. Bone Joint Surg. Am.* 50, 964–972. doi: 10.2106/00004623-196850050-00008
- Gui, L. A., Xin, C. T., Xue, C. S., Lin, F. C., Yu, W., Li, N. W., et al. (1997). Regenerative changes in median nerve defects using various rabbit skeletal muscles. *Nihon Hansenbyo Gakkai Zasshi* 66, 207–213. doi: 10.5025/hansen.66.207
- Gurtler, A., Kunz, N., Gomolka, M., Hornhardt, S., Friedl, A. A., McDonald, K., et al. (2013). Stain-Free technology as a normalization tool in Western blot analysis. *Anal. Biochem.* 433, 105–111. doi: 10.1016/j.ab.2012.10.010
- Hara, Y., Nishiura, Y., Ochiai, N., Sharula, Nakajima, Y., Kubota, S., et al. (2012). New treatment for peripheral nerve defects: reconstruction of a 2 cm, monkey median nerve gap by direct lengthening of both nerve stumps. *J. Orthop. Res.* 30, 153–161. doi: 10.1002/jor.21476
- Hayashi, A., Moradzadeh, A., Hunter, D. A., Kawamura, D. H., Puppala, V. K., Tung, T. H., et al. (2007). Retrograde labeling in peripheral nerve research: it is not all black and white. *J. Reconstr. Microsurg.* 23, 381–389. doi: 10.1055/s-2007-992344
- Ho, C. Y., Yao, C. H., Chen, W. C., Shen, W. C., and Bau, D. T. (2013). Electroacupuncture and acupuncture promote the rat's transected median nerve regeneration. *Evid. Based Comp. Alternat. Med.* 2013:514610. doi: 10.1155/2013/514610
- Hoke, A. (2012). Animal models of peripheral neuropathies. *Neurotherapeutics* 9, 262–269. doi: 10.1007/s13311-012-0116-y
- Hu, N., Wu, H., Xue, C., Gong, Y., Wu, J., Xiao, Z., et al. (2013). Long-term outcome of the repair of 50 mm long median nerve defects in rhesus monkeys with marrow mesenchymal stem cells-containing, chitosan-based tissue engineered nerve grafts. *Biomaterials* 34, 100–111. doi: 10.1016/j.biomaterials.2012.09.020
- Huang, C. T., and Tsai, Y. J. (2016). Docosahexaenoic acid confers analgesic effects after median nerve injury via inhibition of c-Jun N-terminal kinase activation in microglia. *J. Nutr. Biochem.* 29, 97–106. doi: 10.1016/j.jnutbio.2015.11.009
- Irvine, K. A., Ferguson, A. R., Mitchell, K. D., Beattie, S. B., Lin, A., Stuck, E. D., et al. (2014). The irvine, beatties, and bresnahan (IBB) forelimb recovery scale: an assessment of reliability and validity. *Front. Neurol.* 5:116. doi: 10.3389/fneur.2014.00116
- Jager, S. B., Ronchi, G., Vaegter, C. B., and Geuna, S. (2014). The mouse median nerve experimental model in regenerative research. *Biomed. Res. Int.* 2014:701682. doi: 10.1155/2014/701682
- Jamnet, P., Kohler, D., Rahmian-Schwarz, A., Lotter, O., Mager, A., Fornaro, M., et al. (2013a). Expression patterns and functional evaluation of the UNC5b receptor during the early phase of peripheral nerve regeneration using the mouse median nerve model. *Microsurgery* 33, 216–222. doi: 10.1002/micr.22059
- Jamnet, P., Kohler, D., Schaufele, M., Rahmian-Schwarz, A., Lotter, O., Fornaro, M., et al. (2013b). Evaluating the role of Netrin-1 during the early phase of peripheral nerve regeneration using the mouse median nerve model. *Restor. Neurol. Neurosci.* 31, 337–345. doi: 10.3233/rnn-120277
- Jeans, L., Healy, D., and Gilchrist, T. (2007). An evaluation using techniques to assess muscle and nerve regeneration of a flexible glass wrap in the repair of peripheral nerves. *Acta Neurochir. Suppl.* 100, 25–28. doi: 10.1007/978-3-211-72958-8_5
- Jeans, L. A., Gilchrist, T., and Healy, D. (2007). Peripheral nerve repair by means of a flexible biodegradable glass fibre wrap: a comparison with microsurgical epineurial repair. *J. Plast Reconstr. Aesthet. Surg.* 60, 1302–1308. doi: 10.1016/j.bjps.2006.06.014
- Jessen, K. R., and Mirsky, R. (2016). The repair Schwann cell and its function in regenerating nerves. *J. Physiol.* 594, 3521–3531. doi: 10.1113/jp270874
- Jiang, L., Jones, S., and Jia, X. (2017). Stem cell transplantation for peripheral nerve regeneration: current options and opportunities. *Int. J. Mol. Sci.* 18:E94
- Jin, H. J., Bae, Y. K., Kim, M., Kwon, S. J., Jeon, H. B., Choi, S. J., et al. (2013). Comparative analysis of human mesenchymal stem cells from bone marrow, adipose tissue, and umbilical cord blood as sources of cell therapy. *Int. J. Mol. Sci.* 14, 17986–18001. doi: 10.3390/ijms140917986
- Jones, S., Eisenberg, H. M., and Jia, X. (2016). Advances and future applications of augmented peripheral nerve regeneration. *Int. J. Mol. Sci.* 17:E1494
- Juneja, M., Burns, J., Saporta, M. A., and Timmerman, V. (2018). Challenges in modelling the charcot-marie-tooth neuropathies for therapy development. *J. Neurol. Neurosurg. Psychiatry* 90, 58–67. doi: 10.1136/jnnp-2018-318834
- Kanaya, F., Firrell, J. C., and Breidenbach, W. C. (1996). Sciatic function index, nerve conduction tests, muscle contraction, and axon morphometry as indicators of regeneration. *Plast. Reconstr. Surg.* 98, 1264–1271. doi: 10.1097/00006534-199612000-00023
- Kaplan, H. M., Mishra, P., and Kohn, J. (2015). The overwhelming use of rat models in nerve regeneration research may compromise designs of nerve guidance conduits for humans. *J. Mater. Sci. Mater. Med.* 26:226. doi: 10.1007/s10856-015-5558-5554
- Kawai, H., Baudrimont, M., Travers, V., and Sedel, L. (1990). A comparative experimental study of vascularized and nonvascularized nerve grafts. *J. Reconstr. Microsurg.* 6, 255–259. doi: 10.1055/s-2007-1006827
- Kelleher, M. O., Al-Abri, R. K., Lenihan, D. V., and Glasby, M. A. (2006a). Use of a static magnetic field to promote recovery after peripheral nerve injury. *J. Neurosurg.* 105, 610–615. doi: 10.3171/jns.2006.105.4.610
- Kelleher, M. O., Myles, L. M., Al-Abri, R. K., and Glasby, M. A. (2006b). The use of ciliary neurotrophic factor to promote recovery after peripheral nerve injury by delivering it at the site of the cell body. *Acta Neurochir.* 148, 55–60. doi: 10.1007/s00701-005-0631-632
- Kemp, S. W., Cederna, P. S., and Midha, R. (2017). Comparative outcome measures in peripheral regeneration studies. *Exp. Neurol.* 287(Pt 3), 348–357. doi: 10.1016/j.expneurol.2016.04.011

- Kemp, S. W., Phua, P. D., Stanoulis, K. N., Wood, M. D., Liu, E. H., Gordon, T., et al. (2013). Functional recovery following peripheral nerve injury in the transgenic Thy1-GFP rat. *J. Peripher. Nerv. Syst.* 18, 220–231. doi: 10.1111/jns5.12035
- Kettle, S. J., Starritt, N. E., Glasby, M. A., and Hems, T. E. (2013). End-to-side nerve repair in a large animal model: how does it compare with conventional methods of nerve repair? *J. Hand. Surg. Eur.* 38, 192–202. doi: 10.1177/1753193412445119
- Kim, J. K., Chung, M. S., and Baek, G. H. (2011). The origin of regenerating axons after end-to-side neurorrhaphy without donor nerve injury. *J. Plast. Reconstr. Aesthet. Surg.* 64, 255–260. doi: 10.1016/j.bjps.2010.04.033
- Konofaos, P., and Ver Halen, J. P. (2013). Nerve repair by means of tubulization: past, present, future. *J. Reconstr. Microsurg.* 29, 149–164. doi: 10.1055/s-0032-1333316
- Kornfeld, T., Vogt, P. M., and Radtke, C. (2018). Nerve grafting for peripheral nerve injuries with extended defect sizes. *Wien Med. Wochenschr.* 169, 240–251. doi: 10.1007/s10354-018-0675-6
- Krupar, C., Archibald, S. J., and Madison, R. D. (2002). Factors that influence peripheral nerve regeneration: an electrophysiological study of the monkey median nerve. *Ann. Neurol.* 51, 69–81. doi: 10.1002/ana.10054
- La Marca, R., Cerri, F., Horiuchi, K., Bachi, A., Feltri, M. L., Wrabetz, L., et al. (2011). TACE (ADAM17) inhibits schwann cell myelination. *Nat. Neurosci.* 14, 857–865. doi: 10.1038/nn.2849
- Lanza, C., Raimondo, S., Vergani, L., Catena, N., Senes, F., Tos, P., et al. (2012). Expression of antioxidant molecules after peripheral nerve injury and regeneration. *J. Neurosci. Res.* 90, 842–848. doi: 10.1002/jnr.22778
- Lawson, G. M., and Glasby, M. A. (1995). A comparison of immediate and delayed nerve repair using autologous freeze-thawed muscle grafts in a large animal model. The simple injury. *J. Hand. Surg. Br.* 20, 663–700. doi: 10.1016/s0266-7681(05)80131-7
- Lawson, G. M., and Glasby, M. A. (1998). Peripheral nerve reconstruction using freeze-thawed muscle grafts: a comparison with group fascicular nerve grafts in a large animal model. *J. R. Coll. Surg. Edinb.* 43, 295–302.
- Lee, J. M., Tos, P., Raimondo, S., Fornaro, M., Papalia, L., Geuna, S., et al. (2007). Lack of topographic specificity in nerve fiber regeneration of rat forelimb mixed nerves. *Neuroscience* 144, 985–990. doi: 10.1016/j.neuroscience.2006.11.001
- Lee, W. P., Constantinescu, M. A., and Butler, P. E. (1999). Effect of early mobilization on healing of nerve repair: histologic observations in a canine model. *Plast Reconstr. Surg.* 104, 1718–1725. doi: 10.1097/00006534-199911000-00016
- Li, R., Hettinger, P. C., Liu, X., Machol, J. T., Yan, J. G., Matloub, H. S., et al. (2014). Early evaluation of nerve regeneration after nerve injury and repair using functional connectivity MRI. *Neurorehabil. Neural. Repair.* 28, 707–715. doi: 10.1177/1545968314521002
- Lindsey, A. E., LoVerso, R. L., Tovar, C. A., Hill, C. E., Beattie, M. S., and Bresnahan, J. C. (2000). An analysis of changes in sensory thresholds to mild tactile and cold stimuli after experimental spinal cord injury in the rat. *Neurorehabil. Neural. Repair.* 14, 287–300. doi: 10.1177/154596830001400405
- Lopatina, T., Kalinina, N., Karagyaur, M., Stambolsky, D., Rubina, K., Revischin, A., et al. (2011). Adipose-derived stem cells stimulate regeneration of peripheral nerves: BDNF secreted by these cells promotes nerve healing and axon growth de novo. *PLoS One* 6:e17899. doi: 10.1371/journal.pone.0017899
- Magill, C., Whitlock, E., Solowski, N., and Mykatsyn, T. (2008). Transgenic models of nerve repair and nerve regeneration. *Neurol. Res.* 30, 1023–1029. doi: 10.1179/174313208x362497
- Manoli, T., Werdin, F., Gruessinger, H., Sinis, N., Schiefer, J. L., Jaminet, P., et al. (2014). Correlation analysis of histomorphometry and motor neurography in the median nerve rat model. *Eplasty* 14:e17.
- Marchesini, A., Raimondo, S., Zingaretti, N., Riccio, V., Battiston, B., Provinciali, M., et al. (2018). The amnion muscle combined graft (AMCG) conduits in nerves repair: an anatomical and experimental study on a rat model. *J. Mater. Sci. Mater. Med.* 29:120. doi: 10.1007/s10856-018-6126-6125
- Marcioli, M. A., Coradini, J. G., Kunz, R. I., Ribeiro Lde, F., Brancalhão, R. M., and Bertolini, G. R. (2013). Nociceptive and histomorphometric evaluation of neural mobilization in experimental injury of the median nerve. *Sci. World J.* 2013:476890. doi: 10.1155/2013/476890
- Marcioli, M. A. R., Silva, J., Ribeiro, L. F. C., Brancalhão, R. M. C., and Bertolini, G. R. F. (2018). Neurotrophin expression and histomorphometric evaluation in Wistar rats subjected to neural mobilization after compression of the median nerve. *Rev. Bras. Ortop.* 53, 276–280. doi: 10.1016/j.rboe.2018.03.006
- Marotte, L. R. (1974). An electron microscope study of chronic median nerve compression in the guinea pig. *Acta Neuropathol.* 27, 69–82. doi: 10.1007/bf00687242
- Matsuyama, T., Midha, R., Mackinnon, S. E., Munro, C. A., Wong, P. Y., and Ang, L. C. (2000). Long nerve allografts in sheep with cyclosporin A immunosuppression. *J. Reconstr. Microsurg.* 16, 219–225.
- Meirelles Lda, S., Fontes, A. M., Covas, D. T., and Caplan, A. I. (2009). Mechanisms involved in the therapeutic properties of mesenchymal stem cells. *Cytokine Growth Factor Rev.* 20, 419–427. doi: 10.1016/j.cytogfr.2009.10.002
- Metz, G. A., and Whishaw, I. Q. (2002). Cortical and subcortical lesions impair skilled walking in the ladder rung walking test: a new task to evaluate fore- and hindlimb stepping, placing, and co-ordination. *J. Neurosci. Methods* 115, 169–179. doi: 10.1016/s0165-0270(02)00012-2
- Meyers, E. C., Granja, R., Solorzano, B. R., Romero-Ortega, M., Kilgard, M. P., Rennaker, R. L., et al. (2017). Median and ulnar nerve injuries reduce volitional forelimb strength in rats. *Muscle Nerve* 56, 1149–1154. doi: 10.1002/mus.25590
- Michailov, G. V., Sereda, M. W., Brinkmann, B. G., Fischer, T. M., Haug, B., Birchmeier, C., et al. (2004). Axonal neuregulin-1 regulates myelin sheath thickness. *Science* 304, 700–703. doi: 10.1126/science.1095862
- Moges, H., Wu, X., McCoy, J., Vasconcelos, O. M., Bryant, H., Grunberg, N. E., et al. (2011). Effect of 810 nm light on nerve regeneration after autograft repair of severely injured rat median nerve. *Lasers Surg. Med.* 43, 901–906. doi: 10.1002/lsm.21117
- Moimas, S., Novati, F., Ronchi, G., Zacchigna, S., Fregnan, F., Zentilin, L., et al. (2013). Effect of vascular endothelial growth factor gene therapy on post-traumatic peripheral nerve regeneration and denervation-related muscle atrophy. *Gene Ther.* 20, 1014–1021. doi: 10.1038/gt.2013.26
- Mokarram, N., Dymanus, K., Srinivasan, A., Lyon, J. G., Tipton, J., Chu, J., et al. (2017). Immunoengineering nerve repair. *Proc. Natl. Acad. Sci. U.S.A.* 114, E5077–E5084. doi: 10.1073/pnas.1705757114
- Mokarram, N., Merchant, A., Mukhatyar, V., Patel, G., and Bellamkonda, R. V. (2012). Effect of modulating macrophage phenotype on peripheral nerve repair. *Biomaterials* 33, 8793–8801. doi: 10.1016/j.biomaterials.2012.08.050
- Montgomery, K. L., Iyer, S. M., Christensen, A. J., Deisseroth, K., and Delp, S. L. (2016). Beyond the brain: optogenetic control in the spinal cord and peripheral nervous system. *Sci. Transl. Med.* 8:337rv335. doi: 10.1126/scitranslmed.aad7577
- Montoya, C. P., Campbell-Hope, L. J., Pemberton, K. D., and Dunnett, S. B. (1991). The 'staircase test': a measure of independent forelimb reaching and grasping abilities in rats. *J. Neurosci. Methods* 36, 219–228. doi: 10.1016/0165-0270(91)90048-5
- Moore, A. M., Borschel, G. H., Santosa, K. A., Flagg, E. R., Tong, A. Y., Kasurkthi, R., et al. (2012). A transgenic rat expressing green fluorescent protein (GFP) in peripheral nerves provides a new hindlimb model for the study of nerve injury and regeneration. *J. Neurosci. Methods* 204, 19–27. doi: 10.1016/j.jneumeth.2011.10.011
- Muratori, L., Gnani, S., Fregnan, F., Mancardi, A., Raimondo, S., Perroteau, I., et al. (2018). Evaluation of vascular endothelial growth factor (VEGF) and its family member expression after peripheral nerve regeneration and denervation. *Anat. Rec.* 301, 1646–1656. doi: 10.1002/ar.23842
- Muratori, L., Ronchi, G., Raimondo, S., Giacobini-Robecchi, M. G., Fornaro, M., and Geuna, S. (2012). Can regenerated nerve fibers return to normal size? a long-term post-traumatic study of the rat median nerve crush injury model. *Microsurgery* 32, 383–387. doi: 10.1002/micr.21969
- Murray, G. M., Taub, D. R., Mackie, P. D., Zhang, H. Q., Ghosh, S., and Rowe, M. J. (1997). The effects of neonatal median nerve injury on the responsiveness of tactile neurones within the cuneate nucleus of the cat. *J. Physiol.* 505 (Pt 3), 759–768. doi: 10.1111/j.1469-7793.1997.759ba.x
- Nabian, M. H., Nadji-Tehrani, M., Zanjani, L. O., Kamrani, R. S., Rahimi-Movaghar, V., and Firouzi, M. (2011). Effect of bilateral median nerve excision on sciatic functional index in rat: an applicable animal model for autologous nerve grafting. *J. Reconstr. Microsurg.* 27, 5–10. doi: 10.1055/s-0030-1267387
- Navarro, X. (2016). Functional evaluation of peripheral nerve regeneration and target reinnervation in animal models: a critical overview. *Eur. J. Neurosci.* 43, 271–286. doi: 10.1111/ejn.13033

- Nicolino, S., Panetto, A., Raimondo, S., Gambarotta, G., Guzzini, M., Fornaro, M., et al. (2009). Denervation and reinnervation of adult skeletal muscle modulate mRNA expression of neuregulin-1 and ErbB receptors. *Microsurgery* 29, 464–472. doi: 10.1002/micr.20636
- Nikkhah, G., Rosenthal, G., Hedrich, H. J., and Samii, M. (1998). Differences in acquisition and full performance in skilled forelimb use as measured by the 'staircase test' in five rat strains. *Behav. Brain Res.* 92, 85–95. doi: 10.1016/s0166-4328(97)00128-9
- Ochoa, J., and Marotte, L. (1973). The nature of the nerve lesion caused by chronic entrapment in the guinea-pig. *J. Neurol. Sci.* 19, 491–495. doi: 10.1016/0022-510x(73)90045-2
- Oliveira, J. T., Almeida, F. M., Biancalana, A., Baptista, A. F., Tomaz, M. A., Melo, P. A., et al. (2010). Mesenchymal stem cells in a polycaprolactone conduit enhance median-nerve regeneration, prevent decrease of creatine phosphokinase levels in muscle, and improve functional recovery in mice. *Neuroscience* 170, 1295–1303. doi: 10.1016/j.neuroscience.2010.08.042
- Oliveira, J. T., Bittencourt-Navarrete, R. E., de Almeida, F. M., Tonda-Turo, C., Martinez, A. M., and Franca, J. G. (2014). Enhancement of median nerve regeneration by mesenchymal stem cells engraftment in an absorbable conduit: improvement of peripheral nerve morphology with enlargement of somatosensory cortical representation. *Front. Neuroanat.* 8:111. doi: 10.3389/fnana.2014.00111
- Ozalp, T., and Masquelet, A. C. (2008). The role of creating a biological membrane in expediting nerve regeneration for peripheral nerve repairs. *Acta Orthop. Traumatol. Turc.* 42, 130–134. doi: 10.3944/aott.2008.42.2.130
- Ozmen, S., Ayhan, S., Latifoglu, O., and Siemionow, M. (2002). Stamp and paper method: a superior technique for the walking track analysis. *Plast Reconstr. Surg.* 109, 1760–1761. doi: 10.1097/00006534-200204150-00065
- Pace, L. A., Plate, J. F., Mannava, S., Barnwell, J. C., Koman, L. A., Li, Z., et al. (2014). A human hair keratin hydrogel scaffold enhances median nerve regeneration in nonhuman primates: an electrophysiological and histological study. *Tissue Eng. Part A* 20, 507–517. doi: 10.1089/ten.TEA.2013.0084
- Papalia, I., Cardaci, A., d'Alcontres, F. S., Lee, J. M., Tos, P., and Geuna, S. (2007). Selection of the donor nerve for end-to-side neurorrhaphy. *J. Neurosurg.* 107, 378–382. doi: 10.3171/jns-07/08/0378
- Papalia, I., Geuna, S., Tos, P. L., Boux, E., Battiston, B., and Stagno d'Alcontres, F. (2003a). Morphologic and functional study of rat median nerve repair by terminolateral neurorrhaphy of the ulnar nerve. *J. Reconstr. Microsurg.* 19, 257–264. doi: 10.1055/s-2003-40582
- Papalia, I., Magaudo, L., Righi, M., Ronchi, G., Viano, N., Geuna, S., et al. (2016). Epineurial window is more efficient in attracting axons than simple coaptation in a sutureless (Cyanoacrylate-Bound) model of end-to-side nerve repair in the rat upper limb: functional and morphometric evidences and review of the literature. *PLoS One* 11:e0148443. doi: 10.1371/journal.pone.0148443
- Papalia, I., Raimondo, S., Ronchi, G., Magaudo, L., Giacobini-Robecchi, M. G., and Geuna, S. (2013). Repairing nerve gaps by vein conduits filled with lipospiro-derived entire adipose tissue hinders nerve regeneration. *Ann. Anat.* 195, 225–230. doi: 10.1016/j.aanat.2012.10.012
- Papalia, I., Tos, P., Stagno d'Alcontres, F., Battiston, B., and Geuna, S. (2003b). On the use of the grasping test in the rat median nerve model: a re-appraisal of its efficacy for quantitative assessment of motor function recovery. *J. Neurosci. Methods* 127, 43–47.
- Park, J. S., and Hoke, A. (2014). Treadmill exercise induced functional recovery after peripheral nerve repair is associated with increased levels of neurotrophic factors. *PLoS One* 9:e90245. doi: 10.1371/journal.pone.0090245
- Pereira, T., Armada-da Silva, P. A., Amorim, I., Rema, A., Caseiro, A. R., Gartner, A., et al. (2014). Effects of human mesenchymal stem cells isolated from wharton's jelly of the umbilical cord and conditioned media on skeletal muscle regeneration using a myectomy model. *Stem Cells Int.* 2014:376918. doi: 10.1155/2014/376918
- Porrero, C., Rubio-Garrido, P., Avendano, C., and Clasca, F. (2010). Mapping of fluorescent protein-expressing neurons and axon pathways in adult and developing Thy1-eYFP-H transgenic mice. *Brain Res.* 1345, 59–72. doi: 10.1016/j.brainres.2010.05.061
- Raimondo, S., Fornaro, M., Di Scipio, F., Ronchi, G., Giacobini-Robecchi, M. G., and Geuna, S. (2009). Chapter 5: methods and protocols in peripheral nerve regeneration experimental research: part II-morphological techniques. *Int. Rev. Neurobiol.* 87, 81–103. doi: 10.1016/S0074-7742(09)87005-87000
- Ray, W. Z., and Mackinnon, S. E. (2010). Management of nerve gaps: autografts, allografts, nerve transfers, and end-to-side neurorrhaphy. *Exp. Neurol.* 223, 77–85. doi: 10.1016/j.expneurol.2009.03.031
- Ronchi, G., Cillino, M., Gambarotta, G., Fornasari, B. E., Raimondo, S., Pugliese, P., et al. (2017). Irreversible changes occurring in long-term denervated Schwann cells affect delayed nerve repair. *J. Neurosurg.* 127, 843–856. doi: 10.3171/2016.9.jns.16140
- Ronchi, G., Fornasari, B. E., Crosio, A., Budau, C. A., Tos, P., Perroteau, I., et al. (2018). Chitosan tubes enriched with fresh skeletal muscle fibers for primary nerve repair. *Biomed. Res. Int.* 2018:9175248. doi: 10.1155/2018/9175248
- Ronchi, G., Gambarotta, G., Di Scipio, F., Salamone, P., Sprio, A. E., Cavallo, F., et al. (2013). ErbB2 receptor over-expression improves post-traumatic peripheral nerve regeneration in adult mice. *PLoS One* 8:e56282. doi: 10.1371/journal.pone.0056282PONE-D-12-18824
- Ronchi, G., Haastert-Talini, K., Fornasari, B. E., Perroteau, I., Geuna, S., and Gambarotta, G. (2016). The Neuregulin1/ErbB system is selectively regulated during peripheral nerve degeneration and regeneration. *Eur. J. Neurosci.* 43, 351–364. doi: 10.1111/ejn.12974
- Ronchi, G., Jager, S. B., Vaegter, C. B., Raimondo, S., Giacobini-Robecchi, M. G., and Geuna, S. (2014). Discrepancies in quantitative assessment of normal and regenerated peripheral nerve fibers between light and electron microscopy. *J. Peripher. Nerv. Syst.* 19, 224–233. doi: 10.1111/jns.12090
- Ronchi, G., Nicolino, S., Raimondo, S., Tos, P., Battiston, B., Papalia, I., et al. (2009). Functional and morphological assessment of a standardized crush injury of the rat median nerve. *J. Neurosci. Methods* 179, 51–57. doi: 10.1016/j.jneumeth.2009.01.011
- Ronchi, G., Raimondo, S., Varejao, A. S., Tos, P., Perroteau, I., and Geuna, S. (2010). Standardized crush injury of the mouse median nerve. *J. Neurosci. Methods* 188, 71–75. doi: 10.1016/j.jneumeth.2010.01.024
- Ruch, D. S., Deal, D. N., Ma, J., Smith, A. M., Castle, J. A., Walker, F. O., et al. (2004). Management of peripheral nerve defects: external fixator-assisted primary neurorrhaphy. *J. Bone Joint Surg. Am.* 86-A, 1405–1413. doi: 10.2106/00004623-200407000-00007
- Santos, A. P., Suaid, C. A., Fazan, V. P., and Barreira, A. A. (2007). Microscopic anatomy of brachial plexus branches in Wistar rats. *Anat. Rec.* 290, 477–485. doi: 10.1002/ar.20519
- Sayad-Fathi, S., Nasiri, E., and Zaminy, A. (2019). Advances in stem cell treatment for sciatic nerve injury. *Expert Opin. Biol. Ther.* 19, 301–311. doi: 10.1080/14712598.2019.1576630
- Schmitz, C., Eastwood, B. S., Tappan, S. J., Glaser, J. R., Peterson, D. A., and Hof, P. R. (2014). Current automated 3D cell detection methods are not a suitable replacement for manual stereologic cell counting. *Front. Neuroanat.* 8:27. doi: 10.3389/fnana.2014.00027
- Shaikh, S., Shortland, P., Lauto, A., Barton, M., Morley, J. W., and Mahns, D. A. (2016). Sensory perturbations using suture and sutureless repair of transected median nerve in rats. *Somatosens Mot. Res.* 33, 20–28. doi: 10.3109/08990220.2016.1142438
- Shibata, M., Breidenbach, W. C., Ogden, L., and Firrell, J. (1991). Comparison of one- and two-stage nerve grafting of the rabbit median nerve. *J. Hand. Surg. Am.* 16, 262–268. doi: 10.1016/s0363-5023(10)80107-8
- Sinis, N., Di Scipio, F., Schonle, P., Werdin, F., Kraus, A., Koopmanns, G., et al. (2009). Local administration of DFO-loaded lipid particles improves recovery after end-to-end reconstruction of rat median nerve. *Restor. Neurol. Neurosci.* 27, 651–662. doi: 10.3233/rnn-2009-2517
- Sinis, N., Kraus, A., Drakotos, D., Doser, M., Schlosshauer, B., Muller, H. W., et al. (2011a). Bioartificial reconstruction of peripheral nerves using the rat median nerve model. *Ann. Anat.* 193, 341–346. doi: 10.1016/j.aanat.2011.02.018
- Sinis, N., Manoli, T., Schiefer, J. L., Werdin, F., Jaminet, P., Kraus, A., et al. (2011b). Application of two different hemostatic procedures during microsurgical median nerve reconstruction in the rat does not hinder axonal regeneration. *Neurosurgery* 68, 1399–1403. doi: 10.1227/NEU.0b013e3182127bc4
- Sinis, N., Schaller, H. E., Becker, S. T., Lanaras, T., Schulte-Eversum, C., Muller, H. W., et al. (2006). Cross-chest median nerve transfer: a new model for the evaluation of nerve regeneration across a 40 mm gap in the rat. *J. Neurosci. Methods* 156, 166–172. doi: 10.1016/j.jneumeth.2006.02.022
- Sinis, N., Schaller, H. E., Schulte-Eversum, C., Lanaras, T., Schlosshauer, B., Doser, M., et al. (2007). Comparative neuro tissue engineering using different nerve

- guide implants. *Acta Neurochir. Suppl.* 100, 61–64. doi: 10.1007/978-3-211-72958-8_13
- Sinis, N., Schaller, H. E., Schulte-Eversum, C., Schlosshauer, B., Doser, M., Dietz, K., et al. (2005). Nerve regeneration across a 2-cm gap in the rat median nerve using a resorbable nerve conduit filled with Schwann cells. *J. Neurosurg.* 103, 1067–1076. doi: 10.3171/jns.2005.103.6.1067
- Speck, A. E., Ilha, J., do Espirito Santo, C. C., Aguiar, A. S., Jr., Dos Santos, A. R., et al. (2014). The IBB forelimb scale as a tool to assess functional recovery after peripheral nerve injury in mice. *J. Neurosci. Methods* 226, 66–72. doi: 10.1016/j.jneumeth.2014.01.007
- Stossel, M., Rehra, L., and Haastert-Talini, K. (2017). Reflex-based grasping, skilled forelimb reaching, and electrodiagnostic evaluation for comprehensive analysis of functional recovery-The 7-mm rat median nerve gap repair model revisited. *Brain Behav.* 7:e00813. doi: 10.1002/brb3.813
- Strasberg, S. R., Mackinnon, S. E., Genden, E. M., Bain, J. R., Purcell, C. M., Hunter, D. A., et al. (1996). Long-segment nerve allograft regeneration in the sheep model: experimental study and review of the literature. *J. Reconstr. Microsurg.* 12, 529–537. doi: 10.1055/s-2007-1006625
- Sullivan, R., Dailey, T., Duncan, K., Abel, N., and Borlongan, C. V. (2016). Peripheral nerve injury: stem cell therapy and peripheral nerve transfer. *Int. J. Mol. Sci.* 17:E2101
- Sun, Q., Zheng, J., and Zhao, C. (2012). Nerve transplantation and accompanying peripheral vessels for repair of long nerve defect. *Zhongguo Xiu Fu Chong Jian Wai Ke Za Zhi* 26, 832–836.
- Tannemaat, M. R., Verhaagen, J., and Malessy, M. (2008). The application of viral vectors to enhance regeneration after peripheral nerve repair. *Neurol. Res.* 30, 1039–1046. doi: 10.1179/174313208x362514
- Tannenbaum, J., and Bennett, B. T. (2015). Russell and Burch's 3Rs then and now: the need for clarity in definition and purpose. *J. Am. Assoc. Lab. Anim. Sci.* 54, 120–132.
- Terenzio, M., Koley, S., Samra, N., Rishal, I., Zhao, Q., Sahoo, P. K., et al. (2018). Locally translated mTOR controls axonal local translation in nerve injury. *Science* 359, 1416–1421. doi: 10.1126/science.aan1053
- Tos, P., Battiston, B., Nicolino, S., Raimondo, S., Fornaro, M., Lee, J. M., et al. (2007). Comparison of fresh and predegenerated muscle-vein-combined guides for the repair of rat median nerve. *Microsurgery* 27, 48–55. doi: 10.1002/micr.20306
- Tos, P., Calcagni, M., Gigo-Benato, D., Boux, E., Geuna, S., and Battiston, B. (2004). Use of muscle-vein-combined Y-chambers for repair of multiple nerve lesions: experimental results. *Microsurgery* 24, 459–464. doi: 10.1002/micr.20064
- Tos, P., Ronchi, G., Nicolino, S., Audisio, C., Raimondo, S., Fornaro, M., et al. (2008). Employment of the mouse median nerve model for the experimental assessment of peripheral nerve regeneration. *J. Neurosci. Methods* 169, 119–127. doi: 10.1016/j.jneumeth.2007.11.030
- Tountas, C. P., Bergman, R. A., Lewis, T. W., Stone, H. E., Pyrek, J. D., and Mendenhall, H. V. (1993). A comparison of peripheral nerve repair using an absorbable tubulization device and conventional suture in primates. *J. Appl. Biomater.* 4, 261–268. doi: 10.1002/jab.770040308
- Vandesompele, J., De Preter, K., Pattyn, F., Poppe, B., Van Roy, N., De Paep, A., et al. (2002). Accurate normalization of real-time quantitative RT-PCR data by geometric averaging of multiple internal control genes. *Genome Biol.* 3:RESEARCH0034.
- Varejao, A. S., Melo-Pinto, P., Meek, M. F., Filipe, V. M., and Bulas-Cruz, J. (2004). Methods for the experimental functional assessment of rat sciatic nerve regeneration. *Neurol. Res.* 26, 186–194. doi: 10.1179/016164104225013833
- Velanac, V., Unterbarnscheidt, T., Hinrichs, W., Gummert, M. N., Fischer, T. M., Rossner, M. J., et al. (2012). Bcl-1 processing of NRG1 type III produces a myelin-inducing signal but is not essential for the stimulation of myelination. *Glia* 60, 203–217. doi: 10.1002/glia.21255
- Wall, J. T., Kaas, J. H., Sur, M., Nelson, R. J., Felleman, D. J., and Merzenich, M. M. (1986). Functional reorganization in somatosensory cortical areas 3b and 1 of adult monkeys after median nerve repair: possible relationships to sensory recovery in humans. *J. Neurosci.* 6, 218–233. doi: 10.1523/jneurosci.06-01-00218.1986
- Wang, H., Spinner, R. J., Sorenson, E. J., and Windebank, A. J. (2008). Measurement of forelimb function by digital video motion analysis in rat nerve transection models. *J. Peripher. Nerv. Syst.* 13, 92–102. doi: 10.1111/j.1529-8027.2008.00162.x
- Wang, Y., Shan, Q., Meng, Y., Pan, J., and Yi, S. (2017). Mrpl10 and Tbp are suitable reference genes for peripheral nerve crush injury. *Int. J. Mol. Sci.* 18:E263
- Wang, Y. H., Zhang, D. Y., Zhang, P. X., Yin, X. F., Kou, Y. H., Wang, J., et al. (2009). Amplification effects in nerve regeneration after different segment injury: experiment with rabbit median nerve. *Zhonghua Yi Xue Za Zhi* 89, 1645–1649.
- Ward, P. J., Clanton, S. L., II, and English, A. W. (2018). Optogenetically enhanced axon regeneration: motor versus sensory neuron-specific stimulation. *Eur. J. Neurosci.* 47, 294–304. doi: 10.1111/ejn.13836
- Ward, P. J., Jones, L. N., Mulligan, A., Goolsby, W., Wilhelm, J. C., and English, A. W. (2016). Optically-induced neuronal activity is sufficient to promote functional motor axon regeneration in vivo. *PLoS One* 11:e0154243. doi: 10.1371/journal.pone.0154243
- Werdin, F., Grüssinger, H., Jaminet, P., Kraus, A., Manoli, T., Danker, T., et al. (2009). An improved electrophysiological method to study peripheral nerve regeneration in rats. *J. Neurosci. Methods* 182, 71–77. doi: 10.1016/j.jneumeth.2009.05.017
- Whishaw, I. Q., Pellis, S. M., and Gorny, B. P. (1992). Skilled reaching in rats and humans: evidence for parallel development or homology. *Behav. Brain Res.* 47, 59–70. doi: 10.1016/s0166-4328(05)80252-9
- Williams, R. W., and Rakic, P. (1988). Three-dimensional counting: an accurate and direct method to estimate numbers of cells in sectioned material. *J. Comp. Neurol.* 278, 344–352. doi: 10.1002/cne.902780305
- Yin, X. F., Kou, Y. H., Wang, Y. H., Zhang, P., Zhang, H. B., and Jiang, B. G. (2011). Portion of a nerve trunk can be used as a donor nerve to reconstruct the injured nerve and donor site simultaneously. *Artif. Cells Blood Substit. Immobil. Biotechnol.* 39, 304–309. doi: 10.3109/10731199.2011.574636
- Yona, S., and Jung, S. (2010). Monocytes: subsets, origins, fates and functions. *Curr. Opin. Hematol.* 17, 53–59. doi: 10.1097/MOH.0b013e3283324f80
- Zhang, P., Zhang, C., Kou, Y., Yin, X., Zhang, H., and Jiang, B. (2009). The histological analysis of biological conduit sleeve bridging rhesus monkey median nerve injury with small gap. *Artif. Cells Blood Substit. Immobil. Biotechnol.* 37, 101–104. doi: 10.1080/10731190902742620
- Zhang, Z., Johnson, E. O., Vekris, M. D., Zoubos, A. B., Bo, J., Beris, A. E., et al. (2006). Repair of the main nerve trunk of the upper limb with end-to-side neurorrhaphy: an experimental study in rabbits. *Microsurgery* 26, 245–252. doi: 10.1002/micr.20235

Conflict of Interest Statement: The authors declare that the research was conducted in the absence of any commercial or financial relationships that could be construed as a potential conflict of interest.

The handling Editor is currently co-organizing a Research Topic with two of the authors KH-T and GG, and confirms the absence of any other collaboration.

Copyright © 2019 Ronchi, Morano, Fregnan, Pugliese, Crosio, Tos, Geuna, Haastert-Talini and Gambarotta. This is an open-access article distributed under the terms of the Creative Commons Attribution License (CC BY). The use, distribution or reproduction in other forums is permitted, provided the original author(s) and the copyright owner(s) are credited and that the original publication in this journal is cited, in accordance with accepted academic practice. No use, distribution or reproduction is permitted which does not comply with these terms.

Advantages of publishing in Frontiers



OPEN ACCESS

Articles are free to read
for greatest visibility
and readership



FAST PUBLICATION

Around 90 days
from submission
to decision



HIGH QUALITY PEER-REVIEW

Rigorous, collaborative,
and constructive
peer-review



TRANSPARENT PEER-REVIEW

Editors and reviewers
acknowledged by name
on published articles

Frontiers

Avenue du Tribunal-Fédéral 34
1005 Lausanne | Switzerland

Visit us: www.frontiersin.org

Contact us: info@frontiersin.org | +41 21 510 17 00



REPRODUCIBILITY OF RESEARCH

Support open data
and methods to enhance
research reproducibility



DIGITAL PUBLISHING

Articles designed
for optimal readership
across devices



FOLLOW US

@frontiersin



IMPACT METRICS

Advanced article metrics
track visibility across
digital media



EXTENSIVE PROMOTION

Marketing
and promotion
of impactful research



LOOP RESEARCH NETWORK

Our network
increases your
article's readership